Third Edition

PACS-Based Multimedia Imaging Informatics

Basic Principles and Applications

H.K. Huang

with website

WILEY Blackwell

Table of Contents

- Cover
- Foreword 1
  - PACS–Based Multimedia Imaging Informatics 3rd Edition, 2018
- Foreword 2
  - A Thought on PACS and CAD
- Foreword 3
- Preface to the Third Edition
  - The Beginning
  - My Experience
  - The Third Edition
  - The Future Growth
- Preface to the Second Edition
  - My Interest in PACS and Medical Imaging Informatics
  - PACS and Imaging Informatics Development since the 2004 Book
  - PACS and Imaging Informatics, The Second Edition
- Acknowledgments
- H.K. Huang Short Biography
- List of Acronyms
- Part 1: The Beginning: Retrospective
  - 1 Medical Imaging, PACS and Imaging Informatics: Retrospective
    - PART I TECHNOLOGY DEVELOPMENT AND PIONEERS
    - 1.1 Medical Imaging
    - 1.2 PACS and its Development
    - 1.3 Key Technologies: Computer and Software, Storage, and Communication Networks
    - 1.4 Key Technologies: Medical Imaging Related
    - PART II COLLABORATIONS AND SUPPORTS
    - 1.5 Collaboration with Government Agencies, Industry and Medical

Imaging Associations
1.6 Medical Imaging Informatics
1.7 Summary
1.8 Acknowledgments
References
Part 2: Medical Imaging, Industrial Guidelines, Standards, and Compliance
2 Digital Medical Imaging
2.1 Digital Medical Imaging Fundamentals
2.2 Two-Dimensional Medical Imaging
2.3 Three-Dimensional Medical Imaging
2.4 Four-Dimensional, Multimodality, and Fusion Imaging
2.5 Image Compression
Further Reading
3 PACS Fundamentals
3.1 PACS Components and Network
3.2 PACS Infrastructure Design Concept
3.3 Generic PACS-Based Multimedia Architecture and Workflow
3.4 PACS-Based Architectures
3.5 Communication and Networks
Further Reading
4 Industrial Standards: Health Level 7 (HL7), Digital Imaging and Communications in Medicine (DICOM) and Integrating the Healthcare Enterprise (IHE)
4.1 Industrial Standards
4.2 The Health Level 7 (HL7) Standard
4.3 From ACR-NEMA to DICOM
4.4 DICOM 3.0 Standard
4.5 Examples of using DICOM
4.6 DICOM Organizational Structure and New Features
4.7 IHE (Integrating the Healthcare Enterprise)
4.8 Some Operating Systems and Programming Languages useful to

HL7, DICOM and IHE
4.9 Summary of Industrial Standards: HL7, DICOM and IHE
References
Further Reading
5 DICOM-Compliant Image Acquisition Gateway and Integration of HIS, RIS, PACS and ePR
5.1 DICOM Acquisition Gateway
5.2 DICOM-Compliant Image Acquisition Gateway
5.3 Automatic Image Data Recovery Scheme for DICOM Conformance Device
5.4 Interface PACS Modalities with the Gateway Computer
5.5 DICOM Compliance PACS Broker
5.6 Image Preprocessing and Display
5.7 Clinical Operation and Reliability of the Gateway
5.8 Hospital Information System (HIS), Radiology Information System (RIS), and PACS
References
6 Web-Based Data Management and Image Distribution
6.1 Distributed Image File Server: PACS-Based Data Management
6.2 Distributed Image File Server
6.3 Web Server
6.4 Component-based Web Server for Image Distribution and Display
6.5 Performance Evaluation
6.6 Summary of PACS Data Management and Web-based Image Distribution
Further Reading
7 Medical Image Sharing for Collaborative Healthcare Based on IHE XDS-I Profile
7.1 Introduction
7.2 Brief Description of IHE XDS/XDS-I Profiles
7.3 Pilot Studies of Medical Image Sharing and Exchanging for a Variety of Healthcare Services

7.4 Results
7.5 Discussion
Acknowledgements
References
Part 3: Informatics, Data Grid, Workstation, Radiotherapy, Simulators, Molecular Imaging, Archive Server, and Cloud Computing
8 Data Grid for PACS and Medical Imaging Informatics
8.1 Distributed Computing
8.2 Grid Computing
8.3 Data Grid [5]
8.4 Fault-Tolerant Data Grid for PACS Archive and Backup, Query/Retrieval, and Disaster Recovery
References
Further Reading
9 Data Grid for Clinical Applications
9.1 Clinical Trials and Data Grid
9.2 Dedicated Breast MRI Enterprise Data Grid
9.3 Administrating the Data Grid
9.4 Summary
References
Further Reading
10 Display Workstations
10.1 PACS-Based Display Workstation
10.2 Various Types of Image Workstation
10.3 Image Display and Measurement Functions
10.4 Workstation Graphic User Interface (GUI) and Basic Display Functions [3–15]
10.5 DICOM PC-Based Display Workstation Software
10.6 Post-Processing Workflow, PACS-Based Multidimensional Display, and Specialized Post-Processing Workstation
10.7 DICOM-Based Workstations in Progress

References
11 Multimedia Electronic Patient Record (EPR) System in Radiotherapy (RT)
11.1 Multimodality 2-D and 3-D Imaging in Radiotherapy
11.2 Multimedia ePR System in Radiation Treatment
11.3 Radiotherapy Planning and Treatment
11.4 Radiotherapy Workflow
11.5 The ePR Data Model and DICOM-RT Objects
11.6 Infrastructure, Workflow and Components of the Multimedia ePR in RT
11.7 Database Schema
11.8 Graphical User Interface Design
11.9 Validation of the Concept of Multimedia ePR System in RT
11.10 Advantages of the Multimedia ePR system in Radiotherapy for Daily Clinical Practice
11.11 Use of the Multimedia ePR System in RT For Image-Assisted Knowledge Discovery and Decision Making
11.12 Summary
Acknowledgement
References
12 PACS-Based Imaging Informatics Simulators
12.1 Why Imaging Informatics Simulators?
12.2 PACS–ePR Simulator
12.3 Data Grid Simulator
12.4 CAD–PACS Simulator
12.5 Radiotherapy (RT) ePR Simulator
12.6 Image-Assisted Surgery (IAS) ePR Simulator
12.7 Summary
Acknowledgments
References
13 Molecular Imaging Data Grid (MIDG)

13.1 Introduction
13.2 Molecular Imaging
13.3 Methodology
13.4 Results
13.5 Discussion
13.6 Summary
Acknowledgments
References
14 A DICOM-Based Second-Generation Molecular Imaging Data Grid (MIDG) with the IHE XDS-i Integration Profile
14.1 Introduction
14.2 Methodology
14.3 System Implementation
14.4 Data Collection and Normalization
14.5 System Performance
14.6 Data Transmission, MIDG Implementation, Workflow and System Potential
14.7 Summary
Acknowledgments
References
15 PACS-Based Archive Server and Cloud Computing
15.1 PACS-Based Multimedia Biomedical Imaging Informatics
15.2 PACS-Based Server and Archive
15.3 PACS-Based Archive Server System Operations
15.4 DICOM-Compliant PACS-Based Archive Server
15.5 DICOM PACS-Based Archive Server Hardware and Software
15.6 Backup Archive Server and Data Grid
15.7 Cloud Computing and Archive Server
Acknowledgements
References
Part 4: Multimedia Imaging Informatics, Computer-Aided Diagnosis (CAD),

Image'Guide Decision Support, Proton Therapy, Minimally Invasive Multimedia Image-Assisted Surgery, Big Data
16 DICOM-Based Medical Imaging Informatics and CAD
16.1 Computer-Aided Diagnosis (CAD)
16.2 Integration of CAD with PACS-Based Multimedia Informatics
16.3 The CAD–PACS Integration Toolkit
16.4 Data Flow of the three CAD–PACS Editions Integration Toolkit
References
Further Reading
17 DICOM-Based CAD: Acute Intracranial Hemorrhage and Multiple Sclerosis
17.1 Computer-Aided Detection (CAD) of Small Acute Intracranial Hemorrhage on CT of the Brain
17.2 Development of the CAD Algorithm for AIH on CT
17.3 CAD–PACS Integration
17.4 Multiple Sclerosis (MS) on MRI
References
Further Reading
18 PACS-Based CAD: Digital Hand Atlas and Bone Age Assessment of children
18.1 Average Bone Age of a Child
18.2 Bone Age Assessment of Children
18.3 Method of Analysis
18.4 Integration of CAD with PACS-Based Multimedia Informatics for Bone Age Assessment of Children: The CAD System
18.5 Validation of the CAD and the Comparison of CAD Result with Radiologists' Assessment
18.6 Clinical Evaluation of the CAD System for Bone Age Assessment (BAA)
18.7 Integrating CAD for Bone Age Assessment with Other Informatics Systems
18.8 Research and Development Trends in CAD–PACS Integration

Acknowledgements
References
Further Reading
19 Intelligent ePR System for Evidence-Based Research in Radiotherapy
19.1 Introduction
19.2 Proton Therapy Clinical Workflow and Data
19.3 Proton Therapy ePR System
19.4 System Implementation
19.5 Results
19.6 Conclusion and Discussion
Acknowledgements
References
20 Multimedia Electronic Patient Record System for Minimally Invasive Image-Assisted Spinal Surgery
20.1 Integration of Medical Diagnosis with Image-Assisted Surgery Treatment
20.2 Minimally Invasive Spinal Surgery Workflow
20.3 Multimedia ePR System for Image-Assisted MISS Workflow and Data Model
20.4 ePR MISS System Architecture
20.5 Pre-Op Authoring Module
20.6 Intra-Op Module
20.7 Post-Op Module
20.8 System Deployment, User Training and Support
20.9 Summary
References
21 From Minimally Invasive Spinal Surgery to Integrated Image-Assisted Surgery in Translational Medicine
21.1 Introduction
21.2 Integrated Image-Assisted Minimally Invasive Spinal Surgery
21.3 IIA-MISS EMR System Evaluation

21.4 To Fulfill some Translational Medicine Aims
21.5 Summary
21.6 Contribution from Colleagues
Acknowledgement
References
22 Big Data in PACS-Based Multimedia Medical Imaging Informatics
22.1 Big Data in PACS-Based Multimedia Medical Imaging Informatics
22.2 Characters and Challenges of Medical Image Big Data
22.3 Possible and Potential Solutions of Big Data in DICOM PACS-Based Medical Imaging and Informatics
22.4 Research Projects Related to Medical Imaging Big Data
22.5 Summary of Big Data
Acknowledgements
References
Index
End User License Agreement

List of Tables

Chapter 01
Table 1.1 Equipment at IPL, UCLA, 1987.
Chapter 02
Table 2.1 Sizes of some common 2-D, 3-D, and 4-D and fusion medical images.
Chapter 03
Table 3.1 Major functions of the PACS server and archive.
Table 3.2 Major functions of PACS workstations.
Table 3.3 Seven-layer open systems interconnect (OSI) protocols.
Table 3.4 Current available wireless LAN technology.
Table 3.5 Transmission rate of current WAN technology.

Table 3.6 Performance data for different sites connected with international Internet 2.

Table 3.7 Comparison of performance data between sites that utilized the Web 100 tuning protocol (last column) and the same sites using standard Linux without tuning.

Table 3.8 Performance data for IPI connectivity to both PolyU and InCor using a commercial high-speed ISP vendor.

Chapter 04

Table 4.1 DICOM service classes.

Table 4.2 DICOM information object classes.

Table 4.3 Normalized DICOM message service element (DIMSE).

Table 4.4 Composite DICOM message service element (DIMSE).

Chapter 05

Table 5.1 Information transferred among HIS, RIS, and PACS triggered by the PACS server.

Chapter 07

Table 7.1 Time intervals for displaying the first image in a series after issuing an ITI-43 request in the online sharing model.

Table 7.2 Time intervals for displaying the first image in a series after issuing an ITI-43 request in the near-line sharing model.

Table 7.3 Comparisons of three pilot studies in work flows, PACS interfacing, implementation of IHE XDS-I actors, and transactions (S = Standard Implementation, C = Customized Implementation).

Chapter 10

Table 10.1 Advantages and disadvantage of the LCD over the CRT.

Table 10.2 Important software functions in a display WS.

Table 10.3 Description of the user interface icons and toolbars shown in Figure 10.17.

Chapter 13

Table 13.1 Preclinical Molecular Imaging File Formats Collected for

Evaluation from USC Molecular Imaging Center.

Table 13.2 Performance tests measuring the time it takes to archive and retrieve a study dataset from six different preclinical molecular imaging modality types over a 100 mbps network.

Chapter 14

Table 14.1 (A) Molecular imaging datasets systematically collected for evaluation from the USC MIC. (SOP: Service-Object Pair; SC: Secondary Capture).

Table 14.1 (B) List of DICOM tags that are labeled by the MIDG during the upload process.

Table 14.2 Comparison of upload and download performance of first-generation MIDG and second-generation MIDG, using datasets from four preclinical imaging modalities.

Chapter 16

Table 16.1 (A) Topics and numbers of CAD-related presentations at the RSNA meetings, 2000–2008.

Table 16.1 (B) Number of CAD presentations at the RSNA meetings, 2003–2008.

Table 16.2 CAD without PACS and with or without digital input.

Table 16.3 (A) CAD with DICOM PACS: PACS WS Q/R, CAD WS, and detect.

Table 16.3 (B) CAD with DICOM PACS: CAD WS Q/R and detect.

Table 16.3 (C) CAD with PACS: PACS WS with diagnosis software.

Table 16.3 (D) Integration of CAD server with DICOM PACS and/or MIII.

Table 16.4 Comparison of the three CAD–PACS integration editions (SR: Structured Reporting).

Chapter 17

Table 17.1 Details of individual image processing and analysis steps of in the CAD for AIH algorithm, as outlined in Figure 17.1.

Table 17.2 Sample rules used in the knowledge base classification in the

CAD system for AIH on CT brain.

Table 17.3 CAD results based on training data and validation data.

Table 17.4 Average performance indicators included are sensitivity, specificity, positive predictive value, and negative predictive value for different clinician groups with and without CAD support.

Table 17.5 Cases in which clinicians change their diagnostic decision after CAD.

Table 17.6 Tasks and requirements for integrating CAD with PACS systems in the three examples.

Chapter 18

Table 18.1 Images and data contained in the Digital Hand Atlas.

Table 18.2 Clinical reliability of using the three ROIs for BAA in different age groups.

Table 18.3 Mean difference between bone age and chronologic age according to race and sex as assessed by radiologists.

Chapter 19

Table 19.1 Proton therapy data collected from one prostate cancer patient.

Table 19.2 Summary of main pretreatment clinical data (n = 39 patients).

Table 19.3 Summary of follow-up clinical data (*n* = 39 patients).

Table 19.4 Patient new information and treatment plan in comparison to search criteria.

Table 19.5 Comparison of volume percentage of the tumor target and critical structures between previous plan and modified plan of Patient New.

Chapter 20

Table 20.1 Default values for the safe ranges of the patient’s vital signs during MISS operation used as indicators to set off alarms on the real-time intra-op display.

Chapter 21

Table 21.1 Comparison of minimally invasive spinal surgery (MISS)

operation times between the procedure with and without using the EMR system with different number of vertebrae per procedure.

Table 21.2 Comparison between the IIAS platform basic common components (columns 3 and 4) and the customized components in column 2 (SW) and column 4 (C) for a specific surgical application.

List of Illustrations

Chapter 01

Figure 1.1 Robert Steven Ledley (June 28, 1926–July 24, 2012, aged 86).

Figure 1.2 Innovative medical imaging components in the Pattern Recognition Laboratory in the mid-1970s: (A) FIDAC (Film input to Digital Automatic Computer); (B) DRIDAC (Drum Input to Digital Automatic Computer); (C) SPIDAC (Specimen Input to Digital Automatic Computer).

Figure 1.3 Pattern Recognition Laboratory, National Biomedical Research Foundation.

Figure 1.4 The ACTA, with Professor Ledley, the first whole-body CT scanner, with two slices per scan in 4½ min.

Figure 1.5 Top: PACS system and components. Bottom: Imaging informatics platform.

Figure 1.6 (A) Professor Moses Greenfield (March 8, 1916–July 26, 2012, 97 years); (B) Professor Hooshang Kangarloo (Dec 24, 1944–May 15, 2012, 67 years) and his faculty and residents in the pediatric radiology reading room using the PACS three 1K × 1K monitor viewing workstation.

Figure 1.7 Research and clinical components at IPL connected by the Ethernet Communication System. This figure was a historical drawing of the Image Processing Laboratory (IPL), Department of Radiological Sciences at UCLA, IPL established in 1982, and developed the first PACS for clinical operation between 1987 and 1991. Bottom left: the IPL. Right: clinical laboratory. Top right: the PACS workstations at three experimental laboratories in the hospital. This equipment was the beta version of the PACS workstations later installed in the clinical sites. IDs in the bottom of each block were the room no. located at the Department

and the UCLA Hospital.

Figure 1.8 The VAX/11 750 computer. Left: the Gould DeAnza multiple display controller (middle, blue).

Figure 1.9 Large-capacity Optical Disk Jukebox by Kodak and the RAID disks running the AMASS software (right).

Figure 1.10 The first Konica laser film scanner at UCLA, 1984.

Figure 1.11 The first Fuji computed radiography (CR) system in the United States was installed at the Ochsner Clinics, New Orleans; the second system was installed at UCLA in late 1985.

Figure 1.12 The first digital interface unit using a ping-pong buffer and the DR11-W interface technology to transmit CR images in real time to the outside of the CR reader. It was designed and implemented by the UCLA PACS team. The black box is shown in (A). The architecture module was a gateway to the PACS input system in (B). The novelty of the design at that time was the use of the ping-pong buffers to allow the continuous Fuji image data transfer to both the laser film recorder as well as the direct digital capture mechanism of the VAX 11/750 computer.

Figure 1.13 The prototype Konica digital radiography system at the UCLA PACS clinical laboratory. There were three imaging plates in the housing, allowing three consecutive exposures in one examination.

Figure 1.14 (A) The multiple viewing workstations laboratory (WS Lab) at UCLA with multiple-resolution workstations, including two six-monitor display systems (512 × 512), one 1400-line single-monitor system, and one three-monitor display system (1K × 1K). This workstation room was used for the first large-scale study on the quality of image display with different spatial and density resolutions. (B) The first two 2K line monitor display was not yet available at that time, but was later developed by a commercial company, Megascan, and installed in the WS Lab.

Figure 1.15 The NATO ASI [22].

Figure 1.16 Adopted from Professor Irie’s Concept of Medical Record System (MIS) in Hokkadio University Hospital [28,29]

Figure 1.17 The Proceedings of the first SPIE Picture Archiving and Communication Systems (PACS) Conference at San Diego, CA, 1982.

Figure 1.18 Automatic chromosome karyotyping innovation by Professor Ledley in the 1970s, probably the earliest concept in systematic medical imaging informatics. Process steps included medical image acquisition, metaphase cell determination, patient data, interactive display, automatic measurement of chromosomes and karyotyping, the determination of normal vs. abnormal chromosomes, that led to the final diagnosis. PACS components included MACDAC (man–machine interface to digital automatic computer). SPIDAC + VIDAC (video memory) + MACDAC (interface) + IBM360/44 were equivalent of today's Pathology PACS. The new knowledge discovery component showed an example of automatic chromosome analysis—microscopic scanning, detecting two metaphase cells (low resolution), and chromosomes (high), analyzing each chromosome, and karyotyping that could lead to the prenatal diagnosis of birth defects.

Figure 1.19 Some examples of today's (2020s) medical imaging informatics applications of three types of patient treatment—surgery, rehabilitation, and radiation therapy. Upper row use of the medical images from various body parts for three different applications. Lower row for image assisted neurosurgery, neuro-rehabilitation, and radiation therapy for cancer treatment.

Chapter 02

Figure 2.1 (A) Terminology used in medical images: image types, sizes, and number of pixels/image. (N × N): total number of pixels of a 2-D image; (*x*,*y*): coordinates of the pixel in the 2-D image; f (x,y): gray level value in (*x*,*y*), which can be from 8 to 12 bits in the gray level or 24 bits in the color image. The total number of bits per image is commonly denoted by (N × N × 12) or (N × N × 24). For 12 bits/pixel, the pixel value is stored in 2 bytes. (B) 3-D image set: (i) a 3-D spatial image set with *z* as the third dimension; (ii) a 3-D temporal image set with t (time) as the third dimension. (C) 4-D image set. A 4-D image set consisting of sequential 3-D spatial sets with t as the fourth dimension. (D) Fusion images: (i) PET fuses with CT: physiology (color) on anatomy (gray level); (ii) MR (color) fuses with CT (gray level): enhancement of soft tissue definition on anatomy.

Figure 2.2 Illustration of spatial and density resolutions, and signal-to-noise ratio using abdominal CT (Computed tomography) see image (512 × 512 × 12 bits) as an example. (A) Four images with a fixed spatial

resolution (512 × 512), but variable density resolutions (12, 8, 6, and 4 bits/pixel, respectively). (B) The original and three images with a fixed density resolution (12 bits/pixel), but variable spatial resolutions (512 × 512, 256 × 256, 128 × 128, and 32 × 32 pixels, respectively). (C) The abdominal CT image (512 × 512 × 12) shown in (A). Random noises were inserted in 1000 pixels, 10 000 pixels, and 100 000 pixels, respectively. The coordinates of each randomly selected noise pixel within the body region were obtained from a random generator. The new pixel value is selected from a range between 0.7 and 1.3 and that of the original value is determined by a second random generator. Clearly, the quality of the CT image is decreasing progressively, starting from the original.

Figure 2.3 Generic radiology workflow. Note that steps 4, 8, 9, 10, 12, and 14 (→) are replaced by "PACS-based" related systems.

Figure 2.4 (A) Data flow of an upright CR system with non-removable imaging plates. (1) Formation of the latent image on the imaging plates; (2) Imaging plates being scanned by the laser beam; (3) Light photons converted to electronic signals; (4) Electronic signals converted to the digital signals that form a CR image (courtesy of Konica Corporation, Japan). (B) The Fuji CR XG5000 reader (Footprint: 26 × 29 × 58 in.) with a stacker accommodates four image cassettes (left), and image processing workstation and quality assurance monitor (right).

Figure 2.5 (A) A pediatric CR image, with a white background (right arrows) as seen on a video monitor. (B) A better visual quality image after the white background has been automatically removed.

Figure 2.6 (A) Workflow steps in the formation of a digital radiography (DR) image, comparing it with that of a CR image shown, (B) an add-on DR system (Figure 2.4A) and utilizes an existing x-rays unit with the patient bed.

Figure 2.7 A slot-scanning digital mammography system. The slot with 300-pixel width, covers the *x*-direction (arrow) with 4400 pixels, The x-ray beam sweeps in the *y*-direction (arrow), producing over 5500 pixels. Top X: x-ray and collimator housing; Middle C: Breast compressor.

Figure 2.8 A 4 K × 5 K × 12-bit CC view digital mammogram shown on a 2 K × 2.5 K monitor (left). A localized digital mammogram for needle biopsy verification (right).

Figure 2.9 Schematic of a general gamma camera used in nuclear medicine imaging. PMT: Photomultiplier tube; NaI (TI): Thallium-activated sodium iodide.

Figure 2.10 Block diagram of a B-mode ultrasound scanner system. TGC: Time gain compensation; RF: radio frequency; HV: high voltage.

Figure 2.11 Color Doppler ultrasound of blood flow, showing convergent pulmonary vein inflow.

Figure 2.12 Block diagram of a digital microscopic system with a CCD camera connected to the digital chain. The system is mostly used in the pathological environment and digital video endoscopic imaging. A/D: analog to digital. D/A: digital to analog.

Figure 2.13 (A) Schematics of a generic digital endoscope (not to scale) with a CCD camera. A/D: analog to digital. D/A: digital to analog.

Figure 2.13 (B) Endoscopic images of thoracic vertebra 9 and 10 acquired in real time during image-guided minimally invasive spinal surgery. See also Chapters 20 and 21 for minimally invasive image-assisted spinal surgery.

Figure 2.14 Two 3-D image coordinate systems: (A) 3-D spatial image set with z as the third dimension. Images from 1 to z show the anatomical changes of the cross-sectional chest CT images; (B) a 3-D temporal image set with t (time) as the third dimension. Images from 1 to t show the same anatomy as image 1; the difference would be, for example, the flow of the contrast media injected to the patient from time 1 to t.

Figure 2.15 Principle of the Fourier transform (FT) projection theorem for image reconstruction from 180-degree 1-D projections from input energy. (A): Spatial domain: A CT image to be reconstructed from 1,2, …,180 1-D projection energy data, f(x,y) is the image to be reconstructed. (B): Frequency domain: F(0, 0) is the center of the 2-D FT; low-frequency components are located at the center region, and high-frequency components are at periphery. P(x,θ) Left: x-ray projection at angle θ (green), x is the distance from left to right of the projection. F(u, θ): 1-D Fourier transform of P(x, θ); red and green are corresponding projections in the spatial domain, and its 1-D Fourier transforms (1-DF) in the frequency domain, respectively. IFT: inverse Fourier transform.

Figure 2.16 Geometry of the multi-slice computed tomography produces

3-D CT images. The patient axis (parallel to the bed) is in the *z*-direction. The x-ray source (orange), shaped as a collimated cone beam, rotates continuously around the *z*-axis by 360 degrees, in sync with the patient's bed movement in the *z*-direction. The detector system is a combination of detector arrays on a concave surface (not to scale) perpendicular to the x-ray beams. The number of slices per 360-degree rotation is determined by two factors: the number of detector arrays (channels) in the *z*-direction and the method used to recombine the cone beam projection data into transverse sectional projections (Figure 2.15). The standard reconstructed images are in transverse (axial) view perpendicular to the *z*-axis; the projection raw data can also be recombined to reconstruct sagittal, coronal, or oblique view images. If the cone beam does not rotate while the patient's bed is moving, the reconstructed image is equivalent to a digital projection image (scout view).

Figure 2.17 The extent of *z*-dimensional scanning of the entire human anatomy with variable multi-slice scans. In this case, array detectors can range from 4, 16, 64, … 256, or even more are possible images in one scan. For example, in the 256 array detector system, a certain number rotations of the x-ray system can capture the entire heart (256 mm), minimizing the possible heart beat artifacts. Another example, a whole-body CT scanner can also scan the body of the patient from head to toe, with the scanner continuing rotating as the bed moving in the *z*-direction (see Figure 2.16 for the *z*-direction).

Figure 2.18 Data flow components of an X-ray CT scanner. The scanning and data collection times, in general, are shorter than the image reconstruction time. A hardware back-projector unit (green) is used to speed up the reconstruction time. A/D: analog to digital; WS: workstation.

Figure 2.19 (A) 3-D multi-slice CT showing a large right parietal hematoma with edema: (upper left) Transverse; (right) coronal. The bottom images are CT angiograms showing the 2-D sagittal view (left) and the coronal view (right) extracted from the 3-D CT 0.5-mm isotropic dataset. (B) 3-D neurodigital subtraction angiogram: (top two and left bottom) sagittal, coronal, and transverse contrast CT images; (bottom right) 3-D angiogram obtained by tissue and bone subtraction from the 3-D CT images. (C) Multi-planar reconstruction CT images. The 16-slice helical CT of the head and neck was obtained during a bolus of

intravenous contrast administration. Volumetric data were then transferred to a Vitrea 3-D workstation for post-processing, including 3-D volumetric rendering and multiplanar reconstructions (MPR) in the (i) sagittal, (ii) coronal, and (iii) transverse planes. This study was conducted in an adult female with transient ischemic attacks. The patient was found to have significant unilateral internal carotid artery stenosis due to atherosclerotic plaque.

Figure 2.20 (A) 3-D CT dataset can also be used to produce 3-D volume rendering images. Left and right show the anterior–posterior (A–P) and posterior–anterior (P–A) views of the thoracic cage, revealing fractures of ribs 7–10 in the P–A view (courtesy of GE Medical Systems). (B) 3-D CT abdominal dataset obtained by using a 64 multi-slice scanner showing 3-D volume rendering of bone, blood vessels, and kidneys, and in particular, an infrarenal abdominal aortic aneurysm with mural thrombus. The scan protocol used was a 135 kVp, 175 mAs, 325-mm scan range taking 12 seconds (courtesy of Toshiba Medical Systems).

Figure 2.21 Schematic of single photon emission CT (SPECT). Refer to Figure 3.24 for nuclear medicine scanning.

Figure 2.22 Block diagram of a positron emission tomography (PET) system showing two array banks of detectors.

Figure 2.23 (A) Positron emission tomography (PET) study of the brain. 18Ffluorodeoxyglucose (18 F-FDG) was administered to the patient, and approximately 60 minutes later the patient was positioned on a PET scanner and images (i: transverse, ii: coronal, and iii: sagittal) were obtained from the skull apex to the skull base. Causes of cognitive impairment, such as Alzheimer's disease, are among the indications for brain 18 F-FDG PET (courtesy of Dr P. Moin). (B) Images of transverse, coronal, and sagittal orthogonal planes (right to left), as well as the posterior–anterior projection image (leftmost) of the whole-body PET image with fluoride ion ($18\ F^-$).

Figure 2.24 (A) Three scanning modes of 3-D US scanning: (left) linear translation; (middle) tilt scanning; and (right) rotational scanning. (B) 3-D ultrasound image of a 25-week fetal face.

Figure 2.25 Block diagram of a generic magnetic resonance imaging (MRI) system. Dotted line separates the digital domain from the MR signal generation. A/D: analog to digital; D/A: digital to analog; RF:

radio frequency.

Figure 2.26 Data flow of forming an MR image. 2-D: two-dimensional; FID: free induction decay; FT: Fourier transform.

Figure 2.27 Clinical 3 T MR imaging system in a magnetic shielded room at the Health Science Campus, USC.

Figure 2.28 T1 weighted (A) transverse, (B) thin section coronal, and (C) sagittal images from an MRI performed to evaluate a possible structural cause for this patient's recent onset of seizures. Thin-section coronals (B) were obtained (only one is shown to allow better visualization of the hippocampi, a region of interest in the imaging evaluation of seizures. Directions: A: Anterior; P: posterior; R: right; L: left; F: front; B: bottom.

Figure 2.29 Two 3-D fetal 3 T MR images using ultrafast sequences.

Figure 2.30 Two views of 3-D dedicated breast MR angiogram (1.5 T).

Figure 2.31 MRA using a 3 T MRI scanner, approaching image resolution possible withDSA (Digital Subtraction Angiography), DSA (Section 2.3.2.2).

Figure 2.32 MRI DTI Tractographic reconstruction of neural connections via DTI.

Figure 2.33 Principles of the 3-D fluorescence confocal microscope used to generate serial sections of an object of interest from the specimen. *x–y* scanning mirrors guide a laser beam (red lines) that excites objects attached with fluorescent dye molecules (yellow) in the sample (size not to scale). The dichromatic mirror only allows excited light (green) to pass. The optical pinhole mechanism accepts in-focus excited emission light (thick green lines) to be recorded by the detector, and rejects out-of-focus emission (thin green line).

Figure 2.34 (A) 3-D rendering of the skeleton of a rat with a set of 1000 slices scanned by a micro XCT scanner with 50 micro pixels. 500 MB of image data were generated. The skeletal structure demonstrates the 3-D rendering of the display (courtesy of ORNL). (B) Two time series—weeks 1, 2, 3, and 5—of molecular images of a mouse with prostate tumor cells in its bone marrow. The three dimensions are projections of the *x–y* plane over time: (top row) no intervention; the tumor was growing fast after injection to week 5; (bottom row) with chemotherapy the tumor as seen at week 5 starting to respond, and it shrinks

continuously after one week.

Figure 2.35 (A) Two 3-D image coordinate systems: (i) A 3-D spatial image set with z as the third dimension. Images from 1 to z show the anatomical changes of the cross-sectional chest; (ii) A 3-D temporal image set with t (time) as the third dimension. Images from 1 to t show the same anatomy as image 1; the difference would be, for example, the flow of the contrast media injected into the patient from time 1 to t. (B) A 4-D image set consisting of sequential 3-D spatial sets, with t as the fourth dimension. (C) (i) PET fuses with CT: physiology on anatomy; (ii) MR fuses with CT: enhancement of soft tissue definition on anatomy.

Figure 2.36 Dual x-ray energy CT scan in a gantry producing high- and low-energy images that can distinguish between tissue types. Single-energy scan (left) without enough information to differentiate a lipid degeneration (right, inside the white circle), shown nicely in the dark red color coded inside the white circle.

Figure 2.37 Fetal images taken with 2-D, 3-D, and 4-D US imaging. 2-D, 3-D, and 4-D US images can be used to observe and monitor the growth of the fetus before the baby is born. (A) Left, 2-D US image with audio heart beat at the bottom. Two 3-D US images reveal the breathing movement of the chest wall and the stretching of the legs. (B) Sequences of 4-D time frames with 3-D US image frames (not in equal time intervals) showing the movements of the legs, turning of the body, and the face (frames 5, 6, 7), and the movement of the arms and legs.

Figure 2.38 (A) PET-CT system with 64 slices at the Nuclear Medicine Division, Department of Radiology, USC. The gantry houses a 3-D CT and a 3-D PET. (B) Hardware image fusion with a PET-CT combined scanner. The hardware fusion method minimizes patient position change and movement during image registration before fusion. The mockup shows a PET-CT scan of a patient 1 hour after injection of 18-F fluorodeoxyglucose. The patient was positioned in a PET-CT scanner. Workflow steps: (1a) 64 Multi-slice CT followed by (1b) a PET scan; (2) 3-D CT images of a full reconstructed coronal section along with (3) brain transverse, coronal, and sagittal sections; (4) 3-D CT data used to perform attenuation correction of PET data; (5) 3-D PET image reconstruction; (6) 3-D PET images obtained showing a coronal, (7) registered and fused CT and PET images with the corresponding coronal section. The “fused” PET-CT images allow for increased sensitivity in

the detection of neoplastic disease by combining identified abnormal physiologic activity (PET) with precise anatomic localization (CT).

Figure 2.39 PET-CT fusion images of a coronal view of the whole body from a dual gantry PET-CT scanner indicating normal distribution of FDG (18-Ffluorodeoxyglucose); (left) CT image; (middle) PET image; (right) fusion image with pseudo-color lookup table (LUT) PET image (physiology) overlaying CT image (anatomy); FDG accumulation shown in cerebral-cerebellar cortex, myocardium, liver, kidneys, renal pelvis, bone marrow, and urinary bladder.

Figure 2.40 PET-CT hardware combined fusion coronal sectional images with 18 F-FDG. Of the 25 equal spaced 1.0-cm sequential images, 00, 04, 08, 12, 16, 20, and 24 are shown. A sagittal section is also displayed (lower right).

Figure 2.41 Original body CT body image (upper left), followed clockwise by reconstructed images with compression ratios of 4:1, 8:1, 17:1, 26:1, and 37:1 (the full-frame method was used).

Figure 2.42 Two-level 2-D wavelet decomposition of a MR head sagittal image. (A) original image; (B) first-level decomposition into four images, (C) second-level decomposition. In each level, the left upper corner is the smooth image, and the other three quadrants are the detailed images (sharper). Observe in the MRI image, all detailed images in each of the three levels contain visible sharp anatomical information. The image compression is to compress each level according to the characteristic of the anatomy, and the acceptable image compression ratio. The needed quality of the compression depends on the acceptable compression ratio discussed in Section 2.5.2.

Figure 2.43 The 3-D volume dataset after two-level decompositions using the 3-D wavelet transform. Each level is decomposed into eight components. f_0 (left) is the original 3-D dataset, f_1s are the eight first-level decomposition (blue), and f_2s, are the second level decomposition (red). The darker blue set in the middle drawing is the smooth image set, the other seven blue are the sharper image sets. The pink in the rightmost second-level decomposition, darker pink in the upper left is the smooth dataset, and the remaining seven sets are the sharper image sets. f'_1 and f'_2 are the seven sets of higher resolution/sharper data of each level.

Figure 2.44 Performance comparison using 3-D versus 2-D wavelet compression on a 3-D MR head image set. Note that 3-D wavelet transform is superior to the 2-D transform for the same peak signal-to-noise ratio (PSNR).

Figure 2.45 One slice of a 3-D CT volume data compressed with a compression ratio of 20:1 with 3-D wavelet, 2-D wavelet, and cosine transform JPEG compression methods: (A) original image; (B) 3-D wavelet reconstructed image; (C) 2-D wavelet reconstructed image; and (D) JPEG reconstructed image. The square covering the vertebra is used to explain Figure 2.46.

Figure 2.46 (A) Image from Figure 2.45B with an square added on. (B'), (C'), and (D'); subtracted images in an enlarged square region near the vertebra. See also Figure 2.45B. (B') Original – 20:1 3-D wavelet; (C') Original – 20:1 2-D wavelet; and (D') Original – 20:1 JPEG.

Chapter 03

Figure 3.1 Yellow and green boxes: picture archiving and communications system (PACS) basic components. Blue boxes: External information systems including hospital and radiology information systems (HIS/RIS), web servers, and application servers. Data flow: blue lines for internal PACS components connection; green and red: PACS connection to related external information components. Application servers and web servers: for enriching PACS infrastructure to other clinical, research, and educational applications.

Figure 3.2 A generic PACS-based workflow. Compare the PACS-based workflow with the PACS-based components and workflow shown in Figure 3.1, and the classical radiology workflow depicted in Chapter 2, Figure 2.3. QC WS: quality control workstation; RIS: radiology information systems; WSs: workstations.

Figure 3.3 Stand-alone PACS-based model and general data flow. The data flow starts when RIS notifies imaging modality and the PACS server that a patient has registered (1). Images are sent from the modality to the PACS server (2), PACS server archives the images (3) and sends them to WSs automatically (single-headed orange arrows, 4) along with other prefetched images (single-headed orange arrows, 5); images can also be queried/retrieved by the WSs (double-headed orange arrows, 6). All WSs have local storage (7). Diagnostic reports are sent back to the PACS

server or directly to RIS (purple arrow, 8).

Figure 3.4 Client-server PACS-based model and general data flow. The first three data flow steps are the same as those of the stand-alone model. Data flow starts when RIS notifies imaging modality and the PACS server that a patient has registered (1). Images are sent from the modality to the PACS server (2), and PACS server archives the images (3). The client WSs has access to the completed current worklist, as well as the list of prehistorical exams of the same patient. Current images as well as historical images can be retrieved from the worklist for review and viewing (4, 5 double-headed orange arrows). All reviewed images are discarded from the WS after review (6). Diagnostic reports are sent back to the PACS server or directly to RIS (purple arrow, 7), the same as in the stand-alone model (Figure 3.3).

Figure 3.5 Basic teleradiology model. The management center monitors the operation to direct workflow between imaging centers and expert centers.RIS: radiology information system; WS: workstation.

Figure 3.6 The PACS and teleradiology combined model. The top rectangle is the PACS components and workflow (detail from Figure 3.1), and the bottom rectangle is the teleradiology model, modified from Figure 3.5. Red lines show communication between PACS and teleradiology. HIS: hospital information system; RIS: radiology information system; WSs: workstations.

Figure 3.7 Enterprise PACS and ePR system with images. The enterprise data center supports all sites in the enterprise. The primary data center has a secondary data center for backup to avoid a single point of failure (SPOF). The enterprise ePR system is accessible from any ePR Web clients, and allows image distribution of the patient’s electronic record within the enterprise.

Figure 3.8 Correspondence between the seven-layer open systems interconnect (OSI, yellow) and the four-layer Department of Defense (DOD, blue) communication protocols. TCP/IP, light purple in DOD is the most popular in medical imaging and PACS applications. FTP: file transfer protocol.

Figure 3.9 Example of data block transmission from one network node to another node with the DOD TCP/IP. The data block is divided into segments. The figure illustrates how a segment of data (yellow) is

encapsulated with the application header (blue), the TCP header (purple), IP header (pink), and the packet header (green) and the packet trailer (green). All these headers and the trailer (color blocks) are the data transmission overheads.

Figure 3.10 An example of a scheme combining the Gbit Ethernet switch with the asynchronous transfer mode (ATM) optical carrier (OC) -12 for PACS-based multimedia application. Blue: Gbit/s; light green: 100 Mbits/s; pink: 10 Mbits/s; purple: <10 Mbits/s; left: dark green: ATM OC-12 622 Mbits/s; light green: OC-3 155 Mbits/s; bottom left: The Cloud (Chapter 15).

Figure 3.11 Major international interconnection points of Internet2 at the Abilene backbone. Most early International connections to Internet 2 were from a hub near Chicago. OC-48 (2.5 gbits/), OC-192 (10 Gbits/s).

Figure 3.12 Topology of international Internet 2 connectivity between three test sites on three continents linking IPI/USC, Los Angeles, North America; InCor, Sao Paulo, Brazil, South America; and Polytechnic University (PolyU), Hong Kong. Flagtel (DS3) was the ISP vendor connecting IPILab to Hong Kong with points of presence (PoPs) in Tokyo and Hong Kong. The routing path from InCor to PolyU used AMPATH, and the path between IPI and InCor used CLARA. Both AMPATH and CLARA are ISP providers.

Chapter 04

Figure 4.1 DICOM and HL7 standards in the PACS workflow, in which all images and pertinent data needed to be first converted to DICOM and HL7, respectively. PACS basic components (yellow) and data flow (blue: Internal; green and red: external between PACS and other information systems); other information systems (light blue). HIS: hospital information system; RIS: radiology information system.

Figure 4.2 (A) Architecture of the DICOM data communication model and DICOM parts (Sections 4.3.2 and 4.3.3). There are two communication models: the network layers model (left) and the media storage interchange model (right). Both models share the upper-level data structure described in DICOM parts 3–6. In part 7, message exchange is used for communication only, whereas in part 10, file format is used for media exchange. Below the upper levels, the two models are completely different. (B) The simplified DICOM data model of the real world with

four levels: patient, study, series, and images. This simplified model can be extended to more complicated data models for various applications, including ePR, radiation therapy, and surgery.

Figure 4.3 “0008,0000” in the “element tag and value” column is the tag for the 0008 Group. “726” is the value for the Group length, and it means there are 726 bytes in this group. The corresponding binary coding of this tag and value are in the same line in “binary coding” column. The next few lines are the tags and values as well as the corresponding coding for “specific character set,” “SOP class UID,” “modality,” and “study description.” The image pixel data is not in the 0008 Group. Its tag is “7FE0 0010,” and following the tag are the coding for the pixel data. The element tag and value “0008 …” becomes “08 00 …” in binary coding because of the little-endian “byte swapping”.

Figure 4.4 Data flow of a set of CT images from the scanner (left) is sent to the WS (right). Within a device the data flow is called a service; between devices it is called a protocol. DIMSE: DICOM message service elements; IP: Internet protocol; TCP: transfer control protocol.

Figure 4.5 DICOM send and receive operations. The example shows the steps involved in sending a set of CT images from the scanner to the acquisition gateway (see Figure 4.1 for the PACS components involved).

Figure 4.6 DICOM query and retrieve operation. The example shows the steps involved in a WS Q/R a set of images from the server (see Figure 4.1 for the PACS components involved).

Figure 4.7 (A) Demonstration scene during an IHE Integration Workshop in 2006. Over 100 vendors were involved in this worldwide connectathon, and during that year tested 5 technical frameworks with 37 integration profiles at major conferences worldwide, where 15 active national chapters from 4 continents participated. (B) IHE Europe 2016 Connectathon in Bochum, http://connectathon.ihe-europe.net/.

Figure 4.8 IHE framework Infrastructure with nine domains. The IHE IT Infrastructure domain in the center is the major support of the framework (modified by the courtesy of IHE, 2010; Sections 4.7.2 to 4.7.4 are based on existing data from IHE, 2010).

Figure 4.9 Sample “IHE use case”. The four actors and their respective roles are shown.

Figure 4.10 IHE scheduled workflow profile including three systems—HIS, RIS, and PACS—and two acquisition devices—conventional films with a digitizer and a CR.

Figure 4.11 IHE post-processing workflow profile (PWF) for a radiology imaging study. This profile is often used in the integration of images from a third-party WS (Chapter 10) or in the integration of CAD with PACS (Chapters 17 and 18) (source: IHE).

Figure 4.12 IHE key image note (KIN) workflow profile for a radiology imaging study. This profile is often used in PACS-based CAD (see Chapters 16 to 18).

Chapter 05

Figure 5.1 PACS basic components (yellow) and data flow (blue: internal; green and red: external between PACS and other information systems); other information systems (light blue); the color of the gateway (red). HIS: hospital information system; RIS: radiology information system.

Figure 5.2 Schematic of the DICOM-compliant PACS image acquisition gateway with the DICOM C-STORE service–object pairs (SOP) connecting the imaging device service class user (SCU) with the gateway service class provider (SCP).

Figure 5.3 Acquisition gateway components and their workflow. Four elementary components are storage service class provider (SCP), storage service class user (SCU), local image storage, and database management system (DBMS). The three error-handling and image recovery software components (shaded) are query and retrieve (Q/R) SCU, integrity check, and acquisition delete.

Figure 5.4 Gateway computer database management hierarchies for patient, study, series, and image tables. (*) denotes primary key and (#), foreign key.

Figure 5.5 The general processing flow diagram of the automatic DICOM query and retrieve image recovery scheme. The scheme starts by the acquisition computer issuing a C-Find command (purple, upper left). The recovery starts by a C-Move command (lower left, green). Both commands are received by the imaging device’s query/retrieve computer.

Figure 5.6 Connection of the US PACS module with several US scanners

(left, yellow) to the hospital integrated PACS (HI-PACS) gateway, purple). Two gateways are used: US PACS gateway (purple) and HI-PACS gateway (blue).

Figure 5.7 Functions of the DICOM-based PACS broker.

Figure 5.8 Manual switch (inside right) to replace the failed acquisition gateway (yellow). Automatic replacement (left) is preferred (outside left, green).

Figure 5.9 The failsafe tandem gateway system, with the left as the primary gateway. The ePR server hardware in the right with multiple processors; one processor is dedicated as the backup gateway. Two identical gateway software programs are running simultaneously on both the gateway hardware and one processor in the ePR server hardware (see Chapter 20, Figure 20.16 for more details).

Figure 5.10 DICOM (Chapter 4) PACS basic components (yellow) and data flow (blue lines): Internal; green and red: external between PACS and other information systems); other information systems (light blue). The four components to be integrated together in Chapters 4 and 5 are HIS/RIS, database gateway, PACS server and archive, and ePR in orange.

Figure 5.11 A typical HIS system with two categories of software packages: business (top), and administration and clinical operation (bottom). Rectangles are major components in each category. The software package STOR (bottom right), is a trade name (other HIS may use different names) that provides a path for the HIS to distribute HL7 formatted data to the outside world, including PACS.

Figure 5.12 Database-to-database transfer using common data format (HL7) and communication protocol (TCP/IP). Data from HIS is accumulated periodically at STOR (see bottom, Figure 5.11) and broadcast to RIS.

Figure 5.13 The principle of the interface engine. (Left) HL7 textual data; (right) DICOM image data; (bottom) Web-based electronic patient record system (Chapter 11) Electronic patient records (ePR), showing image and textual data, or messages and images. Message standards depicted are: LOINC: logical observation identifier names and codes; NDC: national drug codes; UMDNS: universal medical device nomenclature system; IUPAC: International Union of Pure and Applied Chemistry; HOI: health outcomes institute; UMLS: unified medical

language system; SNOMED: systemized nomenclature of medicine; ICD (ICD-9-CM): the *International Classification of Diseases*, 9th edition, Clinical Modification.

Figure 5.14 Information transfer between the HIS, RIS, and PACS. Numerals represent steps of information transfer explained in Table 5.1.

Figure 5.15 RIS–PACS interface architecture implemented with a database-to-database transfer using a trigger mechanism.

Figure 5.16 RIS–PACS interface with a query protocol. Start at green from left upper blue; PACS query RIS (top); RIS sends request through TCP/IP to RIS (right, yellow); RIS executes query, forwards results, packed and received by the PACS (bottom, blue).

Figure 5.17 Enterprise-wide information systems (IHE) patient reconciliation workflow profile used as an example as the HIS–RIS–PACS interface. Step 1: Yellow boxes and green arrows: trauma patient examination without patient's ID. Step 2: Blue boxes and orange arrows: start at step 8, use the IHE workflow profile to reconcile trauma patient ID and demographic data when they become available.

Chapter 06

Figure 6.1 PACS data management and Web-based image distribution. PACS data management, patient folder management, Web-based server, and wireless remote control of clinical image workflows are related to the four pink color boxes in the PACS components and workflow with Web servers.

Figure 6.2 Several distributed image file servers connected to the PACS server. Each of these servers provides specific applications for a given cluster of users. For example, the physician desktop server WS; purple) are used as an illustration. The concept of the Web server is described in Figure 6.3.

Figure 6.3 Basic architecture of a Web server allowing Web browsers to query and retrieve image/data from PACS through the Web-based server. The DICOM/HTTP interpreter is the key component.

Figure 6.4 Typical query/retrieval session from the Web browser through the Web server, requesting images and related data from the PACS server. The session requires eight steps involving both Web (yellow) and PACS (blue) technologies. The resources required in the Web server (Figure

6.3) for such a session are detailed in the Web broker (middle, orange).

Figure 6.5 Architecture of the component-based Web server for image/data distribution and display (Zhang *et al*., 2003). IIS: Microsoft Internet information server; ASP: active server pages. The concept is moving the image processing and manipulation objects to the browser during viewing. Blue: DICOM technology; yellow: Web technology.

Figure 6.6 Data flow of the query/retrieve operation in the component-based Web server, which preserves the 12 bits/pixel DICOM image in the browser. The DICOM images can be displayed with their full resolution by the display and processing component in the browser. Numerals are the workflow steps. Blue: PACS technology; yellow: Web technology; pink: processing component objects (Zhang *et al*.). (1)–(1)'–(1)": query; (2)–(2)'–(2)"–(3)"–(3)"–(3): retrieve.

Figure 6.7 Component architecture of a diagnostic WS for display and to process DICOM images in a Web-based server. iViewer, iProcessor, and iController are image processing and display interfaces software (Zhang *et al*.). API: application program interface; ODBC: open database connectivity.

Figure 6.8 Workflow of the display and processing (DP) component in a Web-based server for display and processing of DICOM images (Zhang *et al*.).

Figure 6.9 (A) Comparison of the averaged speeds of image loading and display from one to six CR images between a PACS diagnostic WS and a web server distributing images to one client. (B) Averaged speeds of distributing different modality images (CT, MRI, CR) from the Web server to one to four clients. All clients requested the web server at the same time. MB/s: megabytes per second (Zhang *et al*.).

Chapter 07

Figure 7.1 The diagram of actors (boxes) and transactions (lines) used in the XDS-I.b profile.

Figure 7.2 The architecture, major components, and workflows of an XDS-I-based iEHR for image sharing with federated integration.

Figure 7.3 (A) Protocols and data flows for online sharing model in an Edge appliance. (B) Protocols and data flows for the near-line sharing model in Edge appliance.

Figure 7.4 Performance comparison of on-line and near-line sharing models. The time intervals (s) represented by vertical axes (time unit: second) for appearance of the first image of different data series after issuing an ITI-43 request in the IHE X-DS-I-based image sharing platform.

Figure 7.5 The architecture, major components, and data flows of the RSNA Image Sharing Network solution.

Figure 7.6 The architecture of the grid-based XDS-I image sharing system for regional imaging collaborative diagnosis, integrated with an existing EHR system. There are two service groups (#1(top) & #2 (bottom)) in this diagram, and radiologists in hospital B and F (blue) perform the final reporting. The Image manager is the central storage archive, which provides image archiving functions to all hospitals in one district.

Figure 7.7 The data models for the XDS provide and register document set-b. The models are related to submitting the preliminary and final reporting datasets.

Figure 7.8 The two new communication services in the interface integration between the grid-based XDS-I image sharing system and the existing EHR system. (A) The image readiness notification allows information to flow from the XDS registry to an existing EHR system. (B) Different mechanisms are shown for a web-based EHR portal client to access published images from the grid-based XDS-I image sharing system, which is integrated with an existing EHR system.

Figure 7.9 Monthly statistical chart of numbers of imaging studies generated in 18 community hospitals in Xuhui District and the number of studies sent to a remote central hospital for both preliminary and final reporting through the iEHR system from January to December 2014.

Figure 7.10 (A) shows major sites in Shanghai involved with the clinical pilot studies since 2011. Three methods of integrating image sharing described in this chapter: 1) Image sharing for cross-enterprise healthcare with federated integration; 2) XDS-I-based patient-controlled image sharing; and 3) Collaborative imaging diagnosis with electronic health record integration in regional healthcare. The second method, XDS-I, was initiated by and demonstrated at RSNA. There were only few pilot studies implemented in clinical environments described in the first and

third methods. Among them are those hospitals and HMOs in Shanghai, China, with 20 million people.

Figure 7.10 (B) XuHui (lower west) and ZhaBei (upper west), two districts in Shanghai were selected as the third pilot project: Collaborative imaging diagnosis with electronic health record integration in regional healthcare, XuHui District. One of the most prestigious living areas, busy, commercial, and residential centre, also known as Xujiahui. Convergence of five main roads (including Huai Hai Road) in Xujiahui. The famous Jiao tong and Donghua universities are located here, as well as various consulate offices, and the district is density populated, with heavy traffic.

Chapter 08

Figure 8.1 Distributed computing is used to perform a PACS CAD task.

Figure 8.2 Five layers of the grid computing technology.

Figure 8.3 Five-layer grid architecture defined by the Globus Toolkit 4.0: Fabric, connectivity, resource, collective, and application. The left-hand side depicts its correspondence to the open system interconnection (OSI) seven-layer Internet protocol (physical, data link, network, transport, session, presentation, and application layer). The right-hand side describes its functions.

Figure 8.4 The five-layer Data Grid architecture integrating DICOM services and the Globus Toolkit for PACS and MIII applications [4]. Resources (fabric) layer: bottom: the five leftmost clear boxes are existing resources from PACS; Internet 2 (I2); Rede Nacional de Ensino e Pesquisa (RNP2); storage area network (SAN) is for PACS archive (Chapter 15); the clear box Replica Database is a Globus tool; the rightmost metadata database is for fault-tolerant Data Grid and computing grid (shadow) application. Core middleware (connectivity layer and resource layer): The four leftmost boxes are Globus tools used for data management in the PACS Data Grid; the rest are other Globus tools. Replica (shadow) and resource management (green shadow) are also used for the computing grid. User level middleware (collective layer): Metadata catalog service and the Globus info services tool are included for fault tolerance. Both resources are also used for computing grid applications (shadow boxes). Data grid application layer: This consists of the DICOM storage, query, and retrieve services. Light

shaded boxes with bold red external rectangles are DICOM resources, and the metadata database for fault tolerance. Services in these boxes were developed at the Imaging Processing and Informatics Laboratory (IPILab), USC.

Figure 8.5 Existing Data Grid and its three current applications developed at IPILab, USC.

Figure 8.6 Data Grid platform at IPILab used to customize for PACS and MIII applications. The major components are the data grid (DG) grid access point (GAP) and the DICOM GAP for connection to PACS sites, other MIII servers, and the Data Grid simulator. The Data Grid simulator can be used for prototyping other Data Grid applications.

Figure 8.7 Enterprise PACS with three PACS sites (light yellow boxes). Each site has a stand-alone PACS with its own server, WSs, storage area network (SAN) archive, and storage backup, and each site operates independently. An enterprise PACS is when these three PAC systems (or more) are connected together to share images. In an enterprise PACS, a WS at each site can Q/R images from its own SAN for image display. A WS of any three PAC systems can also Q/R images from other sites using an imaging routing mechanism (IRM, yellow box) shown on the left. The weakness of this method of connecting the three PAC systems is that two single points of failure can occur. When a PACS server or the SAN fails, the interconnectivity of the three PAC systems breaks down. On the other hand, the fault-tolerant data grid architecture shown in green can restore each site's backup and their connections to the IRM. It maintains interconnectivity of these three systems in real time without human intervention. There are two types of PACS GAP in this architecture, the DICOM GAP (bottom) and the PACS GAP (middle left). The former is for the PACS WS that uses the DICOM standard for image Q/R, the latter is for DICOM file transfer used by some PACS.

Figure 8.8 General architecture of the fault-tolerance metadata system for the Data Grid. There are three levels of fault tolerance: (top) Multiple grid access points (GAP); (middle) data access interface (DAI) servers; and (bottom) multiple metadata storage nodes.

Figure 8.9 Workflow of the Data Grid during image data archive. Solid black lines (left) show the normal archive and backup operations, the first copy of the image file is sent from the acquisition to its SAN1 P1, and

two backup copies to the Data Grid SAN2 P2, and SAN3 P2 for backup storage through its designated GAP1. Dotted black line shows when GAP 1 fails (red crossed lines), and GAP 2 takes over GAP 1 functions automatically.

Figure 8.10 Workflows of the Data Grid during query/retrieve (Q/R) of an image file. (A) The PACS WS Q/R its own PACS image file or from the Data Grid; (B) the PACS WS Q/R other PACS image file from the Data Grid.

Figure 8.11 Three tasks (upper right, heavy green lines) of the Data Grid during disaster recovery when either a PACS server or the SAN fails. Site 3 is used as an example. Task 1: Allow site 3 PACS WS to Q/R its own images from the Data Grid for continuing clinical operation. Task 2: After server and SAN have been restored, the Data Grid rebuilds P1 of SAN 3 its own images. Task 3: After its server and SAN have been restored, the Data Grid rebuilds P2 of SAN 3, which has the backup images of other PACS connected to the Data Grid. All three tasks are performed without human intervention. Workflows and operations of Figures 8.9, and 8.10 allow the Data Grid to automatically complete the three tasks.

Chapter 09

Figure 9.1 Organizational chart of an imaging-based clinical trial. Radiology core (blue) is responsible for all image-related operations.

Figure 9.2 Typical workflow of the imaging-based clinical trial. The images are sent from field sites (1, 2, …, *n*) to a radiology core (blue), where the images are checked by a quality control (QC) workstation (WS) (point a). Images are stored in the image server (point b). The server archives images in an image repository and stores the metadata of the image in the database (point c). The images in the repository are backed up (point d).

Figure 9.3 Three-cores Data Grid architecture (green) for image backup in clinical trials. Cores A, B, and C have the same setup. The image backup storage (e.g. SAN) in every radiology core is separated into two partitions, P1 and P2. P1 is used for local backup, while P2 is contributed to the Data Grid for backup of images from other cores. Note that the Data Grid has not intruded on the core’s backup operation in the image repository. Figure 9.5 also describes the data migration process from the

current local hard disk backup to P1 of the SAN.

Figure 9.4 Data Grid test bed (green) with three International sites at the Image Processing and Informatics Laboratory (IPI SAN), University of Southern California; the Hong Kong Polytechnic University (PolyU); and the Heart Institute (InCor) at University of São Paulo, Brazil. The test bed used two real clinical trials image sets (MRI T1 and T2 images) for the validation of the Data Grid. IPI (left, blue) is used as the site for testing data migration.GAP: grid access point; P1, P2: partition 1, 2; RAID: redundant array of independent disks.

Figure 9.5 Data migration from existing backup storage to the Data Grid (right, green) during Data Grid deployment. Image migration from the local backup of the radiology core (left, blue) to P1 of the IPI SAN and the Data Grid is through a three-step procedure. In this scenario, after completion of the Data Grid deployment, the SAN becomes the local backup archive for the clinical trials' images of the Laboratory. P1 is the core's own backup, and P2 is used to back up for other cores. GAP: grid access point; T: trial.

Figure 9.6 (A) Left: Relative size of the AURORA dedicated stand-alone breast MRI scanner. Right: Major components of the scanner. (B) Multimodality Web-based viewing workstation: Sagittal MRI, Axial MRI, 3-D US, digital mammography, and CAD Structure reporting. (C) One view of a 3-D MRI study using the AURORA dedicated breast MRI scanner. The patient was in the prone position with her two breasts extruded through the two round openings from the table (courtesy of AURORA, Imaging Technology, Inc.). (D) Imaging data grid (BIDG) platform ready to be connected to three MRI sites. The ePR Web server is an additional component in the data grid (DG) for the enterprise system patient electric records.

Figure 9.7 The DICOM-based enterprise dedicated MRI breast imaging Data Grid (BIDG) is an infrastructure that supports large-scale breast imaging archive and distribution management. The AURORA-dedicated MRI enterprise is used as an example. Compare the similarity between this figure and the general Data Grid architecture shown in Figure 8.11 in Chapter 8. Two additional components in this figure are the ePR Web server and the DICOM conversion unit (DCU) explained in the text (courtesy of AURORA Imaging Technology, Inc.). DB: database; GAP: grid access point; IPILab: Image Processing and Informatics Laboratory,

University of Southern California; SAN: storage area network; WS: workstation.

Figure 9.8 The Breast Imaging Data Grid is based on the IHE XDS-I workflow profile. Left: green, input sources. Right: Consumers.

Figure 9.9 A dedicated breast MRI Data Grid using IHE XDS-I workflow profile was planned and is in progress in Taiwan. Three dedicated breast MRI scanners, each of which is located in a major city: Taipei, Tai-chung and Tan-nan, together with a mobile Data Grid MRI, form the MRI enterprise. The three cites and the mobile are connected to a Taiwan Internet network. The dedicated breast MRI Data Grid is located at the IPILab, USC, and is connected to the International Internet. This figure shows their relative locations and their connectivity.

Figure 9.10 Data Grid workflow with lossless digital signature embedding (LDSE) and HIPAA-compliant auditing system (H-CAS) implemented. Red circle: generate and embed digital signature (DS). Green circle: verify DS. There are two data lines: (1) left middle: imaging source sends image/data to the Data Grid; (2) lower middle: user queries image/data.

Figure 9.11 (A) Top: Simulated LDSE workflow in a clinical trials setting using the Data Grid (Figure 9.4). This simultaneously tests the LDSE verification system and HIPAA-compliant auditing system user authentication. (B) Bottom: LDSE process to assure data integrity. A CT image set is used in this example (see also Chapter 17).

Figure 9.12 Intertwined nature of personal relationships within a Data Grid consisting of three clinical sites. Each site is composed of two groups of shareholders, the administrators and the operators. Double (blue gray) and solid (green and blue) lines are for primary relationships, dotted lines (purple) are for optional relationships. The personal relationships become complex as the number of sites in the Data Grid grows.

Chapter 10

Figure 10.1 PACS-based multimedia imaging informatics basic components (yellow), data flow (blue: internal; green and red: external between PACS and other information systems); other medical imaging informatics systems (light blue), PACS-based workstation (orange red). HIS: hospital Information system; RIS: radiology information system [1].

Figure 10.2 Schematic of a standard PACS-based display workstation (WS) with two image display LCD monitors (2 K or 1 K). The WS is composed of a personal computer (PC), e.g. display hardware boards with image processing capability, image and video memory, dual display LCD monitors (2 K or 1 K), magnetic or RAID disk, and network connections [2].

Figure 10.3 WS data flow of an image from the internal magnetic disk to the display monitor. D/A: digital-to-analog conversion; LUT: lookup table; RAM: random access memory; VRAM: video random access memory.

Figure 10.4 Some commonly used physical test objects and digitally generated test patterns. (A) Physical: A-1, star-shaped line pair pattern embedded in water contained in a circular cylinder; A-2, high-contrast line pair (aluminum against water); A-3, low-contrast line pair (contrast media against water); A-4, aluminum step wedge. (B) Corresponding x-ray images of A; Morie patterns can also be seen in B-1. (C) Digitally generated 512 images: C-1, high-contrast line pair: gray level = 0, 140; width (in pixel) of each line pair = 2, 4, 6, 8, 10, 12, 14, 16, 32, 64, and 128 pixels; C-2, low-contrast line pair: gray level = 0, 40; width in pixel of each line pair = 2, 4, 8, 16, 20 and 28 pixels. The line pair (LP) indicated in the figure shows the width of 16 pixels. (D) Soft copy display of the 1024 Å ~ 1024 Society of Motion Picture and Television Engineers (SMPTE) phantom using the JPEG format (Chapter 6) depicts both contrast blocks (0% black – 100% white), and high-contrast and low-contrast line pairs (four corners, and middle). D-1, display adjusted to show as many contrast blocks as possible, resulting in the low-contrast line pairs barely discernable; D-2, adjusted to show the low-contrast line pairs resulted in indistinguishable contrast blocks (0–40%, and 60–100%).

Figure 10.5 A generic 2 K display WS with two LCD monitors showing the PA (left) and the lateral (right) views of CR chest images of the same patient.

Figure 10.6 Two-monitor 1 K (1600 lines) ICU display WS showing two CR images. Left-hand CRT monitor shows the current image; all previous images can be accessed within 1 second on the right-hand monitor by clicking on the two arrow icons at the (Previous or Next sign). Simple image processing functions are controlled by the icons

located at the bottom of the screens.

Figure 10.7 Magnetic resonance angiography(MRA) imaging, using a 3 T MRI 135–136, is approaching the same image resolution quality as digital subtraction angiography.

Figure 10.8 Four mammograms shown on a two-monitor 2 K digital mammograph teaching WS: (left) left and right craniocaudal views; (middle) left and right mediolateral oblique views; (right) text monitor with icons for image display and manipulation on the WS.

Figure 10.9 Concept of histogram equalization. (A) Region in the center of the chest x-ray with the lung region overexposed, showing relatively low contrast. (B) Histogram of the original chest image. (C) Modified image with the lung region enhanced with histogram equalization. (D) The modified histogram.

Figure 10.10 Results after background removal. (A) Original pediatric CR image with background (arrows, white area near the borders). (B) Corresponding histogram. (C) Same CR image after background removal, displayed with a different LUT based on the new histogram shown in (D). (D) The corresponding histogram of the image shown in (C) with the background removed. All pixels with values greater than 710 in (D) have been removed.

Figure 10.11 Pixel value adjustment for CR images in different body regions: head (H), bone (B), chest (C), and abdomen (A).

Figure 10.12 (A,B) Gamma curves of two monitors; (L) linear response curve of both monitors after the gamma correction.

Figure 10.13 Patient directory with the patient list (with fictitious names), ID, date, and time of the study, modality, procedure, and physician’s name.

Figure 10.14 (A) Single LCD monitor displaying three views of a basic MRI study. (B) Two-LCD monitor WS displaying transverse view on the left and coronal view on the right monitor.

Figure 10.15 A two-LCD monitor WS showing a CT chest examination with the soft tissue window. The first image is the chest scout view of the patient.

Figure 10.16 Two-LCD monitor WS showing an obstetric US

examination of a fetus.

Figure 10.17 Graphical user interface display toolbars and icons.

Figure 10.18 Software architecture of a PC-based display WS.

Figure 10.19 Software data flow in the DICOM-compliant PC-based display workstation. Compare this software workflow with the early WS development shown in Figure 10.2.

Figure 10.20 Three-level hierarchical levels of the patient folders: patient, study, and series level, based on the DICOM data model managed by the display WS. See also Figure 10.21.

Figure 10.21 Patient folders in the WS. Each folder contains three hierarchical levels: patient, study, and series level.

Figure 10.22 Different 3-D orientations resulting in display methods such as multi-planar reconstruction (MPR), maximum intensity projection (MIP), surface-shaded display (SSD), and volume rendering can be visualized. (A) Top: four screenshots of visualization of a patient's heart from multi-slice CT; upper left: sagittal projecting plane of MPR; upper right: coronal projecting plane of MPR; bottom left: axial projecting plane of MPR; bottom right: sagittal MIP. (B) Bottom: a head CT image series constructed to a 3-D volume dataset; upper left: one MPR; upper right: MIP; lower left: MPR; and lower right: SSD.

Figure 10.23 (A) Screen captures of a work list, right: showing the patient study being reviewed; (B) Gallery; (C) viewer; and (D) A manufacturer 3-D display product report.

Figure 10.24 (A) Screen captures of a work list; (B) four breast images from the post-processed 3-D MRI generated by a manufacturer workstation.

Figure 10.25 An example of the EchoPixel True 2½-D image of the abdomen showing the two kidneys, a part of the lower ribs, the vertebra at the back, and other anatomical features.

Figure 10.26 A researcher uses hardware and software tools. Upper right: hand held stylus with red pointer guiding an enlarged anatomical true 3-D feature (red) outside of the true 3-D CT body (middle, gray, and yellow); CT image data box: lower right (black and transparent); other imaging tools, a pair of dark glasses at bottom right.

Figure 10.27 True 3-D medical imaging. New medical visualization protocols and visualization protocols can lead to new knowledge = cognition + intuition. The key is developing new clinical protocols. This figure shows that many anatomical features and components can be extracted from 3-D or 4-D medical images. As an example, a pseudo green object (top left) is being extracted from the inside of the skull by a red color pointer.

Figure 10.28 A computed tomography (CT) image of the head with a basilar aneurysm shows many blood vessels inside the head on a contrast CT angiogram. The large basilar aneurysm (yellow) in the posterior circulation of the head has been software segmented and can be pulled out and looked at in any angle chosen in true 3-D. The hand-held stylus (yellow) allows the user to interact with data at the end of the yellow color ray and move to any desired location in the true 3-D space that is created by the EchoPixel software and ZVR display on the desktop.

Figure 10.29 CT post-kidney transplant. A computed tomography angiography of the abdomen that shows the post kidney transplant. Kidney transplants are usually placed in the pelvis area because of the access to the iliac veins and arteries. In this true 3-D image, a segmentation of the transplanted kidney has been pulled out by software (yellow lint) from its location to be shown in the true 3-D space.

Figure 10.30 MRI of the head with tumors. The MRI head scan shows four tumors registered as blue, red, purple, and green, which have been segmented by software with the true 3-D viewer. The image in the upper left of the screen is a 2-D reference view of the same exact angle that the cut plane is going through on the colored volume. A measure has been made to show the distance from the side of the skull to one of the large tumors. The blue colored tumor has been taken out into the true 3-D space to be able to see it in different views and to measure volume and surface area. Four different colored areas: blue, red, purple, and green, have been identified, each of which can be pulled out individually from the brain to the workspace for study. The hand-held stylus allows the user to interact with the data instantaneously at the WS, and the end of the green color ray is used to move to any desired location in the 3-D space that is created by the stylus. Upper left: CT head image volume, see the part of the aneurysm at the lower left of the CT image volume. Rectangular grid: Used for measurement and direction; blue: An already

extracted partial tumor component in the brain with measurements.

Figure 10.31 (A) Schematic representation of the 3-D printing technique known as fused filament fabrication; a filament (a) of plastic material is fed through a heated moving head (b) that melts and extrudes it, depositing it layer after layer, in the desired shape based on the CT layer data; (c) A moving platform (e) lowers after each layer is deposited. For this kind of technology, additional vertical support structures (d) are needed to sustain overhanging parts. (B) Schematic representation of stereolithography; a light-emitting device (a) (laser or DLP) selectively illuminates the transparent bottom (c) of a tank (b) filled with a liquid photopolymerizing resin; the solidified resin (d) is progressively dragged up by a lifting platform (e) [17]..

Figure 10.32 (A) Preoperative computer-generated 3-D printing segmentation of severe scoliosis, created by the Mount Sinai Hospital Neurosurgery Simulation Core. (B) 3-D printing printed severe thoracolumbar scoliosis with multilevel malsegmentations and type I diastematomyelia for use in presurgical planning and intraoperative visualization. (C) Postoperative computer-generated 3-D segmentation following two-stage corrective surgery, depicting spinal alignment of long-segment posterior fusion (pre- and postoperative images courtesy of the Mount Sinai Hospital Department of Radiology and Dr Anthony Costa, head of the Mount Sinai neurosurgery simulation core.

Chapter 11

Figure 11.1 Generic external beam radiation therapy workflow, including treatment planning and delivery using prostate gland cancer as an example. RT information is scattered at where it is generated. The yellow boxes indicate the RT-related images and data that could be generated in the workflow. Treatment planning steps 1, 2, and 3, and treatment delivery step 6 shown in yellow boxes, are described in the text. Step 2 in the RT treatment plan with radiation dose distribution involves the superposition of the radiotherapy treatment parameters: RT plan, RT structure set, and RT dose upon the corresponding set of computed tomography (CT) images. DRR: digital reconstructed radiograph; DVH: dose–volume histogram.

Figure 11.2 (A) RT structure set (Chapter 9): tumor volume (red), organs at risk (femoral head in green and pink, rectum in purple, bladder in

blue), and body contour. The structures in this diagram have the CT image as their frame of reference and are superimposed on the CT image. (B) RT plan: includes treatment beam details, fractionation scheme, and prescription (above). On the left is a graphic display of information from the RT plan and RT structure set, both superimposed onto the CT image. There are nine radiation beams (attribute of the RT plan), each represented by a red label and three yellow lines in the diagram. (C) RT dose: on the left are the radiation dose data from a TPS. Isodose curves (yellow, pink, green, magenta, and blue) are displayed with reference to the CT image and the tumor volume (red shading) from an RT structure set. (D) Dose volume histogram (DVH): belongs to the RT dose object in (C) for treatment plan evaluation. This is key to evaluating whether proper radiation dose is applied to the target tumor while limiting dose to the surrounding critical healthy tissue and organs. The red line shows that most of the tumor volume receives >7500cGy of radiation dose. Other colors show the dose received by other OARs. (E) Web client application page showing a comparison between the reference image (left) and the electronic portal image (right) used to verify the treatment field. The digital reference image was generated from the CT scans, and the electronic portal image from the linear accelerator. Note that there is an icon marked “X”, to indicate approval by the radiation oncologist. (F) Three different types of RT 2-D images for verification of the treatment accuracy: (left) projectional simulator image with delineator showing the field to be irradiated; (middle) reference digital image reconstructed from CT images; (right) portal images from the linear accelerator. Portal images are compared with the reference images from the simulator or the DRRs to verify the accuracy of the treatment portal.

Figure 11.3 (A) MR-CT image fusion used for more accurate tumor delineation. One image each from the 3-D MRI and the 3-D CT is presented for illustration. (Right) A transverse section of the 3-D MRI volume in a gray-scale LUT showing the brain tumor (arrows). (Left) The corresponding anatomical transverse section of the 3-D CT volume with a gray-scale LUT. Two registration points are used for image registration, one point at the tip of the nose and the second at the posterior skull. Since the CT (512 Å ~ 512) and the MR (256 Å ~ 256) images are of different pixel sizes, the registration requires resizing and scaling to perform a proper mapping. Once the registration is complete, the next step is to display the fused MR and CT images. (B) The MR/CT

fusion screenshot from a PACS workstation showing the fused MR and CT images. A slider bar at the bottom allows interactively viewing of each image overlaid. The fused image shows the CT image (grayish color) as well as the MR image (reddish color) with the preference color washing to enhance the target tumor tissue. The viewed target tumor can be outlined interactively more accurately, as shown by the black contour. Note the difficulty to outline the tumor in the CT image or in the MRI, individually and independently, from Figure 5.7A.

Figure 11.4 RT multimedia ePR software organization. DICOM and HL7 standards are used: the ePR server is Web-based. The yellow boxes are ePR services.

Figure 11.5 RT multimedia ePR low-level data schema. The DICOM data model starts from patient and proceeds to study, series, and RT objects level, which consists of one DICOM diagnosis image object (top) and seven DICOM-RT objects.

Figure 11.6 RT multimedia ePR data model. The left side shows the DICOM image, and right side shows the DICOM-RT. Only five DICOM-RT objects are used in the model. The sixth is the summary, which is a textual file that does not require further processing.

Figure 11.7 RT archive server database schema. The database schema is based on the DICOM data model of the real world. The seven DICOM-RT objects in the blue shaded boxes are integrated within the modality of the series module along with the diagnostic image object (light yellow box) to keep each RT object grouped under a modality similar to the CT or MR. The four light blue boxes are the image, structure, dose, and plan. The two upper darker blue boxes are the beams and the summary record, and the lower one is the brachy record, which is not used for external therapy.

Figure 11.8 (A) Three DICOM RT objects: (i) structure, (ii) plan, and (iii) dose; and (iv) DVH curves (reproduced from Figure 11.2). (B) The three RT treatment records. These objects include the RT beams treatment record, the RT Brachy treatment record, and RT treatment summary record. The figure shows the RT beam treatment record, which records the dose given for each radiation beam at each treatment session (rows). Column 1 shows the date on which the radiation dose was delivered. The other columns show the dose (in monitor units) delivered

to radiation fields 1–11 on a given date. Radiation field numbers 12–15 show a second phase of treatment that consists of only four radiation fields.

Figure 11.9 Structural similarities between the PACS and the DICOM-RT based ePR system. (A) Generic PACS components and data flow; the key PACS components that are successfully utilized today within the radiology workflow. PACS uses diagnostic WS for high-quality viewing, and the PACS Web server and review WS are mostly used for reviewing radiological image studies by referring physicians. (B) Multimedia DICOM-RT ePR system components and data flow. Most of the RT components follow the PACS data model (modules 1–3 relate to the imaging modalities, acquisition gateway, and PACS server, respectively, in A). The ePR system platform (dotted rectangle) is used to extract information from the DICOM-RT server to develop the Web-based ePR system. Note that the RT Web server is more complex in B (refer to Figure 11.10 for detail) when compared with A, since the data contain more complex imaging and informatics data objects, while the Web server in A contains only diagnostic image studies and reports. Also, there are different Web application pages within the RT Web client workstations used by oncologists, radiation therapists, and medical physicists, based on their different needs (modified from original drawing by Dr M. Law).

Figure 11.10 Architecture of the RT Web server of the DICOM-RT ePR system. Six key components are shown within the Web server rectangular domain. Note that the RT Web server is more complex than a PACS Web server, since it must handle the multimedia image and informatics data from the seven DICOM-RT objects in addition to the DICOM diagnostic images from radiology. SCP: Service class provider; SCU: service class user; HTTP: hypertext transfer protocol.

Figure 11.11 Screenshot of a Web client application page on the client WS from the DICOM-RT ePR system prototype developed in the Hong Kong Polytechnic University, showing the timeline overview of a RT patient’s ePR display window. Key data extracted from some DICOM-RT objects are displayed as thumbnail representations for users to and review in more detail using the GUI at the client WS. This patient had a CT scan on June 11, 2002, a dosimetric treatment plan done on June 20, a DRR generated on June 21, and portal image produced on June 26, after

which treatment started immediately on June 26. Six radiation doses were delivered from June 26 to July 2. GUI: Graphical user interface; DRR: digitally reconstructed radiograph.

Figure 11.12 Database scheme of the RT Web application server based on a multimedia ePR system in RT prototype developed at the Hong Kong Polytechnic University. Although the database is generic, it can be modified for other oncology departments with different workflows, treatment plans, and viewing conditions.

Figure 11.13 (A) Website hierarchy of a multimedia ePR system in RT prototype developed at the Hong Kong Polytechnic University. Minor modifications may be needed for other oncology centers with different workflows and display requirements from the users. BEV: Beam's eye view; MLC: multileaf collimator. (B) Workflow of the graphical user interface. Minor modifications may be needed for other oncology centers with different workflows and display requirements from the users.

Figure 11.14 Photograph of the multimedia ePR system in RT prototype implemented within the laboratory environment for evaluation of the RT data objects and workflow. Each component represents the conceptual diagram from Figure 23.5B. From right to left: (1) RT object simulator for DICOM-RT data input; (2) DICOM-RT gateway; (3) DICOM-RT archive server; (4) RT Web-based server (refer to Figure 23.6 for RT Web server architecture); and (5) RT client WS. See also Chapter 12.

Figure 11.15 Sample RT patient record from the multimedia ePR system in which some GUI windows are shown in the RT web client. (A) patient list, stemetil 5 mg tid × 5 (antiemetic medicine, 3 times a day for 5 days); (B) patient visit summary; (C) prescription page; (D) treatment setup page; (E) shielding block position; (F) treatment record; and (G) treatment summary record.

Figure 11.16 Medical Imaging Informatics approach toward development of decision support tools for the DICOM-RT-based ePR system. Steps 1–4 were presented in Figures 23.5B and 23.6; steps 5–9 appearing in this figure are discussed in the text. The long-term results are new and robust features for the ePR system to provide decision support for new patient cases. This methodology can be applied to different cancers, as well as different types of RT treatments, for prompt response from new decision-support tools.

Chapter 12

Figure 12.1 Organization of a MII simulator in the clinical research environment, showing the relationship between HIS/RIS/PACS data flow (upper, red) and the imaging informatics platform (middle, green), and MII simulators (blue). DICOM images and data are transmitted from the PACS server to the imaging informatics server, as well as the Web-based perk system. Processed data from the MII platform are transmitted to the MII simulator for the proper application.

Figure 12.2 The PACS–ePR simulator shown at a RSNA exhibition. Left to right: RIS simulator, modality simulator, DICOM gateway, monitoring system of the data flow of the PACS–ePR simulator operation, PACS simulator, PACS WS, and Web-based ePR simulator and WS [2,3].

Figure 12.3 MIDG simulator workflow and system overview. A molecular imaging facility typically has three major components: preclinical researchers at various remote sites (upper right), molecular animal imaging modalities (lower left), and the imaging informatics facility (lower right).

Figure 12.4 Typical imaging modalities in a small animal imaging research facility.

Figure 12.5 Evaluation of an automatic detection and quantification method of multiple sclerosis (MS) on MRI—configuration of the CAD–PACS simulator and its data flow. Top: The CAD–PACS simulator displayed at the 2007 RSNA annual scientific exhibition in 2007 [16]. The PACS WSs (right) also show the MRI images and 3-D CAD result (color). Bottom: The CAD–PACS integration and workflow steps (numerals). Blue: PACS simulator components. Red: CAD components. Yellow: CAD–PACS toolkit modules.

Figure 12.6 CAD results shown on the PACS WS. Left: DICOM-SR describing the multiple sclerosis. Bottom middle: An MRI image of a patient with multiple sclerosis, and bottom right: The 3-D CAD results of multiple sclerosis in the brain. See also Figure 12.5—the CAD–PACS integration components for the MRI images and CAD result shown on the right.

Figure 12.7 CAD–PACS simulator in a laboratory environment (see also Figure 12.5). Black text: normal clinical workflow.Red text: bone age assessment (BAA) using the CAD–PACS simulator.

Figure 12.8 CAD–PACS simulator in the clinical environment. Population statistics database has been embedded in the clinical workflow. The bone age assessment (BAA) of the child is compared directly with the database for evaluating the health of the child, elevating the role of the simulator Digital Hand Atlas (DHA).

Figure 12.9 System components of laboratory environment. From the right to left: TPS simulator, ePR system, and client WS; the yellow arrows represent the data flow and the direction of the data flow.

Figure 12.10 Architecture and data flow of the RT ePR system. (a) The data gateway is used to receive data. (b) The ePR server has the storage and database to archive and quantify stored data. (c) The decision support tools give users the ability to analyze and interact with treatment plans and patient data to improve treatment for future patients. (d) The visualization module contains all GUIs for user interaction in data acquisition, data storage, data display, and for decision support tools. The numerals represent the data flow steps. KB: knowledge base; GUI: graphical user interface.

Figure 12.11 Improving treatment for a new patient based on treatment plans of previous patients, showing step-by-step simulation of knowledge discovery based on the treatment plans of previous patients.

Figure 12.12 (A) A screenshot of the intelligent treatment plan navigator (ITPN) shows the overlapping region of the 95% isodose curve (orange), the target prostate (pink), and two critical organs: the bladder (yellow) and the rectum (green). Utilization of knowledge discovery results for this patient led to a modification of the original 10-mm beam margin to a smaller 7-mm margin. (B) The dose–volume histogram (DVH) for the original treatment plan with a beam margin of 10 mm shows that 25.70% of the rectum receives a 55 Gy dose. (C) The DVH of the modified treatment plan incorporating a reduced beam margin of 7 mm shows that the volume of the rectum receiving a 55 Gy dose has reduced from the original 25.70% to 18.18%, while maintaining the original dose of 55 Gy to 100% of the prostate.

Figure 12.13 Data flow of the IAS ePR simulator. Minimally invasive spinal surgery (MISS) is used as an example. There are three surgical operation phases: pre-op, intra-op, and post-op, each phase with four data flow steps. Numerals indicate the data flow steps through the three

phases of operation.

Figure 12.14 The IAS ePR simulator in the laboratory environment simulating the pre-op and intra-op of a MISS surgery. Right to left: two pre-op displays, an intra-op live display and two DVD devices feeding simulating data to the intra-op display.

Figure 12.15 (A) The MISS operation room (OR) before the installation of the ePR system. EEG: electroencephalogram; EMG: electromyogram; MRI: magnetic resonance imaging. (B) A snapshot from the real-time intra-op display monitor of the MISS ePR system.

Figure 12.16 (A) Pre-op phase. Left: patient records, right: MRI, and red depicts the lesion to be operated on. (B) Intra-op phase. Top: Live real-time waveforms with inserted labels. Top left: vital signs waveforms with synthesized data per second, and the automatic alert signal. Middle left: EMG. Middle to right: endoscopic and C-arm images. All data are recorded in real time, synced by a system master time clock. IU: integration unit; Pulse OX: pulse oximeter. (C) An automatic screenshot from the intra-op real-time data taken during a specific time (see bottom green marker overlaid by blue on the time axis) prepared for the patient surgical document during the post-opphase. Top left to right: an endoscopic image along with some corresponding digital vital signs. Bottom: time axis showing the duration of the operation time. Red marks automatic default data collection time. Blue: surgeon’s requests during the operation via a foot paddle. Larger green: time of screen shot capture. Some corresponding vital waveforms are also recorded.

Chapter 13

Figure 13.1 (A) MicroPET; (B) MicroCT; (C) MicroMRI; (D) MicroUS; (E) Optical Imaging; (F) Autoradiography (A,B,D,E,F, courtesy of Molecular Imaging Center, University of Southern California (USC); C courtesy of Molecular Imaging Program at Stanford, Stanford University).

Figure 13.2 Sagittal CT, PET, and PET/CT Fusion Image of a mouse (left to right).

Figure 13.3 Traditional molecular imaging and informatics workflow (green arrow: digital data write and blue arrow: digital data read).

Figure 13.4 Implementation scenario of the multi-institution MIDG at the

USC Molecular Imaging Center and IPI Lab with connectivity to collaborator sites.

Figure 13.5 Molecular imaging data model for storing files in the data grid archive.

Figure 13.6 (A) MIDG system architecture, built with services from the Globus Toolkit package, tailored for molecular imaging data application.

Figure 13.6 (B) IPILab data grid five-layer infrastructure integrating Globus Toolkit and DICOM [15,16]. Note that the two core middleware layers (connectivity and resource) correspond to the core middleware layer shown in 13.6(A).

Figure 13.7 Screenshots of the upload (left) and download (right) pages from the MIDG's Web-based user interface.

Figure 13.8 Application layer workflows for archiving and query/retrieving in the MIDG's Web-based user interface.

Figure 13.9 Components and connectivity of the molecular imaging grid architecture, from a molecular imaging site's perspective. The metadata catalog service extracts study-relevant and file-specific metadata; the replica location service handles file-delivery destination mappings; the certificate authorization server gives third-party authority of digital certificates; the data persistence server maintains long-term storage and internal data redundancy; the system monitoring and events auditing server offers real-time monitoring of databases, storage archives, and data movement events; and the storage archive consists of network storage devices with RAID 5 redundancy for local fault tolerance.

Figure 13.10 Overall workflow of the USC Molecular Imaging Center (MIC) with the MIDG showing the novel archiving, data management, and data retrieval data flow methods.

Chapter 14

Figure 14.1 Preclinical molecular imaging workflow with steps that require user interaction with the MIDG identified in gray.

Figure 14.2 MIDG system overview. A molecular imaging facility typically has multiple animal model imaging modalities and works with investigators to perform imaging studies. An informatics research laboratory typically has robust computational hardware and services that

may provide additional data and computational infrastructure for a molecular imaging facility. Preclinical investigators at remote sites connect with these sites via the MIDG to collaborate and utilize preclinical imaging data resources (compare with Figure 13.4 in Chapter 13).

Figure 14.3 Second- generation MIDG software architecture with new OGSA data grid infrastructure.

Figure 14.4 MIDG implementation of the IHE XDS-i integration profile. Red boxes highlight the MIDG hardware components.

Figure 14.5 Geographic location of the three USC sites are the IPILab, MIC, and UTRC sites participating in the multi-site MIDG Evaluation Model. Map provided by Google.

Figure 14.6 Network bandwidth in the three-site MIDG evaluation implementation.

Figure 14.7 Upload performance in the MIDG for a microCT study of a rat animal model. Five repeated tests resulted in standard deviations of 1, 4, and 5 seconds for the conversion, transmission, and registration steps, respectively.

Figure 14.8 Upload performance results for studies uploaded into the MIDG at the USC MIC site. Note that microCT datasets 1 and 2 were not incorporated due to unfavorable distortion of the timescale.

Figure 14.9 Download performance results for studies downloaded from the MIDG at the USC IPILab site. See Figure 14.6 for Internet and WAN speed bandwidth.

Figure 14.10 Fault-tolerance results for a microCT study downloaded from the MIDG at the USC UTRC site.

Figure 14.11 MIDG GUI: administrator’s management page. In addition to the study management ability, administrators can add new fields or edit existing fields for the interface.

Chapter 15

Figure 15.1 PACS basic components (red and yellow) and data flow (blue lines: within PACS; green and orange red lines: external between PACS and other information systems); HIS: hospital information system; RIS: radiology information system.

Figure 15.2 Hierarchical storage systems in PACS ensuring data integrity. Until an individual image has been archived in the permanent storage, such as by local archive digital linear tape (DLT) or Data Grid, two copies are retained in separate storage subsystems. DLT can be an archive system within the PACS; Data Grid (green) is mostly external (see Chapters 8 and 9, which is most likely to be used as a tool in multimedia biomedical imaging informatics).

Figure 15.3 Configuration of the archive system and the PACS network. A DLT for permanent storage or the Data Grid (green, external connection) is used as an example. The archive server is connected to the DLT (light yellow) or the Data Grid (green) and a pair of mirrored database servers. Patient, study, and image directories are in the database, and images are stored in the DLT or externally in the Data Grid. A local Ethernet network connects all PACS storage components, and a high-speed Gbits/s switch (as an example) connects the archive server to 1 K and 2 K WSs, providing fast image display. In addition, the archive server is connected to remote sites via T1, high-speed WAN or high-speed Internet (bottom), the hospital information system (HIS), and the radiology information system (RIS) via departmental and campus Ethernet (top). The PACS gateway can also be connected to Data Grid (green, see Chapters 8 and 9). This figure is based on current PACS storage systems (refer to Section 15.7 on how to use the Cloud computing and archive service approach, vendor-neutral archive technology, gradually replacing the PACS systems).

Figure 15.4 Interprocess communications among the major processes running on a PACS archive server connected to the acquisition gateway, WSs, and storage devices. Compare to the workflow in the DICOM compliant server shown in Figure 15.8 (see also Figure 15.5). HL7: Health Level 7; arch: archive images; arch_ack: archive acknowledge; acq_del: acquisition delete; image_manager: process image information and update PACS database; prefetch: preselect needed images; recv: receive images; ris_recv: receive HL7 message; retrv: retrieve images; send: send images to WSs; stor: store images; wsreq: retrieve requests from WSs.

Figure 15.5 Image communication utilizing DICOM SOP services in PACS. The gateway via the storage SOP service acquires images generated from imaging devices. These images are then transmitted to

the archive server, where they are routed to the permanent archive subsystem and WSs. The archive server supports Q/R SOP service, handling all Q/R requests from WSs (see Figure 15.4). SOP: service-object pair; SCU: service class user; SCP: service class provider.

Figure 15.6 Interprocess communication among the major processes running in a DICOM-compliant acquisition gateway, which supports both push and pull operations for acquiring images from the scanners. The DcmPull process (blue) incorporates the gateway's local database to perform data integrity check, ensuring no missing images from any image sequences during the acquisition process (see also Figure 15.5). DB: database; Dcm: DICOM; Img: image; Q/R: query and retrieve; SCU: service class user; SCP: service class provider.

Figure 15.7 Basic hardware components in a PACS server and archive server with high-speed (HS) Ethernet (Ethn.) for broadband Internet, and small computer system interface II (SCSII) and fiber-optic channels (FO Chan) connections. Blue lines: PACS Intranet; SAN: storage area network with multiple partitions, P1 and P2; WSs: workstations.

Figure 15.8 DICOM PACS server and archive software components and dataflow. The six components are receive, insert, route, send, Q/R-server, and RetrieveSend. green: SCU; orange red: SCP.SCP: service class provider; SCU: service class user; WSs: workstations.

Figure 15.9 Workflow in a DICOM PACS archive server, with CR as an example of an image sent from the acquisition gateway (left), through the server (middle), to the WSs (right). Green and black numerals and lines are the auto-push model; blue are the client and server model with Q/R; (refer to Figure 15.8). SCP: service class provider; SCU: service class user.

Figure 15.10 General architecture of the ASP backup archive server. One DICOM gateway at the ASP site and one PACS gateway at the hospital site are used as the buffers between the two sites. T1 or a higher speed network is used for the broadband WAN. WSs at the hospital site can access PACS images from the ASP, following the route: 1, 2, 3, and 4, should some components in the PACS fail, like the server and the archive. After the PACS components are repaired, the missing images can be recovered via route 5. The image Q/R performance is limited only by the network speed, in this example, the T1, 1.5 Mbits/s. All PACS

data transmitted throughout this architecture should conform to the DICOM protocol standard.

Figure 15.11 Disaster recovery procedures. In a disastrous event, the components shown with crossed marks can be considered unavailable for use. In this scenario, a data migrator can be used physically to export PACS examinations and import them directly into PACS using the appropriate DICOM protocols. After the PACS are repaired, the migrator can be used to feed images back to the PACS server via routes 4 and 5 shown in Figure 15.10.

Figure 15.12 The Open Group has developed a range of models and services. (A) Basic cloud computing model.

Figure 15.12 (B) Providing cloud services.

Figure 15.12 (C) Providing added services.

Figure 15.12 (D) Using cloud services.

Figure 15.12 (E) Internal and external cloud services.

Figure 15.12 (F) Cloud ecosystem.

Figure 15.13 (A) An example of the architecture using a cloud storage service to archive images and other data from the hospital. 1) Images and other data are collected from the imaging modality and WSs (left) using the DICOM C-STORE and C-FIND (left, middle). 2) The collected information is transmitted through the cloud gateway (left, blue) at the hospital, screened by the hospital firewall (middle, red) for the protection of its data integrity. 3) Hypertext transfer protocol (HTTP) representational state transfer (REST; right) are used to categorize the data, then archived them to the proper cloud components master index, slave database, DB, and blobstore. The workflows of these steps are described in Figures 15.14. (B) An example of using PACS cloud services (right) to transmit images and data across two hospitals (left top and bottom). See also Figure 15.13A for terminology and explanation. 1) Hospital A (upper left) activates the DICOM-to-Web-services gateway to request data transmission to Hospital B (lower left). 2) Hospital A starts DICOM services C-STORE, QUERYS, C-FIND, and C-MOVE from modalities and WSs at Hospital A. 3) Gateway A, using the HTTP REST/SOAP, activates STORAGE (blue) to transmit the gateway data to the cloud services consisting of the master index and the cloud slaves. 4)

The cloud service activates C-MOVE (orange) to gateway B (blue) at Hospital B and uses the DICOM C-STORE to wake up its internal storage to archive.

Figure 15.14 (A) PACS cloud storage workflow, left to right—each DICOM object (left) sends the patient study directly to the gateway (middle, blue) that is responsible to store it on the cloud slave (right, blue arrows). See also Figure 15.13. (B) PACS cloud query workflow—using the DICOM devices, the WS (left, blue) sends a query to the gateway (middle, blue) that inquires of the cloud database and the master index (right, blue). The collected results are then combined and returned to the gateway (green), then the WS (left, green). (C) PACS cloud retrieval workflow—cloud (right, green dot) to gateway (middle, green), and gateway to WSs (left, green). See also Figure 15.13B (bottom, red).

Chapter 16

Figure 16.0 PACS data management and Web-based image distribution. PACS data management, patient folder management, Web-based server, and wireless remote control of clinical image workflow are related to the four red boxes in the PACS components and workflow.

Figure 16.1 (A) Demonstration of multi-view CAD. The relatively large, but very subtle lung nodule (dotted circles), located in the right mediastinum region was correctly marked by CAD (triangles) on the lateral view of a chest radiograph, but was not marked by CAD on the PA view. (B) Temporal subtraction image obtained from previous and recent nuclear medicine bone scan images. One cold lesion (solid circle) and two hot lesions (dark dotted circles) on the subtraction image were correctly marked by CAD method. The temporal subtraction image for successive whole-body bone scans has the potential to enhance the interval changes between two temporal images. (C) Image matching from collected nodules in the PACS/MIII or imaging informatics nodule database. Comparison of an unknown case of a mass in a mammogram in the center (blue) with two benign masses on the left and two malignant masses on the right, which may be retrieved from the PACS database. Most observers were able to visually identify the unknown case correctly as being more similar to malignant masses (right, orange) than to benign ones (left, green).

Figure 16.2 Data flow in film-based CAD mammography. Only a single

monitor and single light-box viewer are shown in the diagram.

Figure 16.3 Methods of integrating CAD with DICOM PACS (see also Table 16.3). (A) PACS WS Q/R, CAD WS detect (C-GET is a DICOM service); (B) CAD WS Q/R and detect; (C) PACS WS has CAD software; (D) integration of CAD server with PACS and/or MIII.

Figure 16.4 DICOM SR objects in the DICOM model of the real world. The green SR document is located in the DICOM data module (green box), which is at the same level as the DICOM Image.

Figure 16.5 CAD workflow (red) in the PACS environment (blue) with the CAD–PACS toolkit (purple). See the color code used in Figure 16.6.

Figure 16.6 Rightmost: The concept of four-level CAD–PACS Integration toolkit. Left: CAD–PACS Integration toolkit (purple), Top levels: three CAD-PACS editions (green), and five distinct software modules (yellow), CAD components and results (red/orange), and PACS components (blue). Left: The 1st edition. DICOM-SC utilizes DICOM SC service to view CAD results. This edition is easy to integrate, but the CAD output is not in a database for future retrieval. Middle: The 2nd edition. DICOM-PACS-IHE is utilized for integration with a full PACS. It consists of four CAD-PACS software modules, and allows a PACS manufacturer to integrate an existing CAD into its own PACS. Right: The 3rd edition. DICOM-CAD-IHE is utilized for integration with the CAD server. This component is independent from the PACS manufacturer as long as the PACS WS is DICOM SR compliant. The CAD results can then be viewed at a PACS WS. The 3rd edition is favored by the CAD manufacturers or research laboratories for integration. The three modules i-CAD, Receive-SR, and Display-SR are the same as those in both the DICOM-PACS-IHE and DICOM-CAD-IHE editions. PPM (post-processing manager) allows the integration of CAD results with the PACS server, which are PACS specific and would require PACS vendor's assistance for implementation. In the lower level components, in either PACS or CAD, proper toolkit software modules can be installed in the corresponding system components for CAD-PACS integration.

Figure 16.7 Data flow of the DICOM-PACS-IHE second edition and locations of the four modules (yellow) of DICOM-PACS-IHE in the CAD and PACS components (see also the color code used in Figure

16.4). Numbers represent data-flow steps during the integration. (1) CAD requests; (2) query CAD work list, work item claimed; (3) retrieve images for CAD; (4) work list purpose procedure step in PPM in the process; (5) CAD results; (6) work item PPS completed; (7) retrieve images/CAD results.

Figure 16.8 Data flow of the DICOM-CAD-IHETM third edition shows the locations of the three software modules (yellow) in the CAD SR server and PACS, respectively (see also the color code used in Figure 16.6). The data flow steps are (1) PACS server pushes the CT images to CAD WS for CAD process; (2) CAD WS pushes the DICOM SR CAD results to CAD SR server, which consists of the Receive-SRTM module with a SR database for archiving CAD results; (3) Web-based Display-SRTM at PACS WS queries/retrieves DICOM SR CAD results from CAD SR server; (4) the Display-SR automatically Q/R original images referenced in the DICOM SR CAD results in the PACS server for reviewing both original images and SR. In this edition, the CAD SR server also keeps all CAD results in SR format.

Chapter 17

Figure 17.1 Schematic of the CAD system. Intermediary outputs of an image showing right basal ganglia hemorrhage illustrate the effect of individual steps. Details of individual steps are outlined in Table 17.1.

Figure 17.2 Angle of the mid-sagittal plane obtained by finding the line of symmetry of the body of lateral ventricles. The section containing the body of lateral ventricles (A) is automatically selected as described in text. The central portion of the image is binarized with threshold at CSF attenuation. It is rotated over a range of angles. The differences between the rotated image (B) and its mirror image (C) are obtained (D). The angle that gives the least difference (E) is the angle of the mid-sagittal plane (F).

Figure 17.3 Original image with artifactual increase in signal intensity toward the brain skull interface (A). Horizontal line indicating the position from where the intensity profile (B) is obtained. Image after correction of cupping artifacts (C). Intensity profile along the same horizontal line (D). It can be appreciated by comparison of (B) and (D) that the peak intensity at the pixel position is around 140, because AIH is more prominent after correction of cupping artifacts.

Figure 17.4 Procedure of highlighting asymmetrical high-density region illustrated by the intermediary outputs of the CAD scheme. Original is shown in (A). Flipped image (B) is elastically transformed to reduce the normal structural asymmetry between the two sides of the brain (C). Difference between (A) and the morphological closing transformation of (C) indicates that AIH within the right Sylvian fissure is of higher signal than CSF in the left contralateral Sylvian fissure (D).

Figure 17.5 Comparison of global thresholding of original image after removal of skull and extracranial tissues (A), and thresholding of the combined processing steps including correction of cupping artifacts, image top-hat transformation, and left–right comparison (B). Notice that the result of (B) is much cleaner and more manageable for subsequent processing.

Figure 17.6 Screen capture of the CAD system graphical user interface. Original images are displayed at the left window, while the output images with the overlays of outlined AIH are displayed at the right. Original and output images are displayed in strip mode and linked such that they can be scrolled together for review of the whole image series.

Figure 17.7 Difficult AIH cases. Small AIH are difficult to detect if they are of similar attenuation as adjacent structures or confused with normal variants and artifacts. Examples of some difficult cases (the left column) with their CAD results (the middle column) and magnified views (the right column) are shown. The system identifies AIH by red perimeter outlines. High-density regions that are segmented but subsequently classified as unlikely to be AIH are identified by blue perimeter outlines

Figure 17.8 Screen capture of the graphical user interface used in the ROC observer study. The original images are displayed at the left window in stack mode. The second reading’s output images of CAD are displayed at the right window. An output image that contained the segmented and realigned intracranial contents, and AIH, is outlined. The original and CAD output images are scrolled at the same time.

Figure 17.9 (A) ROC detection of AIH among different clinician groups. EP: emergency physicians; RR: radiology residents; RS: board certified radiology specialists. The lighter colored bars are unaided reading mode; the darker colored bars are CAD-assisted reading mode. Notice that among the 20 readers, all but reader 4 improved their performance with

CAD-assisted reading. (B) Area under the ROC curves of all six curves. CAD can be used to improve the readings, which are the ROC (Az) values, in all three physician groups. Compare each of the three color groups: green, red, and blue. The lighter colored curves represent unaided reading mode (UA); the darker colored curves represent CAD–assisted reading mode.

Figure 17.10 Iterative process in clinical evaluation. Once the CAD is installed in the clinical environment for evaluation, it goes through several phases of iterative processes, shown in green arrows. With this iterative process is completed, the CAD system can be deployed for clinical use.

Figure 17.11 CAD–PACS integration prototype in the laboratory environment showing two systems: the CAD server for AIH, and the PACS simulator. The leftmost component is the CAD server running an AIH case study. Other components are the PACS simulator (see Chapters 7 and 8). The PACS simulator has all the essential components of a real PACS, including a modality simulator, DICOM gateway, PACS server, and PACS WS. It is used for PACS training and for testing the functionality of CAD-PACS integration. The PACS WS is located at the rightmost position, with the same AIH case shown on the monitor of the CAD server. A physician reads the case at the PACS WS with and without CAD-assistance (see also Chapter 12).

Figure 17.12 Manufacturer’s chest CAD report already in DICOM-SR format (left) with referenced image and annotation (right). Annotation (small red circle) in the DICOM-SR allows the user to toggle it on or off (case materials courtesy of General Electric Medical Systems).

Figure 17.13 A manufacturer’s mammography CAD report already in DICOM-SR (left) with referenced image and annotation (right). Note that the DICOM-SR format is different from that of the CAD on CT (red text, shown in Figure 17.12). Annotation (dark crosses) in the DICOM-SR allows the user to toggle it on or off (case materials courtesy of R2/Hologic, Inc).

Figure 17.14 Commonly obtained data from 3-D multiple sclerosis (MS) CAD results. The data include the original 3-D MRI dataset: (A) MRI FLAIR image; (B) CAD detected multiple lesions; (C) radiologist identified lesions (normally not shown in the results, depicted here for

comparison purpose only); (D) color-coded MS lesions on a 2-D image; (E) on two slices; (F) on all slices; (G) quantitative results of all 26 lesions detected by CAD; (H) three oblique views of 2-D images with all 26 MS lesions overlaid. Green color shows the ventricles.

Figure 17.15 Multiple sclerosis (MS) computer-aided diagnosis (CAD) SR template. The SR template is designed following a tree structure starting from the document root, which branches into four parent nodes; each parent node branches to (1 − n) child nodes.

Figure 17.16 Use of the PACS simulator to verify the data flow between the integrated PACS and CAD system. Top: PACS simulator displayed at RSNA Annual Scientific Exhibit from 2000 to 2004. Bottom: Workflow of CAD–PACS integration: PACS simulator components (blue); CAD components (pink); CAD–PACS toolkit modules (yellow). The integration steps in numerals are described in the text. The PACS WS (the rightmost component) displays the original image (middle) from PACS, where the CAD results (right) were obtained. The left monitor shows the CAD–SR (see also Figure 17.17).

Figure 17.17 Multiple sclerosis CAD report in DICOM SR format (left) and a 2-D oblique image (right).

Chapter 18

Figure 18.1 An example of the data-mining process used to locate an average hand image of African-American females from 1 to 12 years of age. (A) The objective is to find the average image (right) from a group of images (left). (B) Example of the average image overlaid on a group of hand images of 11-year-old African-American girls from the database. (C) The average hand images of a group of African-American girls from 1 to 12 years old from a child hand database. One average image is provided per year group; see the example in (B) for the 11-year-old group.

Figure 18.2 Procedure of current clinical practice in BAA for children that is based on comparing the child's hand radiograph with the Greulich & P*yle* Atlas (blue) with data over 70 years old.

Figure 18.3 (A) Procedure for obtaining a hand radiograph and converting it to a digital image. (B) The protocol used to obtain the hand radiograph; the figure shows where the five fingers and the wrist joint should be placed. 1 represents the thumb.

Figure 18.4 Examples of four 14-year-old boys from four different races; their corresponding demographic data and two radiologists' readings are included in the DICOM image header. (A) 14.13-year-old Asian boy; (B) 14.46-year-old African-American boy; (C) 14.79-year-old Caucasian boy; and (D) 14.64-year-old Hispanic boy.

Figure 18.4 (E) A sample collection of hand images in digital atlas, available on-line.

Figure 18.5 Right column: Small charts show the four divided age subsets for (F) girls and (M) boys. These charts provide a road map for use in the study of racial differences during different growth periods. (F) Green indicates 1–5 years of age; blue: 6–9 years; purple: 10–13 years; orange: 14–18 years. (M) Green indicates 1–7 years of age; blue: 8–10 years; purple: 11–15 years; orange: 16–18 years. Left column: Large charts show cross-racial comparison for (F) girls (upper chart), and (M) boys (lower chart). Data are shown only if differences are significant ($P \leq 0.05$). Each racial block was divided into the four age groups described. The plus and minus signs indicated under- and overestimation of bone age, respectively, by radiologists in comparing rows with columns. ASF: Asian girls; ASM: Asian boys; AAF: African-American girls; AAM: African-American boys; CAF: Caucasian girls; CAM: Caucasian boys; HIF: Hispanic girls; HIM: Hispanic boys.

Figure 18.6 Comparisons of three racial female pairs. The *x*-axis shows the chronologic age, the *y*-axis shows the average bone age, and the 45° dotted line shows the normal standard comparison in (A1) Asian girls (ASF) versus Caucasian girls (CAF), (B1) Asian girls versus African-American girls (AAF), and (C1) Hispanic girls (HIF) versus African-American girls. The graphs on the left show the plots of the entire age (1–18 years) range, whereas the graphs on the right (A2, B2, C2) are close-up plots for the third age subset (10–13 years).

Figure 18.7 Comparisons among four racial male pairs: 1. (A1) Hispanic (HIM) versus African-American boys (AAM); 2. (B1) Asian (ASM) versus African American boys 3. (C1) Asian versus Caucasian boys (CAM); and 4. (D1) Hispanic versus Caucasian boys. Left: entire age range (1–18 years); Right: third age subset (11–15 years) (A2, C2, D2); and third and fourth age subsets (11–18 years) (B2).

Figure 18.8 BAA fuzzy logic CAD algorithm workflow consists of eight

regions of interest (ROI): six phalangeal, one carpal bone, and one wrist joint. All regions are automatically detected by the CAD. There are three fuzzy logic systems; the aggregation of the three systems gives the CAD bone age of the child.

Figure 18.9 Top: Features extracted from a phalangeal sub-ROI segmentation from which features are extracted. Bottom: Phalangeal fuzzy subsystems, consisting of six components, each with a module for shape and size features (solid lines), and wavelet features (dash lines). The aggregation of all features from six sub-regions yields the bone age, BA1, of the phalangeal.

Figure 18.10 Example of using the carpal bones region alone to determine the bone age. Steps 1–7 describe the total procedure. The capitate (Cap) and hamate (Ham) bones provide sufficient information to assess the bone age, each with three features: one size (×1), and two shapes, eccentricity (×2) and triangularity (×3). In this example, the bone age, BA2 is 2.75 years. ROI: region of interest; Y: years.

Figure 18.11 Result of wrist region analysis and growth plate segmentation, and the workflow of converting wavelet features into bone age BA3. ROI: region of interest.

Figure 18.12 Fuzzy integration of eight ROIs, phanlangeal (6), carpal bones (1), and wrist (1), to determine the final BAA.

Figure 18.13 Comparison between CAD and pediatric radiologists' (Ped Rad) assessment of bone age. Girls (A); boys (B). Each boy or girl group has six comparisons (1–6): A1, B1. All boys and girls images combined. A2, B2. All images from either all girls or boys. A3–6, B3–6:images from one race from the Digital Health Atlas (DHA). A screenshot from the GUI of the Digital Hand Atlas display component from http://ipilabmysql.usc.edu/newindex.php of the CAD system can assess the system. The user clicks icons on the screen (top right) to specify the data and format in the DHA to be plotted. Dotted line: Radiologists average reading, solid line: CAD assessment. Note that A1 and B1 are identical plots as they contain the same group data from the DHA.

Figure 18.14 Simulated clinical workflow diagram of the BAA CAD system using the PACS simulator (see Chapter 12).

Figure 18.15 Clinical evaluation of the BAA CAD system. The workflow was implemented at the Los Angeles County Hospital (LAC) with the

clinical PACS and CAD server.

Figure 18.16 BAA CAD clinical evaluation Web GUI, as shown on the PACS WS monitor. (A) Step 1. Retrieve a patient's hand image from PACS, and link it with the CAD results in the CAD server database. (B) Step 2. Compare the original image (left) with the best matched Greulich & P*yle* (*G&P*) Atlas image (right). The match criterion is to use the patient's chronologic age to search the *G&P Atlas*, in the order of race, sex, and age, for the image with the closest age in the *G&P Atlas*. (C) Step 3. Compare the original image (left), with the best matched *G&P Atlas* image (center), and the best-matched DHA image (right). The chronologic age, bone age, and the matched DHA age are shown at the top right of the screen within the green ellipse. The CAD accessed child bone age (red dot) compared to the children in the normal range in the DHA is shown in the plot.

Figure 18.17 DICOM SR template for BAA CAD. The template is designed based on the types of output that radiologists require to review.

Figure 18.18 Integrating BAA CAD with DICOM-SR. Left: CAD report in DICOM-SR format based on the design of the SR template. Right: A component in the DICOM-SR that is a plot of the CAD BAA results of a patient (red dot) compared with the normals and ± two standard deviations in the Digital Hand Atlas (see also Figure 18.16C).

Figure 18.19 Workflow steps of integrating the CAD DICOM-SR with the Data Grid. Color code: Data sources and CAD (light blue); Data Grid infrastructure (pink); referring physician and radiology WS (blue); workflow processes (green). There is data Web server (right) and multiple grid access points (GAPs). Data flow: Input to the Data Grid—Images (1) and CAD results in DICOM-SR format (2) move across from left to right through the GAP (left), secured SQL via SSG tunnel requests data to be transmitted using GRIDFTP service for certificate authentication and stored in multiple local repositories (3), and metadata in master grid repository and database (3,4). Output–multiple sites where referring physicians and radiologists view images and DICOM-SR results from WSs by requesting the Data Grid Web server through the GAP (right), which fetches images, and CAD DICOM-SR data (3,4), and perform data mining using either HTTPS or TCP communication protocol (5). Data Grid provides both reliability and redundancy of images and DICOM-SR, and allows secured multiple user-accesses.

Figure 18.20 (A) Operation architecture of a computational grid. Numerals represent the workflow. (B) Three-layer procedure of BAA CAD. (C) Operation workflow of BAA computational services. The MDS allocates the computation requirements according to the available resources in the Data Grid. Numerals represent the workflow. API: application program interface; GRAM: grid resource allocation and management; ROI: region of interest.

Chapter 19

Figure 19.1 Graph showing a comparison between photon depth dose and proton depth dose. The depth dose curve of the thin pencil of beam of protons is shown in red. The blue line demonstrates the spread out proton beam Bragg peak, which allows the dose confined around the tumor and the drop off right after the target, sparing the healthy tissue beyond it. The depth dose curve of an x-ray beam (the modality used today in most hospitals for radiation therapy), which shows the characteristic exponential decrease of the dose with depth is shown in green.

Figure 19.2 Illustration of the proton therapy workflow. Yellow boxes indicate the data (both DICOM objects and data forms) that are generated within the workflow. CT: computed tomography; RT: radiotherapy DICOM object; RT-ION : radiotherapy ion, including protons and heavy ionized particles beam, DICOM object.

Figure 19.3 The architecture of the proton therapy ePR system and its data flow model. The data flow depicts a roadmap of how data can be integrated into the proton therapy ePR system. (A) The data gateway use to receive data. (B) The ePR server has the storage and database to archive and quantify stored data. (C) The decision support tools give users the ability to analyze and interact with treatment plans and patient data to improve treatment for future patient. (D) The visualization module contains all GUI for user interaction in data acquiring, data storage and display and decision support tools. The numerals represent the dataflow steps. CT: computed tomography; KB: knowledge base; RT: radiotherapy; RT ION: radiotherapy ions.

Figure 19.4 Data model consisting of three different primary data types: images, radiotherapy (RT) and RT-ION objects, and clinical data forms. The knowledge base data are added later when the primary data are analyzed and extracted for decision support purposes. DVH: dose–

volume histogram.

Figure 19.5 The system configuration at IPILab, University of Southern California for developing and evaluation.

Figure 19.6 Step-by-step guideline of the clinical example. ePR: electronic patient records; ITPN: intelligent treatment plan navigator; TPS: treatment planning system.

Figure 19.7 Screenshot of knowledge-based search engine query input for Patient New.

Figure 19.8 Screenshot of knowledge-based search results displaying previous patients that have undergone new hypofractionation treatment protocol who have toxicity grades ranging from 0 to 3.

Figure 19.9 Difference in the shapes of the prostates, red contours, of Pt. New (left) and Pt. 21 (right).

Figure 19.10 Screenshot of beam margin configuration of Pt. Demo showing the beam margin of 10 mm around prostate.

Figure 19.11 Screenshot of ITPN showing the overlapping region of the isodose curve 95% (orange), target prostate (pink), and critical organs: rectum (green) and bladder (yellow). The isodose 95% covered the entire prostate.

Figure 19.12 Screenshots DVH curves on the ITPN of Patient (Pt.). New shows 100% volume of prostate receiving 55 Gy, but a decreasing volume percentage of rectum receiving 55 Gy from 25.70% to 18.18%, with the modified hypofractionation plan of 7 mm beam margin being used. The computation is automatically computed by the ITPN shown in the right-hand-most column in Figure 19.3.

Chapter 20

Figure 20.1 Creation of a continuum across the chasm from diagnostic images to treatment. Before, a patient was first diagnosed by imaging techniques, and the surgeon performed the surgery based on the diagnostic results; until recently, it was rare that the surgeon performed the surgery guided (or assisted) by real-time images. The example in MISS shows the surgeon performing the spinal surgery first based on diagnosis from 3-D MRI images (second row, leftmost column under diagnosis, dark blue background box), then under the guidance and

assistance of two real-time imaging techniques: endoscope and DR (fifth row, leftmost column under treatment, light green background box). ICT: information and communication technology.

Figure 20.2 Minimally invasive spinal surgery on cervical, thoracic, and lumbar spines. Upper row: Pre-operation arrows show the areas where the disc protrudes from the spine. Lower row: Post-endoscopy-assisted spinal surgery shows the lesions have been cured.

Figure 20.3 (A) Surgical team assembles outside the OR reviewing the surgical plan before the operation. (B) Surgical team is inside the OR preparing for the MISS procedure.

Figure 20.4 Traditional, present-day image-assisted OR suite for MISS operation with endoscopic imaging system and C-Arm DF for image-assisted operation. Notice the many live monitoring waveform devices scattered around the suite and the surgical video for documentation. In the periphery of the OR are the images, waveforms. and other information used during the operation. With the design and implementation of the ePR described in this chapter, today's suite becomes a real-time image-guided MISS OR (Figure 20.11).

Figure 20.5 (A) Continuous conscious electroencephalogram monitoring with the computerized SNAP device (SNAP index or Bispectral Index monitor) improves anesthesia and reduces drug requirement. (B) Continuous intra-op electromyogram monitoring prevents undue trauma to the spinal nerve to be decompressed. (C) Real-time C-Arm fluoroscopy during surgery for positioning of the endoscopy. (D) Real-time digital video endoscopic images, both static images and video clips.

Figure 20.6 Location of problematic disc marked on the skin, with a small hollow tube (~6 mm) inserted by the surgeon into the disc space (A). The location is verified by the C-Arm image. An endoscope (see the endoscopic image shown in the middle above the insertion) and a variety of MISS surgical instruments can be inserted through the hollow tube, including mini-forceps, curettes, trephines, rasps, burrs, cutters, and other types of probes shown in (B) during the image-assisted operation.

Figure 20.7 Tissue modulation technology, including Holmium yttrium aluminium garnet laser digital equipment and radiofrequency, are among technologies that can be used for thermodiskoplasty. The lasers are used to shrink and tighten the disc and to remove portions of a protruded disc.

The figure shows the laser generators and the right-angle (side-firing) laser probe.

Figure 20.8 Lower left: MRI sagittal view showing the large extruded L4 disc. Upper left and right: The lumbar endoscopic posterior lateral approach showing two endoscopic lumbar discectomy images with the lumbar nerve root in close proximity. Lower right: Removed extruded disc fragments.

Figure 20.9 MISS patient surgical outcome (symptomatic improvements) from 5373 patients performed by Dr J. Chiu at the California Spinal Institute, Thousand Oaks, California.

Figure 20.10 Algorithm of spine care for degenerative and herniated spinal discs, and spinal stenosis. Before MISS, spine care ranged from conservative treatment to pain management to spinal arthroplasty disc replacement or artificial disc, and to open spinal surgery fusion. With MISS, there exists an additional option (yellow ellipse) offered before the patient has to choose between the other two extremes.

Figure 20.11 Schematic of the dynamic multimedia ePR system for image-assisted MISS. The prototype system is running at the MISS OR of CSI with two large liquid crystal displays (LCD), one for the pre-op consultation integrated display and the other for the live intra-op integrated display (compare to the current existing OR shown in Figure 20.4).

Figure 20.12 General workflow of the MISS procedure showing three different stages: before surgery (green), patient preparation at the surgical site and surgical operation (blue), and post-surgery (yellow) [3–18].

Figure 20.13 Data model of the ePR system. It extends the DICOM scheme to accommodate additional surgical information, including live patient waveforms and several standard surgical forms and real-time images. Additional entities (green) were augmented to the ePR imaged-assisted MASS data model [18].

Figure 20.14 Data flow of the ePR system for MISS. There are three time stages—preoperative (Pre-OP), intraoperative (Intra-OP), and postoperative (Post-OP)—and four operational modules—input units, gateway, ePR server and database, and visualization and display, which forms a 3 × 4 matrix. Each numeral represents one event in the data flow [3–19].

Figure 20.15 ePR system architecture showing three operation phases (first column), pre-op, intra-op, and post-op, as well as four operation modules (partitioned and scattered systematically). Some partitioned modules are bundled together for ease of data transfer and tandem backup. The arrows show the data flow during the three phases of operation. The outside light gray color large side-way U band is the display module backbone (Section 20.4.2.4) with five white rectangular box subunits. Inside the opening of the "U" in the dark gray are the integration unit (Section 20.4.2.1), tandem gateway (Section 20.4.2.2), and tandem ePR server (Section 20.4.2.3). Within the gateway and the ePR server, the database and file system software are interrelated and shared by both components.

Figure 20.16 Tandem dual-system backup schema with two hardware pieces: gateway hardware and ePR server hardware. Each hardware piece has two softwares—ePR server software and gateway software—and a tandem database with hard drive for data and metadata archive [18].

Figure 20.17 The home page of the ePR system showing three surgical stages: pre-op, intra-op, and post-op. The pre-op page shows that there are three patients with pre-op consultations; the intra-op and post-op pages show that patient John Doe is being operated on [17,18,20,21].

Figure 20.18 (A) Based on the patient examination, history, and recommendation, a physician assistant creates the surgical procedure planning in the ePR system pre-op module. (B) Oswestry disability index, a survey to identify how the pain in the back or legs is affecting the patient in his/her daily activities.

Figure 20.19 (A) Pre-op authoring module page. The upper left-hand text list depicts the surgical data model showing the studies and procedures. After the user clicks on an item in the list, the proper image, in this case a sagittal MRI, is shown on the right. (B) The neuronavigator tool allows the correlation of the position of the lesion in the sagittal (left) and the axial view (right). The red lines are the two corresponding sagittal and axial sections. (C) The pre-op display organized during patient consultation as seen on the monitor in the OR during intra-op. Top left: From the whiteboard information; Bottom left: Extracted from the patient history summary. Right: Images and annotation during the pre-op consultation (see also Figure 20.11, right). (D) Method of extracting pertinent and concise clinical history information by highlighting

(yellow) from the full report during pre-op editing (compared with C, left). The extracted concise information is shown in (C) during intra-op.

Figure 20.20 Hardware and software interconnectivity diagram for a MISS procedure using the ePR system. During intra-op, live data are continuously displayed on the intra-op monitor. A system default allows the live intra-op data to be acquired at a specific time interval. The surgeon has an option to acquire additional data during the entire course of the operation by pushing the surgeon keypad (green). The IU in the middle column accepts different input devices and sends them to the intra-op live display (lower-right, yellow) [17,18].

Figure 20.21 Example of the intra-op live display as seen on the large monitor in OR (see also Figure 20.11, right). (Top row) Eight waveforms of six vital signs, plus BIS, and IVF with digital values. Alert message on low heart rate (HR) and diastolic pressure; the horizontal axis is time. (Middle row from left to right) Waveform of EMG, endoscopic (Endo) images, and fluoroscopic image; (bottom row): Laser output values.

Figure 20.22 Post-op authoring module displaying a document showing data acquired during the surgery. This page can be synchronized by the surgeon’s post-op dictation. It is in PDF format for easy insertion into the report. The red time marks at the bottom are default intra-op data capture. Blue marks are additional data the surgeons saved during the surgery. The green mark represents the time frame when this page was captured.

Figure 20.23 (A) ePR server installation at the server room of the California Spinal Institute. Dr J. Documet is shown installing the servers. (B) Left: the Integration unit (IU, inside the red ring) installed in the OR, it is connected to various input sources. Middle: Input units cables are connected to the back of the IU. Right: The back of the vital signs device is connected to the back of the IU [17,18].

Figure 20.24 Training of the ePR system for the clinical staff at the California Spinal Institute. (A) Group training in pre-op authoring at the consultation room. (B) One-to-one training at the consultation room on GUI. (C) Training of the IU in the OR for input devices connectivity. The engineer is behind the unit.

Chapter 21

Figure 21.1 Some results of image-assisted minimally invasive spinal surgery at three anatomical locations: lumber, cervical, and thoracic. MRI

was used to assist the surgery. Upper: pre-op, surgical planning. Lower: post-op, after surgery. Red arrows were annotated on the MRI digital images during the pre-op to identify the surgical plan. A greasy black pen was also used to mark the MRI film (left). These results were obtained without the integration of the electronic medical record system.

Figure 21.2 Image-assisted minimally spinal surgery (MISS) operating room (OR) with multiple signal and imaging systems and their corresponding display monitors before its integration with the electronic medical record system. Each staff member in the OR has his/her responsibility to monitor and view a given system(s) during the operation. C-arm x-rays (middle right) and endoscopic imaging (top middle) were used to assist the surgery in real time. PACS transmits MRI and other image data to the OR for viewing. EEG: electroencephalogram.

Figure 21.3 Integration of the EMR with the image assisted minimally invasive spinal surgery operating room. The locations of multiple signal and imaging systems are reorganized properly; two large display monitors were hanged strategically on two opposite walls of the room, one for pre-op data and the other for real-time intra-op data. Every staff member in the room can view both the pre-op and intra-op monitors simultaneously.

Figure 21.4 The workflow of the integrated image-assisted minimally invasive spinal surgery EMR) system in a 3 × 4 matrix. From left to right: Three rows delineate the pre-op, intra-op, and post-op phases. Input data moves through various components, first to the input gateway, the EMR module, and then to the pre-op, the intra-op (real-time), and the post-op (real-time) display monitors. Numerals 1–12 portray the order of the data workflow. The left and the right monitors shown in Figure 21.3 are for the pre-op and intra-op modules. The post-op display shares the intra-op monitor since they are used at two different times. The input gateways are used to standardize all surgical data. The DICOM standard is used. The EMR module is the system that includes the EMR server, monitoring module, and archive database.

Figure 21.5 Integration unit installed in the operating room (left, green). All cables of the input data sources (middle and right) are connected to the unit’s back panel.

Figure 21.6 A page of the pre-op display (see Figure 21.4, Numeral 3).

Left: the patient history; Right: the surgical plan. The graphical user interface (GUI) in the pre-op screen can be used to switch to any other pages at the request of the surgeon at any time pre-op and intra-op.

Figure 21.7 A snapshot of the intra-op monitor in which the anesthesiologist in the foreground is preparing a patient for the surgery. The monitor depicts some preliminary vital signs of the patient, and a C-arm image (right). The endoscopic display portion is not yet on line (see vertical color bars).

Figure 21.8 A snapshot of the intra-op monitor identifies the vital signs and other surgical related signals, as well as an endoscopic and a C-arm x-ray image of a patient.

Figure 21.9 A snapshot depicting the intra-op display monitor of a patient during the minimally invasive spinal surgery with real-time surgical data (see also Figure 21.4, Numeral 7). The integrated EMR system records all information on the screen synchronized by a real-time master clock. Top: patient's vital signs, bispectral index system (BIS), and other related surgical signals. Right: the C-arm X-rays image shows the surgical site of the vertebra. Middle: the endoscopic image depicts a yttrium aluminum garnet (YAG) laser with characteristics shown in the last row, which was used to heat up the lesion. Left: the electromyogram signal shows that the spinal cord response is normal. This *in vivo* dataset had been recorded by the EMR as a part of the surgical document. The digital data including images of this page in the document was converted to an "open standard for electronic document exchange" Adobe Systems' PDF automatically by the EMR as an independent page. This page (can be more pages), along with other relevant data, and the surgeon's dictation comprise the final surgical report.

Figure 21.10 Post-op pages consisting of data from the EMR system default function, and those selected by the surgeon during the operation, which can be displayed and archived. This example is one of the selected pages consisting of two images (left: C-arm, right: endoscopic), seven waveforms, and time marks at a certain time during the surgery. Middle: three red vertical arrow time marks selected by the surgeon during the operation for inclusion in the surgical document (the three red arrows on the top of the waveforms). Bottom: seven waveforms, each color designating a surgical signal. Top: a C-arm x-ray and an endoscopic image at those selected time marks. Similar pages can also be generated

for any system default time marks. The final patient report can be obtained by a click of the mark at the center of the display page. PDF files of this information can be generated automatically as part of the patient document. A red star at the upper left of each image indicates that the image had been included in the PDF file.

Figure 21.11 A mock-up intra-op screenshot mimicking a neurosurgical intra-op display of an integrated image-assisted neurosurgery EMR system. Additional real-time imaging data shown in the bottom are neuro-navigation system output with 3-D images on the left, microscopic image in the middle, and overhead camera image on the right.

Chapter 22

Figure 22.1 Special features of characters of the “five V” features: volume, value, veracity, variety, and velocity in big data of DICOM-based medical imaging informatics: PB: petabyte.

Figure 22.2 Amount of PACS-based image data (terabytes, TB) stored per year from 2008 to 2013 (only 7 months) in the Huadong Hospital, Shanghai. China.

Figure 22.3 Percentage of retrieved historic imaging studies in Huadong Hospital PACS during 2013 (M: month, Y: year).

Figure 22.4 (A) The traditional data storing and processing three-tier infrastructure. (B) Big data in medical imaging and informatics: horizontally scaled and distributed big data processing architecture with multiple middle layers in between acquisition and presentation.

Figure 22.5 (A) A typical architecture of vendor neutral archive-based image storage and sharing solution; (B) Cloud computing-based image storage and sharing solution. See also Chapter 15 for VNA.

Figure 22.6 The five "V" features research performed at the Laboratory for Medical Imaging Informatics of The Shanghai Institute of Technical Physics (LMI/SITP).

PACS-Based Multimedia Imaging Informatics

Basic Principles and Applications

Third Edition

H.K. Huang, D.Sc., FRCR (Hon), FAIMBE

Professor Emeritus of Radiology and Biomedical Engineering
University of Southern California
Honorary Professor, Shanghai Institute of Technical Physics
Chinese Academy of Sciences
Former Chair Professor of Medical Informatics
Hong Kong Polytechnic University
Former Professor
University of California, San Francisco
Former Professor
University of California, Los Angeles

PERPUSTAKAAN PRIBADI AN-NUR SUNARYA

WILEY Blackwell

This edition first published 2019
© 2019 John Wiley & Sons, Inc.

Edition History
Wiley-Blackwell (2e, 2010)

All rights reserved. No part of this publication may be reproduced, stored in a retrieval system, or transmitted, in any form or by any means, electronic, mechanical, photocopying, recording or otherwise, except as permitted by law. Advice on how to obtain permission to reuse material from this title is available at http://www.wiley.com/go/permissions.

The right of H.K. Huang to be identified as the author of this work has been asserted in accordance with law.

Registered Office
John Wiley & Sons, Inc., 111 River Street, Hoboken, NJ 07030, USA

Editorial Office
9600 Garsington Road, Oxford, OX4 2DQ, UK

For details of our global editorial offices, customer services, and more information about Wiley products visit us at www.wiley.com.

Wiley also publishes its books in a variety of electronic formats and by print-on-demand. Some content that appears in standard print versions of this book may not be available in other formats.

Limit of Liability/Disclaimer of Warranty
The contents of this work are intended to further general scientific research, understanding, and discussion only and are not intended and should not be relied upon as recommending or promoting scientific method, diagnosis, or treatment by physicians for any particular patient. In view of ongoing research, equipment modifications, changes in governmental regulations, and the constant flow of information relating to the use of medicines, equipment, and devices, the reader is urged to review and evaluate the information provided in the package insert or instructions for each medicine, equipment, or device for, among other things, any changes in the instructions or indication of usage and for added warnings and precautions. While the publisher and authors have used their best efforts in preparing this work, they make no representations or warranties with respect to the accuracy or completeness of the contents of this work and specifically disclaim all warranties, including without limitation any implied warranties of merchantability or fitness for a particular purpose. No warranty may be created or extended by sales representatives, written sales materials or promotional statements for this work. The fact that an organization, website, or product is referred to in this work as a citation and/or potential source of further information does not mean that the publisher and authors endorse the information or services the organization, website, or product may provide or recommendations it may make. This work is sold with the understanding that the publisher is not engaged in rendering professional services. The advice and strategies contained herein may not be suitable for your situation. You should consult with a specialist where appropriate. Further, readers should be aware that websites listed in this work may have changed or disappeared between when this work was written and when it is read. Neither the publisher nor authors shall be liable for any loss of profit or any other commercial damages, including but not limited to special, incidental, consequential, or other damages.

Library of Congress Cataloging-in-Publication data is available for this book.

ISBN 9781118795736 (hardback)

Cover image: Courtesy of H.K. Huang
Cover design: Wiley

To my wife, Fong, for her support, understanding, and help.

To my daughter, Cammy, for her growing wisdom, ambitious spirit, and an established career.

To my grandchildren Tilden and Calleigh, for their calming innocence.

Foreword 1

PACS–Based Multimedia Imaging Informatics 3rd Edition, 2018

Medical imaging, PACS, and imaging informatics have revolutionized the approach to managing patients in both the inpatient and outpatient settings. While this has been true for many decades, the fusion and integration of medical images of all types, in the current era and in the future, will make these data sources all the more important and powerful. Medical imaging had traditionally been in the domain of radiology in schools of medicine. With the nearly universal use of electronic medical records (EMR), images from all sources can now be brought to bear on the diagnosis, prognosis, and treatment course of individual patients.

Thus, both traditional radiological images as well as pathological, photographic, retinal, and other imaging data can be integrated with genomic and other "omic" information to provide a much more comprehensive view of an individual. They are no longer based on the use of static two- or three-dimensional snapshots of a given aspect of a patient's state but, rather, four- and five-dimensional imaging datasets can now be used to study dynamic processes or changing states for a given patient over time. Images from different patients can be combined, using modern imaging methodologies, to produce population images that better define aspects of a disease, patient groups, or genetic characteristics. Such population images will provide previously unavailable insights into the human state under both normal and pathologic conditions.

Dr H.K. "Bernie" Huang's 3rd edition of his book is a comprehensive survey of the history, current use, and future opportunities for medical imaging, PACS, and imaging informatics. This comprehensive textbook expands upon the first two editions and provides new and previously unpublished information about how medical images and PACS systems will be used in the 21st century. With Dr Huang's vast experience of this topic, he is the ideal individual to develop a comprehensive text of this sort and he has done just that. The four parts of the text carefully organize this vast topic into manageable and appropriately segregated components. Because the textbook includes both a retrospective, providing the reader with insight into how the field developed initially, and a

more futuristic section (Part 4), which provides specific examples and future directions for the use of medical images in computer-aided diagnosis, image-guided decision support, specific types of radiation therapy imaging strategies and image-assisted surgery, the overall content of the text is something that will be useful to students of these disciplines at any level. I also believe that a text of this type would be a valuable learning tool for policy makers who are studying advanced uses of the electronic medical record and insights that can be provided from the data contained in those records.

I have recently had the opportunity to visit facilities that are utilizing image-assisted surgical systems for both open and laparoscopic procedures. These systems incorporate, not only three- and four-dimensional imaging approaches, but also utilize captured real-time images during the procedure to troubleshoot errors and complications. Furthermore, such approaches are now becoming instrumental in designing workflows for managing patients through various types of image-associated therapies. As such, medical imaging has gone from a static early diagnostic tool to a comprehensive component of operational and quality control measures, critical in the modern approach to high-quality, high-throughput, patient care.

I highly recommend this text to students of medical imaging at all levels and particularly to those who are interested in expanding the horizons for the use of medical images and those who would like to advance the field of biomedical imaging informatics, population imaging, and imaging as a tool for quality and workflow management.

Dr Huang has done a superb job in producing an extraordinarily comprehensive text that is well illustrated and continues in the tradition of the previous two editions to be a comprehensive reference for students and practitioners of these disciplines.

John C. Mazziotta, MD, PhD
Vice Chancellor, UCLA Health Sciences
CEO, UCLA Health

Foreword 2

A Thought on PACS and CAD

The concepts of picture archiving and communication systems (PACS) and computer-aided diagnosis (CAD) were introduced in the late 1970s and early 1980s, as digital imaging had been attempted in diagnostic radiology and medical imaging. Bernie Huang is one of the key pioneers who have been very active since the beginning of large-scale research on PACS and CAD, as well as the development of many digital imaging systems. In the beginning, many assumed PACS and CAD to be just a “dream”. However, PACS has grown significantly over the years as the foundation of an infrastructure for image data and medical information in radiology and other branches of medicine. This version of *PACS-based Multimedia Imaging Informatics* by Bernie Huang is the third edition of his book, which is an excellent book for researchers, practitioners, and students in the field of medical imaging, on the subject of informatics and PACS.

However, although CAD had limited success, for example, CAD for detection of breast cancer on mammograms, CAD is still in the early stage of infancy toward its full development in many imaging modalities and different types of examinations. The success of PACS has provided many benefits to physicians and to hospitals, and it has produced a vast database of image information stored in PACS. However, the image information in PACS has not been used extensively and actively, except for comparison of new and previous cases of the same patients and also in research and teaching, which constitutes a small fraction of the image data stored in PACS. Therefore, a vast amount of the images stored in PACS may be considered to be “sleeping” at this time. These images may be used for the development of many CAD schemes for the detection of lesions and for the differential diagnosis of abnormalities in many different imaging modalities by use of new approach such as machine learning and deep-learning convolution neural networks.

In addition, images similar to those of a new clinical case could be identified by searching of clinical cases with known pathology stored in PACS, based on the contents of image information and subjective similarity of images. These are examples of ways in which this book may be used for finding solutions in

radiology and other branches of medicine. This book *PACS-based Multimedia Imaging Informatics* could be a useful source of information leading to a new approach for research and development in CAD and many other fields.

Kunio Doi, Ph.D.
Professor Emeritus, The University of Chicago
Professor Emeritus and Former President
Gunma Prefectural College of Health Sciences
Maebashi, Gunma, Japan

Foreword 3

Dr H.K. “Bernie” Huang's third edition of this book covers a tremendous amount of highly relevant topics in its 22 chapters; and yet it may still be considered as an essential introduction to the overall topic of PACS and Informatics. The organization of the book is such that the reader is presented with both a logical and temporal evolution of medical imaging systems, which demonstrates the general trajectory of these systems. Starting from closed, standalone systems (difficult to imagine now, but this was the state of technology he encountered when he created the first PACS system) and moving to the more integrated systems containing vast amounts of data that will undoubtedly be the sources of “Big Data” that will be explored, mined, and analyzed for years to come.

While medical images provide a tremendous amount of insight into establishing patients’ diagnoses, disease stage, response to therapy, and many other uses, this data is still underutilized. There is still tremendous potential in exploring the integration of this data with other information sources – the multimedia that Bernie refers to – such as radiology reports (free text and structured reporting), Computer-Aided Diagnosis (CAD), quantitative imaging features (radiomics), as well as pathology information, genomics, proteomics, information extracted from other modalities (e.g. circulating tumor cells), and other sources. This book provides unique perspectives into these issues by starting with a brief history (Part 1 – Retrospective), the infrastructure necessary for integration between different systems (Part 2 – Standards and Guidelines), examples of integrated systems (Part 3 – Informatics, Archives, Electronic Patient Record, the Cloud), and then some example applications (Part 4 – CAD, Clinical Decision Support, Big Data).

Therefore, this book is highly recommended for a broad audience of practicing physicians, information scientists, system developers, researchers, and others in healthcare that seek to create and utilize integrated information sources. While at first glance this book may seem to be of primary interest to those in radiological and surgical disciplines, the approaches described here are broader than that and should also be of interest to those in other specialty departments such as pathology, cardiology, and orthopedics. Bernie has created another outstanding text, which will surely stand as both a standard reference and a signpost to the future for years to come.

Michael McNitt-Gray, PhD, DABR, FAAPM, FACR
Professor, Department of Radiological Sciences
Director, Physics and Biology in Medicine Graduate Program
Assistant Vice Chancellor of Research, Radiation Safety
David Geffen School of Medicine at UCLA

Preface to the Third Edition

The Beginning

This is the third edition of the PACS and Imaging Informatics series 2004, 2010 to now 2018 that I have written to discuss the development and growth of medical imaging and PACS-related technology during the past 30 or more years. This series has been written with the help and encouragement of John Wiley & Sons. The 2010 second edition, in particular, using all color figures with text was encouraged and suggested by Mr Thomas Moore, then Senior Editor, so using color has since become the necessary requirement in medical imaging publication.

I learned medical imaging from my Mentor, the late Professor Robert S. Ledley at Georgetown University, Washington, DC, 1966–1980. He also gave me the opportunity to learn and help in developing some original medical imaging systems and the first whole-body CT scanner at Georgetown. During an annual RSNA meeting in the middle of 1970, I had the honor to bring the CT scanner to its first demonstration. These learning experiences have enriched my understanding of medical imaging and its potential applications in biomedical healthcare.

After having left Georgetown, I joined the Departments of Bioengineering and Radiology at the University of Iowa in 1980. Professor Tony Franklin, then the Chair of Radiology, gave me the opportunity to develop my first image processing laboratory during my short stay of two years there. From 1982 to 1992 at the University of California at Los Angeles, I joined the Department of Radiological Sciences and later as a Vice Chair, headed the Biomedical Physics Graduate Program where I initiated and implemented the first in-house PACS. From 1992 to 2000, at the University of California, San Francisco, as a Vice Chair, I taught medical imaging at the University of California, Berkeley, developed the Radiological Informatics Lab, implemented the hospital-integrated PACS, and introduced the concept of imaging informatics. After I retired from the University of California system, from 2000–2012, I joined both the University of Southern California and the Hong Kong Polytechnic University to continue in developing PACS-based medical imaging informatics. At the same time I became a consultant to the Hong Kong Hospital Authority (HKHA),

helping them to develop the total digital hospital operation system in Hong Kong, with 46 public hospitals plus the other 10% private. After 12 years, Hong Kong is running 85–90% total digital patient care, and is now working on the total digital healthcare system.

My Experience

During these past many years, I have had the opportunity to write medical imaging books, and to continue learning and collaborating with many of my colleagues to publish medical imaging and PACS-based related topics including:

An Atlas for Computerized Tomography with Robert Ledley and John Mazziotta, 1977, Williams & Wilkins.

Elements of Digital Radiology: A Professional Handbook and Guide, alone, 1987 Prentice-Hall.

Picture Archiving and Communication Systems in Biomedical Imaging, alone, 1996, VCH Publishers.

Picture Archiving and Communication Systems: Principles and Applications, alone, 1999, Wiley & Sons.

PACS and Imaging Informatics: Principles and Applications, 1st edition, alone, 2004, John Wiley & Sons.

Principles and Advanced Methods in Medical Imaging and Image Analysis, with Atam P. Dhawan and Dae-Shik Kim (eds), 2008.

PACS and Imaging Informatics: Principles and Applications, 2nd edition, alone, 2010, Wiley & Blackwell.

Since the 2000s, several historical reviews of PACS and imaging informatics development from different points of view have been discussed. In 2011, the *European Journal of Radiology* published a series of three articles by Lemke (Europe), Inamura and Jong (Asia), and Huang (North America), who summarized the historical PACS development in the three continents. My article described some medical imaging accomplishments identifying certain inventions in the 1960s and 1970s. These inventions had conceptually defined basic components of PACS guiding the course of its continuous development in the 1980s and 1990s, as well as the subsequent imaging informatics research in the 2000s. Chapter 1 of this new edition provides a detailed description based on my personal perspective.

PACS, digital report, and informatics were originally developed for radiology application to replace film and paper tools. During the past 30 years, these technologies have been integrated and progressed to a must-have radiological diagnosis clinical component for daily use. The original DICOM PACS and informatics technologies are being extended and expanded to many related clinical imaging applications. However, adopting the DICOM standard as a general image-based standard in Internet communications for other types of non-radiological images and signals has some major drawbacks: DICOM is an excellent standard for PACS, but sometimes technically cumbersome and expensive to use due to its inherited heavily constrained rules and overheads. It is time-consuming to display hundreds of images, retrieval, and archives of a patient's record. In addition, there is the potential of image characteristic compatibility between radiology and other types of medical related images. In the early 2010s, in order to minimize these drawbacks, the Radiological Society of North America (RSNA), along with the Integrating Healthcare Enterprise (IHE), initiated the concept of the "Integrating Healthcare Cross-Enterprise Document Sharing – Imaging (IHE XDS-I) profile". Several major manufacturers and research Institutes were invited by RSNA to participate in this initiative. The principles of IHE XDS-I were defined, prototype systems were developed, and medical imaging companies and radiology equipment manufacturers were encouraged to bring their own imaging equipment and/or information systems to connect to the RSNA IHE XDS-I system backbone for a live demonstration. Since then, new methodology has been drastically improved, and compatible IHE XDS-I profile systems have become available for various hospitals to use. IHE XDS-I profile is a major advancement opening up the gateway for Web-based data management and multimedia image distribution.

Because of the success of IHE XDS-I profile since 2010, the PACS climate has changed dramatically. It seems that the future trend of PACS is to be fragmented, so the term is now called "deconstructed PACS". Traditional PACS vendors are now not only focusing their business in the pure PACS market or storage archive solutions, but also on viewing software and imaging workstations. And the storage solution is now called the vendor neutral archive (VNA), which concentrates on storing the image files in the native DICOM file. VNA is also used to store all other kinds of data, including non-radiology images, whether they are DICOM or non-DICOM. PACS vendors still sell PACS because they have knowledge of the radiology workflow, so that their viewing software will embed these workflow features. Most VNA technologies do not know the deeper DICOM fields, so they just extract basic patient information and archive by

using the Web technology and the IHE XDS-I profile. The recent drastic change of the “PACS” concept has inspired and influenced my further understanding of the combination of DICOM, medical imaging, PACS, and informatics.

The Third Edition

This Third Edition of *PACS-Based Multimedia Imaging Informatics* is organized into four parts with 22 chapters.

Part 1 The Beginning: Retrospective

Part 2 Medical Imaging, Industrial Guidelines, Standards, and Compliance

Part 3 Informatics, Data Grid, Workstation, Radiotherapy, Simulators, Molecular Imaging, Archive Server, and Cloud Computing

Part 4 Multimedia Imaging Informatics, Computer-Aided Diagnosis, Image-Guided Decision Support, Proton Therapy, Minimally Invasive Multimedia Image-Assisted Surgery, and Big Data.

In these 22 chapters, materials are based on the revised DICOM-based PACS technology, and new research and development in PACS-based multimedia Imaging informatics during the past eight years. Part 1 is on the retrospective of medical imaging, PACS, and imaging informatics. Part 2, with Chapters 2 to 7, combines modified and current multimedia image informatics, including Health Level 7, IHE, DICOM, HIS, RIS, PACS, ePR, Web-based data management, and IHE XDS-I forming the new foundation for the DICOM-based PACS multimedia imaging informatics.

Part 3 consists of Chapters 8 to 15, presenting the Data Grid, display workstation, radiotherapy, PACS-based imaging informatics simulators, DICOM-based molecular imaging data grid with IHE XDS-I integration profile, and PACS-based archive servers, and cloud computing. Chapter 8 discusses the Data Grid used for PACS and informatics, and Chapter 9 describes how to use the Data Grid for clinical applications, including a dedicated breast magnetic resonance imaging enterprise with the IHE XDS-I technology. Chapter 10 describes display workstations, including two new technologies of true 2½-dimensional and true three-dimensional image display workstations printing. Chapter 11 presents the multimedia electronic patient record system (ePR) in radiotherapy. Chapter 12 describes five PACS-based imaging informatics simulators with their architectures and functions. Chapters 13 and 14 are on the molecular imaging data grid. Chapter 15 is the first to present PACS-based

archive server and the new technology cloud computing for PACS-based imaging informatics.

Part 4 discusses multimedia imaging informatics, computer-aided diagnosis (CAD), image-guide decision support, proton therapy, minimally invasive multimedia image-assisted surgery, and big data. The first three chapters are on CAD, where the general CAD concept is first discussed, followed by two clinical applications including CAD on acute intracranial hemorrhage and multiple sclerosis. A very detail description on bone age assessment (BAA) in children follows. It starts from data collection, to CAD methodology, to the development of a digital hand atlas, to clinical evaluation, and the final step of integration of the BAA CAD system at the Los Angeles County Children Hospital for clinical evaluation. The BAA CAD is available to the public on the book's website. Chapter 19 then follows with an intelligent ePR system for evidence-based research in radiotherapy. The next two chapters are on minimally invasive image-assisted spinal surgery, showing the current technology combining minimally invasive surgery with multimedia imaging informatics technology. The final chapter is on big data, describing how the new concept of big data technology can be used to extend the potential of current and future PACS-based multimedia imaging informatics applications.

The Future Growth

While preparing Edition 3, I also learned that other clinical departments, in addition to using radiological images, had also started using PACS-based technology by imbedding it into their daily clinical practices. Some successful examples are Pathology PACS (Biegel, 2007), Multimedia ePR (electronic Patient Record) System in Radiotherapy (Law, 2009; Le, 2011), Multimedia ePR System for Image-Assisted Spinal Surgery (Documet, 2010), DICOM-Based Molecular Imaging Data Grid (MIDG) with the IHE XDS-i Integration Profile (Lee, 2012), Surgical PACS (SPIE, 2015 Medical Imaging Conference, integration of CAD with PACS) (Doi, 2007), Computer-Aided Diagnosis (CAD) and Image-Guided Decision Support (Le, 2009), and Intelligent ePR for evidence-based research in radiotherapy (Le, 2011), Cardiac PACS Systems (American College of Cardiology, Mtgs, 2012 and 2013), PACS-based Molecular Imaging (Lee, 2011), and others. For these reasons, it is seen that "PACS and Imaging Informatics" research disciplines have gradually broaden to "PACS-based Multimedia Biomedical Imaging Informatics". As a result, the term "PACS-based multimedia" is no longer constrained to text and radiological

images. It encompasses new imaging informatics paradigm, providing physicians and researchers with new tools based on their own clinical specialties and resources to select and consolidate their preferred multimedia as a means of helping their research, and diagnosing and curing patients.

The term “PACS-based multimedia” can loosely mean that any clinical specialist would have the opportunity to extract and integrate the patient’s existing data, images, graphs, tables, reports, 3-D, 4-D, 5-D images, movies, and scripts based on the PACS-based technology, to compose their needed contents in a physician workstation, as well as to view, diagnose, report, and archive. Multimedia can be recorded, played, displayed dynamically, and interactively accessed from information content processing devices such as computerized and electronic device, and can also be part of a live performance. The majority practicing physicians nowadays do have experience in using PACS-based images and reports from medical Web servers and workstations to help them to take care of their patients. By using the PACS-based technology platform, these multimedia PACS-based biomedical imaging informatics can enrich the clinical specialists to facilitate their patient care.

Selected portions of the PACS-based Imaging Informatics series 2004, 2010 and some pre-printed materials in 2017, have been used as lecture materials in undergraduate and graduate courses: “Medical Imaging and Advanced Instrumentation” at UCLA, UCSF, and UC Berkeley; “Biomedical Engineering Lectures” in Taiwan, and the People's Republic of China; “PACS and Medical Imaging Informatics” at the Hong Kong Polytechnic University; and required courses at the “Medical Imaging and Informatics” track at the Department of Biomedical Engineering, School of Engineering, USC. It is my greatest hope that this new edition will continuously be used, not only to provide information and guidelines for those contemplating a PACS-based Imaging Informatics career, but also to inspire others to apply this technology as a tool toward a brighter future for healthcare delivery.

H.K. (Bernie) Huang
South San Francisco, CA; Berkeley Springs, WVA

Preface to the Second Edition

My interest in PACS and Imaging informatics was inspired and deeply influenced by Dr Robert S. Ledley and initially by his book *Use of Computers in Biology and Medicine* (McGraw-Hill, 1965), the first such book combining principles of biology, medicine, and mathematics. After earning degrees in meteorology and mathematics, I worked for IBM and the space industry as a professional programmer for several years. My goal at that time was to become an astronomer. It was during this fork in the road that I came across Ledley's book and was fascinated by the contents and tangible hypotheses. I made an appointment to see him in Washington, DC, and before the end of the visit he offered me a job (I was not looking for one) and convinced me that I should change my interest from astronomy to biomedical imaging. Soon after, I went to work for him at the National Biomedical Research Foundation (NBRF), Georgetown University Medical Center, Washington, DC, from 1966 to 1980. During this period, I also obtained my doctorate in applied mechanics and mathematics, and continued with postdoctoral studies in anatomy, physiology, and radiology.

Dr Ledley guided me through the design and implementation of several revolutionary medical imaging instrumentation, including FIDAC (film input to digital automatics computer), SPIDAC (specimen input to digital automatics computer), and the automatic computerized transverse axial (ACTA) whole-body CT scanner. These instruments were the infants of today's film digitizers, digital microscopes, and multi-slice CT scanners. I also led or worked on research projects in chromosomes karyotyping; classification of pneumoconiosis on chest x-ray films; 3-D image rendering; image subtraction; CT for radiotherapy on bone and body mass densities, diagnosis of pulmonary nodules, and cardiac imaging; and protein sequences medical databases. These projects were predecessors of many of today's medical imaging informatics methodologies and database concepts.

I further benefited from working with Dr Ledley on soliciting for grants, designing a research laboratory, and writing a book. I followed technology transfer from the university research to private industry and entrepreneurship. I had the opportunity to develop innovative interdisciplinary courses combining physical and biological sciences that were taught as electives at Georgetown.

My Interest in PACS and Medical Imaging Informatics

I joined the Departments of Bioengineering and Radiology at the University of Iowa in 1980, where I developed my first image processing laboratory. Although my stay at Iowa was short, the concept of bridging the gap between engineering and medicine that was due to Dr Tony Franklin, then Chair of Radiology, became the mainstay of my academic career. I summarized this learning experience in “Biomedical Image Processing” a single article issue in the *CRC Critical Reviews in Bioengineering* (vol. 5, Issue 3, 1981). From 1982 to 1992, I developed the Medical Imaging Division, headed the Biomedical Physics Graduate Program, and implemented the in-house PACS at UCLA. From 1992 to 2000, I taught medical imaging at UC, Berkeley, developed the Radiological Informatics Lab, implemented the hospital-integrated PACS, and introduced the concept of imaging informatics at UCSF. Since then, I have been overseeing the development of medical imaging informatics at the Hong Kong Polytechnic University (2000—now) and at USC (2000—now). For more than 25 years I have been documenting PACS and imaging informatics research, development, and implementation in a number of books: *Elements of Digital Radiology: A Professional Handbook and Guide* (Prentice-Hall, 1987), *Picture Archiving and Communication Systems in Biomedical Imaging* (VCH Publishers, 1996), *Picture Archiving and Communication Systems: Principles and Applications* (Wiley, 1999), and *PACS and Imaging Informatics: Principles and Applications* (Wiley, 2004).

These earlier books document the developments in new digital technologies that have emerged through the years. The reader not familiar with a certain concept or term in a newer book could find it explained in more detail in an older book.

PACS and Imaging Informatics Development since the 2004 Book

After the 2004 book was published, PACS development trends shifted to imaging informatics, PACS-based CAD, ePR with image distribution, and ePR for therapy and surgery. The milestones were recorded in two special issues that I edited in 2005 and 2007 for the *Journal of Computerized Medical Imaging and Graphics*, as sequels to the special issues on picture archiving and communication systems, in 1991; on medical image databases, in 1996; and on

PACS 20 Years later, in 2003. The previous special issues were mainly on PACS research and development, whereas the two newer issues were on PACS applications. The first was “Imaging Informatics” (2005), and the second was “Computer-Aided Diagnosis (CAD) and Image-Guided Decision Support” (2007).

In the annual RSNA meetings, we have witnessed progressively fewer film-based technical exhibits from the industry, as well as scientific presentations and exhibits by radiologists and scientists throughout these years. At the 2008 RNSA meeting, there were practically none. Many nonclinical presentations and exhibits are now in CAD, imaging informatics related research, ePR, and image-based therapy.

Since the development of PACS has matured, several well-attended annual conferences in PACS, such as CARS, SPIE, and SCAR, have been gradually shifting their interests from PACS to imaging informatics and related topics. The CARS (Computer-Assisted Radiology and Surgery) annual meeting has been changed to a private foundation-sponsored annual congress, with the official journal *JCARS* accepting manuscripts in imaging informatics and image-assisted surgery and treatment. At the SPIE (International Society for Optical Engineering), annual medical imaging conference, the PACS conference track has shifted their sessions to more PACS-driven imaging informatics topics. The SCAR (Society for Computer Applications in Radiology) changed their society name to SIIM (Society for Imaging Informatics in Medicine). The conclusions that can be deduced from such evidence are that PACS has completed its original goal and gradually become a commodity, a *de facto* integrated imaging tool for image-based diagnoses. PACS-based medical imaging informatics has taken over as the next wave of development to better the patient service and improve healthcare.

PACS and Imaging Informatics, The Second Edition

Medical imaging informatics has evolved from developments in medical imaging, PACS, and medical informatics. Medical imaging is the study of human anatomy, physiology, and pathology based on imaging techniques. The picture archiving and communication system (PACS) consists of medical image and data acquisition, storage, and display subsystems integrated by digital networks and application software. PACS facilitates the systematic utilization of

medical imaging for patient care. Medical imaging informatics is a subset of medical informatics that studies image/data information acquisition; processing; manipulation; storage; transmission; security; management; distribution; visualization; image-aided detection, diagnosis, surgery, and therapy; as well as knowledge discovery from large-scale biomedical image/data sets. Over the past six years, we have witnessed rapid advancement in the research and development of medical imaging technology, PACS, and medical informatics. A revolutionary breakthrough has occurred in image-based healthcare methodologies that benefits the patient in ways never before thought possible.

This new edition on PACS and imaging informatics is organized in the introduction and four parts. Altogether, in the 22 chapters, over 60% to 70% of the materials are based on the new research and development in PACS and imaging informatics from the past six years. All chapters of Parts 1 and 2 have been revised, and Chapter 5 is a new chapter. Chapters 3, 4, 8, 9, 11, 12, and 13 have been changed substantially. In Part 3, web-based PACS, fault-tolerant and enterprise PACS have been rewritten, so has the chapter on image security; the PACS clinical implementation, experience, and pitfalls are based on PACS operation over the past six years. In Part 4, some concepts and research topics that appeared piecemeal in the last edition have been greatly expanded and organized into nine chapters, presenting totally new materials on methodology, results, and clinical experience.

As I wrote in the Preface of the last edition, I would be remiss in not acknowledging the debt of gratitude owed to many wonderful colleagues for this adventure in PACS and Imaging Informatics. I thank former chairmen of radiology at various universities, Drs Edmund Anthony Franken, Gabriel Wilson, Robert Leslie Bennett, and Hooshang Kangarloo in the United States; and chairmen and deans, Profs Maurice Yap, George Woo, and Thomas Wong at PolyU, Hong Kong, for their encouragement and generous support. I can never forget my many students and postdoctoral fellows; I have learned much (and continue to learn now) from their challenges and contributions.

Over the past six years, we have received continuous support from many organizations with a great vision for the future: the National Library of Medicine (NLM), the National Institute of Biomedical Imaging and Bioengineering (NIBIB), other Institutes of the National Institutes of Health (NIH), and the US Army Medical Research and Materiel Command. The private medical imaging industry has encouraged and funded many projects from small to large scale, allowing myself and our team to carry out technology transfers from the

academy to the real world. The support from these agencies and manufacturers provided us with opportunities to go beyond the boundaries of current PACS and Imaging Informatics and open up new frontiers for patient care and healthcare delivery.

In 2006, Mr Thomas Moore, who took over the Senior Editorship of Medical Sciences at John Wiley & Blackwell, tempted me to write a new edition with color figures and text. It was like bees and honey. I have had the great pleasure of exchanging humorous emails, conversations, and worked with him and his editorial team in developing the concepts and contents of this manuscript.

Selected portions of the book have been used as lecture materials in graduate courses: “Medical Imaging and Advanced Instrumentation” at UCLA, UCSF, and UC Berkeley; “Biomedical Engineering Lectures” in Taiwan, and the People's Republic of China; “PACS and Medical Imaging Informatics” at the Hong Kong Polytechnic University; and required courses in the “Medical Imaging and Informatics” track at the Department of Biomedical Engineering, School of Engineering, USC. It is my greatest hope that this new edition will not only provide guidelines for those contemplating a PACS career but also inspire others to apply PACS-based imaging informatics as a tool toward a brighter future for healthcare delivery.

H.K. (Bernie) Huang
Agoura Hills, CA; Berkeley Springs, WVA; and Hong Kong

Acknowledgments

Many associates and friends have contributed valuable assistance during the preparation of this Third Edition, in particular, many of my colleagues, researchers, postdoctoral and former graduate students, from whom I have learned the most. Part 1, Chapter 1 was based on the paper entitled “PACS, and imaging informatics: retrospective” published by *Radiological Physics and Technology* on December 2013, (2014) 7: 5–24. The paper was suggested by Professor Kunio Doi, Professor of Radiology, University of Chicago, and the Editor-in-Chief of *Radiological Physics and Technology*. He was kind enough to suggest, comment, and edit my draft and published the paper (Chapter 1).

Chapters 2 to 7 have been revised based on materials from the Second Edition and updates from industrial standards. Most importantly, I am deeply thankful to the contributions from the following individuals: Jianguo Zhang, Chapters (6, 7, 10, 15, 22), Jasper Lee (8, 9, 12, 13, 14), Anh Le (6, 12, 15, 16, 19), Jorge Documet (12, 20, 21), Brent J. Liu (12, 15, 16), Maria Y.Y. Law (11, 12, 19), Aifeng Zhang (12, 18), Tao Chan (12, 17), and Will Johnsen and Ron Schilling from EchoPixel (10).

Also, thanks to Joe Hunziker, and Bruce Haroldson, Magnolia Senior Center, South San Francisco, California for providing me an office to work during regular office hours.

This book was written with the contributions and assistance of the following faculty, colleagues, staff members, and consultants

Jianguo Zhang, PhD
Professor and Director
Medical Imaging Informatics Lab,
Shanghai Institute of Technical Physics
Chinese Academy of Sciences. Shanghai, China

Jasper Lee, PhD, CIIP
Cedars Sinai Medical Center
EIS Enterprise Imaging, Los Angeles

Anh Le, PhD
Assistant Professor and Medical Physicist
Department of Radiation Oncology Jacobs, School of Medicine & Biomedical

Sciences,University at Buffalo, SUNY Roswell Park Comprehensive Cancer, Buffalo, NY

Jorge Documet, PhD
Tradesy Inc., Santa Monica, California

Brent J. Liu, PhD
Associate Professor, Director,
Imaging Processing and Informatics Laboratory,
Department of Biomedical Engineering, USC

Maria Y. Y. Law, PhD, MPhil, BRS, Teach Dip
Professor in Radiation Therapy
Hong Kong Polytechnic University
Tung Wah College, Hong Kong

Aifeng Zhang, PhD
Research Specialist
University of Illinois Chicago

H.K. Huang Short Biography

H.K. (Bernie) Huang, FRCR(Hon), FAIMBE. Professor Emeritus of Radiology and Biomedical Engineering; University of Southern California, USA; Honorary Professor, Shanghai Institute of Technical Physics (SITP), Chinese Academy of Sciences. Former Chair Professor of Medical Informatics, Hong Kong Polytechnic University (2000–2010), Former Professor, University of California, San Francisco, UCSF (1992–1999), and UCLA (1982–1992).

Dr Huang was inducted into the Royal College of Radiologists, London, as an Honorary Fellow, 1992; the American Institute of Medical and Biological Engineering as a Founding Fellow, 1993; the EuroPACS Society as an Honorary Member, 1996; the Honorary President, International CARS Congress, London, 2003; the President of the First Iranian Imaging Informatics Conference, 2007; and an Honorary Member, Iranian Society of Radiologists, 2011. Dr Huang has been a Visiting Professor of many leading universities around the world, and a board member of several medical imaging manufacturers.

Dr Huang pioneered in picture archiving and communication system (PACS) and imaging informatics research. He developed the PACS at UCLA in 1991, and the hospital-integrated PACS at UCSF in 1995, and started imaging informatics research in 1999. Dr Huang has taught at Georgetown University (1971–1980); University of Iowa (1981/1982); and UCLA, Vice Chair and Professor of Radiological Sciences and Program Director of Biomedical Physics Graduate Program, School of Medicine, (1982–1992). He taught medical imaging at the UC Berkeley, and was Professor and Vice Chair of Radiology, UC San Francisco (1992–1999). He was the Chair Professor of Medical Informatics, Hong Kong Polytechnic University (2000–2010) and Professor of Radiology and Biomedical Engineering, University of Southern California (2000–2010). In his career, he has mentored 24 PhD students and over 44 Post Doctoral Fellows from around the world.

Dr Huang’s research interests has been in tele-imaging and telemedicine, fault-tolerant PACS server, Internet 2, PACS-based CAD and surgery, imaging informatics, image recovery after disaster, image integrity, Data Grid and Grid computing, Cloud computing, HIPAA compliance, Patient tracking system, Radiation Therapy Information System, ePR, dedicated breast MRI ePR, image-guided minimally invasive spinal surgery, and imaging informatics simulators.

He has authored, co-authored, and co-edited 10 books, published over 200 peer-reviewed papers, and received several patents. His 2010 book: “PACS and Imaging Informatics, 2nd edition with full color and 1000 pages by Wiley, is the only single-authored textbook in this field. His 3rd edition: “PACS-Based Multimedia Imaging Informatics” will be published by Wiley in 2019.

Dr Huang was an IPO Board of Directors of Medical China, Ltd., Hong Kong in the mid-2000s. He was the Cofounder of the Surgmatix, Inc., USA in 2008; and was co-awarded the “Surgical Data Monitoring and Display System”, US Trademark 079977-0015 and US Patent 8,313,432 B2, 2012. Surgmatix invented the image-assisted minimally invasive spinal surgery ePR system. During the past 30 years, Dr Huang, as an experienced grant administrator, has received over 21 million US dollars in PACS, medical imaging informatics, tele-imaging, and image processing, physics, and informatics related research grants and contracts from the US Federal and State Governments, and private industry. Dr Huang has been an honorary consultant for many national and international hospitals, and imaging manufacturers in the design and implementation of PACS-based imaging Informatics.

List of Acronyms

1-D
one-dimensional

2-D
two-dimensional

3-D
three-dimensional

4-D
four-dimensional

A/D
analog to digital converter

A & E
ambulatory and emergency

ABF
Air Blown Fiber

ACC
ambulatory care center

ACGME
Accreditation Council for Graduate Medical Education

ACR
American College of Radiology

ACR BIRADS
American College of Radiology Beast Imaging Reporting and Data System Atlas

ACR-NEMA
American College of Radiology–National Electric Manufacturer's Association

ADM
acquisition and display module

ADT
admission, discharge, transfer

AE

application entities

AFBUS
volumetric (3-D) automated full breast ultrasound

AFP
alpha-fetal protein—a tumor marker

AIH
acute intracranial hemorrhage

AJCC
American Joint Committee on Cancer

AL
aluminum

AMP
amplifier

AMS
Acquisition Modality Standards Institute

AMS
acquisition modality simulator

AMS
automatic monitoring system

ANL
Argonne National Laboratory

ANOVA
Analysis of Variance

ANSI
American National Standards Institute

AP or PA
anterior-posterior, access point

API
Application Program Interface

APS
antepartum care summary

ARI
access to radiology information

ASCII

American Standard Code for Information Interchange

ASI NATO
Advanced Study Institute

ASIC
Application-Specific Integrated Circuit

ASP
active server pages

ASP
application services provider

AT
acceptance testing

ATL
active template library

ATM
asynchronous transfer mode

ATNA
audit trail and node authentication

AVI
Audio Video Interleave

Az
area under the ROC curve

BAA
bone age assessment

BPP
bit per pixel

BDF
Building Distribution Center

BGO
Bismuth Germanate X-ray detector

BIDG
Breast imaging data grid

BIRN
Biomedical Informatics Research Network

BIS
Bispectral Index System

BME
biomedical engineering

BMI
body mass index

BMP
Bitmap Image File Format

BNC
a type of connector for 10 Base2 cables

BPPC
basic patient privacy consents

Brachy
brachytherapy

CA
certificate authority

CA
continuous available

CaBIG
Cancer Biomedical Informatics grid

CAD
computer-aided diagnosis and detection

CADe
computer-aided detection

CADx
computer-aided diagnosis

CAI
computer-aided instruction

CalREN
California Research and Education Network

CARS
Computer assisted radiology and surgery

CATH

cardiac cath

CC
cancer center

CC
cranio-caudal

CD
compact disk

CCD
charge-coupled device

CCU
coronary care unit

CDA
R2 clinical document architecture, release 2

CDDI
copper distributed data interface

CDR
central data repository

CDRH
Center for Devices and Radiological Health

CDS
clinical decision support

CE-MRI
contrast-enhanced MRI

CEN TC251
Comite Europeen de Normalisation–Technical Committee 251–Healthcare Informatics

CF
computerized fluoroscopy

CFR
contrast frequency response

CHG
charge posting

CHLA
Childrens Hospital Los Angeles

CIE
Commission Internationale de L’Eclairag

CNA
Center for Network Authority

CO_2
carbon dioxide

CMS
clinical management system

CNA
campus network authority

COG
children’s oncology group

COM
component object model

CORBA
common object request broker architecture

COSTAR
computer-stored ambulatory record

CPI
consistent presentation of images

CPU
central processing unit

CR
computed radiography

CRF
central retransmission facility—headend

CRPS
Clinical Patient Record System

CRT
cathode ray tube

CsF
cesium flouride

CSI
California Spine Institute, Thousand Oaks, CA

CSMA/CD
carrier sense multiple access with collision detection

CSS
cascade style sheet

CSU/DSU
channel service unit/data service unit

CT
Computed Tomography

CT
consistent time

CTCAE
Common Terminology Criteria for Adverse Events v3.0

CTN
central test node

CTV
clinical target volume

D/A
digital-to-analog

DAI
data access interface

DASM
data acquisition system manager

DB
a unit to measure the signal loss

DB
database

DB MRI
dedicated breast MRI

DBMS
database management system

DC
direct current

DCM

DICOM

DCT
Discrete Cosine Transform

DCU
DICOM conversion unit

DDR
digital reconstructed radiography

DE
digital envelope

DEC
device enterprise communication

DECRAD
DEC radiology information system

DES
data encryption standard

DEN
distance education network

DF
digital fluorography

DG
data grid

DGS
data grid simulator

DHA
digital hand atlas

DHHS
Department of Health and Human Services

DICOM
Digital Imaging and Communication in Medicine

DICOM-RT
DICOM in radiotherapy

DICOM-SR
DICOM structured report

DIFS

distributed image file server

DIMSE
DICOM message service elements

DIN/PACS
digital imaging network/PACS

DLT
digital linear tape

DM
digital mammography

DMR
diabetic mellitus retinopathy

DMZ
de-militarized Zone

DOD
Department of Defense

DOT
directly observed treatment

DOR
Department of Radiology

DP
display and processing

DQE
Detector Quantum Efficiency

DR
digital radiography

DR11-W
a parallel interface protocol

DRPT
displayable reports

DRR
digitally reconstructed radiograph

DS
digital signature

DS-0

digital service

DSA
digital subtraction angiography

DSA
digital subtraction arteriography

DSC
digital scan converter

DSL
Digital Subscriber List

DSSS
direct sequence spread spectrum

DTD
document type definition

DTI
Diffusion Tensor MRI

DVA
digital video angiography

DVD
digital versatile disks

DVH
dose volume histogram

DVSA
digital video subtraction angiography

DWI
diffusion weighted MR imaging

ebXML
eXtensible markup language used for electronic business

ECDR
eye care displayable report

ECED
eye care evidence document

ECG
electrocardiogram

ECT
emission computed tomography

ECHO
echocardiography

ED
emergency department

ED
evidence documents

EDER
emergency department encounter record

EDGE
enhanced data rates for GSM evolution

EDH
extradural hemorrhage

EDR
emergency department referral

EHR
electronic health record

EIA
electrical industry association

EMG
electromyography

eMR
electronic medical record

EP
emergency physician

EPI
echo-planar imaging

EPI
electronic portal image

EPID
electronic portal imaging device

EP
electrophysiology

ePR
electronic patient record

ESF
edge spread function

EUA
enterprise user authentication

EuroPACS
European Picture Archiving and Communication System Association

EVN
event type segment

EYECARE
eye care

FAA
Federal Aviation Administration

FCR
Fuji CR

FDA
US Food and Drug Administration

FDDI
fiber distributed data interface

FDG
flurodeoxyglucose

FFBA
full frame bit allocation

FFD
focus to film distance

FFDDM
full-field direct digital mammography

FID
free induction decay

FIFO
first-in-first-out

FLAIR
fluid attenuated inversion recovery

FM
folder manager

fMRI
functional MRI

FP
false positive

FPD
flat panel detector

FRS
facial recognition system

FRSS
facial and fingerprint recognition system

FSA
functional status assessment

FT
fault tolerance

FFT
fast Fourier transformation

FTE
full time equivalents

FTP
file transfer protocol

FUSION
image fusion

FWHM
full width at half maximum

G & P
Greulich and Pyle bone development atlas

GAP
Grid Access Point

GEMS

General Electric Medical System

GIF
graphic interchange format

GMAS
Grid Medical Archive Solution

GridFTP
Grid File Transfer Protocol (Globus Toolkit)

GPRS
general packet radio services

GRAM
grid resource allocation and management

GSM
global system for mobile communication

GT4
Globus toolkit Version 4, open source software for grid computing

GTV
gross target volume

GUI
graphic user interface

GW
gateway

HA
high availability

H & D
curve Hurter & Driffield characteristic curve

H-CAS
HIPAA-compliant auditing system

HCC
Health Consultation Center

HCC II
Health Consultation Center II

HELP

health evaluation though logical processing

HII
Healthcare Information Infrastructure

HIM
SS Healthcare Information and Management Systems Society

HIPAA
Health Insurance Portability and Accountability Act

HI-PACS
integrated-PACS

HIS
hospital information system

HISPP
healthcare information standards planning panel

HK HA
Hong Kong Hospital Authority

HKI
D Hong Kong identity card number

HL-7
Health Level 7

HMO
healthcare maintenance organization/hospital management organization

HOI
Health Outcomes Institute

HP
Hewlett Packard

HPCC
high performance computing and communications

HTM
hypertext markup language

HTTP
hypertext transfer protocol

HTTPS
hypertext transfer protocol secured

Hz

Hertz (cycle/sec)

I2
Internet 2

I/O
input/output

IAS
image-assisted surgery

IASS
image-assisted surgery system

IAT
image-assisted therapy

ICD-9-CM
International Classification of Diseases, ninth edition, Clinical Modification

ICH
intracerebral hemorrhage

ICMP
internet control message protocol

ICT
information and communication technology

ICU
intensive care unit

ID
identification

IDCO
implantable device cardiac observation

IDF
intermediate distribution

IDNET
a GEMS imaging modality network

IEC
international electrotechnical commission

IEEE

Institute of Electrical and Electronics Engineers

iEHR
image-enabled EHR

IFT
inverse Fourier transform

IG-MISS
Image guided—minimally invasive spinal surgery

IHE
Integrating of Healthcare Enterprise

IHE-RO
Integrating the Healthcare Enterprise, Radiation Oncology

IHE XDS-I
IHE cross-enterprise document sharing for imaging

IIS
Internet Information Server

IIA-MISS
Integrated image assisted minimally invasive spinal surgeryIIASIntegrated image assisted surgery

IMAC
image management and communication

IMRT
intensity modulated radiation therapy

INC
identifier names and codes

InCor
Heart Institute at the University of San Paulo, Brazil

InfoRAD
Radiology information exhibit at RSNA

IOD
information object definition

IP
imaging plate

IP
internet protocol

IPILab
Image Processing and Informatics Laboratory at USC

IRB
Institute Review Board

IRM
imaging routing mechanism

IRWF
import reconciliation workflow

ISCL
integrated secure communication layer

ISDN
integrated service digital network

ISN
Image Sharing Network

ISO
International Standards Organization

ISO-OSI
International Standards Organization—Open System Interconnection

ISP
internet service provider

ISSN
integrated image self-scaling network

IT
information technology

ITI
IHE Information Technology Infrastructure Profile

ITI-18
ITI transaction of Registry Stored Query

ITI-41
ITI transaction of Provide and Register Document Set-b

ITI-42
ITI transaction of Register Document Set-b

ITI-43

ITI transaction of Retrieve Document Set

ITPN
intelligent treatment planning navigator

ITS
information technology services

IU
integration unit

IUPAC
International Union of Applied Chemistry

IVA
intravenous video arteriography

IVF
intravenous fluid

IVH
intraventricular hemorrhage

IVUS
intravascular ultrasound

JAMIT
Association of Medical Imaging Technology

JAVA
Just another vague acronym (a programming language)

JCAHO
Joint Commission on Accreditation of Healthcare Organizations

JCMIG
Journal of Computerized Medical Imaging and Graphics

JEPG
Joint Photographic Experts Group Image File Format

JIRA
Japan industries association of radiation apparatus

JND
just noticeable difference

JPEG
Joint Photographic Experts Group

KB
knowledge base

KIN
key image note

KOS
Key Object Selection

kVp
kilo-volt potential difference

LAC
Los Angeles County

LAN
local area network

LCD
liquid crystal display

LDMS
legacy data migration system

LDS
Latter-Day Saints Hospital

LDSE loss
less digital signature embedding

LDSERS
lossless digital signature embedding receiving site

LINAC
linear accelerator

L.L
left lower

LLUNC
Loma Linda University Medical Center

LOINC
logical observation identifier names and codes

LP
line pair

LRI
laboratory for radiological informatics

LSB
least significant bit

LSF
line spread function

LSWF
laboratory scheduled workflow

LTCS
LOINC test codes subset

LTVS
location tracking and verification system

LUT
look up table

mA
milli-ampere

MAC
message authentication code

MAMMO
mammography image

MAN
metropolitan area network

MB, Mb
megabytes

MDA
monitoring and discovery system

MDF
message development framework

MDIS
medical diagnostic imaging support systems

MEDICUS
medical imaging and computing for unified information sharing

MFC

Microsoft foundation class

MGH
Massachusetts General Hospital

MHS
Message header segment—a segment used in HL7

MIACS
medical image archiving and communication system

MIC
Molecular Imaging Center, USC Keck School of Medicine

MicroCAT
Micro Computed Axial Tomography

MicroPET
Micro Positron Emission Tomography

MIDG
molecular imaging data grid

MIDS
medical image database server

MIII
medical imaging informatics infrastructure

MIME
multipurpose internet mail extension

MIMI
Multi-modality Multi-resource Information Integration

MIMP
Mediware Information Message Processor—a computer software language for HIS used by the IBM computer

MIP
maximum intensity projection

MIS
Minimally invasive surgery

MISS
minimally invasive spinal surgery

MITRE
a non-profit defense contractor

MISS
minimally invasive spinal surgery

MIU
modality integration unit

MLO
mediolateral oblique view in a mammogram

mmHg
millimeters of mercury

MOD
magnetic optical disk

MODEM
modulator/demodulator

MMR-RO
multimodality registration for radiation oncology

MOD
magnetic optical disk

MP
megapixels

MP
multi-processors

MPEG
motion picture experts group compression

MPR
multi-planar reconstruction

MR
magnetic resonance

mR
milli-Roentgen

MRA
magnetic resonance angiography

MRI
magnetic resonance imaging

MRMC
multiple-reader multiple-case in ROC analysis

MRS/MRSI
magnetic resonance spectroscopic imaging

MS
multiple sclerosis

MS
medical summaries

MSDS
healthcare message standard developers sub-committee

MSH
message header segment

MSM
mobile site module

MTF
modulation transfer function

MTOM
Message Transmission Optimization Mechanism

MUM
mobile unit modules

MUMPS
Massachusetts General Hospital Utility Multi-Programming System—a computer software language

MZH
Mt Zion Hospital, San Francisco

NA
numerical aperture

NANT
new approaches to neuroblastoma therapy

NAPT
National Association for Proton Therapy

NATO ASI
North Atlantic Treaty Organization—Advanced Science Institutes

NCHS

National Center for Health Statistics

NCI
National Cancer Institute

NDC
network distribution center

NDC
national drug codes

NEC
Nappon Electronic Corporation

NEMA
national electrical manufacturers association

NFS
network file system

NGI
next generation internet

NIE
network interface equipment

NIBIB
National Institute of Biomedical Imaging and Bioengineering

NIH
National Institutes of Health

NINT
nearest integer neighbor

NIST
National Institute of Standards and Technology

NK1
next of kin segment

NLM
National Library of Medicine

NM
nuclear medicine

NMSE
normalized mean-square error

NPC

nasopharynx carcinoma

NPfIT
National Program for IT

NPRM
Notice of Proposed Rule Makings

NSF
National Science Foundation

NTPL-S
normal treatment planning-simple

NTSC
national television system committee

NTW
new territories west cluster, Hong Kong

NVRAM
nonvolatile random access memory

OAR
organ at risk

OC
optical carrier

OD
optical density

ODBC
open database connectivity

OFDM
orthogonal frequency division multiplexing

OGSA
open grid services architecture

OML
orbital-meatal line

OP IC
out patient imaging Center

OPT
optical imaging modality

OR
operating room
OS
operating system
OSI
open system interconnection

PA
posterior-anterior
PACS
picture archiving and communication system
PBR
pathology-bearing region
PC
personal computer
PD
postdoctoral
PDA
personal digital assistant
PDF
Portable Document Format
PDI
portable data for imaging
PDQ
patient demographics query
Perl
practical extraction and report language
PET
positron emission tomography
PET-CT
Co-registered PET and CT
PGP
presentation of grouped procedures
PHD

personal health data

PHI
protected health information

PHP
hypertext preprocessor

PHR
personal health record

PI
principal investigator

PICT
Macintosh picture format

PIR
portable data for imaging

PID
patient identification segment

PIR
patient information reconciliation

PIX
patient identifier cross-referencing

PL
plastic

PLUS
PACS local user support

PMS
Philips Medical Systems

PMT
photomultiplier tube

PNG
portable network graphics

POH
Pok Oi Hospital, Hong Kong

PolyU
Hong Kong Polytechnic University

PoP

point-of-presence

PP
post processing

PPI
parallel peripheral interface

PPI-ePR
public private interface–electronic patient record

ppm
parts per million

PPM
post processing manager

PPM
pre-processing manager

PPW
post processing workflow

PPHP
pre-procedural history and physical

PRA
patient record architecture

PRF
pulse repetition frequency

PSA
patient synchronized application

PSA
prostate specific antigen

PSF
point spread function

PSL
photo-stimulable luminescence

PSNR
peak signal-to-noise ratio

PT
proton therapy

PTD

parallel transfer disk

PTV
planning target volume

PV1
patient visit segment

PVM
parallel virtual machine system

PWF
pathology workflow

PWF
post-processing workflow

PWP
personnel white pages

Q/R
query and retrieve

QA
quality assurance

QC
quality control

QED
query for existing data

R&D
research and development

RAID
redundant array of inexpensive disks

RAM
random access memory

RETMA
Radio-Electronics-Television Manufacturers Association

RF
radio frequency

RFD

retrieve form for data capture

RFP
request for proposals

RGB
red, green and blue colors

RID r
request information for display

RIM
reference information model

RIS
radiology information system

RLE
run length encoding

RLS
replica location service in grid computing (Globus Toolkit)

RNp2
Rede Nacional de Ensino e Pesquisa

ROC
receiver operating characteristic

ROI
region of interest

RR
radiology residents

RS
radiology specialists

RS r
receiving site

RS232
recommended electrical device interface standard 232

RSNA
Radiological Society of North America

RT
radiation therapy/radiotherapy

RWF

reporting workflow

S-bus
a computer bus used by SPARC

SAH
subarachnoid hemorrhage

SAN
storage area network

SC
screen captured

SCAR
Society of Computer Applications in Radiology

SCH
student health center

SCP
service class provider

SCSII
small computer systems interface II

SCU
service class user

SD
standard deviations

SDH
subdural hemorrhage

SDK
software development toolkit

SEQUEL
structured English query language

SFVAMC
San Francisco VA Medical Center

SIG
special interest group

SIIM
Society for Imaging Informatics in Medicine

simPHYSIO
simulation physiology

SINR
simple image and numeric report

SJHC
Saint John's Healthcare Center

SMIBAF
super medical image broker and archive facility

SMPTE
Society of Motion Picture and Television Engineers

SMZO
Social and Medical Center East, Vienna

SNOMED
systemized nomenclature of medicine

SNR
signal-to-noise ratio

SOAP
Simple Object Access Protocol

SOBP
Spread Out Bragg Peak

Solaris 2.x
a computer operating system version 2.x used in a SUN computer

SONET
synchronous optical Network

SOP
service-object pairs, DICOM

SPARC
a computer system manufactured by Sun Microsystems

SPECT
single photon emission computed tomography

SPIDAC
Specimen Input to Digital Automatics Computer

SPIE

International Society for Optical Engineering

SPOF
single-point-of failure

SQL
structured query language

SR
structured reporting

SRS/SRT
stereotactic radiosurgery/stereotactic radiotherapy

SS s
ending site

SSE
Semantic searching engine

SSD
surface shaded display

SSG
service selection gateway

SSL
secure socket layer

ST
a special connector for optical fibers

STIP
Shanghai Institute of Technical Physics

STRESS
stress testing

SUN OP
SUN computer operating system

SWF
scheduled workflow

T-rate
data transmission rate

T1
DS-1 private line

TB, Tb
terabyte

TC t
threshold contrast

TCE
teaching file and clinical trial export

TCP/IP
transmission control protocol/internet protocol

TDS
tube distribution system

TFS
teaching file script

TGC
time gain compensation

TIFF
tagged image file format

TLS
transport layer security

TMH
Tuen Mun Hospital, Hong Kong

TMR
triple modular redundancy

TP
treatment plan

TP
true positive

TPS
treatment planning system

TRWF
treatment workflow

UCAID
University Corporation for Advanced Internet Development

UCLA

University of California at Los Angeles

UCSF
University of California at San Francisco

UH
University Hospital

UID
unique identifier

UMDNS
universal medical device nomenclature system

UML
unified medical language system

UMTS
universal mobile telecommunications service

UPS
uninterruptible power supply

URL
uniform resource locator

US
ultrasound

USAVRE
United States Army Virtual Radiology Environment

USC
University of Southern California

UTP
unshielded twisted pair

VA
Department of Veterans Affairs

VAHE
United States Department of Veterans Affairs Healthcare Enterprise Information System

VAMC
VA Medical Center

VAS

visual analog scale

VAX
a computer system manufactured by Digital Equipment Corporation (DEC)

VB
visual basic

vBNS
very high-performance backbone network service

VGA
video graphics array

VI
Visual Indexing

VL
visible light

VM
value multiplicity

VME
a computer bus used by older SUN and other computers

VMS
a computer operating system software used by DEC computers

VNA
Vendor Neutral Archives

VPN
virtual private network

VR
value representation

VR
voice recognition

VRAM
video RAM

VRE
virtual radiology environment

VS
virtual simulator

VTK
visualization toolkit

WADO
web access to DICOM persistent objects

WAN
wide area network

WECA
Wireless Ethernet Compatibility Alliance

WEP
wired equivalent privacy

Wi-Fi
wireless fidelity

WLAN
wireless LAN

WORM
write once read many

WS
workstation

WWAN
wireless WAN

WWW
World Wide Web

XCT
X-ray computed tomography

XD*-LAB
sharing laboratory reports

XDM
cross-enterprise document media interchange,

XDR
cross-enterprise document reliable interchange

XDS
cross-enterprise document sharing

XDS-i
cross-enterprise document sharing for imaging, IHE Integration Profile

XDS-SD
cross-enterprise sharing of scanned documents

XML
Extensible Markup Language

XPHR
exchange of personal health record content

YCbCr
luminance, and two chrominance coordinates used in color digital imaging

YIQ
luminance, in-phase, and quadrature chrominance color coordinates

Part 1
The Beginning: Retrospective

1
Medical Imaging, PACS and Imaging Informatics: Retrospective

CHAPTER MENU

Part I Technology Development and Pioneers

1.1 Medical Imaging

1.1.1 The Pattern Recognition Laboratory and Professor Robert S. Ledley

1.1.2 The ACTA: The Whole Body CT Scanner

1.1.3 Dr Ledley's Lifetime Accomplishments

1.2 PACS and its Development

1.2.1 PACS

1.2.2 The Department of Radiological Sciences and the Biomedical Physics Graduate Program

1.2.3 Professor Moses Greenfield

1.2.4 Professor Hooshang Kangarloo

1.2.5 The Image Processing Laboratory (IPL) at UCLA

1.3 Key Technologies: Computer and Software, Storage, and Communication Networks

1.3.1 The Vax 11/750 Computer System

1.3.2 Multiple Display Controller

1.3.3 Hierarchical Storage System

1.3.4 Personal Image Filing System

1.3.5 Image Compression

1.3.6 Laser Film Printer for X-Ray Images

1.3.7 Asynchronous Transfer Mode (ATM) Communication Technology

1.4 Key Technologies: Medical Imaging Related

1.4.1 Laser Film Scanner
1.4.2 Computed Radiography (CR)
1.4.3 Direct Digital Input from CR to PACS
1.4.4 Digital Radiography
1.4.5 Interactive Display with Multiple Monitors
Part II Collaboration and Supports
1.5 Collaboration with Government Agencies, Industry and Medical Imaging Associations
1.5.1 The US Government Agencies
1.5.2 The Netherlands National Foundation and the UCLA PACS
1.5.3 The NATO Advanced Science Institute (ASI) and the UCLA PACS
1.5.4 Collaboration of the UCLA Team with the US Medical Imaging Industry
1.5.5 Japan Medical Imaging Technology and the UCLA PACS
1.5.6 SPIE, EuroPACS, CARS and UCLA PACS Team
1.5.7 Patents and Copyrights
1.6 Medical Imaging Informatics
1.6.1 Biomedical Informatics
1.6.2 The 1970s Concept: Chromosome Karyotyping
1.6.3 Medical Imaging Informatics Today
1.7 Summary
1.7.1 The Golden Era of Medical Imaging Technology Research Support
1.7.2 After the First 10 Years of PACS
1.7.3 The PACS End Users
1.7.4 The Diligent Contributors
1.8 Acknowledgments
References

PART I TECHNOLOGY DEVELOPMENT AND PIONEERS

Historical reviews of PACS and imaging informatics development have been published in the past from different points of view [1–3]. This retrospective chapter attempts to look at the topic from a different angle by identifying certain basic medical imaging inventions in the 1960s and 1970s, which had conceptually defined basic components of PACS, guiding its course of development into the 1980s and 1990s, as well as subsequent imaging informatics research in the 2000s. In medical imaging, the emphasis was on the innovations in the 1960s and 1970s at Georgetown University in Washington, DC. During the 1980s and 1990s, research and training support from US government agencies and public and private medical imaging manufacturers became available for training of young talent in biomedical physics and for developing the key components required for PACS development. In the 2000s, computer hardware and software as well as communication networks advanced by leaps and bounds, opening the door for medical imaging informatics to flourish. Because many key components required for the PACS operation were developed by the UCLA PACS team and its collaborative partners in the 1980s, this chapter is centered on that aspect. During this period, substantial collaborative research efforts by many individual teams in the United States and Japan are highlighted.

Credit is due in particular to the Pattern Recognition Laboratory at Georgetown University, and the computed radiography (CR) development at the Fuji Electric Corp. in collaboration with Stanford University in the 1970s; the Image Processing Laboratory (IPL) at UCLA in the 1980s to 1990s; as well as the early PACS development at the Hokkaido University, Sapporo, Japan, in the late 1970s; and film scanner and digital radiography developed by Konishiroku Photo Ind. Co. Ltd. (Konica-Minolta), Japan, in the 1980s to 1990s. Major support from the US National Institutes of Health and other federal agencies and private medical imaging industry are appreciated. The NATO (North Atlantic Treaty Organization) Advanced Study Institute (ASI) sponsored the International PACS Conference at Evian, France, in 1990, the contents and presentations of which convinced a half dozen high-level US military healthcare personnel, including surgeons and radiologists, that PACS was feasible and would greatly streamline the current military healthcare services. The impact of the post-conference summary by these individuals to their superiors opened the door to

long-term support of PACS development by the US Military Healthcare Services. PACS and imaging informatics have thus emerged as a daily clinical necessity.

1.1 Medical Imaging

1.1.1 The Pattern Recognition Laboratory and Professor Robert S. Ledley

In the early medical imaging research in the 1960s to 1970s, the two most important innovations allowing the possible development of PACS are probably the digitizer (or scanner), which converts an analog image to a digital image, and the whole-body CT scanner. The former allowed the conversion of analog medical images to digital images, with the latter replacing conventional 2-D x-ray procedures with the use of direct digital acquisition of 3-D body images. With scanners, successful developments included the 35-mm film flying-spot scanner, the x-ray film drum scanner, and the microscopic slide scanner. Among other medical imaging researchers, Prof. Robert S. Ledley can be singled out as a pioneer in this area of research. Ledley was Professor of Physiology and Biophysics and Professor of Radiology at the Georgetown University Medical School, pioneering the use of electronic digital computers in biology and medicine. This section is dedicated to Dr Ledley's lifetime accomplishments. He had a colorful career in research related to medical imaging. He contributed two influential articles in *Science*: "Reasoning Foundations of Medical Diagnosis" in 1959 [4] and "Digital Electronic Computers in Biomedical Science" in 1964 [5]. In 1965, he published the fundamental *Use of Computers in Biology and Medicine* that became a classic in early medical imaging research (Figure 1.1) [6]. In 1960, he founded the National Biomedical Research Foundation (NBRF) to promote the use of computers and electronic equipment in biomedical research. At the NBRF, Ledley pursued several major innovative projects to convert analog images to digital images, including the FIDAC (Film input to digital automatic computer) for 35-mm slides in the 1960s (Figure 1.2A), and the DRIDAC (drum input to digital automatic computer) for x-ray films (Figure 1.2B) in the 1970s. In microscope slides, the SPIDAC (Specimen input to digital automatic computer) automated the analysis of chromosomes in the late 1970s (Figure 1.2C). He established the Pattern Recognition Laboratory at the NBRF, which housed this equipment (Figures 1.2C and 1.3 and Section 1.6.2).

Robert Steven Ledley (June 28, 1926 – July 24, 2012), Professor Emeritus of Physiology and Biophysics, Georgetown University. In 1965, he published *Use of Computers in Biology and Medicine* and established the National Biomedical Research Foundation (NBRF).

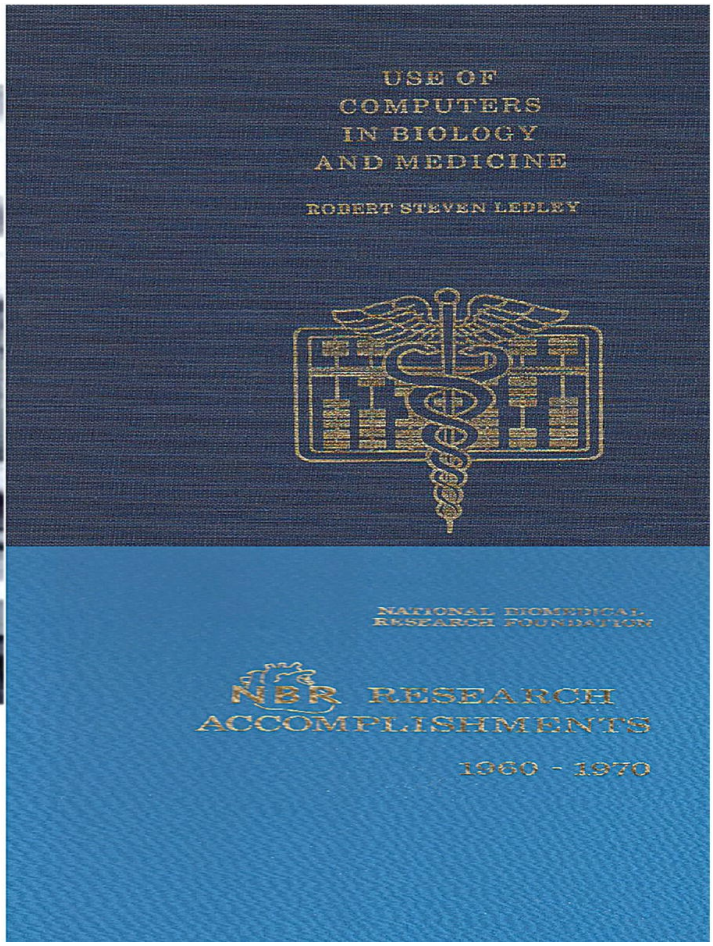

Figure 1.1 Robert Steven Ledley (June 28, 1926–July 24, 2012, aged 86).

(A)

FIDAC

(Film Input to Digital Automatic Computer) 70s

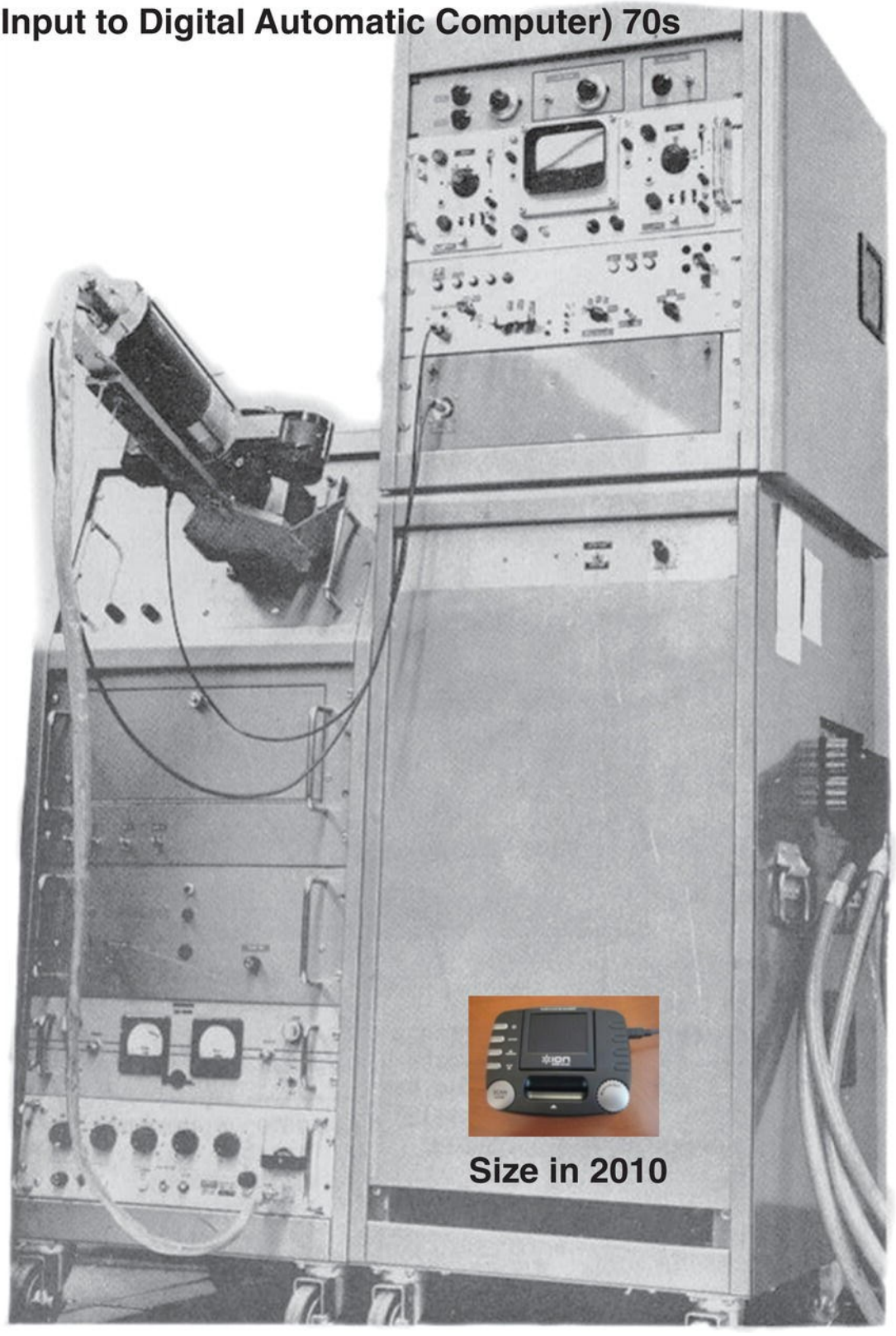

Size in 2010

(B)

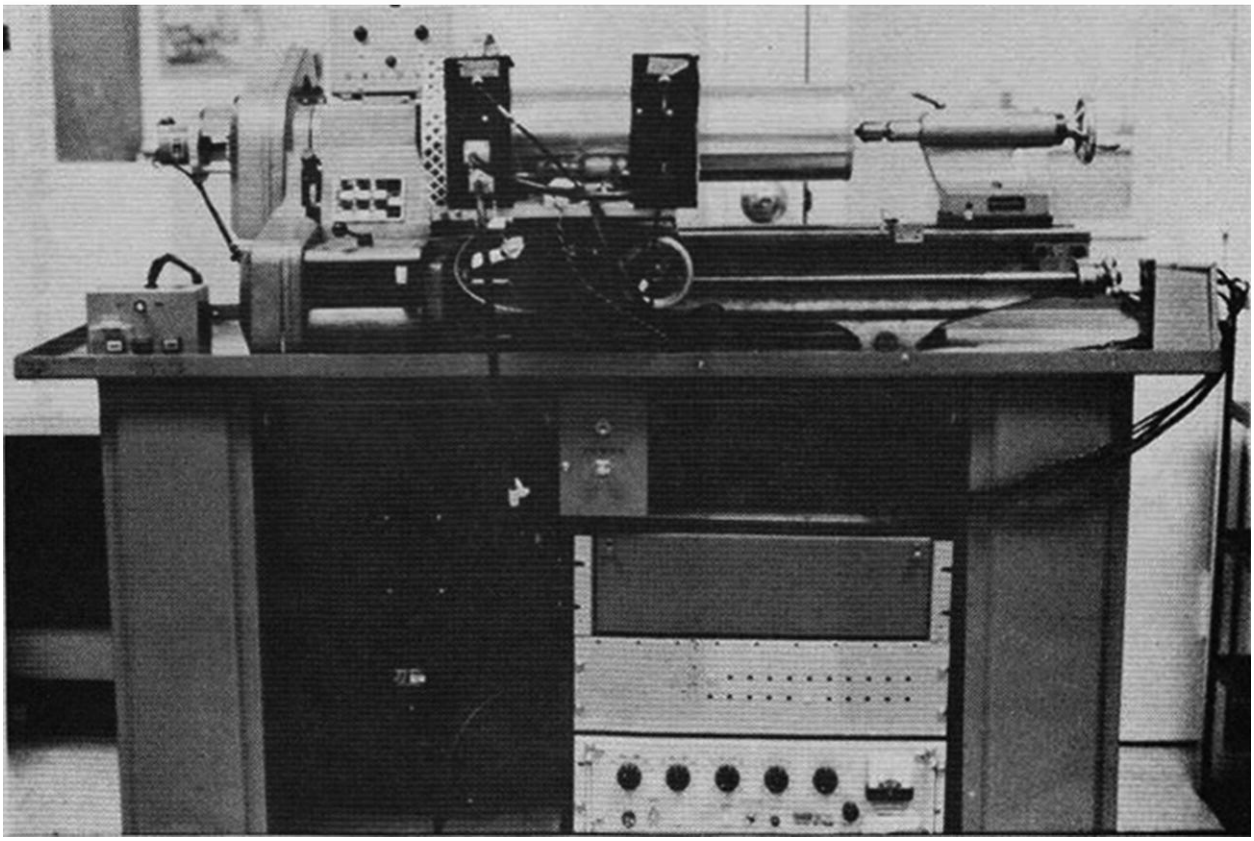

(C)

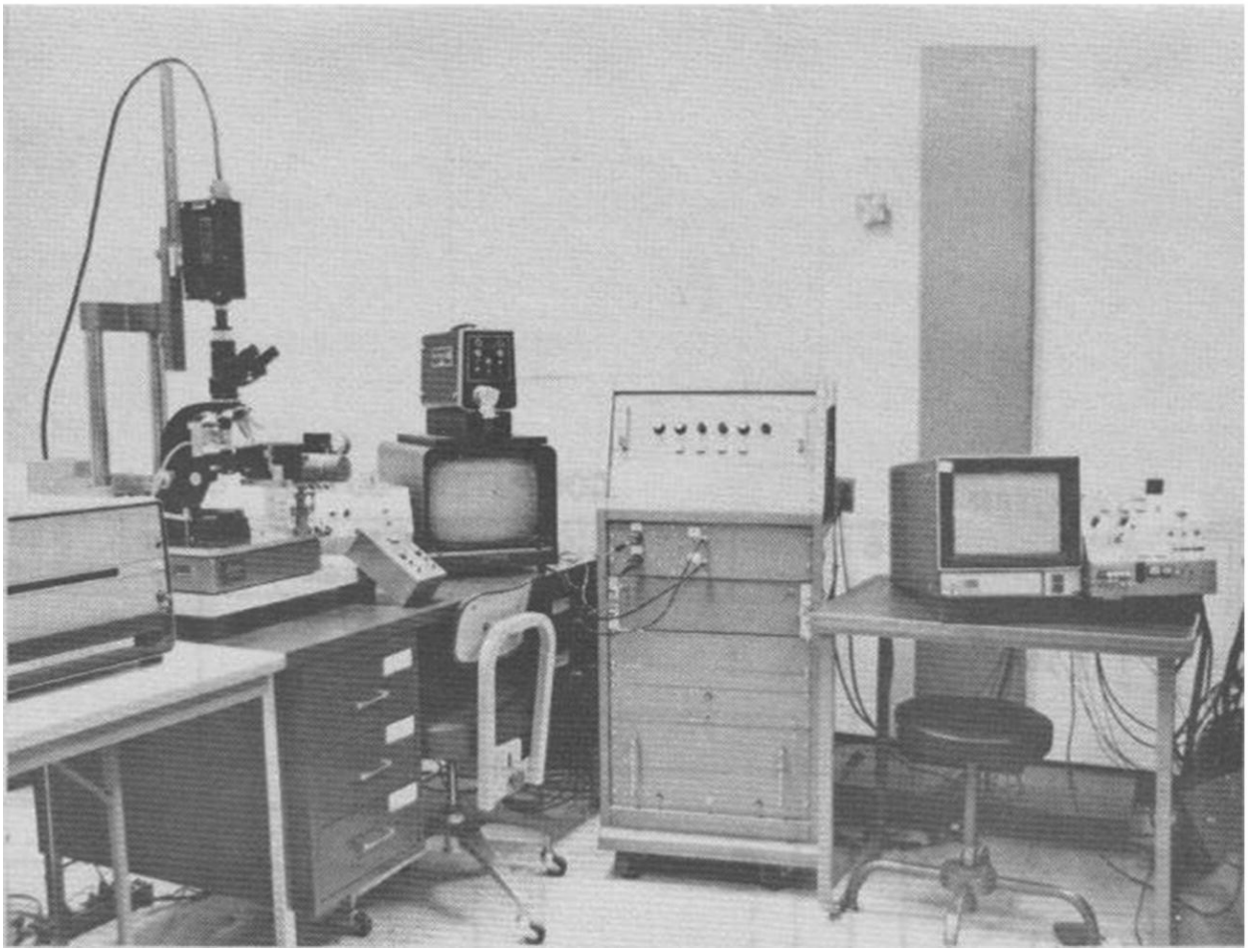

Figure 1.2 Innovative medical imaging components in the Pattern Recognition Laboratory in the mid-1970s: (A) FIDAC (Film input to Digital Automatic Computer); (B) DRIDAC (Drum Input to Digital Automatic Computer); (C) SPIDAC (Specimen Input to Digital Automatic Computer).

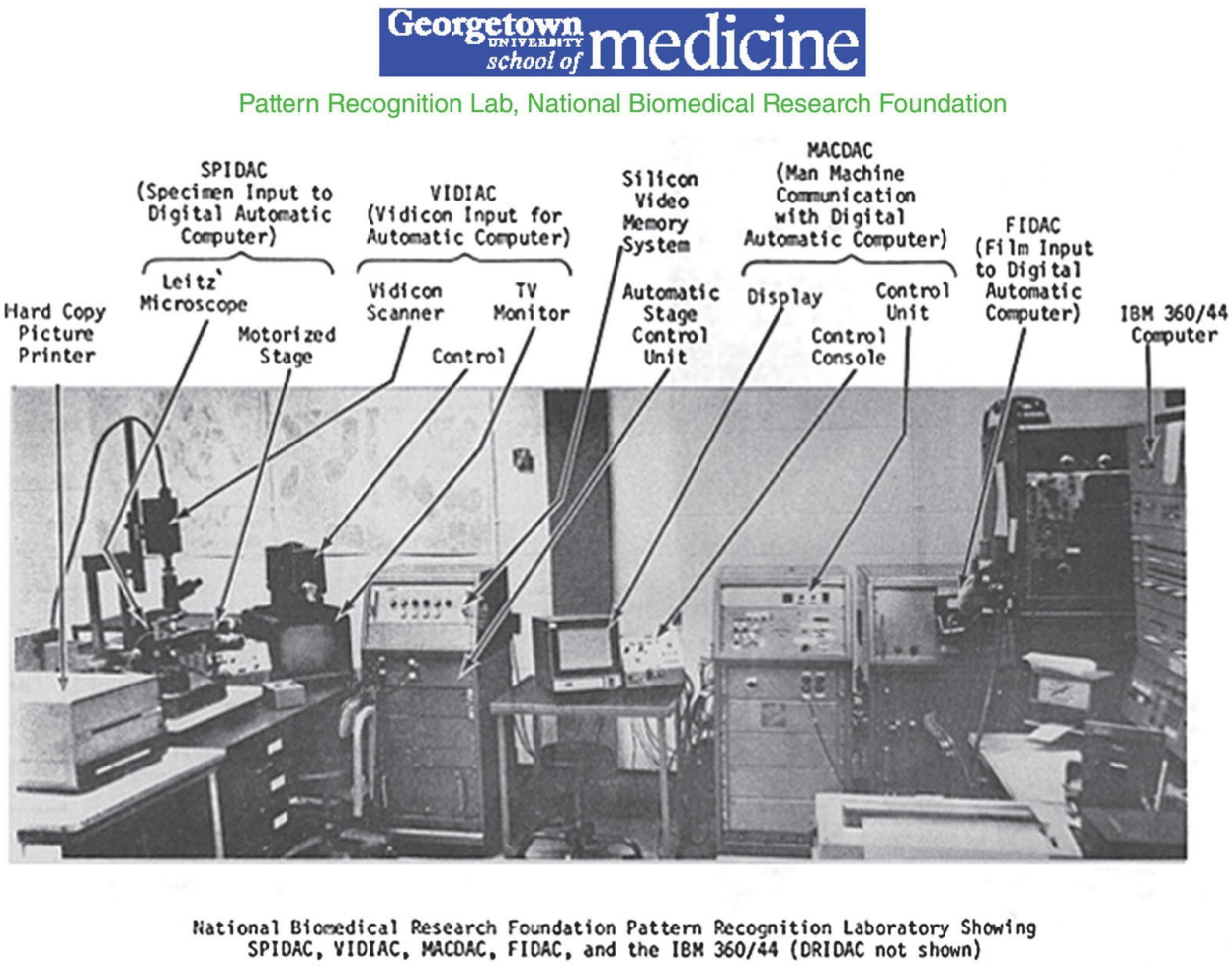

Figure 1.3 Pattern Recognition Laboratory, National Biomedical Research Foundation.

1.1.2 The ACTA: The Whole Body CT Scanner

When Sir Godfrey N. Hounsfield, Nobel laureate, invented the head CT scanner at EMI, UK, in the early 1970s [7], Dr Ledley was also developing the ACTA (automatic computerized transverse axial) scanner, the first whole-body CT scanner, in the mid-1970s (Figure 1.4). In the first available cross-sectional anatomy textbook, published by Williams & Wilkins in 1997, the sectional images in the textbook were obtained from the ACTA scanner at Georgetown University [8]. In the late 1960s, NBRF was affiliated with the Georgetown University Medical School in Washington, DC, as a research laboratory. Ledley became an Emeritus Professor in 2010. Throughout the years, he provided opportunities to many young multidisciplinary open-minded trainees to explore the use of computers and electronics in medicine, by luring them to participate in

his Pattern Recognition Laboratory as interns or research scientists (Figure 1.3). The author, H.K. Huang, was one of these fortunate individuals, who had given up his dream to become an astronomer, and was later mentored by Professor Ledley.

(A)

(B)

Cross-Sectional Anatomy— An Atlas For Computerized Tomography

Robert S. Ledley
H. K. Huang
John C. Mazziotta

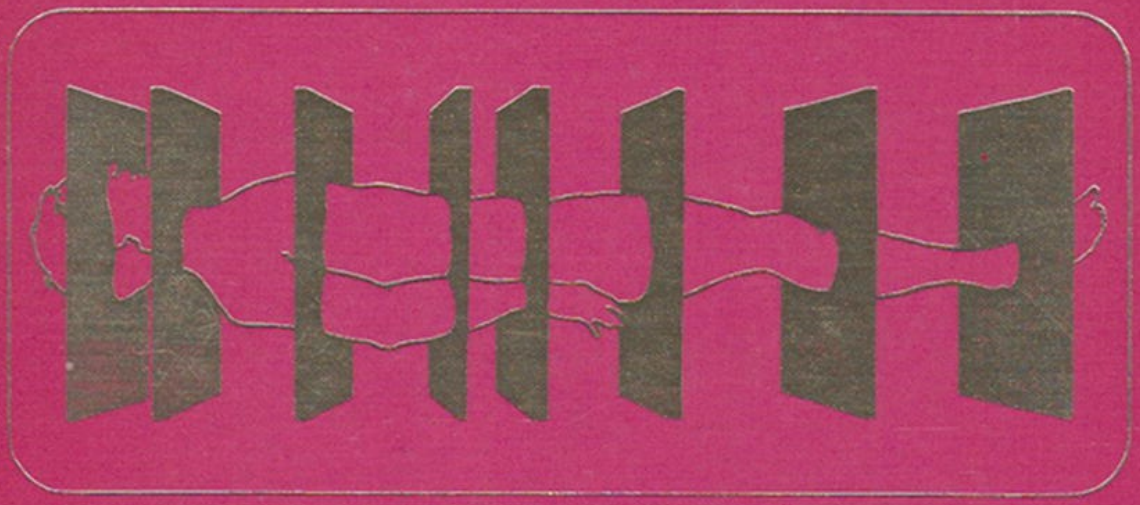

The first Cross-Sectional Atlas
William & Wilkins
1977

Figure 1.4 The ACTA, with Professor Ledley, the first whole-body CT scanner, with two slices per scan in 4½ min.

1.1.3 Dr Ledley's Lifetime Accomplishments

Among many other accomplishments and awards, the first ACTA prototype scanner was displayed at the Smithsonian's National Museum of American History in Washington, DC. The museum also established an archive with relevant materials related to the development of the ACTA. In 1990, Ledley was inducted into the National Inventors Hall of Fame, sponsored by the US Patent and Trademark Office. For pioneering his contributions to biomedical computing and engineering, including the invention of the whole-body CT scanner which revolutionized the practice of radiology, and for his role in developing automated chromosome analysis for prenatal diagnosis of birth defects (Section 1.6.2), he was awarded the National Medal of Technology and Innovation by the US President Bill Clinton in 1997. The National Institutes of Health honored him with a public lecture in 2008: "A Lifetime of Biomedical Computing: A Conversation with Robert Ledley".

Ledley initiated and remained the Editor-in-Chief of four scientific journals from the 1970s until 2012: *Pattern Recognition*, *Computers in Biology and Medicine*, *Computer Languages, Systems and Structures*, and *Computerized Medical Imaging and Graphics*. These journals are still in publication today.

1.2 PACS and its Development

1.2.1 PACS

PACS, based on digital communication, display, and information technology, has revolutionized the practice of radiology and, when combined with medical imaging informatics, greatly enhances clinical practice. The first international conference and workshop on PACS was held at Newport Beach, California, in January 1982, sponsored by the SPIE (International Society for Optical Engineering). Major components of PACS consist of an image and data acquisition gateway accepting images from various modalities, a PACS server and archive for management and storage, and display workstations connected by digital networks. PACS is usually integrated with other healthcare information systems through database gateways; for example, the HIS (Hospital Information System) and the RIS (Radiology Information System), to communicate and manage patient information related to imaging examinations. The top part of

Figure 1.5 depicts the general HIS/RIS/PACS system. This retrospective attempts to identify some of the major components in the early days of PACS development, contributed by the UCLA PACS team and its collaborators, who played major roles in the later success of PACS. Some of these components can be traced back to Professor Ledley's innovations in his Pattern Recognition Laboratory at Georgetown University. Others were the laser film digitizer, computed and digital radiography, direct digital image input to computer memory, interactive display workstations, and the concept of imaging informatics (discussed later in Section 1.6). In order to present these innovations and the cutting-edge technologies, Sections 1.2.2 and 1.2.3 are used as background material to facilitate the subsequent presentation, followed by Sections 1.3 to 1.5: Sections 1.2.2, the Department of Radiological Sciences and the Biomedical Physics Graduate Program, UCLA; Section 1.2.3, the Image Processing Laboratory; Section 1.3, development of computer and software, storage, and communication networks-related key technologies; Section 1.4, development of medical imaging-related key technologies; and Section 1.5, collaboration with government agencies, industry, and medical imaging associations.

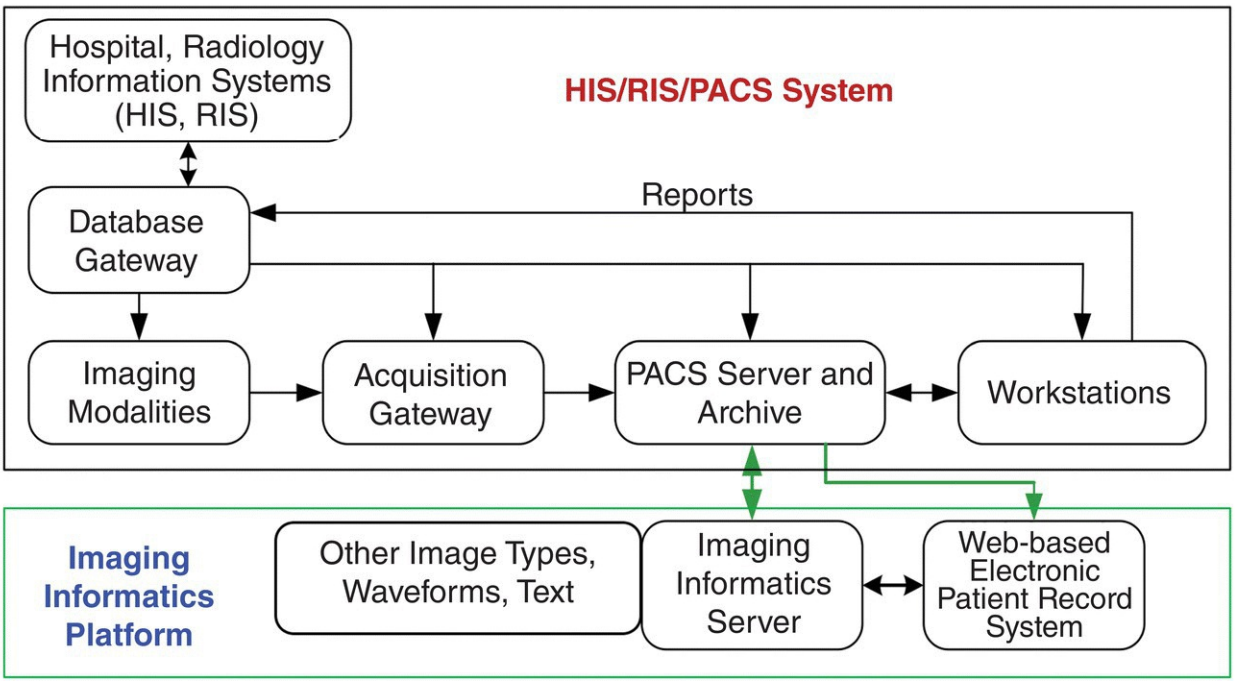

Figure 1.5 Top: PACS system and components. Bottom: Imaging informatics platform.

1.2.2 The Department of Radiological Sciences and the

Biomedical Physics Graduate Program

The Department of Radiological Sciences and the Biomedical Physics Graduate Program, UCLA, was developed in 1987, when PACS was developed at UCLA. The UCLA Medical Center is situated on the south side of the UCLA campus in Westwood Village, California, a community in the Santa Monica foothills, a few miles from the Pacific Ocean. The Medical Center is the primary training facility for diagnostic radiology, including a 4-year resident training program. The Medical Center had over 700 beds, and performed 200 000 diagnostic radiological and nuclear medicine procedures annually in the 1980s. Another facility adjacent to the hospital, the Medical Plaza, provides a resource for training in outpatient radiology. The department has included 23 professors, 7 emeritus professors, 6 associate professors, 16 assistant professors, and many adjunct faculty members. Faculty members include both medical professionals and basic scientists.

The Medical Center also has a Biomedical Physics Graduate Program under the auspices of the Department of Radiological Sciences, which trains MS and PhD candidates in four specialties: biophysics, medical imaging, medical physics, and radiation biology, teaching students from three clinical science departments. Two pioneers, Professor Moses Greenfield, Director of the Biomedical Physics Graduate Program, and Professor Hooshang Kangarloo, Chairman of Radiological Sciences, championed the development of PACS at UCLA, which led to the success of its implementation.

1.2.3 Professor Moses Greenfield

Professor M. Greenfield (Figure 1.6A), Professor Emeritus of Radiological Sciences, was the founder of the Medical Physics PhD program at UCLA. In 1948, UCLA established the Department of Radiological Science, and Greenfield was recruited to establish the Clinical Physics Laboratory inside a clinical department of the Medical School. He later formed and was appointed as the Director of the well-known Medical Physics PhD Program at UCLA from 1960 to 1982. After he retired, Professor H.K. Huang was recruited to be mentored by Greenfield, who was instrumental in expanding the graduate program and adopted its new name, Biomedical Physics Graduate Program, to signify a broadened scope by offering four subspecialties in biophysics/nuclear medicine, medical imaging, radiobiology and experimental radiation oncology, and therapeutic medical physics. Then he transferred to UCSF/UC Berkeley to continue PACS research. Huang pioneered the PACS program and was the

Director of the Graduate Program from 1982 to 1992. Greenfield was asked to assume the position of Acting Director of the Graduate Program from 1992 to 1996. After he became Professor Emeritus, Professor Greenfield continued to participate in the training program until 2010. During his tenure at UCLA, Greenfield cofounded the American Association of Physicists in Medicine (AAPM) and the American College of Medical Physics. He received the William D. Coolidge Award, AAPM, in 1991. *The Journal of Applied Clinical Medical Physics (JACMP)*, published in 2005, was dedicated to his accomplishments in this field.

(A)

(B)

Figure 1.6 (A) Professor Moses Greenfield (March 8, 1916–July 26, 2012, 97 years); (B) Professor Hooshang Kangarloo (Dec 24, 1944–May 15, 2012, 67 years) and his faculty and residents in the pediatric radiology reading room using the PACS three 1K × 1K monitor viewing workstation.

Greenfield received a NIH (National Institutes of Health) training grant in medical physics in the late 1970s. With the graduate program broadened to “biomedical physics” in the 1980s, the training grant was renewed. The NIH Biomedical Physics training grant continues to be renewed by the succeeding directors of the Graduate Program, each as the principal investigator, thus becoming one of the longest training grants in this field supported by NIH. The UCLA Biomedical Physics Program gave more than 266 MSc and PhD degrees (as of 2010), a major contribution to the medical physics profession. Many of the graduates have dedicated their careers to the fields of medical imaging, PACS, and imaging informatics, continuing the research and development efforts.

Dr Greenfield's contribution to PACS and imaging informatics development helps to establish the quality of trainees in the biomedical physics program that provides a pool of young scientists to participate in these fields of research.

1.2.4 Professor Hooshang Kangarloo

Professor H. Kangarloo was Professor of Pediatrics, Radiology, and Bioengineering at UCLA. He was section head of pediatric imaging from 1978 to 1987, director of residency training from 1984 to 1986, and became the first Leo G. Rigler Chair of the Department of Radiological Sciences from 1986 to 1995. Under his chairmanship, UCLA became renowned as a major innovator in PACS. Using integrated computed radiography, CT, MR, and US images, and PACS displaying them on three multiple 1K × 1K monitors, the pediatric PACS was online for daily clinical use in the late 1980s. From 1984 to 2005, Kangarloo was the principal investigator of five NIH-funded R01 grants, a training grant from the National Library of Medicine (NLM) in medical imaging informatics, and a continuously funded Program Project Grant in digital imaging, PACS, and informatics that spanned over 20 years. In 2005, he became Emeritus Professor and Chairman of the Department of Radiological Sciences, and continued leading the research and training program in PACS and medical imaging informatics until 2012.

The major contributions of Professor Kangarloo to PACS and imaging informatics are as follows: as the chair of the Department of Radiological Sciences, he persuaded the clinical faculty to buy into the concept of PACS, and he moved the department from film reading to PACS reading. When he was the division chief, his pediatric radiology division was the first clinical division to use total digital PACS to read radiologic examinations. He mandated that radiology resident training had to include a 2-week rotation in the image processing laboratory for learning PACS. He also encouraged faculty and residents to participate in PACS and imaging informatics research. Figure 1.6B shows Professor Kangarloo with his faculty and residents using the PACS system in the pediatric radiology reading room.

1.2.5 The Image Processing Laboratory (IPL) at UCLA

Professor H.K. Huang was recruited from the Georgetown University to establish the future Image Processing Laboratory (IPL) at UCLA in 1982, supported by the Department of Radiological Sciences. While he was waiting for the position to be vacated by Professor Greenfield's retirement from UCLA, he

set up a smaller-scale image processing laboratory at the Bioengineering Department and the Department of Radiology at the University of Iowa, Iowa City, from September 1980 to April 1982. The original purpose of the UCLA IPL was to assist residents to learn the basic image-processing terminology commonly used in diagnostic radiology. After Professor Huang joined UCLA, the department's research direction gradually shifted to PACS research and development. As a result, the IPL grew steadily. In 1987, the IPL had received several grants related to PACS development from the NIH, collaborative research support from five major imaging equipment manufacturers, and some matching funds from the Department of Radiological Sciences. Many Biomedical Physics Graduate Program's post-doctorates (PDs) and PhD students joined the laboratory, as did five to six post-doctoral fellows from foreign countries. The IPL gradually matured as a research and education laboratory; its members became faculty researchers and PhD students in the Division of Medical Imaging of the Biomedical Physics Graduate Program. The laboratory also offered a formal training program to radiology residents. Table 1.1 is a list of the equipment in the IPL, and Figure 1.7 depicts system components of the laboratory and clinical equipment supporting the PACS operation (data were collected in 1987). The IPL hosted annual visits for participants of the SPIE Annual PACS Conference, Newport Beach, California, from 1987 to 1991 (Section 1.5.6).

Table 1.1 Equipment at IPL, UCLA, 1987.

VAX-11/750 Computer A (7 Mb) and B (6 Mb).
Gou Id IP8500 Image Processor A: The Gou Id IP8500 has 12 512×512 image memories, a real-time (1/30 second) image digitizer, and an image array processor.
Gou Id IP8500 Image Processor B: Same as A but has 20 MB image memory (80 512×512 images).
Storage: Data storage includes six magnetic disk drives (10, 121, 205, and three 456 MB), two optical storage systems, one optical library (166 GB), and a high-speed dual-density magnetic tape drive.
Video Scanner: One video scanner together with the IP8500 can digitize an analog image into a 512×512×8 digital image in 1/30 second; a Mitsubishi 1440×1440×8 video scanner is attached to its own image processor.
Laser Scanner/Printer: Two laser scanners—one can digitize a 14×17 inch x-ray to a 2000×2400×10 bit digital image, and the other to a 1440×1440×8 image. The laser printer can write one or more images into a 4000×5000 pixel

area on 8×10 and 14×17 inch film.
CT Image Processing System: This system consists of PDP-11/44 computer, dual AP-500 array processors, hardwired back-projector, 160-MB disk, tape drive, and a multi-format camera.
PIXAR Image Computer: This 1024 color state-of-the-art image computer is connected to a SUN computer.
Mitsubishi 2048 Image Processor: This image processor is connected to a laser film scanner and two 2048 monitor display station.
Picture Archiving and Communication System: One broadband and one baseband Ethernet communication system connect the laboratory to remote facilities and diagnostic imaging equipment located throughout the department.
Viewing Stations: There are five multiple monitor viewing stations with 512, 1024, and 2048 resolutions.
All computers and image processing equipment are connect through an Ethernet communication system.

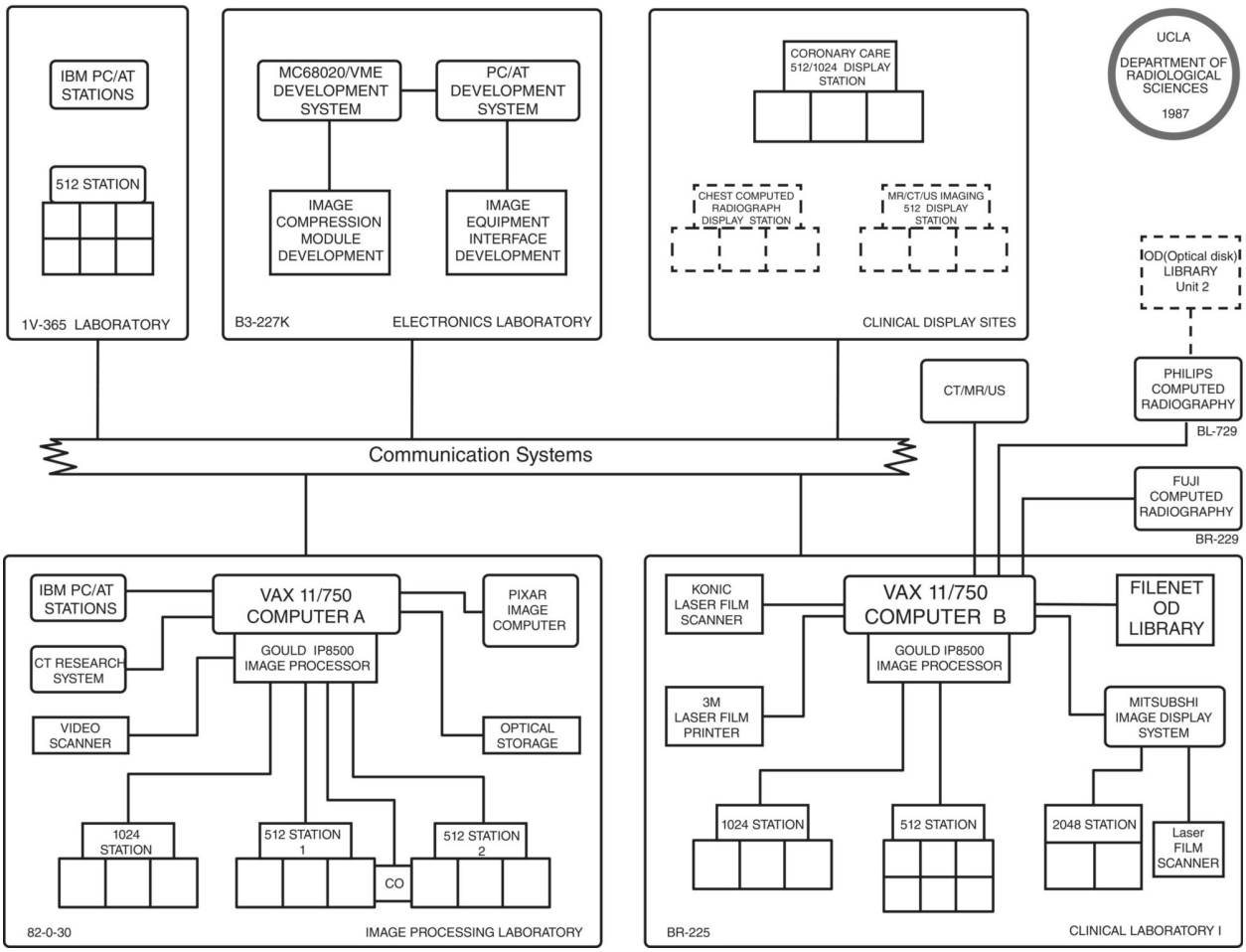

Figure 1.7 Research and clinical components at IPL connected by the Ethernet

Communication System. This figure was a historical drawing of the Image Processing Laboratory (IPL), Department of Radiological Sciences at UCLA, IPL established in 1982, and developed the first PACS for clinical operation between 1987 and 1991. Bottom left: the IPL. Right: clinical laboratory. Top right: the PACS workstations at three experimental laboratories in the hospital. This equipment was the beta version of the PACS workstations later installed in the clinical sites. IDs in the bottom of each block were the room no. located at the Department and the UCLA Hospital.

1.3 Key Technologies: Computer and Software, Storage, and Communication Networks

Many key technologies were not in existence during the early 1980s, but PACS required them for its development. Although most of them have been improved/replaced gradually by more up-to-date technologies, it is instructive for historical purposes to review some of them here (for details, see [9–11]). This section presents a set of computer and software, data storage, and communication networks technologies which were not originally developed for PACS, but were modified for PACS applications. Section 1.4 describes a second set of key technologies developed solely for PACS [12]. In the presentation of these two sets of new key technologies, credit is given to those individuals and/or manufacturers who contributed to the novelty of this accomplishment.

1.3.1 The VAX 11/750 Computer System

The VAX 11/750 computer system was partially supported by the Digital Equipment Corporation (DEC) in 1984, running the VMS operating system, the most advanced mini-computer at that time (Figure 1.7, bottom left and right, and Figure 1.8, left).

Figure 1.8 The VAX/11 750 computer. Left: the Gould DeAnza multiple display controller (middle, blue).

1.3.2 Multiple Display Controller

The Image Processing Controller hardware that could drive a color 1024 monitor (Figure 1.7, bottom left and right, and Figure 1.8, middle, blue, and Figure 1.14, right) was supported by Dr Harold Rutherford of the Gould DeAnza Corp. from January 1984 to January 1989. The controller was modified by the UCLA PACS team to drive three 1024 black-and-white monitors to display three different 1K × 1K PACS (black-and-white) images simultaneously. Hence, it became a high-resolution multimodality image display system.

1.3.3 Hierarchical Storage System

The Hierarchical Storage System project was carried out in collaboration with Kodak in the United States from April 1988 to March 1995, to integrate a large capacity computer Jukebox with many optical disks (14”) (Figure 1.9, left), with the then innovative redundant array of inexpensive disks (RAID) by use of AMASS software (Figure 1.9, right), which was designed by the UCLA PACS

team. This system was still running the UCLA legacy PACS for archiving of historical images until the early 2000s.

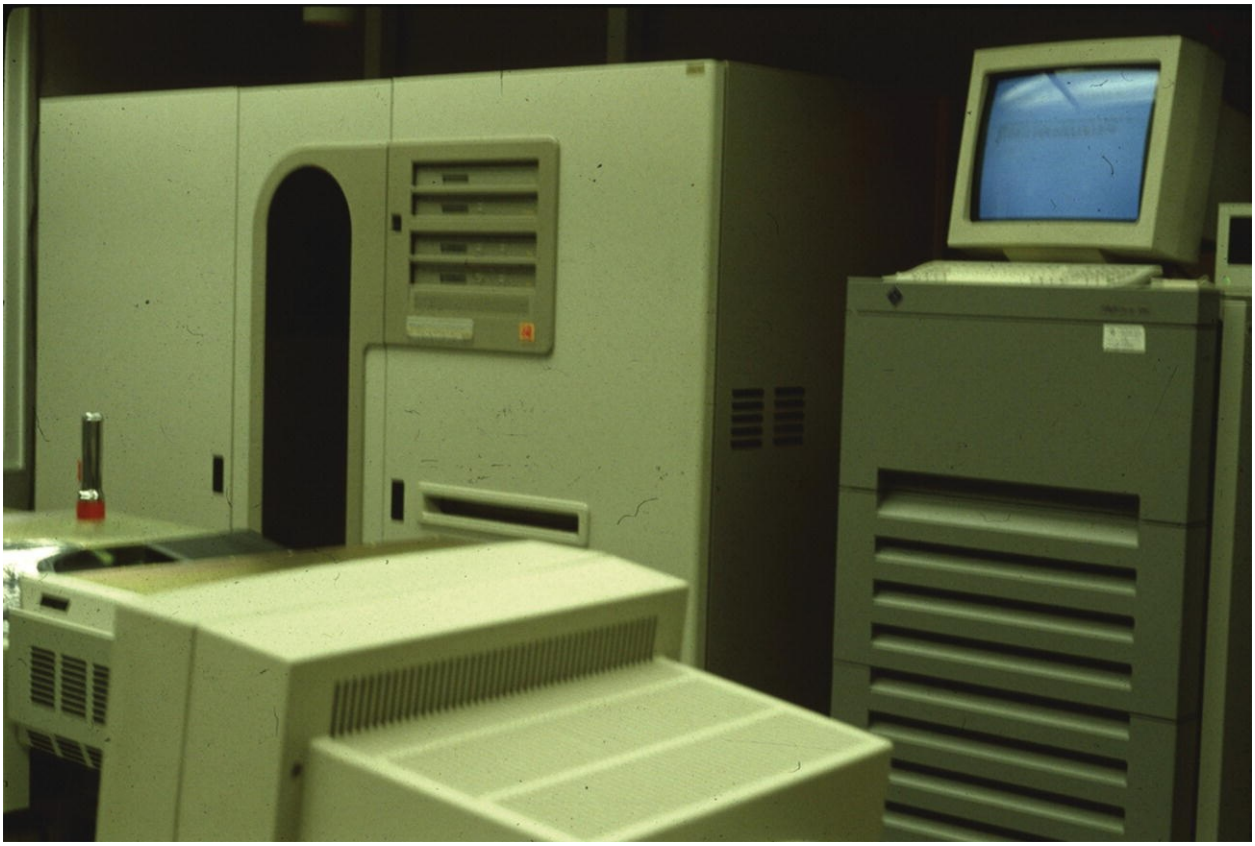

Figure 1.9 Large-capacity Optical Disk Jukebox by Kodak and the RAID disks running the AMASS software (right).

1.3.4 Personal Image Filing System

The Personal Image Filing System, a two-phase collaborative project with Maxell Hitachi, Japan, ran from October 1988 to September 1990, and from October 1992 to September 1994, for the development of an information system using designated storage areas for retrieving/converting data and directories of different-format image archiving in optical and magnetic storage. The result was a US patent awarded to the UCLA team with two Japanese scientists, Sonobe Takeo and Toru Shinagawa, of Maxell Hitachi in 1995 [13].

1.3.5 Image Compression

This Image Compression project was supported by IBM with its massive computer center at San Jose, California, from August 1984 to August 1985, with continuous extension of several years for running of computational intensive

image compression algorithms, which ultimately resulted in the development of the 3-D wavelet compression method for medical images [14,15].

1.3.6 Laser Film Printer for X-Ray Images

Laser Film Printer for x-ray Images was sponsored by 3M Corp., Minneapolis, Minnesota, from October 1986 to September 1988, for printing of PACS output images on film. In the early days of PACS operation, printing of PACS images on film was still necessary for image quality comparison and as an established tradition in clinical wards. For these reasons, the availability of film copy was still required in the beginning of the PACS operation.

1.3.7 Asynchronous Transfer Mode (ATM) Communication Technology

This 2-year collaborative project, Asynchronous Transfer Mode (ATM) communication Technology, with Pacific Bell, CalREN (California Research and Education Network), USA, from March 1994 to December 1996, was used to merge the local area network with the ATM, the then high-speed wide-area network (155 mbits/s) for PACS application in teleradiology. The location of the operation was at the Laboratory for Radiological Informatics, University of California, San Francisco [16], when a component of the UCLA team relocated to UCSF.

1.4 Key Technologies: Medical Imaging Related

Five key technologies in medical imaging required for PACS operation are summarized below. All were developed in long-term collaboration with major medical imaging manufacturers.

1.4.1 Laser Film Scanner

In order to convert millions of already archived x-ray films in every radiology department to digital format for PACS operation, high-resolution 2K × 2K × 12 bits laser film scanners became necessary. The UCLA PACS team collaborated with three major film scanner manufacturers for many years. The first one developed for clinical use was by Konishiroku Photo Ind. Co. Ltd. (it changed its name to Konica in the 1980–1990s, and most recently to Konica-Minolta), Japan. The collaborative research between Konica and UCLA was very extensive and is described in Section 1.5.5 in more detail. Figure 1.10 shows the

first laser film scanner delivered by Konica at UCLA.

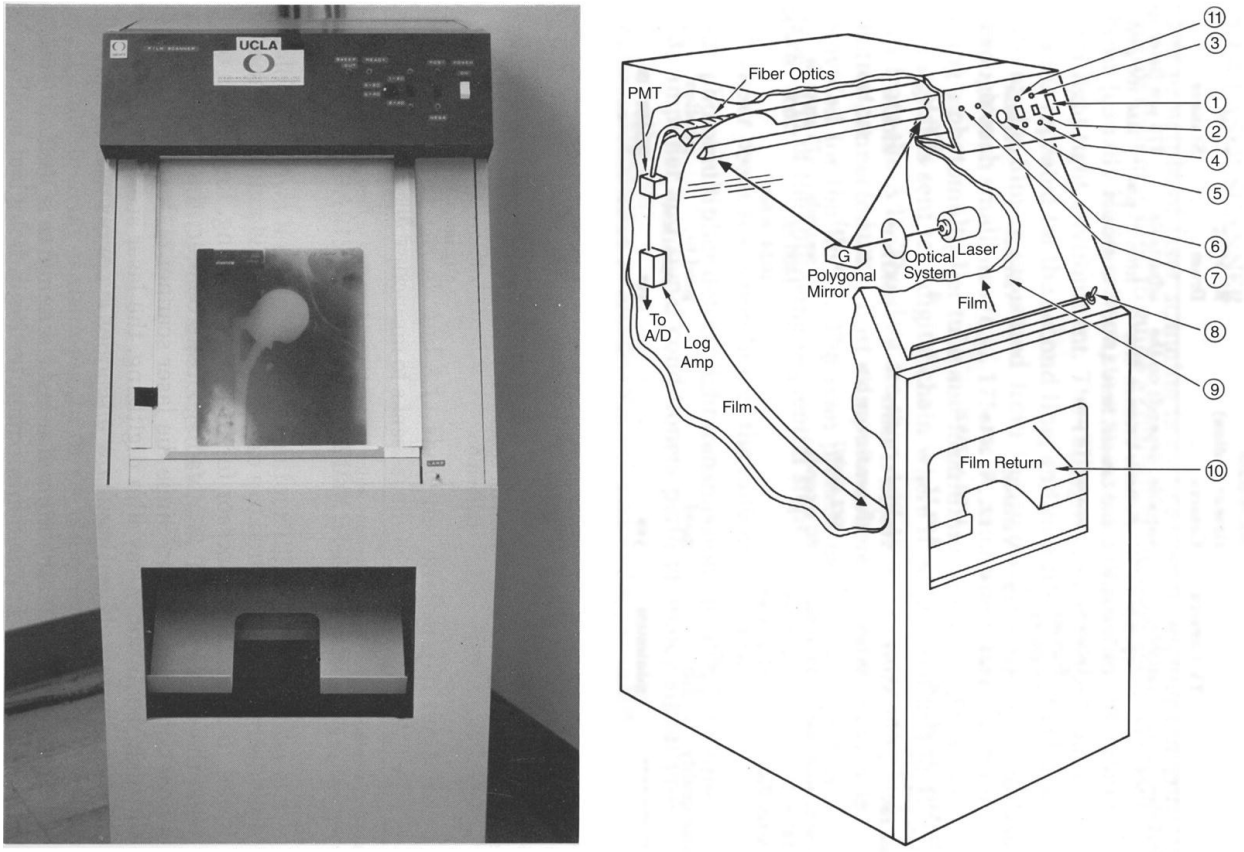

Figure 1.10 The first Konica laser film scanner at UCLA, 1984.

In late 1964, Mr Toshio Abe left Konishiroku, and formed his own company in 1967, named Abe Sekkei, Tokyo, Japan. He had developed the micro-densitometer (1969), drum scanner (1975), and imaging camera for medical applications (1977) (also compared with Professor Ledley's development of scanners discussed in Section 1.1.1). Abe had also developed one of the best laser film scanners for x-ray films and the digital radiography system dominating the Japanese laser scanner market. Since its establishment, Abe Sekkei has maintained a long-term working relationship with the UCLA PACS team.

The UCLA team also collaborated with Lumisys, Silicon Valley, CA. The scanner was used for digitizing archived x-ray films and for comparison of digitized image quality with other scanners.

1.4.2 Computed Radiography (CR)

In the late 1970s and early 1980s, Fuji Electric Corp. was developing a 2-D

computed radiography system in Japan. H. Kado, the chief engineer, was collaborating with Stanford University, Stanford, CA, on its further clinical applications [17,18]. Fuji started to sell its CR in Japan in the early 1980s as a different method of generating an x-ray image by using a laser-stimulated luminescence phosphor plate. However, its output was still printed on laser Fuji film. Dr Bill Angus, the late Senior Vice President of Philips Medical Systems (PMS) of North America, initiated the negotiations to obtain the license for Philips to sell the Fuji CR in Europe and in America under the Philips name. As a result, a similar Fuji CR system was called PMS CR on both continents. The first Fuji CR-101 installed in the United States was at the Ochsner Clinics (now Health System), New Orleans, Los Angeles (Figure 1.11). With the assistance of Dr Angus, Fuji also installed the second Fuji CR-101 system in the United States at UCLA, because Philips was not ready to deliver. Several members of the UCLA PACS team were trained at the Ochsner Clinics by Philips CR physicists. UCLA used the CR-101 in its pediatric radiology section. Later, Philips installed the PCR-901 and PCR-9000 at UCLA.

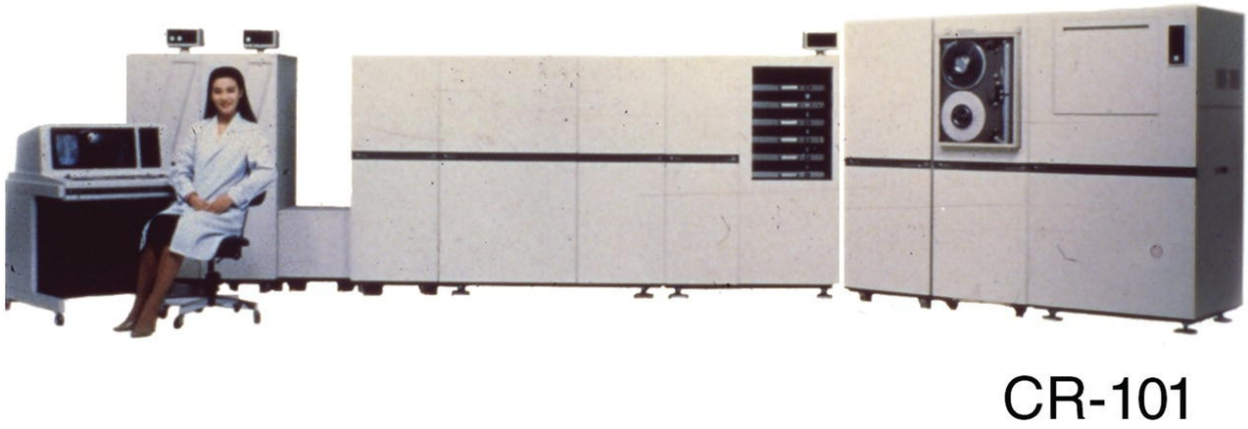

Figure 1.11 The first Fuji computed radiography (CR) system in the United States was installed at the Ochsner Clinics, New Orleans; the second system was installed at UCLA in late 1985.

1.4.3 Direct Digital Input from CR to PACS

The reason UCLA wanted to install the Fuji CR system was not because a laser-stimulated luminescence phosphor could potentially produce a better-quality image on a Fuji film. It was because UCLA contemplated the potential of obtaining a direct digital image from the output of the Fuji CR without the use of film. The advantage was immediately obvious for PACS application.

However, several negotiations with Fuji failed to allow the UCLA team to obtain

the direct digital image output from the Fuji CR, due to industry confidentiality. Several months later, through the influence of Dr Angus of PMS, UCLA developed a long-term research collaboration with PMS from which the UCLA team learned the digital data characteristic of the Fuji CR. This knowledge opened the gate for direct digital images from a CR system that might eliminate the use of a film scanner to scan future x-rays films. This success was a key turning point in shortening the development time of the PACS system. Figure 1.12A shows the black box with two ribbon cables, one connected to the Fuji CR system and the second to the PACS image acquisition computer [19], and its schematic is shown in Figure 1.12B. This project involved in-depth industry collaboration; some of its collaborative arrangements are presented in Section 1.5.5.

(A)

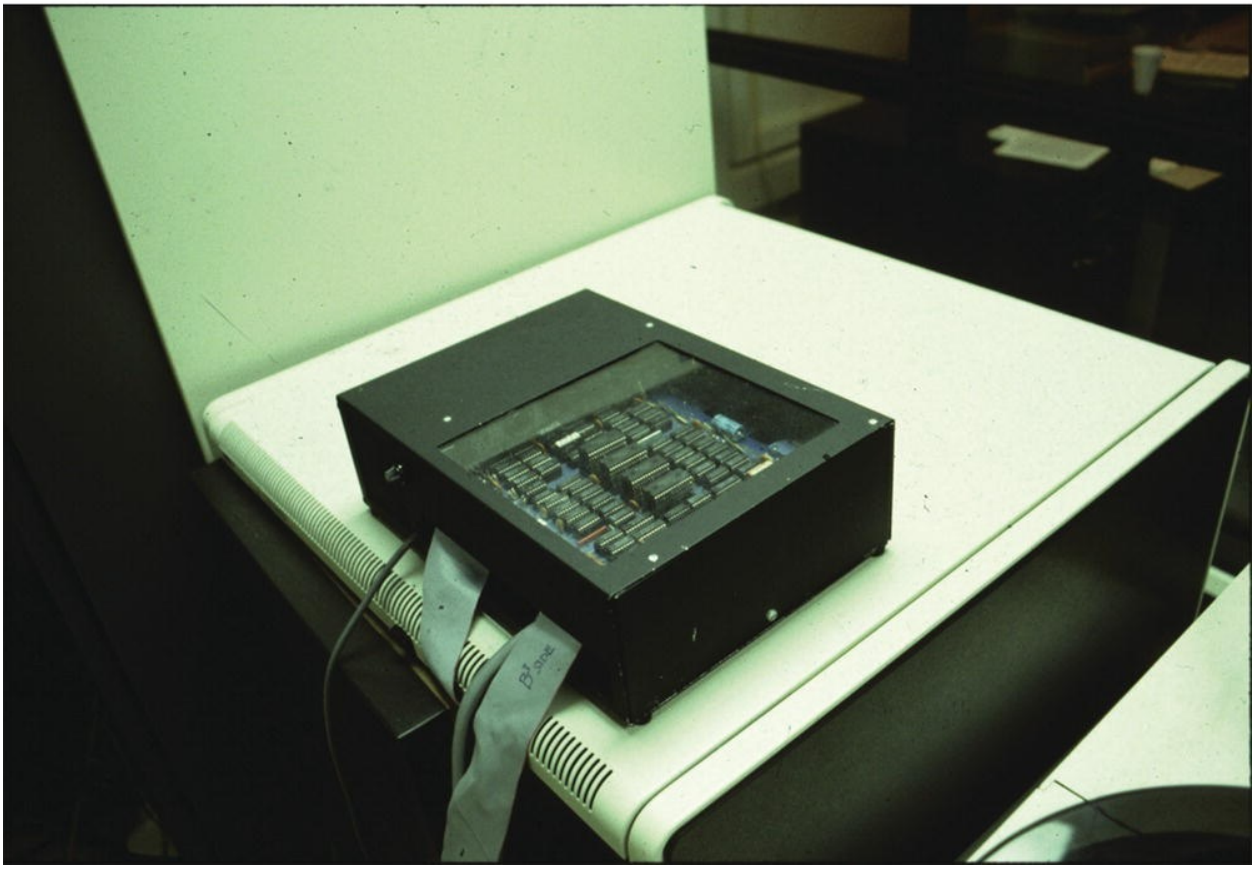

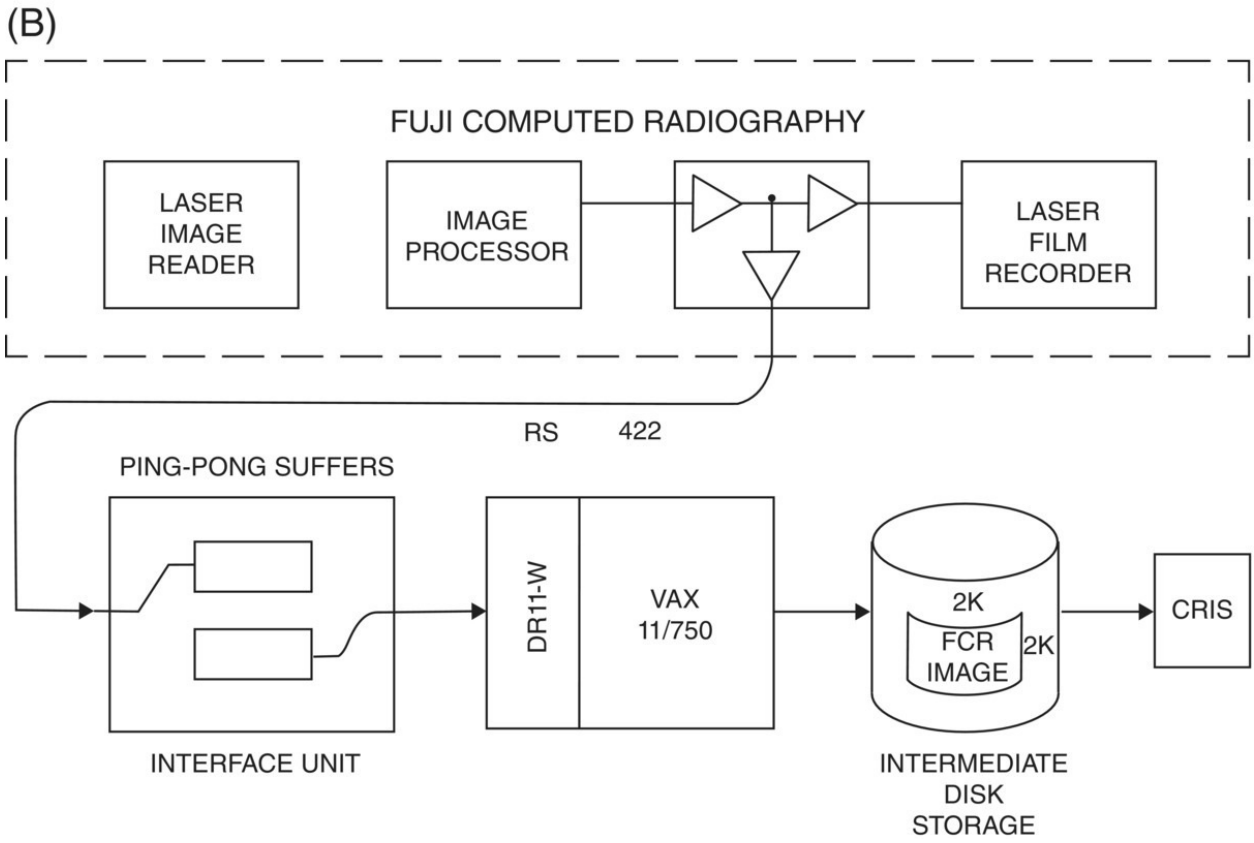

Figure 1.12 The first digital interface unit using a ping-pong buffer and the DR11-W interface technology to transmit CR images in real time to the outside of the CR reader. It was designed and implemented by the UCLA PACS team. The black box is shown in (A). The architecture module was a gateway to the PACS input system in (B). The novelty of the design at that time was the use of the ping-pong buffers to allow the continuous Fuji image data transfer to both the laser film recorder as well as the direct digital capture mechanism of the VAX 11/750 computer.

1.4.4 Digital Radiography

Konica used a laser-stimulated luminescence phosphor plate to develop a prototype digital radiography (DR) system in Japan and shipped it to UCLA for further research and development for clinical use (Figure 1.13). The difference between the Fuji CR and the Konica DR system at that time was that the early Fuji CR required four steps for obtaining a CR image. First, the unexposed laser-stimulated luminescence phosphor plate was exposed to form an x-ray image, a laser beam was used to scan the exposed plate to obtain light photons, which formed a light image, and then the CR film image was produced. The residual light energy in the plate was erased by use of a high-intensity floodlight. These

steps occurred in sequence, and hence a massive instrument was required to house the FCR-101 system, as shown in Figure 1.11. The Konica prototype DR system used the indirect image capture method with a semiconductor laser to scan the plate to collect light photons, and a PMT (photomultiplier tube) and an A/D (analog to digital conversion) coupled together to convert the light photos to form a digital image. There were three imaging plates inside the system, allowing three x-ray exposures per examination. Figure 1.13 depicts the Konica system. Several Konica engineers from Japan and a few UCLA PACS team members worked together to modify the DR system to become a prototype clinical system. Later, Konica developed a new DR system for clinical trials at UCLA.

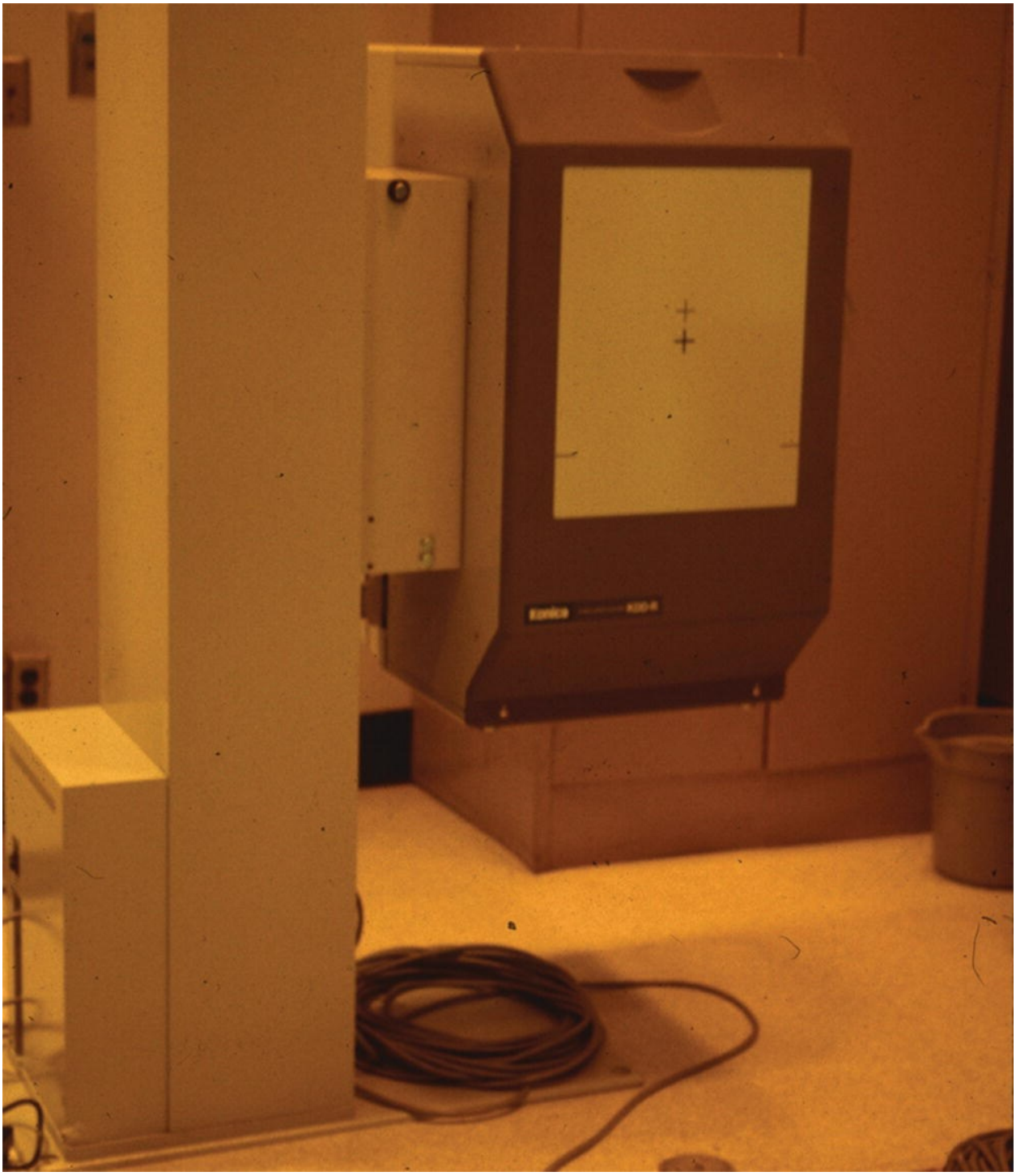

Figure 1.13 The prototype Konica digital radiography system at the UCLA PACS clinical laboratory. There were three imaging plates in the housing, allowing three consecutive exposures in one examination.

1.4.5 Interactive Display with Multiple Monitors

In order to understand the resolution requirement and the number of images needed to display for a given type of radiographic examination, the UCLA team developed workstations of various resolutions and types of display monitors. This ambitious endeavor required many workstations of different kinds. Through the generous support by many image workstation manufacturers, a workstation laboratory was established. Most of the time, the manufacturer loaned the hardware to UCLA, and their engineers worked together with the PACS team to develop the display and controller software. These workstations included two sets of six 512 × 512 monitors (the architecture of this display system was later adopted by Siemens Gammasonics, Inc., Chicago, Illinois, for their PACS system installed at the Danube Hospital, Vienna, Austria, 1990), three 1024 × 1024 monitors (supported by Gould DeAnza), one 1400-line monitor (supported by Mitsubishi, Japan), and two 2048 × 2048 monitors (supported by Megascan). Figures 1.14A,B depict the multiple viewing workstations laboratory at UCLA.

(A)

(B)

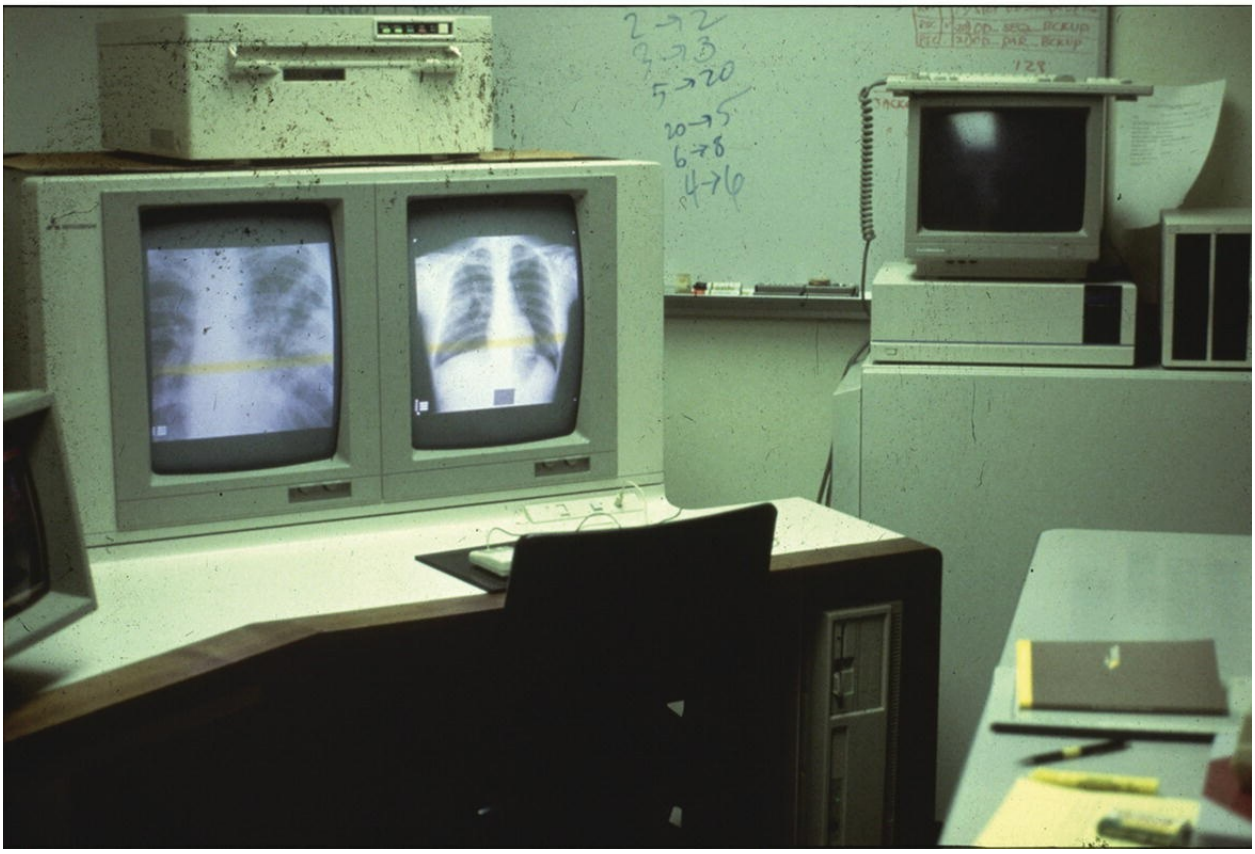

Figure 1.14 (A) The multiple viewing workstations laboratory (WS Lab) at UCLA with multiple-resolution workstations, including two six-monitor display systems (512 × 512), one 1400-line single-monitor system, and one three-monitor display system (1K × 1K). This workstation room was used for the first large-scale study on the quality of image display with different spatial and density resolutions. (B) The first two 2K line monitor display was not yet available at that time, but was later developed by a commercial company, Megascan, and installed in the WS Lab.

PART II COLLABORATIONS AND SUPPORTS

1.5 Collaboration with Government Agencies, Industry and Medical Imaging Associations

In addition to the pioneering work of medical imaging by Professor Robert Ledley, Georgetown University; Professor Moses Greenfield's development of the biomedical physics training program; Professor Hooshang Kangarloo, as both a clinician and scientist to champion PACS R&D; and the PACS team at the Department of Radiological Sciences at UCLA, the success of rapid development of key PACS technologies during the first 10 years had been due to the collaboration with government agencies, industry, and medical imaging associations. Among them were contributions from national and international government agencies, private medical imaging industry, scientific societies, colleagues from academia, and many individuals from these organizations, as described in previous sections. This retrospective chapter attempts to organize their contributions systematically.

1.5.1 The US Government Agencies

The Department of Radiological Sciences, UCLA, was fortunate to receive substantial support from the US NIH (National Institutes of Health), NSF (National Science Foundation), FAA (Federal Aviation Administration), and NCHS (National Center for Health Statistics) for PACS-related research during the first 10 years of PACS development, as follows:

1. from the National Cancer Institute (NCI), NIH: Digital Viewing Stations for Diagnostic Images (6/84–6/87, 8/87–7/92, and 8/92–95), Radiological Image Compression (7/86-6/89), Program Project Grant: PACS in Radiology (5/90-4/95), and Biomedical Physics Training (9/87–8/92 and 9/92–8/97);
2. The National Science Foundation: Parallel Computing Algorithms for 3-D Imaging (7/92–6/94);
3. The Federal Aviation Administration: Image Processing for Automated X-Ray Experimental System (12/83–12/84) and New Detection Concept (9/85–12/87); and
4. National Center for Health Statistics: Film Digitization (5/90–10/97).

Dr Matti Al-Aish, of the Radiation Research Program, NCI (National Cancer Institute), who was the Program Administrator of the UCLA Program Project Grant on behalf of the NCI, presented his impression of UCLA PACS R&D development at the NATO, ASI meeting, “Picture Archiving and Communication Systems (PACS) in Medicine”, Evian, France, October 14–26, 1990 (funded by NATO ASI. see also Section 1.5.3) [20]:

> *At the University of California in Los Angeles (UCLA) … research is in progress on many aspects of PACS in radiology…*
>
> *In conclusion, The UCLA team is striving to design and develop an accurate diagnostic imaging system with rapid throughput of patients, timely reporting and efficient retrieval of patients' radiological examinations. They are investing six years of experience in PACS research in this major undertaking. So far, they have successfully implemented two PACS prototype systems in pediatric radiology and coronary care units. These systems have been used for the past two years in the daily routine of patients' examinations. This success encourages them to plan five additional PACS modules in intensive care units, neuroradiology, urology, and chest radiology. It is heartening to say that upon completion of this project, 35% of the total examination procedure at the Department of Radiology at UCLA will be converted to PACS digital imaging systems.*
>
> *The anticipated success of this research project will usher in a new era in radiological examination, improved patient care and healthcare costs.*

1.5.2 The Netherlands National Foundation and the UCLA PACS

Professor A.R. Bakker of the University of Leiden was also the Director of BAZIS, a non-profit organization that developed and supported the integrated HIS in the Netherlands. This HIS was one of the best systems in the world in the 1980s; it was in use in 7 of 8 university hospitals and some 30 general hospitals in that country. The UCLA PACS team benefited from Professor Bakker, who shared this technology with the team and explained the importance of the integration of PACS with HIS in the future of PACS development. However, Professor Bakker cautioned about the difficulty for the Netherlands and other European countries to develop a PACS system, for two reasons: i) the initial investment was too huge a burden for a European country, and ii) in the 1980s and 1990s, no major imaging manufacturers in Europe would invest in this application [21]. He forecast that the cost of PACS could not be justified for any

Netherlands hospitals to install until the year 2000, when its cost would be equivalent to that of a film-based system. For these reasons, during the first decade of PACS development in Europe, the focus would be on research of PACS components. Professor Bakker encouraged the UCLA team to apply for travel lectureship funds from the National Science Foundation of the Netherlands as a means of exchanging information on PACS technology development during the years ahead.

Through his suggestions and assistance, the UCLA PACS team was successful in receiving two 2-week lecture grants from the Netherlands: i) Information System in National Science, “Digital Radiology in Netherlands Lectures” (10/1985); and ii) National Science Foundation of Netherlands, “Boerhaave Lectures” (10/1988), During the time of these lectures, the UCLA PACS team toured universities in the Netherlands, other research laboratories, and the Philips Medical Systems, exchanging the team’s experience in PACS system integration with the hosts’ specialties in PACS component development. In two lecture tours, the UCLA team always included several members who themselves were visitors to UCLA from different manufacturers, and/or from universities of different countries.

1.5.3 The NATO Advanced Science Institute (ASI) and the UCLA PACS

Among several major PACS international conferences during the first 10 years of PACS development, two deeply influenced the development of PACS. The first was the SPIE Medical Imaging Conference at Newport Beach, California, in 1982, where the name “PACS” was first coined. The second was the NATO ASI-sponsored PACS in medicine conference held in Evian, France, October 14–26, 1990 [22]. The ASI supported NATO countries to conduct innovative research and development projects in the form of sponsoring conferences in a NATO country. The UCLA PACS team, in coordination with Professor Osman Ratib, Digital Imaging Unit, Center of Medical Informatics, University Hospital of Geneva, Switzerland (a cardiologist by training, he also received a PhD in Medical Imaging at UCLA), applied to NATO ASI to host an international conference on PACS. During the second round of the application in 1989, the grant was awarded to the UCLA Medical Imaging Division: NATO ASI, 8/1990, PACS in Medicine. The grant was able to support travel expenses for 2 weeks for 100 participants who had made contributions to PACS-related research in the past, and no admission fee to the ASI was required. The site had to be in one of the NATO countries, and Evian, France, was chosen. More than 150 participants

joined the conference; one-third of them paying their own travel expenses. There were altogether 68 presentations and many small-group workshops. The Conference Proceedings were published in the NATO ASI series [22]. The highlights were:

1. The conference hall had only one public telephone, and there were no TVs or phones in the surrounding dormitory rooms. Each room was spacious and comfortable with private shower. Evian was famous for its excellent drinking water. This countryside accommodation environment resulted in drawing the participants close together and allowing more time for discussions in individual groups. The evening atmosphere was always friendly and candid, with frank discussions on the pros and cons of PACS in medical practice. The NATO Conference created a memorable fraternity of PACS research and development (R&D) in these early days.
2. Almost 75% of the participants had R&D experience in PACS, and 50% of them remained in this area of work 10 years after the NATO Conference. Many of them became leaders in their own area of expertise in PACS and imaging informatics, and in future PACS operation or management.
3. Many chief engineers and management personnel in PACS R&D of major medical imaging manufacturers from Japan and Korea, European countries, and the US joined the conference, but no commercial advertising was done during the meeting.
4. Many presentations summarized the PACS development in a specific country. *The Proceedings of the NATO Conference* published by Springer-Verlag (Berlin and Heidelberg, Germany) in 1991 was one of the most complete documents related to PACS development in each country at that time, with the pros and cons detailed by the presenters (Figure 1.15). As an example, Professor Walter Hruby's presentation on "The Vienna SMZO Project" hinted that his project was almost complete [23]. In April 1992, Professor Hruby opened a new and completely digital radiology department at the Danube Hospital, Vienna, showcasing his PACS system installed by Siemens Gammasonics. Many of the NATO participants were Professor Hruby's guests of honor, subsequently, during the opening ceremony of the digital radiology department of the Danube Hospital.
5. Japan led in PACS development during the first 10 years. Two main reasons might be: i) the pioneering work of Fuji's CR system and Konica's film scanner, and CR and DR systems, and ii) the PACS project was jointly

supported by the Japanese government and the manufacturers. Many Japanese researchers from the universities supported by the government teamed up with their respective supporting manufacturers, to install PACS systems in their affiliated university hospitals. At the NATO conference, they presented their PACS development and experience [22,25,26].

6. Colonel Fred Goeringer, Medical Diagnostic Imaging Support Systems for Military Medicine, and many other military officers of colonel rank, from various healthcare services in the US, also participated. The Digital Imaging Network and Picture Archiving and Communications System (DIN/PACS), RFP (request for proposal) announced in 1986 encouraged the US universities to compete for funding support [24]. After the NATO ASI conference, Goeringer immediately implemented the Army MDIS (Medical Diagnostic Imaging Support Systems) project, which resulted in several large-scale military PACS installations. The MDIS also injected a major stimulus into the PACS industry in the United States and Europe, which led to continuous large-scale PACS R&D efforts (Figure 1.15).

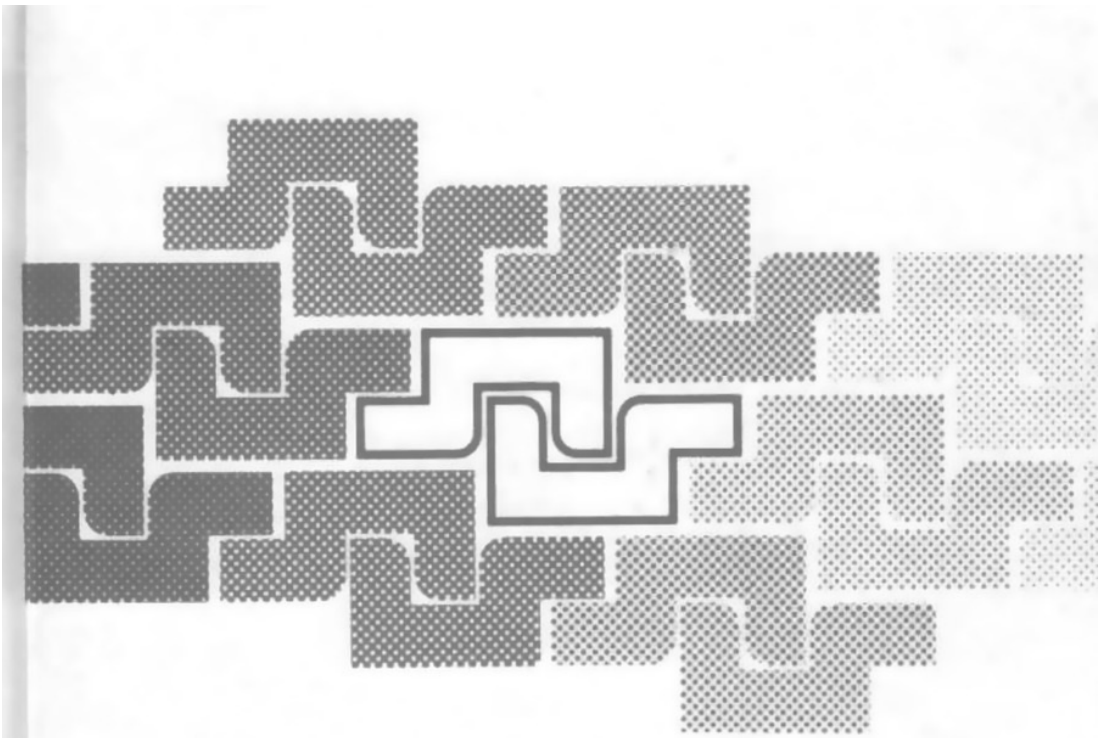

Picture Archiving and Communication Systems (PACS) in Medicine

Edited by
H. K. Huang O. Ratib A. R. Bakker G. Witte

NATO ASI Series

Series F: Computer and Systems Sciences, Vol. 74

Figure 1.15 The NATO ASI [22].

1.5.4 Collaboration of the UCLA Team with the US Medical Imaging Industry

Sections 1.3 and 1.4 presented some key PACS technologies in which the UCLA team collaborated with the US medical imaging industry. In order to appreciate the support of industries, this section summarizes their contribution to the UCLA PACS project systematically in chronological order.

1. Technicare Corporation: CT Image Input to PACS (1/84–1/89);
2. Light Signatures, Inc: Image Processing Research (1/84–1/86);
3. Gould/DeAnza Inc: Image Processing Equipment Evaluation (1/84–1/89);
4. 3M: Laser Film Printer (10/86–9/88);
5. Virtual Imaging: Image Station (5/87–1/89);
6. Polaroid Corporation: Quality Assurance of Laser Imager (7/95–12/96);
7. Pacific Bell, CalREN: ATM High Speed WAN (3/94–12/96);
8. IBM, Folder Manager and PACS Related Research, Topics (84–85 and cont., 1/93–1/95);
9. Kodak: Hierarchical Storage System (4/88–3/95);
10. Philips Medical Systems: Computed Radiography Systems and CR Equipment (7/85–12/86, 5/87–3/89, 9/89–8/92);
11. Megascan: 2K × 2K Workstation (9/87–9/90);
12. Lumisys: high-resolution laser digitizer (9/94–9/99)

1.5.5 Japan Medical Imaging Technology and the UCLA PACS

The UCLA team was in very close collaboration with both Japan academia and the medical imaging industry, including Konica (1984–1993), Mitsubishi Electronic Co. (1985–1989), Maxell Hitachi (1988–1990 and 1992–1994), and Abe Sekkei (1988–2013).

In 1984, Konishiroku (Konica) Photo Ind. Co. Ltd. delivered the first laser film scanner to the IPL, UCLA, followed by CR, then a DR system. Many research

engineers from Konica also came to work with the PACS team, not only on PACS, but also on its clinical operation at various time intervals during the first 10 years of PACS research. The upper management of Konica signed a long-term collaborative contract with the Department of Radiological Sciences at UCLA. Konica wanted their technical key employees to be inspired by some of the Western research spirit and methodology. From the 1982 to the 1990s, the following senior engineers stayed at UCLA for at least 2 years: Dr Hiroshi Takeuchi (post-doctoral fellow in medical imaging), M. Kimura, PhD (post-doctor in medical imaging), and Yoshiyuki Ishimitsu (received his PhD in medical imaging at UCLA).

After the late Dr Bill Angus, senior VP of Philips Medical Systems (PMS), North America, obtained the right for Philips to sell the Fuji FCR system in Europe and North America in 1984, he single-handedly established a working relationship between the UCLA PACS team and Fuji, Japan. Since that time, the PACS team has had a license to work with both Konica and Fuji to benefit from using both companies' CR systems for PACS application. The UCLA team, with Konica and Fuji engineers, abides by a certain set of guidelines, respecting each company's confidentiality, working together without any conflicts or problems. This arrangement led to tremendous advances in PACS development from 1982 to 1992.

During this collaboration between Konica and Fuji within UCLA, and the team's working relationship with other Japanese medical imaging manufacturers, the team often visited Japan and attended national conferences. The team was very well received by the Japanese elite PACS research groups, and they learned a tremendous amount about the Japanese PACS philosophy and methodology [25,26].

Many academic faculty members in Japan contributed to the PACS development during the 1980s, as evidenced by publications in the *Journal of the Japan Association of Medical Imaging Technology* (*JAMIT*, 1983, 1986). Among these members, three deeply influenced the thoughts of the team in developing PACS at UCLA: Morio Onoe, Professor Emeritus, University of Tokyo, in his Opening Special Lecture at the Fifth Symposium on Medical Imaging Technology in Japan, 1986, "Facets of PACS" [27]. He clearly identified four major key technological issues in PACS:

1. short-term and long-term image archive;
2. high-speed image transmission;

3. a more sophisticated image workstation; and
4. standardization.

The UCLA team closely followed his thought processes and guidance during the years of PACS development. In the USA, we have been fortunate to have Professor Steve Horii at the University of Pennsylvania (before, he was at Georgetown University), who has taken up the challenge on standardization, and has since devoted his lifetime to research and teaching to improve the DICOM (Digital Imaging and Communications in Medicine) Standard, which PACS had adopted for many years as the standard for all medical images used in PACS.

The second person was Professor Goro Irie, Radiology Department, Hokkaido University Hospital, Sapporo. The UCLA team had visited his hospital several times in the 1980s, when Professor Irie was developing the Hokkaido University Medical Information System, in which PACS was connected to the HIS and the medical record system, as shown in the bottom of Figure 1.16. He predicted that PACS needed to be connected with the HIS and MIS in order to be accepted as a fully functional digital data healthcare delivery system. Professor Irie lectured to the team on this concept, and some of the team members took his advice seriously. Professor Irie presented his concept, “Clinical Experience—16 months of HU-PACS”, during the NATO ASI [28]. Unfortunately, the UCLA team was unable to carry out such a large-scale project in the 1980s. Instead, they focused first on the PACS development, followed by connecting the PACS to the RIS (radiology information system), then to the HIS in the 1990s. True fulfillment of Professor Irie’s concept did not occur until after 1999, when some UCLA team members were relocated to other institutions, and they had designed a total integration system for the Hong Kong Hospital Authority with 43 public hospitals in the early 2000s. The design included Professor Irie’s original concept, and several years later the total integration system was gradually implemented stepwise. A later chapter in this current edition: “From PACS to Web-based ePR system with image distribution for enterprise-level filmless healthcare delivery” discusses the methodology and some of the results. In [29], Figures 1.5–1.7 describe the details with the number of online hospitals continuously being added in.

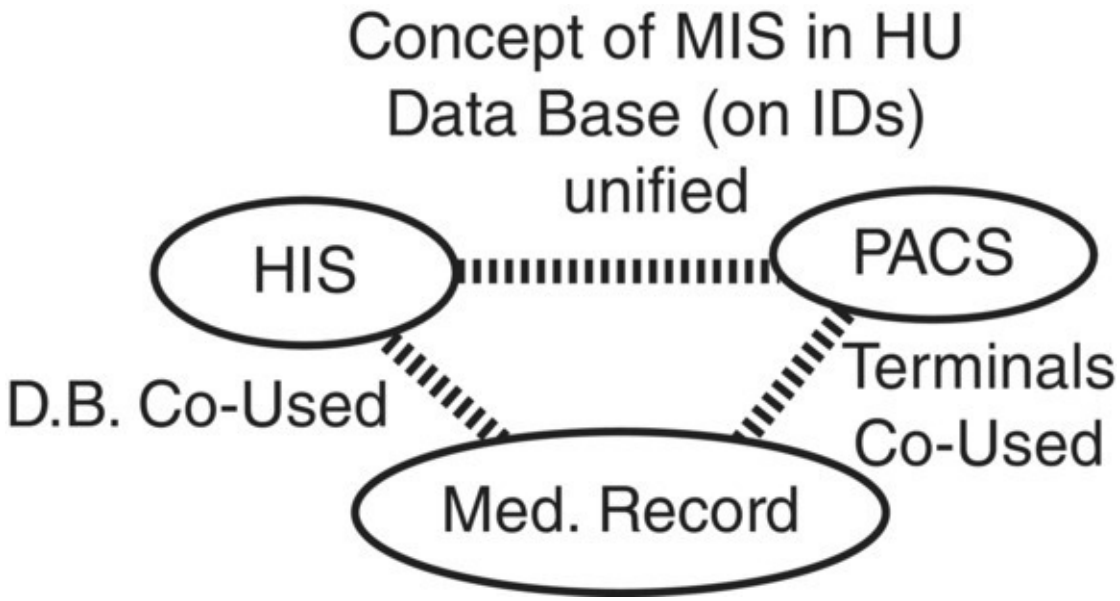

Figure 1.16 Adopted from Professor Irie's Concept of Medical Record System (MIS) in Hokkadio University Hospital [28,29].

The third person was Mr Koyo Matsuda, who worked at Konishiroku (Konica) Photo Ind. Co. Ltd., and left the company in 1984 to work at Abe Sekkei (Section 1.4.1). He established a life-long working relationship and friendship between Abe Sekkei and the UCLA PACS team members. In 1991, a new company, Array Corporation, branched out from Abe Sekkei to extend its business to include computer software. In 1998, the Array Corporation merged with Abe Sekkei, where Mr Toshio Abe and his son Satoshi have been the Chairman and the President, respectively, and Mr Matsuda remains in the merged company. Many original UCLA PACS team members, even though they might have changed careers or relocated to different positions, remain in contact with Array, either in business or friendship.

1.5.6 SPIE, EuroPACS, CARS and UCLA PACS Team

In addition to working with the Japanese medical imaging industry, the UCLA PACS team also worked very closely with three professional conferences, starting when their management established the PACS emphasis in their conferences: SPIE (the International Society for Optical Engineering), Medical Imaging Conferences and Courses (1982), The International European PACS Meeting (EuroPACS (1982), and the Computer-Assisted Radiology and Surgery (CARS) International Congress and Exhibit (1985).

1.5.6.1 SPIE

The first SPIE PACS Conference started in 1982 at Newport Beach, CA (Figure 1.17). The meeting was held there annually until the venue changed to San Diego, CA, in the early 2000s. Since then, it has alternated between San Diego, CA, and Orlando, FL, every other year since the late 2010s. In the early 1980s, when UCLA started its PACS R&D efforts, many participants of SPIE Conferences came to visit the UCLA IPL and the PACS Laboratory. In the mid-1980s, SPIE suggested to the UCLA IPL. who were organizing these visits. that it should become an annual event attached to the SPIE PACS Conference, compliments of the IPL. On a selected evening during the SPIE Conference, a tour bus would take SPIE visitors to UCLA, Westwood, for an evening with show-and-tell and visit all related laboratories, followed by a light snack and open discussion. The bus would then take them back to Newport Beach, where their conference hotels were located. Good will, friendship, and fellowship were generated during this evening event.

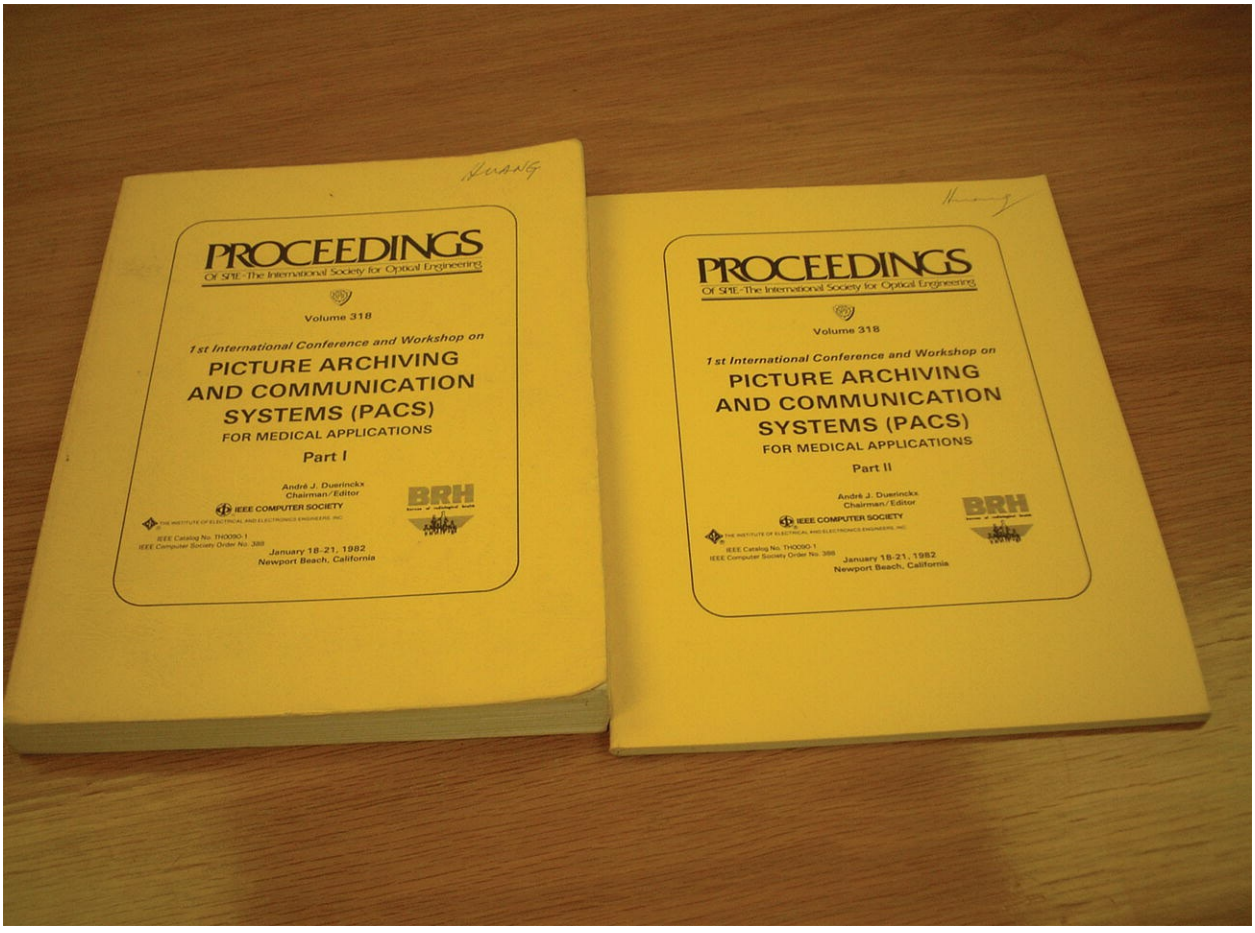

Figure 1.17 The Proceedings of the first SPIE Picture Archiving and Communication Systems (PACS) Conference at San Diego, CA, 1982.

1.5.6.2 EuroPACS

EuroPACS was launched in 1982 as the European PACS Society. Its membership was open to any individual, hospital, or university in European. The Europe PACS philosophy at that time was quite different from that in Japan or the USA, where system integration was the priority. European PACS development was mostly in modeling, simulation, or individual components during the 1980s and early 1990s. The membership of the society was limited. A different host country took turns to sponsor an annual meeting during a summer month. Because of the small membership, the meetings tended to be close-knit; as almost all members and their families met at least once a year, and everybody knew each other well. The discussion was very open, and each country learned what other countries were planning and executing to help each other to progress. Researchers from outside Europe could join as guest members or could be elected as Honorary Members of the EuroPACS Board. The UCLA PACS team began its association with the EuroPACS in 1982, and some members were elected as Honorary Board Members. It was very important for the UCLA PACS members to join the EuroPACS, because they learned much about the philosophy of the EuroPACS and their emphasis and progress. EuroPACS merged in the late 1990s to the early 2000s with CARS and became one of the International Congress and Exhibit members. As of today, many original EuroPACS members still retain a good relationship with the original UCLA PACS team members.

Since PACS now included medical imaging informatics, EuroPACS amended its original name to the European Society of Medical Imaging Informatics (EuSoMII) in 2014.

1.5.6.3 CARS

CARS was established in 1985. Its original name was CAR (computed-assisted radiology); later, the specialty surgery joined the CAR to become CARS. The CARS headquarters is near the Black Forest, Germany, and the Congress met every year, one year always being in Germany (Berlin or other cities), and the other year in a different country, including Japan and the USA. CARS had an annual attendance of about 1000, including the host country’s participants. The CARS Congress includes other conferences: International Society for Computer-Aided Surgery, EuroPACS Meeting, Workshop on Computer-Aided Diagnosis (CAD), and the Computed Maxillofacial Imaging Congress. The UCLA PACS team joined the Program Committee of CARS in 1985, when it was established, and has since contributed substantially to its activities including scientific

presentations, workshop and tutorial presentations, session chairmen, and as the CARS Congress Annual President. CARS allowed the team members to gain more in-depth knowledge of PACS, and also to learn other image-assisted specialties that are necessary for imaging informatics research and development.

1.5.7 Patents and Copyrights

Since 1982, The UCLA PACS team has collaborated with many US and other countries' academic institutions, professional societies, and manufacturers. Many of these collaborations were tightly coupled with the PACS development. Thus, sometimes it was difficult to distinguish which partners should own particular intellectual properties, copyrights, and/or patents. The team had waived its right to apply for any copyrights and/or patents related to PACS project research and development in the 1980s; and their partners had a free hand to pursue their own applications. The first of two examples was interfacing the Fuji CR to the outside world; it was a novel development (see the black box in Figure 1.12 with its caption). Several years later, Fuji used a similar concept to develop its own interface. The second example was the six-monitor display workstation used by Siemens Gammasonics in Professor Hruby's SMZO PACS project, in 1992, as described in Section 1.5.3. The original design of the workstation was by the UCLA team in 1987, as shown in Figure 1.14a with its caption, in the UCLA Workstation Laboratory.

The only exception where the UCLA PACS team applied for a patent, was the US Patent No. 5410676, April 25, 1995. Some UCLA team members received the patent award with collaborators from Maxell Hitachi, the topic of which was not related to PACS, as it was a computer software data storage algorithm [13].

1.6 Medical Imaging Informatics

1.6.1 Biomedical Informatics

Biomedical informatics is loosely categorized into four levels of study: bioinformatics (molecular level), imaging informatics (cellular, tissue, and organ system level), clinical informatics (personal healthcare level), and public health informatics (population level) [30]. Some rudimentary biomedical informatics research and development started as early as the 1990s. However, because medical imaging informatics research requires large-scale medical image/data from PACS (not available until in the late 1980s and the 1990s), enterprise PACS, and integration of PACS with HIS and RIS (not available until in the late

1990s and early 2000s), systematic medical imaging informatics research did not start until the middle of the 2000s (see Chapter 22). The only exception was the automatic chromosome karyotyping imaging informatics system developed by Professor Robert Ledley in the 1970s. He was able to develop such an imaging informatics system for research, because he did not use radiologic images as input data. Instead, in order to acquire a large number of digital images, Ledley used the microscope analog light images from glass slides, and his SPIDAC system, to covert the analog images to digital images.

1.6.2 The 1970s Concept: Chromosome Karyotyping

In the early 1970s, Professors Ledley and Huang developed the SPIDAC in his Pattern Recognition Laboratory (PRL, see Section 1.1.1), and applied it to automatic chromosome karyotyping and analysis. This endeavor could probably be considered as the first systematic medical imaging informatics application. Chromosome karyotypes describe the number, shapes, bands, and contents of chromosomes in a metaphase cell, and how they look under a light microscope. In human genetics, chromosome karyotyping is used to determine whether the chromosomes in the metaphase cell of the mother are normal or abnormal. The results can lead to prenatal diagnosis of birth defects.

A systematic medical imaging informatics platform generally includes two major components: i) the PACS for images and data acquisition, archive, communications, display, and management; and ii) the new knowledge discovery from the PACS data.

In Professor Ledley's PRL, integration of SPIDAC with the VIDAC (video memory) + MACDAC (man–machine interface to digital automatic computer) + IBM360/44 computer could scan a microscope glass slide (Figure 1.18, left), select (Figure 1.18, upper middle), and detect two metaphase cells at low resolution and chromosomes at high resolution), acquire (upper right), display (lower left), and manage metaphase cells data. These functions in the 1970s were almost equivalent to the basic components of an early Pathology PACS in the 2000s (including all the steps shown in Figure 1.18). The medical imaging the informatics component included image processing to analyze and karyotype all possible chromosomes (Figure 1.18, lower right) from each cell in the glass slide, and intelligent components within the cell to determine whether the it was normal, based on information from its chromosome karyotyping, which is the new knowledge discovery component extracted from the image informatics data.

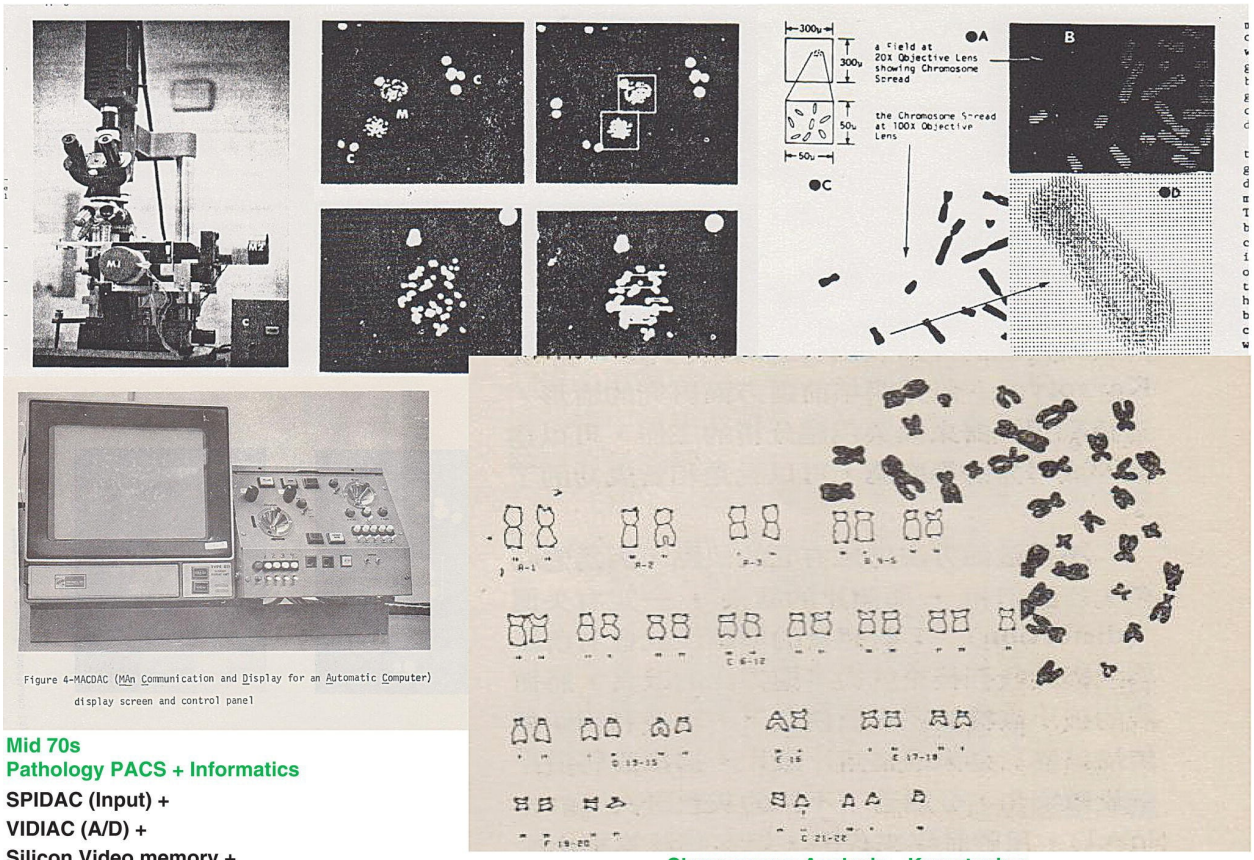

Figure 1.18 Automatic chromosome karyotyping innovation by Professor Ledley in the 1970s, probably the earliest concept in systematic medical imaging informatics. Process steps included medical image acquisition, metaphase cell determination, patient data, interactive display, automatic measurement of chromosomes and karyotyping, the determination of normal vs. abnormal chromosomes, that led to the final diagnosis. PACS components included MACDAC (man–machine interface to digital automatic computer). SPIDAC + VIDAC (video memory) + MACDAC (interface) + IBM360/44 were equivalent of today's Pathology PACS. The new knowledge discovery component showed an example of automatic chromosome analysis—microscopic scanning, detecting two metaphase cells (low resolution), and chromosomes (high), analyzing each chromosome, and karyotyping that could lead to the prenatal diagnosis of birth defects.

1.6.3 Medical Imaging Informatics Today

Figure 1.19 shows three examples of today's medical imaging informatics system components platform that can provide different types of specific clinical

applications:

1. image-assisted neurosurgery;
2. neuro-rehabilitation engineering, and
3. radiation therapy for prostate cancer [30].

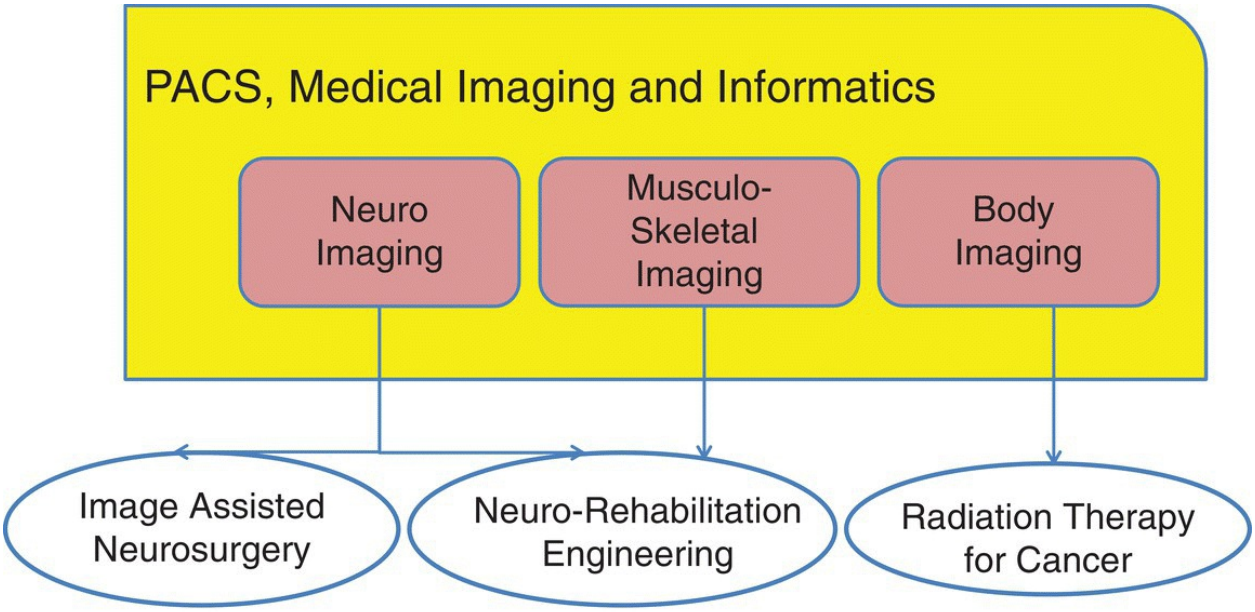

Figure 1.19 Some examples of today's (2020s) medical imaging informatics applications of three types of patient treatment—surgery, rehabilitation, and radiation therapy. Upper row use of the medical images from various body parts for three different applications. Lower row for image assisted neurosurgery, neuro-rehabilitation, and radiation therapy for cancer treatment.

In these examples, the upper three smaller rectangles in the figure represent the PACS imaging components, whereas the lower three rectangles depict the medical imaging informatics components, including image detection and processing, as well as the new knowledge discovery from the PACS imaging data. These examples are to be described in the following chapters in this current edition.

1.7 Summary

The possibility of PACS development during the first 10 years, in the 1980s and 1990s, was ignited by three pioneers' innovations and dedication. In this

retrospective review, we started by introducing the background of three pioneers and explaining their influence on the success of PACS research and developmental efforts, followed by the opportunity of UCLA receiving research support from US federal government agencies. The UCLA PACS team also established a close collaboration with many medical imaging partners in private industry. The time was ripe for the UCLA PACS team to attempt the implementation of PACS components in a clinical system for daily healthcare use.

The influence of three pioneers:

1. Professor Robert Ledley established his Pattern Recognition Laboratory, invented various types of medical imaging scanners, introduced the concept of medical imaging informatics application, and led a group of “can-do followers” in the 1960s and 1970s.
2. Professor Moses Greenfield formed and ran the Biomedical Physics Graduate Program, UCLA, for more than 40 years, where he trained more than 200 graduate students, many of whom selected PACS and imaging informatics as their career path.
3. Dr Hooshang Kangarloo, Professor of Pediatrics, Radiology and Bioengineering, Chairman of Radiological Sciences at UCLA, championed PACS as representing the future of radiology and the future of digital practice in healthcare delivery. He dared to convert his Pediatric Radiology Division from a film to a PACS operation; his division became the first clinical site for clinical service with PACS.

1.7.1 The Golden Era of Medical Imaging Technology Research Support

The 1980s and 1990s were the golden era of receiving support from US government agencies for innovative research and training, especially related to medical high technology development. The funding opportunity was even better if a university could set up a matching program, in the sense that the university would match a certain percentage of the federal amounts. The Department of Radiological Science at UCLA was a well-established and wealthy department in the 1980s and 1990s. With Professor Kangarloo as the chairman, who championed the development of PACS, it would not be too difficult for him to convince the department’s financial committee to accept the PACS concept and agree to support the developmental effort. Once the federal government funded

the UCLA PACS R&D program with the additional departmental support, the US and Japanese medical imaging industry contemplated the opportunity of future collaboration with UCLA, and also contributed to the program. Another major factor in the success of the PACS implementation at UCLA was Professor Greenfield's Biomedical Physics Graduate Program, which recruited many young talents who had physics, engineering, or other physical science majors, and a biomedical science minor. They could either enroll in the graduate program to obtain a PhD degree or join the post-doctoral program to expand their horizon to become faculty members, either at UCLA or at other US and foreign universities, or they returned to their motherlands to seek golden opportunities. The R&D and training resources in the Department of Radiological Sciences were able to support the Graduate Program without much difficulty.

The time was ripe for the implementation of PACS components in a system for daily clinical use. The reasons were as follows: first, the R&D personnel of PACS developers were ready for its implementation. At that time, primary users of PACS were radiology faculty and residents at UCLA. They had been convinced by the PACS champion, Dr Kangarloo, and were eager to try it out. In addition, they had taken the mandatory 2-week PACS training class in the Biomedical Physics Graduate Program. The result was that several PACS modules were clinically online in the late 1980s, and the radiology users were convinced and had not looked back to read a case based on x-ray films for making the radiologic diagnosis.

1.7.2 After the First 10 Years of PACS

After several PACS modules were online for daily clinical use at UCLA, the question was, "Now what?" During the first wave when PACS started in the 1980s, much R&D work was contributed by the UCLA PACS team and its collaborators. With sufficient resources for PACS R&D and with excellent personnel, the time was ripe for the team to expand the PACS capacity to include PACS for multiple-hospital enterprises, PACS integration with HIS and RIS, PACS with the Web server for image distribution, and integration of PACS with the patient record system [30]. However, as the scope of PACS increased, the UCLA PACS team could not handle such multifaceted interests, demands, and requirements. Many of them were too technically mature to be confined to a group project like the PACS, original designed at UCLA. It was time for the team to move on or to let private industry take over the continuation of development. Individuals started to pursue their own interests and domain, and

they also sought other career ventures. Other experts from outside UCLA had different talents and were most definitely qualified to take on some aforementioned PACS applications to flourish.

1.7.3 The PACS End Users

As for the end users of PACS, radiologists and radiology personnel, what was their perspective? Before the high technology scanners became available, and the 1980s and 1990s PACS development era, radiology had been a self-sufficient, low-key, but vital clinical service department, supporting physicians by performing radiological procedures and making diagnoses from x-ray-related examinations. With the advent of US, nuclear medicine, CT, and then MRI developed by the radiological science specialists, and the successful and convenience use of these scanners and PACS for medical diagnoses and clinical service, the prestige of the radiology profession was elevated among healthcare colleagues. Those radiologists who led the development of these scanners and PACS had become leaders in their profession, and the majority of these leaders agreed that PACS technology, if refined and further polished, could one day be another new valuable clinical tool for radiology to contribute to healthcare delivery.

When PACS was first introduced as a clinical tool, because of its cost, and lack of good methods in training the users, human inertia of avoiding teaching the newcomers new techniques, and individual xenophobia, PACS was not well accepted by general radiologists. In addition, PACS still presented many operational handicaps, including image quality on soft copy, archive capacity, image transmission speed, and data security. But leaders in the radiology community felt that the “time was ripe for the pus” to support PACS development. At every annual RSNA (Radiology Society of North America) Assembly since the 1990s, they promoted PACS diligently and formed many subcommittees to resolve the aforementioned shortcomings. Examples of the contributions were in the training of their fellows, residents, and participants in the RSNA assembly in the technology and usage of PACS, setting up the DICOM Standard and the IHE (Integrating of Healthcare Enterprise) Workflow Profiles, defining long-term and short-term archives, requiring HIPAA compliance (Health Insurance Portability and Accountability Act) to include data definition and privacy, security, and integrity, system fault tolerance, and continuous availability. Because of competition, the vendors lowered the cost of the PACS system. The radiology leaders, as a group, contemplated that the time was ripe for their attempt to contribute substantially to the continuing

development of PACS.

1.7.4 The Diligent Contributors

The PACS banner has been carried successfully by many other experts with different skills and backgrounds that led to today's benchmarks for PACS as the daily healthcare baseline tool for data and image distribution to every clinical service in hospitals and by medical practitioners. They are the diligent contributors to PACS. With them, adding on with multimedia medical imaging informatics promises to be the next wave to be recognized and nurtured to success in the near future.

1.8 Acknowledgments

When my former two mentors, Professor Ledley at Georgetown University, and Professor Greenfield at UCLA, as well as my good friend and colleague Emeritus Chairman and Professor Kangarloo at UCLA passed away in the same year, 2012, in memory of these pioneers I delivered a special lecture: "In memory of Three Pioneers in Biomedical Imaging, Medical Physics, and PACS and Informatics" [31], during the 2013 SPIE Annual Medical Imaging Conference—Advanced PACS-based imaging informatics and therapeutic applications, at Lake Buena Vista, Florida, USA. To my surprise, although it was the last afternoon session of the conference, many colleagues with whom we had been working during the past 40 years showed up. After the meeting, some of them suggested that I should write a paper to publicize the past contributions of the pioneers in these fields. Dr Kunio Doi, Professor of Radiology, University of Chicago, and the Editor-in-Chief of *Radiological Physics and Technology* was kind enough to suggest, comment, and edit my presentation and published the paper [32], (Chapter 1 of the current edition) by Springer in 2014. This chapter is dedicated to the late Professors Ledley, Greenfield, and Kangarloo.

References

Most references cited in this chapter were published between the 1960s and 1990s, which reflects the medical imaging and PACS innovations during that era.

1 Huang, H.K. (2011) Short history of PACS Part I: USA. *Euro J Radiol*, 78, 163–176.

2 Lemke, H.U. (2011) Short history of PACS Part II: Europe. *Euro J Radiol*, 78, 177–183.

3 Inamura, K. and Jong, H.K. (2011) History of PACS in Asia: Part III. *Euro J Radiol*, 78, 184–189.

4 Ledley, R.S. and Lusted, L.B. (1950) Reasoning foundations of medical diagnosis. *Science*, 130, 9–21.

5 Ledley, R.S. (1964) High-speed automatic analysis of biomedical pictures. *Science*, 146(3641), 216–223.

6 Ledley, R.S. (1965*) Use of Computers in Biology and Medicine*. New York: McGraw-Hill.

7 Hounsfield, R.N. (1973) Computerized transverse axial scanning (tomography). Part 1: Description of system. *Br J Radiol*, 46, 1016–1022.

8 Ledley, R.S., Huang, H.K. and Mazziotta, J.C. (1977) *Cross-sectional Anatomyan Atlas for Computerized Tomography*. Baltimore, MD: Williams & Wilkins.

9 Huang, H.K. (2003a) Editorial: Some historical remarks on picture and communication systems. *Comp Med Imaging Graph*, 27(I2–3), 93–99.

10 Huang, H.K., Andriole, K., Bazzill, T., Lou, A.S.L. and Wong, A.W.K. (1996) Design and implementation of PACS—the second time. *J Digital Imag*, 9(2), 47–59.

11 Huang, H.K., Wong, A.W.K., Lou, S.L., Bazzill, T.M., *et al*. (1996) Clinical experience with a second generation PACS. *J Digital Imag*, 9(4), 151–166.

12 Huang, H.K. (1999) *Picture Archiving and Communication Systems: Principles and Applications*. New York: Wiley and Sons; p. 521.

13 Huang, H.K., Morioka, C., Osman, R., Cho, P.N.S., Ho, B.K.T., *et al*. (1995) Information system using designating areas for retrieving/converting data and directories of different formats storing in optical and magnetic storage. US Patent No. 5,410,676. April 25, 1995.

14 Lo, S.C. and Huang, H.K. (1976) Compression of radiological images with 512, 1,024, and 2,048 matrices. *Radiology*, 161, 519–525.

15 Wang, J. and Huang, H.K. (1996) Medical image compression by using 3-D wavelet transformation. *IEEE Trans Med Imag*, 15(4), 547–554.

16 Huang. H.K., Arenson, R.L., Dillon, W.P., Lou, A.S.L, Bazzill, T. and Wong, A.W.K. (1995) Asynchronous transfer mode (ATM) technology for radiologic communication. *Am. J. Roentgenol*, 164, 1533–1536.

17 Sonoda. M., Takano. M., Miyahara. J. and Kato. H. (1983) Computed radiography utilizing scanning laser stimulated luminescence. *Radiology*, 148, 833–838.

18 Kado, H. (1986) Storage and display system of computed radiographic images. *Medical Imag Technol*, 4(2)4, 20(4), 280, July.

19 Ho, B.K.T., Morioka, C., Kaabi, L., Taira, R.K., Hayrapetian, A. and Huang, H.K. (1991) Acquisition interface for computed radiography. In: Huang, H.K., Ratib, R., Bakker, A.R., Witte, G. and Chuang, K.S. (eds). *Picture Archiving and Communication System (PACS)*. NATO ASI F Series 74. Berlin, Heidelberg: Springer, pp. 23–33.

20 Al-Aish. M. (1991) NIH supported PACS related research. In: Huang, H.K., Ratib, R., Bakker, A.R., Witte, G. and Chuang, K.S. (eds) *Picture Archiving and Communication System (PACS)*. NATO ASI F Series 74. Berlin, Heidelberg: Springer, pp. 201–206.

21 Bakker, A.R. (1991) PACS and related research in the Netherlands. In: Huang, H.K., Ratib, R., Bakker, A.R., Witte, G. and Chuang, K.S. (eds) *Picture Archiving and Communication System (PACS)*. NATO ASI F Series 74. Berlin, Heidelberg: Springer, pp. 295–299.

22 Huang, H.K., Ratib, O., Bakker, A.R., Witte, G. and Chuang, K.S. (eds) (1991) *Picture Archiving and Communication System (PACS)*. NATO ASI F Series. Berlin, Heidelberg: Springer.

23 Mosser, H., Mandl, A., Urban, M., Hradil, H. and Hruby, W. (1991) The Vienna SMZO Project. In: Huang, H.K., Ratib, O., Bakker, A.R., Witte, G. and Chuang, K.S. (eds). *Picture Archiving and Communication System (PACS)*. NATO ASI Series F, vol. 74. Berlin, Heidelberg: Springer; pp. 247–250.

24 MITRE/ARMY (1986) RFP B52-15645 for University Medical Center Installation Sites for Digital Imaging Network and Picture Archiving and Communication System (DIN/PACS), October 18, 1986.

25 The First International Symposium on PACS and PHD (1983) In: *Proc. Medical Imaging Technology*, vol. 1.

26 The Third International Symposium on PACS and PHD (1986) *Medical Imaging Technology, JAMIT*, 4(2), July.

27 Onoe, M. (1986) Facets of PACS, the Third International Symposium on PACS and PHD. *Medical Imaging Technology, JAMIT*, 4(2), 101.

28 Goro, I. (1991) Clinical experience. 16 Months of HU-PACS. In: Huang, H.K., Ratib, O., Bakker, A.R., Witte, G. and Chuang, K.S. (eds) *Picture Archiving and Communication System (PACS)*. NATO ASI F Series 74. Berlin, Heidelberg: Springer, pp. 183–188.

29 Huang, H.K. (2011) From PACS to Web-based ePR with image distribution for enterprise-level filmless healthcare delivery. *Rad Phys Technol*, 4(2), 91–108.

30 Huang, H.K. (2010) *PACS and Imaging Informatics: Principles and applications*, 2nd ed. Hoboken, NJ: Wiley Blackwell.

31 Huang, H.K. (2013) In memory of three pioneers—Ledley (Biomedical Imaging), Greenfield (Medical Physics) and Kangarloo (PACS and Informatics). In: *Proceedings of Advanced PACS-Based Imaging Informatics and Therapeutic Applications*, 14(41), 86740S1–6.

32 Huang, H.K, (2014) Medical imaging, PACS, and imaging informatics: Retrospective. *Radiol Phys Technol*, published online: December 6, 2013, 7, 5–24.

Part 2
Medical Imaging, Industrial Guidelines, Standards, and Compliance

2
Digital Medical Imaging

CHAPTER MENU

2.1 Digital Medical Imaging Fundamentals
2.1.1 Digital Image
2.1.2 Digital Medical Image
2.1.3 Image Size
2.1.4 Image Display
2.1.5 Density Resolution, Spatial Resolution, and Signal-To-Noise Ratio
2.1.6 Radiology Workflow
2.2 Two-Dimensional Medical Imaging
2.2.1 Conventional Direct Digital 2-D Projection Radiography
2.2.2 Examples of the CR (Computed Radiography) Systems
2.2.3 Full–Field Direct Digital Mammography
2.2.4 Nuclear Medicine Imaging
2.2.5 Two-Dimensional (2-D) Ultrasound Imaging (US)
2.2.6 Two-Dimensional (2-D) Light and Endoscopic Imaging
2.3 Three-Dimensional Medical Imaging
2.3.1 Two-Dimensional Transmission X-Ray Computed Tomography (CT) from 1-D Projections
2.3.2 Transmission X-Ray Computed Tomography (3D-CT)
2.3.3 Emission Computed Tomography (ECT)
2.3.4 Three-dimensional Ultrasound Imaging (3-D US)
2.3.5 Magnetic Resonance Imaging (MRI)
2.3.6 3-D Fluorescence Confocal Microscopy: Light Imaging
2.3.7 3-D Micro Imaging and Small Animal Imaging
2.4 Four-Dimensional, Multimodality, and Fusion Imaging

2.4.1 Basics of 4-D, Multimodality, and Fusion Medical Imaging
2.4.2 4-D Medical Imaging
2.5 Image Compression
2.5.1 Some Terminology
2.5.2 Acceptable Compression Ratio
2.5.3 The Wavelet Transform Method
Further Reading

2.1 Digital Medical Imaging Fundamentals

2.1.1 Digital Image

A digital image is a two-dimensional (2-D) array of non-negative integer function, f(x,y), where $1 \le x \le M$ and $1 \le y \le N$, and M and N are positive integers representing a small square in the image represented by the coordinates (x,y), which is called a picture element, or a pixel, and f(x,y) is its corresponding pixel value. If M = N, then f becomes a square image; most sectional images in a three-dimensional (3-D) image volume used in medicine are square images. If the digital image f(x,y,z) is 3-D, then the picture element is called a voxel. As f(x,y,z) is collected through time t, the collection becomes a four-dimensional (4-D) image set, where the fourth dimension is t. Throughout this book, the symbols f and p are interchangeably; f is used when mathematics is presented, and p is used when a picture or image is being emphasized.

2.1.2 Digital Medical Image

The aforementioned terms are collectively called digitized or digital medical images: digitized if the image is obtained through a digitizer, or digital if it is generated digitally. The pixel (voxel) value (or gray level value, or gray level) can range from 0 to 255 (8-bit), 0 to 511 (9-bit), 0 to 1023 (10-bit), 0 to 2045 (11-bit), and 0 to 4095 (12-bit), depending on the digitization procedure or the medical image generation procedure used. These gray levels represent physical, chemical, and physiological properties of the state of anatomical structures or physiological processes when the image was captured. For example, in an image obtained by digitizing an x-ray film, the gray level value of a pixel represents the optical density of the small square area of the film. In the case of x-ray computed

tomography (XCT), the pixel value represents the relative linear attenuation coefficient of the tissue; in magnetic resonance imaging (MRI), it corresponds to the magnetic resonance signal response of the tissue; in ultrasound imaging, it is the echo signal of the ultrasound beam when it penetrates the tissues; and in an endoscopic image, the pixel values represent the light signals from the camera.

2.1.3 Image Size

A 2-D projection image is the ordered pair (M,N) signals, and the size of the image is the product M × N bits where 2^k represents the gray level range. In sectional images of a 3-D volume, most of the time M = N. The exact dimensions of a digital image sometimes are difficult to specify because of the design constraints imposed on the detector system for various examination procedures. Therefore, for convenience, a 512 × 512 image is called a 512 image, a 1024 × 1024 image a 1 K image, and a 2048 × 2048 image a 2 K image, even though the image itself may not be exactly 512, 1024, or 2048 square. Also, in computers, 12 bits is an odd number for the computer memory and storage device to handle. For this reason, 16 bits or 2 bytes are normally allocated to store a 12 bit data of the pixel. Table 2.1 lists the general sizes of some conventional 2-D, 3-D, and 4-D medical images.

Table 2.1 Sizes of some common 2-D, 3-D, and 4-D and fusion medical images.

2-D Modality	One Image (bits)	No. Images/Examination	One Examination (MB)
Nuclear Medicine (NM)	128 × 128 × 12	30–60	1–2
Digital Subtraction Angiography (DSA)	512 × 512 × 8	30–40	8–10
Digitized Film	2048 × 2048 × 12–1780 × 2160 × 12	1	8
Computed/Digital Radiography	2048 × 2048 × 12-3520 × 4280 × 10	1	8–28
Digital Mammography	2560 × 3328 × 12–4000 ×	4	68–160

	5000 × 12		
Digital Color Microscopy	512 × 512 × 24	1 up	0.8 up
Digital Color Endoscopy	512 × 512 × 24	1 up & movie loop	0.8 up & movie loop
3-D Modality			
Positron Emission CT (PET)—Whole Body	168 × 168 × 16–	500	28
Body Regions	256 × 256 × 16	20 up	2.5 up
Magnetic Resonance Imaging (MRI)	256 × 256 × 12–320 × 320 × 12	Multiple sequences 100–1000	60 up
Head: 3 Sequences—Proton, T1 and T2			
Single Photon Computed Tomography (SPECT)	512 × 512 × 12	Head: 10 up	5 up
Computed Tomography (CT)	512 × 512 × 12	Head: 10 up	5 up
Multislide CT (256 Slides)/Rotation		Body: 40 – 1000	Up to 500 or more
		256/rotation	134
Ultrasound (US)	512 × 512 × 8	30 f/s video	8
Ultrasound True Color	480 × 640 × 24	30 f/s video	28
Ultrasound Pseudo-Color	716 × 537 × 8	30 f/s video	12
4-D Modality Fusion			3-D × time
			2 × images/modality

2.1.4 Image Display

A digital image can be printed on film or paper as a hard copy, or it can be displayed on a cathode ray tube (CRT) video monitor or a liquid crystal display

(LCD) as a soft copy. The soft-copy display is volatile, since the image disappears once the display device is turned off. To display a soft-copy digital medical image, the pixel values are first converted to analog signals, called digital-to-analog (D/A) conversion, similar to conventional video signals used in the television industry. Current software display devices can display up to a 2 K image on one screen. To date, no commercially available display system can handle a 4 K image. In order to display a 4 K image, such as a 4 K digital mammogram, subsample or split-screen methods are used. Figure 2.1A shows a perspective of image size compared with number of pixels in a 128, 256, 512, 1024, 2048, and 4096 image. Figures 2.1B, C and D, respectively, also depict the concept of 3-D and 4-D images, and image fusion.

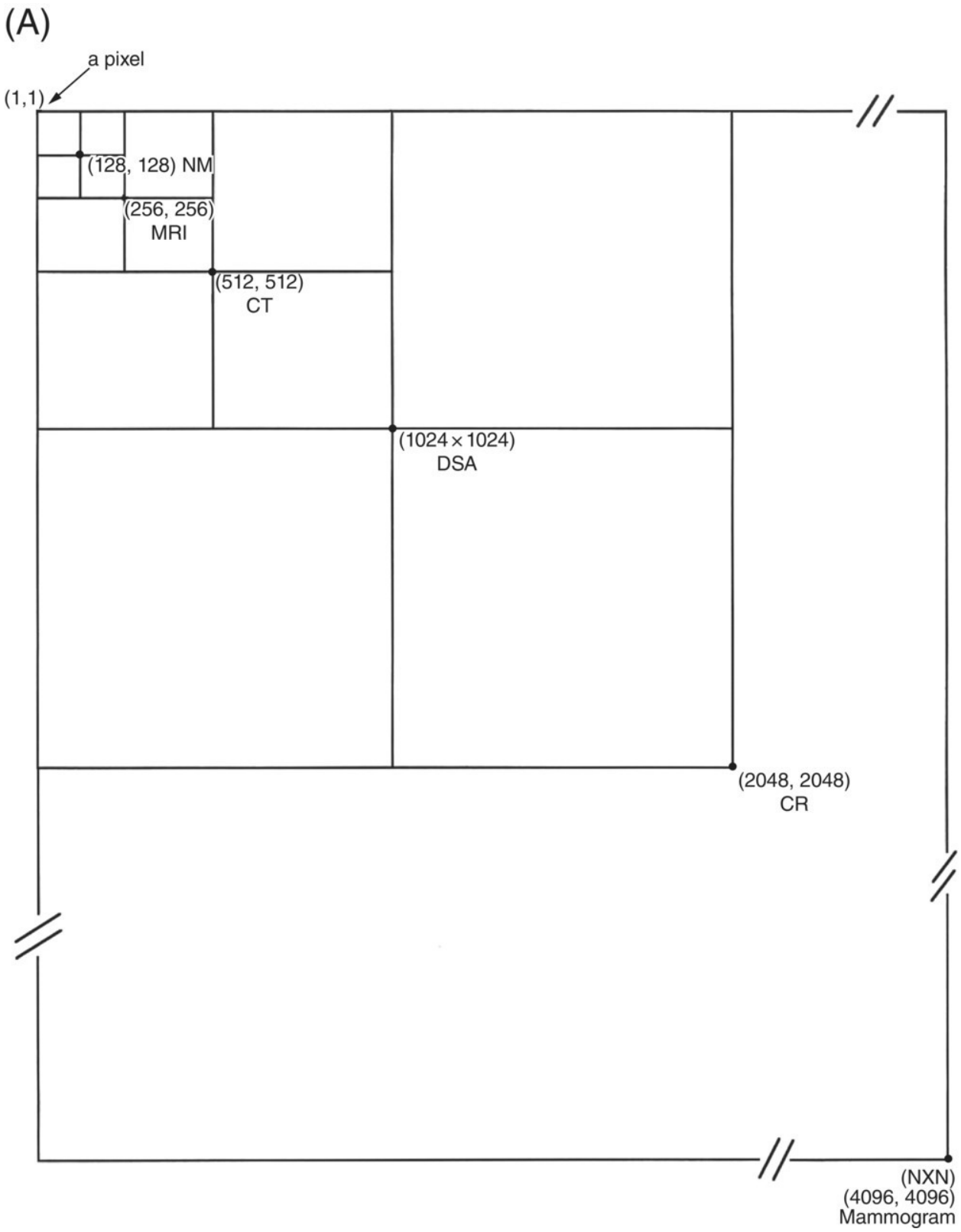
(A)
a pixel
(1,1)
(128, 128) NM
(256, 256)
MRI
(512, 512)
CT
(1024 × 1024)
DSA
(2048, 2048)
CR
(NXN)
(4096, 4096)
Mammogram

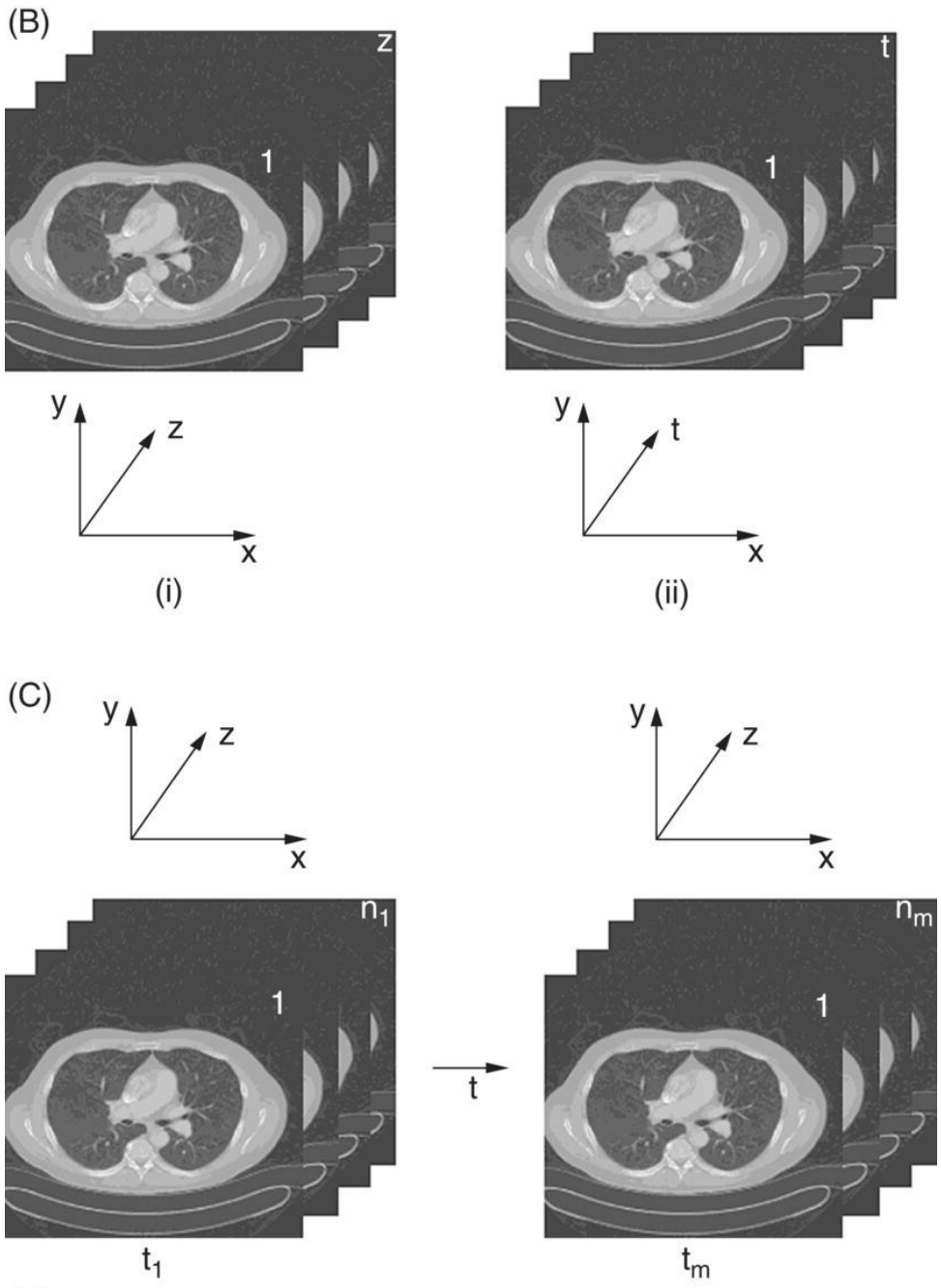
(B)
z
1
t
1
y
z
x
(i)
y
t
x
(ii)
(C)
y
z
x
y
z
x
n_1
1
t
n_m
1
t_1
t_m
(D)
(i)
PET
fuses
CT
PET on CT
(ii)
MR
fuses
CT
MR on CT

Figure 2.1 (A) Terminology used in medical images: image types, sizes, and number of pixels/image. (N × N): total number of pixels of a 2-D image; (*x*,*y*): coordinates of the pixel in the 2-D image; f (x,y): gray level value in (*x*,*y*), which can be from 8 to 12 bits in the gray level or 24 bits in the color image. The total number of bits per image is commonly denoted by (N × N × 12) or (N × N × 24). For 12 bits/pixel, the pixel value is stored in 2 bytes. (B) 3-D image set: (i) a 3-D spatial image set with *z* as the third dimension; (ii) a 3-D temporal image set with t (time) as the third dimension. (C) 4-D image set. A 4-D image set consisting of sequential 3-D spatial sets with t as the fourth dimension. (D) Fusion images: (i) PET fuses with CT: physiology (color) on anatomy (gray level); (ii) MR (color) fuses with CT (gray level): enhancement of soft tissue definition on anatomy.

2.1.5 Density Resolution, Spatial Resolution, and Signal-To-Noise Ratio

The quality of a digital image is generally measured by three parameters: spatial resolution, density resolution, and signal-to-noise ratio. The spatial and density resolutions are related to the number of pixels and the range of pixel values used to represent the object of interest in the image. In a square image N × N × k, N is related to the spatial resolution, and k is the density resolution. A high signal-to-noise ratio means that the image has strong signal with little noise, as a result, the image would please the eyes as seeing a good quality image.

Figure 2.2 demonstrates the concept of spatial and density resolutions of a digital image using a CT body scan (512 × 512 × 12 bits) as an example. Figure 2.2A shows the original and three images with a fixed spatial resolution (512 × 512), but three variable density resolutions (8, 6, and 4 bits/pixel, respectively). Figure 2.2B shows the original and three images with a fixed density resolution (12 bits/pixel), but three variable spatial resolutions (256 × 256, 128 × 128, and 32 × 32 pixels, respectively). Figure 2.2C illustrates the deteriorating quality of the CT body image after noise was introduced. Clearly, in all three cases, the quality of the CT image is decreasing, starting from the original. Spatial resolution, density resolution, and signal-to-noise ratio of the image should be adjusted properly when the image is acquired. A higher resolution image normally requires more storage space to archive and longer time for image processing and transmission.

(A)

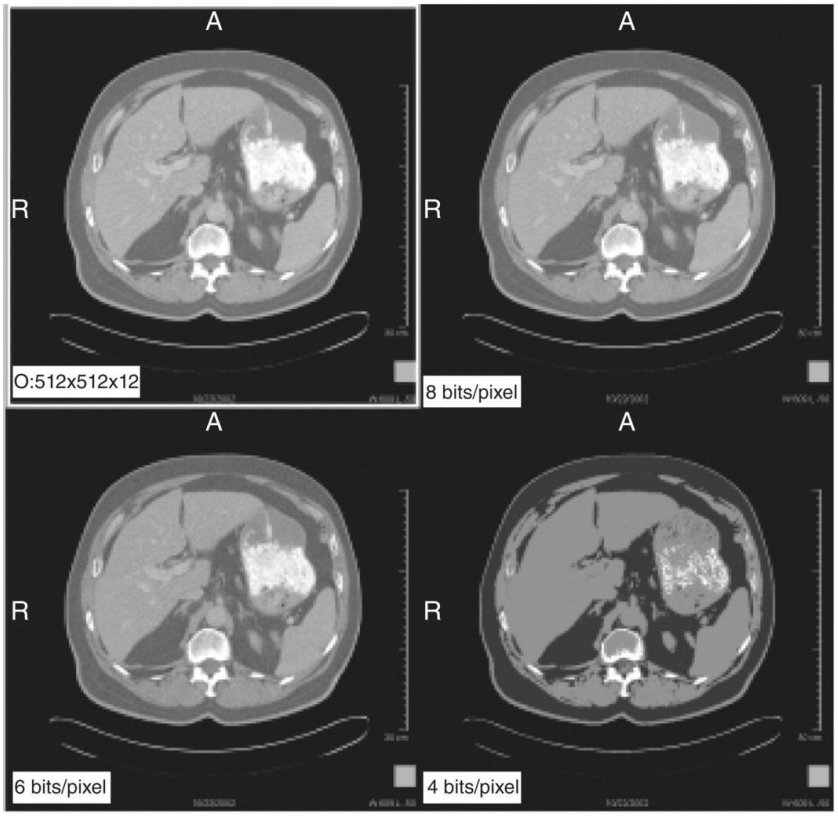
A
R
O:512x512x12
A
R
8 bits/pixel
A
R
6 bits/pixel
A
R
4 bits/pixel

(B)

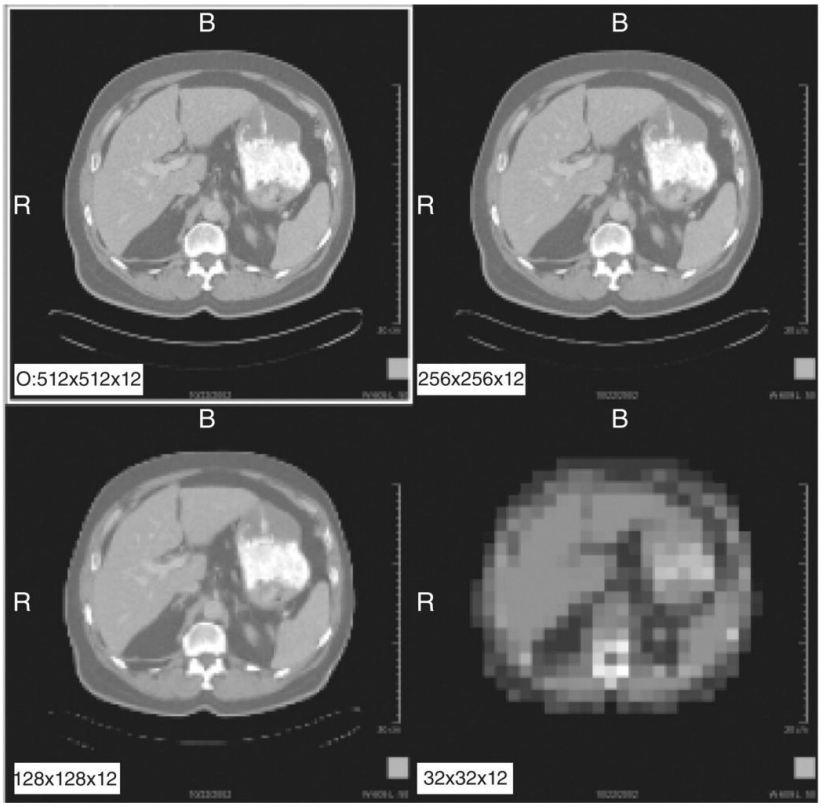
B
R
O:512x512x12
B
R
256x256x12
B
R
128x128x12
B
R
32x32x12

(C)

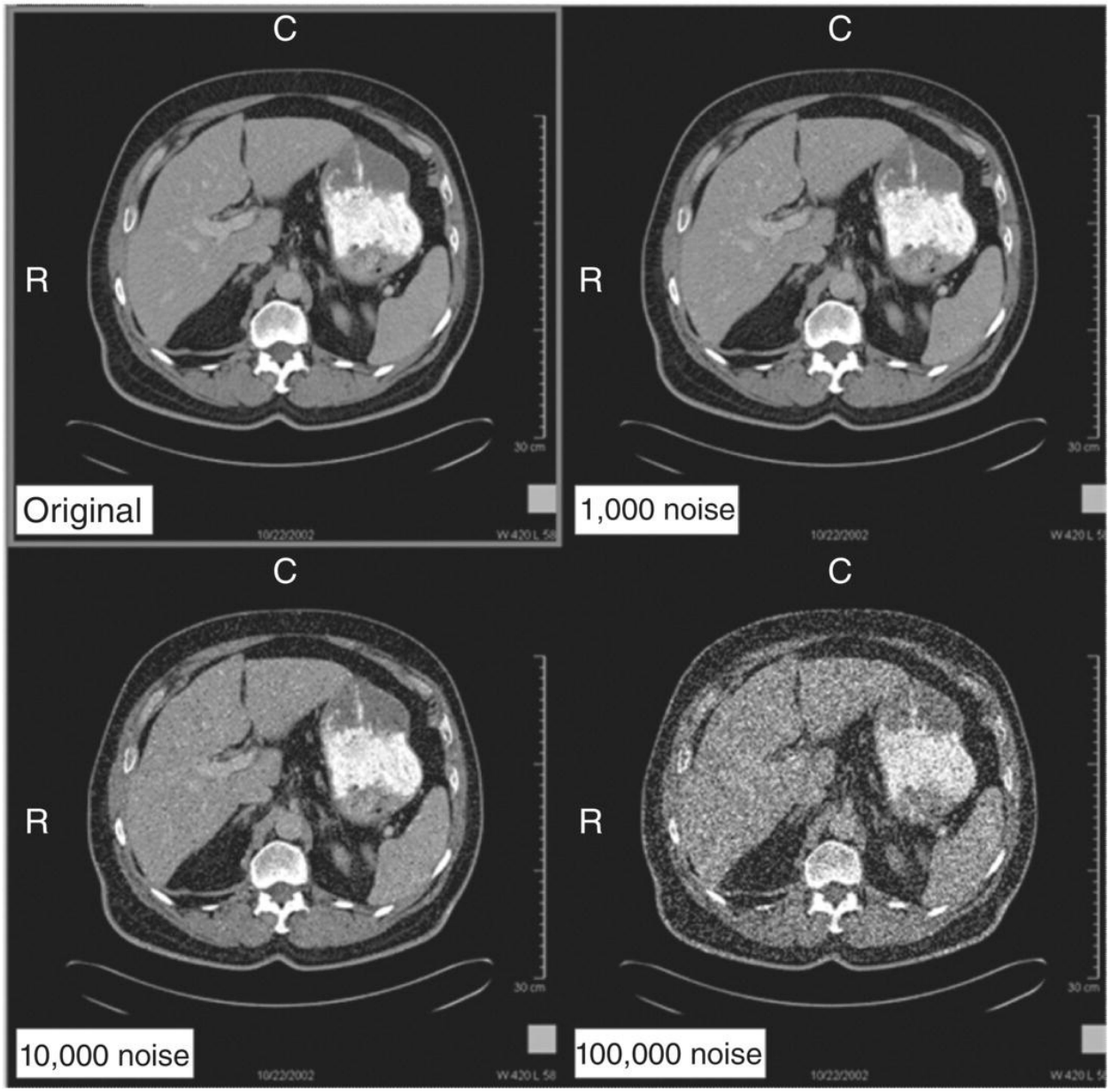

Figure 2.2 Illustration of spatial and density resolutions, and signal-to-noise ratio using abdominal CT (Computed tomography) see image (512 × 512 × 12 bits) as an example. (A) Four images with a fixed spatial resolution (512 × 512), but variable density resolutions (12, 8, 6, and 4 bits/pixel, respectively). (B) The original and three images with a fixed density resolution (12 bits/pixel), but variable spatial resolutions (512 × 512, 256 × 256, 128 × 128, and 32 × 32 pixels, respectively). (C) The abdominal CT image (512 × 512 × 12) shown in (A). Random noises were inserted in 1000 pixels, 10 000 pixels, and 100 000 pixels,

respectively. The coordinates of each randomly selected noise pixel within the body region were obtained from a random generator. The new pixel value is selected from a range between 0.7 and 1.3 and that of the original value is determined by a second random generator. Clearly, the quality of the CT image is decreasing progressively, starting from the original.

2.1.6 Radiology Workflow

Medical Imaging was originally used by radiologists for diagnostic purposes, and for this reason, this subsection first highlights the generic radiology workflow. It is followed by 2-D, 3-D, 4-D, and fusion of high-dimensional images.

PACS-based (picture archiving and communication systems, see Chapter 3) multimedia imaging informatics is a system integration of multimedia imaging informatics with patient imaging, which requires workflow and diagnostic components and procedures. A thorough understanding of the PACS-based multimedia imaging informatics workflow allows efficient system integration, and hence a better PACS-based design for the total hospital operation. The enterprise of the hospital workflow can vary from department to department, and hospital to hospital. For this reason, workflow analysis is the first step in PACS-based integration design and implementation. Figure 2.3 shows the 14 steps of a generic PACS-based workflow design. Among the 14 steps, steps 4, 8, 9, 10, 12, and 14 are not the imaging required.

1. New patient arrives at hospital for radiological imaging examination (exam).
2. Patient registers in radiology area. If the patient is new, they are registered in the hospital information system (HIS).
3. Exam ordered at radiology information system (RIS) upon arrival at radiology registration desk. Exam accession number is automatically assigned, and a requisition is printed and registered.
4. Technologist receives information from clerk and calls the patient in the waiting area for exam.
5. Patient escorted into the modality room.
6. Exam is performed by a technologist.
7. Exam is completed.
8. Clerk pulls out old films if needed, or the patient previous digital imaging

records and reports.

9. Clerk prepares all necessary papers and films or digital images at workstations (WS) for radiologist.
10. Films or images on WS are prepared for radiologist's review.
11. Radiologist reviews images, check examination record, and dictates reports.
12. Transcriptionist types the draft report from the dictation.
13. Radiologist reviews the report and signs it off.
14. Final reports are input into RIS for clinician viewing.

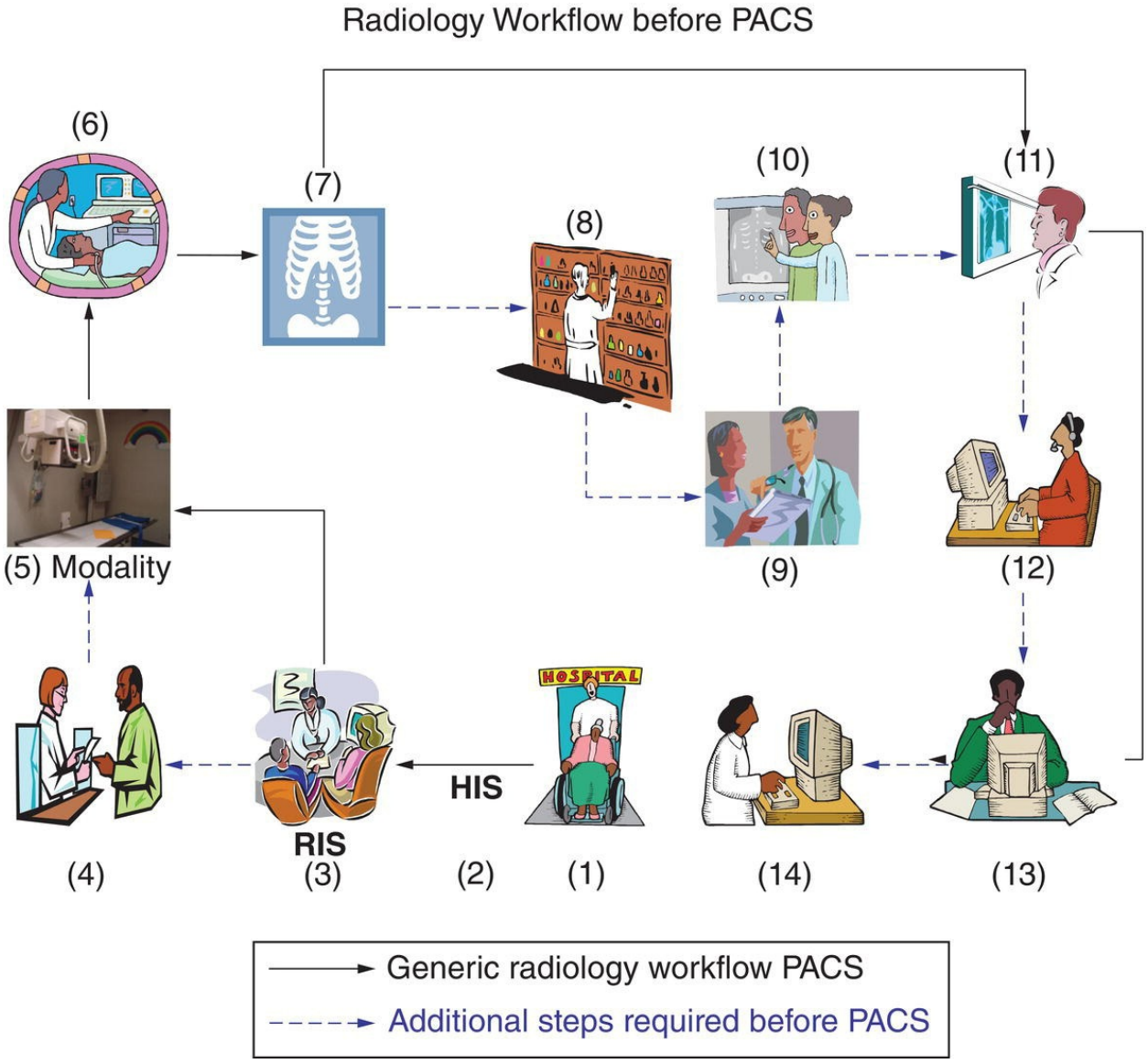

Figure 2.3 Generic radiology workflow. Note that steps 4, 8, 9, 10, 12, and 14

(→) are replaced by “PACS-based” related systems.

2.2 Two-Dimensional Medical Imaging

2.2.1 Conventional Direct Digital 2-D Projection Radiography

Conventional x-ray imaging procedures are used to examine all types of subspecialties in a radiology department, including out-patient, emergency, pediatric, neuroimaging, chest, abdomen, genitourinary, gastrointestinal, cardiovascular, musculoskeletal, extremities, and breasts. In each subspecialty procedure, several major work areas in the department are involved: the x-ray procedure room, image acquisition and display, and the diagnostic area. During the past 20 years, two major methods have been used to examine a patient:

1. the laser-stimulated luminescence plate technology, computed radiography (CR), generating a 2 K × 2 K × 12 bits direct digital image, has replaced the conventional x-ray films for 2-D images; and
2. the 1 K × 1 K × 10 (to 12) bits digital fluorography (DF) system as a method of obtaining and displaying a time series of 2-D images (see also Figure 2.1B (ii)).

2.2.2 Examples of the CR (Computed Radiography) Systems

Figure 2.4A illustrates the data flow of an upright CR system with three nonremovable rotating imaging plates, and Figure 2.4B shows the FCR (Fuji computed radiography) XG5000 system with removable imaging plate and its components, including a reader with a stacker accommodating four image cassettes and a quality assurance display workstation (right).

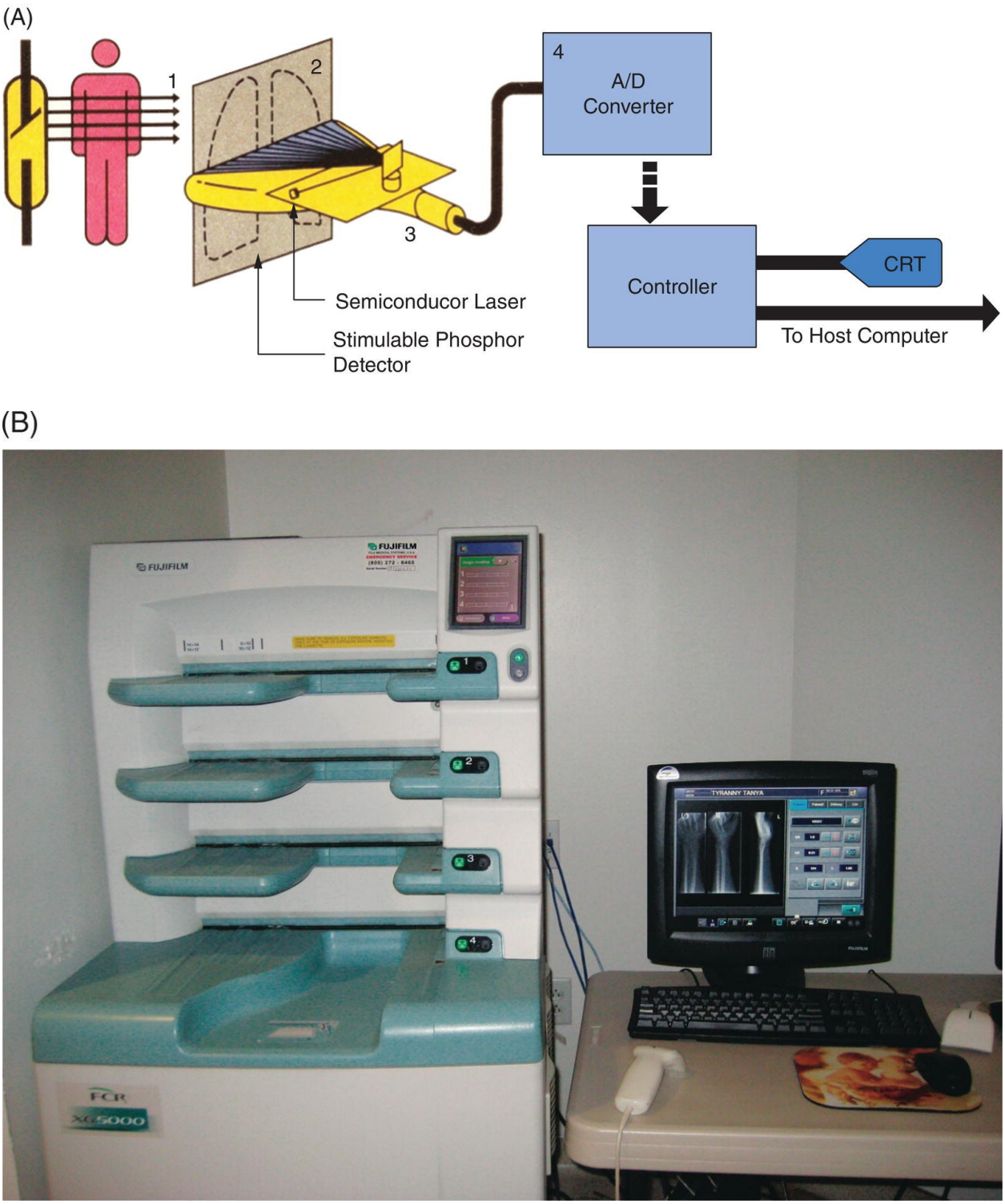

Figure 2.4 (A) Data flow of an upright CR system with non-removable imaging plates. (1) Formation of the latent image on the imaging plates; (2) Imaging plates being scanned by the laser beam; (3) Light photons converted to electronic signals; (4) Electronic signals converted to the digital signals that form a CR

image (courtesy of Konica Corporation, Japan). (B) The Fuji CR XG5000 reader (Footprint: 26 × 29 × 58 in.) with a stacker accommodates four image cassettes (left), and image processing workstation and quality assurance monitor (right).

The CR system has a built-in image background removal function. Under normal operating conditions, images obtained using the projection radiography method would include certain unexposed areas due to x-ray collimation; for example, areas outside the circle of the imaging field in digital fluorography (DF), and areas outside the collimator of CR for skeletal and pediatric radiology. In a digital image, unexposed areas appearing as a white color on a display monitor are defined as the background. Figure 2.5A is a pediatric CR image with a white background appearing on the monitor. Background removal means that the brightness of the background is converted from white to black, and hence the chest image is much clearer on the display monitor. Figure 2.5B shows that the original white background in Figure 2.5A has been automatically removed.

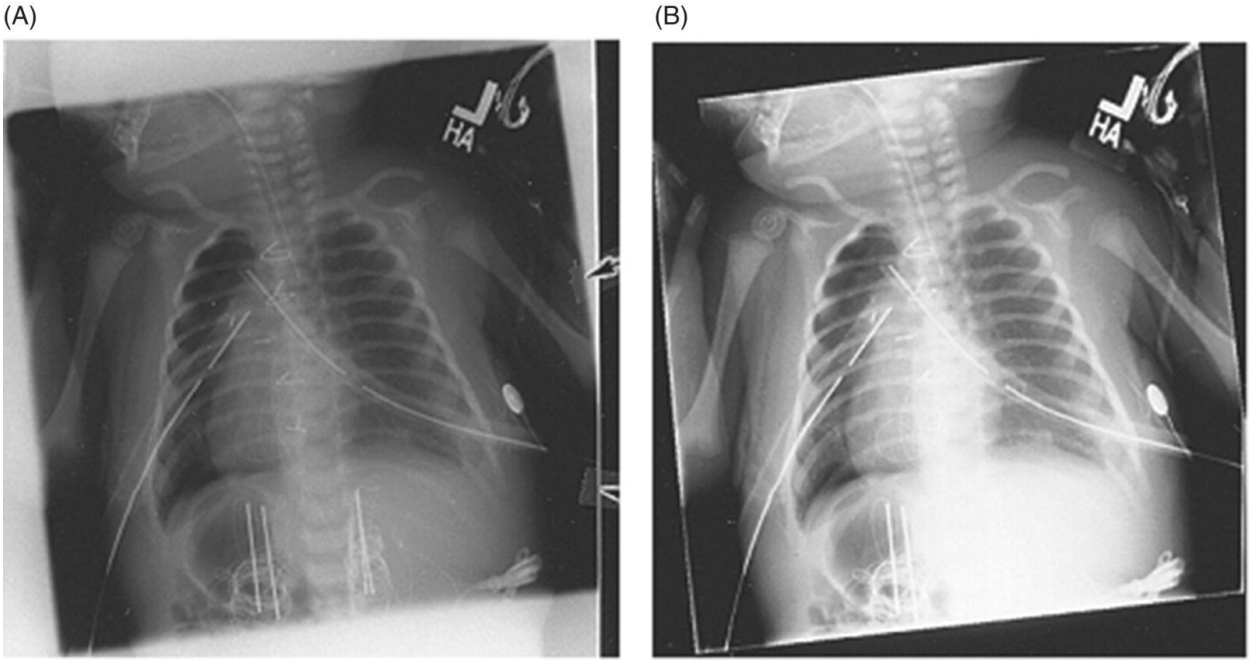

Figure 2.5 (A) A pediatric CR image, with a white background (right arrows) as seen on a video monitor. (B) A better visual quality image after the white background has been automatically removed.

The CR technology can also be added on to a conventional analogy table x-ray system. Figure 2.6B (bottom) illustrates the conventional analogy table bed with the x-ray system, and the add-on DR image acquisition system near the wall to receive and display the DR image. Figure 2.6A shows the CR workflow system).

A typical DR unit produces a 2000 × 2500 × 12-bit image instantaneously after the exposure.

(A)

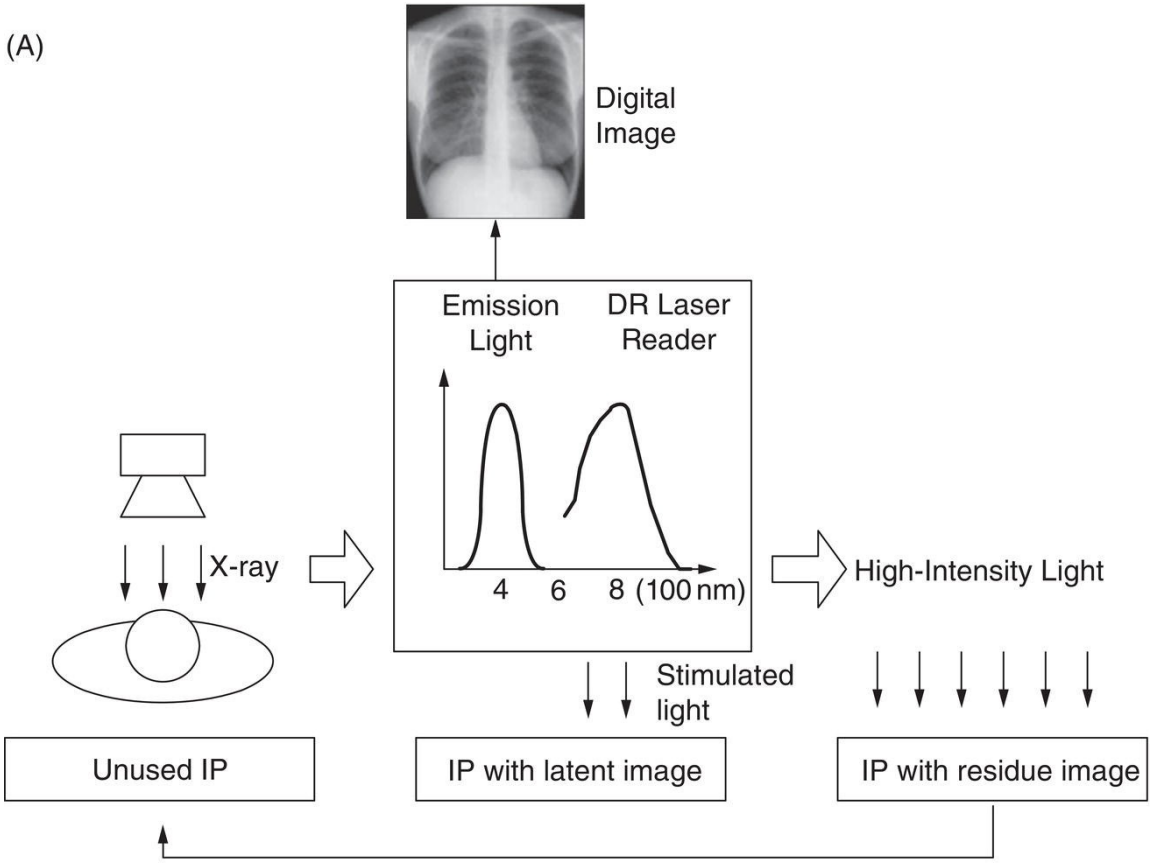
Digital
Image
Emission
Light
DR Laser
Reader
4
6
8 (100 nm)
X-ray
High-Intensity Light
Stimulated
light
Unused IP
IP with latent image
IP with residue image

(B)

Figure 2.6 (A) Workflow steps in the formation of a digital radiography (DR) image, comparing it with that of a CR image shown, (B) an add-on DR system (Figure 2.4A) and utilizes an existing x-rays unit with the patient bed.

2.2.3 Full-Field Direct Digital Mammography

2.2.3.1 Screen/Film Cassette and Digital Mammography

Conventional screen/film mammography produces a very high quality mammogram on an 8 × 10 sq. in. film. However, some abnormalities, like calcification, in the mammogram require 50 μm spatial resolution to be recognized. For this reason it is difficult to use CR or a laser film scanner to convert a film mammogram to a quality digital image, which hinders the possibility of integrating the mammogram directly to a PACS image. Yet mammography examinations account for about 8% of all diagnostic procedures in a typical radiology department. Over the past 15 years, in the USA as well as worldwide, the betterment of women's health has become a major social issue. As a result, joint research efforts between academic institutions and private industry, supported by the US National Cancer Institute and Army Medical Research and Development Command, have propelled the development of some excellent quality digital mammography systems. Many of these systems are in daily clinical use now. In the next section, the principle of digital mammography, a very critical component of total digital imaging operation in a hospital, is described.

2.2.3.2 Slot-Scanning Full-Field Direct Digital Mammography

There are several methods which can be used to develop a full-field direct digital mammogram system, among them the imaging plate technology using a better resolution imaging plate made from different materials with higher quantum efficient detection, as described in the previous section. Another method is the slot-scanning method, which can be a direct or indirect digital radiography system. This section summarizes the hybrid direct slot-scanning method. The slot scanning technology modifies the image receptor of a conventional mammography system by using a slot-scanning mechanism and a detector system.

The slot-scanning mechanism scans a breast with an x-ray fan beam, and the image is recorded by using a charged-couple device (CCD) camera encompassed in a Bucky anti-scatter grid in the mammography unit. Figure 2.7 shows a full-

field direct digital mammography (FFDDM) system developed in the late 1990s. The digital mammography technology has been greatly improved since that time.

The left-hand side of Figure 2.8 shows a 4 K × 5 K × 12-bit digital mammogram obtained with the system shown in Figure 2.7, and the right-hand side of Figure 2.8 depicts a localized smaller size digital mammogram for biopsy purpose. A standard screening mammography examination requires four images, two for each breast (the craniocaudal [CC] and mediolateral oblique [MLO] views. The result is 160 MB of image data.

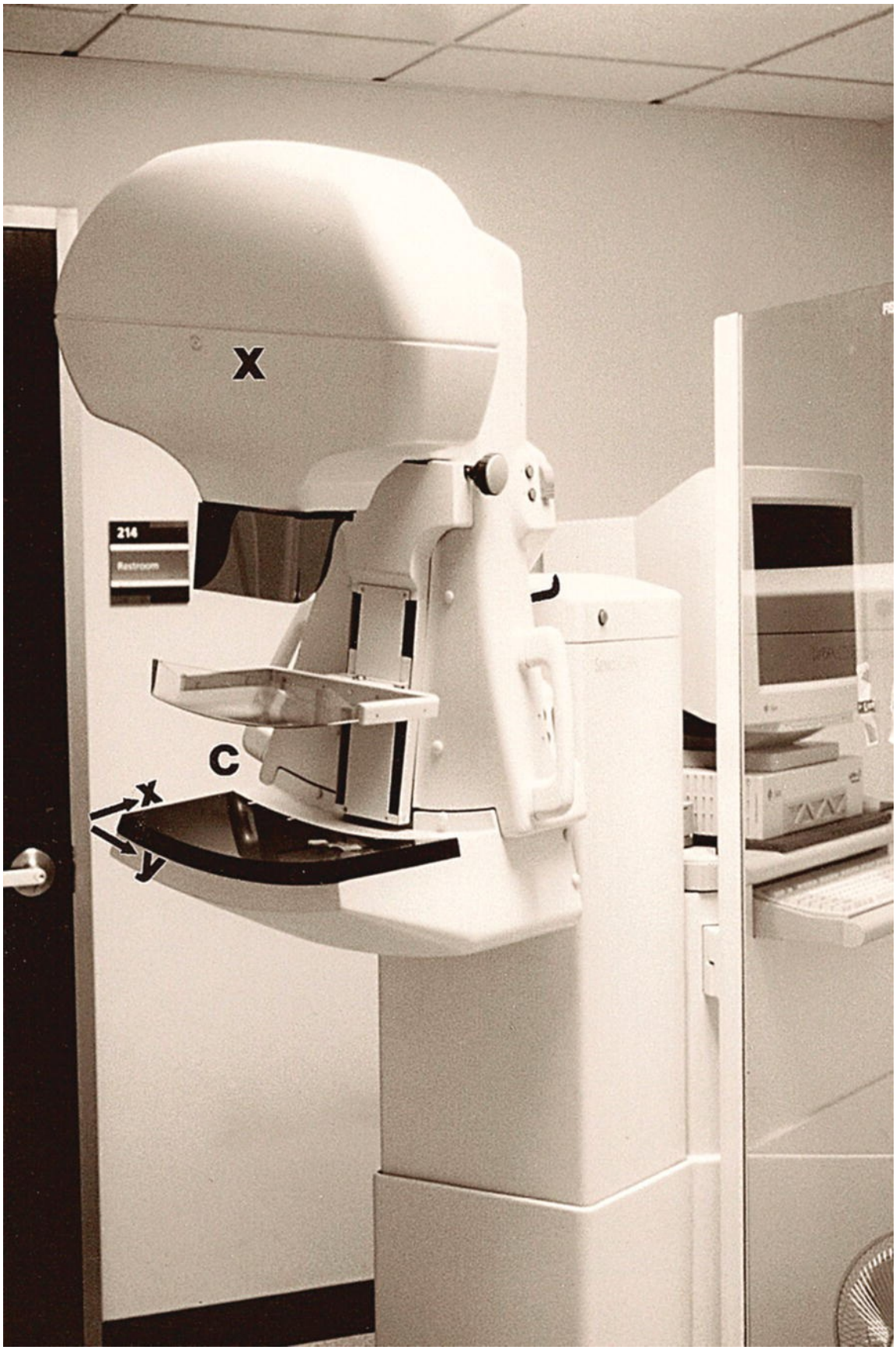
X
214
Restroom
C
x
y

Figure 2.7 A slot-scanning digital mammography system. The slot with 300-pixel width, covers the *x*-direction (arrow) with 4400 pixels, The x-ray beam sweeps in the *y*-direction (arrow), producing over 5500 pixels. Top X: x-ray and collimator housing; Middle C: Breast compressor.

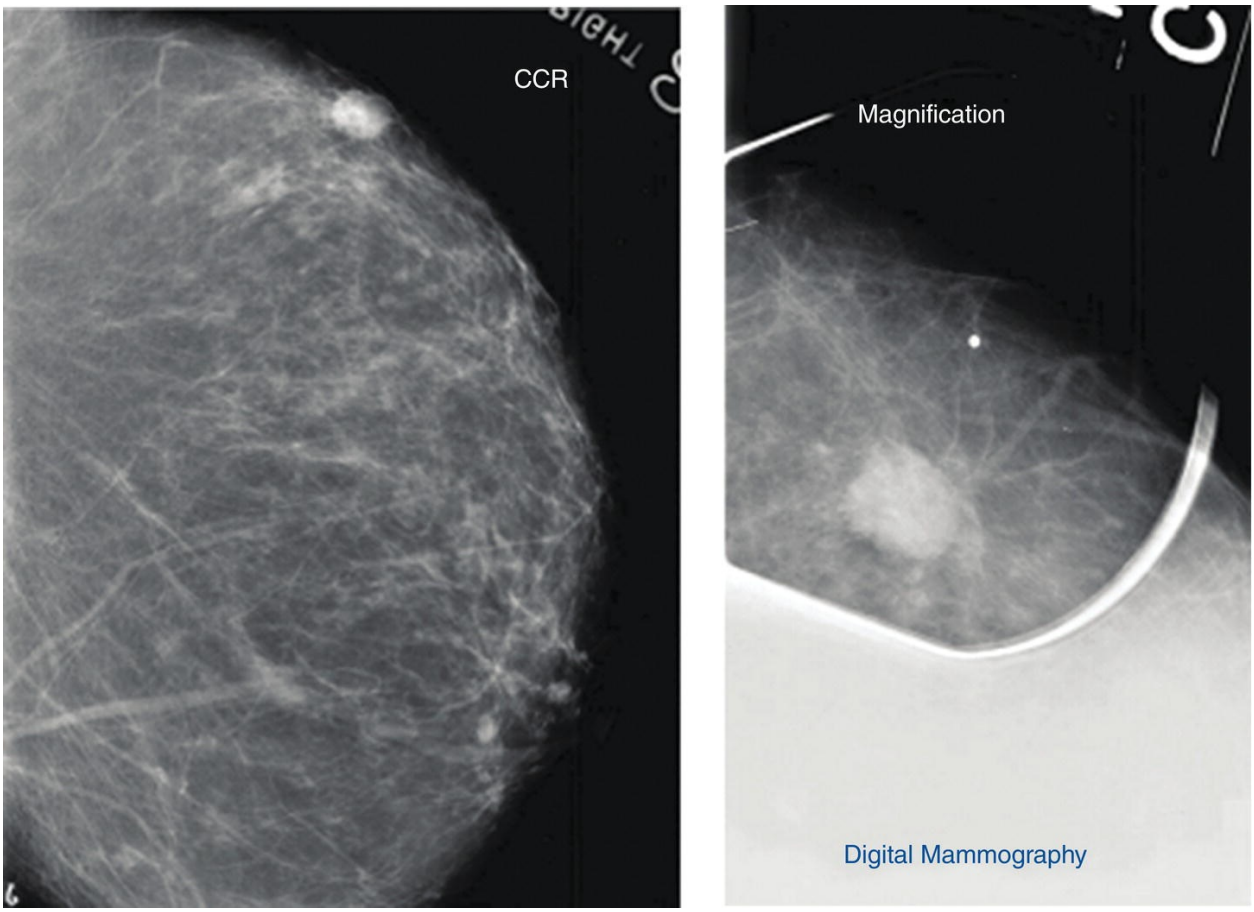

Figure 2.8 A 4 K × 5 K × 12-bit CC view digital mammogram shown on a 2 K × 2.5 K monitor (left). A localized digital mammogram for needle biopsy verification (right).

See Chapter 9, Section 9.2, Dedicated Breast MRI Enterprise Data Grid for other noninvasive breast imaging methods.

2.2.4 Nuclear Medicine Imaging

2.2.4.1 Principles of Nuclear Medicine Scanning

The nuclear imaging (NM) technique can be used to generate both 2-D and 3-D images. In 2-D imaging, a projection image is produced. In 3-D imaging, the combined nuclear imaging and tomography techniques can generate an emission

CT (ECT). This section discusses 2-D NM imaging, and ECT is presented in Section 2.3. The formation of a NM image is by administering a radiopharmaceutical agent that can be used to differentiate between a normal and an abnormal physiological process. A radiopharmaceutical agent consists of a tracer substance and a radionuclide for highlighting the tracer's position. The tracer typically consists of a molecule that resembles a constituent of the tissue of interest, a colloidal substance that is taken up by reticuloendothelial cells, for example, or a capillary blocking agent. A gamma camera (see Section 2.2.4.2) is then used to obtain an image of the distribution of the radioactivity in the organ to be imaged.

The gamma emitter is chosen on the basis of its specific activity, half-life, energy spectrum, and ability to bond with the desired tracer molecule. Its radionuclide half-life is important because, in general, we would like to perform scans in the shortest possible time, while still accumulating sufficient statistically meaningful nuclear decay counts. Furthermore, a reasonably short half-life minimizes the radiation dose to the patient. The energy spectrum of the isotope is important because if the energy emitted is too low, the radiation will be severely attenuated when passing through the body, so the photon count statistics will be poor or scan times unacceptably long. If the energy is too high, there may not be enough photoelectric interaction, so absorption in the detector crystal will be low. Typical isotopes used in nuclear medicine have γ-ray emission energies of 100–400 keV.

2.2.4.2 The Gamma Camera and Associated Imaging System

As with most imaging systems, a nuclear medicine imager (e.g. a gamma camera) contains subsystems for data acquisition, data processing, data display, and data archiving. A computer is used to control the flow of data and coordinate these subsystems into a functional unit. The operator interactively communicates with the computer control via graphical user interface (GUI) or predefined push buttons on the system's control paddle. Figure 2.9 shows a schematic of a generic nuclear medicine gamma camera. Typical matrix sizes of nuclear medicine images are 64 × 64, 128 × 128, or 256 × 256 by 8 to 12 bits, with a maximum of 30 frames per second in cardiac imaging. For example, in gated cardiac mode, useful parameter values such as ejection fraction and stroke volume can be calculated. In addition, the frames of a cardiac cycle can be displayed consecutively and rapidly in cine fashion to evaluate heart wall motion. Unfortunately, some older nuclear imagers do not have the DICOM standard.

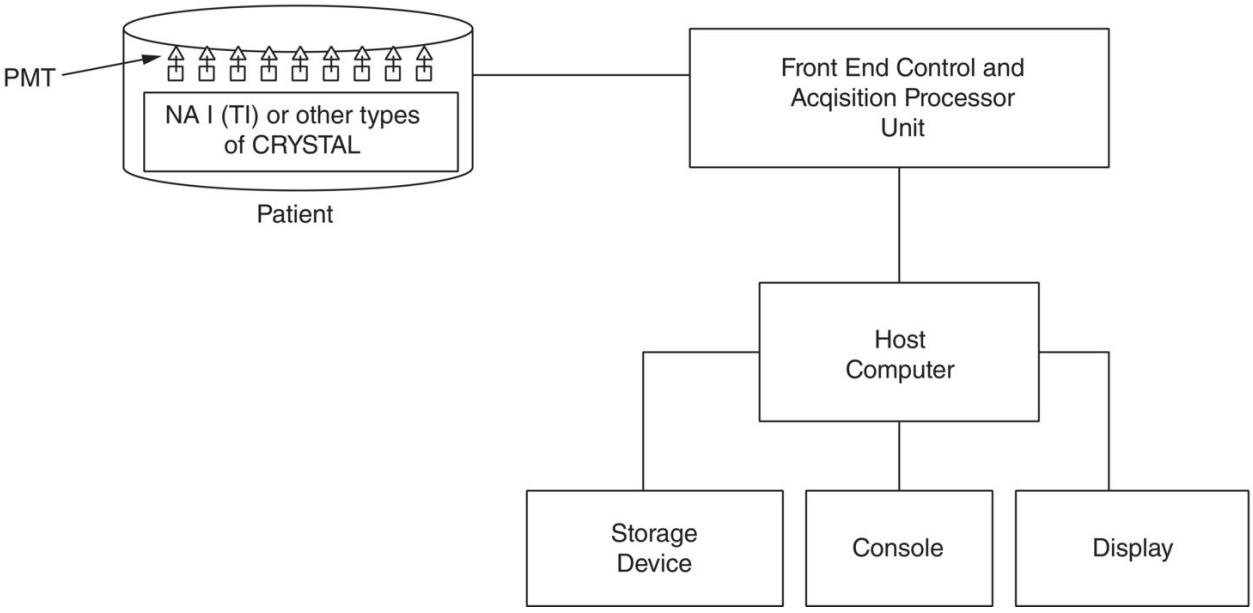

Figure 2.9 Schematic of a general gamma camera used in nuclear medicine imaging. PMT: Photomultiplier tube; NaI (TI): Thallium-activated sodium iodide.

2.2.5 Two-Dimensional (2-D) Ultrasound Imaging (US)

2.2.5.1 B-Mode (Brightness) Ultrasound Scanning

Ultrasound imaging is used in many medical specialties, including obstetrics, gynecology, pediatrics, ophthalmology, mammography, abdominal imaging, and cardiology, as well as for imaging smaller organs such as the thyroid, prostate, and testicles, and in intravascular ultrasound endoscopy (see Section 2.2.6.2). Its wide acceptance is partially due to its noninvasiveness, its use of non-ionizing radiation, and its lower equipment and procedural costs compared with XCT and MRI. An ultrasound examination is often used as the first step in attempting to diagnose a possible ailment due to its noninvasive nature. Recently developed handheld portable US scanners are popular for applications in emergency situations.

External B-mode ultrasound imaging is used to generate a sectional view of an area of interest in the patient, by detecting the amplitudes of acoustical reflections (echoes) occurring at the interfaces of tissues with different acoustical properties. Figure 2.10 shows a general block diagram of a typical B-mode ultrasound scanner. It is made up of a high-voltage pulse generator (top left), a transmitter circuit (left, middle), a receiver circuit with time gain compensation (TGC, top middle), a digital scan converter (DSC, middle right), a video display

monitor (bottom right), a position recorder circuit (middle low), a mechanical scanning arm with position encoders (middle lower, blue), and a transducer (bottom, blue).

In 2-D US, the scanning arm is restricted to the movement in one linear direction at a time. The digital scan converter (DSC) image memory is normally 512 × 512 × 8 bits, in a color Doppler US image, but it can be extended to 512 × 512 × 24 bits.

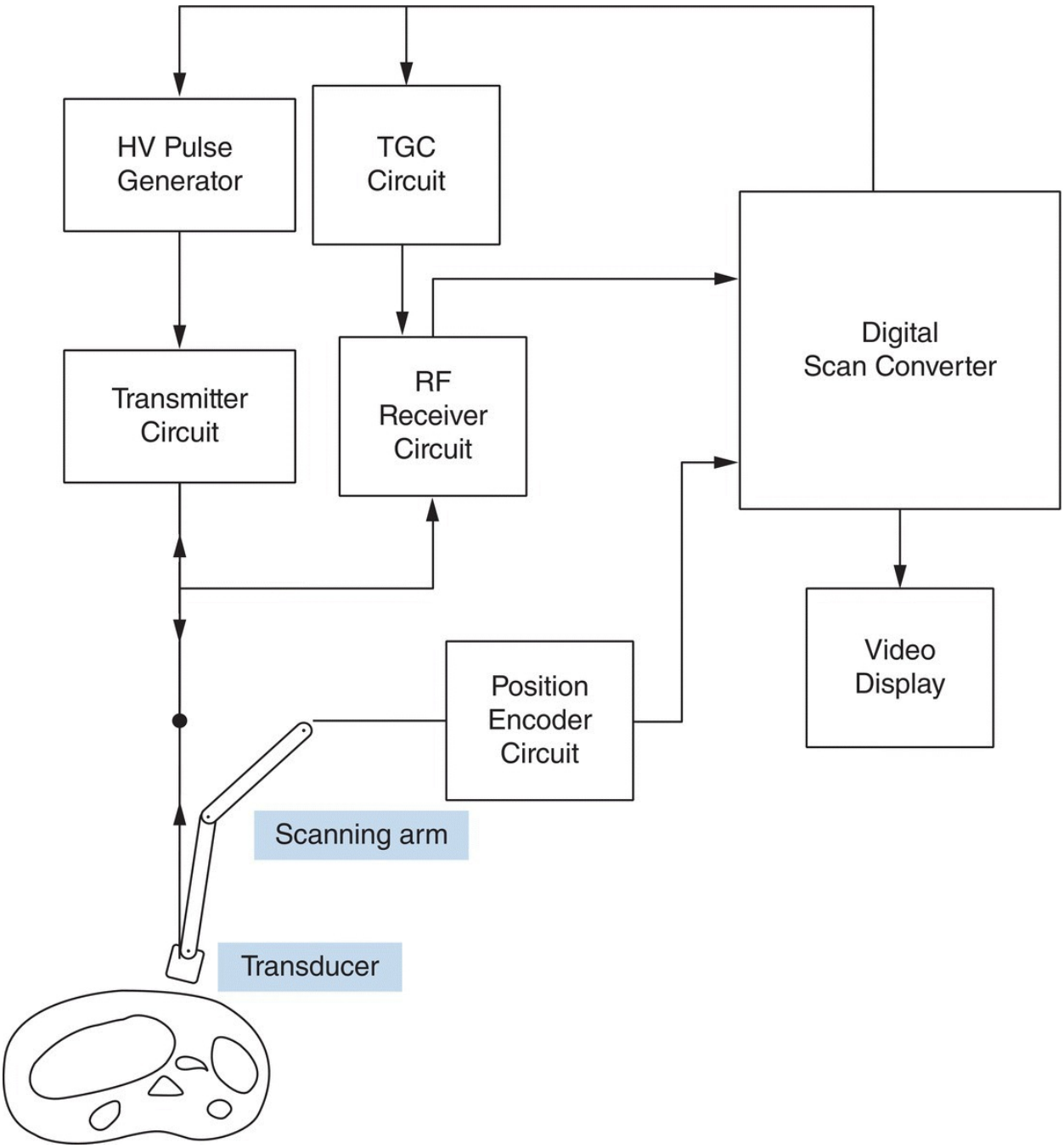

Figure 2.10 Block diagram of a B-mode ultrasound scanner system. TGC: Time gain compensation; RF: radio frequency; HV: high voltage.

2.2.5.2 Sampling Modes and Image Display

Three different sampling modes are available on most 2-D ultrasound units: the survey mode, in which the data stored in the memory is continually updated and displayed; the static mode, in which only maximum US echo signals (values) during a scanning session are stored and displayed; and an averaging mode, in which the average of all scans for a particular scan location are stored and displayed.

Once stored in the memory, the digital data are subjected to post-processing operations of several types. These can be categorized according to changes in the gray level display of the stored image, temporal smoothing of the data, or spatial operations. Gray scale mean and windowing and nonlinear gray scale transformations are common.

The image display is performed by the video processor and controller units (Figure 2.10), which can quickly access the image memory and modulate an electron beam to display the image on a video monitor. The digital scan converter allows for echo data to be read continuously from the fast access image memory.

2.2.5.3 Color Doppler Ultrasound Imaging

Ultrasound scanning using Doppler principle can detect the movement of blood inside the vessels. In particular, it can detect whether the blood is moving away or toward the scanning plane. When several blood vessels are in the scanning plane, it is advantageous to use different colors to represent the blood flow direction and speed with respect to the stationary anatomical structures. Thus, colors coupling with the grayscale ultrasound image results in a duplex Doppler ultrasound image. This coupling permits simultaneously imaging of anatomical structures as well as characterization of circulatory physiology from known reference planes within the body. The resulting image is called color Doppler or color-flow imaging. A color Doppler image needs $512 \times 512 \times 24$ bits. Figure 2.11 shows a color Doppler US blood flow image demonstrating the pulmonary vein inflow convergent.

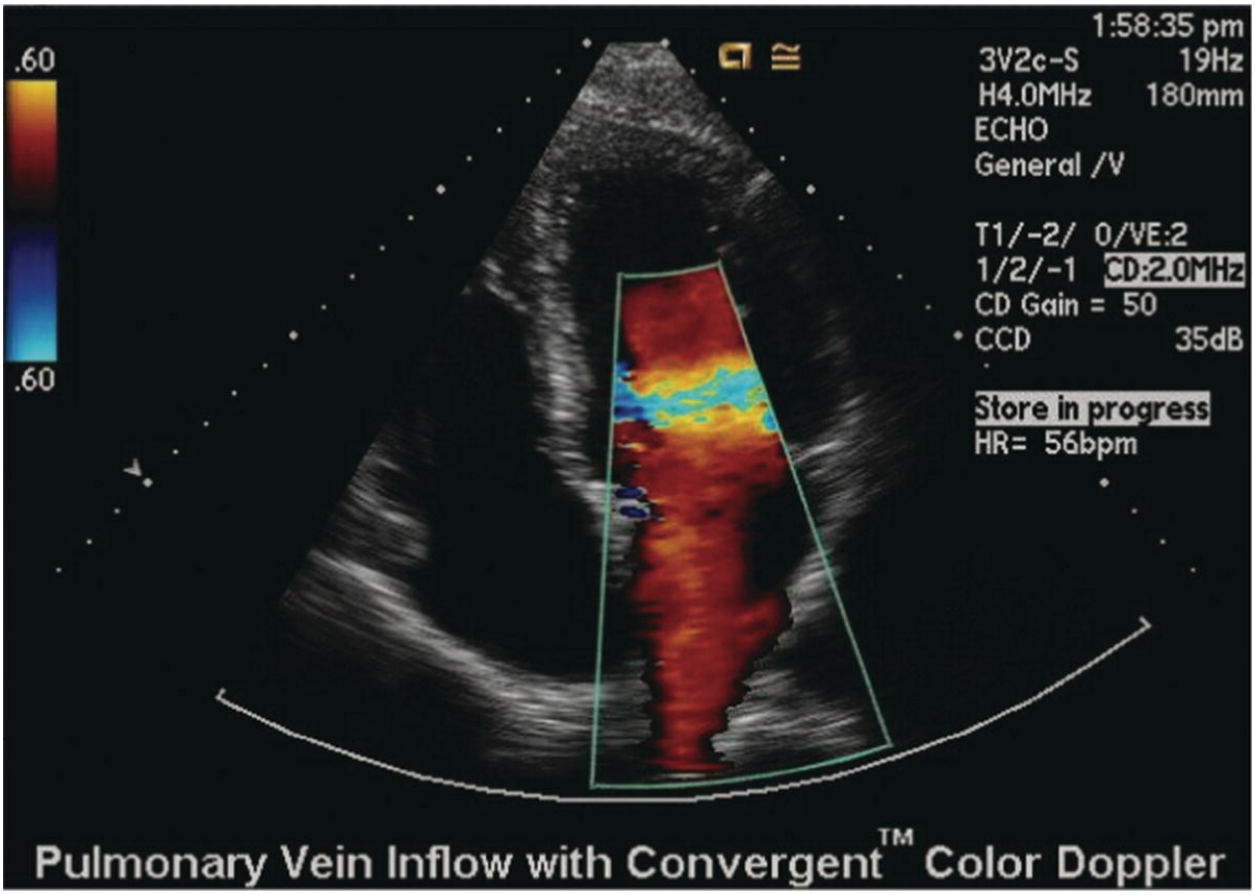

Figure 2.11 Color Doppler ultrasound of blood flow, showing convergent pulmonary vein inflow.

(courtesy of Siemens Medical Imaging Systems: http://www.siemensmedical)

2.2.5.4 Cine Loop Ultrasound

One advantage of ultrasound imaging over other imaging modalities is its noninvasive nature, which permits the accumulation of ultrasound images continuously through time without adverse effects to the patient. Such images can be played back in a cine loop, which can reveal the dynamic motion of a body organ, for example, the heart beat (see Section 2.3.2 on multislice CT). Several seconds of cine loop ultrasound images can produce a very large image file. For example, a 10-second series of color Doppler cine loop ultrasound images will yield $(10 \times 30) \times 0.75 \times 10^6$ bytes (= 225 MB) of image information. In general, unless the study is related to dynamic movement like cardiac motion, very seldom would the complete cine loop be archived. The radiologist or clinician in charge previews all cine loop images but discards most, except the few relevant to be archived as the patient ultrasound records.

2.2.6 Two-Dimensional (2-D) Light and Endoscopic Imaging

2.2.6.1 2-D Light Imaging

Light imaging uses various light sources to generate images for diagnosis or image-guided treatment. Two commonly used digital light imaging systems for medical applications are the microscopy and endoscopy, both systems generating real color images. These two modalities are different to the method used to generate the image. In the former, microscopy, the imaging system is mostly connected to a fluorescence, confocal, or other type of microscope, with the image source from pathological glass slides. The endoscopy is mostly used on the anatomical scale, which involves different types of instrumentation such as a cannula, a miniature light source with a light guide assembly, and a micro-sized CCD camera. They are inserted into the appropriate human organ before the surgical operation. After the light images are obtained, the endoscopic instruments are then extracted from the organ. Both the light imaging system and endoscopy use similar digital chains for image preprocessing, analysis, display, and archive. Figure 2.12 shows a generic workflow of a digital microscopic system.

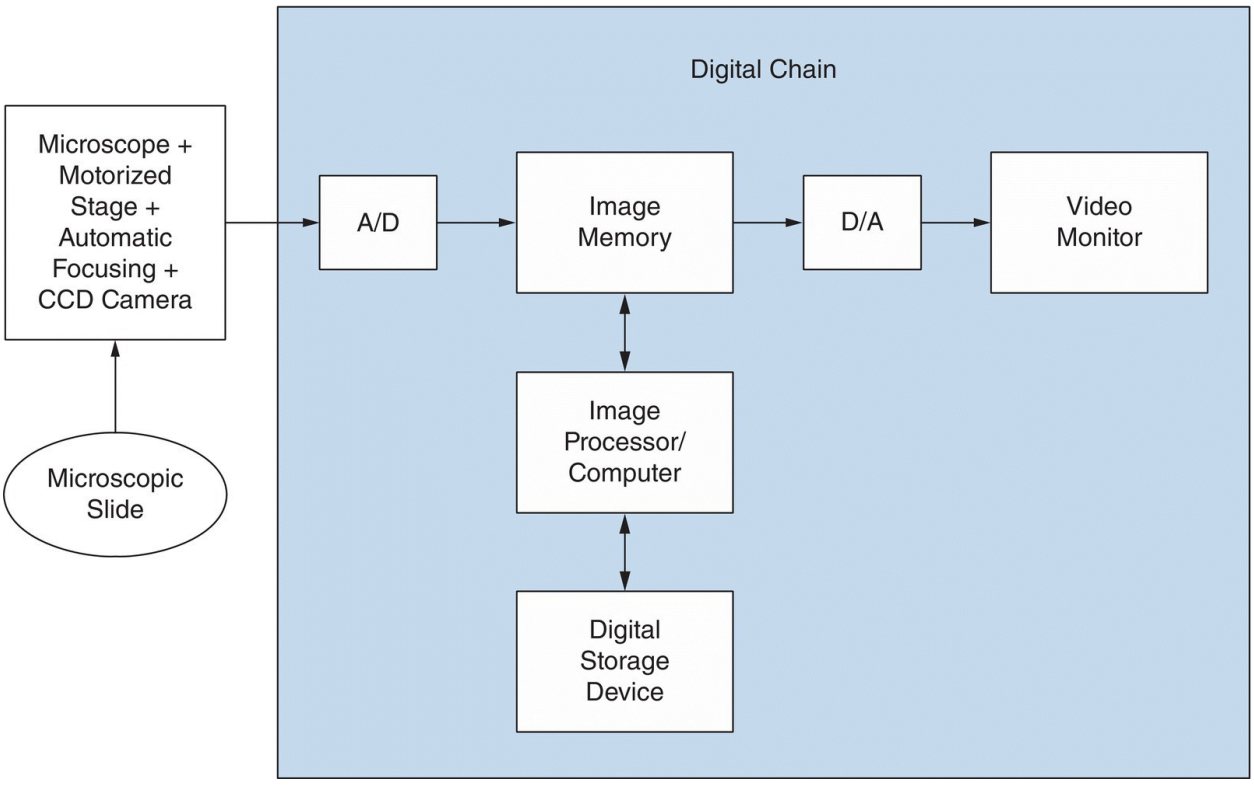

Figure 2.12 Block diagram of a digital microscopic system with a CCD camera connected to the digital chain. The system is mostly used in the pathological

environment and digital video endoscopic imaging. A/D: analog to digital. D/A: digital to analog.

2.2.6.2 2-D Endoscopic Imaging

An endoscopic examination is a visual inspection of the inside of the human body, conducted by inserting an endoscopic tube with a light source and light guides into the lumen. The surgeon can look into the light guides through an eyepiece on the outside of the apparatus or use a CCD camera to capture real-time endoscopic images transferred to an LCD monitor or a workstation, to obtain an accurate diagnosis. If the insertion is, for example, in the throat, tracheobronchial, upper gastrointestinal, colon, spine, and rectum, the procedure is called laryngoscopy, bronchoscopy, gastroscopy, colonoscopy, minimally invasive spinal surgery, and sigmoid scope, respectively. If a digital chain is attached to the light guide so that the image can be seen on a display system, and be archived in a storage device, the system is called a digital endoscope. The digital chain consists of a CCD camera, A/D converter, image memory, computer, display, and endoscopic analysis software. Figure 2.13A illustrates the schematic of a generic digital endoscopic system. Figure 2.13B shows a sequence of four real-time color endoscopic images of thoracic vertebrae 9 and 10 under minimally invasive spinal surgery.

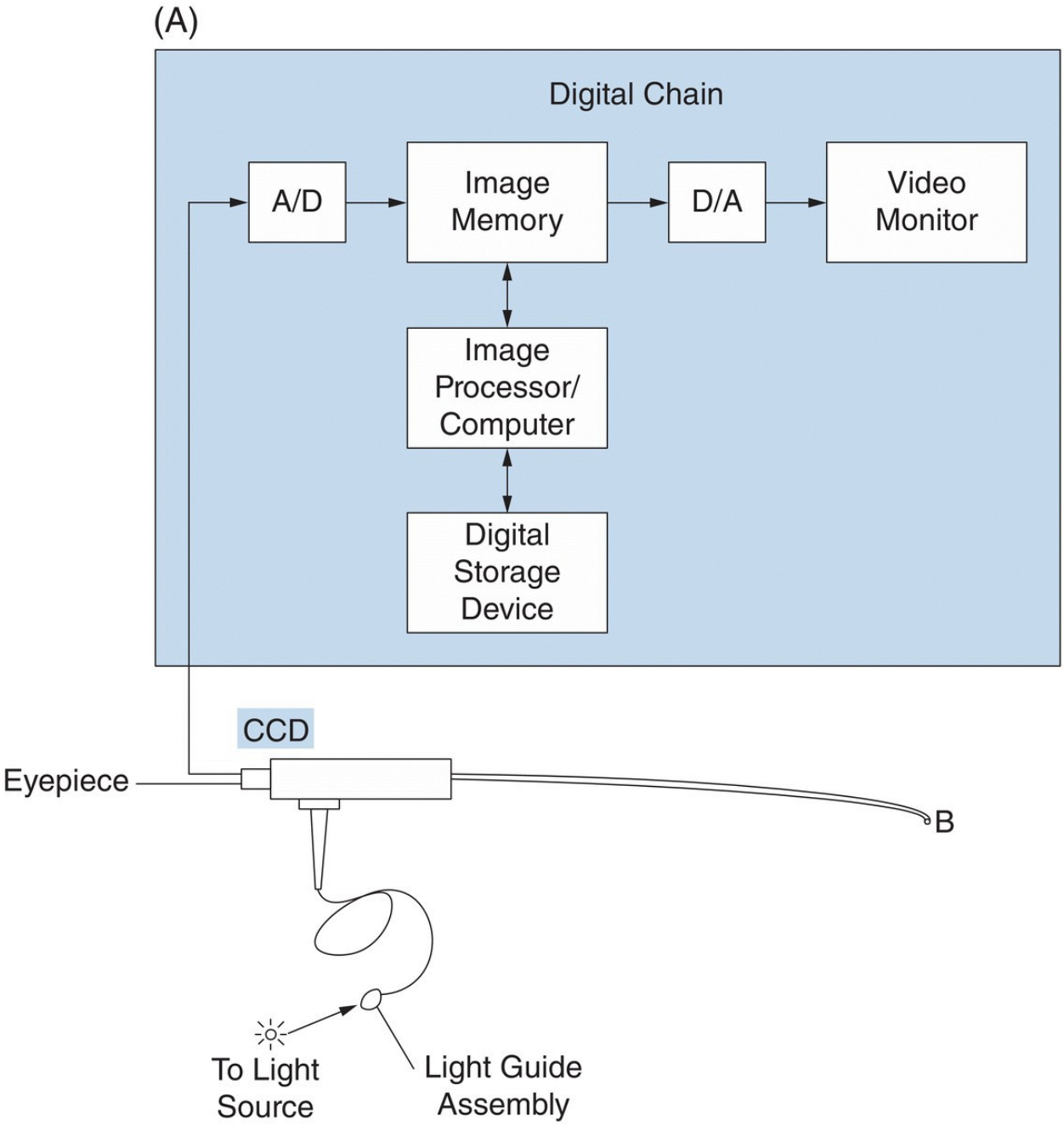

Figure 2.13 (A) Schematics of a generic digital endoscope (not to scale) with a CCD camera. A/D: analog to digital. D/A: digital to analog.

(B)

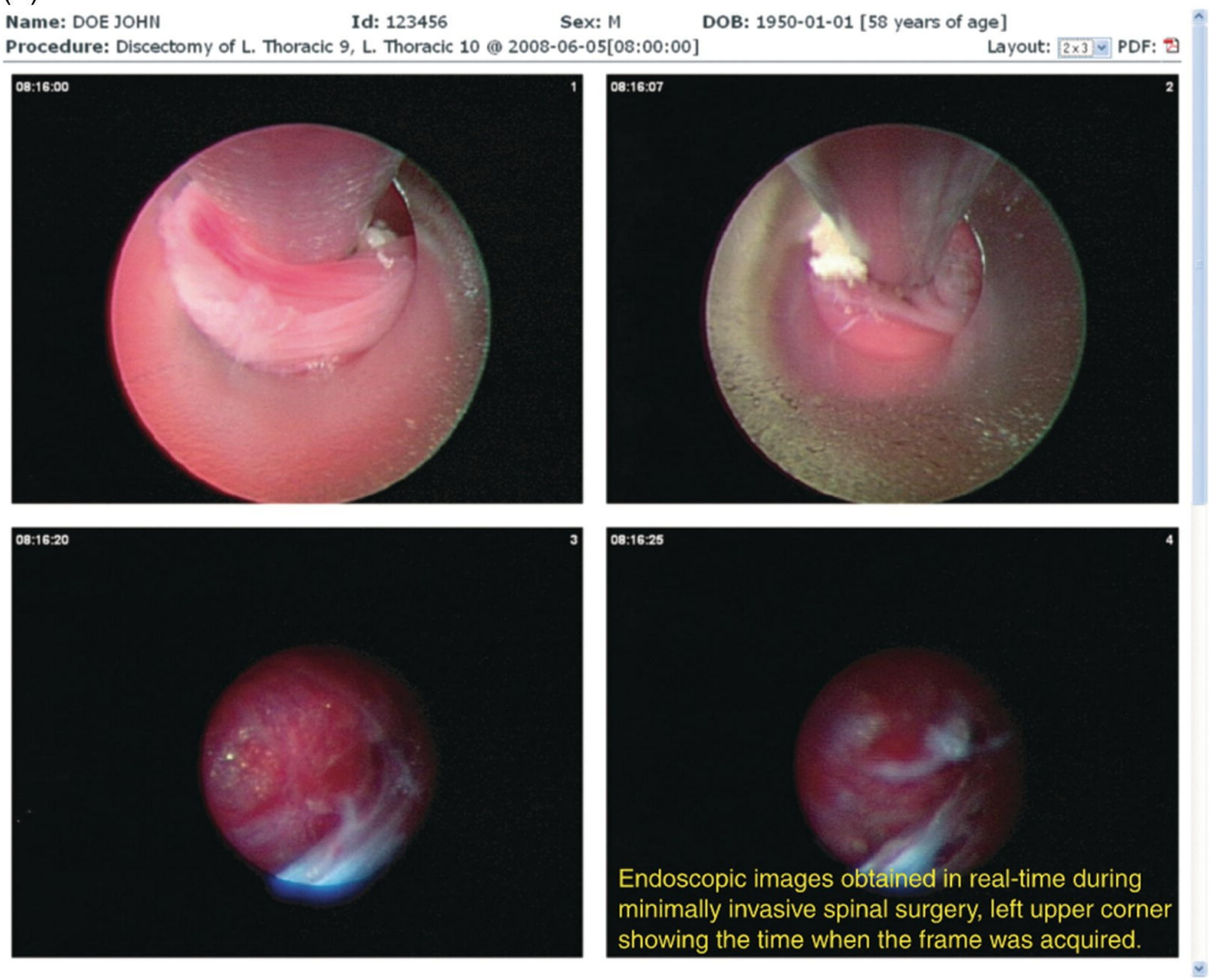

Figure 2.13 (B) Endoscopic images of thoracic vertebra 9 and 10 acquired in real time during image-guided minimally invasive spinal surgery. See also Chapters 20 and 21 for minimally invasive image-assisted spinal surgery.

(courtesy of Dr J Chiu, California Spine Institute)

2.3 Three-Dimensional Medical Imaging

2.3.1 Two-Dimensional Transmission X-Ray Computed Tomography (CT) from 1-D Projections

Most 3-D medical images are generated by using the image reconstruction method, or tomography techniques with data collected from data projections from detectors coupled with various energy sources (Figure 2.14). These energy sources can be from x-rays, single-photon emission, positron emission,

ultrasound, nuclear magnetic resonance (NMR), and light photons. The image so reconstructed is called XCT, single-photon emission tomography (SPECT), positron emission tomography (PET), 3-D ultrasound (3-D US), MRI, or 3-D light imaging, respectively. If the projections are from 1-D data (Figure. 2.15A), then the image formed using the Fourier projection theorem is a 2-D sectional image, f(x,y) (Figure 2.15B). A collection of combined multiple sectional images would generate a 3-D image volume, which has consecutive space gaps in between two consecutive sections. If the projections are 2-D, for example (see Figure 2.16, *z*-direction), where *z* is the body axis, then the reconstructed 3-D image set would be a fully 3-D image volume.

Recent advances in these techniques produce very large 3-D image volume data. It is not unusual to obtain hundreds and even thousands of CT images in one examination. Archiving, transmission, display, and management of these large data volume sets become a technical challenge. Refer to Table 2.1, for the sizes and number of images per examination of these sectional and 3-D imaging modalities.

The next sections present 3-D imaging, including 3-D CT, SPECT, PET, 3-D US, MRI , and 3-D light imaging.

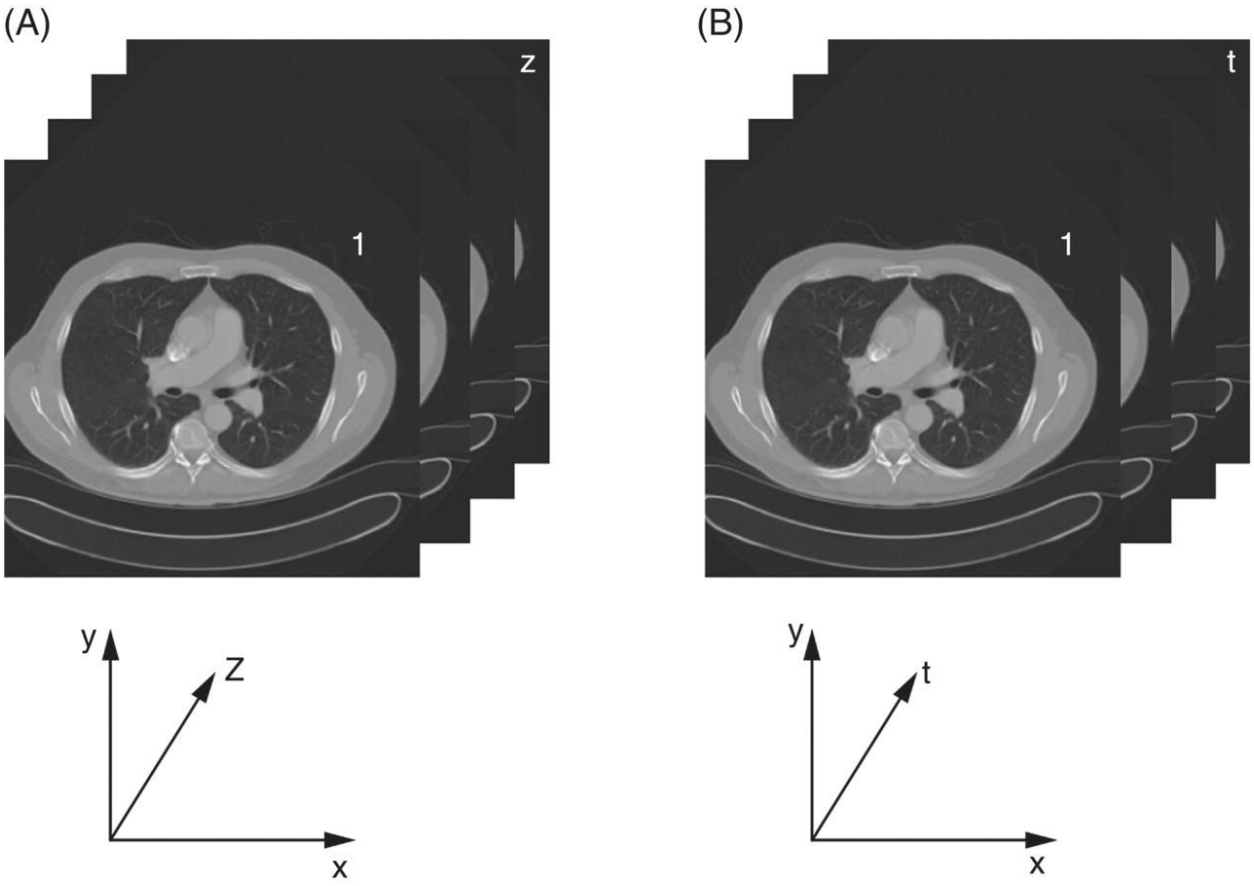

Figure 2.14 Two 3-D image coordinate systems: (A) 3-D spatial image set with z as the third dimension. Images from 1 to z show the anatomical changes of the cross-sectional chest CT images; (B) a 3-D temporal image set with t (time) as the third dimension. Images from 1 to t show the same anatomy as image 1; the difference would be, for example, the flow of the contrast media injected to the patient from time 1 to t.

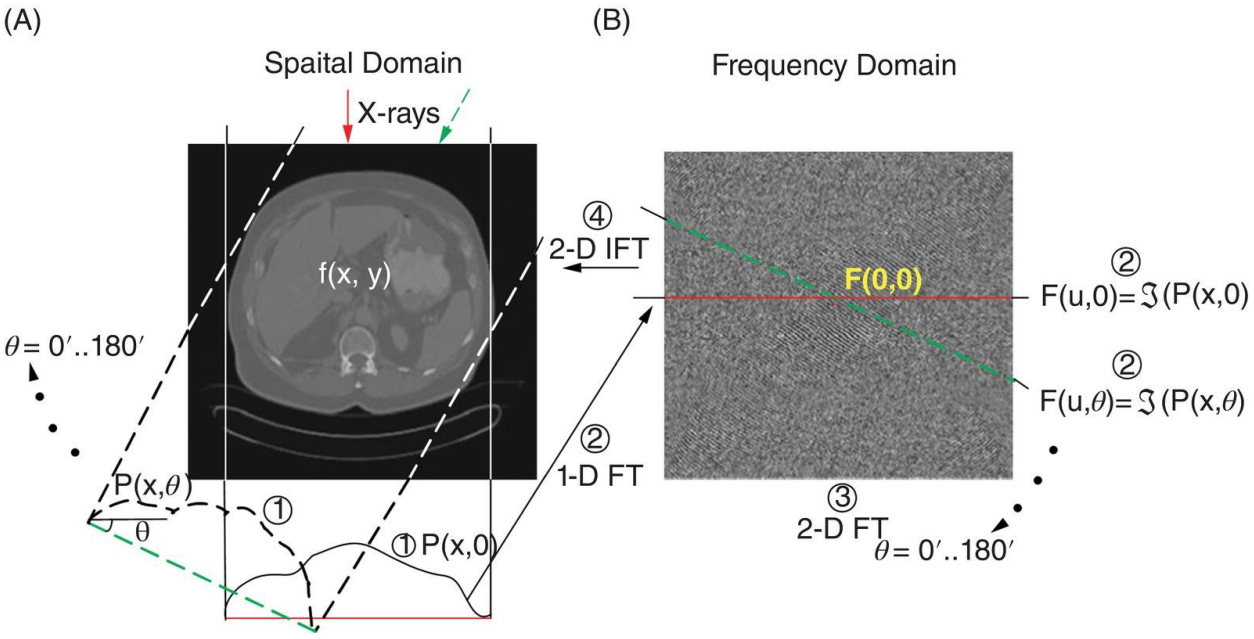

Figure 2.15 Principle of the Fourier transform (FT) projection theorem for image reconstruction from 180-degree 1-D projections from input energy. (A): Spatial domain: A CT image to be reconstructed from 1,2, …,180 1-D projection energy data, f(x,y) is the image to be reconstructed. (B): Frequency domain: F(0, 0) is the center of the 2-D FT; low-frequency components are located at the center region, and high-frequency components are at periphery. P(x,θ) Left: x-ray projection at angle θ (green), x is the distance from left to right of the projection. F(u, θ): 1-D Fourier transform of P(x, θ); red and green are corresponding projections in the spatial domain, and its 1-D Fourier transforms (1-DF) in the frequency domain, respectively. IFT: inverse Fourier transform.

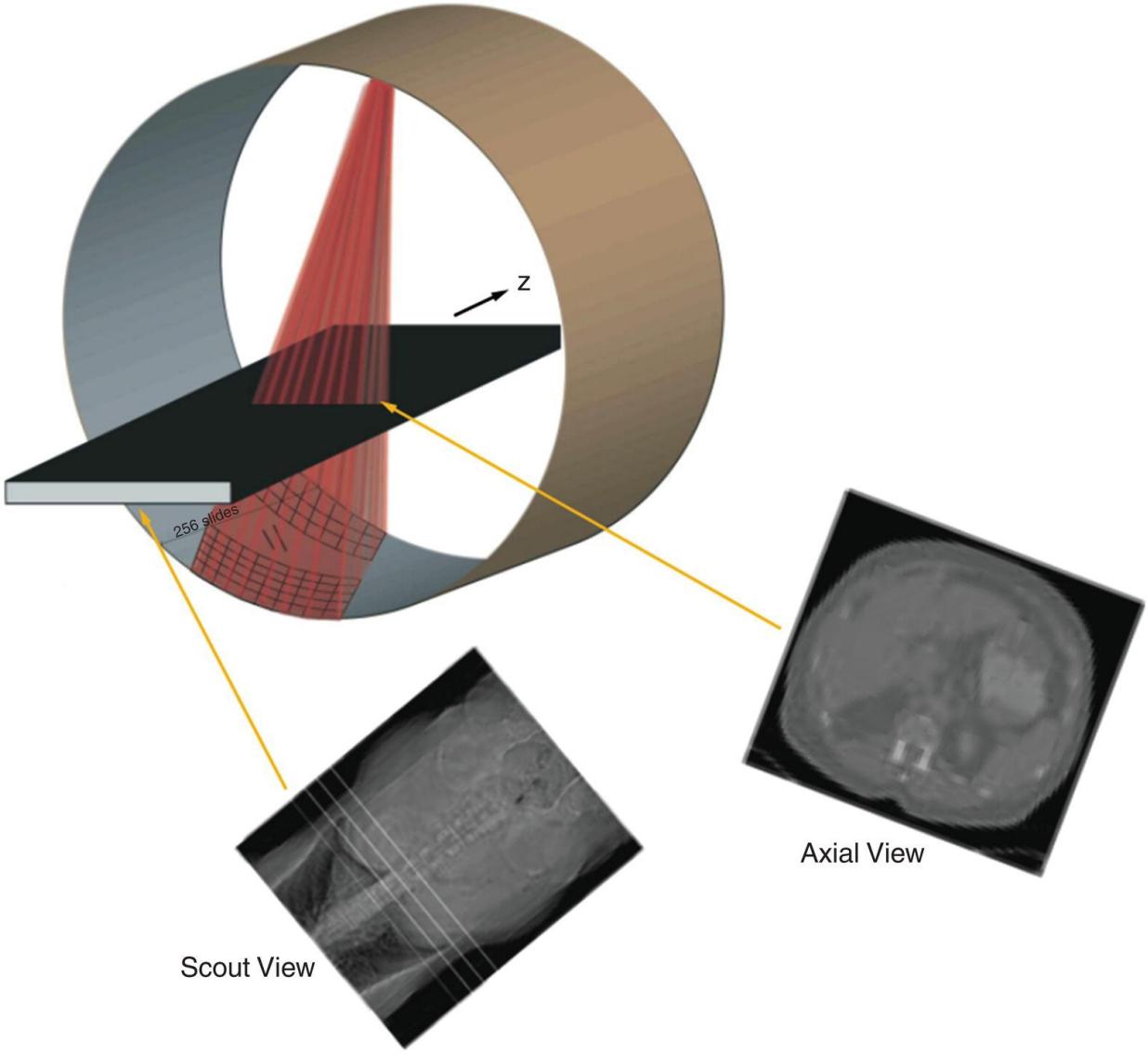

Figure 2.16 Geometry of the multi-slice computed tomography produces 3-D CT images. The patient axis (parallel to the bed) is in the *z*-direction. The x-ray source (orange), shaped as a collimated cone beam, rotates continuously around the *z*-axis by 360 degrees, in sync with the patient's bed movement in the *z*-direction. The detector system is a combination of detector arrays on a concave surface (not to scale) perpendicular to the x-ray beams. The number of slices per 360-degree rotation is determined by two factors: the number of detector arrays (channels) in the *z*-direction and the method used to recombine the cone beam projection data into transverse sectional projections (Figure 2.15). The standard reconstructed images are in transverse (axial) view perpendicular to the *z*-axis; the projection raw data can also be recombined to reconstruct sagittal, coronal, or oblique view images. If the cone beam does not rotate while the patient's bed

is moving, the reconstructed image is equivalent to a digital projection image (scout view).

2.3.2 Transmission X-Ray Computed Tomography (3D-CT)

2.3.2.1 Convention Transmission X-Ray Computed Tomography (CT)

A CT scanner consists of a scanning gantry housing a continuous rotating x-ray tube aligned to a full 180- to 210-degree angle detector unit, and synchronizing them with a movable bed that can receive a specific number of cross-sections of the patient with the scanning gantry. The gantry provides a fixed relative position between the x-ray tube and the detector unit with the section of the patient to be scanned. A scanning mode is the procedure of collecting more than 180-degree x-ray attenuation profiles (projections) from a transverse (cross) section of the body. From these projections, the CT scanner's computer program or back-projector hardware reconstructs the corresponding cross-sectional CT images of the body.

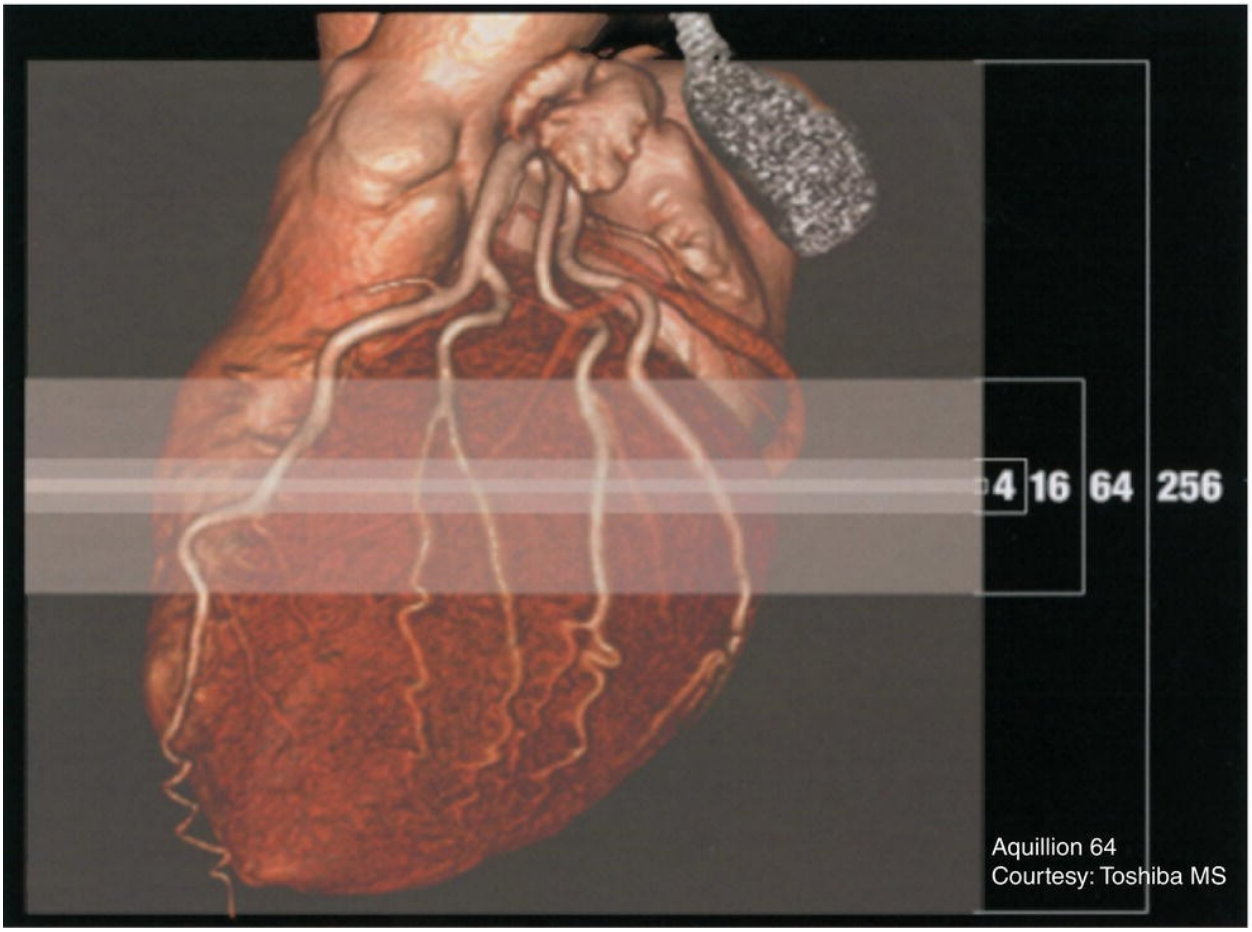

Figure 2.17 The extent of *z*-dimensional scanning of the entire human anatomy with variable multi-slice scans. In this case, array detectors can range from 4, 16, 64, … 256, or even more are possible images in one scan. For example, in the 256 array detector system, a certain number rotations of the x-ray system can capture the entire heart (256 mm), minimizing the possible heart beat artifacts. Another example, a whole-body CT scanner can also scan the body of the patient from head to toe, with the scanner continuing rotating as the bed moving in the *z*-direction (see Figure 2.16 for the *z*-direction).

2.3.2.2 Whole Body CT Scan

Figure 2.17 shows the extent of *z*-dimension scanning of the human anatomy by variable multi-slice scanners currently in the commercial market, with array detectors ranging from 4, 16, 64, to 256. In the 256 array detector system, for example, one full rotation of the x-rays can almost capture the entire heart (256 mm), so this multi-slice architecture can minimize the possible image artifacts due to the heart beat; whereas, in the 16 mm architecture, 16 rotations are required, which will take more time to scan, and hence the chance of more heart movement during the scan.

The scanning speed of the multi-slice CT scanner allows for fast whole body CT, important for studying a patient's trauma in an emergency situation. It will also allow a healthy patient to obtain a routine whole body check-up. The patient's whole body can be scanned from head to toe, when the contiguous CT images are to be used for screening review. In PACS and imaging informatics, such a whole-body scan will result in a very large dataset for a full examination and will require special considerations for archiving and data transmission.

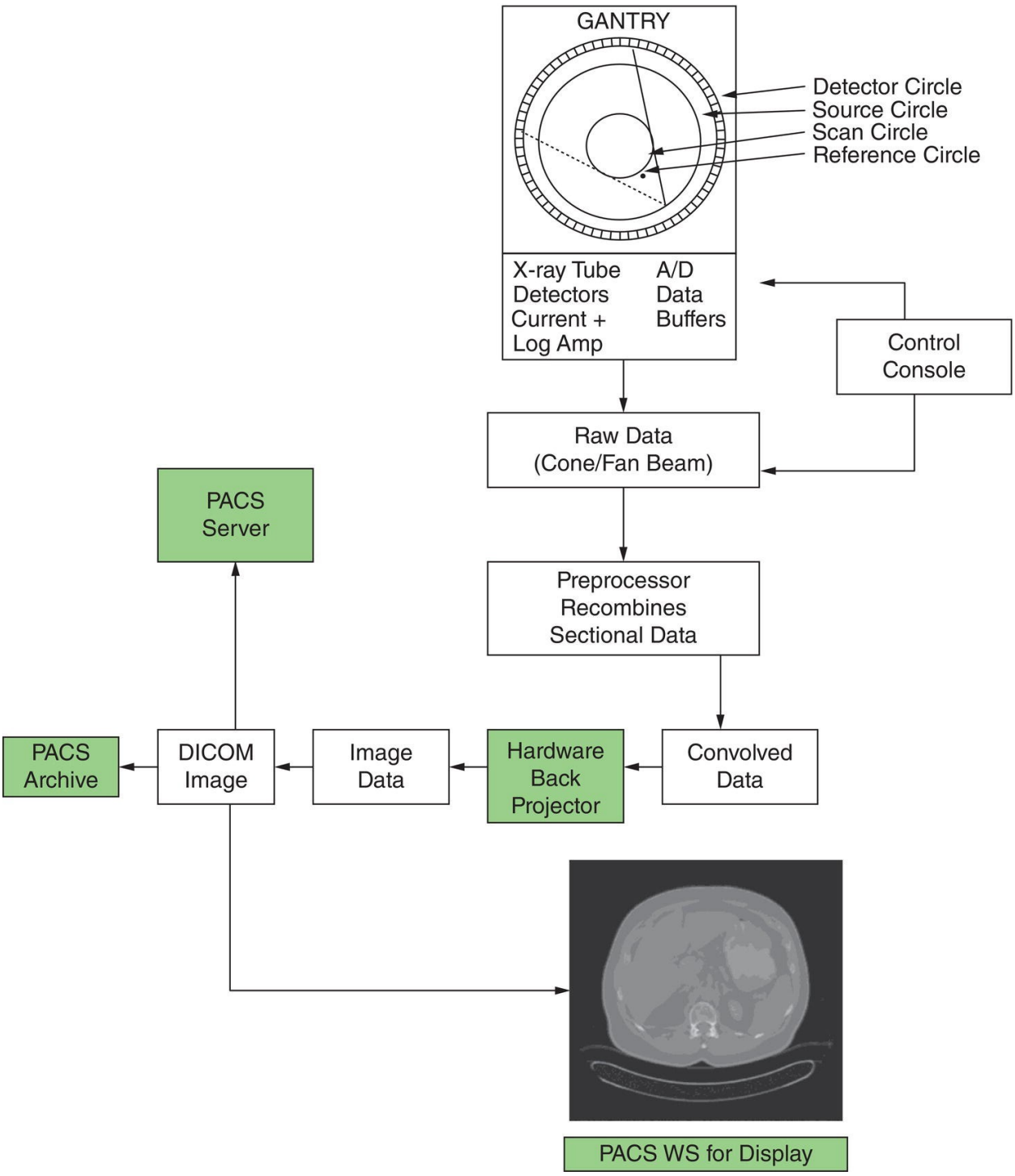

Figure 2.18 Data flow components of an X-ray CT scanner. The scanning and data collection times, in general, are shorter than the image reconstruction time. A hardware back-projector unit (green) is used to speed up the reconstruction time. A/D: analog to digital; WS: workstation.

2.3.2.3 Components and Data Flow of a 3-D CT Scanner

Figure 2.18 shows the main components and the data flow in one of today's CT whole-body scanners, including a gantry housing the x-ray tube, the rotating detector system, signal processing/conditioning circuits, a front-end preprocessor unit for the cone- or fan-beam to correct and recombine data to transverse-sectional projection data, a high-speed computational processor, a hardware back-projector unit, and a video controller for displaying images. The CT number, Hounsfield number, or pixel/voxel value, represents the relative x-ray attenuation coefficient of the tissue in each pixel/voxel of the CT image, defined as:

$$\text{CT number} = \mathrm{K}(\mu - \mu_w)/\mu_w$$

where μ is the attenuation coefficient of the material under consideration, μ_w is the attenuation coefficient of water, and K is a constant set by the manufacturer.

CT numbers in a CT image can be used to compute DICOM-based medical imaging informatics data and computer-aided diagnosis (see later chapters, in particular, Chapters 16, 17, and 18.).

2.3.2.4 CT Image Data

2.3.2.4.1 Isotropic Image and Slice Thickness

Current multi-slice or spiral CT scanners can configure up to 256 or even 512 detectors in an array. In these scanners, multiple slices of 3-D data can be acquired simultaneously for different detector sizes; and 0.75-, 1-, 2-, 3-, 4-, 5-, 6-, 7-, 8-, and 10-mm slice thickness can be reconstructed. If the *x* and *y* resolutions of the pixel are the same as the slice thickness, then the pixel is called a voxel, which is isotropic. So voxels from these transverse, sagittal, and coronal images are isotropic after the multi-planner reconstruction.

2.3.2.4.2 Image Data File Size

Consider a standard chest CT image examination, which covers between 300 and 400 mm generating from 150 to 200 2-mm slices, and up to 600 to 800 0.5-mm slices, depending on the slice thickness, or data sizes from 75 MB up to 400 MB. A whole-body CT scan for screening can produce up to 2500 images or 1250 MB (1.25 GB) of data, with each image being 512 × 512 × 2 bytes.

2.3.2.4.3 CT Image Data Flow and Image Post-processing

Most current CT image post-processing (discussed in Chapters 6 to 22) uses

DICOM-based CT raw data. If these CT images are needed for post processing, the slice thickness reconstructions are performed on the raw data. Sometimes a CT scanner can also have a cone-beam x-ray combined detector system. Once the set of images is acquired in DICOM format (Chapter 4), any future post-processing would also be in DICOM data. This includes multi-planar reconstruction of transverse, sagittal, coronal, and oblique slices. Raw data can also be saved for future reconstruction of the different slice thicknesses. The following demonstrate two examples, Figures 2.19A,B,C show CT angiography , and Figure 2.20 depicts 3-D volume rendering post-processing images, A: thoracic, and B: abdominal.

The reconstruction process is time consuming. Some scanners feature a secondary computer that shares the database and functions as an acquisition host computer. This secondary computer can perform the same post-processing functions, while the scanner continues acquiring new patient data from scanning. This secondary computer also can perform image transmission through the network to PACS or another DICOM destination (e.g. highly specialized 3-D processing workstation), alleviating the acquisition host computer from these functions and thus improving throughput of the system scanning.

(A)

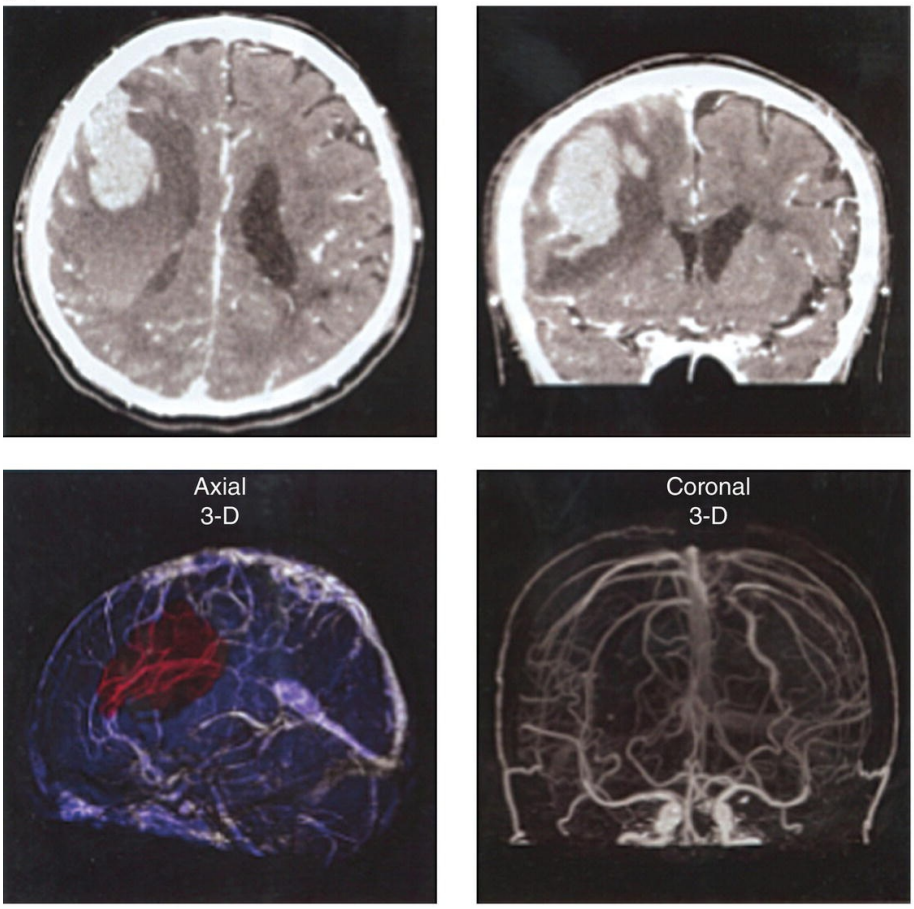

A large right parietal hematoma with edema
135 kV, 130 mAs
Isotropic 0.5 mm

Aquillion 64
Courtesy: Toshiba MS

(B)

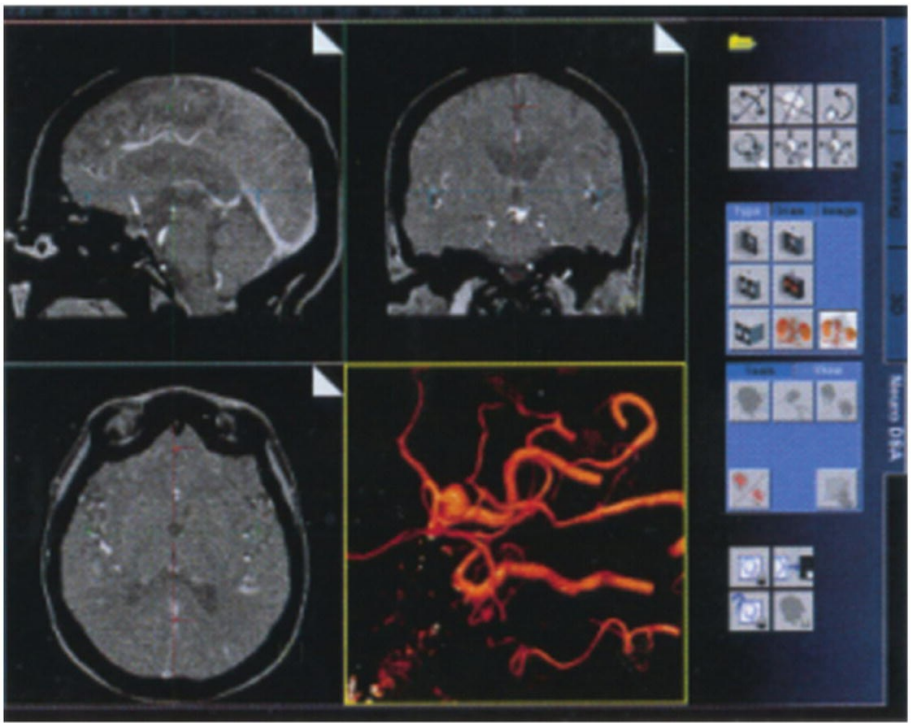

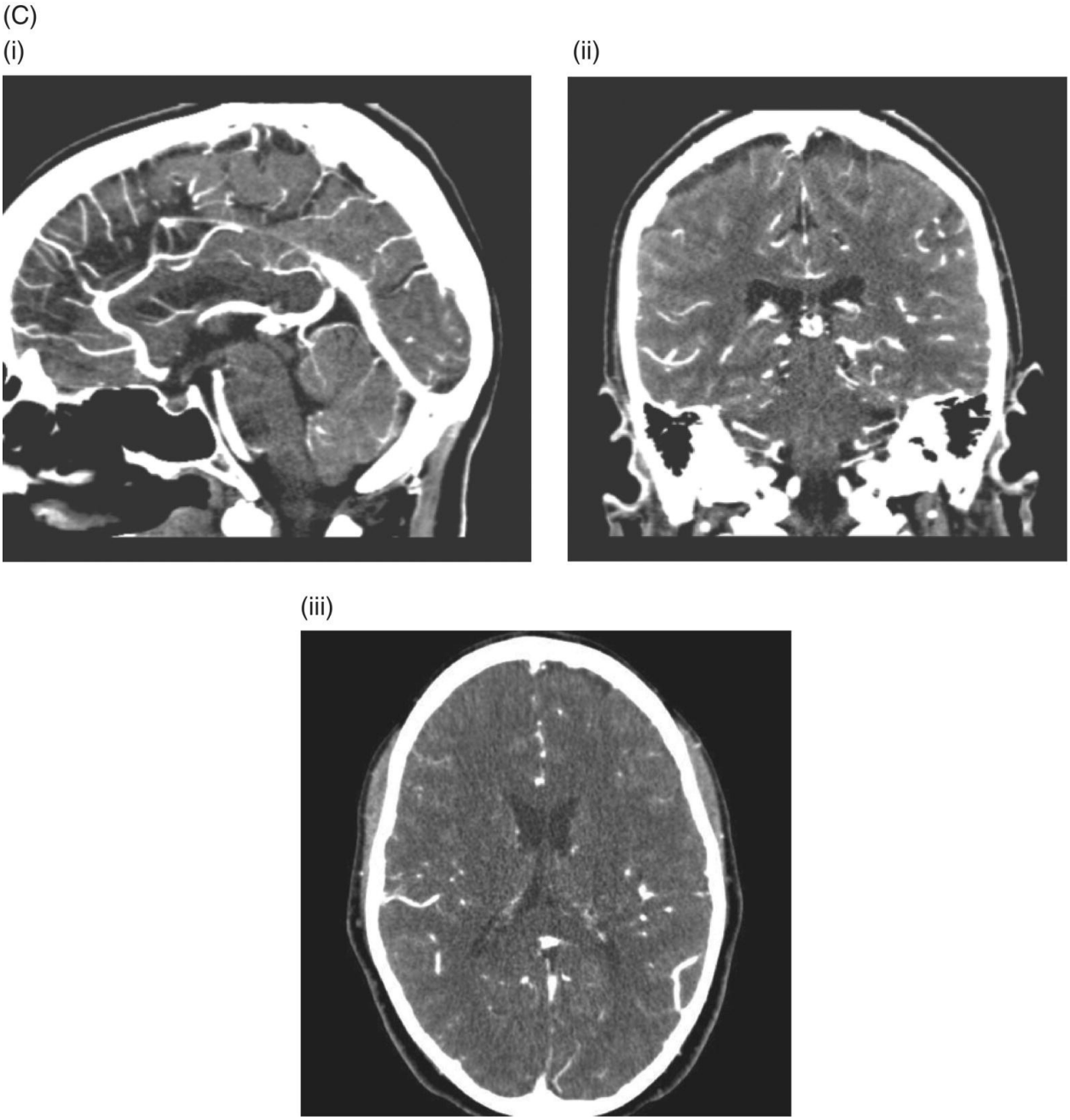

Figure 2.19 (A) 3-D multi-slice CT showing a large right parietal hematoma with edema: (upper left) Transverse; (right) coronal. The bottom images are CT angiograms showing the 2-D sagittal view (left) and the coronal view (right) extracted from the 3-D CT 0.5-mm isotropic dataset.

(courtesy of Toshiba Medical Systems)

(B) 3-D neurodigital subtraction angiogram: (top two and left bottom) sagittal, coronal, and transverse contrast CT images; (bottom right) 3-D angiogram

obtained by tissue and bone subtraction from the 3-D CT images.

(courtesy of Siemens Medical Systems)

(C) Multi-planar reconstruction CT images. The 16-slice helical CT of the head and neck was obtained during a bolus of intravenous contrast administration. Volumetric data were then transferred to a Vitrea 3-D workstation for post-processing, including 3-D volumetric rendering and multiplanar reconstructions (MPR) in the (i) sagittal, (ii) coronal, and (iii) transverse planes. This study was conducted in an adult female with transient ischemic attacks. The patient was found to have significant unilateral internal carotid artery stenosis due to atherosclerotic plaque.

(courtesy of Dr P. Moin)

(A)

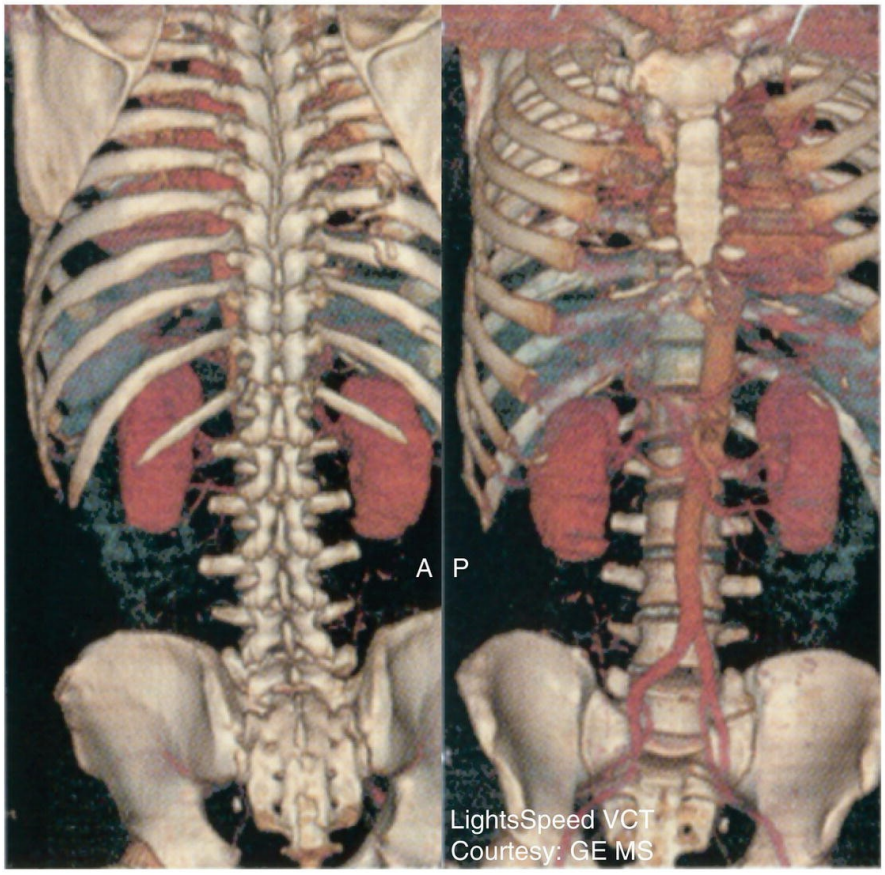

Cage trauma volume render anterior (A) and posterior (P) views reveal fractures posterior 7th–10th ribs.

(B)

Infra-renal abdominal aortic aneurysm with mural thrombus
135 KV, 175 mAs, 0.5 s/rot
325 mm scan range
12 s.

Figure 2.20 (A) 3-D CT dataset can also be used to produce 3-D volume rendering images. Left and right show the anterior–posterior (A–P) and posterior–anterior (P–A) views of the thoracic cage, revealing fractures of ribs 7–10 in the P–A view (courtesy of GE Medical Systems). (B) 3-D CT abdominal dataset obtained by using a 64 multi-slice scanner showing 3-D volume rendering of bone, blood vessels, and kidneys, and in particular, an infrarenal abdominal aortic aneurysm with mural thrombus. The scan protocol used was a 135 kVp, 175 mAs, 325-mm scan range taking 12 seconds (courtesy of Toshiba Medical Systems).

2.3.3 Emission Computed Tomography (ECT)

ECT has many characteristics in common with transmission x-ray CT, but the main difference is the radiation source used for imaging. In ECT, the radionuclide administered to a patient in the form of radiopharmaceuticals, either by injection or by inhalation, is used as the emission energy source inside the body instead of an external x-ray beam. Basically ECT consists of nuclear medicine scanning, as discussed in Section 2.3.7.

Selecting a dose-efficient detector system for an ECT system is important for two reasons. First, the quantity to be measured in ECT involves the distribution of the radionuclide throughout the body, and this quantity changes with time as a result of the flow and biochemical kinetics in the body. Therefore, all necessary measurements must be made in as short a period of time as possible. Second, the amount of isotope administered has to be minimal to limit the dose delivered to the patient. Therefore, detector efficiency is a crucial consideration in selecting the detector system.

The basic principle of image reconstruction is the same in ECT as in transmission CT, except that the signal in ECT is composed of γ-rays that become attenuated during their flight from the emitting nuclei to the detectors. To minimize the contribution from scattered radiation, the ECT uses the characteristics of monoenergetic energy in setting up a counting window to discriminate the lower-energy scattered radiation from the high-energy primary radiation. There are two major categories in ECT: SPECT and PET.

2.3.3.1 Single Photo Emission CT: Rotating Camera System

There are several designs for SPECT, but only the rotating gamma camera system is discussed here (Figure 2.21), because it is commercially available. In a

rotating camera system, the gamma camera is rotated around the object, and the multiple 2-D images series are reconstructed and stored for post-processing. The camera is composed of a large scintillation crystal of diameter 30 to 50 cm and a number of photomultiplier tubes (PMTs) attached to the opposite surface of the crystal. When a γ-ray photon interacts with the crystal, the light generated from the photoelectric effect is uniformly distributed among the neighboring PMTs. By measuring the relative signal of each PMT, the camera can locate the interactive position for each event. The drawback of this system is the difficulty in maintaining a uniform speed of rotation with the rather heavy camera. Figure 2.21 shows the schematic of a SPECT.

Since a typical tomographic study takes 15–20 minutes to accomplish, it is important to maintain patient immobilization. To provide the best sensitivity and resolution, it is desirable to have the camera as close to the patient as possible. Since the dimension of body width is greater than body thickness, an elliptical orbit of rotation of the camera tends to produce a higher-resolution image. Different collimators are used for different applications. In general, the reconstruction algorithm must be modified and the attenuation values corrected for each type of collimator. For example, a single-plane converging collimator will need a fan-beam reconstruction algorithm, and a parallel collimator will need a parallel-beam algorithm.

Today, SPECT is mostly used for studies of the brain, including brain blood volume (^{99m}Tc-labeled blood cells), regional cerebral blood flow (^{123}I-labeled iodoantipyrine or inhaled ^{133}Xe), and physiological condition measurements.

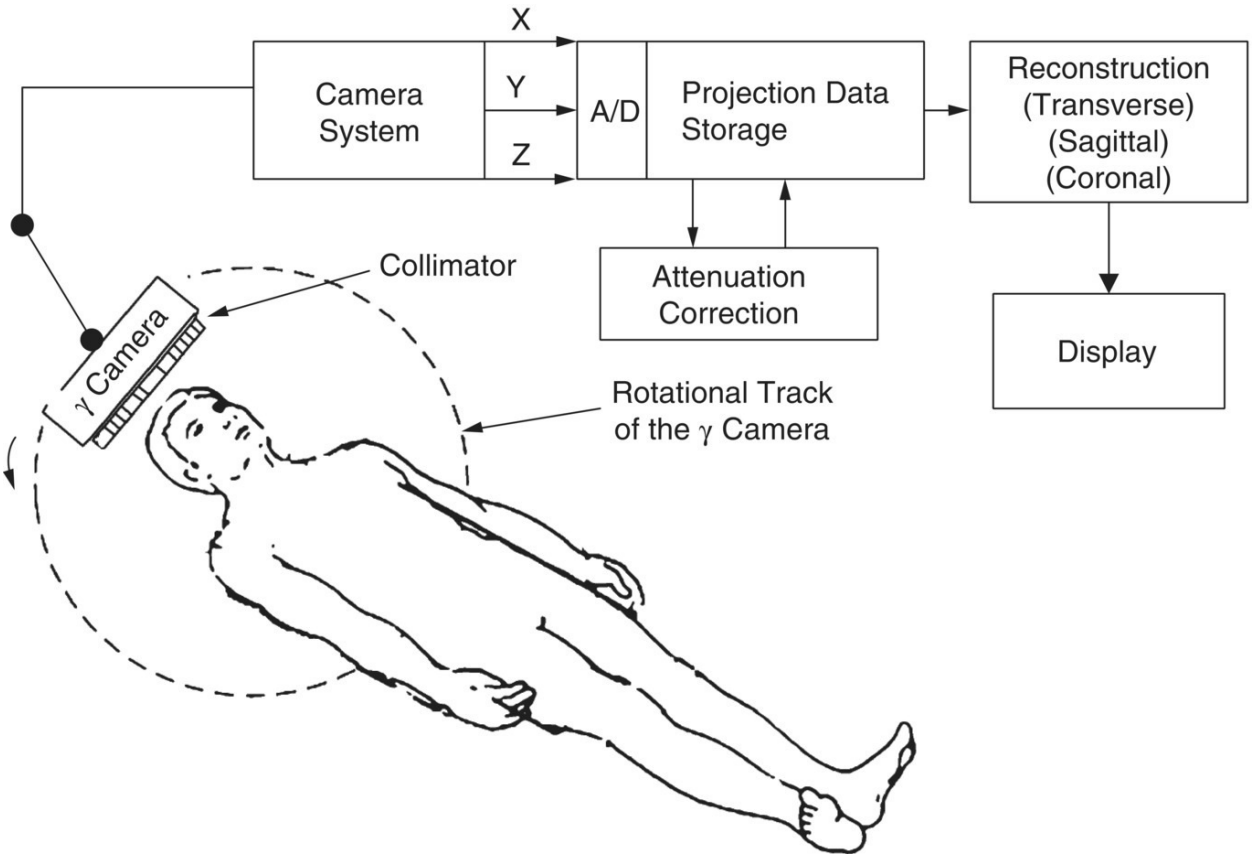

Figure 2.21 Schematic of single photon emission CT (SPECT). Refer to Figure 3.24 for nuclear medicine scanning.

2.3.3.2 Positron Emission Tomography (PET)

PET uses a positron instead of a single photon as the radionuclide source. The positron emitted from the radio nuclide is rapidly slowed down and annihilated, yielding two 511 keV γ-ray photons oriented at 180 degrees to each other. The PET system utilizes this unique property of positrons by employing a detector system that requires simultaneous detection of both photons from annihilation, and thus it avoids the need for collimators. So a pair of detectors is placed at the opposite sides of the patient, and only events that are detected in coincidence are recorded. Simultaneous detection of two annihilation photons by the detector system thus signals the decay of a positron anywhere along a line connecting the two points of detection (Figure 2.22). With this multiple coincidence logic, PET systems have higher sensitivity than SPECT.

The correction of attenuation is easier in PET than in SPECT, due to the probability that the annihilated photons will reach both detectors simultaneously as a function of the thickness of the body between the two opposite detectors.

The correction factor can be obtained by means of a preliminary scan of the body with an external γ-ray source, or by means of a correction table based on a simple geometric shape resembling the attenuation medium to be used. Patient movements, oversimplified geometric shape, and non-uniform medium can cause errors in the correction of attenuation.

Thallium-drifted sodium iodide NaI (T1), bismuth germanate (BGO), and cesium fluoride (CsF) are some materials used for detector. Because of the high energy of the annihilation photon, detector efficiency is a crucial factor in selecting a scintillator for a PET system. Bismuth germanate is the most prominent PET detector material, because of its high detection efficiency, which is due to its high physical density (7.13 g/cm^3) and large atomic number (83), and because of its non-hygroscopicity, which makes for easy packing and minimal afterglow.

A typical whole-body PET scanner consists of 512 BGO detectors placed in 16 circular array banks, with 32 detectors in each bank. During the scanning, the system is capable of wobbling to achieve higher resolution via finer sampling. The image spatial resolutions for the stationary and wobbled modes are 5–6 mm and 4.5–5 mm, respectively.

In the whole-body imaging technique, PET produces tomographic images of the entire body, with equal spatial resolution in the three orthogonal image planes. Since the body longitudinal axis is, in general, longer than the other two axes, the patient bed is required to advance during the scanning process to permit the entire body length to be scanned. A sophisticated data acquisition system in synchrony with the bed motion is necessary to monitor the data collection process. This data collection scheme is similar to that of the multi-slice CT. Figure 2.23A shows the transverse, coronal, and sagittal planes of a PET scan of the brain. Figure 2.23B shows images of the transverse, coronal, and sagittal orthogonal planes, as well as the anterior–posterior projection image of the whole-body PET scan with a fluoride ion isotope ($^{18}F^-$).

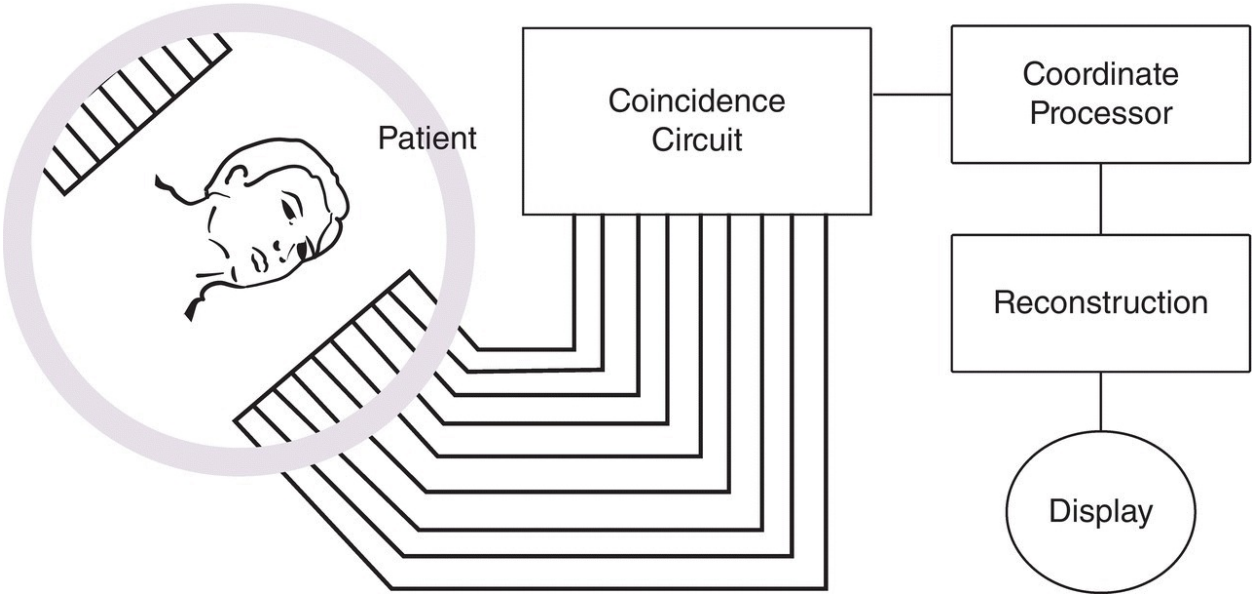

Figure 2.22 Block diagram of a positron emission tomography (PET) system showing two array banks of detectors.

(A)

(i)

(ii)

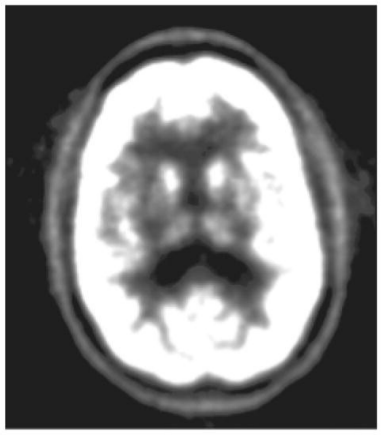

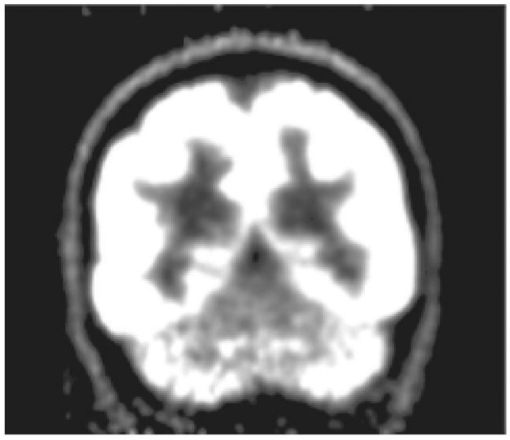

(iii)

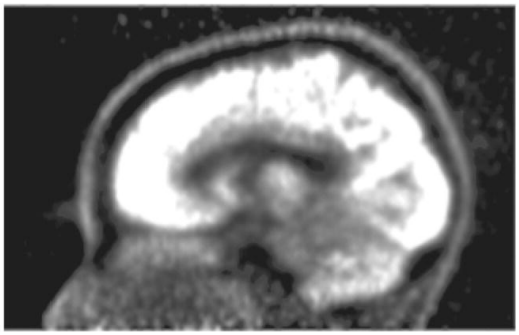

(B)

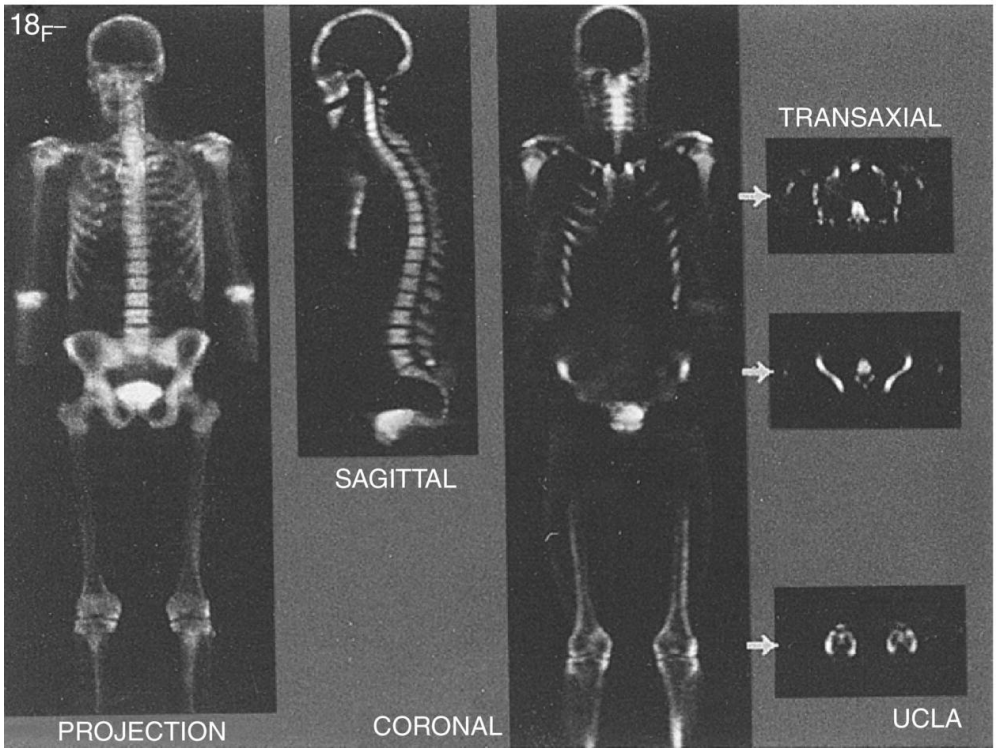

Figure 2.23 (A) Positron emission tomography (PET) study of the brain. 18Ffluorodeoxyglucose (18 F-FDG) was administered to the patient, and approximately 60 minutes later the patient was positioned on a PET scanner and images (i: transverse, ii: coronal, and iii: sagittal) were obtained from the skull apex to the skull base. Causes of cognitive impairment, such as Alzheimer's disease, are among the indications for brain 18 F-FDG PET (courtesy of Dr P. Moin). (B) Images of transverse, coronal, and sagittal orthogonal planes (right to left), as well as the posterior–anterior projection image (leftmost) of the whole-body PET image with fluoride ion ($18\,F^-$).

(courtesy of Dr R.A. Hawkins)

2.3.4 Three-Dimensional Ultrasound Imaging (3-D US)

Compared with other imaging modalities, 2-D US imaging has several limitations; among them are:

1. 2-D US images do not provide a fixed origin that can pinpoint the position of the anatomy and the pathology; and
2. 2-D US images cannot measure the exact volume of a tumor.

3-D US can be used to remove these weaknesses. 3-D US uses a high data rate (15–60 images per second) to collect tomographic plane (or oblique plane) images under the operator's control of the position and orientation of the images. If an array of ultrasound transducers with a fixed center of translation and/or rotation is used to scan the object of interest, the resulting echo signals are similar to those of a sectional CT image. The scanning modes in 3-D US imaging include linear translation 3-D scanning, tilt 3-D scanning, and 3-D motorizing scanning (Figure 2.24A). These 2-D oblique plane images can be recombined according to the scanning mode and direction, forming a 3-D US image set. Such 3-D US images can be used for breast imaging, obstetrics imaging for the fetus, and carotid artery scanning, among other types of scans. Figure 22.4B depicts a 3-D rendering of a 26-week fetal face from a set of 3-D US images.

Another type of 3-D US imaging technique is the endovascular 3-D US, in which a miniature US transducer is inserted into the vascular lumen to perform 3-D US imaging. An example is the intravascular ultrasound (IVUS) technology, which is used to identify blockages in arteries, most commonly near the heart. The technique involves inserting a catheter into the circulatory system through the thigh, and up to the heart, using ultrasound signals to obtain a 3-D map of the

arteries.

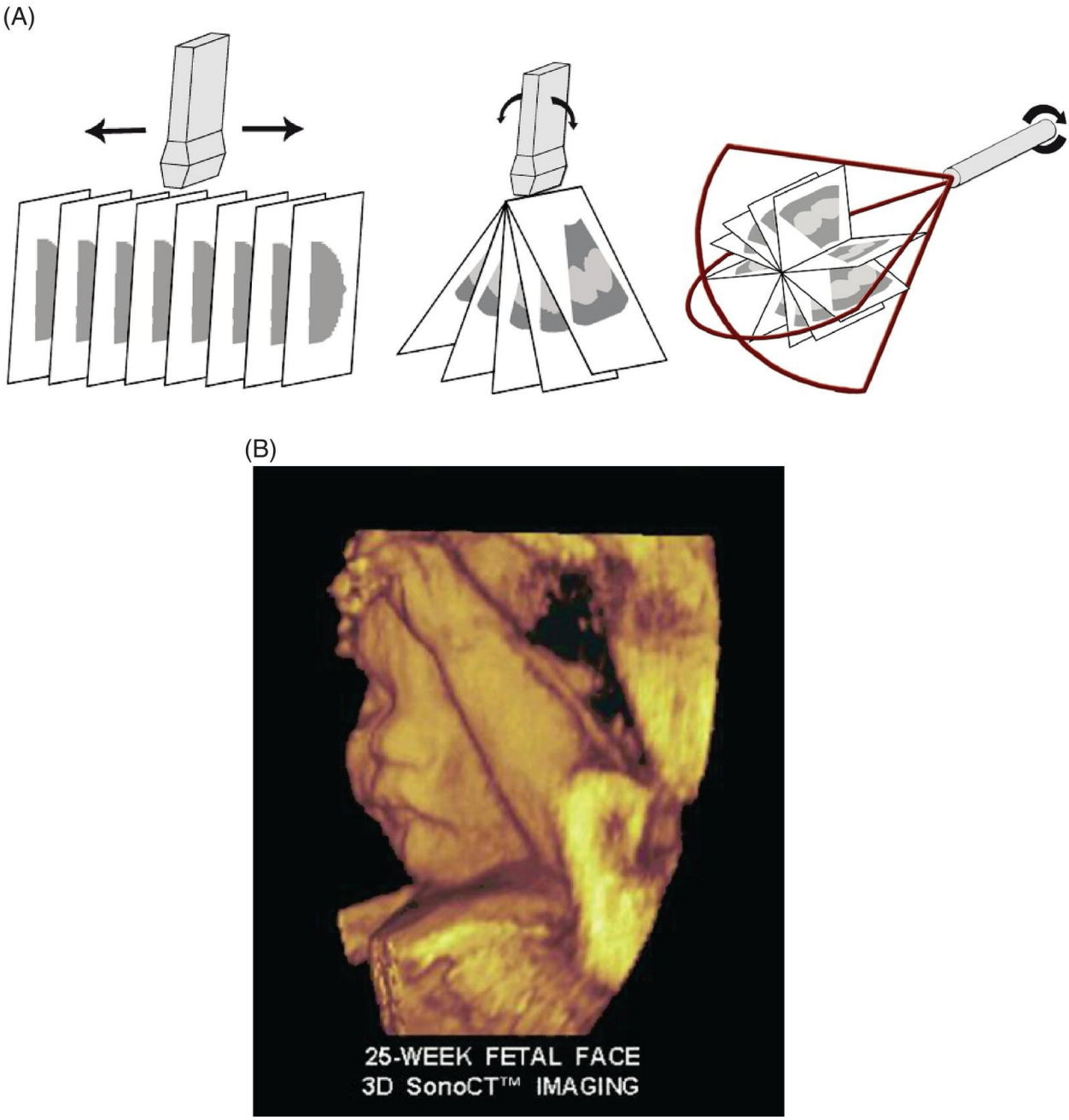

Figure 2.24 (A) Three scanning modes of 3-D US scanning: (left) linear translation; (middle) tilt scanning; and (right) rotational scanning. (B) 3-D ultrasound image of a 25-week fetal face.

(courtesy of Philips Medical Systems: http://www.medical.philips.com/main/products/ultrasound/assets/images/imagelibrary/3d-2295-H5-2–OB-3D.jpg)

2.3.5 Magnetic Resonance Imaging (MRI)

2.3.5.1 MRI Basics

The MRI modality forms images of objects by measuring the magnetic moments of protons using radio frequency (RF) and a strong magnetic field. Information concerning the spatial distribution of nuclear magnetization in the objects is determined from RF signal emission by these stimulated nuclei. The received signal intensity is dependent on five parameters: hydrogen density, spin–lattice relaxation time (T1), spin–spin relaxation time (T2), flow velocity (e.g. arterial blood), and chemical shift.

MRI collects spatial (anatomical) information from the returned RF signals through a filtered back-projection reconstruction or a Fourier analysis and displays it as a 2-D section or a 3-D volume of the objects. There are some distinct advantages to using MRI over other modalities (e.g. CT) in certain types of examination:

1. The interaction between the static magnetic field, RF radiation, and atomic nuclei is free of ionizing radiation; therefore the imaging procedure is relatively noninvasive compared with the use of other ionizing radiation sources.
2. The scanning mechanism is either electrical or electronical, requiring no moving parts to perform a scan.
3. It is possible to obtain 2-D slices of the coronal, sagittal, and transverse planes, and any oblique section, as well as a 3-D data volume.
4. MRI can use various pulse sequences for imaging to enhance different tissues under consideration.

The two disadvantages at present in MRI, as compared with CT images, are that MRI, in general, has lower spatial resolution, whereas CT has better image quality in some body regions. In current clinical practice, MRI and CT have complementary use, each depending on the case examination under investigation.

2.3.5.2 Magnetic Resonance Image Production

Figure 2.25 shows the components for the production, detection, and display of MR signals in a simplified block diagram of a generic MRI system:

1. A magnet to produce the static magnetic B_0 field;

2. RF equipment to produce the magnitude of the RF magnetic field (transmitter, amplifier, and coil for transmitting mode) and then detect the free induction decay (FID) of the nucleus, which is the response of the net magnetization to an RF pulse (coil for receiving mode, preamplifier, receiver, and signal demodulator);
3. x, y, and z gradient power supplies and coils providing the magnetic field gradients needed for encoding spatial position;
4. The electronics and computer facility to orchestrate the whole imaging process (control interface with computer), convert the MR signals to digital data (A/D converter), reconstruct the image (computer algorithms), and display it (computer, disk storage, image processor, and display system).

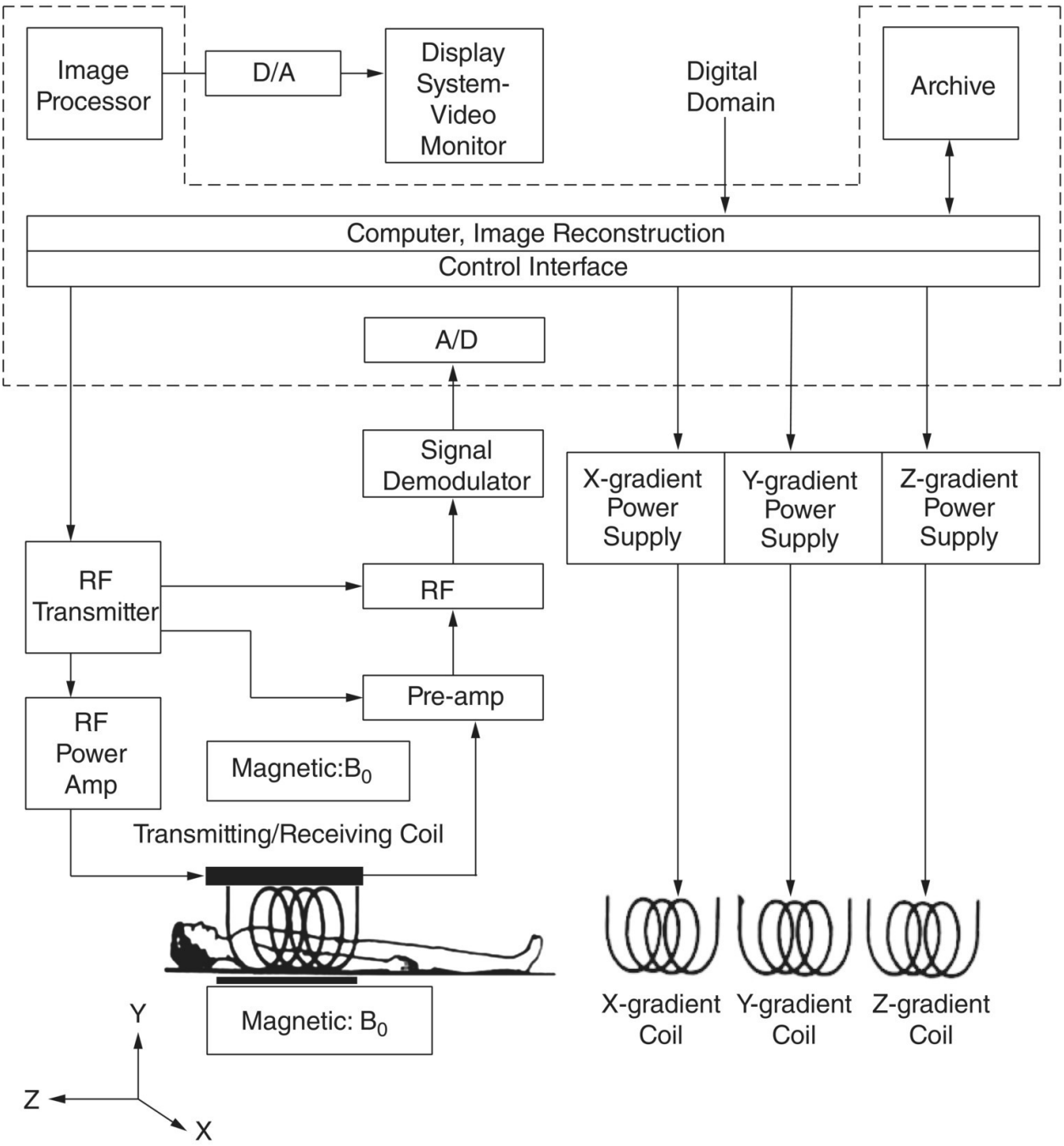

Figure 2.25 Block diagram of a generic magnetic resonance imaging (MRI) system. Dotted line separates the digital domain from the MR signal generation. A/D: analog to digital; D/A: digital to analog; RF: radio frequency.

2.3.5.3 Steps in Producing an MRI

An MRI is obtained by using a selected pulse sequence that perturbs the external magnetic field B_0 (e.g. 1.5 and 3.0 Tesla). This set of images is named based on

the selected pulse sequence. Some useful pulse sequences in radiology applications are therefore spin echo, inversion recovery, gradient echo, and echo planar, as each pulse sequence highlights certain chemical compositions in the tissues under consideration.

A spin-echo pulsing sequence is used to illustrate how an MRI is produced. First, the object is placed inside an RF coil situated in the homogeneous portion of the main magnetic field, B_0. Next, a pulsing sequence with two RF pulses is applied to the imaging volume (hence spin echo). At the same time, a magnetic gradient is applied to the field B_0, in order to identify the relative position of the spin echo free-induction-decay (FID) signals. Note that FID is composed of frequency components. The FID signal is demodulated from the RF signal, sampled with an analog-to-digital converter, and stored in a digital data array for processing. This set of data is analogous to one set of projection data in CT. After the repetition time has elapsed, the pulsing sequence is applied and a new FID is obtained and sampled repeatedly with alternate gradient magnitudes until the desired number of projections is acquired.

During and after data collection, the selected tomographic reconstruction algorithm described in Section 3.1, either the filtered back-projection or 2-D fast Fourier transform (inverse FT), is performed on all the acquired projections (digital FID data). The result is a spin-echo image of the localized magnetization in the spatial domain. The pixel values are related to the hydrogen density, relaxation times, flow, and chemical shift. This procedure can be represented as follows:

$$\text{Frequency spectrum} \xrightarrow{\text{FT}} \text{FID} \xrightarrow{\text{Inverse FT}} \text{Spatial distribution (MR image)}$$

This digital image can then be archived and displayed. Figure 2.26 illustrates the data flow in forming an MRI and Figure 2.27 shows a commercial 3 T MRI scanner through the window of a magnetic field shielded MRI examination room.

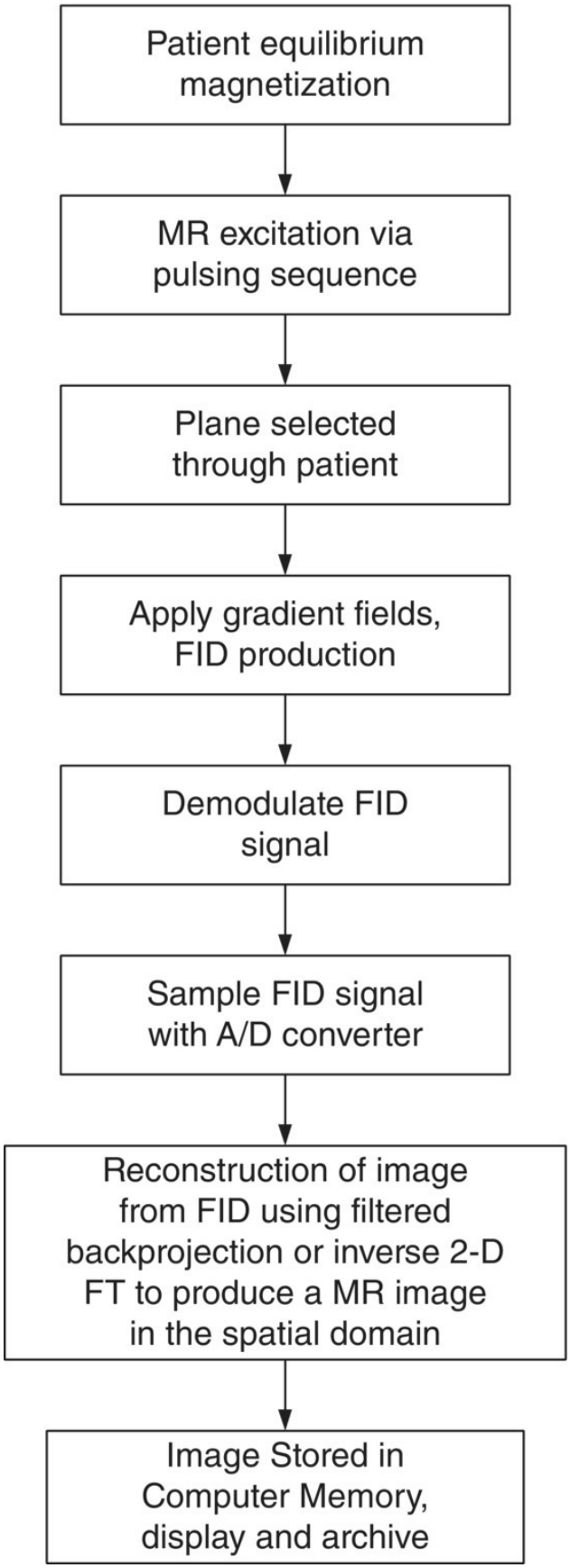
Patient equilibrium magnetization
MR excitation via pulsing sequence
Plane selected through patient
Apply gradient fields, FID production
Demodulate FID signal
Sample FID signal with A/D converter
Reconstruction of image from FID using filtered backprojection or inverse 2-D FT to produce a MR image in the spatial domain
Image Stored in Computer Memory, display and archive

Figure 2.26 Data flow of forming an MR image. 2-D: two-dimensional; FID: free induction decay; FT: Fourier transform.

Figure 2.27 Clinical 3 T MR imaging system in a magnetic shielded room at the Health Science Campus, USC.

2.3.5.4 MR Imaging (MRI)

The MR scanner can reconstruct transverse (similar to CT), sagittal, coronal, or any oblique plane images (Figure 2.28), and 3-D images of other body regions, for examples, 3-D fetus (Figure 2.29) and 3-D breasts (Figure 2.30). Besides reconstructing images in various planes, the MR scanner can selectively emphasize different MR properties of various parts of the anatomy by selecting the relative position of frequency under consideration from the FID. The most commonly used are the T1 and T2, proton density MR images, as well as other combinations. The challenge of MRI is to decipher the abundance of information in FID (ρ_H, T1, T2,) flow velocity, and chemical shift, and to adequately display

them for different types of images.

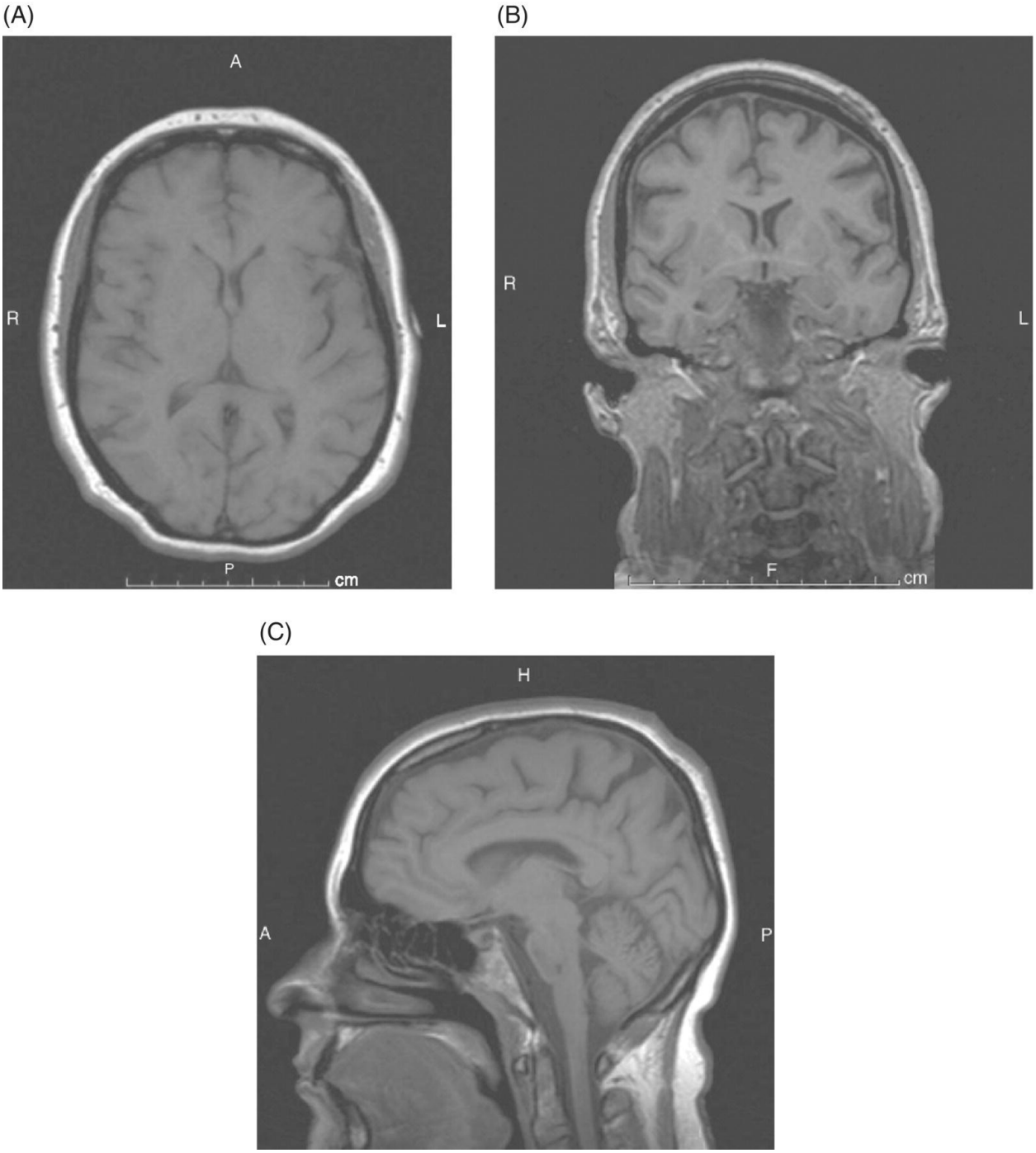

Figure 2.28 T1 weighted (A) transverse, (B) thin section coronal, and (C) sagittal images from an MRI performed to evaluate a possible structural cause for this patient's recent onset of seizures. Thin-section coronals (B) were obtained (only one is shown to allow better visualization of the hippocampi, a region of interest in the imaging evaluation of seizures. Directions: A: Anterior;

P: posterior; R: right; L: left; F: front; B: bottom.

Figure 2.29 Two 3-D fetal 3 T MR images using ultrafast sequences.

(courtesy of National Center for Child Health Development, Tokyo, Japan. *DiagnImag* 8/2004, p. 55

Figure 2.30 Two views of 3-D dedicated breast MR angiogram (1.5 T).

(courtesy of Dr X. Hong, Aurora)

2.3.5.5 Other Types of Images from MR Signals

This section describes several current clinical and work-in-progress MR image types that can be generated from MR signals, and some of them have been used in clinical environment. The emphasis of the discussion is not on the physics and chemistry of the image acquisition, but on the informatics relevant after the images have been acquired. The MR angiography is first considered, followed by other pulse-sequences imaging.

2.3.5.5.1 MR Angiography (MRA)

Current MRI scanners have the capability to acquire 3-D volumetric MR angiogram data. The Fourier nature of 3-D MR data acquisition involves collecting the entire 3-D dataset prior to reconstruction of any of the individual sections. Phase encoding is employed to spatially encode the *y*-axis as well as the *z*-axis position information. The section thickness can be reduced to less than 1 mm, providing a sufficient signal-to-noise ratio. Repetition and echo times are shortened, making it possible to collect large 3-D volumes of high-resolution data or multiple successive lower resolution volumes in 20–40 seconds.

A standard MRA study, similar to other x-rays angiography, but using the MRI energy, can vary from a typical head/neck study of 100 images to a lower extremity runoff study of 2000 images that produces a data size of between 25 and 500 MB. Performance wise, it depends on the scanner hardware and can yield studies that vary in time from 15–40 seconds. Figure 2.31 shows an MRA study containing abdominal slices, using a maximum projection display method to highlight the contrasting blood vessels in the entire study.

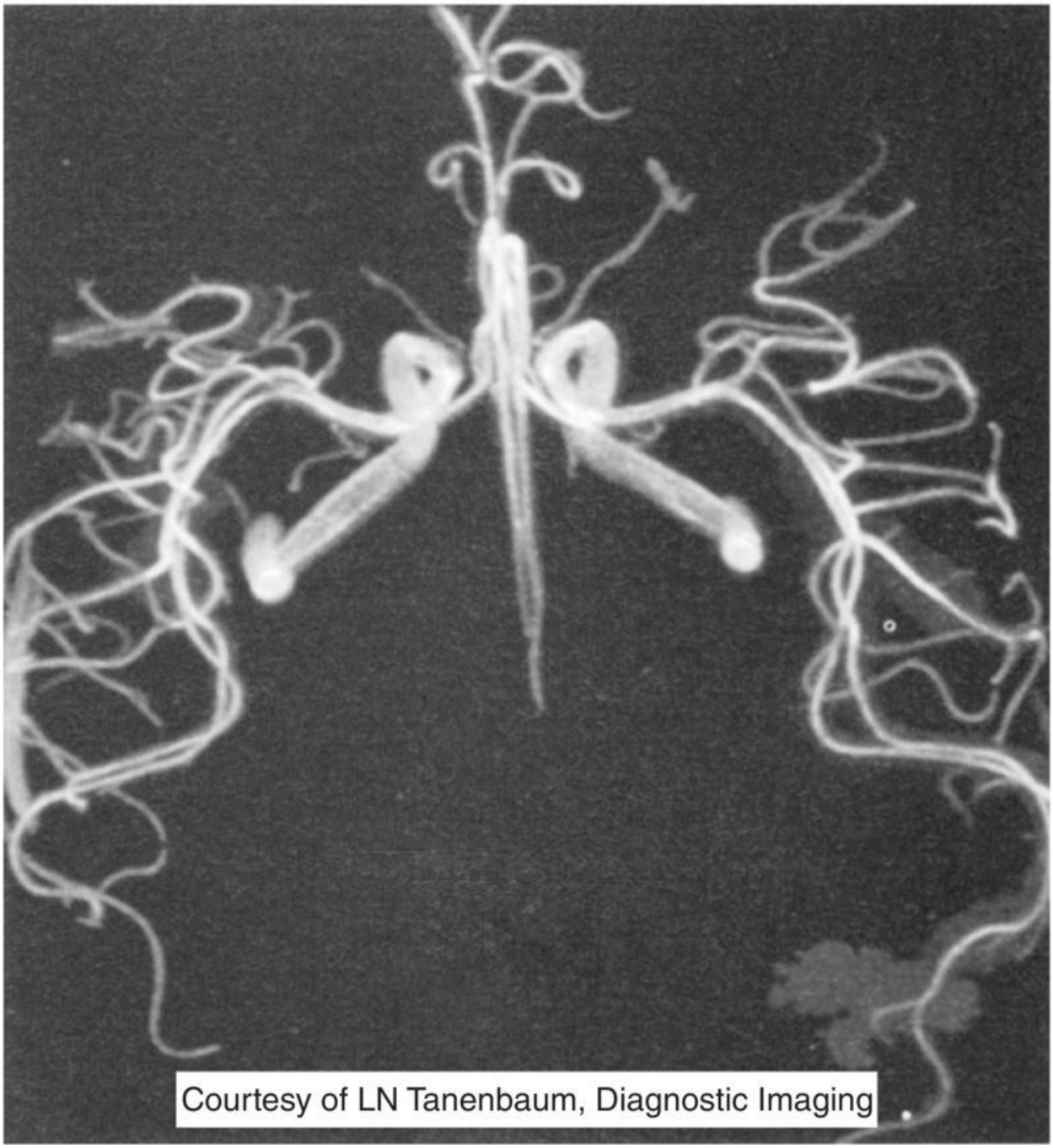

Figure 2.31 MRA using a 3 T MRI scanner, approaching image resolution possible withDSA (Digital Subtraction Angiography), DSA (Section 2.3.2.2).

(courtesy of L.N. Tanenbaum. *DiagnImag* 11/2004, p. 74)

2.3.5.5.2 Other Pulse-Sequence Images

Over the past decade, more than 30–40 pulse sequences were developed to enhance a certain tissue or image contrasts. The major reason for enhancing

pulse sequences is for faster imaging. The idea is to read the signal after RF excitation fast enough before it decays. The latest developments in this direction are in echo-planar imaging (EPI) and spiral imaging readout techniques, which are used for very fast imaging of the heart in motion (cardiac MRI), imaging of multi-voxel chemical profiles, magnetic resonance spectroscopic imaging (MRS and MRSI), and imaging the physiological response to neural activation in the brain (functional MRI, or fMRI). Fast data acquisition and image reconstruction allows 30–60 slices to be obtained in 2–4 seconds. The increase in field strength from today's 1.5 and 3.0 Tesla to even higher Tesla will increase the signal sensitivity signal to noise, SNR), which results in smaller image matrices and thus higher resolution. Based on the pulse sequences, certain imaging protocols and image data characteristics have been established for specific applications. There follows two examples to illustrate the state-of-the-art pulse sequences that are on the verge of being used in daily clinical applications.

Functional MRI (fMRI): Among these new types of images derived from MR, functional MRI is available for daily clinical applications. The image formation consists in 3-D MRI volume acquisition plus selective activation of different functions like motor, sensory, visual, or auditory and their location inside the brain to produce a 4-D fMRI dataset. Typically, an fMRI experiment consists of four series, each taking about 5 minutes with 100 acquisitions. A whole adult brain can be covered by 40 slices with the slice thickness of 3 mm, and each slice can be of 64 × 64 or 128 × 128 voxels. While 2-D and 3-D acquisition techniques exist, in both cases the resulting raw data is a stack of 2-D slices. The average fMRI experiment adds up to 400 volumes, each volume 64 × 64 × 40 × 2 bytes or about 330 KB, amounting to a total of roughly 130 MB. When using 128 × 128 matrices, the total data volume is increased to around 520 MB per study.

Because the DICOM standard (Chapters 4 and 5) is inefficient for many small images like fMRI, the data are mainly reconstructed as a raw data stack and processed offline on a workstation. Therefore standard data communication or processing scheme exists is still lacking. A DICOM standard extension, supplement 49, check DICOM, was introduced in the mid-2002s, but no vendor has yet implemented it for daily clinical operation.

5) *Diffusion Tensor MRI (DTI)*: Another MRI application in neurosciences is diffusion-weighted MR imaging (DWI). DWI uses MR signals based on the structural properties of neural tissue as local water molecular displacements.

One type of DWI is a gradient-direction encoded diffusion tensor imaging (DTI) that can reveal neuroanatomical connections in a noninvasive manner. The implication of the availability of this diagnostic tool is that we may be able to characterize neural tissue properties such as cortical thinning, demyelination, and nerve degeneration and regeneration following injury. Figure 2.32 shows a tractographical reconstruction of neural connections via MRI DTI.

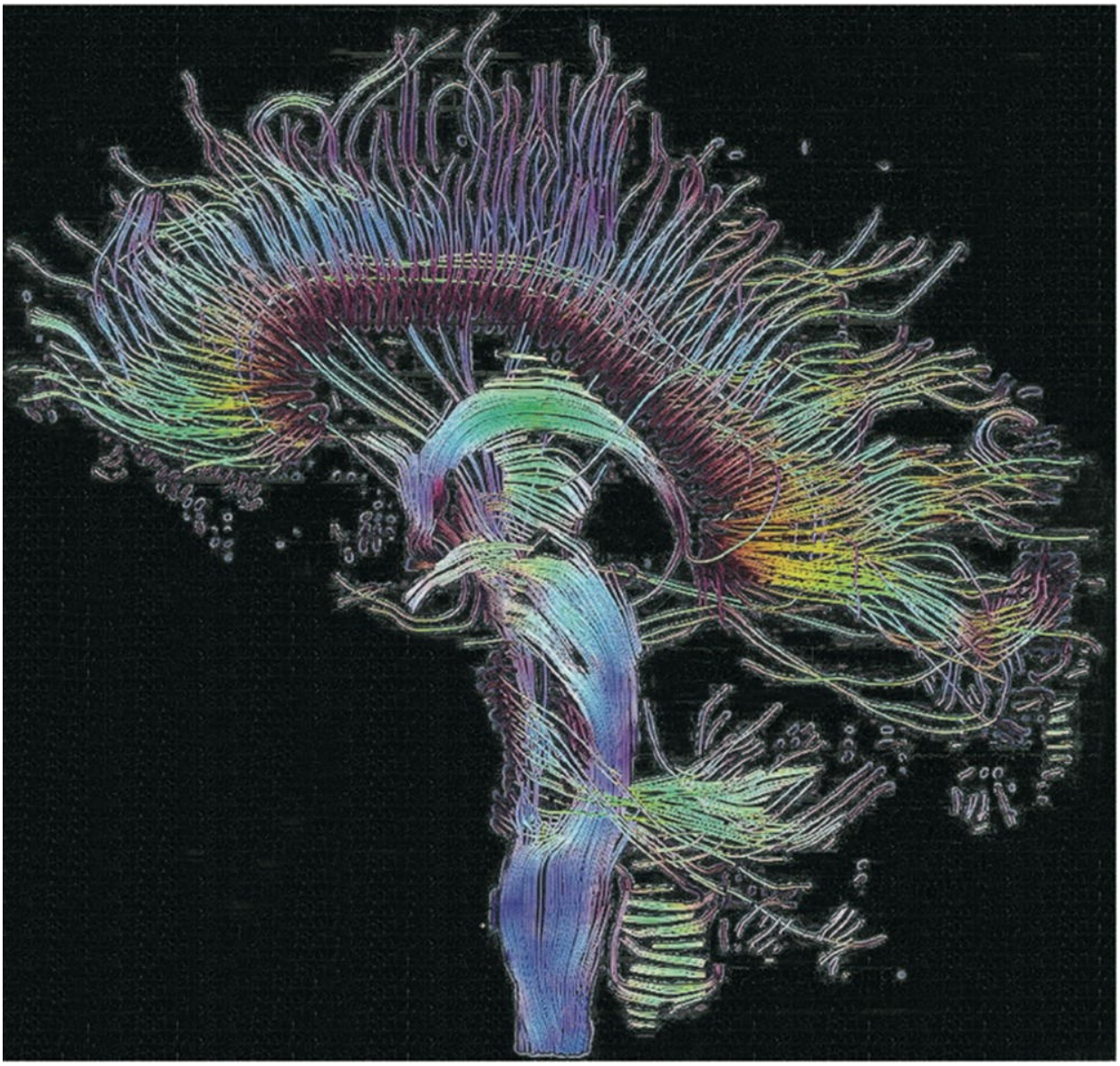

Figure 2.32 MRI DTI Tractographic reconstruction of neural connections via DTI.

Source: https://commons.wikimedia.org/wiki/File:DTI-sagittal-fibers.jpg. By Thomas Schultz [GFDL (http://www.gnu.org/copyleft/fdl.html), CC-BY-SA-3.0 (http://creativecommons.org/licenses/by-

sa/3.0/)

2.3.6 3-D Fluorescence Confocal Microscopy: Light Imaging

A conventional 2-D microscope can be extended to 3-D light imaging using the concept of confocal microscope discussed in Section 2.2.6.1. A schematic diagram of a fluorescence confocal microscope is shown in Figure 2.33. First, the focusing mechanism, a laser beam as the light source (Figure 2.33, left), is used to scan (*x*–*y* scanning mirrors), focus (objective lens), and excite fluorescence objects of interest, in order to obtain depth discrimination from other objects in the sample. Only the in-focus emission from the sample will pass the pinhole mechanism and be recorded by the detector. In operation, the object can be scanned horizontally, point by point, using *x*–*y* scanning mirrors. The pinhole aperture can systematically allow the in-focus emission from the object in contiguous sections in the *z*-direction to pass and be received by the detector. The result is a contiguous 3-D fluorescence image set of the object in the microscope slide, or a 3-D light imaging volume set.

Although the size of a 2-D color microscope image is less than 1 MB, we can extrapolate it to 3-D volumes from many objects of interest in a field, and to many fields in the entire microscope slide; the storage requirement of 3-D light microscopy imaging is enormous. Image storage will be a major challenge to consider in the future.

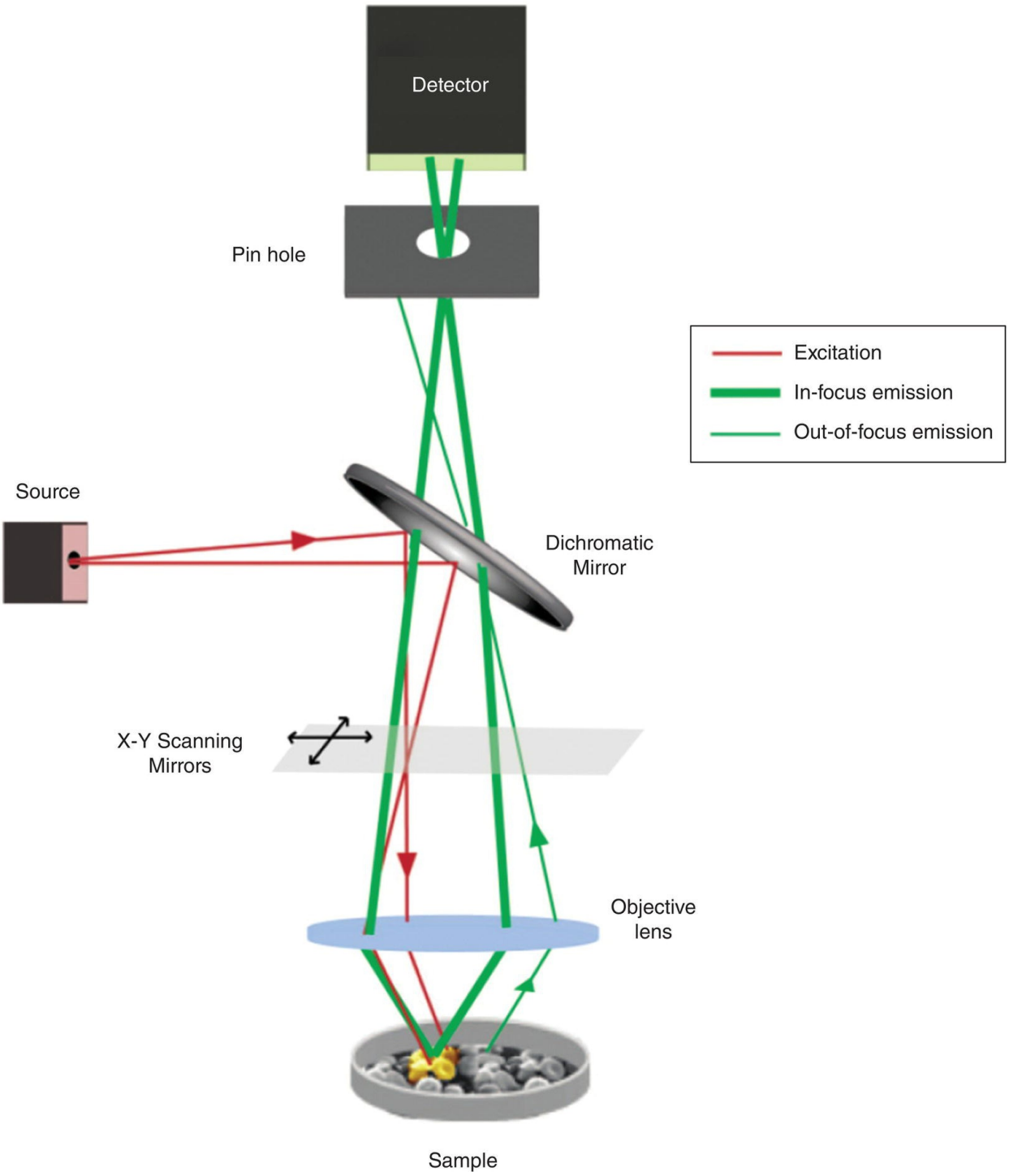

Figure 2.33 Principles of the 3-D fluorescence confocal microscope used to generate serial sections of an object of interest from the specimen. *x–y* scanning mirrors guide a laser beam (red lines) that excites objects attached with fluorescent dye molecules (yellow) in the sample (size not to scale). The dichromatic mirror only allows excited light (green) to pass. The optical pinhole

mechanism accepts in-focus excited emission light (thick green lines) to be recorded by the detector, and rejects out-of-focus emission (thin green line).

(courtesy of M. Fleshman)

2.3.7 3-D Micro Imaging and Small Animal Imaging

Small animal experiments are now performed routinely from bench research to clinical validation. Without the micro imaging, animals have to be sacrificed at each stage of the experiment in order to periodically observe the change of conditions. Micro imaging can have a tremendous impact on the design of animal models, for example, *in vivo* evaluation of the growth of tumors and the effectiveness of drug treatment on the tumors. With the micro scanners, the animal does not have to be sacrificed for validation after each stage of treatment as in the traditional method; the animal can be kept alive under observation during the complete treatment cycle.

CT, MRI, and PET were originally developed mainly for examination of the human body; their design was not intended for small animal studies. Some recent advances in CT, MRI, and PET imaging are in the development of micro-imaging scanners, specially designed for small animal studies involving rats and mice. Major design differences of such micro scanners from clinical sectional imaging systems are their small bore housing of small animals (20–50 g), lower radiation energy input, and smaller size but more sensitive detector system. For a single complete animal experiment, for example, the micro CT scanner can produce 1000 images of 50 μm spatial resolution, or 500 MB of image data. Figure 2.34A shows a 3-D display of a rat scanned by a micro CT scanner with 50-μm resolution, with the skeletal structure emphasized in the display. Figure 2.34B shows the 3-D projection molecular images of a mouse with prostate tumor cells in bone marrow, with time as the third dimension. The top row time series shows no intervention, whereas the bottom rows show chemotherapy intervention. The two time series are from weeks 1, 2, 3, and 5.

With the advancements in small animal scanners, the traditional small animal laboratory will have to be renovated to accommodate these scanners, and this has led to the development of the small animal imaging center. The concept of molecular imaging is discussed in detail in Part 3, Chapters 13, and 14,.

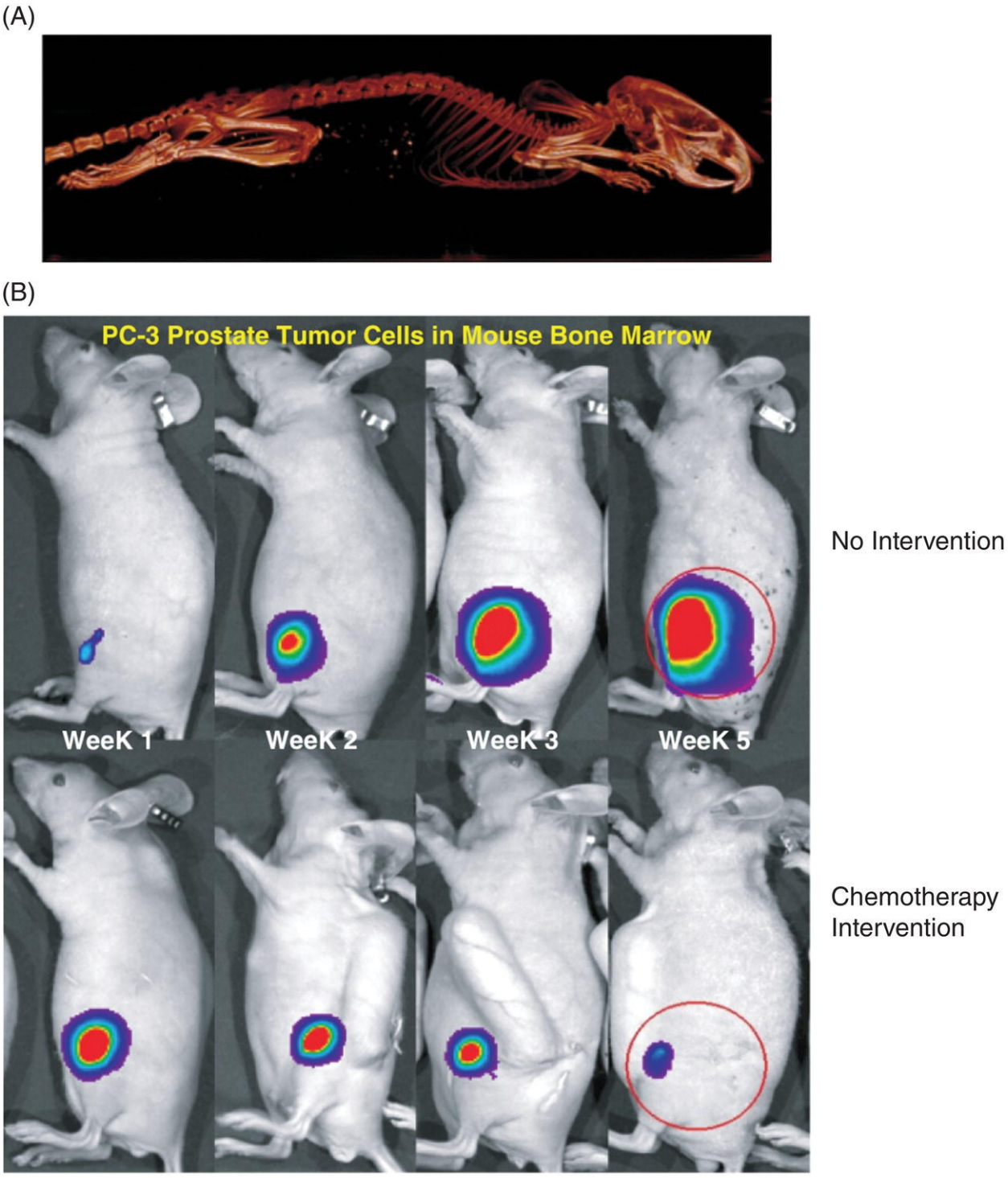

Figure 2.34 (A) 3-D rendering of the skeleton of a rat with a set of 1000 slices scanned by a micro XCT scanner with 50 micro pixels. 500 MB of image data were generated. The skeletal structure demonstrates the 3-D rendering of the display (courtesy of ORNL). (B) Two time series—weeks 1, 2, 3, and 5—of molecular images of a mouse with prostate tumor cells in its bone marrow. The

three dimensions are projections of the *x*–*y* plane over time: (top row) no intervention; the tumor was growing fast after injection to week 5; (bottom row) with chemotherapy the tumor as seen at week 5 starting to respond, and it shrinks continuously after one week.

(courtesy of Drs J. Pinski and G. Dagliyan, Molecular Imaging Center, University of Southern California)

2.4 Four-Dimensional, Multimodality, and Fusion Imaging

2.4.1 Basics of 4-D, Multimodality, and Fusion Medical Imaging

In Sections 2.2 and 2.3, the concepts of 2-D and 3-D imaging were discussed, while this section discusses 4-D imaging. Figure 2.35A revisits two types of 3-D images with *z* and *t*, time, as the third dimension, respectively. With 4-D imaging, which can take several forms, one possible extension from 3-D to the 4-D image is to add the fourth dimension in time "*t*" to the 3-D (x, y, z) spatial imaging, as shown in Figure 2.35B. A 4-D imaging set can also be fused to another 4-D imaging set of identical anatomy and with the same time frames (Figure 2.35C (i), PET on CT), or Figure 2.35C (ii), MR on CT. The fused imaging set "i" and "ii" can be called 4-D multimodality PET fused on CT, and MR fused on CT, respectively. Figure 2.35C presents the basics of 4-D imaging, including its formation, multimodality image registration, fusion, and display.

2.4.1.1 From 3-D to 4-D Imaging

Consider a CT contrast study of the heart of a patient. Figure 2.35B, left, shows a 3-D CT image set taken at time t_1 with 1 to n_1 images; as time "t" continues until a time interval t_m, as the contrast medium travels through the blood stream continuously, a new 3-D CT image set t_m with 1 to n_m is obtained, as depicted in Figure 2.35B, right. The combination of both sets and other possible 3-D CT sets in between t_1 to t_m obtained through time t, form a 4-D imaging set. The contents of this 4-D image set reveal the contrast media distribution through the 3-D anatomy from t_1,…, t_m.

To obtain the 4-D CT imaging shown in Figure 2.35B, the multi-slice CT scanner described in Sections 2.3.2.1 and 2.3.2.2 is used. In this case, the 3-D

CT would first obtain multi-slice CT images "t_1" in one rotation, and the fourth dimension "t" is used to move the patient's bed back to the original scanning position; while the contrast media flows through the heart, the CT would repeat the scan to obtain the next multi-slice images "t_m". This type of data collection of a time interval 4-D image set is useful to follow the patient's blood flow condition during cardiac studies.

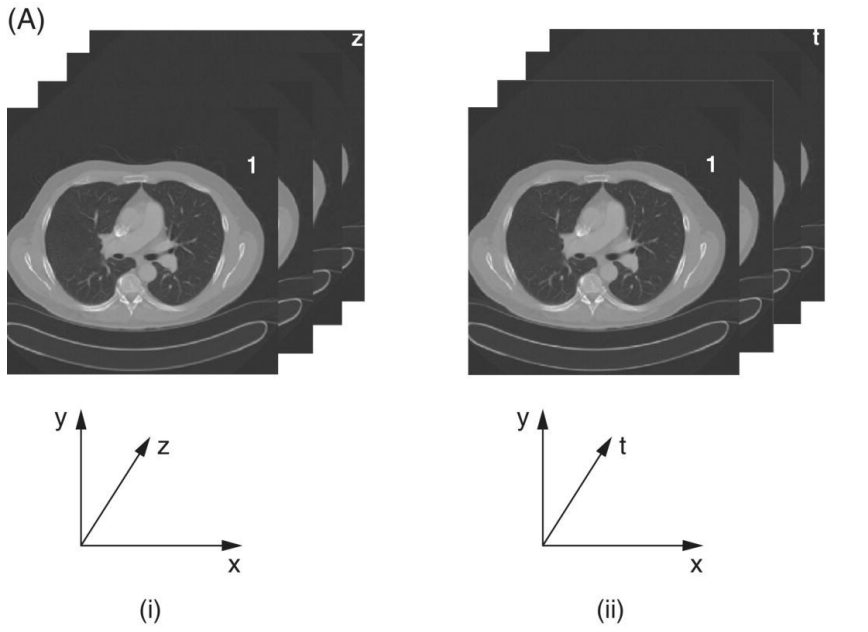
(A)
z
1
t
1
y
z
x
y
t
x
(i)
(ii)

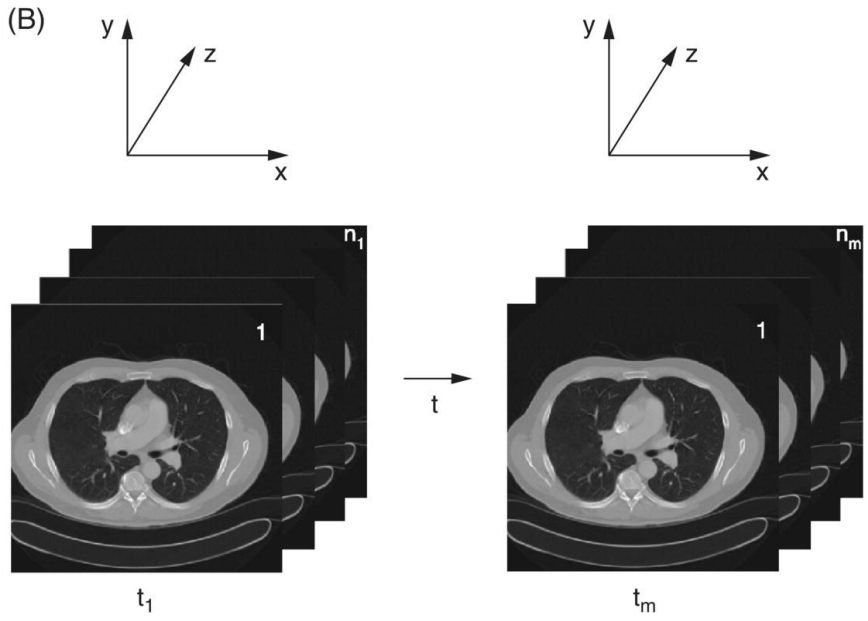
(B)
y
z
x
y
z
x
n_1
1
t
n_m
1
t_1
t_m

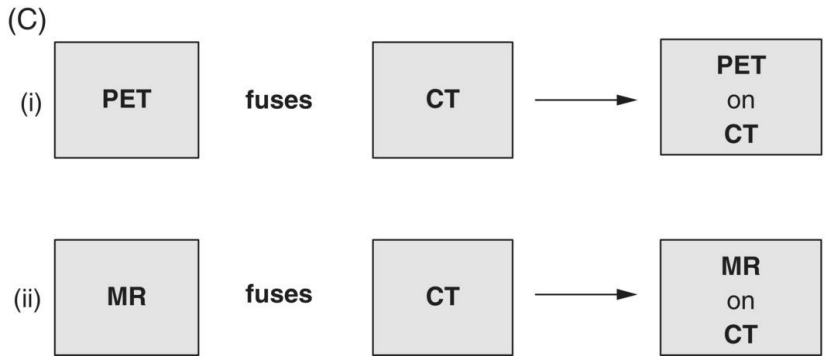
(C)
(i)
PET
fuses
CT
PET
on
CT
(ii)
MR
fuses
CT
MR
on
CT

Figure 2.35 (A) Two 3-D image coordinate systems: (i) A 3-D spatial image set with z as the third dimension. Images from 1 to z show the anatomical changes of the cross-sectional chest; (ii) A 3-D temporal image set with t (time) as the third dimension. Images from 1 to t show the same anatomy as image 1; the difference would be, for example, the flow of the contrast media injected into the patient from time 1 to t. (B) A 4-D image set consisting of sequential 3-D spatial sets, with t as the fourth dimension. (C) (i) PET fuses with CT: physiology on anatomy; (ii) MR fuses with CT: enhancement of soft tissue definition on anatomy.

(adapted from Figure 2.1B –D)

2.4.1.2 Multimodality 3-D and 4-D Imaging

Multimodality imaging loosely means that different imaging modalities are used to examine the same anatomical region of interest. Because different modality imaging techniques can reveal tissue characteristics not obtainable by certain other imaging techniques, information from multimodality images can enhance the patient's diagnostic or therapeutic process. For example, CT can be used to obtain high-resolution anatomical images, whereas PET can be used to obtain *in vivo* physiological images that lack anatomical details. In combination, PET and CT fused images can yield a very powerful two-modality tool for high-quality spatial resolution functional imaging. Certain imaging modalities, such as CT, US, MRI, and PET, can be used for obtaining either 3-D or 4-D images. The second imaging modality with identical anatomy can be used to augment the first imaging modality for diagnosis; conceptually, it is like an added on dimension (but not necessarily in the same time domain) to the original 3-D or 4-D images. To avoid confusion of terminology, this chapter uses the terms "multimodality 3-D" and "multimodality 4-D".

Another type of multimodality imaging is to use the same modality to scan the patient; then the energy used during the scanning is split into two energy levels, such as high and low energies. The images generated by the second energy are then treated as if they are from a second modality. After one scan, two sets of images can be generated, the high- and low-energy image sets.

Figure 2.36 shows the dual energy CT scanning technology in which high- and low-energy images are generated in one scan. Both the high- and low-energy images can be combined to identify the lesion inside the circle as lipid degeneration. Dual energy CT imaging can also be used to identify bone and soft tissues more readily from both images.

Multimodality imaging always produces multiple images of the same anatomical region. In two-modality imaging, it produces two images, as shown in Figure 2.36. In PACS image archive, however, there is the potential for large data accumulation resulting from multimodality imaging.

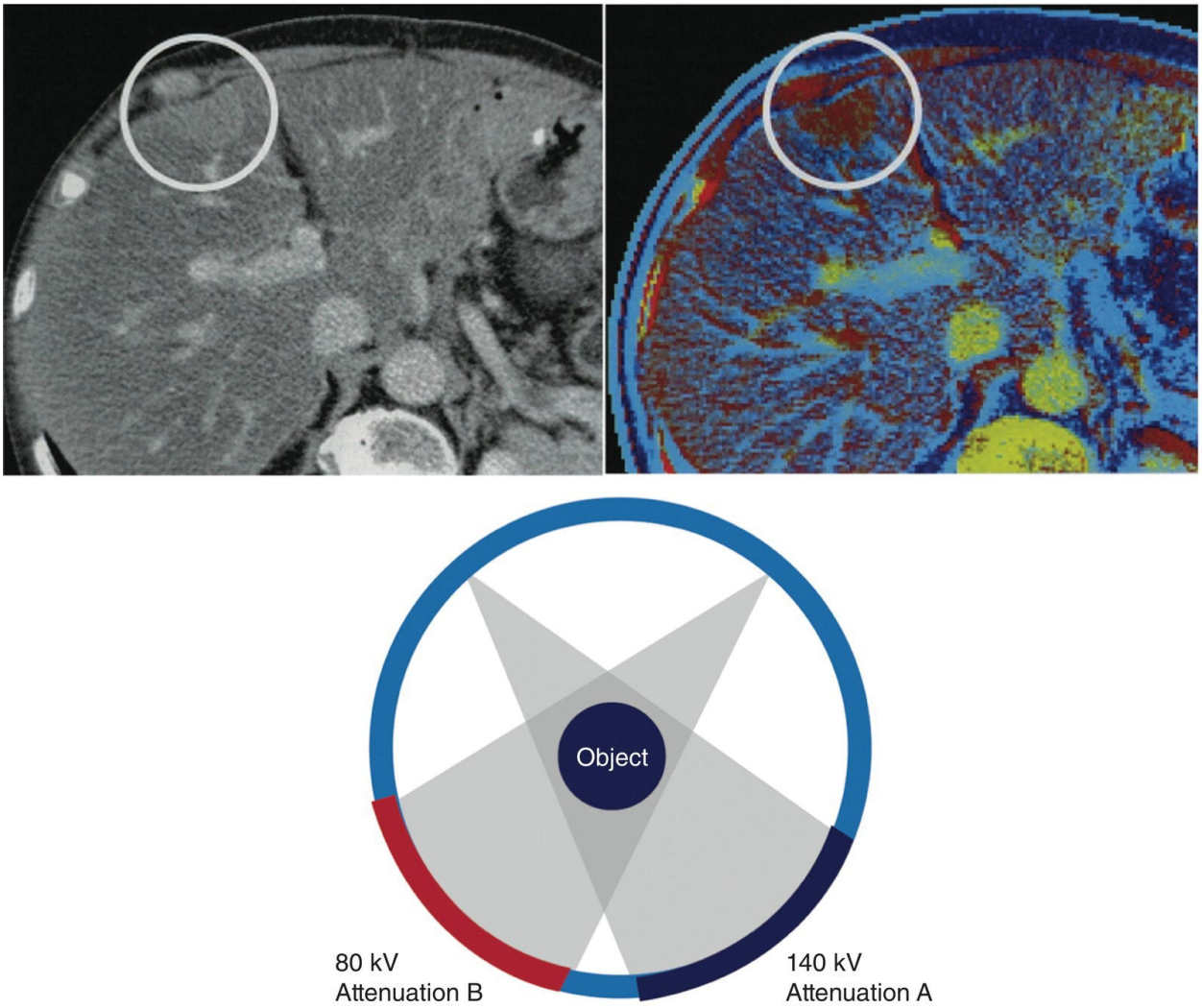

Figure 2.36 Dual x-ray energy CT scan in a gantry producing high- and low-energy images that can distinguish between tissue types. Single-energy scan (left) without enough information to differentiate a lipid degeneration (right, inside the white circle), shown nicely in the dark red color coded inside the white circle.

(courtesy of Siemens Medical Systems)

2.4.1.3 Image Registration

Given two sets of 3-D or 4-D images, in order to maximize their potential use for

enhancing the diagnostic and therapeutic process, they need to be registered, fused, and properly displayed. This section discusses principles of image registration.

Image registration in this context means that two sets of images are aligned and matched, and so coincide either in anatomical outline and structure or in the targeted lesion location and specifics. The former type of registration is called global, and the latter local. The alignment and matching can be 2-D, 3-D, or 4-D. In the case of 2-D, two images are registered section by section; 3-D registration is to align two 3-D volumes. The registration in 4-D not only requires 3-D volume registration, but also for the images to be in sync with the time dimension.

Image registration first defines the reference (or primary) image set, and then transforms the secondary (floating) image set to align, match, and coincide with the reference image set. In general, the higher spatial resolution image is used as the primary image (e.g. CT), and the lower resolution is used as the secondary image (e.g. PET). In the transformation, if only translation and rotation are required, it is called a rigid transformation. On the other hand, if a sub-volume structure in one image set needs to be warped (or deformed) in order to match the other set, then it is called a non-rigid transformation. Rigid body transformation is much easier to perform compared with non-rigid transformation.

2.4.1.4 Image Fusion

After two 3-D image sets have been properly registered, the next step is to overlay the two sets and display the result, a process called image fusion. The basic principle is to overlay the secondary 3-D set by using a lookup table (LUT) on the secondary 3-D set to highlight specific features on the primary 3-D set obtained from its own LUT. Effective LUT pairs have the primary set in gray scale and the secondary in color. Both tables need to use a customized GUI (Chapter 10) to manually adjust the overlaid display by optimizing its effectiveness for the specific application. This customized LUT set can then be used as the default for future display of the same application.

In clinical applications, for example, PET-CT fusion is used to map the physiological parameters from PET onto the more detailed anatomy CT; such as in radiation therapy treatment planning for the prostate gland, to prevent overdosing critical organs. The prostate appearing on the MRI has higher soft tissue definition that allows for a precise maximum dose to be delivered to the

target organ, as it is fused onto the CT, which shows the overall anatomical details. This is a case of image fusion of local anatomy with a high-density resolution (MRI) onto a global anatomy with high spatial resolution (CT) (Chapters 11 and 19). Another radiation therapy application is the overlay of dose distribution onto the anatomy shown on a CT in accordance with a treatment plan.

2.4.1.5 Display of 4-D Medical Images and Fusion Images

Current methods to display 4-D images use video format. If the fourth dimension is time, then the video will show 3-D images with timeframes moving forward and backward. Many commercial products displaying video are readily available for this purpose. If the PACS workstation (WS) does not have these display features (Chapter 10), the 4-D image set may first need to be packaged for post-processing display, then the user can log out from the PACS WS and use some standard web-based video display software.

For image registration and fusion display, the integrated result is to display on the PACS WS, or other specialized post-processing WS (Chapter 10). Take the example of PET-CT. The LUT of PET is in color, and that of CT is in gray scale, each of which has its own GUI. The two GUIs are two sliders allowing for an interactive adjustment of the color for PET and the gray scale for CT. When the two customized GUI sliders have been accepted for a given clinical application, they may be combined as one single slider to facilitate interactive fine-tuning adjustments of the display during viewing.

For more effective imaging registration and fusion results, since the displays have multimodality images, it is advantageous to use a color LCD (liquid crystal display) device, with the gray scale component assigned to the LUT of CT, and the color component to the color LUT of PET.

2.4.2 4-D Medical Imaging

With the time coordinate added to the 3-D space, sectional 3-D images can generate 4-D medical images. The “time” duration of the fourth dimension can mostly be short term. It can be the change of heartbeat, physiological changes of the blood flow, movements of some internal organs, and others. But sometimes the duration can also be long, in minutes, hours, days or weeks, for example, in the case of waiting for an experimental result to obtain molecular images, as shown in Figure 2.34B. Therefore, care needs to be taken to specify the duration of the time parameter when it is the fourth dimension, so that the 4-D image set

is acquired and identified properly.

2.4.2.1 4-D Ultrasound Imaging

In Section 2.3.4, 3-D ultrasound (US) imaging was introduced by using the ultrasound transducer and detector systems. Although the quality of 3-D US images is inferior when compared with that generated by CT and MRI imaging, the advantage of 3-D US, in addition to its noninvasive nature, is that it produces real-time images instantaneously compared with CT and MRI. For this reason, 4-D US imaging with the time as the fourth dimension is mostly practiced during certain critical patient screening and on-line diagnostic applications. There is also an increasing interest in the visualizing of 4-D US data for on-line medical diagnosis.

For example, 4-D maternity US scans would provide expecting eager parents with the very first images of their future baby, from a yawn to the heart beats, arms and legs stretch, and other movements at week 12 and so on. 4-D US imaging can be used to follow the growth of the fetus in the mother's womb, and is the most effective method with dynamic mode in video format. For this reason, integrating 4-D ultrasound imaging with PACS-based operation is especially in demand. Figure 2.37 shows a real time comparison between 2-D, 3-D, and 4-D US fetus images.

(A)

(B)

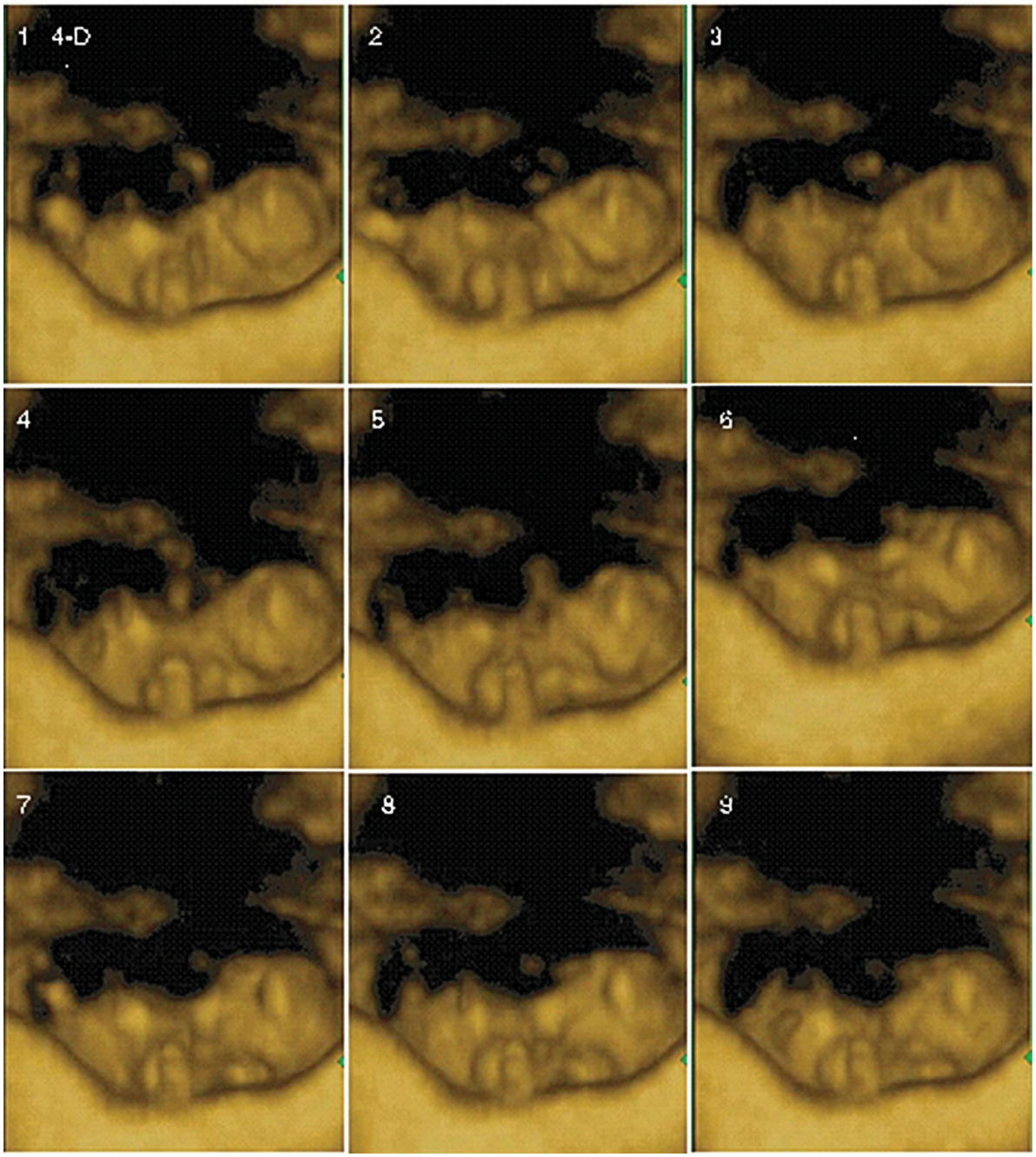

Figure 2.37 Fetal images taken with 2-D, 3-D, and 4-D US imaging. 2-D, 3-D, and 4-D US images can be used to observe and monitor the growth of the fetus before the baby is born. (A) Left, 2-D US image with audio heart beat at the bottom. Two 3-D US images reveal the breathing movement of the chest wall and the stretching of the legs. (B) Sequences of 4-D time frames with 3-D US image frames (not in equal time intervals) showing the movements of the legs, turning of the body, and the face (frames 5, 6, 7), and the movement of the arms and legs.

(courtesy of Dr C. Huang; artwork: A. Sullivan)

2.4.2.2 Selected Data from 4-D X-Ray CT Imaging

Consider the contents in Section 2.4.1.4, and follow the cardiac imaging in Section 2.4.1, then advance one more step and take advantage of this knowledge to define a particular type of 4-D x-ray CT imaging. Recall Figures 2.16 and 2.17, that delineate the multi-slice 3-D CT scanner of the heart with 256 images in one compete rotation of the x-ray system. Suppose that x-ray contrast enhanced media is injected into the patient, with the patient and the bed remaining stationary, and an electrocardiogram gated study of the heart allowing only the x-rays gantry to rotate in sync with the diastole and systole cycles during the heart beat. Assuming the given task is to collect systolic and diastolic 4-D CT data of the heart, then the solution is to follow the method of obtaining the 4-D CT image set with the fourth dimension “times”, but only to acquire those data during the time when it is in sync with the systolic and diastolic cycles during the heart beat.

2.4.2.3 4-D PET-CT Imaging

A 3-D PET-CT scanner is a combination of a CT and a PET scanner within one gantry, so together they generate simultaneously a set of fast 3-D CT images and another set of slower physiological PET images during the scanning process. The CT scan is extremely fast, almost in real time, whereas the PET scanner accumulates the necessary data over the total PET scan duration in minutes, which is not real time. For example, in a whole-body PET scan, it takes about 23 minutes to accumulate 64 multi-slices (Section 2.3.3.2 and Figure 2.22). During this time of data collection, the CT images automatically fuse with the PET images within the two sets of data inside the scanner; this fusion method is called hardware image fusion. Figure 2.38A shows a PET- CT scanner, and Figure 2.38B describes the image fusion data flow. Thus, 3-D PET averages the

image data over the time period that the data are collected. For example, in the gated 4-D PET cardiac study, as discussed in Section 2.4.2.2, the 64 multi-slices first generate the 4-D PET raw dataset at each “time unit”, then the average of these total 23 minutes “time unit” forms the PET final imaging data (Figures 2.39 and 2.40).

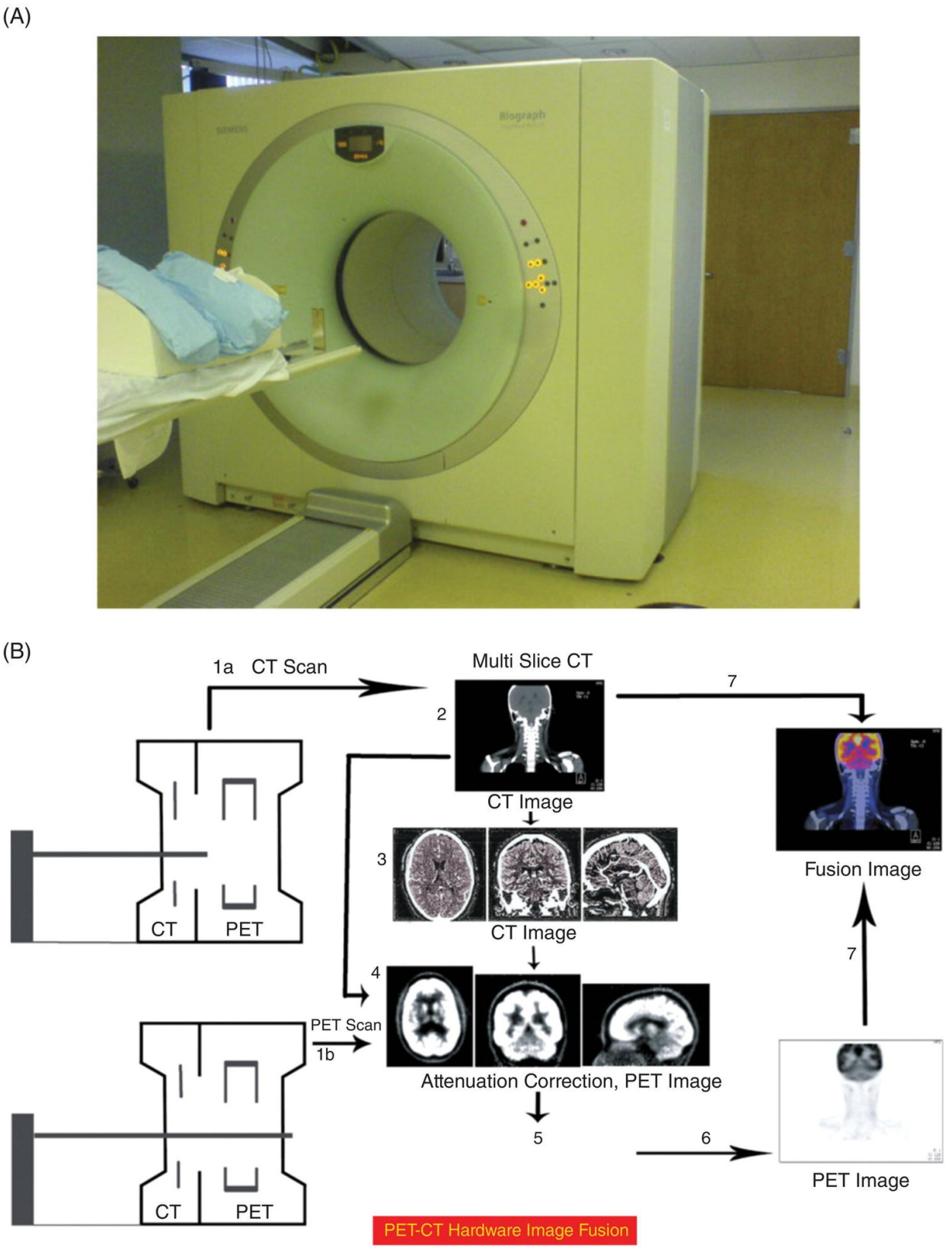

Figure 2.38 (A) PET-CT system with 64 slices at the Nuclear Medicine

Division, Department of Radiology, USC. The gantry houses a 3-D CT and a 3-D PET. (B) Hardware image fusion with a PET-CT combined scanner. The hardware fusion method minimizes patient position change and movement during image registration before fusion. The mockup shows a PET-CT scan of a patient 1 hour after injection of 18-F fluorodeoxyglucose. The patient was positioned in a PET-CT scanner. Workflow steps: (1a) 64 Multi-slice CT followed by (1b) a PET scan; (2) 3-D CT images of a full reconstructed coronal section along with (3) brain transverse, coronal, and sagittal sections; (4) 3-D CT data used to perform attenuation correction of PET data; (5) 3-D PET image reconstruction; (6) 3-D PET images obtained showing a coronal, (7) registered and fused CT and PET images with the corresponding coronal section. The "fused" PET-CT images allow for increased sensitivity in the detection of neoplastic disease by combining identified abnormal physiologic activity (PET) with precise anatomic localization (CT).

(courtesy of Dr P. Moin; artwork by A Sullivan)

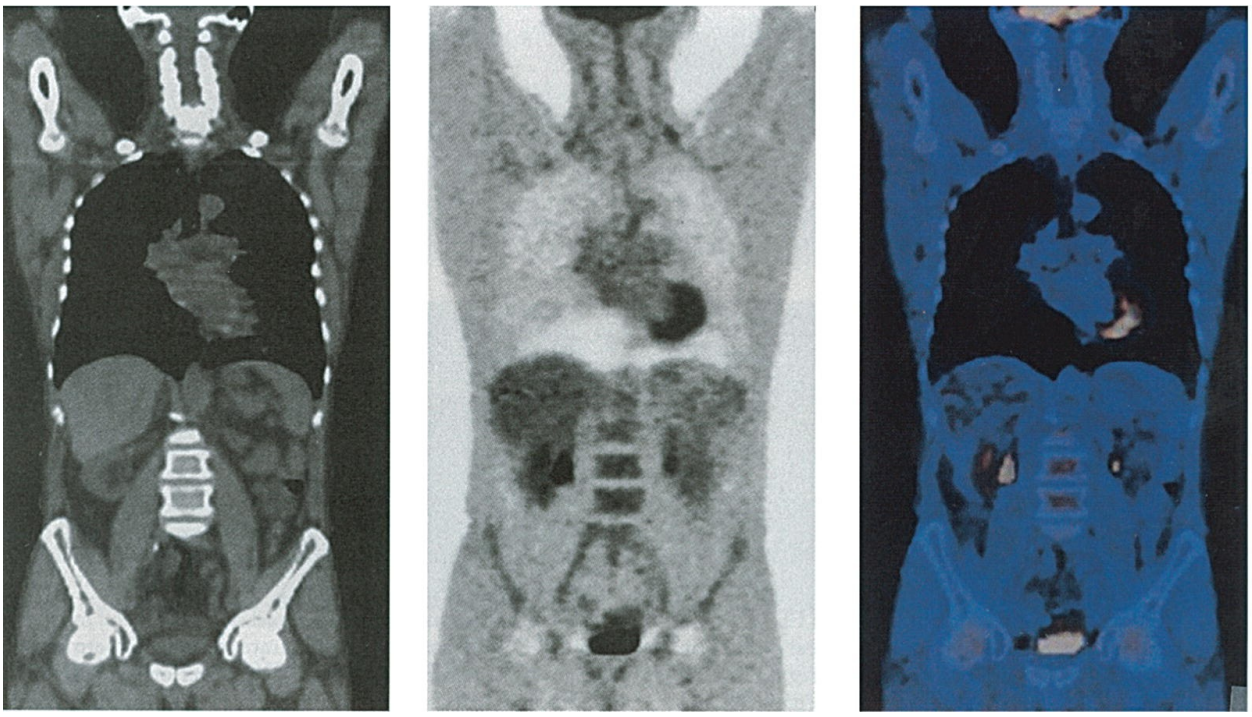

Figure 2.39 PET-CT fusion images of a coronal view of the whole body from a dual gantry PET-CT scanner indicating normal distribution of FDG (18-Ffluorodeoxyglucose); (left) CT image; (middle) PET image; (right) fusion image with pseudo-color lookup table (LUT) PET image (physiology) overlaying CT image (anatomy); FDG accumulation shown in cerebral-cerebellar cortex, myocardium, liver, kidneys, renal pelvis, bone marrow, and

urinary bladder.

(courtesy of Dr R. Shrestha and of L. Kostakoglu *et al*., *Radiographics*, 2004; 24: 1411–1431)

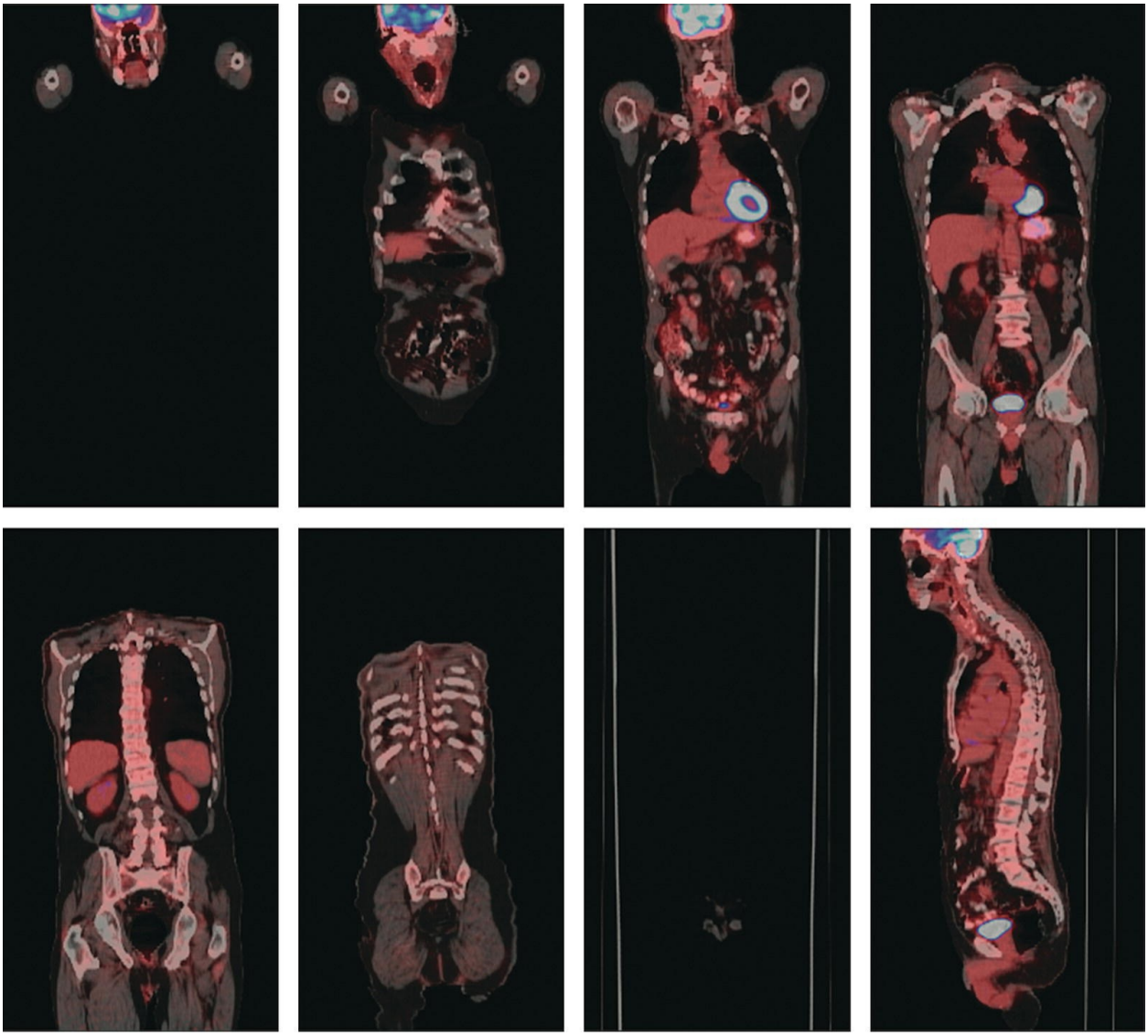

Figure 2.40 PET-CT hardware combined fusion coronal sectional images with 18 F-FDG. Of the 25 equal spaced 1.0-cm sequential images, 00, 04, 08, 12, 16, 20, and 24 are shown. A sagittal section is also displayed (lower right).

(courtesy of M. Fleshman, artwork)

2.5 Image Compression

A compressed medical image can reduce the image size and the capacity of an examination, and also shorten the image/examination transmission time and

lessen its storage requirement. But a compressed image may compromise the image's original quality and affect its diagnostic value. This section briefly touches on the basic concept of image compression and the current preferred image compression method. Only the basic concept of 1-D, 2-D, and 3-D lossy wavelet image compression methods are briefly discussed, along with the original images compared with various compressed ratio images.

2.5.1 Some Terminology

- *Compressed image file*: the compressed image file of any 2-D, 3-D, or 4-D image is a 1-D encoded information data file derived from the original or the transformed image by an image compression technique.
- *Reconstructed image from a compressed image file:* the reconstructed image (or the image set) from a compressed image file is a 2-D rectangular array $f_c(x,y)$, a 3-D data block $f_c(x,y,z)$, or a 4-D $f_c(x,y,z,t)$ image set. The technique used for the reconstruction (or decoding) depends on the method of compression (encoding). In the case of error-free (or reversible, or lossless) compression, the reconstructed image is identical to the original image, whereas in irreversible or lossy image compression, the reconstructed image loses some information of the original image. The term "reconstructed image," which is obtained from a compressed image file, should not be confused with the term "image reconstruction," which is obtained from projections used in computed tomography, as described earlier in this chapter. Thus the reconstructed image in this chapter means that the image is reconstructed from a compressed file.
- *Encoding and decoding*: the term "encoded" is used for the image that has been compressed. The term "decoded" is used for the compressed image that has been reconstructed.
- *Difference image*: the difference image is defined as the subtracted 2-D image, the subtracted 3-D data block, or the subtracted 4-D image sequence between the original and the reconstructed image, $f(x,y) - f_c(x,y)$, $f(x,y,z) - f_c(x,y,z)$, or $f(x,y,z,t) - f_c(x,y,z,t)$. In the case of error-free compression, the difference image is the zero image (image set). In the case of irreversible (lossy) compression, the difference image is the pixel-by-pixel, voxel-by-voxel, or time and voxel-by-voxel differences between the original image and the reconstructed image. The amount of the difference depends on the compression technique used, as well as the compression ratio; the lesser the

difference, the closer is the reconstructed image to the original.

- *Compression ratio*: the compression ratio between the original image and the compressed image file is the ratio between the computer storage required to store the original image versus that of the compressed data file. Thus, a 4:1 compression on a 512 × 512 × 8 = 2097, 152-bit image requires only 524 288 bits of storage, or 25% of the original image storage space. There is another way to describe the degree of compression by using the term “bpp” (bit per pixel). Thus, if the original image is 8 bits/pixel, or 8 bpp, a 4:1 compression means that the compressed image becomes 2 bpp, because the compression ratio computed from pixel-by-pixel or voxel-by-voxel differences between the original and the compressed image is not necessarily an exact number. A 4:1 compression means the acceptable compression is approximate 4:1 (see Section 2.5.2 and Chapter 17).

2.5.2 Acceptable Compression Ratio

A question in imaging compression is: what is the acceptable compression ratio of a given image after it is compressed? Figure 2.41 shows an example using a 2-D CT chest image. Consider the following experiment. Compress a 512 × 512 × 12-bit body CT image with compression ratios 4:1, 8:1, 17:1, 26:1, and 37:1. The original image and the five reconstructed images arranged clockwise are shown in Figure 2.41. It is not difficult to arrange these images in the order of quality. But it is more difficult to answer the question: which compression ratio is acceptable for clinical diagnosis? From the figure it is seen that reconstructed images with compression ratios of less than and equal to 8:1 do not exhibit visible deterioration in image quality. In other words, compression ratio 8:1 or less is visually acceptable in this case. But visually unacceptable does not necessarily mean that it is not suitable for diagnosis, because it depends on which body region and what diseases are under consideration. Receiver operating characteristic (ROC) analysis, described in the next section, is an acceptable objective method used in diagnostic radiology to address this question.

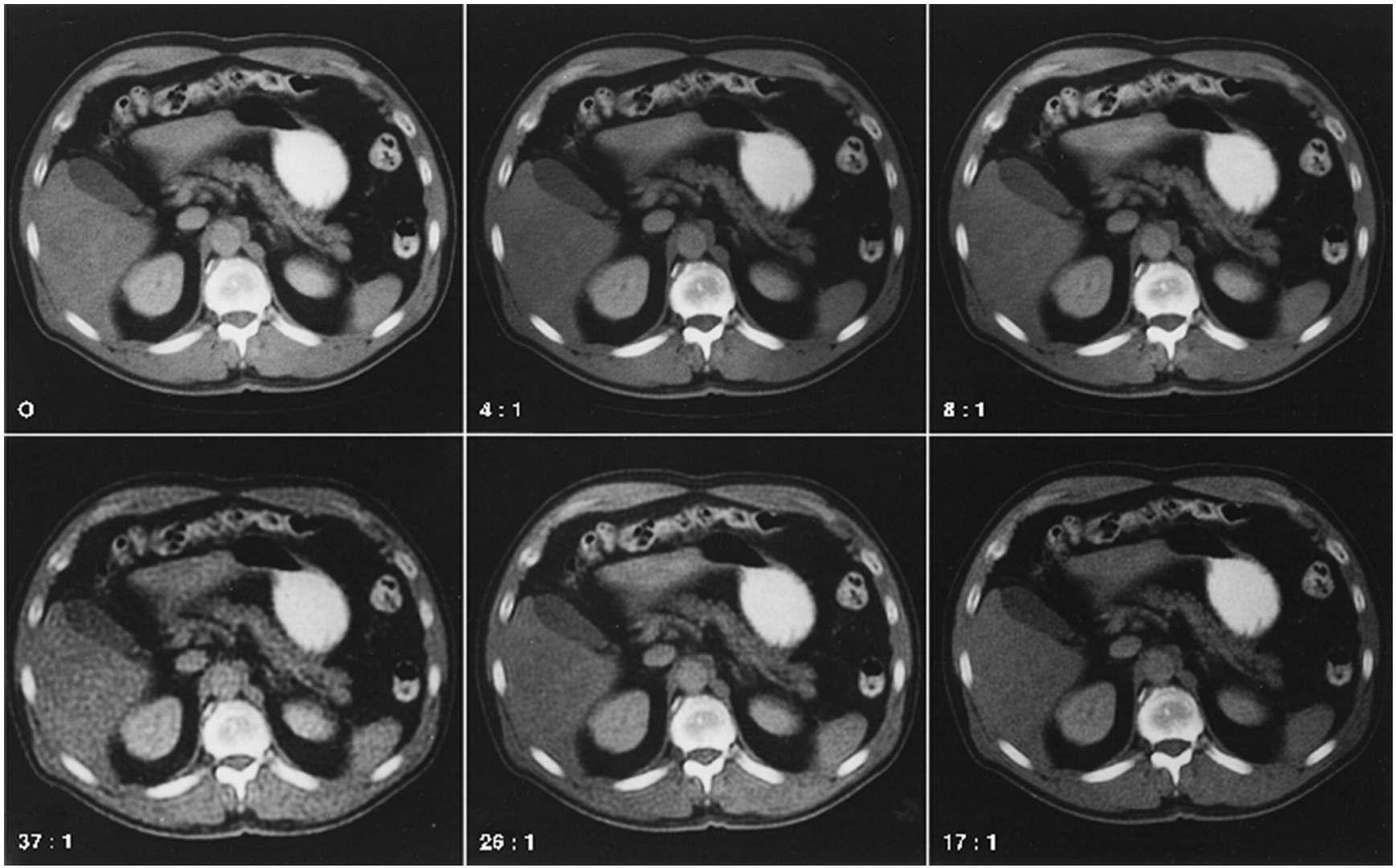
0
4 : 1
8 : 1
37 : 1
26 : 1
17 : 1

Figure 2.41 Original body CT body image (upper left), followed clockwise by reconstructed images with compression ratios of 4:1, 8:1, 17:1, 26:1, and 37:1 (the full-frame method was used).

2.5.3 The Wavelet Transform Method

Using the wavelet transform method to compress medical images has been established and well accepted since the early 2090s. This section briefly highlights its principles. In wavelet transform, it first decomposes a 2-D or 3-D medical image to smoother and sharper components, then compresses these components to an acceptable compressive ratio for the compressed image to be read or stored.

2.5.3.1 2-D Wavelet Transform

A 2-D head MRI image is used as an example, as shown in Figure 2.42A. The method starts to split the MRI into several levels. The first level is to decompose the original MRI image to four sub-images of one-quarter of its original size, each of which retains certain properties of "Image A", shown in Figure 2.42B. The left-upper one-quarter sub-image is called the first-level smooth image; it retains most of the information of Figure 2.42A, with the other three one-quarter sub-images retaining different types of sharper edges information of Figure 2.42A.

The second level decomposition starts from the left-upper one-quarter smooth image (see Figure 2.42B); this one-quarter smooth image is again decomposed into four sub-sub-images of one-quarter of Figure 2.42B, as shown in Figure 2.42C. The left-upper one-quarter sub-sub image is called the smooth image that retains the most information of Figure 2.42B; the rest of three sub-sub-images retain various sharper edges information of the left-upper sub-image Figure 2.42B.

The third, fourth, and further levels can continue to be decomposed as levels 1 and 2; during each process the smooth one-quarter of the previous level will be used. The total number of levels to be decomposed depends on the type of image to be compressed, with the acceptable compression ratio as the final goal. After all levels decomposition has been completed, the image compression can be performed from the data of all the decomposed levels to obtain the compressed MRI image. The 2-D compressed MRI can be reconstructed to obtain the acceptable lossy 2-D MRI.

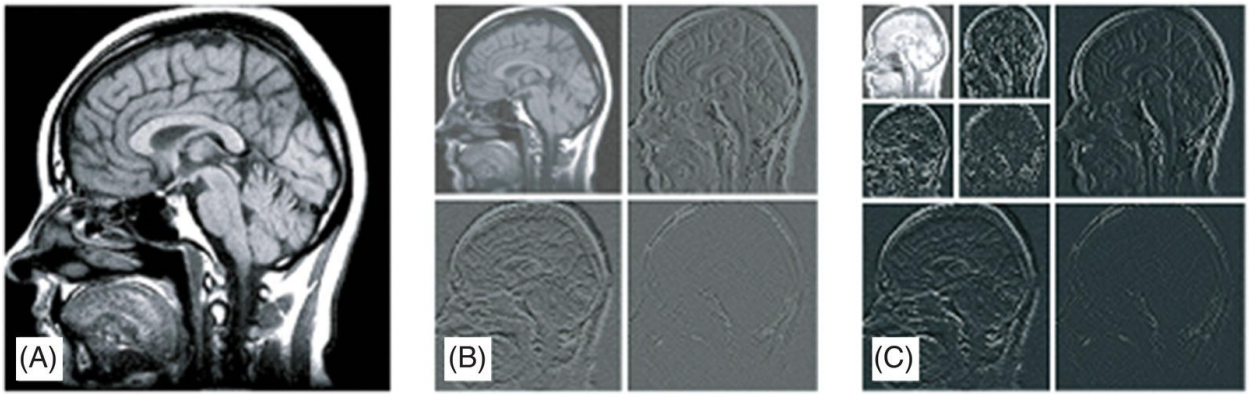

Figure 2.42 Two-level 2-D wavelet decomposition of a MR head sagittal image. (A) original image; (B) first-level decomposition into four images, (C) second-level decomposition. In each level, the left upper corner is the smooth image, and the other three quadrants are the detailed images (sharper). Observe in the MRI image, all detailed images in each of the three levels contain visible sharp anatomical information. The image compression is to compress each level according to the characteristic of the anatomy, and the acceptable image compression ratio. The needed quality of the compression depends on the acceptable compression ratio discussed in Section 2.5.2.

2.5.3.2 3-D Wavelet Transform

In 3-D wavelet transform, the 3-D image set to be compressed first forms a 3-D block, which is an effective geometry to compress a 3-D medical image dataset to achieve higher compression ratio with lesser storage space. Figure 2.43 shows a block diagram of the 3-D wavelet decomposition procedures. In 3-D, the concept of the levels of decomposition is similar to that of the 2-D image wavelet transform shown in Figure 2.42, except that instead of using a 2-D image to decompose the image, the 3-D wavelet method uses a 3-D image block to perform the wavelet decomposition. Figure 2.43 shows two levels of 3-D wavelet transform of an image volume dataset. The original 3-D image block is f_0, the first level f_1 is decomposed into eight components, the left upper (f_1, deep blue) is the "smooth" component of the image data block, and the remaining seven blocks f'_1 (light blue) are the high (sharper, detailed) resolution components. As shown in Figure 2.43, f_1 is further decomposed to level 2 (the rightmost box), with eight smaller volumes labeled f_2 (one smooth) and seven f'_2 s (sharper, detailed). Note that the detailed images f'_1 in level 1 contain one more level 1 high-frequency component than those f'_2 of level 2. Similar to the 2-D MRI image compression, after all necessary levels have been completed, 3-

D image compression can be performed from the data of all decomposed levels that form the compression ratio of the 3-D block. The 3-D compressed data block can be used to reconstruct acceptable 3-D images.

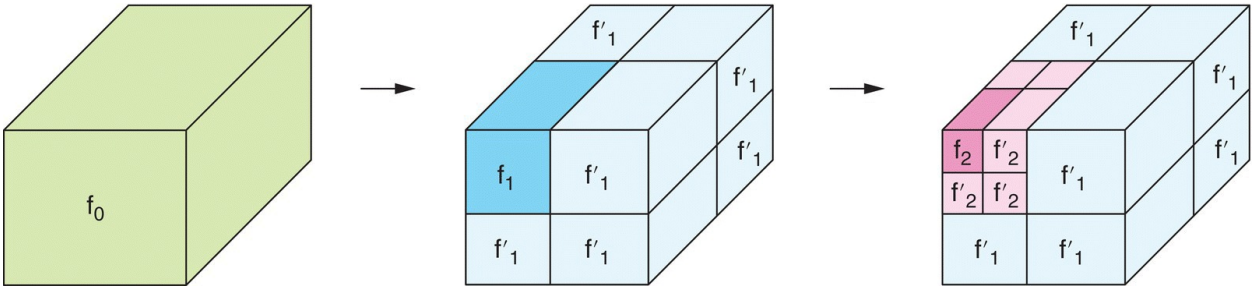

Figure 2.43 The 3-D volume dataset after two-level decompositions using the 3-D wavelet transform. Each level is decomposed into eight components. f_0 (left) is the original 3-D dataset, f_1s are the eight first-level decomposition (blue), and f_2s, are the second level decomposition (red). The darker blue set in the middle drawing is the smooth image set, the other seven blue are the sharper image sets. The pink in the rightmost second-level decomposition, darker pink in the upper left is the smooth dataset, and the remaining seven sets are the sharper image sets. f ’$_1$ and f ’$_2$ are the seven sets of higher resolution/sharper data of each level.

2.5.3.3 Examples of 3-D Wavelet Transform

Two examples are used to demonstrate 3-D wavelet compression results compared with those obtained by other image compression methods. The first example uses a 3-D MRI dataset consisting 124 images with 256 × 256 × 16 bits per image. Both 2-D and 3-D wavelet compressions are used, respectively. The 3-D wavelet compression method is similar to that of the 2-D compression algorithm, except that 2-D wavelet transform is applied to each image slice, whereas 3-D wavelet is applied to a 3-D block. Figure 2.44 compares the compression ratios using the 3-D and 2-D algorithms for a fixed PSNR (peak signal-to-noise ratio); the horizontal axis is the PSNR and the vertical axis shows the compression ratio. This example demonstrates that for the same PSNR, the compression ratio using the 3-D wavelet method is superior to that of the 2-D wavelet.

The second example is to compress a body 3-D CT volume using three different image compression methods, the 3-D wavelet, 2-D wavelet, and cosine transform JPEG compression method. Taking an arbitrary extraction of a CT image, the quality of the reconstructed 20:1 compression ratio images using the

three compression methods (Figure 2.45B, C, and D), respectively, are used to compare against the quality of the original image (Figure 2.45A). The 3-D wavelet compression result is almost of the same quality as the original image, and superior to that from both the 2-D wavelet (Figure 2.45C) and JPEG cosine transform (Figure 2.45D).

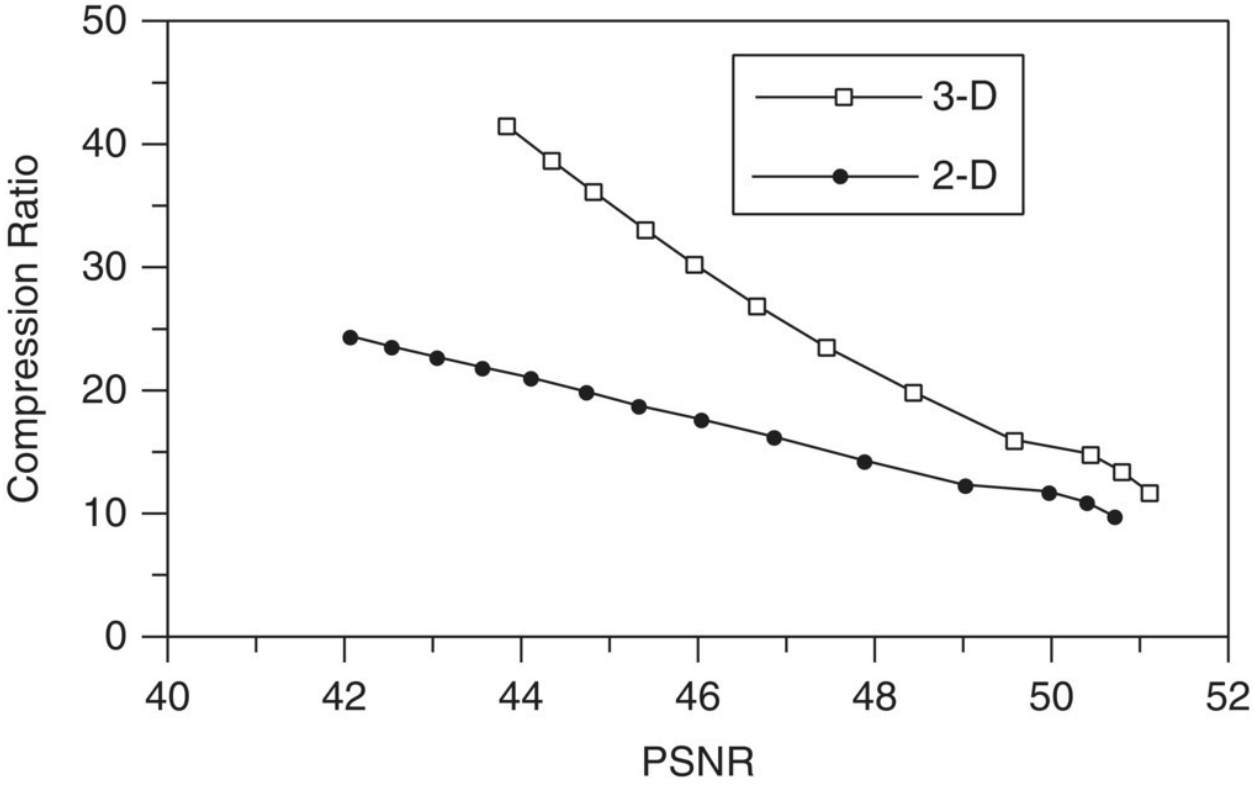

Figure 2.44 Performance comparison using 3-D versus 2-D wavelet compression on a 3-D MR head image set. Note that 3-D wavelet transform is superior to the 2-D transform for the same peak signal-to-noise ratio (PSNR).

The second example uses a 3-D body CT images block to compare the quality of three different image compression methods. By fixing a compression ratio of 20:1, the 3-D wavelet, 2-D wavelet, and DICOM JPEG block (see Chapters 4 and 5) compression methods are used to first compress the CT block, then reconstruct the images from the block and compare the reconstructed CT image quality among the three methods. Figure 2.45A is one of the original images, and Figures 2.45B–D show the results from the three similarly compressed and then reconstructed images from the 3-D image volume block compression results. Figure 24.6 shows the subtracted images in an enlarged square region covering the vertebra (see the square from Figure 2.45A). It is observed that the quality of the 3-D wavelet reconstructed image with a compression ratio of 20:1 is almost

of the same quality as that of the original image, since the difference image contains minimum residual anatomy of the original image (Figure 2.46B'). The 3-D wavelet compression quality is also superior to both results from the 2-D wavelet (Figure 2.46C') and the 2-D JPEG cosine transform (Figure 2.46D').

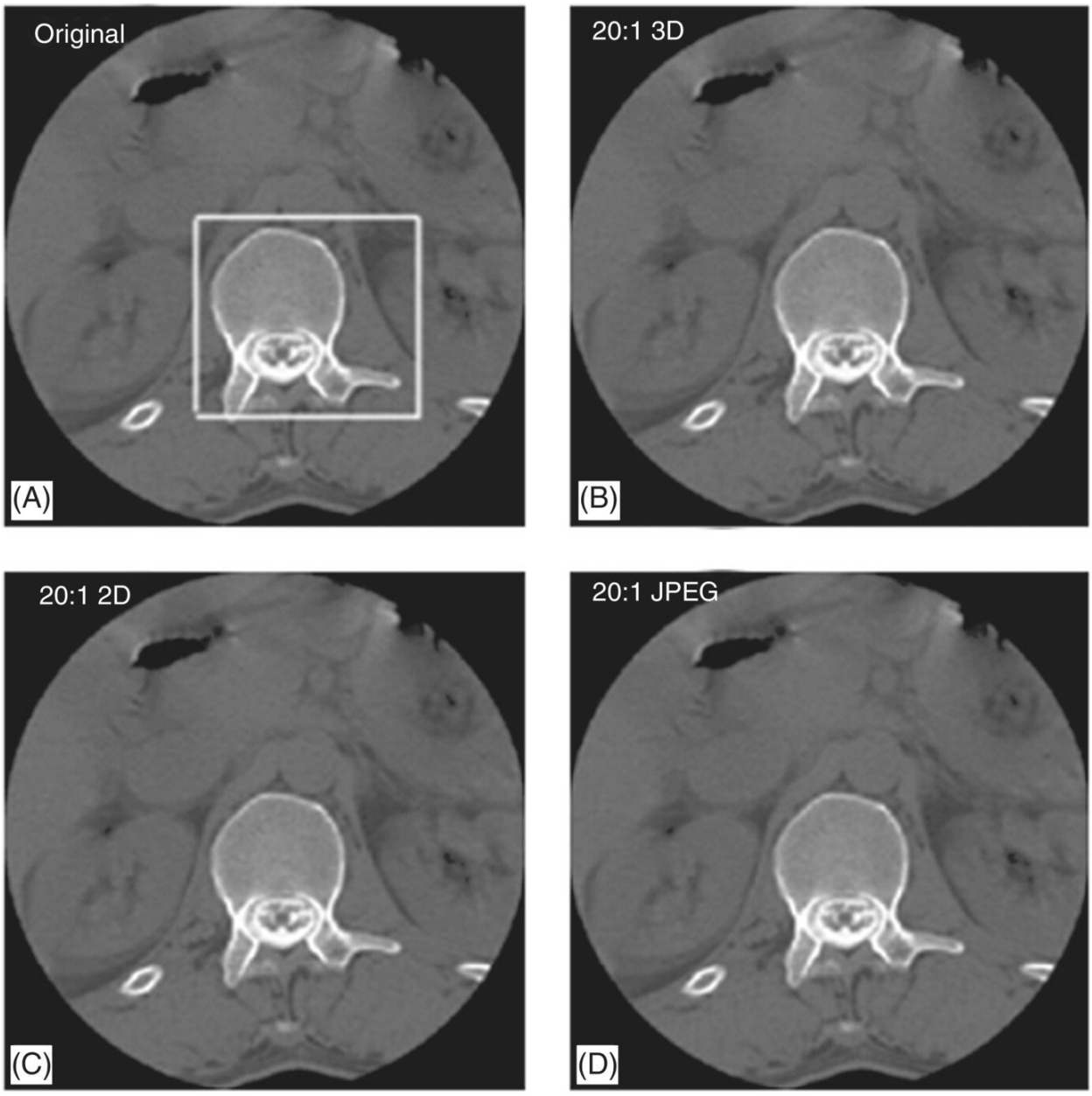

Figure 2.45 One slice of a 3-D CT volume data compressed with a compression ratio of 20:1 with 3-D wavelet, 2-D wavelet, and cosine transform JPEG compression methods: (A) original image; (B) 3-D wavelet reconstructed image; (C) 2-D wavelet reconstructed image; and (D) JPEG reconstructed image. The square covering the vertebra is used to explain Figure 2.46.

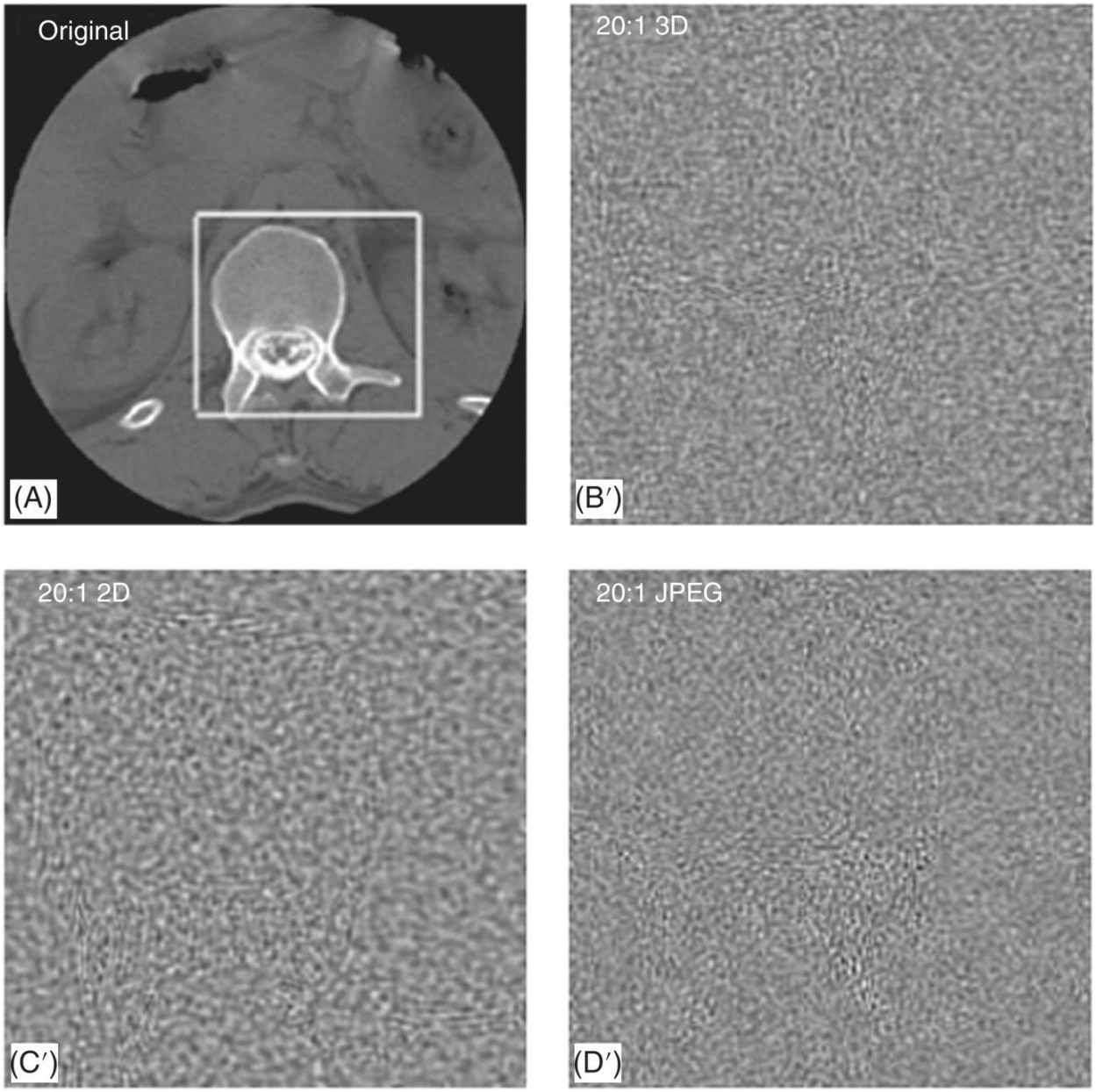

Figure 2.46 (A) Image from Figure 2.45B with an square added on. (B'), (C'), and (D'); subtracted images in an enlarged square region near the vertebra. See also Figure 2.45B. (B') Original – 20:1 3-D wavelet; (C') Original – 20:1 2-D wavelet; and (D') Original – 20:1 JPEG.

Further Reading

Albanesi, M.G. and Lotto, D.I. (1992) Image compression by the wavelet decomposition. *Sig Process*, 3(3), 265–274.

Antonini, M., Barlaud, M., Mathieu, P. and Daubechies, I. (1992) Image coding using wavelet transform. *IEEE Trans Image Process*, 1, 205–220.

Baines, C.J. (1999) A tangled web: Factors likely to affect the efficacy of screening mammography. *J Nat Cancer Inst*, 91, 833–838.

Bankman, I.N. (2008) *Handbook of Medical Imaging Processing and Analysis*, 2nd ed. San Diego: Academic Press.

Barrett, H.H. and Swindell, W. (1981) *Radiological Imaging: The Theory of Image Formation, Detection, and Processing*. San Diego: Academic Press.

Behrens, S., Laue, H., Althaus, M., *et al*. (2007) Computer assistance for MR-based diagnosis of breast cancer: present and future challenges. *J Comp Med Imag Graphics*, 31, 236–247.

Beekman, F.J. and Kachelriesz, M. (2008) Fully 3-D reconstruction of medical imaging. *IEEE Trans Medi Imag*, 27(7), 877–879.

Benedetto, A.R., Huang, H.K. and Ragan, D.P. (1990) *Computers in Medical Physics*. New York: American Institute of Physics.

Bertram, S. (1970) On the derivation of the fast Fourier transform.*IEEE Trans Audio Electroacoust*, 18, 55–58.

Beutel, J., Kundel, H. and Van Metter, R.L. (2000) *Handbook of Medical Imaging, vol. 1: Physics and Psychophysics*. Bellingham, WA: SPIE Press.

Boyd, D., Lockwood, G.A., Byng, J.W., Tritchler, D.L., Yaffe, M.J. (1998) Mammographic densities and breast cancer risk. *Cancer Epid Biomark Prev*, 7, 1133–1144.

Bracewell, R.N. (1956) Strip integration in radio astronomy. *Austr J Phys*, 9, 198–217.

Bracewell, R.N. (1965) *The Fourier Transform and its Applications*. New York: McGraw-Hill.

Brigham, E.O. (1974) *The Fast Fourier Transform. Englewood Cliffs*. Englewood Cliffs, NJ: Prentice-Hall, pp. 148–183.

Burhenne, H.J., Burhenne, L.W., Goldberg, F., *et al*. (1994) Interval breast cancers in the screening mammography program of British Columbia: analysis

and classification. *AJR*, 162, 1067–1071.

Cao, X. and Huang, H.K. (2000) Current status and future advances of digital radiography and PACS. *IEEE Eng Med Bio*, 19(5), 80–88.

Chou, Y.H., Tiu, C.M., Chen, J.Y. and Chang, R.F. (2007) Automatic full-field breast ultrasonography: The past and the future.*J Med Ultrasound*, 15(1), 31–44.

Cochran, W.T., Cooley, J.W., Favin, D.L., *et al*. (1967) What is the fast Fourier transform? *IEEE Trans Audio Electroacoust*, 15, 45–55.

Cohen, A., Daubechies, I. and Feauveau, J.C. (1992) Biorthogonal bases of compactly supported wavelets. *Comm Pure Appl Math*, 45, 485–560.

Curry, T.S., III, Dowdey, J.E. and Murry, R.C. Jr. (1990) *Introduction to the Physics of Diagnostic Radiology*, 4th ed. Philadelphia: Lea and Febiger.

Dhawan, A.P., Huang, H.K. and Kim, D.S. (2008) Future trends in medical and molecular imaging. In: Dhawan, A.P., Huang, H.K. and Kim, D.S. (eds) *Principles and Advanced Methods in Medical Imaging and Image Analysis*. Singapore: World Scientific, pp. 829–843.

Daubechies, I. (1988) Orthonormal bases of compactly supported wavelets. *Comm Pure Appl Math*, 41, 909–996.

Dainty, J.C. and Shaw, R. (1974) *Image Science*, chapter 2. San Diego: Academic Press.

Dhawan, A.T. 2003) *Medical Image Analysis*. Hoboken, NJ: Wiley/IEEE.

Dhawan, A.P., Huang, H.K. and Kim. D-S, (eds) (2008) *Principles and Advanced Methods in Medical Imaging and Image Analysis*. New Jersey, London, Singapore: World Scientific Publishing.

Feldkamp, L.A., Davis, L.C. and Kress, J.W. (1984) Practical cone-beam algorithm. *J Opt Soc Am*, 1, 612–619.

Fenster, A. and Downey, D.B. (2008) Three-dimensional ultrasound imaging. In: Beutel, J., Kundel, H.L. and Van Metter, R.L. (eds) *Handbook of Medical Imaging*, vol 1: *Physics and Psychophysics*. Bellingham, WA; SPIE Press, pp. 463–509.

Gonzalez, R.G. and Wood, R.E. (2002) *Digital Image Processing*, 2nd ed.

Reading, MA: Addison-Wesley.

Hendee, W.R. (2000) Medical imaging for the 21st century. In: Xie, N.Z. (ed.) *Medical Imaging and Precision Radiotherapy*. Guangzhou, China: Foundation of International Scientific Exchange; pp. 24–30.

Hendee, W.R. and Wells, P.N.T. (1997) *The Perception of Visual Information*, 2nd ed. New York: Springer.

Huang, H.K. (1987) *Elements of Digital Radiology: A professional handbook and guide*. Englewood Cliffs, NJ: Prentice-Hall, Inc.

Huang, H.K. (1996) *PACS: Picture Archiving and Communication Systems in Biomedical Imaging*. New York: VCH/Wiley.

Huang, H.K. (1999) *Picture Archiving and Communication Systems: Principles and applications*. New York: Wiley & Sons, p. 521.

Huang, H.K. (2004) *PACS and Imaging Informatics: Principles and Applications*. Hoboken, NJ: John Wiley & Sons, 704 pp.

Huang, H.K. and Lou,S.L. (1999) Telemammography: A technical overview. *RSNA Categorical Course Breast Imag*, 273–281.

Jemal, A., Thomas, A., Murray, T., Thun, M. (2002) Cancer statistics. *CA Cancer J Clin*, 52, 23–57.

Kim, D.S. (2008) Recent advances in functional magnetic resonance imaging. In: Dhawan, A.P., Huang, H.K. and Kim, D.S. (eds). *Principles and Advanced Methods in Medical Imaging and Image Analysis*. Singapore: World Scientific, 267–287.

Kim, D.S. and Ronen, I. (2008) Recent advances in diffusion magnetic resonance imaging. In: Dhwan, A.P., Huang, H.K. and Kim, D.S. (eds). *Principles and Advanced Methods in Medical Imaging and Image Analysis*. Singapore: World Scientific, pp. 289–309.

Kim, Y. and Horii, S.C. (2000) *Handbook of Medical Imaging, vol. 3: Display and PACS*. Bellingham, WA: SPIE Press.

Kuzmak, P.M. and Dayhoff, R.E. (2000) The use of digital imaging and communications in medicine (DICOM) in the integration of imaging into the electronic patient record at the Department of Veterans Affairs. *J Digital Imag*,

13(2 Suppl 1), 133–137.

Law, M.Y.Y. (2005) A model of DICOM-based electronic patient record in radiation therapy. *J Comput Med Imag Graph*, 29, 125–136.

Law, M.Y.Y. (2008) Image guidance in radiation therapy. In: Dhawan, A.P., Huang, H.K. and Kim, D.S. (eds). *Principles and Advanced Methods in Medical Imaging and Image Analysis*. Singapore: World Scientific, pp. 635–662.

Law, M.Y.Y. (2009) DICOM-RT and its utilization in radiation therapy. *J Radiograph*, 29, 655–667.

Law, M.Y.Y. and Huang, H.K. (2003) Concept of a PACS and Imaging Informatics-based Server for Radiation Therapy. *J Comput Med Imag Graph*, 27, 1–9.

Law, M.Y.Y. and Brent, J.L. (2009) DICOM-RT-Based ePR (Electronic Patient Record) Information System for Radiation Therapy. *J Radiograph*, 29, 961–972.

Leondes, C.T. (1997) *Medical Systems Techniques and Applications*. London: Gordon & Breach Science Publishers.

Lightstone, M. and Majani, E. (1994) Low bit-rate design considerations for wavelet-based image coding. *Proc SPIE*, 2308, 501–512.

Long, M. (1996) *Understanding MPEG2 Digital Video Compression*. http://www.mlesat.com/Article7.html

Mallat, S.G. (1989) A theory for multi-resolution signal decomposition: The wavelet representation. *IEEE Trans Pattern Anal Mach Intell*, 11(7), 674–693.

Orel, S.G. and Schnall, M.D. (2001) MR imaging of the breast for the detection, diagnosis, and staging of breast cancer. *Radiology*, 220, 13–30.

Prince, J.L. and Links, J.M. (2006) *Medical Imaging Signals and Systems*. Englewood Cliffs, NJ: Prentice Hall.

Raxche, V., Mansour, M. and Reddy, V., *et al*. (2008) Fusion of three-dimensional X-ray angiography and three-dimensional echocardiography.*Int J CARS*, 2, 293–303.

Ringl, H., Schrnthaner, R., Sala, E., *et al*. (2008) Lossy 3D JPEG2000 compression of abdominal CT images in patients with acute abdominal

complaints. *Radiology*, 248, 476–484.

Robb, R.A. (1995) Three dimensional biomedical imaging. In: *The Calculus of Imaging*. Cambridge, UK: VCH; pp. 188–206.

Robb, R.A. (1997) *Three-Dimensional Biomedical Imaging*. New York: VCH/Wiley.

Rosenfeld, A. and Kak, A.C. (1997) *Digital Picture Processing*, 2nd ed. San Diego: Academic Press.

Rossman, K. (1969) Image quality. *Radiolog Clin N Am*, 7(3); 419.

Solbiati, L. (2008) Image fusion system fast, reliable guide for treatment. *RSNA News* (March), pp. 12–13.

Song, Y. and Li, G. (2008) Current and future trends in radiation therapy. In: Dhawan, A.P., Huang, H.K. and Kim, D.S. (eds). *Principles and Advanced Methods in Medical Imaging and Image Analysis*. Singapore: World Scientific, pp. 745–881.

Sonka, M. and Fitzpatrick, J.M. (2000) *Handbook of Medical Imaging, vol. 2: Medical Imaging Processing and Analysis*. Bellingham, WA: SPIE Press.

Sternick, E.S. (2000) Intensity Modulated Radiation Therapy. In: Xie, N.Z. (ed.) *Medical Imaging and Precision Radiotherapy*. Guangzhou, China: Foundation of International Scientific Exchange, pp. 38–52.

Strang, G. and Nguyen, T. (1995) *Wavelets and Filter Banks*. Boston, MA: Wellesley-Cambridge Press.

Villasenor, J.D., Belzerm, B. and Liao, J. (1995) Wavelet filter evaluation for image compression. *IEEE Trans Image Process*, 4(8), 1053–1060.

Wang, J. and Huang, H.K. (1996) Three-dimensional medical image compression using wavelet transformation. *IEEE Trans Med Imag*, 15(4), 547–654.

Wang, J. and Huang, H.K. (2008) Three-dimensional image compression with wavelet transforms. In: Bankman, I.N. (ed.). *Handbook of Medical Imaging*. San Diego: Academic Press, pp. 851–862.

Winchester, D.P. and Cox, J.D. (1998) Standards for diagnosis and management

of invasive breast carcinoma. *CA Cancer J Clin*, 48, 83–107.

Zanzonico, P. (2008) Multimodality image registration and fusion. In: Dhawan, A.P., Huang, H.K. and Kim, D.S. (eds). *Principles and Advanced Methods in Medical Imaging and Image Analysis*. Singapore: World Scientific, pp. 413–435.

Zhang, J. and Huang, H.K. (1997) Automatic background recognition and removal (ABRR) of computed radiography images. *IEEE Trans Med Imag*, 16(6), 762–771.

Zuckier, L.S. (2008) Principles of nuclear medicine imaging modalities. In: Dhawan, A.P., Huang, H.K. and Kim, D.S. (eds). *Principles and Advanced Methods in Medical Imaging and Image Analysis*. Singapore: World Scientific, pp. 63–98.

PERPUSTAKAAN PRIBADI
AN-NUR
SUNARYA

3
PACS Fundamentals

CHAPTER MENU

3.1 PACS Components and Network
3.1.1 PACS Components
3.1.2 Data and Image Acquisition Gateways
3.1.3 PACS Server and Archive
3.1.4 Display Workstations
3.1.5 Application Servers
3.1.6 System Networks
3.2 PACS Infrastructure Design Concept
3.2.1 Industry Standards
3.2.2 Connectivity and Open Architecture
3.2.3 Data Reliability
3.2.4 Security
3.3 Generic PACS-Based Multimedia Architecture and Workflow
3.4 PACS-Based Architectures
3.4.1 Stand-Alone PACS-Based Model and Data Flow
3.4.2 PACS-Based Client-Server Model and Data Flow
3.4.3 Web-Based Model
3.4.4 Teleradiology Model
3.4.5 Enterprise PACS-Based Multimedia and ePR System with Image Distribution
3.5 Communication and Networks
3.5.1 Network Standards – OSI and DOD
3.5.2 Network Technology
Further Reading

3.1 PACS Components and Network

PACS-based multimedia imaging informatics require some basic components, including a general architecture and system requirements. This chapter consists of four sections: PACS components, infrastructure design, PACS workflow, and communication and networks.

3.1.1 PACS Components

The major components in PACS consist of image and data acquisition gateways, PACS server and archives, and display workstations (WSs), integrated with digital networks. PACS can be further connected to other healthcare information systems by database gateways and communication networks, as shown in Figure 3.1 (see also Chapter 15).

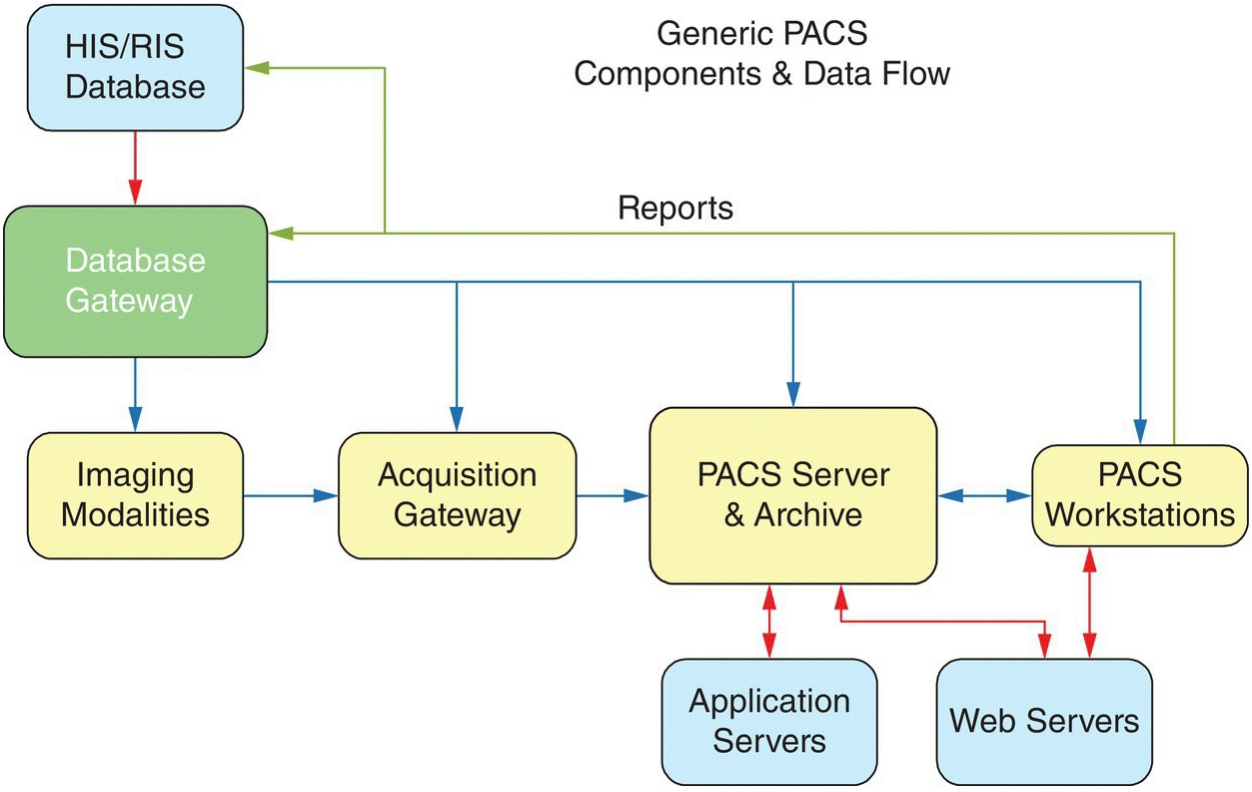

Figure 3.1 Yellow and green boxes: picture archiving and communications system (PACS) basic components. Blue boxes: External information systems including hospital and radiology information systems (HIS/RIS), web servers, and application servers. Data flow: blue lines for internal PACS components

connection; green and red: PACS connection to related external information components. Application servers and web servers: for enriching PACS infrastructure to other clinical, research, and educational applications.

3.1.2 Data and Image Acquisition Gateways

PACS acquires images sent from imaging modalities (devices) and related patient data from the hospital information system (HIS) and the radiology information system (RIS). There are two types of gateways (GW) to the PACS server and archive, the database GW (Figure 3.1, green) for textual data, and the image acquisition GW (Figure 3.1, yellow) for imaging data. A major task in PACS is to acquire images reliably and in a timely manner from each radiological imaging modality via the acquisition GW, and relevant patient data including study support text information of the patient, description of the study, and parameters relevant to image acquisition and processing through the database GW.

Image acquisition is a major task in PACS. The imaging modality is not under the control of a single PACS manager, the imaging modalities being supplied by the manufacturers, each of which has their own DICOM-compliant statements (Chapter 2). Even worse, some older imaging modalities, for example, light imaging from endoscopy and pathology, may not even be DICOM compliant. For the many imaging modalities to connect to a PACS, if not organized well enough, may require labor-intensive work and the cooperation of modality manufacturers. In addition, image acquisition is a slow operation, because patients' examinations are documents involved in the acquisition process. Inevitably it takes the imaging modality and the radiological technician considerable time to acquire the necessary data for image reconstruction and to compile a complete image file (Section 3.4.2). Also, images and patient data generated by the modality sometimes contain format information unacceptable by the on-site PACS operation. To address these problems, an acquisition gateway computer, as some manufacturers call it, the modality integration unit (MIU), is often placed between the imaging modality(s) and the rest of the PACS network to isolate the host computer in the radiological imaging modality from the PACS. Isolation is necessary because traditional imaging device computers lack the necessary communication and coordination software that is standardized within the PACS infrastructure. If the host computers do not contain enough intelligence to associate with the PACS server to recover various errors, the acquisition gateway computer would have to convert the manufacturer specification data from the imaging device, including header format, byte

ordering, and matrix sizes to the PACS standard format, and forward the result to the PACS server or display WSs (see Edition 2, Chapter 7, Section 7.1.1).

3.1.3 PACS Server and Archive

After the acquisition gateway receive images and HIS and RIS data, it forwards them to the PACS server and archive. The PACS server is the engine of the PACS and consists of high-end computers or servers. The PACS server and archive have two major components: a database server and an archive system. Table 3.1 lists some major functions of a PACS server. The archive system can accommodate short-term, long-term, and permanent storage. These components are explained in detail in Chapter 15: PACS-based Server and Cloud Computing.

Table 3.1 Major functions of the PACS server and archive.

- Receives images from examinations (exams) via acquisition gateways
- Extracts text information describing the received exam from the DICOM image header
- Updates the database management system
- Determines the destination workstations to which newly generated exams are to be forwarded
- Automatically retrieves necessary comparison images from historical exams from a cache storage or long-term library archive system
- Automatically corrects the orientation of computed or digital radiography images
- Determines optimal contrast and brightness parameters for image display
- Performs image data compression if necessary
- Performs data integrity check if necessary
- Archives new exams onto long-term archive library
- Deletes images that have been archived from the acquisition gateway
- Services query/retrieve requests from WSs and other PACS controllers in the enterprise PACS
- Interfaces with PACS application servers

3.1.4 Display Workstations

A workstation (WS) includes communication network connection, local database, display, resource management, and processing software. High-quality WSs for radiologists to make primary diagnosis are called diagnostic WSs, while others are generally called review WSs. The fundamental WS operations are listed in Table 3.2.

Table 3.2 Major functions of PACS workstations.

Function	Description
Case preparation	Accumulation of all relevant images and information belonging to a patient examination
Case selection	Selection of cases for a given subpopulation through DICOM query/retrieve
Image arrangement	Tools for arranging and grouping images for easy review
Interpretation	Measurement tools for facilitating the diagnosis
Documentation	Tools for image annotation text, and voice reports
Case presentation	Tools for a comprehensive case presentation, including 3-D image display for a large 3-D file, and fusion images
Image reconstruction	Tools for various types of image reconstruction for proper display

Until several years ago there were four types of display WSs, categorized by their display resolutions:

1. high-resolution (2.5 K × 2 K or higher resolution) liquid crystal display (LCD) for primary diagnosis at the radiology department;
2. medium-resolution (2000 × 1600 or 1600 × 1 K) LCD for primary diagnosis of sectional images and at the hospital wards;
3. physician desktop WS (1 K to 512) LCD; and
4. hard copy/copying WS for copying images onto CD or print on film or paper.

For a stand-alone primary diagnostic WS (Chapter 10), current and historical images are stored on local high-speed disks for fast retrieval. The WS also has access to the PACS server database for retrieving longer-term historical images if needed. Chapter 10 elaborates on the concept and applications of WS, as well

as two concepts currently being developed, 3-D printing and EchoPixel's 2.5-display with a built-in intelligent WS.

Over the past few years, as more affordable WSs became available on the market, the aforementioned WS categories needed to be modified. A good quality PC (personal computer) with 1 K LCD display at a reasonable price is now readily available. The classical PACS WS model has evolved to a client–server model concept. In this model, the terms thick client, thin client, smart client, and fat client emerge have become popular in manufacturers' PACS WS lists. A thick-client PACS WS has local storage and many image processing functions and only needs to communicate with the server occasionally; a thin-client PACS WS, on the other hand, has no local storage, very minimal image processing functions, and needs the support from the server continuously. In between are smart-client and fat-client WSs. This client-server model is discussed further in more detail in Chapter 10.

3.1.5 Application Servers

Application servers (Figure 3.1, light blue) are connected to the PACS server and archive. Through these application servers, PACS data can be filtered to different servers tailored to various applications; for example, a web-based image viewing server (Chapter 6), a radiation therapy ePR server (Chapters 11 and 19), an image-guided surgery ePR server (Chapters 20 and 21), and CAD server (Chapters 16 to 18).

3.1.6 System Networks

A basic function of any computer network is to provide an access path from which end users (e.g. radiologists and clinicians) at different geographic locations can access information (e.g. images and reports) from another location. The required networking data for system design include location and function of each network node, frequency of information passed between any two nodes, cost of transmission between nodes with various speed lines, desired reliability of the communication, and required workflow throughput. The variables in the design include the network topology, communication line capacities, and data flow assignments.

At the local area network (LAN) level, digital communication in the PACS infrastructure design can consist of low-speed Internet (10 Mbits/s signaling rate), medium-speed (100 Mbits/s), or fast (1 Gbit/s) Internet, and high-speed asynchronous transfer mode (ATM) technology (155–622 Mbits/s and up). In

wide area networks (WANs), various digital service (DS) speeds can be used, which range from DS-0 (56 Kbits/s) and DS-1 (T1, 1.544 Mbits/s) to DS-3 (45 Mbits/s) and ATM (155–622 Mbits/s). There is a trade-off between transmission speed and cost.

The network protocol used should be standard, for example, the transmission control protocol/internet protocol (TCP/IP) and DICOM communication protocol (a higher level of TCP/IP, see Chapter 4). A low-speed network is used to connect the imaging modalities (devices) to the acquisition gateway computers, because the time-consuming processes of imaging acquisition do not require high-speed connection. Sometimes several segmented local area Internet branches can be used to transfer data from imaging devices to a gateway (GW) computer. Medium- and high-speed networks are used on the basis of the balance of data throughput requirements and costs. A faster image network is used between GWs and the PACS server, because several GWs may send large image files to the server at the same time. High-speed networks are always used between the PACS server and WSs for fast images distribution to the users.

Process coordination between tasks running on different computers connected to the network is an extremely important issue in PACS-based system networking. The coordination of processes running either on the same computer or on different computers is accomplished by using inter-processor communication methods with socket-level interfaces to TCP/IP. Commands are exchanged as American Standard Code for Information Interchange (ASCII) messages to ensure standard encoding of messages. Various PACS-based related job requests are lined up into the disk resident priority queues, which are serviced by various computer system DAEMON (agent) processes. The Queue software can have a built-in job scheduler that is programmed to retry a job several times by using either a default set of resources or alternative resources if a hardware error is detected. This mechanism ensures that no jobs are lost during the complex negotiation for job priority among processes. Communications and networking is presented in more detail in Section 3.4.

3.2 PACS Infrastructure Design Concept

Four major ingredients in the PACS infrastructure design concept are system standardization, open architecture and connectivity, reliability, and security.

3.2.1 Industry Standards

The first important rule in building a PACS infrastructure is to incorporate as many industry *de facto* standards as possible that are consistent with the overall PACS design scheme. The idea is to minimize the need for customized software. Furthermore, using industry standard hardware and software increases the portability of the system to other computer platforms. For example, the following industry standards, protocols, computer operating systems, programming languages, and workflow profiles should be used in the PACS-based infrastructure design:

1. UNIX operating system;
2. WINDOWS NT/XP operating system;
3. C and C++ programming language;
4. Java (just another vague acronym) programming language platform ;
5. Extensible markup language (XML)for data representation and exchange on the World Wide Web (WWW);
6. SQL (structured query language) as the database query language;
7. X WINDOW platform for graphical user interface (GUI);
8. TCP/IP communication protocols;
9. DICOM (see Chapter 5) standard for image data format and communication;
10. Health Level 7 (HL7; see Chapter 4) for healthcare database information and textual data format exchange;
11. Integrating the Healthcare Enterprise (IHE), (see Chapter 4) for workflow profiles; and
12. ASCII text representation for message passing.

The implications of following these standards and protocols in PACS implementation are several. First, implementation and integration of all future PACS-based components and modules become standardized. Second, system maintenance is easier because the concept of operation of each module looks logically similar to that of the others. Moreover, defining the PACS-based primitive operations serves to minimize the amount of redundant computer code within the PACS-based system, which in turn makes the code easier to debug, understand, and search. It is self-evident that using industrial standard terminology, data format, and communication protocols in PACS design facilitates system understanding and documentation among all levels of PACS-

based developers. Among all standards, HL7 and DICOM (Chapters 4 and 5) are the most important; the former allows interfaces between PACS and HIS/RIS, and the latter interfaces images among various manufacturers. Following the IHE (Chapter 4) workflow profiles allows for smooth PACS-based components interoperation. These topics are discussed in more detail in Chapters 4 and 5.

3.2.2 Connectivity and Open Architecture

If PACS components, modules, and various PACS-based systems in the same hospital or in an enterprise PACS are such that they cannot communicate with each other, then each component will become an isolated system, each with its own images and patient information, and it will become difficult to combine these modules or systems to form a total hospital-integrated PACS-based operation. That is why packaging a mini-PACS system with the purchase of a modality like CT or MR is not a good idea in the longer term.

An open network design is essential, allowing a standardized method for data and message exchange between heterogeneous systems. Because computer and communications technology changes rapidly, a closed architecture would hinder system upgradability. For instance, suppose that an independent imaging WS from a given manufacturer would, at first glance, make a good additional component to an MRI scanner for viewing images. If the WS has a closed proprietary architecture design, then no components except those specified by the same manufacturer can be augmented to the system. Potential overall system upgrading and improvement would become limited. The consideration of connectivity is important, even when a small-scale PACS-based system is planned. To ensure that a contemplated PACS-based system is well designed and allows for future connectivity, the following questions should be considered:

1. Can images from this PACS-based module be transmitted to other modules, and vice versa?
2. Does this module use HL7 standard for textual data and DICOM standard for images?
3. Does the computer in the module use a certain standard communication protocol?

3.2.3 Data Reliability

Data reliability is a major concern in PACS-based multimedia for two reasons. First, a PACS-based system has many components, so the probability of a failing

component is high. Second, because PACS-based multimedia systems manage and display critical patient information, extended periods of downtime cannot be tolerated. In designing a PACS-based multimedia system, it is therefore important to use fault tolerant measures, including error detection and logging software, external auditing programs (i.e. network management processes that check network circuits, magnetic disk space, database status, processer status, and queue status), hardware redundancy, and intelligent software recovery blocks. Some fail recovery mechanisms that can be used include automatic retry of failed jobs with alternative resources and algorithms and intelligent bootstrap routines (a software block executed by a computer when it is restarted), which allow a PACS-based computer to automatically continue operations after a power outage or system failure. Improving reliability needs to be preplanned and is costly; however, it is essential to maintain high reliability of a complex integrated information system.

3.2.4 Security

Data security, particularly the need for patient confidentiality, is an important consideration because of medico-legal issues and the Health Insurance Portability and Accountability Act (HIPAA) mandate. There are, in general, three types of data violation: physical intrusion, misuse, and behavioral violations. Physical intrusion relates to facility security, which can be handled by building the PACS-based multimedia management. Misuse and behavioral violations can be minimized by account control and privilege control. Most sophisticated database management systems have identification and authorization mechanisms that use accounts and passwords. Application programs may supply additional layers of protection. Privilege control refers to granting and revoking the user’s access to specific tables, columns, or views from the database. These security measures provide the PACS-based infrastructure with a mechanism to control access to clinical and research data. With these mechanisms, the system designer can enforce policy as to which persons have access to clinical studies. In some hospitals and clinical settings, for example, referring clinicians are granted image study access only after a preliminary radiology reading has been performed, signed, and attached to the image data. An example of using fingerprint identification and facial verification is given in Chapter 20.

An additional security measure can be implemented in data security and data communication security, in which an image digital signature can be embedded in the image during its storage and transmission. If implemented, this feature will

increase the system software overhead, but data transmission through open communication channels is more secure.

3.3 Generic PACS-Based Multimedia Architecture and Workflow

This section emphasizes PACS-based system workflow and uses a generic PACS system for illustration. For this reason, whenever appropriate, a data workflow scenario is accompanied with the PACS-based model at its introduction. A generic PACS workflow starting from the patient registering in the HIS, RIS ordering examination (exam), technologist performing the exam, to image viewing and reporting by the radiologist, to image archiving, are shown in Figure 3.1, and the PACS-based radiology workflow is delineated in Figure 3.2. From these two figures, it can be see that PACS-based operation has clearly replaced many manual steps in the classic film-based workflow. Follow the PACS workflow numerals shown in Figure 3.2:

1. Patient registers in HIS, with radiology exam ordered in RIS, and exam accession number automatically assigned.
2. RIS outputs HL7 messages of HIS and RIS demographic data to PACS broker/interface engine.
3. PACS broker notifies the archive server of the scheduled exam for the patient.
4. Following pre-fetching rules, historical PACS exams of the scheduled patient are pre-fetched from the archive server and sent to the radiologist's reading WS.
5. Patient arrives at modality. Modality queries the PACS broker/interface engine for the DICOM worklist.
6. Technologist acquires images and sends the PACS exam of images acquired by the modality and patient demographic data to quality control WS in a DICOM format.
7. Technologist prepares the PACS exam and sends to the radiologist at the diagnostic WS as the prepared status.
8. On its arrival at the radiologist's reading WS, the PACS exam is immediately sent automatically to the archive server. Archive server database is updated with the PACS exam as the prepared status.

9. Archive server automatically distributes the PACS exam to the review WSs in the wards, based on patient location as received from the HIS/RIS HL7 message.
10. Reading radiologist dictates a report with the exam accession number on the dictation system. The radiologist signs off on the PACS exam with any changes. The archive database is updated with changes and marks the PACS exam as signed-off.
11. Transcriptionist or auto-dictater fetches the dictation and types a report that corresponds to the exam accession number within RIS.
12. RIS outputs HL7 message of results report data along with any previously updated RIS data.
13. Radiologist queries the PACS broker for previous reports of PACS exams on the reading WSs.
14. Referring physicians query the broker for reports of PACS exams on the review WSs.

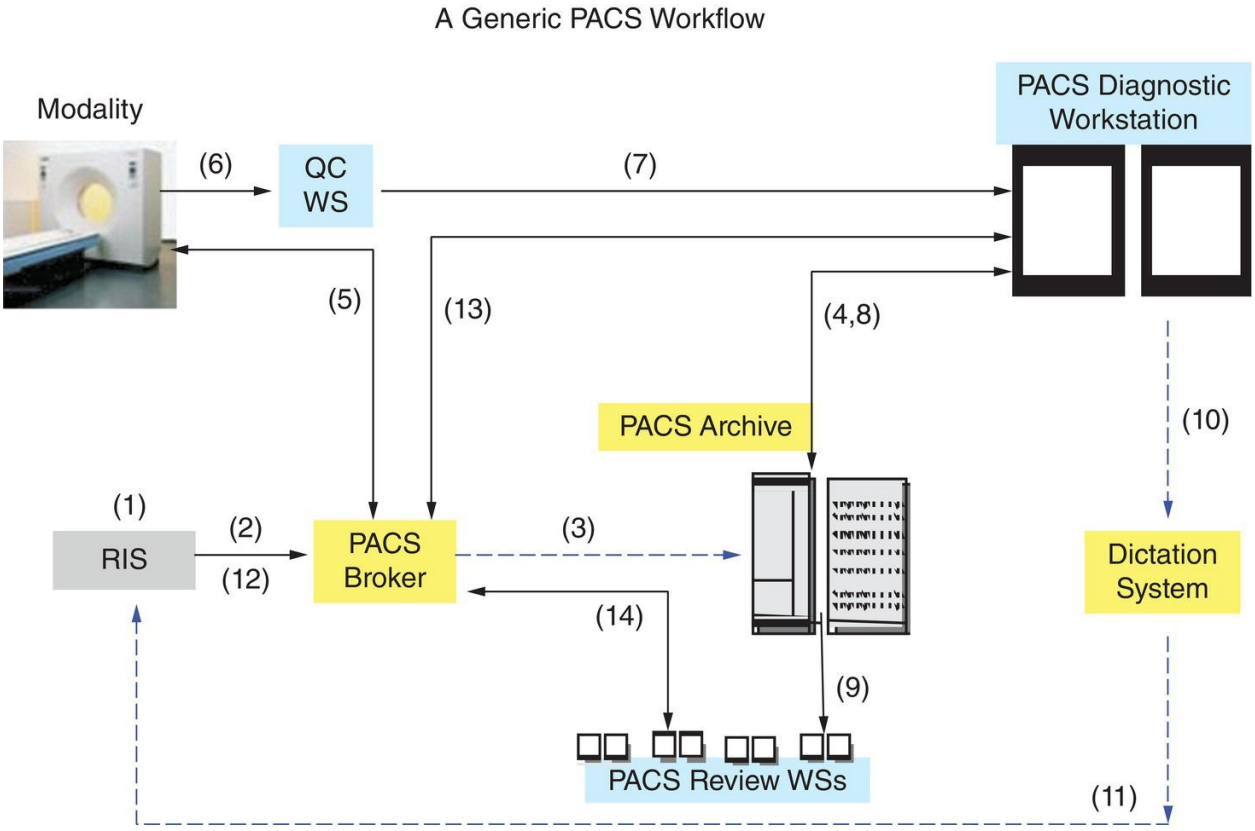

Figure 3.2 A generic PACS-based workflow. Compare the PACS-based workflow with the PACS-based components and workflow shown in Figure 3.1,

and the classical radiology workflow depicted in Chapter 2, Figure 2.3. QC WS: quality control workstation; RIS: radiology information systems; WSs: workstations.

3.4 PACS-Based Architectures

3.4.1 Stand-Alone PACS-Based Model and Data Flow

The stand-alone PACS-based model described here is also called the thick-client model. The three major features of the stand-alone model are:

1. Images are automatically sent to the designated diagnostic and review WSs from the server.
2. WSs can also query/retrieve images from the archive server.
3. WSs have short-term cache storage.

The data workflow of the stand-alone PACS-based model is shown in Figure 3.3. The numerals indicate as follows:

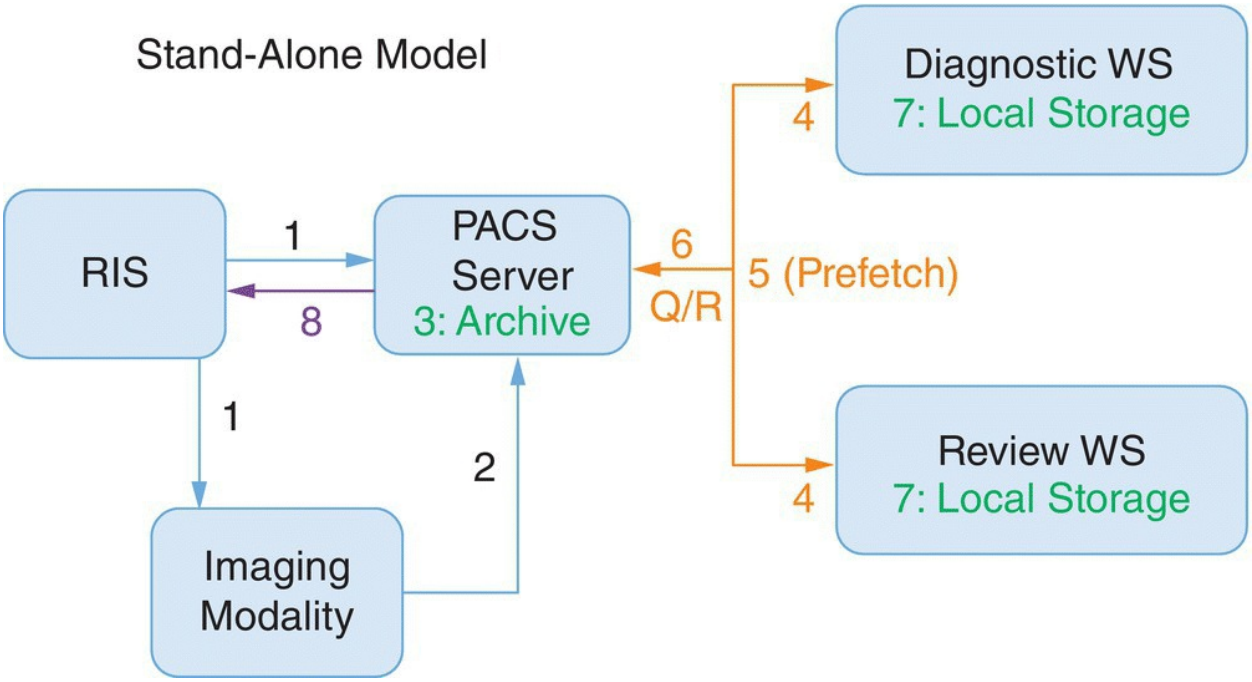

Figure 3.3 Stand-alone PACS-based model and general data flow. The data flow starts when RIS notifies imaging modality and the PACS server that a patient has registered (1). Images are sent from the modality to the PACS server (2), PACS server archives the images (3) and sends them to WSs automatically (single-

headed orange arrows, 4) along with other prefetched images (single-headed orange arrows, 5); images can also be queried/retrieved by the WSs (double-headed orange arrows, 6). All WSs have local storage (7). Diagnostic reports are sent back to the PACS server or directly to RIS (purple arrow, 8).

1. RIS notifies the imaging modality and the PACS server that a patient has registered.
2. After the exam, the modality sends images to the PACS server.
3. PACS server archives the images.
4. Multiple copies of the images are distributed to selected diagnostic and review WSs. The server performs the image distribution function automatically, based on the default setting.
5. Server also prefetches pertinent historical images and sends copies to selected WSs.
6. WSs can also use DICOM query/retrieve function through the server to obtain prepetched images for review. In addition, if automatic prefetching fails, a WS can query/retrieve historical images from the server.
7. Each WS contains a local storage to hold a preset number of PACS exams.
8. WS returns the diagnosis to the server, then to the RIS.

3.4.1.1 Advantages

1. If the PACS server goes down, imaging modalities or acquisition GWs have the flexibility to send images directly to designated WSs, so that radiologists can continue reading new cases.
2. Because multiple copies of the PACS exam are distributed throughout the system, there is less risk of losing PACS image data.
3. Some historical PACS exams will still be available in WSs, because they have local storages.
4. System is less susceptible to daily variations of network performance, because PACS exams are preloaded onto the WS local storage and are available for viewing immediately.
5. Modification to the DICOM header can be performed if necessary during the quality control before archiving.

3.4.1.2 Disadvantages

1. Users must rely on correct image distribution and pre-fetching of historical PACS exams based on the preset default table, which is not possible all the time.
2. Because images are sent to designated WSs, each one may have a different worklist, which makes it inconvenient for radiologists to read/review all exams assigned to him/her at any WS in one setting.
3. Users sometimes need to use query/retrieve function to retrieve pertinent PACS exams from the archive; this task can be a complex function compared with the client/server model.
4. Radiologists may duplicate the reading of the same case from a different WS, because the same exam may be sent to several WSs.

3.4.2 PACS-Based Client–Server Model and Data Flow

The client–server model described here is also called the thin-client model; the three major features of the client–server model are as follows:

1. Images are archived centrally in the PACS server.
2. From a single work list at the client, the WS has a single worklist of all examinations where a user can select the patient and images via the PACS server.
3. WSs have no local storage; images are flushed after reading.

Data flow of the client–server PACS model is shown in Figure 3.4. The numerals indicate the following steps:

1. RIS notifies the imaging modality and the PACS server of a patient registration.
2. After the examination, the modality sends images to the PACS server.
3. PACS server archives the images.
4. Client WSs have access to the complete worklist from where images and exams can be retrieved from the PACS server and archive. For more efficient image retrievals, the worklist can be shortened by a preset filter.
5. Once the examination is selected, images from the PACS archive are loaded directly into the image memory of the client WS for viewing. Pre-fetched

historical exams are loaded to the WS in the same manner.

6. Once the user has completed reading/reviewing the exam, the image data are flushed from the memory, leaving no image data in the image memory of the client WS.
7. WS returns the diagnosis to the server and then to the RIS.

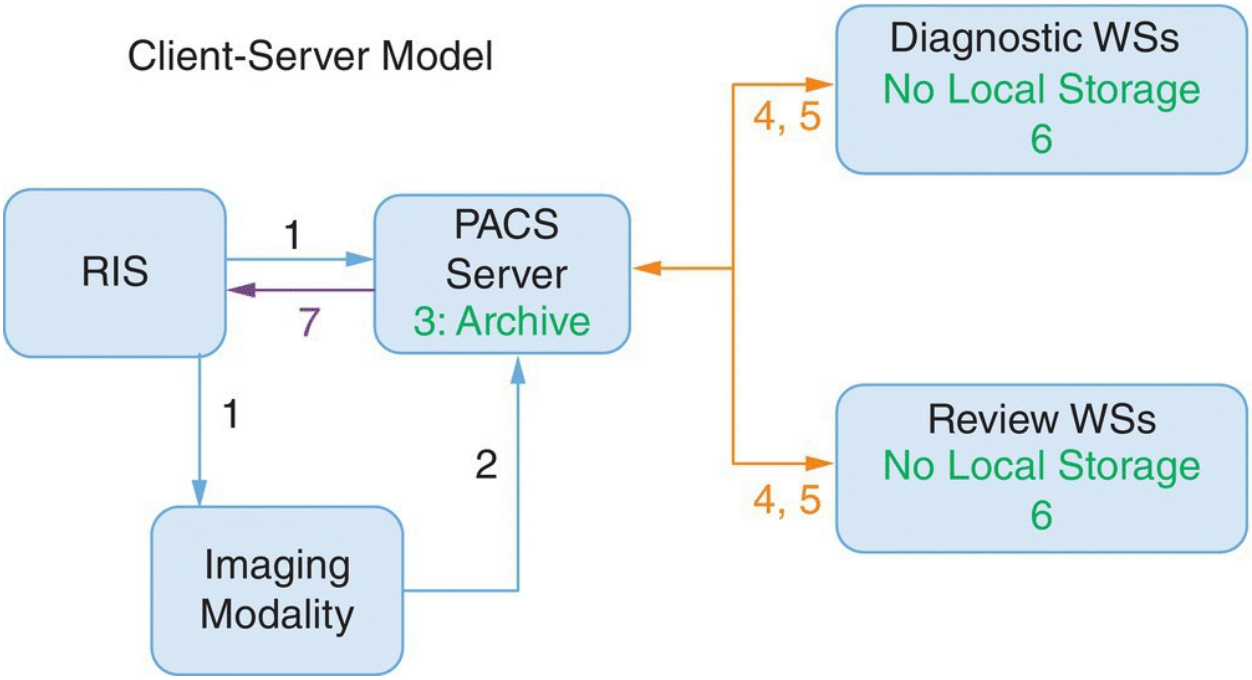

Figure 3.4 Client-server PACS-based model and general data flow. The first three data flow steps are the same as those of the stand-alone model. Data flow starts when RIS notifies imaging modality and the PACS server that a patient has registered (1). Images are sent from the modality to the PACS server (2), and PACS server archives the images (3). The client WSs has access to the completed current worklist, as well as the list of prehistorical exams of the same patient. Current images as well as historical images can be retrieved from the worklist for review and viewing (4, 5 double-headed orange arrows). All reviewed images are discarded from the WS after review (6). Diagnostic reports are sent back to the PACS server or directly to RIS (purple arrow, 7), the same as in the stand-alone model (Figure 3.3).

3.4.2.1 Advantages

1. Any exams are available on any PACS WS at any time, making it convenient to retrieve and to read/review.
2. No pre-fetching or study distribution is needed.

3. No query/retrieve function is needed. The user just selects the exam from the worklist on the client WS and the images are loaded automatically.
4. Because the main copy of a PACS exam is located in the PACS server archive and shared by client WSs, radiologists will know immediately if they are reading the same exam and thus avoid duplicate readings.

3.4.2.2 Disadvantages

1. The PACS server is a single point of failure; if it does go down, the entire PACS is nonfunctional. Then users are not able to view any exams from any client WSs. All newly acquired exams must be held back from the archive at the modalities storage until the server is repaired.
2. Because there are more database transactions in the client–server architecture, the system is exposed to more transaction errors, making it less robust when compared with the stand-alone architecture.
3. The architecture is dependent on network performance, especially when WAN is being used.
4. Modification to the DICOM header in the image for quality control is not possible until the image is archived.

3.4.3 Web-Based Model

The Web-based PACS model has the architecture similar to the client–server model. The main difference is that the client and server software are designed for Web-based applications. A couple of additional advantages of the Web-based model to compare with the client–server model are:

1. The client WS hardware can be platform independently, as long as the Web browser is supported.
2. The system is a completely portable. The Web-based application can be used on site as well as in the home with an Internet connection.

A disadvantage compared with the client–server model is that the system may be limited to the amount of functionality and performance of the Web-based browser. During the past few years, the client–server model and the Web-based model have emerged as the dominant PACS-based models in clinical operation.

3.4.4 Teleradiology Model

3.4.4.1 Pure Teleradiology Model

The Web-based PACS model propels its operation from an enclosed hospital environment to the outside world. The teleradiology model extends medical images to the outside world, as discussed in Chapter 2. Teleradiology is the transmission of radiological patient images and data, such as x-ray, CT, PET, MRI from certain different locations to others, for the purposes of sharing imaging studies with other radiologists and physicians. Teleradiology can be an entirely independent system operated in a pure teleradiology model, as shown in Figure 3.5. This model is better for several imaging centers and smaller hospitals with a radiological examination facility, with not enough in-house radiologists to cover the readings. In this model, the teleradiology management center serves as the monitor of the operation. It receives images from different imaging centers, 1,…, N, keeps a record but not the images, and routes images to different expert centers, 1,…, M, for reading. Reports come back to the management center, where it records the reading and forwards the reports to the appropriate imaging centers. The management center is also responsible for the billing and other administrative functions, such as image distribution and workload balancing. The WAN used for connection between various imaging centers, the management center, and expert centers can be of mixed type, with various performances dependent on requirements and costs. This model is used mostly for night and weekend coverage.

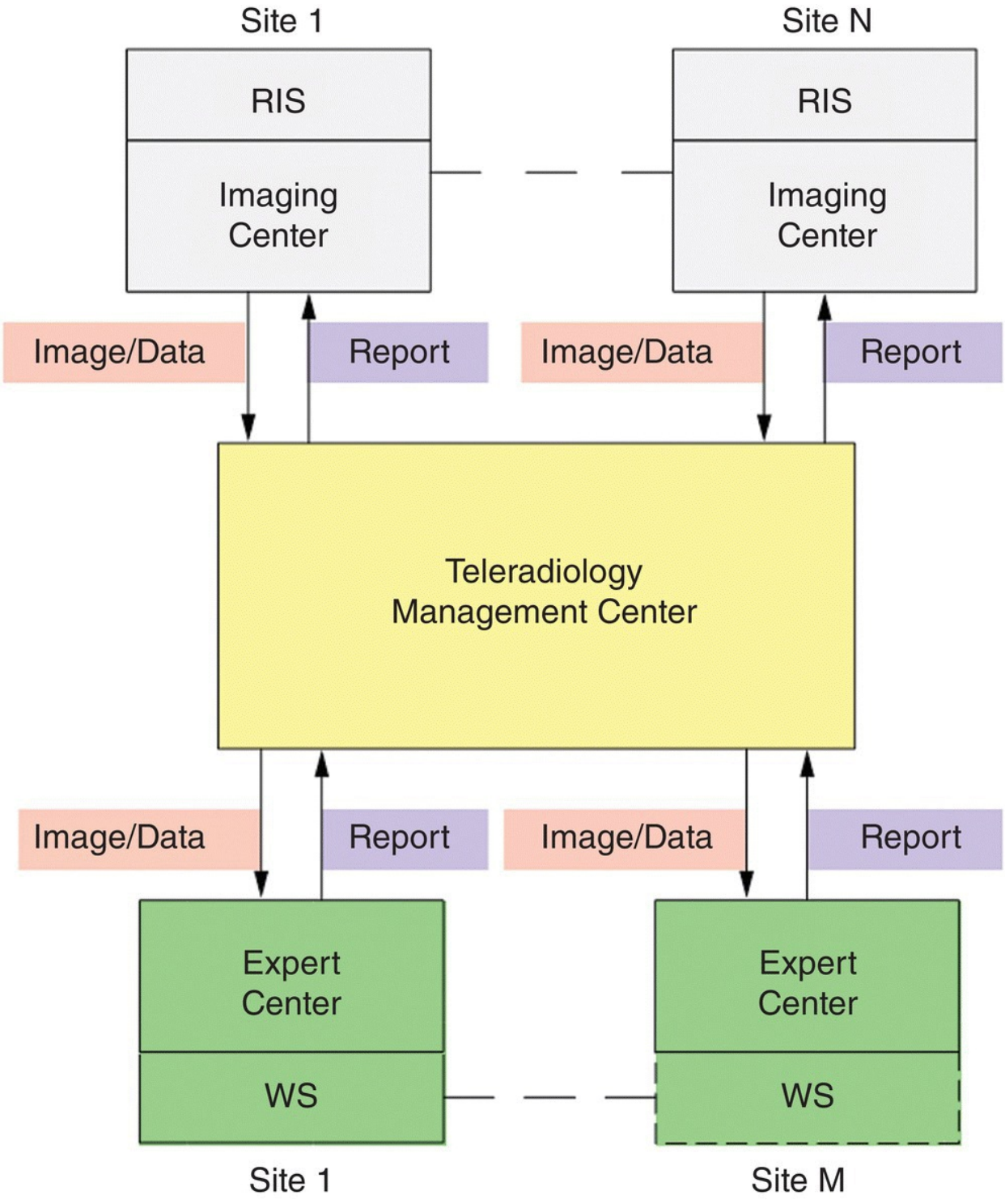

Figure 3.5 Basic teleradiology model. The management center monitors the operation to direct workflow between imaging centers and expert centers.RIS: radiology information system; WS: workstation.

3.4.4.2 PACS and Teleradiology Combined Model

PACS and teleradiology can be combined to form the unit, as shown in Figure 3.6. The two major components are the generic PACS, shown inside the upper dotted rectangle and the pure teleradiology model (Figure 3.6), shown in the lower rectangle. The workflow of this combined model is as follows:

- Radiologists at PACS WSs read exams from the outside imaging centers (step 1).
- After reading by PACS radiologists from its own WSs (step 2), reports are sent to the HIS database via the database gateway for its own record (step 3) and to the expert center (steps 4 and 5), from where the report (step 4) is also sent back to the imaging center.
- PACS can also send its own exams to the outside expert center for reading (step 5). The expert center returns the report to the PACS database gateway (step 6).
- The image center can send images to the expert center for reading, as in the pure teleradiology model (step 7).

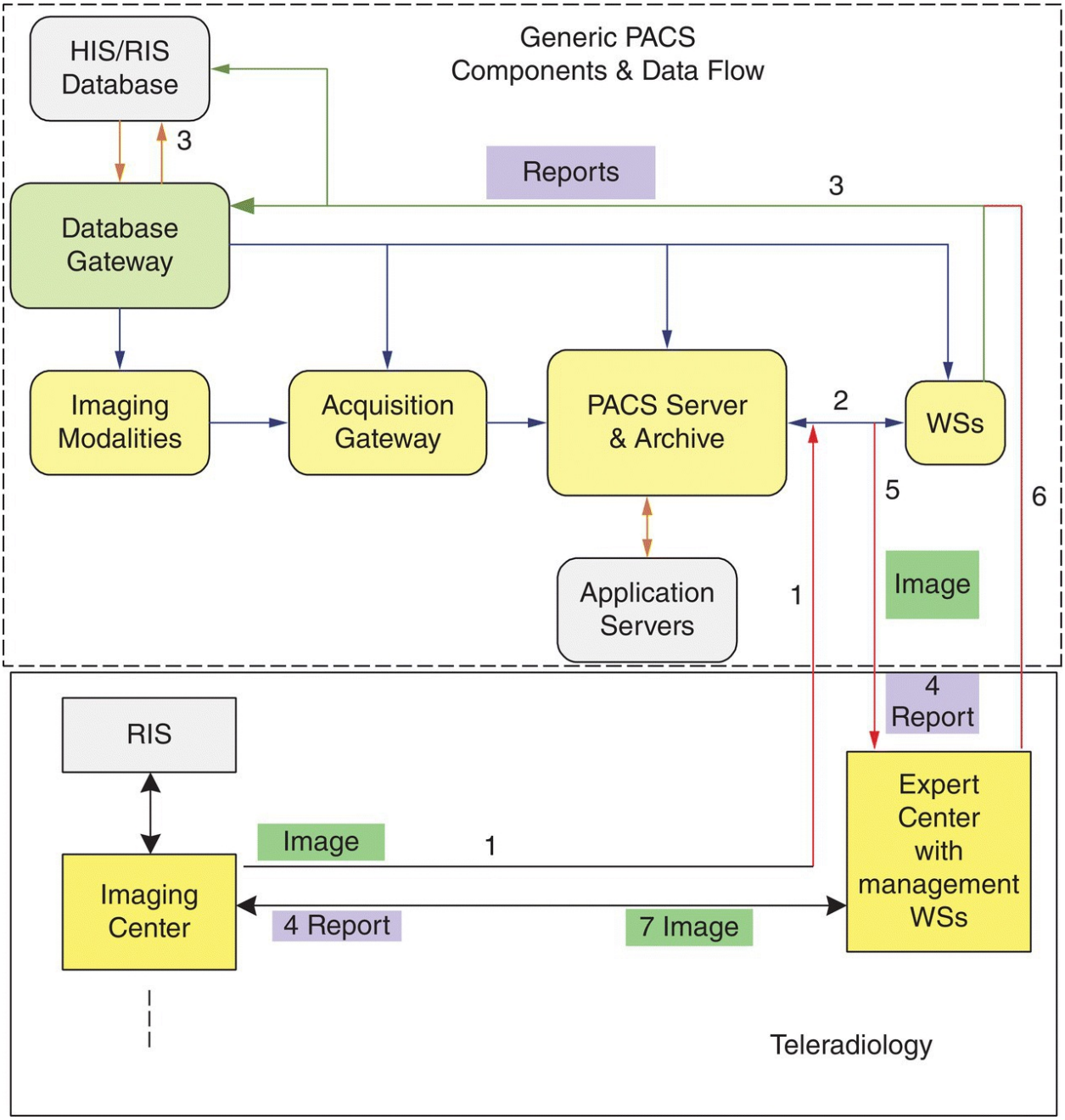

Figure 3.6 The PACS and teleradiology combined model. The top rectangle is the PACS components and workflow (detail from Figure 3.1), and the bottom rectangle is the teleradiology model, modified from Figure 3.5. Red lines show communication between PACS and teleradiology. HIS: hospital information system; RIS: radiology information system; WSs: workstations.

The combined teleradiology and PACS model is mostly used in a healthcare center with these components:

1. satellite imaging centers;
2. multiple affiliated hospitals; and
3. with backup radiology coverage between hospitals and imaging centers.

3.4.5 Enterprise PACS-Based Multimedia and ePR System with Image Distribution

Enterprise PACS is for large-scale PACS-based multimedia systems integration. It has become particularly popular in today's enterprise healthcare delivery system. Figure 3.7 shows the generic architecture of an enterprise PACS. In the generic architecture, three major components are PACS-based multimedia at each hospital in the enterprise, the enterprise data center, and the enterprise ePR. The general workflow is:

1. The enterprise data center supports all PAC systems in the enterprise.
2. Patient images and data from each PACS are sent to the enterprise data center for long-term archive (step 1).
3. Filtered patient data and images from the Web server at each site are sent to the ePR system in the data center (step 2). The ePR system is the master Web-based client-server ePR system with filtered data and images.
4. The data center has a primary data center, backed by the secondary data center (step 3), avoiding a single point of failure (SPOF) in the enterprise PACS.
5. In the data center, the ePR (step 4) is responsible for combining patients' electronic records with images from all sites of the enterprise. The ePR has a backup at the secondary data center (step 5).
6. ePR Web clients throughout the enterprise can access patients' electronic records with images from any sites in the enterprise through the data center ePR system (step 6) or its own site patient through its own Web server (step 7).

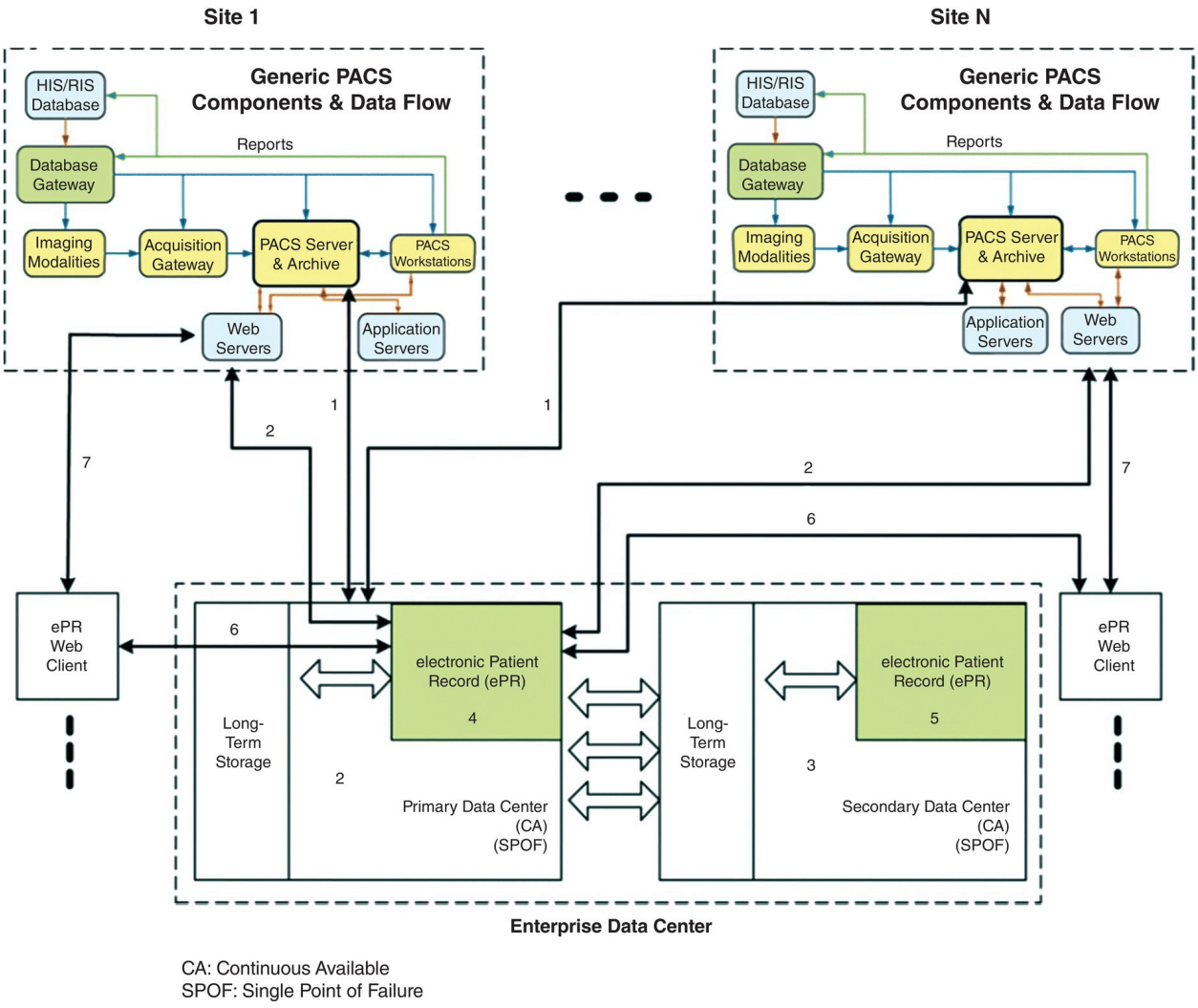

Figure 3.7 Enterprise PACS and ePR system with images. The enterprise data center supports all sites in the enterprise. The primary data center has a secondary data center for backup to avoid a single point of failure (SPOF). The enterprise ePR system is accessible from any ePR Web clients, and allows image distribution of the patient's electronic record within the enterprise.

3.5 Communication and Networks

PACS-based multimedia uses communication and networks for data transmission. Figure 3.1 describes the generic PACS-based multimedia components and workflow. This section emphasizes the importance of communication and networks of PACS-based components interconnecting with other healthcare information systems.

3.5.1 Network Standards – OSI and DOD

The two most commonly used network standards in PACS-based applications are the standard developed by the US Department of Defense (DOD), and the open systems interconnection (OSI) developed by the International Standards Organization (ISO). As shown in Figure 3.8, DOD (right) has four-layer protocol stacks and OSI (left) has seven-layer stacks. In the DOD protocol stacks, the file transfer protocol (FTP) and TCP/IP are two popular communication protocols used widely in medical imaging industry. The seven layers in the OSI protocols are defined in Table 3.3.

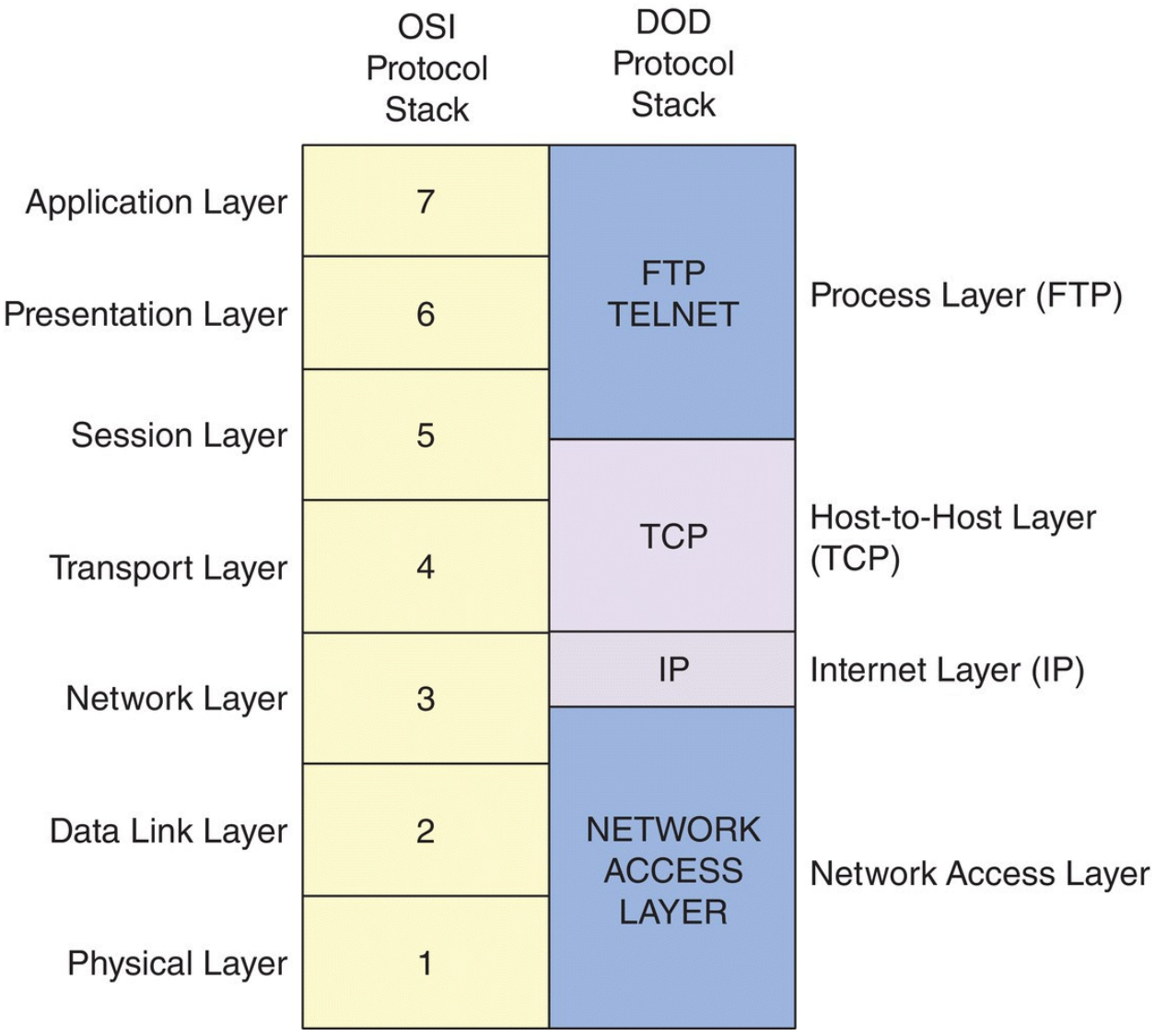

Figure 3.8 Correspondence between the seven-layer open systems interconnect (OSI, yellow) and the four-layer Department of Defense (DOD, blue) communication protocols. TCP/IP, light purple in DOD is the most popular in

medical imaging and PACS applications. FTP: file transfer protocol.

Table 3.3 Seven-layer open systems interconnect (OSI) protocols.

Layer	Protocol	Definition
7	Application Layer	Provide services to users
6	Presentation Layer	Transformation of data (encryption, compression, reformatting)
5	Session Layer	Control applications running on different workstations
4	Transport Layer	Transfer of data between endpoints with error recovery
3	Network Layer	Establish, maintain, and terminate network connections
2	Data link Layer	Medium access control—network access (collision detection, token passing) and network control logical links control—send and receive data messages or packets
1	Physical Layer	Hardware layer

An example is used to explain how data are sent between two nodes in a network using the DOD TCP/IP transmission. Figure 3.9 shows the procedure from the top to bottom (the steps by which a block of data (yellow) is transmitted with protocol information listed in the left of the figure). First, blocks of data are split into segments of data (yellow), whereupon each segment is given, in that order, a packet header, an IP header, a TCP header, followed by the application header (AH), then the data segment, and lastly, a packet trailer. The encapsulated data segment is called a packet with six boxes (see bottom line in Figure 3.9). The packet is then sent, and the process is repeated until the entire block of data (see top line in Figure 3.9) has been transmitted.

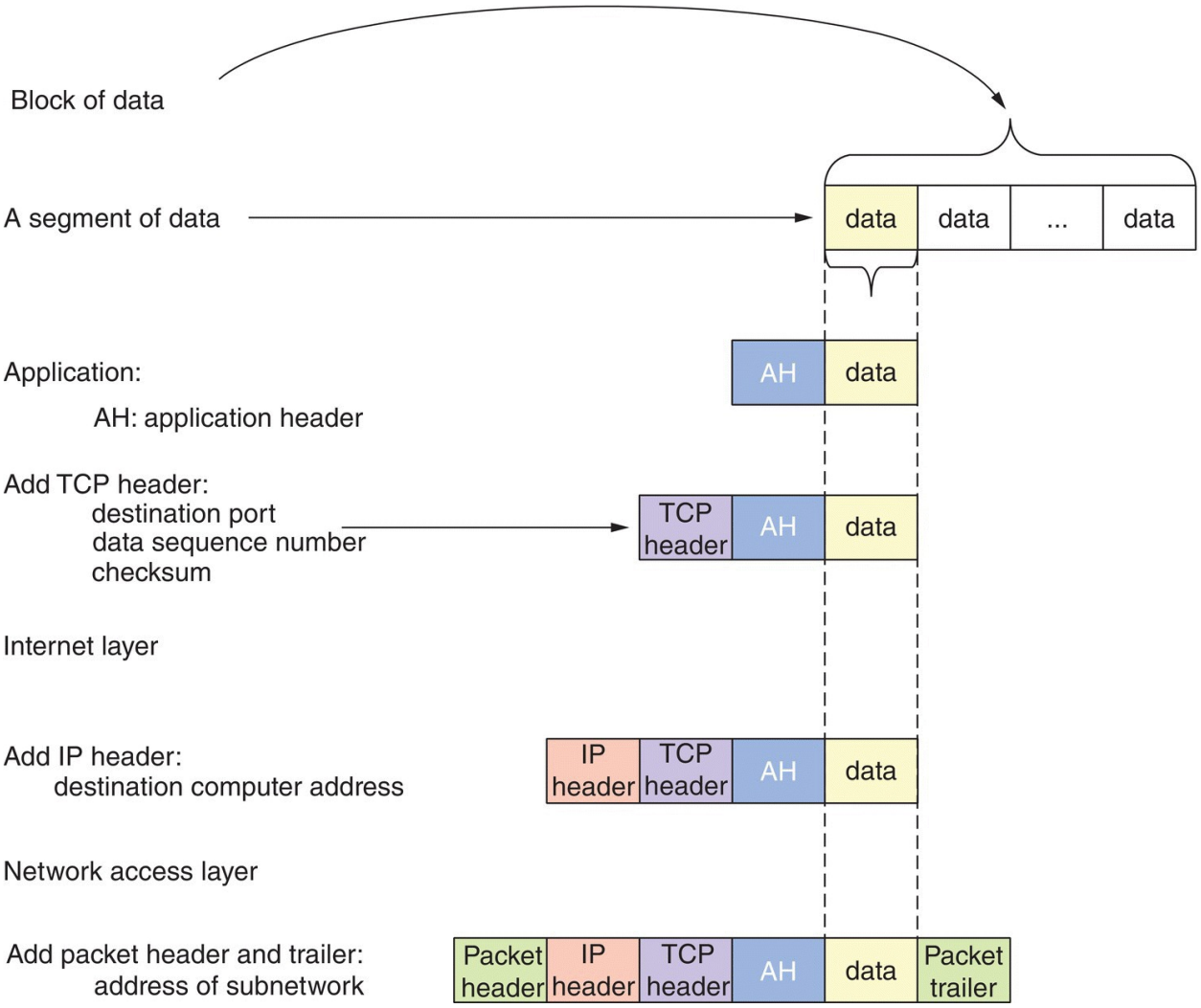

Figure 3.9 Example of data block transmission from one network node to another node with the DOD TCP/IP. The data block is divided into segments. The figure illustrates how a segment of data (yellow) is encapsulated with the application header (blue), the TCP header (purple), IP header (pink), and the packet header (green) and the packet trailer (green). All these headers and the trailer (color blocks) are the data transmission overheads.

In using the TCP/IP, there are two types of transmission overhead: the storage and the time. Storage overheads are the packet header, IP header, TCP header, application header (AP), and the packet trailer. The time overheads are the encoding and decoding processes. While TCP/IP is very reliable, it does add to overheads during the data transmission, which could delay the image transmission time.

3.5.2 Network Technology

Two commonly used network technologies in PACS-based multimedia applications are the Ethernet and the ATM, both running on TCP/IP communication modes. Ethernet is a network system for connecting a number of computer systems to form a LAN, with protocols to control the passing of information and to avoid simultaneous transmission by two or more systems. ATM is a switching technique used by telecommunication networks that uses asynchronous time-division multiplexing to encode data into small, fixed-sized cells. This technology is different from Ethernet or Internet (Section 3.5.2.1), which use variable packet sizes for data or frames.

3.5.2.1 Ethernet and Gigabit Ethernet

3.5.2.1.1 Standard Ethernet

The standard Ethernet (luminiferous ether), is based on IEEE Standard 802.3 carrier sense multiple access with collision detection (CSMA/CD). It operates from 10 Mbits/s to 1 Gbit/s, and can be even higher over half-inch coaxial cables, twisted pair wires, fiberoptic cables, or wireless systems. Another technology, high-definition multimedia interface (HDMI), is a proprietary audio/video interface for transferring uncompressed video data and compressed or uncompressed digital audio data from an HDMI-compliant source device, such as a display controller, to a compatible computer monitor, video projector, digital television, or other display (see Chapter 10, Display Workstation). Data are sent out in packets to facilitate the sharing of the cable. All nodes on the network connect to the backbone cable via the Ethernet switches or hubs. Each packet contains a source address, a destination address, data, and error detection codes. In addition, each packet is prefaced with signal detection and transmission codes that ascertain status and establish the use of the cable.

3.5.2.1.2 Fast Ethernet and Gigabit Ethernet

Advances in fast Ethernet (100 Mbit/s) and gigabit Ethernet (1.0 Gbit/s or higher) switches allow PACS-based multimedia components to obtain very high speed performances. High-speed Ethernet technology is a star topology, much like the ATM (Section 3.5.2). Each switch allows for a certain number of connections to the WSs through a standard 100-Mbits/s board or an adapter board attached to the workstation for a higher-speed connection.

A gigabit Ethernet switch can be branched out to many 100 Mbit/s WSs; and a 100 Mbits/s Ethernet switch can be stepped down to several 10 Mbit/s switches, and many 10 Mbit/s WSs connections, as shown in Figure 3.10.

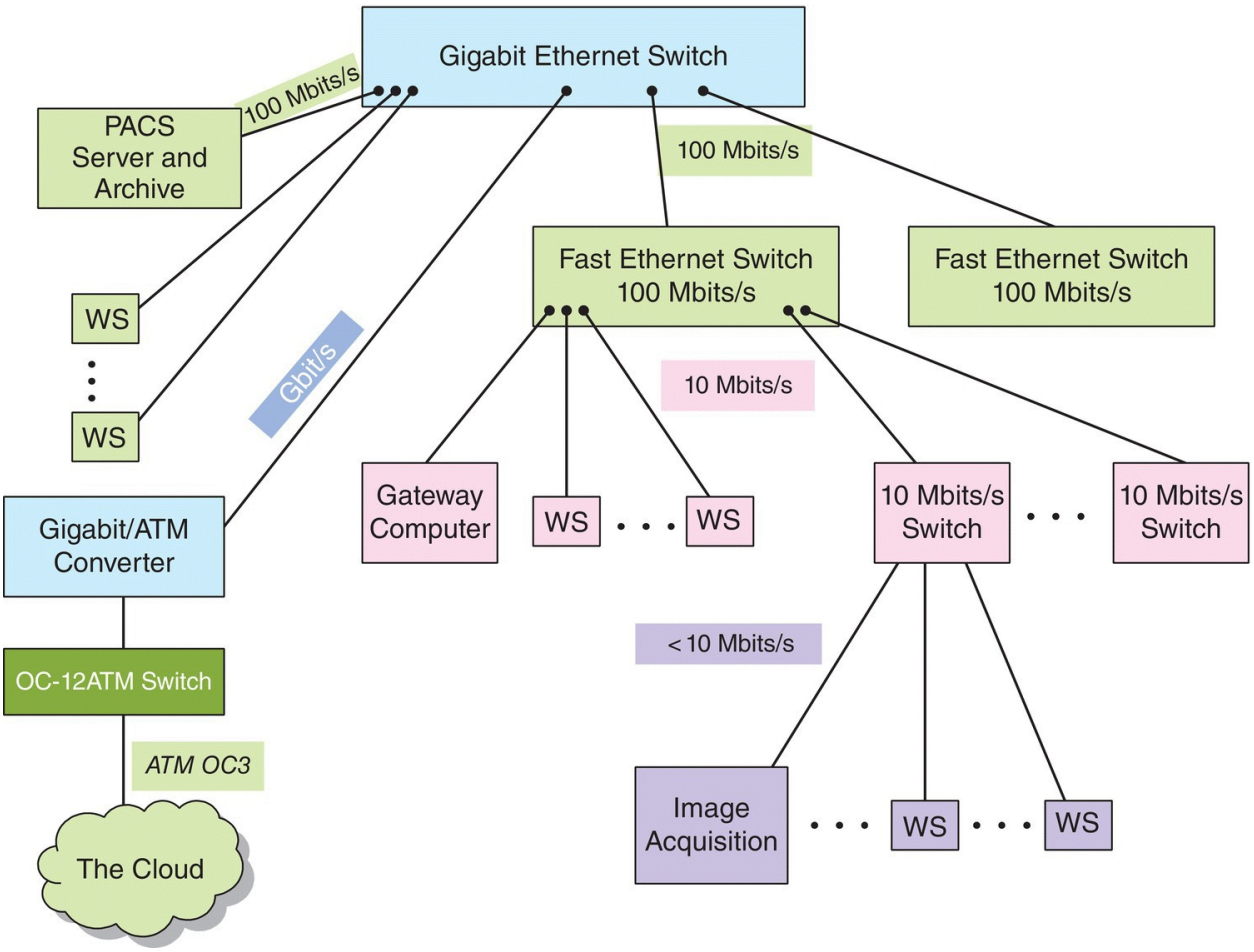

Figure 3.10 An example of a scheme combining the Gbit Ethernet switch with the asynchronous transfer mode (ATM) optical carrier (OC) -12 for PACS-based multimedia application. Blue: Gbit/s; light green: 100 Mbits/s; pink: 10 Mbits/s; purple: <10 Mbits/s; left: dark green: ATM OC-12 622 Mbits/s; light green: OC-3 155 Mbits/s; bottom left: The Cloud (Chapter 15).

3.5.2.2 ATM (Asynchronous Transfer Mode) Technology

Ethernet was originally designed for LAN applications, but radiological imaging communication should have no physical or logical boundaries between LANs and WANs. ATM can step in as a good technology for combining both LANs and WANs. ATM is a method for transporting information that splits data into fixed-length cells, each consisting of 5 bytes of ATM transmission protocol header information and 48 bytes of data information. Based on the virtual circuit-oriented packet-switching theory developed for telephone circuit switching applications, ATM systems were designed on the star topology, in which an ATM switch serves as a hub. The basic signaling rate of ATM is 51.84

Mbit/s, called optical carrier level 1 (OC-1). Other rates are multiples of OC-1, for example, OC-3 (155 Mbit/s), OC-12 (622 Mbit/s), OC-48 (2.5 Gbit/s), OC-192 (10 Gbit/s) and more. In medical imaging and PACS-based multimedia, TCP/IP and DICOM transmission can be used for both LAN and WAN, and the combination of ATM and Gbit/s Ethernet technologies can form the backbone of Internet 2, to be discussed in Section 3.5.2.4.

Because backbone Ethernet is mostly used for LANs, and ATM can be used for both LANs and WANs, it is important to know that the gigabit Ethernet switch can also be used to connect to various ATM switches, providing an interconnection for these two network technologies. Figure 3.10 shows an example of a two-node connection of a Gbit/s Ethernet switch with an ATM OC-12 and together they can achieve up to 500 Mbit/s, sufficient for most medical imaging applications.

3.5.2.3 Wireless Networks

Wireless networks are other emerging technologies used to handle display devices in PACS-based multimedia applications. It is convenient to use for handheld or pocket display WS. A wireless LAN (WLAN) is a type of LAN that uses high-frequency radio waves rather than wires to communicate between nodes. WLANs are based on IEEE Standard 802.11, also known as wireless fidelity (Wi-Fi). IEEE Standard 802.11 was introduced as a standard for wireless LANs in 1997 and is updated to IEEE 802.11-1999. The current standard is also accepted by the American National Standards Institute/ International Standards Organization(ANSI/ISO). Table 3.4 shows the different standards available in this technology.

Table 3.4 Current available wireless LAN technology.

Name	Frequency (GHz)	Maximum Bandwidth(Mbits/s)
802.11a	5	54
802.11b	2.4	11
802.11 g	2.4	54

Among these, IEEE 802.11b is probably the most widely implemented and routinely used wireless LAN today. It operates in the 2.4-GHz band and uses direct sequence spread spectrum (DSSS) modulation. The 802.11b-compliant devices can operate at 1, 2, 5.5, and 11 Mbits/s. The next improvement of 802.11b is 802.11 g, which can increase the bandwidth to 54 Mbits/s within the

2.4-GHz band. Standard 802.11a is another high-speed wireless LAN operating in the 5-GHz band, which uses orthogonal frequency division multiplexing (OFDM). The data rates it supports include 6, 9, 12, 18, 24, 36, 48, and 54 Mbits/s. Standard 802.11a has a range similar to 802.11b in a typical office environment of up to 225 ft. Twelve separate non-overlapping channels are available for 802.11a; therefore data rates higher than 54 Mbits/s can be reached by combining channels. Most laptop computers used in clinical environments are equipped with 54-Mbits/s ports for wireless communication.

In wireless communication technology, the term Wi-Fi is often used. Wi-Fi is a trademark of the Wi-Fi Alliance, founded in 1999 as Wireless Ethernet Compatibility Alliance (WECA), comprising more than 300 companies, whose products are certified by the Wi-Fi Alliance, based on the IEEE 802.11 standards (also called WLAN and Wi-Fi). This certification warrants interoperability between different wireless devices. The alliance was founded because many products did not correctly implement IEEE 802.11 and some included proprietary extensions. This led to incompatibilities between products from different manufacturers.

Another new wireless communication technology, Bluetooth™1, is emerging, in which the Bluetooth Special Interest Group (SIG) has produced a specification for Bluetooth wireless communication devices that are publicly available for the standardization of the technology. Bluetooth devices are characterized by wireless communication using radio waves to transmit and receive data. This technology is specifically designed for short-range (10 meters) communication, thus consuming very little power, and is tailored for small, portable personal devices, like a personal digital assistant (PDA).

3.5.2.4 Ethernet and Internet

The terms “Ethernet” and “Internet” are sometimes confusing if the PACS-based multimedia users are not familiar with the communication technology. The Internet and Ethernet are two totally different things, although they are often found together. Ethernet is a LAN used to connect computers located near to one another. Internet is a WAN that computers further away from each other can connect to in order to access information.

By definition, Ethernet is a term that is used to identify a group of technologies that allow computers to be interconnected, in order to transmit data from one to the other. Ethernet is a physical specification for LANs, also known as IEEE 802.3. It is the cable (or media) hardware that connects computers to other

equipment or to the network routers. Nowadays, most Ethernets take the form of CAT-5 cables, fiber optics, or Wi-Fi (IEEE 802.11). In Ethernet, the term media access control addresses uniquely identify Ethernet network cards (or PCs with built-in Ethernet). Although it is true that every computer that uses Ethernet has a unique media access control address, not all Internet connections are made over Ethernet.

The Internet is a worldwide packet switching network. Since it is based on packets, and Ethernet delivers packets, the carrier for the Internet that most people encounter is Ethernet. Within one building, the Internet is often carried by Ethernet. But over longer distances, other technologies like WANs are used. In the Internet, it is sometime called a global superhighway. This is a collection of physical machines (servers, hosts, etc.) and software (e.g. World Wide Web – www) set up in an interconnected global “web” in multitude ways. For example, if a www site is log in, it means that the Internet is being used because the Web site is identified by its physical media including cables and air waves. Simply put, Ethernet is a physical media for connection among computers; Internet is the network of computers.

Both Ethernet and Internet are types of networks that are used to connect computers. However, the scope and range of these networks differ. The Ethernet is a LAN, which connects computers in a local location. There are thousands and hundreds of thousands of Ethernet networks. The Internet, on the other hand, is one massive WAN that computers further away can connect to in order to access information.

The Internet is the massive global system that connects computer networks around the world. Worldwide, many private, public, academic, business, healthcare, and government networks connect with each other over the Internet to share massive amounts of information, resources, and services. As an example, the Internet is used to access web pages, send emails, listen to music, or watch videos online.

A major difference between Ethernets and the Internet is data security. The Ethernet is usually safe, as it is a closed network. The Internet is mostly open access, with everyone belonging to the same Web site, who can access the data and information online. Unfortunately, this arrangement can open a way for people to hack other computers and to plant viruses.

3.5.2.5 Internet 2

Several years ago, the federal government initiated the Internet 2 WAN

communication technology, which is easy to use as the standard Internet and low cost to operate once the institution is connected to the Internet 2 backbone. It was introduced in the early 2000s and has evolved since then. Most university campuses, academic research laboratories, and some private industrial research laboratories are now equipped with this network connection.

3.5.2.5.1 Image Data Communication

PACS-based multimodality requires high-speed networks to transmit large image files between components. In the case of an intranet, that is, PACS within a medical center, Gbits/s switches and Mbits/s connections to WSs are almost standard in most network infrastructures. Their transmission rates, even for large image files, are acceptable for clinical operation. However, when using the WAN, these rates would not be sufficient. Table 3.5 shows the transmission rates of current WAN technologies.

Table 3.5 Transmission rate of current WAN technology.

Technology	Transmission Rate
• DS-0	56 Kbits/s
• DS-1	56 to (24 × 56) Kbits/s
• DSL	32 Kbits/s to 50 Mbits/s
• DS-1 (T1)	1.5 Mbits/s
• ISDN	56 Kbits/s to 1.5 Mbits/s
• DS-3	28 DS-1 = 45 Mbits/s
• ATM (OC-3)	155 Mbits/s and up
• Internet 2	100 Mbits/s and up

Among these technologies, digital subscriber lines (DSL) has emerged as a reliable technology used by many home office connections, including in small-scale lower-speed teleradiology applications. DSL is a broadband delivery

method using standard copper telephone wires, but many times faster than modem dial-up services. DSL is a system that provides subscribers with continuous, uninterrupted connections to the Internet over existing telephone lines, offering a choice of speeds ranging from 32Kbits/s to more than 50 Mbits/s. Telemedical imaging applications require low-cost and high-speed backbone WANs to carry large amounts of imaging related data for rapid-turnaround interpretation. Current low-cost commercial WAN is too slow for medical imaging application, whereas the high-speed WAN (T1 and up) is too expensive for cost-effective use. Internet 2 technology is a potential candidate for low-cost and high-speed networks for large-scale image data transmission, especially for those medical centers already equipped with Internet 2 technology.

3.5.2.5.2 What Is Internet 2 (I2)?

Internet2 (I2) is a federal government initiative for the integration of higher-speed backbone communication networks (up to 10 Gbits/s) as a means of replacing the current Internet for many applications including medical imaging related data. The nonprofit I2 organization, known as the University Corporation for Advanced Internet Development (UCAID)consortium, was founded in the summer of 1996 and is supported by the National Science Foundation. It is the network infrastructure backbone in the USA for high-speed data transmission. Members of the consortium, consisting of more than 1000 research universities and nonacademic institutes, are now connecting to the I2 backbones. I2 has evolved from several backbones: very high-speed backbone network service(vBNS), Abilene, and the California Research and Education Network(CalREN); and is now consolidated to the current Abilene backbone, shown in Figure 3.11. Some segments can rise from 5.6 Gbits/s, to 6.25 Gbits/s, to 9 Gbits/s performance. Care should be taken to distinguish Internet2 from next-generation Internet(NGI); the former refers to the network infrastructure, whereas the latter refers to various I2-related applications.

Figure 3.11 Major international interconnection points of Internet2 at the Abilene backbone. Most early International connections to Internet 2 were from a hub near Chicago. OC-48 (2.5 gbits/), OC-192 (10 Gbits/s).

(courtesy of Abilene Network, abiline.internet2.edu)

3.5.2.5.3 An Example of I2 Performance

3.5.2.5.3.1 Connection of Three International Sites

In the early 2000s, the Image Processing and Informatics Laboratory (IPILab) and the Exhibit Hall, Main Campus, Los Angeles, University of Southern California (USC); Polytechnic University (Hong Kong), and InCor (Brazil), were connected with I2 and Internet service provider (ISP) vendors (when the I2 link was missing). IPILab and USC counted as two US sites, since performance data could be measured at both sites. Performance values were collected using FTP and DICOM transmission protocols to measure real-world clinical applications of medical images studies. In addition, a repeatable Web 100 tuning protocol was applied to the four sites, effectively improving the performance three to eight times in comparison with the standard configuration. Figure 3.12 shows the network configurations. Tables 3.6, 3.7, and 3.8 show some of the results.

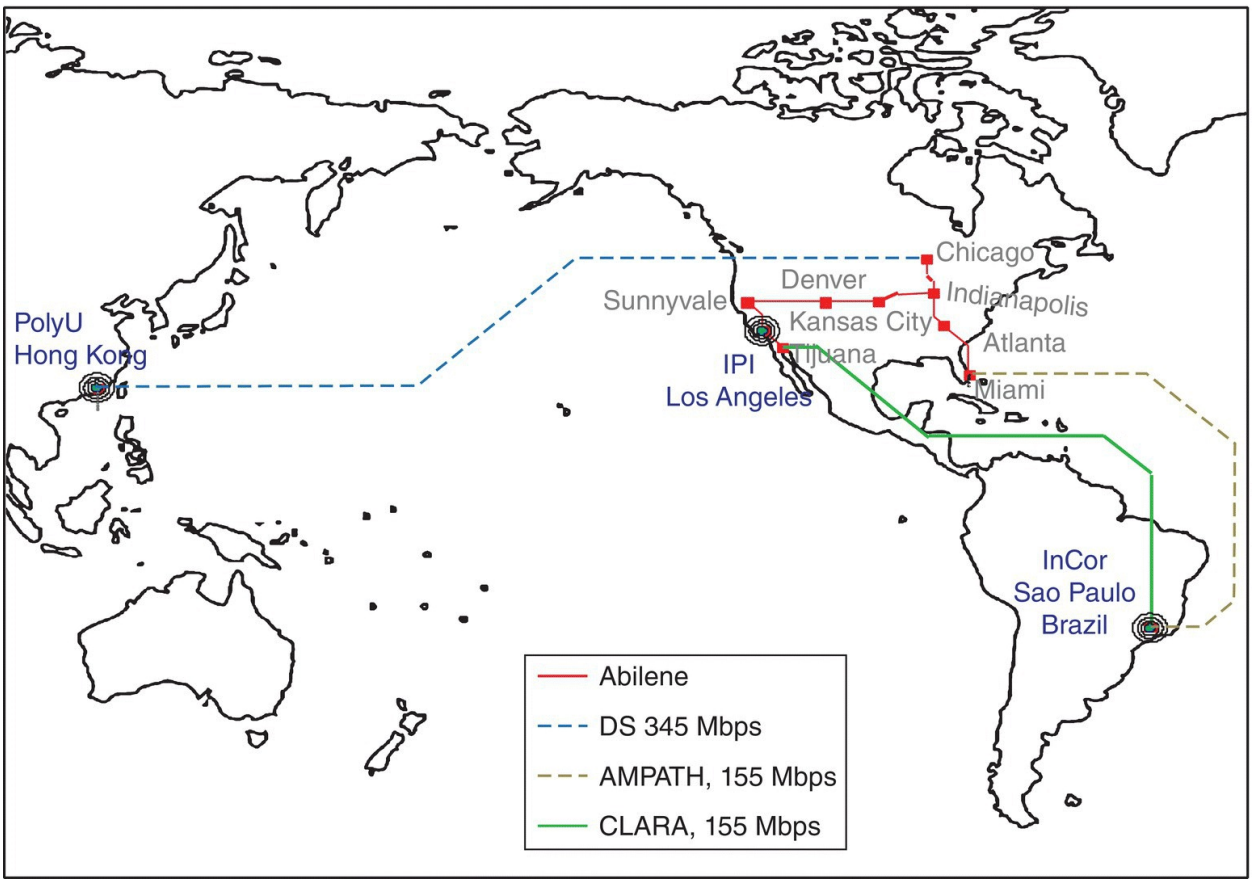

Figure 3.12 Topology of international Internet 2 connectivity between three test sites on three continents linking IPI/USC, Los Angeles, North America; InCor, Sao Paulo, Brazil, South America; and Polytechnic University (PolyU), Hong Kong. Flagtel (DS3) was the ISP vendor connecting IPILab to Hong Kong with points of presence (PoPs) in Tokyo and Hong Kong. The routing path from InCor to PolyU used AMPATH, and the path between IPI and InCor used CLARA. Both AMPATH and CLARA are ISP providers.

Table 3.6 Performance data for different sites connected with international Internet 2.

To	From	IPI	USC/HSC	PolyU	InCor
IPI	FTP (Mbits/s)		28.00*	1.60*	—
	RTT (ms)		—	292*	—
USC/HSC	FTP (Mbits/s)	10.00*		1.78	2.65
	RTT (ms)	—		253	171
PolyU	FTP (Mbits/s)	1.60*	2.80		1.12

	RTT (ms)	292*	254		425
InCor	FTP (Mbits/s)	—	1.50	0.63	
	RTT (ms)	—	172	424	

Note: Round trip times (RTT) in milliseconds and FTP performance times in megabits per second (Mbits/s) were collected. All sites were running standard Linux. The file size used was 7.8 MB. Asterisks show data collected from a different data collection period. A blank line means that no data were collected.

Table 3.7 Comparison of performance data between sites that utilized the Web 100 tuning protocol (last column) and the same sites using standard Linux without tuning.

From	To	Protocol	STD Linux (Mbits/s)	Tuned (Mbits/s)
PolyU	InCor	FTP	0.63	4.40
		DICOM	0.62	9.44
InCor	PolyU	FTP	1.12	3.10
		DICOM	1.50	2.97
PolyU	IPI Lab	FTP	1.63*	9.79*
		DICOM	1.36*	3.06*
IPI Lab	PolyU	FTP	1.60*	9.79*
		DICOM	1.36*	3.06*

Note: Performance data were gathered for both FTP and DICOM file transmissions. Asterisks show data collected from a different data collection period. A blank line means that no data were collected. With the tuning protocol, the performance was three to four times better.

Table 3.8 Performance data for IPI connectivity to both PolyU and InCor using a commercial high-speed ISP vendor.

From	To	RTT (ms)	CT		CR	
			(29 images, 15.5MB)		(2 images, 16 MB)	
			Untuned (Mbits/s)	Tuned (Mbits/s)	Untuned (Mbits/s)	Tuned (Mbits/s)
IPI	PolyU	187	3.09	12.24	3.16	6.61
PolyU	IPI	187	2.3	17.9	2.23	17.67

IPI	InCor	805	0.957	10.78	0.928	13.84
InCor	IPI	831	1.36	2.6	1.7	3.04
Note: Round trip times (RTT) were gathered between sites. One CT study of 29 images with 15.5 MB, and one CR study of two images with 16 MB were used to evaluate the DICOM transmission protocol performance between the sites.						

3.5.2.5.3.2 Some Observations

Results gathered from these measurements showed that even without the Web 100 tuning, performance numbers were comparable to those of a T1 connection (e.g. 1.5 Mbits/s) linking two such geographically distant sites as Brazil and Hong Kong. In addition, these performance numbers were comparable to commercially available high-speed ISPs that require a costly monthly service fee and are subject to fluctuations of performance due to e-commerce traffic—both of which are not characteristics of international Internet 2 connectivity. The performance evaluation showed how three international sites can use international Internet 2 connectivity as well as other non-US research networks, as adequate and acceptable solutions for almost real-time medical imaging transmission.

Further Reading

Abilene Network. http://abilene.internet2.edu/

Arbaugh, W.A., Shankar, N. and Wan, Y.C.J. (2001) Your 802.11 wireless network has no clothes. March 30, 2001. http://www.cs.umd.edu/~waa/wireless.pdf

Borisov, N., Goldberg, I. and Wagner, D. (2001). Intercepting mobile communications: the insecurity of 802.11. *Proceedings of the Seventh Annual International Conference on Mobile Computing and Networking*. July 16–21, 2001. http://www.isaac.cs.berkeley.edu/isaac/mobicom.pdf California Research and Education Network, CalREN2. http://www.calren2.net

Chan, L.W.C., Cao, F., Zhou, M. and Hau, S.K. (2003) Connectivity issues and performance monitoring of international Internet-2 in tele-imaging consultation. Education Exhibit, RSNA 2003.

Chan, L.W.C., Zhou, M.Z., Hau, S.K., Law, M.Y.Y. and Tang, F.H. (2005)

Documet J, international Internet-2 performance and automatic tuning protocol for medical imaging applications. Computer Med Imag Graph, 29, 103–114.

Digital Imaging and Communications in Medicine (DICOM) (1996) Rosslyn, VA: National Electrical Manufacturers' Association. Flagtelecom. http://www.flagtelecom.com

Gast, M.S. (2005) *802.11 Wireless Networks: The Definitive Guide*. 2nd ed. Sebastopol, CA: O'Reilly. Globalcrossing. http://www.globalcrossing.com

http://apps.internet2.edu/rsna2003-demos.html#RemoteTreatmentPlanning

Advanced Networking. Internet2. http://networks.internet2.edu/rons.html

http://www.freesoft.org/CIE/RFC/792/index.htm

http://www.interne2.edu

http://www.novatelwireless.com/pcproducts/g100.html

http://www.siemenscordless.com/mobilephones/s46.html

Huang, C. (2003) Changing learning with new interactive and media-rich learning environments: Virtual Labs Case Study Report. *Comp Med Imag Graph*, 27(2–3), 157–164.

Huang, H.K. (2004) Enterprise PACS and image distribution. *Comp Med Imag Graph*, 27(2–3), 241–253.

Huang, H.K. (2004) *PACS and Imaging Informatics: Basic Principles and Applications*. Hoboken, NJ: John Wiley & Sons, Inc.

Huntoon, W. and Ferguson, J. (2002) Internet2 Presentation—May 2002, in I2 members meeting. http://www.web100.org/docs/Web100I2MM.ppt International Exchange Point in Miami, Florida International University, AMPATH. http://www.ampath.fiu.edu

Internet2 Consortium, UCAID. http://www.internet2.edu

Latina American Cooperation of Advanced Networks, redCLARA. http://www.redclara.net

Liu, B.J., Zhou, Z., Gutierrez, M.A., Documet, J., Chan, L. and Huang, H.K. (2007) International Internet2 connectivity and performance in medical imaging applications: Bridging the Americas to Asia. *J High Speed Networks*, 16(1), 5–20. Making the Choice: 802.11a or 802.11 g.

http://www.80211planet.com/tutorials/article/0,,10724_1009431,00.html

Mogel, G., Cao, F., Huang, H.K., Zhou, M., *et al*. (2002) Internet2 Performance for Medical Imaging Applications, RSNA 2002 Fall Meeting. http://apps.internet2.edu/rsna2002-demos.html

Mogel, G.T., Cao, F., Huang, H.K., Zhou, M., Liu, B.J. and Huang, C. (2002) Internet 2 performance for medical imaging applications: in Internet 2 RSNA Demos. *Radiology*, 225, 752.

Rede Nacional de Ensino e Pesquisa, RNP. http://www.rnp.br

Remote Treatment Planning for Radiation Therapy. Internet2/NLM infoRAD exhibit. RSNA 2003.

Shanmugam, R., Padmini, R. and Nivedita, S. (2002) *Special Edition Using TCP/IP*, 2nd ed. Indianapolis: Que Publishing.

Stahl, J.N., Zhang, J., Zellner, C., Pomerantsev, E.V., Chou, T.M. and Huang, H.K. (2000) Teleconferencing with dynamic medical images. *IEEE Trans Info Tech Biomed*, 4(1), 88–96.

StarLight. http://www.startap.net/starlight/

Summerhill, R. (2004) Internet2 Network infrastructure: Abilene current status and future plans. *GNEW 2004 Meeting*, CERN, Geneva, March 15, 2004.

Tierney, B.L. (2001) TCP tuning guide for distributed application on wide area networks. *Proceedings of the Network Computing*, February 2001.

Verio. http://www.verio.com

Web100 project. http://www.web100.org/

Wi-Fi Alliance home page. http://www.weca.net/

Yu, F., Hwang, K., Gill, M. and Huang, H.K. (2000) Some connectivity and security issues of NGI in medical imaging applications. *J High Speed Networks*, 9, 3–13.

Zhang, J., Stahl, J.N. and Huang, H.K. (2000) Real-time teleconsultation with high-resolution and large volume medical images for collaborative healthcare. *IEEE Trans Info Tech Biomed*, 4(2), 178–185.

Zhou, Z., Gutierrez, M., Documet, J., Chan, L., Huang, H.K. and Liu, B.J.

(2007) The role of a Data Grid in worldwide imaging-based clinical trials. *J High Speed Networks*, 16(1), 21–33.

PERPUSTAKAAN PRIBADI AN-NUR SUNARYA

4
Industrial Standards: Health Level 7 (HL7), Digital Imaging and Communications in Medicine (DICOM) and Integrating the Healthcare Enterprise (IHE)

CHAPTER MENU

4.1 Industrial Standards
4.2 The Health Level 7 (HL7) Standard
4.2.1 Health Level 7
4.2.2 An Example
4.2.3 The Trend in HL7
4.3 From ACR-NEMA to DICOM
4.3.1 ACR-NEMA and DICOM
4.3.2 Digital Imaging and Communications in Medicine (DICOM 3.0)
4.3.3 DICOM Standard PS 3.1 - 2008
4.3.4 DICOM Supplements
4.4 DICOM 3.0 STANDARD
4.4.1 DICOM Data Format
4.4.2 DICOM Model of the Real World
4.4.3 DICOM File Format
4.4.4 Object Class and Service Class
4.4.5 DICOM Services
4.4.6 DICOM Communication
4.4.7 DICOM Conformance
4.5 Examples of using DICOM
4.5.1 Send and Receive

4.5.2 Query and Retrieve
4.6 DICOM Organizational Structure and New Features
4.6.1 DICOM New Features since 2010
4.6.2 DICOM's Organizational Structure
4.6.3 Current DICOM Strategic Document
4.7 IHE (Integrating the Healthcare Enterprise)
4.7.1 History and what is IHE?
4.7.2 IHE Technical Framework and Integration Profiles
4.7.3 Some Examples of IHE Workflow Profiles
4.7.4 The Future of IHE
4.8 Some Operating Systems and Programming Languages useful to HL7, DICOM and IHE
4.8.1 UNIX Operating System
4.8.2 Windows NT/XP Operating Systems
4.8.3 C and C++ Programming Languages
4.8.4 SQL (Structural Query Language)
4.8.5 XML (Extensible Markup Language)
4.9 Summary of Industrial Standards: HL7, DICOM and IHE
References
Further Reading

This Chapter 4 and Chapter 5 provide the basic ingredients for the building blocks for marching forward (Chapter 15). Many PACS-based multimedia imaging informatics chapters included in this third edition are developed from this foundation.

4.1 Industrial Standards

Transmission of images and textual information among healthcare information systems has always been difficult for two reasons. First, information systems use different computer platforms, and second, images and data are generated from various imaging modalities by different manufacturers. With the emerging healthcare industry standards, Health Level 7 (HL7) and Digital Imaging and

Communications in Medicine (DICOM), it has become feasible to integrate all these heterogeneous, disparate medical images and textual data into an organized PACS-based multimedia system. Interfacing multiple healthcare components requires two major ingredients: a common data format and a communication protocol. HL7 is a standard textual data format, whereas DICOM includes data format and communication protocols. In conforming to the HL7 standard, it allows the sharing of healthcare information among hospital information systems (HIS), radiology information systems (RIS), various types of clinical results, PACS, and multimedia. By adapting the DICOM standard, medical images generated from a variety of imaging modalities and manufacturers can be interfaced as an integrated healthcare system. These two standards are discussed first. The third topic covered in this chapter is the Integrating the Healthcare Enterprise (IHE) model used for driving the adoption of standards. With these mandated standards readily available, a champion of IHE can persuade PACS-based multimedia imaging informatics users to adopt and use the standard model. The last topic in the chapter presents the computer operating systems and programming languages commonly used in medical imaging and healthcare information technology. Figure 4.1 shows the DICOM and HL7 standards in the PACS-based multimedia workflow, in which all images and pertinent data need to be first converted to the standards.

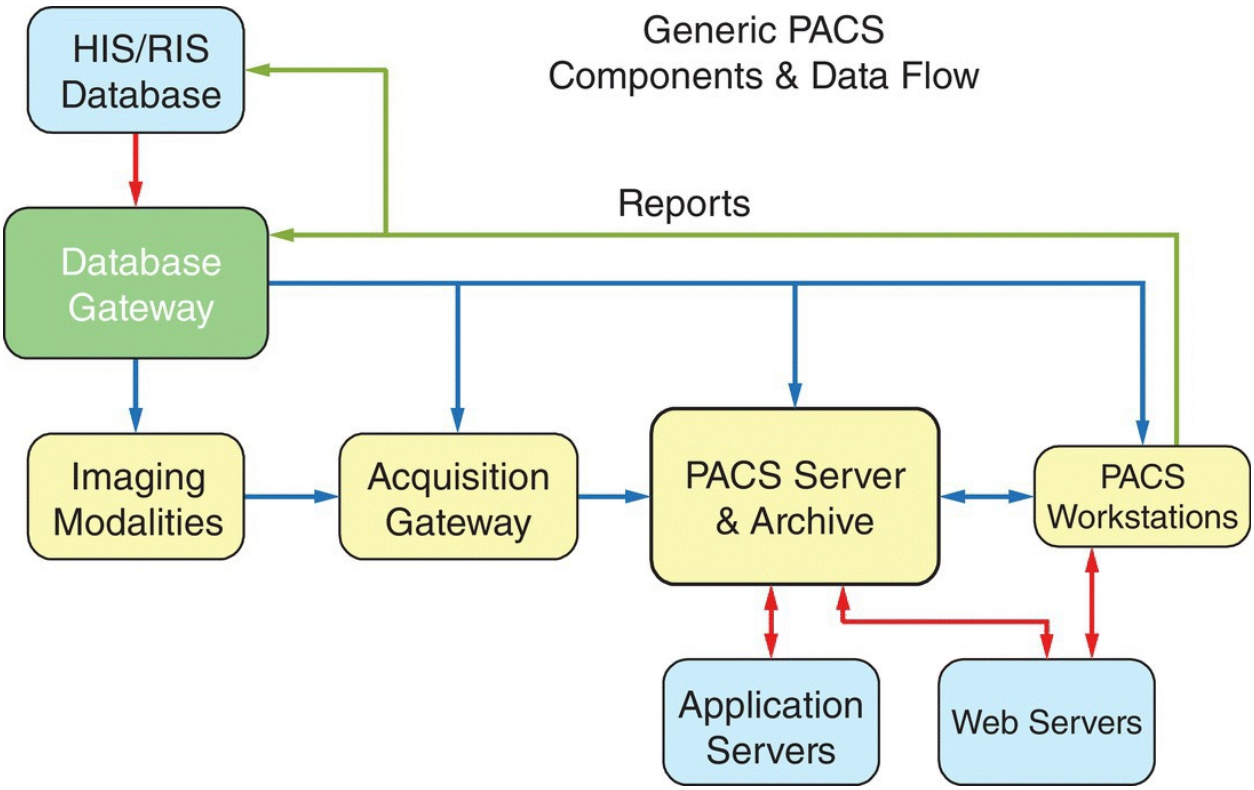

Figure 4.1 DICOM and HL7 standards in the PACS workflow, in which all images and pertinent data needed to be first converted to DICOM and HL7, respectively. PACS basic components (yellow) and data flow (blue: Internal; green and red: external between PACS and other information systems); other information systems (light blue). HIS: hospital information system; RIS: radiology information system.

4.2 The Health Level 7 (HL7) Standard

4.2.1 Health Level 7

Health Level 7 (HL7), established in March 1987, was organized by a user–vendor committee to develop a standard for electronic data exchange in healthcare environments, particularly for hospital applications. The HL7 standard refers to the highest level, the application level, in the seven communication levels model of open systems interconnection (OSI; Chapter 3, Section 3.5.1). The common goal is to simplify the interface implementation between computer applications from multiple vendors. This standard emphasizes data format and protocol for exchanging certain key textual data among healthcare information systems, such as HIS, RIS, and PACS (Chapter 5).

Although HL7 addresses the highest level (level 7) of the OSI model of the International Standards Organization (ISO), it does not conform specifically to the defined elements of the OSI's seventh level (Chapter 3, Section 3.5.1). It conforms to the conceptual definitions of an application-to-application interface placed in the seventh layer of the OSI model. These definitions were developed to facilitate data communication in a healthcare setting. by providing rules to convert abstract messages associated with real-world events into strings of characters comprising an actual message.

4.2.2 An Example

Consider the three popular computer platforms used in HIS, RIS, and PACS, namely the IBM mainframe computer running the VM operating system, the PC Microsoft Windows operating system, and the UNIX system. Interfacing involves the establishment of data links between these three operating systems via TCP/IP (Chapter 3, Section 3.1.6) with HL7 data format as the application layer.

When an event occurs, such as patient admission, discharge, or transfer (ADT),

the IBM computer in the HIS responsible for tracking this event will initiate an unsolicited message to the remote UNIX or Windows server in the RIS that takes charge of the next event. If the message is in HL7 format, UNIX or Windows passes the message, updates its local database automatically, and sends confirmation to the IBM. Otherwise, a “rejected” message is sent.

In the HL7 standard, the basic data unit is a message. Each message is composed of multiple segments in a defined sequence. Each segment contains multiple data fields and is identified by a unique, predefined three-character code. The first segment is the message header segment with the three-letter code “MSH”, which defines the intent, source, destination, and some other relevant information such as message control identification and time stamp. The other segments are event dependent. Within each segment, related information is bundled together based on the HL7 protocol. A typical message, such as patient admission, may contain the following segments, together with their codes:

- MSH—Message header segment;
- EVN—Event type segment;
- PID—Patient identification segment;
- NK1—Next of kin segment;
- PV1—Patient visit segment;

In this patient admission message, the patient identification segment may contain the segment header and other demographic information, such as patient identification number, name, birth date, and gender. The separators between fields and within a field are defined in the message header segment. Here is an example of transactions of admitting a patient for surgery in HL7:

1. Message header segment

   MSH||STORE|HOLLYWOOD|MIME|VERMONT|200305181007|security|

   ADT|MSG00201||| < CR>

2. Event type segment

   EVN|01|200305181005|| < CR>

3. Patient identification segment

   PID|||PATID1234567||Doe∧John∧B∧II||19470701|M||C|

   3976 Sunset Blvd∧Los Angeles ∧CA∧90027||323-681-2888|||||| < CR>

4. Next of kin segment

   NK1|Doe∧Linda∧E||wife| < CR>

5. Patient visit segment

   PV1|1|I|100∧345∧01||||00135∧SMITH∧WILLIAM∧K|||SUR|ADM|

   < CR>

Combining these five segments, these messages translate to: “Patient John B. Doe, II, male, Caucasian, born on July 1, 1947, lives in Los Angeles, was admitted on May 18, 2003 at 10:05 am by Doctor William K. Smith (#00135) for surgery. The patient has been assigned to Room 345, bed 01 on nursing unit 100. The next of kin is Linda E. Doe, wife. The admission, discharge, and transfer (ADT) message 201 was sent from system STORE at the Hollywood site to system MIME at the Vermont site in the same date two minutes after the admission.”

The “|” is the data file separator. If no data are entered in a field, a blank will be used, followed by another “|.”

The data communication between an HIS and an RIS is event driven. When an ADT event occurs, the HIS automatically sends a broadcast message, conformed to HL7 format, to the RIS. The RIS then passes this message and inserts, updates, and organizes patient demographic data into its database according to the event. Similarly, the RIS sends an HL7-formatted ADT message, the examination reports, and the procedural descriptions to the proper PACS-based multimedia imaging informatics component. When the PACS-based component has acknowledged and verified the data, it updates the appropriate databases and initiates any required follow-up actions.

4.2.3 The Trend in HL7

The most commonly used HL7 today is version 2.X, which has many options and thus is flexible. Over the past few years, version 2.X has been developed continuously, and is widely and successfully implemented in healthcare environments. Version 2.X and other older versions use a “bottom-up” approach, beginning with general concepts and adding new features as needed. These new features become options to the implementers so that the standard is very flexible and easy to adapt to different sites. However, these options and flexibility also make it impossible to perform reliable conformance tests of any vendor’s implementation. This forces vendors to spend more time in analyzing and

planning their interfaces to ensure that the same optional features are used in both interfacing parties. There is also no consistent view of the data when HL7 moves to a new version, or of the relationship of those data to other data. Therefore, a consistently defined and object-oriented version of HL7 is needed, which is version 3.

The initial release of HL7 Version 3 was in December 2001. The primary goal of HL7 version 3 is to offer a standard that is definite and testable. Version 3 uses an object-oriented methodology and a reference information model (RIM) to create HL7 messages. The object-oriented method is a “top-down” method. The RIM is an all-encompassing, open architecture design covering the entire scope of healthcare IT, containing more than 100 classes and more than 800 attributes. RIM defines the relationships of each class. RIM is the backbone of HL7 version 3, as it provides an explicit representation of the semantic and lexical connections between the information in the fields of HL7 messages. Because each aspect of the RIM is well defined, very few options exist in version 3. Through the object-oriented method and RIM, HL7 version 3 will improve many of the shortcomings of previous 2.X versions. Version 3 uses extensible markup language; (XML Section 4.7.2.1) for message encoding to increase interoperability between systems. This version has developed the patient record architecture (PRA), an XML-based clinical document architecture. It can also certify vendor systems through the HL7 message development framework (MDF). This testable criterion will verify vendors’ conformance to version 3. In addition, version 3 will include new data interchange formats beyond ASCII and support of component-based technology such as ActiveX and CORBA. As the industry moves to version 3, providers and vendors will face some impact now or in the future.

4.2.3.1 Benefits

1. Version 3 will be less complicated and less expensive to build and to maintain the HL7 interfaces.
2. HL7 messages will be less complex, and therefore analysts and programmers will require less training.
3. HL7 compliance testing will be enabled.
4. It will be easier to integrate different HL7 software interfaces from different vendors.

4.2.3.2 Challenges

1. Adoption of version 3 will be more expensive than the previous version.
2. Adoption of version 3 will take time to replace the existing version.
3. Retraining and retooling will be necessary.
4. Vendors will eventually be forced to adopt version 3.
5. Vendors will have to support both versions 2.X and 3 for some time.

HL7 version 3 offers tremendous benefits to providers and vendors as well as analysts and programmers, but complete adoption of the version 3 standard may take time and effort. HL7 is a nonprofit organization that develops and publishes standards providing a framework for interoperability of health information. It is used by approximately 500 corporate members, representing over 90% of information systems vendors serving healthcare worldwide; it has since been adopted by other countries on a national level, as well as by ISO (International Organization for Standardization).

4.3 From ACR-NEMA to DICOM

4.3.1 ACR-NEMA and DICOM

The American College of Radiology (ACR) and the National Electrical Manufacturers Association (NEMA), created a committee to develop a set of standards to serve as the common ground for various medical imaging equipment vendors. The goal was that newly developed instruments would be able to communicate and participate in sharing medical image information, in particular, within the PACS-based environment. The committee focused chiefly on issues concerning information exchange, interconnectivity, and communications among medical systems, and the ACR-NEMA standard was established in 1982. The first ACR-NEMA version was released in 1985, and specified standards, including point-to-point message transmission, data formatting and presentation, a preliminary set of communication commands, and a data format dictionary. The second version, ACR-NEMA 2.0, published in 1988, was an enhancement of the first version, including both hardware definitions and software protocols, as well as a standard data dictionary. Networking issues were not addressed adequately in either version. For this reason, a new version aiming to include network protocols was released in 1992. Because of the magnitude of changes and additions, it was given a new name: Digital Imaging and Communications in Medicine (DICOM 3.0) [1].

4.3.2 Digital Imaging and Communications in Medicine (DICOM 3.0)

In 1996, a new version was released consisting of 13 published parts that formed the basis of future DICOM new versions and parts. Manufacturers readily adopted this version to their imaging products. Each DICOM document is identified by title and standard number in the form: PS 3.X-YYYY, where “X” is the part number and “YYYY” is the year of publication. Thus PS 3.1-1996 means DICOM 3.0 document Part 1 (Introduction and Overview), released in 1996. Although the complexity and involvement of the standards were increased by many-fold, DICOM remains compatible with previous ACR-NEMA versions. The two most distinguished new features in DICOM compared with the ACR-NEMA standard are adaptation of an object-oriented data model for message exchange and utilization of existing standard network communication protocols. For a brief summary of the ACR-NEMA 2.0, refer to the first edition of this book.

4.3.3 DICOM Standard PS 3.1 - 2008

The DICOM Standard PS 3.1 2008 comprises 18 related but independent parts following ISO directives, and are referred to as:

Part 1: Introduction and Overview;

Part 2: Conformance;

Part 3: Information Object Definitions;

Part 4: Service Class Specifications;

Part 5: Data Structures and Encoding;

Part 6: Data Dictionary;

Part 7: Message Exchange;

Part 8: Network Communication Support for Message Exchange;

Part 9: Point-to-Point Communication Support for Message Exchange (Retired);

Part 10: Media Storage and File Format for Media Interchange;

Part 11: Media Storage Application Profiles;

Part 12: Media Formats and Physical Media-for-Media Interchange;

Part 13: Print Management Point-to-Point Communication Support (Retired);

Part 14: Gray Scale Standard Display Function;

Part 15: Security and System Management Profiles;

Part 16: Content Mapping Resource;

Part 17: Explanatory Information;

Part 18: Web Access to DICOM Persistent Objects (WADO).

Parts 17 and 18 were added to the DICOM standard released in 2004. These two additional parts are used to facilitate the linkage of images with structured reporting, other types of report format and languages, and information annexes. Since these two standards are useful in PACS-based imaging informatics, discussed in Part 4 of this book, the following two paragraphs are extracted from the DICOM document.

- *Part 17: Explanatory Information*

  This DICOM part contains explanatory information in the form of Normative and Informative Annexes. Some of these annexes include the following: Explanation of Patient Orientation; SR (Structured Reporting) Encoding Example; Mammography CAD (Computer-Aided Detection, Diagnosis); Clinical Trial Identification Workflow Examples; Ultrasound Templates; Echocardiography Procedure Reports; and Configuration Use Cases.

- *Part 18: Web Access to DICOM Persistent Objects (WADO)*

  This standard specified a web-based service for accessing and presenting DICOM persistent objects such as images and reports through a simple mechanism from hypertext markup language (HTML) pages or extensible markup language (XML) documents, through hypertext transfer protocol (HTTP) using DICOM unique identifiers (UID's). Data may be retrieved as specified by the requester in a presentation-ready format, e.g. Joint Photographic Experts Group (JPEG), graphics interchange format (GIF), or in native DICOM. It does not support facilities for web searching of DICOM images.

4.3.4 DICOM Supplements

In addition to the base standard of 18 parts, DICOM has final supplements that enhance the existing base standard. Some of the areas covered include handling

PET image fusion data storage, pathology-related and specimen imaging data storage, breast tomosynthesis data storage, cardiac stress testing data storage, surface segmentation and presentation data, and MPEG2 Main Profile/High Level (MP@HL) transfer syntax for high-definition video.

Figures 4.2(A) and (B) summarize the various parts of the DICOM standard PS 3.1 2008 document. In Figure 4.2(A), there are two routes of communication between parts: network exchange on-line communication (left) and media storage interchange off-line communication (right).

4.4 DICOM 3.0 Standard

4.4.1 DICOM Data Format

DICOM data format includes the DICOM model of the real world and DICOM file format. The former is used to define the hierarchical data structure including patient, studies, series, images, and waveforms. The latter describes how to encapsulate a DICOM file ready for a DICOM service-object pair (SOP) service.

Two fundamental components of DICOM are the information object class and the service class. Information objects define the contents of a set of images and their relationship, and the service classes describe what to do with these objects. Tables 4.1 and 4.2 list some service classes and some information object classes. The service classes and information object classes are combined to form the fundamental unit of DICOM called service-object pairs (SOPs). This section describes these fundamental concepts and provides some examples.

Table 4.1 DICOM service classes.

Service Class	Description
Image storage	Provides storage service for data sets
Image query	Supports queries about data sets
Image retrieval	Supports retrieval of images from storage
Image print	Provides hard copy generation support
Examination	Supports management of examinations (which may consist of several series of management images)

Storage resource	Supports management of the network data storage resource(s)

Table 4.2 DICOM information object classes.

Normalized	**Composite**
Patient	Computed radiograph
Study	Computed tomogram
Results	Digitized film image
Storage resource	Digital subtraction image
Image annotation	MR image
	Nuclear medicine image
	Ultrasound image
	Displayable image
	Graphics
	Curve

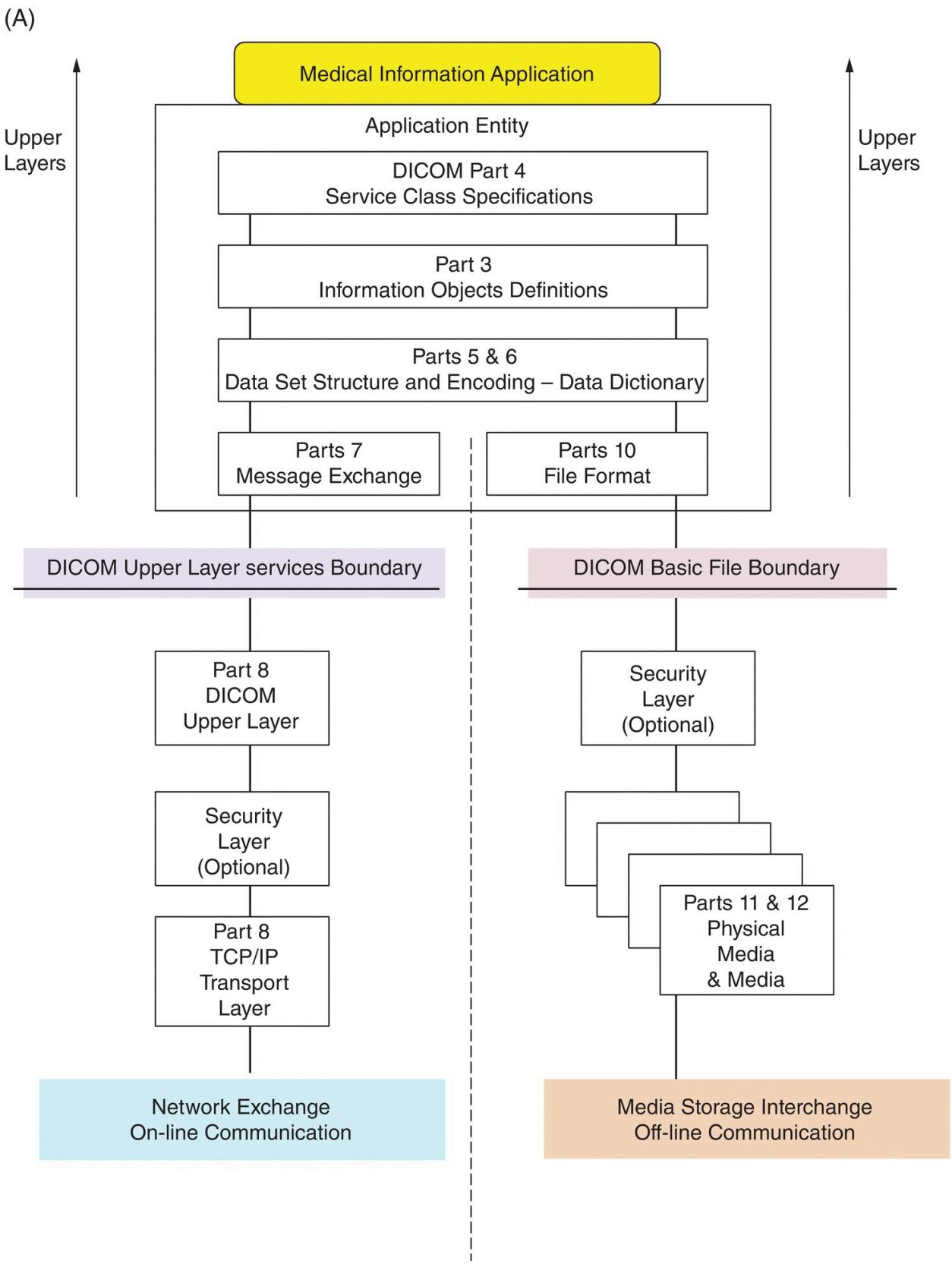
(A)
Medical Information Application
Upper Layers
Application Entity
DICOM Part 4
Service Class Specifications
Part 3
Information Objects Definitions
Parts 5 & 6
Data Set Structure and Encoding – Data Dictionary
Parts 7
Message Exchange
Parts 10
File Format
Upper Layers
DICOM Upper Layer services Boundary
DICOM Basic File Boundary
Part 8
DICOM
Upper Layer
Security
Layer
(Optional)
Part 8
TCP/IP
Transport
Layer
Security
Layer
(Optional)
Parts 11 & 12
Physical
Media
& Media
Network Exchange
On-line Communication
Media Storage Interchange
Off-line Communication

(B)

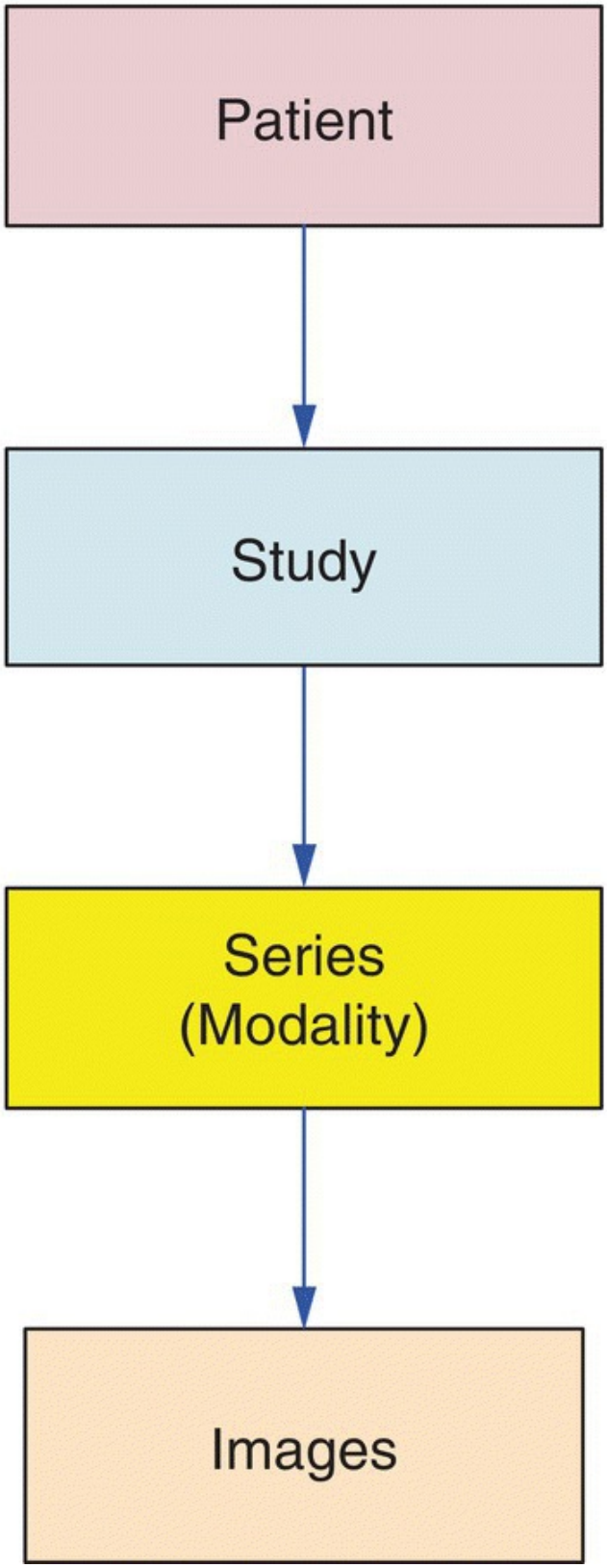

Figure 4.2 (A) Architecture of the DICOM data communication model and DICOM parts (Sections 4.3.2 and 4.3.3). There are two communication models: the network layers model (left) and the media storage interchange model (right). Both models share the upper-level data structure described in DICOM parts 3–6. In part 7, message exchange is used for communication only, whereas in part 10, file format is used for media exchange. Below the upper levels, the two models are completely different. (B) The simplified DICOM data model of the real world with four levels: patient, study, series, and images. This simplified model can be extended to more complicated data models for various applications, including ePR, radiation therapy, and surgery.

4.4.2 DICOM Model of the Real World

The DICOM model of the real world defines several real-world objects in the clinical image arena (patient, study, series, image, etc.) and their interrelationships within the scope of the DICOM standard. It provides a framework for various DICOM information object definitions (IOD). The DICOM model documents four object levels: patient; study; series and equipment; and image, waveform, and structured reporting (SR). Each of these levels can contain several (1 – n or 0 – n) sublevels.

A patient is a person receiving, or registering to receive healthcare services. This person could have had several previous (1 – n) studies already, and may visit the healthcare physician and register to have more (1 – n) studies. For example, a patient has one historical CT chest study and two historical MR brain studies. The patient can also visit the hospital to have a new CR chest study.

A study can be a historical study, a currently performed study, or a study to be performed in the future. A study can contain a few (1 – n) series or several study components (1 – n), each of which can include another few (1 – n) series. For example, an MR brain study may include three series: transaxial, sagittal, and coronal. A study or several (1 – n) studies can also have several scheduled procedural steps to be performed in different modalities. For example, an MRI brain study is scheduled at the MRI scanner, or one MRI study and one CT study are scheduled in an MRI and a CT scanner, respectively. A study can thus include additional results. The results may be in the form of a report or an amendment.

A series or several series can be created by equipment. Equipment is a modality (e.g. MRI scanner) used in the healthcare environment. A series can include

several (0 – n) images or waveforms, SR (structured reporting), documents, or radiotherapy objects (Chapter 11), and so forth. For example, an MR transaxial brain series includes 40 MR brain Images.

An image can be any image from all sorts of modalities, for example, a CT image, MR image, CR image, DR image, US image, NM image, or endoscopic image. A waveform is from the modality generating the waveform output, for example, an ECG waveform from an ECG device. A SR document is a new type of DICOM document for structured reporting. DICOM defines many SR templates to be used in the healthcare environment, for example, a mammography CAD SR template. These topics are discussed in more detail in Section 4.6. Contents of this data model are encoded with necessary header information and tags in a specified format to form a DICOM file. Figure 4.2(B) shows the simplified DICOM data model of the real world. There are several extended DICOM data models for various applications, for example, ePR (electronic patient record, Chapters 5 and 6), radiation therapy ePR (Chapters 11 and 19), and image-assisted surgery (Chapters 20 and 21).

4.4.3 DICOM File Format

DICOM file format defines how to encapsulate the DICOM dataset of a SOP instance in a DICOM file. Each file usually contains one SOP instance. The DICOM file starts with the DICOM file meta-information (optional), followed by the bitstream of the dataset, and ends with the image pixel data if it is a DICOM image file. The DICOM file meta-information includes file identification information. The meta-information uses explicit value representations (VR) transfer syntax for encoding. Therefore the meta-information does not exist in the Implicit VR-encoded DICOM file. Explicit and Implicit VR are two coding methods in DICOM. Vendors or implementers have the option of choosing either one for encoding. DICOM files encoded by both coding methods can be processed by most of the DICOM compliant software. The difference between Explicit VR and Implicit VR is that the former has VR encoding, whereas the latter has no such encoding. For example, an encoding for the element “modality” of CT value in Implicit VR and Explicit VR would be (the first 4 bytes, 08 00 60 00, is a tag):

08 00 60 00 02 00 00 00 43 54 Implicit VR

08 00 60 00 43 53 02 00 43 54 Explicit VR

In the encodings above, the first 4 bytes (08 00 60 00) is a tag. In Implicit VR,

the next 4 bytes (02 00 00 00) are for the length of the value field of the data element, and the last 2 bytes (43 54) are element value (CT). In Explicit VR, the first 4 bytes are also a tag, the next 2 bytes (43 53) are for VR representing code string, one type of VR in DICOM, the next 2 bytes (02 00) are for length of element value, and the last 2 bytes (43 54) are element value.

One dataset represents a single SOP instance. A dataset is constructed of data elements. Data elements contain the encoded values of the attributes of the DICOM object (see DICOM, Section 4.4 on the construction and encoding of a data element and a dataset). If the SOP instance is an image, the last part of the DICOM file is the image pixel data. The tag for image pixel data is 7FE0 0010. Figure 4.3 shows an example of an Implicit VR little-endian (byte swapping) encoded CT DICOM file.

Element Tag and Value	Binary Coding
0008,0000,726	08 00 00 00 04 00 00 00 D6 02 00 00
0008,0005, ISO.IR 100	08 00 05 00 0A 00 00 00 49 53 4F 5F 49 52 20 31 30 30
0008,0016, 1.2.840.10008.5.1.4.1.1.2.	08 00 16 00 1A 00 00 00 31 2E 32 2E 38 34 30 2E 31 30 30 30 38 2E 35 2E 31 2E 34 2E 31 2E 31 2E 32 00
0008,0016, CT	08 00 60 00 02 00 00 00 **43 54**
0008,1030, Abdomen. 1abdpelvis	08 00 30 10 12 00 00 00 41 62 64 6F 6D 65 6E 5E 31 61 62 64 70 65 6C 76 69 73
...	...
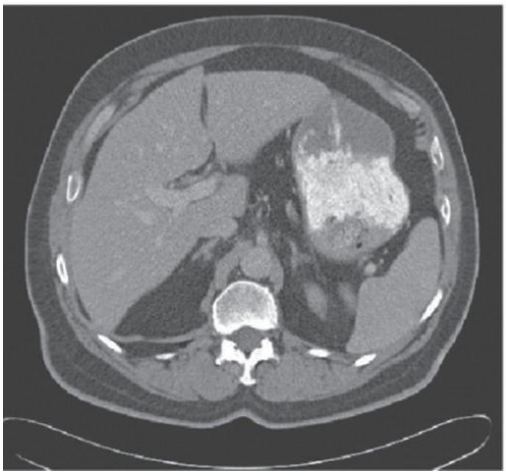	E0 7F 10 00 00 00 00 00 00 00 00 00 00 00 .... 20 00 25 00 1° 00 19 00 1C 00 14 00 2D 00 ....

Figure 4.3 "0008,0000" in the "element tag and value" column is the tag for the 0008 Group. "726" is the value for the Group length, and it means there are 726 bytes in this group. The corresponding binary coding of this tag and value are in

the same line in “binary coding” column. The next few lines are the tags and values as well as the corresponding coding for “specific character set,” “SOP class UID,” “modality,” and “study description.” The image pixel data is not in the 0008 Group. Its tag is “7FE0 0010,” and following the tag are the coding for the pixel data. The element tag and value “0008 …” becomes “08 00 …” in binary coding because of the little-endian “byte swapping”.

4.4.4 Object Class and Service Class

The DICOM object class consists of normalized objects and composite objects. Normalized information object classes include those attributes inherent in the real-world entity represented. The left side of Table 4.2 shows some normalized object classes. Consider two normalized object classes: study information and patient information. In the study information object class, the study date and image time are attributes of this object, because these attributes are inherent whenever a study is performed. On the other hand, patient name is not an attribute in the study information object class, but an attribute in the patient object class. This is because the patient’s name is inherent in the patient information object class on which the study was performed and not in the study itself. The use of information object classes can identify objects encountered in medical imaging applications more precisely and without ambiguity. For this reason, the objects defined in DICOM 3.0 are very precise.

However, sometimes it is advantageous to combine normalized object classes together to form composite information object classes for facilitating operations. For example, the CR image information object class is a composite object, because it contains attributes from the study information object class (image date, time, etc.) and patient information object class (patient’s name, etc.). Table 4.2 (right) shows some composite information object classes.

DICOM uses a UID, 1.2.840.10008.X.Y.Z, to identify a specific part of an object, where the numerals are called the organizational root and X, Y, and Z are additional fields to identify the parts. Thus, for example, the UID for the DICOM explicit values representing little-endian transfer syntax is 1.2.840.10008.1.2.1. Note that the UID is used to identify a part of an object; it does not carry information.

4.4.5 DICOM Services

DICOM services are used for communication of imaging information objects within a device and for the device to perform a service for the object, for

example, to store the object or to display the object. A service is built on top of a set of “DICOM message service elements” (DIMSEs). These DIMSEs are computer software programs written to perform specific functions. There are two types of DIMSEs, one for the normalized objects and the other for the composite objects, as given in Tables 4.3 and 4.4, respectively. DIMSEs are paired in the sense that a device issues a command request and the receiver responds to the command accordingly. The composite commands are generalized, whereas the normalized commands are more specific.

Table 4.3 Normalized DICOM message service element (DIMSE).

Command	Function
N-EVENT-REPORT	Notification of information object-related event
N-GET	Retrieval of information object attribute value
N-SET	Specification of information object attribute value
N-ACTION	Specification of information object-related action
N-CREATE	Creation of an information object
N-DELETE	Deletion of an information object

Table 4.4 Composite DICOM message service element (DIMSE).

Command	Function
C-ECHO	Verification of connection
C-STORE	Transmission of an information object instance
C-FIND	Inquiries about information object instances
C-GET	Transmission of an information object instance via third-party application processes
C-MOVE	Similar to GET, but end receiver is usually not the command initiator

DICOM services are referred to as “service classes”, because of the object-oriented nature of its information structure model. If a device provides a service, it is called a service class provider; if it uses a service, it is a service class user. Thus, for example, a magnetic disk in the PACS server is a service class provider for the server to store images. On the other hand, a CT scanner is the service class user of the magnetic disk in the PACS server to store images. Note that a device can be either a service class provider or a service class user or both,

depending on how it is used. For example, in its routing process that receives images from the scanners and distributes these images to the workstations (WSs), the PACS server assumes the roles of both a storage service class provider and a storage service class user. As a service class provider, it accepts images from the scanners by providing a storage service for these images. On the other hand, the PACS server is a service class user when it sends images to the WS by issuing service requests to the WS for storing the images.

4.4.6 DICOM Communication

DICOM uses existing network communication standards based on the ISO OSI for imaging information transmission (Chapter 3, Section 3.5). The ISO OSI consists of seven layers from the lowest physical (cables) layer to the highest application layer. When imaging information objects are sent between layers in the same device, the process is called a “service”. When objects are sent between two devices, it is called a “protocol”. When a protocol is involved, several steps are invoked in two devices, so it is termed that the two devices are in “association” using DICOM. Figure 4.4 illustrates the data flow of the CT images from the scanner to the WS using DICOM. The numerals represent the steps as follows:

1. CT scanner encodes all images into a DICOM object.
2. Scanner invokes a set of DIMSEs to move the image object from a certain level down to the physical layer in the ISO OSI model.
3. WS uses a counter set of DIMSEs to receive the image object through the physical layer and move it up to a certain level.
4. WS decodes the DICOM image object.

If an imaging device transmits an image object with a DICOM command, the receiver must use a DICOM command to receive the information. DICOM uses TCP/IP for file transmission. On the other hand, if a device transmits a DICOM object with a TCP/IP communication protocol through a network without invoking the DICOM communication, any device connected to the network can receive the data with the TCP/IP protocol. However, a decoder is still needed to convert the DICOM object for proper use. The TCP/IP method is used to send a full resolution DICOM image from the PACS server to the Web server without invoking the DICOM service discussed in Chapter 6.

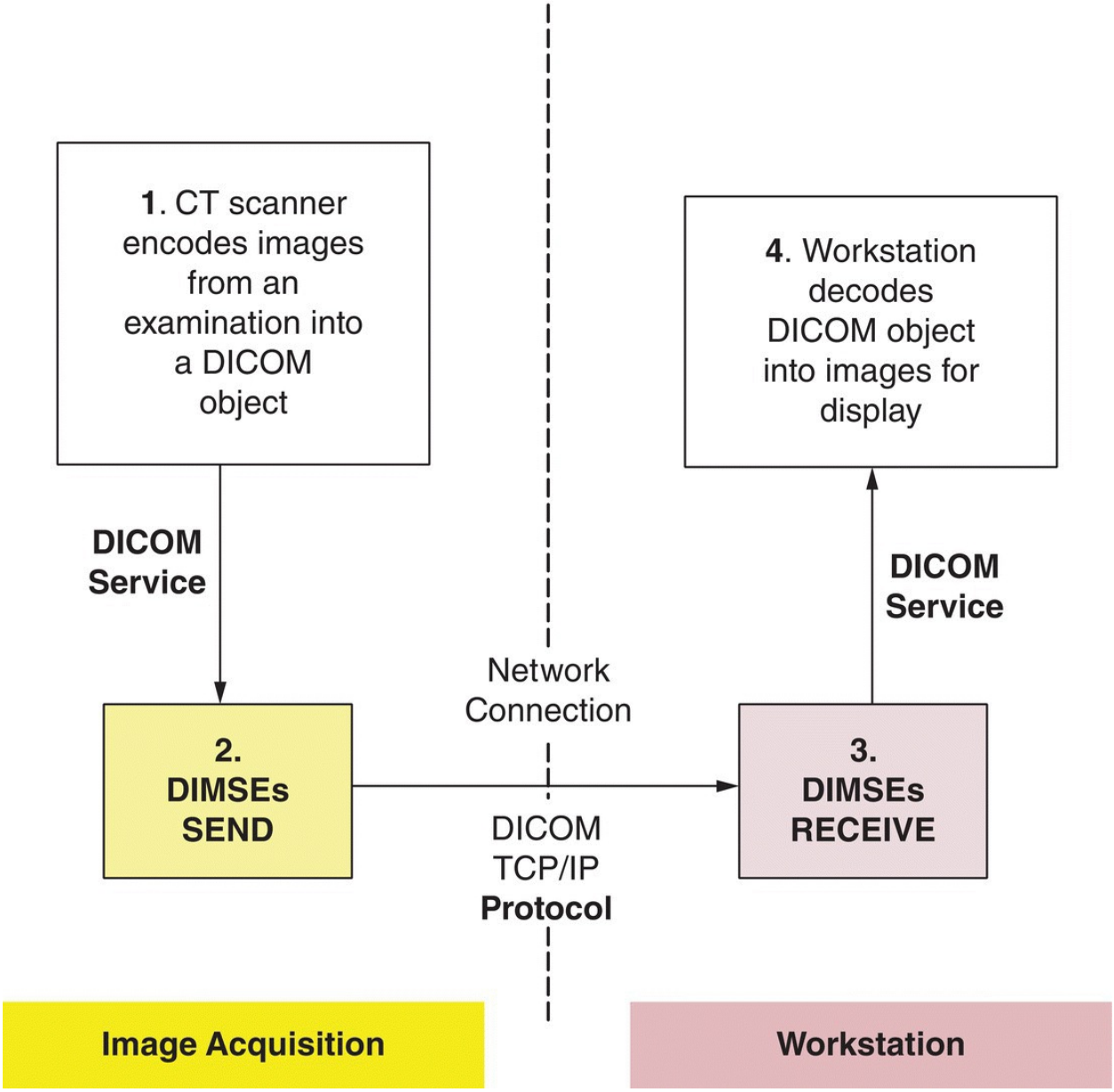

Figure 4.4 Data flow of a set of CT images from the scanner (left) is sent to the WS (right). Within a device the data flow is called a service; between devices it is called a protocol. DIMSE: DICOM message service elements; IP: Internet protocol; TCP: transfer control protocol.

4.4.7 DICOM Conformance

DICOM conformance PS 3.2–1996 is Part 2 of the DICOM document, instructing manufacturers on how to conform their devices to the DICOM standard. In a conformance statement, the manufacturer describes exactly how the device or its associate software conforms to the standard. A conformance

statement does not mean that this device follows every detail required by DICOM; it only means that this device follows a certain subset of DICOM. The extent of the subset is described in the conformance statement. For example, a laser film digitizer needs only to conform to the minimum requirements for the digitized images to be in the DICOM format, but the digitizer should be a service class user (SCU) to send the formatted images to a second device like a magnetic disk, which is a DICOM service class provider (SCP). Thus, if a manufacturer claims that its imaging device is DICOM conformant, it means that any system integrator who follows this manufacturer's conformance document will be able to interface this device with their DICOM-compliant components. In general, the contents of the conformance statement include (quoted from DICOM 2003):

1. The implementation model of the application entities (AEs) in the implementation and how these AEs relate to both local and remote real-world activities.
2. The proposed (for association initiation) and acceptable (for association acceptance) presentation contexts used by each AE.
3. The SOP classes and their options supported by each AE, and the policies with which an AE initiates or accepts associations.
4. The communication protocols to be used in the implementation.
5. A description of any extensions, specializations, and publicly disclosed privatizations to be used in the implementation.
6. A description of any implementation details, which may be related to DICOM conformance or interoperability. (DICOM PS3.2 1996)

4.5 Examples of using DICOM

To an end user, the two most important DICOM services are "send and receive" images and "query and retrieve" images. In this section, two examples are used to explain how DICOM accomplishes these services. Note that the query and retrieve services are built on top of the send and receive services.

4.5.1 Send and Receive

Consider steps involved in sending a CT examination with multiple images from the CT scanner to the DICOM gateway (Figure 4.1) using the DICOM protocol.

Each individual image is transmitted from the CT scanner to the gateway by utilizing DICOM's C-STORE service. In this transmission procedure, the scanner takes on the role of a client as the C-STORE SCU, and the gateway assumes the role of the C-STORE SCP. The following steps illustrate the transmission of a CT examination with multiple images from the scanner to the gateway (Figure 4.5). The CT scanner and the PACS acquisition gateway first establish the connection through DICOM communication "association request and response" commands.

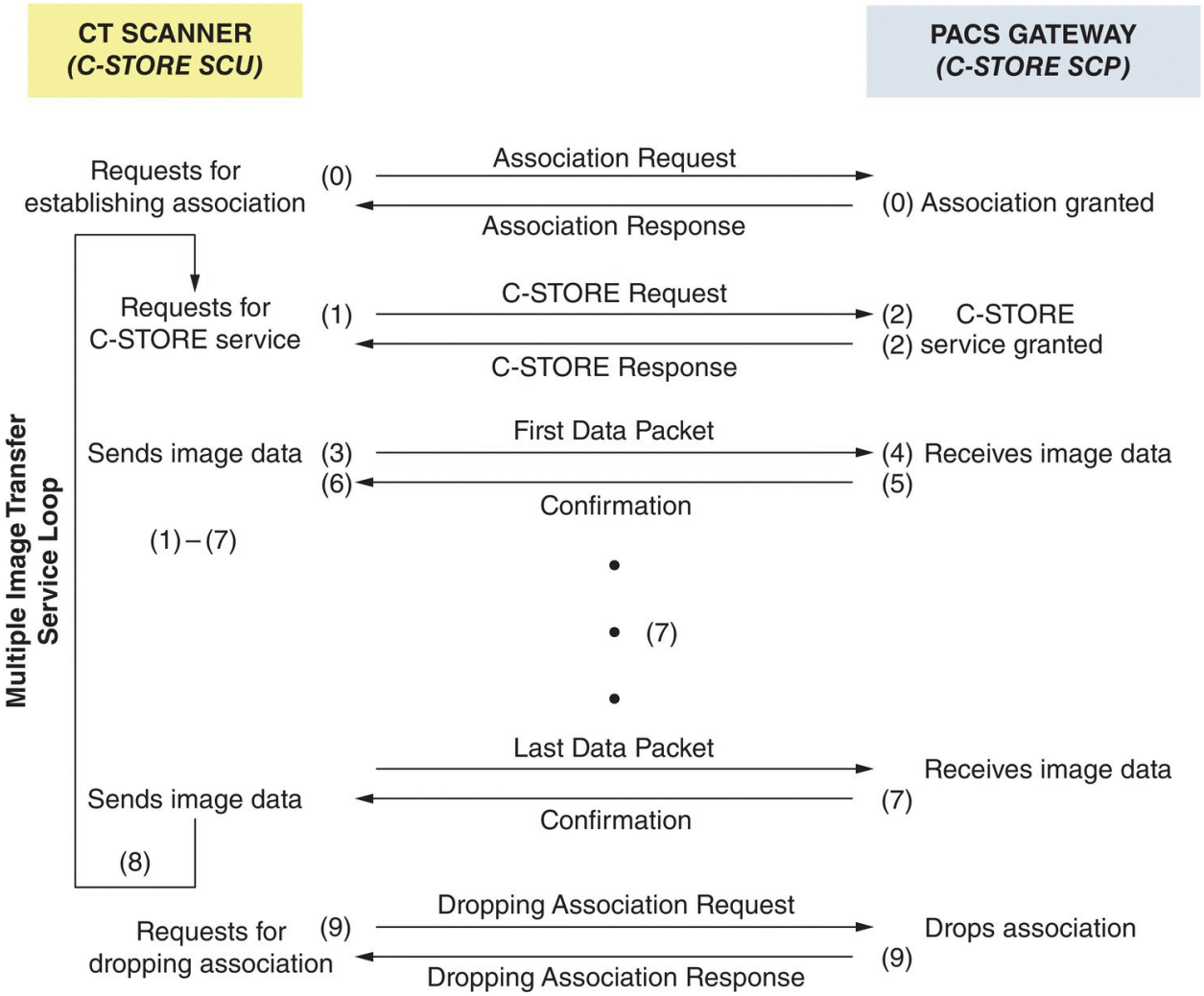

Figure 4.5 DICOM send and receive operations. The example shows the steps involved in sending a set of CT images from the scanner to the acquisition gateway (see Figure 4.1 for the PACS components involved).

1. The invoking scanner (SCU) issues a C-STORE service request to the PACS gateway (SCP).

2. The gateway receives the C-STORE request and issues a C-STORE response to the invoking scanner.
3. The CT scanner sends the first data packet of the first image to the gateway.
4. The gateway performs the requested C-STORE service to store the packet.
5. On completion of the service, the gateway issues a confirmation to the scanner.
6. After receiving the confirmation from the gateway on the completion of storing the packet, the scanner sends the next packet to the PACS controller.
7. Processes 4 to 6 repeat until all packets of the first image have been transmitted from the scanner to the gateway.
8. The scanner issues a second C-STORE service request to the PACS gateway for transmission of the second image. Steps 1 to 7 repeat until all images from the study have been transmitted.
9. The scanner and the PACS gateway issue DICOM communication command "dropping association request and response" to disconnect.

4.5.2 Query and Retrieve

The send and receive service class using the C-STORE is relatively simple compared with the query and retrieve service class. Consider a more complicated example, in which the PACS WS queries the PACS server to retrieve a historical CT examination and to compare with a current study already available at the WS. This composite service class involves three DIMSEs: C-FIND and C-MOVE (Table 4.4), and C-STORE described in the last section. In performing the query/retrieve (Q/R) SOP service, both the WS and the server each have one user and one provider:

	WS	Server
Query/retrieve (Q/R)	User	Provider
C-STORE	Provider	User

Thus in Q/R, the WS takes on the role of user (SCU) and the server functions as the provider (SCP), whereas in C-STORE, the WS has the role of SCP and the server has the function of CSU. Referring to Figure 4.6, after the association between the WS and the server has been established, then:

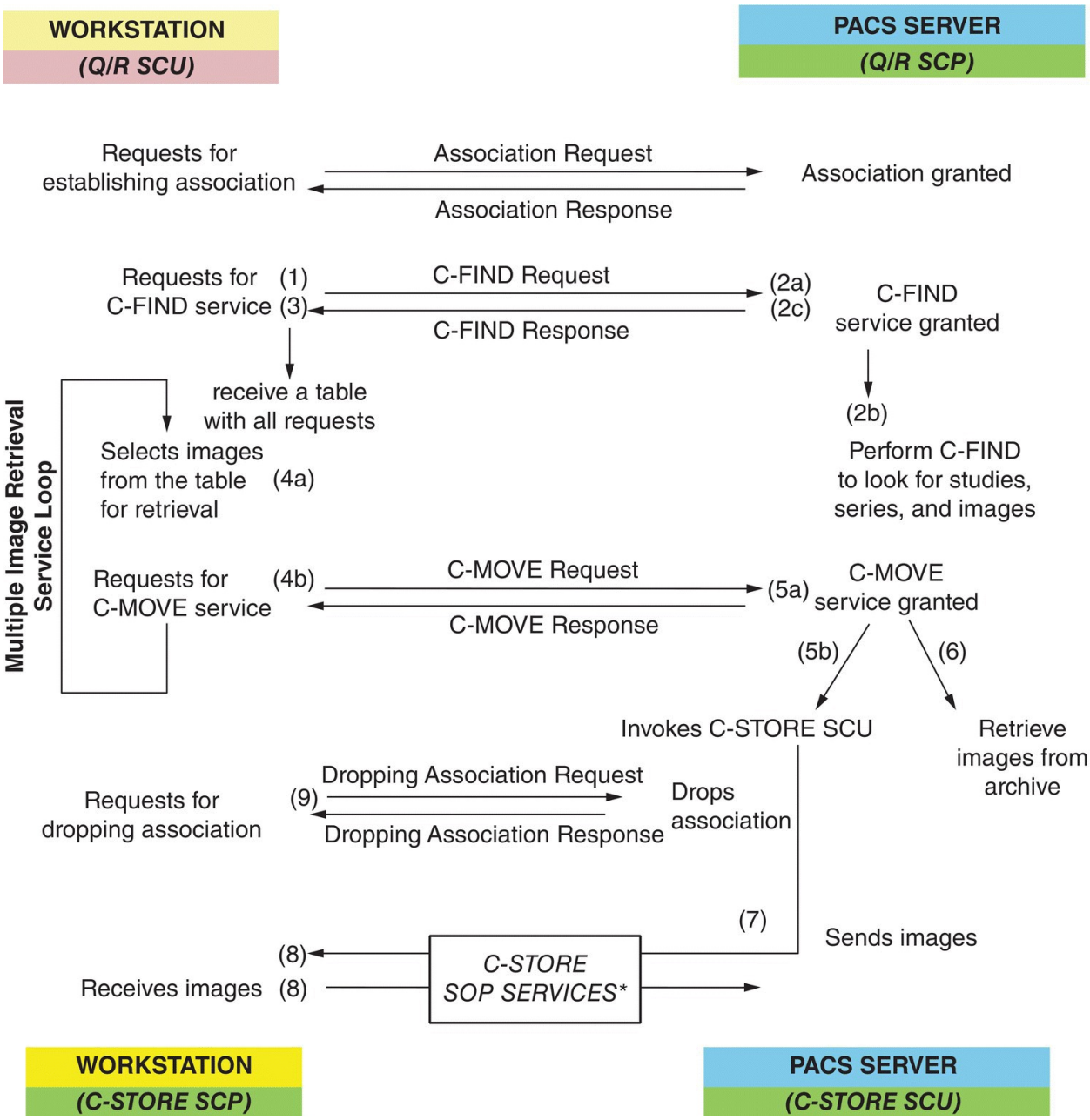

Figure 4.6 DICOM query and retrieve operation. The example shows the steps involved in a WS Q/R a set of images from the server (see Figure 4.1 for the PACS components involved).

1. The PACS WS's Q/R application entity (AE) issues a C-FIND service (Table 4.4) request to the server.
2. The server's Q/R AE receives the C-FIND request from the querying WS (Figure 4.6, 2a); performs the C-FIND service (Figure 4.6, 2b) to look for studies, series, and images from the PACS database; and issues a C-FIND

response to the WS (Figure 4.6, 2c).

3. The WS's Q/R AE receives the C-FIND response from the PACS server. The response is a table with all the requests shown at the WS.
4. The user at the WS selects interesting images from the table (Figure 4.6, 4a) and issues a C-MOVE service (Table 4.4) request for each individual selected image to the PACS server (Figure 4.6, 4b).
5. The server's Q/R AE receives the C-MOVE (Table 4.4) request from the WS (Figure 4.6, 5a) and issues an indication to the server's C-STORE SCU (Figure 4.6, 5b).
6. The server's C-STORE SCU retrieves the requested images from the archive device.
7. The server issues a C-STORE service request to the WS's C-STORE SCP.
8. The WS receives the C-STORE request and issues a C-STORE response to the server. From this point on, the C-STORE SOP service is identical to the example given in Figure 4.5.
9. After the WS retrieves the last image, it issues a "dropping association request" and terminates the association.

4.6 DICOM Organizational Structure and New Features

This section is extracted from the DICOM documents.

4.6.1 DICOM New Features since 2010

DICOM is a dynamic operation and continues updating organization. The latest substantive DICOM update was on June 16, 2010. Several new features and two new parts, 17 and 18, had been added to the DICOM, which are important to the system integration and communication with other input data not in the realm of conventional radiological images. These are visible light images (Section 4.3.9), structured reporting object, content mapping resource, mammography CAD, JPEG 2000 compression (Section 4.6.4.2), waveform information object definition (IOD) (e.g. ECG IOD and cardiac electrophysiology IOD), and security profiles (Chapter 17).

4.6.1.1 Visible Light (VL) Images

The visible light (VL) images IOD for endoscopy, microscopy, and photography has become available for health care. It includes definitions of VL endoscopic image IOD, VL microscopic image IOD, VL slide coordinates microscopic image IOD, VL photographic image IOD, and VL image module. An example is provided in Chapters 20 and 21, which utilizes the DICOM endoscopic image format in minimally invasive spinal surgery.

4.6.1.2 Mammography Computer-Aided Detection (CADe)

One application of the DICOM structured reporting is in mammography computer-aided detection. It uses the mammography CAD output for analysis of mammographic findings. The output is in DICOM structured reporting format (Chapter 17).

4.6.1.3 Waveform IOD

The DICOM waveform IOD was mainly developed for imaging cardiac waveforms, for example, ECG and cardiac electrophysiology. The ECG IOD defines the digitized electrical signals acquired by an ECG modality or an ECG acquisition function within an imaging modality. Cardiac electrophysiology IOD defines the digitized electrical signals acquired by an electrophysiology modality.

4.6.1.4 Structured Reporting (SR)

Object structured reporting is for radiologists to shorten their reporting time. SOP classes are defined for transmission and storage of documents that describe or refer to the images or waveforms or the features they contain. SR SOP classes provide the capability to record the structured information to enhance the precision and value of clinical documents and enable users to link the text data to particular images or waveforms. Chapters 17 and 18 provide examples of using SR to link CAD results in the CAD WS with DICOM images in the PACS server.

4.6.1.5 Content Mapping Resource

The content mapping resource feature defines the templates and context groups used in other DICOM parts. The templates are used to define or constrain the content of structured reporting (SR) documents or the acquisition context. Context groups specify value set restrictions for given functional or operational contexts. For example, Context Group 82 is defined to include all units of

measurement used in DICOM IODs.

The features described in Sections 4.6.1.4 and 4.6.1.5, together with the new features in Part 17 (explanatory information described in Section 4.3.3), lead to the possibility of linking the CAD SR from the CAD WS with the PACS image data in the PACS archive server. These linkages allow radiologists at PACS WSs to read and review CAD results from the CAD server or WSs along with PACS images. Examples of linking CAD results from its WS to DICOM images and being displayed by a PACS WS are given in Chapters 17 and 18.

4.6.2 DICOM's Organizational Structure

DICOM is an independent, international standards development organization administered by NEMA's Medical Imaging and Technology Alliance. The complete Procedures (bylaws) of the DICOM Standards Committee are available on the DICOM Web page at http://dicom.nema.org. Working groups of the DICOM Committee perform the majority of work on the extension of and corrections to the Standard. Working groups are formed by the DICOM Committee to work on a particular classification of tasks. Once formed, working groups petition the DICOM Committee to approve work items for which the working group will execute the plan delineated in the work item. Once the output of a work item (generally a supplement or correction proposal) has been completed, it is submitted to the Base Standards Working Group (WG-06), for their review. Supplements to the standard then go through a public comment period, after which the DICOM Committee authorizes the supplement for letter ballot by DICOM members. Letter ballots require approval by two-thirds of those voting affirmative or negative and return of more than one-half of the ballots sent to members in good standing relative to letter ballots. Since the working groups perform the majority of work on the extension of and corrections to the Standard, the current status and future directions of the DICOM Standard are best represented by review of each working group. (DICOM is located at 1300 North 17th Street, Suite 900 Arlington, VA 22209, United States; tel. +1-703-841-3259; http://dicom.nema.org; email: dicom@medicalimaging.org).

4.6.3 Current DICOM Strategic Document

The purpose of the current DICOM document (revised January 1, 2017) is to provide a summary of the current activities and future directions of the DICOM Standard. The content of the document is largely based on information submitted

by individual working group chairs. The date of the last change of the strategy is marked for each working group; changes to the listing of secretaries and/or co-chairs are made as needed.

The table of contents of the strategic document as of January 30, 2017, listed below provides a summary of the current activities and future directions of the DICOM Standard. The content of this document is largely based on information submitted by individual working group chairs. The date of the last change of the strategy is marked for each working group; changes to the listing of secretaries and/or co-chairs are made as needed. There are 31 working groups:

Contents

- **INTRODUCTION**
- **The DICOM Standards Committee**
- WG-01: Cardiac and Vascular Information
- WG-02: Projection Radiography and Angiography
- WG-03: Nuclear Medicine
- WG-04: Compression
- WG-05: Exchange Media
- WG-06: Base Standard
- WG-07: Radiotherapy
- WG-08: Structured Reporting
- WG-09: Ophthalmology
- WG-10: Strategic Advisory
- WG-11: Display Function Standard
- WG-12: Ultrasound
- WG-13: Visible Light
- WG-14: Security
- WG-15: Digital Mammography and CAD
- WG-16: Magnetic Resonance
- WG-17: 3D Manufacturing

- WG-18: Clinical Trials and Research
- WG-19: Dermatologic Standards
- WG-20: Integration of Imaging and Information Systems
- WG-21: Computed Tomography
- WG-22: Dentistry
- WG-23: Application Hosting
- WG-24: Surgery
- WG-25: Veterinary Medicine
- WG-26: Pathology
- WG-27: Web Technology for DICOM
- WG-28: Physics
- WG-29: Education, Communication and Outreach
- WG-30: Small Animal Imaging
- WG-31: Conformance INTRODUCTION

Readers can obtain details of each working group statement from the DICOM Website.

4.7 IHE (Integrating the Healthcare Enterprise)

4.7.1 History and what is IHE?

4.7.1.1 IHE History

IHE is an initiative by healthcare professionals and industry to improve the way computer systems in healthcare share information. IHE promotes the coordinated use of established standards such as DICOM and HL7 to address specific clinical needs in support of optimal patient care. Systems developed in accordance with IHE communicate with one another better, are easier to implement, and enable care providers to use information more effectively. The vision is to enable seamless and secure access to health information that is usable whenever and wherever needed. Its mission is to improve healthcare by providing specifications, tools, and services for interoperability. IHE engages clinicians, health authorities, industry, and users to develop, test, and implement standards-

based solutions to vital health information needs [2, 3, 4].

In Chapter 9 of the second edition of this book, Siegel and Channin, 2001; Channin *et al*. 2001 a,b [5, 6]; Henderson *et al*. 2001 [7]; Carr and Moore, 2003; Russler, 2006; and other works were summarized. The most up-to-day information on IHE at that time was based on the 2008 Ninth Annual IHE Connectathon, representatives from 70 leading companies gathered to test 136 healthcare information technology (IT) systems. For completeness of IHE development history, this section has re-edited the previous Chapter 9.5 as Chapter 4, Section 4.7 in this current edition. More information can be obtained from IHE@rsna.org(www.rsna, org/IHE and www.himss.org). Figures 4.7A and B show the first Connectathon in 2006, and the most recent in 2016.

(A)

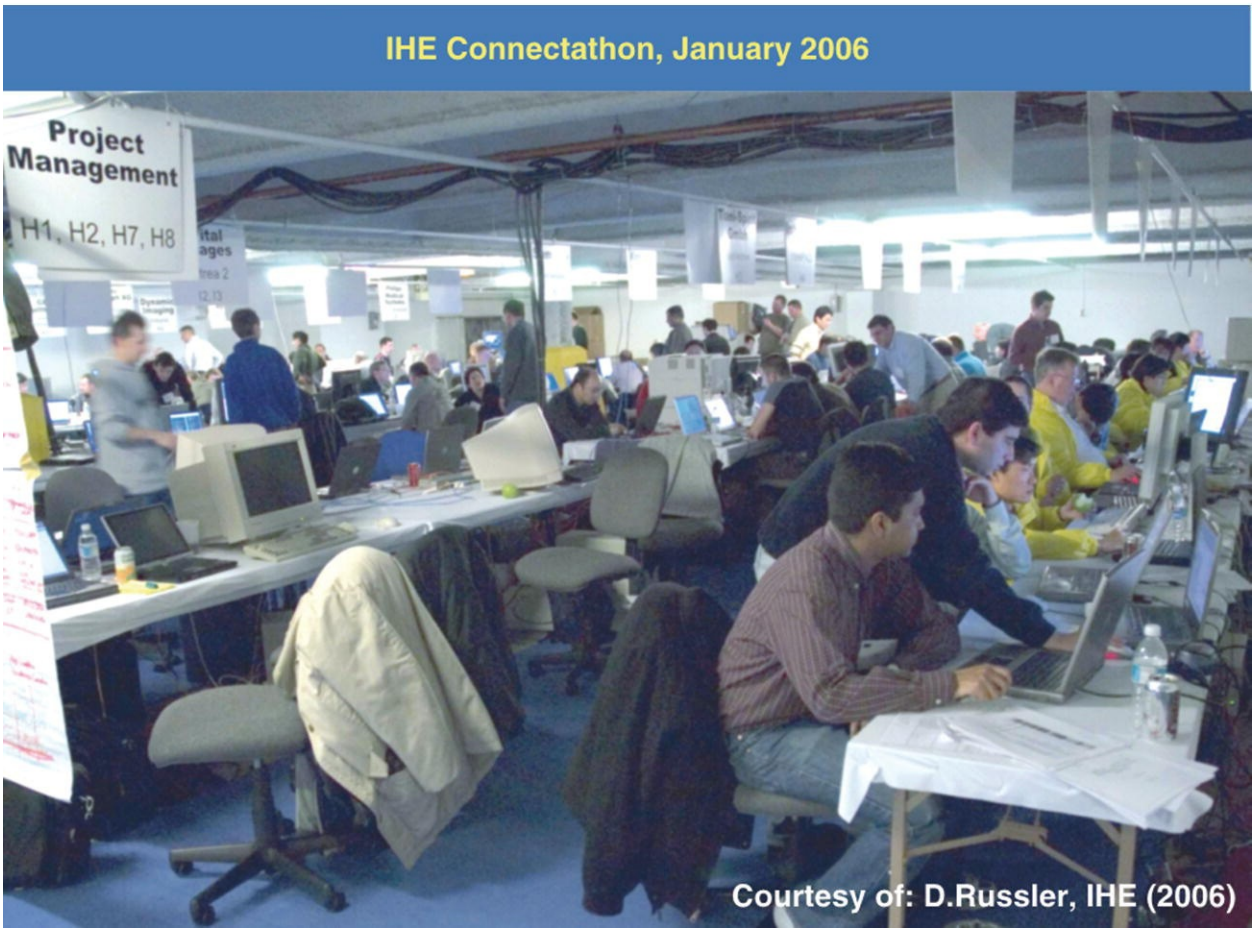

(B)

Figure 4.7 (A) Demonstration scene during an IHE Integration Workshop in 2006. Over 100 vendors were involved in this worldwide connectathon, and during that year tested 5 technical frameworks with 37 integration profiles at major conferences worldwide, where 15 active national chapters from 4 continents participated.

(courtesy of Dr D Russler)

(B) IHE Europe 2016 Connectathon in Bochum, http://connectathon.ihe-europe.net/.

(courtesy of IHE Europe)

4.7.1.2 What is IHE?

This chapter has discussed both HL7 and DICOM standards extensively in previous sections; even with these two standards available, there is still a need of common consensus on how to use them for integrating heterogeneous healthcare information systems smoothly. IHE is not a standard nor a certifying authority;

instead, it is a high-level information model for driving adoption of HL7 and DICOM standards. IHE is a joint initiative of the Radiological Society of North America (RSNA) and the Healthcare Information and Management Systems Society (HIMSS) started in 1998. The mission was to define and stimulate manufacturers to use DICOM and HL-7-compliant equipment and information systems to facilitate daily clinical operations. The IHE technical framework defines a common information model and vocabulary for using DICOM and HL7 to complete a set of well-defined radiological and clinical transactions for a certain task. This common vocabulary and model then facilitates healthcare providers and technical personnel to understand each other better, which then leads to smoother system integration. The first large-scale demonstration was held at the RSNA annual meeting in 1999, and thereafter at RSNA in 2000 and 2001, at HIMSS in 2001and 2002, and annually since at RSNA. In these demonstrations, manufacturers came together to show how their products could be integrated together according to IHE protocols. It is the belief of RSNA and HIMSS that with successful adoption of IHE, life would become more pleasant in healthcare systems integration for both the users and the providers. Chapter 7 in this book discusses some technical methods and examples under various clinical environments, which can be used to perform the system collaboration.

4.7.1.3 IHE Activities

IHE national deployment committees have been established in 17 countries, including Europe, North America, South America, Asia-Pacific, and the Middle East. These countries are sanctioned by IHE International to conduct testing, education, outreach, and collaboration with local health agencies and other deployment-related activities.

Many IHE national deployment committees coordinate their activities through regional groupings. All national deployment committees also participate in the IHE Global Deployment Coordination Committee. This committee meets regularly to coordinate planning of major IHE activities and to share resources and best practices.

In April 2013, IHE International held the first World Summit, hosted by IHE Turkey in coordination with the IHE Europe Connectathon in Istanbul. The gathering brought together leaders of IHE national deployment committees and other stakeholder organizations from 21 countries worldwide. The 17th IHE-Europe Connectathon is scheduled to be held in Venice, Italy from April 3–7, 2017.

4.7.2 IHE Technical Framework and Integration Profiles

4.7.2.1 Data Model, Actors and Integration Profiles

There are three key concepts in the IHE technical framework: data model, actors, and integration profiles:

1. *Data Model*: The data model is adapted from HL 7 and DICOM and shows the relationships between the key frames of reference, e.g., patient, visit, order, and study defined in the framework.
2. *IHE Actor*: An actor is one that exchanges messages with other actors to achieve specific tasks or transactions. An actor, not necessarily a person, is defined at the enterprise level in generic, product-neutral terms.
3. *Integration Profile*: An integration profile is the organization of functions segmented into discrete units. It includes actors and transactions required to address a particular clinical task or need. An example is the scheduled workflow profiles, which incorporate all the process steps in a typical scheduled patient encounter from registration, ordering, image acquisition, and examination to viewing.

IHE integration profiles provide a common language, vocabulary, and platform for healthcare providers and manufacturers to discuss integration needs and the integration capabilities of products. IHE integration profiles started first in the domain of radiology. During the 2003 implementation, there were 12 radiology integration profiles. Since then, IHE has branched out and grown rapidly in different domains, including anatomic pathology, cardiology, eye care, IT infrastructure, laboratory, patient care coordination, patient care devices, radiation oncology, and radiology. These domains are briefly presented in the following subsections.

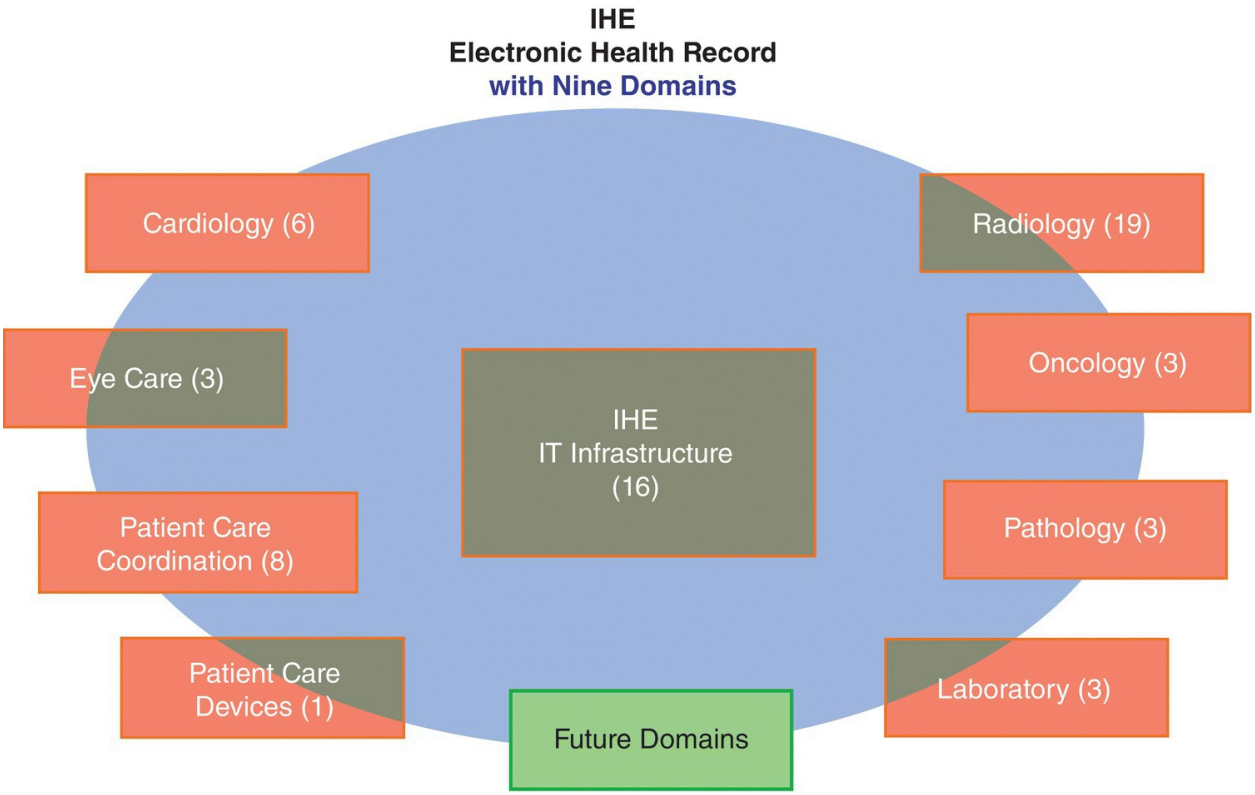

Figure 4.8 IHE framework Infrastructure with nine domains. The IHE IT Infrastructure domain in the center is the major support of the framework (modified by the courtesy of IHE, 2010; Sections 4.7.2 to 4.7.4 are based on existing data from IHE, 2010).

4.7.2.2 IHE Profiles

The development of IHE profiles are organized across an increasing number of clinical and operational domains. These domains are independent and produce their own set of technical framework documents in close coordination with other IHE domains. Many of these domains have only the framework document, and workflow profiles may not yet be available. The following is a list of the current domains and their corresponding profiles, as of 2010. As these numbers of domain and profile will continue to grow, readers should not limit themselves to this list, and should follow the most up-to-day document provided by IHE. Figure 4.8 depicts the organization of the IHE technical framework as of today.

4.7.2.2.1 Domain: Anatomic Pathology

The *Anatomic Pathology Workflow* (PWF) establishes the continuity and

integrity of basic pathology data acquired for examinations being ordered for an identified inpatient or outpatient.

4.7.2.2.2 Domain: Cardiology

1. *Cardiac Cath Workflow (CATH)*: Integrates ordering, scheduling, imaging acquisition, storage, and viewing for cardiac catheterization procedures.
2. *Echocardiography Workflow (ECHO)*: Integrates ordering, scheduling, imaging acquisition, storage, and viewing for digital echocardiography; retrieves ECG for display; provides access throughout the enterprise to electrocardiogram (ECG) documents for review purposes.
3. *Evidence Documents (ED)*: Adds cardiology-specific options to the radiology evidence document profile.
4. *Implantable Device Cardiac Observation (IDCO)*: Specifies the creation, transmission, and processing of discrete data elements and report attachments associated with cardiac device interrogations (observations) or messages.
5. *Stress Testing Workflow (STRESS)*: Provides ordering and collecting multimodality data during diagnostic stress testing procedures.
6. *Displayable Reports (DRPT)*: Distributes “display ready” cardiology clinical reports from the department to the enterprise as a portable document format (PDF) file.

4.7.2.2.3 Domain: Eye Care

1. *Eye Care Workflow (EYECARE)*: Manages eye care workflow including ordering, scheduling, imaging acquisition, storage, and viewing.
2. *Eye Care Evidence Document (ECED)*: Creates, stores, retrieves, and uses objects to record eye care evidence.
3. *Eye Care Displayable Report (ECDR)*: Creates, stores, and retrieves displayable (as a PDF) clinical professional reports.

4.7.2.2.4 Domain: IT Infrastructure

1. *Consistent Time (CT)*: Ensures system clocks and time stamps of computers in a network are well synchronized (median error less than 1 second).
2. *Audit Trail and Node Authentication (ATNA)*: Describes authenticating

systems using certificates and transmitting protected health information-(PHI) related audit events to a repository. This helps sites to implement confidentiality policies.

3. *Request Information for Display (RID)*: Provides simple (browser-based) read-only access to clinical information (e.g. allergies or lab results) located outside the user's current application.
4. *Enterprise User Authentication (EUA)*: Enables single sign-on by facilitating one name per user for participating devices and software.
5. *Patient Identifier Cross Referencing (PIX)*: Cross-references patient identifiers between hospitals, care sites, health information exchanges, etc.
6. *Patient Synchronized Application (PSA)*: Allows selection of a patient in one application to cause other applications on a WS to tune to that same patient.
7. *Patient Demographics Query (PDQ)*: Lets applications query a central patient information server and retrieve a patient's demographic and visit information.
8. *Cross-enterprise Document Sharing (XDS*): Registers and shares electronic health record (EHR) documents between healthcare enterprises, ranging from physician offices to clinics to acute care in-patient facilities.
9. *Personnel White Pages (PWP)*: Provides basic directory information on human workforce members to other workforce members and applications.
10. *Cross-enterprise Document Media Interchange (XDM)*: Transfers XDS documents and metadata over compact disk and USB memory devices, and over email using a zipped attachment.
11. *Cross-enterprise Document Reliable Interchange (XDR)*: Provides a standards-based specification for managing the interchange of documents that healthcare enterprises have decided to explicitly exchange using a reliable point-to-point network communication.
12. *Cross-Enterprise Sharing of Scanned Documents (XDS-SD)*: Defines how to couple legacy paper, film, electronic, and scanner outputted formats, represented within a structured HL7 Clinical Document Architecture Release 2 (CDA) header, with a PDF or plaintext formatted document containing clinical information.
13. *Patient Identifier Cross-reference and Patient Demographics Query for HL7v3*: Extends the patient identifier cross-reference and patient

demographics query profiles leveraging HL7 version 3.

4. *Registry Stored Query Transaction for Cross-enterprise Document Sharing Profile*: Adds a single transaction, stored query, to the XDS profile.
5. *Stored Query*: A large improvement over the existing Query Registry transaction, since it removes the use of SQL.
6. *Retrieve Form for Data Capture (RFD)*: Enables EHR applications to directly request forms from clinical trial sponsors and public health reporting.

4.7.2.2.5 Domain: Laboratory

1. *Laboratory Scheduled Workflow (LSWF)*: Establishes the continuity and integrity of clinical laboratory testing and observation data throughout the healthcare enterprise.
2. *Sharing Laboratory Reports (XD*-LAB)*: Describes a clinical laboratory report as an electronic document.
3. *LOINC Test Codes Subset (LTCS)*: No information available yet.

4.7.2.2.6 Domain: Patient Care Coordination

1. *Medical Summaries (MS)*: Defines the content and format of discharge summaries and referral notes.
2. *Exchange of Personal Health Record Content (XPHR)*: Describes the content and format of summary information extracted from a PHR system for import into an EHR system, and vice versa.
3. *Emergency Department Referral (EDR)*: Allows clinicians to create electronic referrals to the emergency room including the nature of the current problem, past medical history, and medications. Upon arrival of the patient at the emergency department, the patient is identified as a referral, and the transfer document is incorporated into the emergency department information system. This profile builds on medical summaries by adding structures to pass data specific for emergency department referrals such as the estimated time of arrival and method of transport.
4. *Basic Patient Privacy Consents (BPPC)*: Enables XDS affinity domains to be more flexible in the privacy policies that they support, by providing mechanisms to record patient privacy consents, enforcing these consents, and creating affinity domain-defined consent vocabularies that identify

information sharing policies. Pre-procedural history and physical (PPHP) describes the content and format of an electronic preprocedural history and physical document.

5. *Antepartum Care Summary (APS)*: Describes the content and format of summary documents used during antepartum (before childbirth) care.
6. *Functional Status Assessments (FSA)*: Describes the content and format of functional status assessments that appear within summary documents.
7. *Emergency Department Encounter Record (EDER)*: Describes the content and format of records created during an emergency department visit.
8. *Query for Existing Data (QED)*: Allows information systems to query data repositories for clinical information on vital signs, problems, medications, immunizations, and diagnostic results.

4.7.2.2.7 Domain: Patient Care Devices

Device Enterprise Communication (DEC): Communicates data about patient care devices to enterprise applications, such as clinical decision support (CDS), central data repositories (CDRs), and electronic medical records (eMR).

4.7.2.2.8 Domain: Radiation Oncology

1. *Normal Treatment Planning-Simple (NTPL-S)*: Illustrates flow of treatment planning data from CT to dose review.
2. *Multimodality Registration for Radiation Oncology (MMR-RO)*: Shows how radiation oncology treatment planning systems integrate PET and MRI data into the contouring and dose review process.
3. *Treatment Workflow (TRWF)*: Integrates daily imaging with radiation therapy treatments using workflow.

4.7.2.2.9 Domain: Radiology

1. *Scheduled Workflow (SWF)*: Integrates ordering, scheduling, imaging acquisition, storage, and viewing for radiology exams.
2. *Patient Information Reconciliation (PIR)*: Coordinates reconciliation of the patient record when images are acquired for unidentified (e.g. trauma), or misidentified, patients.
3. *Postprocessing Workflow (PWF)*: Provides worklists, status, and results

tracking for post-acquisition tasks, such as computer-aided detection or image processing.

4. *Reporting Workflow (RWF)*: Provides worklists, status, and result tracking for reporting tasks, such as dictation, transcription, and verification.
5. *Import Reconciliation Workflow (IRWF)*: Manages importing images from CDs, hardcopy, for example, and reconciling identifiers to match local values.
6. *Portable Data for Imaging (PDI)*: Provides reliable interchange of image data in a browser.
7. *Nuclear Medicine Image (NM)*: Specifies how nuclear medicine images and result screens are created, exchanged, used, and displayed.
8. *Mammography Image (MAMMO)*: Specifies how mammography images and evidence objects are created, exchanged, used, and displayed.
9. *Evidence Documents (ED)*: Specifies how data objects such as digital measurements are created, exchanged, and used.
10. *Simple Image and Numeric Report (SINR)*: Specifies how diagnostic radiology reports (including images and numeric data) are created, exchanged, and used.
11. *Key Image Note (KIN)*: Lets users flag images as significant (for referral, for surgery, etc.) and adds notes.
12. *Consistent Presentation of Images (CPI)*: Maintains consistent intensity and image transformations between different hard- and soft-copy devices.
13. *Presentation of Grouped Procedures (PGP)*: Facilitates viewing and reporting on images for individual requested procedures (e.g. head, chest, abdomen) that an operator has grouped into a single scan.
14. *Image Fusion (FUS)*: Specifies how systems creating and registering image sets and systems displaying fused images create, exchange and use the image, registration, and blended presentation objects.
15. *Cross-enterprise Document Sharing for Imaging (XDS-I)*: Extends XDS to share images, diagnostic reports, and related information across a group of care sites.
16. *Teaching File and Clinical Trial Export (TCE)*: Lets users flag images and related information for automatic routing to teaching file authoring or

clinical trials management systems.

7. *Access to Radiology Information (ARI)*: Shares images, diagnostic reports, and related information inside a single network.
8. *Audit Trail and Node Authentication (ATNA)*: Radiology option defines radiology-specific audit trail messages.
9. *Charge Posting (CHG)*: Provides timely procedure details from modalities to billing systems.

Of the nine domains, the most well-used and developed is the radiology domain, because radiological imaging has been well used with PACS-based informatics for many years. Of the 19 current workflow profiles, 11 of them were already available in 2003 (see the above list); the 8 new profiles have been developed since 2003. Comparing this list with the 12 workflow profiles available in 2003, only one basic security has been absorbed by other DICOM protocols and IHE workflow profiles. Note that the order of these profiles has been rearranged from the original IHE profiles in 2003.

4.7.3 Some Examples of IHE Workflow Profiles

In this section, four examples of IHE workflow profiles are given. The first example, “IHE use case”, presents four actors and their roles, as described in Figure 4.9. In the figure, the scheduled workflow profile within the radiology domain provides healthcare information that supports efficient patient care workflow in a typical imaging examination. In addition, three more examples depicted in Figure 4.10 (Carr and Moore, 2003), Figures 4.11 and 4.12 in the radiology domain are important for post-processing workflow (PWF), such as 3-D reformats and handling key images (KIN) from imaging studies.

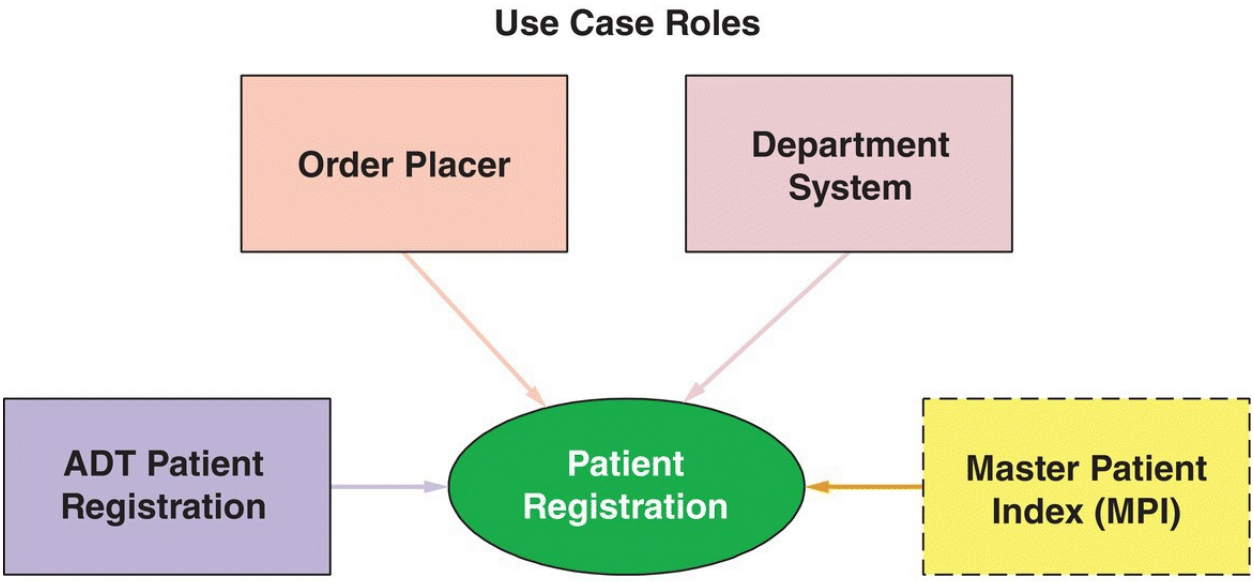

Actor: ADT (admission, discharge, transfer)
Role: Adds and modifies patient demographic and encounter information.
Actor: Order Placer
Role: Receives patient and encounter information for use in order entry.
Actor: Department System
Role: Receives and stores patient and encounter information for use in fulfilling orders by the Department System Scheduler.
Actor: MPI
Role: Receives patient and encounter information from multiple ADT systems. Maintains unique enterprise-wide identifier for a patient.

Figure 4.9 Sample “IHE use case”. The four actors and their respective roles are shown.

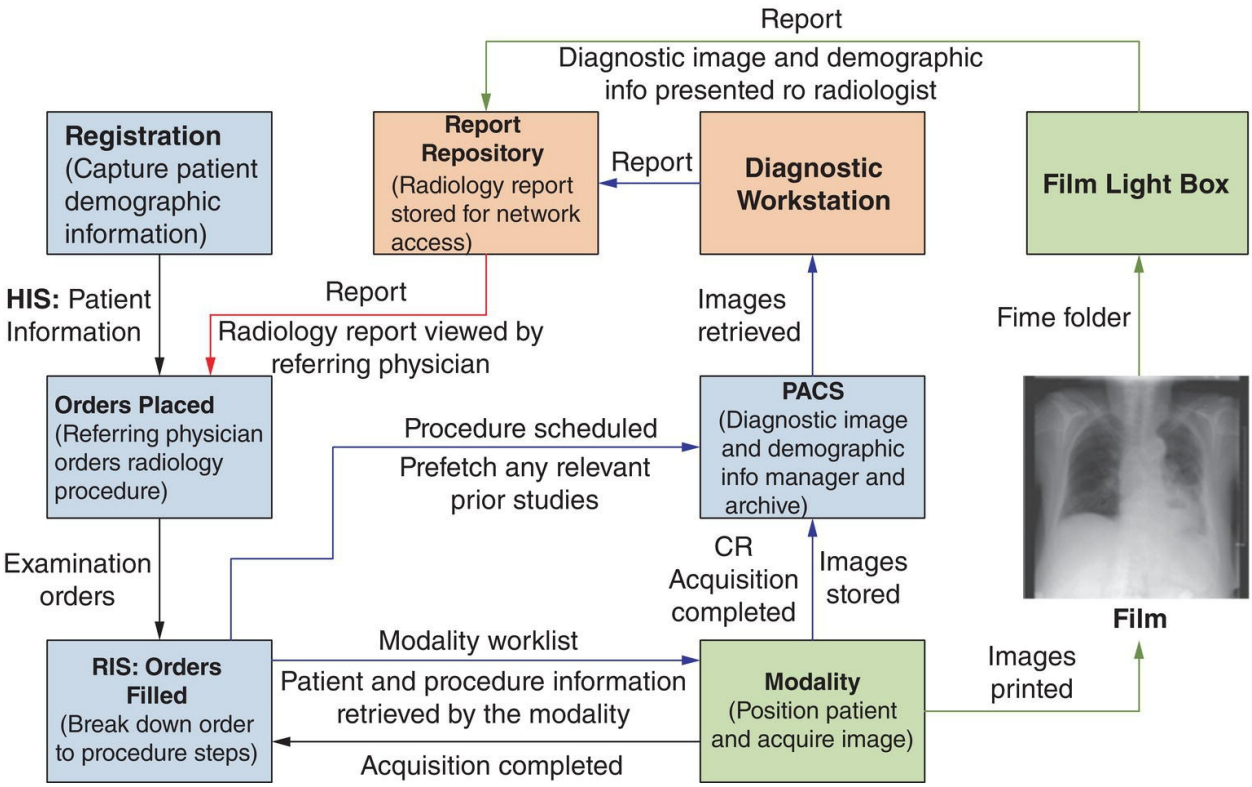

Figure 4.10 IHE scheduled workflow profile including three systems—HIS, RIS, and PACS—and two acquisition devices—conventional films with a digitizer and a CR.

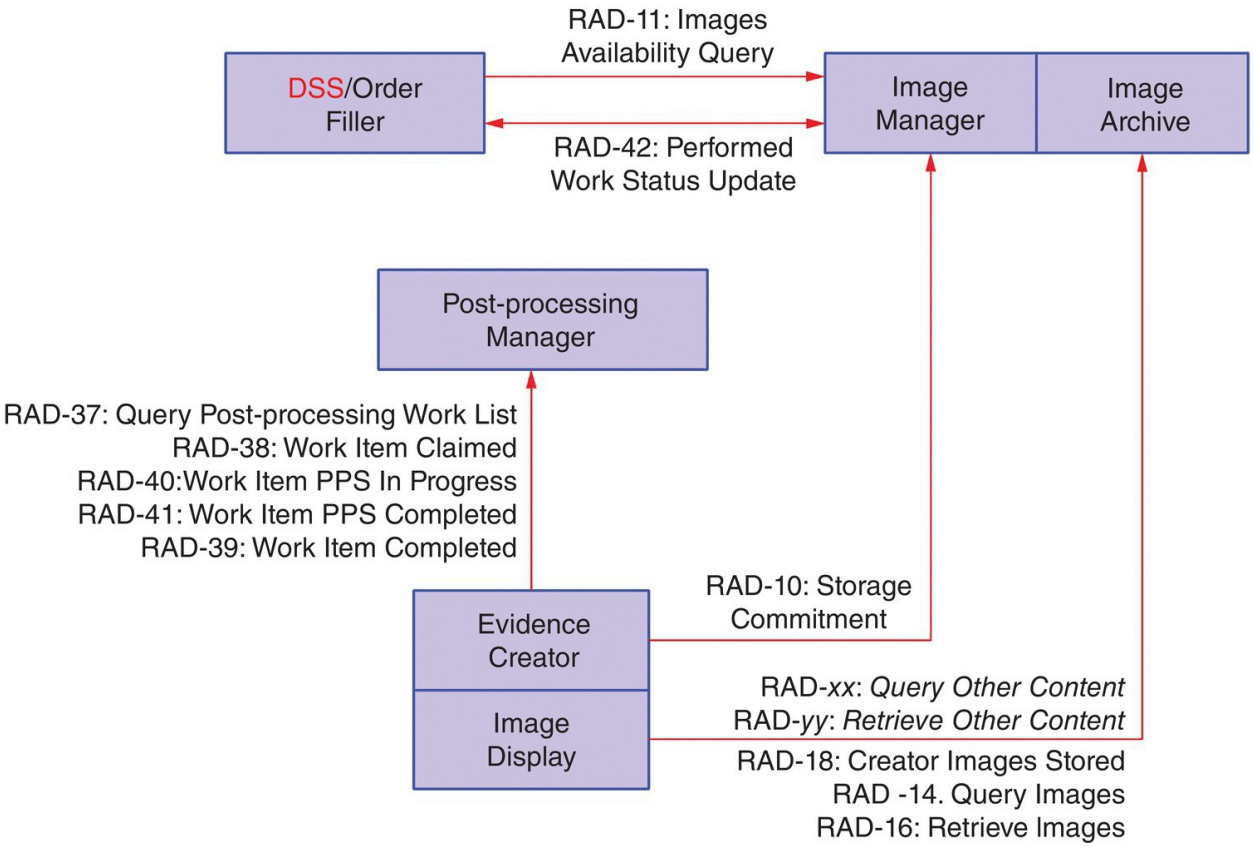

Figure 4.11 IHE post-processing workflow profile (PWF) for a radiology imaging study. This profile is often used in the integration of images from a third-party WS (Chapter 10) or in the integration of CAD with PACS (Chapters 17 and 18) (source: IHE).

4.7.4 The Future of IHE

4.7.4.1 Multidisciplinary Effort

Before 2000, the concentration of the IHE initiative was mainly in radiology. The IHE Strategic Development Committee was formed in September 2001; its members include representatives from multiple clinical and operational personnel, such as cardiology, laboratory, pharmacy, medication administration, and interdepartmental information sharing. Work to identify key problems and expertise in these fields has progressed well. The eight new domains and the expanded domain radiology were presented earlier in Section 4.7.2.2.

4.7.4.2 International Expansion

IHE has expanded internationally. Demonstrations held in Europe and Japan

have received the enthusiastic support of healthcare providers and vendors. Three additional goals have emerged:

1. to develop a process to enable US-based IHE initiative technology to be distributed globally;
2. to document nationally based differences in healthcare policies and practices; and
3. to seek the highest possible level of uniformity in medical information exchange. Figures 4.7A and 4.7B show scenes from the IHE world workshop in 2006 and in 2016.

4.7.4.3 IHE 2020 Vision

Since its inception in 1998, IHE has become a worldwide initiative driving the interoperability of health IT systems. IHE produces standards-based specifications and delivers testing services that enhance the connectivity of IT products and provide the foundation for exchange of health information.

IHE's 2020 vision is to build on its foundation to:

- broaden stakeholder engagement;
- increase awareness and adoption of IHE profiles;
- strengthen support for IHE members, committees, and international deployment organizations;
- broaden testing services to improve product and deployment successes; and
- enhance the organization's independence, governance, and capacity.

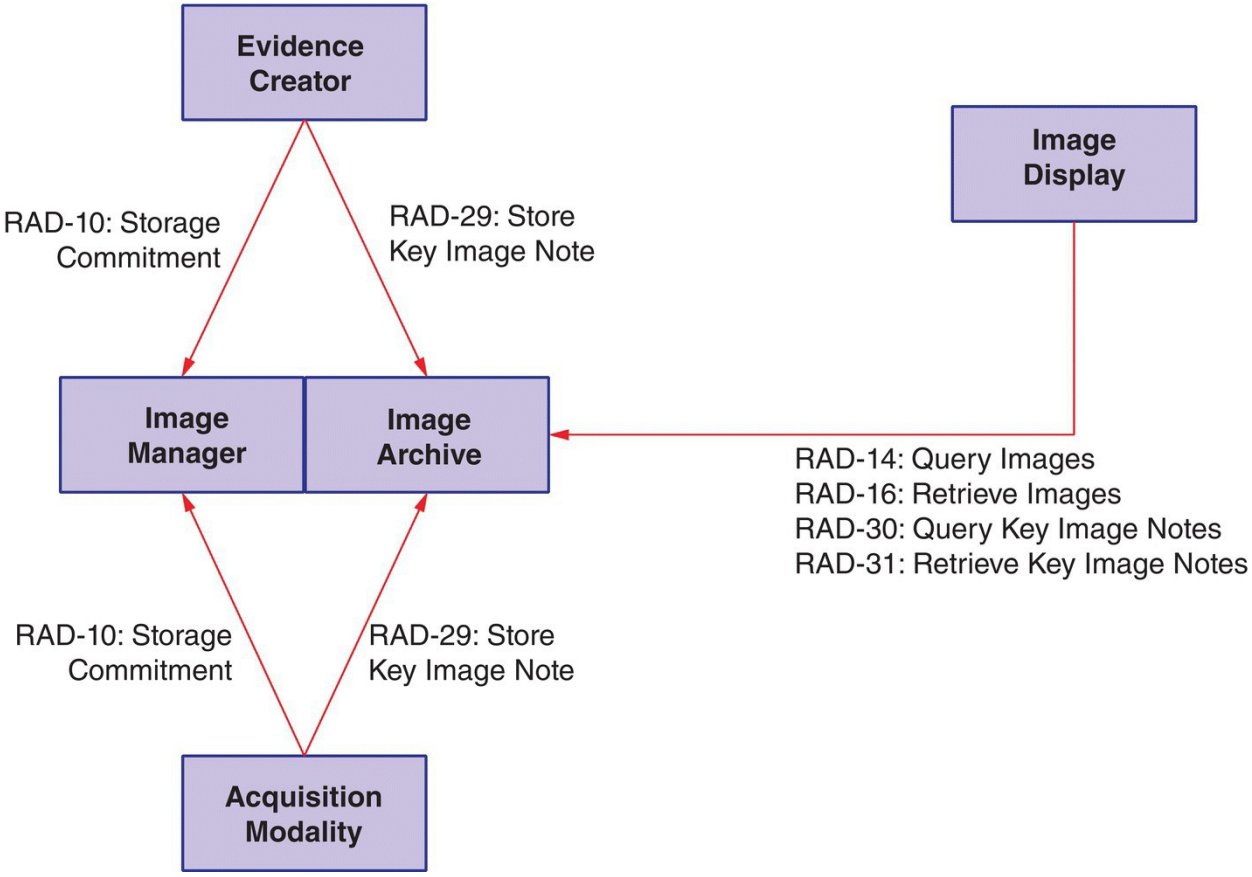

Figure 4.12 IHE key image note (KIN) workflow profile for a radiology imaging study. This profile is often used in PACS-based CAD (see Chapters 16 to 18).

4.8 Some Operating Systems and Programming Languages useful to HL7, DICOM and IHE

In previous sections, some industry standards, protocols, computer operating systems, programming languages, and workflow profiles are mentioned, which are used in PACS-based multimedia imaging informatics infrastructure design and applications. This last section briefly includes five industrial software standards used commonly in PACS-based operation for historically review purposes.

4.8.1 UNIX Operating System

The first UNIX operating system (System V) was developed by AT&T and released in 1983. Other versions of UNIX from different computer vendors

include Berkeley Software Distribution (BSD) by the University of California at Berkeley, Solaris (Sun Microsystems), HP-UX (Hewlett-Packard), Xenix (Microsoft), Ultrix (Digital Equipment Corporation), AIX (International Business Machines), and A/UX (Apple Computers).

Despite its many varieties, the UNIX operating system provides an open system architecture for computer systems to facilitate the integration of complex software systems within individual systems and among different systems. UNIX offers great capability and high flexibility in networking, interprocess communication, multitasking, and security, which are essential to medical imaging applications. UNIX is mostly used in the server, PACS server, gateway, and specialized high-end WSs.

4.8.2 Windows NT/XP Operating Systems

Microsoft Windows NT and XP operating systems run on desktop personal computers (PCs) and are a derivative of the University of California at Berkeley's BSD UNIX. Windows NT and XP, like UNIX, support TCP/IP communications and multitasking, and therefore provide a low-cost software development platform for medical imaging applications in the PC environment. Windows NT is mostly used in WSs and low-end servers.

4.8.3 C and C++ Programming Languages

The C programming language was simple and flexible, and became one of the most popular programming languages in computing. C++, added to the C programming language, is an object-oriented language that allows programmers to organize their software and process the information more effectively than most other programming languages. These two programming languages are used extensively in PACS application software packages.

4.8.4 SQL (Structural Query Language)

Structured Query Language (SQL) is a standard interactive and programming language for querying, updating, and managing relational databases. SQL is developed from Structured English Query Language (SEQUEL), developed by IBM. The first commercially available implementation of SQL was from Relational Software, Inc. (now Oracle Corporation).

SQL is an interface to a relational database such as Oracle and Sybase. All SQL statements are instructions to operate on the database. Hence, SQL is different

from general programming languages, such as C and C++. SQL provides a logical way to work with data for all types of users, including programmers, database administrators, and end users. For example, to query a set of rows from a table, the user defines a condition used to search the rows. All rows matching the condition are retrieved in a single step and can be passed as a unit to the user, to another SQL statement, or to a database application. The user does not need to deal with the rows one by one, or to worry about how the data are physically stored or retrieved. The following are the commands SQL provides for a wide variety of database tasks:

- querying and retrieving data;
- inserting, updating, and deleting rows in a table;
- creating, replacing, altering, and dropping tables or other objects;
- controlling access to the database and its objects; and
- guaranteeing database consistency and integrity.

SQL is adopted by both the American National Standards Institute (ANSI) (1986) and ISO (1987), and many relational database management systems, such as IBM DB2 and ORACLE, support SQL. Therefore, users can transfer all the skills they have gained with SQL from one database to another. In addition, all programs written in SQL are portable among many database systems. These database products have their proprietary extensions to the standard SQL, so very little modification is usually needed for the SQL program to be moved from one database to another. SQL is used most often in the DICOM query/retrieve operation.

4.8.5 XML (Extensible Markup Language)

XML, a system-independent markup language, is becoming the industry standard for data representation and exchange on the World Wide Web, Intranet, and elsewhere. As a simple, flexible, extensible text format language, XML can describe information data in a standard or common format, so that it makes data portable.

Although, like HTML, which has been used extensively over the past 10 years for easy data representation and display, XML uses tags to describe the data, it is significantly different from HTML. First, HTML mainly specifies how to display the data, whereas XML describes both the structure and the content of the data. This means that XML can be processed as data by programs, exchanged among

computers as a data file, or displayed as Web pages, as HTML does. Second, there is a limit in HTML, where only those predefined tags can be used. However, XML is extensible, as mentioned above.

4.9 Summary of Industrial Standards: HL7, DICOM and IHE

This chapter presents two important industrial standards, HL7 for healthcare textual data and DICOM for medical imaging data and communications. HL7 has been a stable standard for many years and is used widely. DICOM has been stabilized and accepted by the medical imaging industry. However, DICOM is still evolving to include other medical specialties, among these, radiation therapy, surgery, cardiology, and pathology. In addition to DICOM, Chapter 7 describes new methods for medical imaging sharing for collaborative healthcare based on IHE XDS-I Profiles.

IHE, on the other hand, is not a standard, but IHE workflow profiles have been developed to promote the use of DICOM and HL7. IHE is also evolving and has been expanded to over nine domains to include IT and other medical specialties such as radiology, radiation therapy, and surgery.

References

1 American Medical Association (2001) *Current Procedural Terminology*. Chicago: AMA.

2 Huff, S.M., Rocha, R.A., McDonald, C.J., *et al*. (1998) Development of the logical observation identifier: names and codes (LOINC) vocabulary. *J Am Med Info Assoc*, 5, 276–292.

3 Russler, D. (2006) Integrating the healthcare enterprise (IHE). Overview in IHE Workshop.

4 Siegel, E.L. and Channin, D.S. (2001) Integrating the healthcare enterprise: A primer—Part 1. *Introduction. RadioGraphics*, 21, 1339–1341.

5 Channin, D., Parisot, C., Wanchoo, V., Leontiew, A. and Siegel, E.L. (2001a) Integrating the healthcare enterprise: a primer. III. What does IHE do for me? *RadioGraphics*, 21, 1351–1358.

6 Channin, D.S., Siegel, E.L., Carr, C., *et al*. (2001b) Integrating the healthcare enterprise: A primer. V. The future of IHE. *RadioGraphics*, 21, 1605–1608. 300 Industrial Standards (HL7 and DICOM) and IHE.

7 Henderson, M., Behel, F.M., Parisot, C., Siegel, E.L. and Channin, D.S. (2001) Integrating the healthcare enterprise: a primer. IV: The role of existing standards in IHE. *RadioGraphics*, 21, 1597–1603.

Further Reading

Carr, C. and Moore, S.M. (2003) IHE: a model for driving adoption of standards. *Comp Med Imag Graph*, 27 (2–3), 137–146.

Channin, D.S. (2001) Integrating the healthcare enterprise: a primer. II: Seven brides for seven brothers: The IHE Integration Profiles. *RadioGraphics*, 21, 1343–1350.

DICOM Standard (2008) http://medical.nema.org/medical/dicom/2008

DICOM Standard (2003) http://www.dclunie.com/dicom status/status.html#BaseStandard 2001. Health Level 7. http://www.hl7.org/

Health Level 7—HL7 Version 3.0: Preview for CIOs, Managers and Programmers. http://www.neotool.com/company/press/199912 v3.htm#V3.0 preview.

International Classification of Diseases, 9th revision (2001) Washington, DC: US Department of Health and Human Services. Publication 91–1260.

Internet Engineering Task Force. http://www.ietf.org

Java web service tutorial. http://java.sun.com/webservices/docs/1.1/tutorial/doc/JavaWS Tutorial.pdf

Oracle8 SQL Reference Release 8.0. Oracle 8 Documentation CD.

Radiological Society of North America Healthcare Information and Management Systems Society (2001) IHE technical framework, year 3, version 4.6. Oak Brook, IL: RSNA, March 2001. Recently Approved Supplements. http://medical.nema.org/

SQL. http://searchdatabase.techtarget.com/sDefinition/0,sid13

gci214230,00.html

XML. http://searchwebservices.techtarget.com/sDefinition/0,sid26 gci213404,00.html

PERPUSTAKAAN PRIBADI AN-NUR SUNARYA

5
DICOM-Compliant Image Acquisition Gateway and Integration of HIS, RIS, PACS and ePR

CHAPTER MENU

5.1 DICOM Acquisition Gateway

5.2 DICOM-Compliant Image Acquisition Gateway

5.2.1 DICOM Compliance

5.2.2 DICOM-Based Image Acquisition Gateway

5.3 Automatic Image Data Recovery Scheme for DICOM Conformance Device

5.3.1 Missing Images and Data

5.3.2 Automatic Image Data Recovery

5.4 Interface of PACS Modalities with the Gateway Computer

5.4.1 PACS Modality Gateway and HI-PACS (Hospital Integrated Gateway)

5.4.2 An Example – Interface the US (Ultrasound) Modality with the PACS Gateway

5.5 DICOM Compliance PACS Broker

5.5.1 Concept of the DICOM Broker

5.5.2 Implementation of a PACS Broker

5.6 Image Preprocessing and Display

5.7 Clinical Operation and Reliability of the Gateway

5.7.1 The Weakness of the Gateway as a Single Point of Failure

5.7.2 A Fail-Safe Gateway Design

5.8 Hospital Information System (HIS), Radiology Information System (RIS), and PACS

5.8.1 Hospital Information System

5.8.2 Radiology Information System
5.8.3 Interfacing PACS with HIS and RIS
References

The image acquisition gateway computer (gateway) with a set of software programs is used as a buffer between image acquisition and the PACS-based multimedia imaging informatics servers [1, 2]. This chapter also relates to Chapter 4 and Chapter 15, Sections 15.1 and 15.7. Figure 5.1 depicts the DICOM-compliance image acquisition gateway (red) in the generic PACS data flow. In this chapter, the terms acquisition gateway computer, gateway computer, acquisition gateway, and gateway have the same meaning [3–8].

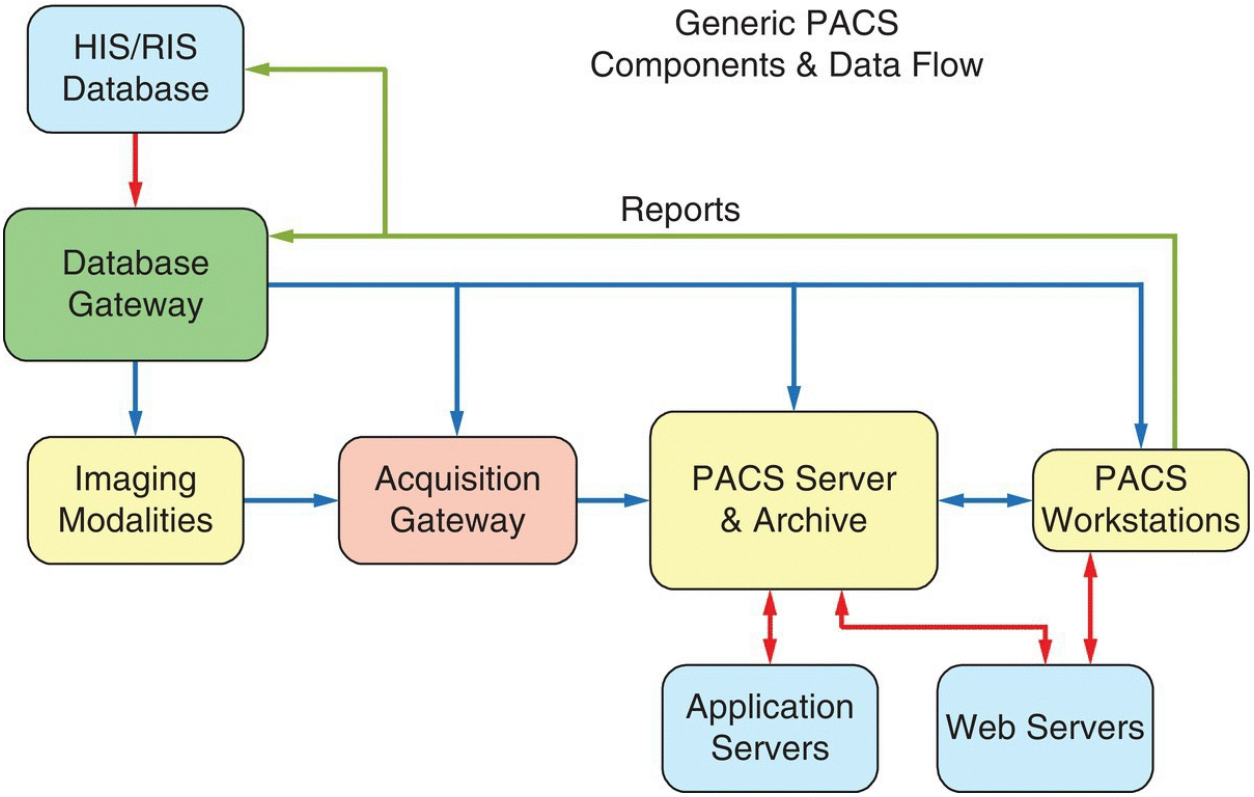

Figure 5.1 PACS basic components (yellow) and data flow (blue: internal; green and red: external between PACS and other information systems); other information systems (light blue); the color of the gateway (red). HIS: hospital information system; RIS: radiology information system.

5.1 DICOM Acquisition Gateway

Several acquisition devices (modalities) can share one gateway computer. The gateway has three primary tasks:

1. to acquire image data from radiological and other energy imaging devices;
2. to convert the data from manufacturer data format to the PACS-based image data standard format (header format, byte-ordering, matrix sizes, etc.) that is compliant with the DICOM data formats; and
3. to forward the image study to the PAC-based server or directly to the PACS workstations (WSs).

Additional tasks of the gateway are some image pre-processing, compression, and data security. An acquisition gateway has the following characteristics:

1. It preserves the image data integrity transmitted from the imaging device.
2. Its operation is transparent to the users and totally or highly automatic.
3. It delivers images timely to the PACS server and WSs.
4. It performs some image pre-processing functions to facilitate image display.

Among all PACS major components, establishing a reliable gateway in PACS is the most difficult task for a number of reasons. First, a gateway must interface with many imaging modalities and PACS modules made by different imaging manufacturers. These modalities and modules have their own image format and communication protocols that can sometimes make the interface task difficult. Even most imaging equipment now follows the DICOM standard; the PACS-based integrator must negotiate several DICOM conformance statements (Chapter 4) for a successful interface. Second, performing radiological examinations with an imaging device requires the operator's input, such as entering the patient's name, identification, accession number, and then forwarding images to WSs and server. During this process, the potential for human error is unavoidable. A very minor error from the input can have a severe impact on the integrity of the PACS data. Third, ideally the gateway should be 100% automatic for efficiency and minimizing system errors.

However, to achieve a totally automatic component without much human interaction and with equipment from varied manufacturers is very challenging. The degrees of difficulty and the cost necessary to achieve this possibility have been the focal issues in PACS-based imaging informatics design. Automated image acquisition from imaging devices to the PACS controller plays an important role in a PACS infrastructure. The word "automatic" is important here,

since relying on labor-intensive manual acquisition methods would defeat the main purpose of PACS. An important measure of the success of an automatic acquisition is its effectiveness in ensuring the integrity and availability of patient images in a PACS system.

Because most imaging devices are now mostly DICOM compliant, this chapter only discusses methods related to the DICOM gateway. For imaging devices that still use a non-DICOM compliant, older interface method such as the endoscopic light imaging, a DICOM converter has to be available in the gateway to comply with the DICOM image format standard. This chapter discusses four topics of interest. The first group of topics relates to the DICOM interface: the DICOM compliant gateway, the automatic image recovery scheme for DICOM conformance imaging devices, interface with other existing PACS modules, and the DICOM broker. Because an imaging gateway also performs certain image pre-processing functions to facilitate image archive and display, the second group of topics considers some image pre-processing functions commonly used in PACS-based informatics. The topic in the third group relates to the concept of multilevel adaptive processing control in the gateway, which ensures the reliability of the gateway as well as the image integrity. This topic is important because, when the acquisition gateway has to deal with DICOM formatting, communication, and many image preprocessing functions, multiple-level processing with a queuing mechanism is necessary. The last topic is on clinical experience with the acquisition gateway.

5.2 DICOM-Compliant Image Acquisition Gateway

5.2.1 DICOM Compliance

DICOM conformance (compliance) by manufacturers is a major factor contributing to the interoperability of different medical imaging systems in the clinical environment. Chapter 4 discusses the DICOM standard, in which it defines the basis of interface mechanism allowing image communication between different manufacturers' systems. With a standardized interface mechanism, the task of acquiring images from the DICOM-compliant imaging systems becomes simpler. Figure 5.2 shows the connection between the imaging device and the acquisition gateway computer.

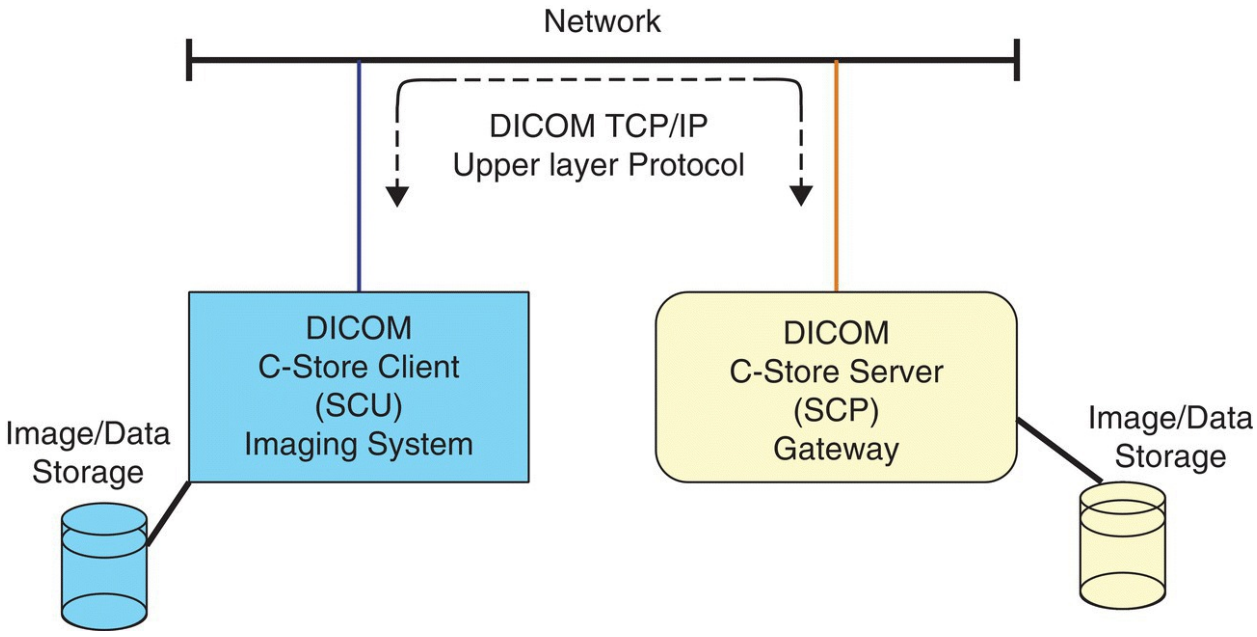

Figure 5.2 Schematic of the DICOM-compliant PACS image acquisition gateway with the DICOM C-STORE service–object pairs (SOP) connecting the imaging device service class user (SCU) with the gateway service class provider (SCP).

The DICOM-compliant imaging device on the left is the C-Store client, and the image acquisition gateway on the right is the C-Store server (Figure 4.5). They are connected by a network running the DICOM TCP/IP transmissions (Section 5.1, Figure 5.8). Regardless of whether a "push" from the scanner or a "pull" from the gateway is used (see also Chapter 3, Section 3.1), one image is transmitted at a time, and the order of transmission depends on the database architecture of the scanner. After these images have been received, the gateway must know how to organize them to form the image series and studies according to the DICOM data model, so that image data integrity is not compromised.

In the gateway, a database management system serves three functions. First, it supports the transaction of each individual image transmitted by the modality and received by the acquisition. Second, it monitors the status of the patient studies and their associated series during the transmission. Third, it provides the basis for the automatic image recovery scheme to detect unsuccessfully transferred images. Three database tables based on the DICOM data model of the real world (Figure 4.2B) are used: patient, study, series, and images. Each table contains a group of records, and each record contains a set of useful data elements. For the study and series database tables, the study name and the series name are the primary keys for searching. In addition, the following major data

elements are recorded:

1. patient name and hospital identification number;
2. dates and times when the study and series were created from the imaging device and acquired from the gateway;
3. the number of acquired images per series;
4. time stamp of each image when it is acquired by the gateway;
5. acquisition status;
6. DICOM unique identification (UID) value for the study and series.

The DICOM standard is used to transmit images, one image at a time; the order of transmission does not necessarily follow the order of scan, series, or study. The image device's "job queue" priority dictates what job needs to be processed next from the scanner's computer, and it is always in favor of the scanning and image reconstruction rather than the communication routine. For this reason, an image waiting in the queue to be transmitted next can be bumped and lose its priority and so be placed in the lower priority waiting queue for a long period of time without being discovered. The result is a temporary loss of images in a series and in a study. If this is not discovered early enough, the images may be lost permanently because of various system conditions; for example, a system reboot, disk maintenance, or premature closing of the patient image file at the gateway. Neither a temporary nor a permanent loss of images is acceptable in PACS operation. An error recovery mechanism is used to automatically regain images that are temporarily lost.

5.2.2 DICOM-Based Image Acquisition Gateway

5.2.2.1 Gateway Computer Components and Database Management

The acquisition gateway shown in Figure 5.3 consists of four elementary software components: database management system (DBMS), local image storage, storage service class provider (SCP), and storage service class user (SCU); and three error handling and image recovery software components: Q/R SCU, integrity check, and acquisition delete. The elementary components are discussed in this section; error handling and image recovery components are discussed in Section 5.3.

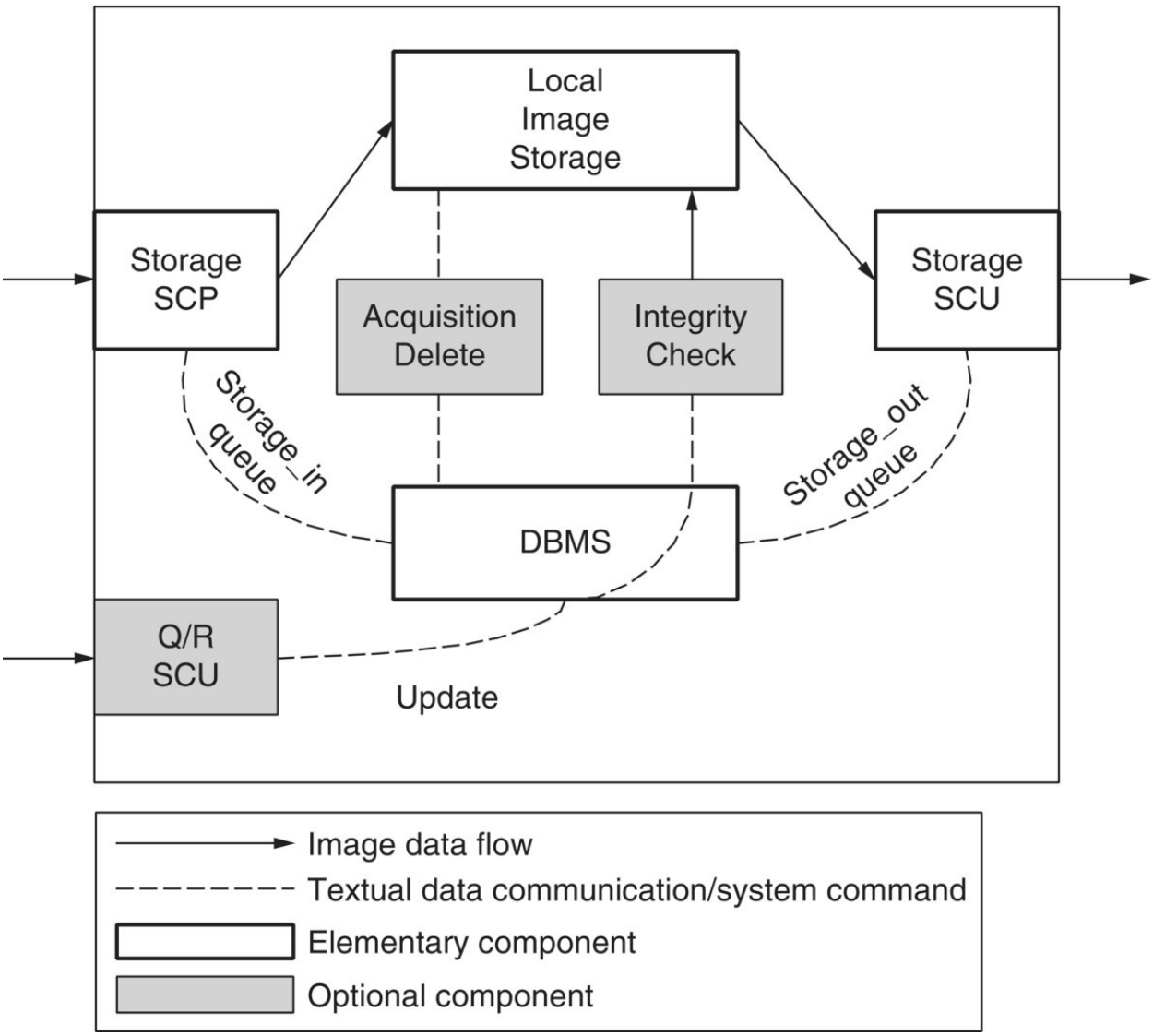

Figure 5.3 Acquisition gateway components and their workflow. Four elementary components are storage service class provider (SCP), storage service class user (SCU), local image storage, and database management system (DBMS). The three error-handling and image recovery software components (shaded) are query and retrieve (Q/R) SCU, integrity check, and acquisition delete.

The local database of the gateway records the textual information about images, problematic images, queues, and imaging devices structurally, and is controlled and managed by the DBMS. Because the textual information will be deleted after the archiving is completed, a small-scale DBMS, such as the Access and MySQL commercial products, is adequate to support normal operation of image acquisition to the gateway. The DBMS mounts extendable database file(s), in

which the textual data are actually stored.

The information about image data can be stored in four tables: patient, study, series, and image (Chapter 4, Figure 4.2B). As shown in Figure 5.4, these tables are linked hierarchically with primary and foreign key pairs. Their primary keys uniquely identify each record in these tables. The primary and foreign keys are denoted by (*) and (#) respectively, in Figure 5.4. The Patient table records some demographic data such as patient ID, name, sex, and birth date. The study and series tables record information such as the date and time when each study and series are created in the imaging device and acquired in the acquisition gateway and the instance UID of each study and series. The study and series instance UIDs are important for image recovery, which is discussed in Section 5.2.3. The image table records generic image information such as orientation, offset, window, and level values of the images stored before and after image pre-processing. The file name and path are defined for each record in the image table, providing a link to the local image storage, which can be used to check the integrity of image stored. The records of problematic images are stored in a set of wrong-image tables, which can be displayed to alert the system administrator through a graphical interface.

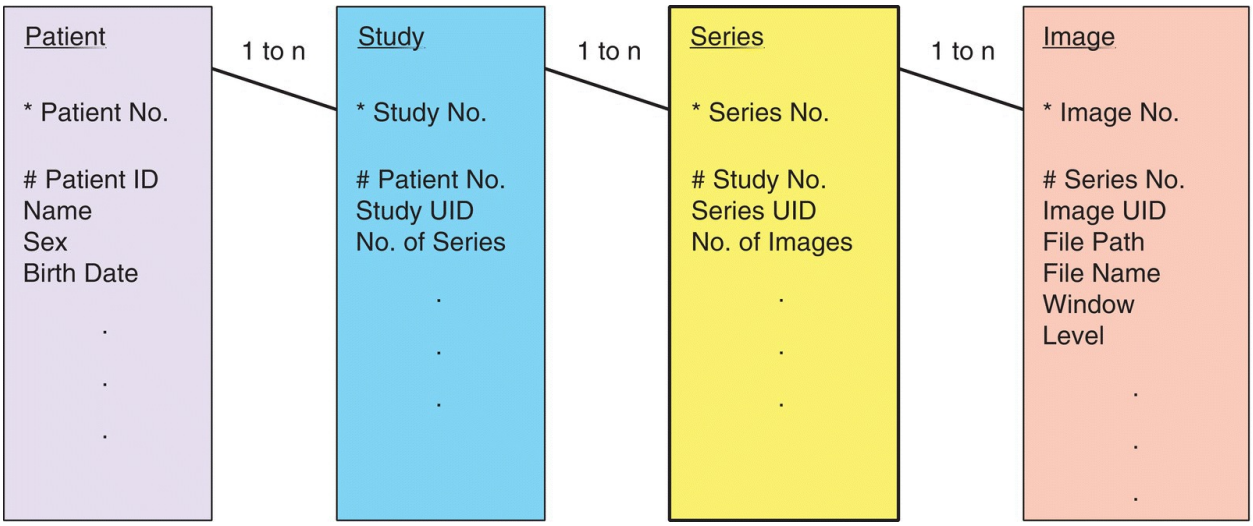

Figure 5.4 Gateway computer database management hierarchies for patient, study, series, and image tables. (*) denotes primary key and (#), foreign key.

5.2.2.2 Determination of the End of an Image Series

If DICOM transmits images one by one from the imaging modality like a CT scanner to the gateway, but not necessarily in order, how does the gateway know when a series or a study is completed and when it should close the study file for

archive or display? The images of a series and/or a study can only be grouped together by a formatting process when the end of series and/or the end of study is determined by the image receiving process. To determine algorithmically the end of a series in a manner both accurate and efficiently is nontrivial. The following section presents three algorithms for determining the end of series and discusses the advantages and drawbacks of these algorithms.

5.2.2.2.1 Algorithm 1: Presence of the Next Series

The first algorithm is to detect the end of a series based on the presence of the next series. This algorithm assumes that the total number of images for the current series would have been transmitted to the gateway before the next series began. In this case, the presence of the first image of the next series indicates the termination of the previous series. The success of the method depends on the following two premises: i) the imaging device transmits the images to the gateway in the order of the scan; and ii) no images are lost during the transmission. Note that the first assumption depends on the specific order of image transmission by the imaging system. If the imaging system transmits the image slices in an ordered sequence, this method can faithfully group the images of a series without errors. On the other hand, if the imaging system transfers the image slices at random, this method may conclude the end of a series incorrectly. Even though we could verify the second assumption by checking the order of the image, whether or not the last image has been transmitted remains unknown to the gateway. Another drawback of this method relates to the determination of the last series of a particular study, which is based on the presence of the first image of the next study. The time delay for this determination could be lengthy, because the next study may not begin immediately after the first series; for example, there may be a delay of the examination from the next patient.

5.2.2.2.2 Algorithm 2: Constant Number of Images in a Given Time Interval

The second method for determining the end of a series is based on a time interval criterion. The hypothesis of this method assumes that an image series should be completed within a certain period of time. By this method, the end of a series is determined when the acquisition time of the first image plus a designated time interval has elapsed. This method is obviously straightforward and simple, but a static time interval criterion is not practical in a clinical environment. Thus, an alternative recourse uses the concept of the constant number of a images in a time interval.

This method requires the recording of the number of acquired images for a given series at two different times, time t_1 and time $t_2 = t_1 + \Delta t$, for some predetermined constant Δt. By comparing the number of images acquired at time t_1 versus the number of images acquired at time t_2, a premise is constructed for determining whether or not the series is complete. If, for example, the number of images is a constant, it concludes that the series is complete; otherwise the series is not yet complete. This process (Δt with number of images verification) is iterated until a constant number of images has been reached. Next, consider how to select Δt: should it be a static or a dynamic number? A short Δt may result in missing images, whereas a long Δt may result in lengthy and inefficient image acquisition. Usually, the first Δt chosen for this method is empirical, depending on the imaging protocols used by the imaging system. For example, if the imaging protocol frequently used in a scanner generates many images per series, then Δt should be long; otherwise, a shorter Δt is preferred. However, it is possible that, for a too short Δt, this method may conclude a series prematurely. This is because in some rare cases the technologist or clinician may interrupt the scanning process in the middle of a series to adjust alignment of the patient or to inject a contrast agent. If the time takes longer than Δt, then images obtained after the procedure would not be grouped into the current series. In a poorly designed DICOM PACS based informatics system, this could result in a severe problem—missing images in a series.

Should Δt be dynamic during the iteration? One thought is that the number of images transmitted from the imaging device to the gateway decreases while the iteration cycle increases. Therefore it seems reasonable that Δt may be reduced proportionally to the number iterations. On the other hand, the number of images transmitted to the gateway may vary with time, depending on the design of the imaging device. For example, an imaging device may be designed to transmit images according to the imaging system workload and priority schedule. If the image transmission process has a low priority, then the number of images transmitted during a period when the system workload is heavy will be lower compared to with the workload is light. In this case, Δt is a variable.

5.2.2.2.3 Algorithm 3: Combination of Algorithm 1 with Algorithm 2

Given the discussion of two algorithms, a combination of both becomes preferable. Algorithm 3 can be implemented into the following three steps:

1. Identify and count the acquired images for a particular series.
2. Record the time stamp whenever the number of acquired images has

changed.

3. Update the acquisition status of the series.

The acquired images can be tracked by using a transaction table designed in association with the series database table discussed in Section 5.2.2.1. It can be first started with the time interval method. Whenever an image is acquired from the imaging device, a record of the image is created in the transaction table identified by the modality type, the imaging system identification, the study number, the series number, the image number, and the acquisition time stamp. A tracking system can be developed based on these records. Three major events from the current iteration are recorded in the transaction table:

1. the number of acquired images;
2. the t_2 value; and
3. the acquisition status declaring the series as standby, ongoing, completed, or image missing.

Here the information regarding the number of acquired images and acquisition status is useful for the maintenance of the image-receiving process. If the series is ongoing, the comparison time is updated for the verification of the number of images during the next iteration.

After the interval method detects the end of a series, it can be further verified by the "presence of the next series" method. If the next series exists in the series database table or the next study exists in the study table, the image series is determined as complete; otherwise one more iteration is executed, and the series remains in standby status. In this case, the end of the series will be concluded in the next iteration regardless of the existence of the next series or study. In general, Δt can be set to 10 minutes. Using this approach, the completeness of an image series is verified by both algorithms and any potential lengthy delay would be minimized.

5.3 Automatic Image Data Recovery Scheme for DICOM Conformance Device

5.3.1 Missing Images and Data

Images can be missing at the gateway computer when they are transmitted from the imaging device. For example, consider a MRI scanner using the DICOM C-

Store client to transfer images with one of the following three modes: auto-transfer, auto-queue, or manual transfer. Only one transfer mode can be in operation at a time. The auto-transfer mode transmits an image whenever it is available, the auto-queue mode transfers images only when the entire study has been completed, and the manual-transfer mode allows the transfer of multiple images, series, or studies. Under normal operation the auto-transfer mode is routinely used and the manual transfer mode is used only when a re-transmission is required. Once the DICOM communication between the image scanner and the gateway has been established, if the technologist changes the transfer mode for certain clinical reasons in the middle of the transmission, some images could be temporarily lost. In the next section, an automatic recovery method for these images is discussed.

5.3.2 Automatic Image Data Recovery

5.3.2.1 Basis for the Image Recovery Scheme

The automatic image recovery scheme includes two tasks: identifying the missing studies, series, or images; and recovering them accordingly. This scheme requires that the gateway can access the scanner image database. These two tasks can be accomplished by using the DICOM query/retrieve service class (Chapter 4, Section 4.5.2) in conjunction with the gateway database described in Section 5.2.2.1 of this chapter. The operation mechanism of the Q/R service involves three other DICOM service classes: C-Find, C-Move, and C-Store. The task of identifying missing studies is through the C-Find by matching one of the image grouping hierarchies, such as study level or series level, between the gateway database and the scanner database. The missing image(s) can be recovered by using the C-Move and the C-Store service classes. The Q/R operation is executed via a client process at the gateway computer and the MRI scanner computer (as an example) as the server.

5.3.2.2 The Image Recovery Algorithm

Figure 5.5 shows the steps of the automatic image recovery algorithm. There are two steps: recover the missing studies, and recover missing series or images.

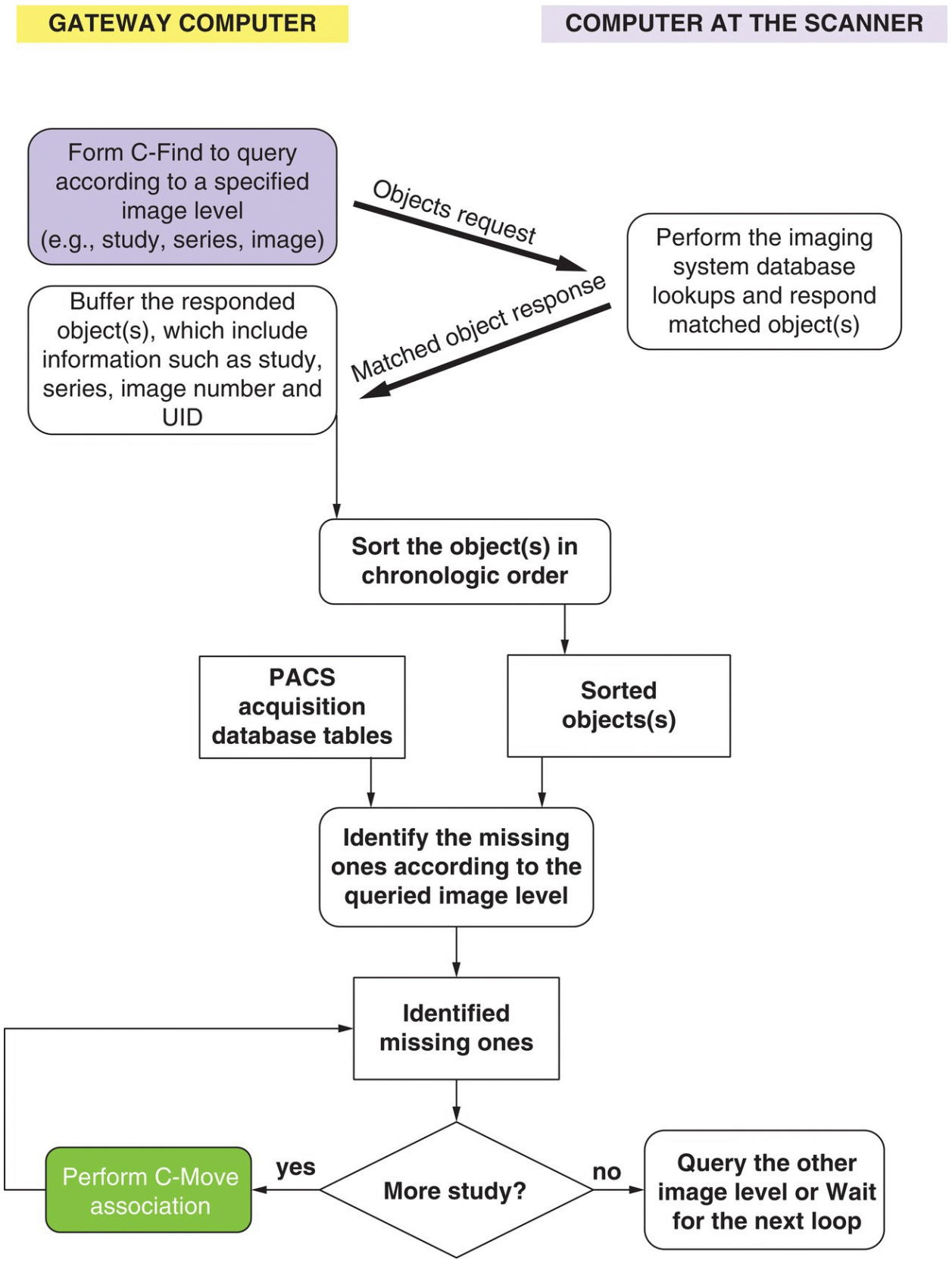

Figure 5.5 The general processing flow diagram of the automatic DICOM query

and retrieve image recovery scheme. The scheme starts by the acquisition computer issuing a C-Find command (purple, upper left). The recovery starts by a C-Move command (lower left, green). Both commands are received by the imaging device's query/retrieve computer.

5.3.2.2.1 Recovery of Missing Study

In this step, the Q/R client encodes a C-Find query object containing the major information elements, such as image study level and a zero-length UID value defined by the DICOM standard. The zero-length UID prompts the Q/R server to return every single UID for the queried level. Then the Q/R server responds with all the matching objects in the scanner database according to the requested image study level. The content of each responding object mainly includes information such as a study number and the corresponding study UID. The information of each responding object is then compared with the records in the gateway database. Those study numbers, which are in the responding objects but not recorded in the PACS gateway database, are considered missing studies. Each of the missing studies can be retrieved by issuing a C-Move object from the gateway, which is equivalent to an image retrieval request. Because the retrieval is study specific, the study UID must be included in the C-Move object explicitly. The scanner, after the C-Move object is received by the Q/R server, relays the retrieval request to the C-Store client. As a result, the study transfer is actually conducted by the C-Store client and server processes.

5.3.2.2.2 Recovery of Missing Series/Image

Recovering missing series or images can be performed with the same recovery mechanism as for the study/image level. The difference between the study level and the series level in the recovery scheme is that a specific study UID must be encoded in the C-Find query object for the series or image level, as opposed to a zero-length UID for the study level.

The records of available images in the scanner database and the gateway database may not synchronize. This situation can happen during a current study when its associated series and images are being generated in the scanner but not yet transferred to the gateway. This asynchronization can result in incorrect identification, because the image recovery process may mistake the current study listed in the scanner database for a missing one, as it has not been transferred to the gateway. To avoid this, the responding objects from the Q/R server are first sorted into chronological order by study creation date and time. If the creation date and time of the most recent study is less than a predefined time interval

compared with the current time, it is considered to be the study being generated by the scanner. Thus, the image recovery process will not identify the most recent study as a missing study.

Algorithms of determination of the end of an image series and automatic image recovery schemes, discussed in Sections 5.2.2 and 5.3, have been implemented by most manufacturers in their 3-D or 4-D imaging acquisition schemes. The image acquisition gateway performance has been improved dramatically over the past few years, but certain human errors may still exist. Should any recovery errors occur, the contents of these sections should provide some clues to provide a solution.

5.4 Interface PACS Modalities with the Gateway Computer

5.4.1 PACS Modality Gateway and HI-PACS (Hospital Integrated Gateway)

Section 5.2 discusses the DICOM image acquisition gateway; this gateway can also be used to interface with a PACS module. A PACS module is loosely defined as a self-contained mini PACS comprising some imaging devices, a short-term archive, a database, some display WSs, and a communication network linking these components together. In practice, the module can function as a self-contained integrated imaging unit in which the WSs can show images from imaging devices. However, without the integration with the general PACS, it remains as an isolated system; images from this isolated PACS module would not be able to communicate with the PACS database, and vice versa. In Section 5.4.2, an example of interfacing the gateway to a PACS module, namely an Ultrasound US module, is given. Another example is discussed in Chapter 9, Section 9.2, Data Grid for a Dedicated Breast MRI Enterprise. Other PACS modules that can also be interfaced with the HI-PACS gateway; examples are: the nuclear medicine PACS module, emergency room module, ambulatory care module, and teleradiology module. The requirements for interfacing these modules are an individual specialized DICOM gateway (i.e. the US gateway, or the MRI gateway) in the respective module with DICOM commands for communication and DICOM format for the image file. Multiple modules can be connected to the HI-PACS by using several pairs of acquisition gateways, as shown in Figures 5.6 and 9.9 in Chapter 9. Both Figures 5.6 and 9.9 are stand-alone modules in their own respective subspecialty areas.

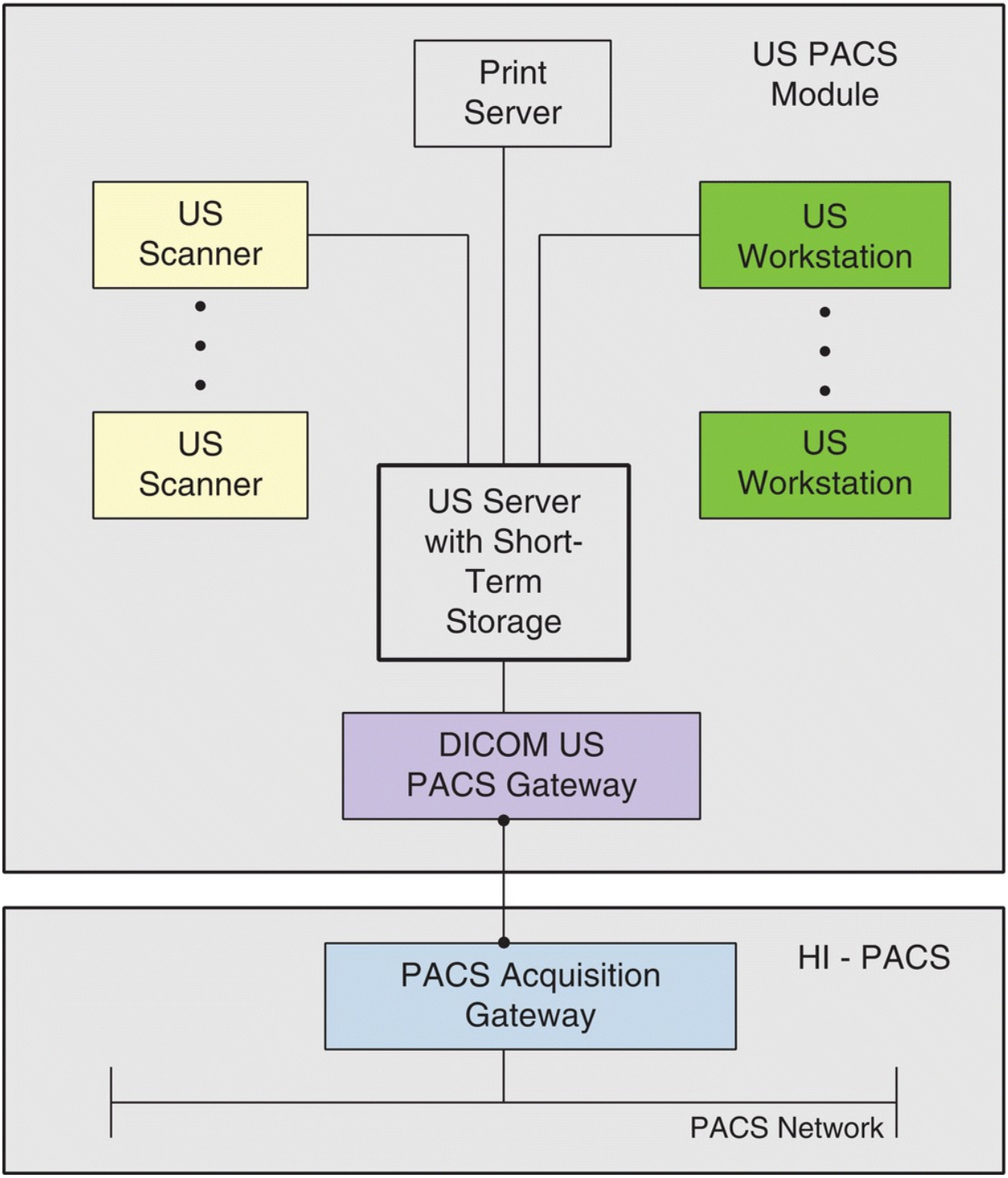

Figure 5.6 Connection of the US PACS module with several US scanners (left, yellow) to the hospital integrated PACS (HI-PACS) gateway, purple). Two gateways are used: US PACS gateway (purple) and HI-PACS gateway (blue).

5.4.2 An Example – Interface the US (Ultrasound) Modality

with the PACS Gateway

An example demonstrating interfacing the gateway to an ultrasound (US) PACS module is shown in Figure 5.6. The US module consists of several US scanners, and some WSs with tailored software for displaying US images, which are connected to an US server with a short-term archive (several weeks) of examinations. There are certain advantages in connecting the US module to a HI-PACS. First, once connected, US images can be appended into the same patient's PACS image folder (or database) and share the general PACS worklist, forming a complete file for long-term archiving. Second, US images can be shown with other modality images in the PACS general display workstations for cross modality comparisons. Third, some other modality images can also be shown in the US module's specialized WSs. In this case, care must be taken, because the specialized WS (e.g. US WS) may not have the full capability to display images from other modalities.

A preferred method of interfacing a PACS module with the HI-PACS is to treat the US PACS module as an imaging device. Two gateways would be needed, one for the US PACS gateway connected to the US server, and a PACS image acquisition gateway connected to the HI-PACS. These two gateways are connected by using the method described in Section 5.4. Figure 5.6 (purple and blue) shows the connection of the two gateways. Each patient's image file in the US server contains the full-sized color or black-and white images (compressed or original), thumbnail (quarter-sized) images for indexing, and image header information for DICOM conversion. In the US gateway computer, several processes are running concurrently. The first process is a daemon constantly checking for new US examinations arriving from scanners. When one is found, the gateway uses a second process to convert the file to the DICOM format. Because a color US image file is normally larger (Chapter 2, Section 2.3.4), a third process compresses it to a smaller file, normally with a 3:1 ratio. The US gateway generates a DICOM send command to transmit the compressed DICOM file to the PACS acquisition gateway computer, by using DICOM TCP/IP transmission. In the PACS acquisition gateway computer, several daemons are also running concurrently. The first is a DICOM command that checks for the DICOM send command from the US gateway. Once the send command is detected, the second daemon checks the proper DICOM format and saves the information in the PACS gateway computer. The third daemon queues the file to be stored by the PACS server's long-term archive.

To request other modality images from an US WS, the patient's image file is first

Q/R from the PACS long-term archive. The archive transmits the file to the HI-PACS gateway, which sends it to the US PACS gateway. This US gateway computer transmits the file to the US server and then to the WS.

5.5 DICOM Compliance PACS Broker

5.5.1 Concept of the DICOM Broker

The PACS broker is the interface between PACS and the radiology information system (RIS), or with the hospital information system (HIS), when the RIS is a component of the HIS. There are very few direct connections between a RIS and PACS, because most current RIS can only output important patient demographic and examination information in HL7 format (Chapter 4, Section 4.4.2), which is a format that most PACS cannot receive or interpret. A PACS broker acts as an interface by processing the HL7 messages received by different RIS systems and mapping the data into easily customizable database tables. The broker then processes the requests by various PACS components and provides the requested components with the proper data formats and contents.

Figure 5.7 shows the architecture and functions of the DICOM-based PACS broker. It receives HL7 messages from the RIS and maps them into its own customizable database tables. PACS components can then request from the broker specific data and formats. These include the DICOM work list for an acquisition modality, scheduled exams for pre-fetching, patient location for automatic distribution of PACS exams to WSs in the hospital ward areas, and radiology reports for PACS viewing WSs.

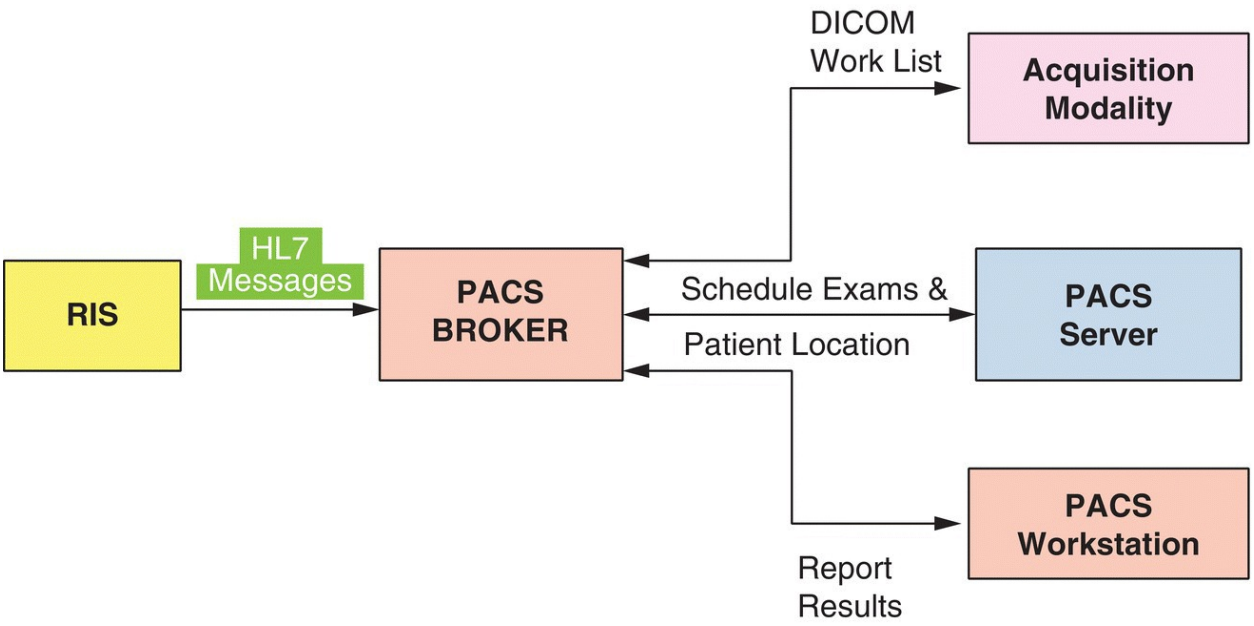

Figure 5.7 Functions of the DICOM-based PACS broker.

5.5.2 Implementation of a PACS Broker

The following example shows how a PACS broker works. Assume the hospital has an RIS and is implementing a PACS, but is missing the interface between the existing RIS with the newly implemented PACS. A broker can be used to act as an interface between the PACS and the RIS as follows.

The RIS outputs HL7 messages triggered by particular events in the radiology workflow; for example, an examination scheduled, dictated, or completed. The broker receives the HL7 messages from the RIS. Following the specifications provided by the RIS, the broker can be pre-configured to map the incoming HL7 message data into various particular fields of its own database tables. The PACS components can now communicate directly with the broker to make requests for information. Some important data that are requested by PACS are:

1. a worklist of scheduled examinations for an acquisition modality;
2. radiology reports and related patient demographic and examination information for PACS-viewing WSs;
3. patient location for automatic distribution of PACS examinations to WSs in the hospital wards; and
4. scheduled examination information for pre-fetching by the PACS server to PACS WSs.

These requests are in addition to general patient demographic data and examination data that are needed to populate a DICOM header of a PACS examination.

5.6 Image Preprocessing and Display

In addition to receiving images from imaging devices, the gateway computer performs certain image pre-processing functions before images are sent to the PACS server or WSs. There are two types of category of pre-processing functions. The first type relates to the image format—for example, a conversion from the manufacturer's format to a DICOM-compliant format of the PACS. This category of pre-processing involves mostly data format conversion, as was described in Chapter 4, Section 4.4. The second category of pre-processing prepares the image for optimal viewing on the PACS WS. To achieve optimal display, an image should have the proper size, good initial display parameters with a suitable lookup table, and proper orientation; any visual distracting background should be removed.

Pre-processing functions should be modified specifically in the sense that each imaging modality has specific sets of pre-processing requirements before the image is sent to the gateway for display. Some pre-processing functions may work well for certain modalities, but poorly for others. Chapter 2 show different types of medical images and their respective pre-processing functions for image display on various WSs, including:

1. computed radiography (CR) and digital radiography (DR)—reformatting, image background removal, and automatic image body part orientation;
2. digitized x-ray images;
3. digital mammography;
4. 2-D and 3-D CT, emission computed tomography (ECT), MRI, and ultrasound imaging; and
5. 4-D, multimodality, and fusion imaging,

Readers are encouraged to refer to these sections and chapters.

5.7 Clinical Operation and Reliability of the Gateway

5.7.1 The Weakness of the Gateway as a Single Point of Failure

During clinical hours, various modality images are continuously sending large amounts of images to the gateway(s); for this reason, the workload of the gateway(s) is very heavy, especially when multiple modalities send all images to one gateway or the gateway shares the computer with other PACS processes, such as image pre-processing. The computer for the gateway may not have enough power to handle the data flow during peak hours. Although the gateway is reliable, it is still potentially a single-point-of-failure component in the PACS-based operation between the modalities and the archive server. Even though there are multiple gateways in PACS, each of which has its own respective assignments in their connection, in general, to switch from one failed gateway to another gateway is mostly a manual procedure. Because DICOM communication needs to set up proper DICOM communication parameters, such as application entities (AE) title, IP address, and port number, it would require an experienced PACS service engineer or administrator to set up and switch gateways correctly and quickly. Fixing a failed gateway might take several minutes to half an hour, and hence it affects the data flow of the PACS. Figure 5.8 shows the manual switching (solid black fonts in the rectangles) between two gateways in PACS. There are two possible solutions. First, use a built-in failsafe mechanism in the imaging device to automatically switch a failing gateway to the other (from yellow to the green box). This built-in failsafe mechanism was developed more than 10 years ago. The second solution, developed about 6–7 years ago, is to develop a failsafe mechanism in the gateway, as discussed in Section 5.7.2.

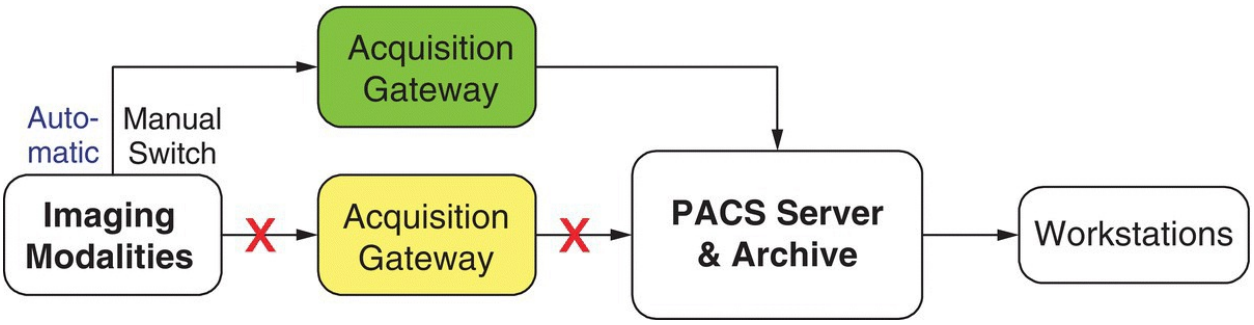

Figure 5.8 Manual switch (inside right) to replace the failed acquisition gateway (yellow). Automatic replacement (left) is preferred (outside left, green).

5.7.2 A Fail-Safe Gateway Design

Because of the possible gateway failure, some DICOM-based PACS

manufacturers change the term “gateway” to DICOM import and export, or multiple integrating unit (MIU). The concept is to bundle several gateways to share the computer load balance and possible single point of failure of the gateway. Some manufacturers also combine the PACS server with the gateways by employing a very powerful server computer with multiple processors.

In this concept, the gateway hardware (Figure 5.9, left) is an independent gateway, and the PACS server (Figure 5.9, right) is a powerful server with enough power to run both server functions as well as the gate software shown in Figure 5.9. A dual-system backup mechanism can be implemented as follows. Two identical gateway software packages, one in the left top and the second in the right second middle of Figure 5.9, are running simultaneously on both the left gateway and one of the right server processes. When input data enter both the gateway hardware and the server hardware, both the gateway and a processor of the server hardware accepts them and allocates them to the DICOM data model database. If the left gateway hardware fails, the designated processor in the ePR server automatically takes over the roles of the gateway hardware, as well as all other software and processes in the ePR server accordingly. No gateway data are lost.

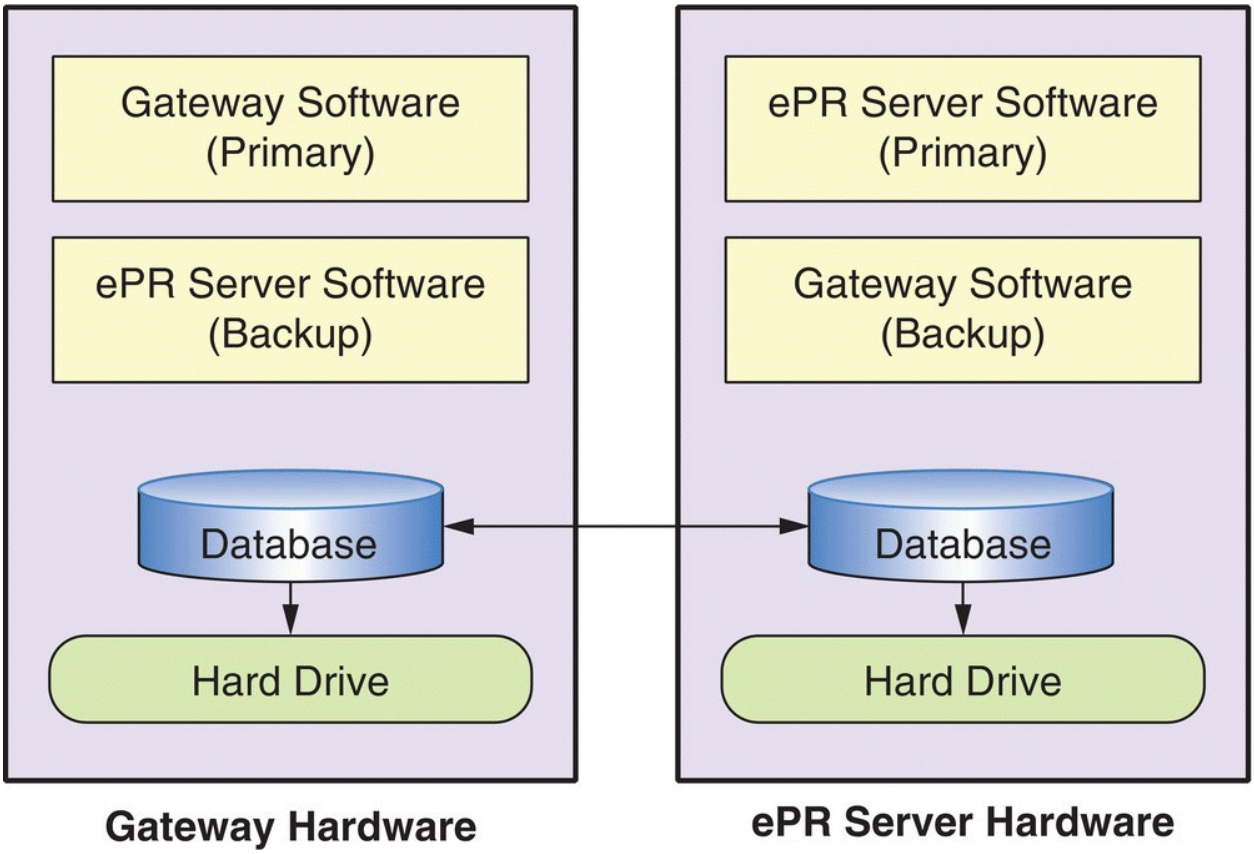

Figure 5.9 The failsafe tandem gateway system, with the left as the primary gateway. The ePR server hardware in the right with multiple processors; one processor is dedicated as the backup gateway. Two identical gateway software programs are running simultaneously on both the gateway hardware and one processor in the ePR server hardware (see Chapter 20, Figure 20.16 for more details).

5.8 Hospital Information System (HIS), Radiology Information System (RIS), and PACS

DICOM-based PACS is an imaging management system that requires pertinent data from other medical information systems for effective operation. Among these systems, data from the HIS and the RIS are the most important. Many functions in the PACS server and archive server, described in Chapters 4 to 6, and ePR rely on data extracted from both HIS and RIS. This section presents some HIS and RIS data that are important to the PACS-based multimedia informatics operation, and discusses how to interface HIS and RIS with PACS to obtain these data. Another topic of interest related to PACS image distribution is ePR, or electronic medical record (eMR), which are discussed in Chapter 11. Figure 5.10 shows the positions of the PACS server and archive, HIS, RIS, and Web-based ePR server in the generic PACS components data flow.

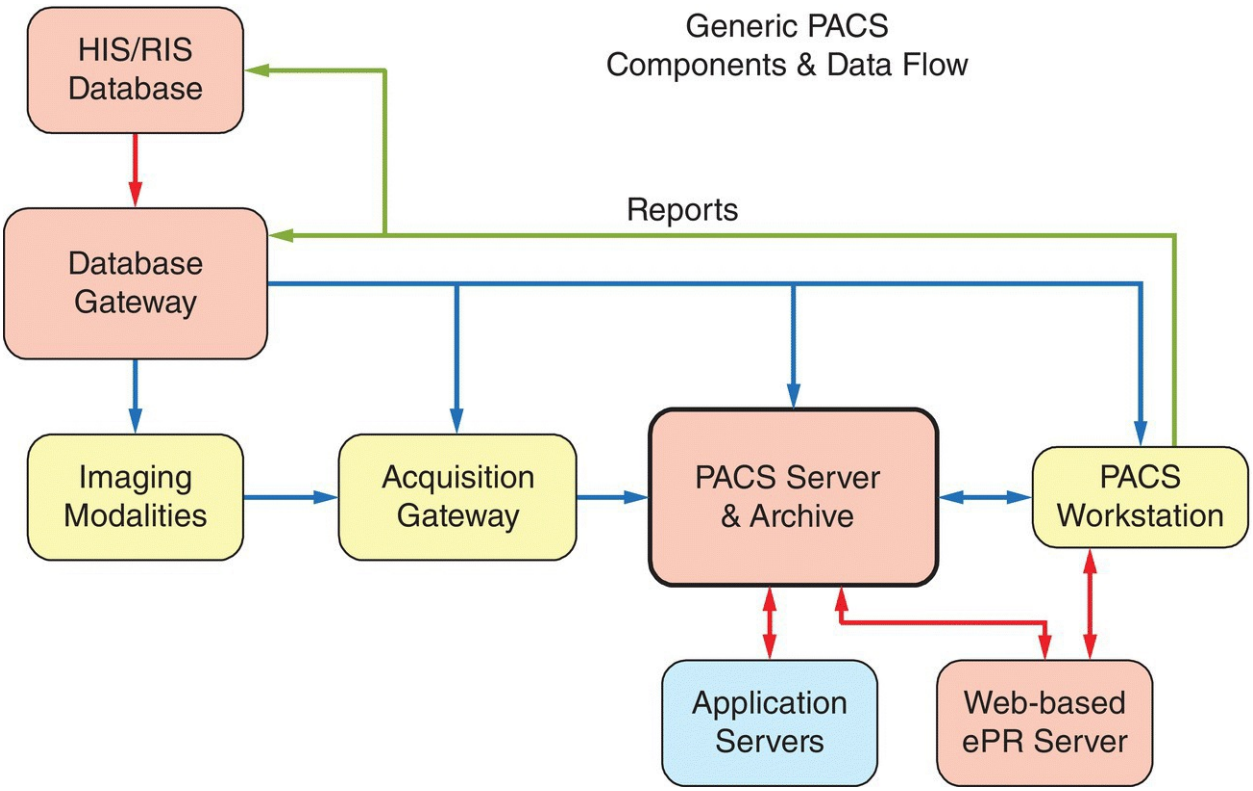

Figure 5.10 DICOM (Chapter 4) PACS basic components (yellow) and data flow (blue lines): Internal; green and red: external between PACS and other information systems); other information systems (light blue). The four components to be integrated together in Chapters 4 and 5 are HIS/RIS, database gateway, PACS server and archive, and ePR in orange.

5.8.1 Hospital Information System

The HIS is a computerized management system for handling three categories of tasks in a healthcare environment:

1. Support clinical and medical patient care activities in the hospital.
2. Administer the hospital's daily business transactions (financial, personnel, payroll, bed census, etc.).
3. Evaluate hospital performances and costs, and project the long-term forecast.

Most clinical departments in a healthcare center, mainly radiology, pathology, pharmacy, and clinical laboratories, have their own specific operational requirements that differ from the general hospital operations. For this reason, special information systems may be needed in these departments. Often, these information systems are under the umbrella of the HIS, which supports their

operations. However, there are also departments that have different workflow environments that may not be covered by the HIS. So they may need their own separate information systems and must develop mechanisms to integrate data between these systems and the HIS. Such is the case in RIS, which began as a component of HIS; later, independent RIS systems were developed because of the limited support from HIS in handling the special data and information required by the radiology operation. However, the integration of these two systems is extremely important for the healthcare center to operate as a total functional entity.

A large-scale HIS consists of mainframe computers and software. The computers are purchased through computer companies offering service and maintenance contracts that include system upgrades. The software can be contracted to a large software company with customized HIS related packages, or they can be home-grown systems. The software is developed progressively by integrating many commercial products over many years. A home-grown system may contain many reliable legacy hardware and software components, but through years of use, their technology may become outdated. Almost all HIS systems were developed through the integration of many information systems, starting from the days when healthcare data centers were first established. While older components might have been replaced by newer systems, the older components can still be in operation. Therefore, to interface HIS to PACS, extra care should be taken to understand not only new but also older technologies to circumvent such a legacy problem. Figure 5.11 shows main components of a typical HIS.

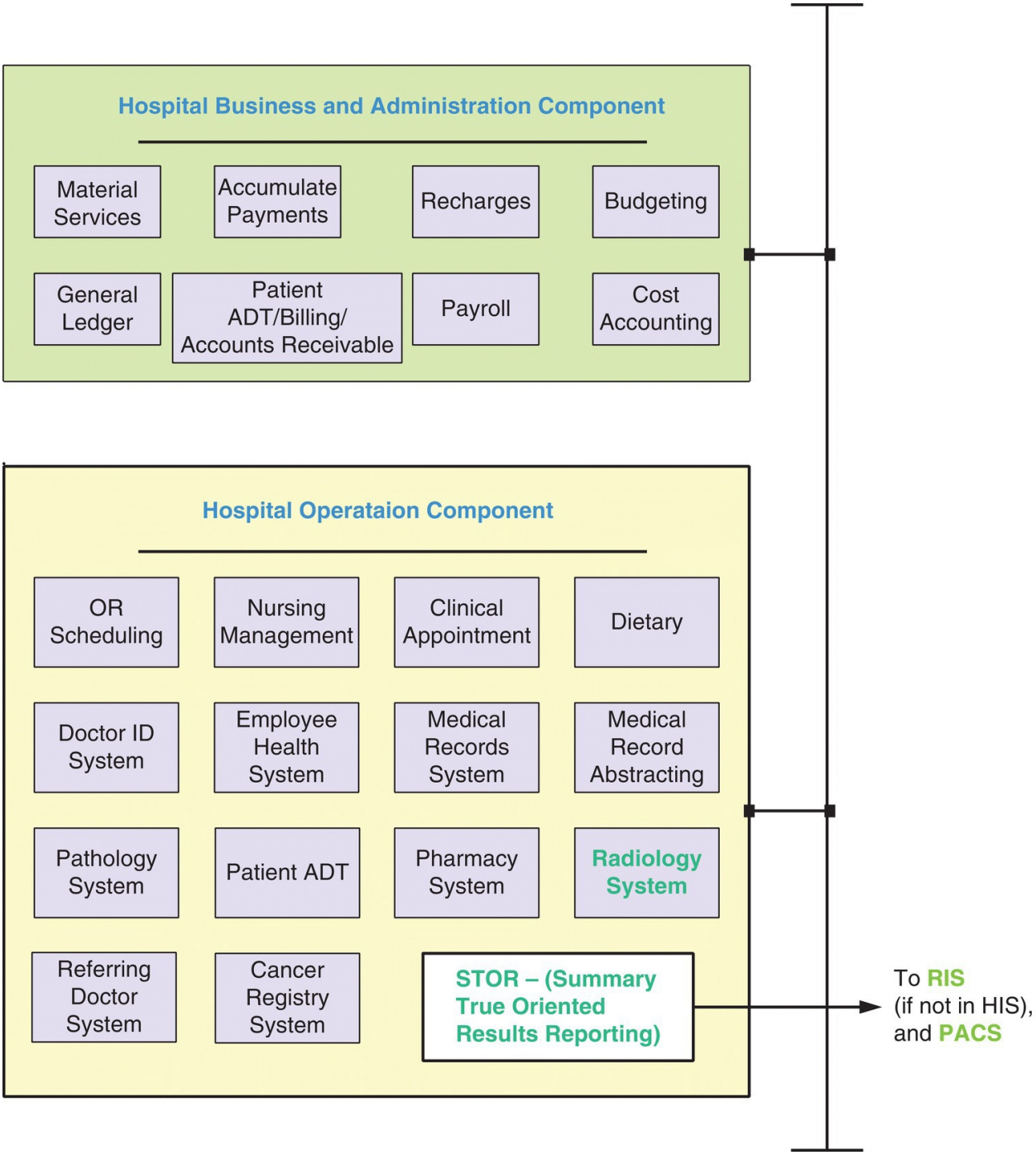

Figure 5.11 A typical HIS system with two categories of software packages: business (top), and administration and clinical operation (bottom). Rectangles are major components in each category. The software package STOR (bottom right), is a trade name (other HIS may use different names) that provides a path for the HIS to distribute HL7 formatted data to the outside world, including PACS.

Notice in Figure 5.11 that, in addition to clinical operations, the HIS supports the hospital's and healthcare center's business and administrative functions. It provides automation for such events as patient registration, admission, discharge, and transfer (ADT), as well as patient accounting. It also provides on-line access to patient clinical results (e.g. laboratory, pathology, microbiology, pharmacy, and radiology). The system broadcasts the patient demographics in real time, and when it encounters information with the HL7 standard (Chapter 4, Section 4.2), it moves the information to the RIS. By way of these paths, ADT and other pertinent data can be transmitted to the RIS and the PACS.

5.8.2 Radiology Information System

The RIS is designed to support both the administrative and clinical operation of the radiology department to reduce administrative overheads, and to improve the quality of radiological examination service. Therefore the RIS manages general radiology patient information, from schedule, examination, to reporting. The RIS configuration is similar to that of HIS, except that it is much smaller in scale. RIS equipment consists of a computer system with peripheral devices such as RIS WSs (normally without image display capability), printers, and barcode readers. Most independent RIS are autonomous systems with limited access to HIS. Some HIS offer embedded RIS as a subsystem with a higher degree of integration.

The RIS maintains many types of patient- and examination-related information. Patient-related information includes medical, administrative, patient demographics, and billing information. Examination-related information includes procedural descriptions and scheduling, diagnostic reporting, patient arrival documentation, film location, film movement, and examination room scheduling. When integrated with PACS, it includes patient-related PACS data and workflow.

The major tasks of the system include:

- processing patient and film (image) folder records.
- monitoring the status of patients, examinations, and examination resources.
- scheduling of examinations.
- creating, formatting, and storing diagnostic reports with digital signatures.
- tracking film (soft-copy) folders.
- maintaining timely billing information.

- performing profile and statistics analysis.

The RIS interfaces to PACS based on the HL7 standard through TCP/IP over the Ethernet on a client–server model using a trigger mechanism. Events such as examination scheduling, patient arrivals, and examination begin and end times can trigger the RIS to send previously selected information (i.e. patient demographics, examination description, diagnostic report, etc.) associated with the event to the PACS in real time.

5.8.3 Interfacing PACS with HIS and RIS

There are two methods of transmitting data between information systems: through database-to-database transfer, and with an interface engine.

5.8.3.1 Database-to-Database Transfer

The database-to-database transfer method allows two or more networked information systems to share a subset of data by storing them in a common local area. For example, the ADT data from the HIS can be reformatted to the HL7 standard and broadcasted periodically to a certain local database in the HIS. A TCP/IP transmission can be set up between the HIS and the RIS, allowing the HIS to initiate the local database and broadcast the ADT data to the RIS through either a pull or a push operation. This method is most often used to share information between the HIS and the RIS, as shown in Figure 5.12.

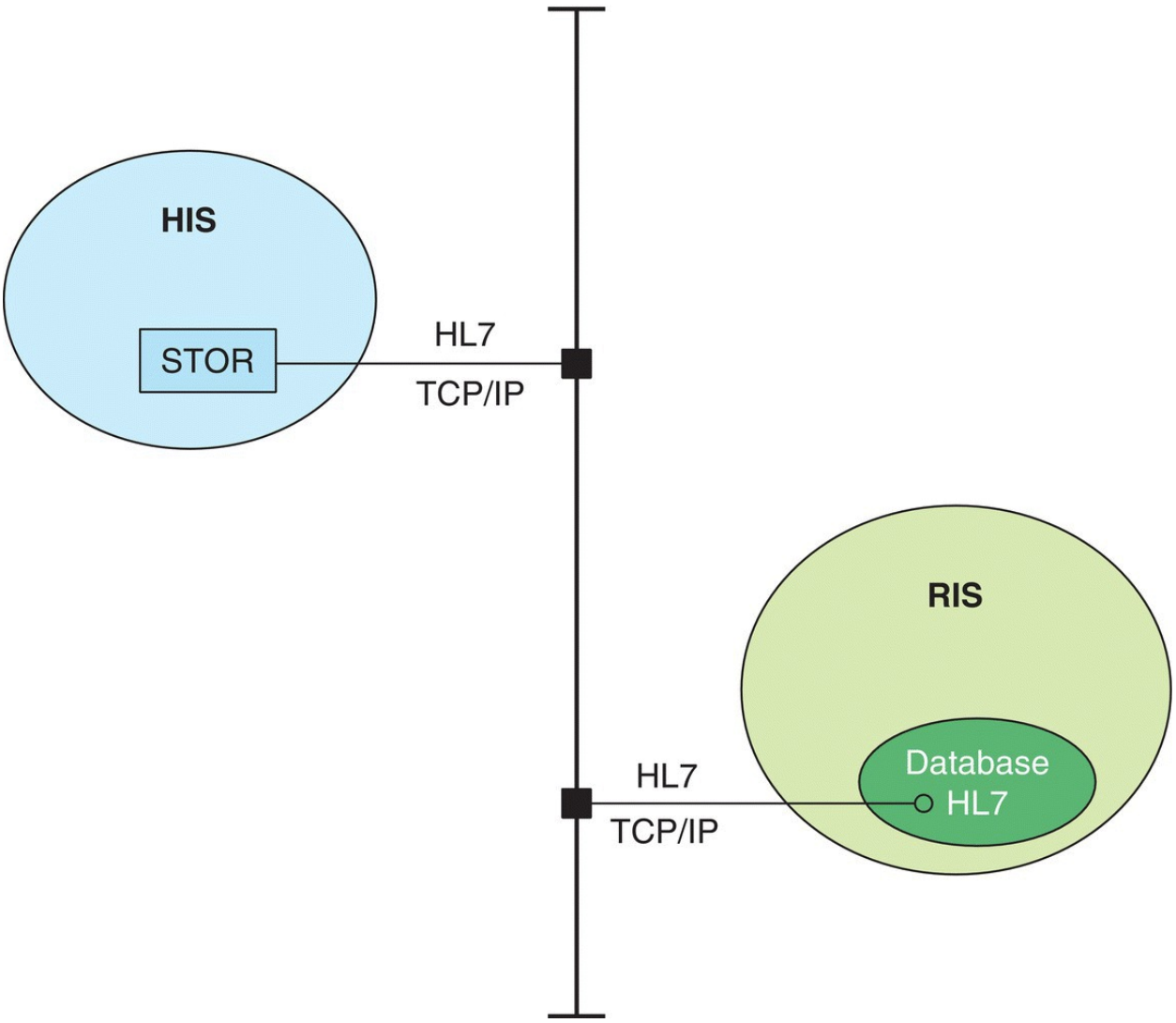

Figure 5.12 Database-to-database transfer using common data format (HL7) and communication protocol (TCP/IP). Data from HIS is accumulated periodically at STOR (see bottom, Figure 5.11) and broadcast to RIS.

5.8.3.2 Interface Engine

An interface engine provides a single interface and language to access distributed data in networked heterogeneous information systems. In operation, it appears that the user is operating on a single integrated database from their WS. In the interface engine, a query protocol is responsible for analyzing the requested information, identifying the required databases, fetching the data, assembling the results in a standard format, and presenting them at the requested WS. Ideally, all these processes are transparent to the user and carried out without affecting the autonomy of each database system. To build a universal

interface engine is not a simple task. Most currently available commercial interface engines are tailored to limited specific information systems. Figure 5.13 illustrates the concept of an interface engine for HIS, RIS, and PACS integration.

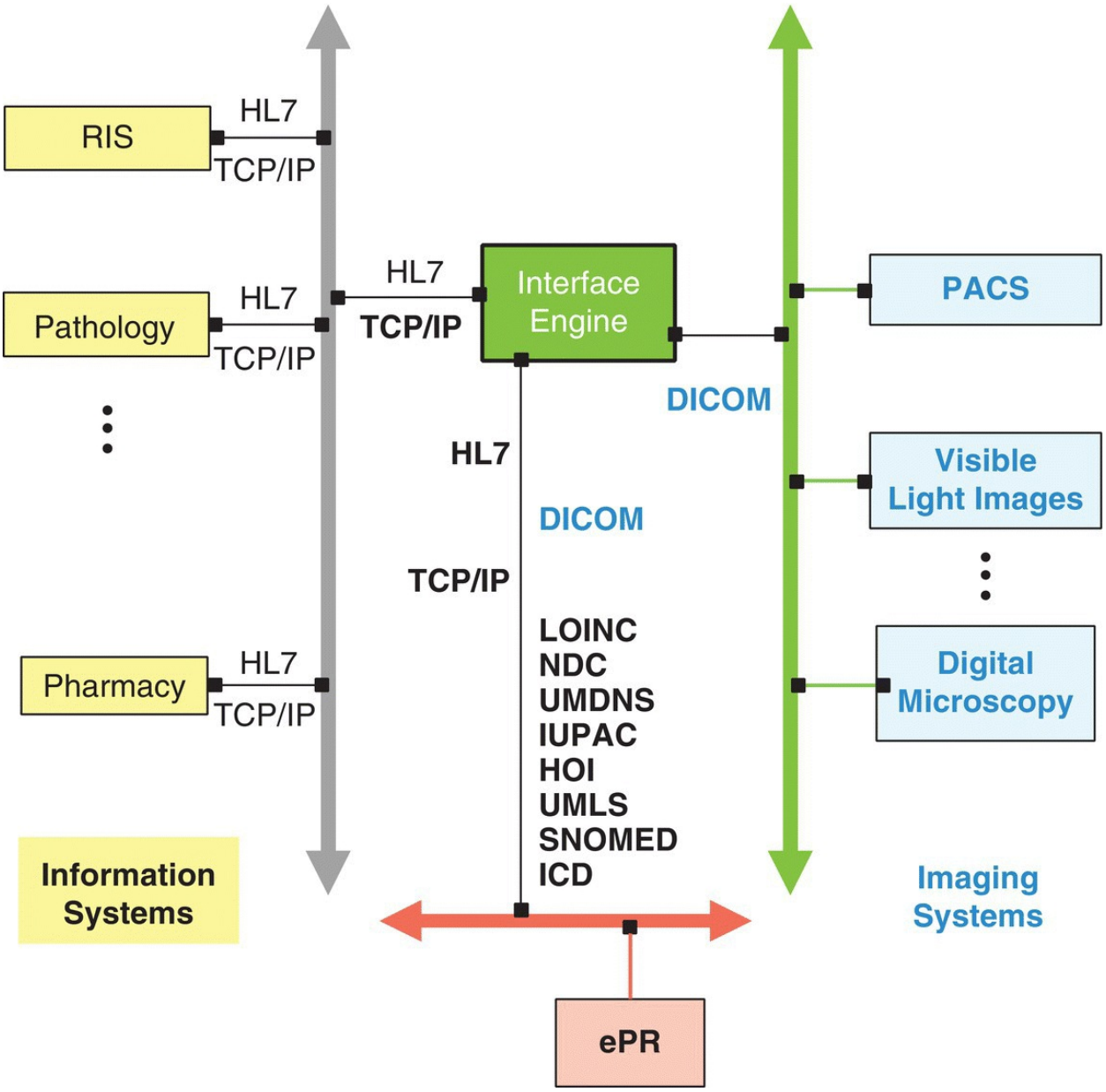

Figure 5.13 The principle of the interface engine. (Left) HL7 textual data; (right) DICOM image data; (bottom) Web-based electronic patient record system (Chapter 11) Electronic patient records (ePR), showing image and textual data, or messages and images. Message standards depicted are: LOINC: logical observation identifier names and codes; NDC: national drug codes; UMDNS: universal medical device nomenclature system; IUPAC: International Union of

Pure and Applied Chemistry; HOI: health outcomes institute; UMLS: unified medical language system; SNOMED: systemized nomenclature of medicine; ICD (ICD-9-CM): the *International Classification of Diseases*, 9th edition, Clinical Modification.

5.8.3.3 Rationale of Interfacing PACS with HIS and RIS

In a hospital environment, interfacing the PACS, RIS, and HIS has become necessary to manage data and patient workflow, PACS images, RIS administration, and research and training. To interface HIS, RIS, and PACS together, some guidelines are required:

1. Each system (HIS, RIS, PACS) remains unchanged in its configuration, data, and functions.
2. Each system is extended to both hardware and software, to allow each system to communicate with the other systems.
3. Only data are shared; functions remain local. For example, RIS functions cannot be performed at the PACS or at the HIS WS. Keeping each system specific and autonomous simplifies the interface process, because database updates are not allowed at a global level.

Following these guidelines, successfully interfacing HIS, RIS, and PACS requires the following steps:

1. Identify the subset data that will be shared by other systems. Set up access rights and authorization.
2. Convert the subset data to HL7 standard form. This step, consisting of designing a high-level presentation, solving data inconsistencies, and naming conventions, can be accomplished by using a common data model and data language and by defining rules of correspondence between various data definitions.
3. Define the protocol of data transfer (e.g. TCP/IP or DICOM).

5.8.3.4 Common Data in HIS, RIS and PACS

The system software in the PACS server and archive server, described in Chapter 15, Sections 5.2 to 5.6, requires certain data from HIS and RIS that are necessary for it to archive images and associated data in permanent storage, and distribute them to WSs correctly and in a timely fashion. Figure 5.14 illustrates data common to the HIS, RIS, and PACS. Table 5.1 describes data definition, the

origin and the destination, and the action that triggers the system software functions.

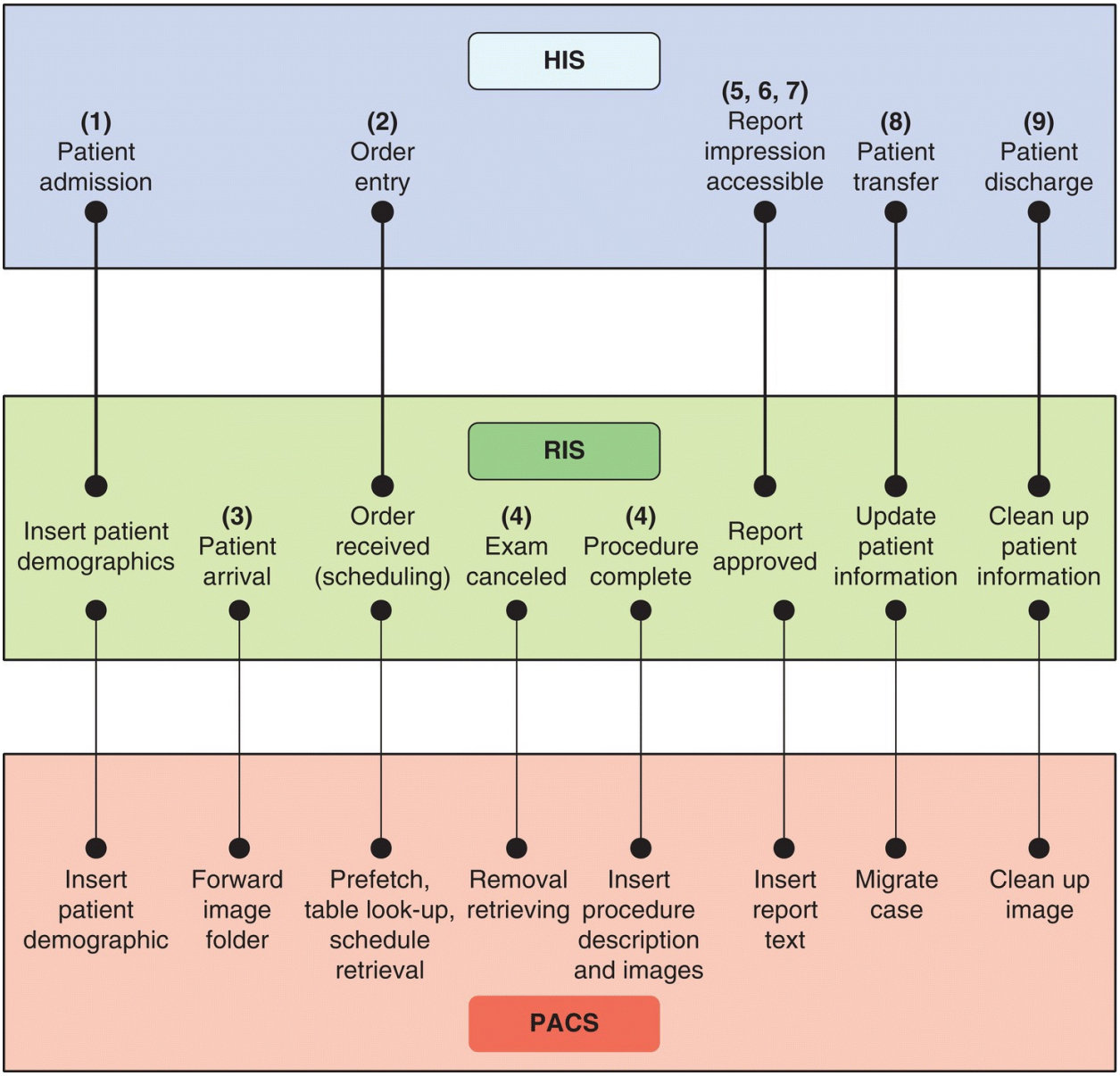

Figure 5.14 Information transfer between the HIS, RIS, and PACS. Numerals represent steps of information transfer explained in Table 5.1.

Table 5.1 Information transferred among HIS, RIS, and PACS triggered by the PACS server.

Events	Message	From	To	Action	Location
(1) Admission	Previous images/reports	HIS/RIS	PACS server	Preselect images and reports,	WS at FL, RR

				transfer from permanent archive to workstations (WS)	
(2) Order entry	Previous images/reports	RIS	PACS server, scanner	Check event (I) for completion	WS at FL, RR
(3) Arrival	PT arrival	RIS	PACS server, scanner	Check events (1) and (2) for completion	WS at FL, RR
(4) Examination complete	New images	Scanner	RIS, PACS server	New images to Folder Manager, WS	Temporary archive; WS at FL, RR
(5) Dictation	“Wet” reading	RR	Digital dictaphone	Dictation recorded on DD or VR, digital report to Folder Manager and to WS	DD or VR; WS at FL, RR
(6) Transcript	Preliminary report	RR	RIS, PACS Server	Preliminary report to RIS, temporary archive and to WS, dictation erased from DD	RIS; temporary archive; WS at FL, RR
(7) Signature	Final report	RR	RIS, PACS server	Final report to RIS, to WS, and to temporary archive. Prelim report erased.	RIS: temporary archive; WS at FL, RR
(8) Transfer	Patient transfer	HIS/RIS	PACS server	Transfer image files	WS at new location
(9) Discharge	Images, report	HIS/RIS	PACS server	Patient folder copied from	WS at FL, RR;

				temporary to permanent storage, patient folder erased from WS	temporary and permanent storage

5.8.3.5 Implementation of RIS–PACS Interface

The RIS–PACS interface can be implemented by either the trigger mechanisms or the query protocol described below.

5.8.3.5.1 Trigger Mechanism Between Two Databases

The PACS is notified of the following events in HL7 format when they occur in the RIS: ADT, order received, patient arrived, examination canceled, procedure completed, and report approved. The application level of the interface software waits for the occurrence of one of these events and triggers the corresponding data to be sent. The communication level transfers the HL7 file to the PACS server with the processes send (to PACS) and ris_recv. The PACS server receives this file and archives it in the database tables for subsequent use. Figure 5.15 shows the trigger mechanism interface. The trigger mechanism is used in a systematic and timely fashion when a small amount of predefined information from the RIS is required from the PACS. In addition to requiring additional storage allocation in both databases, this method is tedious for information updating and is not suitable for user queries.

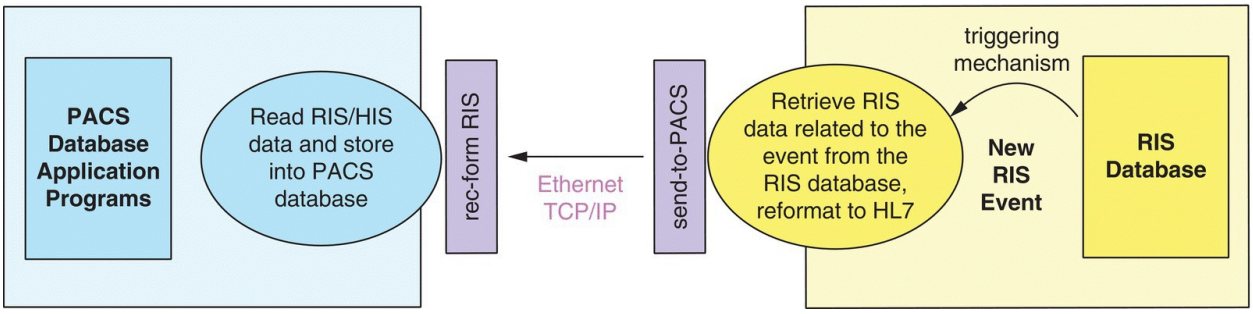

Figure 5.15 RIS–PACS interface architecture implemented with a database-to-database transfer using a trigger mechanism.

5.8.3.5.2 Query Protocol

The query protocol allows access to information from the HIS, RIS, and PACS databases by using an application-layer software on top of these heterogeneous database systems. From a PACS WS, users can retrieve information uniformly

from any of these systems and automatically integrate them to the PACS database. Figure 5.16 illustrates the query protocol. The DICOM Q/R service class described in Chapter 4, Section 4.5.2, is one method to implement such a query mechanism. The application-layer software utilizes the following standards:

- SQL as the global query language;
- a relational data model as the global data model;
- TCP/IP communication protocols; and
- HL7 data format.

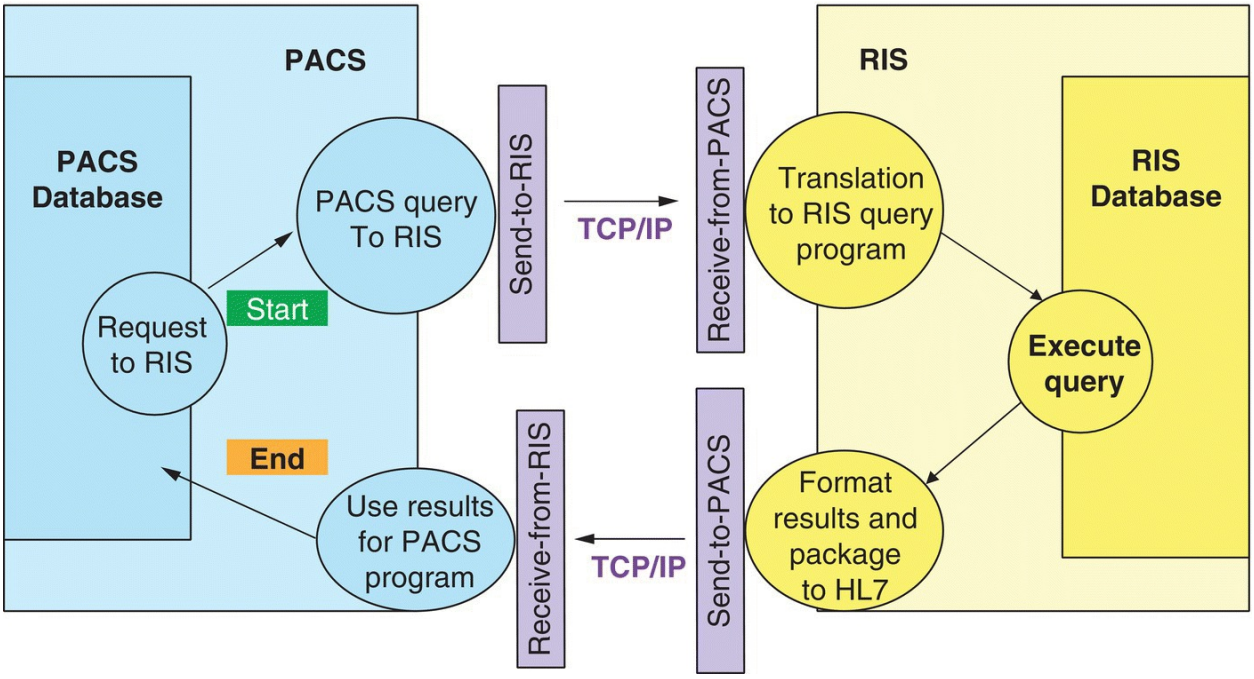

Figure 5.16 RIS–PACS interface with a query protocol. Start at green from left upper blue; PACS query RIS (top); RIS sends request through TCP/IP to RIS (right, yellow); RIS executes query, forwards results, packed and received by the PACS (bottom, blue).

5.8.3.6 An Example: The IHE (integrating the healthcare enterprise) Patient Information Reconciliation Profile

The hospital enterprise level IHE patient information (Chapter 4, Section 4.7) can be used to combine different data: ADT in HIS, RIS in radiology, and DICOM image management and archive in PACS. These combined data can be used to explain how the ePR workflow can benefit from the integration of HIS,

RIS, ePR, and PACS data. This integration profile can extend the scheduled workflow profile by providing the means to match images acquired for an unidentified patient with the patient's registration and order history. An example is a trauma case in which the patient examination and images had been obtained in the emergency room and then archived in the PACS HIS, RIS database, but without the patient ID. Once the patient's ID is identified, the patient information reconciliation profile can insert the patient's ID and allow it to subsequently reconcile to the patient database, as shown in Figure 5.17. Information systems involved in this integration profile are:

- enterprise-wide information systems (IHE) that manage patient registration and services ordering (ADT/registration system, HIS);
- radiology departmental information systems that manage department scheduling (RIS) and image management/archiving (PACS); and
- acquisition modalities.

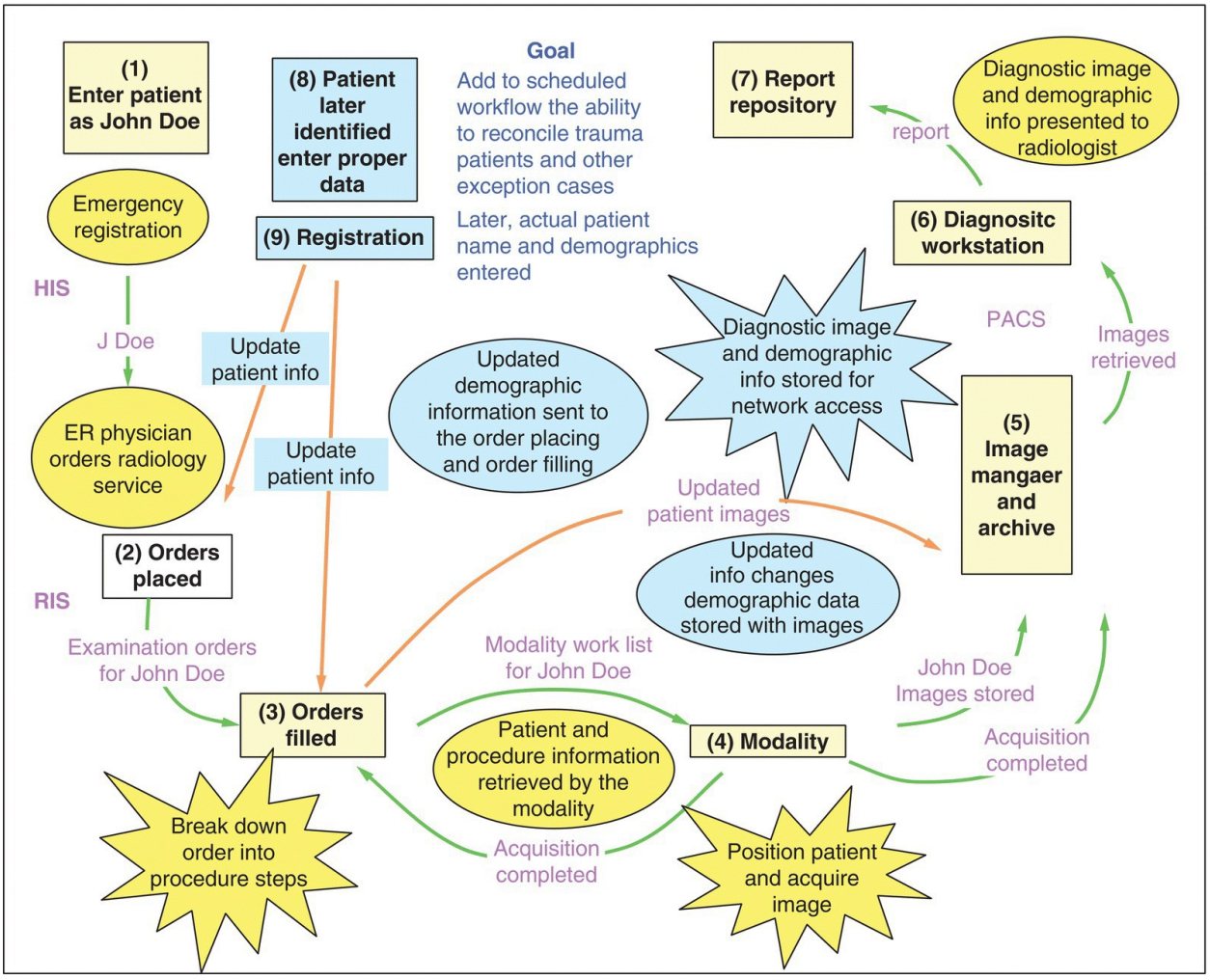

Figure 5.17 Enterprise-wide information systems (IHE) patient reconciliation workflow profile used as an example as the HIS–RIS–PACS interface. Step 1: Yellow boxes and green arrows: trauma patient examination without patient's ID. Step 2: Blue boxes and orange arrows: start at step 8, use the IHE workflow profile to reconcile trauma patient ID and demographic data when they become available.

References

1 Herrewynen, J. (2002) *Step-by-step integration. Decisions in Imaging Economics* (December 2002). Also: www.imagingeconomics.com/library/200212-13.asp

2 Huang, H.K. (1996) Towards the digital radiology department. *Eur J Radiol*, 22, 165.

3 Huang, H.K., Andriole, K., Bazzill, T., Lou, A.S.L. and Wong, A.W.K. (1996) Design and implementation of a picture archiving and communication system: The second time. *J Digital Imag*, 9(2), 47–59.

4 Huang, H.K., Wong, A.W.K., Lou, S.L., Bazzill, T.M., *et al*. (1996) Clinical experience with a second generation PACS. *J Digital Imag*, 9(4), 151–166.

5 Huang, H.K. (2001) PACS, informatics, and the neurosurgery command module. *J Mini Invasive Spinal Tech*, 1, 62–7.

6 Huang. H.K. (2003) Enterprise PACS and image distribution. *Comp Med Imag Graph*, 27(2–3), 241–53.

7 Huang, H.K. (2008) Utilization of medical imaging informatics and biometric technologies in healthcare delivery. *Intern J Comp Asst Rad Surg*, 3, 27–39.

8 Law. M. and Huang, H.K. Concept of a PACS and imaging informatics-based server for radiation therapy. *Comp Med Imag Graph*, 27, 1–9.

PERPUSTAKAAN PRIBADI AN-NUR SUNARYA

6
Web-Based Data Management and Image Distribution

CHAPTER MENU

6.1 Distributed Image File Server: PACS-Based Data Management
6.2 Distributed Image File Server
6.3 Web Server
6.3.1 Web Technology
6.3.2 Concept of the Web Server in PACS Environment
6.4 Component-based Web Server for Image Distribution and Display
6.4.1 Component Software Technologies
6.4.2 Architecture of Component-based Web Server
6.4.3 Data Flow of the Component-based Web Server
6.4.4 Component-based Architecture of the Display Workstation
6.5 Performance Evaluation
6.6 Summary of PACS Data Management and Web-based Image Distribution
Further Reading

6.1 Distributed Image File Server: PACS-Based Data Management

This chapter presents DICOM-based medical imaging informatics. For convenience, Figure 6.1, already delineated in previous chapters, is reiterated here to remind readers of the PACS data management integrated with the Web-based image distribution and display.

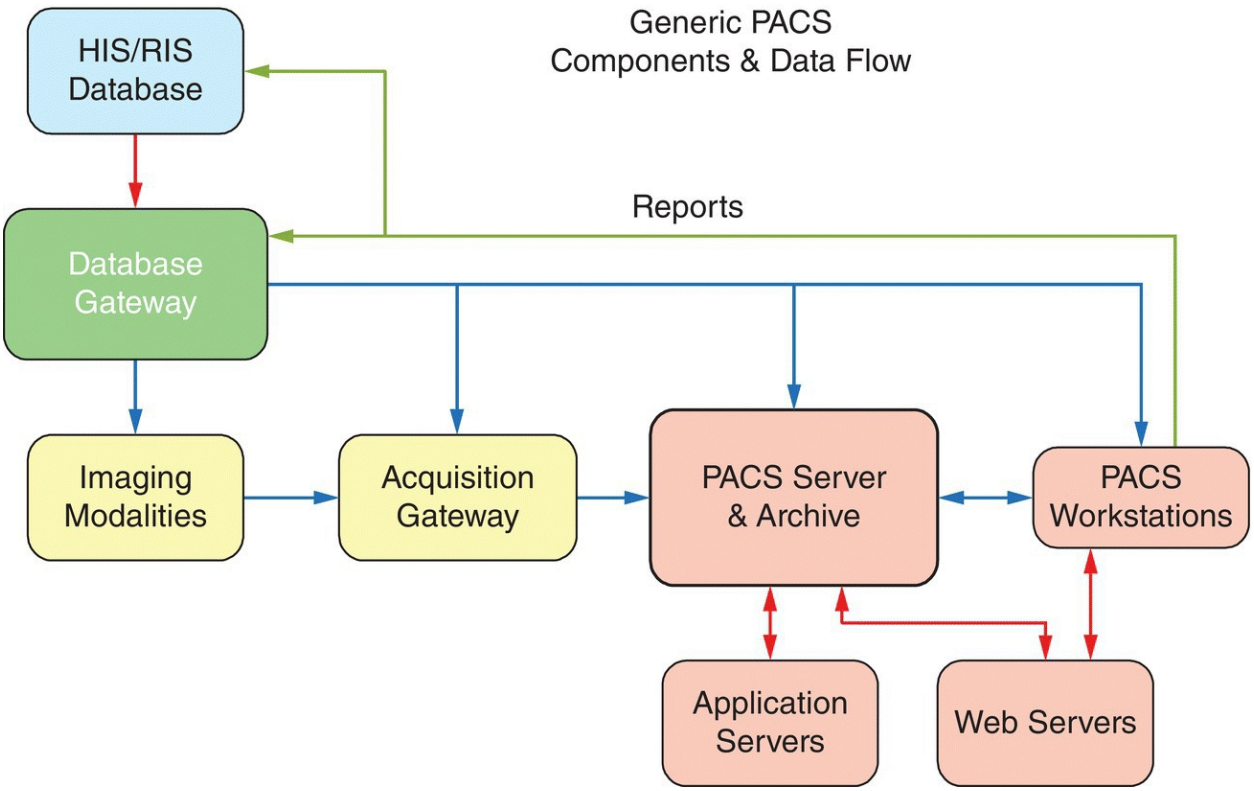

Figure 6.1 PACS data management and Web-based image distribution. PACS data management, patient folder management, Web-based server, and wireless remote control of clinical image workflows are related to the four pink color boxes in the PACS components and workflow with Web servers.

6.2 Distributed Image File Server

PACS was developed to meet the needs of image management in the radiology department. As the PACS concept evolved, the need for using PACS for other clinical applications increased. For this reason, the hospital-integrated PACS design includes distributed image file servers to provide integrated image and textual data for other clinical departments in the medical center and for the entire healthcare enterprise.

The PACS components and data flow shown in Figure 6.1 represent an open architecture design. The display component can accommodate many types of workstations (WSs). However, as the number of WSs (e.g. physician desktop WSs) increases, each with its own special applications and communication protocols, numerous queries and retrievals generated by the more active WSs will affect the performance of the PACS server. Under these circumstances, distributed image servers linked to the PACS server should be accounted for in

the PACS infrastructure to alleviate the workload of the server. For example, Figure 6.2 (gray floor), shows an extension of Figure 6.1, delineating a multiple-image server design connecting the PACS server to a particular physician's desktop computer. During the past 10 years, Web-based image distribution has become a standard and is useful for image distribution because of the easy-to-use Web technology, as well as the fact that its potential integration with ePR infrastructure is enormous. Section 6.3 discusses the Web-based image/data distribution concept, its infrastructure design, and applications.

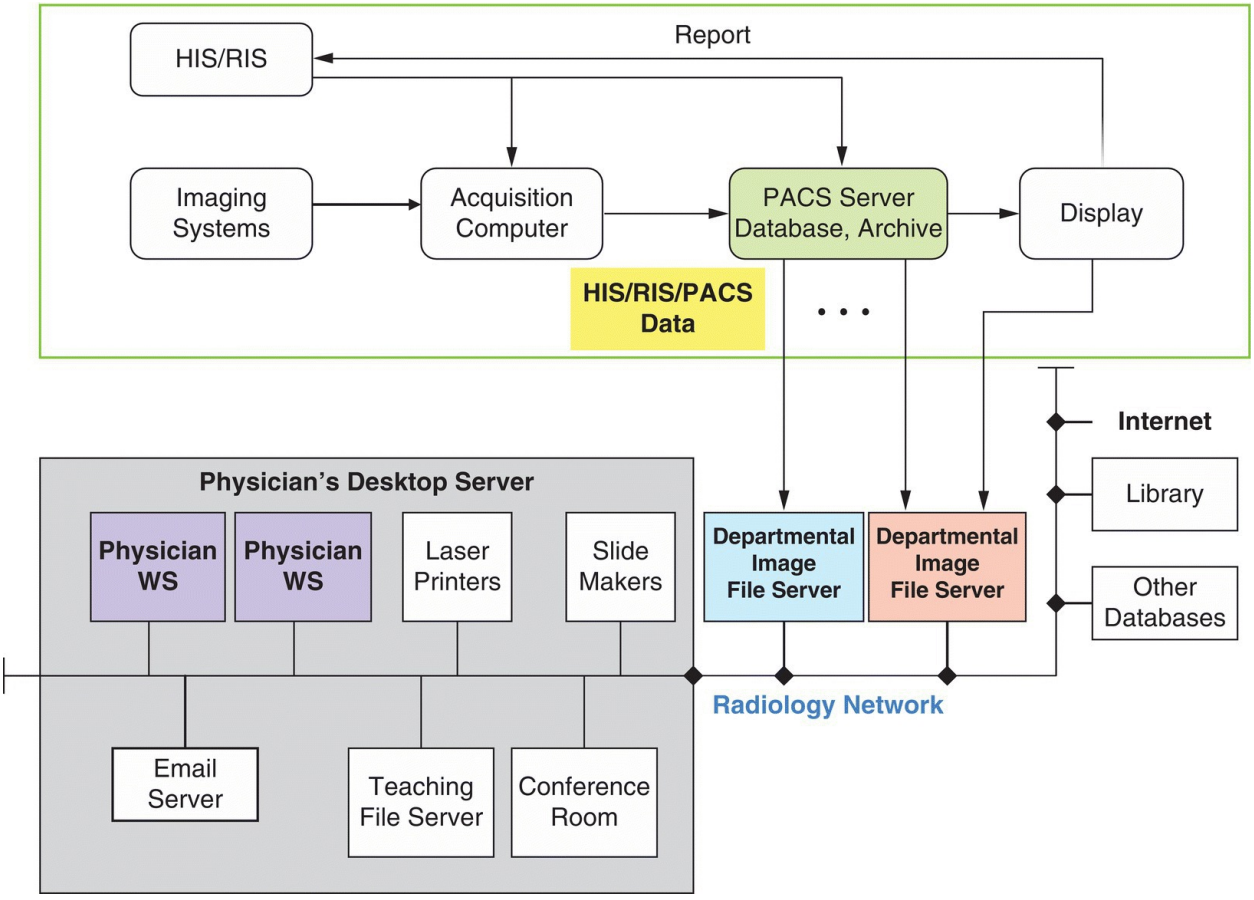

Figure 6.2 Several distributed image file servers connected to the PACS server. Each of these servers provides specific applications for a given cluster of users. For example, the physician desktop server WS; purple) are used as an illustration. The concept of the Web server is described in Figure 6.3.

6.3 Web Server

The previous subsection describes the concept of the distributed image file server, which provides easy access to PACS image/data for different

applications. In this subsection on the Web Server, an image file server design based on the World Wide Web technology allows easy access to PACS and informatics image/data for both inter- and intra-hospital DICOM-based medical imaging informatics applications.

6.3.1 Web Technology

This section first briefly reviews the development of Web technology over the past few years, followed by the presentation of a Web-based image file server for PACS-based informatics application.

The Internet was developed by the US government originally for military applications. Through the years, its use was extended to many other applications. The Internet can be loosely defined as a set of computers connected by various wiring methods, which through transmission control protocol/Internet protocol (TCP/IP) transmit information to each other using a public communication network. The Intranet, on the other hand, is a private Internet that transmits information within an administrative entity through a secured network environment. The World Wide Web is a collection of Internet protocols that provide easy access to many large databases through Internet connections.

The Web is based on the hypertext transfer protocol (HTTP), which supports the transmission of hypertext documents on all computers accessible through the Internet. The two most popular languages used for Web applications, which allow for the display of formatted multimedia documents independent of the computers used, are the hypertext markup language (HTML) and Java language (just another vague acronym; Sun Microsystems, Mountain View, CA). Currently, the extensible markup language (XML) has been used extensively for image and text standards. Nowadays, most Web browsers, such as Microsoft's Internet Explorer and Netscape Navigator, support JPEG (Joint Photo-graphics Experts Group; 24 bits for color images) or graphics interchange format, GIF; 8 bits) for image rendering. Although PNG is good for storing line drawings, text, and iconic graphics at a small file size, it is not convenient to be used for large scale medical imaging applications.

In Web terminology, there is the Web server and clients (or sites, or browsers). The Web site uses trigger processes to access information from the Web server through the HTTP. For the past few years, applications of Web technology have been extended to healthcare information applications. Some Web sites now support access to textual information from ePR systems. These Web-based systems can be categorized according to their characteristics, such as

completeness and detail of the information model, methods of coupling between the Web-based and legacy hospital information systems, quality of the data, and the degree of customization.

The use of the Web server as a means to access PACS image/data has been implemented by academic centers, medical imaging manufacturers, and network companies. In the next section, the design of a Web-based image file server is discussed for the PACS-based medical imaging informatics environment, as a means to access PACS image/data both intra- and inter-hospital, and their users' applications.

6.3.2 Concept of the Web Server in PACS Environment

Consider a Web-based image file server, as shown in Figure 6.3. It must:

1. support Web browsers connected through the Internet;
2. allow interpretation of queries from the browser written in HTML or Java and convert the queries to DICOM and HL7 standards;
3. support DICOM query and retrieve (Q/R) service–object pair (SOP) to query and retrieve image/data from the PACS server; and
4. provide a translator to convert DICOM images and HL7 text to HTTP.

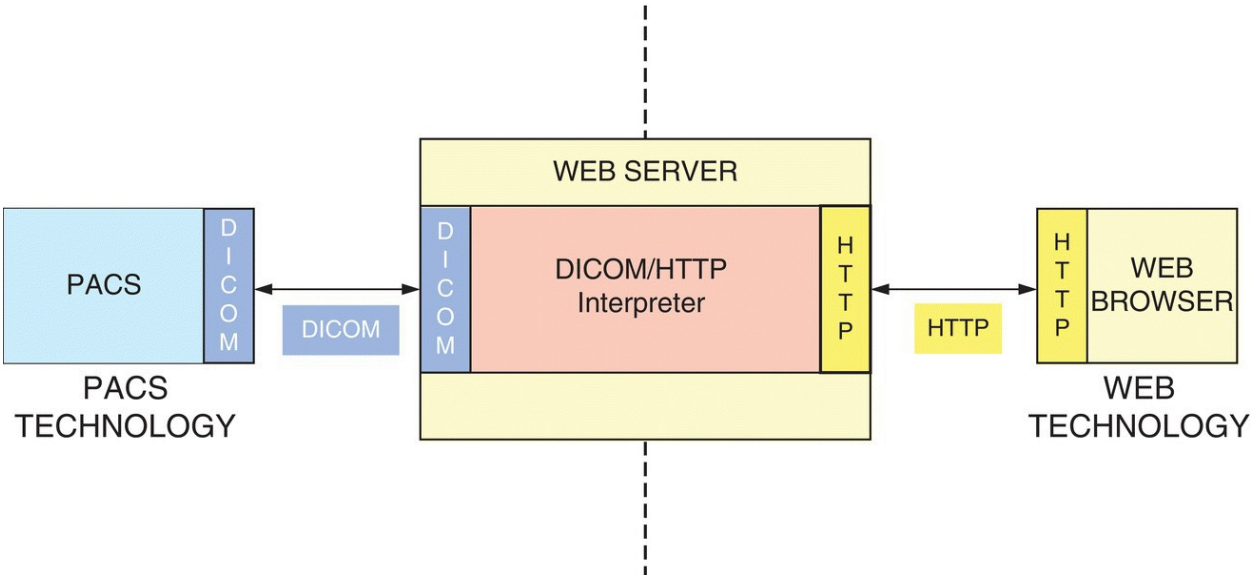

Figure 6.3 Basic architecture of a Web server allowing Web browsers to query and retrieve image/data from PACS through the Web-based server. The DICOM/HTTP interpreter is the key component.

Figure 6.3 shows the basic architecture of a Web server allowing Web browsers to query and retrieve PACS image/data. Figure 6.4 illustrates the eight basic steps involved in a typical Q/R session from the Web browser to the Web server for image/data stored in the PACS server and archive system. Note that in step 8 (Figure 6.4), the image forwarder can only return 8 bits/pixel, which is not the full resolution of DICOM images. In order to obtain a 12 bits/pixel full DICOM image resolution, it is necessary to use the component-based technology, which is discussed in Section 6.4.

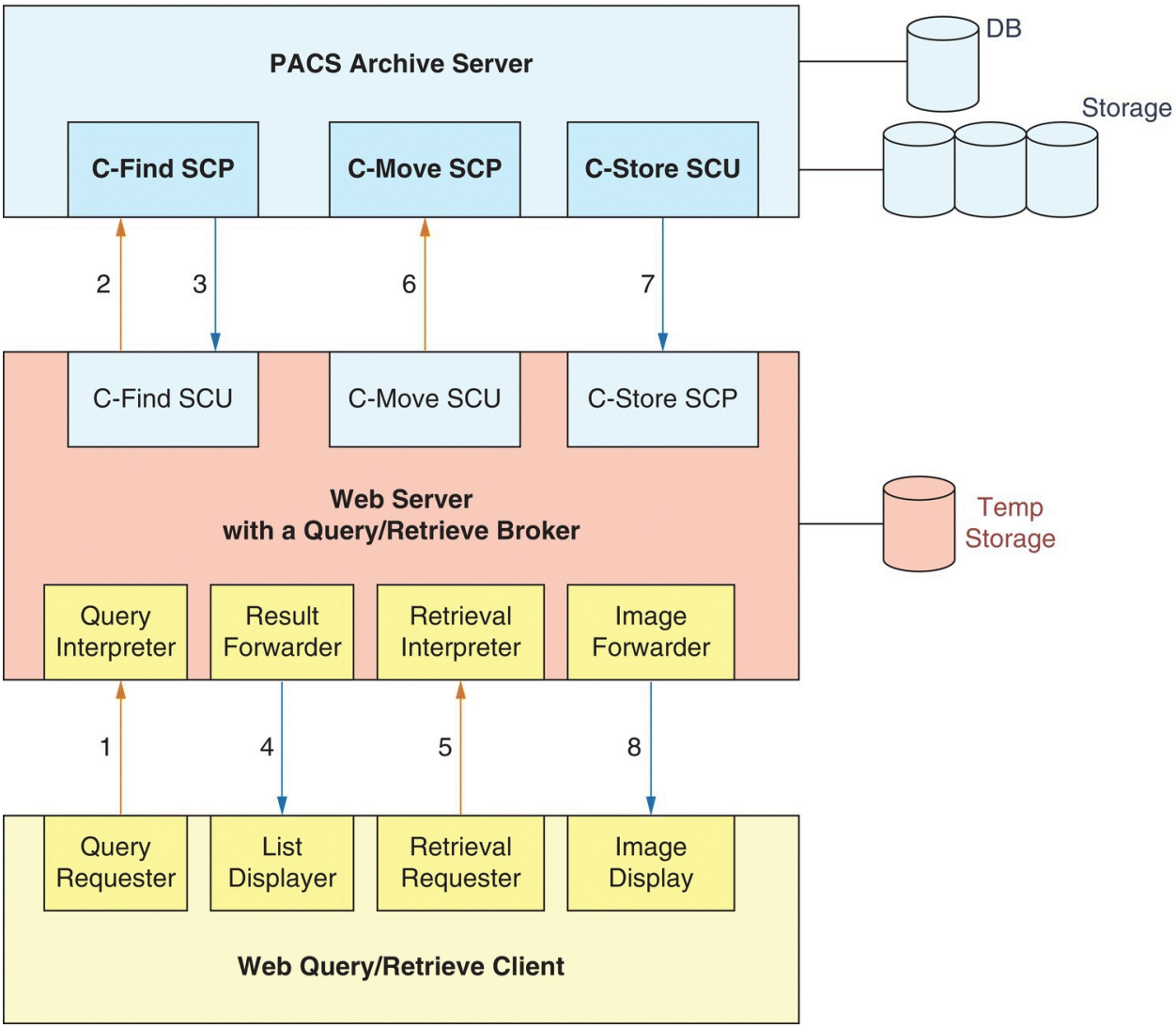

Figure 6.4 Typical query/retrieval session from the Web browser through the Web server, requesting images and related data from the PACS server. The session requires eight steps involving both Web (yellow) and PACS (blue) technologies. The resources required in the Web server (Figure 6.3) for such a session are detailed in the Web broker (middle, orange).

The Web server is an elegant concept utilizing existing Internet technology available in everybody's desktop computer to access PACS image/data. It works very well in Intranet environments, because most Intranets now use well-designed high-speed gigabit Ethernet switches, which have sufficient bandwidth for medical image transmission. However, there are certain drawbacks in using the current Internet for WAN applications, for two reasons. First, the response time for image transmission from the Internet is normally too slow, because of the constraint of the conventional WAN speed. As a result, it is useful only if the number and size of images retrieved are both small, or to use the in-house gigabit transfer rate, which is becoming much faster and cheaper to use now. Another drawback is that Web technology is not designed for high-resolution gray-scale image display, especially when a real-time look-up table operation is required. In this case, the waiting time for image display and manipulation would be too long to be acceptable. In the next section, an example of a Web-based image distribution in the clinical DICOM-based environment is discussed.

6.4 Component-based Web Server for Image Distribution and Display

This section discusses a component-based Web server for multimedia imaging informatics. This method, combining both Web and PACS technologies, can preserve the original 12 bits/pixel medical image quality and display the full-resolution DICOM images on Web client WSs using a display and processing software component.

6.4.1 Component Software Technologies

Traditional software development requires an application executable to be compiled and linked to their dependencies. Every time a software developer wishes to use different processing logics or new capabilities, it must modify and re-compile the primary application to support them. As a result, it requires additional resources for software development, which inhibits fast turnaround time of the product and costs more. Component software technologies, now widely used in current software engineering, especially in enterprise-level software development, were introduced into software development to alleviate these problems. Component technologies usually consist of two parts: the component software architecture and the component software itself.

The component software architecture is a static framework or skeleton (structure

or set of conventions) that provides the foundation for the component software to build on. The architecture defines how the parts relate to each other, including constraints governing how they can relate. The software components are generally any software (or subsystems) that can be factored out and has the potential for standardizing or reusing exposed interface. Such systems generally use their interfaces (importing/exporting) to provide special functions and services or to interact with other components or software modules.

Three component software technologies are used widely: Common Object Request Broker Architecture (CORBA@ BASIC); the JavaBeans (Java); and the Component Object Model (COM), or Active X www.Microsoft.com/technet. The latter two are best supported and more often used in Microsoft Windows platforms, such as Windows 98, Windows 10 and 11, Windows 2000, or XP.

6.4.2 Architecture of Component-based Web Server

Consider a Web-based PACS image/data distribution server based on the component architecture and the DP (display and processing) component, described in Section 6.4.4. The XML is used for text messages exchanged between the browsers and web server. Other standard components are the Microsoft Internet Information Server (IIS) as the Web server; Internet Explorer (5.0 or higher) with Microsoft Edge as the default browser supported by the component-based Web server, and the Active X Plug-in Pro from Ncompass. Figure 6.5 shows the component-based Web server architecture (see also Figure 6.3 for the general PACS–Web interface). In this architecture, the image processing and manipulation functions are moved to the browser side during the image viewing (Figure 6.3, right; see Section 6.4.4). The active server page (ASP) objects, as Web-accessing interfacing objects, bridge the components distributed in the Web server (DICOM services and image database) and the browser display and processing (DP) component, and make them interoperate with each other.

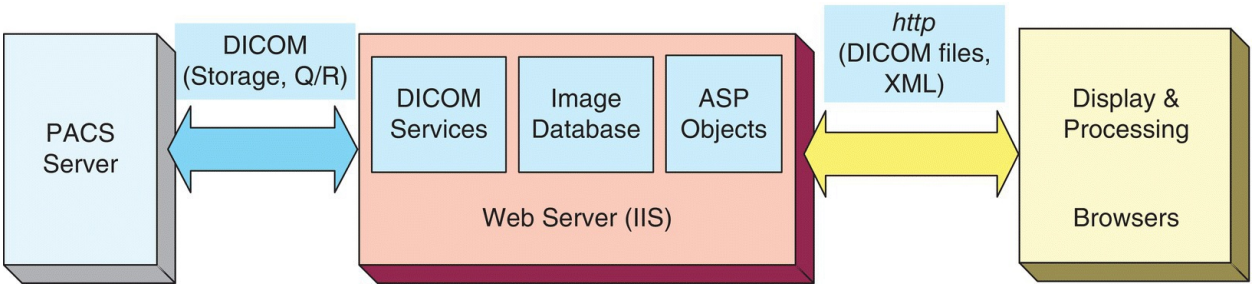

Figure 6.5 Architecture of the component-based Web server for image/data

distribution and display (Zhang *et al*., 2003). IIS: Microsoft Internet information server; ASP: active server pages. The concept is moving the image processing and manipulation objects to the browser during viewing. Blue: DICOM technology; yellow: Web technology.

6.4.3 Data Flow of the Component-based Web Server

The Active X control component of display and processing first resides in the Web server as a cabinet file. It can be downloaded to any browser to access images in the Web server and registers as a plug-in object in the client computer. A client can use a browser the first time to access the web pages containing ASP objects in the Web server. Later, the user can display and process DICOM images managed by the Web server in the same way as in a component-based diagnostic WS (Section 6.4.4).

6.4.3.1 Query/Retrieve DICOM Image/Data resided in the Web Server

When the user wants to use the browser to access DICOM images managed by the image database in the Web server (Figure 6.5, middle), the browser sends the HTTP request to the Web server using a multipurpose internet mail extension (MIME) message (XML format, encoded by the processing component). The Web server decodes the XML-formatted message, queries its local database with SQL based on the content of the XML message, compiles the queried results (including patient/study/series/image/files information) to XML format, and sends the HTTP response with the XML-formatted MIME message to the browser.

The browser then requests the Web server (Figure 6.5, right) to send the DICOM files, pointed by the uniform resource locator (URL) in the request message, to the browser, based on the user selection from the patient list. The Web server decodes the XML message sent from the browser and uploads the DICOM files to the browser through the HTTP response, in which the type and content of the MIME message are the binary and DICOM files. The browser or DP component receives the DICOM files, decodes the files, and displays the images. Note that the full resolution of the image pixel is preserved and this guarantees that the user can manipulate the images in the same way as in a single-monitor diagnostic WS.

6.4.3.2 Query/Retrieve DICOM Image/Data resided in the PACS Archive Server

Users can also query and retrieve the DICOM images stored in the PACS archiving server by using the browser. The operation and the communications between the browser and Web server for PACS image Q/R are similar to those of the Web server image. However, the interoperation between the Web server and PACS server is through DICOM services. For example, when the XML formats the query message sent from a client browser and received by the Web server, the message is then posted to the component of the DICOM communication service, and converted to a DICOM query object and sent to the PACS server through the DICOM C-Find service by the DICOM component. When the DICOM component receives the queried result from the PACS server, it converts it to an XML message, and sends the XML message to the browser through the Web server.

For the retrieval operation, the data flow is similar to that of the query, but the DICOM communication services between the Web server and the PACS server are C-Move and C-Store. Figure 6.6 shows the data flow of the Q/R operation between the browser, the Web server, and the PACS server. In Figure 6.6, (1)–(1)'–(1)" denotes the query procedure, and (2)–(2)'–(2)"–(3)"–(3)'–(3) denotes the retrieval procedure.

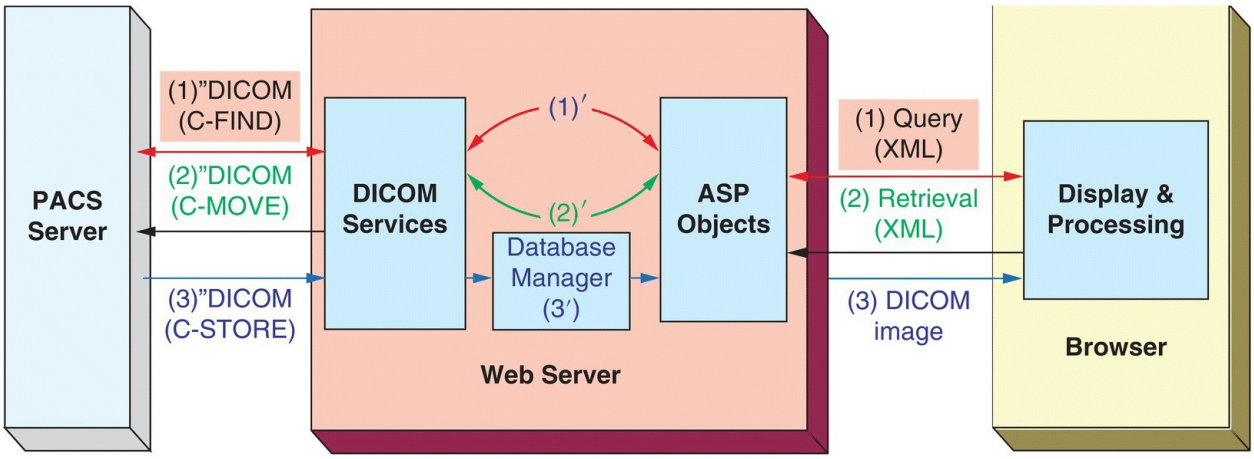

Figure 6.6 Data flow of the query/retrieve operation in the component-based Web server, which preserves the 12 bits/pixel DICOM image in the browser. The DICOM images can be displayed with their full resolution by the display and processing component in the browser. Numerals are the workflow steps. Blue: PACS technology; yellow: Web technology; pink: processing component objects (Zhang *et al.*). (1)–(1)'–(1)": query; (2)–(2)'–(2)"–(3)"–(3)"–(3): retrieve.

There is certain similarity in the Q/R operation by the browser using the DICOM protocol and format and that using the Web protocol and format. The difference

is that (described in Section 6.4) 12 bits/pixel is preserved, whereas in the Section 6.3, the Web image format only allows 8 bits/pixel (Figure 6.4), where step 8 can only return 8 bits/pixel, because of the Web component technologies being used.

6.4.4 Component-based Architecture of the Display Workstation

The purpose of the component-based workstation (WS) is to augment Web-based technologies for displaying and processing full-resolution (12 bits) DICOM images, which the standard Web-based technology cannot do. The component software architecture of the Web-based WS consists of four components:

1. DICOM communication component;
2. image database component;
3. image processing, and display component; and
4. graphic user interface (GUI) component.

All these components are integrated into one computer with image cache memory and hard disks, as well as a powerful central processing unit(CPU) with high-speed network interface. They are interoperated through the standardized or privately defined component interfaces, as shown in Figure 6.7.

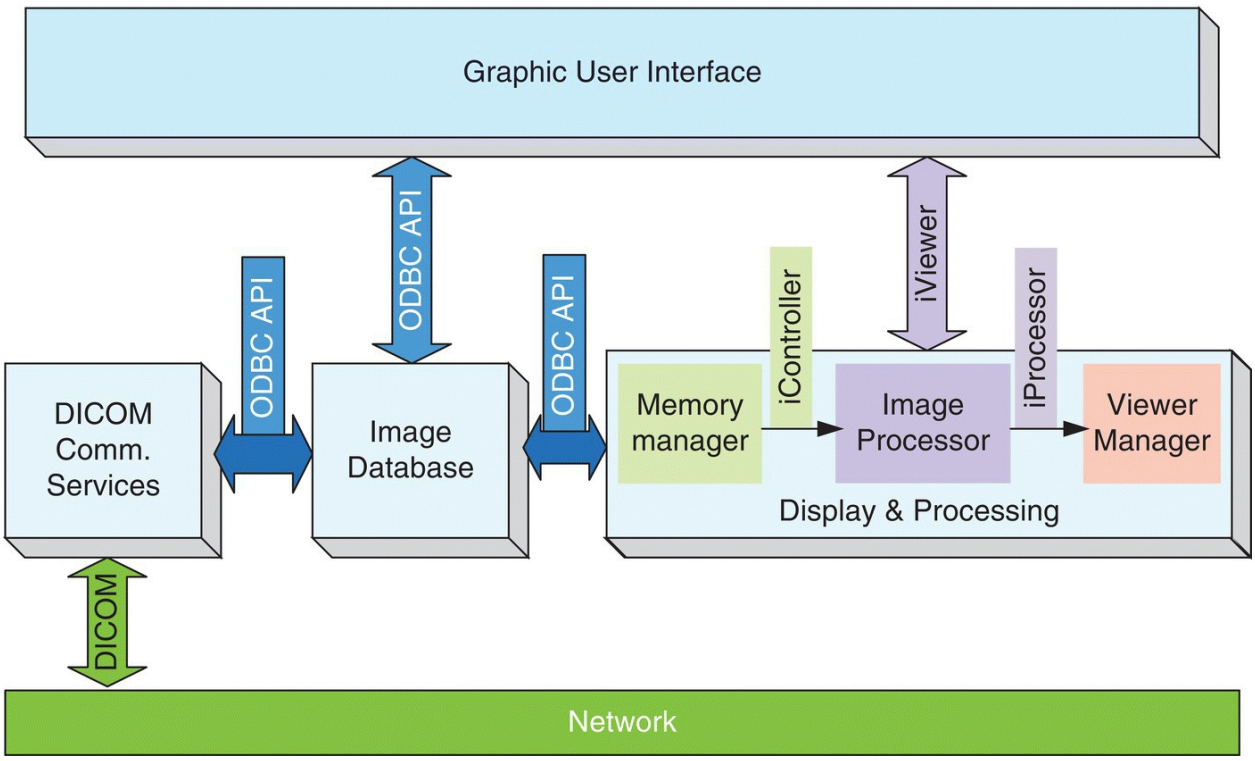

Figure 6.7 Component architecture of a diagnostic WS for display and to process DICOM images in a Web-based server. iViewer, iProcessor, and iController are image processing and display interfaces software (Zhang *et al.*). API: application program interface; ODBC: open database connectivity.

An example is given here to show a component-based diagnostic display WS based on the active template library (ATL) to develop the components of DICOM communication services, and image database and Microsoft foundation classes (MFC) to develop the components of GUI and the key component of display and processing. The standardized interfaces used in the WS are DICOM and open database connectivity (ODBC)compliant. The three software programs: iViewer, iProcessor, and iController, are for image processing and display interfaces.

There are three kinds of object arrays and one memory bulk object inside the component of display and processing (DP):

1. the array of processing objects;
2. the array of viewing objects; and
3. the array of window objects; the bulk memory storing image objects is managed by the memory manager.

The interoperation and data exchanges between these object arrays are done through the interfaces of iController, iProcessor, and iViewer, shown in Figure 6.8. There is also a message queue that collects the messages generated from different windows and dispatches them to the proper image processing pipelines, which are formed by the three objects of processing, viewing, and window.

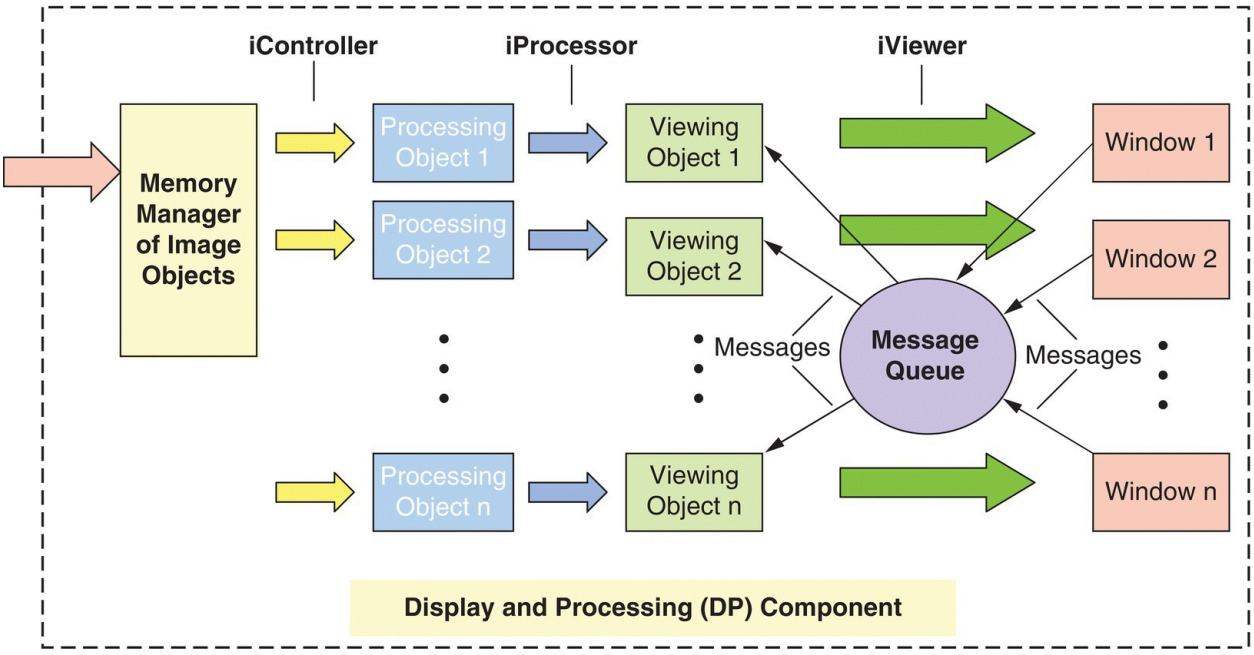

Figure 6.8 Workflow of the display and processing (DP) component in a Web-based server for display and processing of DICOM images (Zhang *et al*.).

Internally, the display and processing (DP) component creates an event-driven window environment to let users use different input devices, such as mouse and keyboard, to manipulate the images displayed and processed through the windows and pipelines in the component with multi-threading processing capability. Because the window objects inside the component can be attached to different display devices through the proper software run-time configuration, this component-based display architecture can be implemented in different display systems.

The DP component uses the Active X control component technology. This component can perform all major display functions found in a PACS diagnostic WS and supports multi-monitor display systems. It also can be reused in different Windows platforms and applications. The DP component can be plugged into any Web browser to interact with the component-based Web server, described in previous sections, to display and manipulate DICOM images.

6.5 Performance Evaluation

Because the browser's DP component preserves full-resolution DICOM images and provides most required diagnostic functions, the client WS can be treated as a regular PACS WS for both diagnosis and review, except that the Q/R images are through the Web-based technology. When this technology was introduced in 2002 and 2003, the question raised was: How would such a DP component in the client's browser built on top of the web-based technology perform in terms of image loading and display time compared with that of a standard web client display? Two experiments were performed 10 years ago (Zhang *et al.*, 2003), with results shown in Figure 6.9. The experiments used two workstations, one with a standard PACS diagnostic WS and the other a component-based Web display system. Both used the same DP component with 100 Mbits/s Ethernet connected to gigabyte Ethernet switch under a controlled research environment.

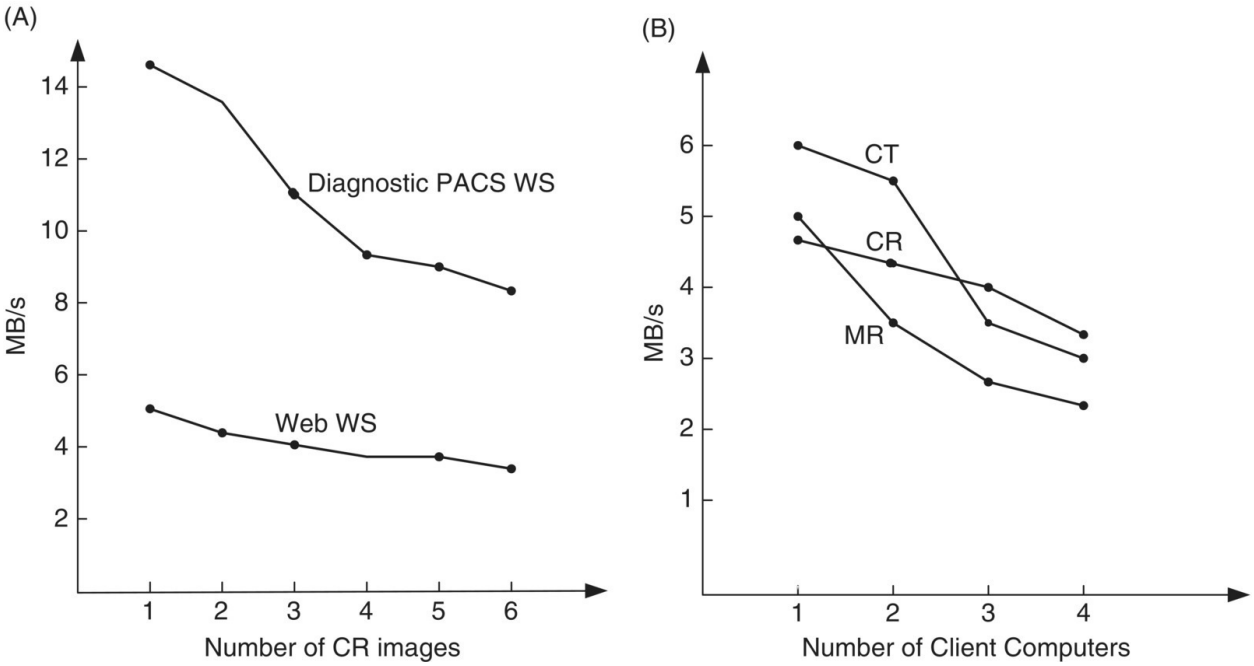

Figure 6.9 (A) Comparison of the averaged speeds of image loading and display from one to six CR images between a PACS diagnostic WS and a web server distributing images to one client. (B) Averaged speeds of distributing different modality images (CT, MRI, CR) from the Web server to one to four clients. All clients requested the web server at the same time. MB/s: megabytes per second (Zhang *et al.*).

Figure 6.9A shows the loading and display speed of one to six CR images to both the web and the PACS diagnostic WSs. Figure 6.9B depicts the loading and

display speed for the web server to distribute different modality images (CT, CR, MRI) to one to four clients.

From Figure 6.9A it can be seen that the speed of image loading and display in the diagnostic WS was reduced from 15 MB/s to 8 MB/s with more CR images selected. On the other hand, the speed of image loading and display from the Web server to the Web clients remained at 4 MB/s, with only a slight decrease. Figure 6.9B allows two interesting observations. One is that the shapes of the speed curves, which slope downward in the loading and displaying of different modality images with an increasing number of clients, are almost the same, and that these shapes are somewhat close to those measured from the diagnostic display WS shown in Figure 6.9A. The second observation is that the loading speeds of the CT and MR images drop a little faster than that of the CR images. These results can be used to estimate the performance of image loading and display between the PACS WS and the Web WS with full DICOM viewing capability. For details of the explanation, see Zhang *et al*., 2003.

Currently, there are two general models used in radiology departments: one is organ-based, and the other is modality-based. For an organ-based radiology operation, the store-forward image delivery method is often used, but for modality-based radiology departments, the query-retrieval method is preferred to obtain images from PACS.

As the Web technology and the speed of Intra- and Internet transmission have improved tremendously during the past 10 years, Web technology is going to remain in PACS-based multimedia imaging informatics applications.

6.6 Summary of PACS Data Management and Web-based Image Distribution

This chapter started with Sections 6.1 and 6.2, Distributed Image File Server, from PACS-based data management to Web-based image distribution. Five major topics were covered: PACS data management, distributed image file server, Web server, component-based Web server for image distribution and display, and Web workstation performance evaluation.

Further Reading

Andrade R, Wangenheim A, Bortoluzzi MK. Wireless and PDA: a novel strategy

to access DICOM-compliant medical data on mobile devices. Int J Med Inform 71(2–3): 157–163; 2003 [Section 3].

Bosak J. (1997) XML, Java, and the future of the Web. World Wide Web J., 2, 4, 219–227.http://www.ibiblio.org/pub/sun-info/standards/xml/why/xmlapps.htm. [Section 3.1]

Cao X, Hoo KS, Zhang H, et al. Web-based multimedia information retrieval for clinical application research, SPIE Proc 4323: 350–358; 2001. [Section 4].

Cedara, I. View. http://www.cedara.com/ (accessed 13 March 2018).

CORBA® BASICS. http://www.omg.org/gettingstarted/corbafaq.htm (accessed 13 March 2018).

Datcard PACScube. http://www.datcard.com (accessed 13 March 2018).

Huang HK, Wong WK, Lou SL, et al. Clinical experience with second-generation hospitalintegrated picture archiving and communication system. J Digit Imag 9: 151–166; 1996.

Huang HK. Display Workstation In: PACS basic principles and applications New York: Wiley-Liss Press; 1999.

Huang HK, Huang C. Internet 2. Adv. Imaging Oncol. Adm. (October): 52–58; 2003.

Huang HK, Cao F, Liu BJ, et al. Fault-tolerant PACS server design. SPIE Med. Imaging 4323–14: 83–92; 2001.

Java component architecture. http://java.sun.com/products/javabeans/ (accessed 13 March 2018).

Kim Y, Horii SC Handbook of Medical Imaging Vol. 3: Display and PACS. Bellingham, WA: SPIE Press; 2000.

Liu BJ, Huang HK, Cao F, et al. Clinical experiences with an ASP model backup archive for PACS image. Radiology 225(P): 313; 2002.

Liu BJ, Huang HK, Cao F, et al. A complete continuous-availability (CA) PACS archive server solution. RadioGraphics 24: 1203–1209; 2004.

Liu BJ, Chao S, Documet J, et al. Implementation of an ASP model offsite backup archive for clinical images utilizing Internet 2. SPIE Med. Imaging 5748:

224–231; 2005.

Moore, L., Richardson, B.R., and Williams, R.W. (2002). The USU medical PDA initiative: the PDA as an educational tool. Proceedings of AMIA Symposium. pp. 528–532.

NCompass ActiveX Plugin Proc. http://www.ncompasslabs.com/ (accessed 13 March 2018).

Ratib O, McCoy M, McGill R, Li M, Brown A. Use of personal digital assistants for retrieval ofmedical images and data on high-resolution flat panel displays. RadioGraphics 23(1): 267–272; 2003.

Sakusabe T, Kimura M, Onogi Y. On-demand server-side image processing for Web-based DICOM image display. SPIE Proc. 3976: 359–367; 2000.

Siemens PACS. http://www.medical.siemens.com (accessed 13 March 2018).

Yaghmai V, Salehi SA, Kuppuswami S, Berlin JW. Rapid wireless transmission of head CT images to a personal digital assistant for remote consultation. Acad. Radiol. 11(11): 1291–1293; 2004.

Zhang J, Stahl JN, Huang HK, et al. Real-time teleconsultation with high resolution and large volume medical images for collaborative health care. IEEE Trans. Inf. Technol. Biomed. 4: 178–186; 2000.

Zhang J, Zhou Z, Zhuang J, et al. Design and implementation of picture archiving and communication system in Huadong Hospital. SPIE Proc. 4323: 73–82; 2001.

Zhang J, Sun J, Stahl JN. PACS and Web-based image distribution and display. Comput. Med. Imaging Graph. 27(2–3): 197–206; 2003.

7
Medical Image Sharing for Collaborative Healthcare Based on IHE XDS-I Profile

CHAPTER MENU

7.1 Introduction

7.2 Brief Description of IHE XDS/XDS-I Profiles

7.3 Pilot Studies of Medical Image Sharing and Exchanging for a Variety of Healthcare Services

7.3.1 Pilot Study 1: Image Sharing for Cross-Enterprise Healthcare with Federated Integration

7.3.2 Pilot Study 2: XDS-I-Based Patient-Controlled Image Sharing Solution

7.3.3 Pilot Study 3: Collaborative Imaging Diagnosis with Electronic Healthcare Record Integration in Regional Healthcare

7.4 Results

7.4.1 Pilot Study 1: Image Sharing for Cross-Enterprise Healthcare with Federated Integration

7.4.2 Pilot Study 2: XDS-I-Based Patient-Controlled Image Sharing Solution

7.4.3 Pilot Study 3: Collaborative Imaging Diagnosis with Electronic Healthcare Record Integration in Regional Healthcare

7.5 Discussion

7.5.1 Comparisons of Three Pilot Studies

7.5.2 Security Issues

7.5.3 Performance and Storage

7.5.4 Extension of XDS-I Profile-Based Image Sharing

Acknowledgements

References

PACS, digital reporting, and informatics were originally developed for radiology application to replace film and paper tools. During the past 30 years, these technologies have been integrated and progressed to a must-have radiological diagnosis clinical component for daily use. The original DICOM PACS and informatics technologies are also being extended to many related clinical imaging applications. However, adopting DICOM as a general image-based standard in Internet communications for other types of non-radiological images and signals has some major drawbacks: DICOM is often technically cumbersome to use due to its inherited heavily constrained rules and overheads; it is expensive in terms of its finances, as well as the time requirement for image compatibility, display, retrieval, and storage.

In the early 2010s, in order to minimize these drawbacks, RSNA along with the Integrating Healthcare Enterprise (IHE), initiated the Integrating Healthcare Enterprise Cross-Enterprise Document Sharing – Imaging (IHE XDS-I) profile). Several manufacturers and research Institutes were invited by RSNA to participate in this initiative. The principles of IHE XDS-I were defined, prototype systems were developed, and radiology manufacturers were encouraged to bring in their own imaging equipment or information systems to connect to the RSNA IHE XDS-i system backbone for live demonstration. Open on-hand live demonstrations have been given to more than 50 000 participants during each year's RSNA Annual Scientific Assembly and Meeting in Chicago, a time period spanning from 2010 until now. It has been one of the most successful demonstrations at RSNA. Since then, instrumented by Professor Jiangou Zhang and his team, the methodology has been drastically improved, and prototype systems have been installed in several hospitals for clinical use in Shanghai, China.

This chapter summarizes the basis of three methods of integrating image sharing described at RSNA and those prototypes used in various hospitals. The first method is Image Sharing for Cross-Enterprise Healthcare with Federated Integration, which was implemented in Huadong Hospital and Shanghai Sixth People's Hospital within the Shanghai Shen-Kang Hospital Management Center; the second method is the XDS-I-based Patient-Controlled Image Sharing Solution, which was implemented by the RSNA team in the United States; and the third method, a pilot study, is Collaborative Imaging Diagnosis with Electronic Health Record (EHR)Integration in Regional Healthcare, which was implemented in two districts in Shanghai. The design and development of the

latter demonstrates the new image accessing method, components, and data model such as Retrieve Imaging Document set 69 (RAD-69)/Web access to DICOM persistent objects (WADO) hybrid image retrieval, RSNA Clearinghouse, and extension of metadata definitions in both the submission set and the XDS Registry.

7.1 Introduction

Healthcare professionals (e.g. referring physicians, radiologists, surgeons, oncologists) benefit from a coordinated method for locating, accessing, and archiving relevant medical documents, including imaging information. The creation and subsequent use of these documents may span several care delivery organizations and may be performed separately over different time periods. Thus, there is a strong motivation to implement electronic healthcare record (EHR) systems as information exchange platforms for regionally coordinated healthcare services [1].

The major challenge with EHR implementation is the integration of different information systems with different information models and platforms. To solve this integration problem, the Integrating Healthcare Enterprise (IHE) [2] has defined an integration profile, known as cross-enterprise document sharing (XDS), to regulate medical record sharing, queries, and retrievals among different document source systems and end applications in a clinical affinity domain: a shared set of policies and infrastructure for exchanging documents [3]. There was some research being done on how to use the XDS profile to federate the multiple clinical affinity domains [4], and how to enable the outsourcing of XDS architectural parts to a public domain with secured data exchange [5]. The XDS-I profile is a supplement to the IHE XDS profile, which extends and specializes XDS to support exchanges of imaging “documents”, specifically sets of DICOM instances (including images, evidence documents, and presentation states) and diagnostic imaging reports, and providing them in a ready-for-display format [6]. The IHE XDS-I profile proposed an architecture model of cross-enterprise medical image sharing for almost 10 years since version “a” was released in 2005, but few clinical implementations of this model have been reported.

In the past few years, some research groups had studied implementation methods of XDS-I profile and have produced some preliminary results [7]. In this chapter, a more complete and systemic presentation of the image sharing and exchanging solutions for three image sharing scenarios based on IHE XDS-I profile is

described. In addition, this chapter evaluates if these solutions can determine whether the IHE XDS-I profile can serve as a foundation for medical image-sharing solutions across different regional healthcare providers. These three scenarios include:

a. long-term healthcare management across multiple hospitals and clinics;
b. patient-controlled image exchange between healthcare providers and image data end-users; and
c. tele-collaboration for image diagnosis across multiple regional care hospitals.

In order to support these pilot studies, a new image accessing method is introduced, including system components and data model, such as RAD-69/WADO hybrid image retrieval, RSNA Clearinghouse, and extension of metadata definitions in both the submission set and the XDS registry. In the following sections, these three pilot studies are presented, together with the results, and the discussion of some key issues that may impact the clinical implementation of XDS-I profile.

7.2 Brief Description of IHE XDS/XDS-I Profiles

One key technical problem for continuity of patient care is the identification of an appropriate method for sharing and exchanging patient records among various hospitals and healthcare providers. To solve this integration problem, several different architectural approaches and programs have been developed; for example, the National Program for IT in the UK [8] and the Canadian Health Infoway in Canada [9]. The IHE has defined an integration profile termed IHE XDS to standardize medical record publication, query, and retrieval among document source systems and consuming applications.

Currently, the IHE XDS integration profile has evolved to version “b”, due to the maturation of Web services standards for intra- and inter-enterprise integration and associated support from an increasing number of platforms and vendors, both commercial and open-source. The b version presents a number of enhancements for image exchange, including metadata expressed in the extensible markup language (XML) used for electronic business (ebXML), Registry 3.0 [10], which is used for XDS transactions, and an updated simple object access protocol (SOAP 1.2) [11]. It also retains the legacy SOAP 1.1, but it uses the W3C message transmission optimization mechanism with XML-

binary optimized packaging (MTOM/XOP) [12], instead of the legacy SOAP with attachments mechanism, for providing and registering a document set "online". In addition, it provides a new transaction with a SOAP binding that uses MTOM/XOP for retrieval of XDS documents [11,12]. Similarly, the XDS-I profile [6] was updated to the b version (XDS-I.b). Figure 7.1 shows the diagram of actors and transactions used in the XDS-I.b profile [6].

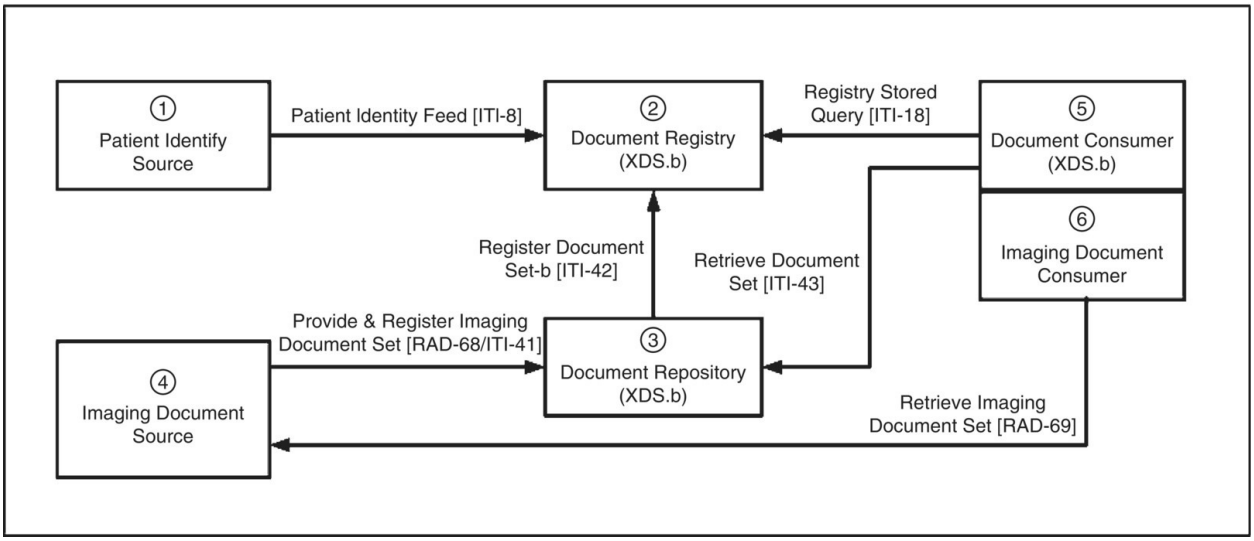

Figure 7.1 The diagram of actors (boxes) and transactions (lines) used in the XDS-I.b profile.

From Figure 7.1, it can be seen that there are six key actors (rectangles) and five major transactions (arrows) in the XDS-I.b profile [6]. The six key actors are: 1. Patient Identify Source, 2. Document Registry, 3. Document Repository, 4. Imaging Document Source, 5. Document Consumer, and 6. Imaging Document Consumer. The five major transactions are Provide and Register Document Set-b (ITI-41), Register Document Set-b (ITI-42), Registry Stored Query (ITI-18), Retrieve Document Set (ITI-43), and Retrieve Imaging Document Set (RAD-69). All these key actors and transactions are clearly defined and described in IHE XDS.b/XDS-I.b profiles [3,6].

In the following sections, we describe how to use the actors and transactions defined in the IHE XDS-I.b profile to design and build different image-sharing solutions that meet the requirements of a variety of regional collaborative healthcare services.

7.3 Pilot Studies of Medical Image Sharing and

Exchanging for a Variety of Healthcare Services

7.3.1 Pilot Study 1: Image Sharing for Cross-Enterprise Healthcare with Federated Integration

7.3.1.1 Background

The EHR provides an information exchange platform for regionally coordinated healthcare services. Owing to the rapid growth of major cities around the world (for example, Shanghai city has reached 20 million), the imbalance between healthcare supply and demand has become an important issue. The local government intends to ameliorate this problem by developing an image-enabled EHR (iEHR) that allows sharing between specific hospitals. The challenges involved in designing and developing this iEHR system are the complicated city healthcare system, the different kinds of affinity domains, and the many different kinds of service models currently in the healthcare system. Shanghai Shen-Kang Hospital Management Center (SSKHMC) is a hospital management organization (HMO) that manages 34 large hospitals in Shanghai. This organization intends to build an iEHR system to enable sharing patient healthcare information among these hospitals. To that end, the city aims to evaluate several different technical solutions. In this chapter, Shanghai is used as an example to illustrate the implementation methods of medical image sharing for collaborative healthcare based on IHE XDS-I method.

The first candidate technical solution was to adopt the IHE XDS-I integration profile [6] as a technical guide for building a prototype iEHR with a federated model for proof of concept. For this proof, the iEHR must integrate with the hospital PACS and the radiology information system (RIS). In addition, it must consider security issues, the protocols for interfacing with different vendors' PACS/RIS, and the operating models.

7.3.1.2 Image Sharing Architecture, Components and Workflows

In Shanghai, Huadong Hospital and Shanghai Sixth People's Hospital were chosen as the pilot study to evaluate the design concept and implementation of an iEHR system based on IHE XDS-I.b profile (See Figure 7.10). The architecture of the major components of the iEHR is shown in Figure 7.2. The PACS/RIS used for pilot testing in Huadong Hospital is from a local PACS vendor, Simed Technologies Inc. [13], which provides DICOM C-Store SCU/SCP services for pilot testing. The PACS/RIS used for pilot testing in the

Sixth People's Hospital was GE Centricity PACS [14], which provided DICOM C-Store SCU/SCP services and also offered a WADO services for pilot testing. The pilot testing network was set up across Huadong Hospital, the Sixth People's Hospital, and the SSKHMC data center through a dedicated virtual private network(VPN) with a bandwidth of 100 MB.

The designed system used typical XDS-I components, including the XDS.b registry, repository, patient identifier cross-referencing (PIX) manager, imaging document consumer (iEHR client), and the Edge appliance. These components were set in a demilitarized zone (DMZ) and functioned as an imaging document source actor and a protocol interfacing adaptor for the hospital PACS/RIS and iEHR systems. All transactions of the IHE XDS-I.b were implemented in the iEHR and conformed to the standards of the National Institute of Standards and Technology document-sharing test facility [15].

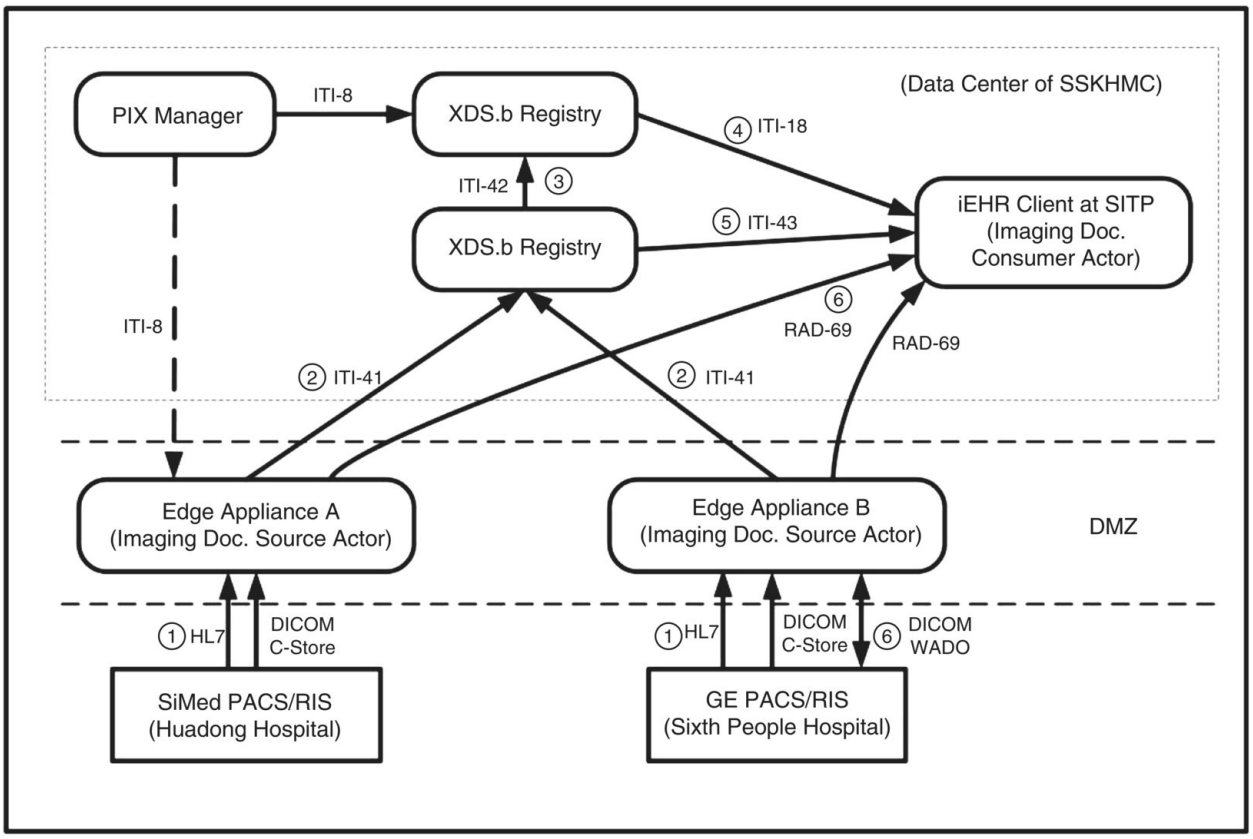

Figure 7.2 The architecture, major components, and workflows of an XDS-I-based iEHR for image sharing with federated integration.

There were two methods for processing the submitted DICOM image data in Edge appliances. One method was to store the DICOM image data in the Edge appliance for later direct retrieval, and when requested from an iEHR client

(imaging document source); this was called on-line retrieval. The other method was to delete the image data in the Edge appliance, and then retrieve image data from the local PACS through IHE RAD-69 and DICOM WADO, on-flying sequentially each time the iEHR client requested the image data from the Edge appliance. The IHE RAD-69 and DICOM WADO hybrid retrieval was first developed specifically for this study in Edge appliances, and was called near-line retrieval.

The typical workflow for testing was to register the imaging document data (DICOM images and related reports) by transferring the data from the hospital PACS/RIS to the XDS-I sharing infrastructure, then, as the iEHR client, to find and retrieve the Image document.

7.3.1.2.1 A. Image Registering

1. DICOM image studies were sent from the PACS to the Edge server through a DICOM C-Store service; reports in Clinical Document Architecture, release 2 (CDA R2) or plain text, were sent from the RIS through an HL7 (Figure 7.2). In Edge appliance A of Huadong Hospital, the DICOM image studies were stored for later online retrieval, when requested from the iEHR client (imaging document source). In Edge appliance B of the Sixth People's Hospital, the DICOM image studies are deleted after registering.
2. The Edge appliance extracts specific metadata information—unique iIdentifiers (UIDs) for patients/studies/series/images—from studies and reports and creates an image manifest defined in the DICOM KOS [6]. It also retrieves a global identifier (global ID) from the PIX manager and creates the submission set, which contains the manifest, DocEntry metadata, and submission set metadata defined by the XDS-I profile [6]. Then, it submits the submission set to the XDS repository through ITI-41.
3. The XDS Repository stores the DICOM manifest and DocEntry metadata in the database, creates the object UID (OID) for each document in the submission set, and forwards the DocEntry metadata, OIDs, and uniform resource locator (URL) of the repository to the XDS registry through ITI-42.

7.3.1.2.2 B. Image Querying and Retrieval

1. The iEHR client (imaging document consumer actor) uses the global ID (from the PIX manager) to query the XDS registry through an XDS query (ITI-18) transaction. Then, the XDS registry searches the registry database and returns a list of OIDs (created when the document was stored in the

repository).

2. The iEHR client parses the queried results to allow the user to make a selection and to initiate the retrieval procedure (ITI-43, Figure 7.2). The retrieval request is sent to the XDS repository, which retrieves the image manifest (DICOM key object selection, KOS) or the report, in CDA R2 format. Then, the repository parses the manifests to obtain the UIDs of the studies/series/images and the URLs of Edge appliance A or B (image source actors that store and manage the image studies). Then, the iEHR client initiates a RAD-69 transaction to retrieve images from Edge appliance A or B.
3. When Edge appliance A is accessed by the iEHR client, it returns the image instances to the iEHR client through an RAD-69 response. When Edge appliance B is accessed, it first converts the RAD-69 transaction request to a DICOM WADO request, then it retrieves the image instances from a PACS of the Sixth People's Hospital (GE Centricity PACS v.3.5), and sends the retrieved image instances to the iEHR client through an RAD-69 response.

7.3.1.3 Key Issues Identified in Pilot Testing

The architecture and workflows of XDS-I-based image sharing for cross-enterprise healthcare were accomplished. However, there were some key issues that required evaluation and discussion before embarking on clinical implementation.

7.3.1.4 Image Sharing Models

One issue was that the choice of image sharing models affects the strategy for integrating the XDS-I infrastructure with the local PACS. In the present study, two sharing models were tested for exchanging data between the local PACS/RIS and the XDS-I image sharing infrastructure. The network settings and communication protocols of these two models are shown in Figure 7.3.

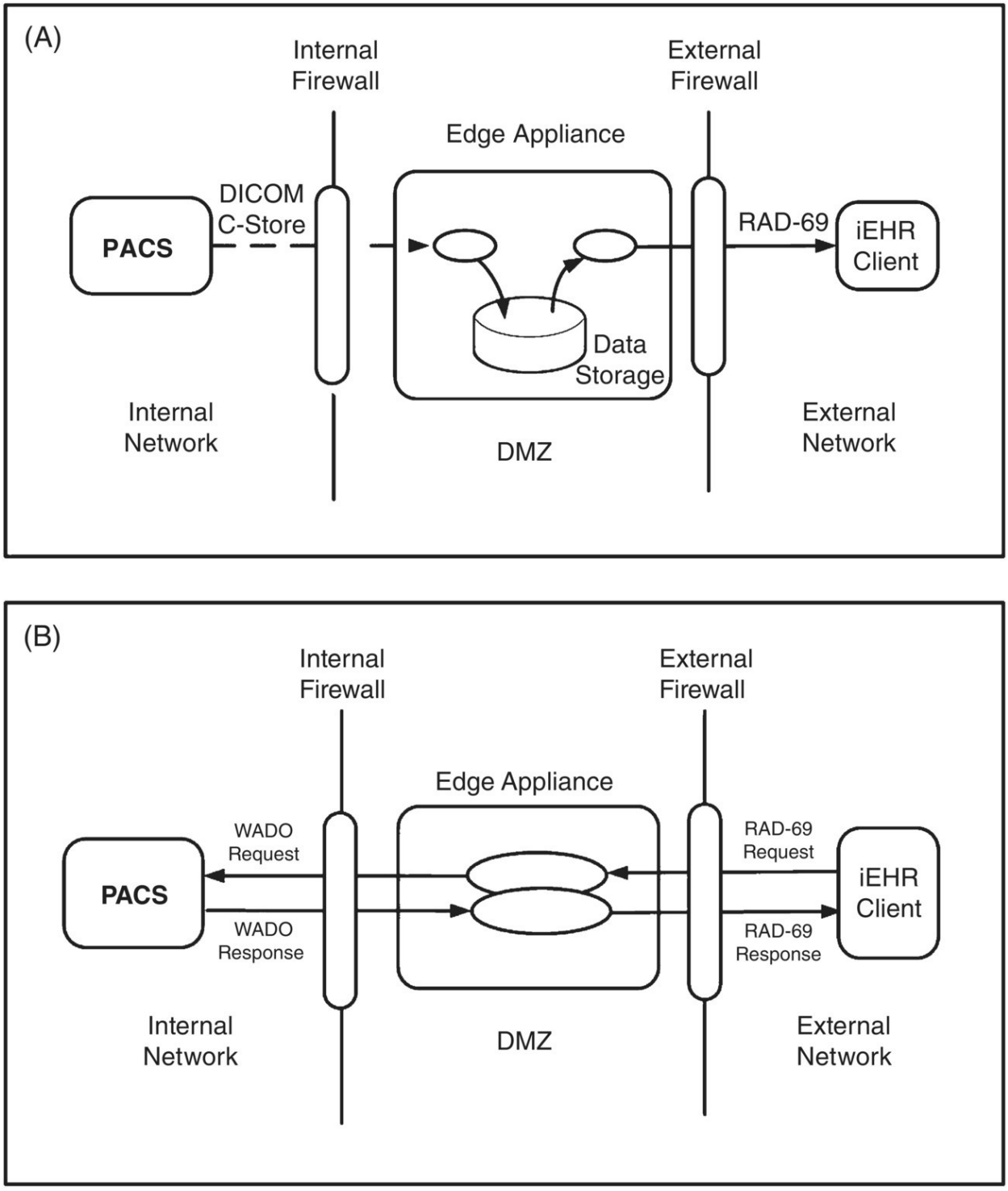

Figure 7.3 (A) Protocols and data flows for online sharing model in an Edge appliance. (B) Protocols and data flows for the near-line sharing model in Edge appliance.

The first model used on-line sharing (Figure 7.3A), which pushed or copied

shared data from the local PACS/RIS to the Edge appliance (Edge appliance A in Figure 7.2), and then registered the data in the XDS-I registry and repository. In this model, the iEHR client could retrieve the image data from the edge appliance directly, with the RAD-69 transaction. In addition, the shared image data was stored in the local Edge server located in the hospital DMZ, and it was fully managed by XDS-I infrastructure. In this model, the local Edge appliance was capable of storing and managing the image data for long-term use. However, this model increased the storage cost, because the image data was duplicated in the local PACS and in the Edge appliance.

The second model used near-line sharing (Figure 7.3B), which registered and stored the metadata and shared the image data manifested in the registry and repository. Thus, the iEHR client could only indirectly retrieve the image data stored in the local PACS/RIS by accessing it through the Edge appliance (Edge appliance A in Figure 7.2) with an RAD-69 and WADO. In this sharing model, the data were stored in the hospital, and fully managed by the hospital PACS. This model saved on storage cost, but it could impact image retrieval performance, because the images must be retrieved first from the local PACS and sent to the Edge server, and then sent to remote consumers. Thus, the retrieval rate was affected by local PACS performance and the security settings.

7.3.1.5 Performance

Another key issue in designing image sharing solutions is the image transmission performance, particularly the rate of image retrieval in on-demand mode of image transmission. In this case, it is most important to measure the interval time from request to arrival of the first retrieved image, as this time interval is the objective compared with measuring the retrieval time of the entire study transmission. In the IHE XDS-I-based image sharing design, we could expect the two sharing models to have different retrieval performances. For this reason, it was decided to compare their retrieval rates.

The hardware configuration of the Edge appliance in the Huadong Hospital DMZ comprised a Dell Poweredge 2950 with dual 2.5-GHz CPUs, 8 GB of RAM, and dual network adaptors. It was set up as an on-line sharing model; therefore, it stored the shared image studies in local storage, and pre-registered the image studies in the registry and repository, located in the Shen-Kang data center, through ITI-41 and ITI-42. The Edge appliance in the Sixth People's Hospital DMZ had the same hardware configuration as that at Huadong Hospital. It was set up as a near-line sharing model; therefore, it stored the

shared image studies in a GE Centricity PACS server, and pre-registered the image studies in the registry and repository, located in the Shen-Kang data center, through ITI-41 and ITI-42. The iEHR client was also set up in a test site of Shen-Kang HMO. For the test, the collection of one computed tomography (CT) study with one series of 200 DICOM images (image size $512 \times 512 \times 2$ bytes), one magnetic resonance (MR) study with one series of 100 DICOM images (image size $256 \times 256 \times 2$ bytes), one digital radiography (DR) study with one series of two DICOM images (image size $2000 \times 2500 \times 2$ bytes), and one ultrasound (US) study with one series of 27 DICOM images (image size $768 \times 1024 \times 1$ bytes), were used.

For the testing procedures, the iEHR client performed an ITI-18 stored query, an ITI-43 document (image manifest) retrieval, and it extracted UIDs for studies/series/images. Then it performed RAD-69 retrievals from the Edge appliances of Huadong Hospital and the Sixth People's Hospital. The time intervals between the ITI-43 request and the first retrieved image of a series through the RAD-69 were measured. For each study or series dataset, three-time testing and measuring of the time intervals between the ITI-43 request and the first retrieved image of a series through the RAD-69 were performed. The time intervals of three-time testing for each study dataset were almost the same, so the testing results were reproducible, but measured interval times of three-time testing were still averaged as a performance result. The retrieval performances of the on-line and near-line sharing models were compared. Tables 7.1 and 7.2, and Figure 7.4 show the results.

Table 7.1 Time intervals for displaying the first image in a series after issuing an ITI-43 request in the online sharing model.

Modality	Time for 1st request (s)	Time for 2nd request (s)	Time for 3th request (s)	Average time for displaying 1st image (s)
MR	2.014	1.912	2.002	1.976
CT	2.386	2.376	2.381	2.381
DR	1.823	1.681	1.777	1.76
US	1.144	1.142	1.136	1.14

Table 7.2 Time intervals for displaying the first image in a series after issuing an ITI-43 request in the near-line sharing model.

Modality	Time for 1st request (s)	Time for 2nd request (s)	Time for 3rd request (s)	Average time for displaying 1st image (s)
MR	2.494	2.112	2.331	2.312
CT	2.783	2.762	2.621	2.721
DR	3.682	3.521	3.611	3.605
US	1.191	1.183	1.201	1.192

The performance comparison from Tables 7.1 and 7.2, as well as Figure 7.4, showed that the on-line sharing model had a faster image retrieval rate than the near-line sharing model for different kinds of images. However, the retrieval time difference between the on-line and the near-line models were only 0.05 s for US and 0.34 s for CT data. This result is explained by it taking longer to transfer an image from the GE WADO to RAD-69 in the Edge appliance, than to read an image from a local disk in the Edge appliance. Another interesting result from Figure 7.4is that the difference of interval times for retrieving DR/CR between online sharing and near-line sharing models was much larger than that of CT/MR/US. The explanation of this result is that it takes longer to retrieve one (first image in a series) DR/CR image from PACS by using WADO, compared to CT/MR/US, as the image size of single DR/CR is larger than that of CT/MR/US.

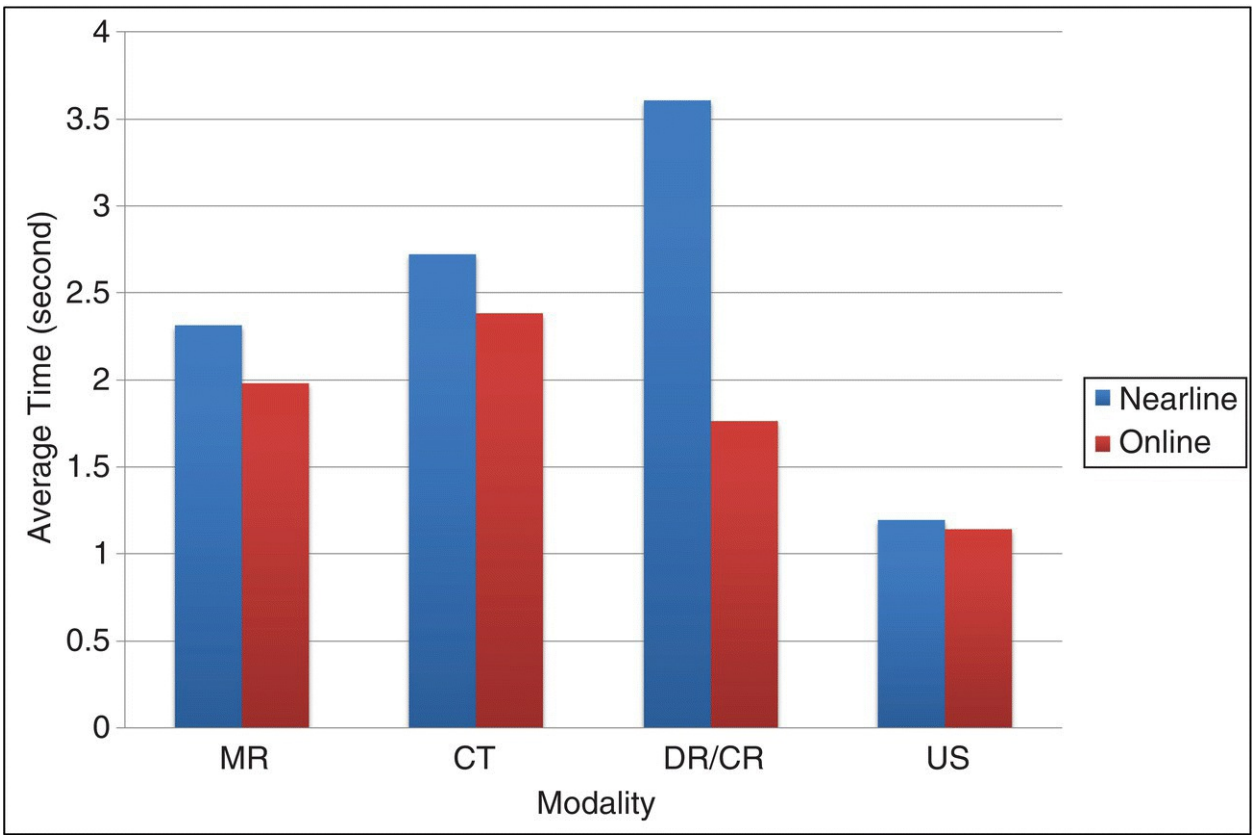

Figure 7.4 Performance comparison of on-line and near-line sharing models. The time intervals (s) represented by vertical axes (time unit: second) for appearance of the first image of different data series after issuing an ITI-43 request in the IHE X-DS-I-based image sharing platform.

7.3.2 Pilot Study 2: XDS-I-Based Patient-Controlled Image Sharing Solution

7.3.2.1 Background

Most XDS-I-based image sharing solutions focus on image transfer between radiologists and physicians. However, it is also common for patients to share imaging examinations with doctors. Typically, patients receive copies of their medical imaging examination on a compact disk (CD). The intent is that patients give the CDs to specialists, who can then view the images on their personal computers. Sharing data through CDs has many disadvantages, including corruption, damage, loss, and incompatibility between operating systems, which causes difficulty and frustration. An on-line method could replace the CD approach.

The National Institute of Biomedical Imaging and Bioengineering (NIBIB) supported a patient-centered image sharing solution, the RSNA Image Sharing Network (ISN) project with five participating academic sites, named the RSNA team: the Mayo Clinic, Mount Sinai Medical Center, the University of Chicago, the University of California San Francisco, and the University of Maryland [16–18], which was based on the IHE XDS-I.b profile. This solution gives the patient control over how imaging examinations should be shared; it leverages a cloud-based "clearinghouse", which was designed and developed collaboratively with lifeIMAGE Inc. [19]. The clearinghouse coordinates to transfer imaging examinations from Edge servers of hospitals/clinics to personal health record (PHR) systems [20,22,23].

7.3.2.2 The RSNA Image Sharing Network Solution

The RSNA ISN solution has three major components (Figure 7.5) [20]: the Edge server, the clearinghouse, and the PHR. The global ID of a patient in the RSNA ISN solution is a hash key, which comprises a PIN specified by the patient and an RSNA ID that is mapped to the local patient medical record number. Combining these values into a hash key ensures a high degree of security. Similarly, all transactions between the Edge servers, clearinghouse, and PHRs are encrypted with a standard secure socket layer (SSL), which provides secure communications over the public Internet.

The Edge server is designed to receive the image study and reports from a hospital PACS and RIS through DICOM and HL7 services. It creates a document submission set that contains a report formatted in CDA R2 , a DICOM KOS manifest, and DICOM objects. It submits this document set to the clearinghouse through an ITI-41 transaction.

The clearinghouse architecture is based on the IHE XDS-I.b profile and is shown in Figure 7.5. The clearinghouse acts as an XDS.b document registry, document repository, XDS-I.b imaging document source, DICOM image manager, and a PIX manager. It receives the document submission set from the Edge servers through ITI-4; it parses out the DICOM objects and stores them in the image manager; and it resets the manifest to make the pointers within the manifest point to the image manager (i.e. the internal source actor). Image data are encrypted with a 256-bit ASA algorithm. As per standard XDS, the PHR can query and retrieve data from the clearinghouse with standard IHE ITI-18, ITI-43, and RAD-69 transactions.

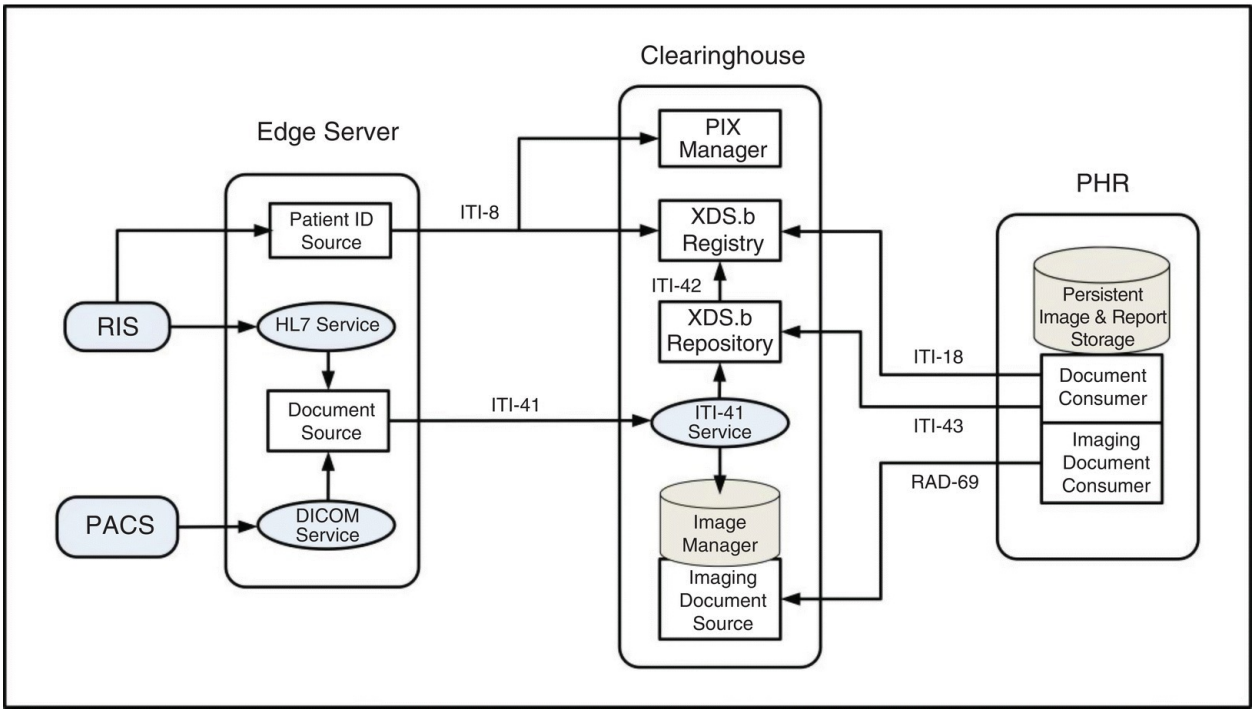

Figure 7.5 The architecture, major components, and data flows of the RSNA Image Sharing Network solution.

The clearinghouse has an audit and monitoring manager that tracks auditing events that ensure compliance with the Health Insurance Portability and Accountability Act (HIPAA) [21] and all ITI transactions; it also monitors source site connections, PHR connections, data volumes, the number of studies, the type of studies, and the volume of pixels stored in the clearinghouse. This audit and monitoring manager is useful in managing the system from the perspectives of both clinical function and technical operation.

PHRs act as XDS.b document consumers and imaging document consumer actors. PHRs use the global ID to retrieve images from the clearinghouse, and have an embedded viewer that allows patients, consulting physicians, or specialists to review images. The PHRs also notify the clearinghouse PIX manager of any cross-referenced patient RSNA IDs.

7.3.2.3 Patient-Controlled Workflow in the RSNA Image Sharing Network [18]

1. Patients are asked whether they want to use the RSNA ISN to obtain image studies, and which examinations they want to push to the network. They are either given an RSNA ID or they use a previously assigned RSNA ID. The patient is asked to provide a PIN to associate with the specific imaging

studies. Finally, they are asked to provide a contact email for notification.

2. Order information is sent to the Edge server via HL7. This order information is maintained in the Edge server database and allows an on-site staff member to search for and select the imaging examination that the patient wants to submit to the clearinghouse. This examination is queued up for submission to the clearinghouse.
3. Once all the requested examinations and results are queued up, the Edge server retrieves the images from the local PACS and the reports from the examination database.
4. The Edge server creates a document submission set, which contains a CDA-formatted report, a DICOM KOS manifest, and DICOM objects. The Edge server transmits the dataset to the clearinghouse. At the same time, an email is sent to the patient to notify them that images are available.
5. Upon receipt of the email, the patient logs in to their PHR account and uses the RSNA ID and PIN to retrieve the images and reports from the clearinghouse. The material is deposited into his/her PHR account.
6. After a fixed period of time, the images and reports are deleted from the clearinghouse.

7.3.2.4 Key Features of the RSNA Image Sharing Network Solution

The RSNA image sharing network solution has a number of key features that differentiate it from standard XDS-I solutions, like the one used in the federated integration model described earlier, and they are:

1. A patient determines whether a study is transferred to the PHR. In the federated model, patients do not have control over what is submitted and shared.
2. Imaging examinations must be explicitly submitted to the clearinghouse by an on-site user. In the federated model, all studies are always uploaded automatically.
3. ITI-41 is used to transfer reports, manifests, and DICOM objects. In a standard XDS-I domain, like the federated model, only manifests and reports are submitted (with ITI-41) to the document repository/registry. The DICOM objects (images) remain with the imaging document source.
4. The clearinghouse is unique, because it groups the XDS registry and

repository actors with an image manager and an imaging document source actor. In contrast, standard XDS-I domains separate the document repository from the image manager and imaging document source actors.

5. A secure global ID is used as a token that comprises the RSNA ID and a user-specified PIN. This ensures that only patients (or individuals that know the PIN) can discover and retrieve patient information. In a standardized XDS-I domain, like the federated model, the global ID is generated by the PIX manager, but it is mapped to a local medical record number, and thus it is open to all users.
6. A transient storage infrastructure is implemented that only stores patient exam information for a limited period of time. The assumption is that information transferred to a PHR can be permanently stored by the patient. Standard XDS-I domains, like the federated model, provide permanent access to patient information; they lack a mechanism for deleting data.

The clearinghouse is hosted by lifeIMAGE, in a HIPPA-compliant data center, in the United States. It went into production in 2011, and has successfully transferred many patient examinations over the Internet from large institutions to patient PHRs. It has proven to be extremely reliable, and it has gained acceptance in more than five institutions.

7.3.3 Pilot Study 3: Collaborative Imaging Diagnosis with Electronic Healthcare Record Integration in Regional Healthcare

7.3.3.1 Background (see Figure 7.10)

In medium or large populated cities in China, there are multiple administration districts. In each district, the health administration typically manages public hospitals that are small (around 50 beds) or medium-sized (200–800 beds). In general, the large hospitals have higher service quality and more medical expert resources than smaller hospitals. However, small hospital service quality may not be recognized, even though they are equipped with high-quality imaging modalities. With the rapid growth of city populations, balancing healthcare supply and demand has become a serious issue. Most patients prefer to go to large hospitals to see doctors when they are sick, despite the high cost. This results in overloading the large hospitals and neglecting the smaller hospitals.

To improve healthcare service quality, to balance healthcare resources between

large and small hospitals, and to reduce costs, each district health administration has begun to build an iEHR system. This undertaking will allow hospitals to share patient medical records and encourage patients to visit small hospitals for initial evaluations and preliminary diagnoses. For example, they can have an imaging examination at the small hospital, then senior radiologists in large hospitals can make the final imaging diagnosis through a regional healthcare information exchange platform, like the iEHR system.

In each district, large hospitals provide collaborative diagnostic services to multiple small hospitals, so those hospitals form a collaborative healthcare service group. There may be multiple collaborative healthcare service groups in one district. Thus, image sharing and collaborative systems must support multiple imaging service groups to provide collaborative imaging services in one health administration domain with one iEHR system.

For these reasons, a method and implementation solution for iEHR systems, based on the IHE XDS-I integration profile, combined with the grid concept [22], was designed (see also Chapters 8 and 9). This grid-based XDS-I image sharing system was used to provide collaborative diagnostic service among four hospitals (one large and three small) in the Zhabei District of Shanghai. This section describes the third pilot study of the extension of data models for XDS/XDS-I transactions to meet the new requirements of regional collaborative imaging diagnosis with multiple service groups. The method integrated the XDS-I-based image sharing system with an existing EHR system to achieve iEHR systems in two districts of Shanghai.

7.3.3.2 XDS-I-Based Regional Collaborative Imaging Sharing Solution with an Existing Electronic Healthcare Record System

This third pilot study, the XDS-I-based image sharing and collaborative system, was to fulfill the following requirements:

1. The system should provide the same workflows for each imaging service group as the previous EHR system.
2. Access to patient imaging studies, before their final report delivery, should only be available to hospitals that are peers of the diagnostic service requester and service provider; later, they can be published to other hospitals in the same district.
3. The same interfacing component (Edge appliance) should be used to interface and communicate with the hospital PACS/RIS [22].

4. It should be integrated with the district iEHR system.

Figure 7.6 shows the architecture of this grid-based, XDS-I image sharing system for regional imaging collaborative diagnosis. The interfaces between the Edge appliance and local PACS/RIS and the operating workflows of this system are presented in [22]. In this pilot study, the data models for XDS/XDS-I transactions to support collaborative diagnoses between peer hospital radiologists in each of multiple service groups were extended, and integrated imaging documents into an existing EHR system.

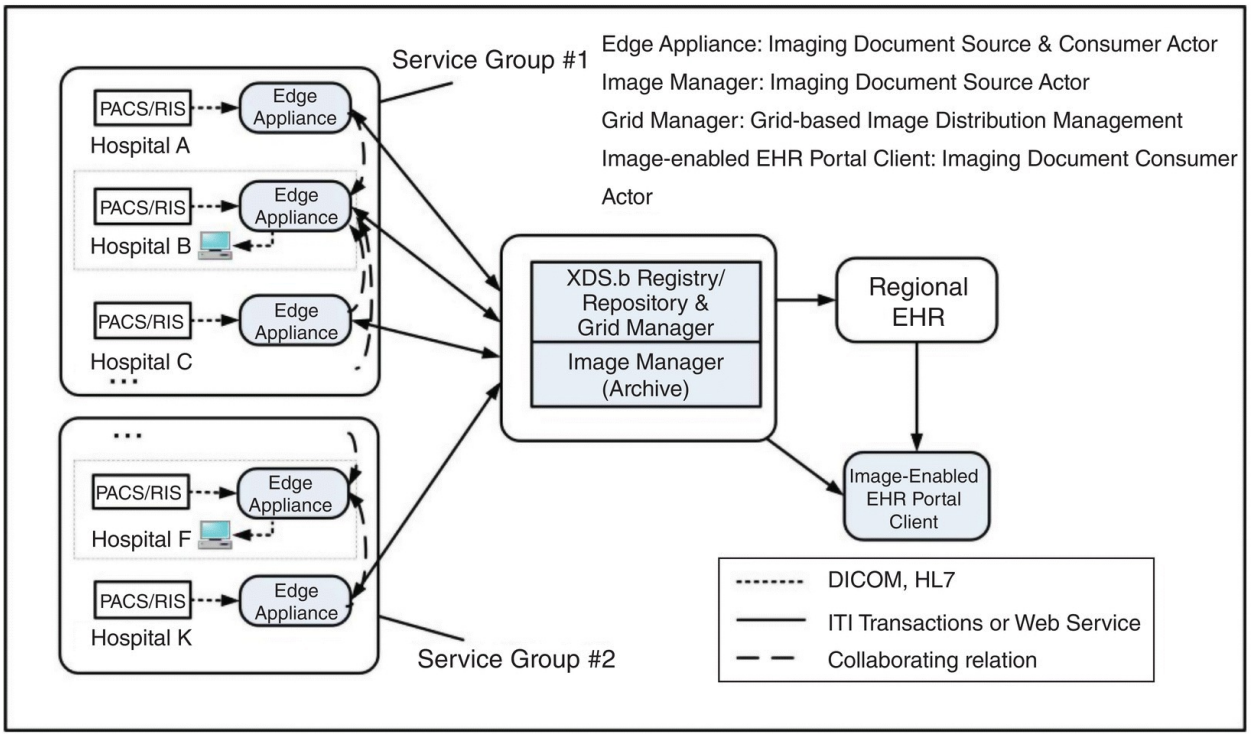

Figure 7.6 The architecture of the grid-based XDS-I image sharing system for regional imaging collaborative diagnosis, integrated with an existing EHR system. There are two service groups (#1(top) & #2 (bottom)) in this diagram, and radiologists in hospital B and F (blue) perform the final reporting. The Image manager is the central storage archive, which provides image archiving functions to all hospitals in one district.

The XDS affinity domains described in XDS/XDS-I.b profiles allow all facilities, hospitals, and service providers with equal access to published patient medical records, when there is no specific access control role applied to documents. The data models for the XDS provide and register document set-b (ITI-41) to support peer-to-peer collaborative imaging diagnoses across multiple service groups were extended (Figure 7.7). These data models are related to the

submission of preliminary and final reporting datasets during a collaborative diagnosis.

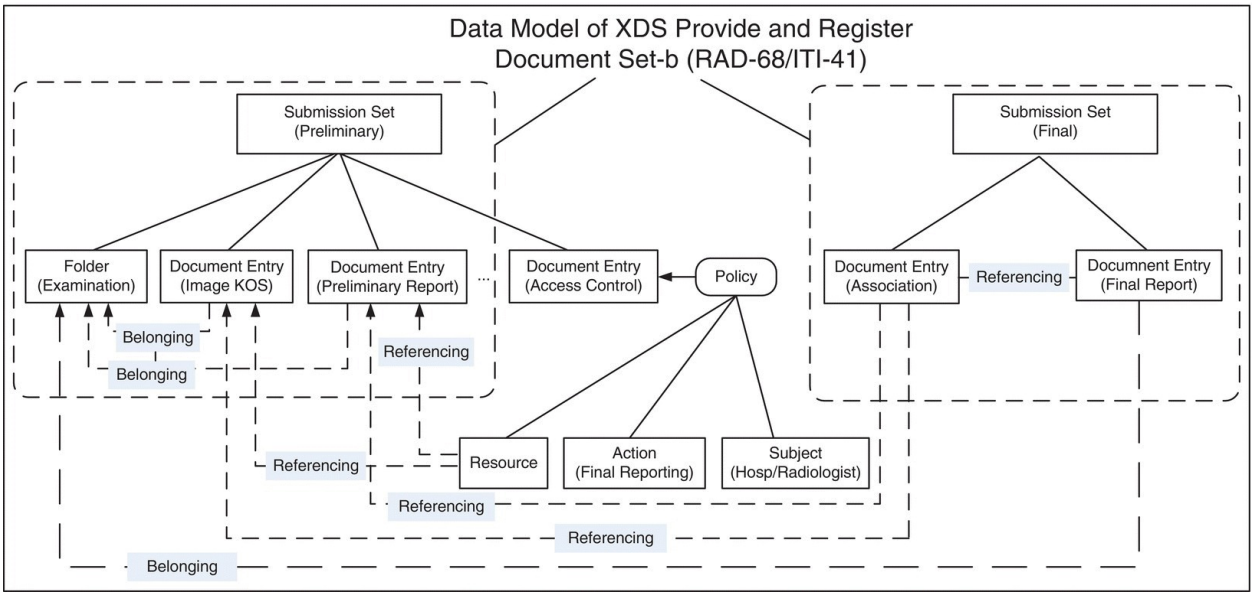

Figure 7.7 The data models for the XDS provide and register document set-b. The models are related to submitting the preliminary and final reporting datasets.

The preliminary submission set for the Provide and Register Document Set-b in the collaborative diagnosis model included an examination folder, document entries of image KOS, a preliminary report and order, and a document entry access control. The access control was created based on extensible access control markup language (XACML). It possesses the properties of an access control policy, for a remote subject (hospital/radiologist), who should take action (perform final reporting) on a resource (reference to an image KOS and preliminary report). The access control was referenced when accessing an image KOS and preliminary report.

After the image was downloaded to a remote site or hospital, and a final report was performed by a senior radiologist [22], the final report was submitted to the XDS repository and registry, through the IT-41. Moreover, it was associated with an image KOS, replaced the preliminary report previously submitted to repository and registry, and was included in the examination folder of the preliminary submission set.

The final report and related image KOS could be published and integrated into the regional, existing EHR system by changing the access control policy, and sending metadata to the EHR system, through the image readiness notification Web service. The metadata included the patient global UID (e.g. social security

number), the preliminary submission set UID, and the document entry UID of the examination record or imaging document.

Figure 7.8 shows the interface integration between the grid-based XDS-I image sharing system and the existing EHR system. There are two new communication services in this integration. Figure 7.8A shows how the image readiness notification service sends communications from the XDS registry to the existing EHR system. Figure 7.8B shows the Web-based image accessing service sending communications from an EHR portal client to the grid-based XDS-I image sharing system.

After the image readiness notification is sent to an existing EHR system, an EHR portal client can query the patient record list from the EHR system, select image records from the list, and retrieve the reports or image studies from the grid-based, XDS-I image sharing system.

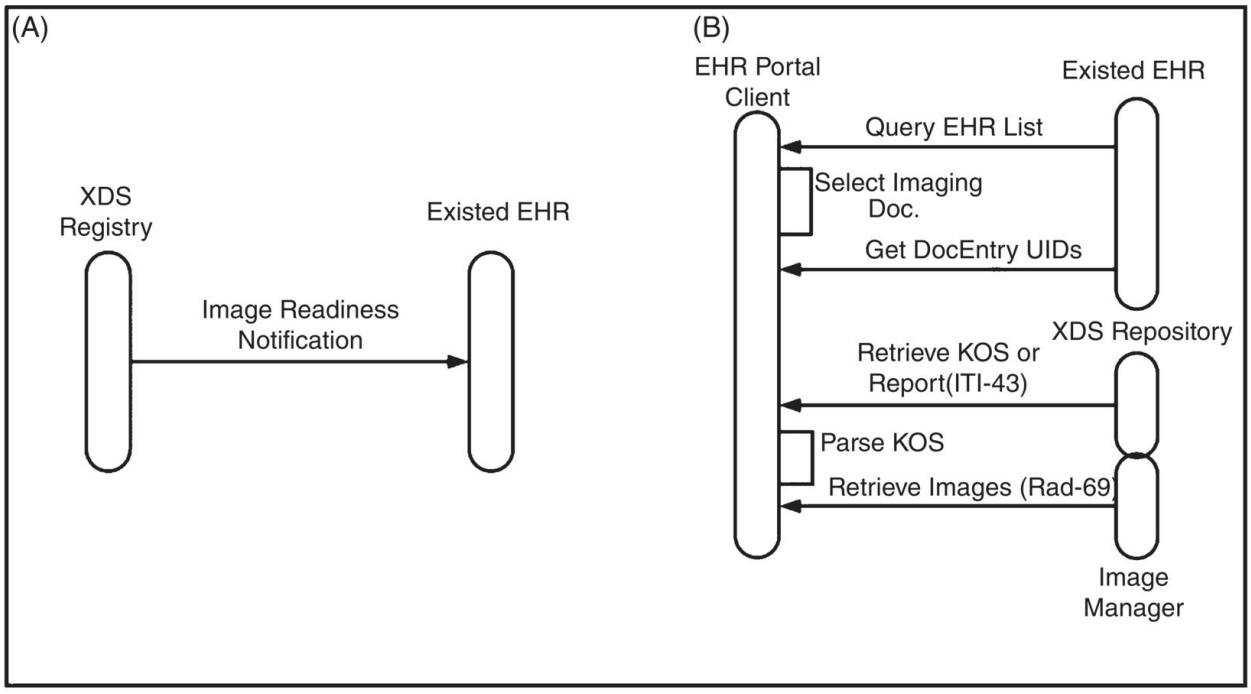

Figure 7.8 The two new communication services in the interface integration between the grid-based XDS-I image sharing system and the existing EHR system. (A) The image readiness notification allows information to flow from the XDS registry to an existing EHR system. (B) Different mechanisms are shown for a web-based EHR portal client to access published images from the grid-based XDS-I image sharing system, which is integrated with an existing EHR system.

7.3.3.3 Imaging Sharing Implementation for Collaborative Diagnosis and Integration with Existing EHR

A new XDS-I-based image sharing solution for multiple collaborative imaging diagnostic centers was implemented in two districts of Shanghai city, the Zhabei District and the Xuhui District. The Zhabei District has 10 community hospitals that perform preliminary reports on radiological examinations, and 2 central hospitals that perform final diagnostic reports upon request from the 10 community hospitals. The Xuhui District has 18 community hospitals that perform radiological imaging examinations, but all preliminary and final reports are currently performed by one of four central hospitals. The image sharing processes of the two districts are logically the same, but there is a difference in the submission set. The content of the preliminary submission set in the Zhabei District is the same as that described in Figure 7.7. However, the preliminary submission set in the Xuhui District is different, because it only contains the examination folder, the image KOS, the order, and the access control document; it does not contain the preliminary report.

Figure 7.9 shows the monthly statistical chart of numbers of imaging studies generated in 18 community hospitals of Xuhui District and the number of studies sent to remote central hospital for both preliminary and final reporting through the iEHR system from January to December 2014. From Figure 7.9, it can be seen that almost 90% (84% ~ 100%) of studies had been sent to remote senior radiologists for final reporting through iEHR system, except for March (64%), when there were 2163 studies being done for screening purpose and not needing to do final reporting according to the agreement between community hospitals and central hospitals in Xuehui District.

The third pilot study, integration of the XDS-I-based image sharing systems in both Zhabei and Xuhui districts, Shanghai, China, with the existing EHR system installed by a third party, has been designed, implemented, and in clinical operation. Both the new XDS-I-based image sharing system for multiple collaborative imaging diagnoses and the integration with existing EHR system have been clinically operating for more than two years.

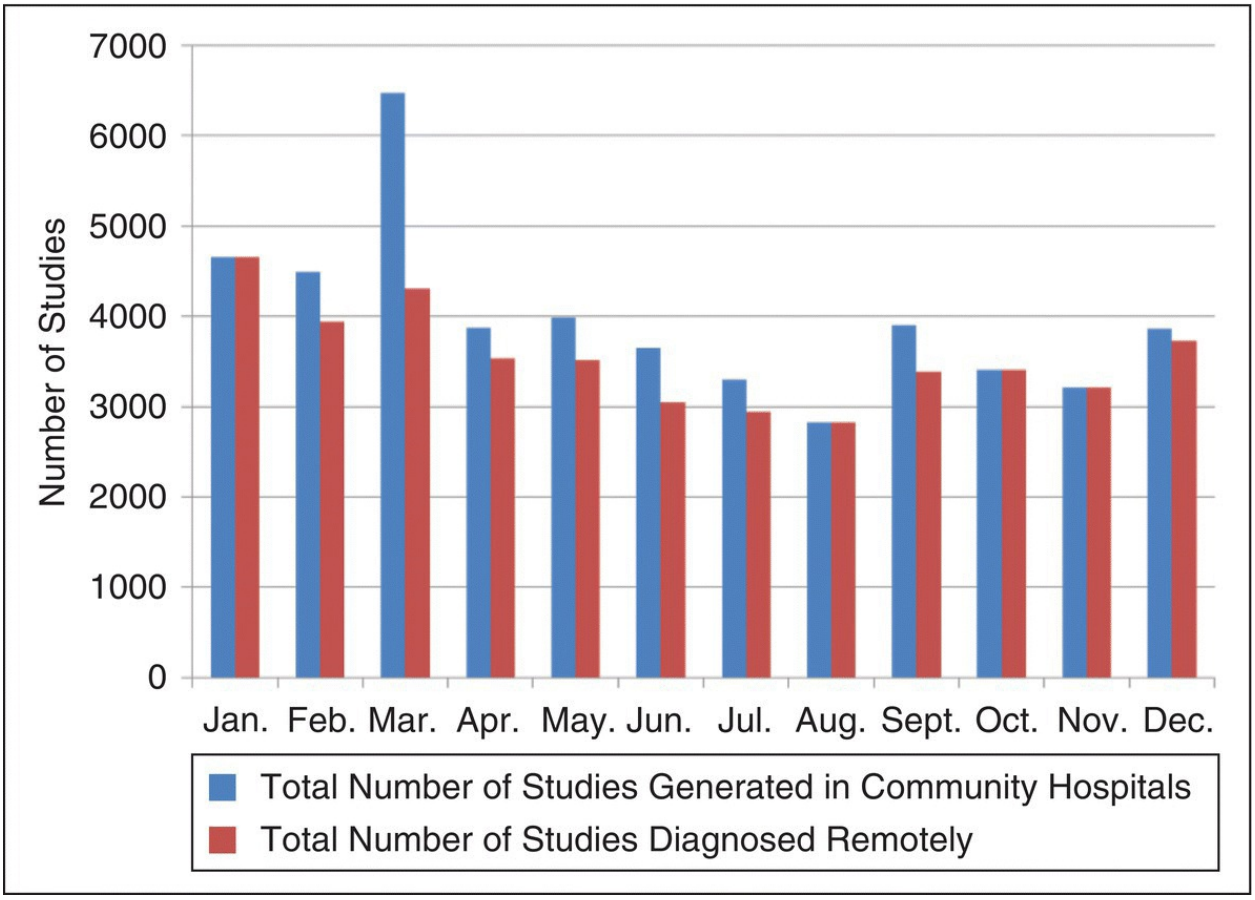

Figure 7.9 Monthly statistical chart of numbers of imaging studies generated in 18 community hospitals in Xuhui District and the number of studies sent to a remote central hospital for both preliminary and final reporting through the iEHR system from January to December 2014.

7.4 Results

This chapter presents three pilot studies of image sharing for cross-enterprise healthcare that were based on the IHE XDS-I profile. In order to support these pilot studies, a new image accessing method for RAD-69/WADO hybrid image retrieval, new components for the RSNA clearinghouse, and a data model for the extension of metadata definitions in both the submission set and the XDS registry have been introduced.

7.4.1 Pilot Study 1: Image Sharing for Cross-Enterprise Healthcare with Federated Integration

Huadong Hospital and Shanghai Sixth People's Hospital were chosen for testing

of image sharing for cross-enterprise healthcare with federated integration within the Shen-Kang Hospital Management Center, to evaluate the design concept and implementation of an iEHR system based on the IHE XDS-I.b profile. In order to retrieve image studies stored securely in local PACS from outside hospitals, the IHE RAD-69 and DICOM WADO hybrid retrieval method was first developed specifically for this study in an Edge appliance to support the near-line sharing model.

Major components and system architecture of image sharing with federated integration, and tested image transmission performance of two sharing models, on-line sharing model and near-line sharing mode, for exchanging data between the local PACS/RIS and the XDS-I image sharing infrastructure, were designed and developed. The performance comparison demonstrated that the on-line sharing model had a faster image retrieval rate than the near-line sharing model, for different kinds of images due to the protocol of WADO being used in near-line sharing. However, the retrieval time difference between the on-line and near-line models were only less than 1 second per case for most kinds of image data.

7.4.2 Pilot Study 2: XDS-I-Based Patient-Controlled Image Sharing Solution

A patient-centered image sharing solution (RSNA ISN), which was implemented by the RSNA team [16–18], was investigated. The RSNA ISN was designed based on the IHE XDS-I.b profile, and leveraged a cloud-based clearinghouse developed by Professor Jianguo Zhang collaborating with LifeIMAGE. From analyzing work and data flows, system components and architecture, as well as the transactions used for RSNA ISN, a number of key features that differentiate RSNA ISN from standard XDS-I solutions, like the one used in the federated integration model described above, were identified by Professor Zhang's team. This solution allows patient control over how imaging examinations are shared. It leverages a cloud-based clearinghouse to transfers imaging examinations from hospitals/clinics to PHR systems.

7.4.3 Pilot Study 3: Collaborative Imaging Diagnosis with Electronic Healthcare Record Integration in Regional Healthcare

A method and the implementation solution to support multiple imaging service groups to provide collaborative imaging services in one health administration

domain with one iEHR system was introduced by Professor Zhang and his team.

In this study, the team extended the data model for the XDS provide and register document set-b (ITI-41) with the access control on the shared image objects and reports based on XACML, to support peer-to-peer collaborative imaging diagnoses across multiple service groups. These data models are related to the submission of preliminary and final reporting datasets during a collaborative diagnosis. Two interfaces to integrate the grid-based XDS-I image sharing system with the existing EHR system were defined. These two services guaranteeing the seamless communications between an EHR server, EHR portal clients, and the grid-based XDS-I image sharing system were defined. This new XDS-I-based image sharing solution for multiple collaborative imaging diagnostic centers in two districts of Shanghai city, the Zhabei District and the Xuhui District, and integrated with existing EHR systems, which were built by a third party, were implemented. Both the new XDS-I-based image sharing system for multiple collaborative imaging diagnosis and the integration with the existing EHR system have been clinically operating for more than two years. According to the statistical study in Xuhui District in 2014, almost 90% (84% ~ 100%) of imaging studies scanned in community hospitals have been sent to remote senior radiologists for final reporting through the new XDS-I-based image sharing system.

(A)

Figure 7.10 (A) shows major sites in Shanghai involved with the clinical pilot studies since 2011. Three methods of integrating image sharing described in this chapter: 1) Image sharing for cross-enterprise healthcare with federated integration; 2) XDS-I-based patient-controlled image sharing; and 3) Collaborative imaging diagnosis with electronic health record integration in regional healthcare. The second method, XDS-I, was initiated by and demonstrated at RSNA. There were only few pilot studies implemented in clinical environments described in the first and third methods. Among them are those hospitals and HMOs in Shanghai, China, with 20 million people.

Professor Zhang's Lab, Shanghai Institute of Technical Physics, Chinese Academy of Sciences (SITP) (center)

Pilot project 1: Image sharing for cross-enterprise healthcare with federated integration.

Sha Huadong Hospital (middle lower) and Shanghai Sixth People's Hospital (leftmost) within the Shanghai Shen-Kang Hospital Management Center

(rightmost).

Pilot projects 3: Collaborative imaging diagnosis with electronic healthcare integration in regional healthcare. Image sharing in two districts.

Zhabei District: 10 community hospitals with red examination and report, and two central hospitals with final diagnostic report upon request. Xuhui District: 18 community hospitals with red examination, all preliminary and final reports performed by one of four central hospitals.

(B)

Figure 7.10 (B) XuHui (lower west) and ZhaBei (upper west), two districts in Shanghai were selected as the third pilot project: Collaborative imaging

diagnosis with electronic health record integration in regional healthcare, XuHui District. One of the most prestigious living areas, busy, commercial, and residential centre, also known as Xujiahui. Convergence of five main roads (including Huai Hai Road) in Xujiahui. The famous Jiao tong and Donghua universities are located here, as well as various consulate offices, and the district is density populated, with heavy traffic.

ZhaBei District. Shanghai Train Station is in this district, and at night is called Ever Bright City. High-quality developments recently completed there include Kerry Ever Bright City and Henderson Ever Bright City.

7.5 Discussion

7.5.1 Comparison of Three Pilot Studies

Three pilot studies of image sharing for cross-enterprise healthcare that were based on the IHE XDS-I profile were evaluated. There were some differences in these three studies in implementation of IHE XDS-I proposed image sharing architecture model. Table 7.3 compares these three studies in data flow, PACS interface, and implementation of IHE XDS-I.b actors and transactions. Table 7.3 Pilot Study 1 shows that the image upload data flow was automatically set to send the manifest of image studies to the repository and register. In registry, and image query and retrieval was controlled based on user on-demand mode. All of transactions of Pilot Study 1 were implemented in standard ITI transactions. The major differences of Pilot Study 1 to Pilot Studies 2 and 3 were interfaced with PACS and image sharing models between PACS and the Edge appliance. There were two sharing models, online sharing and near-line sharing in Pilot Study 1.

In Pilot Study 2, both data flows of image upload and query/retrieval were controlled by patients. Except for the ITI-41 transaction, data flow was customized to be implemented to transfer both manifest and DICOM image data from the local Edge server to the clearinghouse; all other transactions were standardized implementation. The interfacing service of local PACS to Edge server was DICOM C-Store.

Table 7.3 Comparisons of three pilot studies in work flows, PACS interfacing, implementation of IHE XDS-I actors, and transactions (S = Standard Implementation, C = Customized Implementation).

Workflows, Interfaces, IHE XDS-I	Pilot Study 1	Pilot	Pilot Study 3

Actors and Transactions			**Study 2**	
Image Upload		Automatic	Patient-Control	Workflow-Driven
Image Query/Retrieval		On-Demand	Patient-Control	Workflow-Driven
PACS Interfacing Services		DICOM C-Store/WADO	DICOM C-Store	DICOM C-Move/ C-Store
XDS. b Registry	Meta Data Model	S	S	C
	ITI-18 Trans.	S	S	C
XDS.b Repository	ITI-41	S	C	C
	ITI-42	S	S	S
	ITI-43	S	S	S
Imaging Doc. Source	ITI-41	S	C	C
	RAD- 69	S	S	S
Imaging Doc. Consumer	ITI-43	S	S	S
	RAD- 69	S	S	S

In Pilot Study 3, the data flows of image upload and query/retrieval were driven by collaboration workflows between local and remote hospitals. The metadata model of registry and ITI-41/18 transactions were customized to be implemented, based on collaboration requirements. All other transactions were performed by standard ITI transactions. The interfacing services of local PACS to Edge server was DICOM C-Move and C-Store, which were triggered by collaboration events.

7.5.2 Security Issues

Security issues typically involve privacy, authentication, data integrity, traceability, verifiability, reliability, and so on. In healthcare information exchange, the most important security issue is to protect patient healthcare information during image data sharing. Protection is generally implemented with SSL-based secure communication and data encryption for data transmission and management, when public networks are used for data exchanges.

The XDS-I.b profile adopted a Web service-based data transmission protocol,

such as MTOM/XOP, for ITI/RAD-69 transactions [11,12]. These protocols facilitate the use of SSL-based secure communication channels for transactions between the participating actors defined in the XDS-I.b profile. The RSNA team and LifeIMAGE have implemented SSL-based transactions for ITI-9/ITI-18/41/43/RAD-69 in the XDS-I-based clearinghouse for patient-controlled image sharing. There, SSL authentication is bidirectional between the clearinghouse, the Edge servers, and the PHR.

Also, for security reasons, hospital PACS/RIS are typically not allowed to be accessed directly by outside applications, like the iEHR client. Therefore, to integrate the local PACS/RIS and XDS-I infrastructures with security features, the Edge appliances are located in the DMZ, where they function as imaging document source actors (Figures 7.2 and 7.3).

7.5.3 Performance and Storage

In the federated solution of XDS-I-based image sharing, the online sharing model achieved faster image data retrieval and had more secure features than the near-line sharing model. However, these features were possible because the image data were duplicated and stored in the Edge appliance. This duplication represents an issue for long-term archiving and sharing across multiple healthcare enterprises in a large city like Shanghai. In contrast, the near-line sharing model does not require extra storage, but performance may be reduced compared with the on-line sharing model. Also, the security of the near-line sharing model may be weaker than that of the on-line sharing model, because the local PACS must be accessed by the Edge appliance. Thus, an internal firewall must be set up to support bi-directional communications between the local PACS network and the DMZ network.

7.5.4 Extension of XDS-I Profile-Based Image Sharing

In large cities or districts, there are multiple healthcare groups with close imaging collaborations between individuals in each group, and these healthcare groups are managed by a single administration. Therefore, to implement regional image sharing, the workflow or data flow should be compatible with the existing healthcare infrastructure. Unfortunately, the XDS-I profile does not provide a workflow management description or scenario; thus, it is difficult to apply the XDS-I profile directly in designing an image sharing system for a specific set of source actors and consumer actors.

This study presented a new approach that extended the XDS-I profile to support

different image sharing scenarios. For example, the metadata model of the XDS-I profile, combined with this extension with a grid-based implementation of XDS-I, can be extended [22] to support collaborative image diagnosis workflows between peer hospital radiologists in multiple service groups. Another example is to integrate the imaging document metadata into an existing EHR system, and the primary advantage of this new design is that the regional image sharing infrastructure is consistent with the XDS-I profile. Thus, most transactions could use the IHE ITI standard transactions, but some privately defined metadata and slots would be included in the XDS registry and submission set.

In the context of the RSNA ISN, several specific designs in both the metadata and the ITI transactions based on the XDS-I image sharing solution were investigated. These designs ensured that the solution met both the requirements of patient-controlled sharing and the requirements of HIPPA compliance in the Internet operating environment.

This chapter demonstrates that the XDS-I-based image sharing designs and implementations are able to be used successfully in three scenarios of image sharing applications. Thus, it shows that the XDS-I profile is flexible, and that it can be considered to suit a variety of image sharing applications for regional healthcare.

In order to use this profile and architecture models efficiently, certain customizations need to be considered during the system design and implementation, which can impact the performance and security strategy of implementation. Some examples are localized metadata definitions in the submission set, the XDS registry, and extensions of the standard ITI transactions.

Acknowledgements

The efforts of RSNA allowed the completion of its initiative, which results in the availability of the technology permitting manufacturers to implement the IHE XDS-I profile for various hospitals to be used. The company lifeIMAGE received support from the RSNA team to organize a research group with technical experts and manufacturers participating in the demonstration. Dr Peter Bak, faculty of McMaster University, Canada, who collaborated with Professor Jianguo Zhang, Director of the Medical Imaging Informatics Laboratory, the Shanghai Institute of Technical Physics, the Chinese Academy of Sciences, assisted lifeIMAGE to complete the project on time during the first

demonstration at RSNA in 2010. Professor Zhang and Dr Bak [23] extend the concept of medical image sharing for collaborative healthcare based on IHE XDS-I profile to further PACS and imaging informatics applications.

References

1 Zhang, J. (2008) DICOM image secure communication with internet protocols. In: *Teleradiology* (S. Kumar and E. Krupinski, eds). Berlin, Heidelberg: Springer, pp. 33–46.

2 Siegel, E. and Channin, D. (2001) Integrating the healthcare enterprise: a primer. Part 1: Introduction, *RadioGraphics*, 21, 1339–1441.

3 ACC/HIMSS/RSNA (2014, March) Integrating the Healthcare Enterprise Cross Enterprise Document Sharing. Available at: http://wiki.ihe.net/index.php?title=Cross-Enterprise Document_Sharing

4 Dogac, A., *et al*. (2007) Enhancing IHE XDS for federated clinical affinity domain support. *IEEE Transactions on Information Technology in Biomedicine*, 11(2), 213–221.

5 Ribeiro, L.S., *et al*. (2013) XDS-I Outsourcing proxy: Ensuring confidentiality while preserving interoperability. *IEEE Journal of Biomedical and Health Informatics*, 18(4), 1404–1412.

6 ACC/HIMSS/RSNA (2014, March) Integrating the Healthcare Enterprise Cross Enterprise Document Sharing for imaging. Available at: http://wiki.ihe.net/index.php?title=Cross-enterprise_Document_Sharing_for_Imaging

7 Zhang, J., *et al*. (2014) Medical imaging document sharing solutions for various kinds of healthcare services based on IHE XDS/XDS-I profiles. *SPIE Proceedings*, 9039, 90390B.

8 Crompton, P. (2007) The national programme for information technology—an overview. *J Vis Commun Med*,. 30, 72–77.

9 Catz, M. and Bayne, J. (2003) Canada health infoway—a pan-Canadian approach. *AMIA Ann Symp Pro*, 2003, 807.

10 ebXML Registry Information Model Version 3.0, OASIS Standard 2, 2005.

Available at: http://docs.oasis-open.org/regrep-rim/v3.0/

11 SOAP Message Transmission Optimization Mechanism. Available at: http://www.w3.org/TR/soap12-mtom

12 XML-binary Optimized Packaging (2005). Available at: http://www.w3.org/TR/2005/REC-xop10-20050125/

13 Simed Medical Information Technologies Inc. Available at: http://www.simed.com.cn

14 GE Healthcare. Available at: http://www3.gehealthcare.com/en/…PACS…/Centricity_PACS

15 NIST Document Sharing Test Facility. Available at: http://ihexds.nist.gov/

16 Mendelson, D.S. (2011) Image sharing: Where we've been, where we're going. *Appl Radiol*, 40(11), 6–10.

17 Langer, S.G. *et al*. (2015) The RSNA Image Sharing Network. *J Digit Imaging*, 28(1), 53–61.

18 RSNA Image Share Network Reaches First Patients (2011). Available at: http://www.rsna.org/NewsDetail.aspx?id=2409

19 Life Image Inc., Available at: http://www.lifeimage.com

20 RSNA Image Share Network Executive Overview. Available at: http://www.rsnaimageshare.org/downloads/3.0/RSNAImageShareNetworkExecut

21 Health Insurance Portability and Accountability Act (HIPAA). Available at: http://en.wikipedia.org/wiki/Health_Insurance_Portability_and_Accountability_A

22 Zhang, J., *et al*. (2011) Grid-Based Implementation of XDS-I as part of image-enabled EHR for regional healthcare in Shanghai. *Int J CARS*, 6, 273–284.

23 Zhang, J., *et al*. (2015) Medical image sharing for collaborative healthcare based on IHE XDS-I profile. *J Med Imag*, 2(4), 0465011–13.

Part 3
Informatics, Data Grid, Workstation, Radiotherapy, Simulators, Molecular Imaging, Archive Server, and Cloud Computing

PERPUSTAKAAN PRIBADI AN-NUR SUNARYA

8
Data Grid for PACS and Medical Imaging Informatics

CHAPTER MENU

8.1 Distributed Computing

8.1.1 The Concept of Distributed Computing

8.1.2 Distributed Computing in PACS and Medical Imaging Environment

8.2 Grid Computing

8.2.1 The Concept of Grid Computing

8.2.2 Current Grid Computing Technology

8.2.3 Grid Technology and the Globus Toolkit

8.2.4 Integrating DICOM Technology with the Globus Toolkit

8.3 Data Grid

8.3.1 Data Grid Infrastructure in the Image Processing and Informatics Laboratory (IPILab)

8.3.2 Data Grid for the Enterprise PACS

8.3.3 Roles of the Data Grid in the Enterprise PACS Daily Clinical Operation

8.4 Fault-Tolerant Data Grid for PACS Archive and Backup, Query/Retrieval, and Disaster Recovery

8.4.1 Archive and Backup

8.4.2 Query/Retrieve (Q/R)

8.4.3 Disaster Recovery—Three Tasks of the Data Grid when the PACS Server or Archive Fails

References

Further Reading

Two consecutive chapters (Chapters 8 and 9) are devoted to the topic of the Data Grid. The first chapter presents the concept of the Data Grid and its applications in PACS and medical imaging informatics. It starts with the concept of distributed computing, grid computing, and the Data Grid, and then leads to the use of a data grid for PACS and medical imaging informatics, which includes medical imaging data archive and backup, query/retrieval (Q/R), and fault-tolerant recovery. Chapter 9 discusses the use of the Data Grid in clinical applications related to PACS and imaging informatics.

8.1 Distributed Computing

8.1.1 The Concept of Distributed Computing

The basic concept of distributed computing is to network several related computers together to complete a task [1, 2]. The total workload can be divided into smaller pieces for each computer to work on. In principle, when *n* computers are networked together, the total processing time to execute and complete the task can be reduced to 1/*n* of each single computer's processing time. It should be noted that this theoretical limit is unlikely to be achieved because of various unavoidable overheads; for example, data communication latency, and various network communication speeds connected to each computer.

There are two important factors affecting the design of a distributed computing schema. The first is the processor speed variations of different computers. This factor would require the implementation of a mechanism in the distributed computing schema to balance the workload by assigning faster computers to work more, otherwise, the performance of distributed computing would be burdened by the slower computers. Data communication speed is another factor to consider. Lower speed networks assigned to each computer in the distributed computing would also limit performance.

In general, a minimum requirement for distributed computing is a networked computer system; for example, the parallel virtual machine (PVM) with software that can coordinate the computers in the system to work coherently to solve a certain problem. After a similar PVM system is installed in all computer systems, we can start the PVM task from any computer. Other computers can be added to or deleted from the PVM task interactively or by a software call to reconfigure the virtual machine.

Figure 8.1 shows an example of how distributed computing can be used during a

PACS operation [3]. The master workstation (WS) requests a 3-D volume image dataset from the PACS database and assigns 3-D blocks to several slave workstations (WSs) sharing a computational function to perform computer-aided diagnoses (CAD). Each slave WS returns its results to the master WS, which compiles all results to complete the task. The Data Grid, a component of grid computing, is a concept evolved from distributed computing.

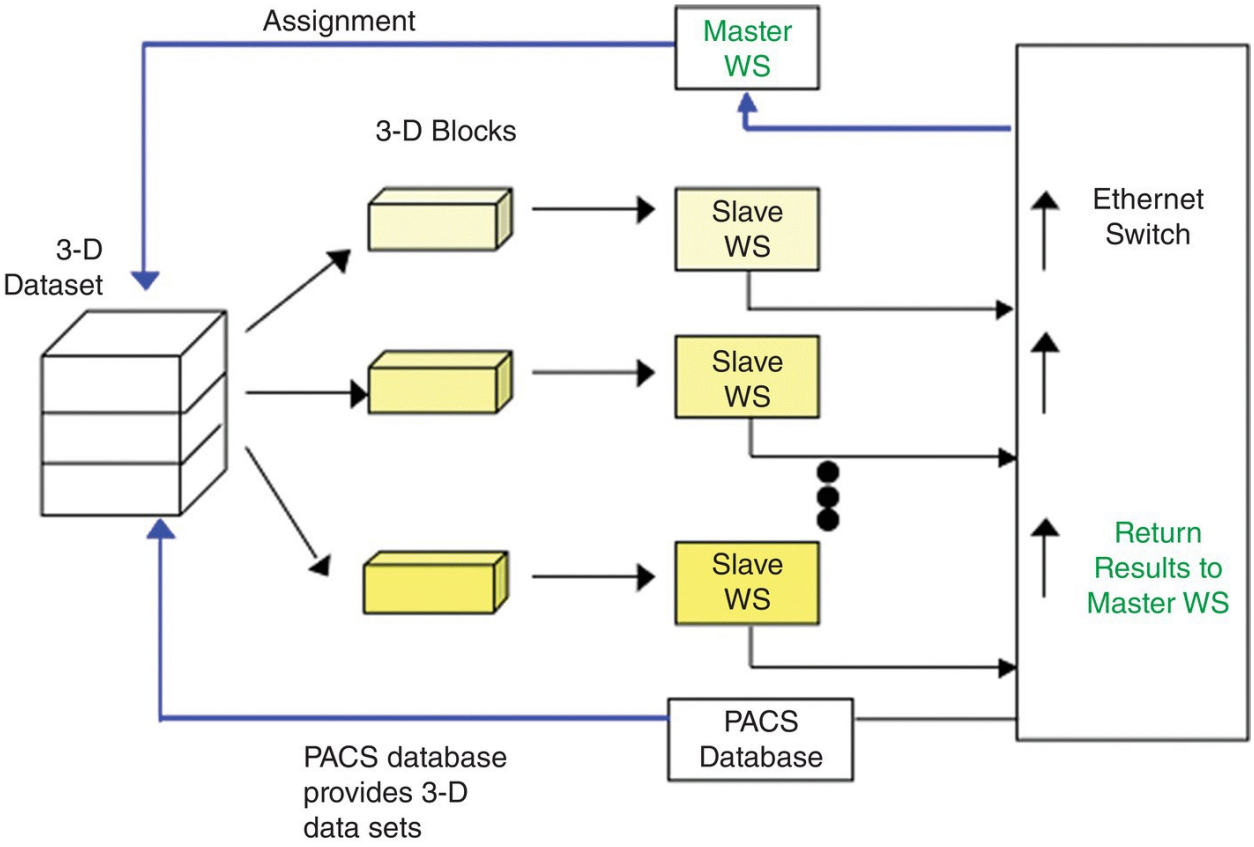

Figure 8.1 Distributed computing is used to perform a PACS CAD task.

(courtesy of Dr J. Wang)

8.1.2 Distributed Computing in PACS and Medical Imaging Environment

Each image WS in a PACS, when it is not in active use, consumes only a minimum of its capacity for running background processes. As the number of image WSs grows, this excessive computational power can be exploited to perform value-added image processing functions for PACS. Image processing is used extensively in the preprocessing stage, which does not require as much computational power as in unsharp masking and background removal in computed radiography (CR), but it has not been used extensively in image post-

processing, like CAD applications. One reason is that pre-processing can be done quickly through the manufacturer's imaging modality hardware and software, which is application specific, and the execution time is fast. On the other hand, post-processing depends on the image WS which, in general, does not provide hardware image processing functions beyond such simple functions as lookup table, zoom, and scroll. For this reason, at the image WS, the user seldom uses time-consuming image processing functions, even though some, like unsharp masking, CAD, and image fusion, are necessary and effective. The multi-image WS PACS environment and medical imaging informatics infrastructure (MIII) connected with many servers and WSs suggest the configuration of distributed computing and, for image processing, the advantage to be gained if the extensive computational power were available at the WSs and servers. Conceptually, distributed computing should raise interest in image processing applications to the extent that there will be a demand for image post-processing tools that can improve medical service by providing near real-time performance at the image WSs. Currently, heavier image processing functions, such as 3-D rendering and CAD on specially designed post-processing WS, are used in the clinical environment.

As in distributed computing, several networked PACS WS could be used for computationally intensive image processing functions, by distributing the workload to these WSs. Thus, the image processing time could be reduced at a rate inversely proportional to the number of WSs used. Distributed computing requires that several WSs be linked to a high-speed network; these conditions are within the realm of PACS and MIII in the number of available WSs and gigabit intra-Ethernet technologies. Figure 8.1 shows how distributed computing in a PACS and MIII network environment would process a 3-D dataset.

Notice in the figure that if, for data security purposes, the computation is for the encode/decode digital signature of the 3-D image volume, and if some slave WSs do not have the encryption software, grid computing can be used to send the encryption software (middleware) with the individual 3-D block datasets to the slave WSs.

8.2 Grid Computing

8.2.1 The Concept of Grid Computing

Grid computing represents the latest exciting computing technology to evolve from the familiar realm of parallel, peer-to-peer and client–server models, and

distributed computing. Grid computing includes many of the concepts of distributed computing and networked computing. In distributed computing, a given task is performed by distributing it to several networked computers (Figure 8.1). Grid computing has one addition ingredient—the middleware—that goes with the data while it is being distributed. Middleware can be computational resources, a software package, a security check, some display functions, or even additional data to facilitate the designated computer if it does not have the necessary resources for the task. For example, if a image content indexing task is being requested that depends on high-power computational algorithms, the middleware that goes with the image data will contain the necessary computational algorithms. Grid computing also has more organization than distributed computing, and each grid within the grid framework may have different resources and even data. When needed, the administrative federation of the grid networked computers can poll resources from different grids for a specific task. Grid computing in medical imaging informatics applications is still in progress, but MIII should include grid computing as a resource in its infrastructure plan.

8.2.2 Current Grid Computing Technology

Grid computing is the integrated use of geographically distributed computers, networks, and storage systems to create a virtual computing system for solving large-scale, data-intensive problems in science, engineering, and commerce. A grid is a high-performance hardware and software infrastructure providing scalable, dependable, and secure access to the distributed resources. Unlike distributed computing and cluster computing, the individual resources in grid computing maintain administrative autonomy and are allowed system heterogeneity; this aspect of grid computing guarantees scalability and vitality. The grid's agreed-upon standards must therefore remain open and scalable. A formal taxonomy, composed of five layers (as shown in Figure 8.2) has been created to ensure its standardization:

1. *Fabric layer*: The lowest layer includes the physical devices or resources, such as computers, storage systems, networks, sensors, and instruments.
2. *Connectivity layer*: The layer above the fabric layer includes the communication and authentication protocols required for grid network transactions, such as the exchange of data between resources, and the verification of the identity of users and resources.
3. *Resource layer*: This layer contains connectivity protocols to enable the

secure initiation, resource monitoring, and control of resource-sharing operations.

4. *Collective layer*: The layer above the resource layer contains protocols, services, and application programming interfaces (API) to implement transactions among resources, such as resource discovery, and job scheduling.
5. *User application layer*: This highest layer calls on all other layers for applications.

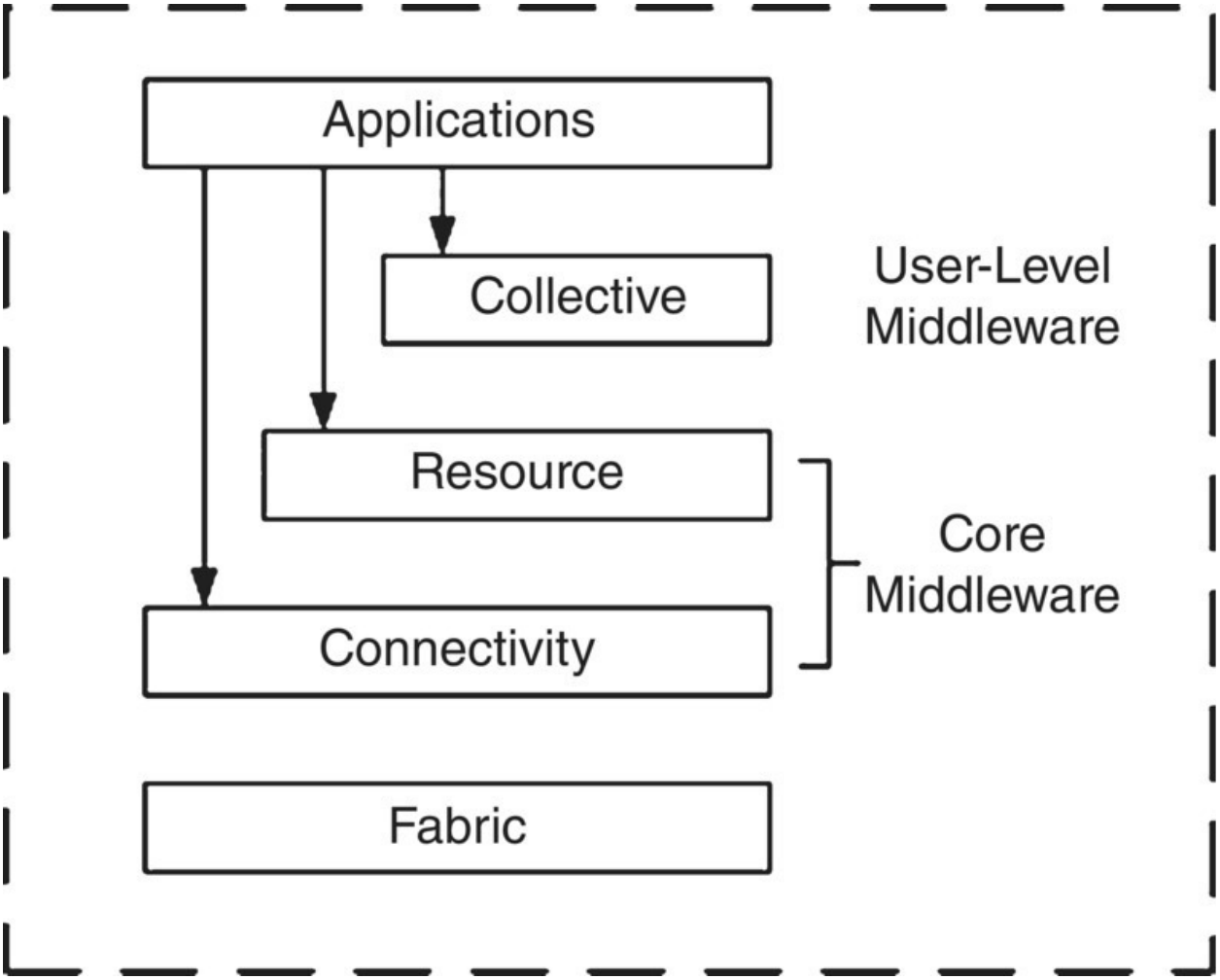

Figure 8.2 Five layers of the grid computing technology.

At its core, grid computing is based on an open set of standards and protocols—such as the open grid services architecture (OGSA). The grid computing provides the user with the following types of service:

1. Computational services support specific applications on distributed

computational resources, such as supercomputers. A grid for this purpose is often called a computational grid.

2. Data services allow the sharing and management of distributed datasets. A grid for this purpose is often called a Data Grid.
3. Application services allow access to remote software and digital libraries, and provide overall management of all applications running.
4. Knowledge services provide for the acquisition, retrieval, publication, and overall management of digital knowledge tools.

There are several large-scale grid projects underway worldwide: the Ninf from the Tokyo Institute of Technology; Globus from Argonne National Laboratory (ANL), University of Chicago, and Information Science Institute, University of Southern California (USC); Gridbus from the University of Melbourne; the European Data grid, and others. Ten years ago there was only limited investigation into the impact of this emerging technology in biomedical imaging, with an exception being a project called e-Diamond, which is a grid-enabled federated database of annotated mammograms. However, nowadays, there are quite a few grid computing and Data Grid applications in medical imaging.

8.2.3 Grid Technology and the Globus Toolkit

Grid computing is based on an open set of standards and protocols in its core infrastructure. OGSA is used as an example to discuss the computational services and the data services (Section 8.2.2) of the Globus Toolkit 4.0 co-developed by Argonne National Laboratory, University of Chicago and the Information Sciences Institute, University of Southern California, for PACS and medical imaging informatics applications.

Figure 8.3 shows the five layers of the grid computing technology defined by the Globus Toolkit 4.0 and the layers correspondence with the open system interconnection (OSI)architecture.

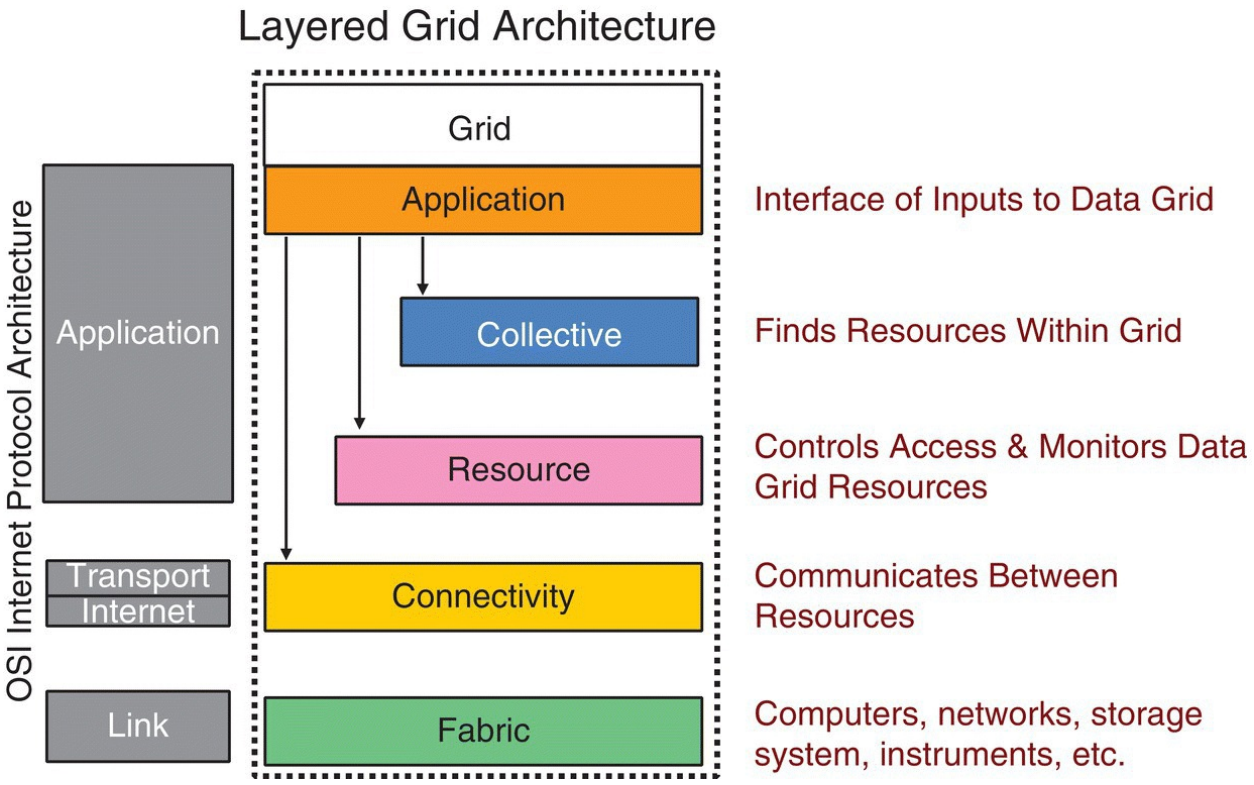

Figure 8.3 Five-layer grid architecture defined by the Globus Toolkit 4.0: Fabric, connectivity, resource, collective, and application. The left-hand side depicts its correspondence to the open system interconnection (OSI) seven-layer Internet protocol (physical, data link, network, transport, session, presentation, and application layer). The right-hand side describes its functions.

8.2.4 Integrating DICOM Technology with the Globus Toolkit

The Globus Toolkit can be used for specific PACS operations by integrating it with a selected customized subset of DICOM resources. For example, Globus can be customized as a fault-tolerant archive system and a computational grid for enterprise PACS operations. Section 8.3 in this chapter presents the Data Grid for image processing and enterprise PACS and it role in daily clinical operation. Section 8.4 describes a fault-tolerant data grid for PACS archive, backup, Q/R, and disaster recovery. The PACS fault-tolerant archive includes topics in PACS image storage, backup archive, and disaster recovery operations using the DICOM image store's Q/R services through the data grid.

Figure 8.4 describes the resources and tools available in each of the five layers after the integration. The majority of these tools are directly from Globus, and

others are through customization using DICOM services. Figure 8.4 also depicts the positions of these DICOM services and the metadata in the Globus grid's five-layer infrastructure. The customized components are shaded, and the colored boxes indicate components developed at the IPILab, USC.

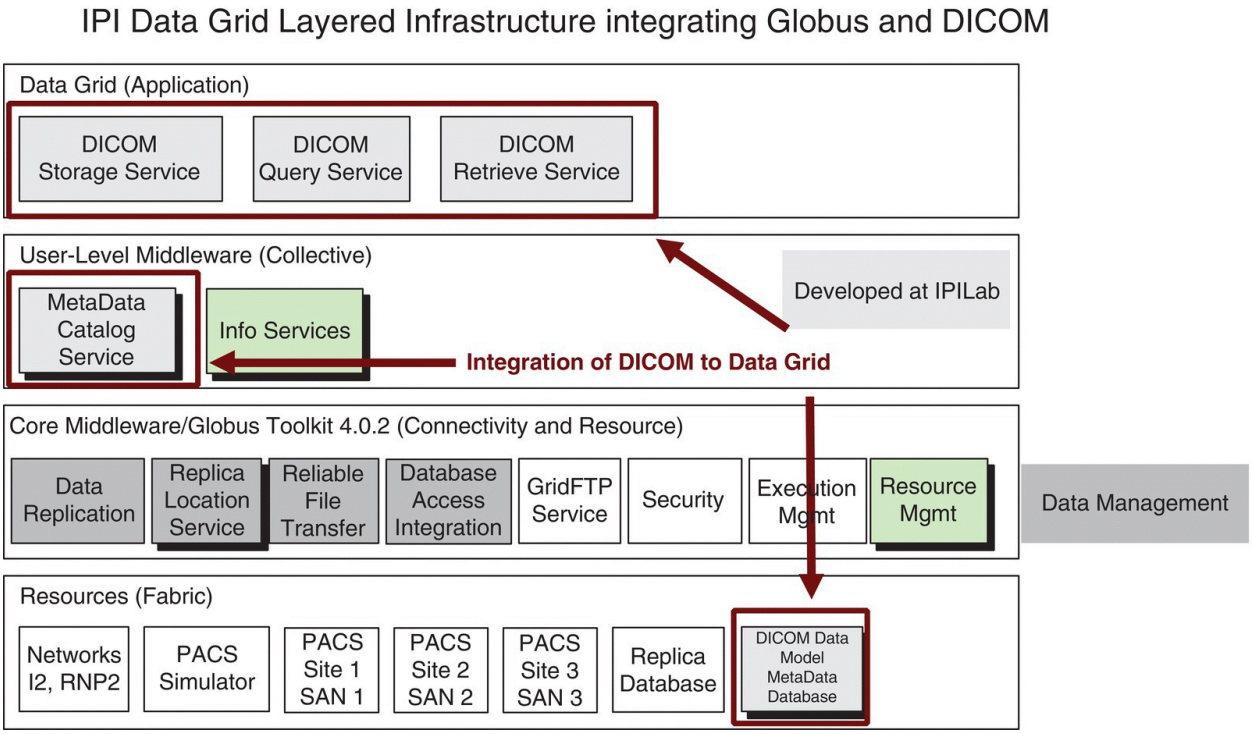

Figure 8.4 The five-layer Data Grid architecture integrating DICOM services and the Globus Toolkit for PACS and MIII applications [4]. Resources (fabric) layer: bottom: the five leftmost clear boxes are existing resources from PACS; Internet 2 (I2); Rede Nacional de Ensino e Pesquisa (RNP2); storage area network (SAN) is for PACS archive (Chapter 15); the clear box Replica Database is a Globus tool; the rightmost metadata database is for fault-tolerant Data Grid and computing grid (shadow) application. Core middleware (connectivity layer and resource layer): The four leftmost boxes are Globus tools used for data management in the PACS Data Grid; the rest are other Globus tools. Replica (shadow) and resource management (green shadow) are also used for the computing grid. User level middleware (collective layer): Metadata catalog service and the Globus info services tool are included for fault tolerance. Both resources are also used for computing grid applications (shadow boxes). Data grid application layer: This consists of the DICOM storage, query, and retrieve services. Light shaded boxes with bold red external rectangles are DICOM resources, and the metadata database for fault tolerance. Services in these boxes were developed at the Imaging Processing and Informatics

Laboratory (IPILab), USC.

8.3 Data Grid [5]

Three topics are presented in this section: data grid infrastructure at IPILab, use of a data grid for a large-scale enterprise PACS operation, and the role of the data grid in the enterprise PACS daily clinical operation.

8.3.1 Data Grid Infrastructure in the Image Processing and Informatics Laboratory (IPILab)

Figure 8.4 illustrates the integration of DICOM image store and DICOM image Q/R in the application layer of the Globus Toolkit to form the Data Grid (top layer) for fault-tolerant storage backup of multiple PAC systems. Figure 8.5 depicts the existing Data Grid with the integrated Globus Toolkit and DICOM services (green) presented in Figure 8.4 at IPILab. The existing Data Grid is ready to be used for PACS and medical imaging informatics applications with customized software. Some of the key customized software, including PACS and DICOM grid access point (GAP; see Figure 8.6, white boxes), storage area network (SAN), metadata database, replica database, grid services, and data grid simulator, are illustrated in Figure 8.6.

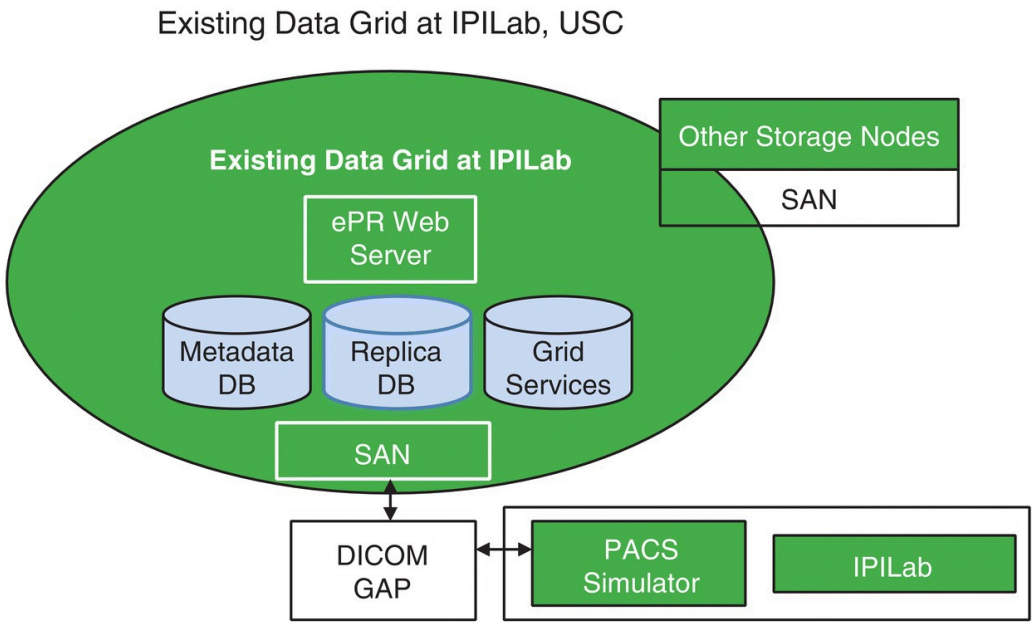

Figure 8.5 Existing Data Grid and its three current applications developed at IPILab, USC.

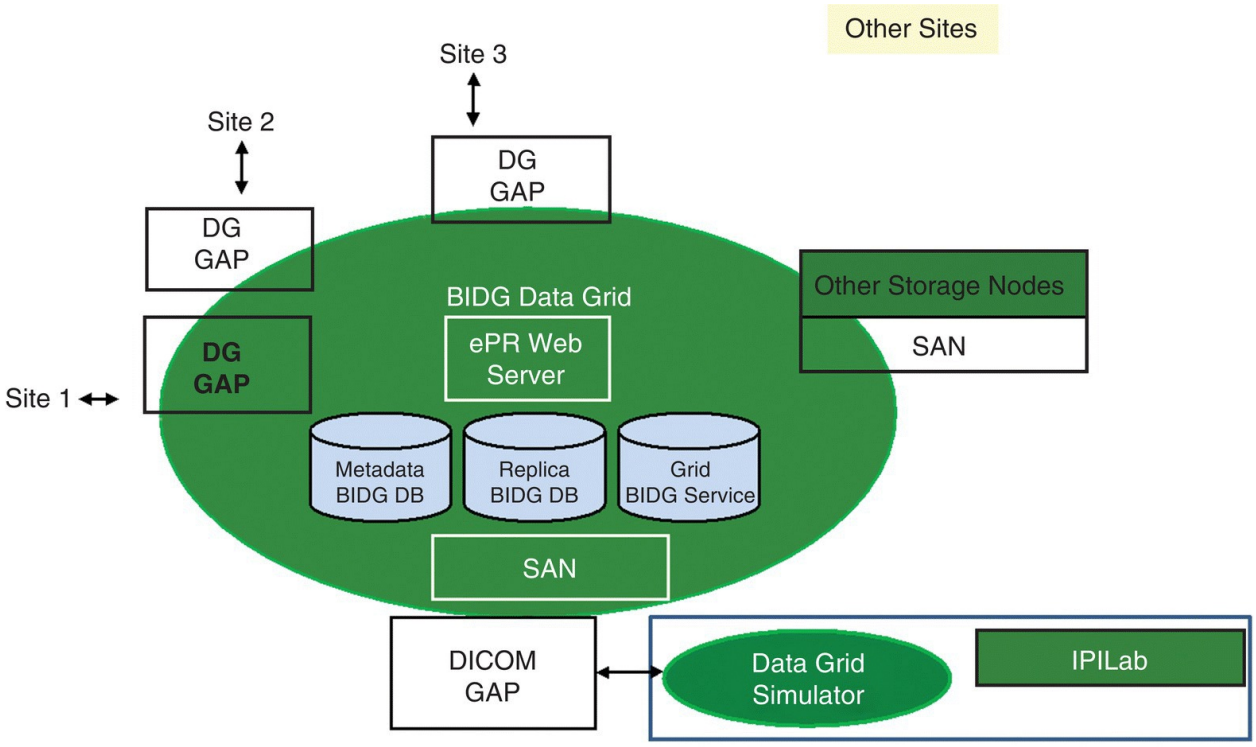

Data Grid Platform at IPILab, USC

Figure 8.6 Data Grid platform at IPILab used to customize for PACS and MIII applications. The major components are the data grid (DG) grid access point (GAP) and the DICOM GAP for connection to PACS sites, other MIII servers, and the Data Grid simulator. The Data Grid simulator can be used for prototyping other Data Grid applications.

8.3.2 Data Grid for the Enterprise PACS

The Data Grid can be used in a large-scale enterprise PACS operation for multiple applications. The example, shown in Figure 8.7 are three PACS sites (three light yellow boxes) plus a research site at IPILab (green box) used for monitoring the operation. Three applications used for demonstration are the image/data archive, Q/R, and fault tolerance of the server and archive disaster recovery.

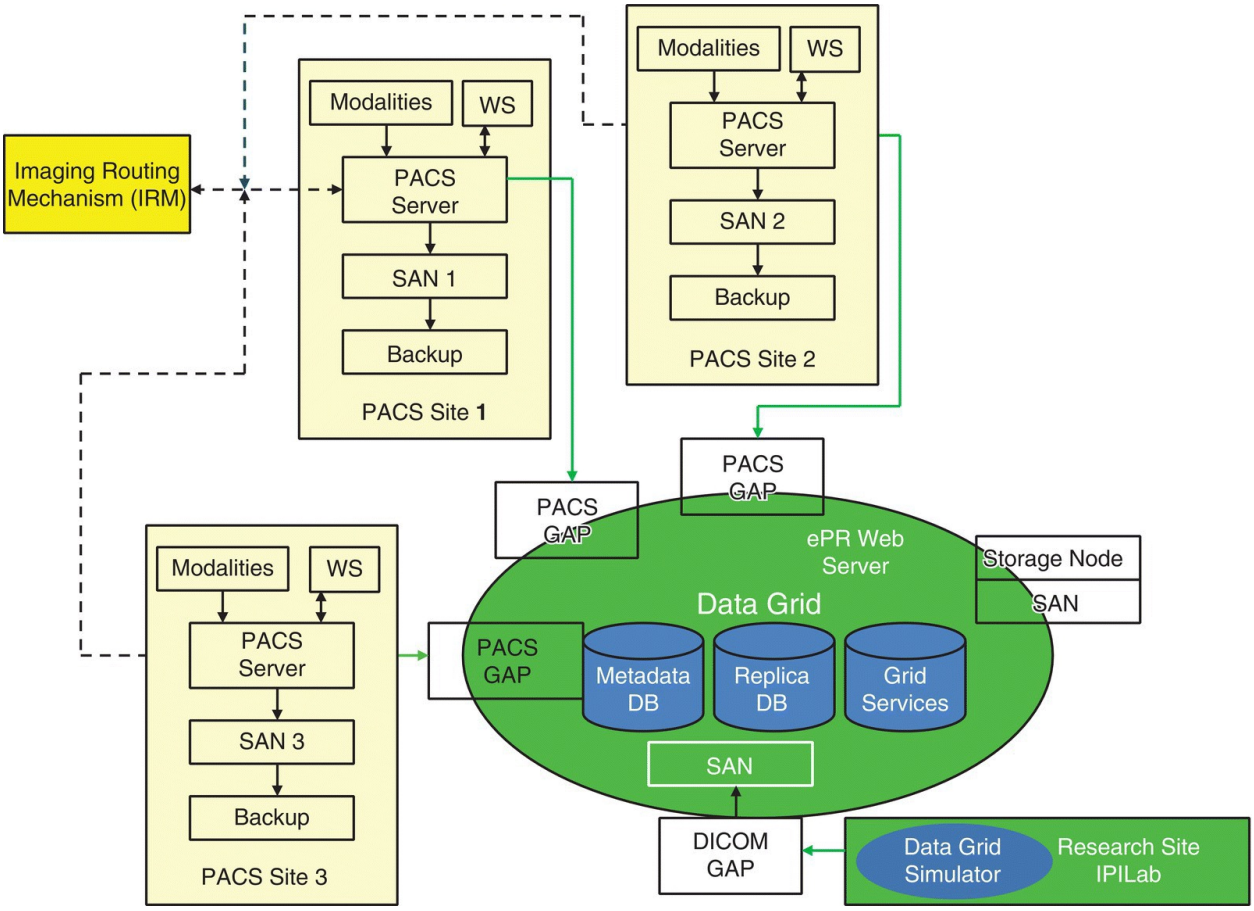

Figure 8.7 Enterprise PACS with three PACS sites (light yellow boxes). Each site has a stand-alone PACS with its own server, WSs, storage area network (SAN) archive, and storage backup, and each site operates independently. An enterprise PACS is when these three PAC systems (or more) are connected together to share images. In an enterprise PACS, a WS at each site can Q/R images from its own SAN for image display. A WS of any three PAC systems can also Q/R images from other sites using an imaging routing mechanism (IRM, yellow box) shown on the left. The weakness of this method of connecting the three PAC systems is that two single points of failure can occur. When a PACS server or the SAN fails, the interconnectivity of the three PAC systems breaks down. On the other hand, the fault-tolerant data grid architecture shown in green can restore each site's backup and their connections to the IRM. It maintains interconnectivity of these three systems in real time without human intervention. There are two types of PACS GAP in this architecture, the DICOM GAP (bottom) and the PACS GAP (middle left). The former is for the PACS WS that uses the DICOM standard for image Q/R, the latter is for DICOM file transfer used by some PACS.

The operation environment is as follows: The enterprise PACS system consists of three PACS sites operating independently as three separate PACS, each supporting its own clinical operation. Each site has a stand-alone PACS with its own server WSs. Any WS in a PACS site can Q/R images from its own SAN to display image data. In addition, any WS of any of the three PACS can Q/R images from other PACS sites using a Web client imaging routing mechanism (IRM, deep yellow), with dotted lines connection, as shown in Figure 8.7.

There are several disadvantages to using this method of integrating multiple PACS operations:

1. The two single points of failure (SPOFs) in each PACS are the server and the SAN archive, assuming that the networks have back up.
2. If the server of a PACS goes down, its WS would not be able to retrieve images from the SAN of its own PACS or review images of other PACS, because the workflow (see dotted lines workflow arrows in Figure 8.7) relies on the availability of the PACS server.
3. If the SAN of a PACS goes down, two things could happen. First, its WS would not be able to view its own images from the SAN. Even though the PACS may have a backup archive, it would take time for the information technology (IT)team to bring the backup on line and supply images to its own WS. This is because most of the backup storage nowadays is low cost, and the priority is to preserve a second copy of the archived data instead of immediately failover to support a continuing operation. The backup is to switch the function to take over the primary operation. Second, a WS from other PACS would not be able to Q/R images from this PACS.

Two major goals of the data grid in this application are, therefore, to minimize the impact due to the failure of the server or the SAN of each PACS, which is described in the next section.

8.3.3 Roles of the Data Grid in Enterprise PACS Daily Clinical Operation

The PACS data grid can be designed to link the three sites together with the following two functions:

1. to support the archive and the backup, and disaster recovery for all the three sites; and
2. to allow a WS of any site to retrieve and review image/data from any other

PACS sites.

Among these functions, the more critical responsibility of the fault-tolerant Data Grid is to take care of each PACS own archive, backup, and disaster recovery, although its role in image distribution and to receive images from other PACS is also extremely useful.

Figure 8.7 illustrates the architecture of the DICOM-imbedded Data Grid located at the IPI, USC (or at any site with sufficient capability); SANs are located at the three clinical PACS as shared storage resources. The three primary components in the Data Grid are:

1. *Storage node*: Resources from the three PACS, including the SAN 1, SAN 2, and SAN 3 (see Figure 8.4, resources layer; and Figure 8.7, three yellow boxes), provide storage resources for the Data Grid. Each SAN has one copy of every image for a given PACS.
2. *Database*: A grid service that keeps track of metadata as well as file locations of different storage nodes within the Data Grid. Dynamic and robust access to data is provided by the data access interface (DAI) in the Globus Toolkit integrated with the database (Figure 8.7, three light blue cylinders inside the Data Grid [green]).
3. *Metadata database*: Metadata contain all DICOM image header and data model information extracted from an image when it is acquired from the imaging modality. This information is organized and stored in the metadata database (Figure 8.4), which provides all necessary information about the image, including a pointer to where the image is located in the Data Grid SANs. Upon a proper query, any image data in the metadata database can be retrieved by the WS through the GAP. The metadata database without backup databases can be a single point of failure in the Data Grid. For this reason, a middle layer, called the DAI in the Globus Toolkit server, is added in-between GAPs and metadata storage nodes. There are thus two layers in the metadata database, the multiple DAI servers and multiple metadata storage nodes (or SANs), as shown in Figure 8.8, which allow multiple GAPs to access multiple DAI servers and multiple metadata storage nodes. The three main functions of the DAI server are centralization of metadata access, replication of metadata into multiple storage nodes, and handling metadata for different PACS archives.
4. *PACS or DICOM GAP*: A service provides access data within the Data Grid with DICOM compliant storage and query/retrieve capabilities for the WS of

any PACS. There are multiple PACS GAPs in the Data Grid (see Figure 8.7, connected to WSs of each PACS and embedded in the Data Grid) that can be used as backup for each other.

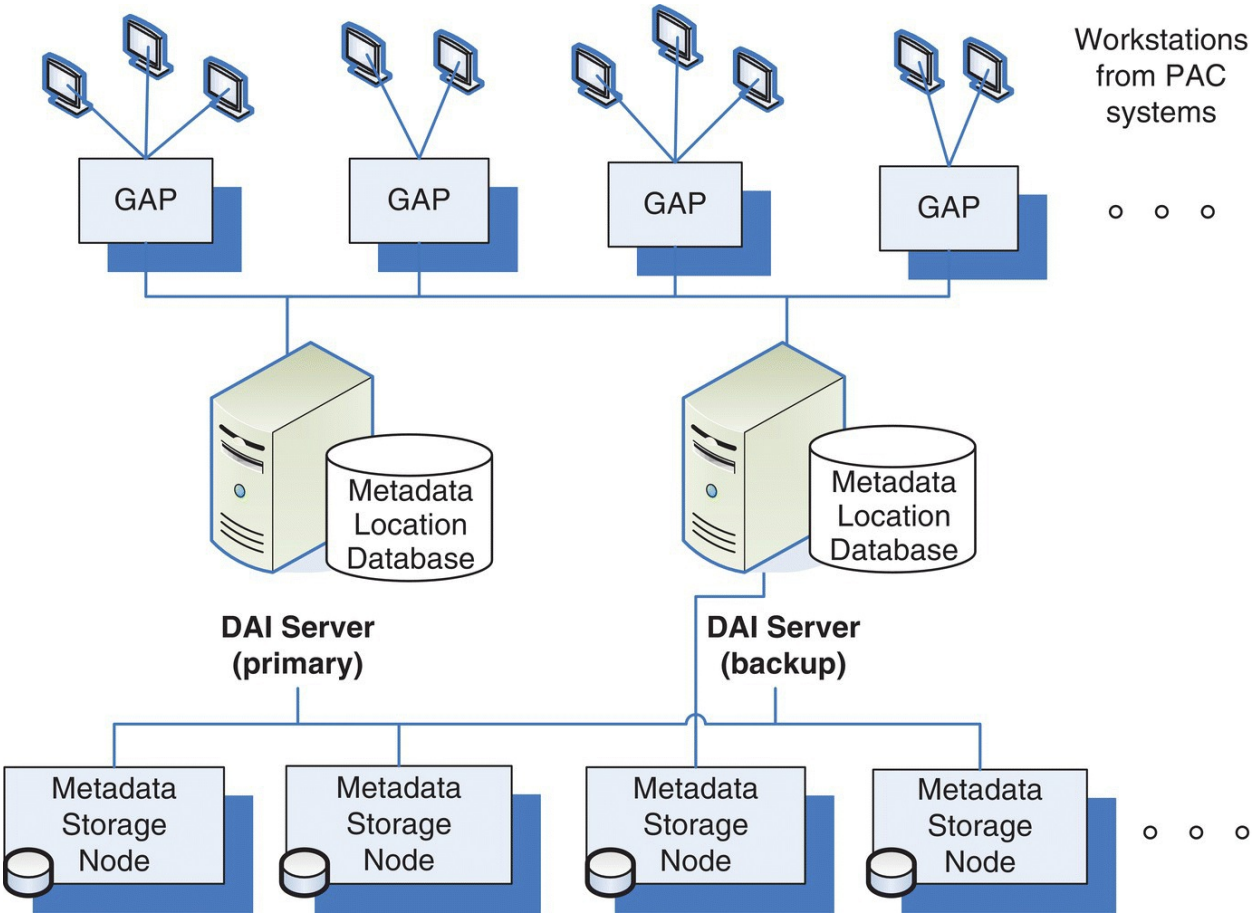

Figure 8.8 General architecture of the fault-tolerance metadata system for the Data Grid. There are three levels of fault tolerance: (top) Multiple grid access points (GAP); (middle) data access interface (DAI) servers; and (bottom) multiple metadata storage nodes.

(courtesy of J. Lee)

8.4 Fault-Tolerant Data Grid for PACS Archive and Backup, Query/Retrieval, and Disaster Recovery

In Figure 8.7, ignore the IRM (deep yellow) and the dotted line connections to the three PACS sites (light yellow), and consider the three PACS sites that are now fully connected (green lines) to the Data Grid (green). In each PACS, the

SAN has been partitioned into P1 and P2, with P1 for its own PACS images/data storage and P2 for contribution to the other two PAC systems for their backup copies. As the enterprise fault-tolerant PACS Data Grid, it has three major responsibilities:

1. Archives its own image/data and backs it up with two extra copies at P2 of two other PACS SANs.
2. Queries/retrieves image/data from other PAC systems.
3. Performs disaster recovery when either its server or SAN goes down.

8.4.1 Archive and Backup

Under normal conditions of operation (Figure 8.9, left, solid lines), the first copy of the image acquired at site 1 is sent to partition 1 (P1) of its own SAN, the second and third backup copies are sent using the GAP 1 to P2 of SAN 2 and P2 of SAN 3 contributed by other PACS sites to the Data Grid. The fault-tolerance (FT) of the GAP can be demonstrated by the dotted lines in the figure. During the backup procedure, supposing that GAP 1 fails (red crossed lines), then the Data Grid would automatically assign GAP 2 to replace GAP 1. GAP 2 would then complete the task original assigned to GAP 1 by storing copy 2 to P2 of SAN 2, and P2 of SAN 3.

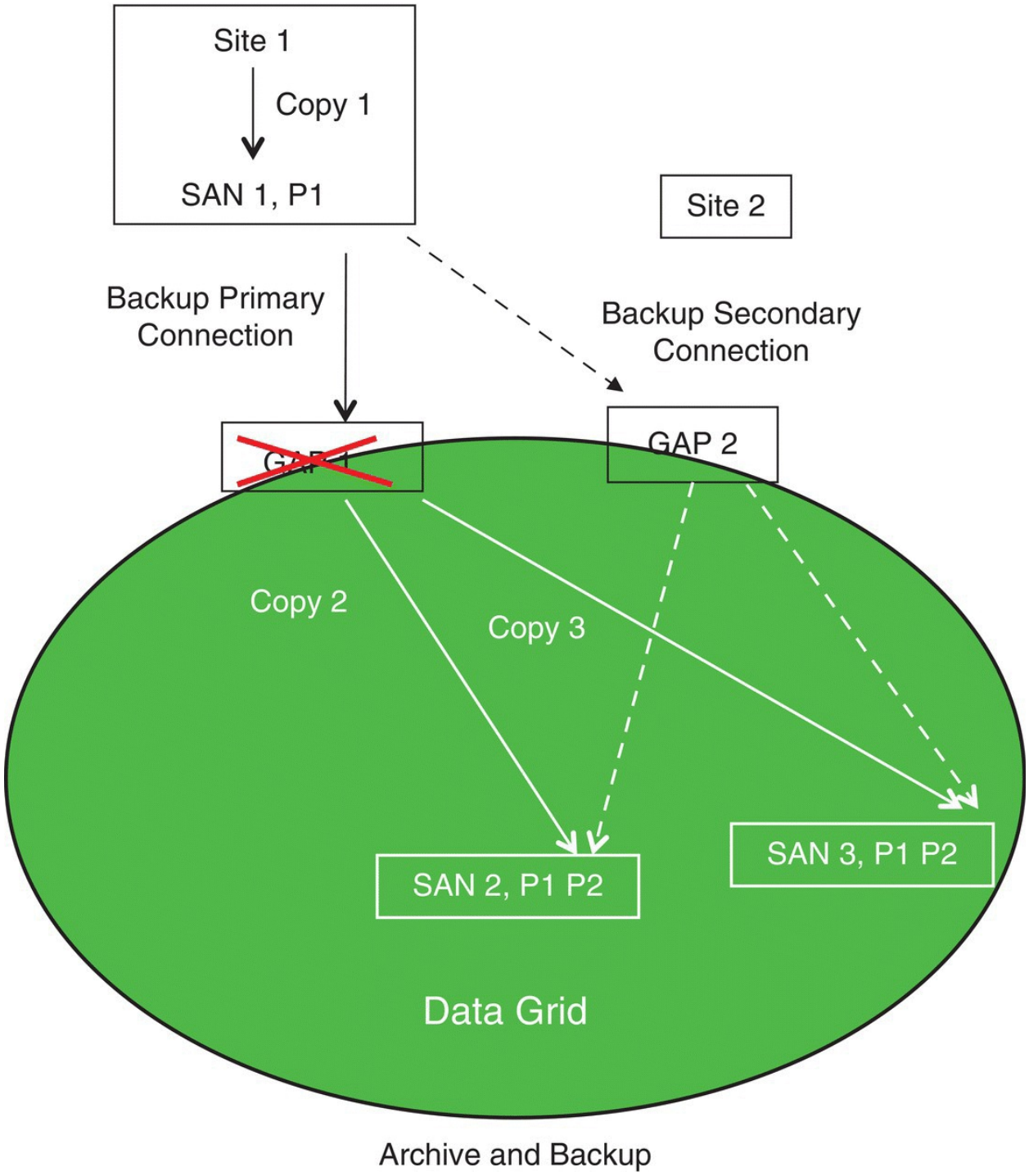

Figure 8.9 Workflow of the Data Grid during image data archive. Solid black lines (left) show the normal archive and backup operations, the first copy of the image file is sent from the acquisition to its SAN1 P1, and two backup copies to the Data Grid SAN2 P2, and SAN3 P2 for backup storage through its designated GAP1. Dotted black line shows when GAP 1 fails (red crossed lines), and GAP 2 takes over GAP 1 functions automatically.

8.4.2 Query/Retrieve (Q/R)

There are two scenarios in image Q/R:

1. *Q/R its own PACS image file*: Refer to Figure 8.10A where the solid lines (left) show the normal operation of DICOM Q/R from WS at site 1. If the image file is in its own SAN 1 P1, then it is a normal PACS operation. But if SAN 1 P1 fails, Q/R will go to its PACS backup through GAP 1 to either SAN 2 P2 or SAN 3 P2. Then Q/R will initiate GAP 1 to the Data Grid to query and then retrieve the image file from the storage nodes, in this example, SAN 2, P2. On the other hand, if during the process SAN 2 fails (red crossed lines), the Data Grid identifies SAN 3, P2, from which the file is then retrieved (blue dotted lines). If during the off-site Q/R, GAP 1 fails, GAP 2 will replace the function of GAP 1, as described in Figure 8.9.
2. *Q/R other PACS image file*: The Q/R goes to GAP 1 to query, then retrieve the image file from SAN 2 P1, as shown in Figure 8.10B. If SAN 2 fails (red lines), then Data Grid will automatically switch to SAN 3 P1, from which the file is then retrieved (blue dotted lines). If GAP 1 fails, GAP 2 will replace the function of GAP 1, as described in Figure 8.9.

(A)

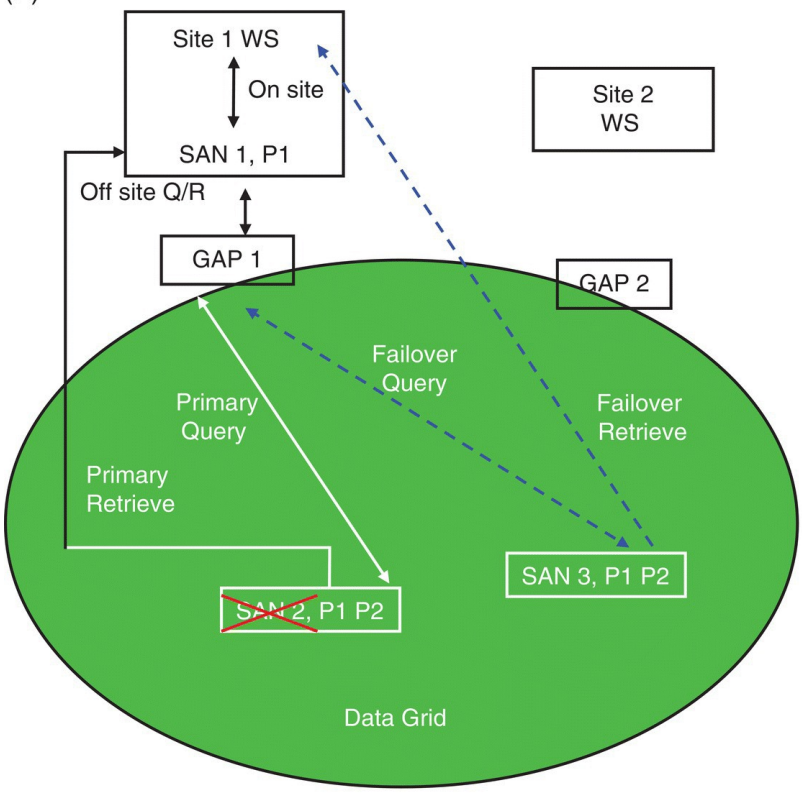

Query/Retrieve its own image file

(B)

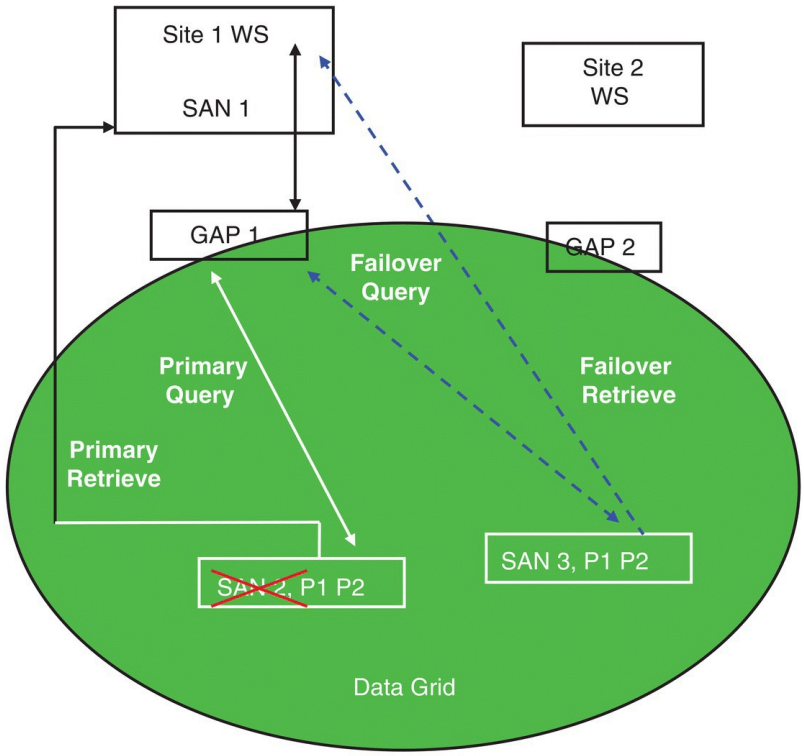

Query/Retrieve image file from other PACS

Figure 8.10 Workflows of the Data Grid during query/retrieve (Q/R) of an image file. (A) The PACS WS Q/R its own PACS image file or from the Data Grid; (B) the PACS WS Q/R other PACS image file from the Data Grid.

8.4.3 Disaster Recovery—Three Tasks of the Data Grid when the PACS Server or Archive Fails

In the Data Grid architecture shown in Figure 8.7, there are two single points of failure at each site, the server/archive and the SAN storage device. When any of these two points fails, or both fail, the Data Grid has to overcome three major tasks (disaster recovery) in order to be fault tolerant.

First, it has to maintain continuous clinical operation allowing WSs at this PACS site to Q/R images from its backup in the Data Grid. Second, after the server and the SAN have been repaired, the Data Grid has to rebuild the SAN P1 at this site for its own primary archive. Third, it has to rebuild the backup archive SAN P2 that contributes to other PACS in the enterprise for their backup. Figure 8.11 describes, using site 3 as an example, these three tasks when the server and/or SAN fail (red crossed lines). SAN 3 is partitioned into P1 and P2. P1 is the archive for its own site and P2, in green fonts, is site 3's SAN storage resource committed to the Data Grid for other sites' backup archive. Task 1 has the highest priority among the three tasks shown in heavy green lines. All three tasks are performed automatically without human intervention. The archive's backup Q/R functions described earlier can be used to complete all three tasks.

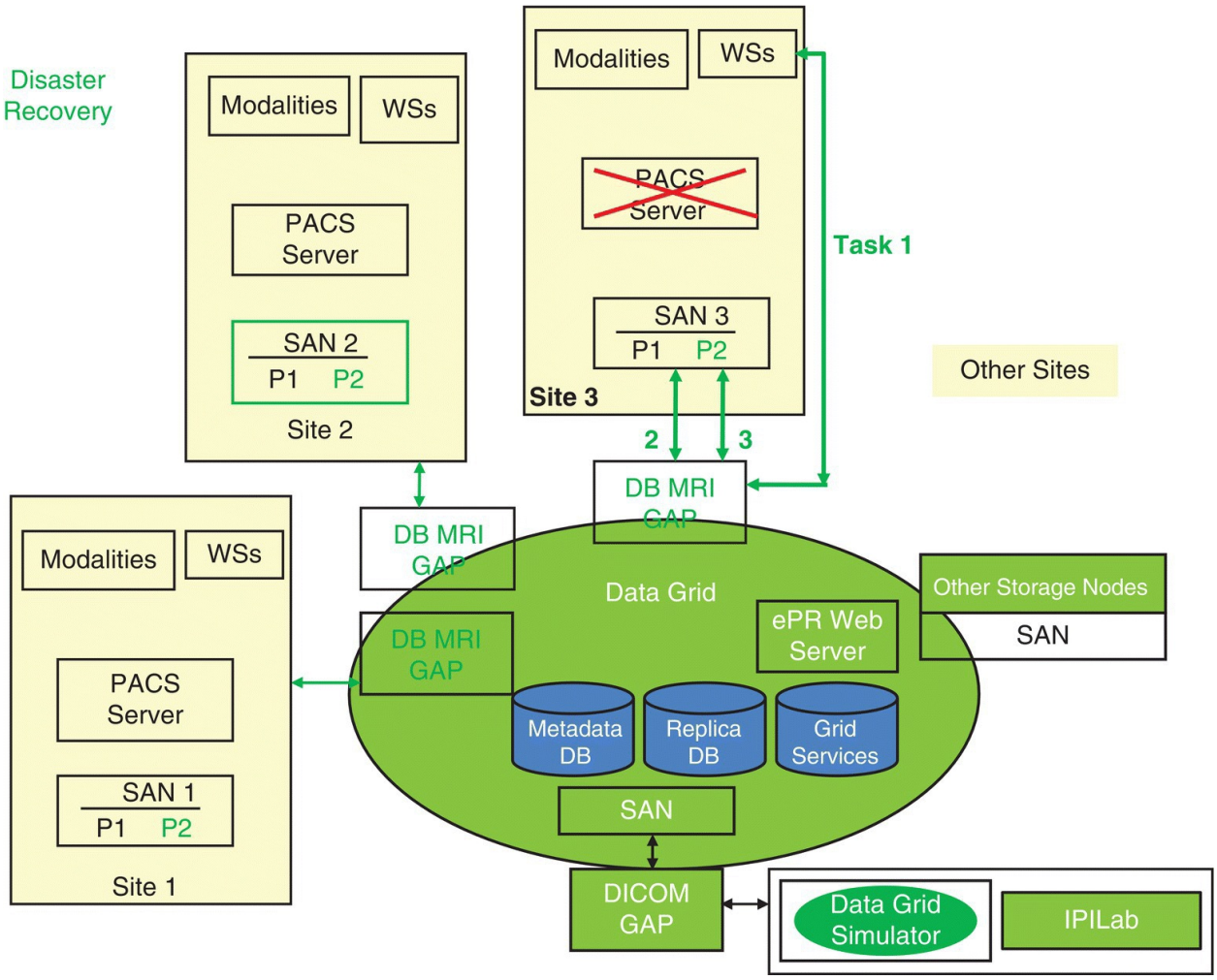

Figure 8.11 Three tasks (upper right, heavy green lines) of the Data Grid during disaster recovery when either a PACS server or the SAN fails. Site 3 is used as an example. Task 1: Allow site 3 PACS WS to Q/R its own images from the Data Grid for continuing clinical operation. Task 2: After server and SAN have been restored, the Data Grid rebuilds P1 of SAN 3 its own images. Task 3: After its server and SAN have been restored, the Data Grid rebuilds P2 of SAN 3, which has the backup images of other PACS connected to the Data Grid. All three tasks are performed without human intervention. Workflows and operations of Figures 8.9, and 8.10 allow the Data Grid to automatically complete the three tasks.

References

1 Allcock, W., Bresnahan, J., Kettimuthu, R., Link, M., Dumitrescu, C., *et al.* (2005) The Globus striped GridFTP framework and server. *Proc Super Comput*,

November 12–18, Seattle, WA: ACM, 1–11.

2 alRen, http://www.cenic.org/calren/index.htm, accessed on March 14, 2006.

3 Brown, M.S., Shah, S.K., Pais, R.C., Lee, Y., McNitt-Gray, M.F., *et al*. (2005) Database design and implementation for quantitative image analysis research. *IEEE Trans. Info Techno Biomed*, 9, 99–108.

4 Chan, L.W., Zhou, M.Z., Hau, S.K., Law, M.Y. and Tang, F.H. (2005) Documet J. International Internet-2,performance and automatic tuning protocol for medical imaging applications. *Comput Med Imag Graph*, 29, 103–114.

5 Chervenak, A., Foster, I., Kesselman, C., Salisbury, C. and Tuecke. S. (2001) The Data Grid: towards an architecture for the distributed management and analysis of large scientific datasets. *J Net Comput Appl*, 23, 187–200.

Further Reading

HARNET. http://www.jucc.edu.hk/jucc/content harnet.html, accessed March 14, 2006.

HIPAA Security Standard. http://www.hipaadvisory.com/regs/finalsecurity/

http://searchdomino.techtarget.com/news/article/0,289142,sid4m gci912158,00.html

https://cabig.nci.nih.gov/overview

http://wiki.ihe.net/index.php?title=Cross Enterprise Document Sharing

http://www-03.ibm.com/grid/pdf/fsgmas.pdf

http://dev.globus.org/ wiki/Incubator/MEDICUS

Huang, H.K., Zhang, A., Liu, B., Zhou, Z., *et al*. (2005) Data Grid for large-scale medical image archive and analysis. *Proceedings of the 13th ACM International Conference on Multimedia*, pp. 1005–1013.

Huang, H.K. (2004) *PACS and Imaging Informatics: Basic Principles and Applications*. Hoboken, NJ: Wiley.

Internet2, http://www.internet2.edu/, accessed March 14, 2006.

King, N.E. (2006) Information systems and healthcare XVII: operational stakeholder relationships in the deployment of a data storage grid for clinical image backup and recovery. *CommAssoc Info Sys*, 23(1), http://www.globus.org/solutions/data_replication/, accessed March 14, 2006.

Law, M.Y. and Zhou, Z. (2003) New direction in PACS education and training, *Comput Med Imag Graph*, 27, 147–156.

Liu, B., Zhou, Z. and Huang, H.K. (2005) A HIPAA-compliant architecture for securing clinical images. *SPIE Med Imag Conf Proc PACS and Imaging Informatics*.

Liu, B., Zhou, Z. and Documet, J. (2005) Utilizing Data Grid architecture for the backup and recovery of clinical image data. *Comput Med Imag Graph*, 29, 95–102.

Liu, B.J., Cao, F., Zhou, M.Z., Mogel, G. and Documet, L. (2003) Trends in PACS image storage and archive. *Comput Med Imag Graph*, 27, 165–174.

Liu, B.J., Zhou, Z., Gutierrez, M.A., Documet, J., Chan, L. and Huang, H.K. (2007) International Internet2 connectivity and performance in medical imaging applications: bridging Americas to Asia. *J High Speed Networks*, 16(1), 5–20.

McNitt-Gray, M.F., Aramato, S.G., Clarke, L.P., McLennan, G., Meyer, C.R. and Yankelevitz, D.F. (2002) The lung imaging database consortium: creating a resource for the image processing research community. *Radiology*, 225, 739–748.

Meinert, C.L. (1986) *Clinical Trials: Design, Conduct, and Analysis*. Oxford: Oxford University Press.

Moge, G.l., Huang, H.K., Cao, F., Zhou, Z., Dev, P., *et al*. (2002) NGI performance in teleradiology applications. *Proc. SPIE Med Imag*, 3, 25–30.

Ouchi, N.K. (1977) System for recovering data stored in failed memory unit. US Patent 714/5, 714/6, m714/807.

Piantadosi, S. (1997) *Clinical Trials: A Methodologic Perspective*. New York: Wiley.

Redundant Array of Independent Disks (RAID). http://en.wikipedia.org/wiki/Redundant array of independent disks, accessed March 14, 2006.

RNP2. http://www.rnp.br/en/, accessed March 14, 2006.

Schopf, J.M. and Nitzberg, B. (2002) Grids: top ten questions. *Sci Progr*, 10, 103–111.

Syslog (2007) http://www.loriotpro.com/Products/SyslogCollector/SyslogDataSheet ENv3.php, accessed December 2007.

TeraGrid. http://www.teragrid.org/, accessed March 14, 2006.

Zhou, X.Q., Huang, H.K. and Lou, S.L. (2001) Authenticity and integrity of digital mammography images. *IEEE Trans. Med Imag*, 20(8), 784–791.

Zhou, Z., Liu, B. and Huang, H.K. *et al*. (2005) A RIS/PACS simulator integrated with the HIPAA-compliant auditing toolkit. *SPIE Med Imag Conf Proc*.

Zhou, Z., Huang, H.K. and Liu, B. (2005) Digital signature embedding for medical image integrity in a Data Grid off-site backup archive. *SPIE Med Imag Conf Proc PACS and Imaging Informatics; SPIE Publication*.

Zhou, Z., Documet, J., Chan, L., *et al*. (2006) *The Role of a Data Grid in Worldwide Imaging-Based Clinical Trials*. USC UPU: Marina del Rey.

Zhou, Z., Liu, B.J., Huang, H.K. and Zhang. J. (2005) Educational RIS/PACS simulator integrated with the HIPAA compliant auditing (HCA) toolkit. *Proc SPIE Med Imag*, 6, 491–500.

9
Data Grid for Clinical Applications

CHAPTER MENU

9.1 Clinical Trials and Data Grid

9.1.1 Clinical Trials

9.1.2 Image-Based Clinical Trials and Data Grid

9.1.3 The Role of a Radiology Core in Imaging-Based Clinical Trials

9.1.4 Data Grid for Clinical Trials – Image Storage and Backup

9.1.5 Data Migration: From Backup Archive to Data Grid

9.1.6 Data Grid for Multiple Clinical Trials

9.2 Dedicated Breast MRI Enterprise Data Grid

9.2.1 Data Grid for a Dedicated Breast MRI Enterprise

9.2.2 Functions of an Enterprise Dedicated Breast Imaging MRI Data Grid (BIDG)

9.2.3 Components in the Enterprise Breast Imaging Data Grid (BIDG)

9.2.4 Breast Imaging Data Grid (BIDG) Workflows in image Archive and Backup, Query/Retrieve, and Disaster Recovery

9.2.5 Development of a Dedicated Breast MRI Data Grid Based on IHE XDS-I Workflow Profile

9.3 Administrating the Data Grid

9.3.1 Image/Data Security in Data Grid

9.3.2 Sociotechnical Considerations in Administrating the Data Grid

9.4 Summary

References

Further Reading

9.1 Clinical Trials and Data Grid

9.1.1 Clinical Trials [1]

The first section in this chapter provides some common understanding of clinical trials, followed by the role of radiology in imaging-based clinical trials, the use of a data grid for clinical trials, and administrating the Data Grid.

Clinical trials are used to evaluate the effectiveness and safety of a particular therapy, medication or medical device, by monitoring their effects on large groups of people. Clinical research trials may be conducted by government health agencies such as National Institutes of Health (NIH), researchers affiliated with a hospital or university medical program, independent researchers, or private industry.

Usually volunteers are recruited, although in some cases research subjects may be paid. Subjects are generally divided into two or more groups, including a control group that does not receive the experimental treatment, receives a placebo (inactive substance) instead, or receives a tried-and-true therapy for comparison purposes.

Typically, government agencies approve or reject new treatments based on the results of clinical trial. While important and highly effective in preventing obviously harmful treatments from coming to market, clinical research trials are not always perfect in discovering all adverse effects, particularly effects associated with long-term use and interactions between experimental drugs and other medications. For some patients, clinical research trials represent an avenue for receiving promising new therapies that would not otherwise be available. Patients with difficult to treat or currently “incurable” diseases, such as AIDS or certain types of cancer, may want to pursue participation in clinical research trials if standard therapies are not effective. Clinical research trials are sometimes lifesaving.

There are four possible outcomes from a clinical trial:

1. *Positive trial*: The clinical trial shows that the new treatment has a large beneficial effect and is superior to standard treatment.
2. *Non-inferior trial*: The clinical trial shows that the new treatment is equivalent to standard treatment. Also called a non-inferiority trial.
3. *Inconclusive trial*: The clinical trial shows that the new treatment is neither clearly superior nor clearly inferior to standard treatment.

4. *Negative trial*: The clinical trial shows that a new treatment is inferior to standard treatment.

9.1.2 Image-Based Clinical Trials and Data Grid

The medical imaging component of PACS-based informatics has become an important tool in clinical trials used to evaluate the effectiveness and safety of medications or medical devices by monitoring their effects on large groups of people. It is because images provide a unique and fast diagnosis with visual observance and quantitative assessment. A typical imaging-based clinical trial consists of:

1. a well-defined, rigorous clinical trial protocol;
2. a radiology core that has a quality control mechanism, a biostatistics component, and an archive server for storing and distributing data and analysis results; and
3. many field sites that generate and send clinical trial image studies to the radiology core.

With an ever-increasing number of clinical trials, it becomes a great challenge for a radiology core that handles multiple clinical trials to have a robust server to administrate multiple trials, as well as to satisfy the requirements to quickly distribute information to participating radiologists/clinicians worldwide to assess the trial results. The Data Grid, as a grid computing technology, can satisfy the aforementioned requirements of imaging-based clinical trials.

9.1.3 The Role of a Radiology Core in Imaging-Based Clinical Trials

Medical imaging is taking on a prominent role in the early detection and quantization of new diseases or the change in diseases. Multiple imaging-based clinical trials provide the required number of cases examined by using images from unbiased populations required to test new diagnostic, therapeutic techniques, or agents. Through the years, although the methodology and protocols of clinical trails have gradually improved, Figure 9.1 remains as a good representation of a general organization chart of a medical imaging-based clinical trial. The radiology core in this figure has the responsibilities of collecting imaging data from multiple field sites with quality control, and an archive server for storing and distributing trial results to field sites. The field sites recruit patients and generate images and send to the radiology core, as

depicted in Figure 9.2.

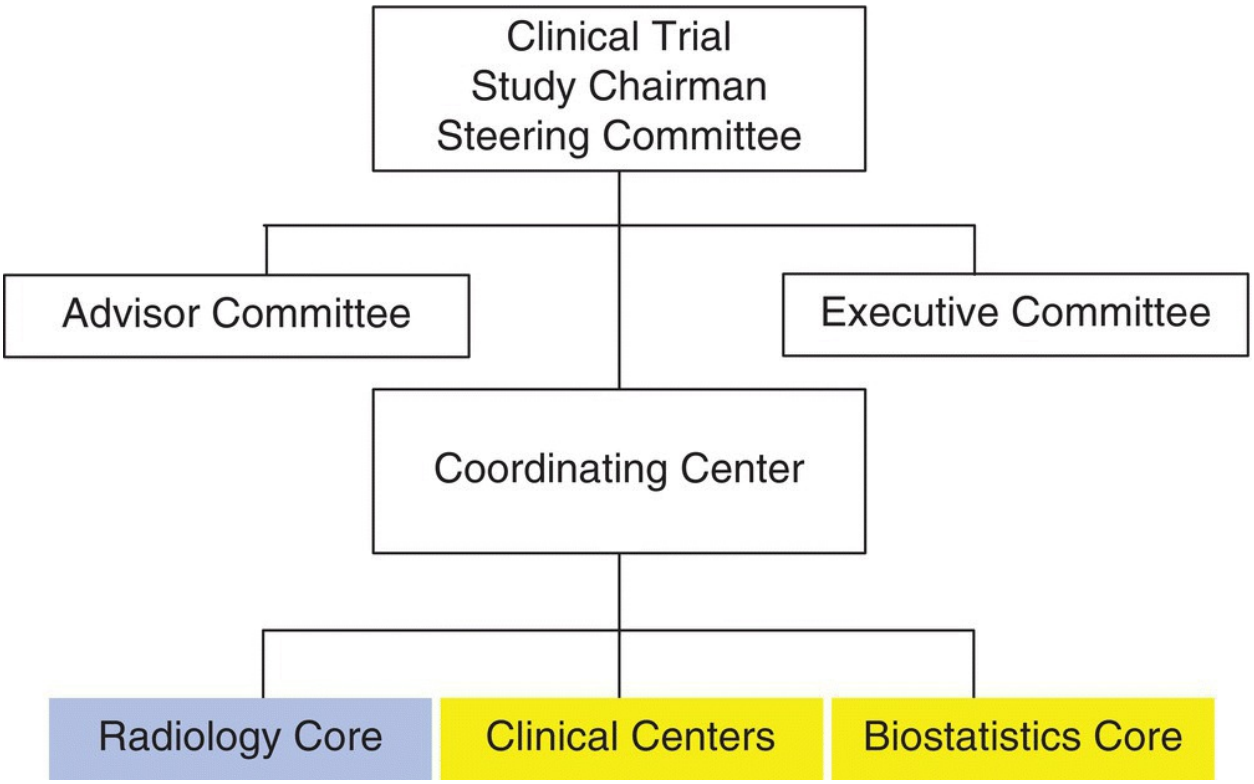

Figure 9.1 Organizational chart of an imaging-based clinical trial. Radiology core (blue) is responsible for all image-related operations.

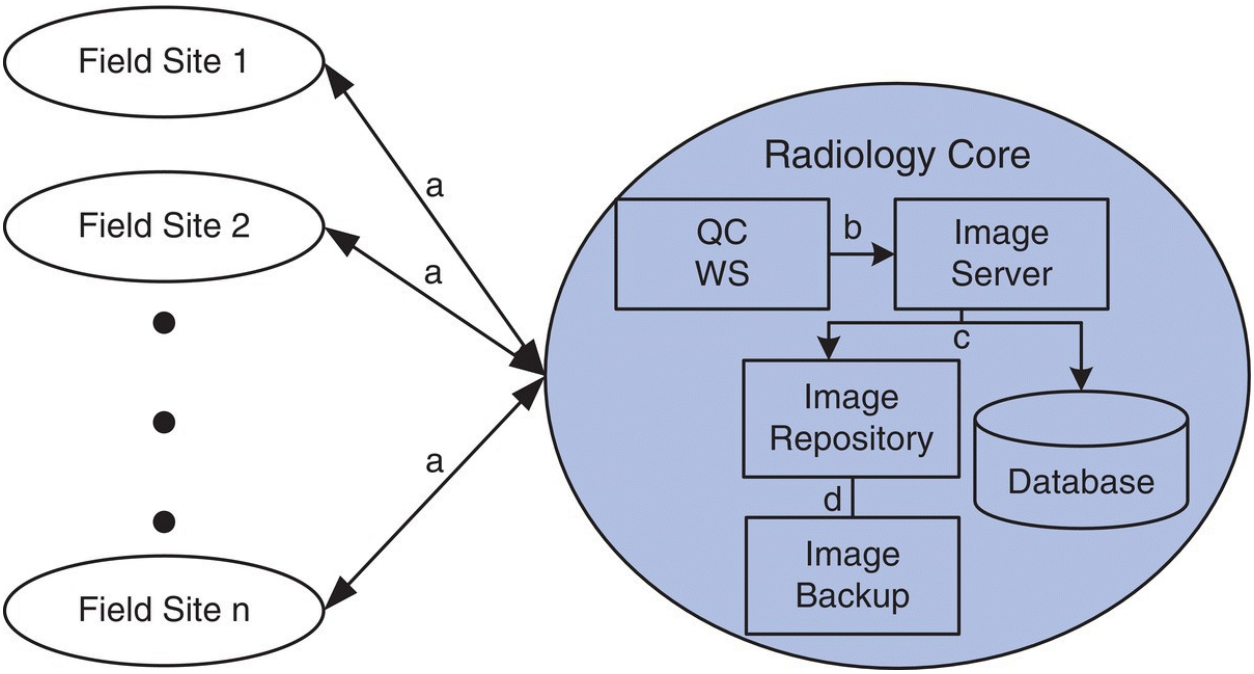

Figure 9.2 Typical workflow of the imaging-based clinical trial. The images are

sent from field sites (1, 2, …, *n*) to a radiology core (blue), where the images are checked by a quality control (QC) workstation (WS) (point a). Images are stored in the image server (point b). The server archives images in an image repository and stores the metadata of the image in the database (point c). The images in the repository are backed up (point d).

The general workflow of an imaging-based clinical trial with three Cores A, B, and C is shown in Figure 9.3 (for now, ignore the Data Grid infrastructure component in green color). There are four steps in this figure:

1. There could be 1 – *n* field sites in a radiology core, which generate DICOM format image data related to the patients enrolled in a specific clinical trial and transmit the image data to the radiology core (Figures 9.1 and 9.2) through various digital networks or storage media, such as a CD or SAN). The image data are anonymized before they are distributed to various sites.
2. The images received by the radiology core go through a QC (quality control) WS (workstation) to assure image quality; for example, regarding patient positioning during the imaging examination, scanning localization, equipment calibration, acquisition parameters, and patient demographic information. Once the quality of the images is approved, the images are sent to a centralized image server.
3. The image server extracts the metadata from the DICOM header of the image and stores the metadata and related patient information in the database of a data repository, such as a redundant array of independent disks(RAID). The images are distributed to assigned radiologists of field sites worldwide to make the diagnosis. The diagnosis results, usually a quantity, are returned and stored in the metadata database.
4. The images stored in the repository are backed-up in an off-line manual storage device.

This workflow and setup at the radiology core can satisfy a small number of clinical trials. With the ever-increasing number of clinical trials, it becomes a great challenge for a radiology core that handles multiple clinical trials to have a robust server to administrate multiple trials, as well as satisfying the requirements to quickly distribute information to participating radiologists/clinicians worldwide to assess trials' results. In addition, different clinical trials can vary in the parameters of results. A dynamic database model is necessary for the image server in the radiology core to accommodate new clinical trials. All these issues underline the need for a new infrastructure that

can satisfy the requirements of imaging-based clinical trials. The Data Grid, described in the previous section, is an emerging image storage and distribution computing technology that is an ideal solution to this new demand.

9.1.4 Data Grid for Clinical Trials – Image Storage and Backup

In order to form a Data Grid for clinical trials, participating radiology cores have to join a Data Grid confederation, something similar to the enterprise PACS discussed in Sections 8.3 and 8.4 of Chapter 8. In this section, three radiology cores are modeled to illustrate the Data Grid concept using a DICOM store for image data and backup, query/retrieve, and recovery, as shown in Figure 9.3. The premises are that during the implementation phase, the Data Grid cannot affect the current radiology core data storage backup operation, and that once the Data Grid is in operation, the existing radiology core storage backup can be dismantled and the radiology core workflow replaced by the Data Grid. The Data Grid concept can be extended to support more than three radiology cores.

Consider Figure 9.3 with the three cores A, B, and C, now they are connected to the Data Grid infrastructure (green) for clinical trials. The image backup storage (e.g. SAN) in every radiology core is separated into partitions P1 and P2; P1 is for local radiology core backup, while P2 is contributed to the Data Grid to form a virtual large backup storage for other radiology cores participating in the Data Grid. The image server in each core sends a second copy of the image to the Data Grid, which automatically replicates it into two additional copies stored in the other two cores. In this case, images from core A will also be stored in P2 at cores B and C. This will ensure fault tolerance (FT) within the Data Grid in case a storage resource is unavailable. Remember, in the current operating radiology core without the Data Grid, the backup uses standard hard disks, as shown in Figure 9.2. With the Data Grid, the archive and backup, query/retrieve, and disaster recovery procedures are taken care of by following the Data Grid workflow described in Figures 8.9, 8.10 and 8.11 in the previous chapter.

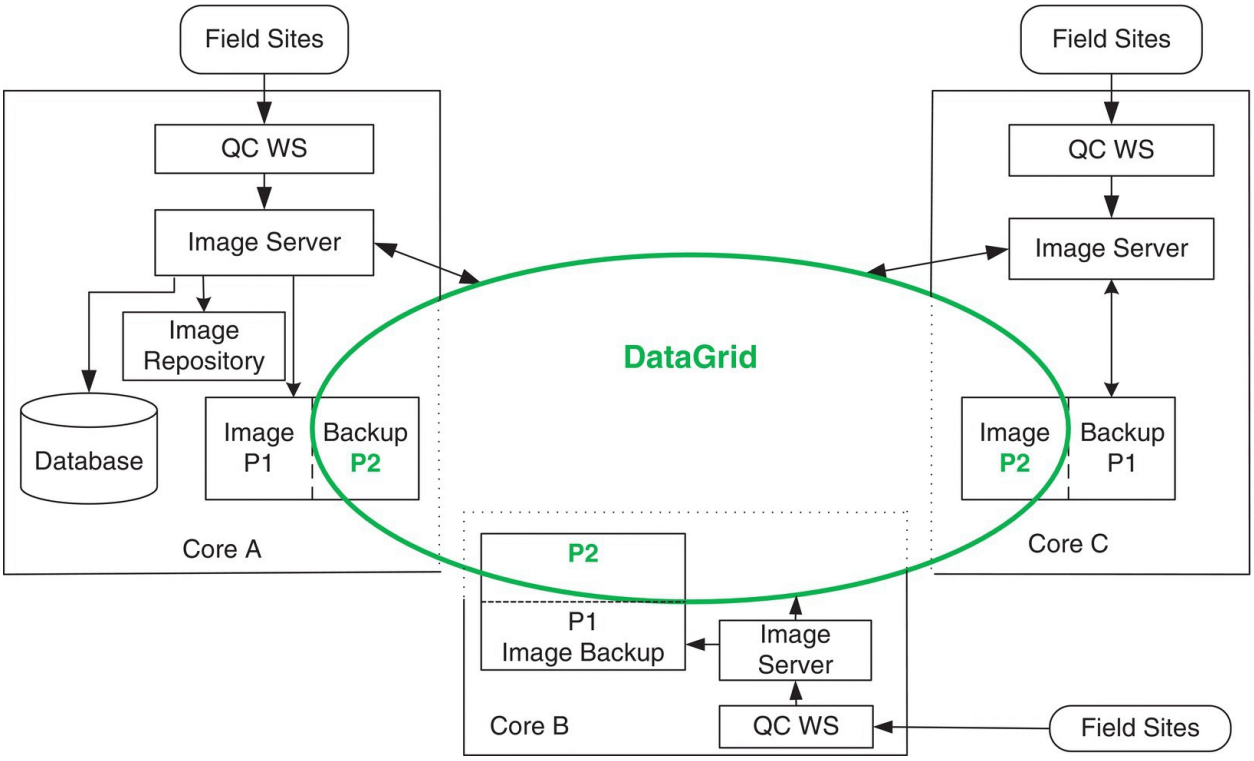

Figure 9.3 Three-cores Data Grid architecture (green) for image backup in clinical trials. Cores A, B, and C have the same setup. The image backup storage (e.g. SAN) in every radiology core is separated into two partitions, P1 and P2. P1 is used for local backup, while P2 is contributed to the Data Grid for backup of images from other cores. Note that the Data Grid has not intruded on the core's backup operation in the image repository. Figure 9.5 also describes the data migration process from the current local hard disk backup to P1 of the SAN.

9.1.5 Data Migration: From Backup Archive to Data Grid

To replace the existing storage backup while the Data Grid is being deployed, a data migration process has to be introduced. This subsection discusses two data migration steps to:

1. start to archive all new images to its own SAN; and
2. replace the existing local backup in the radiology core to the Data Grid.

Following the Data Grid configuration described in Figure 9.3, then Figures 9.4 and 9.5 can be used to demonstrate how to migrate images from the local backup to the Data Grid.

The clinical trial radiology core test bed with three international sites is used as an example. They are at the Image Processing and Informatics Laboratory

(IPILab), University of Southern California; the PACS Lab, Hong Kong Polytechnic University (PolyU); and the Heart Institute (InCor), University of Sãao Paulo, Brazil. All three sites have the same version of the Globus Toolkit integrated with DICOM services and are connected with the International Internet 2 [2]. The IPILab SAN in core A (Figure 9.4, left) is used as a Data Grid confederation for illustration purpose [3].

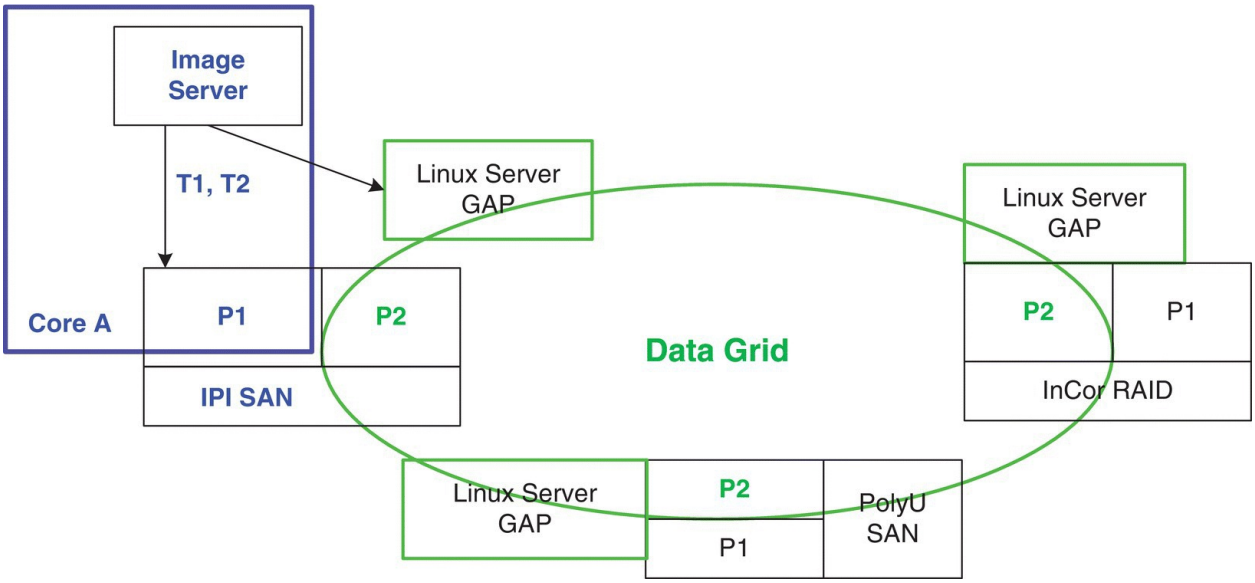

Figure 9.4 Data Grid test bed (green) with three International sites at the Image Processing and Informatics Laboratory (IPI SAN), University of Southern California; the Hong Kong Polytechnic University (PolyU); and the Heart Institute (InCor) at University of São Paulo, Brazil. The test bed used two real clinical trials image sets (MRI T1 and T2 images) for the validation of the Data Grid. IPI (left, blue) is used as the site for testing data migration.GAP: grid access point; P1, P2: partition 1, 2; RAID: redundant array of independent disks.

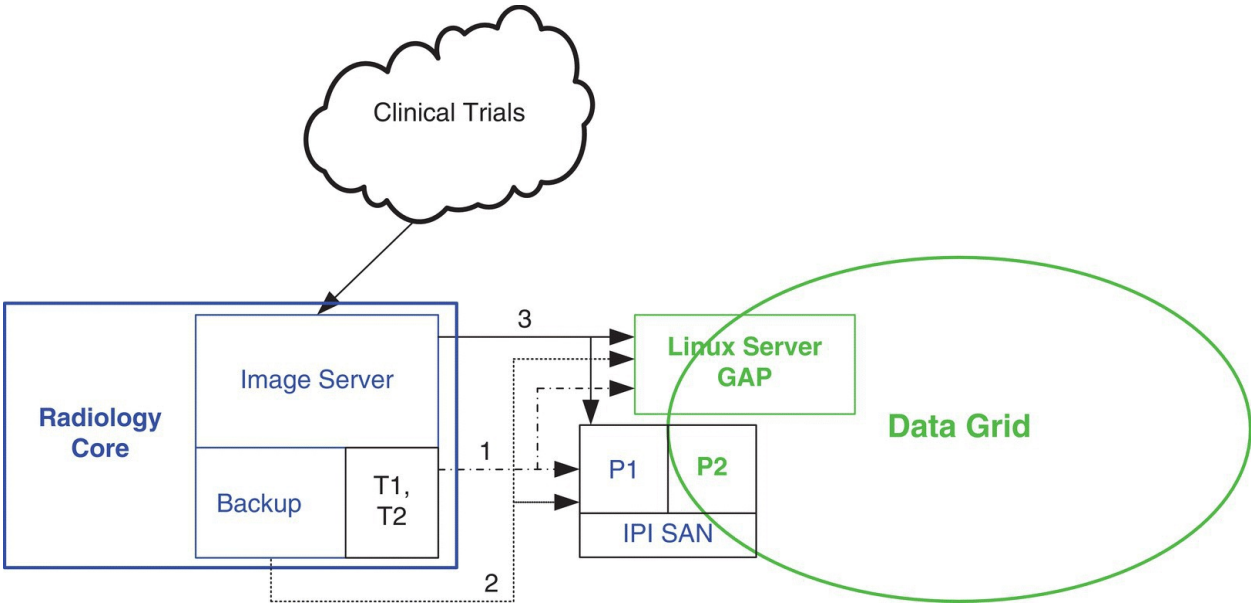

Figure 9.5 Data migration from existing backup storage to the Data Grid (right, green) during Data Grid deployment. Image migration from the local backup of the radiology core (left, blue) to P1 of the IPI SAN and the Data Grid is through a three-step procedure. In this scenario, after completion of the Data Grid deployment, the SAN becomes the local backup archive for the clinical trials' images of the Laboratory. P1 is the core's own backup, and P2 is used to back up for other cores. GAP: grid access point; T: trial.

1. Following the workflow shown in Figure 9.5, two clinical trials (T1 and T2) start with a small number of enrolled patients. For any new image received by the image server sent by a clinical trial site (Figure 9.2), one copy of the image is stored within the radiology core's existing local backup storage. The local backup sends a copy to P1 of the IPILab SAN as the archive in the core, which is designated as the migrated new images from the existing local backup to its SAN (IPI SAN), one image at a time. Meanwhile, the local backup also sends a copy to the Linux server (grid access point, GAP) at the Data Grid for backup. The Data Grid will maintain two copies of the image in two remote storage areas (see Figure 9.4, two P2s at PolyU and InCor).
2. Once all testing and evaluation of step 1 are satisfactory, one copy is sent of all historical backup images of the same patient enrolled in T1 and T2 in the local backup to P1 of the IPILab SAN, and another copy is sent to the Linux server at the Data Grid, which replicates it to two more copies stored at P2s of two remote cores. Step 1 continues if more new images are coming in during step 2.

3. When step 2 is completed, IPILab SAN P1 has all backup images of trials T1 and T2, both new and historical. The image server then stops sending images to the local backup. But the image server will begin to send any new images of trials T1 and T2 to P1 of the SAN as the local archive, and also send a copy to the Data Grid for backup, which replicates two copies in two P2s of other cores. The data migration procedure for trials T1 and T2 is completed, and traditional local backup at the core can be dismounted.

9.1.6 Data Grid for Multiple Clinical Trials

With the use of more digital imaging modalities, such as digital mammography, multiple slices CT, MRI, and US images in clinical trials, as well as the ever-increasing number of clinical trials, the current informatics system infrastructure of the radiology core becomes saturated. It is no longer able to handle multiple trials satisfying the requirements of fault tolerance in image data, and analyzing results to quickly distribute images and reports to worldwide experts involving in the trials.

This section discusses the use of Data Grid for the radiology core in clinical trials. A Data Grid test bed with three international sites for backup of clinical trial images from multiple imaging cores has been presented with a data migration scheme. The Data Grid concept has several advantages to multiple trial databases:

1. fault tolerance;
2. data and result sharing; and
3. dynamic creation and modification of the data model to support any new trial or change of trials.

In addition to using the Data Grid for clinical trials, the radiology/imaging cores inside the Data Grid can be embedded so that the computer process or analysis software from multiple cores can be shared and be fault tolerant. The ultimate goal of the Data Grid in clinical trials is to provide a large virtual distributed fault-tolerant data system for a variety of clinical trials to store, backup, and share images and results among multiple clinical trials. Such a Data Grid infrastructure would allow trials images and results to be pooled and mined for hidden knowledge, which could eventually improve clinical trials outcomes. Since the use of the Data Grid in clinical trials is a relatively new concept, extensive current research results are given in references provided in this chapter.

9.2 Dedicated Breast MRI Enterprise Data Grid

This section presents the concept and the implementation of a dedicated breast MRI enterprise Data Grid.

9.2.1 Data Grid for a Dedicated Breast MRI Enterprise

During the past decade, healthcare centers have emerged in specialized women's health needs, particularly in breast imaging. Many breast imaging centers perform all types of breast imaging examinations, including digital mammography (DM), ultrasound imaging (US), 3-D US, US biopsy, and MRI. All these imaging modalities are dedicated to specialized breast imaging, except the MRI. The reason is that the MRI modality calls for very expensive imaging equipment, so it is not cost-effective to have a general MRI system to take care of only breast imaging. This situation has created a niche in the development of the dedicated breast (DB) MRI scanner, a relatively lower-cost MRI scanner compared with whole-body MRI, yet it provides the required quality for breast imaging. However, because DB MRI is lower in cost compared with a generalized MRI system, it may not have the common DICOM connectivity, file format and structure, and backup archive to be readily integrated into the daily PACS and informatics operation. During the past few years, DB MRI has found a market in breast imaging centers, due to the cost of a DB MRI becoming financial affordable by a breast imaging center or MRI manufacturers making a profit-sharing arrangement with the centers. In certain favorable situations, a manufacturer may even finance a geographic region with DB MRI systems to establish DB MRI enterprises. Under these situations, a Data Grid has become an ideal add-on component to help the DB MRI centers to integrate the purchased centers with other types of breast imaging modalities. In the case of enterprise DB MRI, the manufacturer may manage many DB MRI systems in a region, and even in multiple regions. The next section presents the concept of Data Grid for the DB MRI enterprise.

9.2.2 Functions of an Enterprise Dedicated Breast Imaging MRI Data Grid (BIDG)

The DICOM-based enterprise dedicated MRI breast imaging Data Grid (BIDG) is an infrastructure that supports the management of large-scale breast imaging archive and distribution. The Aurora Imaging Technology, Inc. (www.auroramri.com) dedicated breast MRI enterprise system is used as an example. The BIDG has the following functions:

1. It archives AURORA 3-D dedicated breast MRI images, and patient records related to the MRI study, including other modality type breast images in DICOM format and diagnostic reports.
2. The Data Grid provides fault tolerance to all archived data.
3. The BIDG also utilizes DICOM structured report standard and Integrating Healthcare Enterprise (IHE) workflow profiles linking special quantitative.
4. DICOM metadata, reports, and breast images comprise the patient's record distributed through the Data Grid.
5. Within an AURORA enterprise BIDG, any site can access patient records, including images and reports from other sites, provided that permission has been granted by the enterprise. In addition, access rights to patient records from different sites can be controlled through security protocols within the BIDG.
6. Following item 4, any Aurora workstation (WS) can display dedicated AURORA 3-D breast MRI images from other sites, including the quantitative metadata through a DICOM structured report.

9.2.3 Components in the Enterprise Breast Imaging Data Grid (BIDG)

Three dedicated breast MRI systems in the enterprise BIDG are used as an example. The left-hand side of Figure 9.6A depicts the relative size of a standalone Aurora dedicated BIDG MRI scanner, and the right-hand side, major components of the scanner. Figure 9.6B shows multimodality web-based AURORA viewing workstation (left to right) delineating sagittal MRI, axial MRI, 3-D US, digital mammogram, and lower, CAD structured reporting. Figure 9.6C shows one rotating view of a 3-D MRI study, and Figure 9.6D delineates the BIDG platform ready for its connection to three MRI sites. Figure 9.7 shows the connection of three AURORA MRI scanners (yellow) to the BIDG (green) of an enterprise BIDG. Compare the similarity of the Data Grid architecture in this figure to Figure 8.11 (three PACS) in the previous chapter.

The four main components in the enterprise BIDG are:

1. *SAN with P1 and P2 partitions*: The SAN device at each site is divided into two partitions, P1 and P2. P1 is used for its own patients' records, and P2 contributes to the other two sites for their backup archive within the BIDG.
2. Each image from each site has three copies, one in its own SAN P1 and two

SANs P2 for the two other sites that are stored within the BIDG. However, while P2 in each SAN is physically located in the SAN of the site, logically, once P2 is committed to the BIDG for the other site's backup, it serves only to this BIDG (see Figure 9.7, where all P2s designate storage nodes are dedicated to the BIDG).

3. *The DICOM Conversion Unit (DCU)*: The DCU converts AURORA 3-D MRI images or any other related breast images (DM, US, etc.) of the patient to the DICOM standard, if necessary. It also converts a specialized MRI report to DICOM structured reporting (SR) format, allowing the linkage between the report, images, and quantitative metadata. This feature allows:
    a. tracking patient progress from multiple studies;
    b. performing data mining for patient outcome analysis; and
    c. developing breast imaging teaching files. The converter also coverts AURORA 3-D MRI DICOM images to AUROR WS display format.
4. *Dedicated Breast (DB) MRI and DICOM Grid Access Point (GAP)*: The DB MRI GAP (black box with green fonts) provides storage and query/retrieve services for any DICOM-compliant WS of any MRI system to access data within the Data Grid. There are multiple GAPs in the Data Grid (see Figure 9.7, green fonts) and can be used as backups for each other. The DICOM GAP provides the transfer of DICOM files from other DICOM-compliant breast imaging modality. If the AURORA enterprise conforms to the DICOM standard already or in the foreseeable future, the DICOM GAP may not be necessary.
5. *Database Services*: A service that keeps track of DICOM metadata, as well as file locations of different storage nodes within the Data Grid (see components within the green ellipse in Figure 9.7). Dynamic and robust access to data is provided by the data aAccess interface (DAI) in the Globus Toolkit integrated with the database (see Figure 8.8 in the previous chapter).

9.2.4 Breast Imaging Data Grid (BIDG) Workflows in image Archive and Backup, Query/Retrieve and Disaster Recovery

Figure 9.7 depicts the general connection to the three sites and workflow of the BIDG (compare with Figure 8.11 in the last chapter). The three major functions in the BIDG, image archive and backup, query/retrieve, and automatic disaster

recovery, are similar to those shown in Figures 8.9, 8.10, and 8.11 in the previous chapter, respectively. Site 3 (middle top) is used to demonstrate the image disaster recovery. An ePR Web server (white rectangular box inside the green color ellipse box) is added to the Data Grid to demonstrate the use of ePR as a means of managing the patient data of the BIDG at the enterprise level.

(A)

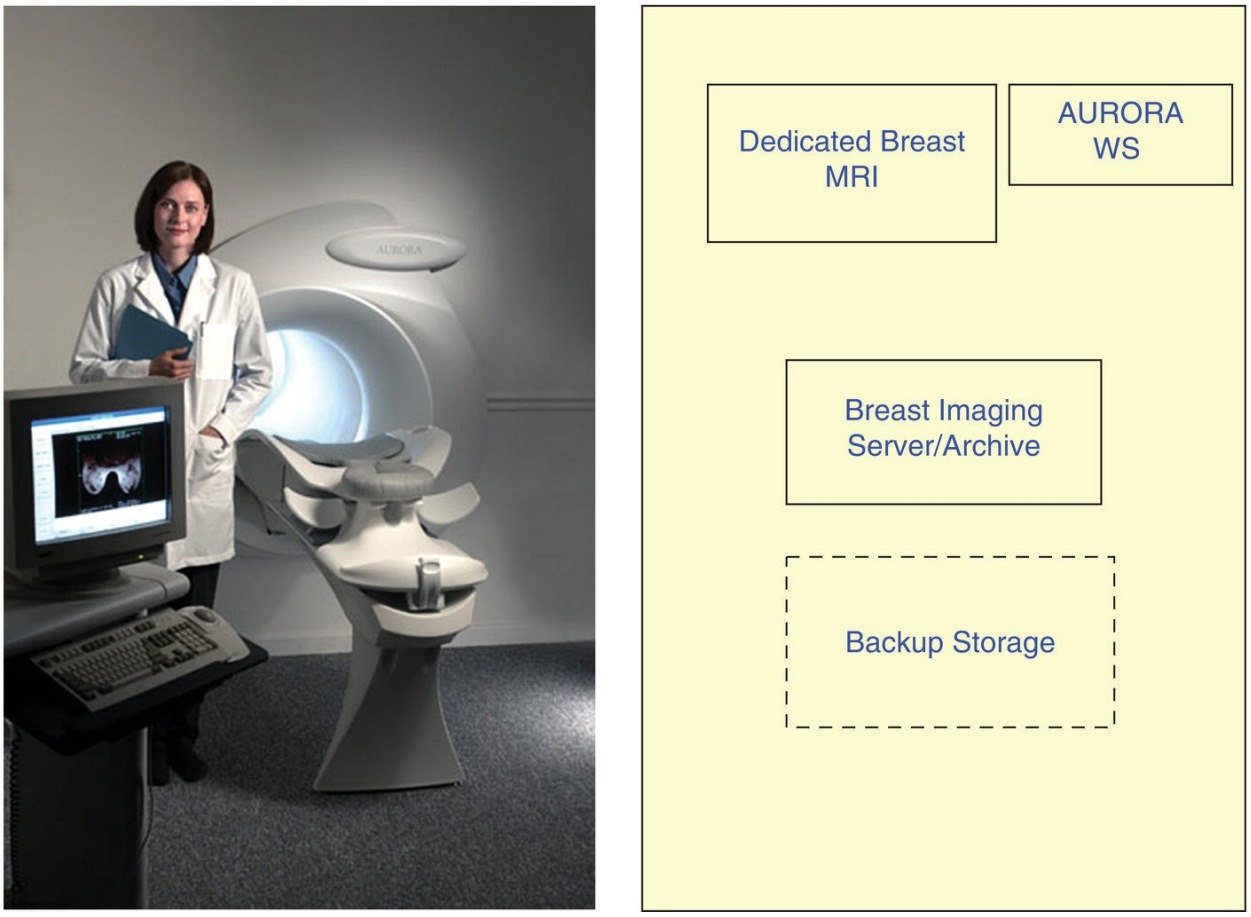

(B)

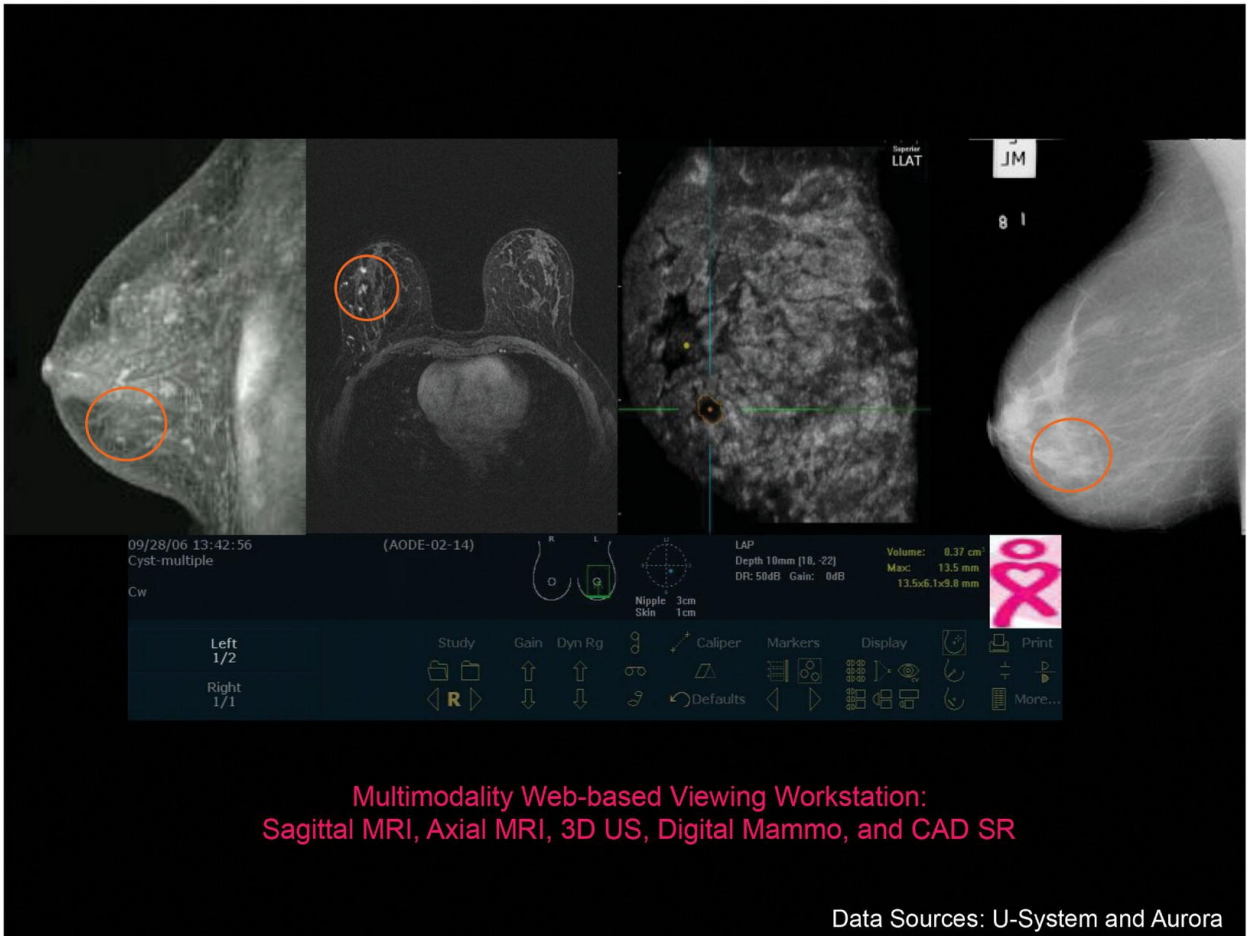
LLAT
JM
09/28/06 13:42:56
Cyst-multiple
Cw
(AODE-02-14)
LAP
Depth 10mm [18, -22]
DR: 50dB Gain: 0dB
Volume: 0.37 cm³
Max: 13.5 mm
13.5x6.1x9.8 mm
Nipple
Skin
3cm
1cm
Left
1/2
Right
1/1
Study
Gain
Dyn Rg
Caliper
Markers
Display
Print
Defaults
More...
Multimodality Web-based Viewing Workstation:
Sagittal MRI, Axial MRI, 3D US, Digital Mammo, and CAD SR
Data Sources: U-System and Aurora

(C)

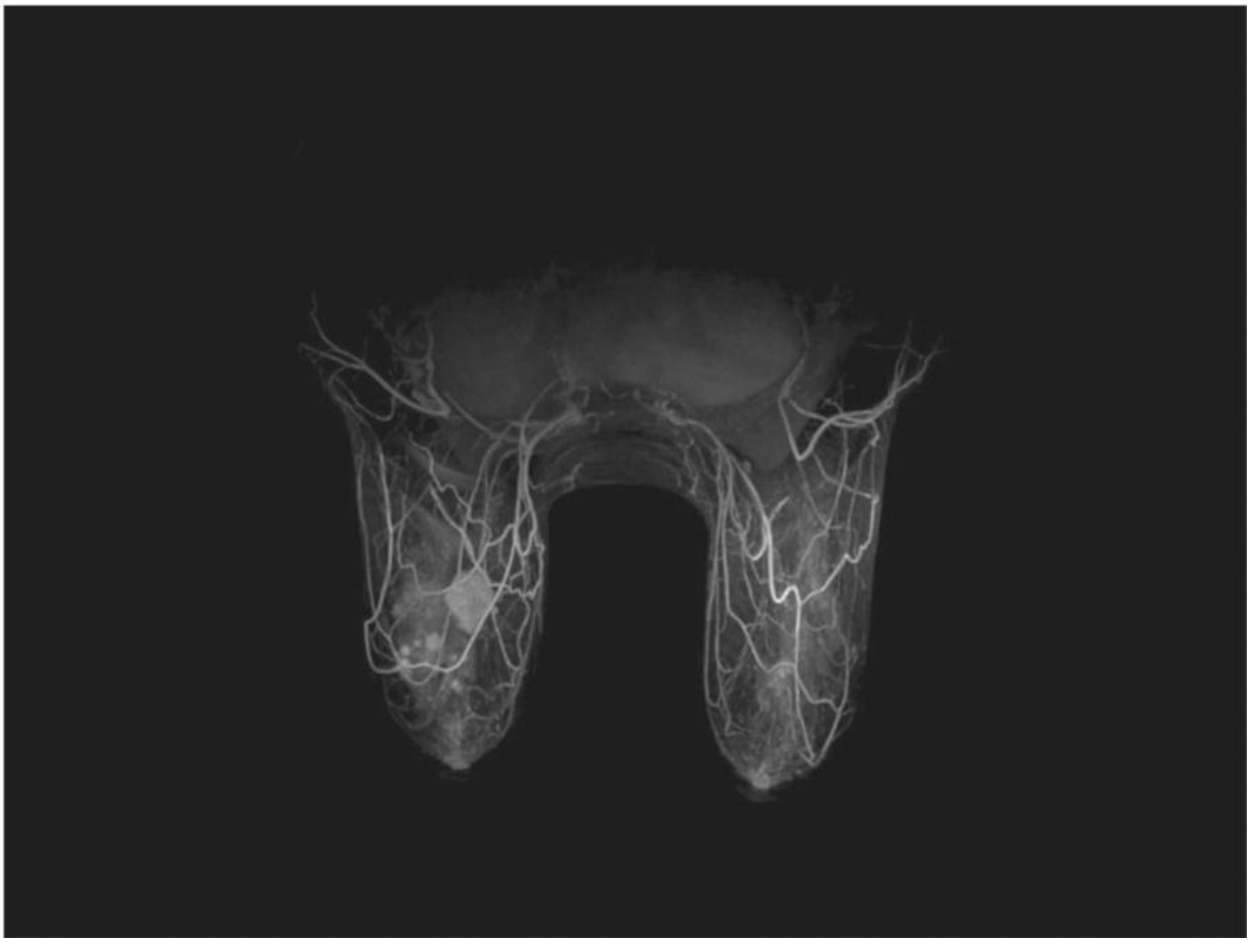

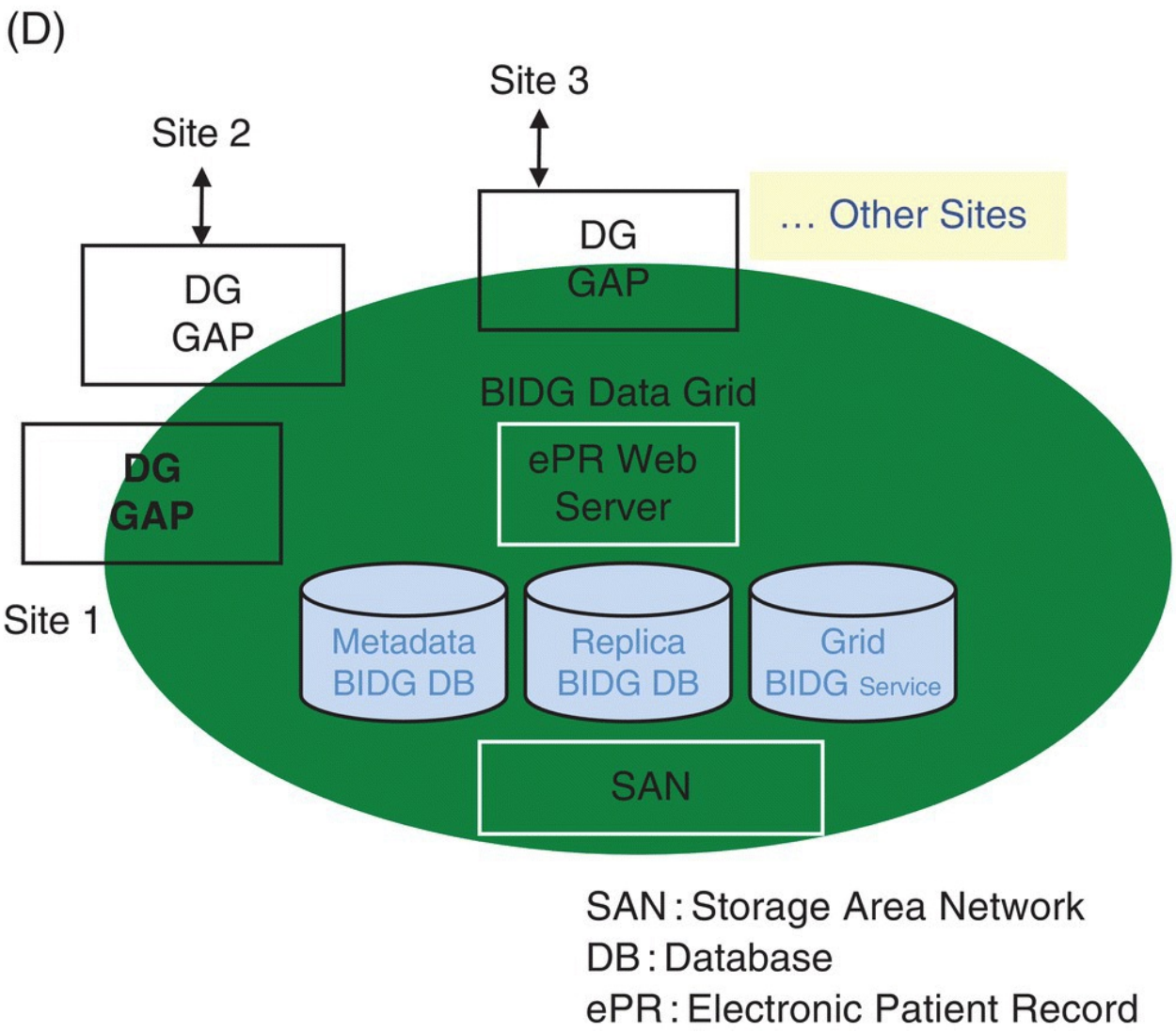

Figure 9.6 (A) Left: Relative size of the AURORA dedicated stand-alone breast MRI scanner. Right: Major components of the scanner. (B) Multimodality Web-based viewing workstation: Sagittal MRI, Axial MRI, 3-D US, digital mammography, and CAD Structure reporting. (C) One view of a 3-D MRI study using the AURORA dedicated breast MRI scanner. The patient was in the prone position with her two breasts extruded through the two round openings from the table (courtesy of AURORA, Imaging Technology, Inc.). (D) Imaging data grid (BIDG) platform ready to be connected to three MRI sites. The ePR Web server is an additional component in the data grid (DG) for the enterprise system patient electric records.

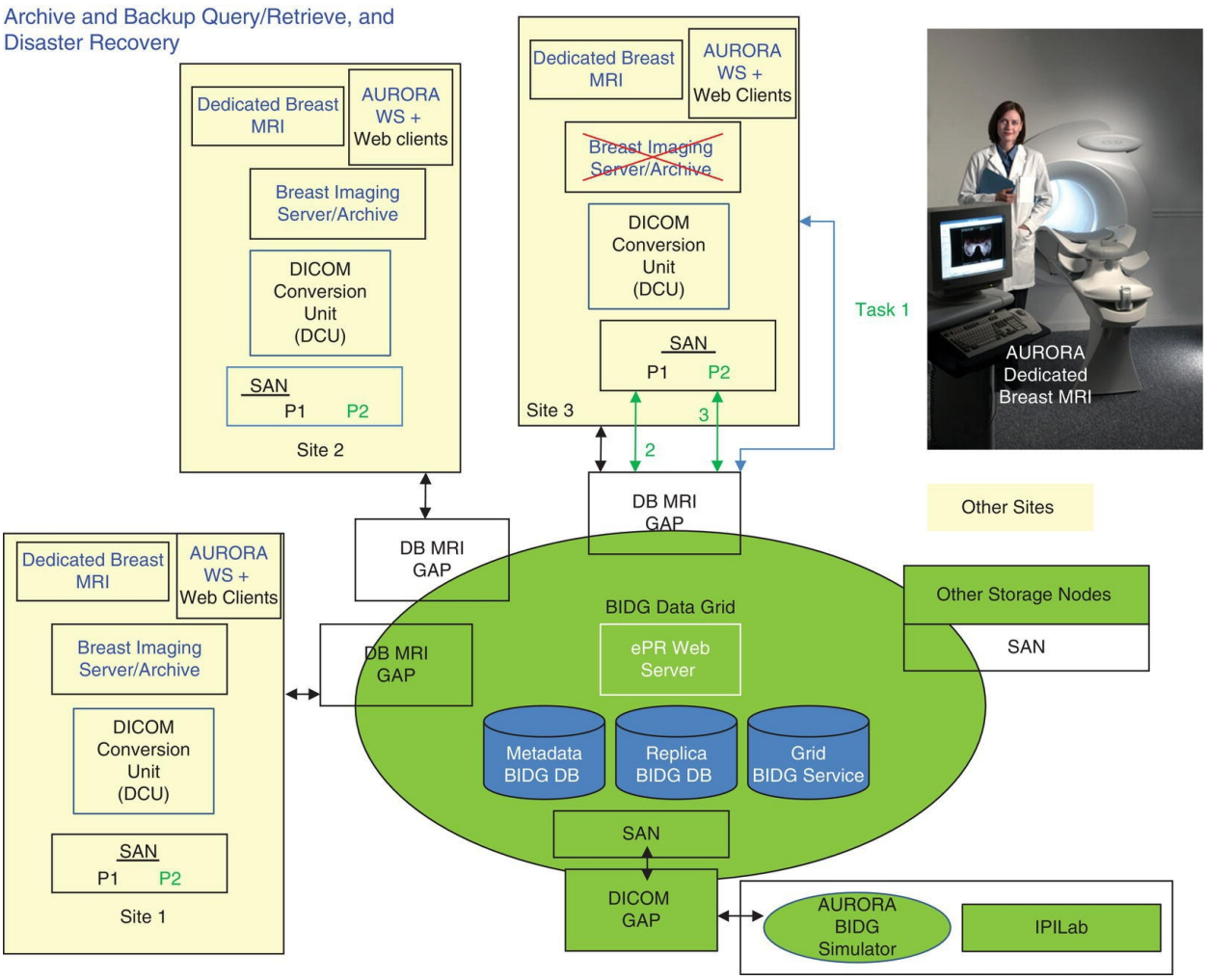

Figure 9.7 The DICOM-based enterprise dedicated MRI breast imaging Data Grid (BIDG) is an infrastructure that supports large-scale breast imaging archive and distribution management. The AURORA-dedicated MRI enterprise is used as an example. Compare the similarity between this figure and the general Data Grid architecture shown in Figure 8.11 in Chapter 8. Two additional components in this figure are the ePR Web server and the DICOM conversion unit (DCU) explained in the text (courtesy of AURORA Imaging Technology, Inc.). DB: database; GAP: grid access point; IPILab: Image Processing and Informatics Laboratory, University of Southern California; SAN: storage area network; WS: workstation.

9.2.5 Development of a Dedicated Breast MRI Data Grid Based on IHE XDS-I Workflow Profile

9.2.5.1 Purpose

The utilization of dedicated breast (DB) MRI is increasing in the diagnostic evaluation of suspicious breast findings. As more imaging centers implement DB MRI, the need for clinical research-oriented data mining and remote real-time patient screening is becoming more apparent. The BIDG is a distributed and dedicated breast MRI data grid system based on the IHE XDS-I workflow profile that addresses the DICOM-compliance, fault-tolerance, and data privacy needs of sharing breast MRI studies over WAN and between multiple users. It delivers large MRI studies securely and robustly across broadband connectivity to researchers, trained radiologists, and surgeons at multiple sites, using efficient grid technology, all the while providing internal queue handling, load balancing, and rules-based archive management. When the BIDG Data Grid was first developed, 2009–2013, the IHE XDS-I workflow profile was not readily available for large-scale clinical use. This section describes how to connect BIDG with the IHE XDS-I and use it for the enterprise dedicated breast Imaging MRI Data Grid.

9.2.5.2 Method

The BIDG system consists of distributed Web services that receive, archive, manage, distribute, and display breast MR studies and reports for multiple users at geographically remote sites. The hardware components include user workstations and a grid node server at each site, a centralized grid management server, a web-based BIDG ePR user interface for visualizing breast MRIs and reports, and two or more large-capacity storage devices at predetermined locations. The workflow within the BIDG, including different types of breast images, diagnoses, US biopsy results, and reports, is based on the IHE XDS-I workflow profile for optimized image data registration, discovery, and delivery (Figure 9.8). To review the IHE XDS-I, some of the information here was excerpted from the IHE Wiki [4]:

> *Cross-Enterprise Document Sharing (XDS) is focused on providing a standards-based specification for managing the sharing of documents between any healthcare enterprise, ranging from a private physician office to a clinic to an acute care in-patient facility and personal health record systems. This is managed through federated document repositories and a document registry to create a longitudinal record of information about a patient within a given clinical affinity domain. These are distinct entities with separate responsibilities:*
>
> 1. *A Document Repository is responsible for storing documents in a*

transparent, secure, reliable and persistent manner and responding to document retrieval requests.

2. *A Document Registry is responsible for storing information about those documents so that the documents of interest for the care of a patient may be easily found, selected and retrieved irrespective of the repository where they are actually stored.*
3. *Documents are provided by one or more Document Sources.*
4. *They are then accessed by one or more Document Consumers.*

Benefits of this development are: to Facilitate management of the Electronic Health Record.

The Cross-Enterprise Document Sharing (XDS) Integration Profile is a workflow profile of IHE9. An enterprise level healthcare system adopting this profile can use the Data Grid concept to implement its operation.

XDS aims to provide a standards-based specification for managing document sharing with any healthcare enterprise, ranging from a private physician office, to a clinic, an acute care inpatient facility, and personal health record systems. XDS is managed through a federation of document repositories. A document registry maintains patients' medical histories and can create a record of information about a patient for a given clinical need. The four distinct entities are the Document Repository, for storing documents, which is provided by Document Sources, and the Document Registry, which provides information about the documents, and is accessed by Document Consumers. The file transfer mechanism can be HTTP, HL7, or DICOM. Since XDS is a profile or a document transfer model, the responsibilities of data management and fault tolerance are left to the healthcare organization. Potential users are national EHR healthcare centers supported by regional health information organizations, and others. Figure 9.8 shows the IHE cross-enterprise frameworks.

IHE International is composed of more than 175 member organizations (as of May, 2016) from around the world, committed to improving the interoperability of healthcare information systems. An organization that becomes a member of IHE International may designate representatives to participate in Domain Committees and National/Regional Deployment Committees relevant to its interests.

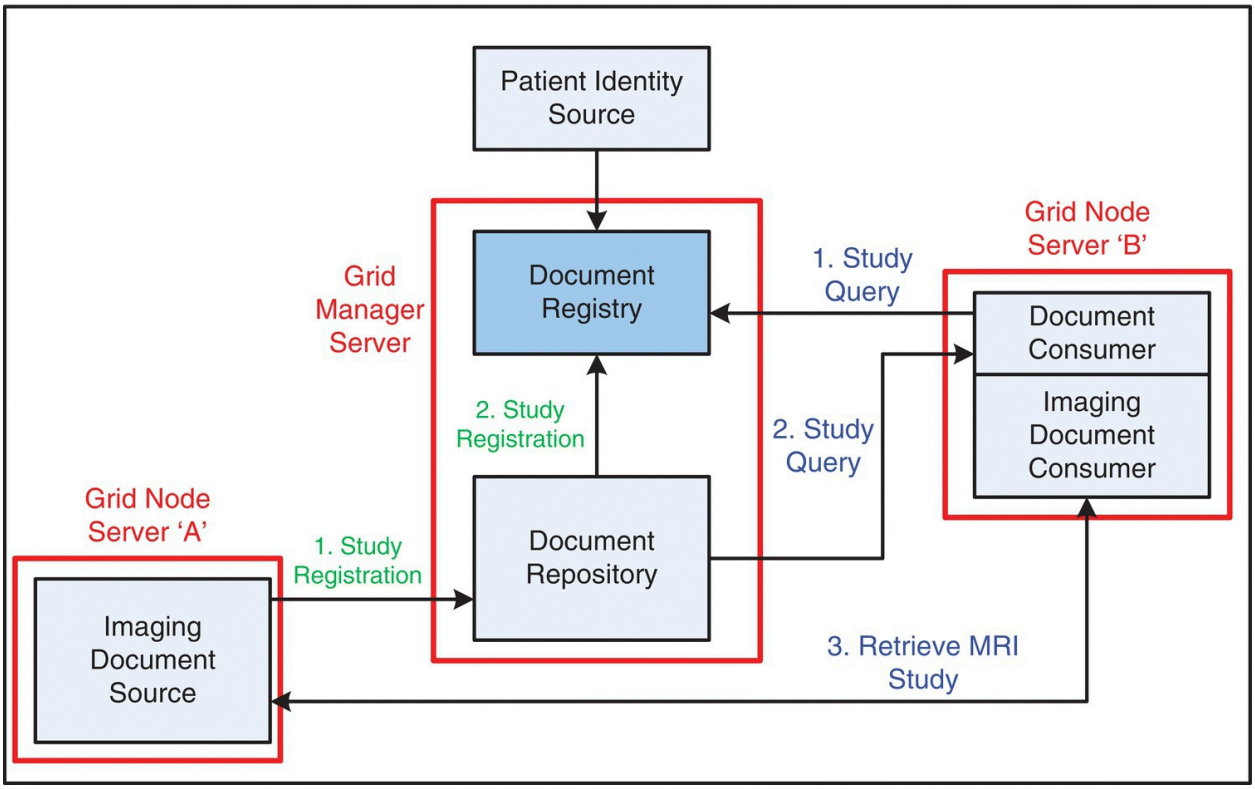

Figure 9.8 The Breast Imaging Data Grid is based on the IHE XDS-I workflow profile. Left: green, input sources. Right: Consumers.

With a DICOM-compliant front-end interface and grid-enabled management services on the grid management server, grid node servers are the thin-client gateways at each site that receive and provide dedicate breast MRI studies. Imaging technicians at breast MRI workstations send their studies to a local grid node server that acts as the image document source, in reference to the XDS-i workflow profile. Researchers and clinicians at participating BIDG sites can then search, retrieve, and visualize these MRI studies via the web-based BIDG ePR user interface. This ePR Web server communicates, over DICOM, query and retrieve requests to a grid node server, which thereby acts as the image document consumer in the XDS-I workflow profile. The grid management server takes the role of the document registry and document repository of the XDS-I workflow profile by coordinating and disseminating data sharing information to these grid node servers over customized fault-tolerant Web services.

Evaluation of the BIDG system demonstrates the technology and workflow proposed to accommodate the unique challenges of a distributed dedicated breast MRI infrastructure. Anonymized breast MRI studies are transmitted into a grid

node server and archived to multiple storage devices within the BIDG implementation for evaluation. Continued functionality and performance metrics are obtained by retrieving the MRI studies via the web-based BIDG ePR system using fault-tolerant testing scenarios.

9.2.5.3 Development of a Dedicated Breast MRI Data Grid Enterprise with IHE XDS-I Workflow Profile

The BIDG system is a total archiving and display solution for dedicated breast MRI clinical research and enterprise healthcare applications. It utilizes workflow-oriented grid services for sharing of breast MRI studies and reports of breast cancer patients. The developed BIDG system was implemented and tested in a laboratory setting at theIPILab, University of Southern California. Expected results of this study were demonstrated successfully, including the system's archiving, distribution, and fault-tolerant data management of the design. A dedicated breast MRI data grid using the IHE XDS-I workflow profile was also planned and is in progress in Taiwan. Three dedicated breast MRI scanners, each of which is located in a major city: Taipei, Tai-chung and Tan-nan, and a mobile DG MRI unit are included; these components form the Taiwan breast MRI enterprise. The three cites and the mobile are connected to a Taiwan Internet network. The dedicated breast MRI Data Grid is located at the IPILab, USC, connected to the International Internet. Figure 9.9 shows their relative locations and their connectivity.

Figure 9.9 A dedicated breast MRI Data Grid using IHE XDS-I workflow profile was planned and is in progress in Taiwan. Three dedicated breast MRI scanners, each of which is located in a major city: Taipei, Tai-chung and Tan-nan, together with a mobile Data Grid MRI, form the MRI enterprise. The three cites and the mobile are connected to a Taiwan Internet network. The dedicated breast MRI Data Grid is located at the IPILab, USC, and is connected to the International Internet. This figure shows their relative locations and their connectivity.

9.3 Administrating the Data Grid

Two topics are now discussed relating to administrating the data grid: the data security, and sociotechnical consideration.

9.3.1 Image/Data Security in Data Grid

Image/Data security in PACS and informatics were discussed previously in the

Second Edition, and similar data security methodology can be extended to the Data Grid. Although backup policies and grid certificates generally guarantee privacy and authenticity of GAPs, there is still a lack of acceptable methods to guarantee that the sensitive DICOM images and data have not been compromised, altered, or corrupted while at clinical trial sites or at the enterprise level during data and image transmission across the public domain. This section provides a general framework toward achieving full image storage and transfer security within the Data Grid, by utilizing DICOM image authentication and the HIPAA-compliant auditing system (H-CAS) discussed in Chapter 17 [5].

The 3-D lossless digital signature embedding (LDSE) procedure involves a private 64-byte signature that is embedded into each original DICOM image volume, whereby the signature can be extracted and verified at the receiving end, following the DICOM transmission [6]. The H-CAS is required to monitor embedding and verification events, and also allows monitoring of other grid activity. The H-CAS system federates the logs of transmission and authentication events at each GAP and stores it in a HIPAA-compliant database. The auditing toolkit is installed at the local GAP and utilizes Syslog, a client–server standard for log messaging over an Internet protocol (IP) network, to send messages to the H-CAS centralized database. By integrating digital image signatures and centralized logging capabilities, DICOM image integrity within the medical imaging and informatics Data Grid can be monitored and guaranteed without loss of any image quality. Figure 9.10 shows the locations of LDSE and H-CAS when an image source sends images to a location, and the user queries image/data from the Data Grid.

Figure 9.11A describes the workflow involved for a clinical trial (Section 9.1) utilizing the IPILab data storage grid with LDSE embedding and verification. The red (darker) dots represent the embedding procedure of the digital signature into DICOM images. The green (lighter) dots represent the physical workflow locations where the digital signature is extracted and verified for image integrity. The H-CAS system receives LDSE logs from all GAPs and storage nodes using Syslog messaging and secure socket layer (SSL)encryption. A Web-based monitoring application can also be developed to communicate with the H-CAS database and can function as the audit layer’s monitoring tool and user interface for the system administrator. Figure 9.11B uses a 3-D CT image set as an example to illustrate the LDSE to assure data integrity.

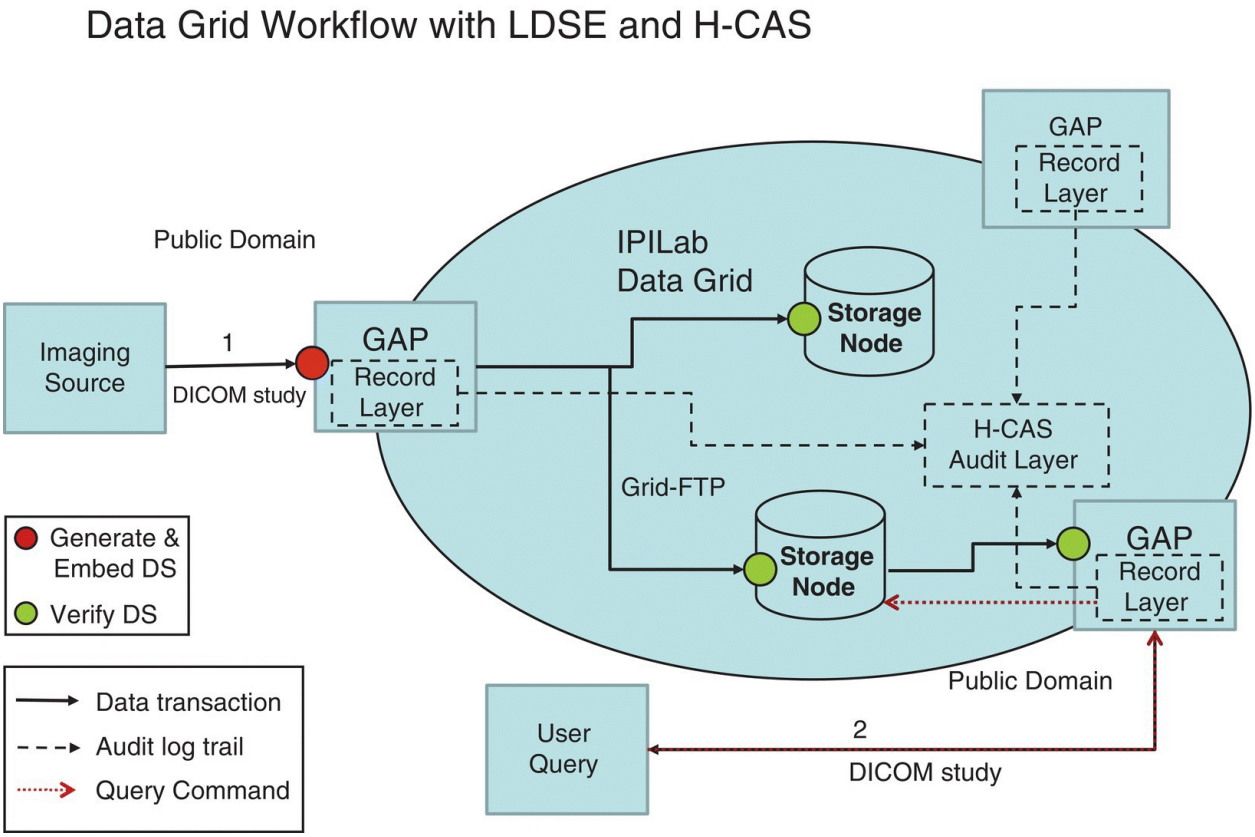

Figure 9.10 Data Grid workflow with lossless digital signature embedding (LDSE) and HIPAA-compliant auditing system (H-CAS) implemented. Red circle: generate and embed digital signature (DS). Green circle: verify DS. There are two data lines: (1) left middle: imaging source sends image/data to the Data Grid; (2) lower middle: user queries image/data.

(A)

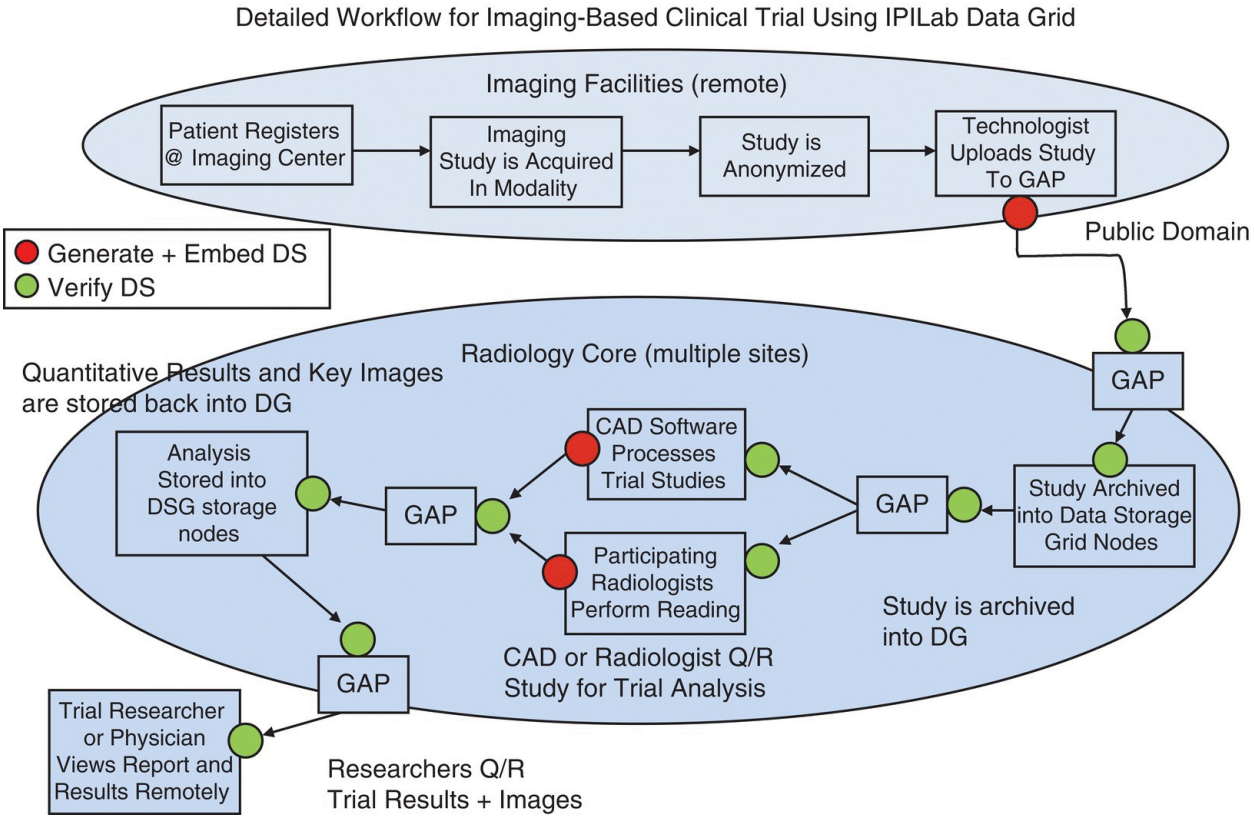
Detailed Workflow for Imaging-Based Clinical Trial Using IPILab Data Grid
Imaging Facilities (remote)
Patient Registers @ Imaging Center
Imaging Study is Acquired In Modality
Study is Anonymized
Technologist Uploads Study To GAP
Public Domain
Generate + Embed DS
Verify DS
Radiology Core (multiple sites)
Quantitative Results and Key Images are stored back into DG
GAP
CAD Software Processes Trial Studies
Analysis Stored into DSG storage nodes
GAP
GAP
Study Archived into Data Storage Grid Nodes
Participating Radiologists Perform Reading
Study is archived into DG
GAP
CAD or Radiologist Q/R Study for Trial Analysis
Trial Researcher or Physician Views Report and Results Remotely
Researchers Q/R Trial Results + Images

(B)

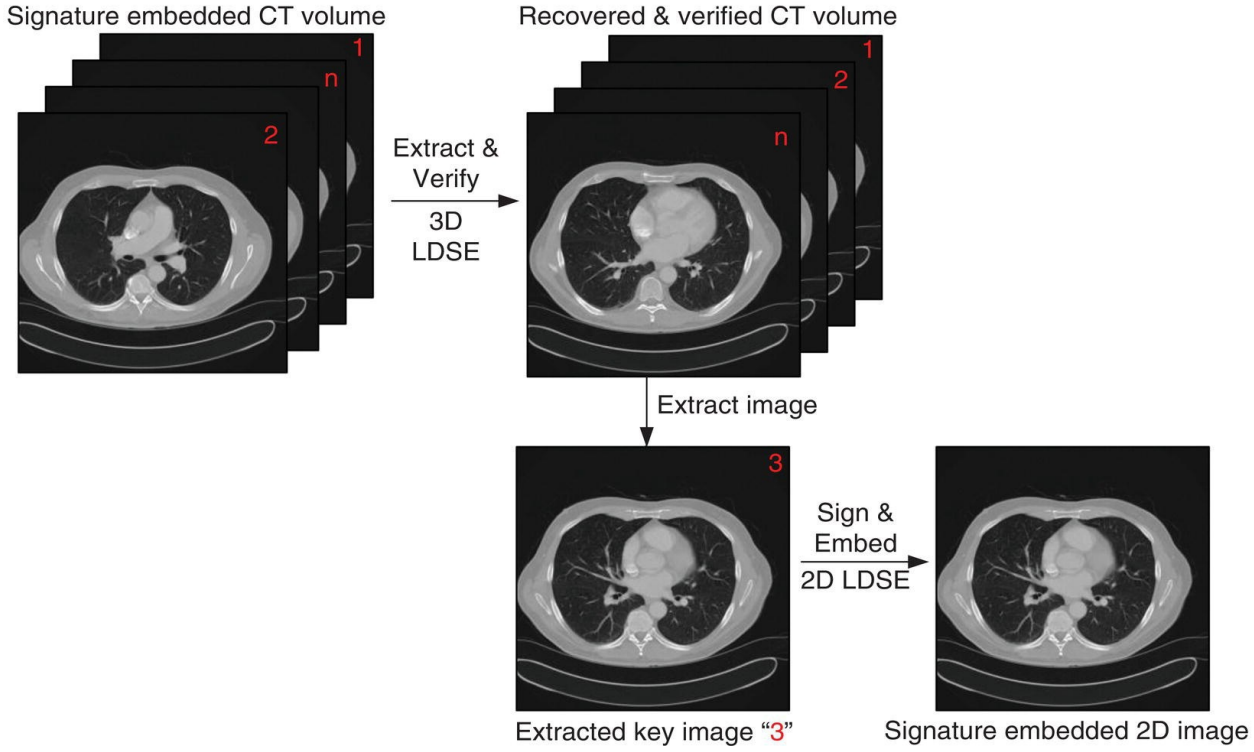
Signature embedded CT volume
1
n
2
Extract & Verify
3D LDSE
Recovered & verified CT volume
1
2
n
Extract image
3
Extracted key image "3"
Sign & Embed
2D LDSE
Signature embedded 2D image

Figure 9.11 (A) Top: Simulated LDSE workflow in a clinical trials setting using the Data Grid (Figure 9.4). This simultaneously tests the LDSE verification system and HIPAA-compliant auditing system user authentication. (B) Bottom: LDSE process to assure data integrity. A CT image set is used in this example (see also Chapter 17).

9.3.2 Sociotechnical Considerations in Administrating the Data Grid

9.3.2.1 Sociotechnical Considerations

A Data Grid, when used correctly, is a cost-effective backup and disaster recovery solution for large-scale enterprise PACS and medical imaging informatics applications. Geographic separation provides fault tolerance against localized disasters. Pooling of storage resources across organizations against localized disasters is facilitated by the low marginal costs of SAN technology. However, the control and administration of the Data Grid is now spread across multiple organizations, which increases the complexity of a Data Grid deployment. There are now multiple stakeholders networked together in a series of relationships that must agree on every operational detail.

The introduction of a Data Grid means that stakeholders in various organizations are now linked together over issues such as security, service level agreements, and liability in the event of a security breach. Many other issues should be considered, such as human issues on allocating responsibility for managing and operating the hardware and software of the Grid, policy issues on to how much storage will be shared and how much bandwidth can be used, and the administrative issues on the allocation of costs and protection against liability.

King (2006) [7] studied the intertwined personnel relationships within a Data Grid linking three clinical sites. Each site is composed of two groups of shareholders, the administrators and the operators shown in Figure 9.12. Before there was a Data Grid, the personnel relationships at the sites were straightforward, as indicated in the figure by the double line and the hexagons labeled 1–1, 2–2, and 3–3 for administrators and operations personnel working side by side. After the Data Grid was added, $3^2 = 9$ new primary relationships resulted, as shown in the original three double lines plus six solid lines. In addition, there is potential for $3 \times 2 = 6$ optional relationships, as marked by the dotted lines. The personnel relationship grows as the number of sites n grows, so there will be n^2 new primary relationships, and $n \times 2 = 2n$ optional relationships.

Clearly, Data Grid administration has potentially become a complex issue.

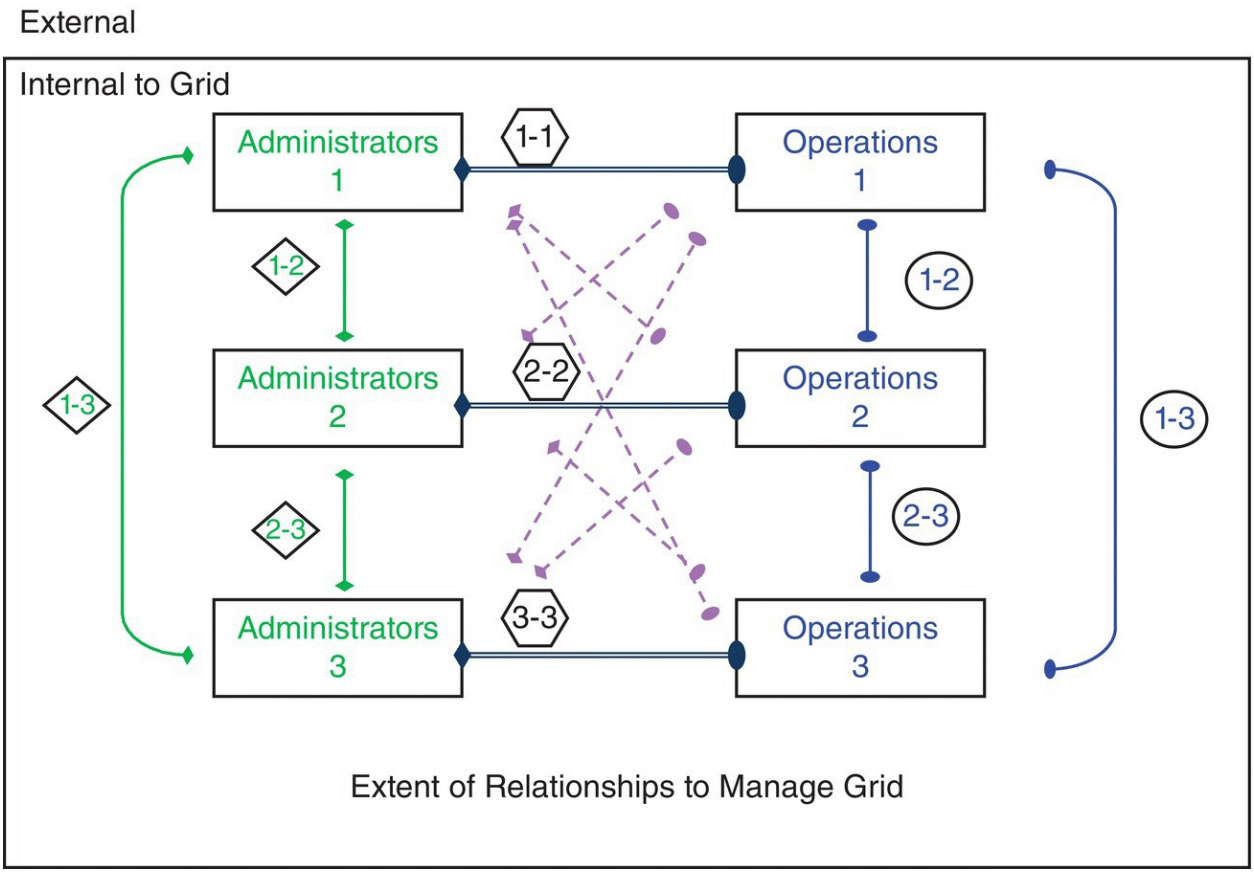

Figure 9.12 Intertwined nature of personal relationships within a Data Grid consisting of three clinical sites. Each site is composed of two groups of shareholders, the administrators and the operators. Double (blue gray) and solid (green and blue) lines are for primary relationships, dotted lines (purple) are for optional relationships. The personal relationships become complex as the number of sites in the Data Grid grows.

(courtesy of Dr N. King)

9.3.2.2 Is Data Grid for Me?

Data Grid indeed may not be suitable for every clinic and/or enterprise, especially for those clinics that have a culturally independent operation philosophy and aversion to external risk. However, Data Grid is suitable for large-scale enterprise level PACS and medical imaging informatics applications. Examples are enterprise PACS, enterprise imaging center, healthcare maintenance PACS operation, dedicated breast imaging enterprise operation, and radiology core in a large-scale image-based clinical trials, as discussed in

previous sections.

An independent clinical service that prefers to operate independently may join a suitable Data Grid organization to take advantage of fault-tolerant backup and disaster recovery of its image/data, without contributing their own data storage and personnel to the Data Grid administration by signing a business contract. This arrangement can avoid Data Grid's administrative complexity and necessary security relationships by negotiating a contractual agreement. The security protection is similar to that of the application service provider (ASP) model discussed in Chapter 16.

9.4 Summary

The research and development of Data Grid has advanced remarkably over the past 10 years. In the first section, the principles of Data Grid are discussed, followed by distributed computing, grid computing, and the grid computing open source Globus Toolkit. As a total, they evolve and form the foundation of the powerful Data Grid infrastructure that can benefit to advance PACS-based medical imaging informatics applications. In the second section, the fault-tolerant concept with three tasks in image data archive/backup, query/retrieval, and disaster recovery using Data Grid are discussed along with two Data Grid applications for image-based clinical trials and to advance dedicated breast MRI enterprise development.

References

1 Chow, S.C. and Liu, J.P. (2004) *Design and Analysis of Clinical Trials: Concepts and Methodologies*. Hoboken, NJ: Wiley.

2 Foster, I. (2005) Globus Toolkit Version 4: Software for Service-Oriented Systems. New York: Springer, pp. 2–13.

3 Foster, I. (2002) The grid: a new infrastructure for 21st century science. *Phys Today*, 55, 42–47.

4 http://wiki.ihe.net/index.php?title=Cross Enterprise Document Sharing

5 Conducting a HIPAA security audit. Digital Imaging and Communications in Medicine (DICOM) 2004. http://medical. nema.org/dicom/2004.html, accessed March 14, 2006.

6 Fridrich, J., Goljan, M. and Du, R. (2002) Lossless data embedding—new paradigm in digital watermarking. *EURASIP J Appl Sig Proc*, (2), 185–196.

7 King, N.E. (2006) Information systems and healthcare XVII: operational stakeholder relationships in the deployment of a data storage grid for clinical image backup and recovery. *CommAssoc Info Sys*, 23(1), http://www.globus.org/solutions/data_replication/, accessed March 14, 2006.

Further Reading

HARNET. http://www.jucc.edu.hk/jucc/content harnet.html, accessed March 14, 2006.

HIPAA Security Standard. http://www.hipaadvisory.com/regs/finalsecurity/

http://searchdomino.techtarget.com/news/article/0,289142,sid4mgci912158,00.html

https://cabig.nci.nih.gov/overview

http://www-03.ibm.com/grid/pdf/fsgmas.pdf

http://dev.globus.org/ wiki/Incubator/MEDICUS

Huang, H.K., Zhang, A., Liu, B., Zhou, Z., *et al*. (2005) Data Grid for large-scale medical image archive and analysis. *Proceedings of the 13th ACM International Conference on Multimedia*, pp. 1005–1013.

Huang, H.K. (2004) *PACS and Imaging Informatics: Basic Principles and Applications*. Hoboken, NJ: Wiley.

Internet2, http://www.internet2.edu/, accessed March 14, 2006.

Law, M.Y. and Zhou, Z. (2003) New direction in PACS education and training, *Comput Med Imag Graph*, 27, 147–156.

Liu, B., Zhou, Z. and Huang, H.K. (2005) A HIPAA-compliant architecture for securing clinical images. *SPIE Med Imag Conf Proc PACS and Imaging Informatics*.

Liu, B., Zhou, Z. and Documet, J. (2005) Utilizing Data Grid architecture for the backup and recovery of clinical image data. *Comput Med Imag Graph*, 29, 95–102.

Liu, B.J., Cao, F., Zhou, M.Z., Mogel, G. and Documet, L. (2003) Trends in PACS image storage and archive. *Comput Med Imag Graph*, 27, 165–174.

Liu, B.J., Zhou, Z., Gutierrez, M.A., Documet, J., Chan, L. and Huang, H.K. (2007) International Internet2 connectivity and performance in medical imaging applications: bridging Americas to Asia. *J High Speed Networks*, 16(1), 5–20.

McNitt-Gray, M.F., Aramato, S.G., Clarke, L.P., McLennan, G., Meyer, C.R. and Yankelevitz, D.F. (2002) The lung imaging database consortium: creating a resource for the image processing research community. *Radiology*, 225, 739–748.

Meinert, C.L. (1986) *Clinical Trials: Design, Conduct, and Analysis*. Oxford: Oxford University Press.

Moge, G.l., Huang, H.K., Cao, F., Zhou, Z., Dev, P., *et al*. (2002) NGI performance in teleradiology applications. *Proc. SPIE Med Imag*, 3, 25–30.

Ouchi, N.K. (1977) System for recovering data stored in failed memory unit. US Patent 714/5, 714/6, m714/807.

Piantadosi, S. (1997) *Clinical Trials: A Methodologic Perspective*. New York: Wiley.

Redundant Array of Independent Disks (RAID). http://en.wikipedia.org/wiki/Redundant array of independent disks, accessed March 14, 2006.

RNP2.http://www.rnp.br/en/, accessed March 14, 2006.

Schopf, J.M. and Nitzberg, B. (2002) Grids: top ten questions. *Sci Progr*, 10, 103–111.

Syslog (2007) http://www.loriotpro.com/Products/SyslogCollector/SyslogDataSheet ENv3.php, accessed December 2007.

TeraGrid. http://www.teragrid.org/, accessed March 14, 2006.

Zhou, X.Q., Huang, H.K. and Lou, S.L. (2001) Authenticity and integrity of digital mammography images. *IEEE Trans. Med Imag*, 20(8), 784–791.

Zhou, Z., Liu, B. and Huang, H.K. *et al*. (2005) A RIS/PACS simulator integrated with the HIPAA-compliant auditing toolkit. *SPIE Med Imag Conf*

Proc.

Zhou, Z., Huang, H.K. and Liu, B. (2005) Digital signature embedding for medical image integrity in a Data Grid off-site backup archive. *SPIE Med Imag Conf Proc PACS and Imaging Informatics; SPIE Publication*.

Zhou, Z., Documet, J., Chan, L., *et al*. (2006) *The Role of a Data Grid in Worldwide Imaging-Based Clinical Trials*. USC UPU: Marina del Rey.

Zhou, Z., Liu, B.J., Huang, H.K. and Zhang. J. (2005) Educational RIS/PACS simulator integrated with the HIPAA compliant auditing (HCA) toolkit. *Proc SPIE Med Imag*, 6, 491–500.

10
Display Workstations

CHAPTER MENU

10.1 PACS-Based Display Workstation
10.1.1 Image Display Hardware
10.1.2 Image Display Board
10.1.3 Display Monitor
10.1.4 Resolution
10.1.5 Color Display
10.2 Various Types of Image Workstation
10.2.1 Diagnostic Workstation
10.2.2 Review Workstation
10.2.3 Analysis Workstation
10.2.4 Digitizing, Printing, and CD Copying Workstation
10.2.5 Interactive Teaching Workstation
10.2.6 Desktop Workstation
10.3 Image Display and Measurement Functions
10.3.1 Zoom and Scroll
10.3.2 Window and Level
10.3.3 Histogram Modification
10.3.4 Image Reverse
10.3.5 Distance, Area, and Average Gray Level Measurements
10.3.6 Optimization of Image Perception in Soft Display
10.3.7 Montage: Selected Sets of Images with Particular Pathology and/or Features
10.4 Workstation Graphic User Interface (GUI) and Basic Display Functions

10.4.1 Basic Software Functions in a Display Workstation
10.4.2 Workstation User Interface
10.5 DICOM PC-Based Display Workstation Software
10.5.1 Software System
10.5.2 Software Architecture
10.5.3 Software Modules in the Application Interface Layer
10.6 Post Processing Workflow, PACS-Based Multidimensional Display, and Specialized Post-Processing Workstation
10.6.1 Post Processing Workflow
10.6.2 PACS-Based Multidimensional Image Display
10.6.3 Specialized Post-Processing Workstation
10.7 DICOM-based Workstations in Progress
10.7.1 Intelligence Workstation
10.7.2 3-D Printing
10.7.3 Summary
References

Among all PACS components, the display workstation (WS) is the one that all radiologists and clinicians are familiar with. PACS-based WSs in the radiology department are of the highest quality, allowing radiologists and clinicians to make primary diagnoses from the images compared with other peripheral WSs not within the radiology department. This chapter gives details of the WS design, hardware and software, ergonomics, features, utilization, and future development prospects. Figure 10.1 depicts the WS in the PACS-based multimedia data flow.

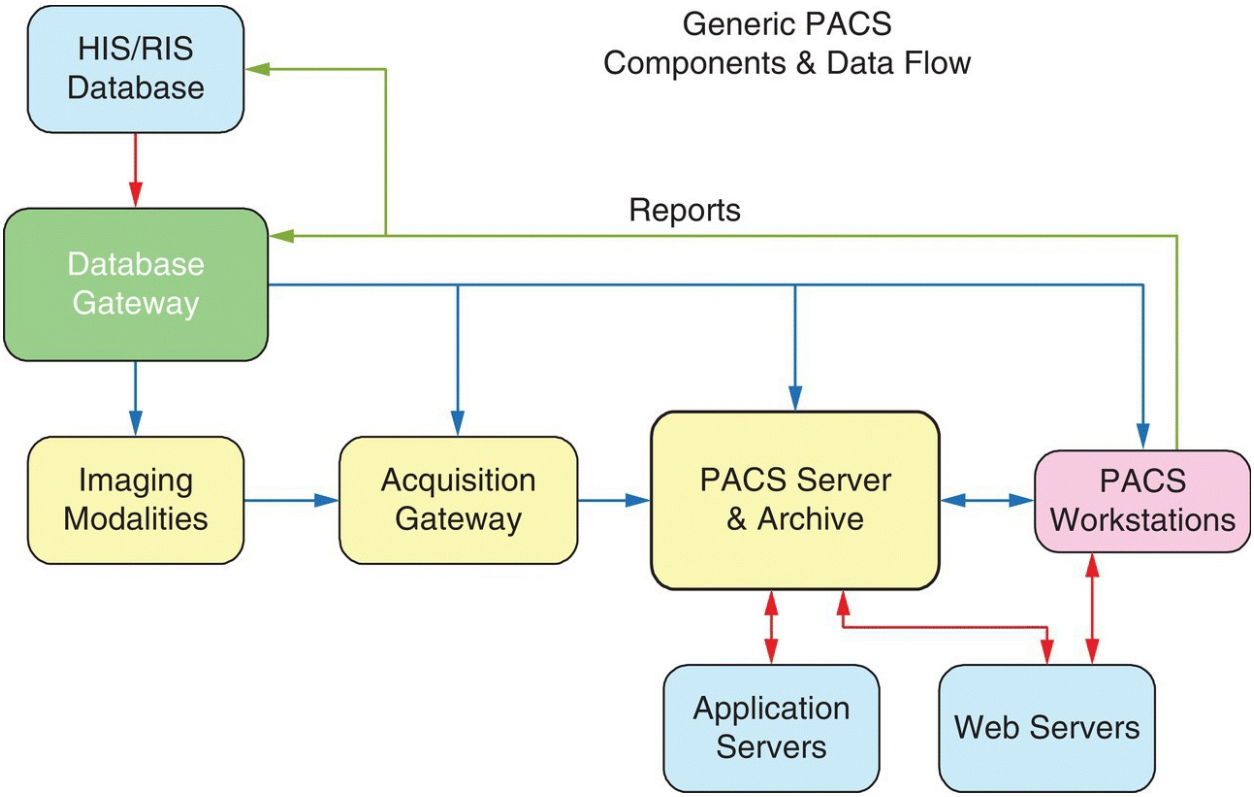

Figure 10.1 PACS-based multimedia imaging informatics basic components (yellow), data flow (blue: internal; green and red: external between PACS and other information systems); other medical imaging informatics systems (light blue), PACS-based workstation (orange red). HIS: hospital Information system; RIS: radiology information system [1].

10.1 PACS-Based Display Workstation

10.1.1 Image Display Hardware

The WS is the interactive component in the PACS-based multimedia system that healthcare providers use for reviewing images and relevant patient information from which patient diagnosis is made. The interpreted results become the diagnostic report that feeds back to the hospital and radiology information systems (HIS, RIS) as a permanent patient record along with the images. In this chapter, the terms softcopy workstation, display workstation, image workstation, or just workstation (WS) are used interchangeably. In the past, the conventional method of viewing radiological images from films is by handling them on an alternator or a light box. The advantages of an alternator are its large surface area, high luminance, and convenience in use, with these images being called

hard copy images.

A WS consists of four major hardware components: a computer, image display boards, display monitors, and local storage devices. A communications network and application software connect these components with the DICOM-based PACS server. The computer and image display boards are responsible for transforming the image data for visualization on the monitors.

Magnetic disks and RAID are used on local storage devices. The communications network is used for transmitting images into and out of the WS. Figure 10.2 shows a schematic of a typical two-monitor WS based on a personal computer (PC). Section 10.1.2 describes the image display board and the display monitor in more detail.

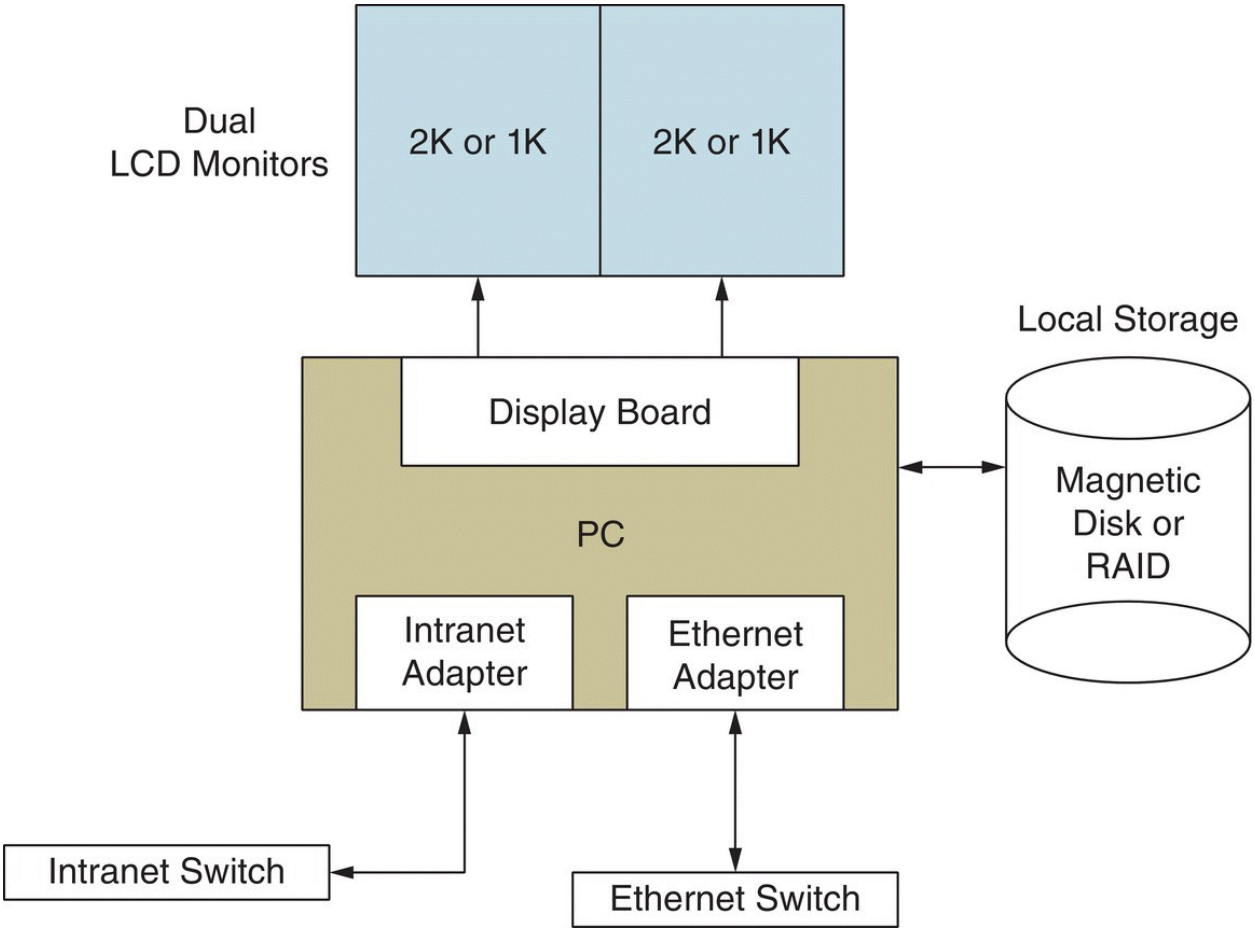

Figure 10.2 Schematic of a standard PACS-based display workstation (WS) with two image display LCD monitors (2 K or 1 K). The WS is composed of a personal computer (PC), e.g. display hardware boards with image processing capability, image and video memory, dual display LCD monitors (2 K or 1 K), magnetic or RAID disk, and network connections [2].

10.1.2 Image Display Board

The image display board has two components: a processing unit and an image memory. The image memory is used to supplement the computer memory to increase the storage capacity for images and to speed up the image display. There are two types of computer memory, random access memory (RAM) and video RAM (VRAM). RAM usually comes with the computer and is less expensive than VRAM. VRAM has a very high input/output rate and is used to display images or graphics. A WS usually has more RAM than VRAM. In a PACS WS, typical numbers are 1 GB RAM and 64 MB VRAM, or more.

An image file in the WS, coming either from the PACS archive server or from the internal disk, is first stored in the RAM. If the RAM is not large enough to store the entire image file, it is split between the RAM and the disk, and so disk I/O and RAM swapping is required. In this case, the image display speed will be slower. It is therefore advantageous to have a larger RAM to increase the display speed. After some operations, the processed image is moved to the VRAM before it is shown on the monitor. Figure 10.3 shows the data flow of an image from the internal magnetic disk to the display memory. Sometimes the terms “4 megapixel” or “5 megapixel” are used for a display board, which represent its capability of displaying a full 2 K × 2 K or 2.5 K × 2 K image, respectively. Color images and graphic overlay require 24 bits/pixel.

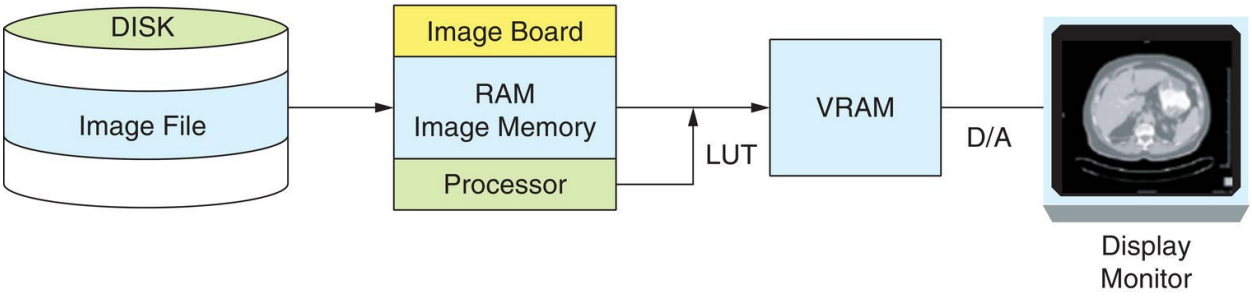

Figure 10.3 WS data flow of an image from the internal magnetic disk to the display monitor. D/A: digital-to-analog conversion; LUT: lookup table; RAM: random access memory; VRAM: video random access memory.

10.1.3 Display Monitor

The cathode ray tube (CRT) has been commonly replaced by the liquid crystal (LCD) flat-panel monitor, which has been used to display arbitrary types of PACS-based medical images since 2001. Table 10.1 shows the advantages and disadvantages of the LCD and the CRT monitor.

Table 10.1 Advantages and disadvantage of the LCD over the CRT.

LCD Advantages versus CRT Disadvantages	
LCD Advantage	CRT Disadvantage
Much thninner	Thicker
Light	Heavy
Consumes 4.2A for four-head system	Consumes 7A for four-head system
Maximum luminance 500 cd/m^2 (nice in bright rooms)	Maximum luminance 300–450 cd/m^2
Flat display	Display surface is not flat
LCD Disadvantages versus CRT Advantages	
LCD Disadvantage	CRT Advantage
Contrast only 500:1 (narrow viewing angle)	Contrast 2000:1 (narrow viewing angle)
Contrast only 45:1 (45° viewing angle)	Contrast 1000:1 (45° viewing angle)
Screen artifact due to black between pixels	Smooth transition between pixels
Only 15,000 hours until backlight replacement (although replacement is less than new unit)	30,000 hours until CRT replacement

10.1.4 Resolution

The resolution of a display monitor is estimated by measuring the total number of lines in the image. For example, the “1 K monitor” has 1024 lines per image on the monitor, and “2 K” has 2048 lines. In the strict sense of the definition, however, it is not sufficient to specify spatial resolution simply in terms of the number of lines available, because the actual resolving power of the monitor may be less. Consider a digitally generated line pair pattern (black and white lines in pairs; Figure 10.4). The maximum displayable number of a 1 K monitor is 512 line pairs. However, in reality, the monitor itself may not be able to resolve 1024 alternating black and white lines in both the vertical and the horizontal directions, because of the design of the instrumentation.

(A)

A-1

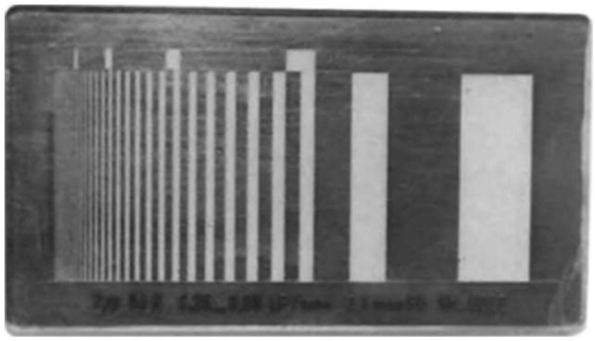

A-2

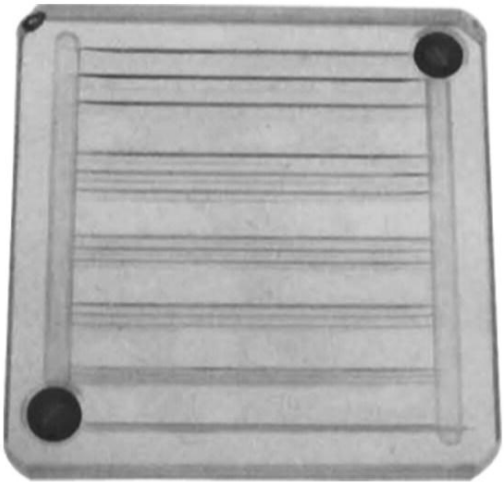

A-3

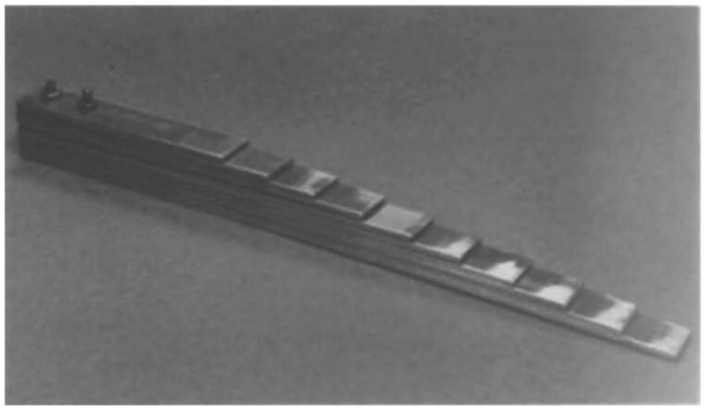

A-4

(B)

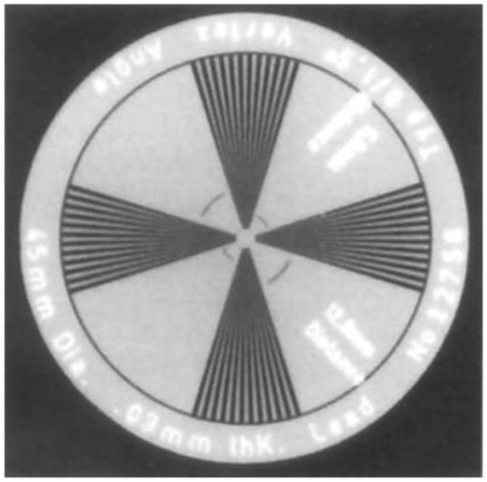

B-1

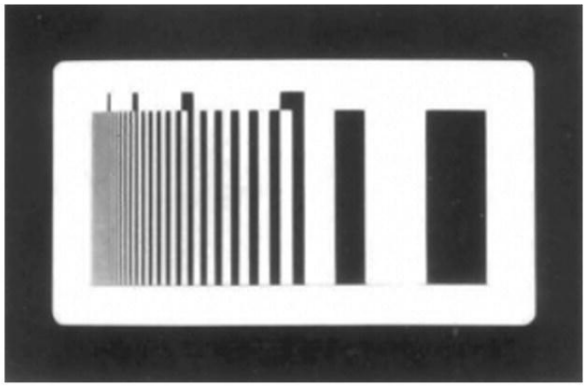

B-2

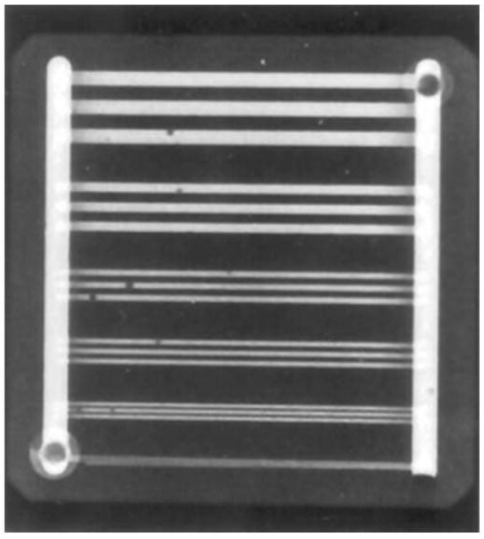

B-3

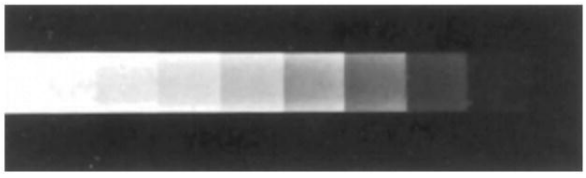

B-4

(C)

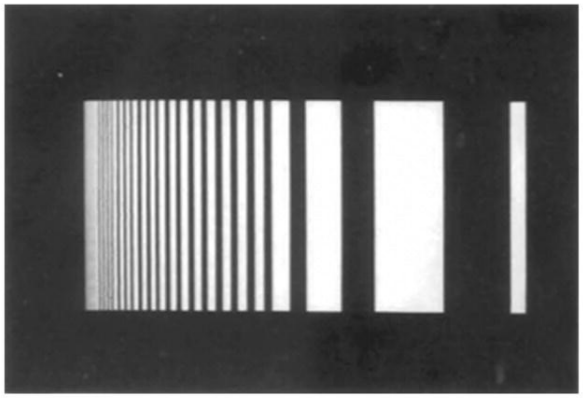

C-1

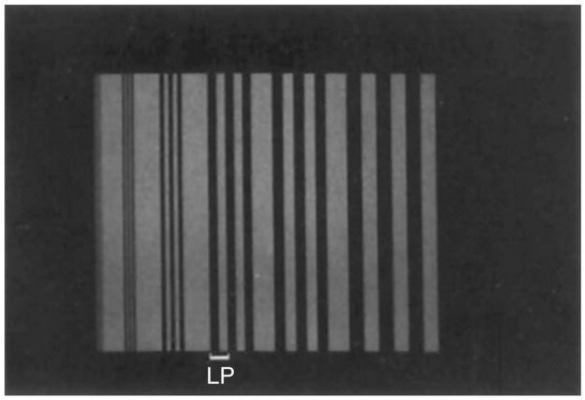

C-2

(D)

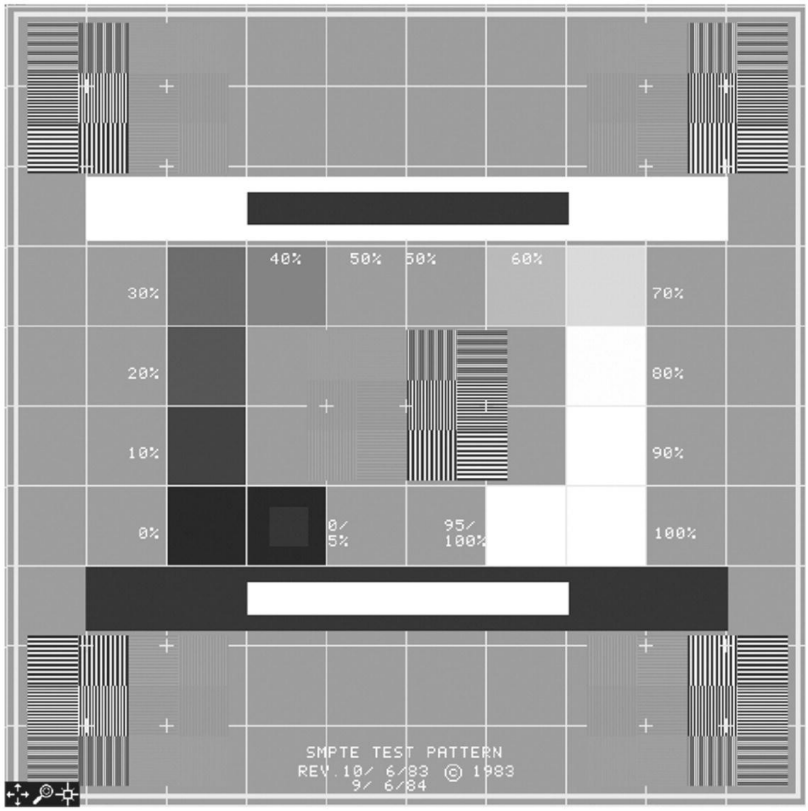
40%
50%
50%
60%
30%
70%
20%
80%
10%
90%
0%
0/
5%
95/
100%
100%
SMPTE TEST PATTERN
REV.10/ 6/83 © 1983
9/ 6/84

D-1

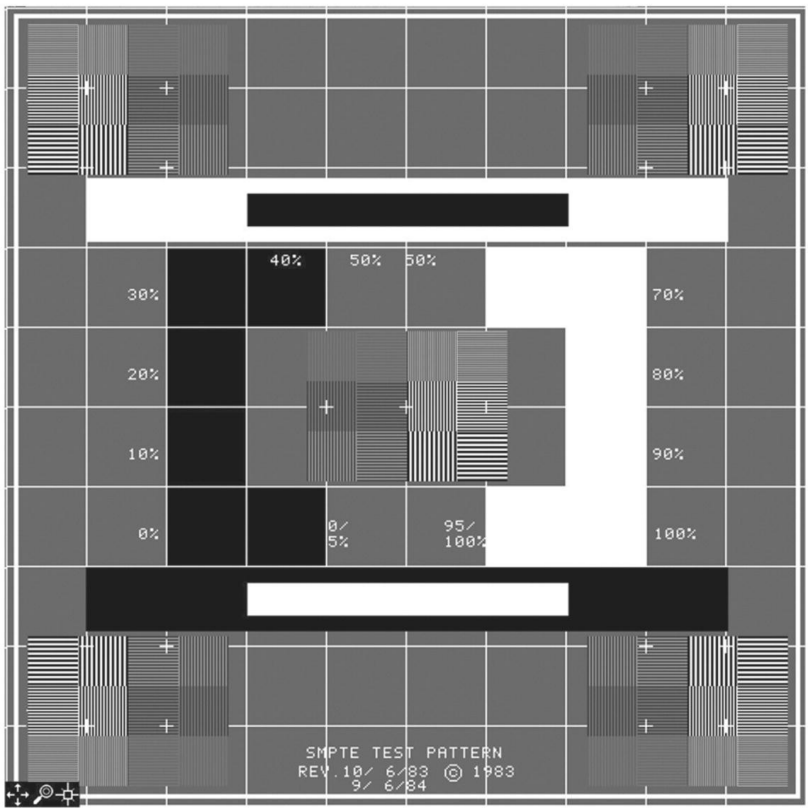
40%
50%
50%
30%
70%
20%
80%
10%
90%
0%
0/
5%
95/
100%
100%
SMPTE TEST PATTERN
REV.10/ 6/83 © 1983
9/ 6/84

D-2

Figure 10.4 Some commonly used physical test objects and digitally generated test patterns. (A) Physical: A-1, star-shaped line pair pattern embedded in water contained in a circular cylinder; A-2, high-contrast line pair (aluminum against water); A-3, low-contrast line pair (contrast media against water); A-4, aluminum step wedge. (B) Corresponding x-ray images of A; Morie patterns can also be seen in B-1. (C) Digitally generated 512 images: C-1, high-contrast line pair: gray level = 0, 140; width (in pixel) of each line pair = 2, 4, 6, 8, 10, 12, 14, 16, 32, 64, and 128 pixels; C-2, low-contrast line pair: gray level = 0, 40; width in pixel of each line pair = 2, 4, 8, 16, 20 and 28 pixels. The line pair (LP) indicated in the figure shows the width of 16 pixels. (D) Soft copy display of the 1024 Å ~ 1024 Society of Motion Picture and Television Engineers (SMPTE) phantom using the JPEG format (Chapter 6) depicts both contrast blocks (0% black – 100% white), and high-contrast and low-contrast line pairs (four corners, and middle). D-1, display adjusted to show as many contrast blocks as possible, resulting in the low-contrast line pairs barely discernable; D-2, adjusted to show the low-contrast line pairs resulted in indistinguishable contrast blocks (0–40%, and 60–100%).

Several techniques are also available for the measurement of resolution. A simpler and commonly used method employs a test pattern that consists of varying widths of line pair objects in vertical, horizontal, and sometimes radial directions (Figure 10.4). It should be noted that this visual approach in measuring the resolution of the total display-perception system, including the visual acuity of the observer, is prone to subjective variations.

Other techniques include the scanning spot photometer, slit analyzer, and measurement of the modulation transfer function (MTF). One additional factor worthy of mentioning is that resolution is a function of location on the monitor. Therefore the resolution specification must describe the location of the monitor as well as the luminance uniformity of the monitor. For these reasons, the display monitor of a PACS-based image requires routine maintenance servicing using a Society of Motion Picture and Television Engineers (SMPTE)phantom.

10.1.5 Color Display

The majority of radiographic images are monochromatic; however, other types of medical images, such as Doppler US, nuclear medicine, PET, light, molecular, and endoscopic images, do use colors for enhancement. In addition, recent developments in image-assisted therapy and image-assisted minimally invasive surgery use extensive color graphics superimposed on monochromatic images

for illustration purposes. To display a color image, three image memories (red, green, blue) are needed. The composite video controller combines these three memories to form a color display (see Edition 2, Section 3.9, Figure. 3.29). Today, color LCD monitors are of excellent quality for color medical image display.

10.2 Various Types of Image Workstation

Image WSs can be loosely categorized into six types based on their applications: diagnostic, review, analysis, digitizing and printing, interactive teaching, and desktop research WSs.

10.2.1 Diagnostic Workstation

A diagnostic WS is used by radiologists to make the primary diagnosis. The WS has the best quality, fast display time (1–2 seconds for the first image), with many user-friendly display functions. In addition, if the WS is used for displaying projection radiographs, multiple 2 K monitors are needed for images comparison. On the other hand, if the WS is used for CT, MRI, and US images, multiple 1 K monitors are sufficient. A diagnostic WS requires a dictation phone for voice dictation. The WS provides software to append the digital voice report to the images. If the radiologist inputs the report him/herself, the DICOM structured reporting function should be available with the WS. Figure 10.5 shows a generic 2 K WS with two LCD monitors showing P–A and lateral views of two computed radiography (CR) chest images.

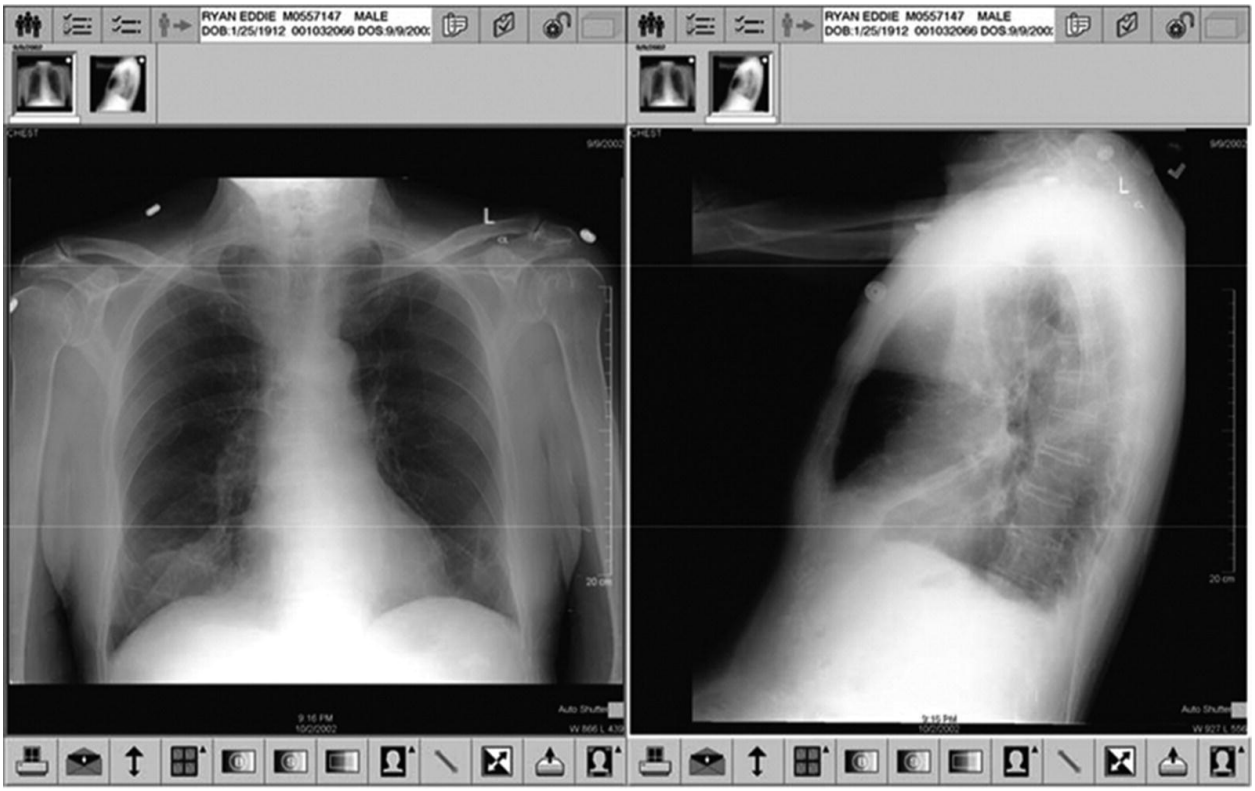

Figure 10.5 A generic 2 K display WS with two LCD monitors showing the PA (left) and the lateral (right) views of CR chest images of the same patient.

10.2.2 Review Workstation

A review WS with two display monitors is used by radiologists and referring physicians to review cases in the hospital wards or outpatient facilities. The dictation or the transcribed report should already be available with the corresponding images at the WS. A review WS may not require 5 megapixel monitors, because images have already been read by the radiologist through the diagnostic WS. With the report already available, the referring physicians can use the 3 megapixel or even the 1 K monitors to visualize the pathology from the monitors. Diagnostic and review WSs can be combined as one single unit, sharing both diagnostic and review functions like the old day alternator. Figure 10.6 shows a generic two-monitor 1 K (1600 lines × 1024 pixels) video WS used in the intensive care unit (ICU).

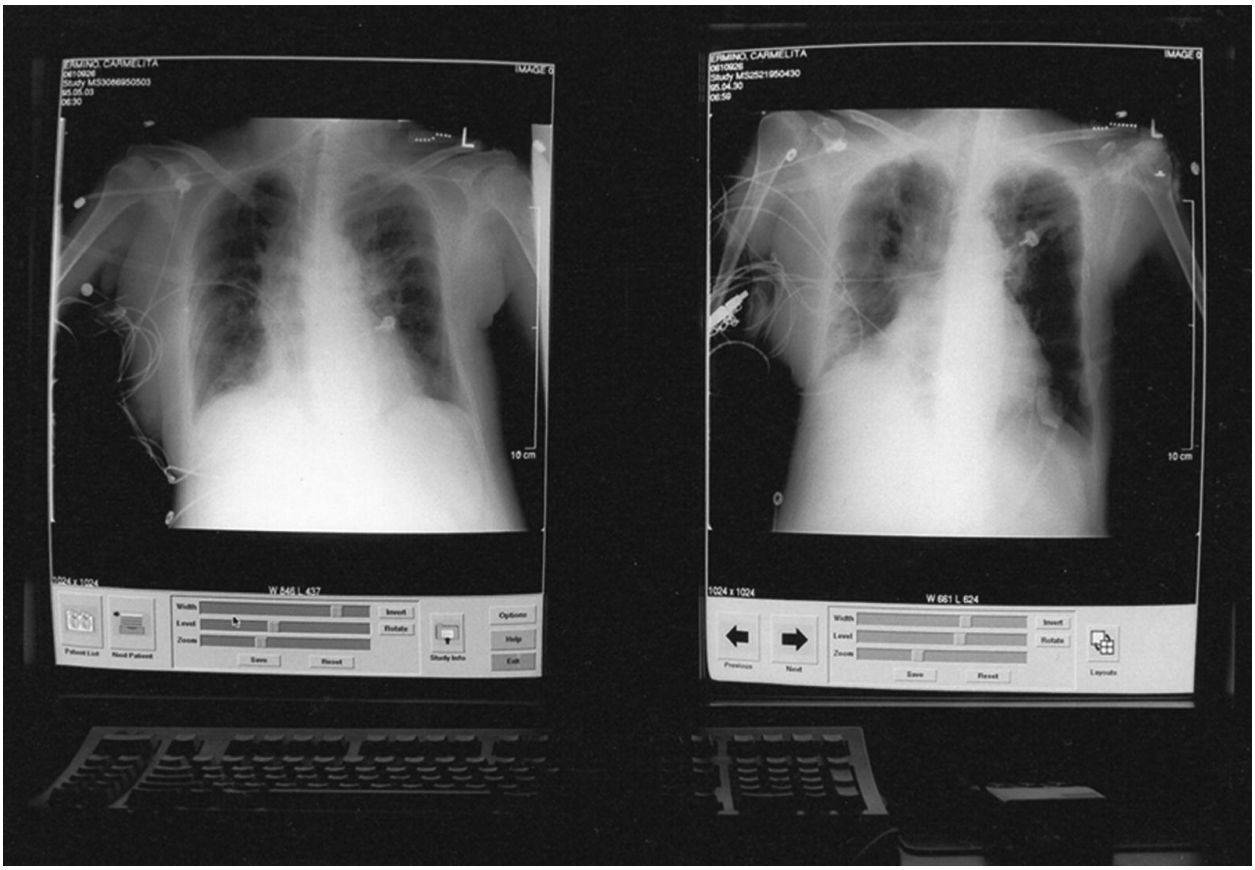

Figure 10.6 Two-monitor 1 K (1600 lines) ICU display WS showing two CR images. Left-hand CRT monitor shows the current image; all previous images can be accessed within 1 second on the right-hand monitor by clicking on the two arrow icons at the (Previous or Next sign). Simple image processing functions are controlled by the icons located at the bottom of the screens.

10.2.3 Analysis Workstation

An analysis WS differs from the diagnostic and review WSs, in that the former is used to extract useful parameters from images. Some parameters are easy to extract from a simple region of interest (ROI) operation, which can be done from a diagnostic or review WS; others (i.e. blood flow measurements from DSA, 3-D reconstruction from sequential CT images) are computationally intensive and require an analysis WS with a more powerful image processor and high-performance software. Figure 10.7 is an example showing a magnetic resonance angiography (MRA) study containing abdominal slices, using a maximum projection display method to highlight the contrasting blood vessels in the entire study.

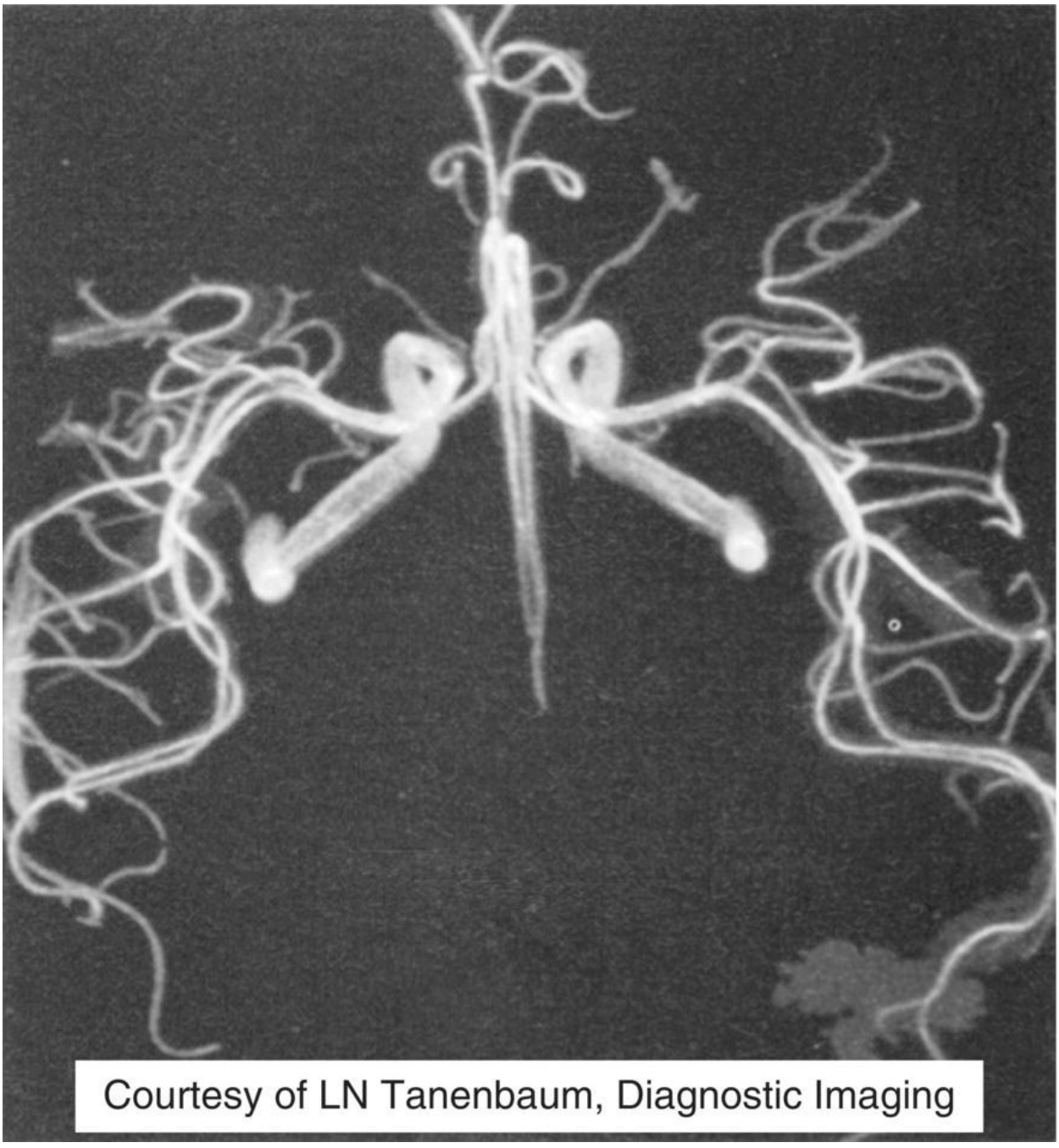

Figure 10.7 Magnetic resonance angiography(MRA) imaging, using a 3 T MRI 135–136, is approaching the same image resolution quality as digital subtraction angiography.

(courtesy of L.N. Tanenbaum, *Diag Imag*)

10.2.4 Digitizing, Printing, and CD Copying Workstation

The digitizing and printing WS is for radiology department technologists or film

librarians who must digitize historical films and films from outside the department. The WS is also used for printing soft copy images to hard copy on film or paper, and for copying images onto a CD for distribution. In addition to the standard WS components already described, the WS also needs to connect to a laser film scanner, a laser film imager, a good-quality paper printer, or a CD copier. The paper printer is used for pictorial report generation from the diagnostic, review, and editorial and research WSs. A 1 K display monitor for quality control purposes would be sufficient for this type of WS.

10.2.5 Interactive Teaching Workstation

A teaching WS is used for interactive teaching. It emulates the role of teaching files in the film library, but with more interactive features. Figure 10.8 shows a digital mammography teaching WS for breast imaging.

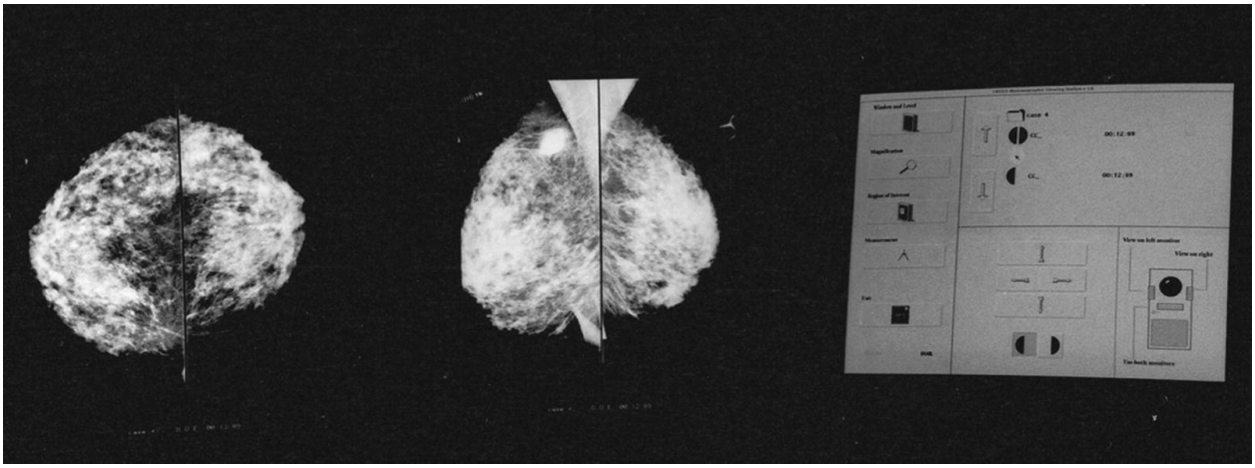

Figure 10.8 Four mammograms shown on a two-monitor 2 K digital mammograph teaching WS: (left) left and right craniocaudal views; (middle) left and right mediolateral oblique views; (right) text monitor with icons for image display and manipulation on the WS.

10.2.6 Desktop Workstation

The desktop WS is for physicians or researchers to generate lecture slides and teaching and research materials from images and related data in the PACS database. The WS uses standard desktop computer equipment to facilitate the user's daily workload. The desktop WS can also be used as a web client to access images and related information from a Web server connected to the PACS server and archive server.

Image WSs that directly interact with radiologists and physicians are the most

important and visible component in a PACS. To design them effectively, a thorough understanding of the clinical operation environment requirements is necessary.

In later sections and chapters, wherever appropriate, additional image WS types are presented, including post-processing workflow and CAD-related WSs, and mobile PDA WSs for image management and distribution.

10.3 Image Display and Measurement Functions

This section discusses some commonly use image display functions, manipulation, and measurement methods used in WSs.

10.3.1 Zoom and Scroll

Zoom and scroll is an interactive command to manipulate via a trackball, mouse, or keyboard to adjust the contrast and brightness of the image displayed on the monitors. The user first uses the trackball to scroll around the image, and center at the ROI on the screen. The ROI is used to magnify by pressing a designated button to perform the image zoom. The image becomes blockier as the zoom factor is magnified.

Although it is useful to magnify and scroll the image on the screen, the field of view decreases in proportion to the square of the magnification factor. Magnification is commonly performed via pixel replication or interpolation. In the former, one pixel value repeats itself several times in both the horizontal and vertical directions; in the latter, the pixel value is replaced by interpolation of its neighbors. For example, to magnify the image to two times by replication is to replicate the image 2×2 times.

10.3.2 Window and Level

The window and level function allows the user to control the grouping and interval of gray levels to be displayed on the monitor. The center of this interval is called the level value, and the range is called the window value. The selected gray level range will be distributed over the entire dynamic range of the display monitor; thus, using a smaller window value will increase the contrast of the resulting image to increase it on the screen. Gray levels present in the image outside the defined interval are clipped to either black or white (or both), according to the sides of the interval on which they are positioned. The user can also use a trackball, mouse, or keyboard to control this function. Window and

level operations can be performed in real time by using a fast lookup table (LUT) image processor.

10.3.3 Histogram Modification

A function very useful for enhancing the display image is using a histogram modification, from which each pixel value can then be modified on the original image based on the histogram.

An example is the histogram equalization, in which the shape of the modified histogram is adjusted to be as uniform (i.e. the number of pixels per value) as possible for all gray levels. The rescaling factor (or the histogram equalization transfer function) is given by:

$$g = (g_{max} - g_{min}) P(f) + g_{min} \tag{10.1}$$

where g is the output (modified) gray level, g_{max} and g_{min} are the maximum and minimum gray level of the modified image, respectively, f is the input (original) gray level, and $P(f)$ is the cumulative distribution function (or integrated histogram) of f.

Figure 10.9 shows an example of modifying an overexposed (too dark) chest x-ray image in the lungs with the histogram equalization method. In this example, the frequency of occurrence of some lower gray level values in the modified histogram has been changed to zero to enforce uniformity. It is seen that some details in the lung have been restored.

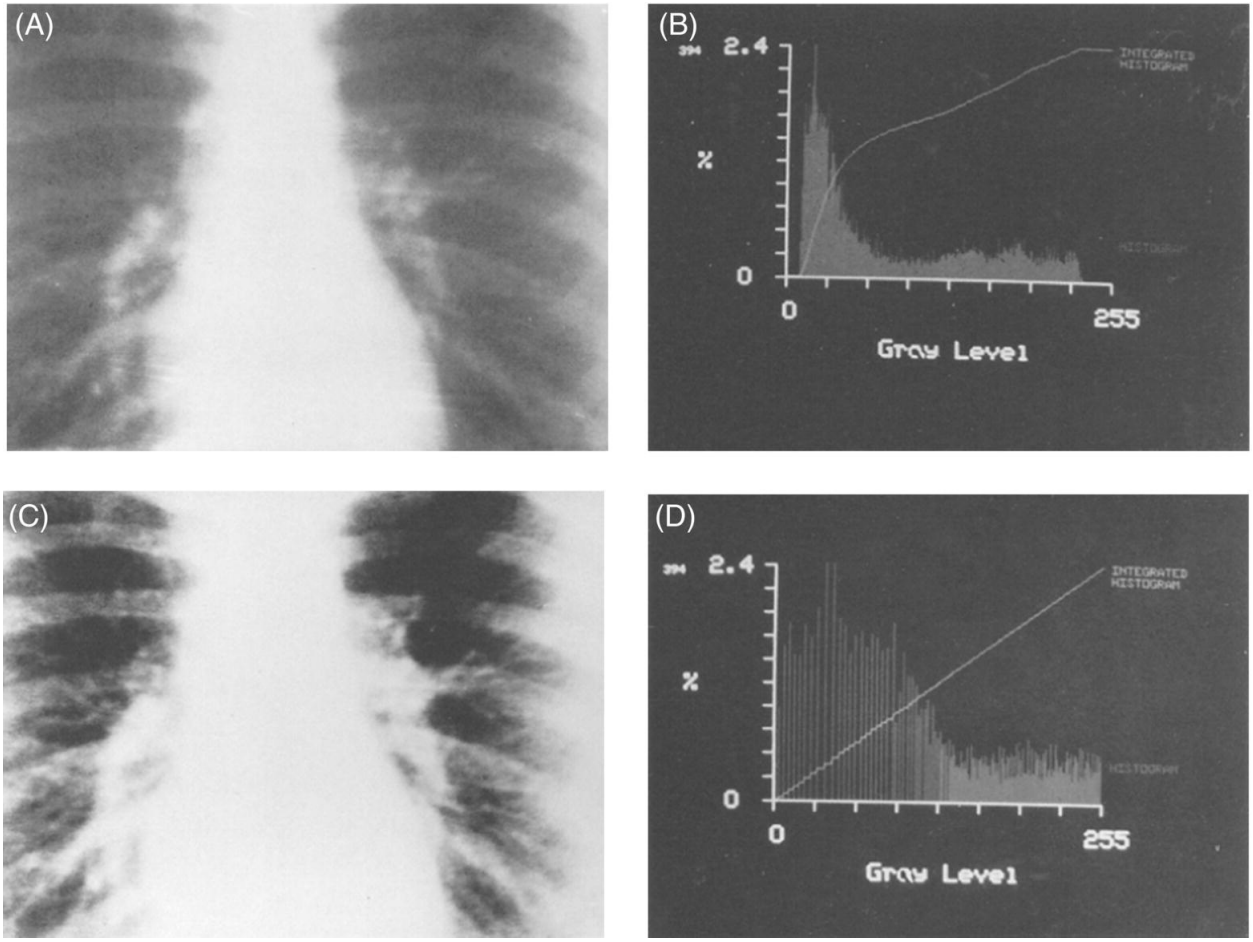

Figure 10.9 Concept of histogram equalization. (A) Region in the center of the chest x-ray with the lung region overexposed, showing relatively low contrast. (B) Histogram of the original chest image. (C) Modified image with the lung region enhanced with histogram equalization. (D) The modified histogram.

10.3.4 Image Reverse

A LUT can be used to reverse the dark and light pixels of an image. In this function, the LUT is loaded with a reverse ramp such that for an 8-bit image, the value 255 becomes 0, and 0 becomes 255, and so forth. Image reverse is used to locate external objects—for example, intrathoracic tubes in ICU x-ray examinations.

10.3.5 Distance, Area, and Average Gray Level Measurements

The following three simple measurement functions are important for immediately interactive quantitative assessment while the clinicians and

radiologist are reading an image, because these functions allow the user to perform physical measurement with the image displayed on the monitor by calibrating the dimensions of each pixel to a pre-assigned physical units or the gray level value to the optical density. These are:

1. The distance between two points in the image can be measured by moving the cursor over the points.
2. The optical density of an area of interest in the image can be obtained by moving the cursor around this area, then averaging the total pixel values.
3. An interactive procedure allows the user to trace a region of interest from which the area can be averaged and the standard deviation gray level can be computed.

10.3.6 Optimization of Image Perception in Soft Display

The following are three sequential steps to optimize the image display: remove the unnecessary background, determine the anatomical ROI, and correct for the gamma response of the monitor based on the ROI.

10.3.6.1 Background Removal

To display CR or digital radiography (DR), the importance of using the method of background removal was discussed in Figures 2.5A and B, Chapter 2, Section 2.2. In this chapter, Figures 10.10A–D show a CR image with two different backgrounds and their corresponding histograms. After the background image of the Figure 10.10A has been removed, the original histogram Figure 10.10B becomes histogram Figure 10.10D, which has no pixel values over 710. The new display image becomes Figure 10.10C, which has a better visual quality than that of Figure 10.10A.

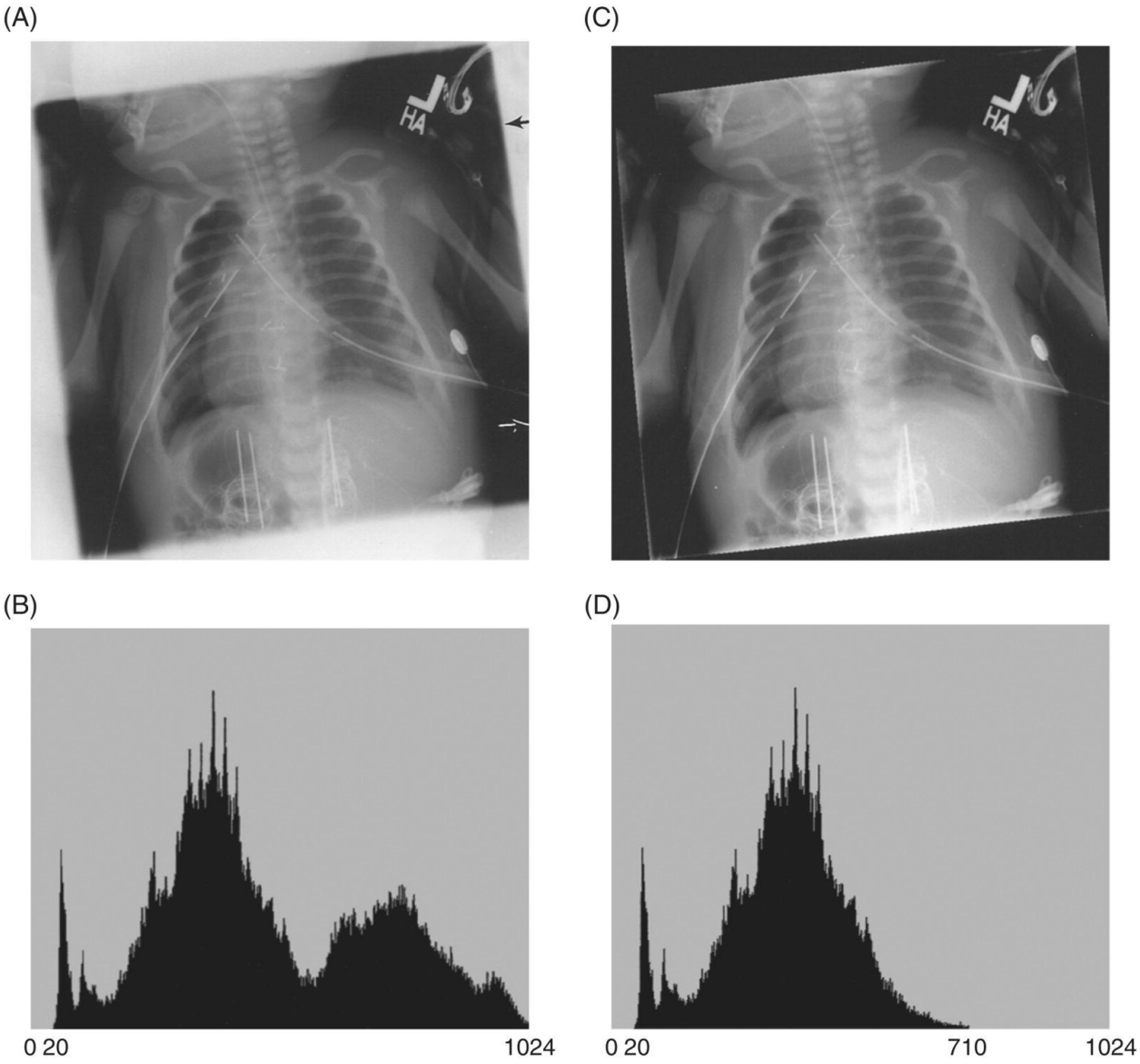

Figure 10.10 Results after background removal. (A) Original pediatric CR image with background (arrows, white area near the borders). (B) Corresponding histogram. (C) Same CR image after background removal, displayed with a different LUT based on the new histogram shown in (D). (D) The corresponding histogram of the image shown in (C) with the background removed. All pixels with values greater than 710 in (D) have been removed.

10.3.6.2 Anatomical Regions of Interest

It is necessary to adjust the display based on the anatomical regions of interest, because the tissue contrast varies in different body regions. For example, in CT chest examinations, it is an advantage to use the lung, soft tissue, and bone

window LUTs to highlight the lungs, heart tissue, and bone, respectively. This method has been used since the dawn of body CT imaging. By the same token, in CR and DR, there are also specially designed LUTs for different body regions. Figure 10.11 shows the four transfer curves used to adjust for the pixel values in the head, bone, chest, and abdomen regions in CR.

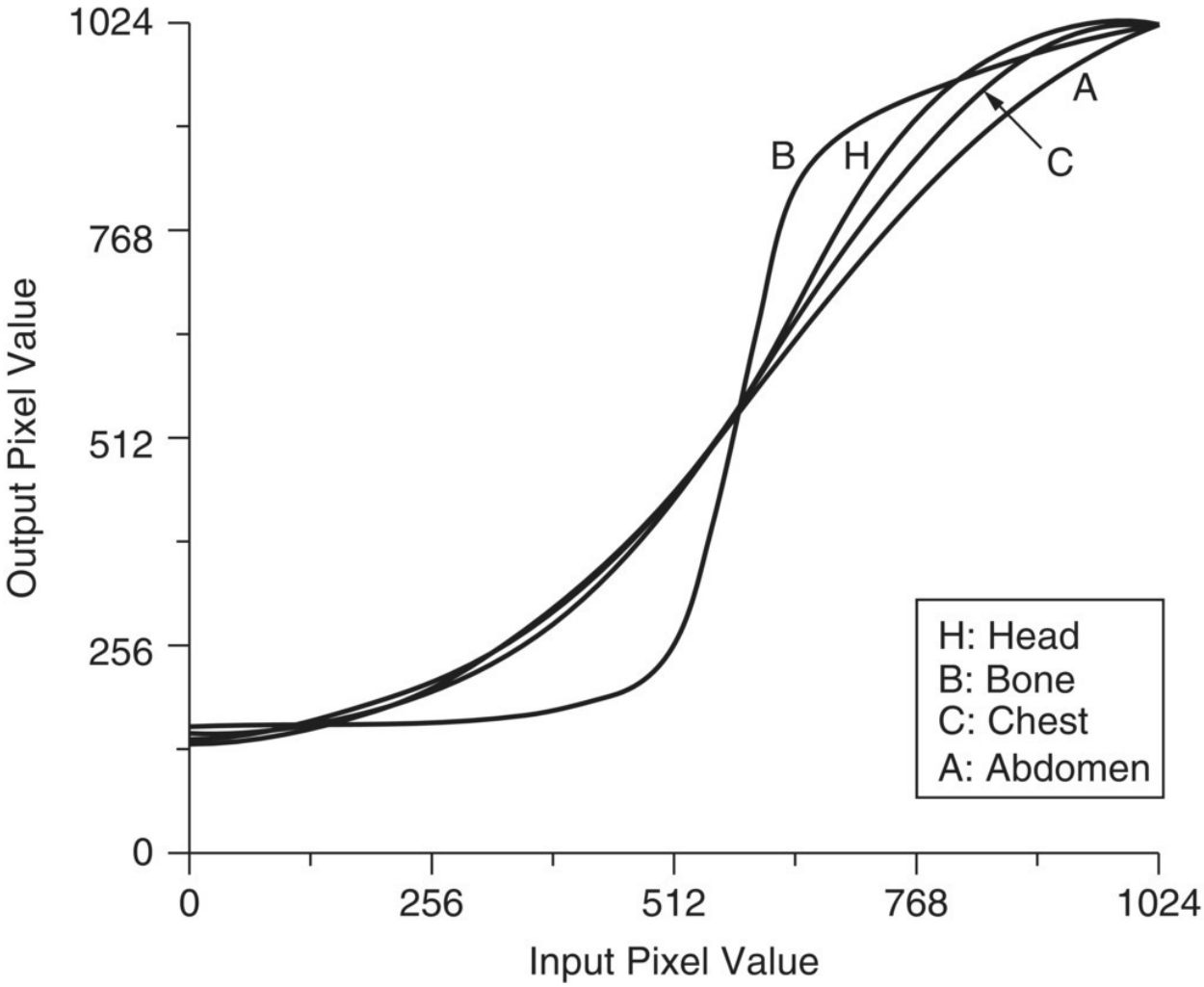

Figure 10.11 Pixel value adjustment for CR images in different body regions: head (H), bone (B), chest (C), and abdomen (A).

(courtesy of Professor J. Zhang)

10.3.6.3 Gamma Curve Correction

The pixel value versus its corresponding brightness in a monitor (either CRT or LCD) is the gamma curve, which is nonlinear and differs from monitor to monitor. An adjustment of this gamma curve to a linear curve would improve the visual quality of the image. For a new monitor, a calibration procedure is

necessary to determine this gamma curve, which is then used to modify the LUT. Figure 10.12 shows the gamma curve from two different types of monitor and their linear correction. A monitor must be recalibrated periodically to maintain its performance.

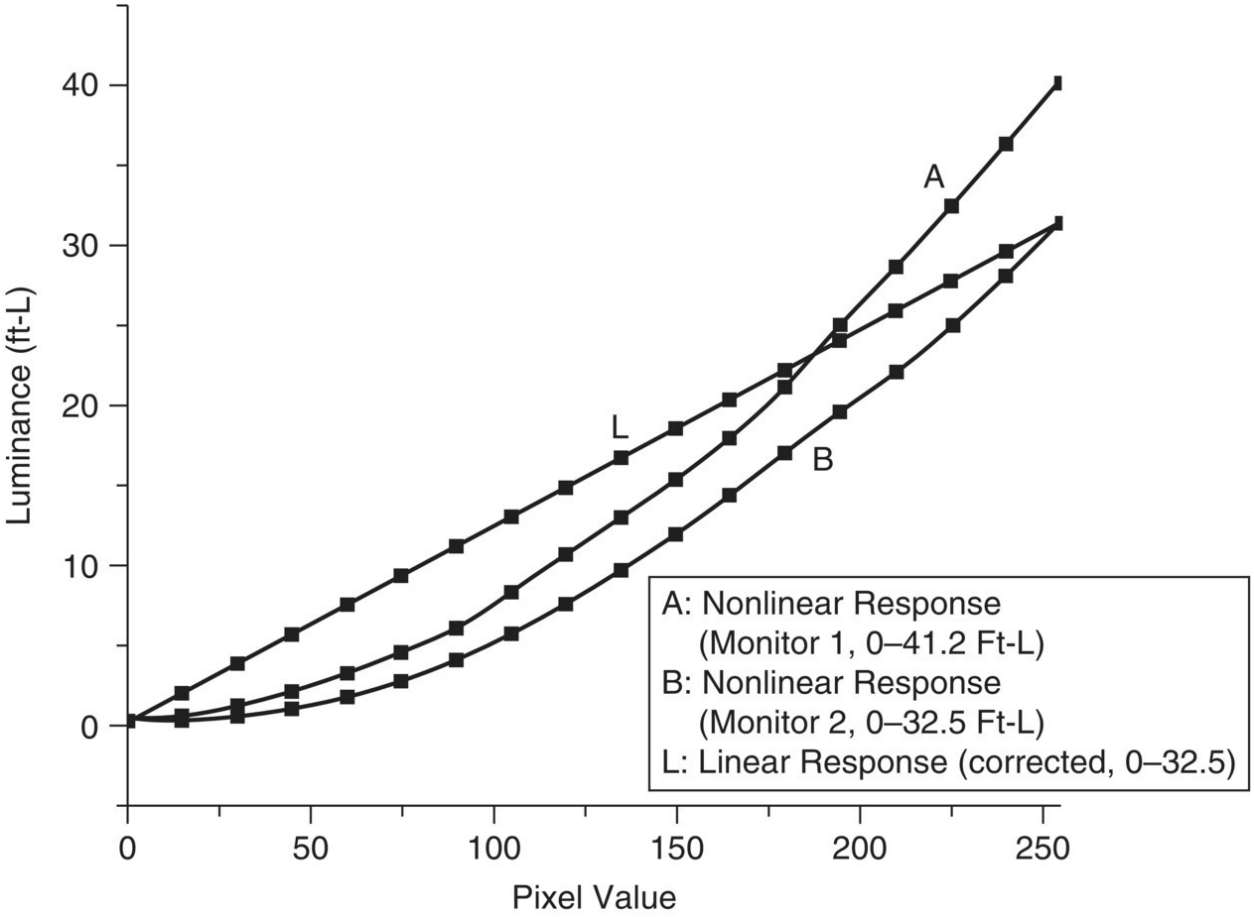

Figure 10.12 (A,B) Gamma curves of two monitors; (L) linear response curve of both monitors after the gamma correction.

(courtesy of Dr J. Zhang)

10.3.7 Montage: Selected Sets of Images with Particular Pathology and/or Features

A montage represents a selected set or sets of individual images from a CT, MRI, US, or any other modality image series for display. Such groupings are useful, because generally only a few images from most image series show the particular pathology or features of interest to the referring physicians or radiologists. For example, an average MRI examination may contain half a dozen sequences with an average of 30 images per sequence, which gives rise to 180 images in the

study. A typical montage would reduce them to 20 images, containing the most significant features representing the examination. So typically only 10% of the images taken from an examination are essential and the rest are supplemental. A montage image collection selected by the radiologist and physician would group the most important images on a single (or multiple) display screen. Each image selected in the montage can be tagged in its own DICOM header for future quick reference and display.

10.4 Workstation Graphic User Interface (GUI) and Basic Display Functions [3–15]

10.4.1 Basic Software Functions in a Display Workstation

Some basic software functions described in Section 10.3 are necessary in a WS to facilitate its operation. These functions are easy to use with a single click on the mouse at the patient's directory, study list, and image processing icons on the monitors. The keyboard is used for retrieving information not stored in the WS's local disks. In this case, the user types in either the patient's name or ID number or a disease category as the key for searching information from the archive. Table 10.2 lists some basic software functions required in a WS. Among these functions, the most often used are: select patient, sort patient directory, library search, select image, cine mode, zoom/scroll, and window and level. Results of using some of these functions are shown in Figures 10.13 to 10.16. Figure 10.13 shows the patient directory with the patient list (with fictitious names), ID, date and time of the study, modality, procedure, and the physician's name. The leftmost column is a read icon to delineate whether the study had been read by a radiologist. Figure 10.14A shows a single monitor displaying three views of an MRI study, and Figure 10.14B is a two-monitor workstation displaying a sequence of transverse view on the left and a coronal view on the right monitor. The bottom icon's graphic user interface (GUI) row describes their functions. Figure 10.15 shows a two-monitor WS of a CT chest examination using the soft tissue window. Figure 10.16 provides a two-monitor view of an obstetric US examination showing a fetus.

Table 10.2 Important software functions in a display WS.

Function	Description
Directory	

Patient directory	Name, ID, age, sex, date of current exam
Study list	Type of exam, anatomical area, date studies taken
Display	
Screen reconfiguration	Reconfigures each screen for the convenience of image display
Monitor selection	Left, right
Display	Displays images according to screen configuration and monitor selected
Image manipulation	
Dials	Brightness, contrast, zoom, and scroll
LUT	Predefined lookup tables (bone, soft tissue, brain, etc.)
Cine	Single or multiple cine on multi-monitors for CT and MRI
Rotation	Rotates an image
Negative	Reverses gray scale
Utilities	
Montage	Selects images to form a montage
Image discharge	Deletes images of discharged patients (a privileged operation)
Library search	Retrieves historical examinations (requires keyboard operation)
Report	Retrieves reports from RIS
Measurements	Linear and region of interest

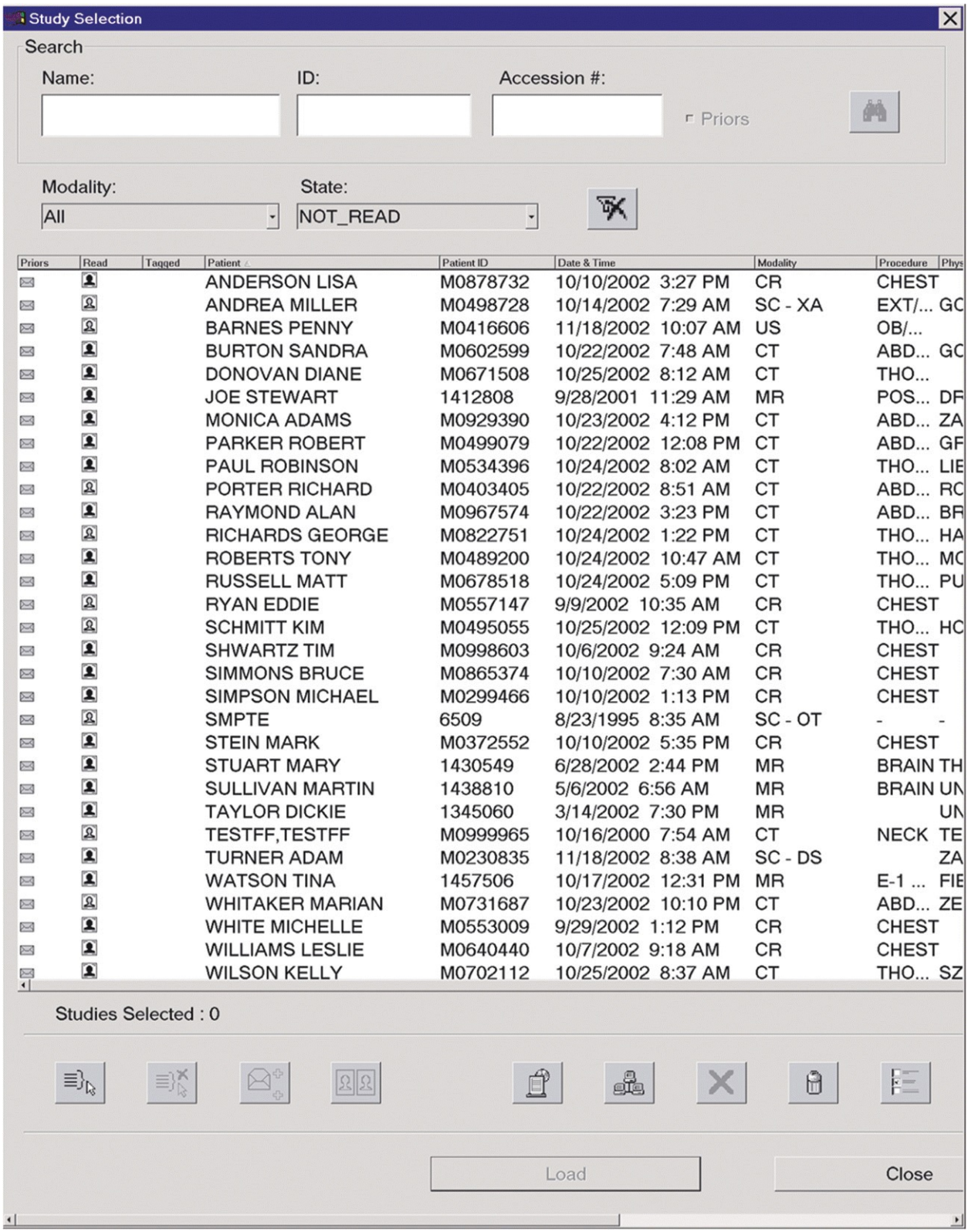

Figure 10.13 Patient directory with the patient list (with fictitious names), ID, date, and time of the study, modality, procedure, and physician's name.

(A)

JOE STEWART 1412808 MALE
DOB:1/25/1996 E-00679270 DOS:9/28/2(
9/28/2001
A
R
H
R
H
A

(B)

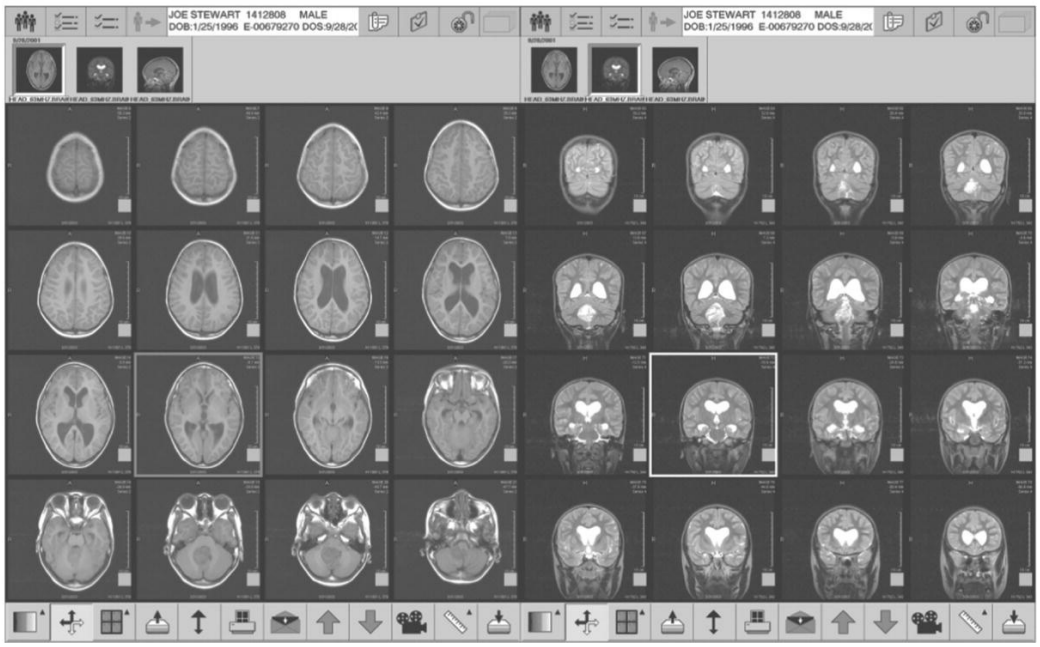
JOE STEWART 1412808 MALE
DOB:1/25/1996 E-00679270 DOS:9/28/2(
JOE STEWART 1412808 MALE
DOB:1/25/1996 E-00679270 DOS:9/28/2(

Figure 10.14 (A) Single LCD monitor displaying three views of a basic MRI study. (B) Two-LCD monitor WS displaying transverse view on the left and coronal view on the right monitor.

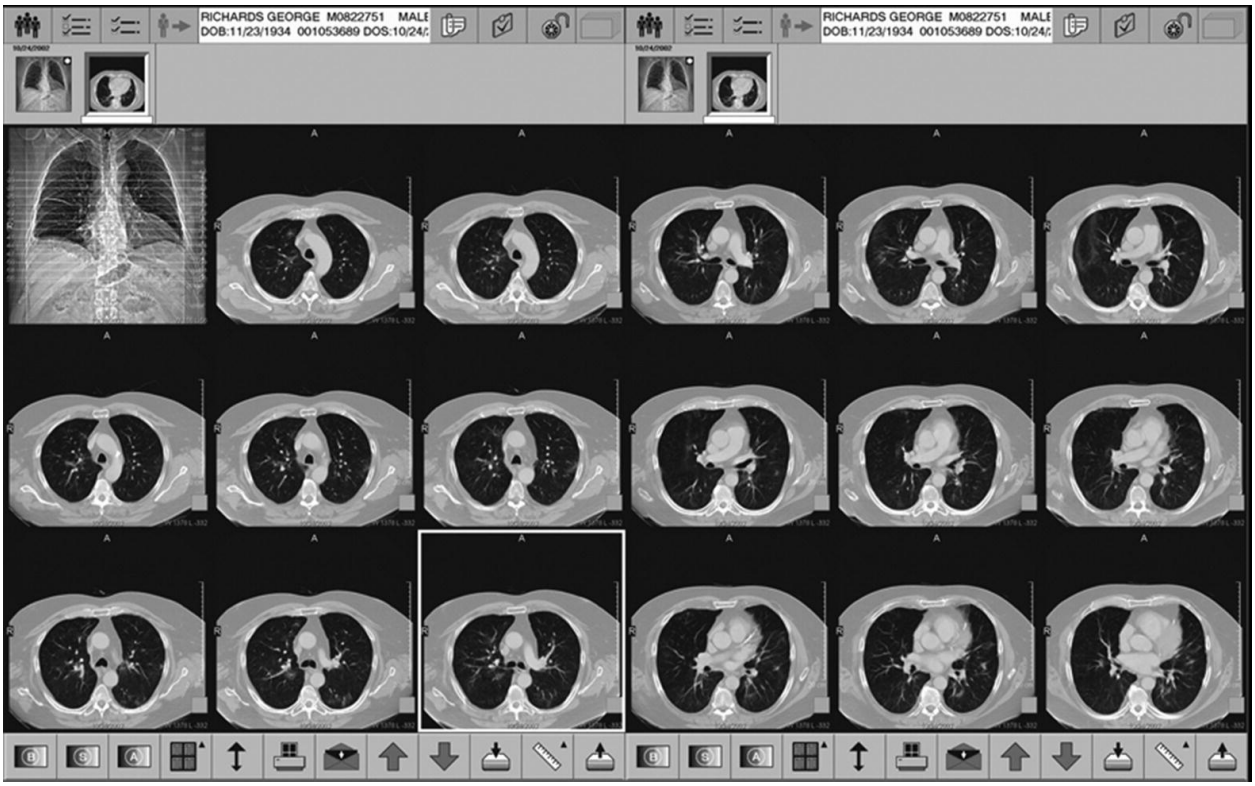

Figure 10.15 A two-LCD monitor WS showing a CT chest examination with the soft tissue window. The first image is the chest scout view of the patient.

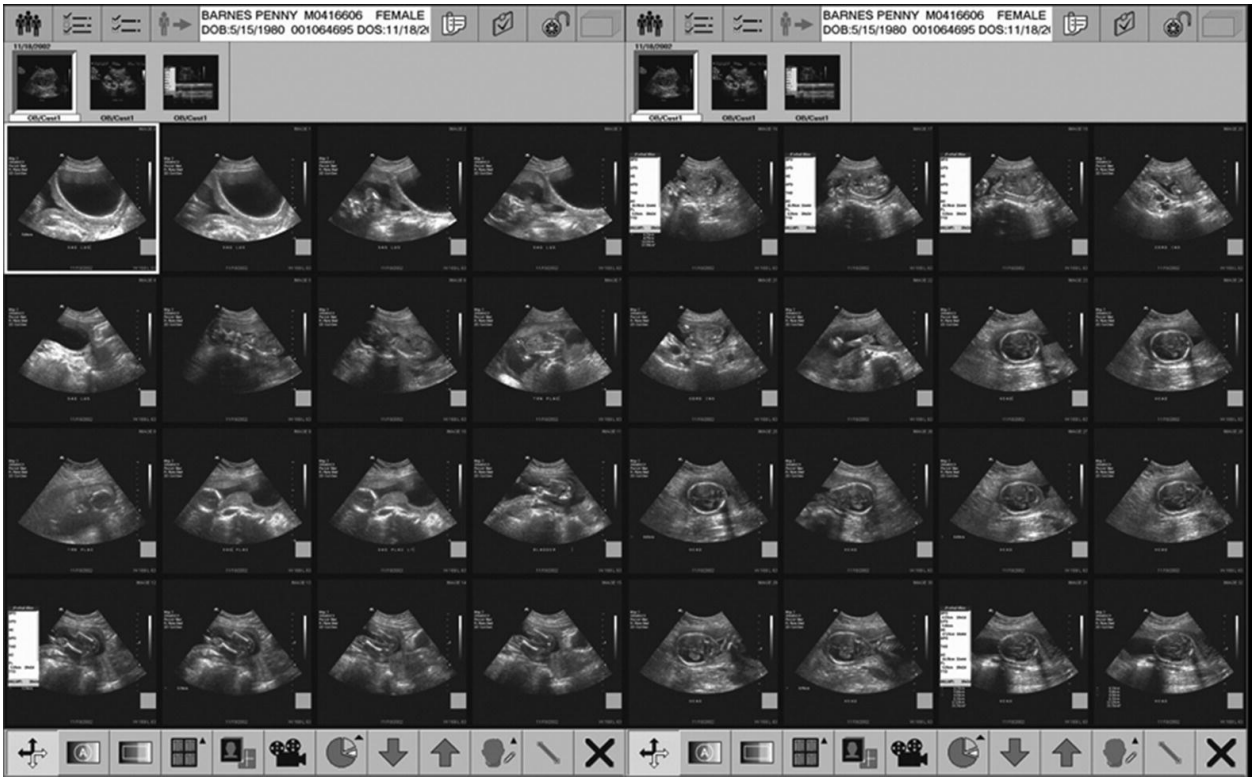

Figure 10.16 Two-LCD monitor WS showing an obstetric US examination of a fetus.

10.4.2 Workstation User Interface

Most PACS manufacturers have implemented the aforementioned display and measurement functions in their WSs in the form of a library. The user can use a pull-down manual to customize their preferred interface at the WS. The 12 icons at the bottom of each display window in Figures 10.13 to 10.16 provide examples of customized user interface icon toolbars designed by the user using a pull-down manual. Figure 10.17 shows these 12 icons, and their descriptions are given in Table 10.3.

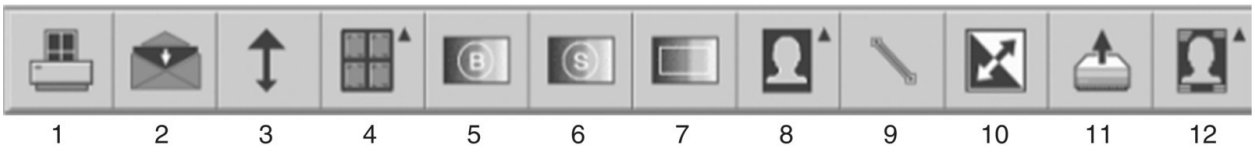

Figure 10.17 Graphical user interface display toolbars and icons.

Table 10.3 Description of the user interface icons and toolbars shown in Figure 10.17.

1. Print the selected image
2. Save the selected image
3. Zoom in and out of the image
4. Show a list of display layouts and set the layout
5. Set the bone window/level
6. Set the soft tissue window/level
7. Set the auto display window/level
8. Edge enhancement filter
9. Image measurement functions
10. Invert the image
11. Reset the image display
12. Select the text level in the image (a lot of text, some, minimum)

10.5 DICOM PC-Based Display Workstation Software

Most display WSs discussed in the Second Edition of *PACS and Imaging Informatics*, 2010 was based on the PC, either Windows 98 and upwards, or the XP operation system. The WSs discussed in this current edition include more up-to-date developments based on the Windows 10 Version 1607 and Windows Server 2016(Window XP (codename Whistler) - Window 7).

This trend is natural for the integration of PACS-based multimedia imaging informatics and the electronic patient record (ePR), since the latter is mostly based on a PC-based system. For this reason, no DICOM PC-based hardware is discussed. In this section, a more up-to-date architecture of the DICOM PC-based display WS software is discussed.

10.5.1 Software System

The PC-based software can be developed on a Microsoft Windows or XP platform and in the Visual C/C++ programming environment. WinSock communication over TCP/IP, Microsoft foundation class (MFC libraries, standard image processing library, University of California, Davis, DICOM

Library, and Windows-based PACS application program interface (API) libraries can be used as development tools. The user interface of the display WS is icon/menu driven with a user-friendly graphical interface.

10.5.2 Software Architecture

The architecture of the software system is divided into four layers, as shown in Figure 10.18: application interface layer (top, green), application libraries layer (blue), system libraries layer (yellow), and operating system (OS) driver layer (purple), with the OS over the hardware layer (reddish).

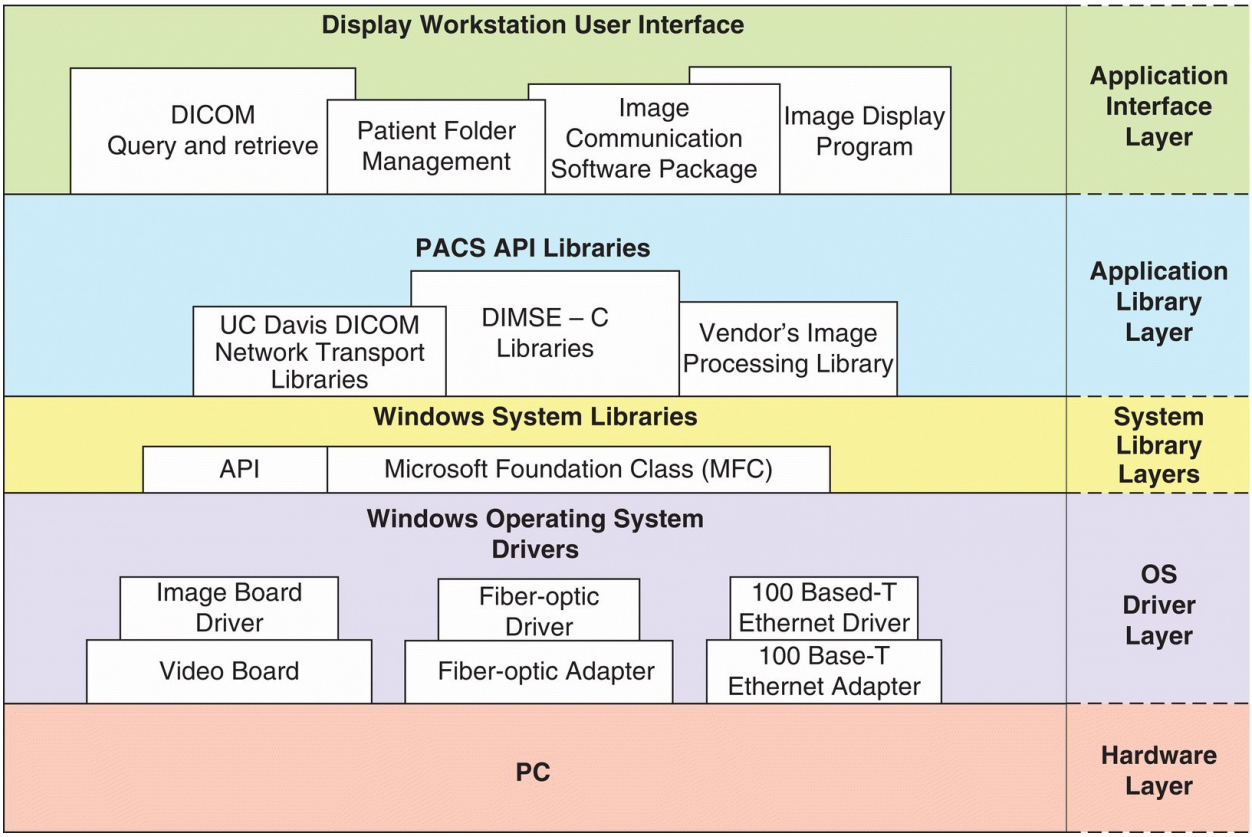

Figure 10.18 Software architecture of a PC-based display WS.

(courtesy of M. Lei, J. Zhang, and X. Wong)

The application interface layer (green) is the top layer of the software system that interfaces with the end user of the display WS. This layer is composed of four modules:

1. image communication software package;
2. patient folder management;

3. image display program; and
4. DICOM query/retrieve software package.

The layer directly supports any application that requires accessing PACS-based radiological and radiotherapy, and optical image.

In the application library layer (blue), the PACS API libraries provide all library functions to support four modules in the application interface layer. Here, the University of California, Davis, DICOM Network Transport libraries and DIMSE-C libraries ensure DICOM communication protocols and functions, as well as taking care of the specific vendor's image processing library supplying library functions for image display of the workstation.

The system library layer (yellow) is responsible for providing Windows system libraries, application library layer functions, and Microsoft foundation class(MFC) to serve as a developmental platform. Also, the OS driver layer (purple) provides Windows OS and its drivers for connecting with hardware components, which include the vendor's driver for its image board, and optical fiber or high-speed Ethernet communication ports. Software data flow between these layers of the software is shown in Figure 10.19.

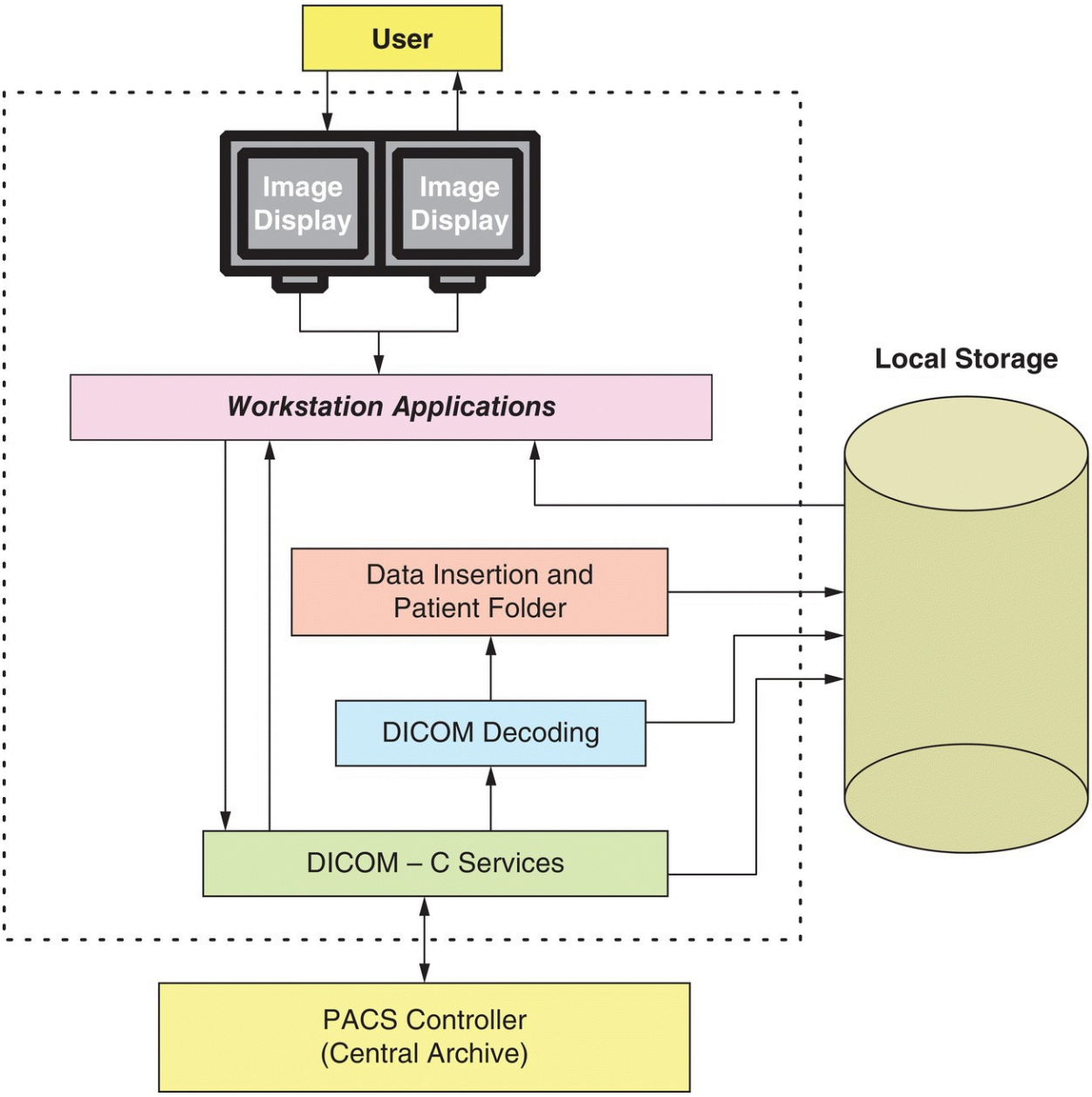

Figure 10.19 Software data flow in the DICOM-compliant PC-based display workstation. Compare this software workflow with the early WS development shown in Figure 10.2.

(courtesy M. Lei, J. Zhang, and X. Wong)

10.5.3 Software Modules in the Application Interface Layer

In the early developed WS, the user has access only to the application interface layer, which is composed of four modules: image communication, a patient folder management, image display program, and query and retrieve modules.

10.5.3.1 Image Communication

The module is responsible for supporting DICOM services with DICOM protocols over TCP/IP to perform two DICOM services: storage service class provider (SCP), and storage service class user (SCU). The DICOM services include C-Echo for verification, C-Store for storage, C-Find for querying, and C-Move for retrieving.

10.5.3.2 Patient Folder Management

The patient folder management module manages the local storage with hierarchical, or tree-structure, directories to organize patient folders within the WS. The DICOM decoder is used to extract patient demographic data and examination records from the header of a DICOM image. The reformatter of the module changes the image from DICOM format to the vendor's image board format for display. The extracted image data, via the DICOM decoder and the reformatter, is inserted into an individual patient folder. A patient folder follows the DICOM data model, which contains three hierarchical levels: patient, study, and series level. The hierarchy starts with a root directory in the local storage system of the WS. Figure 10.20 depicts a diagram of the DICOM data model patient folder infrastructure.

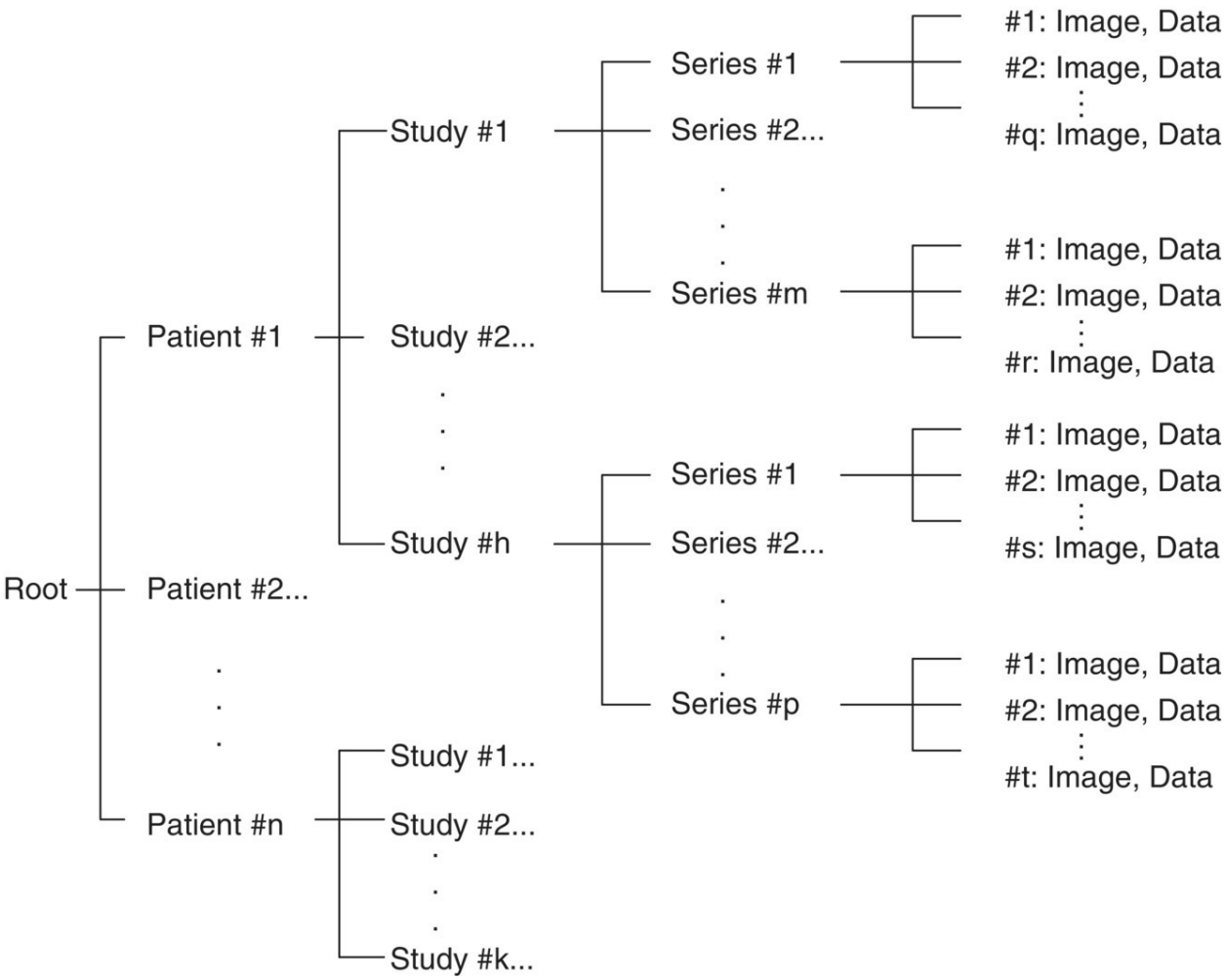

Figure 10.20 Three-level hierarchical levels of the patient folders: patient, study, and series level, based on the DICOM data model managed by the display WS. See also Figure 10.21.

(courtesy of M. Lei, J. Zhang, and X. Wong)

A patient's folder is automatically created in the WS on receipt of the first image of the patient. Subsequent images from individual studies and series are inserted into the patient folder accordingly. The patient folder can be automatically deleted from the WS based on certain aging criteria, such as the number of days since the folder was created or discharge or transfer of the patient. Figure 10.21 presents the interface of three hierarchical levels of patient folders.

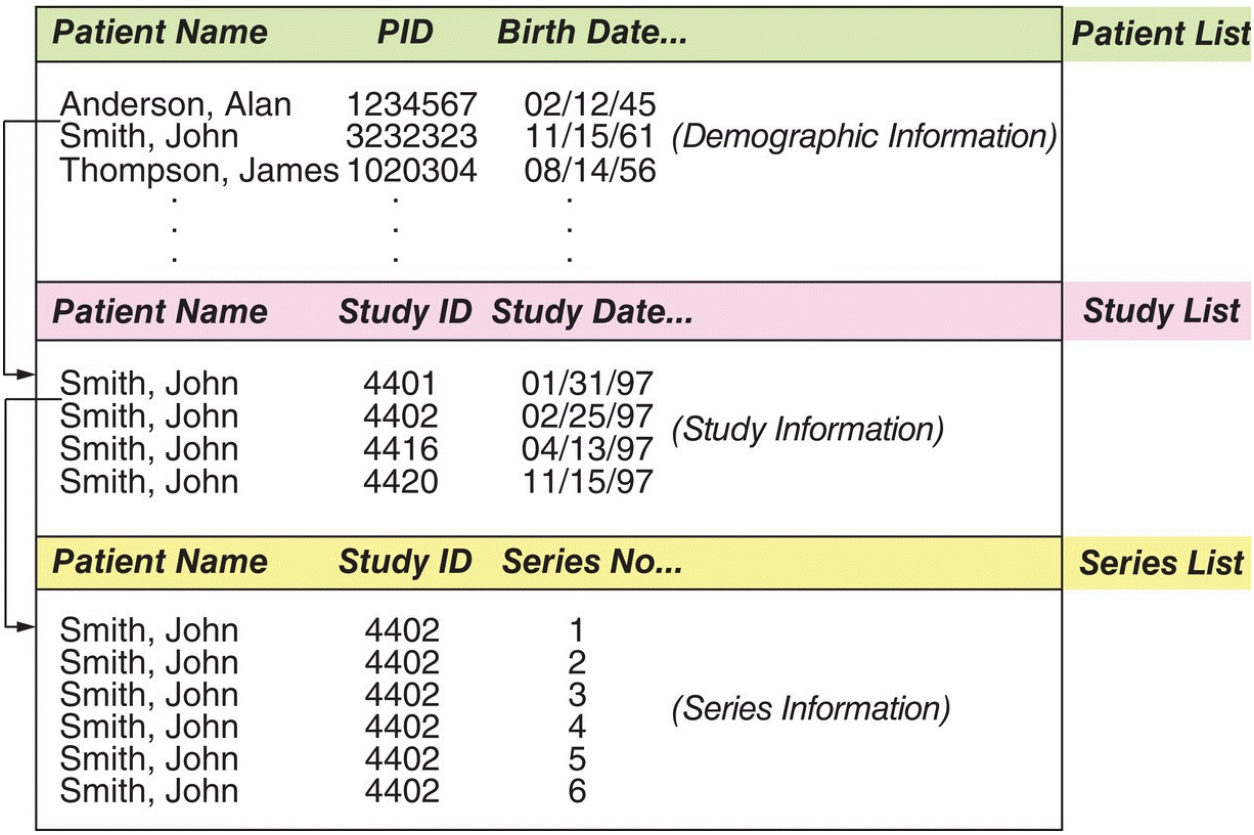

Figure 10.21 Patient folders in the WS. Each folder contains three hierarchical levels: patient, study, and series level.

(courtesy of M. Lei, J. Zhang, and X. Wong)

10.5.3.3 Image Display Program

The image display program supports both single and dual large 1600 × 1280 (up to 2.5 K × 2.K) resolution portrait LCD monitors to display patient information and radiological images. Images with the vendor image board header format in a patient folder can be displayed via the image display program. The screen layout of the WS should be user adjustable, with one image on one monitor, two on one, four on one, etc. The display program supports multimodality display for most DICOM-based multimedia medical images and informatics data, including CT, MR, US, CR/DR, multimodality, and light images in the sense that one monitor can display one modality while the second monitor's is for other modality images.

Image manipulation functions such as zoom, pan, rotation, flip, window and level adjustment, and invert are also included. Automatic defaulted window and level preset function is used during imaging loading to minimize the

manipulation time. Real-time zoom and contrast adjustment is easily performed by using the WS mouse.

10.5.3.4 Query and Retrieve

This module is a DICOM query/retrieve (Q/R) service class user to query and retrieve patient studies from the PACS long-term archive or directly from radiological and surgical related imaging systems. The Q/R module supports DICOM C-Echo, C-Store, C-Find, and C-Move services. With this module, the WS has the access capability to Q/R service class providers, which use the Q/R information models of patient root and study root.

10.6 Post-Processing Workflow, PACS-Based Multidimensional Display, and Specialized Post-Processing Workstation

10.6.1 Post-Processing Workflow

Current development of multidimensional imaging technology leads to the requirement of inventing new types of storage methods as well as display WSs. A single examination may generate hundreds on multidimensional images. With these multimodality images per examination, radiologists, surgeons, radiation therapists, and physicians face the time constraint of completing their daily workload. The trend is to intelligently extract focused qualitative and quantitative results from these images and display them effectively and optimally on the workstation. The image storage issue has been discussed in previous chapters and will be continuously mentioned in later chapters. The rest of this section focuses on some innovative methods for image display.

To circumvent voluminous images per study, research laboratories around the world have developed new methods for display and production by manufacturers. The common term used in this approach is called post-processing workflow (PPW). It has two components:

1. a post-processing WS to receive images and data from their sources, and process them accordingly; and
2. a workflow to integrate the post-processed data and export results to the PACS-based multimedia informatics WSs for viewing.

The post-processing WS can be one that performs a multidimensional image

display or a CAD workstation (see Chapters 16–18) with complex algorithms for information retrieval, feature extraction, and computer diagnosis. To integrate CAD results to PACS-based multimedia imaging informatics, Chapter 16 presents a general-purpose CAD PACS integration toolkit. Some post-processing image products may not require the same US Food and Drug Administration (FDA) approval as that needed from some CAD products, because in the former the manufacturer does not change the PACS images and data, but only displays them differently. Thus, their products can get to the marketplace faster. Geniune CAD products do require FDA approval, and the time required from perceiving the concept to the market place may take years. The following two sections discuss two methods that focus on PPW of multidimensional image display. The first method is to integrate a software toolkit into the PACS-based WS, and the second method is to use the vendor provided specific display WS.

10.6.2 PACS-Based Multidimensional Image Display

As multi-slice CT (128–256 slices) and 3-D MRI modalities are used widely in radiological, radio therapeutic, and surgical imaging studies. The image numbers per series are increased from a few of hundreds to many thousands, and these huge amounts of medical image data are generated daily. The traditional 2-D image display modes, such as multiple window layout, pan, static stack, or dynamic stack, are not sufficient for physicians to handle so many images in one or two display screens at the same time. The new 3- and 4-D image display functions have become common diagnostic tools for viewing these images. As many of these studies generate isotropy images in all directions, physicians can view and analyze image structures and pathology from all directions with different 3-D orientations, resulting in methods such as multi-planar reconstruction (MPR), maximum intensity projection (MIP), surface-shaded display (SSD), or volume rendering.

In these types of display, interactive manipulation is essential to obtain the optimal visualization effect. The 3-D image WSs should provide enough, easy-to-use GUI to users when rendering volume and time (4-D) image data. Free and easy to change the visual angle (free multi-planar reconstruction (MPR)) and to set the rendering pattern is advantageous. Furthermore, in favor of the widespread application of medical image visualization in the clinical environment, a small and flexible 3-D display software framework to plug in the existing PACS WS is suitable for radiologists and physicians to use. This is because there is usually a lack of computing power in the PACS-based WS's clinical environment. This section provides the concept of a software

visualization toolkit (VTK), consisting of the aforementioned functions for displaying multidimensional images, which can easily be applied to a medical image WS or Web-based network application. Once the toolkit is installed in the PACS WS, it provides a straightforward PPW between the multidimensional images input data and the PACS-based WS display. Figures 10.22A shows some MPR and MIP displays of a cardiac CT study, and Figure 10.22B depicts a head CT MPR, MIP displays, and an SSD rendering pattern.

(A)

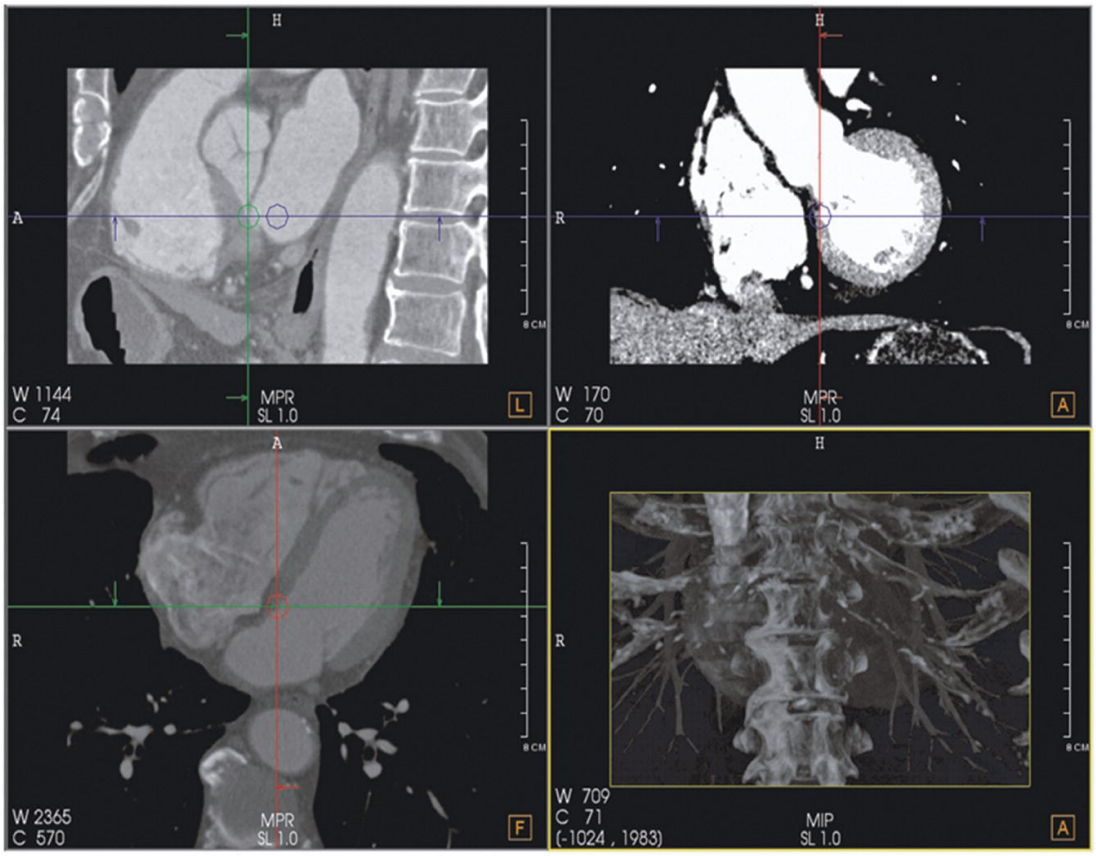
H
A
W 1144
C 74
MPR
SL 1.0
L
H
R
W 170
C 70
MPR
SL 1.0
A
A
R
W 2365
C 570
MPR
SL 1.0
F
H
R
W 709
C 71
(-1024 , 1983)
MIP
SL 1.0
A

(B)

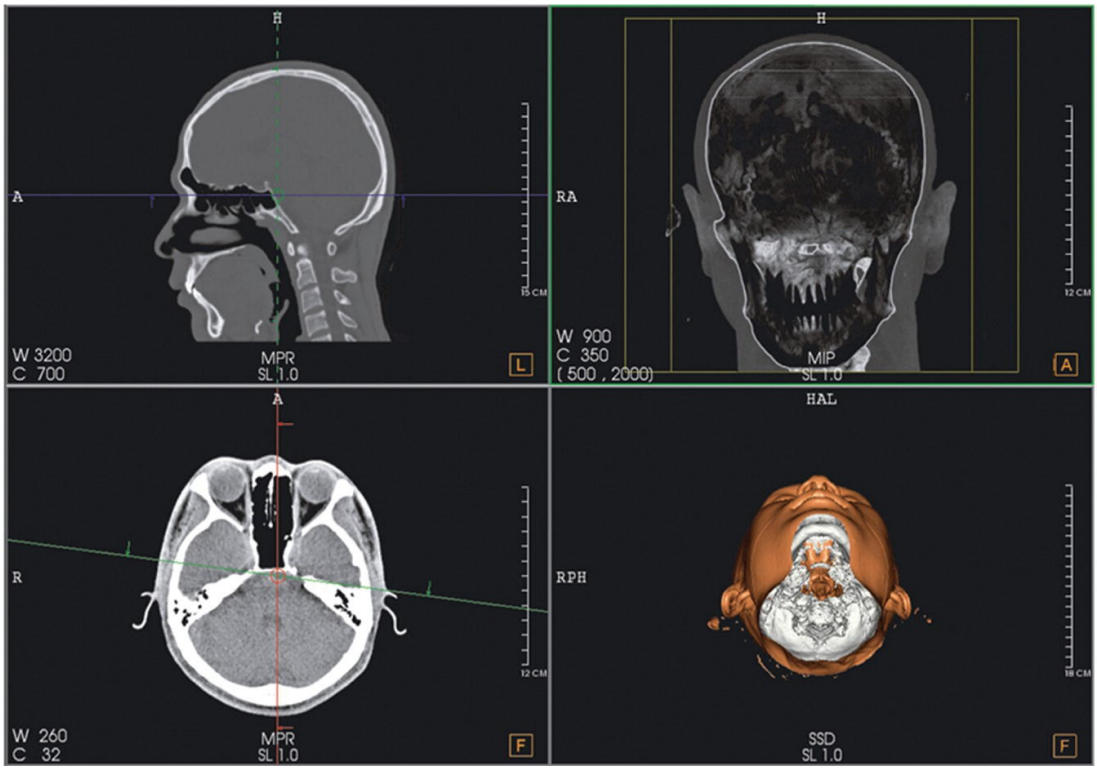
H
A
W 3200
C 700
MPR
SL 1.0
L
H
RA
W 900
C 350
(500 , 2000)
MIP
SL 1.0
A
A
R
W 260
C 32
MPR
SL 1.0
F
HAL
RPH
SSD
SL 1.0
F

Figure 10.22 Different 3-D orientations resulting in display methods such as multi-planar reconstruction (MPR), maximum intensity projection (MIP), surface-shaded display (SSD), and volume rendering can be visualized. (A) Top: four screenshots of visualization of a patient's heart from multi-slice CT; upper left: sagittal projecting plane of MPR; upper right: coronal projecting plane of MPR; bottom left: axial projecting plane of MPR; bottom right: sagittal MIP. (B) Bottom: a head CT image series constructed to a 3-D volume dataset; upper left: one MPR; upper right: MIP; lower left: MPR; and lower right: SSD.

(courtesy of Dr J. Zhang)

10.6.3 Specialized Post-Processing Workstation

There are at least half a dozen manufacturers who produce specialized post-processing WSs. Each of them has their own specialties and market niche of applications. Since these WSs have more computational power, they can produce faster, more comprehensive data, and better-quality displays, but the current penalty for post-processing is the lack of its communications among the workflow, the WS, and the PACS-based data input and display. As of now, most post-processing workstations can accept DICOM push functions and compute the necessary algorithms on the WSs. But to transfer post-processing results directly back to PACS-based multimedia imaging informatics WS for direct display is still not convenient. Currently, most of the "push back" is still manual, requiring the radiologist, clinician, and technologist to transfer to screenshot data manually; from there, the result is then dictated and/or screenshot as a report. This situation is "what you see is what you get," as the real post-processing data are not linked to the PACS-based WS, and only the screenshot is. Screenshot is a very preliminary technology in DICOM. There is yet a product developed by vendors that can be easily connected to the DICOM structured reporting method linking the direct post-processing data to the PACS-based WS (Chapters 16–18). Figures 10.22 to 10.24 show some screenshot results from the post-processing WSs.

(A)

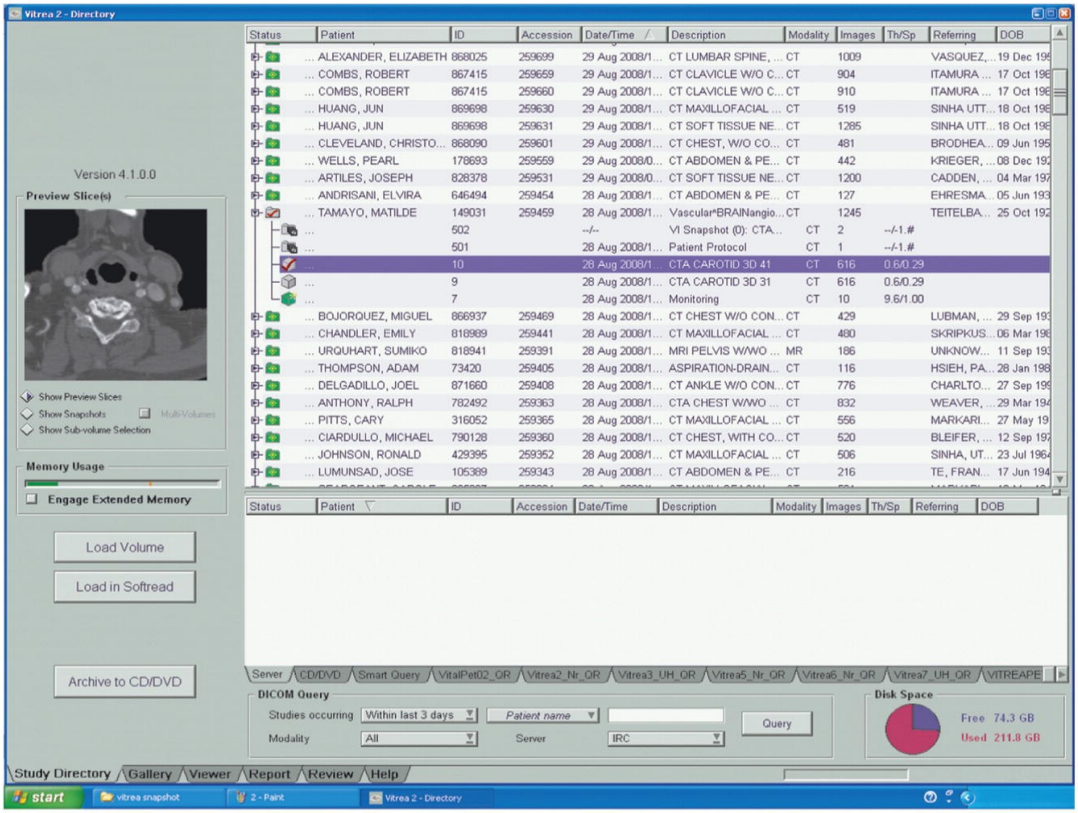
Vitrea 2 - Directory
Version 4.1.0.0
Preview Slice(s)
Show Preview Slices
Show Snapshots
Multi-Volumes
Show Sub-volume Selection
Memory Usage
Engage Extended Memory
Load Volume
Load in Softread
Archive to CD/DVD
Status
Patient
ID
Accession
Date/Time
Description
Modality
Images
Th/Sp
Referring
DOB
ALEXANDER, ELIZABETH 868025 259699 29 Aug 2008/1... CT LUMBAR SPINE, ... CT 1009 VASQUEZ,... 19 Dec 19
COMBS, ROBERT 867415 259659 29 Aug 2008/1... CT CLAVICLE W/O C... CT 904 ITAMURA ... 17 Oct 19
COMBS, ROBERT 867415 259660 29 Aug 2008/1... CT CLAVICLE W/O C... CT 910 ITAMURA ... 17 Oct 19
HUANG, JUN 869698 259630 29 Aug 2008/1... CT MAXILLOFACIAL ... CT 519 SINHA UTT... 18 Oct 19
HUANG, JUN 869698 259631 29 Aug 2008/1... CT SOFT TISSUE NE... CT 1285 SINHA UTT... 18 Oct 19
CLEVELAND, CHRISTO... 868090 259601 29 Aug 2008/1... CT CHEST, W/O CO... CT 481 BRODHEA... 09 Jun 19
WELLS, PEARL 178693 259559 29 Aug 2008/0... CT ABDOMEN & PE... CT 442 KRIEGER, ... 08 Dec 19
ARTILES, JOSEPH 828378 259531 29 Aug 2008/0... CT SOFT TISSUE NE... CT 1200 CADDEN, ... 04 Mar 19
ANDRISANI, ELVIRA 646494 259454 28 Aug 2008/1... CT ABDOMEN & PE... CT 127 EHRESMA... 05 Jun 19
TAMAYO, MATILDE 149031 259459 28 Aug 2008/1... Vascular*BRAINangio... CT 1245 TEITELBA... 25 Oct 19
502 --/-- VI Snapshot (0): CTA... CT 2 --/-1.#
501 28 Aug 2008/1... Patient Protocol CT 1 --/-1.#
10 28 Aug 2008/1... CTA CAROTID 3D 41 CT 616 0.6/0.29
9 28 Aug 2008/1... CTA CAROTID 3D 31 CT 616 0.6/0.29
7 28 Aug 2008/1... Monitoring CT 10 9.6/1.00
BOJORQUEZ, MIGUEL 866937 259469 28 Aug 2008/1... CT CHEST W/O CON... CT 429 LUBMAN, ... 29 Sep 19
CHANDLER, EMILY 818989 259441 28 Aug 2008/1... CT MAXILLOFACIAL ... CT 480 SKRIPKUS... 06 Mar 19
URQUHART, SUMIKO 818941 259391 28 Aug 2008/1... MRI PELVIS W/WO ... MR 186 UNKNOW... 11 Sep 19
THOMPSON, ADAM 73420 259405 28 Aug 2008/1... ASPIRATION-DRAIN... CT 116 HSIEH, PA... 28 Jan 19
DELGADILLO, JOEL 871660 259408 28 Aug 2008/1... CT ANKLE W/O CON... CT 776 CHARLTO... 27 Sep 19
ANTHONY, RALPH 782492 259363 28 Aug 2008/1... CTA CHEST W/WO ... CT 832 WEAVER, ... 29 Mar 19
PITTS, CARY 316052 259365 28 Aug 2008/1... CT MAXILLOFACIAL ... CT 556 MARKARI... 27 May 19
CIARDULLO, MICHAEL 790128 259360 28 Aug 2008/1... CT CHEST, WITH CO... CT 520 BLEIFER, ... 12 Sep 19
JOHNSON, RONALD 429395 259352 28 Aug 2008/1... CT MAXILLOFACIAL ... CT 506 SINHA, UT... 23 Jul 19
LUMUNSAD, JOSE 105389 259343 28 Aug 2008/1... CT ABDOMEN & PE... CT 216 TE, FRAN... 17 Jun 19
Server
CD/DVD
Smart Query
VitalPet02_OR
Vitrea2_Nr_OR
Vitrea3_UH_OR
Vitrea5_Nr_OR
Vitrea6_Nr_OR
Vitrea7_UH_OR
VITREAPE
DICOM Query
Studies occurring
Within last 3 days
Patient name
Modality
All
Server
IRC
Query
Disk Space
Free 74.3 GB
Used 211.8 GB
Study Directory
Gallery
Viewer
Report
Review
Help
start
vitrea snapshot
2 - Paint
Vitrea 2 - Directory

(B)

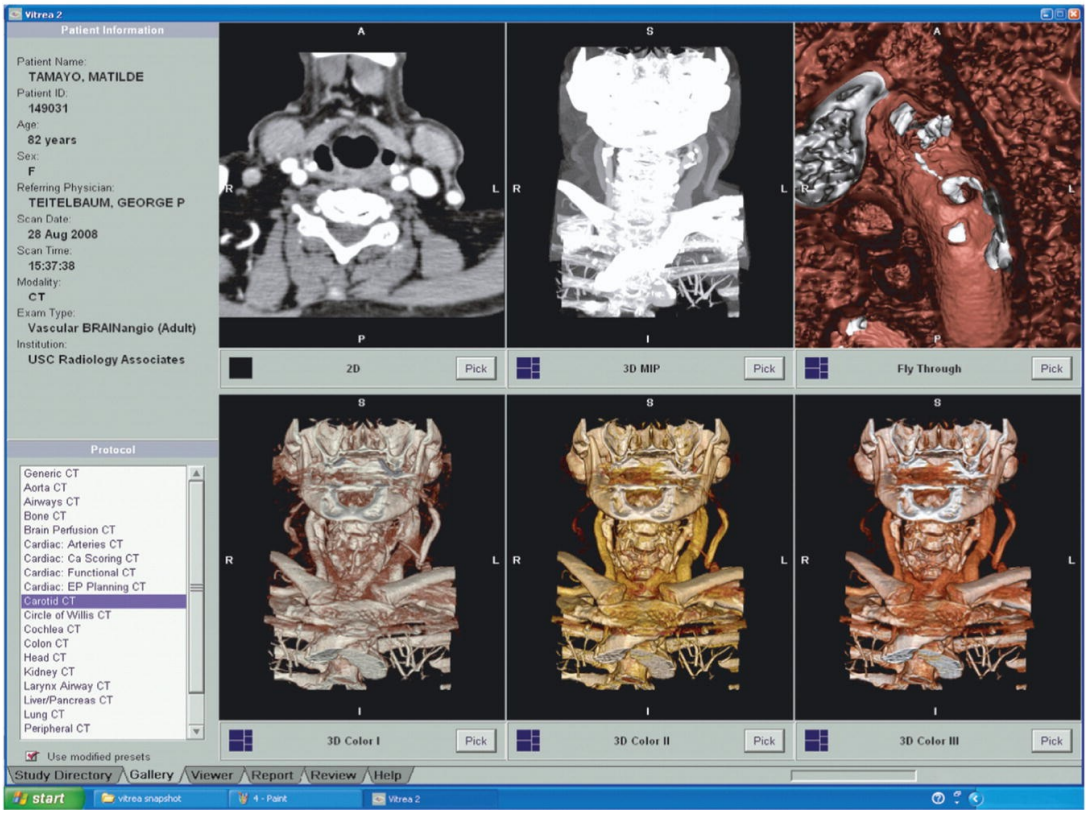
Vitrea 2
Patient Information
Patient Name:
TAMAYO, MATILDE
Patient ID:
149031
Age:
82 years
Sex:
F
Referring Physician:
TEITELBAUM, GEORGE P
Scan Date:
28 Aug 2008
Scan Time:
15:37:38
Modality:
CT
Exam Type:
Vascular BRAINangio (Adult)
Institution:
USC Radiology Associates
Protocol
Generic CT
Aorta CT
Airways CT
Bone CT
Brain Perfusion CT
Cardiac: Arteries CT
Cardiac: Ca Scoring CT
Cardiac: Functional CT
Cardiac: EP Planning CT
Carotid CT
Circle of Willis CT
Cochlea CT
Colon CT
Head CT
Kidney CT
Larynx Airway CT
Liver/Pancreas CT
Lung CT
Peripheral CT
Use modified presets
2D
Pick
3D MIP
Pick
Fly Through
Pick
3D Color I
Pick
3D Color II
Pick
3D Color III
Pick
Study Directory
Gallery
Viewer
Report
Review
Help
start
vitrea snapshot
4 - Paint
Vitrea 2

(C)

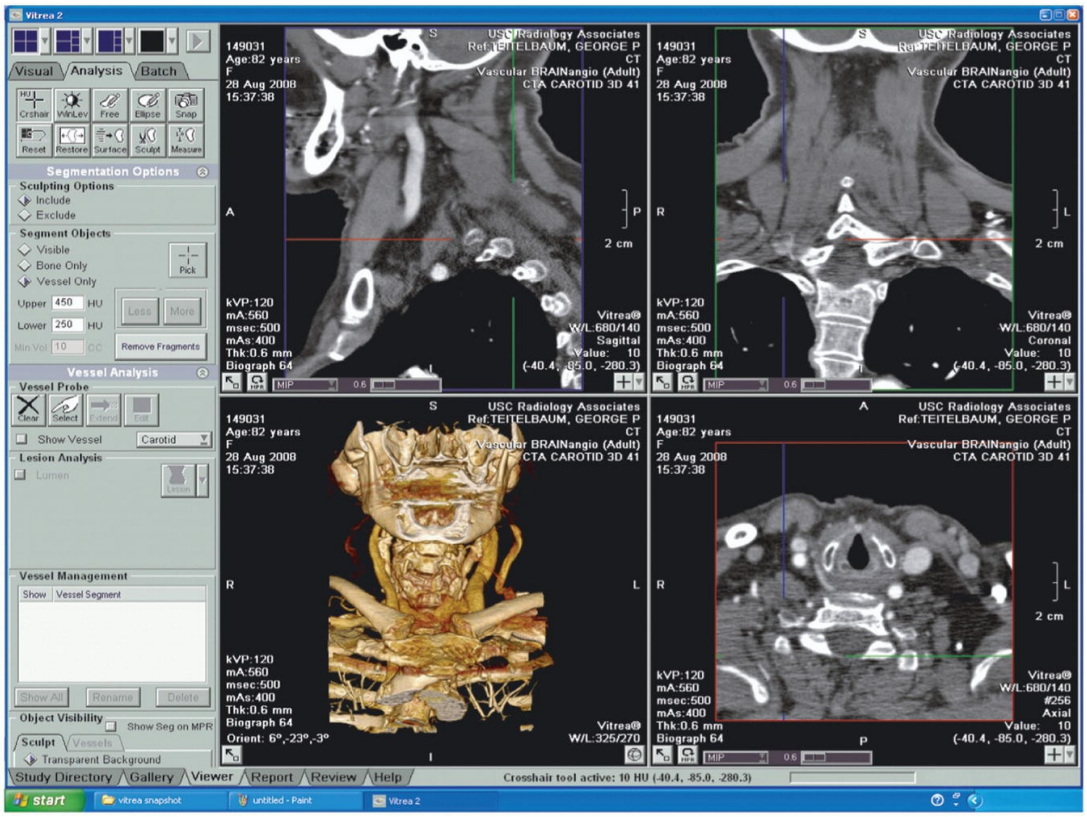
Vitrea 2
Visual
Analysis
Batch
Segmentation Options
Sculpting Options
Include
Exclude
Segment Objects
Visible
Bone Only
Vessel Only
Pick
Upper 450 HU
Lower 250 HU
Less
More
Remove Fragments
Vessel Analysis
Vessel Probe
Clear
Select
Extend
Edit
Show Vessel
Carotid
Lesion Analysis
Lumen
Vessel Management
Show
Vessel Segment
Show All
Rename
Delete
Object Visibility
Show Seg on MPR
Sculpt
Vessels
Transparent Background
149031
Age:82 years
F
28 Aug 2008
15:37:38
USC Radiology Associates
Ref:TEITELBAUM, GEORGE P
CT
Vascular BRAINangio (Adult)
CTA CAROTID 3D 41
kVP:120
mA:560
msec:500
mAs:400
Thk:0.6 mm
Biograph 64
Vitrea®
W/L:680/140
Sagittal
Coronal
Axial
Value: 10
(-40.4, -85.0, -280.3)
W/L:325/270
Orient: 6°,-23°,-3°
2 cm
Study Directory
Gallery
Viewer
Report
Review
Help
Crosshair tool active: 10 HU (-40.4, -85.0, -280.3)
start
vitrea snapshot
untitled - Paint
Vitrea 2

(D)

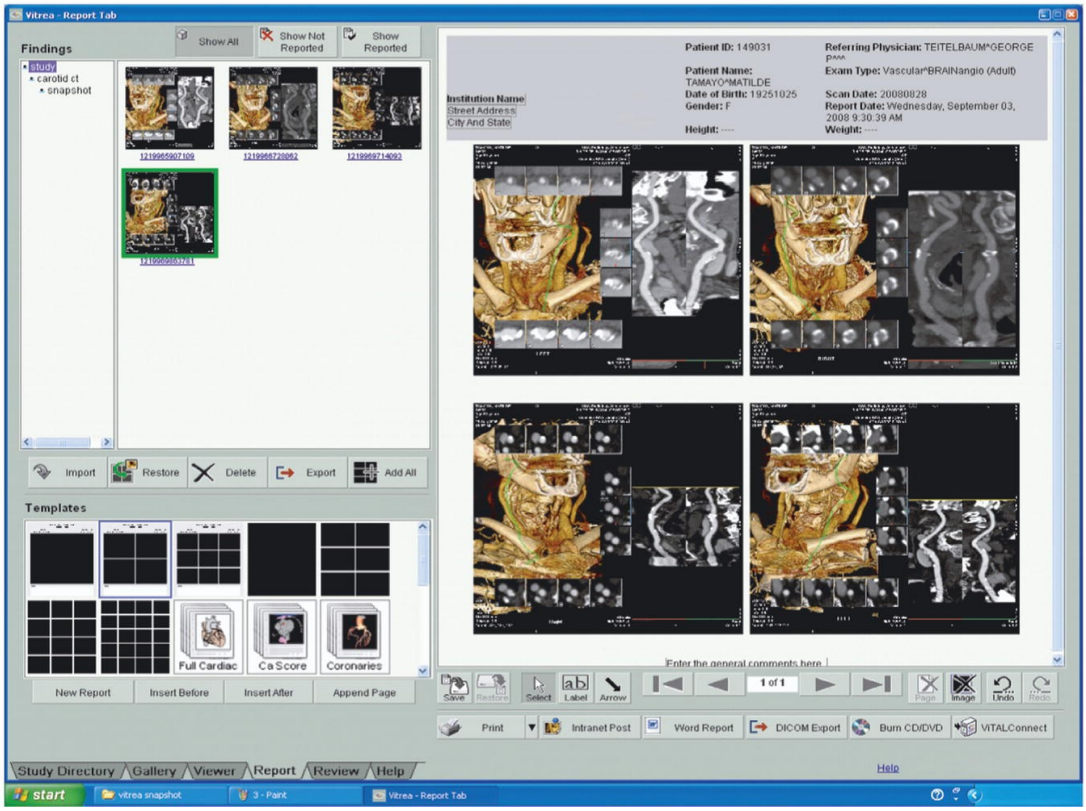
Vitrea - Report Tab
Findings
Show All
Show Not Reported
Show Reported
Study
carotid ct
snapshot
Import
Restore
Delete
Export
Add All
Templates
Full Cardiac
Ca Score
Coronaries
New Report
Insert Before
Insert After
Append Page
Patient ID: 149031
Patient Name: TAMAYO^MATILDE
Date of Birth: 19251025
Gender: F
Height: ----
Referring Physician: TEITELBAUM^GEORGE P^^^
Exam Type: Vascular^BRAINangio (Adult)
Scan Date: 20080828
Report Date: Wednesday, September 03, 2008 9:30:39 AM
Weight: ----
Institution Name
Street Address
City And State
Enter the general comments here
1 of 1
Print
Intranet Post
Word Report
DICOM Export
Burn CD/DVD
VITALConnect
Help
Study Directory
Gallery
Viewer
Report
Review
Help
start
vitrea snapshot
3 - Paint
Vitrea - Report Tab

Figure 10.23 (A) Screen captures of a work list, right: showing the patient study being reviewed; (B) Gallery; (C) viewer; and (D) A manufacturer 3-D display product report.

(courtesy of Dr B. Guo)

(A)

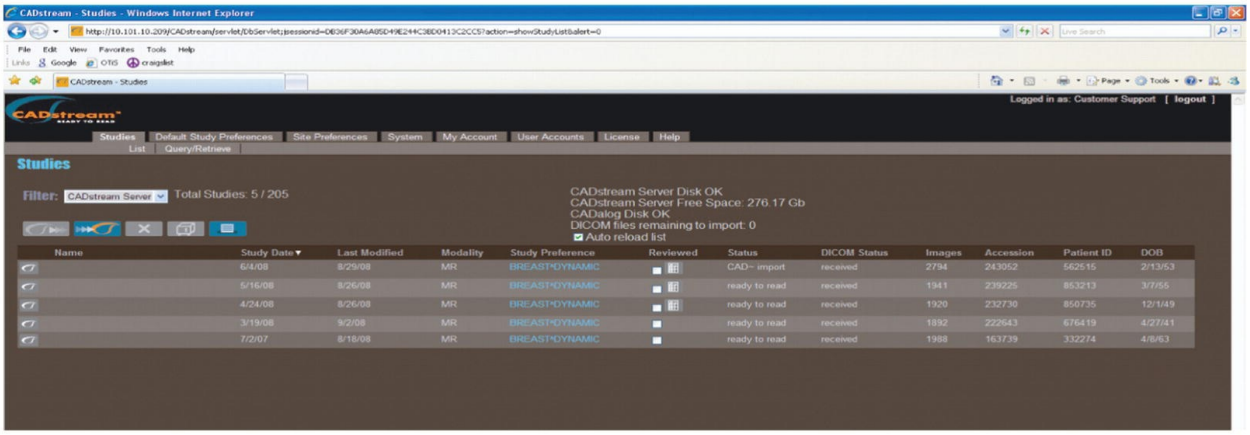

(B)

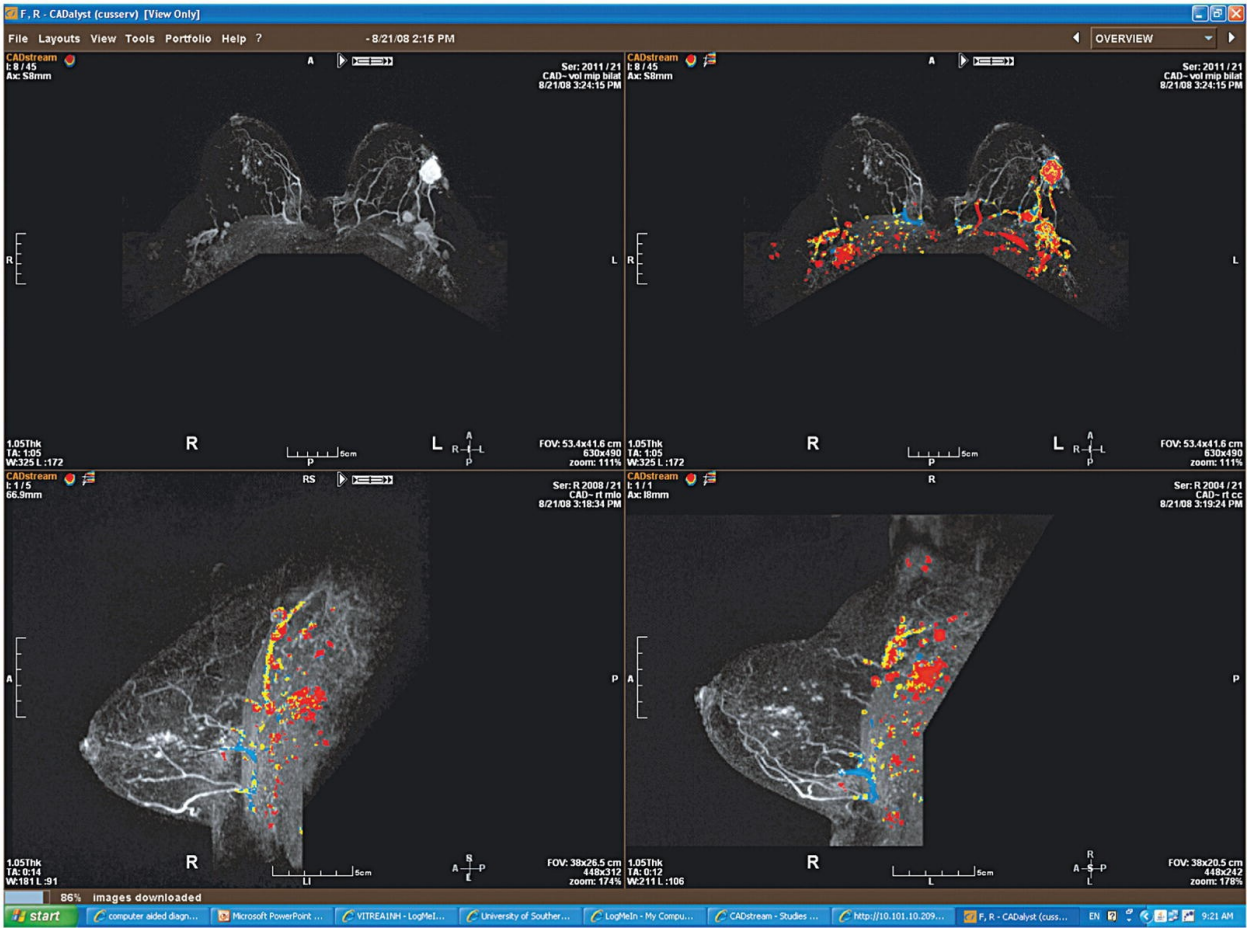

Figure 10.24 (A) Screen captures of a work list; (B) four breast images from the post-processed 3-D MRI generated by a manufacturer workstation.

(courtesy of Dr B. Guo)

10.7 DICOM-Based Workstations in Progress

10.7.1 Intelligence Workstation

10.7.1.1 "True 2½-D" and "True 3-D" Image Workstations

Medical images can be generated in two, three and four dimensions, as described in Chapter 2. However, existing display WSs can only display two dimensions. Many display methods have been developed allowing users to view 2-D image series as if they are 3-D images. An example is watching 3-D movies at the theater with special eye glasses. Chapter 2, Section 6, and Chapter 10, Figures 10.22 to 10.24, depict some 2-D, 3-D, and 4-D images as examples. During the past few years, two new concepts have been gradually developed. First, the concept of "true 2½-D" and "true 3-D" medical images on 2-D monitors are being displayed and operated at some Radiology departments, and second, the 3-D printing based on 3-D CT, MRI, and US images is presented. Sections 10.7.1.1 to 10.7.1.3 discuss true 2/½-D and true 3-D, and Section 10.7.2 discusses 3-D printing.

Recently, true 3-D, a powerful tool that has gained FDA approval for certain clinical applications, allows physicians to better analyze medical images, and provides more accurate diagnoses and assistance in the planning of complex therapies and surgical procedures. A vendor named EchoPixel, recently associating with Hewlett Packard computer technology, developed true 3-D using virtual reality solution, which has been on the market since early 2015. The FDA approval of the EchoPixel system allows its use for medical diagnostic and planning purposes. The true 3-D system creates holographic 3-D medical images that can be viewed in real time, a potential benefit for radiologists, physicians, surgeons, radiotherapists, and researchers. Figure 10.25 shows a 2½-D image display on the 2-D WS; 2½-D in the sense that the dispay does not show independent true 3-D anatomomic components on the image.

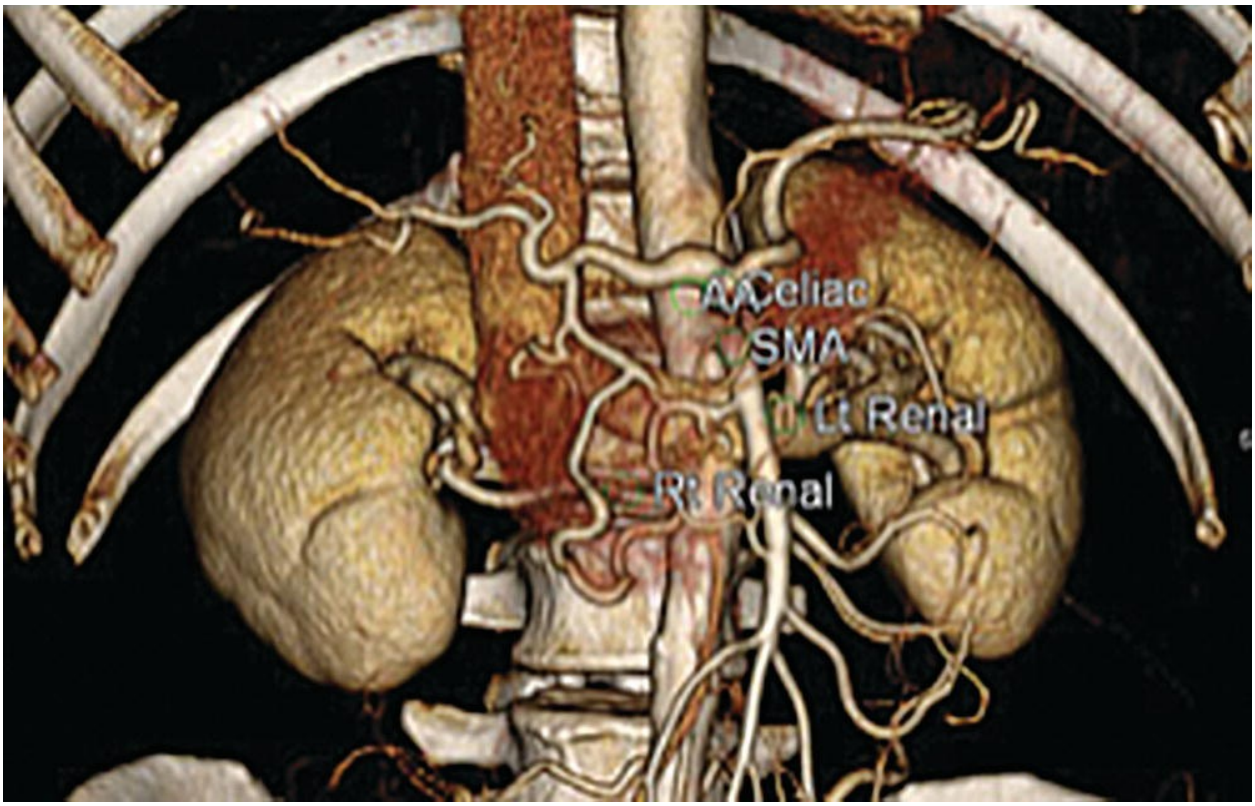

Figure 10.25 An example of the EchoPixel True 2½-D image of the abdomen showing the two kidneys, a part of the lower ribs, the vertebra at the back, and other anatomical features.

(courtesy of EchoPixel)

10.7.1.2 Characteristics of "True 2½-D" and "True 3-D"

True 3-D is an advanced medical visualization software solution. It offers physicists an unprecedented opportunity to view and interact with patient tissues and organs in a true 3-D in front of the 2-D WS, as if they are real physical 3-D objects. Some of the advantages of true 3-D are:

1. *Real-time, Interactive Virtual Reality System*: True 3-D moves beyond the 2-D flat screen displaying real patient anatomy in an open 3-D space, with instant response and seamless interaction capabilities.
2. *Optimal Image Strategy*: Anatomical information is tailored to be procedure-specific, easily accessible, and unobstructed.
3. *Effortless Interpretation*: True 3-D provides the required visual context, with no extraneous information, significantly lowering the cognitive load in doctors.

4. *Engaging User Interface*: It is intuitive to use. Specialized tools enable users to directly grasp, dissect, and size key clinical features with one move.
5. *Advanced Protocols and Sharing*: Expert-derived protocols facilitate specific procedures, allowing physicians to create rich data, share it with others, and improve the utility of the system across the network of users.

Figure 10.25 shows an example of an EchoPixel 2½-D image of the abdomen.

As a case study, Professor Judy Yee, MD (Vice Chair of the Department of Radiology and Biomedical Imaging at UCSF and Chief of Radiology at San Francisco Veterans Affairs Health Care System), uses the EchoPixel system at her 3-D Imaging Lab. In one case, she created thin slices of a CT scan. Each of the images appears 3-D on the flat screen. It can morph into video "fly-through" views, enhancing polyps, lesions, and other precancerous anomalies. Yee also refines this revolutionary blend of advanced graphical software and scanning technology—known as CT colonography or virtual colonoscopy—as a far less invasive and easier-to-interpret alternative to conventional colonoscopies.

Figures 10.26 and 10.27 demonstrate some EchoPixel true 3-D techniques and some of its software and hardware tools.

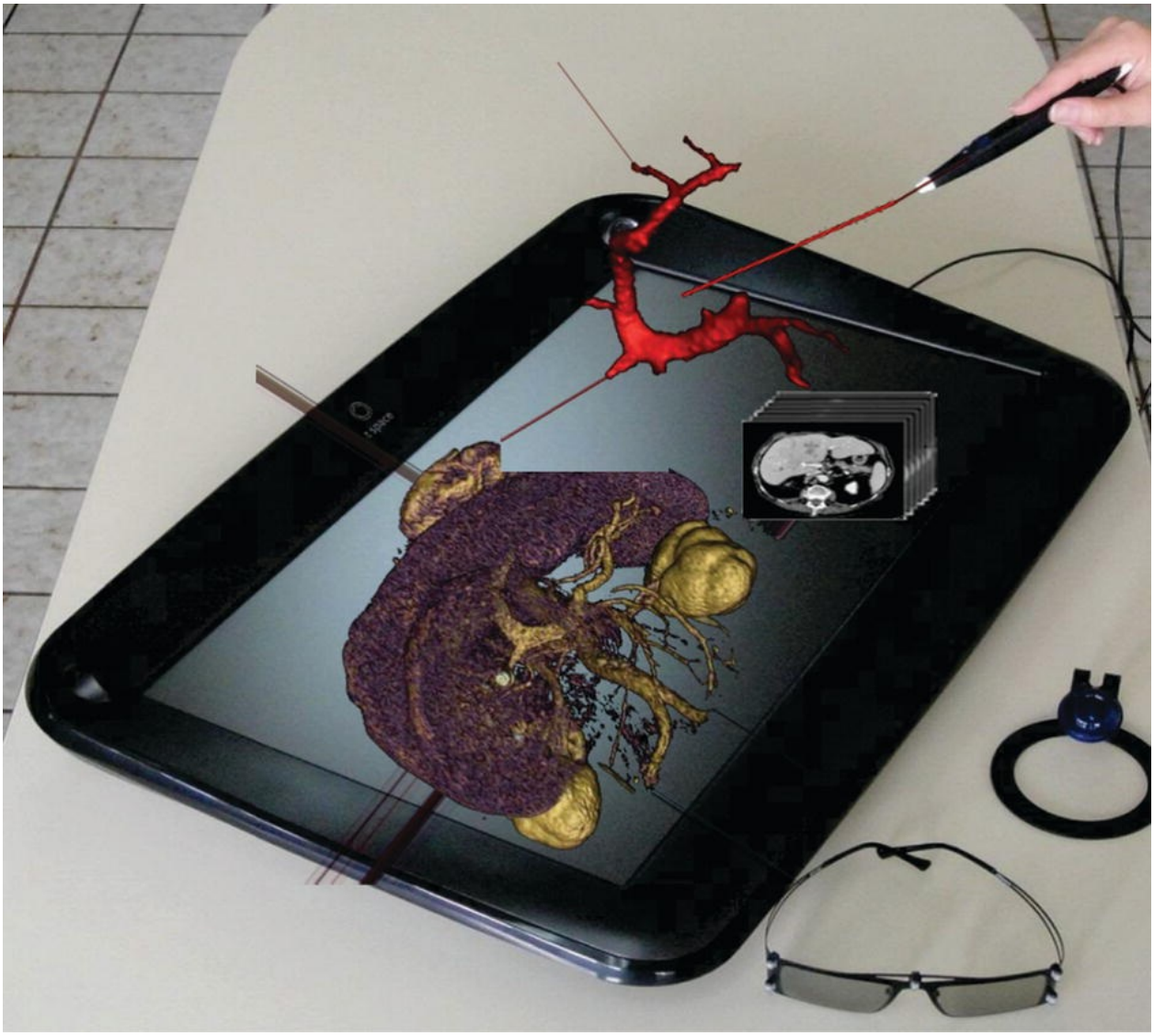

Figure 10.26 A researcher uses hardware and software tools. Upper right: hand held stylus with red pointer guiding an enlarged anatomical true 3-D feature (red) outside of the true 3-D CT body (middle, gray, and yellow); CT image data box: lower right (black and transparent); other imaging tools, a pair of dark glasses at bottom right.

(courtesy of researchers, EchoPixel)

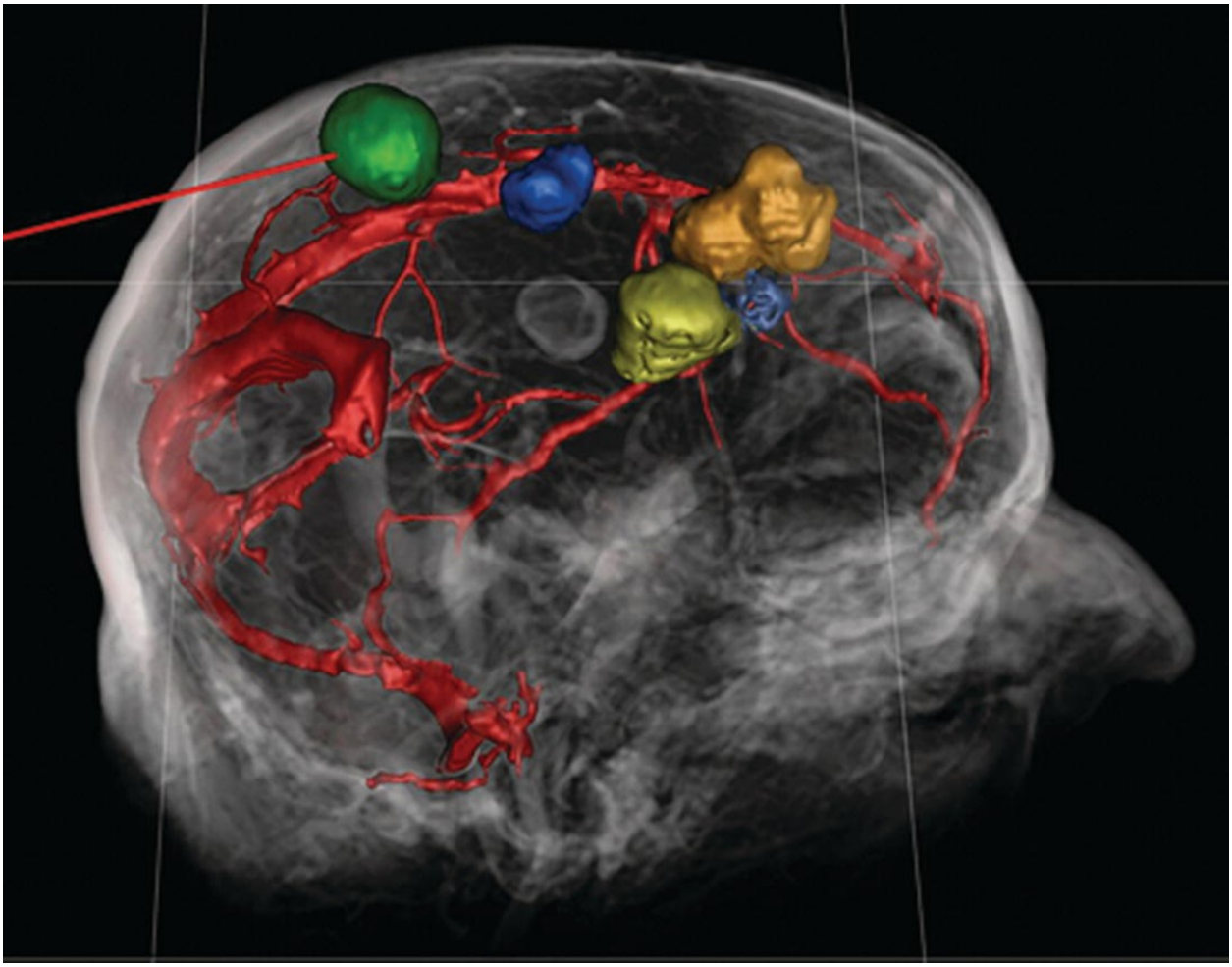

Figure 10.27 True 3-D medical imaging. New medical visualization protocols and visualization protocols can lead to new k nowledge = cognition + intuition. The key is developing new clinical protocols. This figure shows that many anatomical features and components can be extracted from 3-D or 4-D medical images. As an example, a pseudo green object (top left) is being extracted from the inside of the skull by a red color pointer.

(courtesy of EchoPixel researchers and collaborators)

10.7.1.3 Would "True 3-D" Work?

During the past 4–5 years, preliminary experiences with the true 3-D from some individual radiologists, surgeons, radiotherapists, and cardiologists demonstrate that the system has a higher degree of confidence, less uncertainty, and more accurate information, which provided them with better reliability and a faster operating tool. For researchers and users in the DICOM-based multimedia imaging informatics field, they feel the system provides them with better

knowledge to further their inventing and developing. Sections 10.7.1.1 and 10.7.1.2 describe some true 3-D capabilities, Figures 10.28 to 10.30 in this section demonstrate three actual clinical cases: CT head with basilar aneurysm, CT post-transplant kidney, and MRI head with tumors that were recently performed by EchoPixel clinical partners (courtesy of Ron Schilling, PhD, and Will Johnsen, Researcher, EchoPixel) [16].

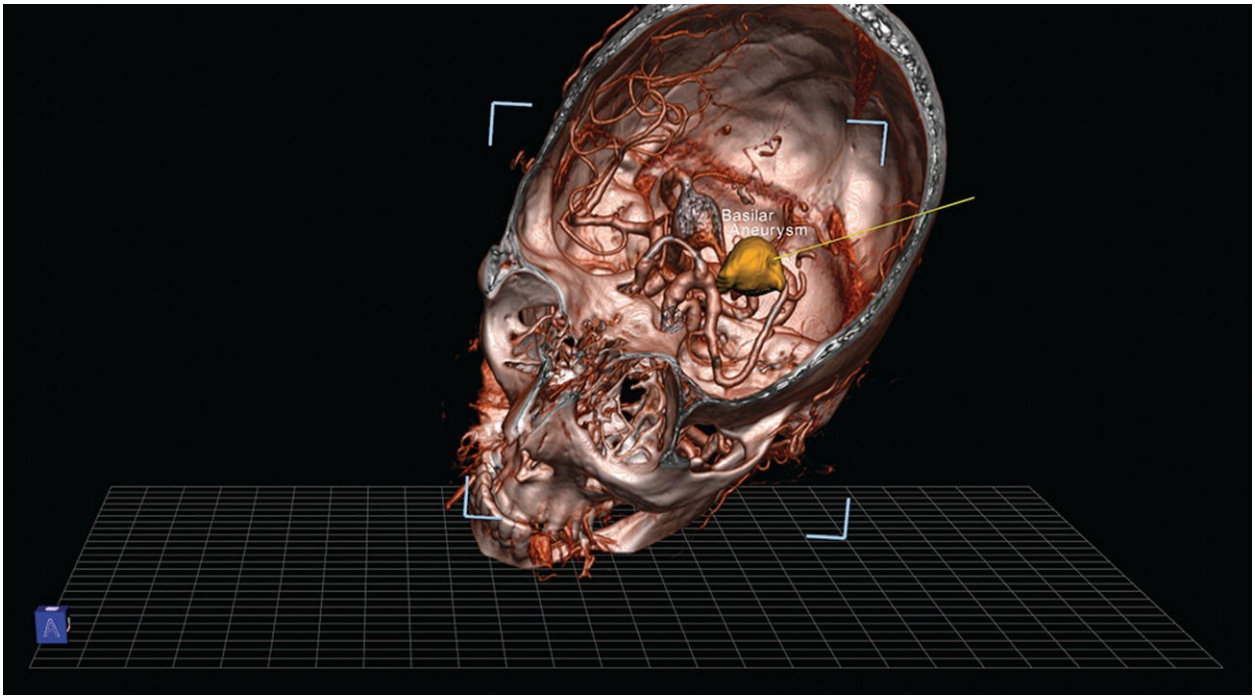

Figure 10.28 A computed tomography (CT) image of the head with a basilar aneurysm shows many blood vessels inside the head on a contrast CT angiogram. The large basilar aneurysm (yellow) in the posterior circulation of the head has been software segmented and can be pulled out and looked at in any angle chosen in true 3-D. The hand-held stylus (yellow) allows the user to interact with data at the end of the yellow color ray and move to any desired location in the true 3-D space that is created by the EchoPixel software and ZVR display on the desktop.

(courtesy of Ron Schilling, PhD, and Will Johnsen, Researcher, EchoPixel)

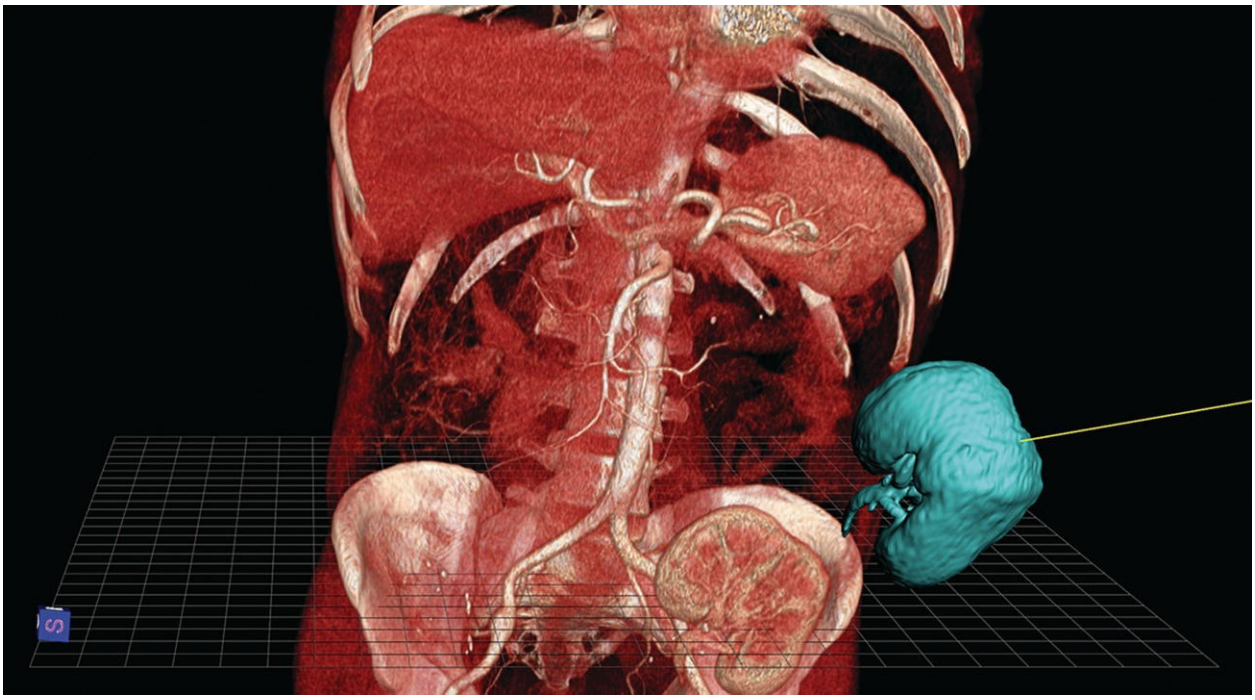

Figure 10.29 CT post-kidney transplant. A computed tomography angiography of the abdomen that shows the post kidney transplant. Kidney transplants are usually placed in the pelvis area because of the access to the iliac veins and arteries. In this true 3-D image, a segmentation of the transplanted kidney has been pulled out by software (yellow lint) from its location to be shown in the true 3-D space.

(courtesy of Ron Schilling, PhD, and Will Johnsen, Researcher, EchoPixel)

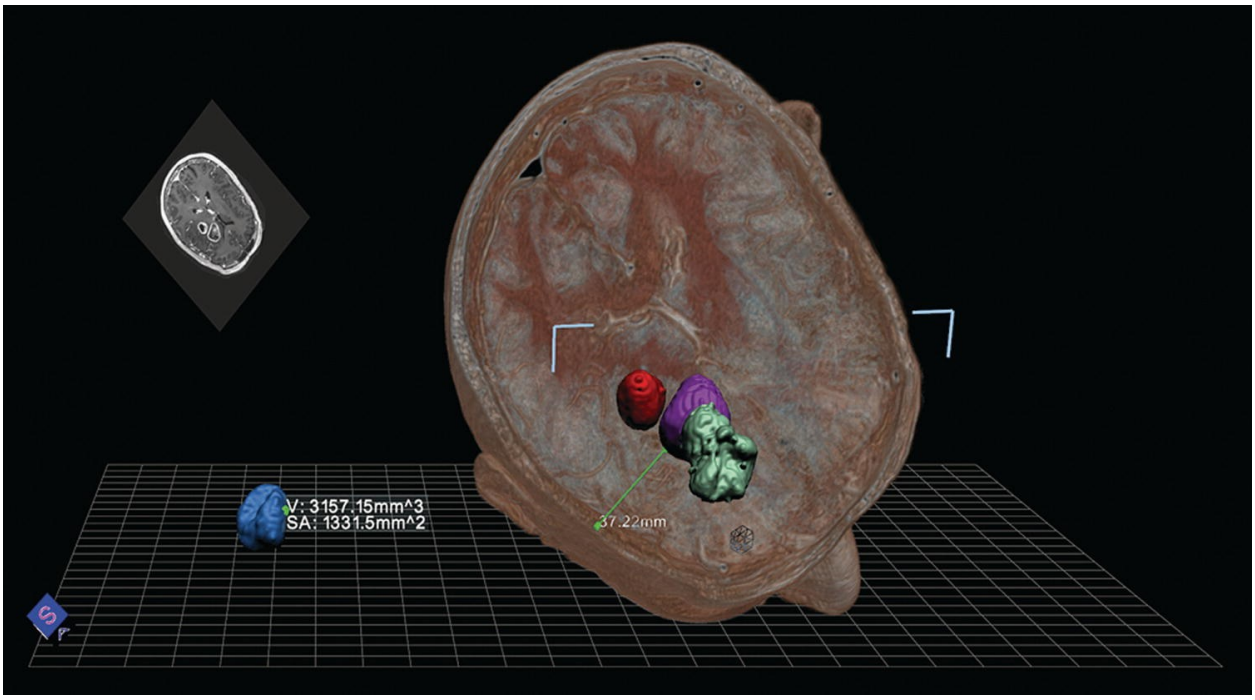

Figure 10.30 MRI of the head with tumors. The MRI head scan shows four tumors registered as blue, red, purple, and green, which have been segmented by software with the true 3-D viewer. The image in the upper left of the screen is a 2-D reference view of the same exact angle that the cut plane is going through on the colored volume. A measure has been made to show the distance from the side of the skull to one of the large tumors. The blue colored tumor has been taken out into the true 3-D space to be able to see it in different views and to measure volume and surface area. Four different colored areas: blue, red, purple, and green, have been identified, each of which can be pulled out individually from the brain to the workspace for study. The hand-held stylus allows the user to interact with the data instantaneously at the WS, and the end of the green color ray is used to move to any desired location in the 3-D space that is created by the stylus. Upper left: CT head image volume, see the part of the aneurysm at the lower left of the CT image volume. Rectangular grid: Used for measurement and direction; blue: An already extracted partial tumor component in the brain with measurements.

(courtesy of Ron Schilling, PhD, and Will Johnsen, Researcher, EchoPixel)

10.7.2 3-D Printing

10.7.2.1 3-D Printing Technology

Three-dimensional printing technology, also known as additive manufacturing,

refers to processes used to create a 3-D object, in which layers of material are formed under computer control to create a 3-D object. In the case of medical imaging, it can be 3-D CT and MRI, or any other 3-D medical image. Since objects can be of almost any shape or geometry, they can be produced by using digital model data from a 3-D model or any electronic data sources such as a medical imaging scanner; 3-D printing quality and accuracy depends on many factors. Therefore, to obtain the required quality of the 3-D printing, one needs to know in advance the output data precision requirement. The term “3-D printing” originally referred to a process that deposits a binder material onto a powder bed with inkjet printer heads layer by layer. Since the quality requirement in medical imaging is very stringent, 3-D printing requires data pixel and voxel precision, as well as how to use the software to guide the print. The next section describes some 3-D printing terminology and methods, and concludes with a successful 3-D scoliotic spine model to aid pre-surgical planning in a child.

10.7.2.2 Terminology and Methods

This section discusses two different but similar concepts to develop 3-D printing, which are “fused filament fabrication”, as shown in Figure 10.31A, and “stereolithography”, as shown in Figure 10.31B. The processes of both 3-D printing concepts start from printing the head to the middle of the body. It should be clear that the first “print” layer is the lowest body part, then follows the head. The quality of the 3-D printing is determined by three factors: the value of each voxel (or pixel), the thickness of each slice, and the method of dropping the next continuous layer on the previous existing layers. The 3-D printing software controls the full completion of these layers. Figure 10.31A depicts the first method in 3-D printing, starting from the lower body part, moving up to the head. Figure 10.31B shows the upside down 3-D printing, with the last layer of the body starting first, with the head last. Various transparent colors can be distributed onto the probable pixels or voxels, depending on the data values. The finished product is a 3-D printing. Both methods have their advantages and disadvantages.

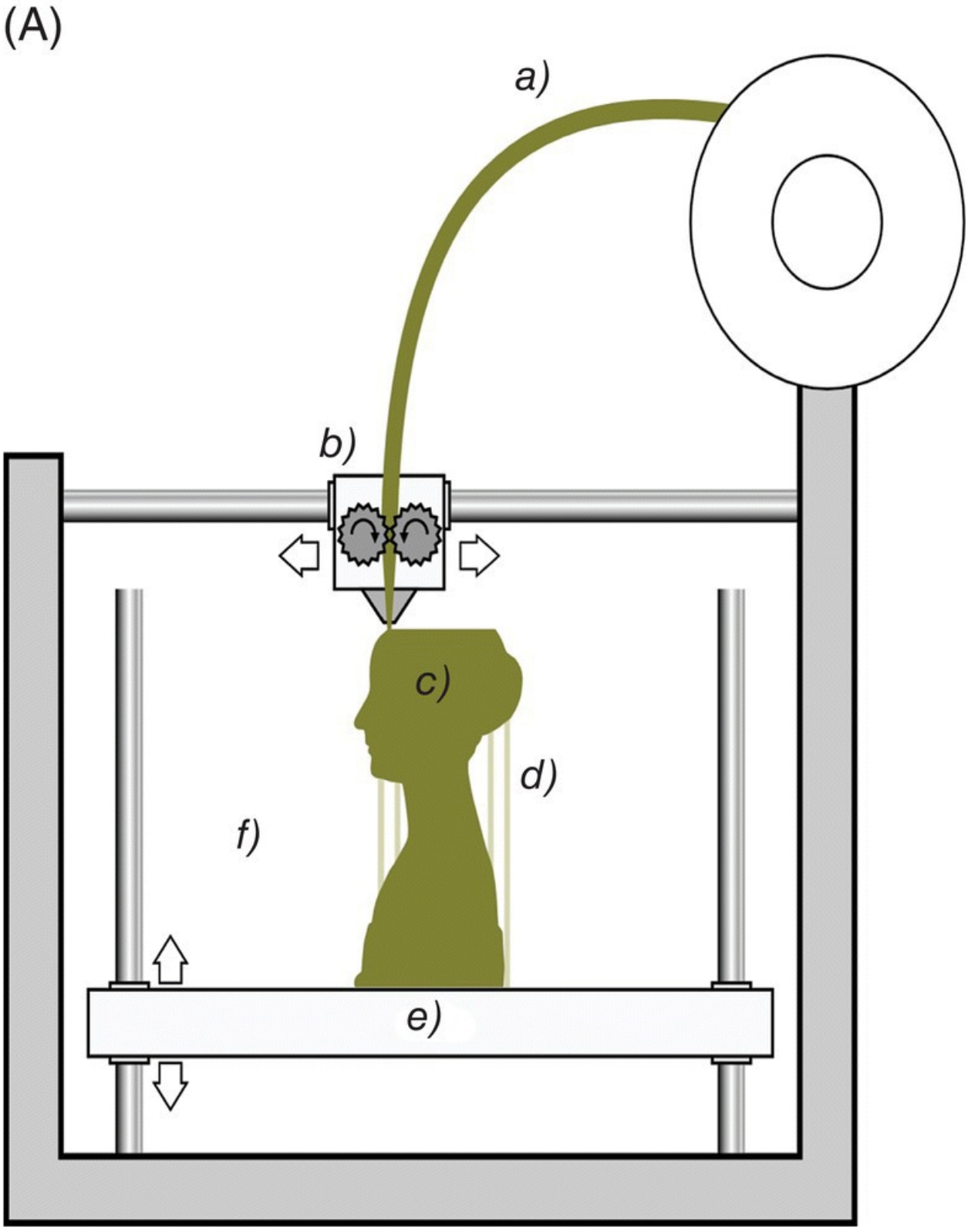
(A)
a)
b)
c)
d)
e)
f)

(B)

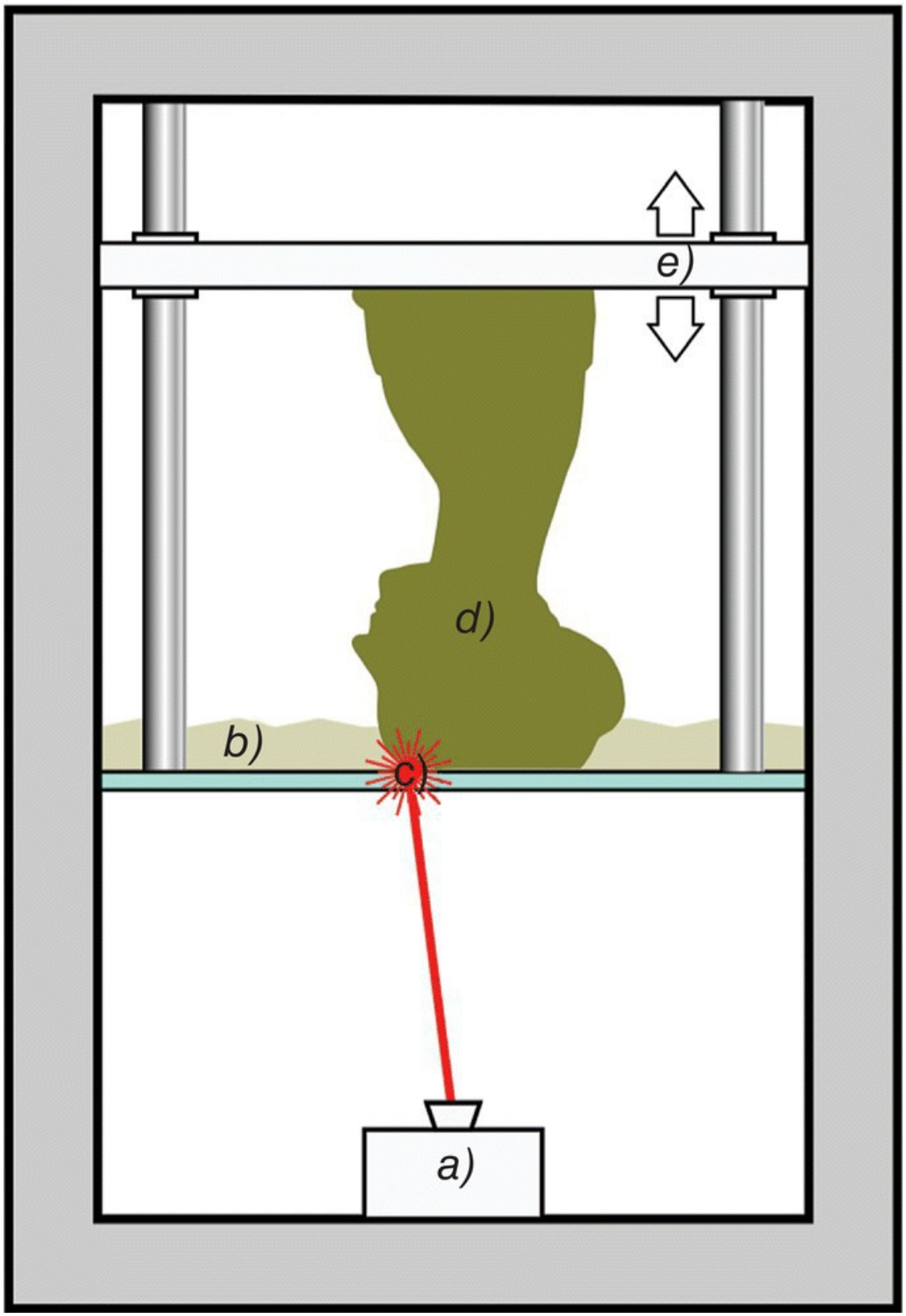

Figure 10.31 (A) Schematic representation of the 3-D printing technique known as fused filament fabrication; a filament (a) of plastic material is fed through a heated moving head (b) that melts and extrudes it, depositing it layer after layer, in the desired shape based on the CT layer data; (c) A moving platform (e) lowers after each layer is deposited. For this kind of technology, additional vertical support structures (d) are needed to sustain overhanging parts. (B) Schematic representation of stereolithography; a light-emitting device (a) (laser or DLP) selectively illuminates the transparent bottom (c) of a tank (b) filled with a liquid photopolymerizing resin; the solidified resin (d) is progressively dragged up by a lifting platform (e) [17]..

10.7.2.3 Use of 3-D Printing: An Example of a Successful Presurgical Planning for Scoliotic Spine

This example relates to an 8-year-old girl with a scoliotic spine, whose 3-D body CT images had been obtained. Radiologist Javin Schefflein, MD, presented this case at the 2016 Annual RSNA Conference in Chicago. Dr Schefflein discussed the production methods for the 3-D printing model created at New York's Mount Sinai Hospital, and worked closely with researchers at Mount Sinai's neurosurgical simulation core. Figure 10.32A shows the preoperative computer-generated 3-D printing of segmentation of severe scoliosis, and Figure 10.32B depicts 3-D printing of the severe thoracolumbar scoliosis.

(A)

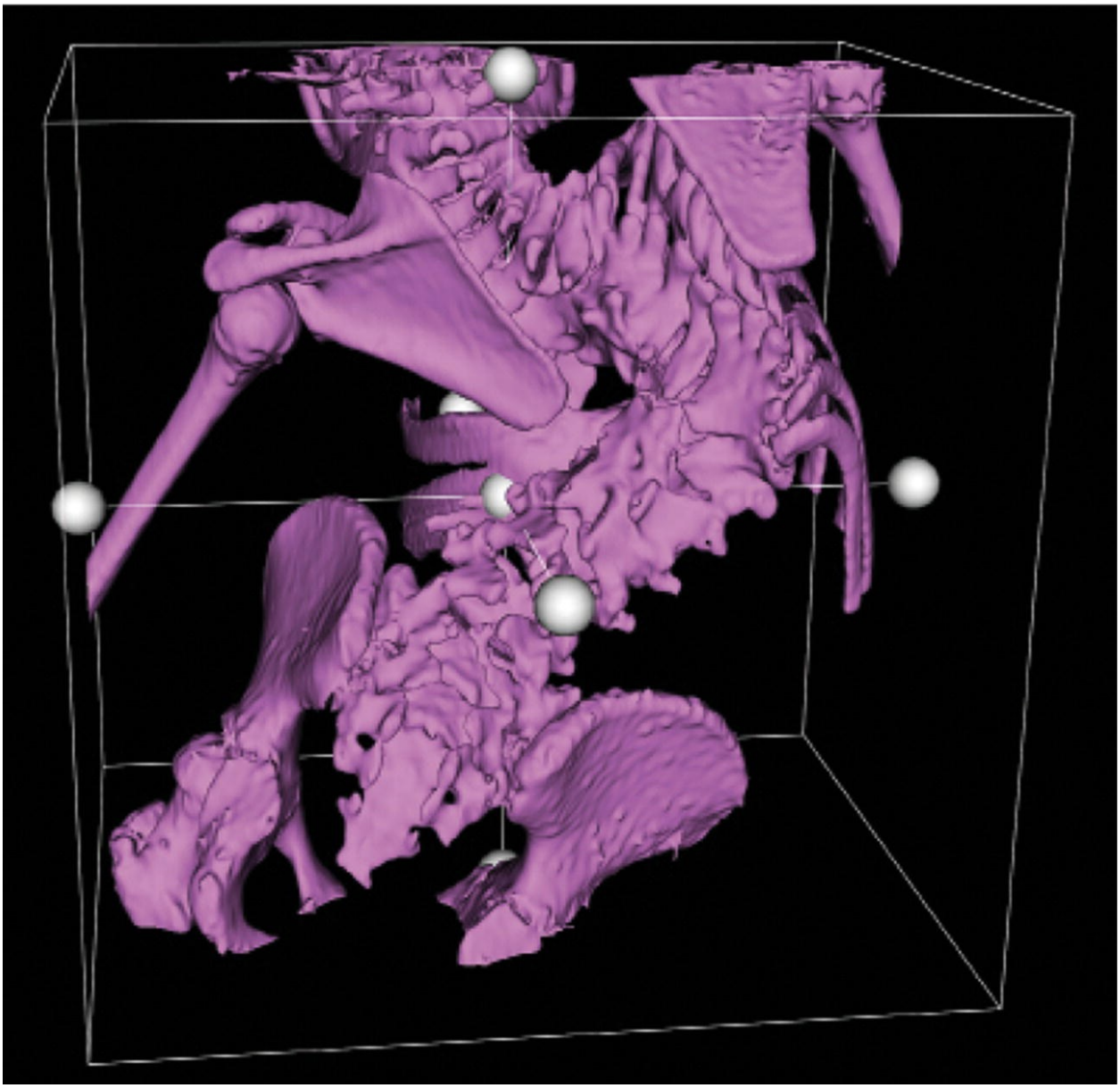

(B)

(C)

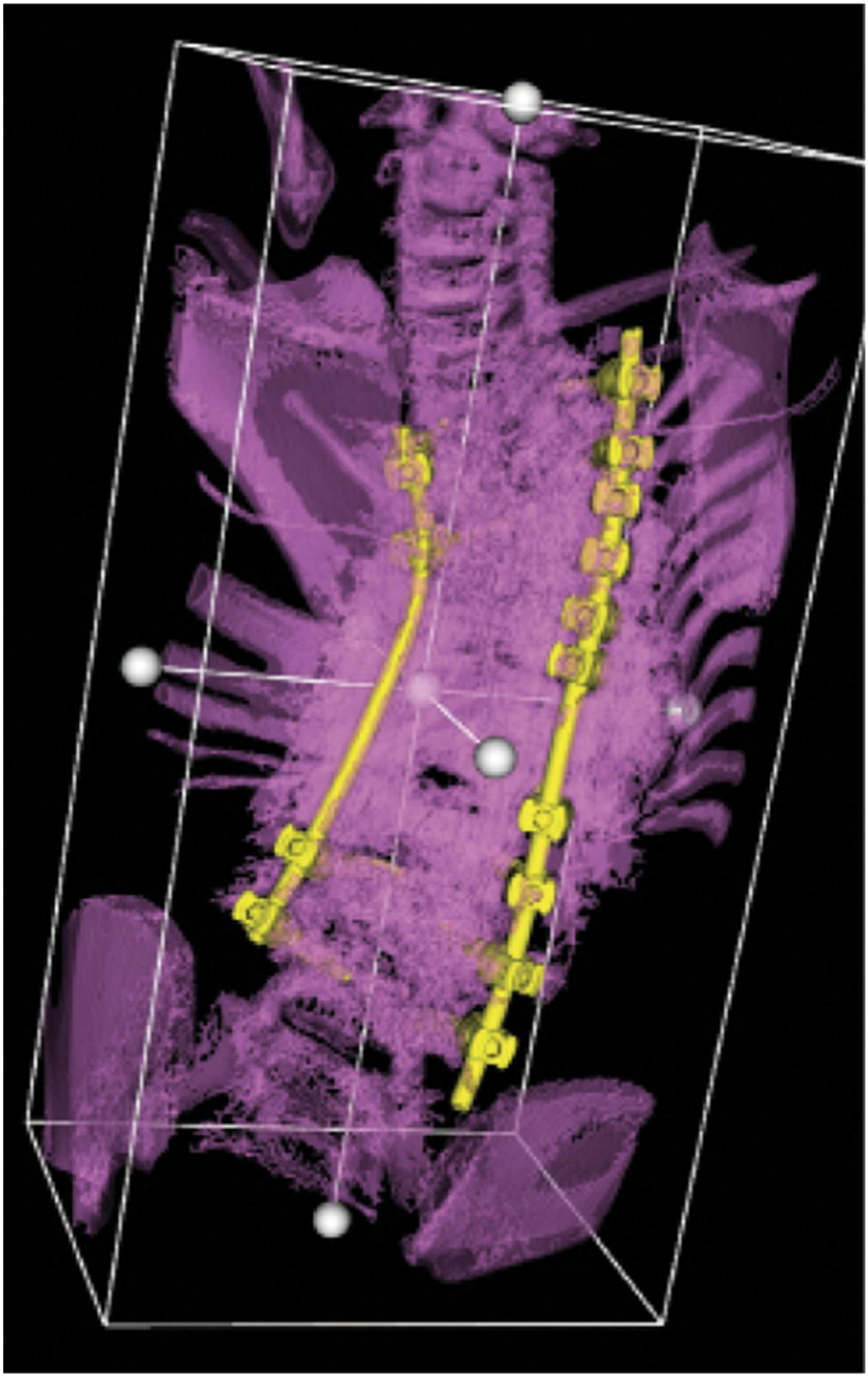

Figure 10.32 (A) Preoperative computer-generated 3-D printing segmentation of severe scoliosis, created by the Mount Sinai Hospital Neurosurgery Simulation Core.

(courtesy of *RSNA Insider*, April 2017)

(B) 3-D printing printed severe thoracolumbar scoliosis with multilevel malsegmentations and type I diastematomyelia for use in presurgical planning and intraoperative visualization.

(image courtesy of the Mount Sinai Hospital Department of Radiology and the Rapid Prototyping Center. Description courtesy of Elizabeth Gardner, *RSNA Insider*, April 2017)

(C) Postoperative computer-generated 3-D segmentation following two-stage corrective surgery, depicting spinal alignment of long-segment posterior fusion (pre- and postoperative images courtesy of the Mount Sinai Hospital Department of Radiology and Dr Anthony Costa, head of the Mount Sinai neurosurgery simulation core.

(courtesy of Elizabeth Gardner: *3-D Scoliotic Spine Model Aids Pre-Surgical Planning in 8-year-old Girl*, and courtesy of *RSNA Insider*, April 2017)) [18]

A 3-D model was used to plan two-stage surgery involving T12–L2 laminectomy, resection to the midline bony spur at L1, intradural exploration to de-tether the spinal cord, asymmetric pedicle subtraction osteotomy at T1–L1 to straighten the curvatures, and long-segment posterior fusion with instrumentation from T2–L5. The model was also used during surgery to help surgeons to visualize steps in the procedure. Because of the detail of the 3-D printing model, as the child underwent the two-stage surgery, a member of the surgical staff held up and manipulated the model so that the surgeon could visualize the portions of all spinal anatomy that were not visible at a given point in the procedure.

The operation, according to Dr Scheffein, was a complete success. Figure 10.32C shows the postoperative computer-generated 3-D printing segmentation following two-stage corrective surgery. In terms of creating the model itself, the process took more than 10 hours, including scanning (10 minutes), segmenting (3 hours), printing 5 hours), and drying/hardening time (2 hours).

This subsection was extracted from Elizabeth Gardner's RSNA article: *3-D Scoliotic Spine Model Aids Pre-Surgical Planning in 8-year-old Girl*, and courtesy of *RSNA Insider*, April 2017. Figures 10.32 A, B, and C are originally from Javin Schefflein, MD, and RSNA, April 2017.

10.7.3 Summary

The PACS-based multimedia imaging informatics display WS is used by almost every healthcare provider who has the need to use and study a patient's medical images while learning and working in diagnostic and treatment processes. During these processes, many and various background users will encounter the WS, and, for these reasons, its design and use have to be simple and easy to use. This chapter discusses the concept of the WS and its design and use, both in hardware and software with examples. Different categories of WS and their functions are presented. Recipe book types of manual are presented to those who want to use and build a WS for their own specialty use. This chapter introduce the two most recently developed technologies, in Sections 10.7.1 "True 3-D" and 10.7.2, "3-D Printing", with examples.

References

1 Gardner, E. (2017) 3-D Scoliotic Spine Model Aids Pre-Surgical Planning in 8-year-old Girl (courtesy of RSNA Insider, April 1, 2017).

2 ISO/IEC 15444-1. JPEG2000 image coding system. Part 1: Core coding system.

3 Shuai, J., Sun, J. and Zhang, J. (2008) A Novel multidimensional medical image display framework based on Visualization Toolkit. *SPIE*, 6919: 12–22.

4 Junichi, H. (2005) An implementation of JPEG 2000 interactive image communication system. *Circuits and Systems, IEEE Int Symp*, 6, 5922–5925.

5 Kruglinski, D.J., Wingo, S. and Shepherd, G. (1998) *Programming Visual C++*, 5th edition. Redmond: Microsoft Press.

6 Li, M., Wilson, D., Wong, M. and Xthona, A. (2003) The evolution of display technologies in PACS applications. *Comp Med Imag Graphics*, 27: 175–184.

7 Prandolini, R., Colyer, G. and Houchin, S. (2000) 15444-9:2004 JPEG 2000image coding system—Part 9: Interactivity tools, APIs and protocols—JPIP. Final Publication Draft Revision 3, ISO/IEC

8 JTC 1/SC29/WG 1N3463. November 2004.

9 Schroeder, W., Avila, L. and Hoffman, W. (2000) Visualizing with VTK: A tutorial. *IEEE Computer Graphics and Applications*, 20(5), 20–27.

10 Schroeder, W., Martin, K. and Lorensen, B. (1997) *The Visualization Toolkit, An Object-Oriented Approach To 3D Graphics*, 2nd edition. Clifton Park, NY: Kitware Inc.

11 Taubman, D. and Marcellin, M. (2002) *JPEG2000: Image Compression Fundamentals, Standards and Practice*. Dordrecht, Kluwer Academic.

12 Taubmana, D. and Prandolini, R. (2003) Architecture, philosophy, and performance of JPIP: Internet protocol standard for JPEG2000. *Int Symp on Visual Comm Image Process* (VCIP2003).

13 The Visualization Toolkit. http://www.vtk.org

14 VTK 5.1.0 Documentation. http://www.vtk.org/doc/nightly/html

15 Yuan, T., Cai, W., Sun, J. and Zhang, J. (2008) A novel strategy to access high resolution DICOM medical images based on JPEG2000 interactive protocol. *SPIE in Medical Image*, 6919, 12–22.

16 Ron Schilling, Develop the true 3-D EchoPixel system, RSNA, April 2017, Courtesy of Dr. Ron Schilling, Chief Executive Officer, EchoPixel, San Jose, California, USA.

17 Eric Barnes. 4 steps to high-quality 3D printing for radiology, Description Courtesy of Eric Barnes, staff writer. Courtesy of RSNA Insider, April 2017.

18 Elizabeth Gardner: 3-D Scoliotic Spine Model Aids Pre-Surgical Planning in 8-year-old Girl, Courtesy of RSNA Insider, April 2017

11
Multimedia Electronic Patient Record (EPR) System in Radiotherapy (RT)

CHAPTER MENU

11.1 Multimodality 2-D and 3-D Imaging in Radiotherapy
11.1.1 Radiotherapy Workflow
11.1.2 2-D and 3-D RT Image Registration
11.1.3 Fusion of 3-D MRI and 3-D CT Images for RT Application
11.2 Multimedia ePR System in Radiation Treatment
11.2.1 Radiotherapy and Minimally Invasive Surgery
11.2.2 Multimedia ePR System for Radiotherapy
11.3 Radiotherapy Planning and Treatment
11.4 Radiotherapy Workflow
11.5 The ePR Data Model and DICOM-RT Objects
11.5.1 The ePR Data Model
11.5.2 DICOM-RT Objects
11.6 Infrastructure, Workflow and Components of the Multimedia ePR in RT
11.6.1 DICOM-RT Based ePR System Architecture Design
11.6.2 DICOM-RT Object Input
11.6.3 DICOM-RT Gateway
11.6.4 DICOM-RT Archive Server
11.6.5 DICOM-RT Web-Based ePR Server
11.6.6 RT Web Client Workstation (WS)
11.7 Database Schema
11.7.1 Database Schema of the RT Archive Server
11.7.2 Data Schema of the RT Web Server

11.8 Graphical User Interface Design
11.9 Validation of the Concept of Multimedia ePR System in RT
11.9.1 Integration of the ePR System
11.9.2 Data Collection for the Prototype System
11.9.3 Multimedia Electronic Patient Record of a Sample RT Patient
11.10 Advantages of the Multimedia ePR system in Radiotherapy for Daily Clinical Practice
11.10.1 Communication between Isolated Information Systems and Archival of Information
11.10.2 Information Sharing
11.10.3 A Model of Comprehensive Electronic Patient Record
11.11 Use of the Multimedia ePR System in RT For Image-Assisted Knowledge Discovery and Decision Making
11.12 Summary
Acknowledgement
References

11.1 Multimodality 2-D and 3-D Imaging in Radiotherapy

11.1.1 Radiotherapy Workflow [1–30]

External beam radiotherapy (RT) calls for treatment planning as well as treatment delivery. Over 90% of the workload in radiation therapy is dedicated to planning radiotherapy and this involves an intensive image and computer graphic process. In the RT planning process, patient information is needed to plan a treatment; image registration is also needed to identify the regions to be treated, and markers are used to align images. Multimodality images from projection x-rays, computed tomography (CT), magnetic resonance imaging (MRI), positron emission tomography (PET), and linear accelerator are used for tumor localization and organ identification. Images must include the shape, size, and location of the targets and the radiosensitive vital organs. Sometimes 3-D and 2-D images must be fused to better identity the outlines of the tumor and

adjacent organ’s anatomy. The images are then overlaid with computer graphics derived from the treatment plan and the dose distribution, to verify that the site of delivery of a uniform high dose will target the tumor and avoid adjacent critical structures. Next, carefully monitoring of the treatment, optimization, and dose calculation is essential for successful patient treatment outcomes. In all these processes, PACS and imaging informatics technologies are used extensively. Radiation therapy is prepared for the individual patient, so it is important that informatics are employed to optimize RT workflow and patient treatment outcomes. The RT workflow in Figure 11.1 depicts a generic treatment plan and delivery of prostate cancer treatment. The multimodalities of the imaging component of RT treatment planning and delivery includes, in particular, (1) image acquisition, (2) field planning at the treatment planning system, (3) generation of digitally reconstructed radiography (DRR), and (6) verification: comparing portal image and reference DRR image at step (3), described in the yellow boxes of the workflow. The informatics component is discussed in more detail in the following sections.

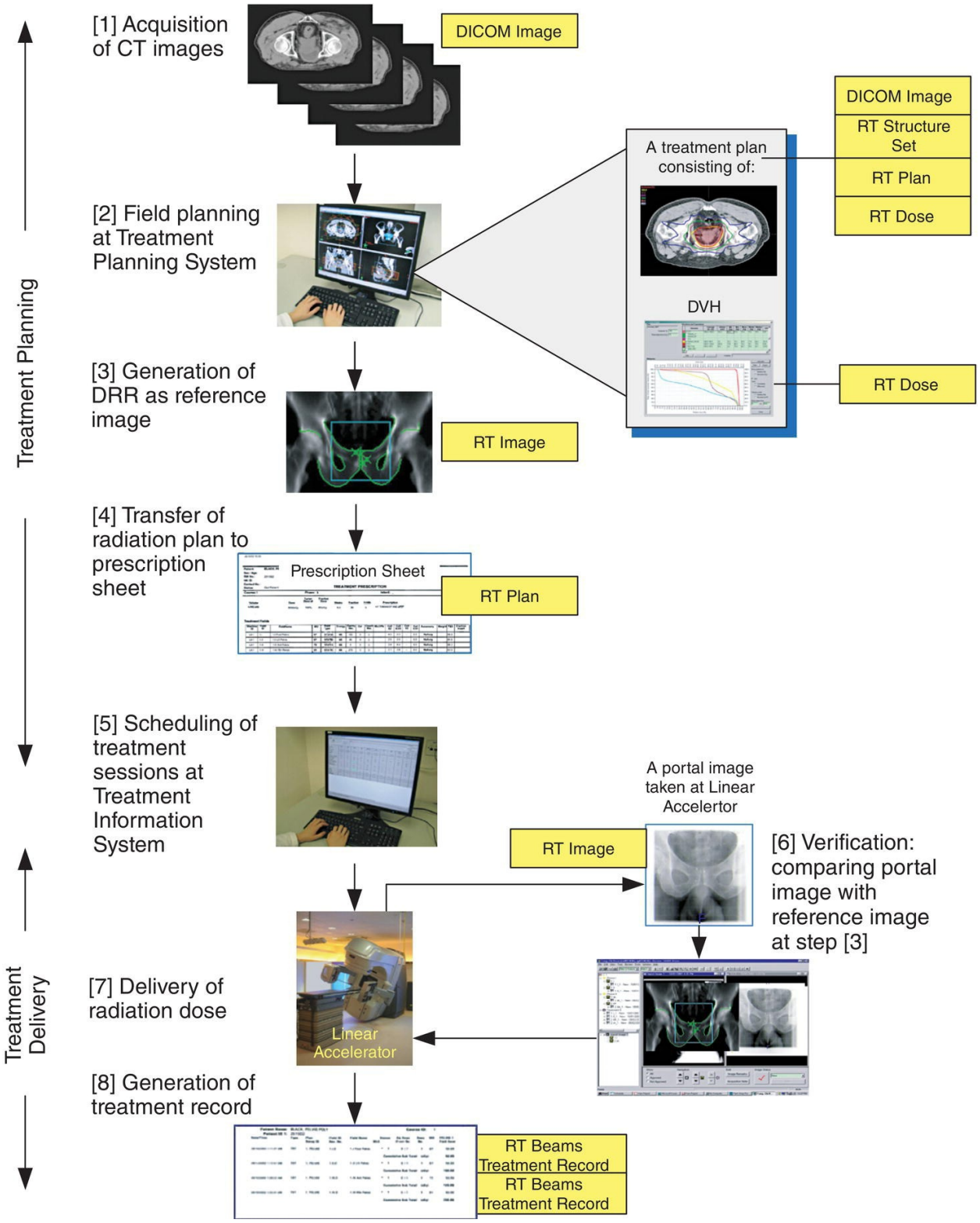

Figure 11.1 Generic external beam radiation therapy workflow, including treatment planning and delivery using prostate gland cancer as an example. RT information is scattered at where it is generated. The yellow boxes indicate the

RT-related images and data that could be generated in the workflow. Treatment planning steps 1, 2, and 3, and treatment delivery step 6 shown in yellow boxes, are described in the text. Step 2 in the RT treatment plan with radiation dose distribution involves the superposition of the radiotherapy treatment parameters: RT plan, RT structure set, and RT dose upon the corresponding set of computed tomography (CT) images. DRR: digital reconstructed radiograph; DVH: dose–volume histogram.

(courtesy of Dr M. Law)

11.1.2 2-D and 3-D RT Image Registration [31–35]

11.1.2.1 Imaging Component in Treatment Planning – Steps 1 to 5

The objective of a treatment plan is to deliver as high and uniform as possible a radiation dose to the prostate tumor-bearing site, but as little as possible dose to the surrounding healthy tissues, especially the surrounding critical and radiosensitive structures. In this example, these are the urinary bladder and the rectum of the patient with prostate cancer.

To start with the workflow, the oncologist orders a set of CT images of the patient's pelvis, either in the CT simulator (a CT scanner) at the radiation oncology department or a CT scanner at the radiology department. The patient's information is delivered to the CT simulator room where the radiation therapist sets the patient up in his treatment position for scanning.

Step 1: Pelvic CT images (Figure 11.1, step 1) are generated as DICOM images (Chapter 4) and stored either in a PACS or the workstation there.

Step 2: The acquired CT images are transferred to a computerized treatment planning system (TPS) for radiation field planning. Previous available diagnostic images—CT, MRI, or PET images—are also retrieved as a reference to aid in the delineation of tumor volume. Image registration and fusion may be needed in this step (see Section 11.1.3.3 for an example). At the TPS workstation, the tumor volume and the organs at risk (OARs) (urinary bladder and rectum) are delineated interactively by a medical physicist (Figure 11.2A). Treatment fields of appropriate size and gantry/collimator angles are positioned (Figure 11.2B). The TPS computes the radiation dose distribution within the bodily region to be treated (Figure 11.3C). A dose–volume histogram (DVH) may be generated to show the dose received by the tumor and OARs (Figure 11.3D).

Step 3: DRR images similar to x-ray projection images are reconstructed from the CT slices to show the treatment field positions (Figure 11.1, step 3, and Figure 11.2E).

Step 4: The finished plan is presented to the radiation oncologist for evaluation and approval. If the plan is found to be satisfactory, the oncologist prescribes the treatment in the RT prescription sheet.

Step 5: A treatment record with all treatment details is prepared with the prescription. Treatment sessions are scheduled at the treatment information system.

(A)

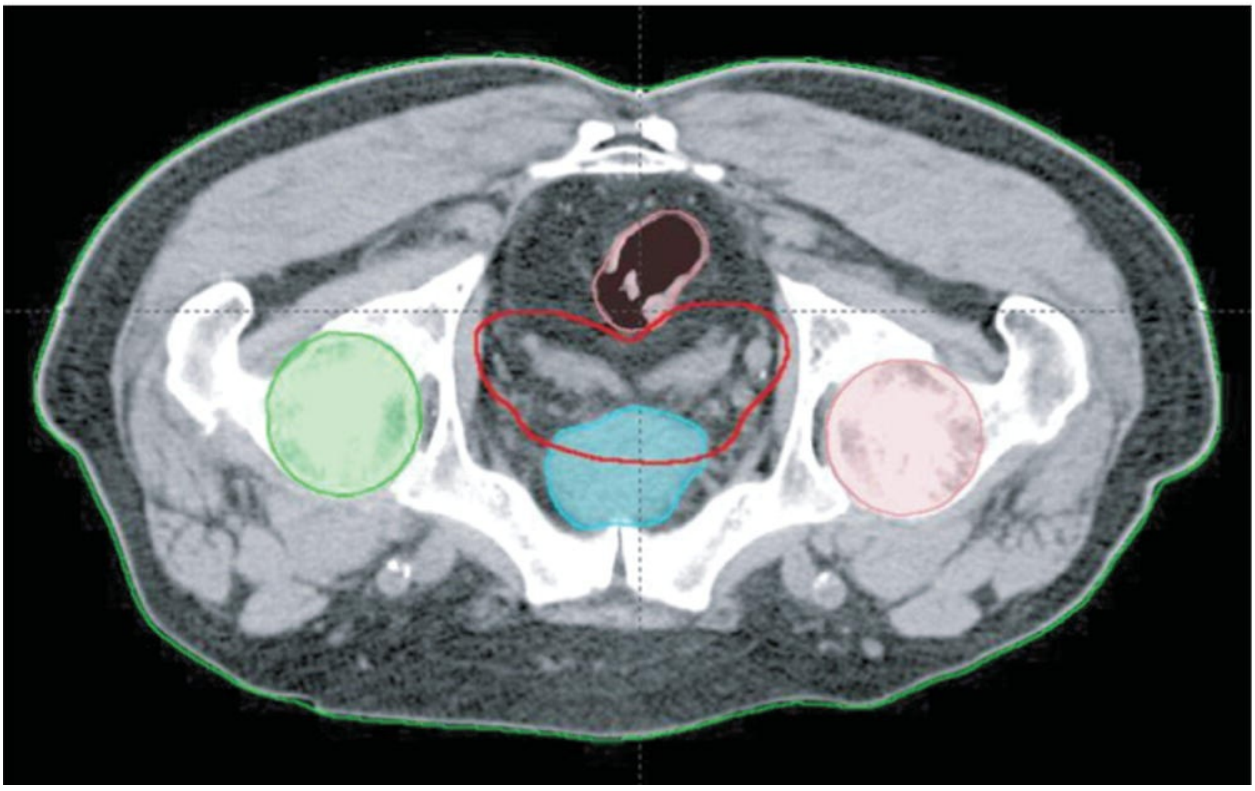

(B)

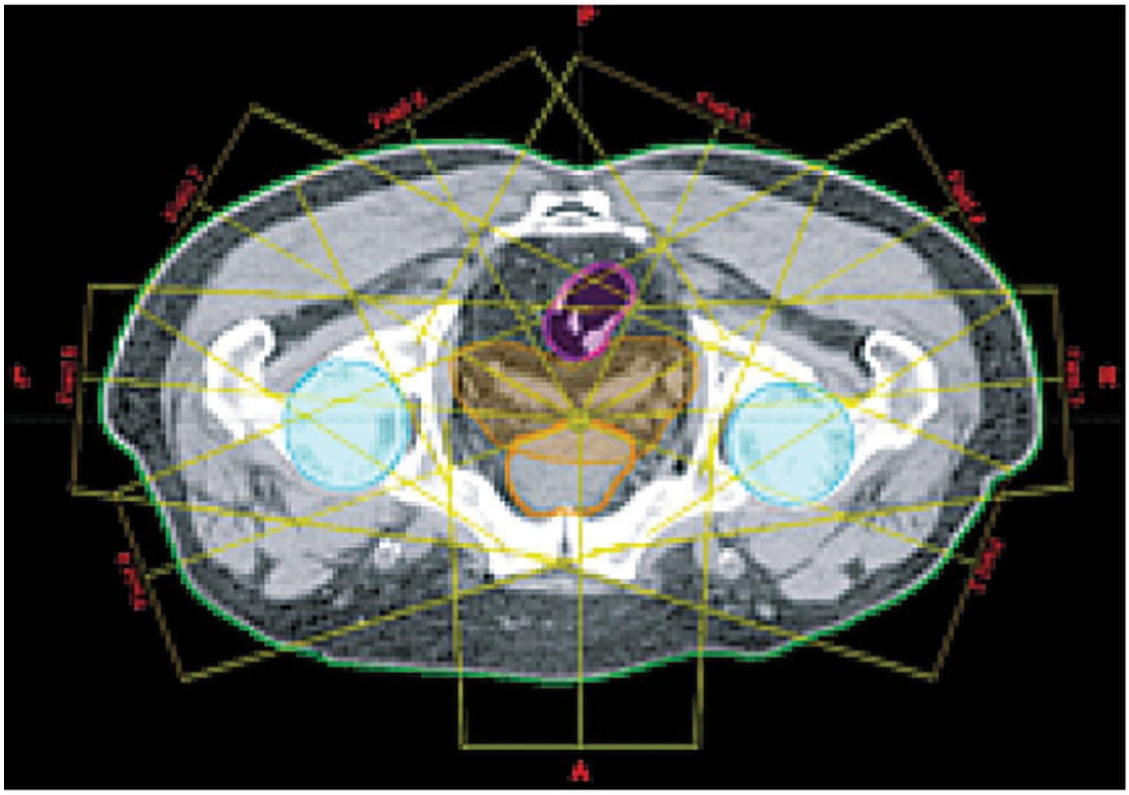

(C)

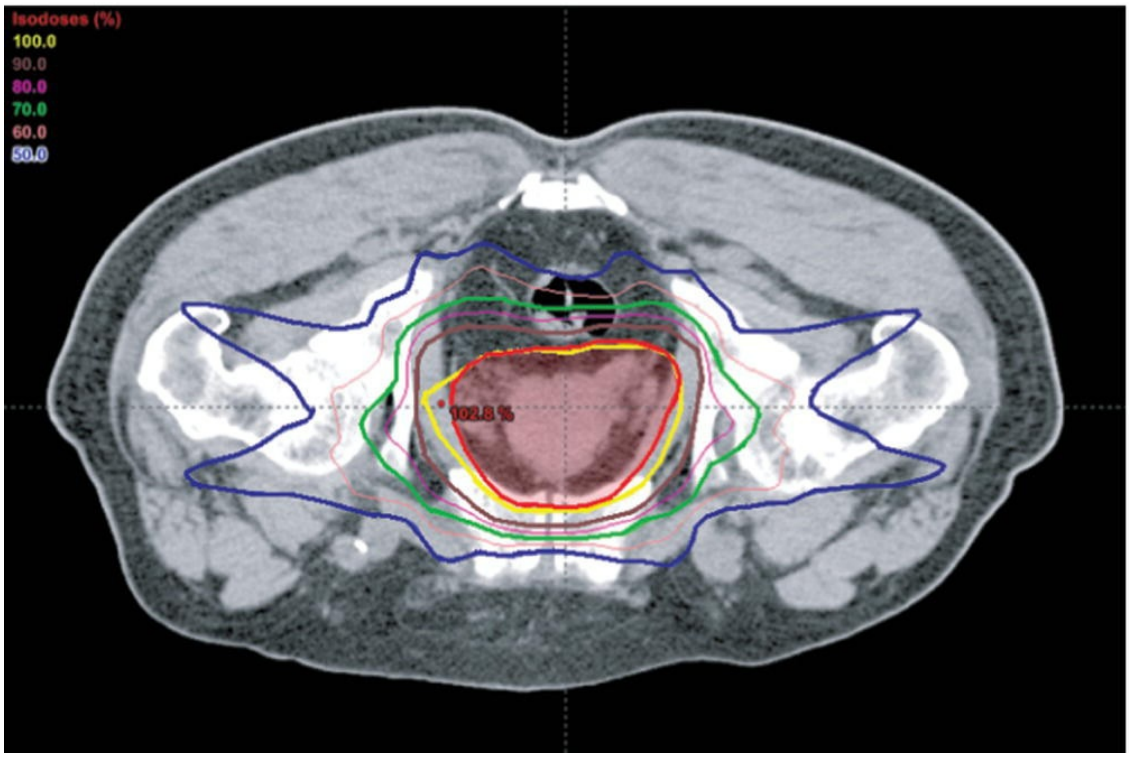

(D)

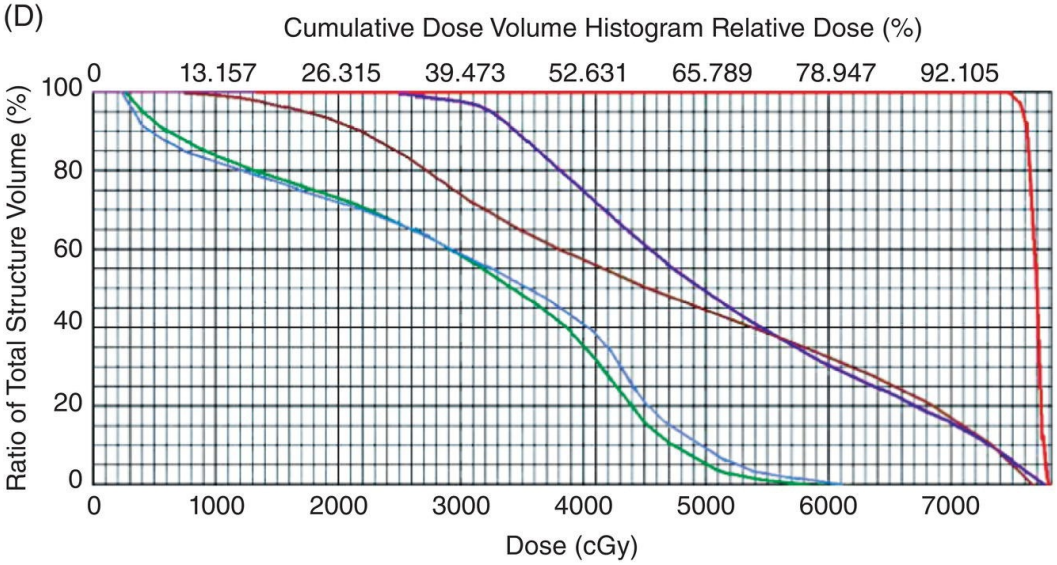
Cumulative Dose Volume Histogram Relative Dose (%)
0
13.157
26.315
39.473
52.631
65.789
78.947
92.105
Ratio of Total Structure Volume (%)
100
80
60
40
20
0
0
1000
2000
3000
4000
5000
6000
7000
Dose (cGy)

(E)

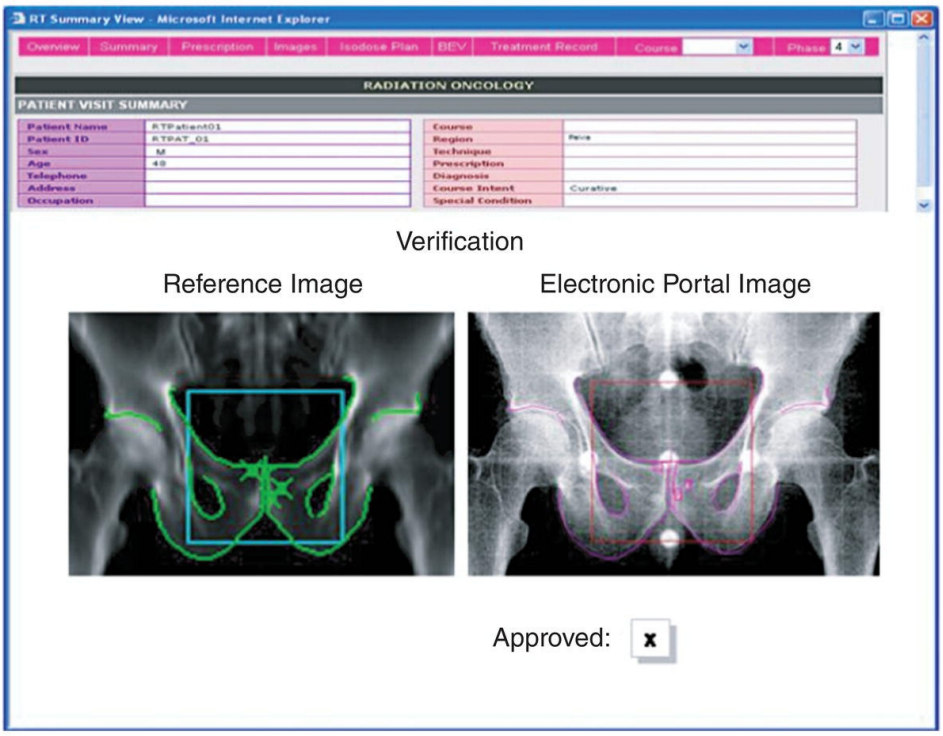
RT Summary View - Microsoft Internet Explorer
Overview
Summary
Prescription
Images
Isodose Plan
BEV
Treatment Record
Course
Phase
RADIATION ONCOLOGY
PATIENT VISIT SUMMARY
Patient Name
Patient ID
Sex
Age
Telephone
Address
Occupation
Course
Region
Technique
Prescription
Diagnosis
Course Intent
Special Condition
Curative
Verification
Reference Image
Electronic Portal Image
Approved:
x

(F)

Figure 11.2 (A) RT structure set (Chapter 9): tumor volume (red), organs at risk (femoral head in green and pink, rectum in purple, bladder in blue), and body contour. The structures in this diagram have the CT image as their frame of reference and are superimposed on the CT image. (B) RT plan: includes treatment beam details, fractionation scheme, and prescription (above). On the left is a graphic display of information from the RT plan and RT structure set, both superimposed onto the CT image. There are nine radiation beams (attribute of the RT plan), each represented by a red label and three yellow lines in the diagram. (C) RT dose: on the left are the radiation dose data from a TPS. Isodose curves (yellow, pink, green, magenta, and blue) are displayed with reference to the CT image and the tumor volume (red shading) from an RT structure set. (D) Dose volume histogram (DVH): belongs to the RT dose object in (C) for treatment plan evaluation. This is key to evaluating whether proper radiation dose is applied to the target tumor while limiting dose to the surrounding critical healthy tissue and organs. The red line shows that most of the tumor volume receives >7500cGy of radiation dose. Other colors show the dose received by other OARs. (E) Web client application page showing a comparison between the reference image (left) and the electronic portal image (right) used to verify the treatment field. The digital reference image was generated from the CT scans, and the electronic portal image from the linear accelerator. Note that there is an icon marked “X”, to indicate approval by the radiation oncologist. (F) Three different types of RT 2-D images for verification of the treatment accuracy: (left) projectional simulator image with delineator showing the field to be irradiated; (middle) reference digital image reconstructed from CT images; (right) portal images from the linear accelerator. Portal images are compared with the reference images from the simulator or the DRRs to verify the accuracy of the treatment portal.

(courtesy of Dr M. Law)

(A)

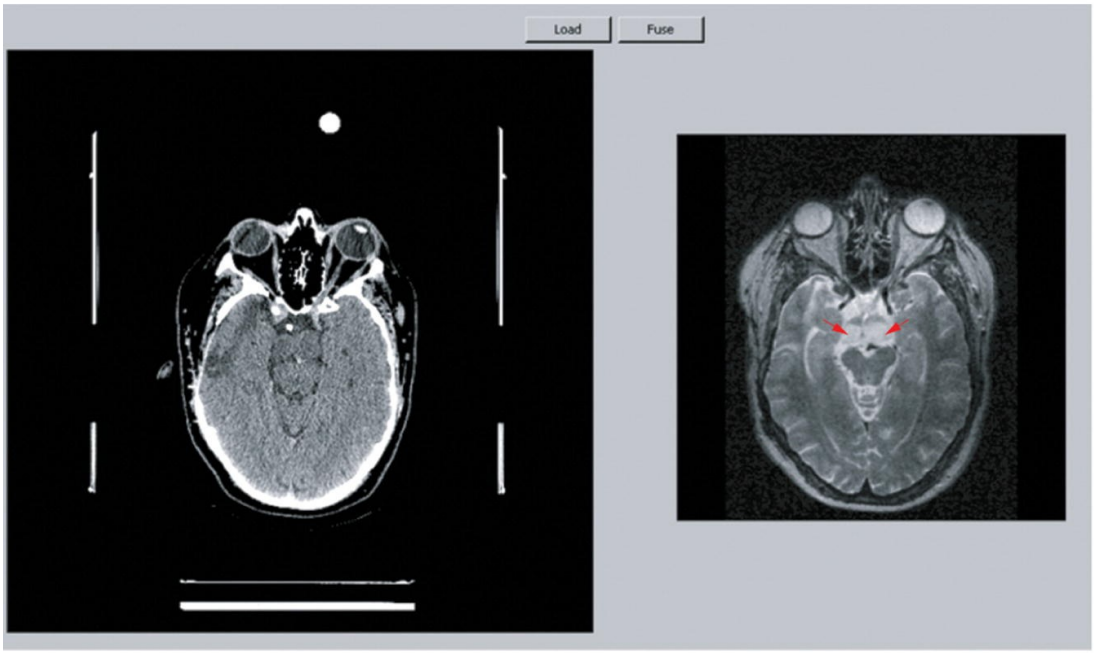

(B)

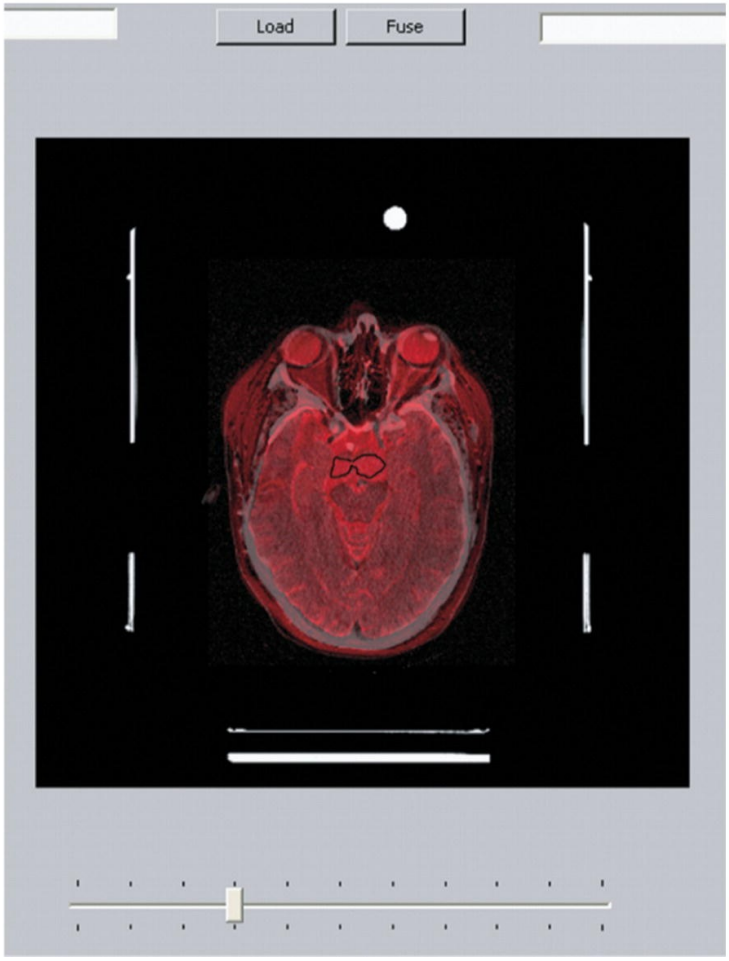

Figure 11.3 (A) MR-CT image fusion used for more accurate tumor delineation. One image each from the 3-D MRI and the 3-D CT is presented for illustration. (Right) A transverse section of the 3-D MRI volume in a gray-scale LUT showing the brain tumor (arrows). (Left) The corresponding anatomical transverse section of the 3-D CT volume with a gray-scale LUT. Two registration points are used for image registration, one point at the tip of the nose and the second at the posterior skull. Since the CT (512 Å ~ 512) and the MR (256 Å ~ 256) images are of different pixel sizes, the registration requires resizing and scaling to perform a proper mapping. Once the registration is complete, the next step is to display the fused MR and CT images. (B) The MR/CT fusion screenshot from a PACS workstation showing the fused MR and CT images. A slider bar at the bottom allows interactively viewing of each image overlaid. The fused image shows the CT image (grayish color) as well as the MR image (reddish color) with the preference color washing to enhance the target tumor tissue. The viewed target tumor can be outlined interactively more accurately, as shown by the black contour. Note the difficulty to outline the tumor in the CT image or in the MRI, individually and independently, from Figure 5.7A.

(courtesy of Drs J. Documet and B. Liu)

11.1.2.2 Imaging Component in Treatment Delivery – Step 6

At step 6 shown in Figure 11.1, the approved treatment plan is transferred to the radiation treatment unit or linear accelerator (LINAC). Before the radiation treatment can begin, the treatment plan with respect to the DRR (which serves as a reference image) needs to be verified at the LINAC for accuracy in terms of field sizes, setup, and shielding positions, and so on. For such verification, a portal image by an electronic portal imaging device (EPID, a device installed in the LINAC for taking digital portal images) is taken at the LINAC. It is then compared with the reference DRR images described in step 3 (Figure 11.2E). When the portal images are found to match the reference images in aligning with the treatment field, the oncologist approves the verification. Radiation treatment can then proceed in accord with step 7. Otherwise, a repeat portal image may be requested. Usually the patient is treated five times a week for seven to eight weeks. Each treatment beam is recorded at each treatment session, as well as the cumulative dose to date described in step 8. Over the course of treatment, the patient will have weekly verification images acquired to ensure the accuracy of the treatment.

11.1.2.3 2-D and 3-D Image Registration

In Figure 11.1, steps 1, 2, and 3 describe how to use several 2-D and 3-D imaging processing methods to expedite the RT workflow from treatment planning; and step 6 presents how to verify the portal image with the reference image for treatment delivery. For the patient with prostate cancer shown in Figure 11.1, the following steps recapitulate the RT workflow, with attention paid to the image registration:

1. Exam of the pelvic using the CT simulator.
2. A physicist uses a computer treatment planning system (TPS) to generate the outlines of the tumor and adjacent organ from the CT images interactively (Figure 11.2A); then planning of the radiation treatment begins (Figure 11.2B). TPS computes the radiation dose distribution of the target cancer and organs (Figure 11.2C) and the DVH (Figure 11.2D). This information are converted to computer graphics and overlaid on the proper CT images (Figure 11.2C), and as DVH plots of the individual organs in the vicinity of the tumor (Figure 11.2).
3. The TPS reconstructs DRR (digitally reconstructed radiographs) (Figure 11.2E, left) using conical geometry because of the cone-beam x-ray output of the CT scanner, which yields 2-D DRR (see image caption).
4. Three different types of RT 2-D images used for verification of the treatment accuracy are shown in Figure 11.2F: projection simulator image with the delineator showing the field to be irradiated (left), the reference DRR reconstructed from the CT images (middle), and portal images from the linear accelerator (right). Portal images are used to compare them with reference images from the simulator or the DRRs and thus to verify the accuracy of the treatment portal, shown in Figures 11.2E and F.
5. These DRRs are used to compare with electronic portal images of the patient taken from an electronic portal imaging device in the LINAC for patient positioning in the LINAC.

Critical to these processes are:

1. various image reconstruction methods from 3-D data to 2-D images;
2. image registration algorithms between the 2-D DRRs and portal images;
3. proper coordinates transformation between computer graphic outlines and the overlay on 3-D CT images. Because different imaging modalities in RT

generate different images, each with its own image format, data collection using a standardization format is a critical consideration in the PACS related informatics environment.

11.1.3 Fusion of 3-D MRI and 3-D CT Images for RT Application

Step 2, Section 11.1.2 discusses the acquired CT images, which are transferred to a computer treatment planning system (TPS) for radiation field planning, and that previous diagnostic images, CT, MRI, or PET images are also retrieved as a reference in the delineation of tumor volume. In the prostate cancer example, there was no previous CT, MRI, or PET (see Chapter 2, Section 2.4.1.4) to be retrieved to aid in the delineation of the tumor's volume.

In this section is an example of a brain tumor in which the patient had both CT and MRI examinations (Figures 11.3A and B). In this case, this set of head CT images provides a simpler anatomy structure of the head and brain for this application to appreciate the concept of image fusion, which is considered as the primary image set; although MRI can delineate a better separation between the tumor and brain tissues, which is assigned to the secondary image set. The challenge of this example is to fuse the secondary 3-D MRI volume with the primary 3-D CT volume to gain more accurate tumor delineation. The first step is to perform the image registration between the 3-D MRI and the 3-D CT sets.

Recall that in Chapter 2, the concepts of "image registration" and "image fusion" were discussed, where image registration required transforming the secondary 3-D MR image set (Figure 11.3A, right) to align, match, and correspond with the reference 3-D CT image set (Figure 11.3A, left). After two 3-D image sets have been properly registered, the next step is to fuse the two 3-D image sets by overlaying them, one over the other, and displaying the result. Each one, sectional image from the 3-D MRI and the other from 3-D CT, is used as shown in Figure 11.3A. One of the most effective lookup table (LUT) pairs is to have the primary in gray scale and the secondary in color. Thus the MRI 3-D set using a reddish LUT highlighting the brain tumor outline is overlaid onto the 3-D CT set with a gray-scale LUT, with the result shown in Figure 11.3B. After satisfaction from the viewing, the target tumor can be outlined interactively with more accuracy, as shown by the black contour. Note the difficulty to outline the tumor using either the CT image or the MRI alone (Figure 11.3A). This concept is revisited in this chapter to describe how image fusion results can be integrated with other imaging informatics methods to facilitate RT planning and treatment.

11.2 Multimedia ePR System in Radiation Treatment

11.2.1 Radiotherapy and Minimally Invasive Surgery

Multimedia ePR systems for patient treatment includes two different types of patient treatments: radiation therapy (Chapters 11 and 19), and minimally invasive surgery (Chapters 20 and 21). Chapter 11 considers the planning and treatment for radiotherapy.

11.2.1.1 Background

Information in an electronic patient record (ePR) system for radiation therapy consists of text, images, and graphics. In this chapter, the term ePR is used for convenience. To enable the exchange of patient information between systems within an institution and across institutions, the DICOM standard should be used. This chapter describes a DICOM-RT ePR system for information exchange and sharing. The system is based on Web technology and uses a server as the common platform for archiving all RT-related multimedia information and for the distribution and viewing of ePR images/data.

11.2.1.2 Fundamental Concept

Fundamental to the functioning of multimedia ePR in clinical treatment is that the input data from other information systems should not only be textual and diagnostic images but should also include various patient's forms, 2-D clinical waves, identification pictures and finger prints, surgical video, and so forth, all in their original data formats. Data can come from different clinical and treatment departments, including radiation therapy and surgery within the hospital or the entire enterprise. The multimedia perk captures these data, stores the pointers in the ePR database for immediate and future retrieval, and presents them in proper display format and media. The multimedia functions in the ePR take the system design requirements out of the textual and images boundaries and into much broader spectra.

11.2.1.3 Infrastructure and Basic Components

A general purpose multimedia ePR system is difficult to design, since so much ground has to be covered and considered. However, for a small-scale mission-oriented multimedia ePR system, the design can be more manageable. To this

end, we restrict the multimedia ePR design to two particular applications, radiation therapy and surgery.

First, once the type of treatment is specified, the goals and boundary of the multimedia ePR can be defined. The ePR is mostly software operated on the well-defined treatment method, operational environment, system hardware, diagnostic systems, treatment devices, and display media. Once all these parameters are clarified and defined, the software can be designed according to the specific treatment. The software infrastructure of the ePR system generally consists of the following components:

1. software organization;
2. database schema;
3. data model;
4. data flow model;
5. display.

With these components as the base, the next two sections provide the software infrastructure for radiation therapy and surgery, respectively.

11.2.2 Multimedia ePR System for Radiotherapy

11.2.2.1 Background

Comprehensive clinical image data and relevant information is crucial in image intensive radiotherapy (RT) for the planning and treatment of cancer. Multiple stand-alone systems utilizing technological advancements in imaging, therapeutic radiation, and computer treatment planning systems acquire key data during the RT treatment course of a patient. Currently, the data are scattered in various RT information systems throughout the RT department. Scattered data can compromise an efficient clinical workflow, since the data crucial to a clinical decision may be time consuming to retrieve, temporarily missing, or even lost. An integrated image-based radiation therapy plan and a multimedia ePR system treatment method are needed to improve the treatment workflow and the efficiency of therapy process.

RT planning and treatment is normally a long-term process, requiring weeks or several months for the patient to return for multiple treatments. Real-time data acquisition is not necessary but multimedia is essential, and the static multimedia ePR model would fit into this clinical environment.

11.2.2.2 Basic Components

11.2.2.2.1 The ePR Software Organization

The purpose of multimedia perk server for RT is to organize all related images/data from image-intensive RT into one unified ePR system that facilitates longitudinal radiotherapy for a patient. The images used are from both radiological diagnostic imaging systems and from radiotherapy systems.

The DICOM RT standard is available for the integration of all RT objects under one standard. The ePR software organization following the DICOM-RT is shown in Figure 11.4.

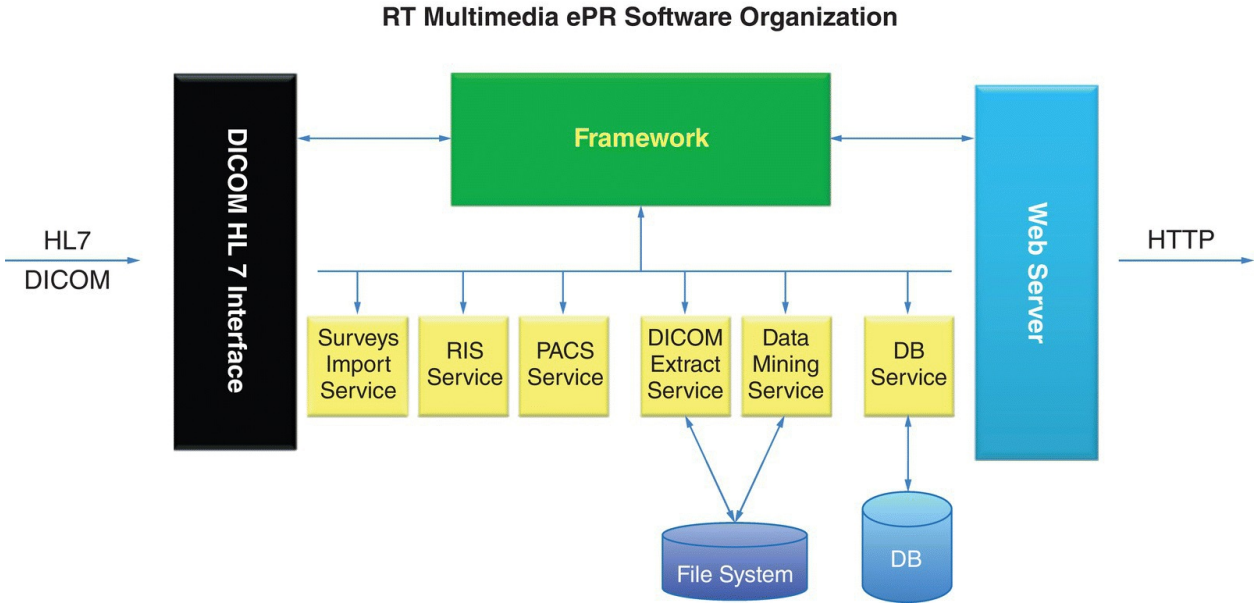

Figure 11.4 RT multimedia ePR software organization. DICOM and HL7 standards are used: the ePR server is Web-based. The yellow boxes are ePR services.

11.2.2.2.2 Database Schema

A low-level data schema is depicted in Figure 11.5. From left to right, if follows the DICOM model, starting from the patient, study, series to RT object level, in which there are seven DICOM-RT objects: images, dose, structure set, plan, beams record, brachy record, and summary. In addition, there are the diagnosis images from the diagnostic systems.

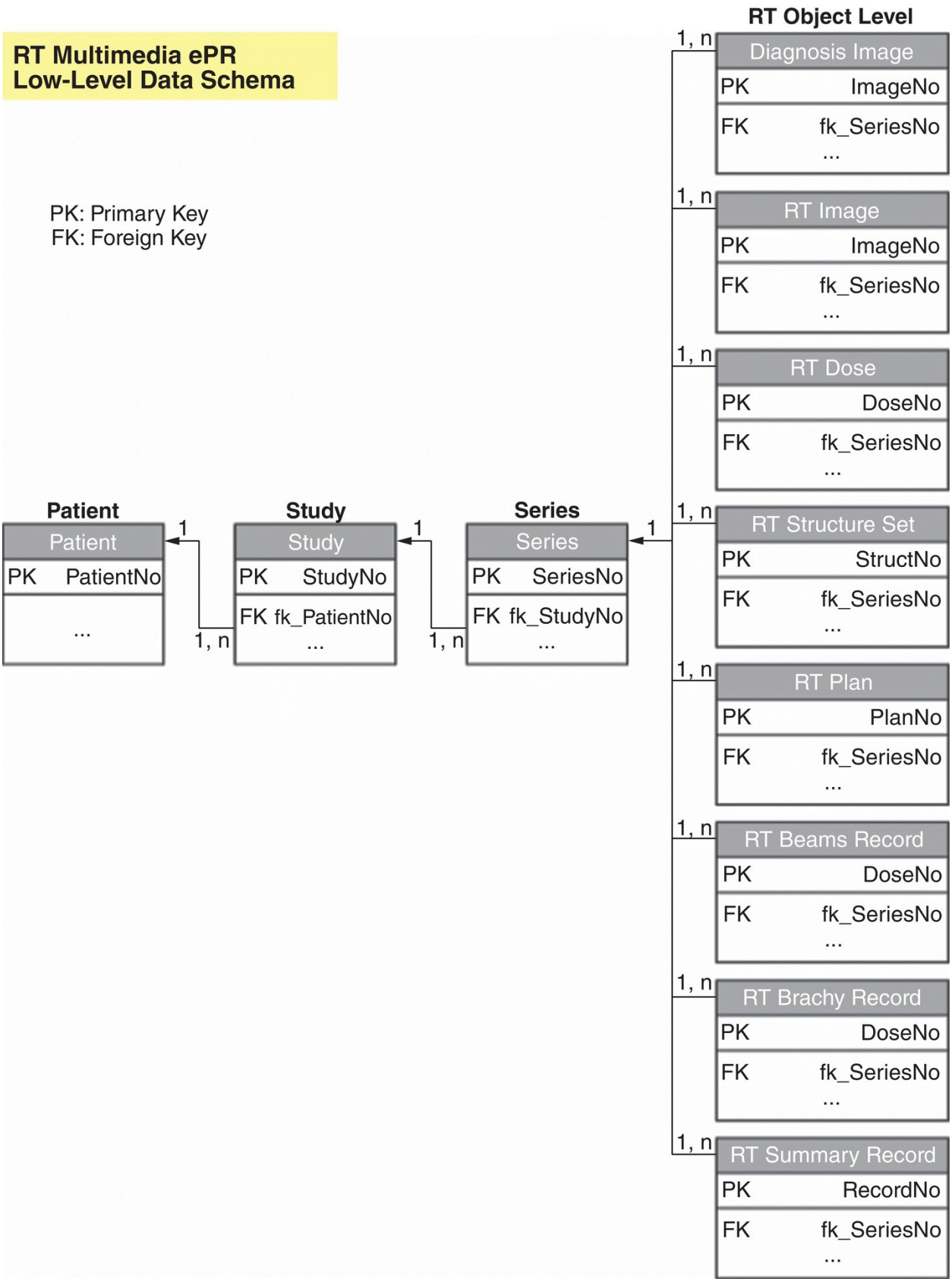
RT Multimedia ePR
Low-Level Data Schema
PK: Primary Key
FK: Foreign Key
RT Object Level
Patient
Study
Series
Patient
PK PatientNo
...
Study
PK StudyNo
FK fk_PatientNo
...
Series
PK SeriesNo
FK fk_StudyNo
...
1
1, n
Diagnosis Image
PK ImageNo
FK fk_SeriesNo
...
RT Image
PK ImageNo
FK fk_SeriesNo
...
RT Dose
PK DoseNo
FK fk_SeriesNo
...
RT Structure Set
PK StructNo
FK fk_SeriesNo
...
RT Plan
PK PlanNo
FK fk_SeriesNo
...
RT Beams Record
PK DoseNo
FK fk_SeriesNo
...
RT Brachy Record
PK DoseNo
FK fk_SeriesNo
...
RT Summary Record
PK RecordNo
FK fk_SeriesNo
...

Figure 11.5 RT multimedia ePR low-level data schema. The DICOM data model starts from patient and proceeds to study, series, and RT objects level, which consists of one DICOM diagnosis image object (top) and seven DICOM-RT objects.

11.2.2.2.3 Data Model

The ePR data model is shown in Figure 11.6, in which the study level consists of seven DICOM-RT objects, excluding the summary and brachy record. The former is a textual file that does not require further processing. The latter is not considered in standard planning and treatment for radiotherapy.

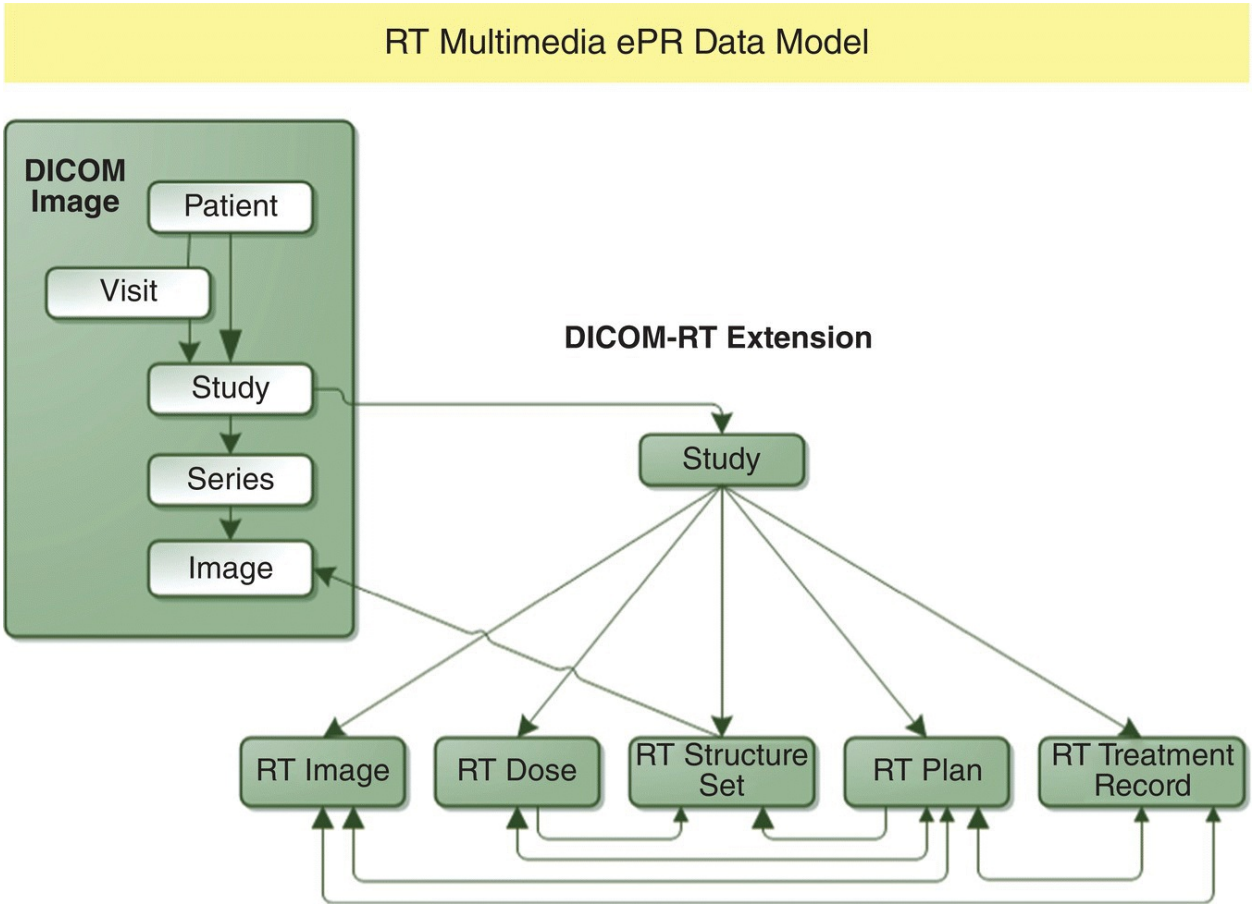

Figure 11.6 RT multimedia ePR data model. The left side shows the DICOM image, and right side shows the DICOM-RT. Only five DICOM-RT objects are used in the model. The sixth is the summary, which is a textual file that does not require further processing.

11.2.2.2.4 Data Flow Model

Data flow of the multimedia ePR for radiotherapy is discussed in this section, with a real example describing the workflow steps of the model.

11.3 Radiotherapy Planning and Treatment

Radiotherapy (RT) uses radiation for the treatment of diseases that usually are malignant. Before delivering the dose of radiation, careful treatment planning is needed. This ensures that the target tumor volume is accurately irradiated while the neighboring normal tissue is spared as much as possible. Such treatment planning results in isodose treatment plans superimposed on CT images illustrating the radiation dose distribution in the irradiated volume, dose volume histograms, treatment parameters, and treatment records. It can be seen that in radiation therapy, not only radiological images are involved; graphics and textual information are generated. For convenience, see Figure 11.1 for a quick review of the RT workflow, which gives a summary of the work and data involved in radiation therapy. DICOM-RT standard is used to integrate all such information originated from other RT systems.

The DICOM standard is the cornerstone to the successful implementation of PACS in radiology. Following the implementation of DICOM format, seven DICOM radiotherapy (RT) objects in DICOM format have been ratified by the DICOM Committee for transmission and storage of radiotherapy multimedia information. The RT archive server database schema, shown in Figure 11.7, consists of seven DICOM-RT objects (Figure 11.7).

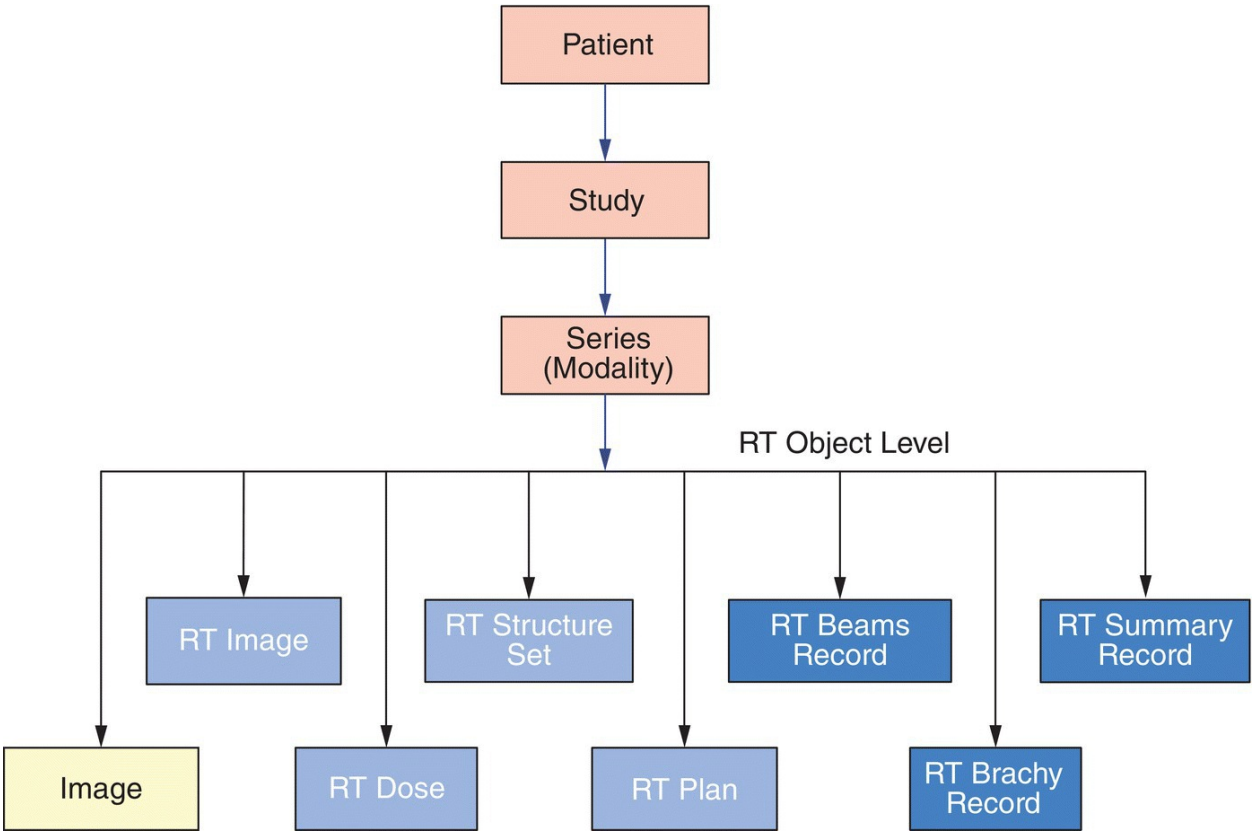

Figure 11.7 RT archive server database schema. The database schema is based on the DICOM data model of the real world. The seven DICOM-RT objects in the blue shaded boxes are integrated within the modality of the series module along with the diagnostic image object (light yellow box) to keep each RT object grouped under a modality similar to the CT or MR. The four light blue boxes are the image, structure, dose, and plan. The two upper darker blue boxes are the beams and the summary record, and the lower one is the brachy record, which is not used for external therapy.

11.4 Radiotherapy Workflow

External beam radiotherapy (RT) involves treatment planning and treatment delivery. It makes up over 90% or the workload in radiation therapy and is an image and computer graphic intensive process. Patient imaging information is needed in the RT planning process, image registration to identify regions to be treated, and markers to align images to ensure treatment setup accuracy. Multimodality images from projection x-rays, CT, MRI, and PET are used for tumor localization and critical organ identification. These include the shape, size, and location of the targets and radiosensitive vital organs. Sometimes images

from different modalities need to be fused for better tumor and critical organ identification. From such information, treatment planning generates computer graphics and radiation dose distribution that overlay the images to ensure the delivery of a uniform high dose to target tumors but not to adjacent critical structures. In addition to careful monitoring of treatment, optimization and dose calculation are essential for successful patient treatment outcomes.

During all these processes, PACS and imaging informatics technologies are used extensively. Radiation therapy emphasizes the individual patient treatment process and has not, until recently, taken advantage of informatics to improve workflow and patient treatment outcomes. Figure 11.1 depicts a generic workflow of RT, including treatment planning and delivery, using a prostate cancer treatment plan and delivery as an example. In this section, we present the multimodalities imaging component of RT treatment planning and delivery, in particular, following the numerals in Figure 11.1, (1) image acquisition, (2) field planning at the treatment planning system, (3) generation of DRR , and (6) verification by comparing portal image and reference DRR, described in the yellow boxes of the workflow.

11.5 The ePR Data Model and DICOM-RT Objects

11.5.1 The ePR Data Model

To develop an ePR, a conceptual data model of the clinical department is required and this in turn determines how patient data are physically represented in the database. To develop the conceptual data model, the radiation therapy workflow from which the data required are defined should first be reviewed. At the same time, the views of the users (radiation oncologists, medical physicists, and radiation therapists) are collected. From these views, the conceptual data model can be increasingly refined with more details. The model is based on the daily operation mode in a radiation therapy department and the users' requirements. The data in the model are parsed from the DICOM images and DICOM-RT objects. When an object is inserted, a link is created at the corresponding location in the table. The output data and the links in the model form the foundation of the design of GUI display windows.

11.5.2 DICOM-RT Objects

Using prostate cancer RT planning and treatment as an example, we describe some DICOM-RT objects (also refer to Section 11.1.1):

1. SRT structure set information object (Figure 11.8(A)(i); see also Figure 11.2A): This object defines a set of areas of significance in radiation therapy, such as body contours, tumor volumes—gross target volume (GTV), clinical target volume (CTV), and planning target volume (PTV)—organs at risk (OARs), and other regions of interest. In prostate cancer, the target volume is the prostate gland and the extension of the cancer around the gland. The OARs are the urinary bladder, the rectum, and the heads of the femur. Each structure will be associated with a frame of reference, with or without reference to the diagnostic images.
2. Plan information object (Figure 11.8A(ii); see also Figure 11.2B): Treatment planning is a process to determine how best the radiation beam should be placed, so that an optimum dose distribution can be delivered. It involves localization of the tumor and OARs, and the design of radiation beams and their dose weighting with respect to the PTV and OARs. A clinical treatment plan may refer to the totality of structures marked on the CT image, the beam positions and beam sizes, and the dose distribution displayed on the image. In the DICOM-RT standard, information about the structures are contained in the structure set object and the dose distribution in the dose object, which requires the coordinates for indication of their positions. Thus the plan object only refers to the textual information in treatment plans, whether generated manually, by a virtual simulation system, or by a treatment planning system. Such information includes treatment beam parameters, fractionation scheme, prescription, accessories used, and patient setup in external beam or brachytherapy.
3. Dose information object (Figure 11.8A(iii); see also Figure 11.2C): The distribution of radiation dose for a treatment is represented by the isodose lines expressed in percentage or in dose units (gray). The isodose lines can be displayed in relation to the tumor volume and OARs and superimposed on images. This object contains such radiation dose data from TPS. It allows the transmission of a 3-D array of dose data as a set of 2-D dose planes. Examples are the isodose distribution dose data either in relation to the corresponding CT or MR image or on their own and the DVH (Figure 11.8A(iv); see also Figure 11.2D).
4. Image information object (Figure 11.8B): In contrast to the DICOM image object, where the different image types are contained in objects for different modalities, the RT image information object specifies the attributes of those images that are “acquired or calculated using conical geometry” in

radiotherapy. Examples are projection simulator images, portal images acquired at linear accelerators, or DRR generated from CT scans at TPS.

5. Beams treatment record information object: This object contains mainly textual data that specify a treatment sessions report generated by a treatment verification system during a course of external beam treatment or treatment information during treatment delivery. Such information includes machine, radiation type and energy used, date and time of treatment, external beam details, treatment beam accessories, treatment fraction detail, the monitor units (dose), calculated dose, cumulative dose, verification image taken, and optional treatment summary. Each treatment is represented by an instance of a beam's treatment record. Figure 11.8B provides an example of a RT beam treatment record.

(A)

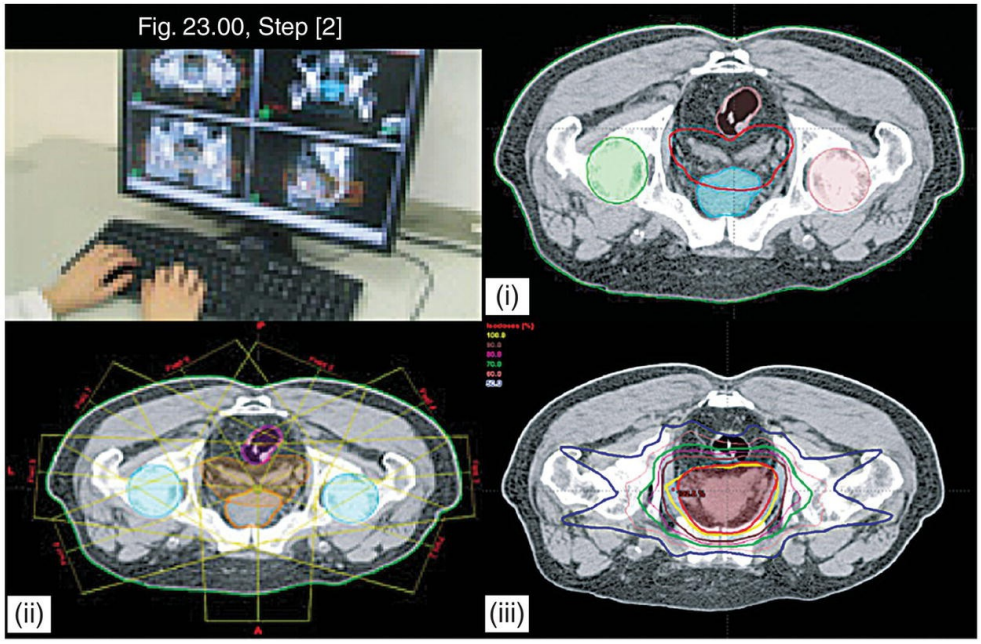

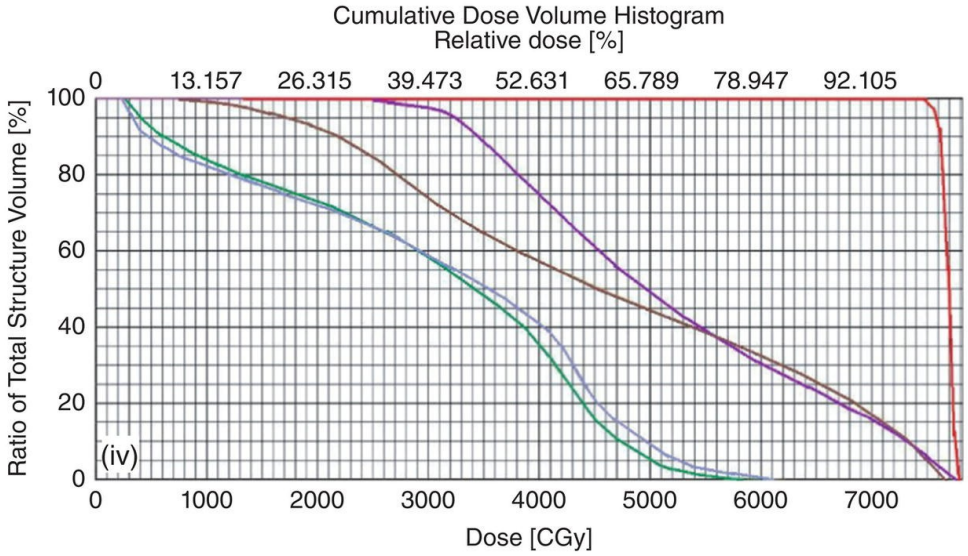

(B)

Field	1	2	3	4	5	6	7	8	9	10	11	12	13	14	15
Wedge	3RW60	3RW45	4RW45	4RW45	4RW45							3RW30	1VW15		3RW45
Date\MU	128	94	187	47	47	75	15	166	30	15	15	128	67	20	104
2002/6/26	128	94	187	47	47	75	15	166	30	15	15				
2002/6/27	128	94	187	47	47	75	15	166	30	15	15				
2002/6/28	128	94	187	47	47	75	15	166	30	15	15				
2002/6/29	128	94	187	47	47	75	15	166	30	15	15				
2002/7/1	128	94	187	47	47	75	15	166	30	15	15				
2002/7/2	128	94	187	47	47	75	15	166	30	15	15				
2002/7/3	128	94	187	47	47	75	15	166	30	15	15				
2002/7/4	128	94	187	47	47	75	15	166	30	15	15				
2002/7/5	128	94	187	47	47	75	15	166	30	15	15				

2002/7/19												128	67	20	104
2002/7/20												128	67	20	104
2002/7/22												128	67	20	104
2002/7/23												128	67	20	104
2002/7/24												128	67	20	104

Figure 11.8 (A) Three DICOM RT objects: (i) structure, (ii) plan, and (iii) dose; and (iv) DVH curves (reproduced from Figure 11.2). (B) The three RT treatment records. These objects include the RT beams treatment record, the RT Brachy treatment record, and RT treatment summary record. The figure shows the RT beam treatment record, which records the dose given for each radiation beam at each treatment session (rows). Column 1 shows the date on which the radiation dose was delivered. The other columns show the dose (in monitor units) delivered to radiation fields 1–11 on a given date. Radiation field numbers 12–15 show a second phase of treatment that consists of only four radiation fields.

(courtesy of Dr M. Law)

Together with the DICOM RT objects shown in Figures 11.8A and B, the DICOM RT descriptions of the prostate cancer radiation therapy plan and treatment of a patient's can be defined.

11.6 Infrastructure, Workflow and Components of the Multimedia ePR in RT

The mission of the ePR system is that all RT-related information for a patient can be viewed within a system (i.e. with the pertinent multimedia information of treatment plans, graphs, images, records, and clinician's remarks) from different sources, to form an ePR with the data standardized in DICOM-RT.

11.6.1 DICOM-RT-Based ePR System Architecture Design

The DICOM data model is used as the base for designing the multimedia ePR system in RT. Figure 11.9A shows the general PACS model being used today and Figure 11.9B depicts the model of the multimedia ePR system in RT; observe the similarity of both models. The ePR in RT consists of three major components: the DICOM-RT objects input, the DICOM-RT gateway, and the DICOM-RT-based perk system platform (dotted rectangle). The ePR platform consists of three modules, the DICOM-RT archive server, the RT Web server, and the Web-based client workstations (WSs). Note that the RT Web server has to handle more complex multimedia data than the Web server in PACS (Figure 11.9A).

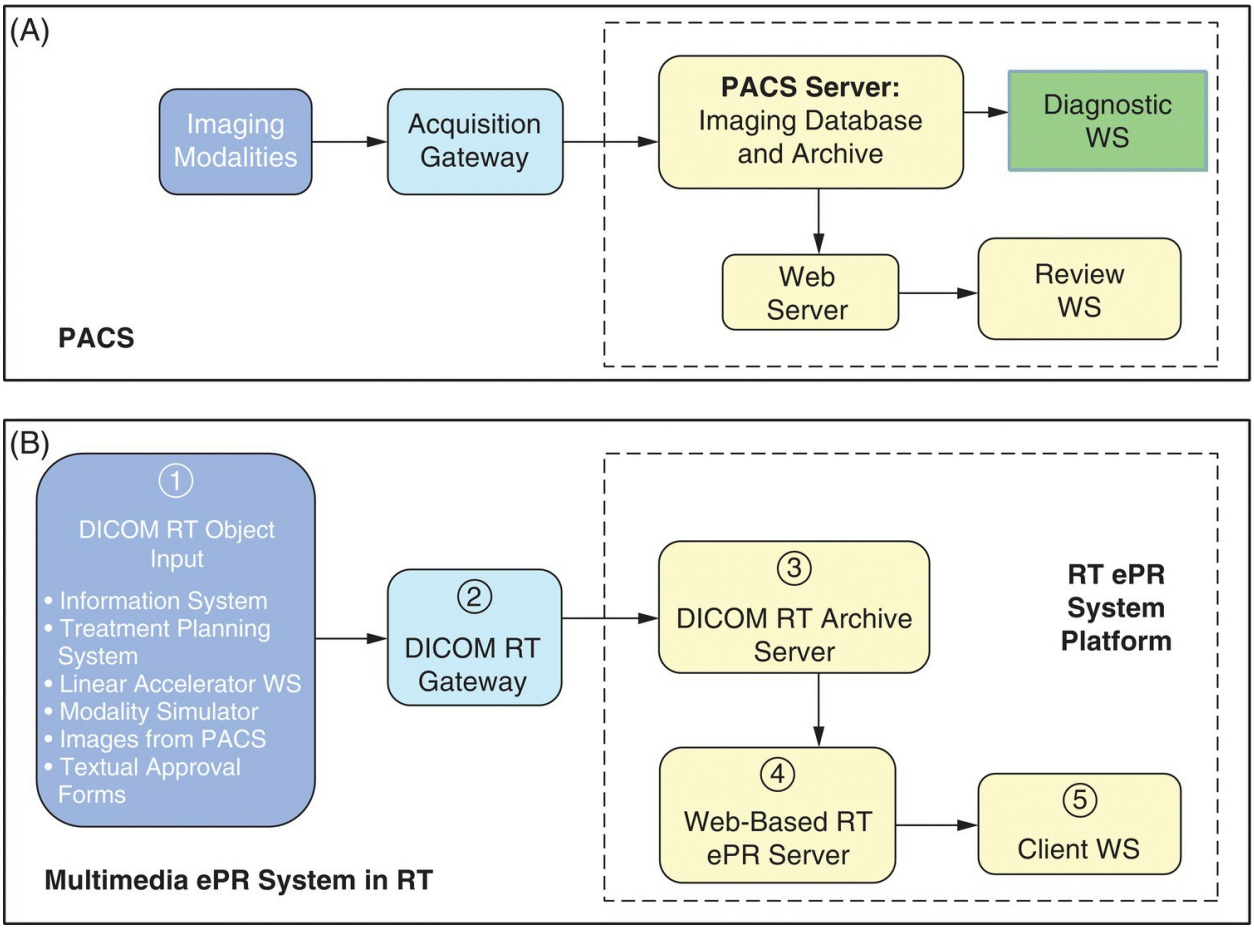

Figure 11.9 Structural similarities between the PACS and the DICOM-RT based ePR system. (A) Generic PACS components and data flow; the key PACS components that are successfully utilized today within the radiology workflow. PACS uses diagnostic WS for high-quality viewing, and the PACS Web server and review WS are mostly used for reviewing radiological image studies by referring physicians. (B) Multimedia DICOM-RT ePR system components and data flow. Most of the RT components follow the PACS data model (modules 1–3 relate to the imaging modalities, acquisition gateway, and PACS server, respectively, in A). The ePR system platform (dotted rectangle) is used to extract information from the DICOM-RT server to develop the Web-based ePR system. Note that the RT Web server is more complex in B (refer to Figure 11.10 for detail) when compared with A, since the data contain more complex imaging and informatics data objects, while the Web server in A contains only diagnostic image studies and reports. Also, there are different Web application pages within the RT Web client workstations used by oncologists, radiation therapists, and medical physicists, based on their different needs (modified from original drawing by Dr M. Law).

11.6.2 DICOM-RT Object Input

The workflow diagram shown in Figure 11.1 identifies all DICOM-RT objects. They can come from any RT information systems, treatment planning system, linear accelerator WS, modality simulator, PACS, and in addition pertinent information related to the patient in the hospital information system (HIS) depicted in Figure 11.9B.

These systems are connected by the Internet and departmental Intranet communication networks. Preselected DICOM and DICOM-RT objects are first identified by each system and then either pushed to, or pulled by, the DICOM-RT gateway shown in Figure 11.9B. Other functional requirements (e.g. treatment plan approval by radiation oncologists) in the workflow review in textual format are converted into the system technical details based on the DICOM-RT object definitions and the data flow of the objects and entered by radiographic technicians to the gateway also. The DICOM standard service classes, such as DICOM storage and query/retrieve, are incorporated into each component of the ePR information system.

11.6.3 DICOM-RT Gateway

After receiving the RT objects, the DICOM-RT gateway (Figure 11.9B) extracts information from the objects and puts them into the data model as required in the DICOM-RT archive server. It also converts any nonstandard data objects to the standard required by the DICOM-RT server. The outputs of the gateway are packaged DICOM and DICOM-RT objects, which are automatically pushed by the gateway to the RT archive server.

11.6.4 DICOM-RT Archive Server

Following the DICOM hierarchical structure, a database schema for the DICOM-RT archive server (Figure 11.9B) can be constructed. It consists of four levels (patient, study, RT series, and RT objects) with 11 modules, as represented by the colored boxes in Figure 11.7. The schema follows the DICOM data model of the real world and includes the seven DICOM-RT data objects and the DICOM diagnostic images. It is important to that most current PACS do not support DICOM-RT objects (except DICOM-RT image), because of the need to have a more elaborated internal schema for a RT archive server. PACS manufacturers are beginning to incorporate the DICOM-RT objects to gradually migrate their PACS server to be compatible with the RT archive server.

In the ePR in RT, the RT server is used mostly for management and storage for RT objects rather than for processing the RT data (attributes) encapsulated in the objects, which is in contrast to the functions of the PACS server. Upon receiving DICOM-RT objects and images from the DICOM-RT gateway, the RT server abstracts only the essential aspects of the entities for the necessary transactions, and autoroutes all the data to the RT Web server (Figure 11.9B) to be processed for display on the RT Web client WS.

11.6.5 DICOM-RT Web-Based ePR Server

While the RT archive server is responsible for storage and transmission of DICOM images and DICOM-RT objects, the RT Web server (Figure 11.9B) receives the objects, decodes them to the corresponding position in the RT Web database, and organizes the data into the Web viewing mode for display in the client workstations (Figure 11.10). In this sense, the Web server is the "brain" for the RT multimedia ePR system, since all actions are processed here.

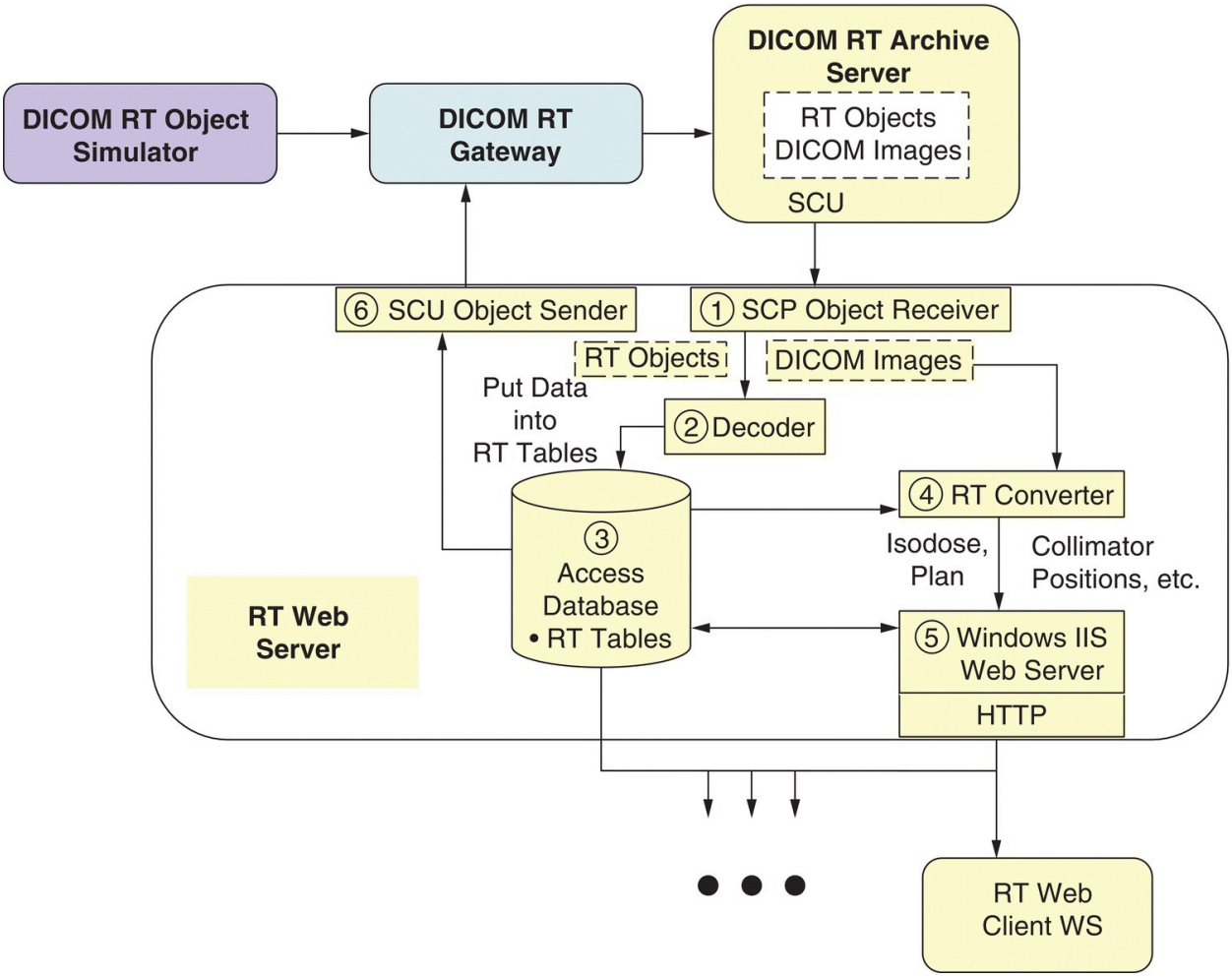

Figure 11.10 Architecture of the RT Web server of the DICOM-RT ePR system. Six key components are shown within the Web server rectangular domain. Note that the RT Web server is more complex than a PACS Web server, since it must handle the multimedia image and informatics data from the seven DICOM-RT objects in addition to the DICOM diagnostic images from radiology. SCP: Service class provider; SCU: service class user; HTTP: hypertext transfer protocol.

There are six major components in the RT Web server, as shown in Figure 11.10. Following the numerals in the figure, the workflow process between the DICOM-RT archive server and the RT Web server is as follows:

DICOM-RT objects and DICOM diagnostic images are sent by the DICOM-RT archive server through the DICOM service class user (SCU) service (Chapter 4) to the RT Web server (SCU is a built-in service in the DICOM-RT archive server). The images are received by the object receiver:

1. using DICOM service class provider(SCP). RT objects are translated by a decoder;
2. and the data are arranged in the RT tables and RT database;
3. the data from the tables, e.g., RT structures and RT dose, are superimposed on the corresponding positions of the DICOM images by the RT converter;
4. and be sent by the Web server;
5. to the client workstations using hypertext transfer protocol(HTTP). When the RT Web server has generated the new data needed to update the DICOM-RT archive server, e.g., a revision in the treatment plan by the oncology, the object sender;
6. the RT Web server will be called upon to perform the task. In this case, it uses the DICOM SCU service to send the updated objects to the RT archive server via the DICOM-RT gateway for storage. The updated information will be in a queue to update the DICOM-RT archive server, which completes the data loop.

The DICOM standard has grouped various RT attributes into modules and object DICOM information object definitions(IODs). The overall database schema of the RT Web server adopts what is defined by the DICOM data model and consists of 72 tables (in its prototype) to facilitate Web viewing in the client WSs. This information includes key data items such as treatment plan parameters, beam records, isodose curves, regions of interest (ROIs), including

the tumor volume and organs at risk (OAR) contours, and DVH (Figures 11.2 and 11.8).

These data are parsed from the DICOM-RT objects as needed, to be displayed in the Web client WSs. The data objects from the Web-based server can be used to develop quantified knowledge and metadata, which can be added to the database schema. Further outcomes data can be added to the overall database schema. Thus, it is important to design the database schema to be as flexible as possible to extend it for knowledge base and outcome data that are not part of the DICOM standard.

11.6.6 RT Web Client Workstation (WS)

For the RT Web client WSs (Figure 11.9B), the GUI is designed for users to access information within the database according to the functional requirements for radiation therapists, dosimetrists, physicists, and oncologists. Based on the user requirements documentation, all necessary data required are included in the database tables of the Web server. The RT workflow also serves to drive the GUI design. Figure 11.11 depicts the timeline window of a cancer patient's RT planning and treatment overview.

Electronic Patient Record - Internet Explorer provided by Dell

http://10.100.6.6/rtweb/RTVSummary.asp?pid=RTPAT_01

Overview | Summary | Prescription | Images | Isodose Plan | BEV | Treatment Record | Course 1 | Phase 4

RADIATION ONCOLOGY

PATIENT VISIT SUMMARY

Patient Name	RTPatient01	Course	1
Patient ID	RTPAT_01	Region	Prostate
Sex	Male	Technique	
Age	52	Prescription	
Telephone		Diagnosis	
Address		Course Intent	Curative
Occupation		Special Condition	

Year	2002	2002	2002	2002	2002	2002	2002	2002	2002
Day-Month	11-Jun	20-Jun	21-Jun	26-Jun	27-Jun	28-Jun	29-Jun	01-Jul	02-Jul
DICOM Image									
CT/CT Sim									
MR									
RT Image									
Simulator Image									
DRR									
Portal Image									
Treatment Plan									
Verification Status									
No. of Treatment				1	2	3	4	5	6
Brachy Record									
Treatment Status									
Comment									
Setup Photo									

Review Update: Continue RT / Suspend RT / Stop RT / Completed

Review Notes:

Reviewer: Dr. S. Lee

Enter

Internet | Protected Mode: Off | 100%

Figure 11.11 Screenshot of a Web client application page on the client WS from the DICOM-RT ePR system prototype developed in the Hong Kong Polytechnic University, showing the timeline overview of a RT patient's ePR display window. Key data extracted from some DICOM-RT objects are displayed as thumbnail representations for users to and review in more detail using the GUI at the client WS. This patient had a CT scan on June 11, 2002, a dosimetric treatment plan done on June 20, a DRR generated on June 21, and portal image produced on June 26, after which treatment started immediately on June 26. Six radiation doses were delivered from June 26 to July 2. GUI: Graphical user interface; DRR: digitally reconstructed radiograph.

11.7 Database Schema

The macro aspect of the multimedia ePR in RT, including infrastructure, system components, and workflow, has been discussed. In Figure 11.7, the high-level of the ePR database schema was presented. The next step is to consider the micro aspect of the ePR, namely the data schema in the RT database. The database schema refers to how data are physically represented. It is concerned with data structures, file organization, and mechanism for the operation of the system and data storage. From the data flow diagram shown in Figure 11.9B, it can be seen that the ePR system has two databases, one for the RT archive server and the other for the RT Web-based server. The former is for management and storage of DICOM objects (including DICOM-RT objects and DICOM images), and the latter is first for partition of the collected DICOM-RT objects data and then the server parses them strategically to be viewed by users at the Web client.

11.7.1 Database Schema of the RT Archive Server

The Web-based RT ePR server component can be designed as a three-tier client–server architecture. In the three-tier architecture, a middle tier is added between the user interface client environment and the database management server environment (see the dotted box in Figure 11.9B). For this design, the three tiers are:

1. the RT archive server, which provides such functions as managing, archiving, and transferring of the DICOM images and DICOM-RT objects;
2. the RT Web-based server, focusing on processing the planning and treatment data of the patient; and
3. the RT Web client, which presents the patient's record.

DICOM is an object-oriented standard. The external aspects (operation) of an object are separated from the internal details of the data, which are hidden from the outside world (information hiding). This organization allows identification of the object, or any operations on the object first, and delays the implementation of details. Also, changes to the internal details at a later stage will not affect the applications that use it, provided that the external aspects remain unchanged. In this way, the database server only needs to identify what an object is and what it does (the DICOM-RT archive server). The internal details or the data structure of an object can be implemented or processed later in the application server (the Web-based RT server). This is the way in which the PACS server was designed; hence, it has a simple data model for the operations of its objects. Such a design can also be adopted for the ePR system, that is, the DICOM-RT archive server only manages the essential aspects of the RT objects and leaves the implementation of details to the RT Web server. Thus, the DICOM-RT archive server has only the basic database schema, based on the first few levels of the DICOM hierarchical structure (Figure 11.7), namely “patient,” “study,” “series,” and its RT objects and diagnostic images.

11.7.2 Data Schema of the RT Web Server

For implementing the details of the DICOM-RT objects using the Web-based RT server, a data model, different and more elaborated than that of the RT server, is required. The basic data structures are given in the DICOM standard documents. How the data are used depends on the actual application at the client WS, which in turn determines how much is included in the data model. From the user requirements collected earlier (Section 11.5.1), the physical data model for the Web server can be designed and implemented following the DICOM standard, as shown in Figure 11.12.

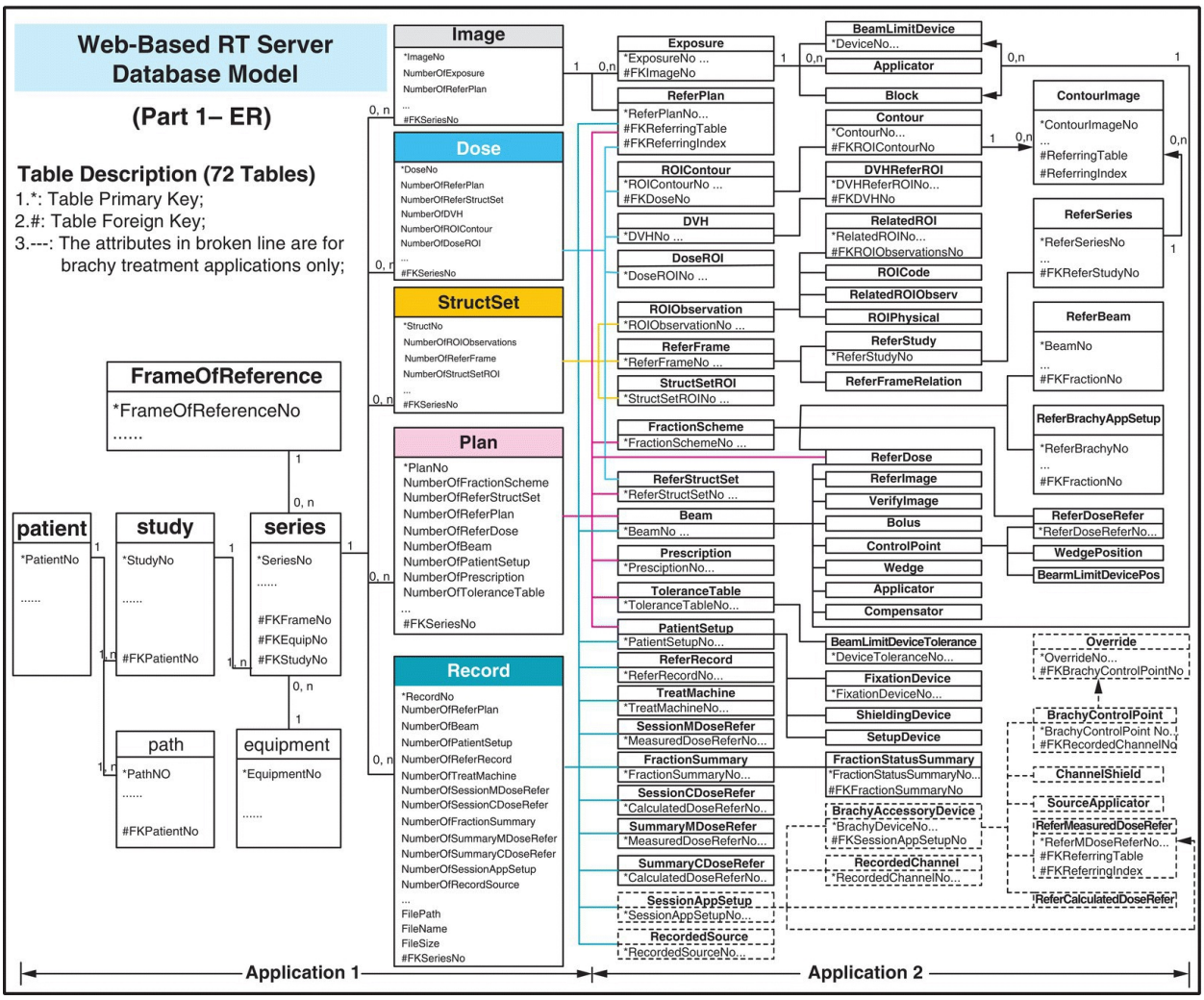

Figure 11.12 Database scheme of the RT Web application server based on a multimedia ePR system in RT prototype developed at the Hong Kong Polytechnic University. Although the database is generic, it can be modified for other oncology departments with different workflows, treatment plans, and viewing conditions.

(courtesy of Professor M. Law)

11.8 Graphical User Interface Design

The user interface presents the patient's information to the users and is an important part of the ePR. The design of the interface can be based on the survey of the user requirements mentioned in Section 11.5.1. Radiation therapists and oncologists should be involved in the design process. Figure 11.13A shows the hierarchical structure of the user interface windows and the functions served by

each window, the detail of which can be referred to in Figure 11.13B [28]. The user interface can be implemented by using the standard GUI software package; for example, the interactive functions of the Visual Basic (VB) scripts embedded in the active server page(ASP), a feature of the Window Internet Information Server.

(A)

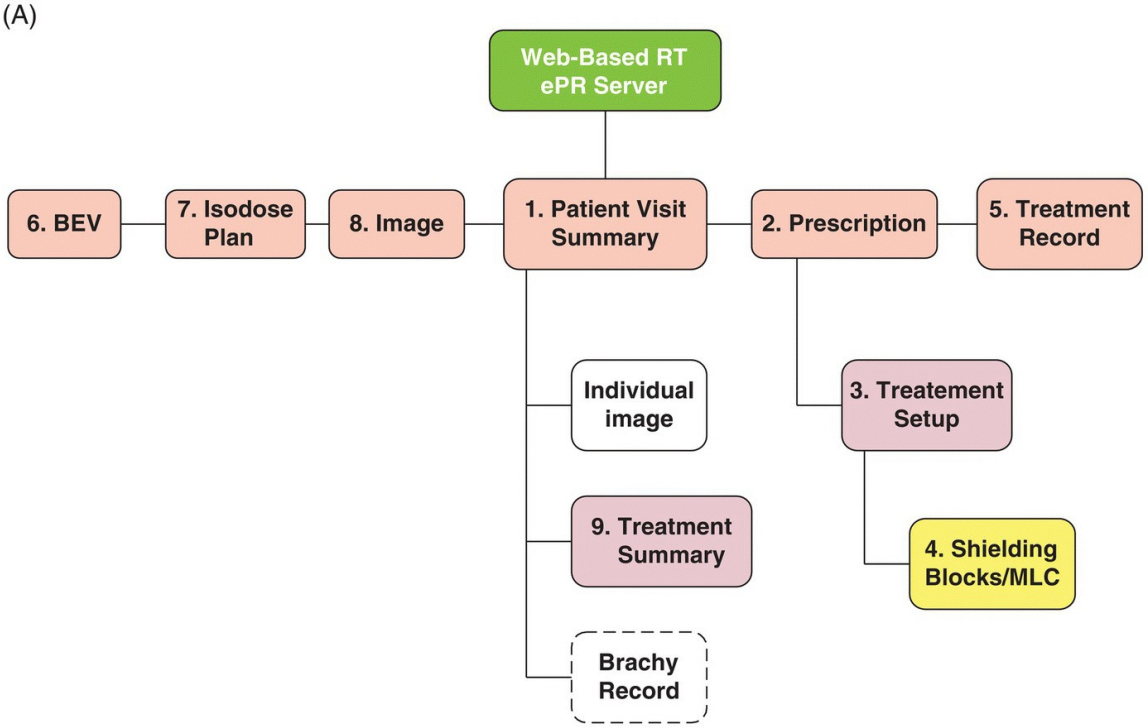
Web-Based RT ePR Server
6. BEV
7. Isodose Plan
8. Image
1. Patient Visit Summary
2. Prescription
5. Treatment Record
Individual image
3. Treatement Setup
9. Treatment Summary
4. Shielding Blocks/MLC
Brachy Record

(B)

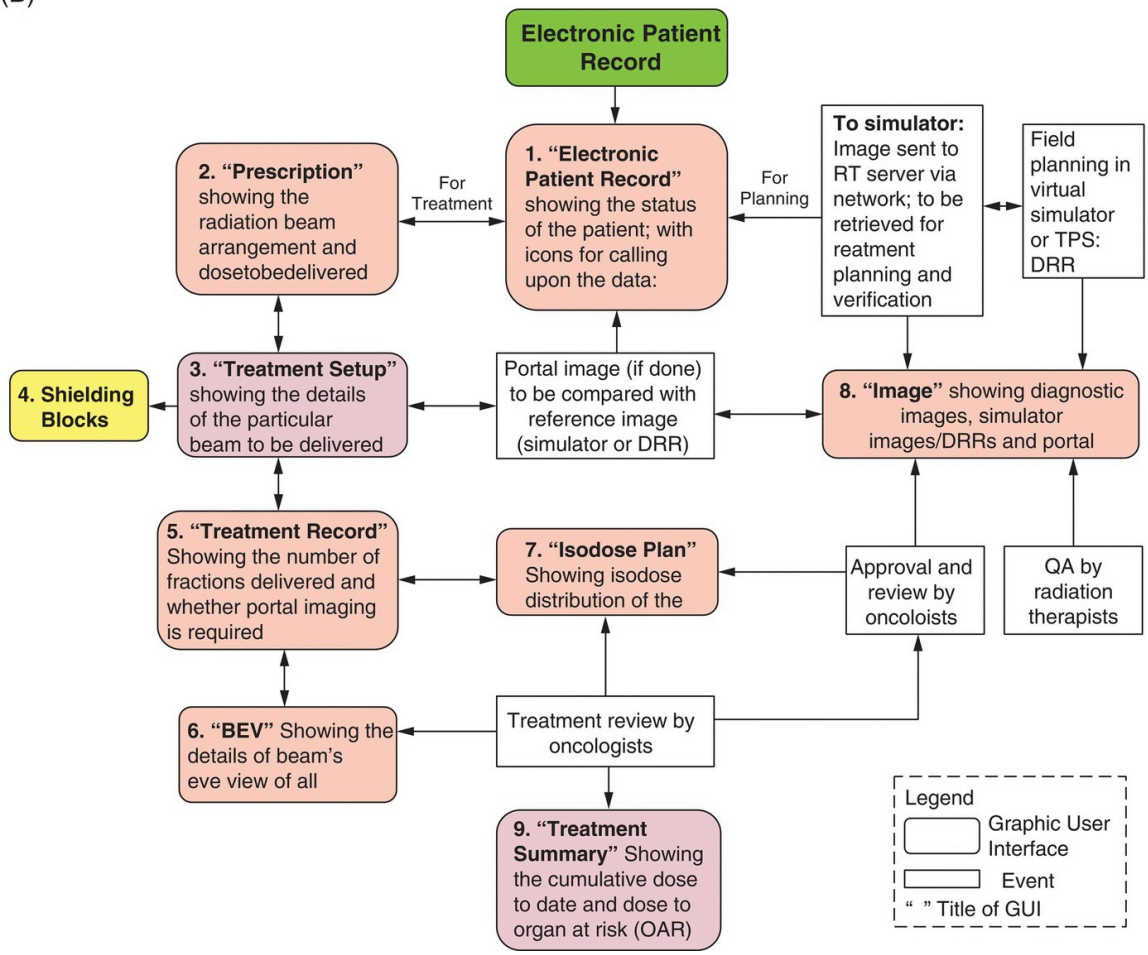
Electronic Patient Record
1. "Electronic Patient Record" showing the status of the patient; with icons for calling upon the data:
2. "Prescription" showing the radiation beam arrangement and dosetobedelivered
For Treatment
For Planning
To simulator: Image sent to RT server via network; to be retrieved for reatment planning and verification
Field planning in virtual simulator or TPS: DRR
4. Shielding Blocks
3. "Treatment Setup" showing the details of the particular beam to be delivered
Portal image (if done) to be compared with reference image (simulator or DRR)
8. "Image" showing diagnostic images, simulator images/DRRs and portal
5. "Treatment Record" Showing the number of fractions delivered and whether portal imaging is required
7. "Isodose Plan" Showing isodose distribution of the
Approval and review by oncoloists
QA by radiation therapists
6. "BEV" Showing the details of beam's eve view of all
Treatment review by oncologists
9. "Treatment Summary" Showing the cumulative dose to date and dose to organ at risk (OAR)
Legend
Graphic User Interface
Event
" " Title of GUI

Figure 11.13 (A) Website hierarchy of a multimedia ePR system in RT prototype developed at the Hong Kong Polytechnic University. Minor modifications may be needed for other oncology centers with different workflows and display requirements from the users. BEV: Beam's eye view; MLC: multileaf collimator. (B) Workflow of the graphical user interface. Minor modifications may be needed for other oncology centers with different workflows and display requirements from the users.

(courtesy of Dr M. Law)

11.9 Validation of the Concept of Multimedia ePR System in RT

11.9.1 Integration of the ePR System

11.9.1.1 The RT ePR Prototype

The concept of the multimedia ePR system in RT presented in previous sections was tested by Professor M. Law at the Hong Kong Polytechnic University, where she has used and developed a prototype ePR system since 2004. The prototype has the five major components shown in Figure 11.14 (Chapter 12), from right to left, the RT object simulator, DICOM-RT gateway, RT archive server, Web-based RT server, and RT client WS (Figure 11.9B). In this section, the prototype system that supports the concept of the multimedia ePR system in RT is discussed.

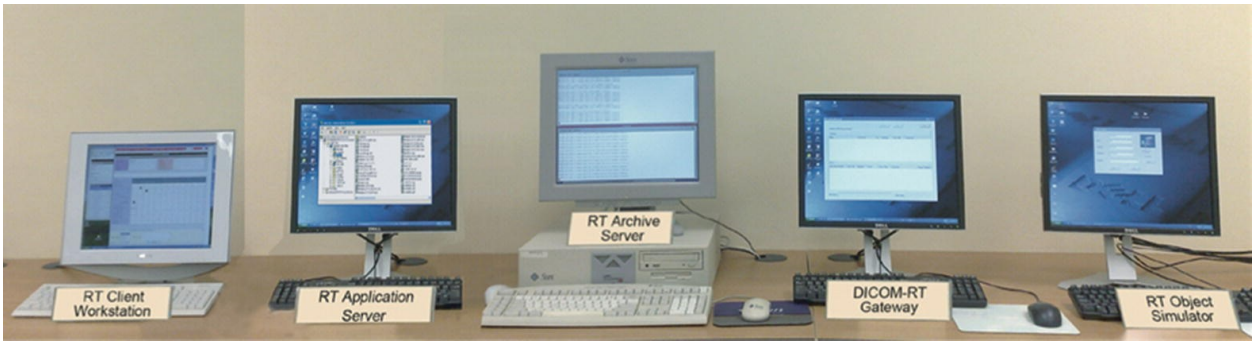

Figure 11.14 Photograph of the multimedia ePR system in RT prototype implemented within the laboratory environment for evaluation of the RT data objects and workflow. Each component represents the conceptual diagram from Figure 23.5B. From right to left: (1) RT object simulator for DICOM-RT data input; (2) DICOM-RT gateway; (3) DICOM-RT archive server; (4) RT Web-

based server (refer to Figure 23.6 for RT Web server architecture); and (5) RT client WS. See also Chapter 12.

(courtesy of M. Law).

11.9.1.2 Hardware and Software

All components in the prototype are PC-based, except for the RT archive server, which is a SUN Ultra 2 computer with an SCSI hard disk and 100 MB Ethernet adapter operating under Sun OS 5.8. The software includes SUN Workshop Compilers CC++, PACS Programming Library, and Oracle8i release 8.1.7 database management system. A Microsoft Access 2000 database was used as the database for the RT web server (Figure 11.10). For distributing RT information, a web server, a Windows Internet information server was used and the data were sent using the hypertext transfer protocol (HTTP). Microsoft Access 2000 was used for the database.

11.9.1.3 Graphical User Interface (GUI) in the WS

The prototype RT Web server system comprises a Web-based display and database structure designed in-house. The front end includes the data objects, structure, and communication protocol, and the back end consists of encoding and decoding with open standards (Figures 11.13). The user interface windows for the Web client WS were created with embedded interactive functions. Within the Web application server, graphical illustrations such as dosimetric plans were created, stored, and displayed in JPEG format. They result from the overlays of the DICOM CT image, RT structure set, RT plan, and RT dose objects. The DICOM standard inherently provides cross-referencing among these objects. Decoding and encoding software applications were developed, based on theinformation object definitions(IODs) of DICOM. For multiple data items that are required on the same display, such as the dosimetric plan, the DICOM objects containing the target volumes, organs at risk, and isodose distribution are decoded to and encoded from the database records of the coordinates in the Web application server based on the definition of the DICOM sequences. Those Web-based displays are achieved by plotting coordinates onto the referenced CT image.

11.9.2 Data Collection for the Prototype System

Different types of RT files (DICOM and non-DICOM) were collected from RT vendors and clinical departments. DICOM files include CT and MRI, digitized

simulator and portal images, RT plan, RT structure set, and RT dose. Non-DICOM files include treatment planning files and the treatment record in textual format, and the portal image in tiff/bitmap format. The names of patients were anonymized. The non-DICOM files were translated to DICOM format. After testing the files for successful transmission through the laboratory computer components, the DICOM files were grouped into folders to form 10 virtual patients, so that their electronic records could be displayed in the Web client. The virtual patients' information was successfully transmitted, stored, and viewed at the RT Web client. Using the user interface windows, we next illustrate the ePR of one of the patients stored in the archive server.

11.9.3 Multimedia Electronic Patient Record of a Sample RT Patient

A patient, whose name is RTPatient01, with a Hong Kong Identity card number (HKID) of RTPat_01, was planned for a course of radiotherapy. He has finished all the earlier treatment planning procedures and is now receiving the radiation treatment. He comes back for this treatment. At the reception desk for the treatment unit, the receptionist or radiation therapist calls up the patient query page and types in the patient's HKID number, or just "RT" against the HKID, to search for the patient's detail. The list of patients beginning with HKID number of "RT" is shown (Figure 11.15A). In the database, only two patients are listed with a beginning "RT," so only two patients' names are shown; RTPatient02 is the other patient. The same page and search procedure can be used when a patient revisits the department for planning procedures or goes to see a radiation oncologist for review or to receive further radiation treatment.

(A)

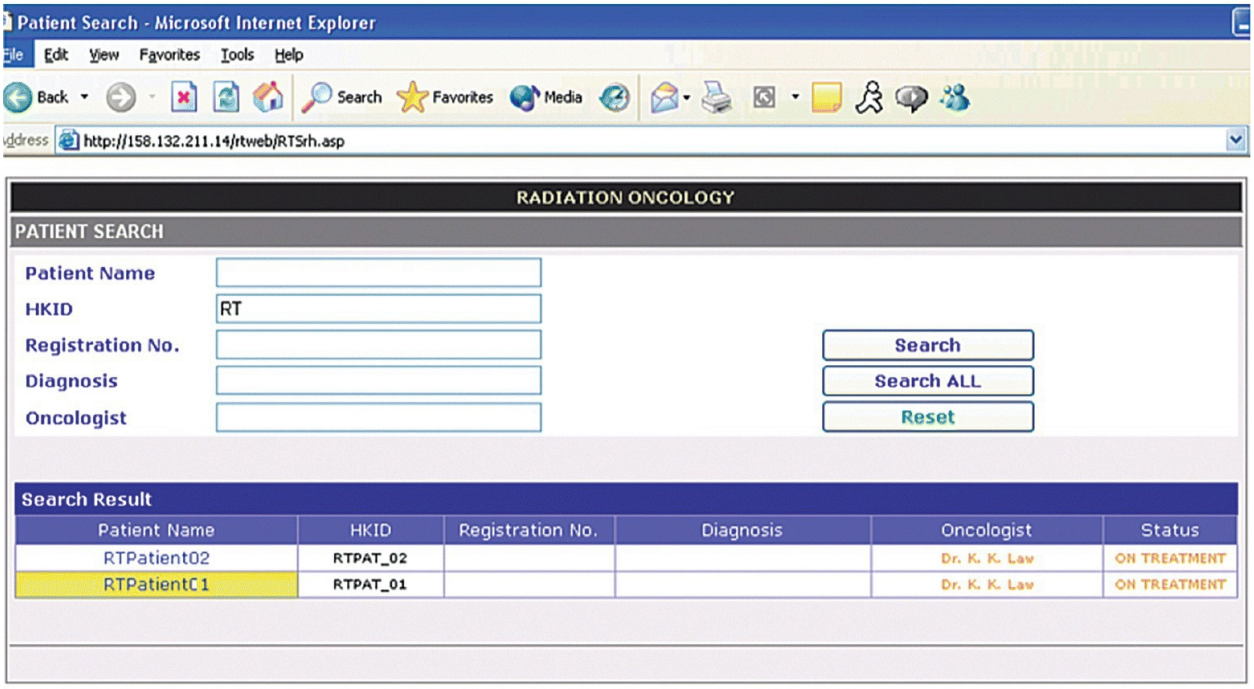
Patient Search - Microsoft Internet Explorer
File Edit View Favorites Tools Help
Back Search Favorites Media
http://158.132.211.14/rtweb/RTSrh.asp
RADIATION ONCOLOGY
PATIENT SEARCH
Patient Name
HKID
RT
Registration No.
Diagnosis
Oncologist
Search
Search ALL
Reset
Search Result
Patient Name
HKID
Registration No.
Diagnosis
Oncologist
Status
RTPatient02
RTPAT_02
Dr. K. K. Law
ON TREATMENT
RTPatient01
RTPAT_01
Dr. K. K. Law
ON TREATMENT

(B)

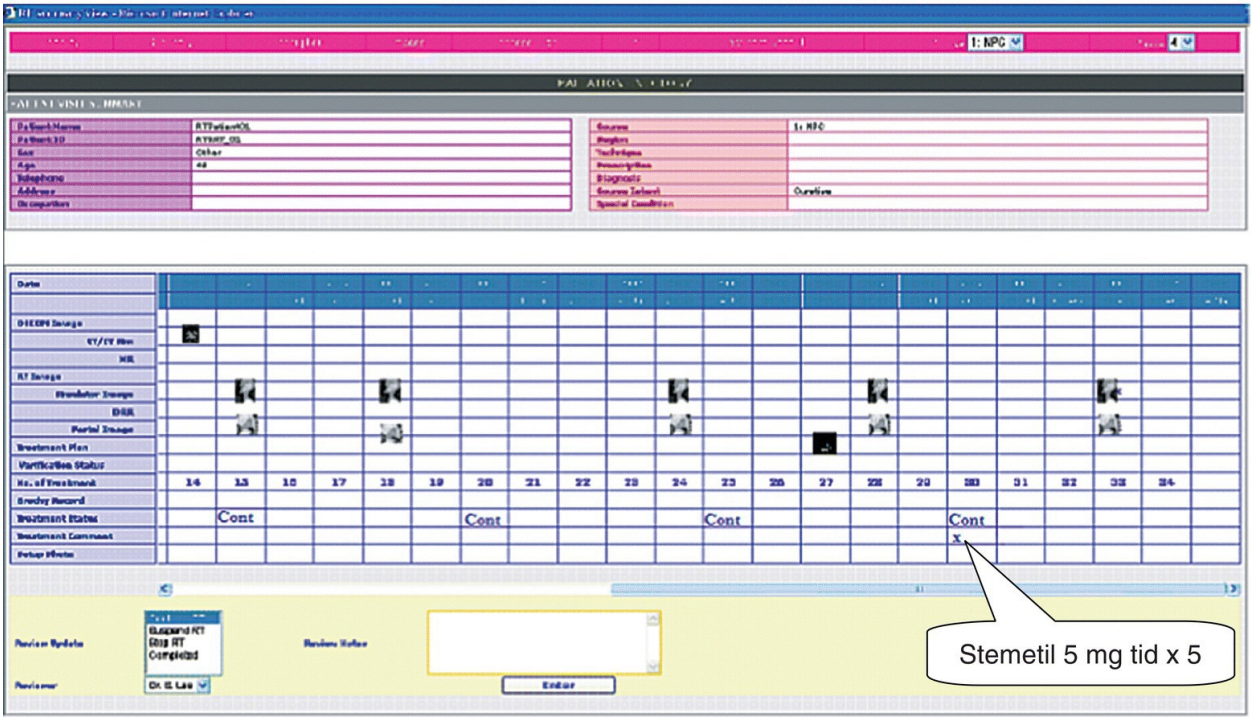
Cont
Cont
Cont
Cont
Stemetil 5 mg tid x 5

(C)

RT Summary View - Microsoft Internet Explorer

Overview | Summary | Prescription | Images | Isodose Plan | BEV | Treatment Record | Course 1: NPC | Phase 4

RADIATION ONCOLOGY

PATIENT VISIT SUMMARY

Patient Name	RTPatient01	Course	1: NPC
Patient ID	RTPAT_01	Region	
Sex	Other	Technique	
Age	48	Prescription	
Telephone		Diagnosis	
Address		Course Intent	Curative
Occupation		Special Condition	

Prescription

Course 1: NPC

Region	Dose (Gy)	Tumer dose at	Fraction Dose (Gy)	Weeks	Fractions	Fr/wk	Prescription detail	Oncologist in charge
-	70	100%	2	-	35	-	-	Dr. K. K. Law

Phase	Machine ID Radiation type	Field ID	Field Name	Field size (cm)	Gantry Angle	Collimator Angle	Wedge/ Accessories	MU
4	MX2_LA2 X	24	Left	9 X 6.5	90°	305°	1VW	67
4	MX2_LA2 X	25	Right 7 P 5 S	9.2 X 7	263°	55°	4RW30	129
4	MX2_LA2 X	26	Ant	9 X 8	0°	0°	2VW	69
4	MX2_LA2 X	27	Ant 35 I	8 X 15	35°	0°	-	157
4	MX2_LA2 X	28	Sup 1 P	11.5 X 14	269°	0°	4RW45	212

(D)

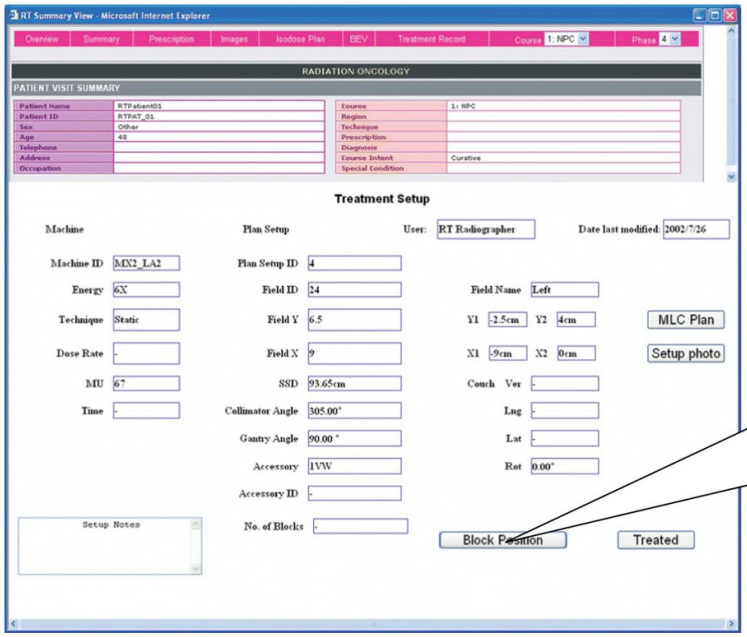

(E)

(F)

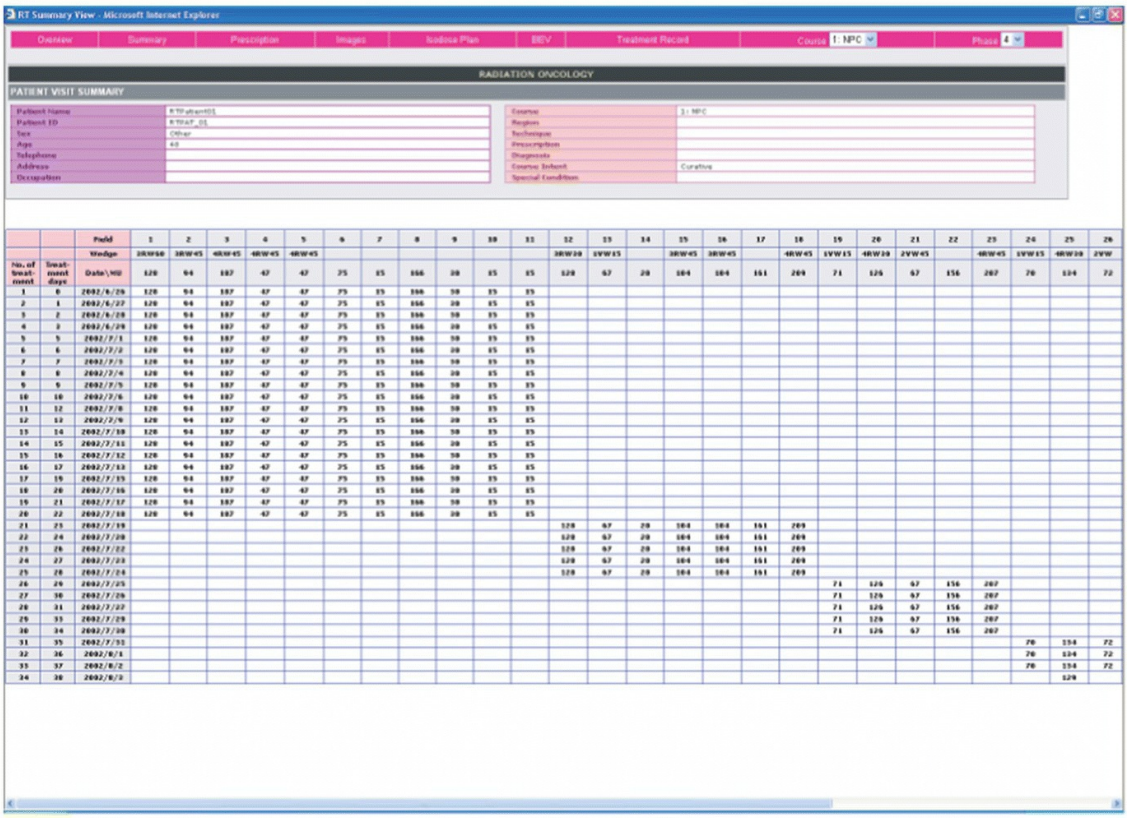
RT Summary View - Microsoft Internet Explorer
Overview
Summary
Prescription
Images
Isodose Plan
BEV
Treatment Record
Course 1: NPC
Phase 4
RADIATION ONCOLOGY
PATIENT VISIT SUMMARY

(G)

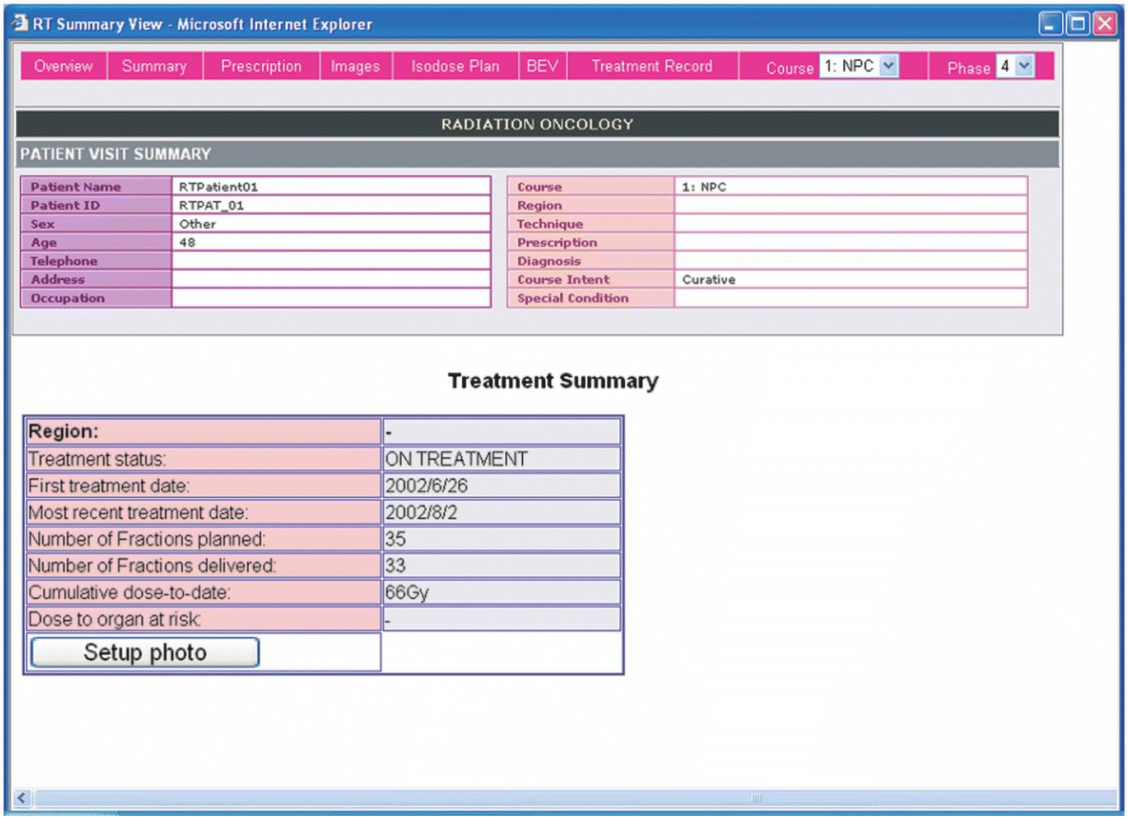
RT Summary View - Microsoft Internet Explorer
Overview
Summary
Prescription
Images
Isodose Plan
BEV
Treatment Record
Course 1: NPC
Phase 4
RADIATION ONCOLOGY
PATIENT VISIT SUMMARY
Patient Name RTPatient01
Patient ID RTPAT_01
Sex Other
Age 48
Telephone
Address
Occupation
Course 1: NPC
Region
Technique
Prescription
Diagnosis
Course Intent Curative
Special Condition
Treatment Summary
Region: -
Treatment status: ON TREATMENT
First treatment date: 2002/6/26
Most recent treatment date: 2002/8/2
Number of Fractions planned: 35
Number of Fractions delivered: 33
Cumulative dose-to-date: 66Gy
Dose to organ at risk: -
Setup photo

Figure 11.15 Sample RT patient record from the multimedia ePR system in which some GUI windows are shown in the RT web client. (A) patient list, stemetil 5 mg tid × 5 (antiemetic medicine, 3 times a day for 5 days); (B) patient visit summary; (C) prescription page; (D) treatment setup page; (E) shielding block position; (F) treatment record; and (G) treatment summary record.

(courtesy of Dr M. Law)

A click on the patient's name, RTPatient01, pops up on the patient's visit summary (Figure 11.15B) with all the procedures done. The radiation therapist or the radiation oncologist can then, at a glance, learn the status of the patient. In this case, in the treatment status row, the latest comment from the radiation oncologist is "Cont. RT," meaning to continue with the treatment. If the visit is to consult the oncologist, the same visit summary can be used for the oncologist to add their comments about the patient. Pointing at the treatment comment is the balloon containing the oncologist's comments.

To prepare the patient for treatment, the radiation therapist needs to refer to the patient's prescription. In the toolbar at the top of the window is a list of functions the users can click on to switch between pages in searching the information about the patient as needed. One of the function buttons is "prescription." A click on the "prescription" reveals the prescription page with all the essential details about the treatment prescription (Figure 11.15C), including the radiation fields to be treated.

Clicking on any of the buttons in the field ID (column 3) leads to the setup details for that radiation field. In this case, field 24 is to be treated, the field ID "24" is clicked and that leads to the setup page where greater detail about the treatment plan is provided (Figure 11.15D). On the treatment setup page, a click on the block position button shows the shielding block, as in Figure 11.15E.

Similarly, a click to the MLC plan button (right-hand side) will call up the MLC shape. From the recommendation of a clinical radiation therapist, a button is added to link to any photo that is taken related to the setup.

When the radiation dose for a field is delivered, a click on the "treated" button will update the field in the treatment record (Figure 11.15 F). When all the fields prescribed for the day are treated, the cumulative dose in the treatment record will be added and the summary record will also be updated (Figure 11.15G).

Some buttons of the toolbar at the top of each page provide a link to the stated information. For example, "summary" leads to the treatment summary record

window (Figure 11.15G), “images” leads to all the images of the patient for the particular course, and “isodose plan” leads to the window showing the distribution of radiation dose around the marked target volume and other nearby anatomical structures on the cross-sectional CT images. Examples of some images, isodose plan, and other types of data displayed on the Web WS from other virtual patients are shown in Figures 11.8 and Figure 11.11.

11.10 Advantages of the Multimedia ePR system in Radiotherapy for Daily Clinical Practice

11.10.1 Communication between Isolated Information Systems and Archival of Information

In a radiotherapy department, there are often different isolated information systems with only small scope and for single-purpose applications. They usually come with the purchase of individual applications, like one system for brachytherapy, and another system for stereotactic radiotherapy/radiosurgery (SRT/SRS). They often stand alone, having little interface with other RT systems. A BrainLab workstation for SRT/SRS has its own storage for the plans performed at its WS. For conventional radiotherapy, the treatment plans are stored in the conventional TPS and the treatment records in another information system. A patient whose treatment involves all three WSs will have treatment information in three different places. Currently, such treatment information is normally “linked” by a paper record or folder of the patient. This has not taken into account the hardcopy films of images that are stored separately in the film library, as is very common in radiotherapy departments. Were the paper record to be lost, the patient treatment information would be “disintegrated.” Using the DICOM and DICOM-RT standards, the multimedia ePR system integrates patient information from different systems and a live summary of the patient’s treatment record can be displayed as required. This can help archive patient information from different systems and save effort and time in searching for records and films, as well as guarding against such loss.

11.10.2 Information Sharing

Most hospital information systems and subsystems have been organization-oriented or system-oriented rather than patient oriented. This means that to query the medical information about a particular patient, we may need to go through several systems. Also patient data collected in these systems are generally not

widely available for immediate integration, due to the differences in formats between WSs and systems. This situation becomes worse if consultation is required across institutions. The lack of an integrated database causes discontinuities in care and often results in redundant questioning or, worse, clinical decisions based on incomplete data. It also limits the ability to conduct clinical and research queries, including the creation of patient cohorts for prospective or retrospective studies. The multimedia ePR system in RT provides a platform for information sharing.

11.10.3 A Model of Comprehensive Electronic Patient Record

With the DICOM standard, PACS, and IHE now having matured, researchers are working toward incorporating medical images such as radiology images, endoscopy images, and microscopy images into the electronic patient records. However, the radiation therapy plans and records have not been taken care of, since a system does not yet exist with a common standard integrating multimedia that includes text, images, and graphics. This is because, other than being image intensive, radiation therapy is highly technical, and its use of radiation also involves radiobiological factors. All of these parameters have to be recorded for future reference in the management of cancer patients treated by radiation therapy. Hence, other than textual information, all related treatment plans and images need to go into the patient's record. The DICOM-RT standards are now set. It is a matter of implementation and refinement before radiotherapy information can be, like other images, linked to the electronic patient record to make it complete. The integrated concept and prototype system described in this chapter is a starting point to this initiative of completing the comprehensive electronic patient record.

11.11 Use of the Multimedia ePR System in RT For Image-Assisted Knowledge Discovery and Decision Making

Currently, in RT, the practical use of imaging informatics tools is limited. DICOM is mostly used for transmitting PACS images to a RT system, and treatment planning systems are limited to dose computations and graphical data displays. Pertinent RT data results do not have a standardized protocol. The concept and prototype of the multimedia ePR system in RT address and can

remedy these shortcomings. In addition, the ePR system in RT can support image-assisted knowledge discovery and decision making. Figure 11.16 shows an overview of the methodology for developing image assisted knowledge discovery and decision support based on the infrastructure of the multimedia ePR system in RT. Steps 1 to 4 in the leftmost column of Figure 11.16 refer to the multimedia ePR system. Assuming that RT data objects are integrated and standardized within the ePR, steps 5 and 6 represent the development of knowledge extracted from the standardized RT objects. The knowledge defined is based on clinical RT workflow scenarios, where the expert user assesses data to make a decision.

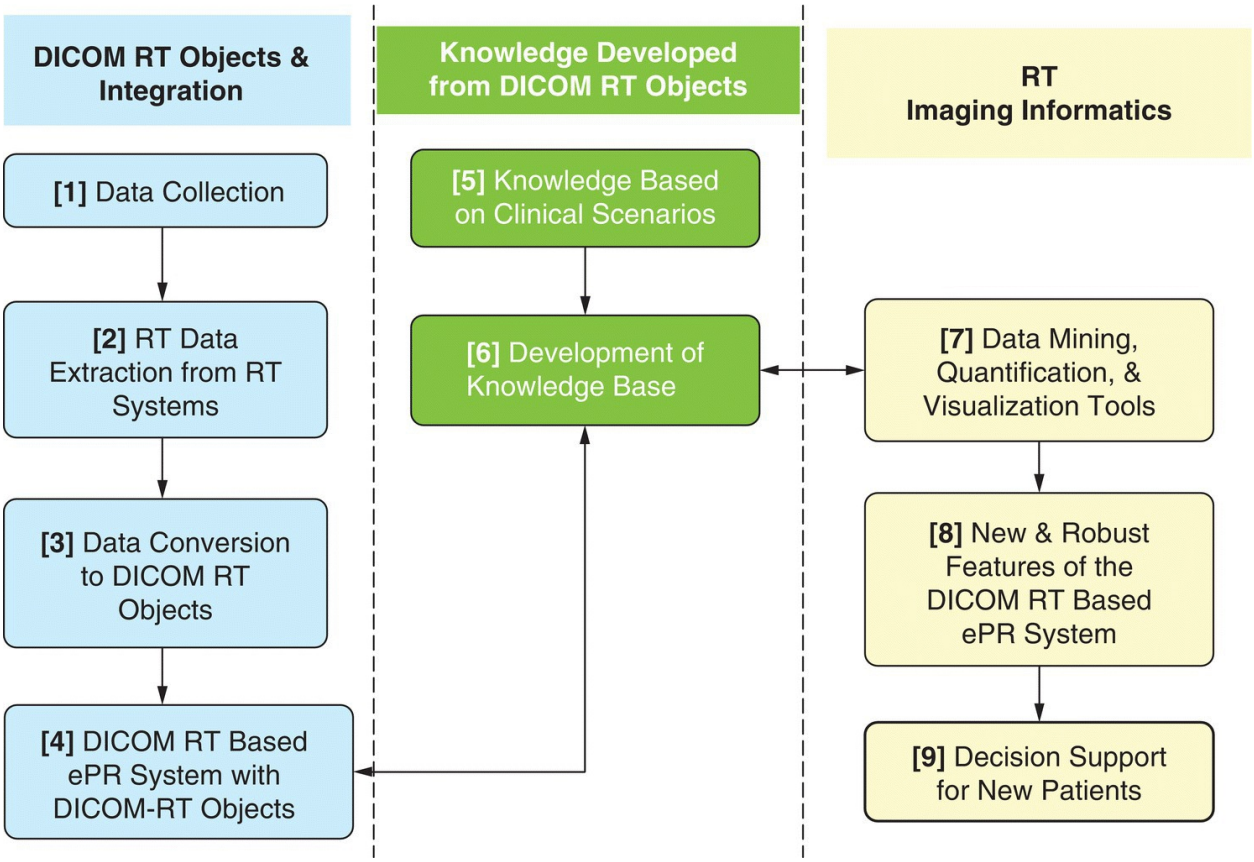

Figure 11.16 Medical Imaging Informatics approach toward development of decision support tools for the DICOM-RT-based ePR system. Steps 1–4 were presented in Figures 23.5B and 23.6; steps 5–9 appearing in this figure are discussed in the text. The long-term results are new and robust features for the ePR system to provide decision support for new patient cases. This methodology can be applied to different cancers, as well as different types of RT treatments, for prompt response from new decision-support tools.

(courtesy of Dr B. Liu)

Step 7 represents the development of decision-support tools based on the knowledge base. These tools can be data mining, quantification, or visualization tools for the knowledge database, and can assist in the decision making of the expert user within the RT workflow. The end result is represented at steps 8 and 9, where the tools naturally become new and robust features of the ePR and assist in the decision support for new cases once the historical data and knowledge are collected. Chapter 19 presents a proton therapy ePR system as an example, to introduce the concept of image knowledge discovery and decision support using the imaging informatics methodology based on the ePR in RT, which is a current trend of research in radiation therapy.

11.12 Summary

All radiation therapy manufacturers are moving toward implementing their information systems from a generated electronic patient record, be it complete or not. Nevertheless, such ePRs are still in vendor-specific formats that may not be easily read by other systems. A major impeding factor is that DICOM-RT records are still not implemented in most cases. This chapter provides the concept and framework for integrating all multimedia RT information using the DICOM and DICOM-RT standards. Discussed are the image-intensive radiation therapy workflow, the DICOM-RT standard, the RT database schema, and the infrastructure and components of the multimedia ePR system in RT. This chapter used the prototype multimedia ePR system in RT, developed at the Hong Kong Polytechnic University, to demonstrate the concept and components in the ePR system. Easy-to-use graphical user interface windows in the Web client WS are emphasized. Utilization of the multimedia ePR system to support image-assisted knowledge discovery and decision making tools is the current trend in radiation therapy image informatics research.

This chapter presents that RT is image and informatics intensive and requires input from multimedia. However, none of the input is required in real time. The time lag of receiving and integrating the data can be from seconds to minutes, hours, or even days; the importance criterion is data integration. Thus, this criterion satisfies the condition of “static multimedia” discussed in this chapter. In Chapters 20 and 21, the concept of multimedia ePR in minimally invasive image-based spinal surgery is described, where the criteria are not only data integration, but also some data acquisition and integration in real time during the surgery. This type of multimedia ePR can be classified as “dynamic multimedia.”

Acknowledgement

Professor Maria Y.Y. Law originated the concept of ePR system in radiation therapy at the Hong Kong Polytechnic University, where she also developed a prototype ePR system for system validation.

References

1 Bidgood, W.D. and Horii, S.C. (1992) Introduction to the ACR-NEMA DICOM Standard. *Radiographics*, 12, 345–355.

2 Connolly, T. and Begg, C. (1998) *Database Systems: A Practical Approach to Design, Implementation, and Management*, 2nd edition. Reading, MA: Addison Wesley.

3 Dennis, A., Wixom, B.H. and Roth, R.M. (2006) *Systems Analysis Design*, 3rd edition. Hoboken, NJL Wiley.

4 DICOM in radiotherapy. http://medical.nema.org/dicom/geninfo/brochure/

5 DICOM Part 3: Information object definitions. http://medical.nema.org/dicom/2007/

6 DICOM Standard 2003. http://medical.nema.org/dicom/2003.html

7 DICOM Supplement 11: Radiotherapy objects, 1997.

8 DICOM Supplement 15: Visible light image for endoscopy, microscopy, and photography.

9 DICOM Supplement 29: Radiotherapy treatment record and media extensions; 1999.

10 DICOM Supplement 30: Waveform interchange.

11 DICOM Supplement 48: Intravascular ultrasound (IVUS).

12 DICOM Supplement 91: Ophthalmic photography SOP classes.

13 DICOM Supplement 102: Radiotherapy extensions for ion therapy.

14 DICOM Supplement 110: Ophthalmic coherence tomography (OCT) storage SOP class.

15 DICOM Supplement 122: Specimen identification and revised pathology.

16 Horii, S.C. (1997) Part Four: A nontechnical introduction to DICOM.*Radiographics*, 17. 1297–1309.

17 Huang. H.K. (2004) *PACS and Imaging Informatics: Basic Principles and Applications*. Hoboken, NJ: Wiley-Liss.

18 IHE-Radiation Oncology Technical Framework, vols 1–2. Draft for trial implementation. *ASTROIntegrating the Healthcare Enterprise*, August 18, 2007.

19 Johns, M.L. (2002) *Information Management for Health Professions*, 2nd edition. Australia: Albany, NY: Delmar.

20 Kushniruk, A. (2002) Evaluation in the design of health information systems: Application of approaches emerging from usability engineering. *Comp Biol Med*, 32, 141–914.

21 Kuzmak, P.M. and Dayhoff, R.E. (2000) The use of digital imaging and communications in medicine (DICOM) in the integration of imaging into the electronic patient record at the Department of Veterans Affairs. *J Digit Imag*, 13(2 suppl 1), 133–137.

22 Law, M.Y.Y., Huang, H.K., Zhang, X. and Zhang, J. (2002) DICOM and imaging informatics-based radiation therapy server. *Proc SPIE CD-ROM, Med Imag*, 4685, 160–167.

23 Law, M.Y.Y. and Huang, H.K. (2003) Concept of a PACS and imaging informatics-based server for radiation therapy.*Comput Med Imag Graph*, 27(1), 1–9.

24 Law, M.Y.Y. and Zhou, Z. (2003) New direction in PACS training. *Comput Med Imag Graph*, 27, (2–3), 147–156.

25 Law, M.Y.Y., Huang, H.K., Zhang, X. and Zhang, J. (2003) The data model of a PACS-based DICOM radiation therapy server. *Proc SPIE on CD-ROM, Med Imag*, 5033, 118–129.

26 Law, M.Y.Y. (2004) The design and implementation of a DICOM-based integrated radiotherapy information system. PhD thesis. Chinese Academy of Sciences.

27 Law, M.Y.Y., Huang, H.K., Chan, C.W., Zhang, X. and Zhang, J. (2004) A

DICOM-based radiotherapy information system. *Proc SPIE on CD-ROM, Med Imag*, 5371, 118–129.

28 Law, M.Y.Y. (2005) A model of DICOM-based electronic patient record in radiation therapy. *J Comput Med Imag Graph*, 29, 125–136.

29 Law, M.Y.Y. and Liu, B.J. (2009) DICOM-RT and its utilization in radiation therapy. *Radiographics*, 29, 655–667.

30 Law, M.Y.Y., Liu, B.J. and Chan, L. (2009) A DICOM-RT-based ePR (Electronic Patient Record) information system for radiation ePR in Radiation Therapy. *Radiographics*, 29, 961–972.

31 Nagata, Y., Okajima, K., Murata, R., *et al*. (1996) Development of an integrated radiotherapy network system. *Int J Radiat Oncol Biol Phy*, 34, 1105–1111.

32 Palta, J.R., Frouhar, V.A. and Dempsey, J.F. (2003) Web-based submission, archive, and review of radiotherapy data for clinical quality assurance: a new paradigm. *Int J Radiat Oncol Biol Phys*, 57(5), 1427–1436.

33 Ratib, O., Swiernik, M. and McCoy, J.M. (2003) From PACS to integrated EMR. *Comput Med Imag Graph*, 27(2–3), 207–215.

34 Schultheiss, E.T., Coia, L.R., Martin, E.E., Lau, H.Y. and Hanks, G.E. (1997) Clinical applications of picture archival and communications systems in radiation oncology. *Sem Radia Oncol*, 7, 39–48.

35 Wasson, C.S. (2006) *System Analysis, Design, and Development: Concepts, Principles, and Practices*. Hoboken, NJ: Wiley.

PERPUSTAKAAN PRIBADI AN-NUR SUNARYA

12
PACS-Based Imaging Informatics Simulators

CHAPTER MENU

12.1 Why Imaging Informatics Simulators?

12.1.1 Background

12.2 PACS–ePR Simulator

12.2.1 What is a PACS–ePR Simulator?

12.2.2 What does a PACS–ePR Simulator do?

12.2.3 PACS–ePR Simulator Components and Data Flow

12.2.4 Using the PACS–ePR Simulator as the Basis for Developing other Imaging Informatics Simulators

12.3 Data Grid Simulator

12.3.1 What is a Data Grid Simulator?

12.3.2 Data Grid Simulator (DGS) Components and their Connectivity

12.3.3 Molecular Imaging Data Grid (MIDG) Simulator

12.3.4 Current Trends in Imaging Informatics Data Grid with Cloud Computing Design

12.3.5 The Use of Cloud Computing Services in the Archive Architecture

12.4 CAD–PACS Simulator

12.4.1 The Concept of CAD–PACS Integration

12.4.2 The CAD–PACS Simulator

12.4.3 Components and Functions

12.4.4 Using a CAD–PACS Simulator to Facilitate the Evaluation of CAD Algorithms

12.4.5 Simulator: From the Laboratory Environment to Clinical Evaluation

12.5 Radiotherapy (RT) ePR Simulator
12.5.1 Concept of the RT ePR Simulator
12.5.2 Components and Features
12.5.3 RT ePR Simulator Architecture
12.5.4 Simulation of Knowledge Discovery
12.5.5 Role of the RT ePR Simulator
12.6 Image-Assisted Surgery (IAS) ePR Simulator
12.6.1 Role of the ePR Simulator in Image-assisted Surgery
12.6.2 IAS ePR Simulator Data Flow
12.6.3 Workflow of the Simulator
12.6.4 The IAS ePR Simulator in a Laboratory Environment
12.6.5 From IAS ePR Simulator to the Clinical MISS ePR System
12.6.6 Other Potential IAS ePR Simulators
12.7 Summary
Acknowledgments
References

12.1 Why Imaging Informatics Simulators?

A medical imaging informatics infrastructure (MIII) platform is an organized method of selecting tools and synthesizing data from hospital systems, with the aim of developing an imaging-based diagnosis or treatment system. Evaluation and analysis of these systems can be made more efficient by designing and implementing imaging informatics simulators. This chapter introduces the MIII platform and provides the definition of treatment/diagnosis systems, while primarily focusing on the development of the related simulators.

A medical imaging informatics (MII) simulator in this context is defined as a system integration of many selected imaging and data components from the MIII platform and clinical treatment protocols, which can be used to simulate patient work and data flows, starting from diagnostic procedures to the completion of treatment. In these processes, DICOM and HL7 standards, IHE workflow profiles, and Web-based tools are emphasized. From the information collected in the database of a specific simulator, evidence-based medicine can be

hypothesized to choose and integrate optimal clinical decision support components.

Other relevant, selected clinical resources, in addition to data and tools from the HIS/RIS/PACS and ePRs platform, may also be tailored to develop the simulator. These resources can include image content indexing, 3-D rendering with visualization, data grid and cloud computing, computer-aided diagnosis (CAD) methods, specialized image-assisted surgical and radiotherapy technologies.

This chapter presents five simulators. The PACS–ePR simulator with image distribution is the cradle of the other four simulators. It supplies the necessary PACS-based ingredients and data security for the development of the four other simulators: the Data Grid simulator for molecular imaging, CAD–PACS, radiotherapy simulator, and image-assisted surgery (IAS) simulator. The purpose and benefits of each simulator with respect to its clinical relevance are presented.

The concept, design, and development of these five simulators have been implemented in laboratory settings for education and training. Some of them have been extended to clinical applications in hospital environments.

12.1.1 Background

MII emphasizes the study of medical images and data. The prevalent medical imaging and data-related systems are PACS, HIS, RIS, electronic patient records (ePR) with image and data distribution, Data Grid (DG), and cloud computing technologies for archive. Some MII methods for imaging-based diagnosis and treatment include CAD, IAS, and image-assisted therapy (IAT).

The MIII platform is an organized method of collecting these data and technologies to develop a certain clinical diagnosis or treatment application. In the process of integrating the images/data, tools and technologies, the DICOM and HL7 standards, IHE workflow profiles, and Web-based tools are normally used. Figure 12.1 shows the organization of this integration [1].

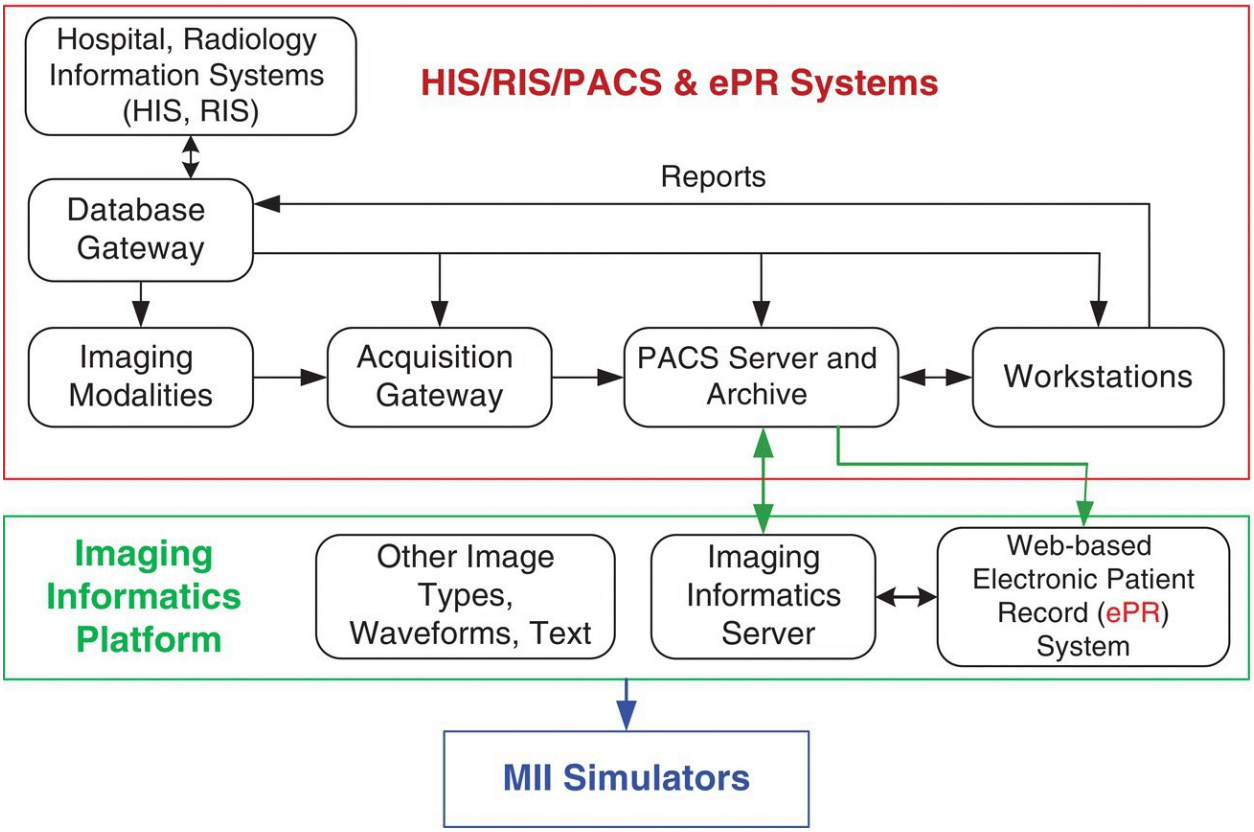

Figure 12.1 Organization of a MII simulator in the clinical research environment, showing the relationship between HIS/RIS/PACS data flow (upper, red) and the imaging informatics platform (middle, green), and MII simulators (blue). DICOM images and data are transmitted from the PACS server to the imaging informatics server, as well as the Web-based perk system. Processed data from the MII platform are transmitted to the MII simulator for the proper application.

An MII simulator in this context is defined as a system integration of many appropriable selected image and data components from the MIII platform, along with certain clinical protocols that can be assembled together to simulate the patient work and data flows, starting from diagnostic procedures to the completion of a treatment. For example, a PACS simulator can be used to predict how the PACS would function under a given clinical environment, and a CAD–PACS simulator can be used to predict how a CAD method would function in a given PACS environment. Similarly, other imaging informatics simulators can be used to predict certain outcomes before a clinical system is developed. The advantage of using the MIII platform is that once the platform is established, it can be expanded to develop other similar types of simulators.

In order to develop MII simulators, we must study the operations of MII system components in the real clinical environment and mimic their functions in a laboratory environment. Most of the imaging informatics systems described in this chapter are novel research systems that are constantly evolving. Apart from the PACS simulator, every other simulator is built with the intention of trying to simulate new and innovative research-engendered informatics systems to examine their interactions and integration with existing informatics systems such as HIS, RIS, and PACS, as well as to analyze their performance to evaluate their effectiveness without disrupting actual clinical operations.

The MII simulators mentioned in this chapter do not attempt to carry out system evaluation, but rather enable and facilitate researchers and clinicians to evaluate MII systems more efficiently by providing tools to enhance research workflow.

Readers are encouraged to peruse the publications referenced throughout this chapter for a detailed evaluation of the associated systems being simulated. The aim of this chapter is to point out the rationale behind developing imaging informatics simulators, to describe how such simulators can be developed, and to explain their benefits and applications. A thorough description of the methods involved in implementing MII simulators will empower readers to use such simulators for testing their specific applications.

12.2 PACS–ePR Simulator

12.2.1 What is a PACS–ePR Simulator?

The PACS–ePR simulator is a comprehensive training tool designed to emulate a 24/7 clinical PACS system in a laboratory environment. It allows the user to learn basic PACS–perk concepts and provides the opportunity for hands-on experience without compromising the stability and security of the clinical PACS–ePR system.

12.2.2 What does a PACS–ePR Simulator do?

The function and data flow of the PACS–ePR simulator begins with the acquisition modality simulator (AMS). This simulates the acquisition of various medical images types, such as computed tomography (CT), magnetic resonance imaging (MRI), computed radiography (CR), and ultrasound or US) and stores DICOM examinations in the DICOM gateway, and then the PACS server. In addition to storing and archiving the images, the PACS server also distributes the

examinations to the viewing workstation (WS) via a query/retrieve function. The WS archives the examinations into a local database and can also distribute them to a Web-based ePR server.

12.2.3 PACS–ePR Simulator Components and Data Flow

The simulator consists of four main components that represent the essential functions of a typical clinical PACS–ePR:

1. RIS and acquisition modality simulator (AMS);
2. DICOM gateway;
3. PACS server and ePR server;
4. Workstations.

Through these components, trainees can observe clinical PACS–ePR operations, trace the data flow step by step, and identify possible image data flow bottlenecks. Because the PACS–ePR simulator is independent, users can also manually induce failures to any component and observe the impact on the PACS–ePR operation. This provides trainees with a better understanding of the system workflow in a safe, simulated learning environment, without impacting the clinical workflow of the actual systems. Figure 12.2 depicts the PACS–ePR simulator shown during several Radiological Society of North America (RSNA) annual scientific exhibits.

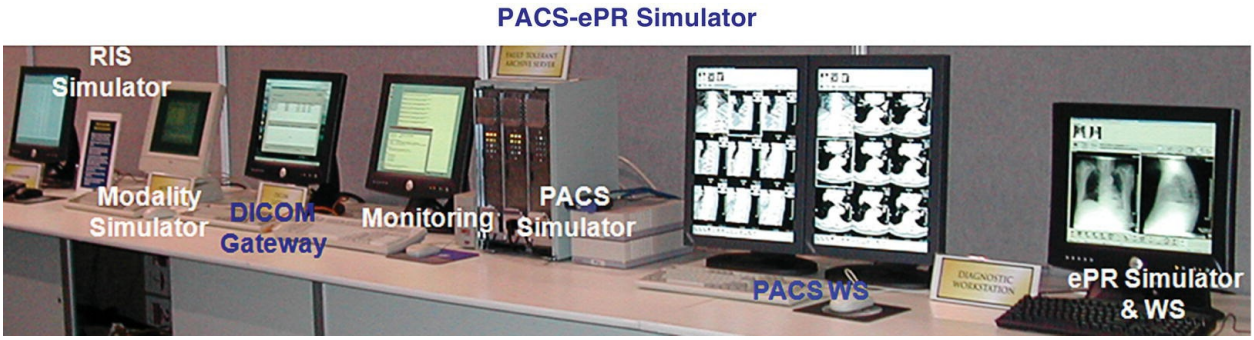

Figure 12.2 The PACS–ePR simulator shown at a RSNA exhibition. Left to right: RIS simulator, modality simulator, DICOM gateway, monitoring system of the data flow of the PACS–ePR simulator operation, PACS simulator, PACS WS, and Web-based ePR simulator and WS [2,3].

12.2.4 Using the PACS–ePR Simulator as the Basis for Developing other Imaging Informatics Simulators

The PACS–ePR simulator encompasses a large segment of the image/data and tools used for imaging informatics applications. It forms the basis for the other four simulators discussed in this chapter. The DG simulator replaces the PACS archive server using DG technology to achieve storage fault tolerance and to reduce its cost. The CAD–PACS simulator integrates CAD results to act as a secondary reader in the PACS data flow to assist the radiologist during the diagnostic process. IAS and IAT simulators extract subsets of PACS patients who require surgery or radiotherapy, respectively, forming the image data sources of the two clinical Web-based ePR systems. These four simulators use the PACS–ePR image/data, DG, CAD methods, and surgical and radiotherapy treatment protocols to form the basis for specific imaging informatics applications.

12.3 Data Grid Simulator

12.3.1 What is a Data Grid Simulator?

The Data Grid (DG) is used for large-scale enterprise PACS–perk and imaging informatics system operations. It employs storage from multiple sites in the enterprise to share the primary and backup image/data archives of the entire system. In order to achieve storage fault tolerance, three copies of every image are normally used. Combining the DG with cloud computing technology, the storage locations can be remotely hosted by professional enterprise archiving centers. In this case, availability of reliable high-speed networking is essential.

12.3.2 Data Grid Simulator (DGS) Components and their Connectivity

Depending upon the application of the Data Grid simulator (DGS), its components and their connections can vary. The DGS is designed to emulate a specific PACS–ePR or an imaging informatics data archive application. The DICOM standard is used as the data structure and format. Three major functions of the DGS are archive and backup, query/retrieve, and disaster recovery. Some applications of DGS are a DG for a fault-tolerant image archive, image-based multiple site clinical trials, data migration from the backup to the primary archive, dedicated breast MRI enterprise DG, and molecular imaging DG [4–7]. For example, a PACS–perk DGS with multiple simulated sites can have the following functions: to support the archive, backup, and disaster recovery for all sites, and to allow a workstation (WS) from a site to retrieve and review

image/data from any other sites.

12.3.3 Molecular Imaging Data Grid (MIDG) Simulator

The Molecular Imaging Data Grid **(**MIDG) provides data archiving, management, and distribution for small animal (preclinical) imaging facilities [8]. The system employs grid technologies and a custom graphical user interface (GUI) to promote experimental data sharing and to expedite data management workflows by imaging informatics technologies. The simulator consists of the three major components shown in Figure 12.3. A general small animal facility with many researchers performing experiments at multiple sites (upper right) sharing the imaging equipment (see Figure 12.4, lower left) and imaging informatics resource including archiving, retrieval, and processing (lower right). In order to facilitate data sharing between research sites and the multimodality small animal imaging facility, images are first converted to the DICOM format. The standardization allows data to be distributed through the grid infrastructure via the grid node server at each participating site connected to the DG [9].

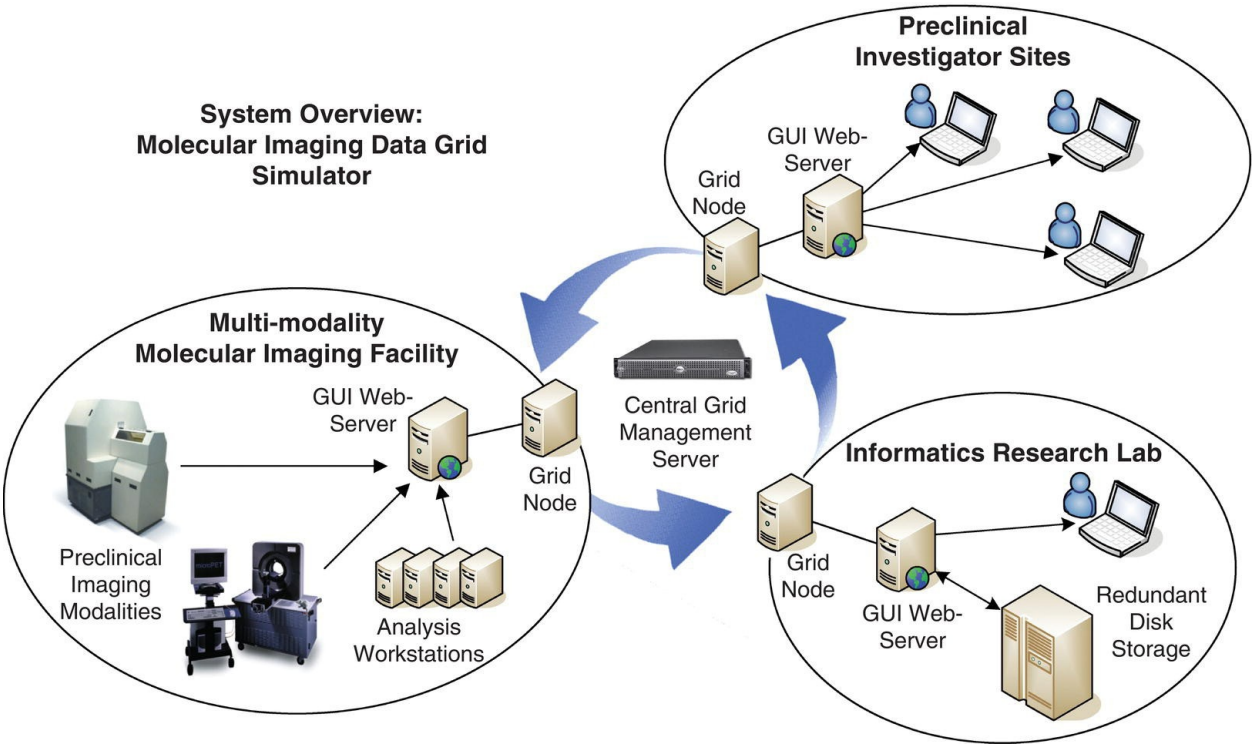

Figure 12.3 MIDG simulator workflow and system overview. A molecular imaging facility typically has three major components: preclinical researchers at various remote sites (upper right), molecular animal imaging modalities (lower left), and the imaging informatics facility (lower right).

Figure 12.4 Typical imaging modalities in a small animal imaging research facility.

12.3.4 Current Trends in Imaging Informatics Data Grid with Cloud Computing Design

12.3.4.1 OGSA and IHE XDS-I

The existing medical Data Grid (DG) takes advantage of the open source Globus toolkits [6]; however, it has two major drawbacks—the lack of easy to use documentation and heavy overhead of the software. For medical imaging applications, the trends are to continue taking advantage of the open grid services architecture (OGSA) principles [7–9], but to abandon the Globus toolkit that has been commonly used in most current data grid designs. The MIDG simulator was originally designed using the Globus toolkit, but has been implemented based on the OGSA and IHE workflow profiles, in particular the cross-enterprise document sharing for imaging (XDS-I) profile. The result was a replacement of the Globus toolkit with a DICOM-handling infrastructure based on Web services. Performing a study registration, replication or retrieval no longer requires DICOM middleware to make a call first to the Globus toolkit for

file delivery responsibilities. Furthermore, the DICOM metadata database and file localization databases are now a single database, thus leading to fewer and less complex database queries. Finding all metadata relevant to a study, including its physical storage location within the MIDG, is now done in a single filtered query. This centralized architecture culminates in a more extensible design, which can support system-wide process monitoring and rules-based data backup policies.

12.3.5 The Use of Cloud Computing Services in the Archive Architecture

The OGSA principles require enterprise partners contributing storage to the DG. With the readily available archive infrastructure in cloud computing services, storage contribution by DG partners in the enterprise PACS–ePR becomes less important. Examples of available Internet-based scalable and fault-tolerant Blobstore data management are the Google App Engine [10], Microsoft Windows Azure [11], Amazon Web Services [12], and Eucalyptus [13]. The "blob" is unstructured data (value) stored in a container, and the lookup is performed through a text key. For multimedia PACS–perk data, Blobstore is very attractive for its storage application. Once the storage is secured using the Blobstore through a service provider, a PACS–ePR system will no longer need a local archive component. Conceptually, the use of cloud computing for PACS–ePR is simple; the cloud computing services replace the DG. However, in order to do so at this point of time, the concept of the OGSA principles still needs to be augmented in the cloud services for DICOM-based PACS–ePR applications [14].

12.4 CAD–PACS Simulator

12.4.1 The Concept of CAD–PACS Integration

CAD systems and PACS are separate stand-alone systems, requiring proprietary software to view CAD results or to separate CAD-specific WSs. Integrating CAD with PACS means integrating the CAD results with the PACS workflow, thereby enabling the clinician to view CAD results on a PACS WS [15]. The workflow consists of the following steps:

1. Integrating the CAD system within the PACS workflow.
2. The CAD result is treated as a new imaging modality in the DICOM data

model and is then integrated into the PACS workflow.

3. The clinician uses DICOM structured reporting(SR) to retrieve and view CAD results at the PACS WS, where the CAD results will overlay the relevant diagnostic images.
4. The CAD–PACS integration toolkit is available in the literature [16]. To use it requires the modification of the existing pre-processing manager (PPM) software of the PACS server and the use of the DICOM SR.

12.4.2 The CAD–PACS Simulator

The CAD–PACS simulator can be used to learn how to integrate a CAD system with a PACS that complies with DICOM and SR standards. The simulator possesses the following characteristics:

1. The integration process uses standardized imaging informatics methodology.
2. The PACS DICOM data model and workflow treat the CAD output as an individual surrogate imaging modality.
3. The utilization of DICOM-SR and IHE integration profiles are used to display CAD output in the PACS WS environment.

The CAD–PACS simulator can simulate and validate an automated workflow of integrating CAD systems in clinical PACS environments using standardized imaging informatics methodology. The simulator utilizes DICOM- SR and IHE integration profiles to display CAD output in the PACS environment.

12.4.3 Components and Functions

1. PACS simulator:
   a. Modality simulator
   b. PACS–ePR archive simulator
   c. Display WS
2. CAD server (on virtual machine);
3. SR server (on virtual machine).

The CAD–PACS simulator consists of three system components: PACS–ePR simulator, CAD server and WS, and SR server and PACS display WS. The top of Figure 12.5 shows the CAD–PACS simulator. It is equipped with the CAD–

PACS toolkit [16] to handle the integration between the CAD components and PACS, including the creation of DICOM-SR objects based on a customized template for each CAD application, as well as data exchange (send/query/retrieve) and Web-based display of DICOM SR objects.

12.4.4 Using a CAD–PACS Simulator to Facilitate the Evaluation of CAD Algorithms

The workflow for evaluating a CAD algorithm can be enhanced by integrating it with the PACS–ePR simulator using three available proprietary software modules: i-CAD, Receive-SR, and Display-SR [16]. This integration workflow is shown at the bottom of Figure 12.5. The simulator furnishes researchers and clinicians with valuable tools to assist in evaluating the CAD algorithm more efficiently. For instance, data collection efficiency is much improved by enabling a communications interface between the CAD server and both the input sources —the modality simulator and the PACS server. In addition, the SR server enables the storage of CAD results as DICOM-SR, a standardized format. This allows the CAD results to be displayed on DICOM compliant WSs for review by clinicians. Figure 12.6 shows CAD results displayed on the PACS WS (right) and DICOM-SR (left). The example presents an automatic detection and quantification method of multiple sclerosis (MS) on MRI.

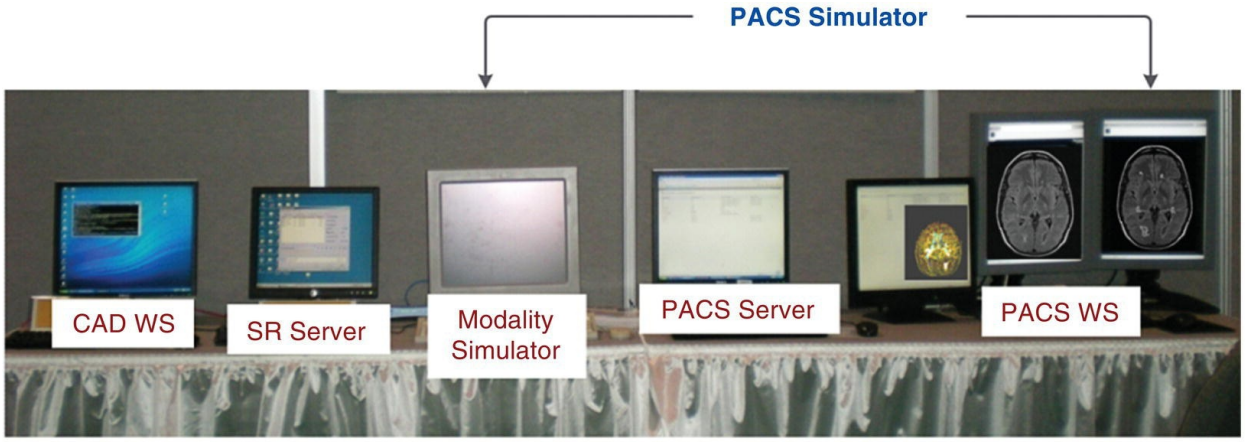

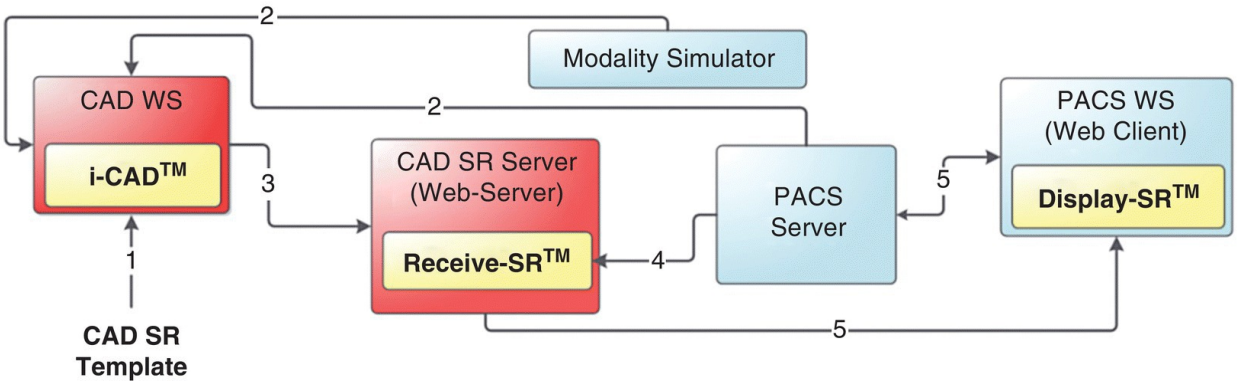

Figure 12.5 Evaluation of an automatic detection and quantification method of multiple sclerosis (MS) on MRI—configuration of the CAD–PACS simulator and its data flow. Top: The CAD–PACS simulator displayed at the 2007 RSNA annual scientific exhibition in 2007 [16]. The PACS WSs (right) also show the MRI images and 3-D CAD result (color). Bottom: The CAD–PACS integration and workflow steps (numerals). Blue: PACS simulator components. Red: CAD components. Yellow: CAD–PACS toolkit modules.

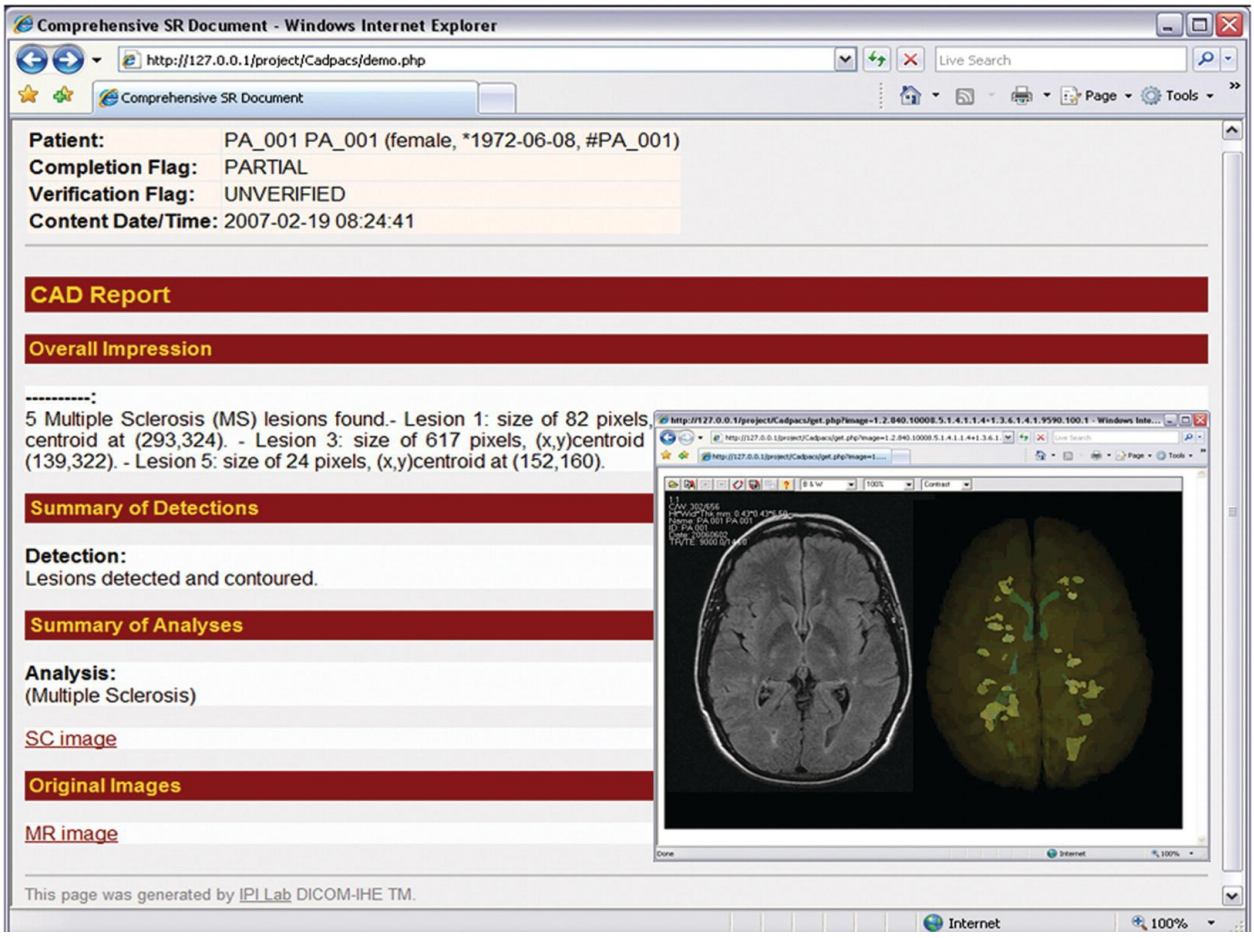

Figure 12.6 CAD results shown on the PACS WS. Left: DICOM-SR describing the multiple sclerosis. Bottom middle: An MRI image of a patient with multiple sclerosis, and bottom right: The 3-D CAD results of multiple sclerosis in the brain. See also Figure 12.5—the CAD–PACS integration components for the MRI images and CAD result shown on the right.

12.4.5 Simulator: From the Laboratory Environment to Clinical Evaluation

Using a simulator, a CAD algorithm can first be tested in the laboratory setting and then continue to be evaluated in the clinical environment. The bone age assessment of children [17–20] is used as an example to present the CAD–PACS simulator system workflow. A routine health examination of children's growth needs certain normal growth and development standards for comparison. A left hand and wrist radiograph provides a dependable indicator of developmental status through bone growth observations of a child. Bone age assessment (BAA) is a clinical procedure in pediatric radiology to evaluate the stage of skeletal maturity based on a left hand and wrist radiograph. Figure 12.7 depicts the bone age assessment of a hand radiograph in the laboratory seating. Figure 12.8 shows that the simulator has been integrated with the PACS clinical workflow, where the CAD bone age result has been incorporated in the clinical assessment with the population health statistics.

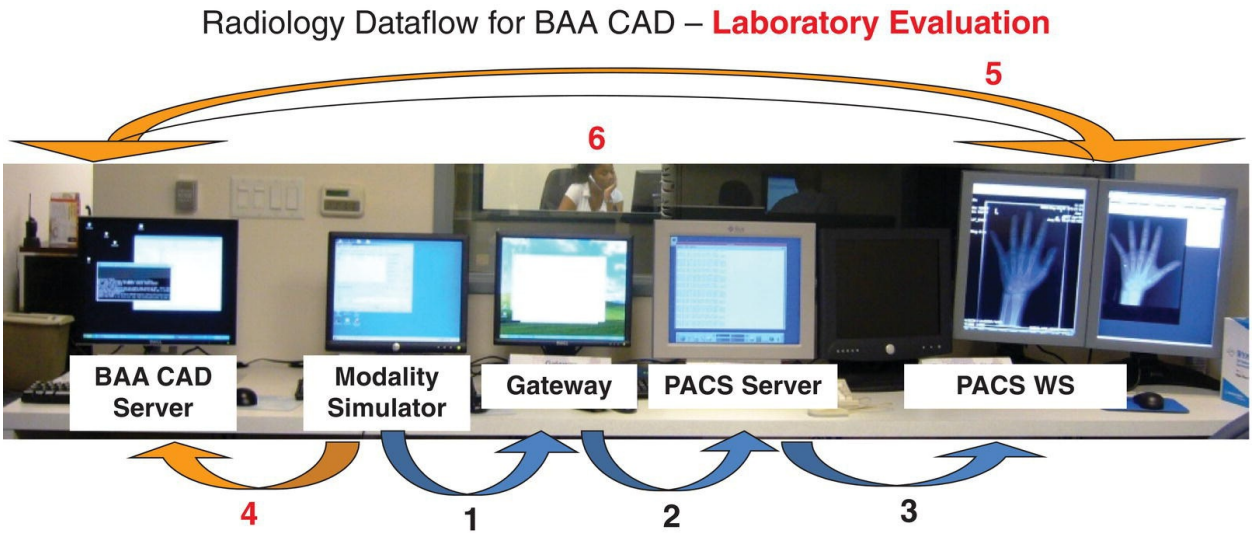

Figure 12.7 CAD–PACS simulator in a laboratory environment (see also Figure 12.5). Black text: normal clinical workflow.Red text: bone age assessment (BAA) using the CAD–PACS simulator.

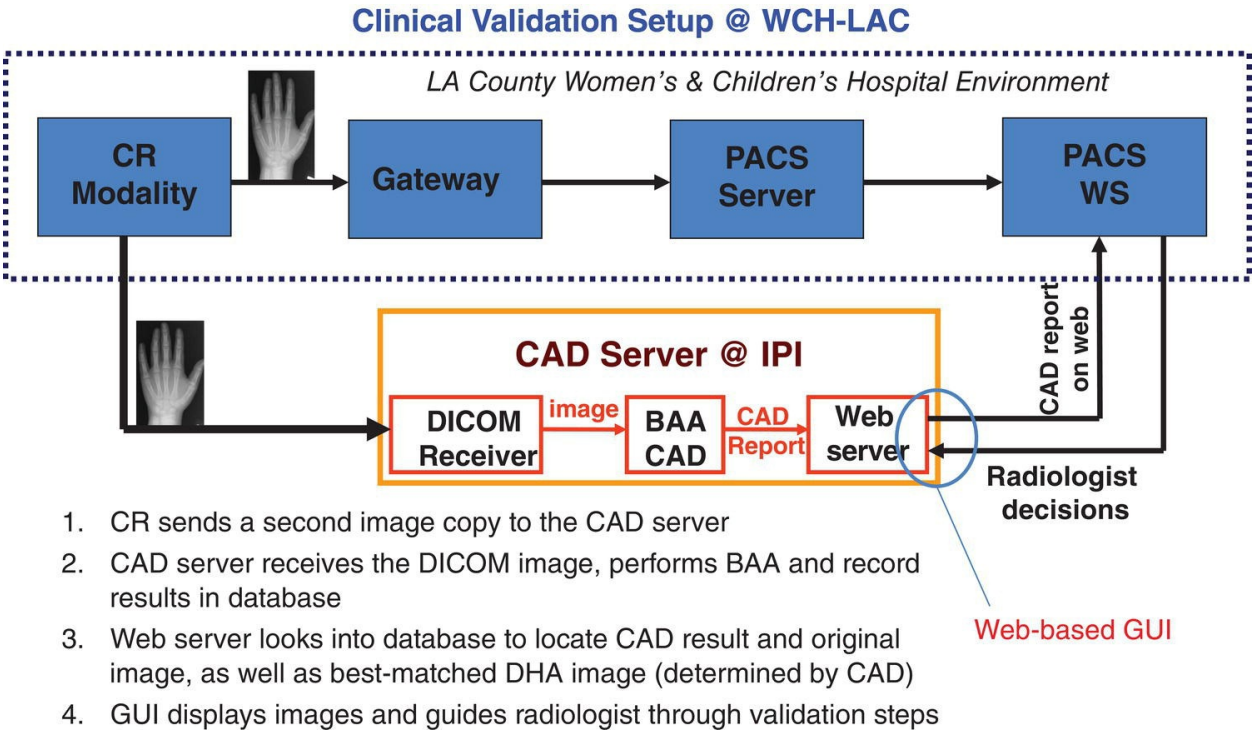

Figure 12.8 CAD–PACS simulator in the clinical environment. Population statistics database has been embedded in the clinical workflow. The bone age assessment (BAA) of the child is compared directly with the database for evaluating the health of the child, elevating the role of the simulator Digital Hand Atlas (DHA).

12.5 Radiotherapy (RT) ePR Simulator

12.5.1 Concept of the RT ePR Simulator

The radiotherapy (ePR) simulator emulates a clinical scenario where a system could improve the efficiency of data integration and data mining in the research related to outcomes analysis and new treatment protocols in radiotherapy. It centralizes all relevant clinical and treatment plan data from all four main steps in radiotherapy: consultation, treatment planning, treatment delivery, and follow-up [21]. Currently, the RT ePR simulator utilizes data from prostate cancer patients treated with hypofractionation dose protocol proton beam therapy. Each dataset includes an initial data form, DICOM files (CT images, RT, and radiotherapy ion DICOM objects), and patient follow-up data forms.

12.5.2 Components and Features

Figure 12.9 shows the system components of the RT ePR, which consists of three subsystems: i) the treatment planning system (TPS) simulator; ii) the ePR system; and iii) the client WS. The TPS simulator, which is the Odyssey treatment planning software non-clinical version 4.2, simulates the data flow of DICOM objects to the ePR system [21]. The ePR system is the main component of the RT ePR simulator and responsible for data input, storage, quantification, display, and distribution. The client WS allows users to perform online clinical data input and to access patient data through the Web interface and test the functionalities of the simulator [22,23].

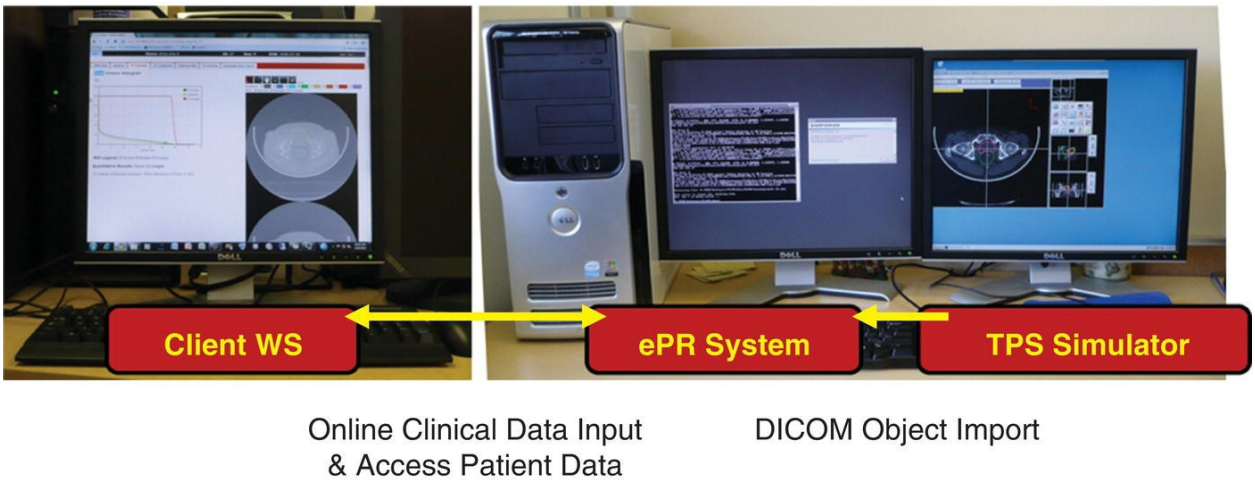

Figure 12.9 System components of laboratory environment. From the right to left: TPS simulator, ePR system, and client WS; the yellow arrows represent the data flow and the direction of the data flow.

12.5.3 RT ePR Simulator Architecture

The RT ePR is a Web-based system that can also be used to complement the current TPS in a radiotherapy department. The RT ePR simulator consists of four main components: the data gateway, the ePR server, decision support tools, and visualization and display tools, as shown in Figure 12.10.

There are three steps of data flow in the RT ePR system (numerals in Figure 12.10):

1. The data are first obtained from each treatment step and then imported to the data gateway.
2. After the data are received, they will be transferred to the ePR server for archive and further quantification.
3. The quantified data from DICOM RT objects and clinical data are then used by decision support tools to perform data mining and knowledge discovery functions. At each step of the data flow, the user can interact with the system using the GUIs provided by the visualization and display component.

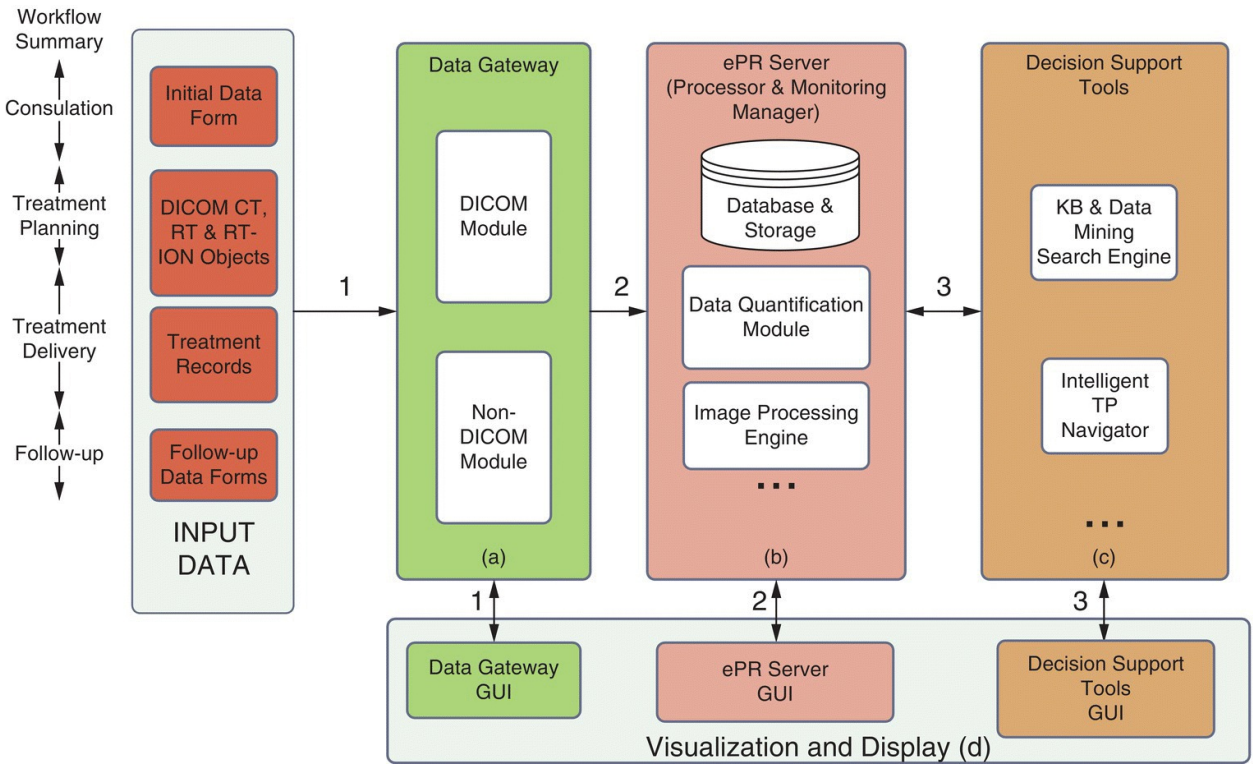

Figure 12.10 Architecture and data flow of the RT ePR system. (a) The data gateway is used to receive data. (b) The ePR server has the storage and database to archive and quantify stored data. (c) The decision support tools give users the ability to analyze and interact with treatment plans and patient data to improve treatment for future patients. (d) The visualization module contains all GUIs for user interaction in data acquisition, data storage, data display, and for decision support tools. The numerals represent the data flow steps. KB: knowledge base; GUI: graphical user interface.

12.5.4 Simulation of Knowledge Discovery

The RT ePR simulator can study several clinical outcomes. This example discusses how the simulator retrieves knowledge from previous patients' data through data mining. Figure 12.11 describes the step-by-step simulation of knowledge discovery utilizing the RT ePR system to improve the treatment plan of a new patient based on previous patients' treatment plans.

An example is the use of the simulator to improve a patient's treatment plan based on knowledge discovery. Figure 12.12 shows a screenshot of results obtained from the RT ePR simulator. Based on the knowledge discovery, the beam margin has been modified from 10 mm to 7 mm, resulting in reduced doses to two critical organs and yet maintaining the dose delivered to the target

volume.

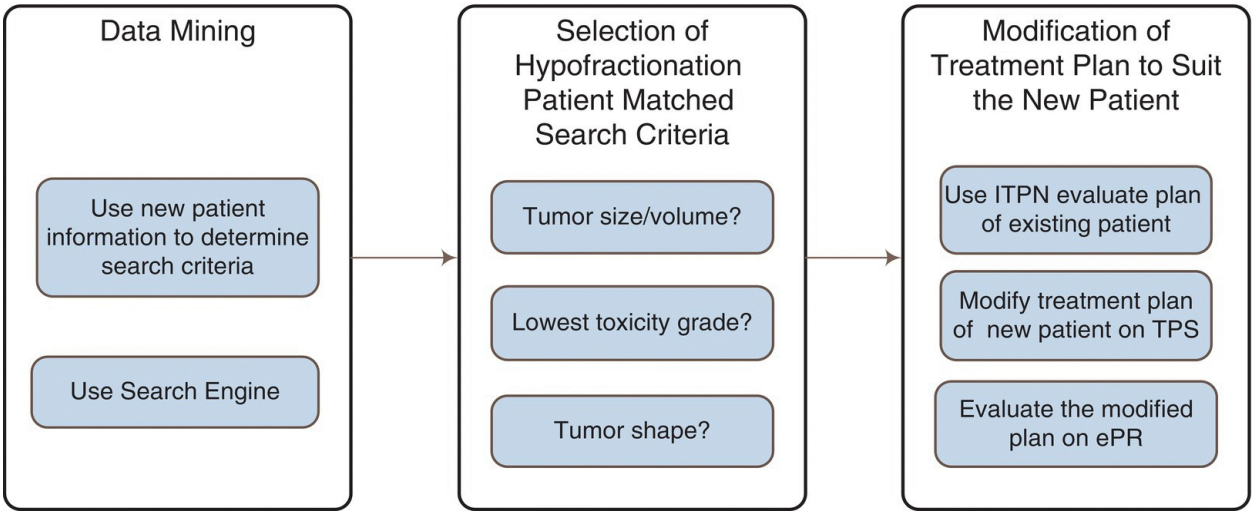

Figure 12.11 Improving treatment for a new patient based on treatment plans of previous patients, showing step-by-step simulation of knowledge discovery based on the treatment plans of previous patients.

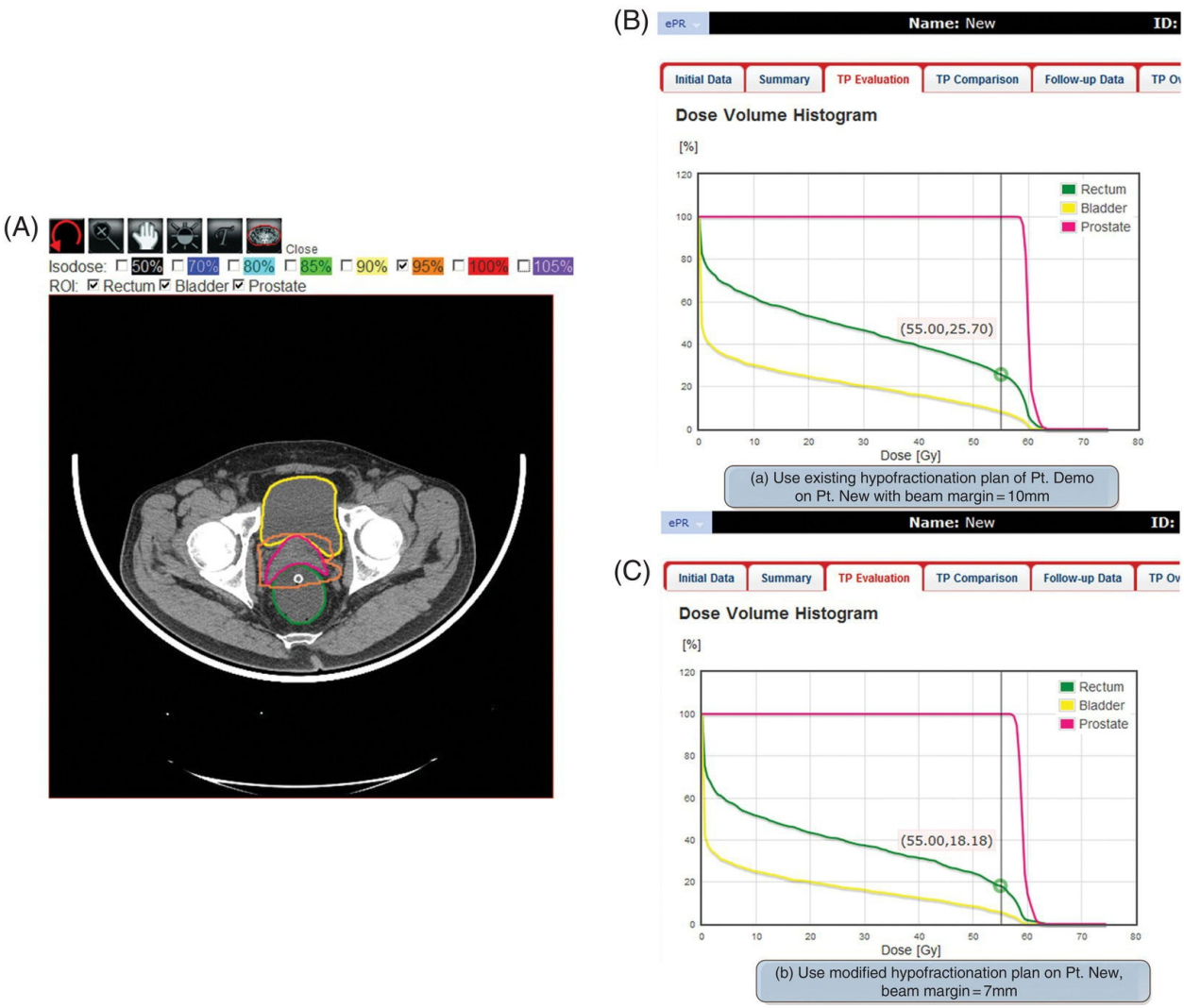

Figure 12.12 (A) A screenshot of the intelligent treatment plan navigator (ITPN) shows the overlapping region of the 95% isodose curve (orange), the target prostate (pink), and two critical organs: the bladder (yellow) and the rectum (green). Utilization of knowledge discovery results for this patient led to a modification of the original 10-mm beam margin to a smaller 7-mm margin. (B) The dose–volume histogram (DVH) for the original treatment plan with a beam margin of 10 mm shows that 25.70% of the rectum receives a 55 Gy dose. (C) The DVH of the modified treatment plan incorporating a reduced beam margin of 7 mm shows that the volume of the rectum receiving a 55 Gy dose has reduced from the original 25.70% to 18.18%, while maintaining the original dose of 55 Gy to 100% of the prostate.

12.5.5 Role of the RT ePR Simulator

The RT ePR simulator discussed here plays the role of a radiation treatment

planning decision support method based on knowledge accumulated from previous patients' treatments in the database. This add-on knowledge can help the oncologist to prescribe a better treatment plan for a new patient under the similar treatment by maximizing the target volume dose and at the same time minimizing the dose to critical organs. In addition, the method may also reduce the normal time required to finalize the treatment plan. Although the data shown in this example consisted of proton beam therapy data, the simulator can also be used for other types of radiotherapy beams.

12.6 Image-Assisted Surgery (IAS) ePR Simulator

12.6.1 Role of the ePR Simulator in Image-Assisted Surgery

Currently, the following weaknesses exist in IAS:

1. Patient clinical forms and data from surgical devices in the operation room, including various pre- and postsurgical textual data, waveforms, and multiple sources of images and video are scattered.
2. The pre-op, intra-op, and post-op workflows do not have a single system guided by a master time clock during data acquisition, management, and distribution.
3. There is no systematic method to analyze patient outcomes based on surgical workflow.
4. There are no data organization and image display system to record the live real-time intraoperation data.

The IAS ePR simulator can be used to minimize these shortcomings. [24]

12.6.2 IAS ePR Simulator Data Flow

The surgical data workflow of the IAS ePR simulator is shown in Figure 12.13. It has three time phases (first column: pre-op, intra-op, and post-op), each with four data flow steps: data collection, data standardization and preprocessing at the gateway, fault tolerance ePR archive and monitoring operations, and image/data visualization.

12.6.3 Workflow of the Simulator

The IAS ePR simulator (minimally invasive spinal surgery is used as an example) has three time phases:

1. *Pre-op phase*: This is the phase before the operation, which includes patient consultations and planning of the surgery. Features of this phase include patient registration, PACS image acquisition, surgical procedure creation and scheduling, preparation of navigation tools, key image selection and annotations, surgical whiteboard data, and pain surveys.
2. *Intra-op phase*: occurs during the operation. The system acquires, archives, and displays various live data from peripheral surgically related devices in real time. Some of the archived information during pre-op will also be used for later review and surgical documentation. These data include biometric verification of patients just prior to surgery, real-time alerts of vital signs using a rules-based system, digital acquisition and integration of video, images, and waveform data from various input devices. Some of these selected data are recorded in real time in a digital storage device, which will be used to emulate the data collection during the intra-op phase of the simulator.
3. *Post-op phase*: is for the creation of a clinical report of the surgical procedure from the data gathered at the pre-op and intra-op phases. Clinical reports can be generated from the post-op authoring module using these data. Vital signs and pain survey data can also be collected during the post-op phases.

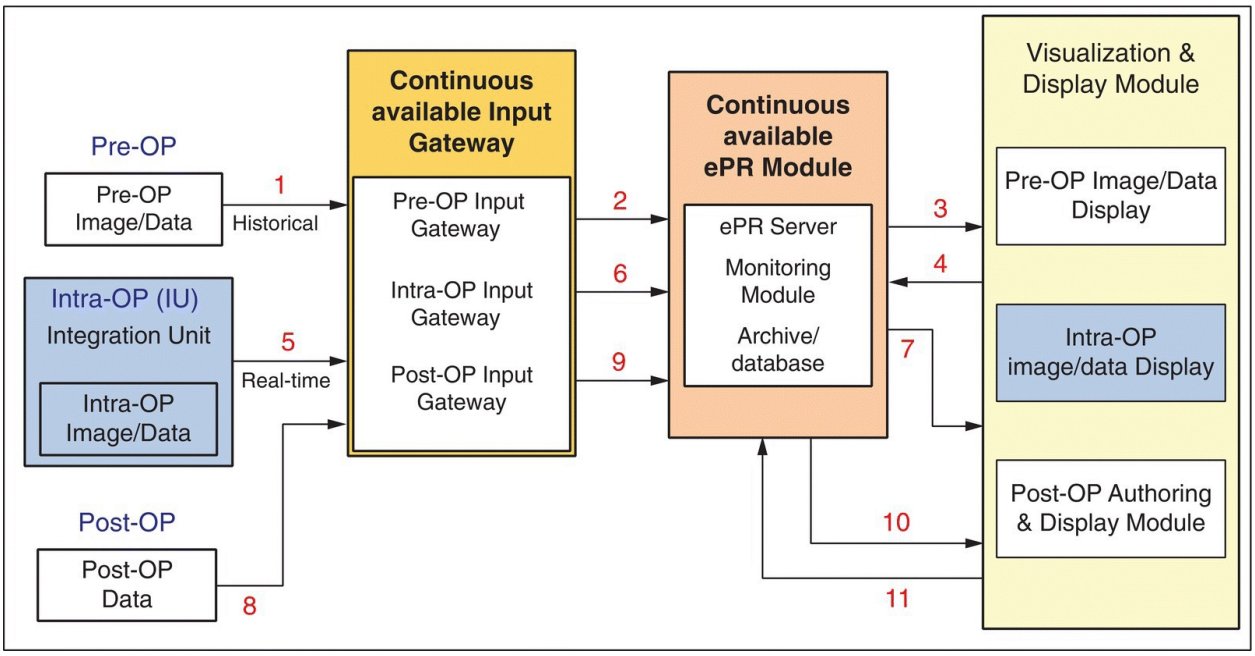

Figure 12.13 Data flow of the IAS ePR simulator. Minimally invasive spinal surgery (MISS) is used as an example. There are three surgical operation phases: pre-op, intra-op, and post-op, each phase with four data flow steps. Numerals indicate the data flow steps through the three phases of operation.

12.6.4 The IAS ePR Simulator in a Laboratory Environment

Figure 12.14 shows a portion of the simulator laboratory in the IPILab at the University of Southern California, depicting the major components of the IAS ePR simulator. The simulator was enabled to simulate the operation of two phases: pre-op (two large display monitors on the right) and intra-op (one larger monitor in the corner of the room). The two leftmost smaller monitors are two DVD devices, one of which fed simulated EMG and vital signs and the other fed endoscopic video and C-arm radiographs to the intra-op display monitor. A master time clock manages the data flow during the operation. The simulated data used were recorded during a minimally invasive spinal surgery (MISS) patient surgery from the live MISS ePR system.

Figure 12.14 The IAS ePR simulator in the laboratory environment simulating the pre-op and intra-op of a MISS surgery. Right to left: two pre-op displays, an intra-op live display and two DVD devices feeding simulating data to the intra-op display.

12.6.5 From IAS ePR Simulator to the Clinical MISS ePR System

The IAS ePR simulator was developed in 2009. Since then, a MISS ePR system has been implemented for daily clinical use at the California Spine Center, starting in 2010. The MISS system was designed based on a more robust simulator architecture. Figure 12.15A shows the clinical environment of the spinal surgery operation room before the IAS ePR system was installed, and Figure 12.15B depicts a snapshot of the intra-op 52” display monitor showing a real-time capture from the MISS ePR system [25]. Figures 12.16A–C depict the snapshots of some pre-op data, intra-op live images and waveforms, and post-op patient documentation, respectively.

(A)

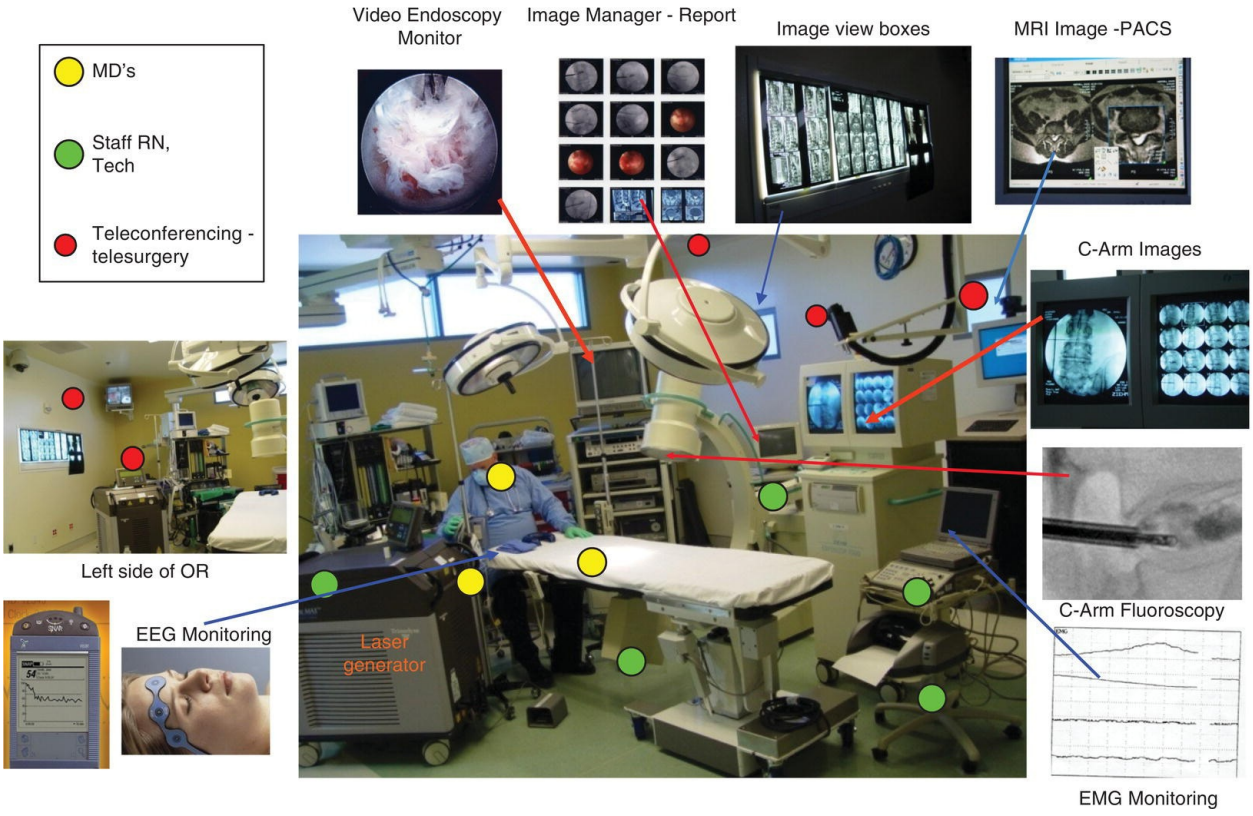
MD's
Staff RN, Tech
Teleconferencing - telesurgery
Video Endoscopy Monitor
Image Manager - Report
Image view boxes
MRI Image -PACS
C-Arm Images
Left side of OR
EEG Monitoring
Laser generator
C-Arm Fluoroscopy
EMG Monitoring

(B)

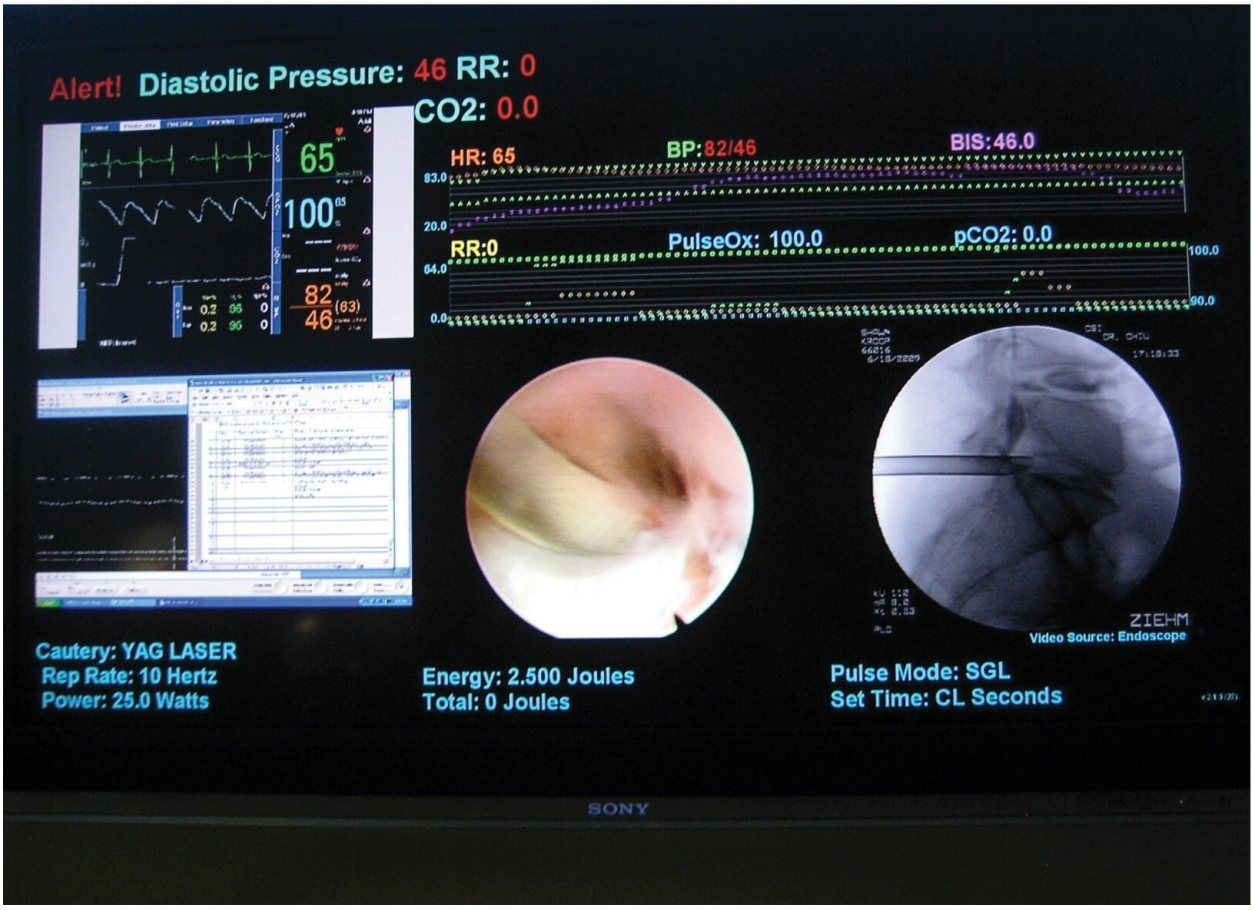

Figure 12.15 (A) The MISS operation room (OR) before the installation of the ePR system. EEG: electroencephalogram; EMG: electromyogram; MRI: magnetic resonance imaging.

(Courtesy of Dr John Chiu.)

(B) A snapshot from the real-time intra-op display monitor of the MISS ePR system.

(A)

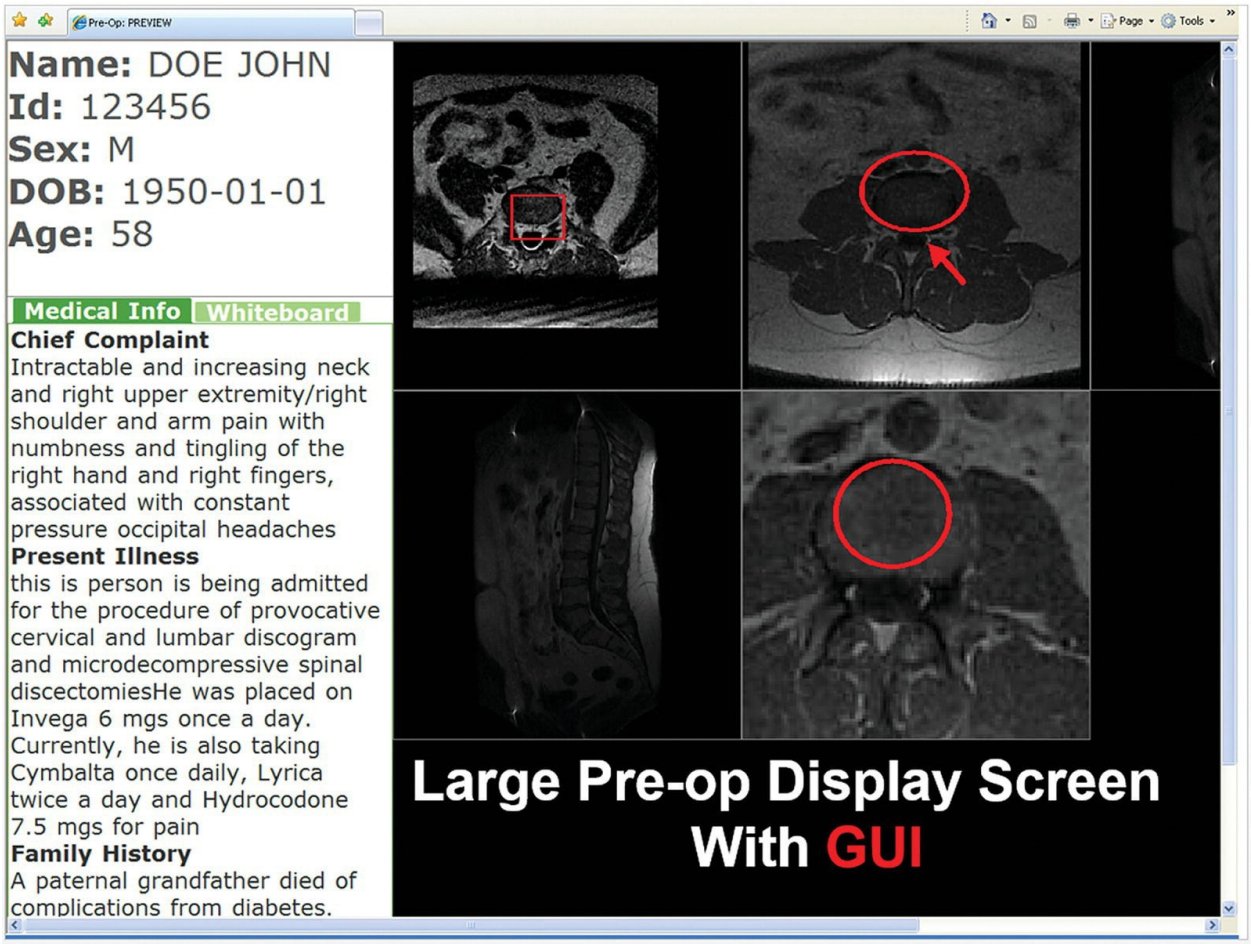
Pre-Op: PREVIEW
Page
Tools
Name: DOE JOHN
Id: 123456
Sex: M
DOB: 1950-01-01
Age: 58
Medical Info
Whiteboard
Chief Complaint
Intractable and increasing neck and right upper extremity/right shoulder and arm pain with numbness and tingling of the right hand and right fingers, associated with constant pressure occipital headaches
Present Illness
this is person is being admitted for the procedure of provocative cervical and lumbar discogram and microdecompressive spinal discectomiesHe was placed on Invega 6 mgs once a day. Currently, he is also taking Cymbalta once daily, Lyrica twice a day and Hydrocodone 7.5 mgs for pain
Family History
A paternal grandfather died of complications from diabetes.
Large Pre-op Display Screen With GUI

(B)

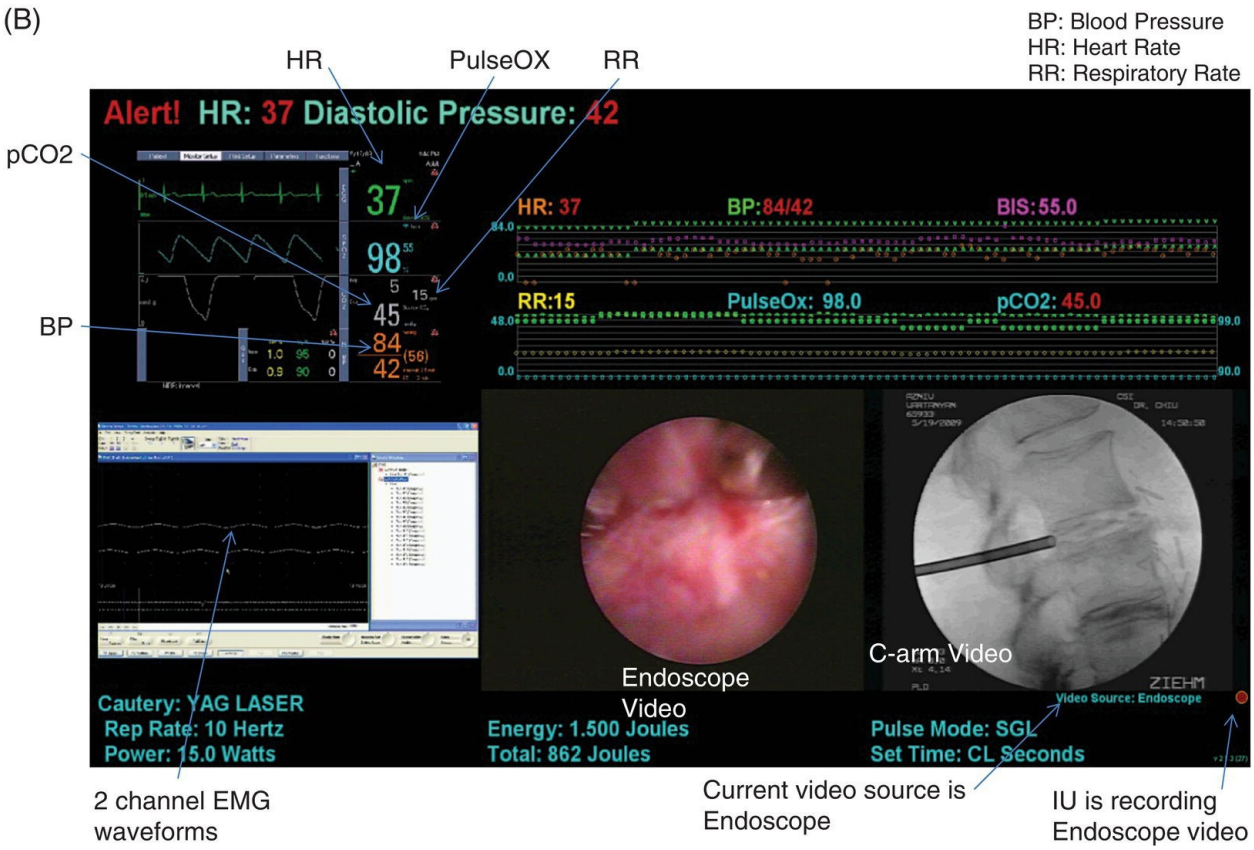
BP: Blood Pressure
HR: Heart Rate
RR: Respiratory Rate
HR
PulseOX
RR
pCO2
BP
Alert! HR: 37 Diastolic Pressure: 42
37
98
45
84 (56)
42
HR: 37
BP:84/42
BIS:55.0
RR:15
PulseOx: 98.0
pCO2: 45.0
Cautery: YAG LASER
Rep Rate: 10 Hertz
Power: 15.0 Watts
Endoscope Video
Energy: 1.500 Joules
Total: 862 Joules
C-arm Video
Video Source: Endoscope
Pulse Mode: SGL
Set Time: CL Seconds
2 channel EMG waveforms
Current video source is Endoscope
IU is recording Endoscope video

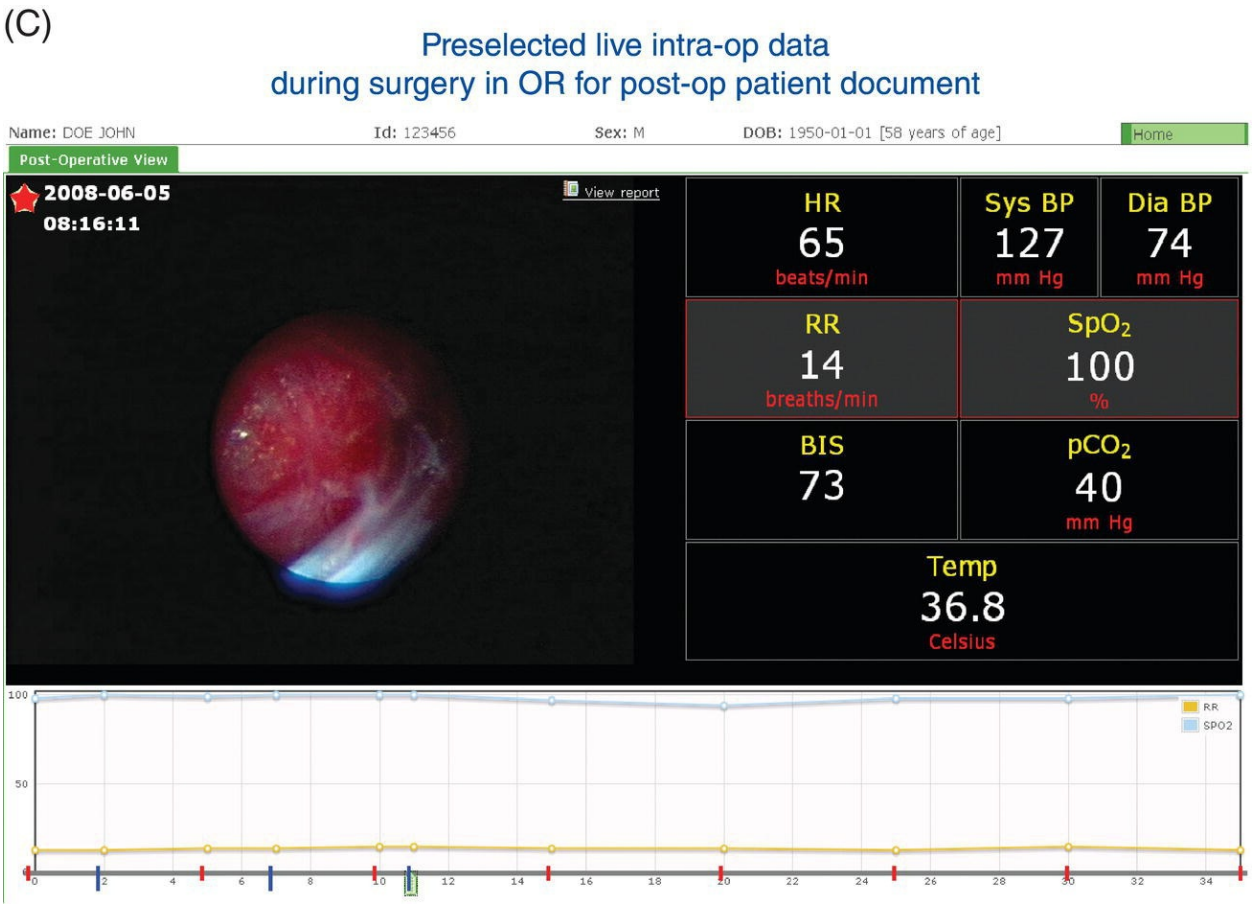

Figure 12.16 (A) Pre-op phase. Left: patient records, right: MRI, and red depicts the lesion to be operated on. (B) Intra-op phase. Top: Live real-time waveforms with inserted labels. Top left: vital signs waveforms with synthesized data per second, and the automatic alert signal. Middle left: EMG. Middle to right: endoscopic and C-arm images. All data are recorded in real time, synced by a system master time clock. IU: integration unit; Pulse OX: pulse oximeter. (C) An automatic screenshot from the intra-op real-time data taken during a specific time (see bottom green marker overlaid by blue on the time axis) prepared for the patient surgical document during the post-opphase. Top left to right: an endoscopic image along with some corresponding digital vital signs. Bottom: time axis showing the duration of the operation time. Red marks automatic default data collection time. Blue: surgeon's requests during the operation via a foot paddle. Larger green: time of screen shot capture. Some corresponding vital waveforms are also recorded.

12.6.6 Other potential IAS ePR Simulators

The first IASePR simulator was developed for MISS. Several versions later, a

clinical MISS ePR system was implemented for daily use. The concept and infrastructure of the IAS perk simulator can be used to develop other specific IAS perk systems. Examples are knee arthroscopic ePR, IAS maxillofacial ePR, and image-assisted neurosurgery ePR. In these potential IAS ePR systems, the data flow shown in Figure 12.13 can be followed closely and modified according to each specific clinical workflow. However, four overall components will need to be modified: image input devices, the ePR surgical database, display, and graphical user interface. The degree of difficulty in system development among these three IAS systems is in ascending order, especially in neurosurgery, because complex image navigation and guidance systems will be involved [26]. Chapter 21 discusses this topic in more detail.

12.7 Summary

An MII simulator in this context is defined as a system integration of many imaging and treatment components, which can be used to simulate a segment of the patient workflow and data flow, starting from diagnostic processes to the completion of a specific treatment. In this clinical continuum, it may sometimes be easier and more advantageous to develop only a subsection of the complete data flow for particular applications.

The concept of an imaging informatics simulator originates from the diagnostic PACS–ePR simulator in the 1990s, which was developed as an educational tool for learning the basics of PACS and ePR with image distribution. Use of the data grid technology for primary and backup image archives in PACS prompts an extension of the PACS–ePR simulator to emphasize the fault tolerance data archive, which leads to the data grid simulator development. With the introduction of cloud computing, the necessity of on-site storage components of the data grid becomes less important, as it can be replaced by cloud storage service.

CAD has been accepted as a potential secondary diagnostic reader in current radiology. Combining CAD results with PACS–ePR images in the diagnostic workflow would facilitate the viewing process, hence the need of CAD and PACS integration. The CAD–PACS simulator was thus introduced by augmenting the DICOM structured reporting and IHE workflow profiles.

In order to complete the clinical continuum, the scope of MII simulators must be expanded to include specific treatment applications. Two examples have been presented—the radiotherapy (RT) ePR simulator and the IAS ePR simulator.

Since every clinical treatment is patient specific, a treatment-related simulator is best developed based on an ePR platform; for example, the RT ePR and IAS ePR simulators.

Each of the five simulators presented in this chapter can be used to improve the education and learning of MII. They cover the spectrum from data collection to clinical diagnosis and treatment. Trainees equipped with this new vocabulary and knowledge may take advantage of them to innovate more effective and efficient diagnostic tools and image-guided treatments for better clinical service and research advancement.

Acknowledgments

The concept of MII simulators was conceived when the IPILab was established at the University of Southern California in 2000. The PACS simulator was first exhibited at the RSNA in 2002, and all simulators described in this chapter have been exhibited over the years thereafter there. Many graduate students, fellows, colleagues, and collaborators, while visiting short or longer terms at the Laboratory, have contributed substantially to the early development and the subsequent improvement of related technology to these simulators.

References

1 Huang, H.K. (2010) *PACS and imaging informatics: principles and applications*, 2nd edition. Hoboken, NJ: Wiley & Blackwell.

2 Zhou, Z., Law, M.Y., Huang, H.K., Cao, F., Liu, B.J. *et al*. (2003) Educational RIS/PACS simulator with web-based image distribution and display system. *SPIE Med Imaging*, 5033, 139–147.

3 Law, M.Y.Y. and Zhou, Z. (2003) New direction in PACS education and training. *Comput Med Imaging Graph*, 27, 147–56.

4 Huang, H.K., Zhang. A., Liu, B., Zhou. Z., *et al*. (2005) Data grid for large-scale medical image archive and analysis. In: *Proceedings of the 13th ACM International Conference on Multimedia*, pp. 1005–1013.

5 Liu, B., Zhou, Z. and Documet, J. (2005) Utilizing data grid architecture for the backup and recovery of image data. *Comput Med Imaging Graph*, 29, 95–102.

6 Lee, J., Documet, J., Liu, B. and Huang, H.K. (2010) A data grid and Web-based ePR solution for mobile dedicated breast MRI scenario, RSNA Education Exhibit INE1223-SUA.

7 Lee, J., Documet, J., Liu, B.J., Park, R., Tank, A. and Huang, H.K. (2011) MIDG-emerging grid technologies for multi-site preclinical molecular imaging research communities. *Int J Comput Assist Radiol Surg*, 6(2), 285–296.

8 Lee, J., Zhang, J., Park, R., Dagliyan, G., Liu, B. and Huang, H.K. (2012) A DICOM-based 2nd generation molecular imaging data grid implementing the IHE XDS-I integration profile. *Int J Comput Assist Radiol Surg*, 7(4), 533–545.

9 Lee, J. (2011) Molecular Imaging Data Grid (MIDG) for multi-site small animal imaging research based on OGSA and IHE XDS-I. PhD Dissertation, USC, August.

10 App Engine (GAE): http://code.google.com/appengine/

11 Windows Azure Platform: http://www.microsoft.com/windowsa zure/

12 Amazon Web Services (AWS): http://aws.amazon.com/

13 Eucalyptus: http://www.eucalyptus.com

14 Silva, L.A., Costa, C. and Oliveira, J.L. (2011) A PACS archive architecture supported on cloud services. *Int J Comput Assist Radiol Surg*, doi:10.1007/s11548-011 0625-x

15 Doi, K. and Huang, H.K. (2007) Computer-aided diagnosis CAD and image-guided decision support. *Comput Med Imaging Graph*, 31, 195–197. http://www.sciencedirect.com/science/article/ pii/S0895611107000237

16 Le, A., Liu, B.J. and Huang, H.K. (2009) Integration of computer-aided diagnosis/detection (CAD) results in a PACS environment using CAD-PACS toolkit and DICOM SR. *Int J Comput Assist Radiol Surg*, 4, 317–329.

17 Dhawan A.P., Huang. H.K., Kim, D.-S. (2008) Trends future in medical and molecular imaging. In: *Principles and Advanced Methods in Medical Imaging and Image Analysis, Chapter 31*. Singapore: World Scientific Publications, pp. 829–843.

18 Huang, H.K. (2008) Utilization of medical imaging informatics and biometric technologies in healthcare delivery. *Int J Comput Assist Radiol Surg*, 3, 27–39.

19 Gertych, A., Zhang, A., Sayre, J.W., Pospiech-Kurkowska, S. and Huang, H.K. (2007) Bone age assessment of children using a Digital Hand Atlas. *Comput Med Imaging Graph*, 31, 322–331.

20 Zhang, A., Sayre, J.W., Vachon, L., Liu, B.J. and Huang, H.K. (2009) Cross racial differences in growth patterns of children based on bone age assessment. *Radiology*, 290, 228–235.

21 Law, M. and Huang, H.K. (2003) Concept of a PACS and imaging informatics-based server for radiation therapy. *Comput Med Imaging Graph*, 27, 1–9.

22 Le, A. (2010) Mining using a radiation treatment plan navigator in an ePR system for minimizing radiation toxicity due to escalated dose in proton therapy for prostate cancer. PhD Dissertation, USC, August 2010

23 Le, A., Liu, B., Schulte, R. and Huang, H.K. (2011) Intelligent ePR for evidence-based research in radiotherapy: An example in proton therapy for prostate cancer. *Int J Comput Assist Radiol Surg*, 6(6), 769–784.

24 Huang, H.K. (2001) PACS, informatics, and the neurosurgery command module. *J Mini Invasive Spinal Tech*, 1, 62–67.

25 Documet, J. (2009) An electronic patient record (ePR) system for image-assisted minimally invasive spinal surgery. PhD Dissertation, USC, August 2009

26 Documet, J., Le, A., Liu, B.J., Chiu, J. and Huang, H.K. (2010) A multimedia electronic patient record (ePR) system for image-assisted minimally invasive spinal surgery. *Int J Comput Assist Radiol Surg*, 5(3), 195–209.

13
Molecular Imaging Data Grid (MIDG)

CHAPTER MENU

13.1 Introduction

13.2 Molecular Imaging

13.2.1 Preclinical Molecular Imaging Modalities

13.2.2 Preclinical Molecular Imaging Informatics

13.2.3 A Molecular Imaging Data Grid (MIDG)

13.3 Methodology

13.3.1 Preclinical Molecular Imaging Data Model

13.3.2 Molecular Imaging Data Grid Software Architecture

13.3.3 Molecular Imaging Data Grid Connectivity and Workflow

13.4 Results

13.4.1 Experimental Setup

13.4.2 Preclinical Molecular Imaging Datasets for Evaluation of the MIDG

13.4.3 MIDG Performance Evaluation

13.4.4 Current Status and the Next-Generation MIDG based on IHE XDS-i Profile

13.5 Discussion

13.5.1 Comparing Existing Data Grids in Healthcare Informatics

13.5.2 Comparing Current Solutions in Preclinical Molecular Imaging Informatics

13.6 Summary

Acknowledgments

References

Molecular imaging is the visualization and identification of specific molecules in anatomy for insight into metabolic pathways, tissue consistency, and tracing of solute transport mechanisms. It is a relatively new field in medical imaging research that has been propagating research discoveries in biology, medicine, disease studies, proteomics, and radiopharmaceutical development, by using in vivo biomarkers to visualize and quantify cellular and molecular content and activity. Small animal imaging facilities throughout medical research institutions have been growing in their number of investigator studies as well image data volume per study.

This chapter presents the molecular imaging data grid (MIDG), which utilizes emerging grid technologies in preclinical molecular imaging to facilitate data sharing and discovery between preclinical molecular imaging facilities and their collaborating investigator institutions, to expedite translational sciences research. Grid-enabled archiving, management, and distribution of animal-model imaging datasets, helps preclinical investigators to monitor, access, and share their imaging data remotely, and promote preclinical imaging facilities to share published imaging datasets as resources for new investigators. As a result, it can lead to interdisciplinary translational clinical research in medicine and clinical practice, which is increasingly interested in cellular and molecular biology activity at the preclinical levels, employing molecular imaging methods on animal models.

The system architecture of the MIDG is described in a four-layer diagram. A data model for preclinical molecular imaging datasets is also presented, based on imaging modalities currently used in a molecular imaging center. The MIDG system components and connectivity are presented, followed by the description of workflow steps for grid-based archiving, management, and retrieval of preclinical molecular imaging data.

13.1 Introduction

Molecular imaging studies using animal models are necessary steps in biological medical research and new therapy discoveries that are focused on cellular and molecular pathways. Researchers from multidisciplinary laboratories and institutions use imaging modalities and software resources provided by preclinical molecular imaging facilities to plan, acquire, post-process, visualize, and analyze their experimental animal model studies [1]. However, the data from these preclinical imaging studies are currently isolated to investigator folders on primitive storage solutions, lacking systematic distributive data infrastructure

with metadata-enriched archiving, study-centric management, and multi-institutional access [2]. This chapter addresses the application, design, and an implementation of emerging grid technologies (see Chapters 8 and 9 on the Data Grid) to tackle these informatics challenges. The objectives are to enable preclinical molecular imaging facilities to share their imaging datasets as resources for new investigations, and to equip preclinical investigators with infrastructure to remotely monitor, share, and access animal model imaging data.

13.2 Molecular Imaging

13.2.1 Preclinical Molecular Imaging Modalities

Molecular imaging is the visualization, localization, and characterization of biological processes at the cellular and molecular levels within intact living organisms. The multiple image-capture techniques in molecular imaging reflect pharmacokinetic pathways and in vivo mechanisms of disease within the context of physiologically authentic environments [3]. Investigators of interdisciplinary sciences such as pharmaceuticals, cancer research, proteomic studies, and image engineering, are increasingly dependent on molecular imaging to test their hypothesis before moving on in their translational research. With promising clinical benefits in personalized medicine, molecular imaging techniques are increasingly being utilized in animal-model trials and medical research experimentation [4].

The imaging modalities in preclinical molecular imaging are similar in design to clinical radiology modalities, but have smaller gantries and higher spatial resolution for small animal imaging. Figure 13.1 shows six common small-animal imaging modalities available in preclinical molecular imaging today. Figure 13.2 shows a sample dataset from a co-registered PET/CT imaging study of a nude mouse with a prostate cancer tumor [5].

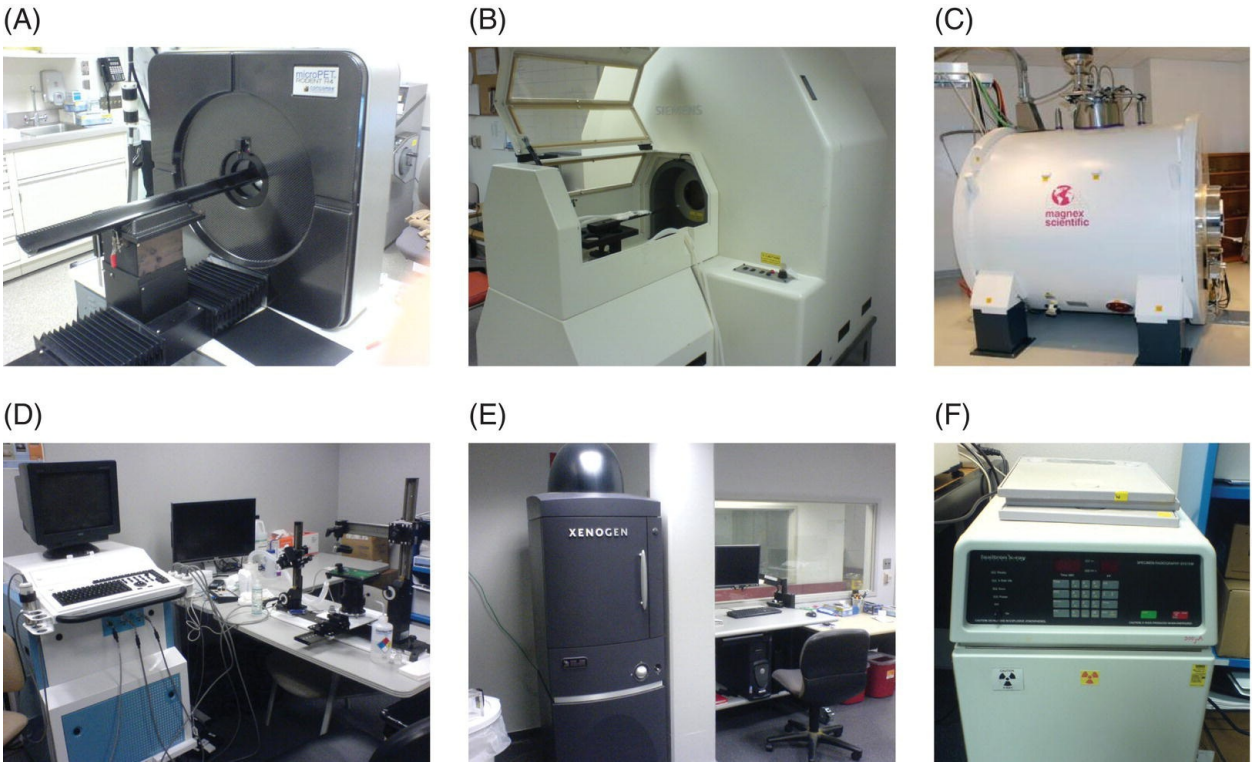

Figure 13.1 (A) MicroPET; (B) MicroCT; (C) MicroMRI; (D) MicroUS; (E) Optical Imaging; (F) Autoradiography (A,B,D,E,F, courtesy of Molecular Imaging Center, University of Southern California (USC); C courtesy of Molecular Imaging Program at Stanford, Stanford University).

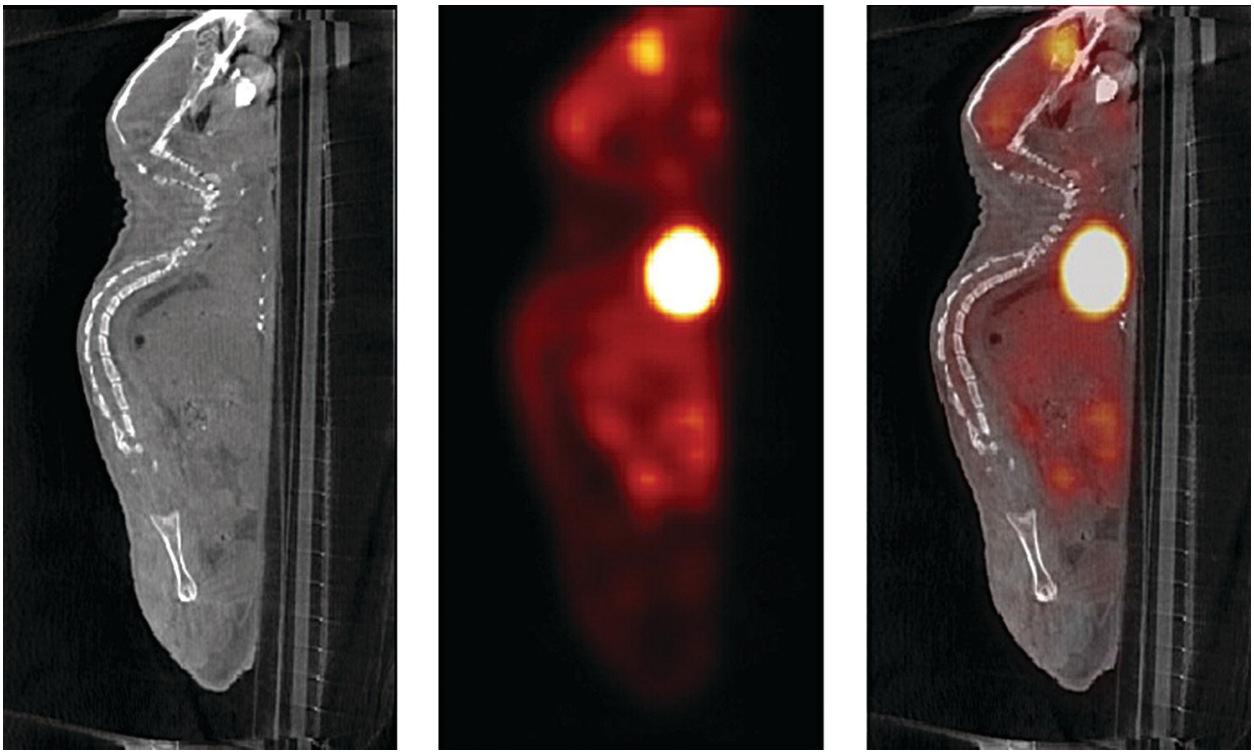

Figure 13.2 Sagittal CT, PET, and PET/CT Fusion Image of a mouse (left to right).

(courtesy of Molecular Imaging Center, USC)

13.2.2 Preclinical Molecular Imaging Informatics

Preclinical molecular imaging provides valuable insight into, otherwise unseen, molecular pathways and disease progression in animal-model anatomy through in vivo image acquisition, visualization, quantification, and analysis [1,3]. Due to high capital and operational costs, these preclinical imaging modalities, computing resources, and trained imaging staff are typically convened into dedicated preclinical imaging facilities. In 2008, there were an estimated 150 preclinical molecular imaging facilities in the United States, of which the majority were located in medical schools to serve both on-campus and local investigators [6].

The investigative imaging workflow at these facilities, overviewed in Figure 13.3, go from study planning and scheduling, to preparing animals for scans, to post-processing acquisition data, to visualization and analysis on dedicated workstations (WSs), and, if no further scans are required, to archive and distribute the resulting datasets. Investigators travel to preclinical imaging facilities, even after image acquisitions are completed, to organize, analyze, and

collect their data. Because molecular imaging systems and data formats are still changing, the data archives for preclinical molecular imaging facilities are primitively tied to the imaging modalities, staff, and computational software [7]. The current challenges in molecular imaging informatics are to organize and distribute these data archives to multiple investigator sites in a secured data infrastructure, so that investigators can readily access and contribute new data from their own laboratories [8]. This chapter presents an informatics data grid method to meet these challenges.

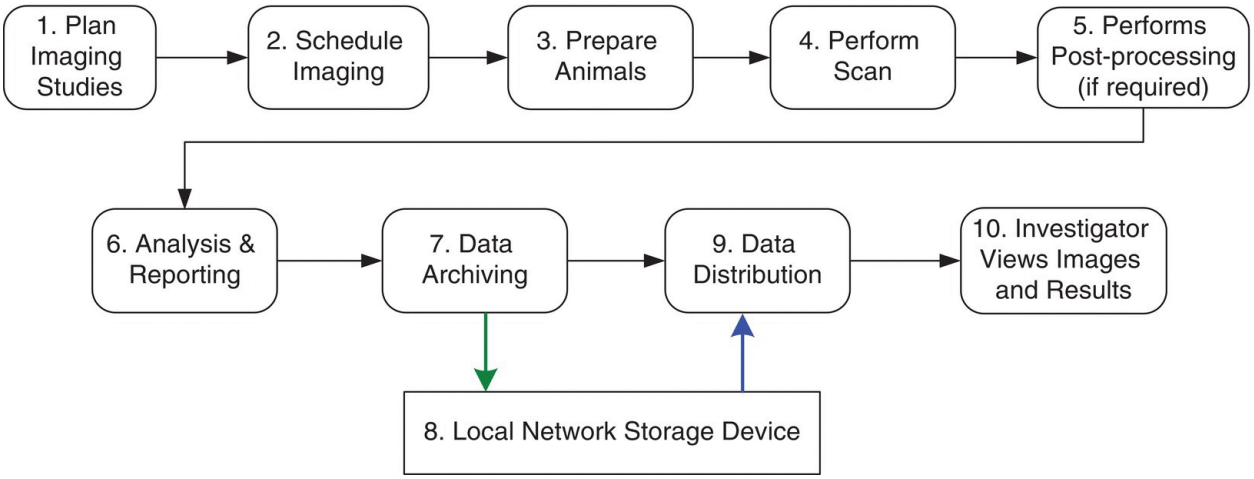

Figure 13.3 Traditional molecular imaging and informatics workflow (green arrow: digital data write and blue arrow: digital data read).

The informatics systems of preclinical molecular imaging can be categorized into image post-processing and data management. Although efforts have been devoted to the automation of computational workflows, data archiving and data dissemination in preclinical imaging facilities have been comparatively primitive, due to informatics challenges caused by non-standardized data formats, complex experimental metadata, and antiquated storage infrastructure [9–11].

13.2.3 A Molecular Imaging Data Grid (MIDG)

An MIDG has been developed at the IPILab and deployed at the USC Molecular Imaging Center, which needed a better way of documenting, searching, and distributing its experimental image data for its growing number of investigators. Previous methods of documenting studies and imaging parameters were on log books written by technicians. Previous methods of saving image data were on stacks of DVDs and external hard drives. Previous methods of data distribution used DVDs and portable flash drives, or email. As the quantity and complexity

of experimental datasets increased, the USC Molecular Imaging Center lacked an integrated informatics infrastructure to expedite their multimodality imaging dataflow.

The objective of the MIDG is to provide a study-centric archive infrastructure for preclinical molecular imaging communities with a Web-based user interface for uploading, monitoring, searching, and downloading preclinical molecular imaging datasets. The novelty of using data grid technology is in its ability to deliver large imaging datasets securely and efficiently across a wide-area-network (WAN) [12]. Designing a metadata database and user interface for preclinical molecular imaging workflows, and integrating them with a data grid infrastructure creates a unique data sharing platform for preclinical molecular imaging research communities. Figure 13.4 demonstrates how the MIDG improves image data sharing among interdisciplinary preclinical molecular imaging research communities.

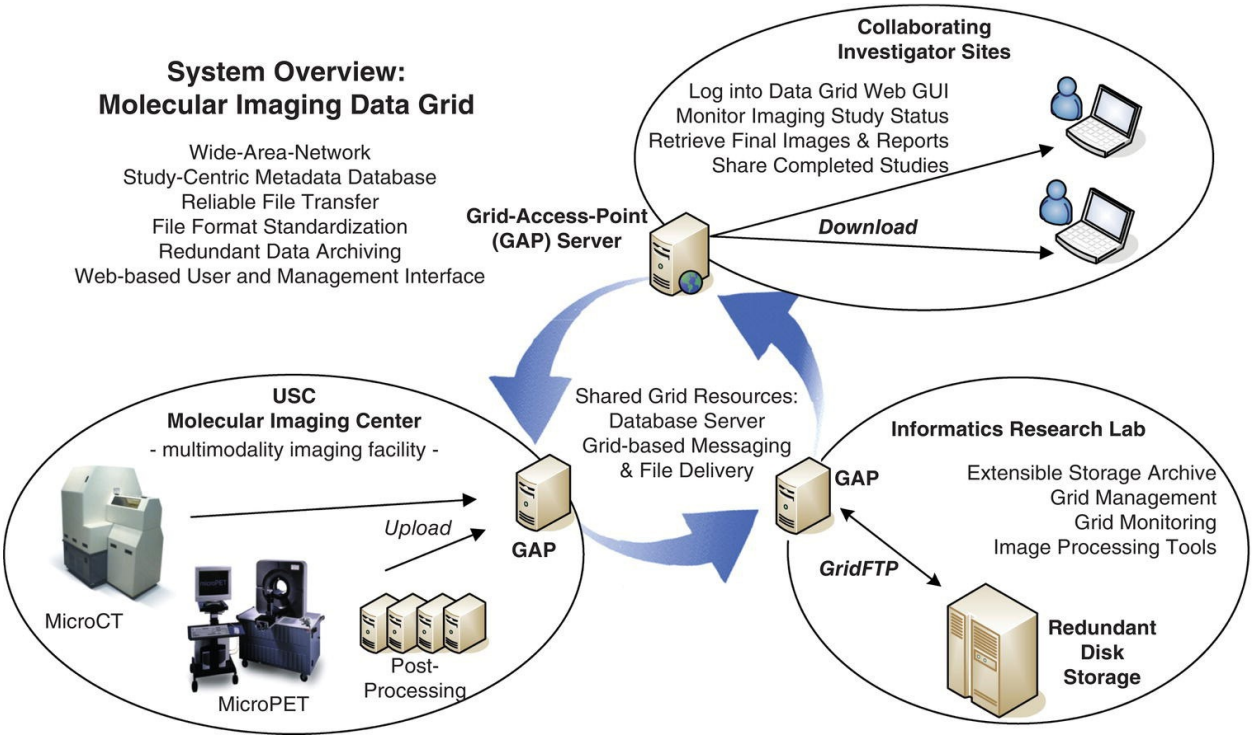

Figure 13.4 Implementation scenario of the multi-institution MIDG at the USC Molecular Imaging Center and IPI Lab with connectivity to collaborator sites.

13.3 Methodology

Building on the existing models of preclinical molecular imaging facilities and

the experience of the IPILab in data grid systems for enterprise radiology, an MIDG for preclinical molecular imaging datasets was designed for preclinical molecular imaging communities. This system was evaluated at the USC campus in 2012, and later published [24] involving the USC Molecular Imaging Center and the IPILab. The primary steps in design were to define a preclinical molecular imaging data model with a study-centric database, and to build components of the data grid architecture around that data model.

13.3.1 Preclinical Molecular Imaging Data Model

A data model for preclinical molecular imaging identifies data formats and relational structure of the data. The preclinical molecular imaging data model presented here is arranged in a study, session, group, scan, and file hierarchy. The file formats in preclinical molecular imaging vary by individual facility's modalities, software, and storage policies, but all files fall within the acquisition, post-processing, and distributed files categories. Figure 13.5 shows this data model with sample files based on modalities, software, and workflow at the USC Molecular Imaging Center. This preclinical imaging data model is reflected in the metadata database for the MIDG.

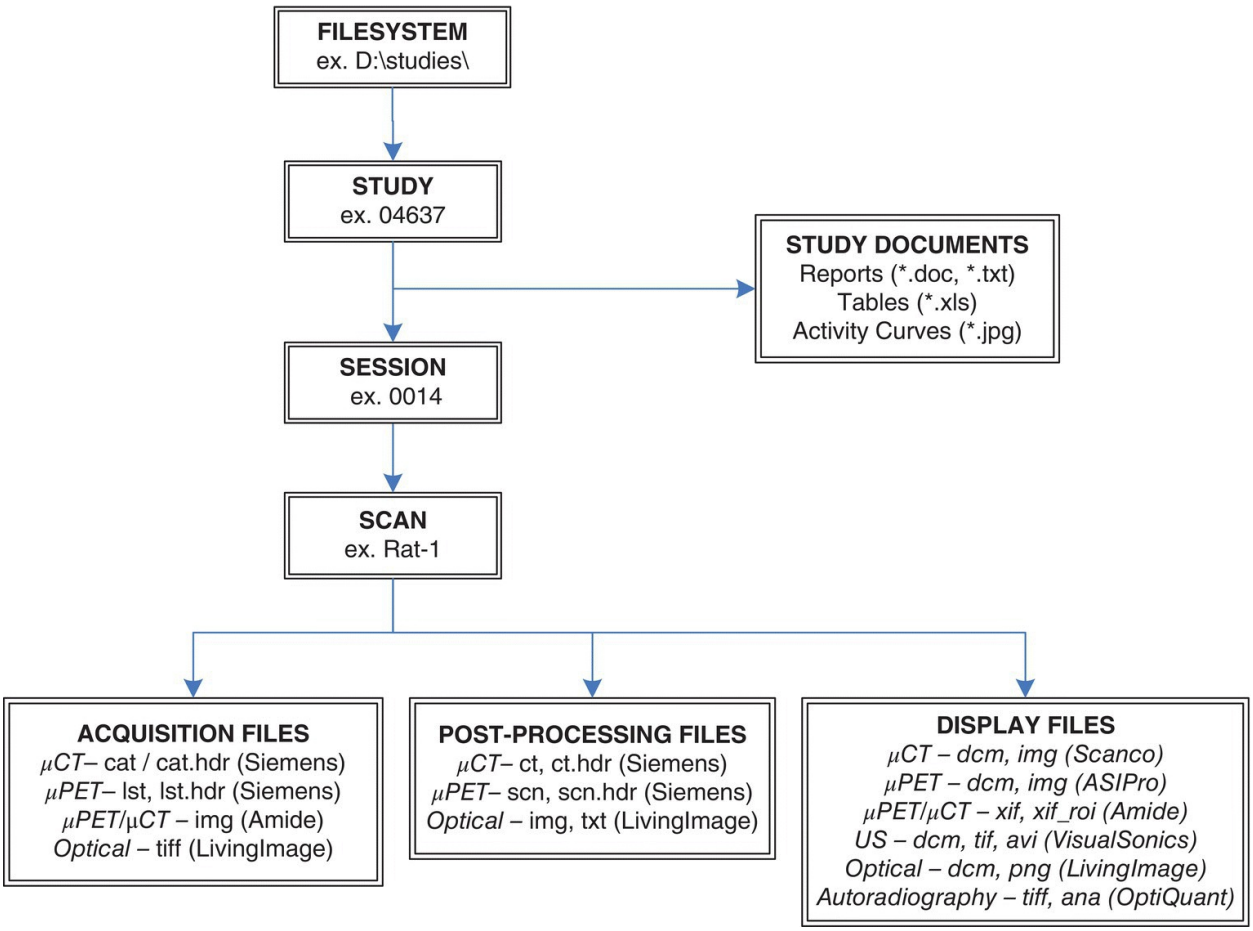

Figure 13.5 Molecular imaging data model for storing files in the data grid archive.

In its current design, the MIDG is customized to support file types provided by the USC Molecular Imaging Center. It converts all 2-D viewable image formats (JPEG, TIFF, PNG, PDF) to the DICOM format, so that final distributed files are standardized and prepared for interaction with external DICOM-compliant systems. File formats that cannot be converted to DICOM, such as raw acquisition files and proprietary files, are also registered into the MIDG, but are not physically copied into the remote storage archives of the grid. Non-DICOM files are kept at the originating facility's storage, where they are most frequently accessed, and are sourced directly to remote sites when queried upon.

13.3.2 Molecular Imaging Data Grid Software Architecture

The system architecture for an MIDG is organized into four layers – application, user-level middleware, core middleware, and fabric. Certain components of this architecture are adaptations to previous medical imaging data grid work done at

the USC IPILab [13,14]. It also uses the secure grid infrastructure provided by the Globus Toolkit version 4.0, an open source software package with file management services and secure file delivery protocols [15]. Figure 13.6A below shows the architecture of the MIDG, and is contrasted with Figure 13.6B to demonstrate design similarities and differences of this new data grid for archival and distribution of preclinical molecular imaging images. In Figure 13.6A, the blocks in orange identify the new software components of the MIDG, and the grid access point (GAP) services at the user-level middleware are highlighted in green.

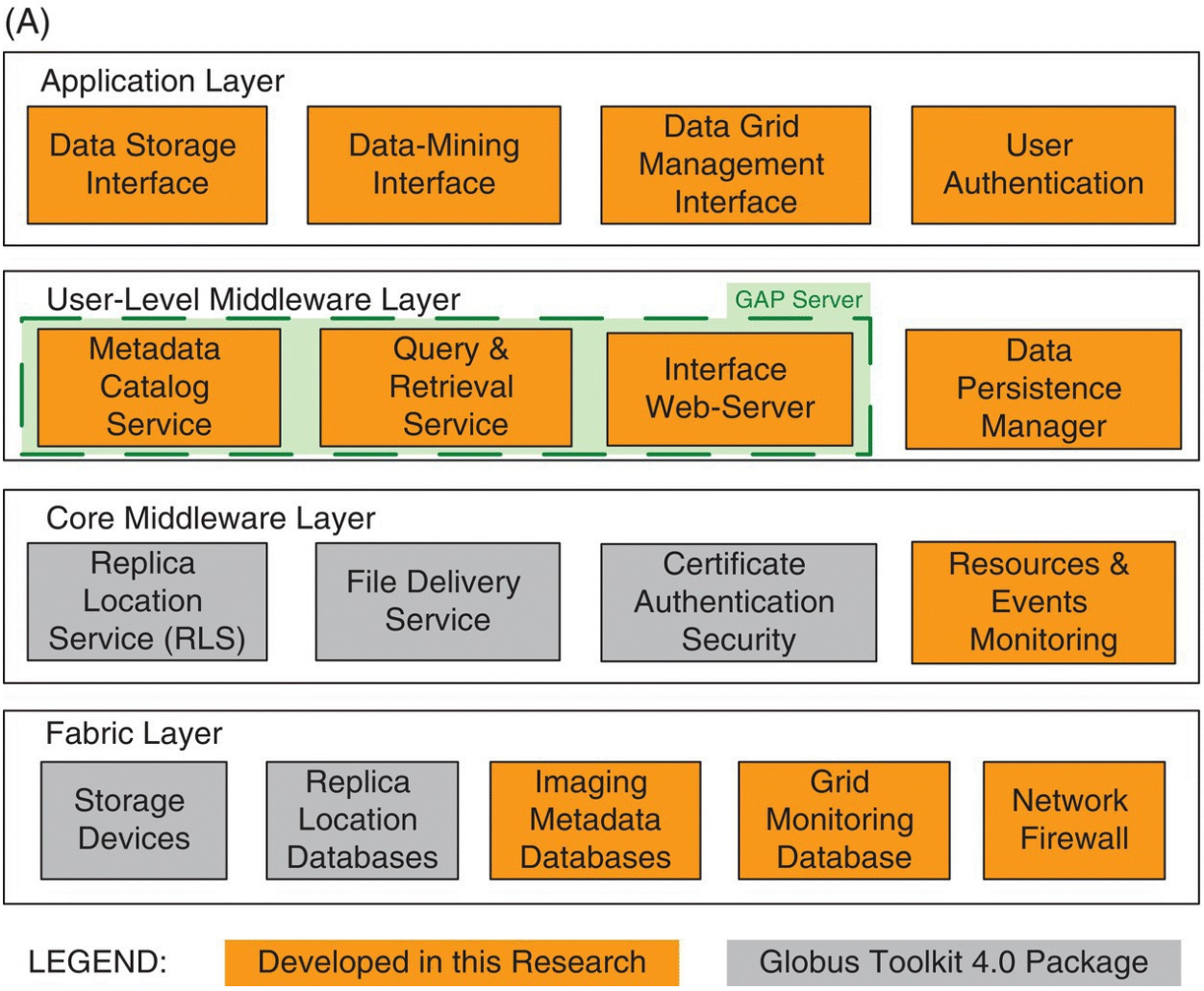

Figure 13.6 (A) MIDG system architecture, built with services from the Globus Toolkit package, tailored for molecular imaging data application.

The core middleware layer of the MIDG also utilizes the Globus Toolkit packages, but a Resources and Events Monitoring service has been implemented to monitor and audit data exchange among preclinical investigators and imaging

facility staff. The picture archiving and communication system (PACS) simulator in Figure 13.6B has been removed, because preclinical imaging workflows do not utilize PACS at this time.

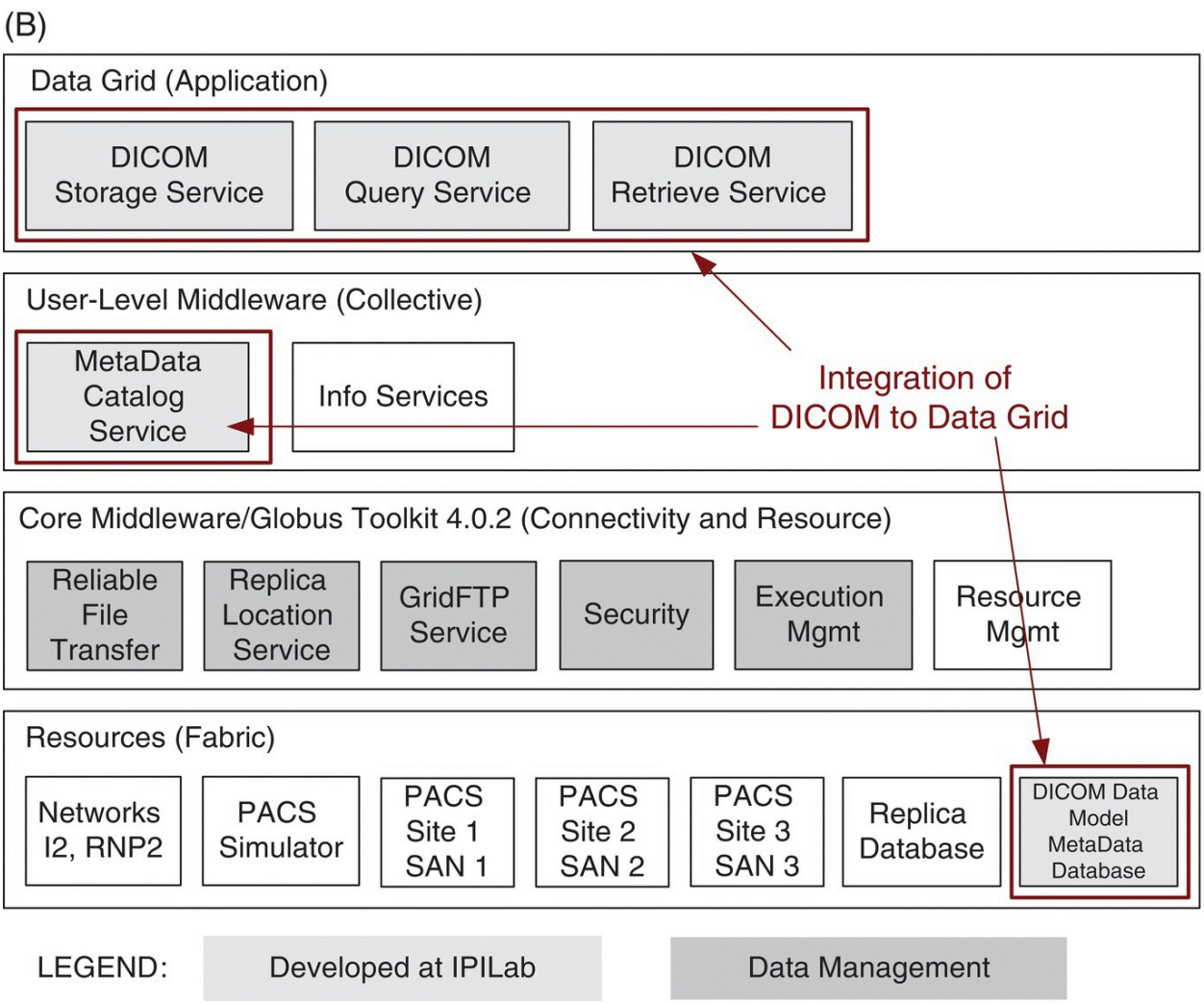

Figure 13.6 (B) IPILab data grid five-layer infrastructure integrating Globus Toolkit and DICOM [15,16]. Note that the two core middleware layers (connectivity and resource) correspond to the core middleware layer shown in 13.6(A).

The new components of the MIDG architecture shown in Figure 13.6A are now presented in more detail in the following sections.

13.3.2.1 Application Layer

With non-standardized data formats and communications protocols in preclinical molecular imaging informatics, the application layer was implemented with

Web-based user interfaces for archiving, monitoring, retrieving, and managing experimental imaging datasets within the MIDG. Unlike the DICOM-compliant data grid for radiology, where external DICOM-compliant systems store, query, and retrieve imaging studies with limited user accountability, the Web-based user-level interfaces enable user-level control, such that study registration, data upload, study sharing, and dataset retrieval are restricted to authorized users only over the secure HTTP protocols between user WSs and local GAP servers. Only authorized grid managers also have an interface to monitor user activity and configure the local GAP services (Figure 13.7).

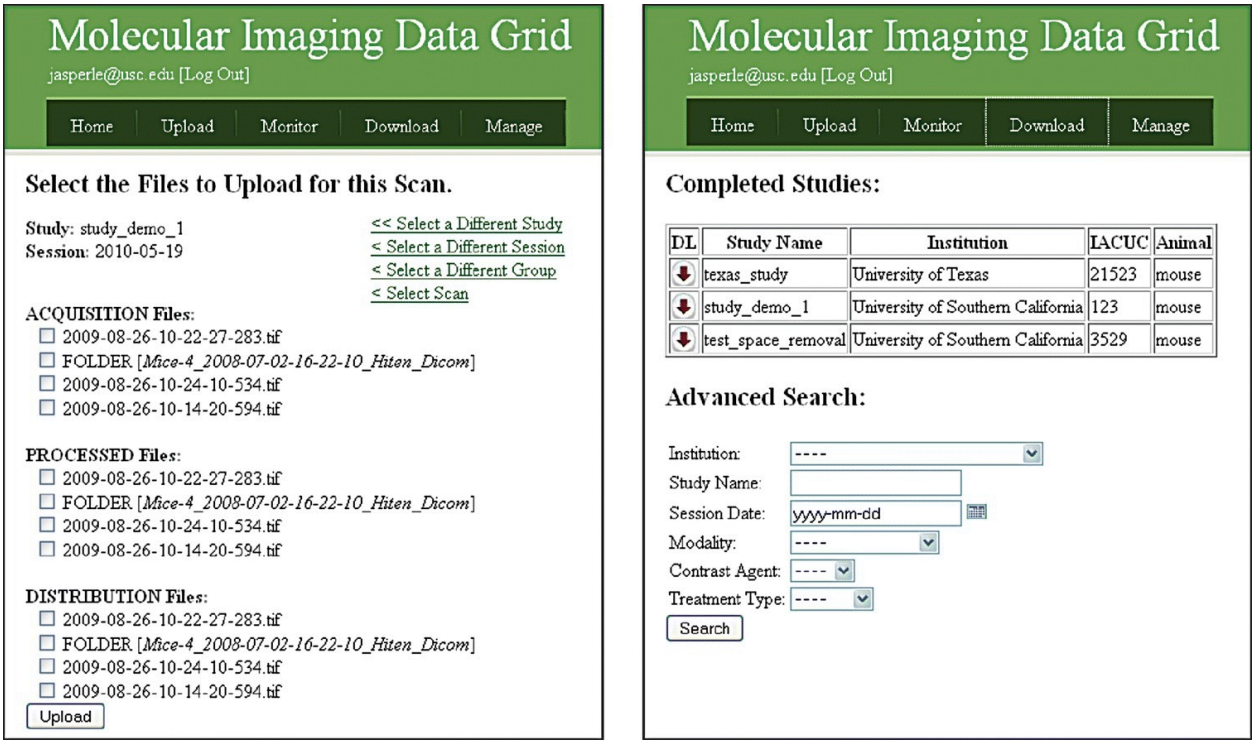

Figure 13.7 Screenshots of the upload (left) and download (right) pages from the MIDG's Web-based user interface.

(copyright USC IPILab, 2010)

The primary features of the application interfaces are uploading of preclinical molecular imaging data files, reviewing and sharing of uploaded studies, searching for publicly shared studies based on filtered experimental parameters, and retrieval of imaging datasets from the data grid's storage archives. The MIDG is shown in Figure 13.8.

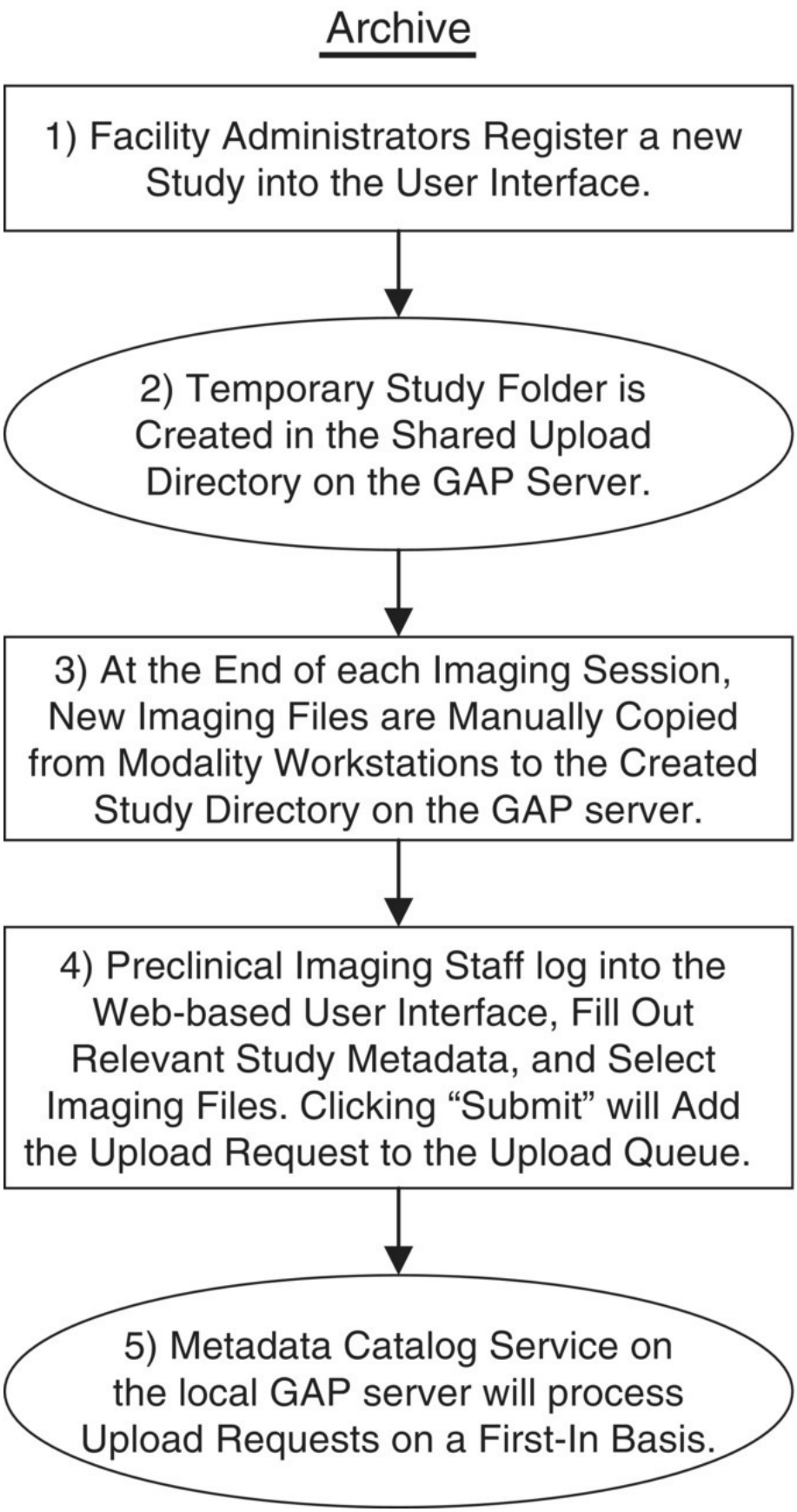
Archive
1) Facility Administrators Register a new Study into the User Interface.
2) Temporary Study Folder is Created in the Shared Upload Directory on the GAP Server.
3) At the End of each Imaging Session, New Imaging Files are Manually Copied from Modality Workstations to the Created Study Directory on the GAP server.
4) Preclinical Imaging Staff log into the Web-based User Interface, Fill Out Relevant Study Metadata, and Select Imaging Files. Clicking “Submit” will Add the Upload Request to the Upload Queue.
5) Metadata Catalog Service on the local GAP server will process Upload Requests on a First-In Basis.

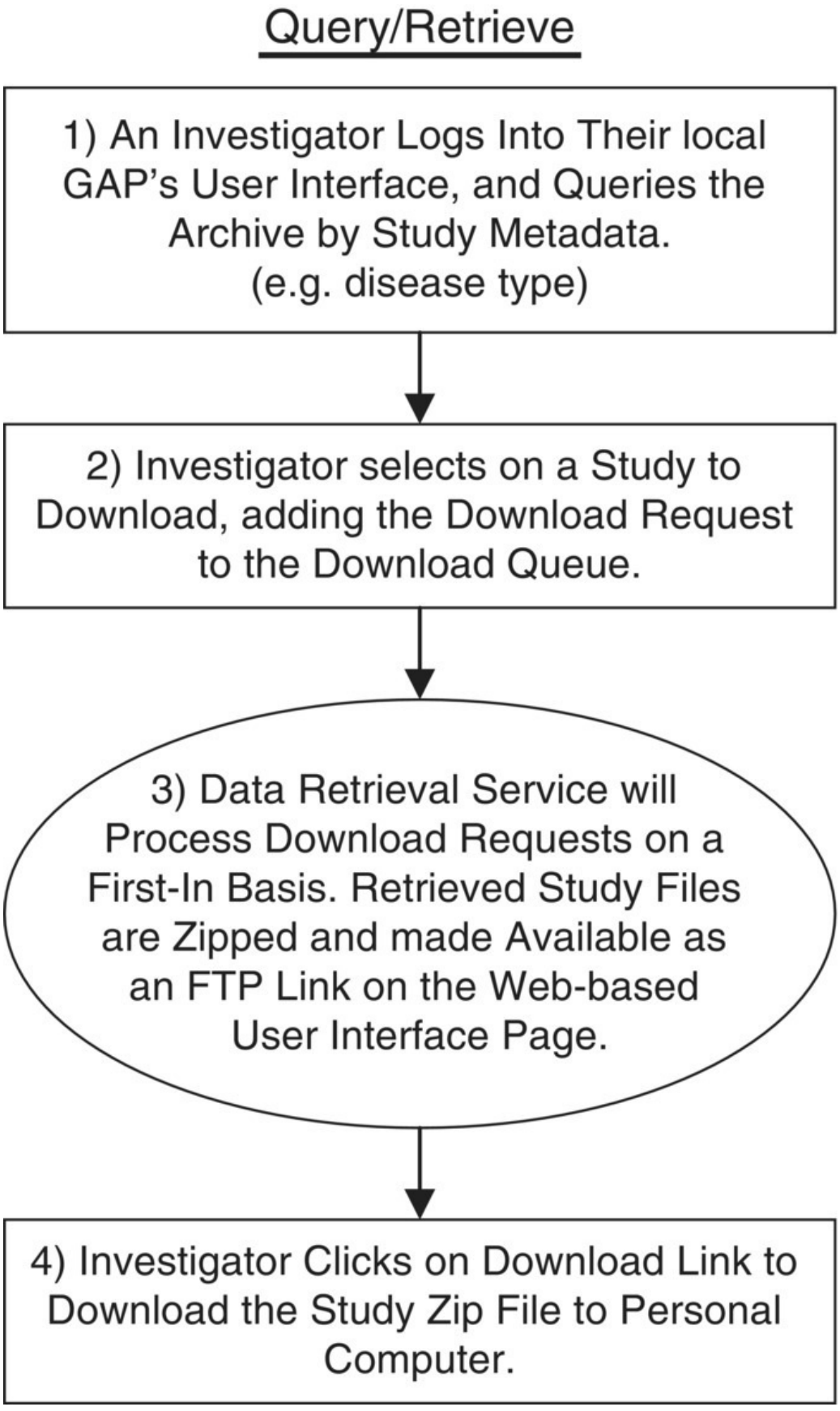
Query/Retrieve
1) An Investigator Logs Into Their local GAP's User Interface, and Queries the Archive by Study Metadata. (e.g. disease type)
2) Investigator selects on a Study to Download, adding the Download Request to the Download Queue.
3) Data Retrieval Service will Process Download Requests on a First-In Basis. Retrieved Study Files are Zipped and made Available as an FTP Link on the Web-based User Interface Page.
4) Investigator Clicks on Download Link to Download the Study Zip File to Personal Computer.

Figure 13.8 Application layer workflows for archiving and query/retrieving in the MIDG's Web-based user interface.

13.3.2.2 User-Level Middleware Layer

There are three major components in the user-level middleware layer: the GAP server, the collision management, and the data persistence manager.

13.3.2.2.1 GAP

GAP servers (Figure 13.6A, green) are placed behind network firewalls at each participating grid site, so only grid messaging and grid file transfer ports are allowed to pass to the Internet. When GAP servers receive new molecular imaging study data and files from the Web-based user interfaces, metadata attached with incoming files are updated to the metadata database by the metadata catalog service, and then physically distributed to one or more of the external grid storage archives over the WAN using core middleware services. To retrieve imaging files from the grid, the data retrieve service processes user selected requests from the Web-based interfaces and initiates a secure gridFTP transfer to pull data files stored in the grid archives back into its local cache, so users can download them locally from the GAP server. Both of these GAP services are written in Java.

13.3.2.2.2 Collision Management

To handle user traffic at the GAP services, there is a queuing mechanism at each GAP for uploading and downloading requests from users so that only one request is handled at a time. Furthermore, data files are not made available for download until upload has been completed and confirmed. If users from two institutions are requesting to download the same image file, there is not a conflict because each GAP server handles its own user requests. However, if one user is attempting to download a file while an administrative user at another institution is trying to delete that file, the delete request will not be queued, because verification is done to make sure that file is not already listed on the download queue.

13.3.2.2.3 Data Persistence Manager

Data files are archived redundantly in a molecular imaging grid at multi-site storage device destinations based on configurations in each metadata catalog service, to allow reliable access to shared data. This data redundancy is

maintained by data persistence managers installed at each storage archive, initiating transmission of local data files to remote storage archives as a third-party manager using gridFTP. The data persistence manager monitors the availability of a remote storage archive during off-peak hours and tries to repopulate missing data files. Upon successful transmission, databases are updated to reflect the added file copy. This method creates an automated disaster recovery mechanism for all data files archived in the MIDG.

13.3.2.3 Core Middleware Layer

The core middleware layer provides critical communications and data management services for the user-level middleware layer, and relies heavily on the Globus Toolkit API packages, particularly the components shown in gray in Figure 13.6A. The Globus Toolkit provides secure file management and delivery across the multi-site infrastructure via its replica location service (RLS), certificate authentication protocols, and gridFTP file delivery services [17]. These software services can be implemented redundantly at multiple remote servers to provide continuously available operations and resources.

The resources and events monitoring software in the MIDG are used to monitor grid hardware resources, and auditing of data handling events is essential. This is necessary to maintain the integrity of experimental research data, services, and investigators in the MIDG. A dedicated monitoring and auditing server maintains its own database to audit the status of all hardware resources, and major events from the users and middleware services.

13.3.2.4 Fabric Layer

The components making up the fabric layer in the grid architecture are the storage devices, databases, and network firewalls. In setting up a storage device for the molecular imaging grid, the amount of storage space allocated by a site is determined by all participating sites archiving data in the same MIDG, thereby requiring discussion and planning between parties. There are three main databases in the imaging grid—the molecular imaging metadata database, the RLS databases, and the grid monitoring and auditing database.

Based on experiences from previous data grid implementations, the metadata database and monitoring and auditing database are kept separate from the core middleware services due to performance degradation issues [18]. Nonetheless, all three databases are critical resources to the grid’s operations and are implemented on dedicated database servers with redundancy methods and secure

socket layer (SSL) communications support.

13.3.3 Molecular Imaging Data Grid Connectivity and Workflow

The network connectivity of the MIDG is shown in Figure 13.9 from the perspective of a molecular imaging site. The pale blue area encapsulates the molecular imaging site's devices and the gray cloud area encapsulates the components of the MIDG that are located outside the WAN. A network firewall, shown in amber, is required at each molecular imaging site to protect the local area network (LAN) devices.

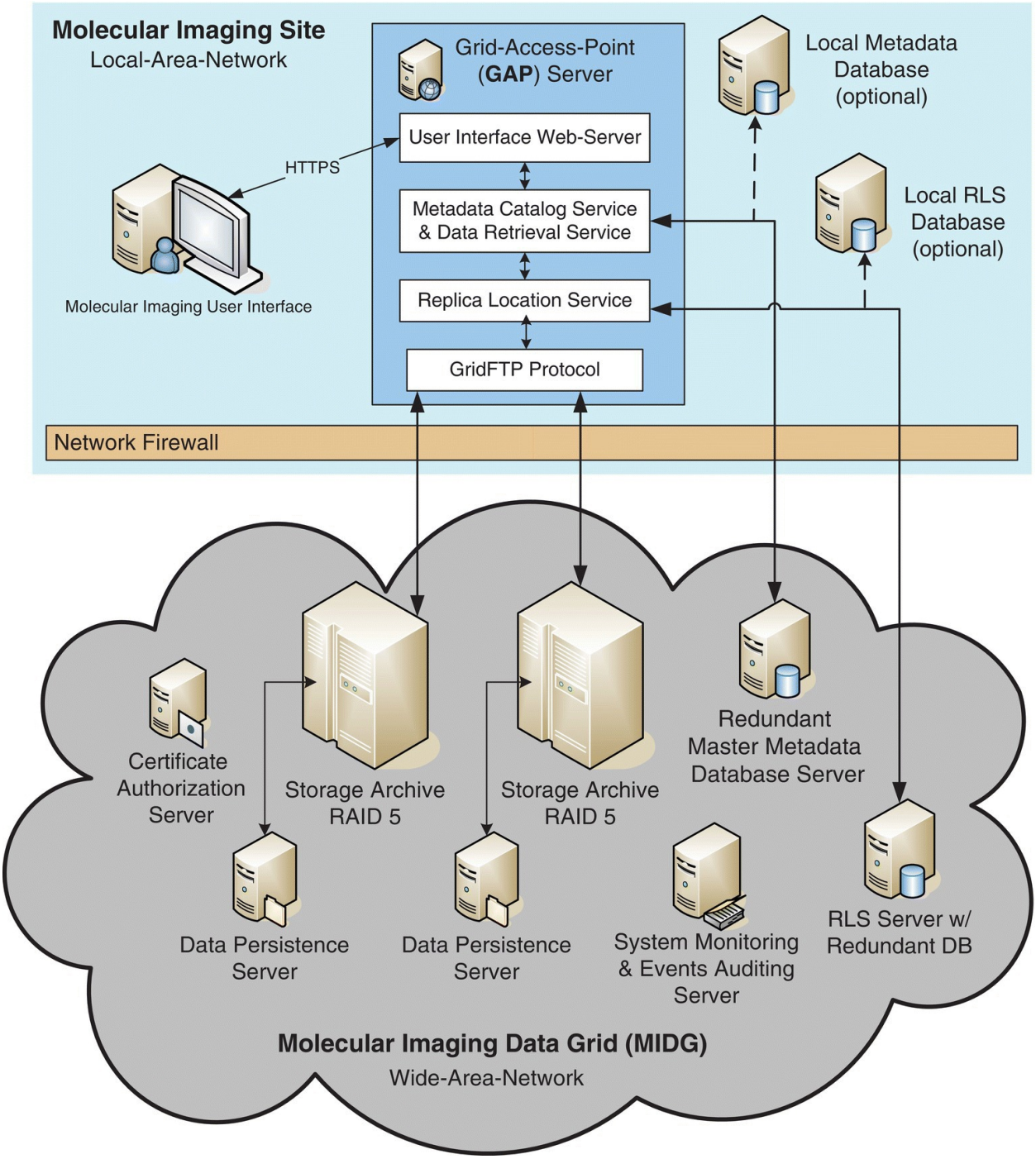

Figure 13.9 Components and connectivity of the molecular imaging grid architecture, from a molecular imaging site's perspective. The metadata catalog service extracts study-relevant and file-specific metadata; the replica location service handles file-delivery destination mappings; the certificate authorization server gives third-party authority of digital certificates; the data persistence server maintains long-term storage and internal data redundancy; the system

monitoring and events auditing server offers real-time monitoring of databases, storage archives, and data movement events; and the storage archive consists of network storage devices with RAID 5 redundancy for local fault tolerance.

The workflow for data archiving, management, and distribution of preclinical molecular imaging, presented in Figure 13.3, changes with a grid-enabled MIDG infrastructure. This new workflow is shown in Figure 13.10. The colored arrows depict these three specific data flows, and the gray regions mark the MIDG components that have been integrated into the original preclinical molecular imaging workflow.

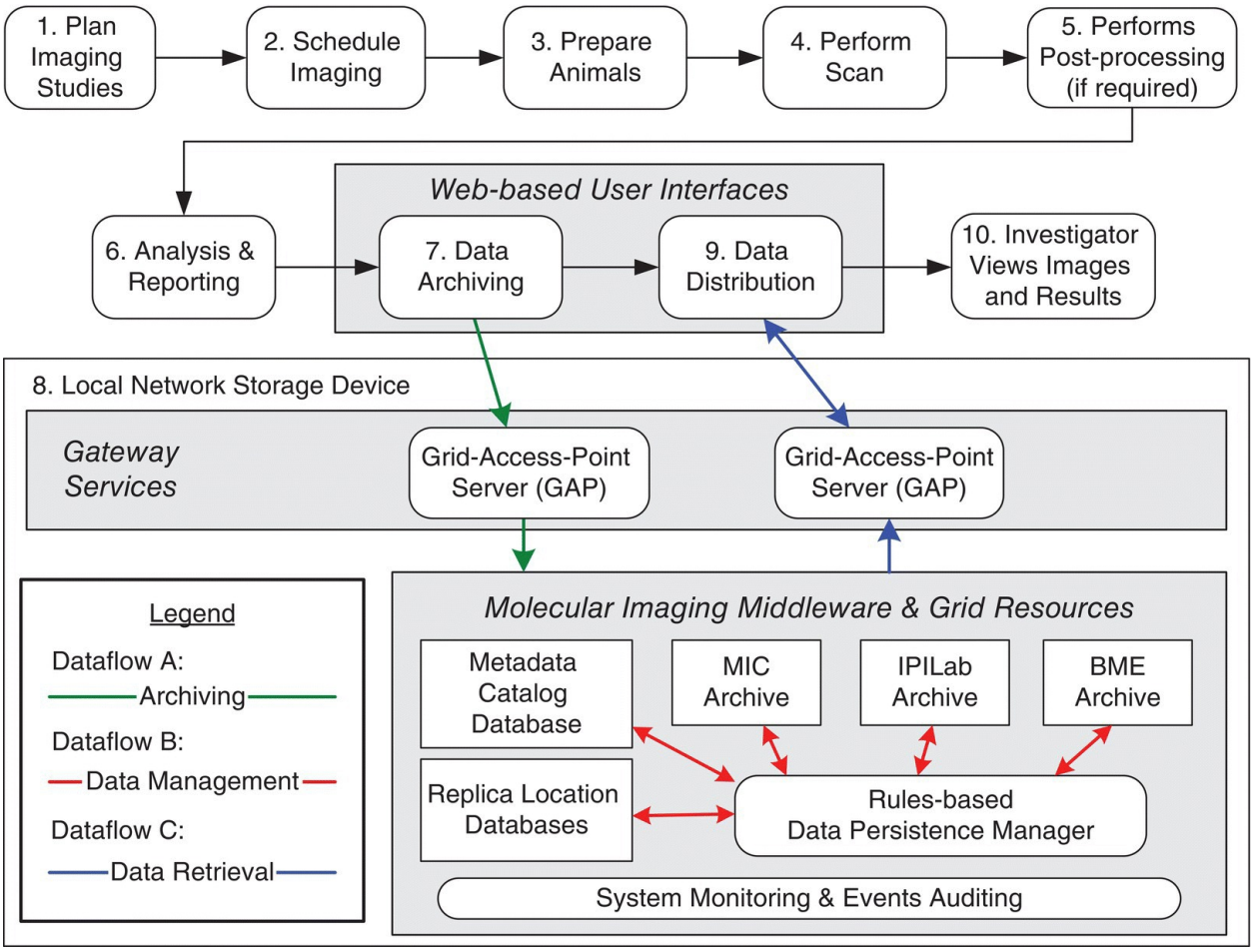

Figure 13.10 Overall workflow of the USC Molecular Imaging Center (MIC) with the MIDG showing the novel archiving, data management, and data retrieval data flow methods.

In step 7 of Figure 13.10, molecular imaging files and study metadata are uploaded into local GAP servers and transmitted securely into remote grid storage archiving sites. Within the grid, data files are monitored and maintained

by the data persistence manager in order to maintain continuous data availability through replication and long-term storage. In step 9, investigators can query for animal-model imaging data from multiple collaborative sites and download datasets into their WSs through a single Web-based user interface of the MIDG.

13.4 Results

13.4.1 Experimental Setup

Initial evaluation of the MIDG has been completed at the USC's Molecular Imaging Center and IPILab using VMware [19] environments. A GAP server has been installed on a Dell Precision PC located on the Molecular Imaging Center's LAN. The remaining hardware components of the MIDG are being run at the IPILab on a dedicated Dell PowerEdge server with VMware Server 2.0. Network connectivity speeds between the Molecular Imaging Center and IPILab is 100 mbps data upload speed. The objectives of the evaluation were to measure the robustness in multiple file format support, and to obtain quantitative estimates of the duration each process takes.

13.4.2 Preclinical Molecular Imaging Datasets for Evaluation of the MIDG

Sample preclinical molecular imaging datasets were collected at the USC Molecular Imaging Center from six preclinical imaging modalities – microCT, microPET, PET-CT, optical imaging, ultrasound, and autoradiography (Figure 13.3). Each modality has a unique combination of acquisition, post-processed, and final viewable files and formats. These datasets listed in Table 13.1, identified by the USC Molecular Imaging Center as necessary files for long-term archiving and/or distribution to their investigators, were selected for evaluation of the MIDG. In this evaluation, only native DICOM (images and formats able to be converted to DICOM were used (see Table 13.1).

Table 13.1 Preclinical Molecular Imaging File Formats Collected for Evaluation from USC Molecular Imaging Center.

	MicroCAT	**MicroPET**	**PET-CT**	**Optical Imaging**	**US**	**Autoradiography**
Acquisition	CAT	LST	–	TIFF	–	TIFF
	CAT.HDR	LST.HDR		TXT		ANA

Post-Processing	IMG	IMG	DCM (PET)	–	–	–
	IMG.HDR	IMG.HDR	DCM (CT)			
Distributed	DCM	DCM	JPG	PNG	DCM	TIFF
	PDF		XIF	PDF	TIFF	PDF
			XLS		AVI	
			PDF		PDF	

13.4.3 MIDG Performance Evaluation

Initial tests of the MIDG can be done by measuring the time it takes to download collected sample datasets into the MIDG. The measured time for uploading a study dataset starts when users click on the “Submit” button in the Web-based user interface, and ends when all selected study files have been received and marked as completed by the metadata catalog service. This completion signifies that the uploaded study has been successfully processed and moved to its storage destination in the MIDG, and is available for download. The amount of time it takes to copy imaging datasets from modality WS to the shared study folder on the GAP server was not measured, because it does not differ from the existing archiving methods.

The measured time for downloading a study dataset starts when users click on the “Download” button in the Web-based user interface, and ends when an FTP link to the zipped study file appears on the Web-based user interface. Initial test results for one study from each of the five modality types are shown in Table 13.2.

Table 13.2 Performance tests measuring the time it takes to archive and retrieve a study dataset from six different preclinical molecular imaging modality types over a 100 mbps network.

	MicroCAT	**MicroPET**	**PET-CT**	**Optical Imaging**	**US**	**Autoradiography**
# of Files in Animal Scan	461	63	3	4	3	2
Total Size	130 MB	2 MB	206	105 KB	578	8.9 MB

			KB		KB	
Failures	none	none	none	none	none	none
Collisions	none	none	none	none	none	none
Archiving Time (m:ss)	5:18	0:35	0:10	0:14	0:12	0:22
Retrieval Time (m:ss)	1:56	0:14	0:05	0:04	0:06	0:07

From these initial performance tests, qualitative results and quantitative performance times can be seen for all six preclinical modality types. The qualitative results are based on success of transmission of the sample datasets, both to and from the MIDG. Testing scenarios include simultaneous uploading and downloading events to test for potential collision handling. Upon refinement of the MIDG system, all sample datasets used in the evaluation were able to be archived and retrieved without failure or colliding traffic. The average length of time for retrieval was half the time it took for archiving the same dataset. The modality types with a few DICOM files had a performance time under half a minute, whereas larger scan datasets such as the 461 DICOM files in a microCAT scan took upwards of 5 minutes to archive and 2 minutes to retrieve for download.

13.4.4 Current Status and the Next-Generation MIDG based on IHE XDS-i Profile

The current MIDG system supports all DICOM file formats; its performance is as shown in Table 13.2. Although DICOM compliance in the MIDG creates a standardized image output that makes preclinical molecular imaging data more accessible to external user software, the challenge to standardize all data formats in preclinical molecular imaging is inevitable. Also, even if to convert all non-DICOM file formats, such as proprietary raw acquisition files from the microCAT modality, and AVI videos from the ultrasound modality is possible, the conversion process is a tedious and time-consuming task. Thus, improving the user-level and core-level middleware of the molecular data grid architecture is necessary. The next chapter introduces an innovative technology—“Medical Imaging sharing for collaborative healthcare based on IHE-i developed for clinical radiology informatics application”—as a means of supporting non-DICOM files across the WAN to alleviate the drawback of the MIDG methodology described in this chapter [23,24].

13.5 Discussion

13.5.1 Comparing Existing Data Grids in Healthcare Informatics

Over the past decade in healthcare, there have been a handful of national and international efforts to realize grid-based systems in biomedical research involving imaging data, such as Europe's ActionGrid and United States' Biomedical Informatics Research Network (BIRN) [20,21]. The difference between the MIDG and these existing methods is in its application and project scope. The MIDG applies data grid technology to preclinical molecular imaging facilities, a specific biomedical imaging research community that has not been addressed before. Furthermore, the scope of MIDG is focused on small communities of preclinical molecular imaging researchers, centered around a few, if not only one, preclinical molecular imaging facility and its affiliated investigator institutions. The scope of the MIDG is purposely kept small to enable comprehensive customization for study metadata and supported file formats, and to empower preclinical molecular imaging facilities to become imaging cores with accessible historical datasets. Nonetheless, a common theme in these grid-based projects is the need for data standardization, user-interfaces, metadata databases, grid-based data delivery, and extendable infrastructure for multiple sites [22]. The MIDG takes these challenges into consideration, and creates a unique preclinical molecular imaging informatics infrastructure with a workflow, data model, and user interfaces that can readily be integrated into larger scoped initiatives such as BIRN in the future.

13.5.2 Comparing Current Solutions in Preclinical Molecular Imaging Informatics

Previous work at other preclinical molecular imaging facilities has been done to facilitate preclinical molecular imaging workflow by developing Web-based data management interfaces for staff and investigative users within their respective institutions. At UCLA's Crump Institute for Molecular Imaging, a Web-based interface is implemented on campus for investigators to schedule scan sessions in advance and request their own datasets to be made available on university-wide file servers [9]. The physical data archive consists of network file servers that organize datasets under individual investigator folders. At Case Western Reserve University, a Web-based multi-modality multi-resource information integration (MIMI) system has been developed to integrate staff, investigator,

and data workflows. Its functionality ranges from scheduling, to data cataloging, to billing. The MIMI system also has a database for documenting user, equipment, project, and billing information. However, they also tackle archiving and retrieval using share file servers and investigative folders [6]. Retrieval of data files from these previous informatics solutions remains institutionalized and investigator centric. Thus, off-campus access, contribution, and discovery of new or historic preclinical molecular imaging datasets are discouraged with current storage infrastructure [8]. As the value of interinstitutional collaboration and the volume of molecular imaging data generated in preclinical trials increases, the need for multi-institutional data sharing infrastructure and study-centric data management is becoming more relevant. The MIDG stands up to these challenges.

13.6 Summary

Data grid technology is an integrative informatics platform that has been used in many research arenas for organizing and sharing large datasets among collaborating institutions. Preclinical molecular imaging facilities can become imaging cores within a multidisciplinary research community, such that medical investigators, basic sciences researchers, and medical imaging engineers can discover, contribute, and manage preclinical molecular imaging data remotely. This chapter presents the MIDG to demonstrate a novel method for archiving and disseminating preclinical molecular imaging data. A multi-modality data model was defined, and the system architecture of the MIDG was presented. A three-site research test-bed within the University of Southern California, to evaluate the MIDG system based on data provided by the USC Molecular Imaging Center, has been deployed [23]. Initial evaluation has been performed in VMware environment to measure quantitative performance times for archiving and retrieving imaging study datasets from the MIDG. By building upon features and services of grid technology, and DICOM imaging standards and IHE workflow profiles, the accessibility of disparate animal-model molecular imaging datasets by users outside a molecular imaging facility’s LAN can be improved. Productivity of research for translational sciences investigators are thereby improved through streamlining experimental dataflow.

Acknowledgments

This chapter is contributed by Dr Jasper Lee and his colleagues while he was

completing his PhD degree at USC. The National Institute of Biomedical Imaging and Bioengineering, NIH awarded the T32 Training Grant #EB004308 to the IPILab, USC, which supported Lee's research.

References

1 de Kemp, R.A., Epstein, F.H., Catana, C., *et al*. (2010) Small-animal molecular imaging methods. *J Nucl Med*, 51(Suppl 1), 18S–32S.

2 Jakobovits, R., Soderland, S., Taira, R., *et al*. (2000) Requirements of a Web-based experiment management system. *AMIA Annual Symposium Proceedings*, pp. 374–378.

3 Massoud, T. and Gambhir, S. (2003) Molecular imaging in living subjects: seeing fundamental biological processes in a new light. *Genes & Development*, 17(5), 545–580.

4 Yang, J., Yang, M., Arabnia, H. and Deng, Y. (2008) Genomics, molecular imaging, bioinformatics, and bio-nano-info integration are synergistic components of translational medicine and personalized healthcare research. *BMC Genomics*, 9(Suppl 2), I1.

5 Molecular Imaging Center, Department of Radiology, Keck School of Medicine, University of Southern California, Los Angeles, CA. http://mic.usc.edu Accessed June 20, 2010.

6 Szymanski, J. (2008) An integrated informatics infrastructure for pre-clinical research-IT support, unpublished PhD thesis, Case Western Reserve University.

7 Peng, H. (2008) Bioimage Informatics: a new area of engineering biology. *Bioinformatics*, 24(17), 1827–1836.

8 Anderson, N., Lee, E., Brockenbrough, J., *et al*. (2007) Issues in biomedical research data management and analysis: needs and barriers. *Journal of the American Medical Informatics Association*, 14. 478–488.

9 Stout, D.B., Chatziioannou, A.F., Lawson, T.P., *et al*. (2005) Small animal imaging center design: the facility at the UCLA Crump Institute for Molecular Imaging. *Mol Imaging Bio*, 7(6), 393–402.

10 Yang, Y., Tai, Y.C. and Siegel, S. (2004) Optimization and performance

evaluation of the microPET II scanner for *in vivo* small-animal imaging. *Phys Med Biol*, 49(12), 2527–2545.

11 Swedlow, J.R. and Eliceiri, K.W. (2009) Open source bioimage informatics for cell biology. *Trends Cell Biol*, 19(11), 656–660.

12 Foster, I. and Kesselman, C. (1999) *The Grid: Blueprint for a New Computing Infrastructure*. Massachusetts: Morgan Kaufmann, pp. 259–278.

13 Huang, H.K. (2008) Utilization of medical imaging informatics and biometrics technologies in healthcare delivery. *Int J CARS*, 3, 27–39.

14 Huang, H.K., Zhang, A., Liu, B.J., *et al*. (2005) Data grid for large-scale medical image archive and analysis. *Proceedings of the 13th* ACM *International Conference on Multimedia*, pp. 1005–1013.

15 Foster, I., Kesselman, C., Nick, J. and Tuecke, S. (2002) The Physiology of the Grid: An Open Grid Services Architecture for Distributed Systems Integration. Globus. www.globus.org/alliance/publications/papers/ogsa.pdf Accessed July 17, 2009.

16 DICOM Standard. http://medical.nema.org/ Accessed April 14, 2010.

17 Globus Toolkit (2006) Data Management: Key Concepts. Globus. http://www-unix.globus.org/toolkit/docs/4.0/data/key/index.html Accessed September 18, 2009.

18 Estrella, F., Hauer, T., McClatchey, R., *et al*. (2007) Experiences of engineering grid-based medical software. *Int J Med Inform*, 76(8), 621–632.

19 Vmware, Inc. http://www.vmware.com/products/server/ Accessed June 20, 2010.

20 Maojo, V. and Tsiknakis, M. (2007) Biomedical informatics and health grids: a European perspective. *IEEE Engineering in Medicine and Biology Magazine*, 26(3), 34–41.

21 Biomedical Informatics Research Network (2009) About: Overview. http://www.birncommunity.org Accessed October 20, 2009.

22 Flanders, A.E. (2009) Medical image and data sharing: are we there yet? *RadioGraphics*, 29(5), 1247–1251.

23 Lee, J., Documet, J., Liu, B.J., Park, R., Tank, A. and Huang, H.K. (2011) MIDG-emerging grid technologies for multi-site preclinical molecular imaging research communities. *Intern J Comp Asst Rad & Surg*, 6, 285–296.

24 Lee, J., Zhang, J., Park, R., Grant, D., Liu, B. and Huang, H.K. (2012) A DICOM-based 2nd generation molecular imaging data grid implementing the IHE XDS-I integration Profile, *Intern J Comp Asst Rad & Surg*, 7, 533–545.

PERPUSTAKAAN PRIBADI AN-NUR SUNARYA

14
A DICOM-Based Second-Generation Molecular Imaging Data Grid (MIDG) with the IHE XDS-i Integration Profile

CHAPTER MENU

14.1 Introduction

14.1.1 Concept of the Second-Generation MIDG (Molecular Imaging Data Grid)

14.1.2 Preclinical Molecular Imaging Workflow of the Second-Generation MIDG

14.1.3 MIDG System Overview

14.2 Methodology

14.2.1 Second-Generation MIDG

14.2.2 Service-Oriented Design Architecture Based on OGSA Principles

14.2.3 Implementation of IHE XDS-i in the MIDG

14.2.4 Rules-Based Backup of Studies to Remote Storage Devices within the MIDG

14.3 System Implementation

14.3.1 Multi-Center Connectivity and the Three Site Test-bed

14.3.2 Evaluation

14.3.3 Hardware Requirements

14.3.4 Software Requirements

14.3.5 Network Bandwidths

14.4 Data Collection and Normalization

14.4.1 Data Collection

14.4.2 Data Normalization

14.5 System Performance

14.5.1 Upload Performance
14.5.2 Download Performance
14.5.3 Fault Tolerance
14.6 Data Transmission, MIDG Implementation, Workflow and System Potential
14.6.1 Data Transmission Performance within the MIDG
14.6.2 Implementing the MIDG
14.6.3 Improved Molecular Imaging Research Workflow
14.6.4 System Potential
14.7 Summary
14.7.1 The USC Second-Generation MIDG
14.7.2 Comparing Existing Data Grids in Healthcare Informatics
14.7.3 Comparing Current Preclinical Molecular Imaging Informatics Methods
14.7.4 Future Research and Development Opportunities in MIDG
14.7.5 Future Research and Development Opportunities
Acknowledgments
References

Chapter 13 presented the concept and methodology of the molecular imaging data grid (MIDG) to demonstrate a novel method for archiving and disseminating preclinical molecular imaging data. DICOM compliance in the MIDG creates a standardized image output that makes preclinical molecular imaging data more accessible to external user software. However, the challenge to standardize all data formats in preclinical molecular imaging is inevitably insurmountable. This chapter describes a second-generation MIDG replacing the Globus Toolkit with new system architecture by inserting the Integrated Healthcare Enterprise (IHE) cross-enterprise document sharing for imaging (XDS-i) integration profile. Implementation and evaluation were conducted using a three-site interdisciplinary test-bed at the University of Southern California (USC).

The second-generation MIDG design architecture replaces the initial design's Globus Toolkit with dedicated Web services and XML-based messaging for

dedicated management and delivery of multimodality DICOM imaging datasets. The XDS-i integration profile from the field of enterprise radiology informatics was adopted into the MIDG design, because streamlined image registration, management, and distribution dataflow are likewise needed in preclinical imaging informatics systems, as in enterprise PACS application. Implementation of the second-generation MIDG was demonstrated at the USC Molecular Imaging Center (MIC) and two other campus sites with specified hardware, software, and network bandwidth.

Evaluation of the MIDG involves data upload, download, and fault-tolerance testing scenarios, using multi-modality animal imaging datasets collected at the USC MIC. The upload, download, and fault-tolerance tests of the MIDG were performed multiple times using 12 collected animal study datasets. Upload and download times demonstrated reproducibility and improved real-world performance. Fault-tolerance tests showed that automated failover between Grid Node Servers has minimal impact on normal download times.

By first building upon the 1st generation concepts and experiences, the second-generation MIDG system improves accessibility of disparate animal-model molecular imaging datasets to users outside a molecular imaging facility's local-area-network (LAN), using a new architecture, data flow, and dedicated DICOM-based management Webservices. Productivity and efficiency of preclinical research for translational sciences investigators has been further streamlined for multi-center study data registration, management, and distribution.

14.1 Introduction

An MIDG was developed at the USC in 2009 to address the lack of systems integration in the animal imaging research community for archiving and disseminating the growing volume of diverse animal imaging studies. Although animal imaging facilities have various ways to archive and disseminate their investigator's datasets, data management techniques at many current facilities rely on network storage devices that are limited in data management solutions due to non-standardized preclinical data formats and inefficient data delivery methods with limited user access control [1,2].

At modern animal imaging research facilities, such as the UCLA Crump Institute for Molecular Imaging, workflow management solutions are in place to automate post-processing of raw image files between on-site software

workstations (WSs). However, storage and distribution of these datasets is kept internally on secure storage area network (SAN) devices, where facility staff managers organize datasets under investigator named folders. Similar archiving servers are set up at Stanford's Molecular Imaging Program (MIPS). Off-site investigators needing access to these file servers must create a virtual private network (VPN) account with the university, which can be tedious to maintain and slow in file transmission across wide area networks (WAN). Even with on-campus access to these file servers, investigative data search functionality is primarily limited to primary investigator names and experiment dates, owing to the lack of captured study metadata. The specific informatics challenges addressed by this first-generation MIDG were standardization of preclinical data objects, capturing unstructured study metadata, and seamless data distribution methods [3].

14.1.1 Concept of the Second-Generation MIDG (Molecular Imaging Data Grid)

This chapter presents a second-generation MIDG, with a revised data distribution method based on the IHE XDS-i integration profile (see Chapter 7). In the first MIDG design, sophisticated data management services were a challenge to develop without more detailed process monitoring and error handling. In addition, implementation required that all nodes in an existing MIDG had to be updated whenever a new site joined, because security certificates and destination mappings were not centrally managed. Lastly, preliminary laboratory tests revealed unacceptable upload and download times of common imaging study datasets. The second-generation MIDG replaces the first generation's open source software, the Globus Toolkit [4], with DICOM-compliant file management web-services to reduce system complexity and optimize dataflow performance for registration, management, and delivery of preclinical imaging studies. Evaluation of this second-generation MIDG design has been performed at the USC using a multi-center test-bed.

14.1.2 Preclinical Molecular Imaging Workflow of the Second-Generation MIDG

The preclinical imaging workflow is a 10-step process that begins with study design planning between investigators and a preclinical imaging facility, and ends with data distribution of imaging and analysis results for research. The complete molecular imaging workflow is shown in Figure 14.1, with steps that

require user interaction with the MIDG via the MIDG's graphical user interface (GUI), colored in gray (compared with steps 2, 7, 9) and in orange (step 8) in Figure 13.3 of Chapter 13).

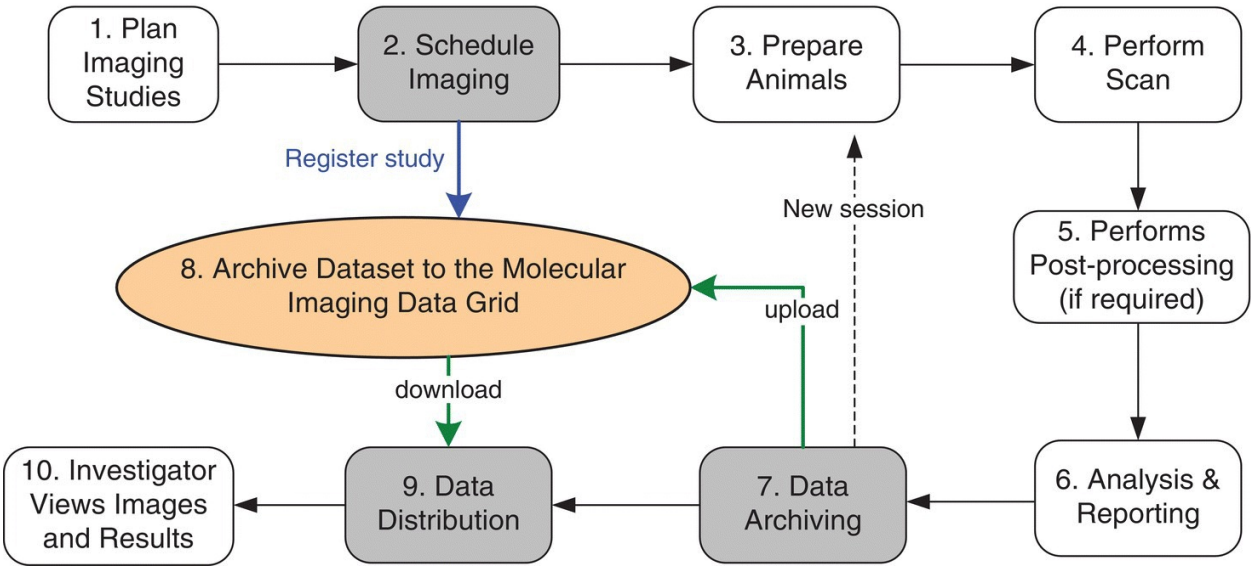

Figure 14.1 Preclinical molecular imaging workflow with steps that require user interaction with the MIDG identified in gray.

Once study subjects and protocols are identified in step 1 of Figure 14.1, investigators can schedule one or more scans with the imaging facility via the MIDG GUI. In steps 7 and 8, physical imaging files are uploaded and archived into the MIDG. Then in step 9, the preclinical datasets can be retrieved by authorized investigators at any MIDG site using the search and download feature of the MIDG GUI.

Data privacy for each study is handled by assigning users specific access to a study in step 2. Consequently, users of the MIDG can only upload data in step 7 to studies and download studies in step 9 that they have been given access to in step 2.

14.1.3 MIDG System Overview

The MIDG is a data management solution that captures structured metadata and catalogues incoming imaging files in a standardized DICOM format [5], the de facto file format of medical imaging files for radiology. The MIDG automatically converts incoming JPEG, BMP, TIFF, and PDF files to metadata-enriched DICOM files before archiving to physical storage, so that users can query and retrieve their preclinical data directly at their site. The distributed

connectivity of an MIDG is demonstrated in Figure 14.2 via an interdisciplinary three-site example. The four hardware components making up the MIDG system design are the MIDG GUI Web-servers, Grid node servers, storage devices (lower right), and a centralized grid management server (middle).

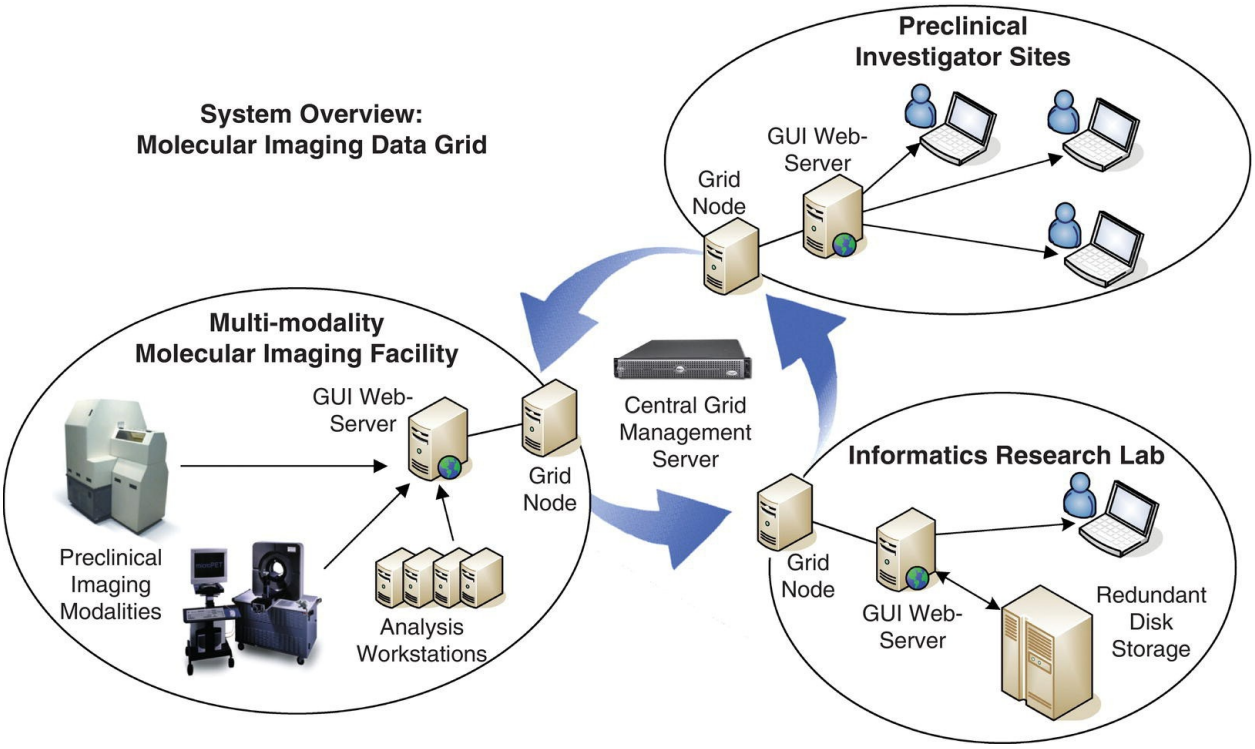

Figure 14.2 MIDG system overview. A molecular imaging facility typically has multiple animal model imaging modalities and works with investigators to perform imaging studies. An informatics research laboratory typically has robust computational hardware and services that may provide additional data and computational infrastructure for a molecular imaging facility. Preclinical investigators at remote sites connect with these sites via the MIDG to collaborate and utilize preclinical imaging data resources (compare with Figure 13.4 in Chapter 13).

A Web-based user interface enables multiple simultaneous users at each site's LAN to utilize the MIDG. Furthermore, user computers on the same LAN as the GUI Web server can copy-and-paste imaging studies to and from their personal computers for upload and download, respectively. Investigators at a MIDG site connect to their local GUI Web server via the web browser on their user WS to upload, monitor, download, and manage their preclinical imaging study datasets. Investigators can download studies from the MIDG onto their own computers as physical DICOM files, organized within series folders. Then, using DICOM-

compliant software, investigators can open these DICOM files for display and analysis.

14.2 Methodology

14.2.1 Second-Generation MIDG

The second-generation MIDG still adheres to the industry defined open grid services architecture (OGSA) principles [6], but it now implements architecture and dataflow based on radiology's Integration the Healthcare Enterprise (IHE) XDS-i. A major difference in the second-generation MIDG design is the replacement of the Globus Toolkit with a DICOM-handling infrastructure built using Web services. Performing a study registration, replication, or retrieval no longer requires DICOM middleware to make a call to the Globus Toolkit for file delivery responsibilities. Furthermore, the DICOM metadata database and file localization databases are now a single database, leading to fewer and less complex database queries. Finding all metadata relevant to a study, including its physical storage location within the MIDG, is now done in a single filtered query. This centralized architecture culminates in a more extensible design that can support system-wide processes monitoring and rules-based data backup policies.

To improve performance, multi-threaded delivery of up to five images per instance maximizes the use of bandwidth for large imaging studies such as CT, while also avoiding time-consuming and computationally intensive compression requirements of the first-generation MIDG, which zips up an entire DICOM series into one deliverable file. Another feature that improves performance is centralized queue handling, which enables prioritization and load balancing of simultaneous incoming requests based on requests from the grid node server. In summary, customized Web-services, integrated databases, centralized queue handling, faster file delivery mechanism, improved automated backup, and high-level data management services all work together to improve upon the first-generation MIDG.

14.2.2 Service-Oriented Design Architecture Based on OGSA Principles

The concept of service-oriented design involves the distinct separation of loosely coupled tasks that are relatively autonomous in logic, stateless in relation to each

other, and reusable for different tasks [7]. The first official OGSA document was distributed in early 2005 by authoring members of the Global Grid Forum and was utilized in many applications of grid-based research [8]. As shown in Figure 14.3, the second-generation MIDG architecture's gateway, grid-middleware, and resources layers have been reconciled into a single package that is implemented with Java J2EE Web services interacting with one another over SOAP messaging protocol (SOAP), XML document encoding, and Web Services Definition Language service definitions (compare with Figure 13.6A in Chapter 13). The second-generation MIDG architecture embodies the grid concepts set forth by the OGSA, to enable design extensibility and interoperability of services.

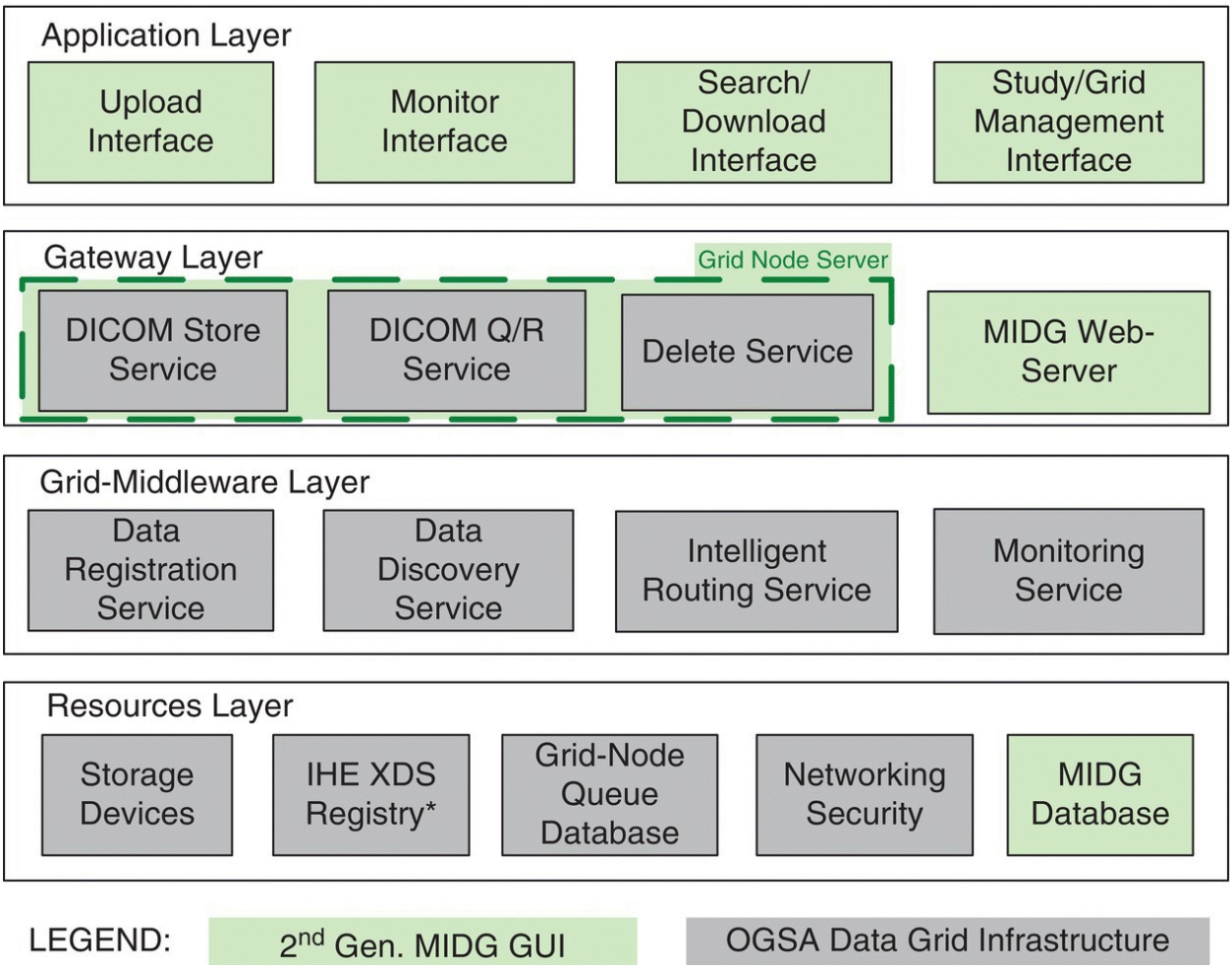

Figure 14.3 Second- generation MIDG software architecture with new OGSA data grid infrastructure.

14.2.3 Implementation of IHE XDS-i in the MIDG

The XDS-i integration profile from the field of enterprise radiology informatics

was adopted into the MIDG design, because streamlined image registration, discovery, and delivery dataflow are likewise needed in preclinical imaging informatics systems [9,10]. In 2005, the IHE defined the XDS-i integration profile to specify a methodology for registration, discovery, and delivery of medical image data between vendor-agnostic imaging systems in enterprise healthcare environments (see Chapter 7) [11]. As with its other integration profiles in the radiology framework, the IHE XDS-i profile is an industry supported model promoting interoperability between healthcare systems and sites. The second-generation MIDG infrastructure implements the XDS-i workflow, handling preclinical imaging datasets in fewer steps and with fewer components than the previous MIDG design based on the Globus Toolkit.

The MIDG workflow for uploading and downloading medical imaging data between a data providing site, central archiving registry, and a data consuming site is shown in Figure 14.4. The figure's components represent actors specified in the IHE XDS-i integration profile and the red boxes depict how these actors are represented by MIDG hardware components (Figure 14.2). The arrows mark the interactions between these components, starting with imaging datasets being sent into the imaging document source, grid node server "A". Note that the patient identity source component in the XDS-i profile is not covered in the MIDG design, because investigator identities are expected to be consistent across all participating MIDG sites, and do not need to be normalized to a global patient identifier such as in enterprise radiology environments. The GUI components of the MIDG design are not depicted in Figure 14.4, because it is a high-level application not within the scope of the IHE XDS-i integration profile.

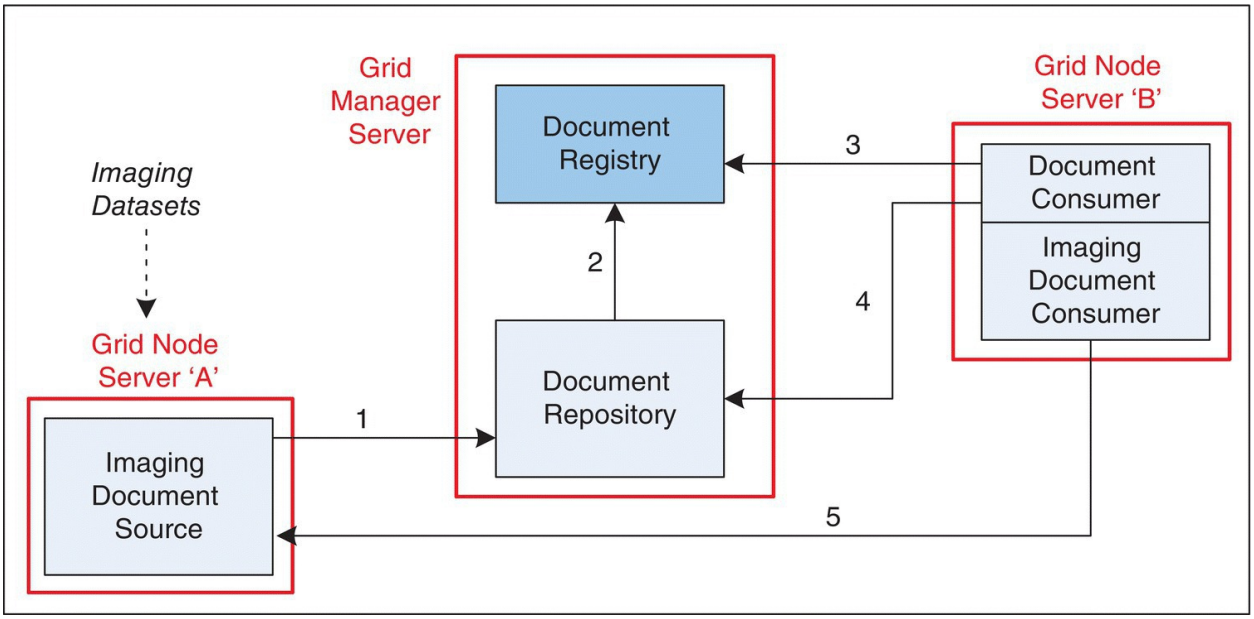

Figure 14.4 MIDG implementation of the IHE XDS-i integration profile. Red boxes highlight the MIDG hardware components.

Uploading imaging datasets is carried out in workflow steps 1 and 2 of Figure 14.4. When preclinical imaging datasets are uploaded to a grid node server A as a DICOM imaging study from a MIDG GUI Web server, grid node server A sends a SOAP message containing the incoming DICOM study's textual metadata as an XML document to the grid manager server's data registration service, represented by the document repository. The received XML document is then parsed and entered into the XDS registry database that also resides on the grid manager server.

Downloading imaging datasets is carried out in workflow steps 3, 4, and 5 of Figure 14.4. When DICOM query and retrieve requests for a particular study dataset are sent to grid node (see Chapter 7) server "B" from an MIDG Web-Server, the DICOM query/retrieve service on grid node server B queries the document registry database on the Grid Manager server for instances of XML documents describing that particular molecular imaging study. Returned XML documents in step 4 tell the DICOM query/retrieve service where to retrieve imaging files corresponding to the particular study of interest. In step 5, grid node server B initiates a GridFTP transfer on grid node server A via the SOAP message to deliver the requested files back to itself, the acting imaging document consumer.

14.2.4 Rules-Based Backup of Studies to Remote Storage Devices within the MIDG

The grid manager server has an intelligent routing service that is configured for multi-site backup purposes and long-term data storage migration. An intelligent routing service triggered by a rule "X" initiates replication of molecular imaging files from grid node server A to grid node server B, which registers the received files back to the grid manager server via a SOAP message. If rule X in the intelligent routing service is a migration event for long-term storage, then a delete request is then sent to the delete service on grid node server A to remove the original file(s) that were replicated to grid node server B. This separation of data registration services and data backup services means less computational load during the initial data upload process at the grid node servers, and timely backup event scheduling at the central grid manager server.

14.3 System Implementation

14.3.1 Multi-Center Connectivity and the Three Site Test-bed

The purpose of the multi-center MIDG implementation at the USC is to demonstrate application and feasibility of the MIDG design in a real-world test across a WAN region with variable network bandwidth.

14.3.1.1 The Three Site Test-Bed

The three sites in the MIDG multi-site model are the USC MIC, located on the USC Health Sciences Campus; the IPILab, located at the USC Annenberg Research Park; and the Ultrasound Transducer Resource Center (UTRC), part of the Department of Biomedical Engineering, located on the USC main campus, shown in Figure 14.5.

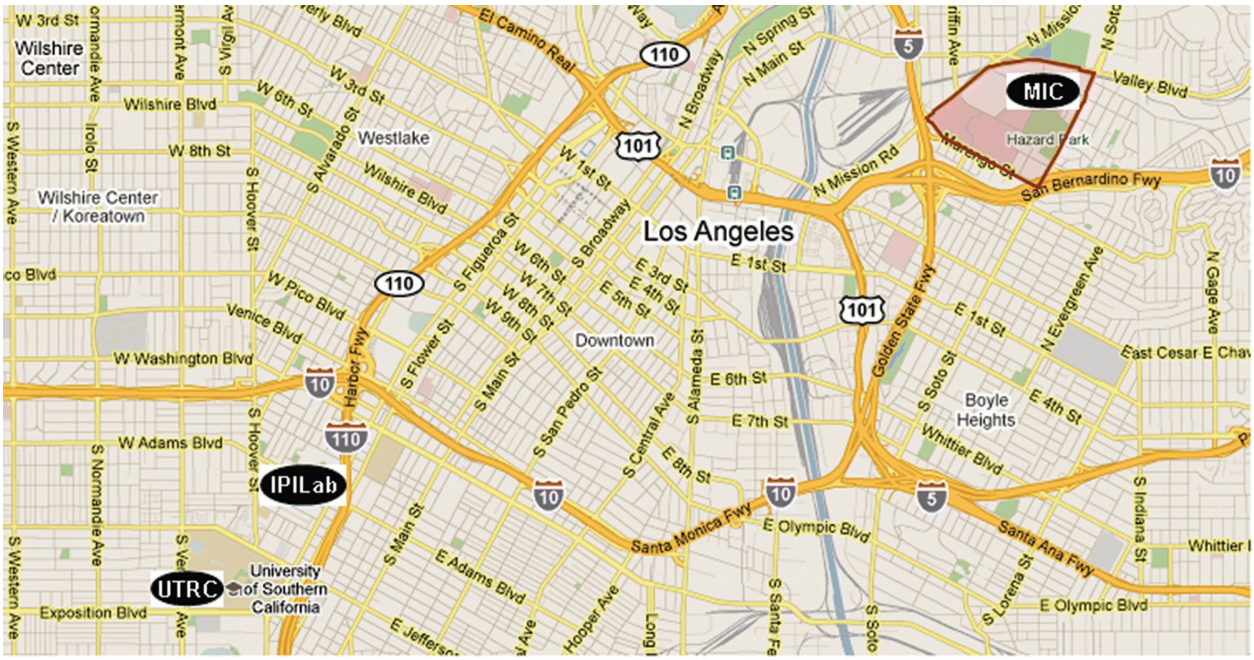

Figure 14.5 Geographic location of the three USC sites are the IPILab, MIC, and UTRC sites participating in the multi-site MIDG Evaluation Model. Map provided by Google.

14.3.1.2 USC Image Processing and Informatics Lab (IPILab)

The USC IPILab is the informatics research and development site behind the MIDG system. With experience in medical informatics projects, ranging from a

PACS simulator to a web-based ePR solution for multimedia data in surgical suites, colleagues at the IPILab have the knowledge and resources to establish the MIDG management site for the multi-site MIDG implementation. The central grid manager server and MIDG database is hosted in a dedicated server facility with adequate facility, backup power supply, and high-speed network bandwidth for efficient data transmission.

14.3.1.3 USC Molecular Imaging Center (MIC)

The USC Molecular Imaging Center is a multi-modality molecular imaging (MIMI) facility, with trained staff and dedicated imaging systems to help research into molecular imaging and personalized medicine for the future clinical environment. Available imaging modalities to investigators include the Siemens MicroPET R4, Siemens MicroCAT II, Xenogen IVIS 200 optical imaging system, VisualSonics Vevo 770 ultrasound system, and Faxitron MX-20 autoradiography system (see Chapter 13, Figure 13.1). Each modality is operated by trained staff using dedicated software on the accompanying WS for image acquisition, post-processing, image display, and certain quantitative image analysis. Every month, the MIC receives an average of five new experimental studies from investigators inside and outside of the USC and generates an estimated 1 terabyte of data per year. In this MIDG multi-site implementation, the MIC site represents the primary imaging data provider and its users help upload collected sample datasets during the evaluation scenarios.

14.3.1.4 USC Ultrasound Transducer Resource Center (UTRC) at the Biomedical Engineering (BME) Department

The UTRC is located in the BME Department, a building with many biomedical research laboratories ranging from medical device prototyping to medical image processing research. The UTRC is an ultrasound transducer research lab conducting research, fabrication, and training on ultrasound transducer design in medical imaging applications for academic investigators and outside private institutions. The UTRC is an exemplary remote molecular imaging research site that can contribute animal research data to the MIDG and benefit from a multi-site MIDG infrastructure and data-sharing research community. In this implementation of the multi-site MIDG model, a grid node server and MIDG web-server at the UTRC is set up to simulate how an investigator at a remote imaging research institution can download and contribute molecular imaging data from their computer with a simple laptop computer.

14.3.2 Evaluation

The multi-center MIDG evaluation steps are:

1. Upload molecular imaging studies to the MIDG from the MIC site, in order to measure study upload performance. In addition to the total time for archival, three sub-process times are also measured: data format conversion to DICOM; transmission of dataset files across WAN; and registration of studies into the central XDS-i repository on the grid manager server at the IPILab.
2. Download the newly uploaded molecular imaging studies from a remote site, the IPILab, to measure study retrieval time across the WAN. This download is performed on the investigator WS at the IPILab via the MIDG GUI.
3. Download the same molecular imaging studies a second time, again at the IPILab, to compare WAN and LAN download performances. After step 2, the IPILab's grid node server has a local copy.
4. Shutdown the IPILab's grid node server to simulate a failure of a data-providing site within the MIDG. Then, attempt to download the studies at a third site, the UTRC, to validate and test MIDG download failover. The total time to download at the UTRC's investigator WS determines whether a delay occurs when one of two data source sites fails (IPILab's grid node server) or becomes unavailable prior to a download attempt at a third data-consuming site.

14.3.3 Hardware Requirements

The hardware used in the multi-center MIDG implementation at USC is shown in Figure 14.5 and includes two Dell PowerEdge 2970 servers, two Dell Dimension 9150 desktop PCs, and a Dell Vostro PC. The central grid manager server is hosted at the USC IPILab on a Dell PowerEdge server, the grid Node Server is hosted on the second Dell PowerEdge server, and the GUI Web server is hosted on a Dell Dimension PC. At the MIC and UTRC sites, VMware [12] was used to consolidate the grid node server and GUI Web server onto a single hardware PC for ease of deployment. The three simulated investigator WSs at these sites are browser-enabled PCs with LAN connectivity to their site's GUI Web server.

14.3.4 Software Requirements

Setting up the MIDG requires installation of prerequisite software and databases. Both the grid manager server and each grid node server require a Java application server to host their Web services and database. The GUI Web server requires Apache2 with hypertext preprocessor support, and a PostgreSQL database. The grid node servers require the application server to host Web services, including the DICOM request and data handling, as well as an MySQL database for process queue handling and local configurations. The grid manager server requires the application server to host Web services, which interact with an Oracle database, to implement XDS-i registry services, rules-based data management services, and process monitoring and fault-tolerance services.

14.3.5 Network Bandwidths

The optimal data transfer speed between remote sites is determined by the limiting upload and download bandwidths at the data provider and consumer sites, respectively. An understanding of the actual bandwidths at the three USC sites may provide insight into the results of the distributed multi-site MIDG evaluation. Figure 14.6 shows the measured WAN bandwidth for each site and also the theoretical LAN bandwidth between grid node server and GUI Web server. Note that the LAN bandwidth was not quantitatively measured at this time, and is susceptible to innate overhead of gigabit switches and VMware hardware virtualization.

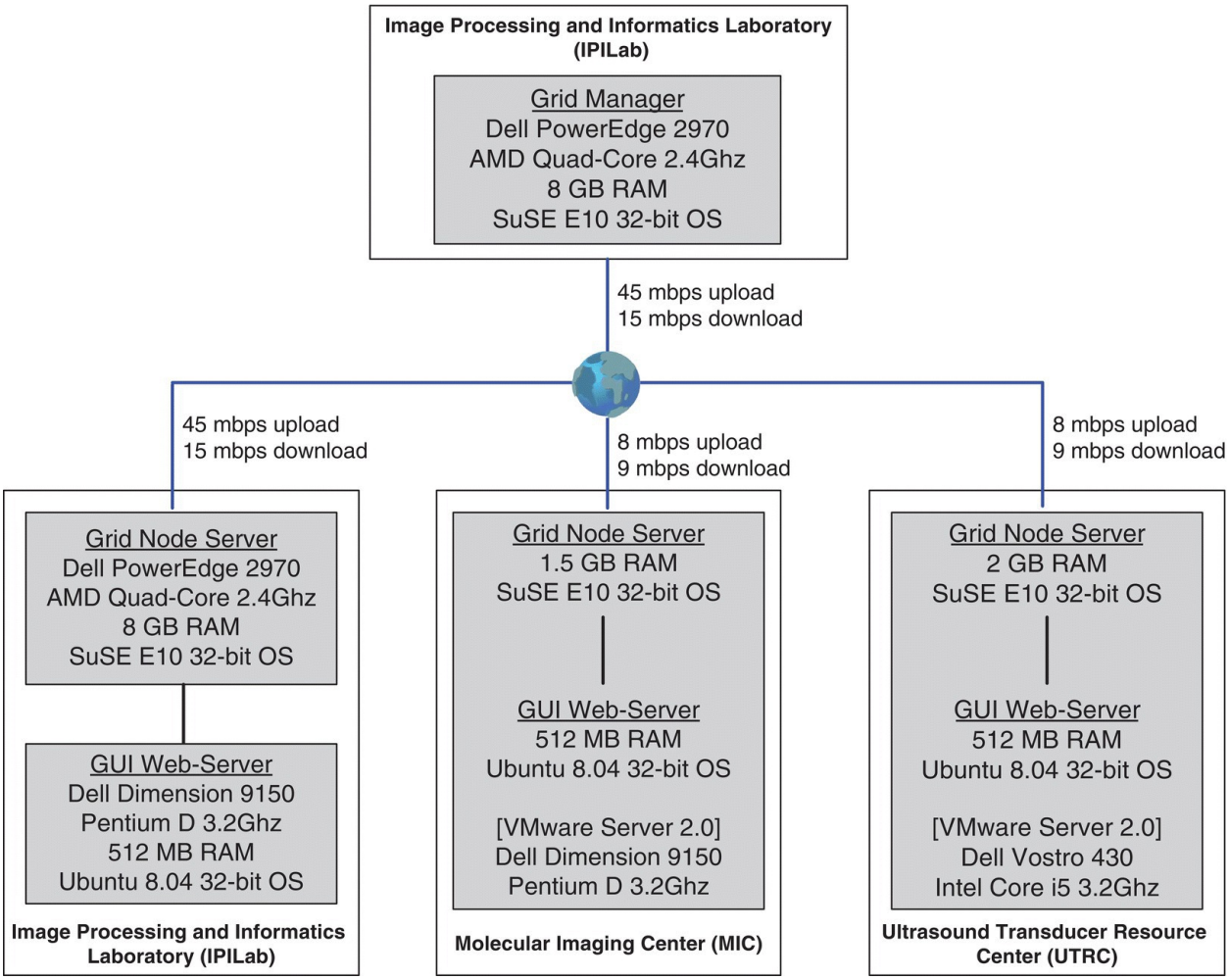

Figure 14.6 Network bandwidth in the three-site MIDG evaluation implementation.

14.4 Data Collection and Normalization

14.4.1 Data Collection

Preclinical imaging studies from six modalities were collected from the USC MIC to evaluate the three-site MIDG implementation [1]. Table 14.1A lists these 12 study datasets with relevant metadata, forming a basis for later discussion of file transfer speed results. Dataset sizes depend on a variety of factors, such as modality type, animal type, animal region of -interest (ROI), file format, number of files, and image resolutions. Note that due to the availability of the IHE XDS-I, an important column named DICOM SOP class (column 4) was systematically introduced to specify the type of DICOM object being created by the MIDG's DICOM standardization process. A list of DICOM tags that are labeled by the

MIDG during the upload process demonstrates the completeness of DICOM data in the MIDG using the IHE XDS-I integration profile. Table 14.1B lists and describes the DICOM tags that are modified by the MIDG GUI Web server before being archived to a grid node server.

Table 14.1 (A) Molecular imaging datasets systematically collected for evaluation from the USC MIC. (SOP: Service-Object Pair; SC: Secondary Capture).

Study Name	Modality Type	Original Formats	DICOM SOP Class	No. of Files	Total Dataset Size
CT 1	MicroCT	DICOM-CT	CT	461	130 MB
CT 2	MicroCT	DICOM-CT	CT	480	138 MB
Pet 1	MicroPET	DICOM-PET	PET	63	2.09 MB
Pet 2	MicroPET	DICOM-PET	PET	63	2.09 MB
PETCT 1	Co-registered MicroPET/CT	JPEG	SC	3	216 KB
PETCT 2	Co-registered MicroPET/CT	JPEG	SC	11	1.20 MB
OPT 1	Optical	TIFF	SC	4	914 KB
OPT 2	Optical	TIFF	SC	5	2.97 MB
US 1	Ultrasound	DICOM-US Multi-Frame	Multi-Frame	1	44.9 MB
US 2	Ultrasound	TIFF	US	3	6.6 MB
AR 1	Autoradiography	TIFF	SC	1	8.38 MB
AR 2	Autoradiography	TIFF, BMP, JPEG	SC	4	10 MB

Table 14.1 (B) List of DICOM tags that are labeled by the MIDG during the upload process.

DICOM Tag	Tag ID	VR	Description
Media Storage SOP Class UID	0002,0002	UI	Same as SOP Class UID
Transfer Syntax	0002,0010	UI	Supported Transfer Syntax:

			[Implicit VR Little Endian = 1.2.840.10008.1.2] [Explicit VR Little Endian = 1.2.850.10008.1.2.1] [Explicit VR Big Endian = 1.2.840.10008.1.2.2] [JPEG Baseline, 1.2.840.10008.1.2.4.50] [RLS Lossless = 1.2.840.10008.1.2.5]
SOP Class UID	0008,0016	UI	Supported SOP Classes: [SC Image = 1.2.840.10008.5.1.4.1.1.7] [CT Image = 1.2.840.10008.5.1.4.1.1.2] [PET Image = 1.2.840.10008.5.1.4.1.1.128] [US MF = 1.2.840.10008.5.1.4.1.1.3.1] [MR Image = 1.2.840.10008.5.1.4.1.1.4]
SOP Instance UID	0008,0018	UI	SeriesUID.FileID
Study Date	0008,0020	DA	Study Date, in the form of yyyymmdd
Series Date	0008,0021	DA	Session Date, in the form of yyyymmdd
Accession Number	0008,0050	SH	StudyUID without the periods in the middle.
Modality	0008,0060	CS	Modality Type Abbreviations: CT, PT, OPT, US, AR
Manufacturer	0008,0070	LO	Modality Manufacturer Name
Institution	0008,0080	LO	Investigator's Institution
Referring Physician	0008,0090	PN	Investigator's Full Name
Study Description	0008,1030	LO	Study Description
Series Description	0008,103E	LO	Scan Comments
Department	0008,1040	LO	Investigator's Department
Operators' Name	0008,1070	PN	Imaging Technician's Full Name
Model Name	0008,1090	LO	Modality Manufacturer's Model Name
Patient Name	0010,0010	PN	Animal Subject's Name
Patient ID	0010,0020	LO	Investigator ID
Patient Sex	0010,0040	CS	Animal Subject’s Sex, M or F (has to be

			uppercase)
Patient Age	0010,1010	AS	Animal Subject's Age, nnnD, nnnW, nnnM, nnnY
Patient Weight	0010,1030	DS	Animal Subject's Weight in kg
Patient Species Description	0010,2201	LO	Animal Type (e.g. mouse, rabbit, etc.)
Clinical Trial Committee	0012,0081	LO	Clinical Trial Protocol Ethics Committee Name = IACUC
Clinical Trial Approval Number	0012,0082	LO	Clinical Trial Protocol Ethics Committee Approval Number
Exam Part	0018,0015	CS	Animal Imaging ROI, Body Part
Contrast Agent	0018,0010	LO	Radiopharmaceutical Biomarker (ex. FDG)
Study ID	0020,0010	SH	Same as Accession Number
Study UID	0020,000D	UI	1.2.StudyID
Series UID	0020,000E	UI	StudyUID.ScanID (note: sessionID and groupID are not accounted for)

14.4.2 Data Normalization

The MIDG Web-based GUI allows investigators to upload new imaging files into the MIDG as DICOM, JPEG, BMP, TIFF, or PDF formats (Column 4). The MIDG Web server then converts these file formats to DICOM with study metadata that has been entered for initial study registration (Figure 14.1). With similarities and differences between molecular imaging research and clinical radiology environments, mapping the molecular imaging study metadata to DICOM header tags, originally intended for patient studies, required some further customization. Nonetheless, the predefined DICOM unique identifiers (UID), such as service-object pair (SOP) Class UID and transfer syntax UID, remained in conformance with the DICOM standard.

Although only a few fields in the DICOM header are required for successful storage within the MIDG, additional preclinical study metadata is captured by the GUI's study registration process and inserted into the DICOM file for the benefit of searching. Deviating from the clinical DICOM data model, the "Referring Physician" tag has been allocated to the investigator's full name, because investigators play a synonymous role in requesting an imaging

examination. Furthermore, the investigator's ID was used in the "Patient ID" tag instead of an animal ID, because molecular imaging studies in research put little emphasis on individual animal models. In stark contrast with clinical radiology, where patients are the focus and owners of imaging studies, investigators are the owners of imaging studies and animals are simply tools in a study. Placing the investigator's ID into the Patient ID enables DICOM-compliant software to sort imaging studies by investigators rather than a multitude of different animal identifiers. The other patient-related tags, such as patient name and patient age, however, remain affiliated with the actual animal subject of the imaging scan. In summary, the DICOM data model adapted for preclinical imaging studies in the MIDG is a hybridization of investigator and animal subject metadata.

14.5 System Performance

14.5.1 Upload Performance

The 12 sample datasets listed in Table 14.1A were uploaded into the multi-center MIDG at the USC MIC site. Measurement of the upload process requires higher temporal resolution (Figure 14.7), so two microCT studies were used for its larger dataset sizes of 130 MB and 138 MB. Because the dataflow consists of three major steps, four time values were recorded during the upload process – data format conversion, file transmission, metadata registration, and total upload time. Over five repeated upload tests for the two microCT studies, the conversion, transmission, and registration process resulted in standard deviations of 1, 4, and 5 seconds, respectively. This 3% margin of variability in the total microCT upload times show that the MIDG upload process is reproducible.

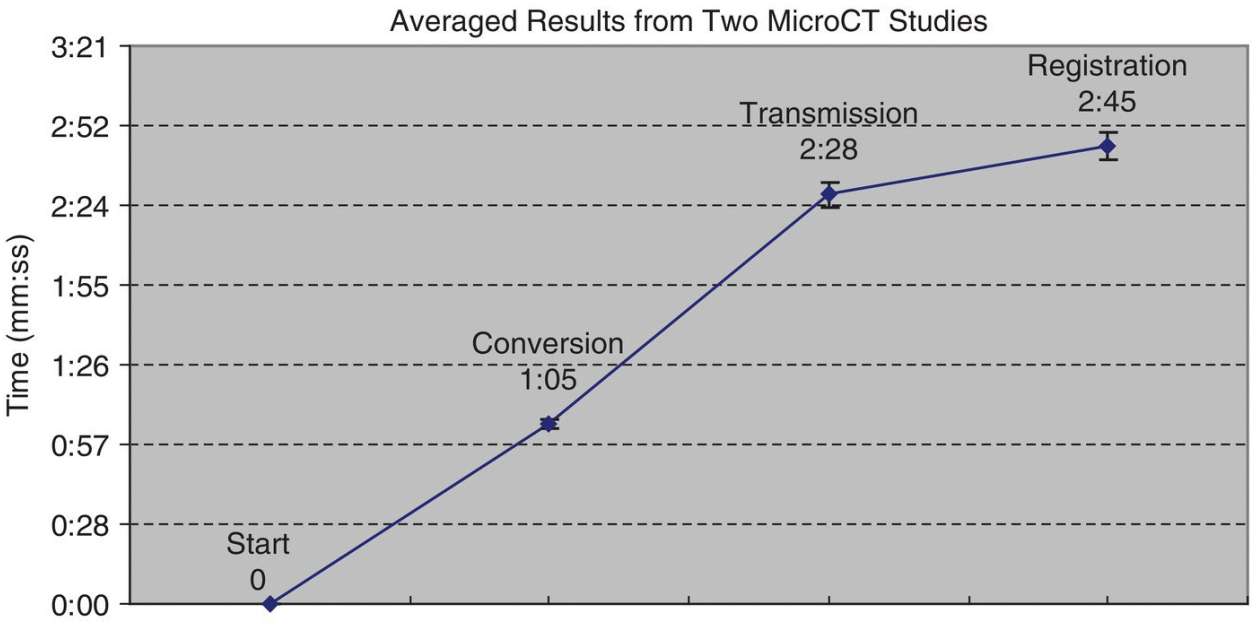

Figure 14.7 Upload performance in the MIDG for a microCT study of a rat animal model. Five repeated tests resulted in standard deviations of 1, 4, and 5 seconds for the conversion, transmission, and registration steps, respectively.

During the conversion step, incoming imaging files are converted to the DICOM format with proper study metadata inserted into the header fields. Then the transmission step sends the converted DICOM image files from the GUI Web server to the local grid node server via DICOM. This DICOM transmission step is initiated by a Java program on the GUI Web server, executing a "dcmsnd" command-line call provided by DCM4CHE to send all converted DICOM files [13]. Note in Figure 14.7 the transmission time for a 130 MB MicroCT study on a 100 mbps LAN took 1 minute and 23 seconds, which is significantly longer than the 10.4 seconds theoretically expected. Explanations for this experienced delay include hindered hardware and bandwidth performance due to hosting both virtual machines on a single desktop PC, DICOM communications overhead for each of the 460+ file transmissions, and record logging of all textual output from the dcmsnd command-line call.

Once arriving at the grid node server, its DICOM storage service constructs and sends a SOAP message to the grid manager's study registration Web service to register the files and location of the study. Note that the upload dataflow is almost entirely carried out over a site's LAN between user WSs, GUI Web server, and the local grid node server. Only during the registration step is a SOAP message sent over the WAN to the grid manager server.

Figure 14.8 shows the upload times for the remaining 10 study datasets for

comparison. With the exception of one ultrasound study, total upload times for these datasets did not exceed 10 seconds for datasets with a size of less than 10 MB. The ultrasound study “US 1” took 41 seconds to complete upload, because it was a large multi-frame DICOM file of 45 MB size. Variability in upload times between studies of comparable size and file count may be attributed to unrelated background processes running on the VMware server host computer at MIC.

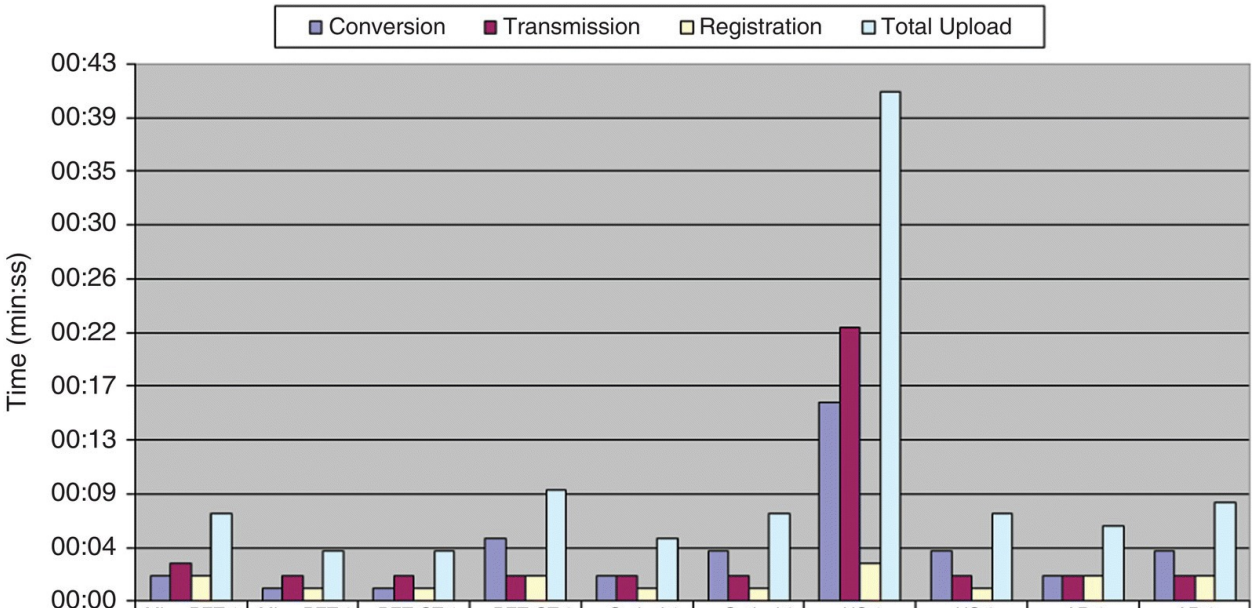

	MicroPET 1 2.09 MB 63 files	MicroPET 2 2.09 MB 63 files	PET-CT 1 216 KB 3 files	PET-CT 2 1.20 MB 11 files	Optical 1 914 KB 4 files	Optical 2 2.97 MB 5 files	US 1 44.9 MB 1 files	US 2 6.6 MB 3 files	AR 1 8.38 MB 1 files	AR 2 10 MB 4 files
Conversion	00:02	00:01	00:01	00:05	00:02	00:04	00:16	00:04	00:02	00:04
Transmission	00:03	00:02	00:02	00:02	00:02	00:02	00:22	00:02	00:02	00:02
Registration	00:02	00:01	00:01	00:02	00:01	00:01	00:03	00:01	00:02	00:02
Total Upload	00:07	00:04	00:04	00:09	00:05	00:07	00:41	00:07	00:06	00:08

Figure 14.8 Upload performance results for studies uploaded into the MIDG at the USC MIC site. Note that microCT datasets 1 and 2 were not incorporated due to unfavorable distortion of the timescale.

14.5.2 Download Performance

To evaluate data retrieval across the WAN, the study datasets previously uploaded to the MIC site were downloaded to the IPILab using the MIDG GUI. The download dataflow has two major steps—localization and delivery of files from a source grid node server to the requesting grid node server over gridFTP protocol, and then the DICOM sends these files to the MIDG GUI Web server over the DICOM C-Move protocol. However, the later step is inconsequential compared with the first if the requested dataset is located at a remote site, and if the GUI Web server and grid node server are deployed on a single VM host

server with 100 mbps internal bandwidth. In the download results shown in Figure 14.9, each dataset was retrieved twice to compare data retrieval over the WAN with data retrieval over the LAN. The first download attempt for each study ranged from 46 seconds to 1 minute and 27 seconds, taking significantly longer than the second attempts, because delivery of datasets required localization, initiation, and transmission across the WAN. The second attempts were faster by a magnitude of 10 for most, because studies were being retrieved over the LAN from the grid node server to the GUI Web server.

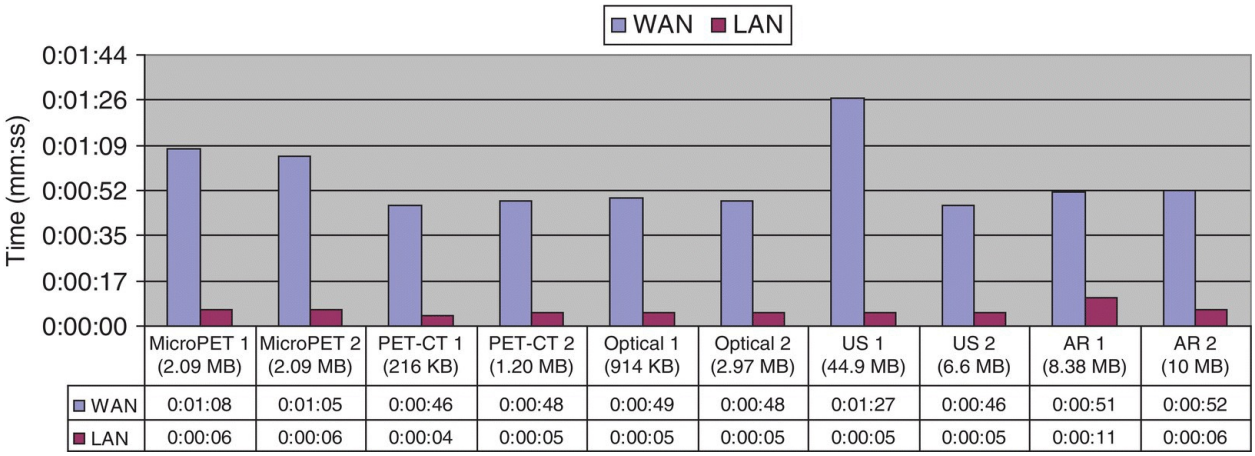

	MicroPET 1 (2.09 MB)	MicroPET 2 (2.09 MB)	PET-CT 1 (216 KB)	PET-CT 2 (1.20 MB)	Optical 1 (914 KB)	Optical 2 (2.97 MB)	US 1 (44.9 MB)	US 2 (6.6 MB)	AR 1 (8.38 MB)	AR 2 (10 MB)
WAN	0:01:08	0:01:05	0:00:46	0:00:48	0:00:49	0:00:48	0:01:27	0:00:46	0:00:51	0:00:52
LAN	0:00:06	0:00:06	0:00:04	0:00:05	0:00:05	0:00:05	0:00:05	0:00:05	0:00:11	0:00:06

Figure 14.9 Download performance results for studies downloaded from the MIDG at the USC IPILab site. See Figure 14.6 for Internet and WAN speed bandwidth.

14.5.3 Fault Tolerance

To evaluate the failover mechanism of the MIDG, there must be at least two copies of a dataset in the three-site MIDG implementation. At this point in the evaluation, that requirement is met, because the 12 datasets are available on both the MIC and IPILab's grid node servers. Fault tolerance was tested by downloading a 130 MB microCT study at the USC UTRC site, through the UTRC's GUI Web server. Three download tests were performed to simulate different scenarios: normal, grid node server failure, and data corruption. After each attempt, the UTRC's grid node server was cleared of all local studies, so that datasets must be re-retrieved from a remote site over the WAN. The first scenario established the normal baseline performance without simulated failure. The second scenario simulated failure of a remote grid node server by shutting down the MIC's grid node server before attempting to download the microCT study at the UTRC. The third scenario simulated data corruption by manually deleting the MIC's local study files before attempting to download the microCT

at the UTRC. The results, shown in Figure 14.10 demonstrate that failure at the grid node server has minimal impact on overall download times, but missing or corrupted datasets required additional detection services that delay remote download times at a third MIDG site by 1 minute 50 seconds.

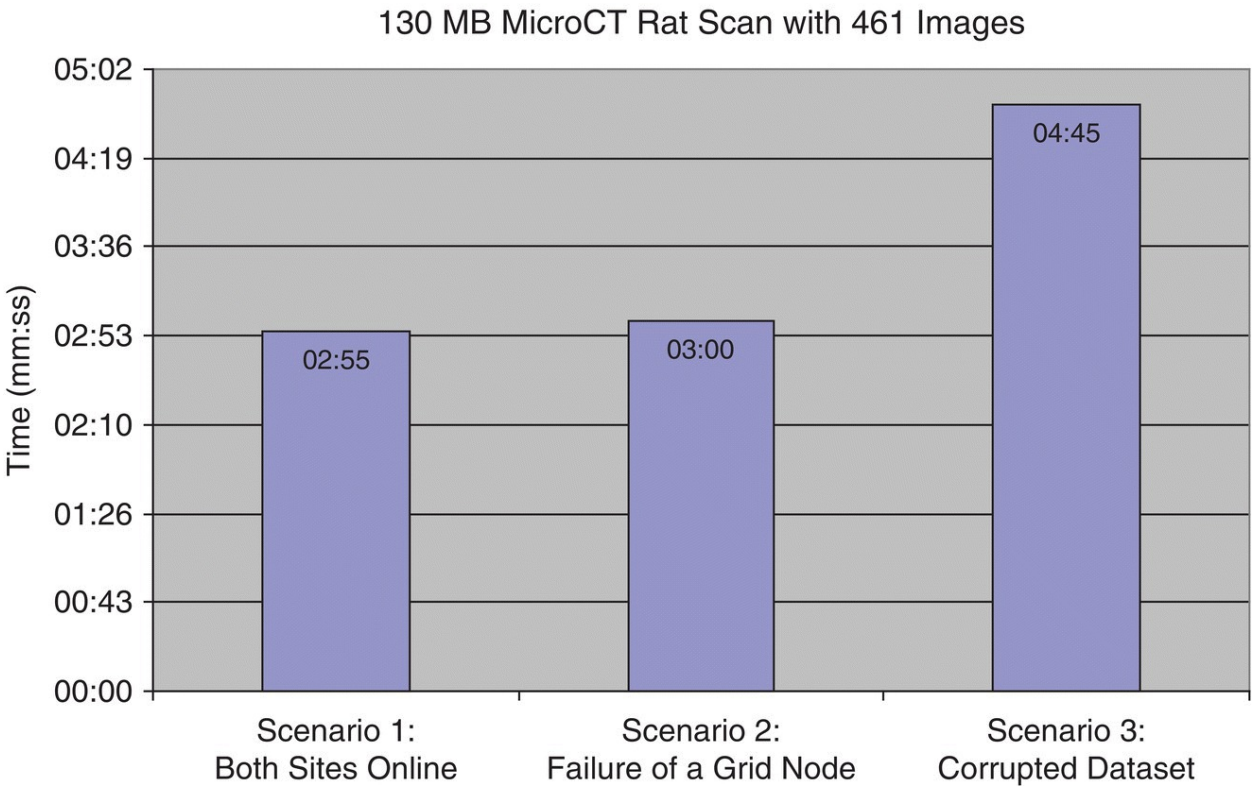

Figure 14.10 Fault-tolerance results for a microCT study downloaded from the MIDG at the USC UTRC site.

14.6 Data Transmission, MIDG Implementation, Workflow and System Potential

14.6.1 Data Transmission Performance within the MIDG

The second-generation MIDG system demonstrates successful implementation and improved performance results over the first MIDG design. Table 14.2 shows a comparison of upload and download times for the same four studies, taking significantly less time in the second-generation MIDG system. For consistency, Table 14.2 measurements were all taken in a laboratory environment at the IPILab using the same LAN and hardware resources. The only negative percent change was seen in the download time of an autoradiography study at –57.1%.

Because these timed values are true measurements that often vary slightly between iterations, a possible explanation for this inconsistency is unspecified simultaneous background operations on the hardware that do not belong to the MIDG software.

Table 14.2 Comparison of upload and download performance of first- generation MIDG and second-generation MIDG, using datasets from four preclinical imaging modalities.

	MicroCAT	MicroPET	PET-CT	Autoradiography
No. of Files	461	63	3	2
Total Size	130 MB	2 MB	206 KB	8.9 MB
Upload (1st Gen.)*	5:18	0:35	0:10	0:22
Upload (2nd Gen.)	2:45	0:07	0:04	0:06
Upload Speedup	48.1%	80%	60%	72.7%
Download (1st Gen.)	1:56	0:14	0:05	0:07
Download (2nd Gen.)	0:11	0:06	0:04	0:11
Download Speedup	90.5%	57.1%	20%	–57.1%

*Measured times are shown in mm:ss format.

14.6.2 Implementing the MIDG

Implementing the second-generation MIDG at a molecular imaging facility requires installation of grid node servers and a grid manager server, and the integration of GUI Web server with any existing data storage device. Because the GUI Web server caches studies in a unique directory structure, it requires its own dedicated directory in the data storage device. The MIDG also requires configuration of the grid node servers and grid management server, because every molecular imaging facility has different modalities and data-archiving policies. Once these server configurations are completed, GUI parameters, such as supported modality types and available contrast agents, must be entered into the MIDG GUI, so that staff and investigators can begin registering new imaging studies into the MIDG. Figure 14.11 demonstrates the GUI configuration page, which is accessible to MIDG administrative users. Once the MIDG is implemented, historic imaging studies can be migrated into the MIDG by imaging staff or investigators via the registration and upload process in the MIDG GUI.

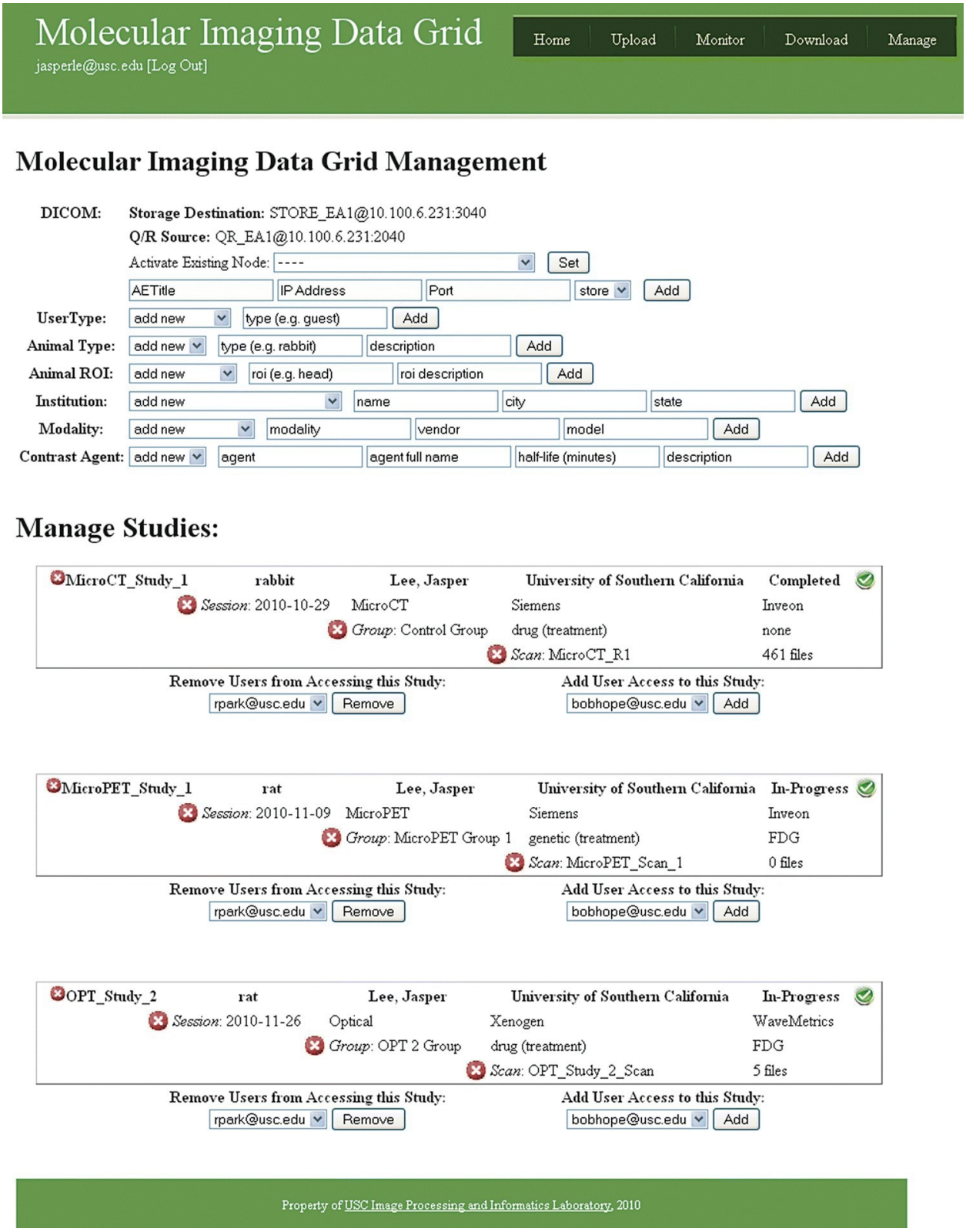

Figure 14.11 MIDG GUI: administrator's management page. In addition to the study management ability, administrators can add new fields or edit existing

fields for the interface.

14.6.3 Improved Molecular Imaging Research Workflow

The MIDG expedites data exchange in multidisciplinary research communities by handling the discovery, contribution, and management of imaging data for molecular imaging facilities, consequently providing time and cost savings for imaging staff and investigators. Secured access and transmission of study data across WAN to remote investigators relieves imaging facility staff from having to maintain and manage data dissemination, such as FTP user accounts or burning of DVDs. Investigators can now log in, search, and download their preclinical datasets from their local MIDG user interface without requesting it from the MIDG staff. Since distribution of imaging datasets to remote investigators is not a primary service of the preclinical molecular imaging facility, automating the data distribution process with the MIDG gives more time for imaging facility staff to conduct scans and also more time for investigators to analyze their preclinical data.

14.6.4 System Potential

The ability of the MIDG to catalogue and search imaging study data also has the potential to assist administrative operations as an imaging facility's workload and/or number of users increase. Often, the task of scheduling and billing a preclinical imaging study is complicated by non-centralized study information. With the MIDG, comprehensive preclinical study metadata can be recorded and accessed through a single user interface. The study monitoring capability of the MIDG GUI creates a summarized list of study metadata and completed datasets that can easily be exported as a PDF report page. The realizable benefits are general study planning and billing via the MIDG customized user-interface for molecular imaging facilities.

14.7 Summary

14.7.1 The USC Second-Generation MIDG

Data grid technology is an integrative informatics platform, which has been used in research for organizing and sharing large datasets among collaborating institutions and laboratories [3,14]. In this chapter, the second-generation MIDG demonstrates a novel method for archiving and disseminating preclinical molecular imaging data while complying with the DICOM imaging standard and

IHE XDS-i integration profile. The MIDG system architecture and multi-center interdisciplinary test-bed is designed and implemented to evaluate the MIDG system based on preclinical imaging datasets provided by the USC MIC. Evaluation has been performed to measure quantitative performance times for archiving and retrieving imaging study datasets from the MIDG. Building upon its first-generation design and technology, the second-generation MIDG improves accessibility of disparate animal-model molecular imaging datasets to users outside a molecular imaging facility's LAN with new workflow and dedicated DICOM-based management Web services. More detailed information of the second-generation MIDC can be obtained from Lee's dissertation [15]. Productivity and efficiency of preclinical research for translational sciences investigators is streamlined for multi-center study data registration, management, and distribution.

14.7.2 Comparing Existing Data Grids in Healthcare Informatics

Over the past decade in healthcare, there has been a handful of national and international efforts to realize grid-based systems in biomedical research involving imaging data, such as Europe's ActionGrid and the United States' Biomedical Informatics Research Network (BIRN) [16]. The difference between the MIDG and these existing methods is in its application and project scope. The MIDG applies a novel and unique data grid technology to preclinical molecular imaging facilities, a specific biomedical imaging research community that has not been addressed before. Furthermore, the scope of MIDG is focused on a cluster of preclinical molecular imaging researchers, centered around a few, if not one, preclinical molecular imaging facility and its affiliated investigator institutions.

The scope of the MIDG is purposely kept small to enable comprehensive customization for study metadata and supported file formats, and to empower preclinical molecular imaging facilities to become imaging cores with accessible historical datasets. Nonetheless, a common theme in these grid-based projects is the need for data standardization, user interfaces, metadata databases, grid-based data delivery, and extendable infrastructure for multiple sites [2]. The MIDG takes these challenges into consideration, and creates a unique preclinical molecular imaging informatics infrastructure with a workflow, data model, and user interfaces that can readily be integrated into larger scoped initiatives in the future.

14.7.3 Comparing Current Preclinical Molecular Imaging Informatics Methods

Previous work at other preclinical molecular imaging facilities has been done to facilitate preclinical molecular imaging workflow by developing web-based data management interfaces for staff and investigative users within their respective institutions. To name several, at UCLA's Crump Institute for Molecular Imaging, a Web-based interface is implemented on campus for investigators to schedule scan sessions in advance and request their own datasets to be made available on university-wide file servers [17]. The physical data archive consists of network file servers that organize datasets under individual investigator folders. At Case Western Reserve University, a Web-based MIMI system has been developed to integrate staff, investigator, and data workflows. Its functionality ranges from scheduling, to data cataloging, to billing. The MIMI system also has a database for documenting user, equipment, project, and billing information. However, it also tackles archiving and retrieval using share file servers and investigative folders [18]. Retrieval of data files from these previous informatics solutions remains institutionalized and investigator centric. Thus, off-campus access, contribution, and discovery of new or historic preclinical molecular imaging datasets are discouraged with current storage infrastructure [1]. As the value of inter-institutional collaboration and the volume of molecular imaging data generated in preclinical trials increases, the need for multi-institutional data sharing infrastructure and study-centric data management is becoming more relevant. The MIDG stands up for these challenges.

14.7.4 Future Research and Development Opportunities in MIDG

The next steps to further develop the second-generation MIDG are to continue evaluation of the multi-site MIDG model using live molecular imaging studies at the USC or other research MICs, to improve system robustness across all currently supported imaging data formats. Furthermore, affiliated molecular imaging research sites that consistently utilize the USC MIC may be added to the current three-site USC implementation, to form a larger molecular imaging research community and to promote collaboration and data-sharing outside of the USC community.

Development of the MIDG GUI and data grid infrastructure can also continue to address the concerns mentioned in the evaluations by the MIC staff. The current upload workflow in the GUI can be expedited using predefined templates for

common preclinical imaging studies, such that study, session, group, or scan descriptions do not have to be re-entered by users for multi-animal imaging experiments. The GUI can also be extended for scheduling and billing at molecular imaging facilities using its current metadata database. The data grid infrastructure can be further developed to address current limitations in data format support, namely raw image acquisition data files and proprietary post-processing files. By implementing an alternative data transfer protocol between the MIDG GUI Web server and grid node server, these non-DICOM files and its affiliated metadata can be archived into the MIDG.

14.7.5 Future Research and Development Opportunities

Another tangible parallel approach would be to utilize the existing technology of radiology PACS and the GUI component from the MIDG to bridge current clinical imaging vendors with preclinical research applications. The IPILab and MIC have received grant funding from the Los Angeles Basin Clinical and Translational Science Institute to pilot a feasibility project entitled, "Development of a novel imaging and informatics platform for translational small animal and molecular imaging research." The objectives are to build a DICOM conversion gateway with GUI capability that receives preclinical imaging datasets and stores them in an attached clinical PACS. The bigger picture is to prompt current PACS vendors to extend their market share and resources into molecular imaging research fields, which have similar imaging data content, study workflows, and billing procedures.

As presented in Chapter 1 (Ref. 16), grid technologies can be categorized into a data grid and a computational grid. With intensive image post-processing algorithms being used in preclinical molecular imaging research, the MIDG can be interfaced with a computational grid that exchanges pre- and post-processed imaging data from a remote site. Currently, there are many vendor-provided grid computing infrastructures that can run grid-based post-processing software, such as Amazon's Elastic Compute Cloud [19]. The MIDG GUI can be further developed as a Web portal that can automate post-processing requests between the MIDG and external grid computing infrastructures.

Moreover, although DICOM compliance in the MIDG creates a standardized image output of molecular imaging datasets for external DICOM-compliant distribution, analysis, and viewing software tools, the challenge of converting all input molecular imaging data files to DICOM may eventually be too complex, if not futile, if vendors persist in their proprietary data formats for raw acquisition

files. Modality, analysis, and post-processing software vendors in the molecular imaging field are gradually recognizing a need for vendor-agnostic interoperability of their output imaging data, but DICOM may not be the only standard format used in the future. For this reason, a future MIDG design may forego data format normalization responsibilities by replacing the DICOM converting middleware with direct uploading and downloading Web services. In this design, incoming and outgoing datasets will require a method other than DICOM to correlate study-centric metadata to its dataset of physical imaging files. A GUI will still be needed to input study, session, group, and scan information, but performance can be improved by consolidating the MIDG database with the grid manager database, and the MIDG Web server with each grid node server. The basic infrastructure and workflow will remain similar to the current MIDG design, but services regarding data context and processing will be optimized with XML-based manifest metadata files.

The data grid infrastructure of the MIDG can be utilized in other biomedical informatics applications such as the breast imaging data grid, which interconnects imaging data and radiologists from multiple breast cancer screening institutions to enable real-time tele-radiology diagnostics. As an example, the development of a Web-based electronic patient record (ePR) system for breast cancer screening patients with multiple breast imaging studies, including dedicated breast MRI, is being conducted. The concept is to integrate the ePR application layer interface with the DICOM-compliant data grid infrastructure used in the MIDG. Together, they comprise the breast imaging data grid electronic patient record for multimodality breast imaging studies (see Chapter 9, Sections 9.2.2 to 9.2.4).

Acknowledgments

This chapter was contributed by Dr Jasper Lee and his colleagues while he was completing his PhD degree at the USC. The National Institute of Biomedical Imaging and Bioengineering, NIH, awarded the T32 Training Grant #EB004308, and the Telemedicin and Advanced Technology Research Center (TATRC), US Army Medical Research and Materiel Command research Grant #2007011185 were awarded to the IPILab, USC, which supported Lee’s research.

References

1 Anderson, N., Lee, E., Brockenbrough, J., *et al*. (2007) Issues in biomedical

research data management and analysis: needs and barriers. *Journal of the American Medical Informatics Association*, 14, 478–488.

2 Flanders, A.E. (2009) Medical image and data sharing: Are we there yet? *RadioGraphics*, 29(5), 247–251.

3 Lee, J., Documet, J., Liu, B.J., Park, R., Tank, A. and Huang. H.K. (2011) MIDG-emerging grid technologies for multi-site preclinical molecular imaging research communities. *Intern J Comp Asst Rad & Surg*, 6, 285–296.

4 Foster, I. (2006) Globus Toolkit Version 4: software for service-oriented systems. *J. Comput. Sci. & Technol*, 21(4), 513–520.

5 NEMA (2009) DICOM Standard, Part 3: Information Object Definition. http://medical.nema.org/ Accessed July 15, 2009

6 Foster, I., Kesselman, C., Nick, J. and Tuecke, S. (2002) The Physiology of the Grid: An Open Grid Services Architecture for Distributed Systems Integration. Globus. www.globus.org/alliance/publications/papers/ogsa.pdf Accessed July 17, 2009

7 Erl, T. (2005) *Service-Oriented Architecture (SOA): Concepts, Technology, and Design*. New Jersey: Prentice Hall.

8 Foster, I., Kishimoto, H., Savva, A., *et al*. (2005) The Open Grid Services Architecture, Version 1.0. Global Grid Forum. http://www.gridforum.org/documents/GFD.30.pdf Accessed November 11, 2009.

9 Mendelson, D.S., Bak, P., Menschik, E. and Siegel, E. (2008) Image exchange: IHE and the evolution of image sharing. *RadioGraphics*, 28, 1817–1833.

10 Zhang, J., Zhang, K., Yang, Y., *et al*. (2010) Grid-based implementation of XDS-I as part of image-enabled EHR for regional healthcare in Shanghai. *Int J CARS*. doi: 10.1007/s11548-010-0522-8.

11 IHE (2006) Radiology Technical Framework Supplement 2005/2006. http://www.ihe.net/Technical_Framework/upload/IHE_RAD-TF_Suppl_XDSI_TI_2005-08-15.pdf Accessed October 12, 2010

12 VMware, Inc (2010) VMware Server: Getting Started with Virtualization Risk-Free. http://www.vmware.com/products/server/ Accessed October 25,

2010.

13 DCM4CHE (2008) Overview of DCMSND. http://www.dcm4che.org/confluence/display/d2/dcmsnd Accessed January 18, 2010

14 Lee, J., Zhang, J., Park, R., Grant, D., Liu, B. and Huang, H.K. (2012) A DICOM-based 2nd generation molecular imaging data grid implementing the IHE XDS-I integration Profile. *Intern J Comp Asst Rad & Surg*, 7, 533–545.

15 Lee, J. (2011) Molecular Imaging data grid (MIDG) for multi-site small animal imaging research based on OGSA and IHE XDS-i., PhD Dissertation, University of Southern California, May 2011.

16 Biomedical Informatics Research Network. About: Overview [cited October 30, 2009] Available from: http://www.birncommunity.org

17 Stout, D.B., Chatziioannou, A.F., Lawson, T.P., *et al*. (2005) Small animal imaging center design: the facility at the UCLA Crump Institute for Molecular Imaging. *Mol Imaging Bio*, 7(6), 393–402.

18 Szymanski, J. (2008) An Integrated Informatics Infrastructure for Pre-clinical Research-IT Support. Unpublished PhD Thesis, Case Western Reserve University.

19 Amazon Elastic Compute Cloud (Amazon EC2) [cited February 18, 2010] Available from: http://aws.amazon.com/ec2/

PERPUSTAKAAN PRIBADI AN-NUR SUNARYA

15
PACS-Based Archive Server and Cloud Computing

CHAPTER MENU

15.1 PACS-Based Multimedia Biomedical Imaging Informatics
15.2 PACS-Based Server and Archive
15.2.1 Image Management Design Concept
15.2.2 Functions of the PACS Server and Archive Server
15.2.3 RIS and HIS Interface
15.3 PACS-Based Archive Server System Operations
15.4 DICOM-Compliant PACS-Based Archive Server
15.4.1 Advantages
15.4.2 DICOM Communications in PACS Environment
15.4.3 DICOM-Compliant Image Acquisition Gateways
15.5 DICOM PACS-Based Archive Server Hardware and Software
15.5.1 Archive Hardware Components
15.5.2 Archive Server Software
15.6 Backup Archive Server and Data Grid
15.6.1 Backup Archive Using an Application Service Provider (ASP) Model
15.6.2 General Architecture
15.6.3 Data Recovery Procedure
15.7 Cloud Computing and Archive Server
15.7.1 Change of the PACS Climate
15.7.2 Cloud Computing
15.7.3 Cloud Computing Service Models and Cloud Storage
15.7.4 An Example of Using Cloud Storage for PACS Archive

15.7.5 Summary of Cloud Computing and Archive Server
Acknowledgements
References

PACS server and archive is a major component of PACS-based multimedia imaging informatics, whenever the HL7, DICOM standards, and Integrating the Healthcare Enterprise (IHE) are used in PACS-related components. The DICOM standard is reliable and is used in most PACS operations, regardless of whether manufacturers' PACS archive or vendor neutral archives (VNA) are used. This chapter reviews the fundamental PACS Server and the DICOM-compliant PACS archive server, and introduces cloud computing and the cloud server.

15.1 PACS-Based Multimedia Biomedical Imaging Informatics

The second edition of this text discusses the classical PACS server and archive data architecture design. The contents emphasize radiological images and text reports based on PACS. In addition, it also discusses the potential use of PACS technology to directly benefit other clinical specialties in addition to radiology. During the past 6–7 years, in addition to use radiological images and reports to help the diagnosis of their patients, other clinical departments also discovered that PACS technology can be directly utilized and imbedded into their daily clinical practices. Some successful examples, to name a few, are Pathology PACS [1], Multimedia electronic Patient Record (ePR) System in Radiation Therapy [2,3], Multimedia ePR System for Image-Assisted Spinal Surgery [4], DICOM-based Molecular Imaging Data Grid (MIDG) with the IHE XDS-i Integration Profile [5], Surgical PACS [SPIE, 2015 Medical Imaging Conference], integration of Computer-Aided Diagnosis (CAD) with PACS [6,7], CAD and Image-Guided Decision Support [6], Cardiac PACS Systems [American College of Cardiology, Meetings, 2012 and 2013], PACS-based Molecular Imaging [8], and others.

For this reason, the PACS and imaging informatics research discipline is gradually broadening to PACS-based multimedia biomedical imaging informatics. As a result, the term "PACS-based multimedia" is no longer constrained to text and radiological images, but also encompasses a new imaging informatics paradigm providing physicians and researchers with new tools based

on their clinical specialties and resources, to select and consolidate their preferred multimedia as a means to help their research, diagnose, and cure their patients.

The term “PACS-based multimedia” also means that any clinical specialist has the opportunity to extract and integrate the patient’s existing data, images, graphs, tables, reports, three-, four-, and five-dimensional images, movies, and scripts based on PACS-based technology to compose contents on a physician’s workstation (WS), as well as to view, diagnose, report, and archive. Multimedia can be recorded, played, displayed dynamically, and interactively accessed from information content processing devices such as computerized and electronic devices, as well as being part of a live performance. Multimedia devices are electronic media devices used to store and experience multimedia content, but distinguished from mixed media in fine art. By including audio, for example, it has a broader scope. The term “rich media” is synonymous with interactive multimedia.

Today, the majority of practicing physicians have experience in using PACS images and reports from certain medical Web servers and WSs to help them to care for their patients. Using the PACS technology platform, these multimedia PACS-based biomedical images and informatics can enrich the clinical specialist's ability to facilitate their patient care.

This chapter first reviews the basic concepts of PACS server and archive, followed by reiterating the meaning of DICOM medical imaging informatics, and the Web-based server in the PACS environment and image distribution. The last section introduces cloud computing and the cloud server as the emerging PACS-based multimedia biomedical informatics technology.

15.2 PACS-Based Server and Archive

This section discusses the PACS-based central node, the engine of the PACS which has two major components: the PACS server and the archive. The former, consisting of the hardware and software architecture, directs the data flow in the entire PACS by introducing inter-process communication. The latter provides a hierarchical image storage management system for short-, medium-, and long-term image archiving. Figure 15.1 shows the positions of the PACS server and archive in the PACS data flow. The connections of the PACS server and archive to the four major gateways are: i) the acquisition gateway, where images of and data about the patient originate; ii) application servers; iii) Web servers; and iv)

PACS WSs. These four gateways open up channels and connectivity for PACS-based technology to multimedia biomedical imaging informatics applications.

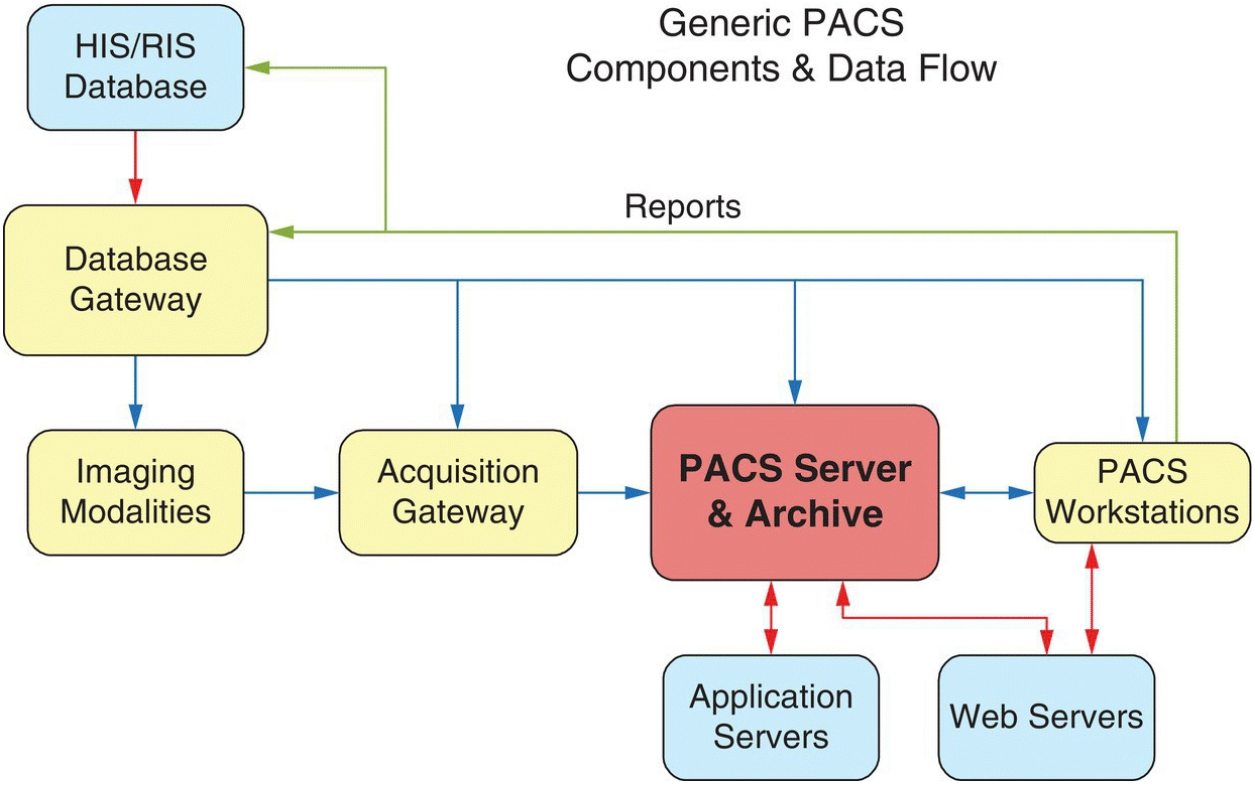

Figure 15.1 PACS basic components (red and yellow) and data flow (blue lines: within PACS; green and orange red lines: external between PACS and other information systems); HIS: hospital information system; RIS: radiology information system.

Section 15.2.1 describes the design concept and implementation strategy of the PACS central node (image management design concept), Section 15.2.2 presents functions of the PACS server and the archive server, and Section 15.2.3 describes the RIS and HIS interfaces to PACS. Section 15.3 presents the PACS archive server system operations. Section 15.4 shows the DICOM-compliant PACS archive server, and in Section 15.5, its hardware and software. Section 15.6 describes the concept of the backup archive server and the roles of the Data Grid. Section 15.7 introduces cloud computing and archive server.

15.2.1 Image Management Design Concept

Two major aspects should be considered in the design of the PACS image management and storage system: data integrity, which promises no loss of images and data once they are received from the PACS-based imaging systems;

and its operation efficiency, which minimizes access time of images display on the WSs.

15.2.1.1 Local Storage Management via PACS Intercomponent Communication

To ensure data integrity, the PACS always retains at least two copies of an individual image in separate storage devices, until the image has been archived successfully to the long-term storage device (e.g. an optical disk or tape library). Figure 15.2 shows the various storage systems used in the PACS. This backup scheme is achieved via the PACS intercomponent communication, which can be broken down as follows (Figure 15.1):

- *At the radiological imaging devices*: Images are not deleted from the imaging devices local storages until technologists have verified the successful archiving of individual images via the PACS connections. In the event of failure of the acquisition process or of the archive process, images can be re-sent from imaging devices to the PACS.
- *At the acquisition gateway computer*: Images in the acquisition gateway computer acquired from the imaging device remain in its local disk storage until the archive system has acknowledged to the gateway that a successful archive has been completed. These images are then deleted from the local disks residing in the gateway, so that storage space from these disks can be reclaimed.
- *At the PACS server and archive server*: Images arriving at the archive server from various acquisition gateways are not deleted until they have been successfully archived to the permanent storage. On the other hand, all archived images are stacked in the archive server's cache disks and will be deleted based on their aging criteria (e.g. number of days from when the examination had been performed; or discharge or transfer of the patient).
- *At the workstations (WS)*: In general, images stored in the designated WS will remain there until the patient is discharged or transferred. Images in the PACS archive can be retrieved from any WS via the DICOM query/retrieve (Q/R) command. In the thin client architecture, WS has no storage for images, so once the user has reviewed the images, they are deleted automatically.

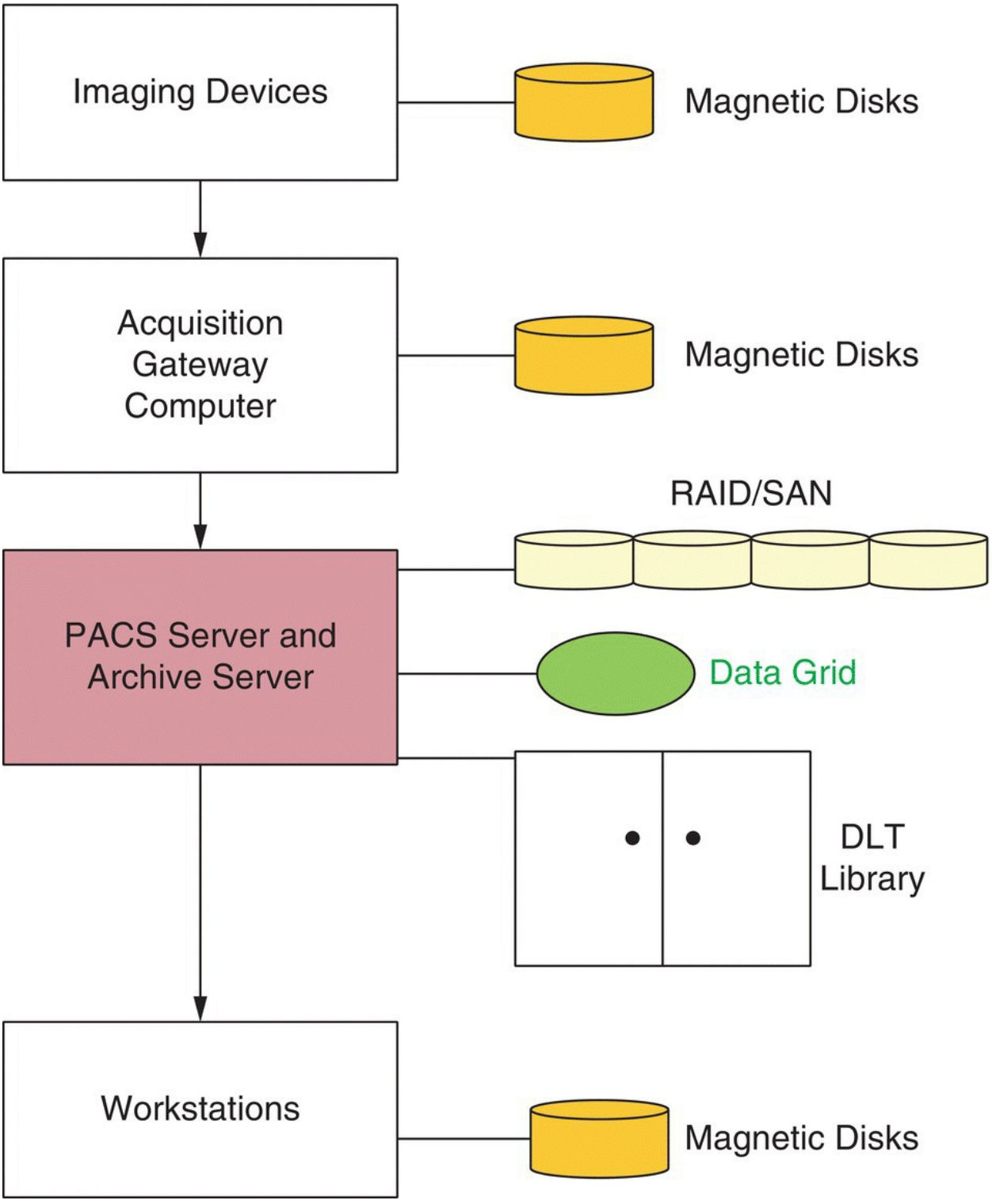

Figure 15.2 Hierarchical storage systems in PACS ensuring data integrity. Until an individual image has been archived in the permanent storage, such as by local archive digital linear tape (DLT) or Data Grid, two copies are retained in separate storage subsystems. DLT can be an archive system within the PACS;

Data Grid (green) is mostly external (see Chapters 8 and 9, which is most likely to be used as a tool in multimedia biomedical imaging informatics).

15.2.1.2 PACS Server and Archive System Configuration

The PACS-based server and the archive server consist of four components: i) an archive server; ii) a database; iii) a storage system (redundant array of inexpensive disks, RAID, storage area network, SAN, digital linear tape, DLT), an image library or connection to the external Data Grid); and iv) a communication network (Figure 15.3). Attached to the archive system through the communication network are various gateways and WSs. Images acquired through the gateways from various imaging devices are transmitted to the archive server, from where they are archived to the storage system and routed to the appropriate WSs. In the thin client model, WS has no storage, and all images reside in the storage system. Refer to Section 15.7 on the VNA, which is an emerging storage technology. First understanding the PACS basic storage infrastructure will facilitate the migration of the PACS archive system in the future.

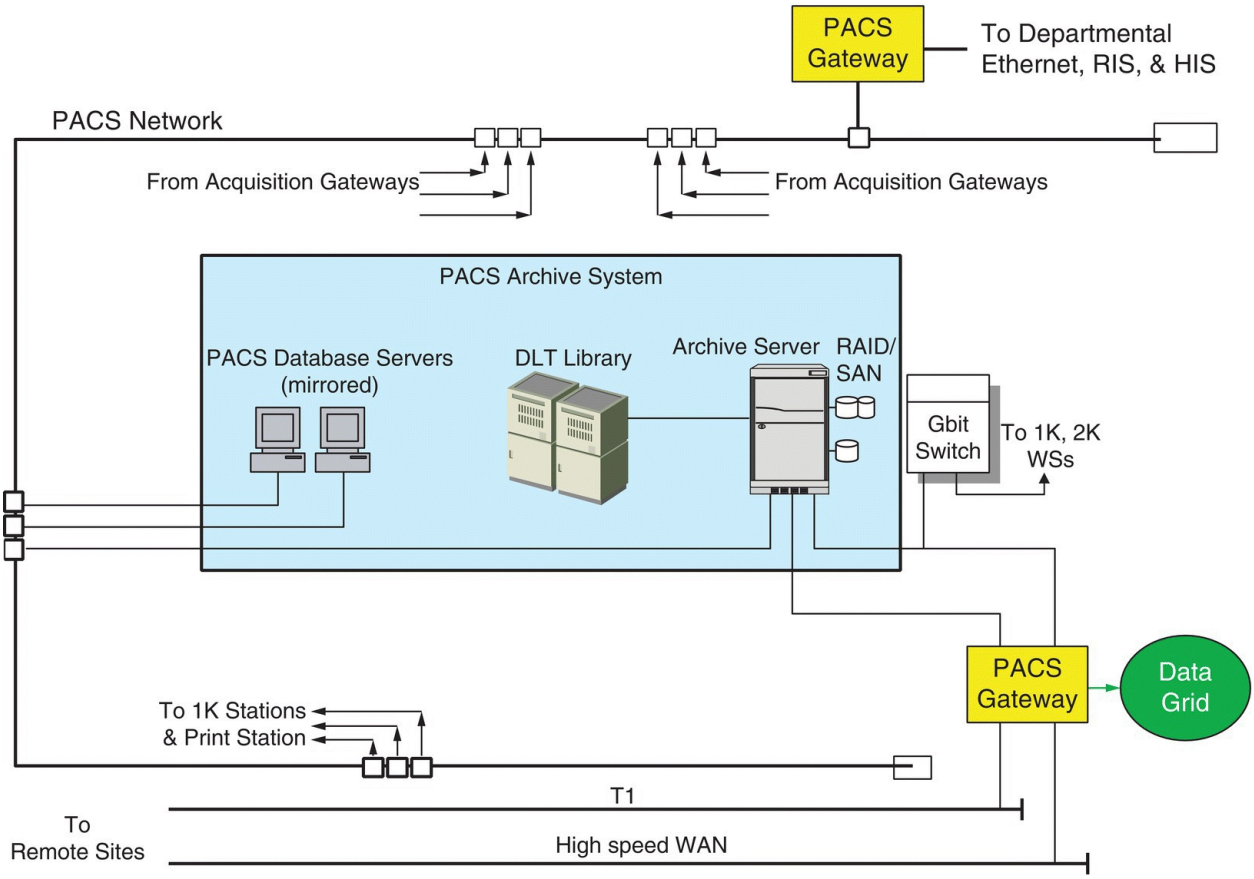

Figure 15.3 Configuration of the archive system and the PACS network. A DLT for permanent storage or the Data Grid (green, external connection) is used as an example. The archive server is connected to the DLT (light yellow) or the Data Grid (green) and a pair of mirrored database servers. Patient, study, and image directories are in the database, and images are stored in the DLT or externally in the Data Grid. A local Ethernet network connects all PACS storage components, and a high-speed Gbits/s switch (as an example) connects the archive server to 1 K and 2 K WSs, providing fast image display. In addition, the archive server is connected to remote sites via T1, high-speed WAN or high-speed Internet (bottom), the hospital information system (HIS), and the radiology information system (RIS) via departmental and campus Ethernet (top). The PACS gateway can also be connected to Data Grid (green, see Chapters 8 and 9). This figure is based on current PACS storage systems (refer to Section 15.7 on how to use the Cloud computing and archive service approach, vendor-neutral archive technology, gradually replacing the PACS systems).

15.2.1.2.1 The Archive Server

The archive server consists of multiple powerful central processing units (CPUs), small computer systems interface II (SCSII) data buses, and network interfaces (Ethernet and WAN). With its redundant hardware configuration, the archive server can support multiple processes running simultaneously, and image data can be transmitted over different data buses and networks. In addition to its primary function of archiving images, the archive server associated with the PACS server acts as a PACS manager, directing the flow of images within the entire PACS from the gateway to various destinations such as the archive, WSs, and print stations. The archive server uses its large-capacity array of inexpensive disks (RAID) as a data cache, capable of storing several months' worth of images acquired from different imaging devices. For example, a small 20-GB disk, without using compression, can hold up to 500 computed tomography (CT), 1000 magnetic resonance (MRI), and 500 computed radiography (CR) studies. Each CT or MRI study consisted of a sequence of images from one examination with each CR study comprising one exposure. The calculation was based on the average study sizes in the field, in MB: CT, 11.68; MR, 3.47; and CR, 7.46. Nowadays, large RAIDs with several terabytes are being used in the archive server, especially in the client/server model [9]. The magnetic cache disks configured in the archive server should sustain high data throughput for the read operation, which provides fast retrieval of images from the RAID.

15.2.1.2.2 The Database System

The database system consists of redundant database servers running identical reliable commercial database systems (e.g. Sybase, Oracle) with structured query language (SQL) utilities. A mirror database with two identical databases can be used to duplicate the data during every PACS transaction (not images) involving the server. The data can be queried from any PACS computer via the communication networks. The mirroring feature of the system provides the entire PACS database with uninterruptible data transactions that guarantee no loss of data in the event of system failure or disk crash. Besides its primary role of image indexing to support the retrieval of images, the database system is necessary to interface with the RIS and the HIS, allowing the PACS database to collect additional patient information from these two healthcare databases.

15.2.1.2.3 The Archive Storage

The archive storage consists of multiple storage devices, usually large RAID, SAN, DLT, and an external Data Grid. The archive server allows concurrent storage and retrieval operations on all these devices. The storage must have a large storage capacity of many terabytes and support mixed storage media. Redundant power supply is essential for uninterrupted operation. The average overall throughputs for read and write operations between the magnetic disks of the archive server and the storage devices should be at least 100 MB/s.

15.2.1.2.4 The Backup Archive

To build reliability in the PACS server, a backup archive system should be used. Two copies of identical images can be saved through two different paths in the PACS network to two archive systems. Ideally the two systems should be located in two different buildings to prevent loss in the case of natural disaster. The backup archive has become a very important consideration, as many healthcare providers are relying on PACS for their daily operation; Section 15.6 discusses a backup archive model using the Data Grid.

15.2.1.2.5 Communication Networks

The PACS archive system is connected to the PACS local area network (LAN), Intranet, or the WAN. The PACS LAN consists of high-speed Ethernet with gigabits/switches and routers. The WAN provides connection to remote sites and can consist of T1 and higher capacity networks and WANs. The PACS high-speed Intranet transmits large-volume image data from the archive server to 1 K

and 2 K WSs. Hundreds of Mbits/s Ethernet can be used for interconnecting slower speed components to the PACS server, including acquisition gateway computers, RIS, and HIS, and as a backup to the Gbit/s Ethernet. Failure of the high-speed network automatically triggers the archive server to reconfigure the communication networks so that images can be transmitted to the 1 K and 2 K display WSs over slower-speed Ethernet without interruption.

15.2.2 Functions of the PACS Server and Archive Server

In the multimedia PACS-based server and archive server, processes of diverse functions run independently and communicate simultaneously with other processes using client-server programming, queuing control mechanisms, and job-prioritizing mechanisms. Figure 15.4 shows the interprocess communications among major processes running on the PACS server and archive. Because the functions of the server and the archive are closely related, the term “archive server” is used to represent both. Major tasks performed by the archive server include image receiving, image stacking, image routing, image archiving, studies grouping, platter management, RIS interfacing, PACS database updating, image retrieving, and image prefetching. The following subsections describe the functionality carried out by each of these tasks. Whenever appropriate, the DICOM standard is highlighted in these processes.

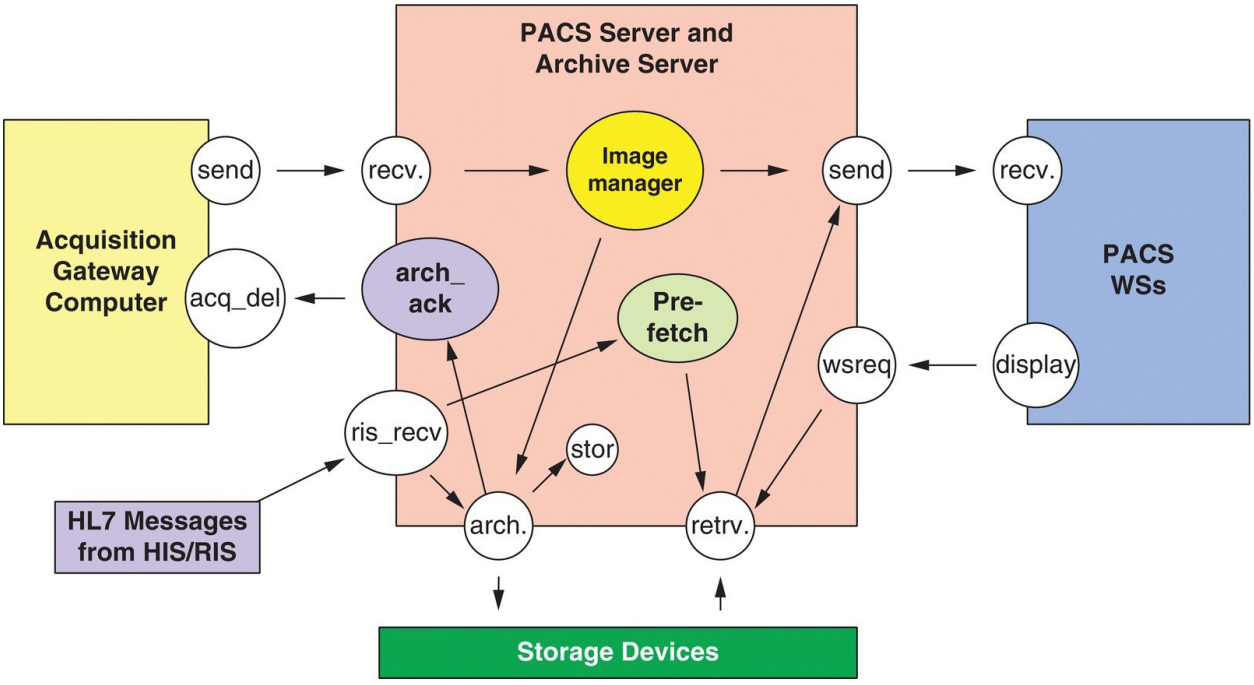

Figure 15.4 Interprocess communications among the major processes running on a PACS archive server connected to the acquisition gateway, WSs, and

storage devices. Compare to the workflow in the DICOM compliant server shown in Figure 15.8 (see also Figure 15.5). HL7: Health Level 7; arch: archive images; arch_ack: archive acknowledge; acq_del: acquisition delete; image_manager: process image information and update PACS database; prefetch: preselect needed images; recv: receive images; ris_recv: receive HL7 message; retrv: retrieve images; send: send images to WSs; stor: store images; wsreq: retrieve requests from WSs.

There are nine major functions in the PACS server and archive server:

1. Image receiving
2. Image stacking
3. Image routing
4. Image archiving
5. Study grouping
6. RIS and HIS interfacing
7. PACS database updates
8. Image retrieving.
9. Image pre-fetching.

These functions are the basic PACS server and archive server functions used in almost all PACS systems.

15.2.3 RIS and HIS Interface

The archive server accesses data from HIS/RIS through a PACS gateway computer. The HIS/RIS relays a patient admission, discharge, and transfer (ADT) message to the PACS, only when a patient is scheduled for an examination in the radiology department or when a patient in the radiology department is discharged or transferred. Forwarding ADT messages to PACS not only supplies patient demographic data to the PACS, but also provides information that the archive server needs to initiate the image pre-fetch, image archive, and studies grouping tasks. Exchange of messages among these heterogeneous information systems can use the HL7 standard data format running TCP/IP transmissions on a client–server basis, as described in Section 3.4.2. The multimedia PACS-based archive server is able to use HIS information to include data from other clinical specialties.

In addition to receiving ADT messages, PACS retrieves examination data and diagnostic reports from the RIS. This information is used to update the PACS database, which can be queried and reviewed from any WS. Chapter 13 presents the RIS, HIS, and PACS interface in more detail.

The RIS and HIS interfacing is the communication method used between the HIS and RIS chosen by the hospitals. The imaging modalities manufacturers chosen by the radiology department are responsible for connecting the imaging devices to the PACS-based systems designated by the hospital [9].

15.3 PACS-Based Archive Server System Operations

The PACS-based server operates on the 24/7/365 service. All operations in a well-designed PACS should be software driven and automatic and should not require any manual operational procedures. The only non-automatic procedures are removal of old or insertion of new storage media in the off-line archive operation. Even this process was minimized several years ago by the introduction of larger storage devices with periodic preventive maintenance service.

A fault-tolerant mechanism in the archive system is used to ensure data integrity and minimize system downtime. Major features of this mechanism include:

1. an uninterruptible power supply (UPS) system that protects all archived components, including the archive server, database servers, and archive library from power outages;
2. a mirrored database system that guarantees the integrity of the data directory;
3. if the DLT library is used for long-term archiving, multiple tape drives and robotic arms that provide uninterrupted image archival and retrieval in the event of failure of a tape drive or robotic arm;
4. a central monitoring system that automatically alerts quality control staff via wireless mobile phone or pagers, to remedy any malfunctioning archive components or processes;
5. spare parts for immediate replacement of any malfunctioning computer components, which include network adapter boards and routers, SCSII or better controllers, and the multi-CPU system board (archive server);
6. a 4-hour turnaround manufacturer’s on-site service that minimizes system

down time due to hardware failure of any major archive component.

In Chapter 16, the concept of fault-tolerant PACS operation is presented in more detail. Refer to the emerging technology in Section 15.7, which describes how to use cloud computing to replace some existing current PACS archive server functions by using Cloud archiving services.

15.4 DICOM-Compliant PACS-Based Archive Server

15.4.1 Advantages

The purpose of the Digital Imaging and Communications in Medicine (DICOM) standard described in Section 9.4 is to promote a standard communication method for heterogeneous imaging systems, allowing the exchange of images and associated information among them. By using the DICOM standard, a PACS will be able to interconnect its individual components together and allow the acquisition gateways to link to imaging devices. However, imaging equipment vendors often select only a subset of DICOM compliant statements for implementation (Section 9.4.4) for their own convenience, which may lead to difficulties for interoperation for these imaging systems. A well-designed DICOM-compliant PACS server can use two mechanisms to ensure the system integration. One mechanism is to connect to the acquisition gateway computer with DICOM, providing reliable and efficient processes of acquiring images from imaging devices. The other is to develop specialized gateway software allowing interoperability of multi-vendor imaging systems. Both mechanisms can be incorporated into the DICOM-compliant PACS system. Chapters 7–10 describe the basic principles of these two mechanisms at the component level. In this section, these mechanisms at the system level, based on the knowledge learned from those chapters, are elaborated upon.

15.4.2 DICOM Communications in PACS Environment

In Section 9.4.5, two major DICOM communication service–object pair (SOP) classes for image communications are discussed: the storage service class and the Q/R service class:

- *Storage service class*: allows a PACS application running on system A (for examination, a CT, scanner) to play the role of a storage service class user (SCU) that initiates storage requests and transmits images to system B (i.e.

an acquisition gateway computer), which serves as a storage service class provider (SCP), accepting images to its local storage device.

- *Q/R service class*: allows PACS applications running on system A (i.e. a WS) to play the role of a Q/R SCU that queries and retrieves images from system B (i.e. an archive server), which serves as a Q/R SCP, processing query and retrieval requests.

Figure 15.5 illustrates the communication of images utilizing the storage service class and Q/R service class in a PACS environment. These two service classes can be used to develop a DICOM-compliant PACS server.

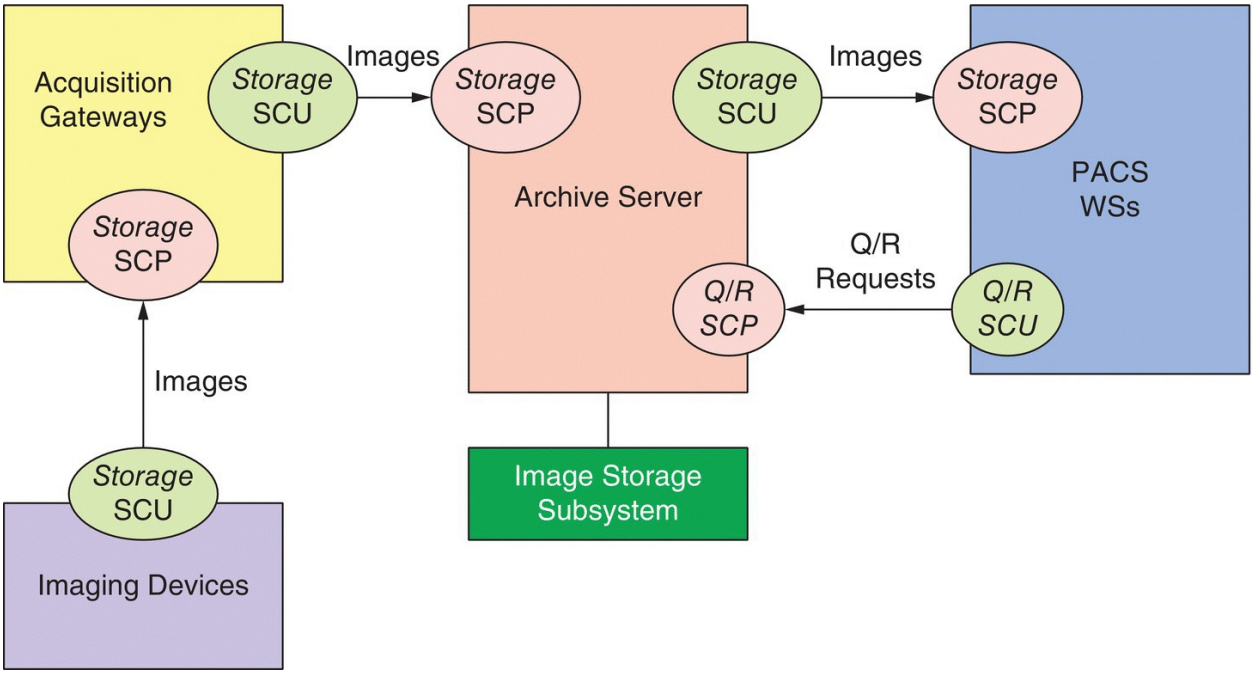

Figure 15.5 Image communication utilizing DICOM SOP services in PACS. The gateway via the storage SOP service acquires images generated from imaging devices. These images are then transmitted to the archive server, where they are routed to the permanent archive subsystem and WSs. The archive server supports Q/R SOP service, handling all Q/R requests from WSs (see Figure 15.4). SOP: service-object pair; SCU: service class user; SCP: service class provider.

15.4.3 DICOM-Compliant Image Acquisition Gateways

A DICOM-compliant acquisition gateway can be used to provide a reliable and efficient process for acquiring images from imaging devices. The DICOM-compliant software running on a gateway should support two types of image

acquisition, the push-mode and the pull-mode operations (see Section 10.2.1).

The push-mode operation utilizes DICOM's storage SOP service. An imaging device such as a CT scanner takes the role of a storage SCU, initiating storage requests. The requesting gateway (storage SCP) accepts these requests and receives the images. The pull-mode operation utilizes DICOM's Q/R SOP service.

The gateway plays the role of a Q/R SCU, initiating query requests, selecting desired images, and retrieving images from an imaging device (Q/R SCP). The pull-mode operation requires the image acquisition process to incorporate with the local database to perform data integrity checks in the gateway computer. This checking mechanism ensures that no images are lost during the acquisition process.

Figure 15.6 summarizes the characteristics of these two modes of operation. In the pull mode, the ImgTrack process in the gateway performs data integrity checks by the following procedure:

1. queries study information from the scanners;
2. generates acquisition status table;
3. periodically checks acquisition status of individual image sequences; and
4. invokes DcmPull process to retrieve images from the scanners.

The DcmPull process, when invoked by the ImgTrack process, retrieves the desired images from the scanner and updates the acquisition status table accordingly. Both push and pull modes are used in the acquisition gateway; the choice is dependent on the operating conditions at the clinical site.

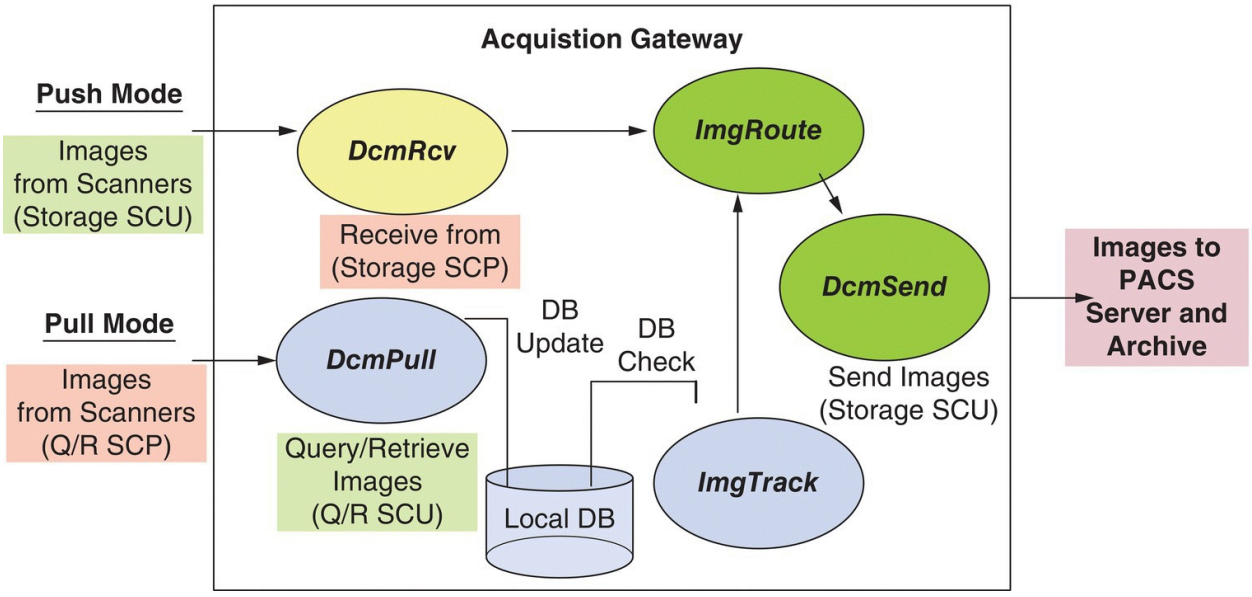

Figure 15.6 Interprocess communication among the major processes running in a DICOM-compliant acquisition gateway, which supports both push and pull operations for acquiring images from the scanners. The DcmPull process (blue) incorporates the gateway's local database to perform data integrity check, ensuring no missing images from any image sequences during the acquisition process (see also Figure 15.5). DB: database; Dcm: DICOM; Img: image; Q/R: query and retrieve; SCU: service class user; SCP: service class provider.

15.5 DICOM PACS-Based Archive Server Hardware and Software

This section discusses the system architecture with generic hardware and basic software components of a DICOM PACS-based archive server.

15.5.1 Archive Hardware Components

The PACS server and archive server generic hardware component consists of the PACS server computers, peripheral archive devices, and fast Ethernet interface and SCSII and fiber-optics channels. For large PACS, the server computers used are mostly UNIX-based machines. The fast Ethernet interfaces the PACS archive server to the high-speed Ethernet networks where gateways and WSs are connected. The SCSII and fiber-optic channels integrate peripheral storage devices with the PACS archive server. The main storage devices for PACS server include magnetic disk, RAID, SAN, DLT, and CD/DVD. PACS separates its images according to the time it had been acquired, with the current ones

relegated to the short-term storage device, and very historical ones to the long-term storage. In-between time image storage would depend on the clinical need.

RAID and SAN, because of their fast access speed and reliability, are used for the short-term archive device in PACS, specifically in the client and server architecture. Because of its large data storage capacity and relatively lower cost, DLT is mostly used for long-term and off-site archive. Figure 15.7 shows an example of the server connection to the DLT with the SCSII, and RAID and SAN with the fiber-optic channels, and to other PACS components with high-speed Ethernet. Many different kinds of storage devices are available for PACS application, including RAID, SAN, DLT, and some others.

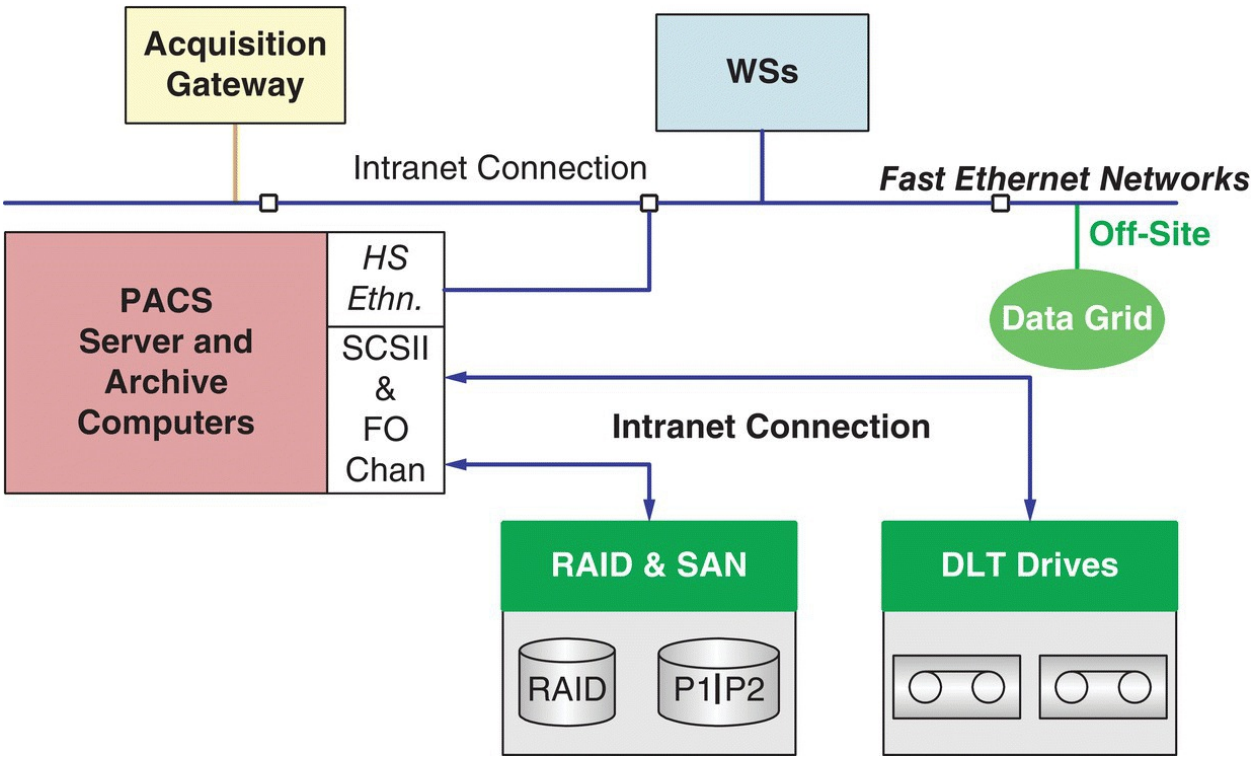

Figure 15.7 Basic hardware components in a PACS server and archive server with high-speed (HS) Ethernet (Ethn.) for broadband Internet, and small computer system interface II (SCSII) and fiber-optic channels (FO Chan) connections. Blue lines: PACS Intranet; SAN: storage area network with multiple partitions, P1 and P2; WSs: workstations.

15.5.2 Archive Server Software

PACS archive server software is DICOM compliant and supports the DICOM storage service and Q/R service classes. Through DICOM communication, the archive server receives DICOM studies/images from the acquisition gateway,

appends study information to the database, and stores the images in the archive device, including the RAID, SAN, and DLT. It receives the DICOM Q/R request from WSs and sends back the Q/R result (patient/study information or images) to WSs. The DICOM services supported by the PACS Server are C-Store, C-Find, and C-Move (see Section 9.4.5). All software implemented in the archive server should be coded in standard programming languages—for example, C and C++ on the UNIX open systems architecture. PACS server software is composed of at least six independent components (processes), including receive, insert, routing, send, Q/R server, and RetrieveSend. It also includes a PACS database. These processes run independently and simultaneously and communicate with other processes through queue control mechanisms. Figure 15.8 delineates the PACS archive software components and data flow (compare with Figure 15.4, which shows the general interprocess communications in a PACS server).

Figure 15.9 shows an example of the DICOM PACS archive server data flow illustrating a CR image moves from the gateway (left), to the server (center, 1–14), to WSs (right).

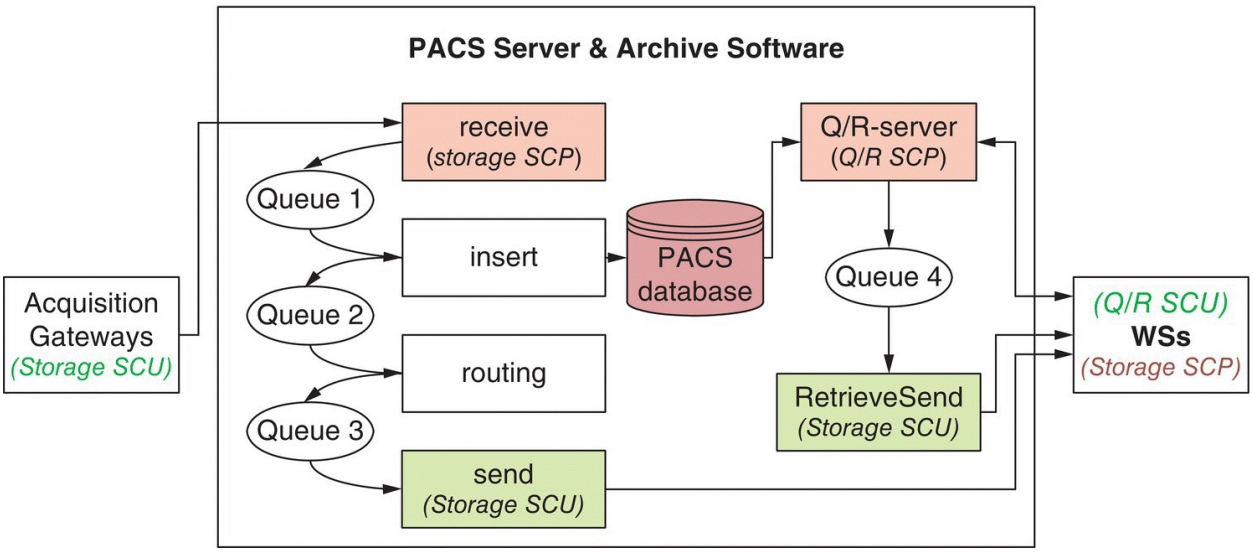

Figure 15.8 DICOM PACS server and archive software components and dataflow. The six components are receive, insert, route, send, Q/R-server, and RetrieveSend. green: SCU; orange red: SCP.SCP: service class provider; SCU: service class user; WSs: workstations.

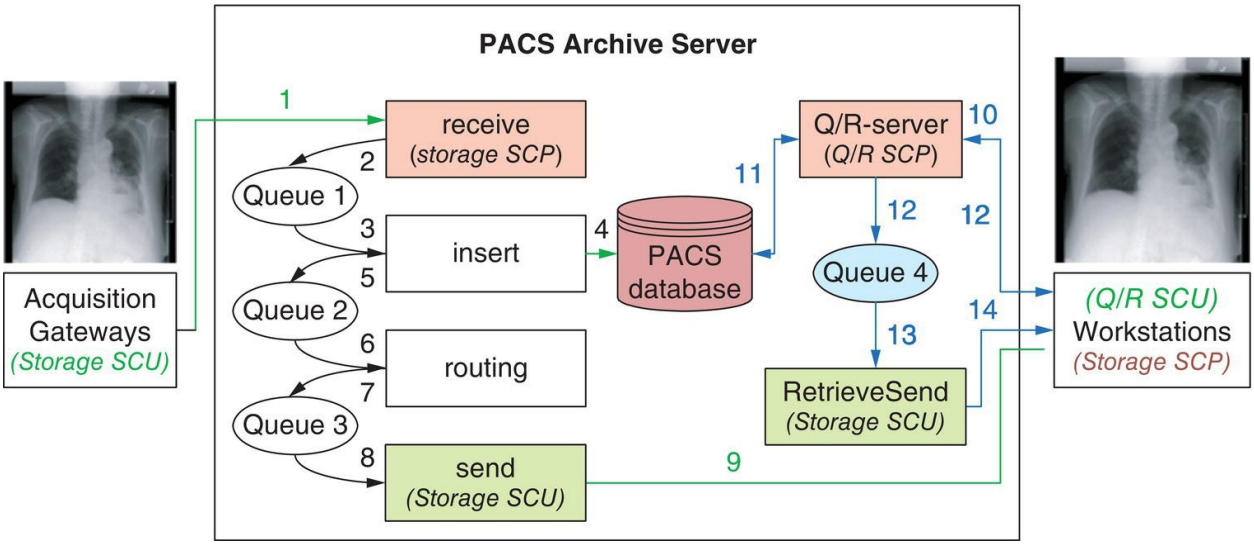

Figure 15.9 Workflow in a DICOM PACS archive server, with CR as an example of an image sent from the acquisition gateway (left), through the server (middle), to the WSs (right). Green and black numerals and lines are the auto-push model; blue are the client and server model with Q/R; (refer to Figure 15.8). SCP: service class provider; SCU: service class user.

15.6 Backup Archive Server and Data Grid

Two major components in the PACS server and archive are the PACS server and the archive server. When the PACS server fails, a system reboots or a backup server may solve most of the problems, then no data are lost. However, when the archive server fails, data in the storage may be damaged and can lead to a loss of image data. Three methods of backup archive are to be discussed. The classical backup archive using an application service provider (ASP) model is presented in Sections 15.6.1 to 15.6.3. The second backup method is to use the Data Grid. During the past 10 years, Data Grid technology, described in Chapters 8 and 9, has improved tremendously, with its usefulness for data storage on a par with, and even with better service and lower cost, than the backup archive server method. Section 15.7 presents a third method, Cloud storage, the most innovative model of storage technology today. To use the cloud storage service, understanding the terminology and workflow processes described in previous sections are necessary.

15.6.1 Backup Archive Using an Application Service Provider (ASP) Model

The PACS archive server is the most important component in a PACS; even though it may have the fault tolerance feature, chances are that the server could still occasionally fail. A backup archive server is necessary to guarantee its uninterrupted service. The backup archive server can be short term (3 months) or long term. The functions of a backup archive server are two-fold: maintaining the PACS continuous operation and preventing loss of image data. Data loss is especially troublesome, because if a major disaster occurs, it is possible to lose an entire hospital's PACS data. In addition, the scheduled downtimes to the main PACS archive could impact the continuity of a filmless institution's operation. Few current PACS archives provide a disaster recovery scheme. Furthermore, current general disaster recovery solutions vary in their approach toward creating redundant copies of PACS data.

One novel approach is to provide a short-term fault-tolerant backup archive server using the ASP model at an off-site location. The ASP backup archive provides instantaneous, automatic backup of acquired PACS image data and instantaneous recovery of stored PACS image data, all at a low operational cost, because it utilizes the ASP business model. In addition, should the downtime event render the network communication inoperable, a portable solution should be using a data migrator, which is a portable laptop computer with a large-capacity hard disk that contains DICOM software for exporting and importing PACS image exams. The data migrator can be used to populate PACS examinations that were stored in the backup archive server. During the emergency, the migrator can be inserted manually to the clinical PACS WS system within hours, allowing the radiologists to continue to read previous PACS examinations until new replacement hardware arrives and is installed, or until a scheduled downtime event has been completed.

15.6.2 General Architecture

Figure 15.10 shows the general architecture of the ASP backup archive integrated with a clinical PACS. The hospital with a PACS and the ASP site are connected via an inexpensive T1 line or very high-speed broadband WAN. At the hospital site, any new examination acquired and archived in PACS is also transferred to an additional DICOM gateway at the hospital via the clinical PACS server. The DICOM gateway, much like a PACS acquisition gateway in the PACS system, is crucial in maintaining the clinical workflow between the hospital and the ASP supported site. It provides a buffer and manages the network transfers of the PACS exams by queuing the network transfer jobs to the ASP site. The DICOM gateway transfers an exam through the T1 (or higher-

speed network) router across the T1 line to a receiving T1 router at the off-site ASP. At the off-site ASP PACS backup storage site, a second gateway receives the PACS examinations and queues them for storage in a fault-tolerant backup archive server. The backup archive should be designed as a fault-tolerant storage device (see Chapter 16).

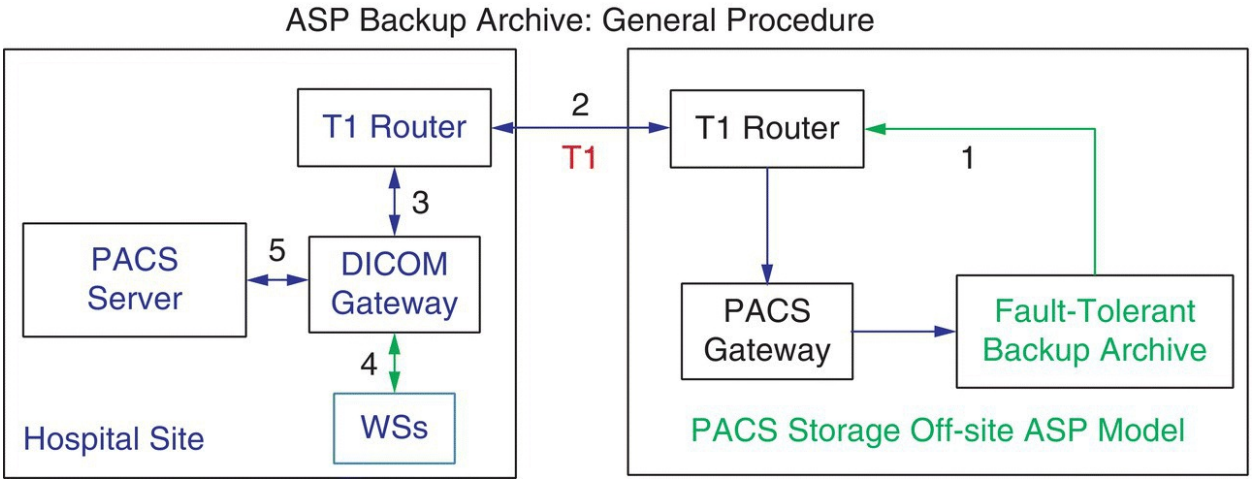

Figure 15.10 General architecture of the ASP backup archive server. One DICOM gateway at the ASP site and one PACS gateway at the hospital site are used as the buffers between the two sites. T1 or a higher speed network is used for the broadband WAN. WSs at the hospital site can access PACS images from the ASP, following the route: 1, 2, 3, and 4, should some components in the PACS fail, like the server and the archive. After the PACS components are repaired, the missing images can be recovered via route 5. The image Q/R performance is limited only by the network speed, in this example, the T1, 1.5 Mbits/s. All PACS data transmitted throughout this architecture should conform to the DICOM protocol standard.

15.6.3 Data Recovery Procedure

Figure 15.11 shows the recovery procedure of the PACS during a scheduled downtime, or an unscheduled downtime such as a disaster. There are two scenarios: network communication still functioning between two sites, but no network connection. If connectivity between the two sites is live, then backup PACS examinations can be migrated back to the hospital site and imported directly into the PACS with DICOM compliant network protocols. In most disaster scenarios, there is the high likelihood that connectivity between the two sites is not functional. In this case, the backup PACS examinations are imported into the hospital PACS with a portable data migrator. The data migrator exports

PACS exams from the backup archive. It is then physically brought on site (this scenario works best if the off-site location in the same metropolitan area as the hospital) to the hospital and the PACS examinations are imported directly into a WS or temporary server. The data migrator is DICOM compliant, which means that the PACS examinations can be imported without any additional software or translation once the PACS server is up and running.

In addition, the data migrator contains up-to-date PACS data, because it is always synchronized with the clinical PACS workflow. In either scenario, radiologists and physicians would have the previous and current PACS examinations to continue with normal clinical workflow readings (with some delay due to download images from the migrator) until replacement hardware is installed, and the hospital PACS archive storage and server are brought back on line.

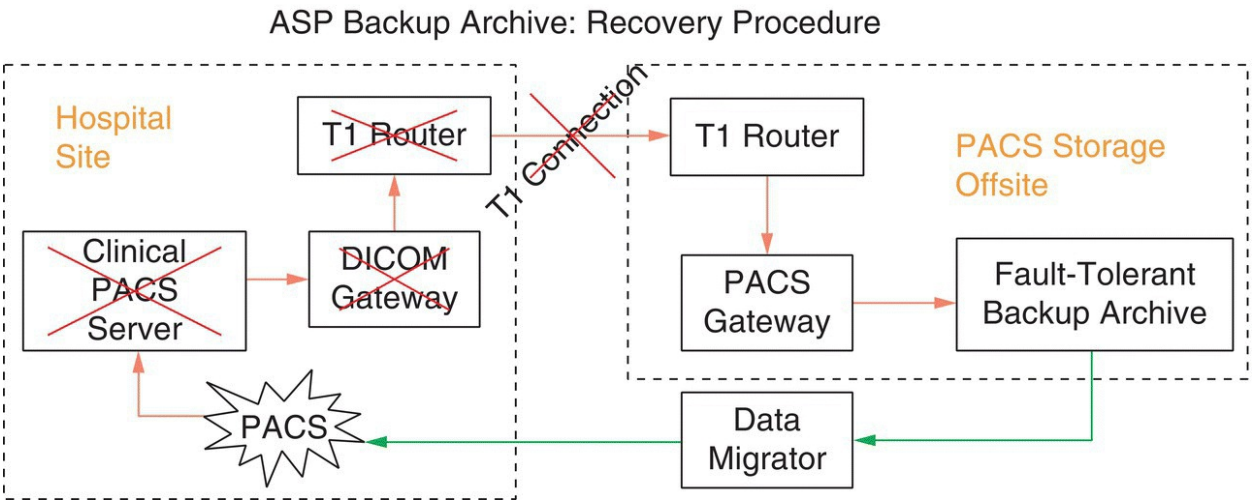

Figure 15.11 Disaster recovery procedures. In a disastrous event, the components shown with crossed marks can be considered unavailable for use. In this scenario, a data migrator can be used physically to export PACS examinations and import them directly into PACS using the appropriate DICOM protocols. After the PACS are repaired, the migrator can be used to feed images back to the PACS server via routes 4 and 5 shown in Figure 15.10.

Section 15.7 describes the emerging cloud computing and archive server technology. Combining the DICOM-compliant PACS-based archive server with the cloud archive server service, they form ideal paired technologies to resolve the backup archive situation, because the existence of the DICOM standard (see Section 15.7.4) is used for the image and data transmission [9].

15.7 Cloud Computing and Archive Server

15.7.1 Change of the PACS Climate

Since 2010, the PACS climate has changed dramatically. Professor Brent Liu has taught graduate courses in PACS and Imaging Informatics for more than 15 years at the University of Southern California, as well as managing and consulting large-scale PACS operation in both the academic and private hospitals. He did an informal survey with a few of the large vendors (Fuji, Siemens and others) and spoke to close colleagues during the 2015 meeting of the RSNA about the current PACS industry landscape. Based on his survey and observations, the following points are recognized as the future trends of PACS:

1. PACS is now broken into pieces. The term is called “deconstructed PACS”.
2. Traditional PACS vendors are focusing their marketing only on the viewing software and not the storage solution.
3. Storage solutions are now called the VNA technology, which concentrates on storing the image files in the native DICOM file.
4. VNA is also used to store all other kinds of data, including non-radiology images, whether they are DICOM or non-DICOM.
5. PACS vendors still sell PACS because they have knowledge of the radiology workflow, so their viewing software will embed these workflow features (e.g. study protocols, automatic hanging protocols, decoding the DICOM header).
6. Most VNA technologies do not employ the deeper DICOM fields, but just extract basic patient information and archive using Web technology and the IHE XDS-I.b profile (see Chapter 7).

Together with the background materials discussed in Sections 15.1 to 15.6, it becomes meaningful to present Section 15.7 leading to the novel topics on cloud computing and storage technology. Together with the emerging cloud computing and current existing PACS-based biomedical imaging informatics technologies, as a whole, they achieve a higher advanced level, not only to better servicing of radiology, but also to other clinical applications.

15.7.2 Cloud Computing

Cloud computing generally represents the practice of using a network of remote

servers hosted on the Internet to store, manage, and process data, rather than a local server or a personal computer. In the 1990s, telecommunications companies, who previously offered primarily dedicated point-to-point data circuits, began offering virtual private network (VPN) services with comparable quality of service, but at a lower cost. By switching the communication traffic as they saw fit to balance server use, the network industry could use overall network bandwidths more effectively and began to use the cloud symbol to denote the demarcation point between what the provider was responsible for and what users were responsible for. The cloud computing industry extended this boundaries to cover all servers as well as the network infrastructure. Since 2000, Cloud computing has marched into industrial existence. Examples are: Amazon introduced its Elastic Compute Cloud in 2006; Microsoft announced its Azure in 2008, renamed Microsoft Azure in 2014; IBM announced the IBM SmartCloud in 2011; and Oracle introduced the Oracle Cloud in 2011, etc. (contents and examples are selectively extracted for PACS and biomedical informatics applications) [10–14].

15.7.3 Cloud Computing Service Models and Cloud Storage

15.7.3.1 Cloud Computing Service Models

Current available cloud computing providers offer their "services" according to different models, of which the three standard models are infrastructure as a service (IaaS), platform as a service (PaaS), and software as a service (SaaS). These models offer increasing abstraction; they are thus often portrayed as layers in a stack: infrastructure-, platform- and software-as-a-service, but these need not be related. For example, we can provide SaaS implemented on physical machines (bare metal), without using underlying PaaS or IaaS layers, and conversely we can run a program on IaaS and access it directly, without wrapping it as SaaS (adapted from *Wikipedia*, August, 2016).

The National Institute of Standards and Technology (NIST)[1] definition of cloud computing defines these three service models as:

1. *Software as a Service*: The capability provided to the consumer is to use the provider's applications running on a cloud infrastructure. The applications are accessible from various client devices, through either a thin client interface, such as a Web browser (e.g. Web-based email), or a program interface. The consumer does not manage or control the underlying cloud infrastructure including network, servers, operating systems, storage, or even

individual application capabilities, with the possible exception of limited user-specific application configuration settings.

2. *Platform as a Service*: The capability provided to the consumer is to deploy onto the cloud infrastructure consumer-created or acquired applications created using programming languages, libraries, services, and tools supported by the provider. The consumer does not manage or control the underlying cloud infrastructure including network, servers, operating systems, or storage, but has control over the deployed applications and possibly configuration settings for the application-hosting.
3. *Infrastructure as a Service*: The capability provided to the consumer is to provision processing, storage, networks, and other fundamental computing resources, where the consumer is able to deploy and run arbitrary software, which can include operating systems and applications. The consumer does not manage or control the underlying cloud infrastructure, but has control over operating systems, storage, and deployed applications; and possibly limited control of select networking components (e.g. host firewalls).

15.7.3.2 Cloud Storage

Cloud Storage is a cloud computing model in which data are stored on remote servers accessed from the Internet, or “cloud.” It is maintained, operated, and managed by a cloud storage service provider on a storage server, which are built-on virtualization techniques. The multimedia data, including biomedical images and other types of data, are stored in logical pools, the physical storage spans multiple servers (and often locations), and the physical environment is typically owned and managed by a hosting company, VPN services, or hospitals. These providers or the PACS owners are responsible for keeping the data available and accessible instantaneously, the physical environment protected, as well as the system running. Biomedical images, informatics data, and electronic patient record)(ePR) from the users or organizations can buy or lease storage capacity from the service providers to store, organized, or utilize these multimedia data. Cloud storage services may be accessed through a co-located cloud computer service, a Web service application programming interface (API), or by applications that utilize the interface, such as cloud desktop storage, a cloud storage gateway, or Web-based content management systems.

15.7.3.3 Role of the National Institute of Standards and Technology(NIST)

After years of planning and 15 drafts of the National Institute of Standards and Technology's (NIST) working definition of cloud cComputing, the 16th and final definition was published as *The NIST Definition of Cloud Computing* (NIST Special Publication 800-145). Cloud computing is a relatively new business model in the computing world. According to the official NIST definition:

> Cloud computing is a model for enabling ubiquitous, convenient, on-demand network access to a shared pool of configurable computing resources (e.g. networks, servers, storage, applications, and services) that can be rapidly provisioned and released with minimal management effort or service provider interaction.

The NIST definition lists five essential characteristics of cloud computing: on-demand self-service, broad network access, resource pooling, rapid elasticity or expansion, and measured service. It also lists three “service models” (software, platform, and infrastructure), and four “deployment models” (private, community, public, and hybrid) that together categorize ways to deliver cloud services. The definition is intended to serve as a means for broad comparisons of cloud services and deployment strategies, and to provide a baseline for discussion from what is cloud computing to how to best use cloud computing.

15.7.3.4 Role of the Open Group

The Open Group is a global consortium that enables the achievement of business objectives through IT standards:

> It leads the development of open, vendor-neutral IT standards and certifications, with more than 500 member organizations with diverse membership that spans all sectors of the IT community—customers, systems and solutions suppliers, tool vendors, integrators and consultants, as well as academics and researchers. Their responsibilities are to:
>
> - capture, understand, and address current and emerging requirements, and establish policies and share best practices;
> - facilitate interoperability, develop consensus, and evolve and integrate specifications and open source technologies;
> - offer a comprehensive set of services to enhance the operational efficiency of consortia; and
> - operate the industry’s premier certification service.
>
> The mission of The Open Group is to drive the creation of Boundaryless

Information Flow™ achieved by:

- working with customers to capture, understand and address current and emerging requirements, establish policies, and share best practices;
- working with suppliers, consortia, and standards bodies to develop consensus and facilitate interoperability, to evolve and integrate specifications and open source technologies;
- offering a comprehensive set of services to enhance the operational efficiency of consortia; and
- developing and operating the industry's premier certification service and encouraging procurement of certified products.

The Open Group has developed and initiated the following models and services:

A. The basic cloud computing model is shown in Figure 15.12A. Servers, storage, applications, and services are accessed via a common network. They are shared between organizations, and accessed by users or applications. The users may be members of the organizations working on-premises, remote workers, customers, or members of the general public.

B. Providing Cloud Service

   The provider of a cloud service has control over a set of resources, and makes them available to consumers of the service in a way that has the essential characteristics of cloud computing.

C. Providing Added Services

   The consumer of a cloud service may use it to provide an added service. The added service is used by the customers of the provider of the added service, not by the provider itself.

D. Using Cloud Services

   An end-user organization, its customers, and other people that interact with it see the cloud software services, rather than the servers or storage. Those services may be provided by the cloud provider, or by added service providers. There may be several clouds, several cloud providers, and several added service providers.

E. The cloud services that support the business processes can be inside the organization, in an internal private cloud, or outside it, in a public cloud

or virtual private cloud. Or they can be in a hybrid cloud, a combination of public and private clouds.

F. Cloud Ecosystems

An ecosystem exists where participants in a defined market have integrated business processes and use common standards for exchange of information, products, and services.

Cloud computing enables providers and consumers of products and services to interact more easily, because they are freed from the drudgery of providing the necessary IT support. This encourages the creation and growth of ecosystems in which companies co-operate effectively to meet the needs of society. The benefits of cloud computing extend not just to individual businesses, but to business as a whole.

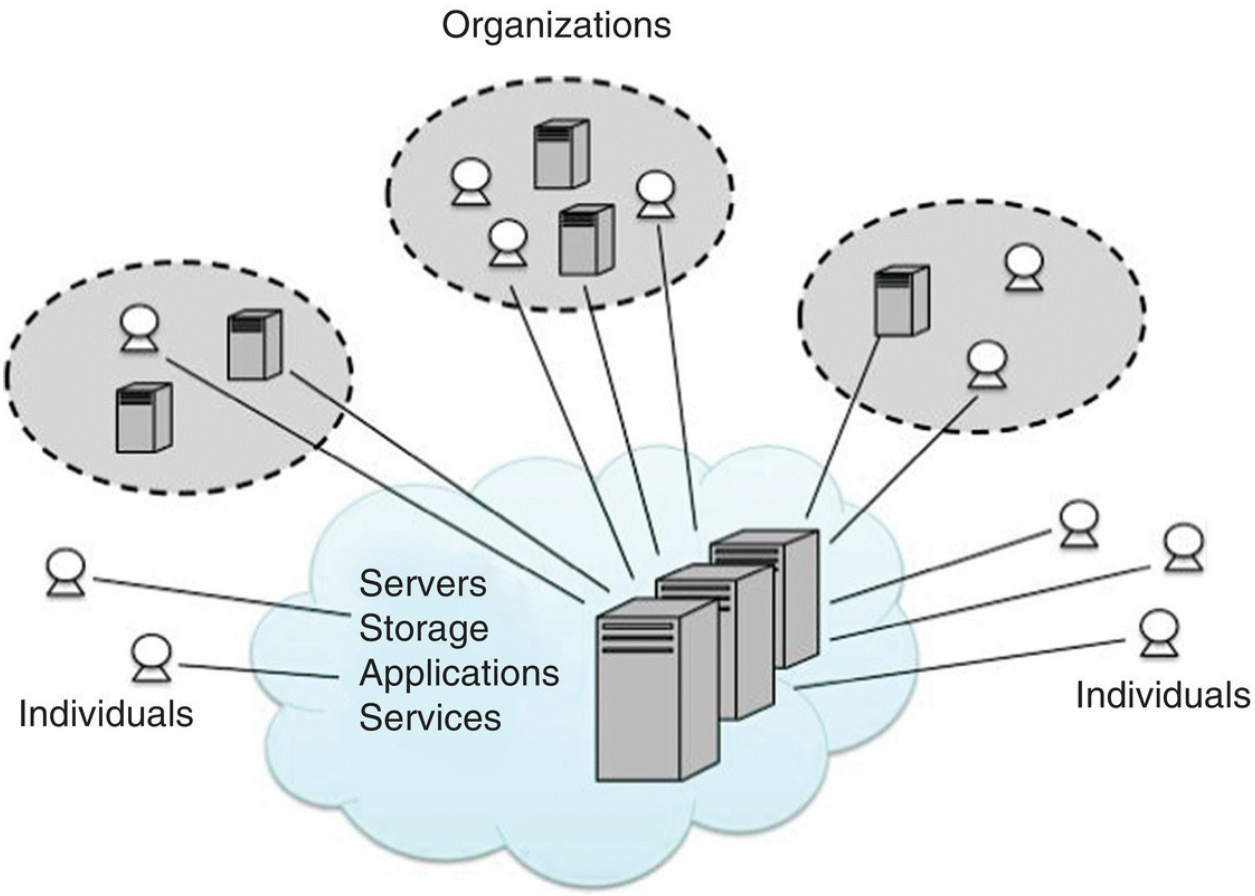

Figure 15.12 The Open Group has developed a range of models and services. (A) Basic cloud computing model.

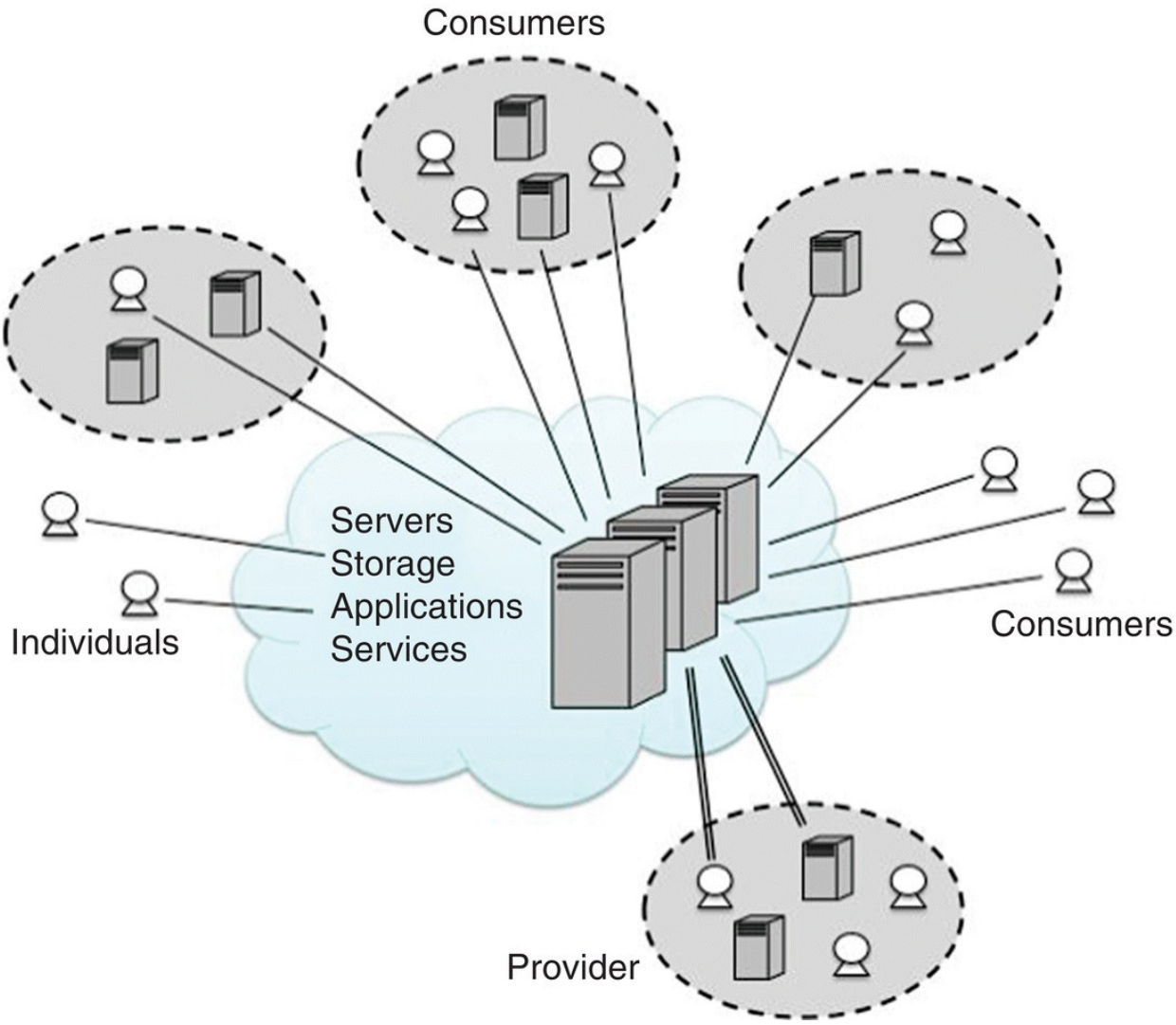

Figure 15.12 (B) Providing cloud services.

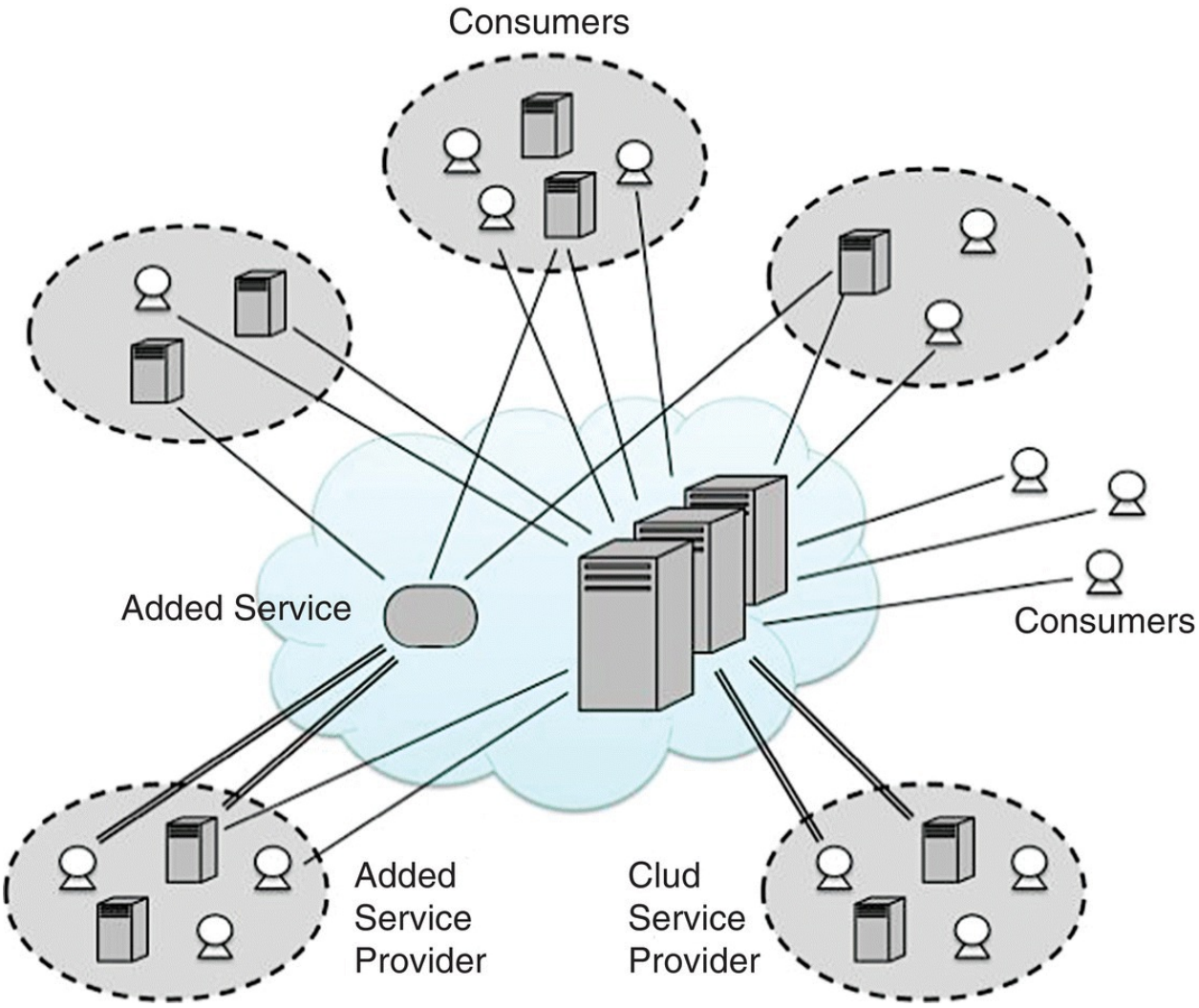

Figure 15.12 (C) Providing added services.

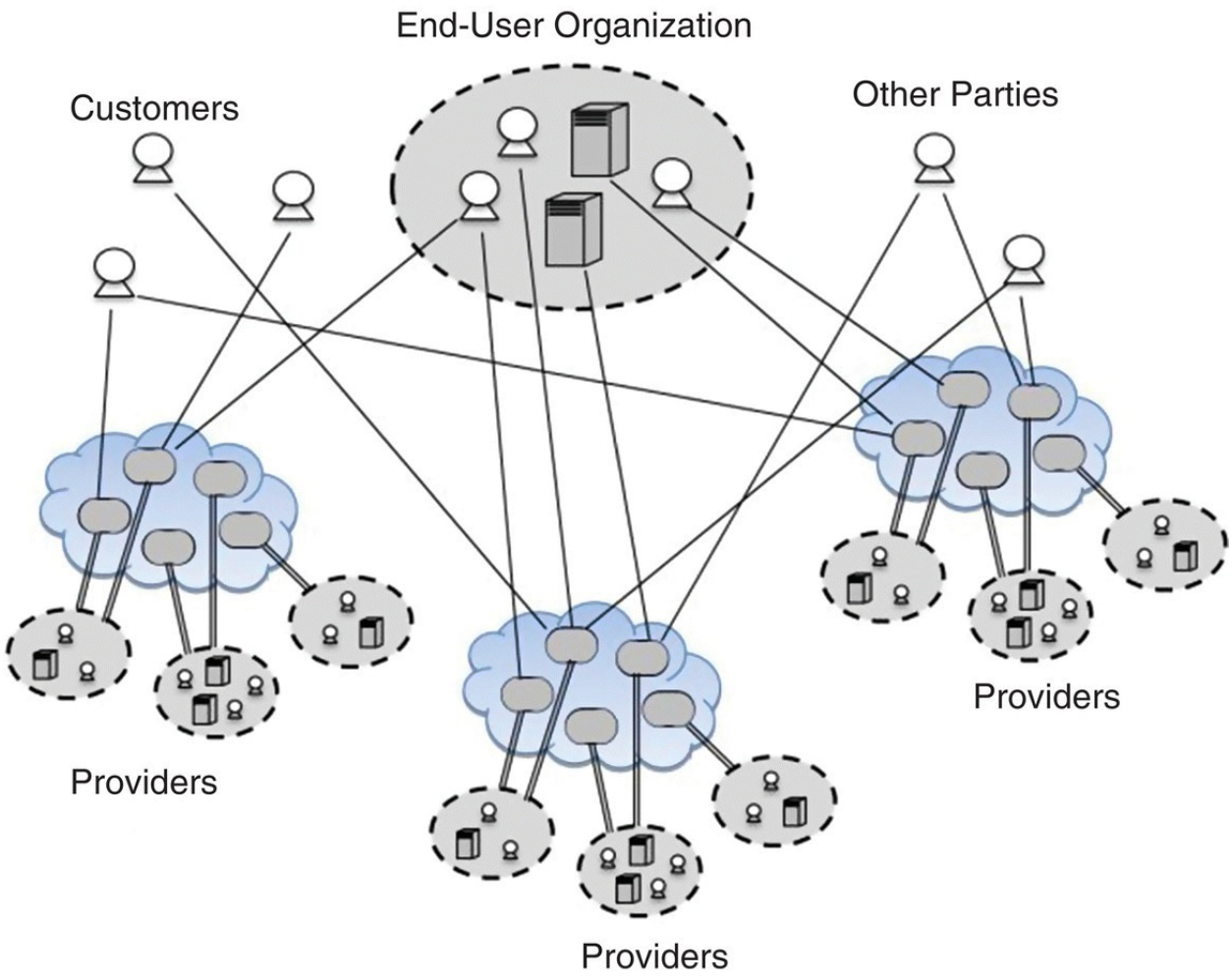

Figure 15.12 (D) Using cloud services.

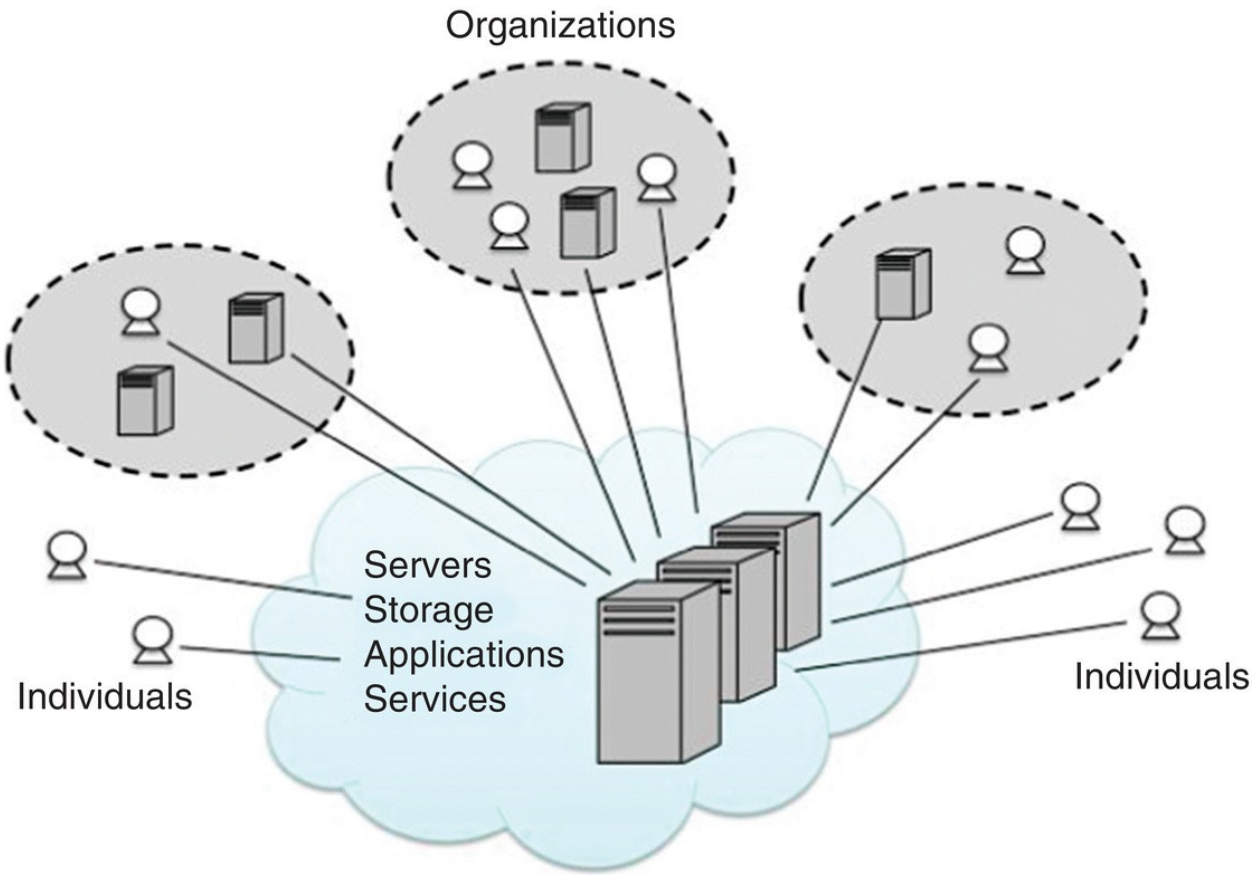

Figure 15.12 (E) Internal and external cloud services.

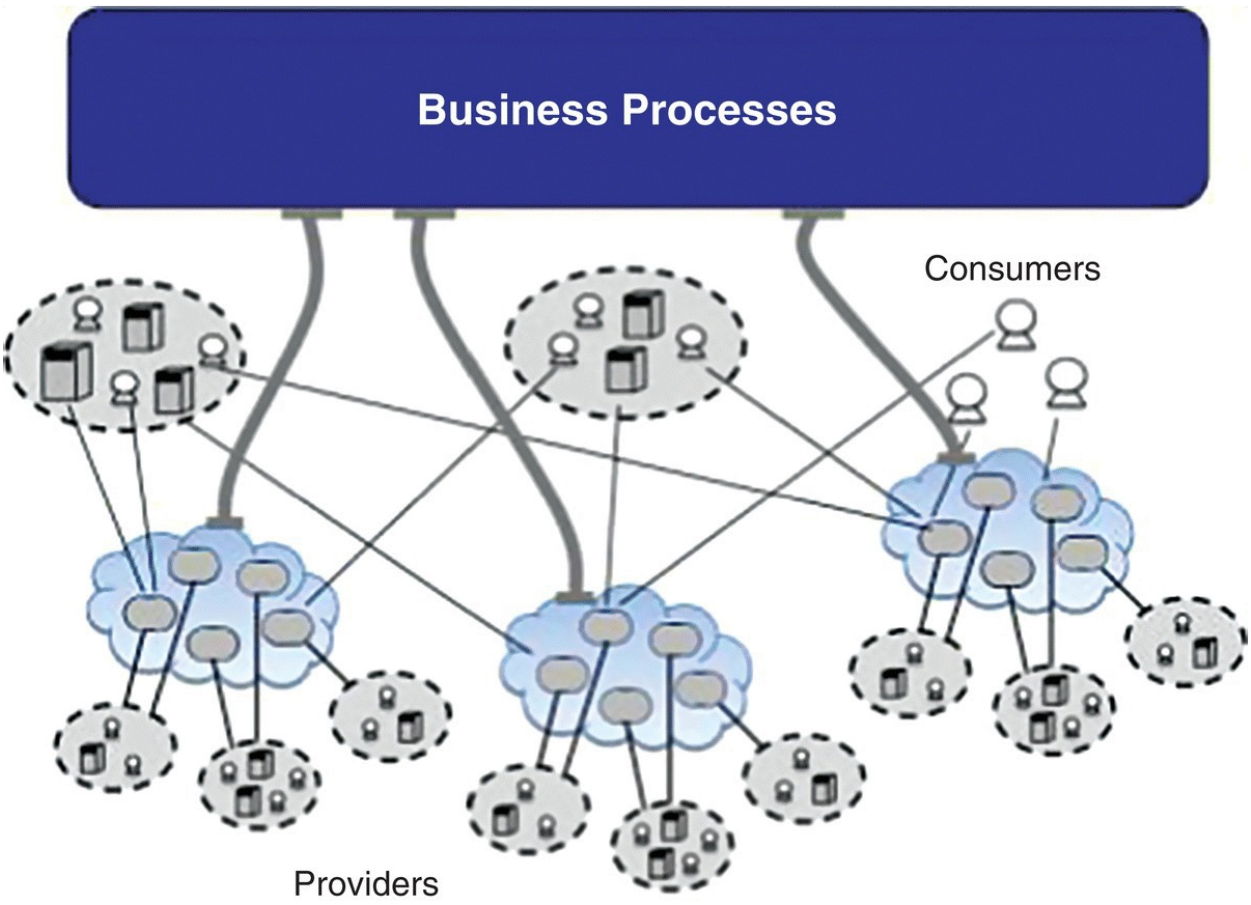

Figure 15.12 (F) Cloud ecosystem.

This section is courtesy of the Open Group, in Public Domain. For more details, refer to the following Website: www.opengroup.org/cloud computing for business/what.htm

15.7.4 An Example of Using Cloud Storage for PACS Archive

15.7.4.1 The Experiment

Dr L.B. Silva, *et al*. performed an experiment in their laboratory using cloud storage technology for a PACS-based image archive in 2011. Taking advantage of the novel technology, the architecture of a cloud-based PACS archive with data privacy, integrity, and availability was developed. The experiment used two independent cloud storage service providers, Google Storage and Amazon S3, and a standard LAN PACS storage device from the laboratory. Each of the three common identical DICOM services with storage and Q/R were installed to each of the three storage systems, Google, Amazon, and LAN PACS storage device.

Operational metrics of several medical imaging modalities were used as a means to compare the performance of these three archive systems (see Silva reference for results) [18-20].

15.7.4.2 PACS Cloud Architecture

The PACS cloud architecture was devised to minimize typical cloud storage weaknesses. Particular emphasis was given to the separation of private data element manipulation from demanding computational operations. The developed solution was based on three major components, a gateway at the hospital and two outside components from the cloud computing archive service. One side of the gateway at the hospital connected internally to image acquisition devices and WSs. The gateway was also connected to the outside archive server with a master index, which was a part of the patient image information, and a cloud slave consisting of the slaves DB (Database and blobstores). Figure 15.13A depicts a typical cloud storage service, in which the hospital relies on an outside cloud storage device to archive its images and related data, for example patient's hospital information and radiology image examination reports.

Figure 15.13B shows how to utilize the cloud storage service(s) with multiple components (Cloud Slaves, Master Index, Databases, and Blobstore) to support enterprise level operation with multiple hospitals, each of which has various specialty physicians, and different types of patients (see also Sections 15.4 and 15.5 and Section 7.4.3 in Chapter 7).

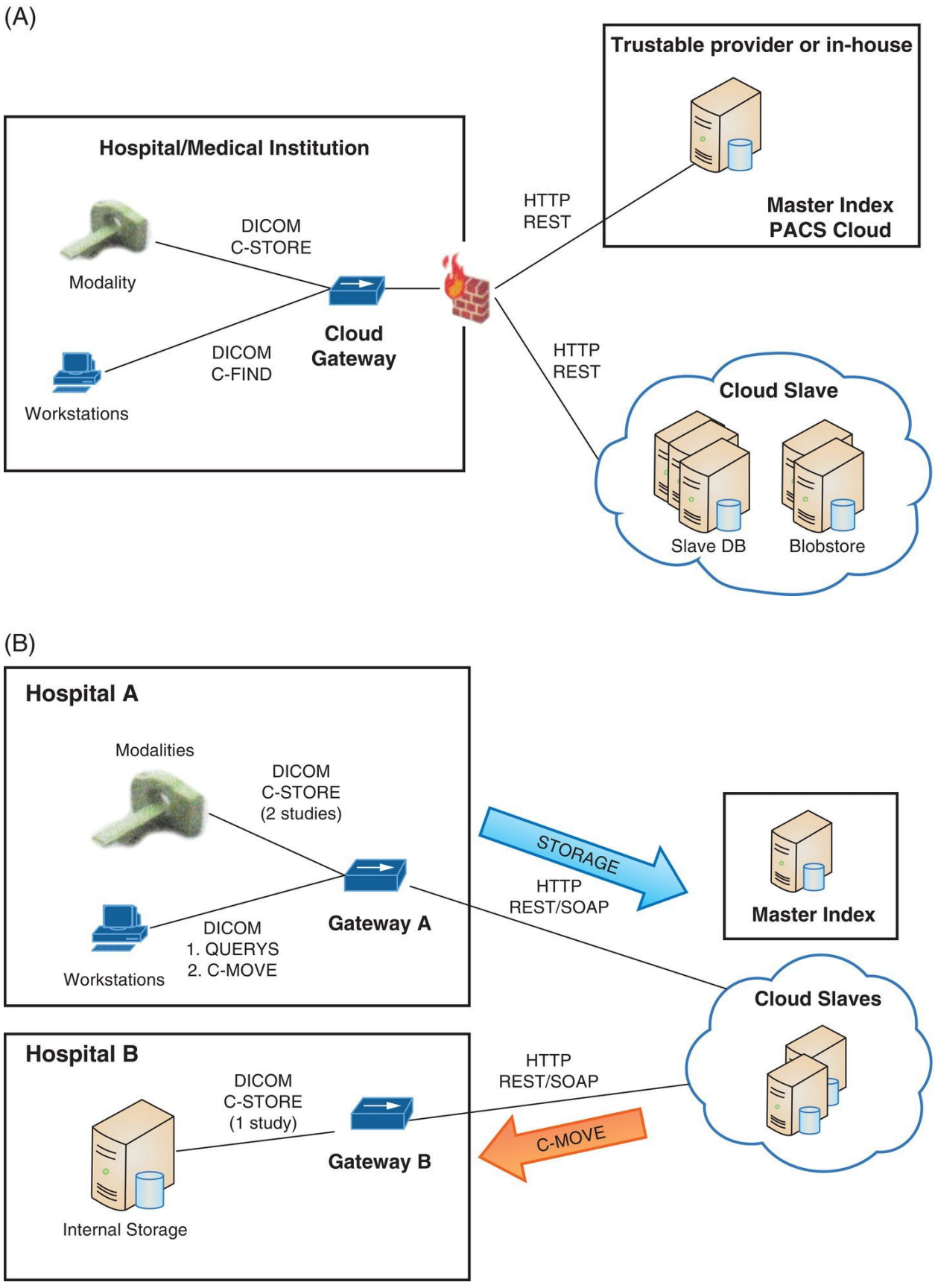
(A)
Trustable provider or in-house
Master Index
PACS Cloud
Hospital/Medical Institution
Modality
DICOM
C-STORE
HTTP
REST
Cloud
Gateway
DICOM
C-FIND
Workstations
HTTP
REST
Cloud Slave
Slave DB
Blobstore
(B)
Hospital A
Modalities
DICOM
C-STORE
(2 studies)
STORAGE
HTTP
REST/SOAP
Master Index
Gateway A
DICOM
1. QUERYS
2. C-MOVE
Workstations
Cloud Slaves
Hospital B
HTTP
REST/SOAP
DICOM
C-STORE
(1 study)
C-MOVE
Gateway B
Internal Storage

Figure 15.13 (A) An example of the architecture using a cloud storage service to archive images and other data from the hospital. 1) Images and other data are collected from the imaging modality and WSs (left) using the DICOM C-STORE and C-FIND (left, middle). 2) The collected information is transmitted through the cloud gateway (left, blue) at the hospital, screened by the hospital firewall (middle, red) for the protection of its data integrity. 3) Hypertext transfer protocol (HTTP) representational state transfer (REST; right) are used to categorize the data, then archived them to the proper cloud components master index, slave database, DB, and blobstore. The workflows of these steps are described in Figures 15.14.

(B) An example of using PACS cloud services (right) to transmit images and data across two hospitals (left top and bottom). See also Figure 15.13A for terminology and explanation. 1) Hospital A (upper left) activates the DICOM-to-Web-services gateway to request data transmission to Hospital B (lower left). 2) Hospital A starts DICOM services C-STORE, QUERYS, C-FIND, and C-MOVE from modalities and WSs at Hospital A. 3) Gateway A, using the HTTP REST/SOAP, activates STORAGE (blue) to transmit the gateway data to the cloud services consisting of the master index and the cloud slaves. 4) The cloud service activates C-MOVE (orange) to gateway B (blue) at Hospital B and uses the DICOM C-STORE to wake up its internal storage to archive.

15.7.4.3 PACS Cloud Storage Service Workflow, Data Query and Retrieve

There are two important steps in activating the cloud storage service: the cloud storage workflow (Figure 15.14A,B), and data Q/R functions (Figure 15.14C).

The gateway at the hospital uses the DICOM devices alerting imaging modalities and WSs to transmit image and data, as shown in Figures 15.13 and 15.14A (left and middle, blue). Figure 15.14B, through the left and middle solid lines, shows the transferred DICOM information from the gateway (middle), then the gateway using the solid blue lines, sends data through the Internet connection to the cloud storage, consisting of a cloud slave blobstore with storage data, cloud slave database with slave database metadata, and master index with references (blue solid lines). In addition, the cloud storage (dotted green lines), acknowledges to the gateway that the cloud storage has received data from the outside hospitals [21].

When a qualified hospital requests data and images from the cloud storage service, Figure 15.13B (thick red arrow) delineates the query, and Figure 15.14C

depicts the reverse process (dotted green lines).

Note that when multimedia data are stored in the cloud storage, the stored data are not in the same format as the medical images and reports, since these data have been converted by HTTP REST format and with data encryption during the processes.

(A)

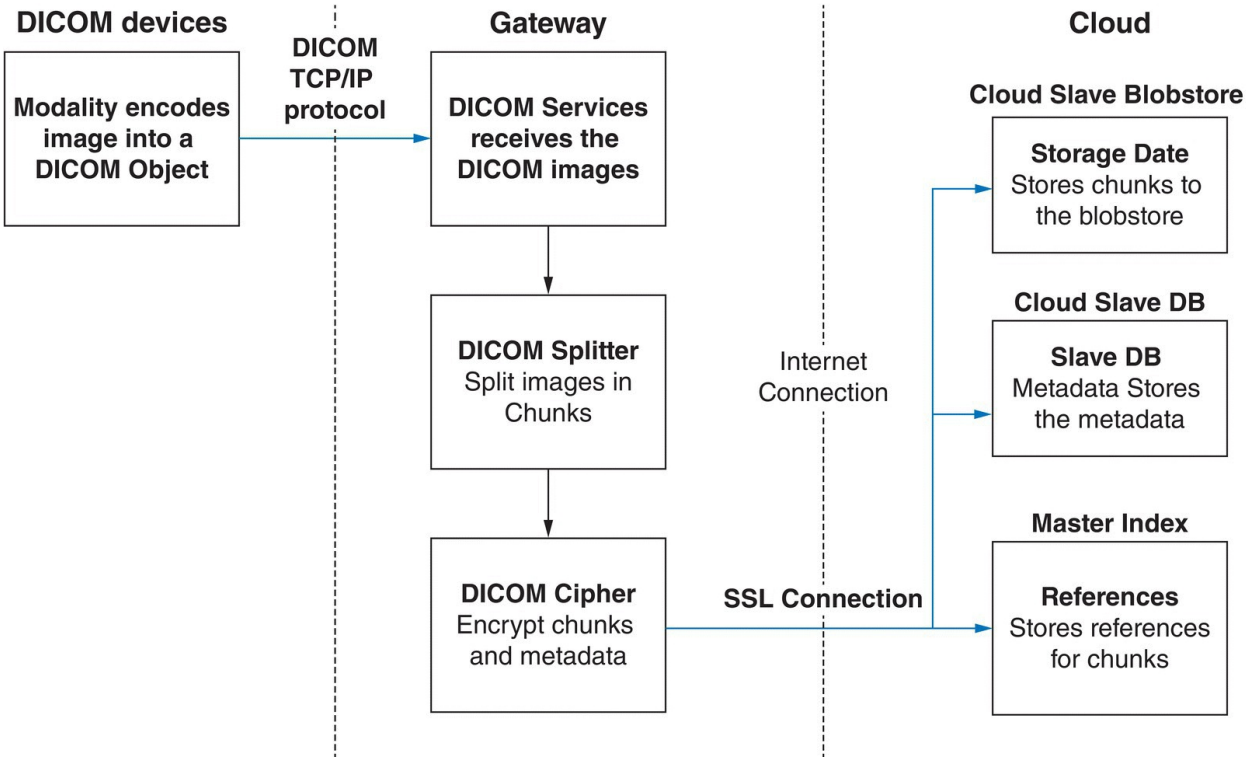

(B)

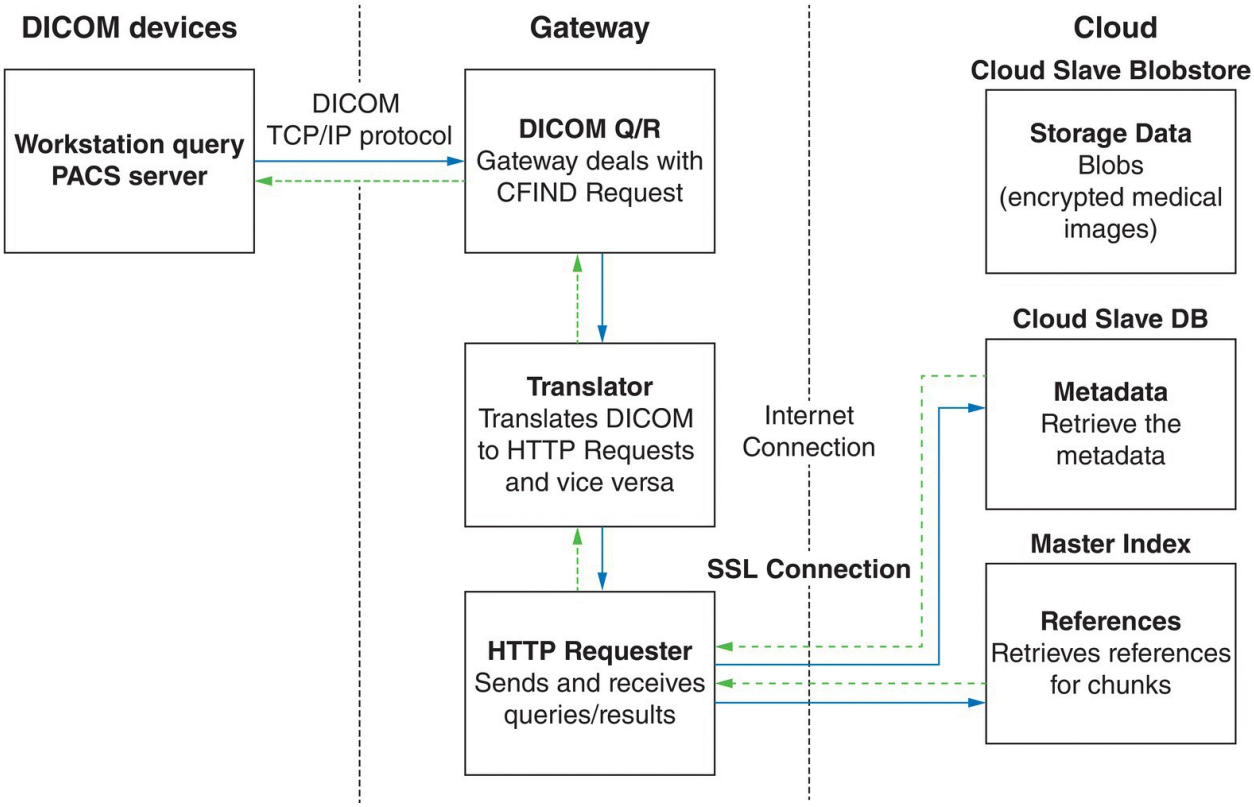
DICOM devices
Gateway
Cloud
Workstation query PACS server
DICOM TCP/IP protocol
DICOM Q/R
Gateway deals with CFIND Request
Cloud Slave Blobstore
Storage Data
Blobs
(encrypted medical images)
Cloud Slave DB
Translator
Translates DICOM to HTTP Requests and vice versa
Internet Connection
Metadata
Retrieve the metadata
Master Index
SSL Connection
HTTP Requester
Sends and receives queries/results
References
Retrieves references for chunks

(C)

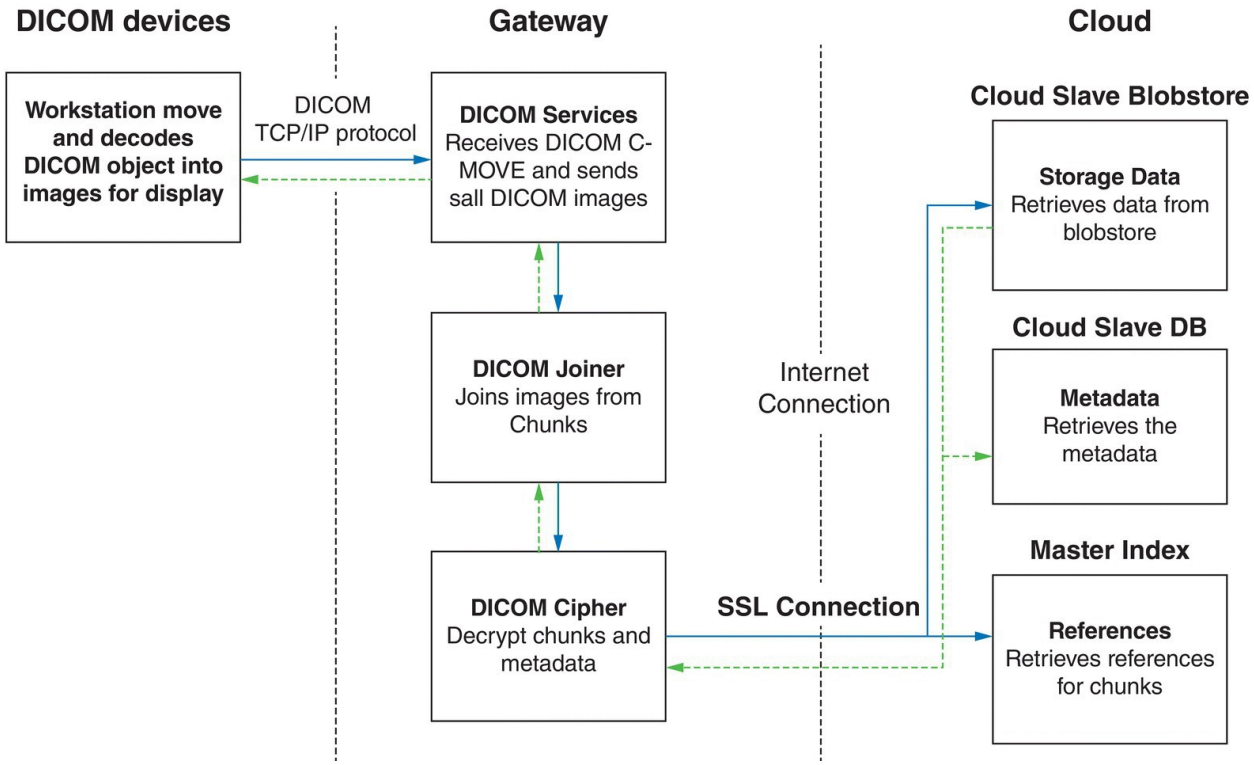
DICOM devices
Gateway
Cloud
Workstation move and decodes DICOM object into images for display
DICOM TCP/IP protocol
DICOM Services
Receives DICOM C-MOVE and sends sall DICOM images
Cloud Slave Blobstore
Storage Data
Retrieves data from blobstore
Cloud Slave DB
DICOM Joiner
Joins images from Chunks
Internet Connection
Metadata
Retrieves the metadata
Master Index
DICOM Cipher
Decrypt chunks and metadata
SSL Connection
References
Retrieves references for chunks

Figure 15.14 (A) PACS cloud storage workflow, left to right—each DICOM object (left) sends the patient study directly to the gateway (middle, blue) that is responsible to store it on the cloud slave (right, blue arrows). See also Figure 15.13. (B) PACS cloud query workflow—using the DICOM devices, the WS (left, blue) sends a query to the gateway (middle, blue) that inquires of the cloud database and the master index (right, blue). The collected results are then combined and returned to the gateway (green), then the WS (left, green). (C) PACS cloud retrieval workflow—cloud (right, green dot) to gateway (middle, green), and gateway to WSs (left, green). See also Figure 15.13B (bottom, red).

15.7.5 Summary of Cloud Computing and Archive Server

Section 15.7 presents the concept of PACS-based archive server using the cloud computing technology. Both DICOM and non-DICOM images and data are stored in the cloud computing archive server, regardless of whether originating from the radiology PACS or any data from other clinical specialty examinations for both archive and retrieve purposes. PACS-based cloud technology grants interoperability with DICOM or non-DICOM devices and acts as a traditional PACS archive from the client's perspective. This characteristic of PACS is very powerful and valuable, to be preserved and maintained in the archive, since many fundamental properties of the patients were obtained from the HIS and RIS during their examinations. Furthermore, from the administrator's point of view, it greatly reduces information technology (IT) infrastructure and brings new management facilities to the enterprise level institutions to share various patient information, images, reports, and data throughout the enterprise infrastructure.

Cloud computing is an emerging solution that promises high scalability of infrastructures, software, and applications, according to a "pay-as-you-go" business model. This approach has motivated and propagated the current storage solution concept: VNA, which uses cloud computing technology to replace the current PACS archive and retrieve method. In addition to RIS and HIS, and radiology images and data, cloud computing and archive server technology appears to be accepting multimedia PACS-based imaging informatics input, DICOM or non-DICOM, so promises to be a potential emerging technology for the VNA solution.

Acknowledgements

Section 15.7 of this chapter presents the recent advances of cloud technology, and the trend of deconstructed PACS and the VNA. During the past 6 years, NIST and the Open Group have both contributed tremendously to its development: the definitions and guidelines from NIST, and the suggested models and services, and the leadership role from the Open Group. Together, they have propelled cloud computing and archive services technology to the current stage. Professor B. Liu at USC diligently surveyed and investigated the PACS's current state-of-the-art during the 2015 RSNA. In discussions with his colleagues and business associates, they recognize the trend of future PACS business models and foresee the potential opportunity in developing multimedia imaging and informatics archive and retrieve service models. Dr Silva's group pioneered the cloud computing retrieval and archive experiment in 2011, where they demonstrated the possibility of scalability of infrastructures, software, and applications, according to a "pay-as-you-go" business model. During our discussion of their experiment, I was fortunate to have Dr Silva contribute Figures 15.13 and 15.14 from their publication.

References

1 Biegel, J. (2007) *Evolution of PACS as a Model to Predict Adoption of Digital Pathology*. McKesson Medical Imaging Group, Presentation, October 23, 2007.

2 Law, Y.Y., Liu, B.J. and Chan, L. (2009) A DICOM-RT-based ePR (Electronic Patient Record) information system for radiation ePR in radiation therapy. *RadioGraphics*, 29, 961–972.

3 Le, A., Liu, B., Schulte, R. and Huang, H.K. (2011) Intelligent ePR for evidence-based research in radiotherapy: An example in proton therapy for prostate cancer, *Intern J. Comp Asst Rad & Surg*, 6(6), 769–784.

4 Documet, J., Le, A., Liu, B.J., Chiu, J. and Huang, H.K. (2010) A multimedia Electronic Patient Record (ePR) system for image-assisted minimally invasive spinal surgery. *Intern J. Comp Asst Rad & Surg*, 5(3), 195–209.

5 Lee, J., Zhang, J., Park, R., Grant, D., Liu, B. and Huang H.K. (2012) A DICOM-based 2nd generation molecular imaging data grid implementing the IHE XDS-I integration profile. *Intern J Comp Asst Rad & Surg*, 7, 533–545.

6 Le, A., Liu, B. and Huang, H.K. (2009) Integration of computer-aided diagnosis/detection (CAD) results in a PACS environment using CAD–PACS

toolkit and DICOM SR. *Intern J. Comp Asst Rad & Surg*, 4, 317–329.

7 Doi, K. and Huang, H.K. (2007) Computer-aided diagnosis (CAD) and image-guided decision support. Editorial. *J Computer Med Imag Graph*, 31, 195–197.

8 Lee, J., Documet, J., Liu, B.J., Park, R., Tank, A. and Huang, H.K. (2011) MIDG-Emerging grid technologies for multi-site preclinical molecular imaging research communities. *Intern J Comp Asst Rad & Surg*, 6, 285–296.

9 Huang, H.K. (2010) *PACS and Imaging Informatics Basic Principles and Applications*, 2nd edition. Hoboken, NJ: Wiley & Blackwell.

10 Amazon Simple Storage Service: https://s3.amazonaws.com/

11 Amazon Webservices (AWS): http://aws.amazon.com/

12 Amazon Web Services LLC (2009) Case studies: TC3 health.Web page: http://aws.amazon.com/solutions/case-studies/tc3-health/

13 Benjamin, M., Aradi, Y. and Shreiber, R. (2010) From shared data to sharing workflow: merging PACS and teleradiology. *Eur J Radiol*, 73(1), 3–9.

14 Bennett, S., Bhuller, M. and Covington, R. (2009) Architectural strategies for Cloud computing. Oracle: http://www.oracle.com/technetwork/topics/entarch/architecturalstrategies-for-cloud-128191.pdf

15 Rosenthal, A., Mork, P., Li, M.H., Stanford, J., Koester, D. and Reynolds, P. (2010) Cloud computing: a new business paradigm for biomedical information sharing. *J Biomed Inform*, 43(2), 342–353.

16 Schutze, B., Kroll, M., Geisbe, T. and Filler, T.J. (2004) Patient data security in the DICOM standard. *Eur J Radiol*, 51(3), 286–289.

17 Sharma, A., Pan, T., Cambazoglu, B.B., Gurcan, M., Kurc, T. and Saltz, J. (2009) VirtualPACS–a federating gateway to access remote image data resources over the grid. *J Dig Imag*, 22(1), 1–10.

18 Eucalyptus: [http://www.eucalyptus.com]

19 Google App Engine (GAE): [http://code.google.com/appengine/]. Google Storage for Developer: http://code.google.com/apis/storage/

20 HIPAA: http://www.rx2000.org/KnowledgeCenter/hipaa/hipfaq.htm

21 Silva, L.A.B., Carlos, C., Oliveira, J.L. (2011) A PACS archive architecture supported on cloud services, *Int J CARS*, June, 2011.

Note

1 The National Institute of Standards and Technology (NIST) is a measurement standards laboratory, and a non-regulatory agency of the United States Department of Commerce. Its mission is to promote innovation and industrial competitiveness. NIST's activities are organized into laboratory programs that include Nanoscale Science and Technology, Engineering, Information Technology, Neutron Research, Material Measurement, and Physical Measurement [15–17].

Part 4
Multimedia Imaging Informatics, Computer-Aided Diagnosis (CAD), Image'Guide Decision Support, Proton Therapy, Minimally Invasive Multimedia Image-Assisted Surgery, Big Data

Prologue – Chapters 16, 17 and 18

PERPUSTAKAAN PRIBADI AN-NUR SUNARYA

16
DICOM-Based Medical Imaging Informatics and CAD

CHAPTER MENU

16.1 Computer-Aided Diagnosis (CAD)

16.1.1 CAD Overview

16.1.2 CAD Research and Development (R&D)

16.1.3 Computer-Aided Detection and Diagnosis (CAD) without PACS

16.1.4 Conceptual Methods of Integrating CAD with DICOM PACS and MIII

16.2 Integration of CAD with PACS-based Multimedia Informatics

16.2.1 The Need for CAD-PACS Integration

16.2.2 DICOM Standard and IHE Workflow Profiles

16.2.3 DICOM Structured Reporting (DICOM SR)

16.2.4 IHE Profiles

16.3 The CAD–PACS Integration Toolkit

16.3.1 Current CAD Workflow

16.3.2 Concept

16.3.3 The Infrastructure

16.3.4 Functions of the Three CAD-PACS Editions

16.4 Data Flow of the three CAD–PACS Editions Integration Toolkit

16.4.1 DICOM-SC, 1st Edition

16.4.2 DICOM–PACS–IHE, Second Edition

16.4.3 DICOM–CAD–IHE, Third Edition

References

Further Reading

The first three chapters in Part 4 relate to PACS-based computer-aided detection and diagnosis (CAD). The DICOM-based PACS is a mature technology in healthcare delivery for daily clinical imaging service and data management. CAD employs computer methods to obtain quantitative measurements from medical images and clinical information to assist clinicians in assessing a patient's clinical state more objectively. CAD needs image input and related information from PACS to improve its accuracy; and PACS would benefit from CAD online results from the workstation (WS) and as a second reader to assist physicians during their decision-making process. Currently, these two technologies, PACS-based informatics and CAD, remain as separate independent systems, with only minimal system integration. In this chapter, contents of these next three chapters is intertwined with their rich technologies, methods, and standardization, as well as the Health Level 7 (HL7), DICOM and its structured reporting (SR), Integrating the Healthcare Enterprise (IHE), and Health Insurance Portability and Accountability Act compliance in developing a general universal concept of integrating CAD with PACS-based medical image informatics in the daily clinical environment.

16.1 Computer-Aided Diagnosis (CAD)

This chapter presents DICOM-based medical imaging informatics and CAD. For convenience purposes, Figure 16.0 is used for PACS and CAD terminology.

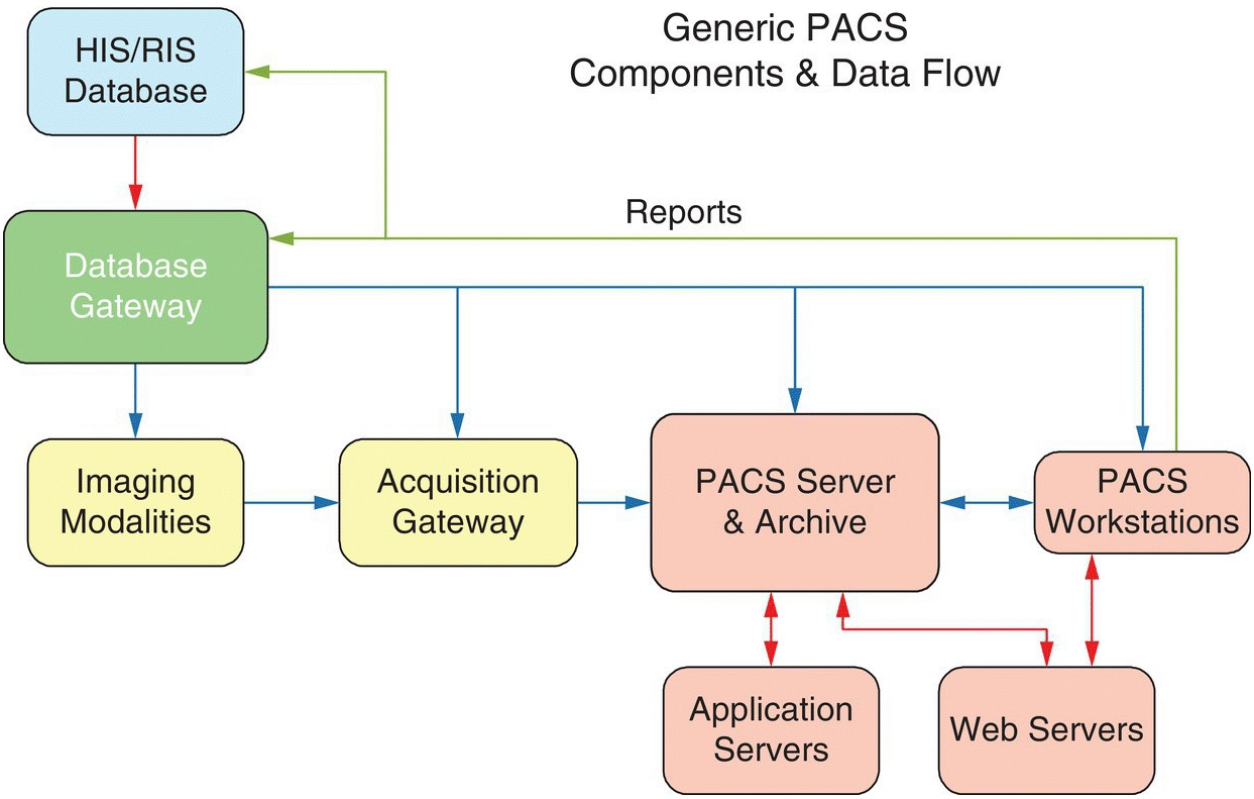

Figure 16.0 PACS data management and Web-based image distribution. PACS data management, patient folder management, Web-based server, and wireless remote control of clinical image workflow are related to the four red boxes in the PACS components and workflow.

16.1.1 CAD Overview

Computer-aided detection (CAD), or computer-aided diagnosis (CADx), research started in the early 1980s and has gradually evolved as a clinical support tool. In mammography, CAD has in fact become a part of the routine clinical operation for the detection of breast cancers in many medical centers and screening sites in the United States. In addition, various CAD schemes have been developed for detection and classification of many different kinds of lesions obtained with the use of various imaging modalities. This is because the concept of CAD is broad, and also can assist radiologists by providing the computer output as a “second opinion.” The usefulness and practicality of CAD, however, depends on many factors, including the availability of digital image data, computer power, and high-quality display and image-archiving systems. It is apparent that CAD needs to be integrated into a part of PACS to become effective to assist clinical practice.

Image-based knowledge discovery and decision support by the use of CAD has become a new trend in research, which translates CAD diagnostic results to assist in short- and long-term patient treatments. PACS was developed more than 30 years ago and has become an integral part of daily clinical operations. Integration of CAD with PACS can take advantage of the image resources in PACS to enhance the value of CAD. CAD applications can therefore be merged into the mainstream for image-aided clinical practice. CAD has become one of the major research subjects in medical imaging informatics and diagnostic radiology. With CAD, radiologists and clinicians use the computer output as a "second opinion" to make the final decisions. CAD, based on computer algorithms, is a concept that has been taken into account equivalently to the roles of physicians, yet the performance of CAD does not have to be comparable to or better than that of physicians, but needs to be complementary to that by physicians. Figure 16.0 (used in several other chapters) refreshes the basic architecture of generic PACS components and its data flow [1–6].

16.1.2 CAD Research and Development (R&D)

CAD research and development (R&D) can be loosely divided into five categories, based on research methods and clinical use:

1. *CAD algorithms research and development*: This category covers general CAD algorithms development in chest radiography, mammography, MR breast imaging, thin-slice CT nodules, and multidimensional medical imaging in organs and diseases. The algorithm development is mostly for general purpose applications. This category attracts most CAD R&D interest. Professor Kunio Doi at the University of Chicago extensively reviewed these types of research, and among them are recent advances that merge CAD with other technologies, as shown in Figure 16.1: multi-view chest radiographs, temporal subtraction of nuclear medicine bone scans, and database search for separating a benign versus malignant mass in mammograms.
2. *Target CAD applications*: This category focuses on CAD application for a specific aliment on a specific imaging modality in a certain clinical environment. In other words, the CAD method may not necessarily be developed for a general clinical setting, but it is used to assist the healthcare provider, at the critical moment in a particular time and space, to obtain a more accurate and timely diagnosis. An example is CAD of small acute intracranial hemorrhage (AIH) on a brain CT, which has been developed for patients in the emergency room suspected of non-penetrating brain injury

when a neuroradiologist may not be readily available to read the CT images (see Chapter 17).

3. *Decision support*: Decision support means that the CAD method developed contributes to a component of a larger CAD system for achieving a common goal. The goal could be an assessment process or contribution to decision support toward a final diagnosis or a treatment plan. An example is in bone age assessment of children using CAD on a hand radiograph (see Chapter 18). In this case, the bone age assessment is based on multiple CAD algorithms on three different regions of the hand, the phalangeal, carpal bone, and the wrist joint region.
4. *CAD system and evaluation*: This category considers a complete CAD system that contains several CAD algorithms, one for each part of the body anatomy for a local decision support. Each algorithm can be a CAD algorithm mentioned in category 3. Together they form a CAD system for achieving a common diagnostic or assessment goal. In the case of bone age assessment, the combination of phalangeal, carpal, and wrist joint bone results is assembled using a fuzzy logic method to derive the final bone age.
5. *Security and CAD–PACS integration*: Integration of CAD and PACS requires the consideration of data security and the method of integration. Data security is necessary to ensure the integrity of images sent to the CAD algorithm for processing, and the integrity of the CAD output data sent back to the WS for reading and archiving in the PACS environment. The method of integration considers how to transfer images from PACS to CAD for processing and to return the CAD results to PACS most efficiently.

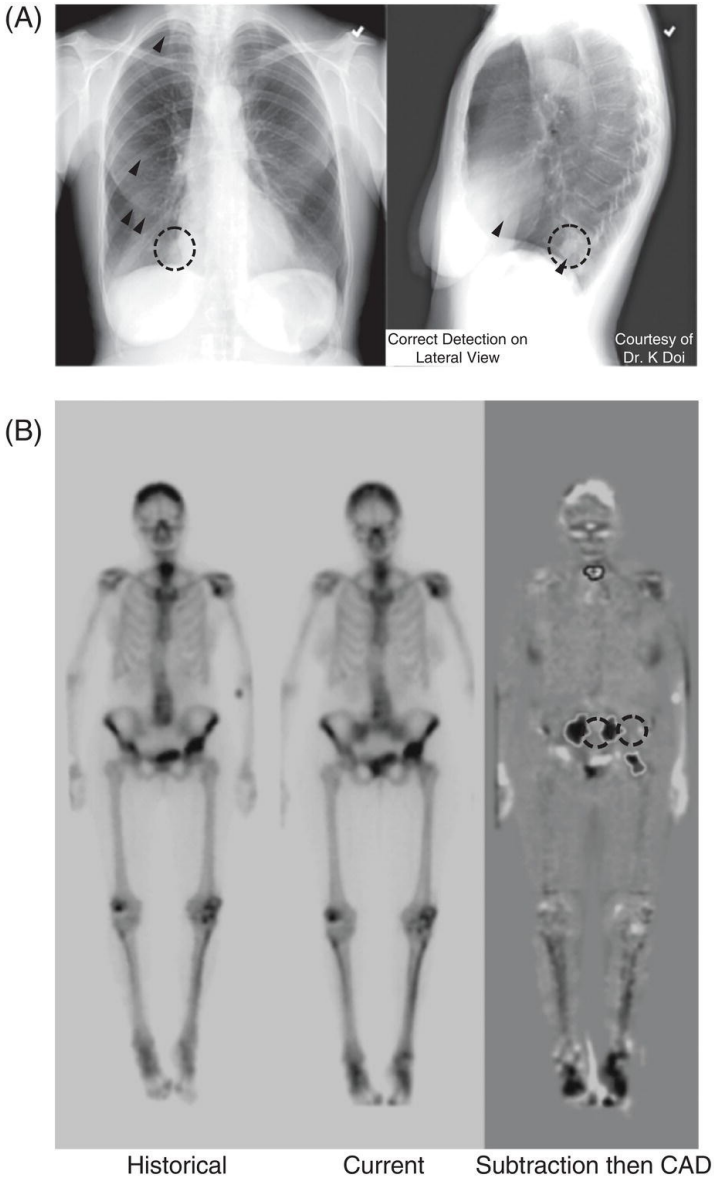
(A)
Correct Detection on Lateral View
Courtesy of Dr. K Doi
(B)
Historical
Current
Subtraction then CAD
(C)
Database in PACS
Unknown
Benign
Malignant

Figure 16.1 (A) Demonstration of multi-view CAD. The relatively large, but very subtle lung nodule (dotted circles), located in the right mediastinum region was correctly marked by CAD (triangles) on the lateral view of a chest radiograph, but was not marked by CAD on the PA view. (B) Temporal subtraction image obtained from previous and recent nuclear medicine bone scan images. One cold lesion (solid circle) and two hot lesions (dark dotted circles) on the subtraction image were correctly marked by CAD method. The temporal subtraction image for successive whole-body bone scans has the potential to enhance the interval changes between two temporal images. (C) Image matching from collected nodules in the PACS/MIII or imaging informatics nodule database. Comparison of an unknown case of a mass in a mammogram in the center (blue) with two benign masses on the left and two malignant masses on the right, which may be retrieved from the PACS database. Most observers were able to visually identify the unknown case correctly as being more similar to malignant masses (right, orange) than to benign ones (left, green).

(courtesy of Dr K. Doi)

For example, Doi tracked the CAD R&D progress between 2000 and 2008 [6] based on computer algorithms, as shown in Tables 16.1A and B based on the Radiological Society of North America (RSNA)annual presentations in this field of study. The progression in the table shows the increasing interest and acceptance by the radiological community throughout the years, in using CAD for assisting clinical diagnosis in various body regions. It is commonly agreed that the integration of CAD with PACS will lead to the emergence of CAD applications into mainstream image-aided clinical practice, in both diagnosis and treatment.

Table 16.1 (A) Topics and numbers of CAD-related presentations at the RSNA meetings, 2000–2008.

	2000	**2001**	**2002**	**2003**	**2004**	**2005**	**2006**	**2007**	**2008**
CAD	55	86	134	191	161	165	167	192	227
Digital mammograms	12	15	20	25	27	22	34	44	31
Lung cancer screening	6	12	19	21	17	7	18	10	10
CR/DR/FPD*	14	20	14	25	18	16	27	24	9

* CR/DR/FPD: Computed radiography/digital radiography/flat-panel detector

Table 16.1 (B) Number of CAD presentations at the RSNA meetings, 2003–

2008.

	2003	2004	2005	2006	2007	2008
Chest	94	70	48	62	72	73
Breast	37	48	49	47	39	51
Colon	17	15	30	25	32	24
Brain	10	9	17	12	13	20
Liver	9	9	9	8	8	22
Skeletal	9	8	5	7	11	6
Vascular, and other[a]	15	2	7	6	17	31
Total	191	161	165	167	192	227

[a] Cardiac, prostate, pediatric, dental PACS.

16.1.3 Computer-Aided Detection and Diagnosis (CAD) without PACS

16.1.3.1 CAD without PACS and without Digital Image

The computer-aided detection or diagnosis engine can stand alone as a PACS-based application server, or it can be organized as a medical imaging informatics infrastructure (MIII) resource. The purpose is to use image post-processing to derive additional parameters to aid the physician as a second reader to improve diagnostic performance. Traditional CAD is performed off line in the sense that an image set of a patient is acquired from a given modality, either through a peripheral device or network transmission, from which image processing is performed to extract relevant parameters. These parameters are then used to provide additional information to pinpoint sites of potential pathology in the image set to alert the physician. The derived parameters are not appended to the images for later retrieval. These procedures are performed without taking advantage of the PACS resource.

An example of a film-based CAD is the one used in mammography. In this film-based CAD (Figure 16.2), screen/film mammograms are digitized, sub-sampled, and fed to a processor that contains the CAD algorithms for detection of microcalcification, masses, and other abnormalities. Results from the CAD are superimposed onto the sub-sampled digitized mammogram and displayed (see Figure 16.2, red dots) on a specific CAD WS with a standard set of monitor(s),

which may not be of the quality to make primary diagnosis on a digital mammogram. An expert radiologist with mammography training displays the film mammogram on the light box viewer (see Figure 16.2, blue color) to visually compare it with the sub-sampled digitized mammograms with detected lesions on the WS. This off-line CAD method is a two-step process requiring special hardware and software to accomplish the detection process. Such a CAD system consists of a film digitizer, a WS, a CAD processor, and a mammography film light-box viewer for comparing the CAD result with the original film mammogram.

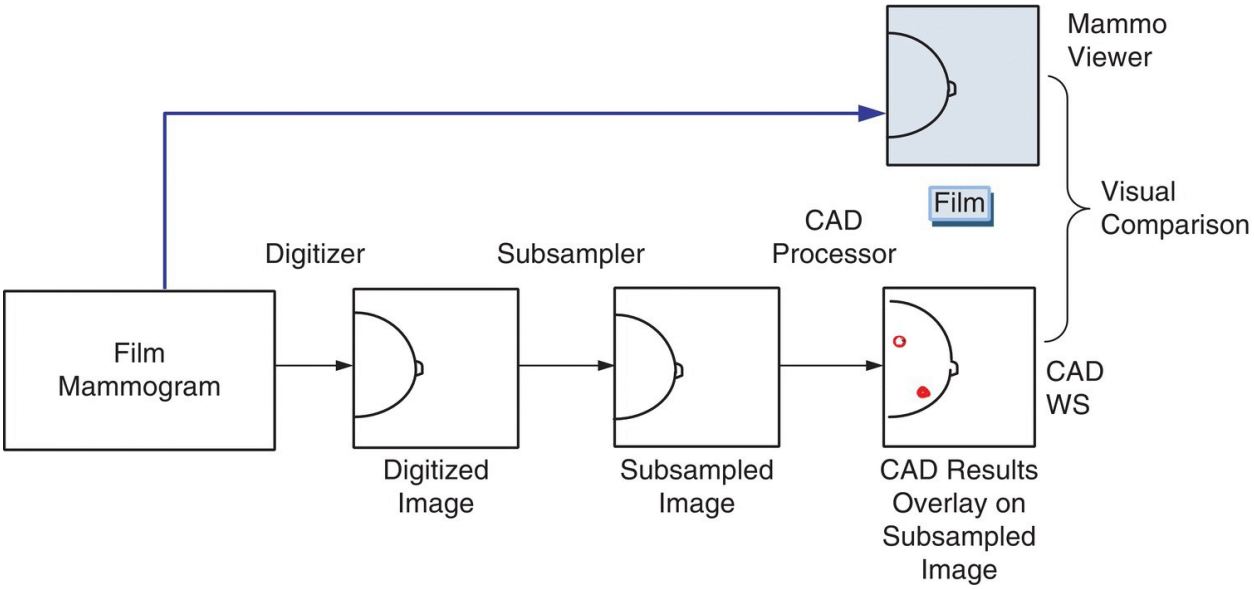

Figure 16.2 Data flow in film-based CAD mammography. Only a single monitor and single light-box viewer are shown in the diagram.

CAD can be integrated into a PACS or MIII environment by taking advantage of the existing resources in its storage, retrieval, communication networks, and display components. Figure 16.2 depicts the data flow in film-based CAD mammography (see Chapter 18).

16.1.3.2 CAD without PACS but with Digital Image

CAD without PACS can use either direct digital input or film with a digitizer. In either case, CAD is an off-line isolated system. Table 16.2 lists the procedure in performing CAD in such a system. The film-based CAD system for mammography shown in Figure 16.2 is an example.

Table 16.2 CAD without PACS and with or without digital input.

- Collect films or digital images based on patient's record
- Digitize films or develop an interface program to read digital images
- Input images to the CAD workstation (WS)
- CAD algorithm
- Return results to CAD WS

16.1.4 Conceptual Methods of Integrating CAD with DICOM PACS and MIII

Integration of CAD with DICOM PACS can use the following four approaches. In the three approaches described below, CAD is connected directly to the PACS, whereas the fourth approach is to use a stand-alone CAD server connected to either the PACS or the MIII, or both.

16.1.4.1 PACS WS Q/R, CAD WS Detect

In this approach, the PACS WS queries and retrieves (Q/R) images from the PACS database and the CAD WS performs the detection. Table 16.3A and Figure 16.3A illustrate the steps in the CAD. This method involves the PACS server, the PACS WS, and the CAD WS. A DICOM C-store (see Chapter 5) function must be installed in the CAD WS.

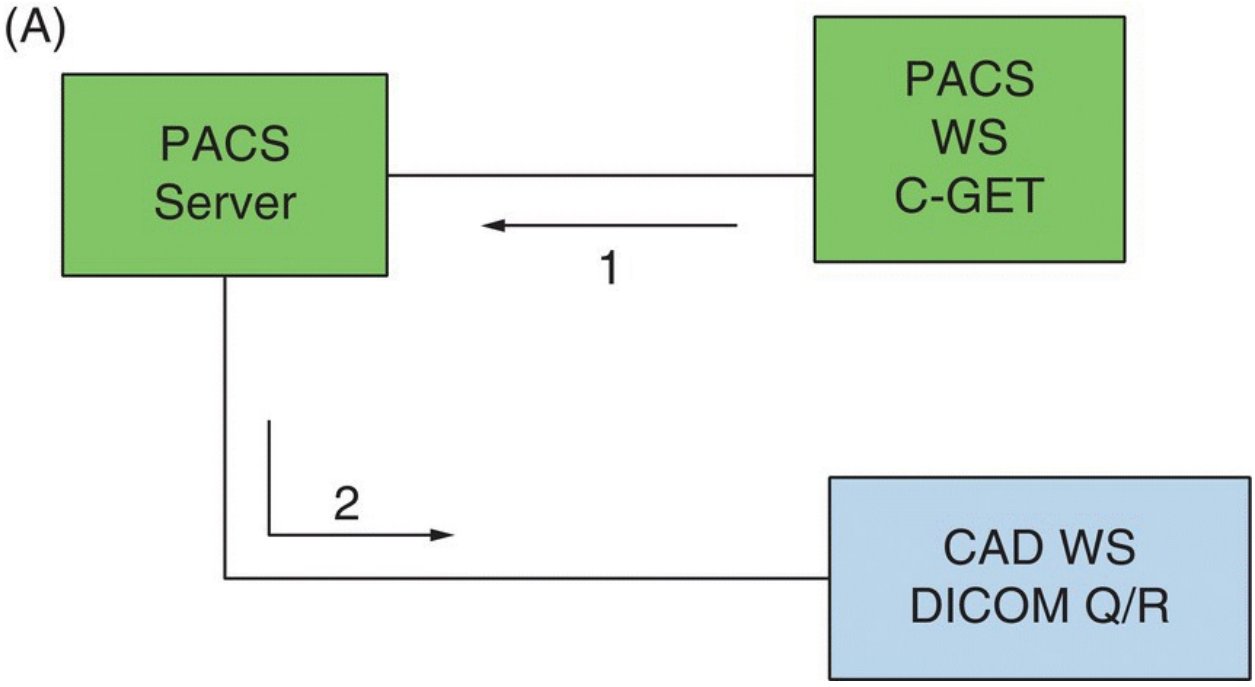

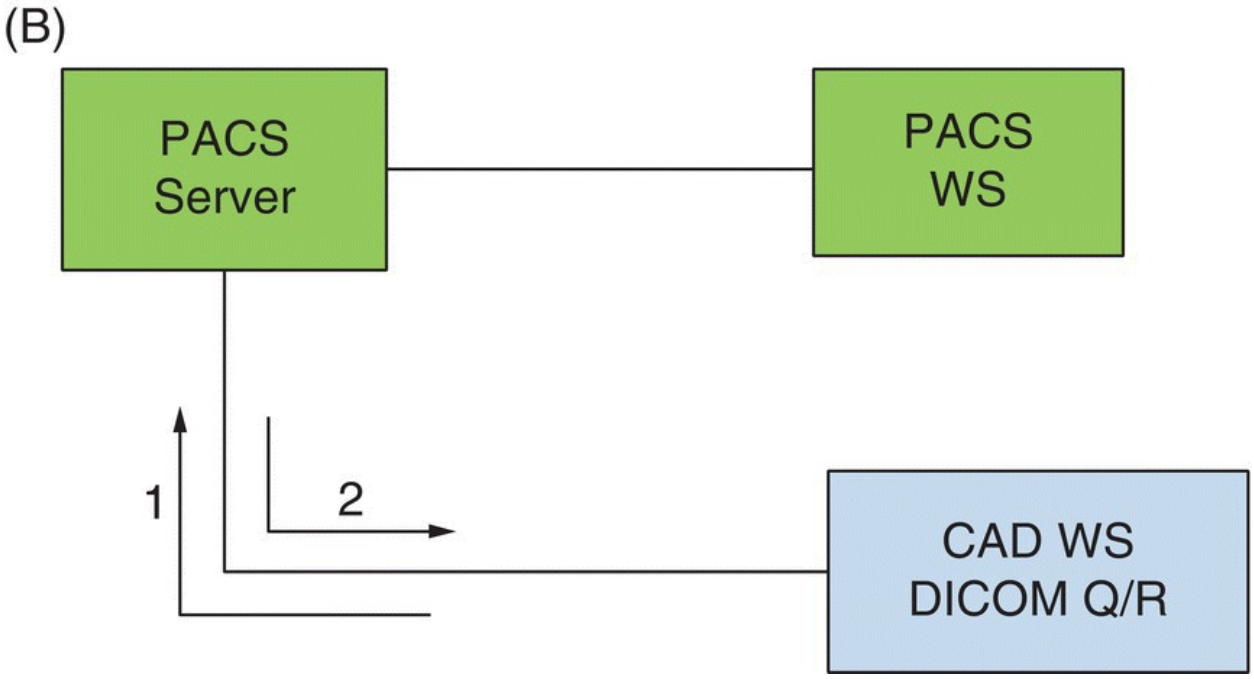
(B)
PACS
Server
PACS
WS
1
2
CAD WS
DICOM Q/R

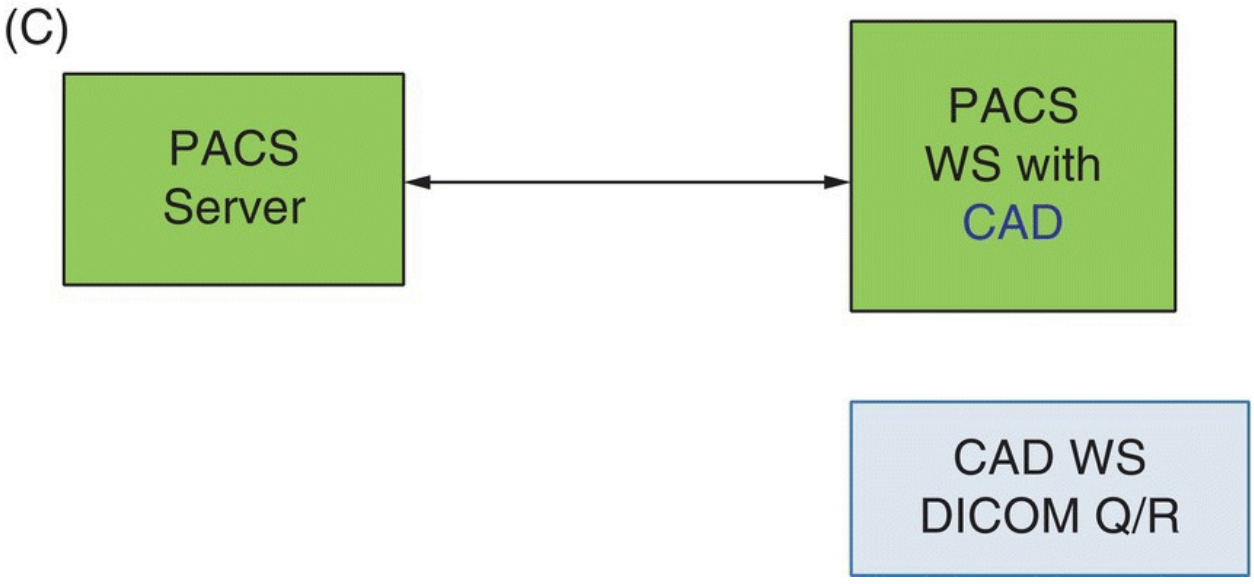
(C)
PACS
Server
PACS
WS with
CAD
CAD WS
DICOM Q/R

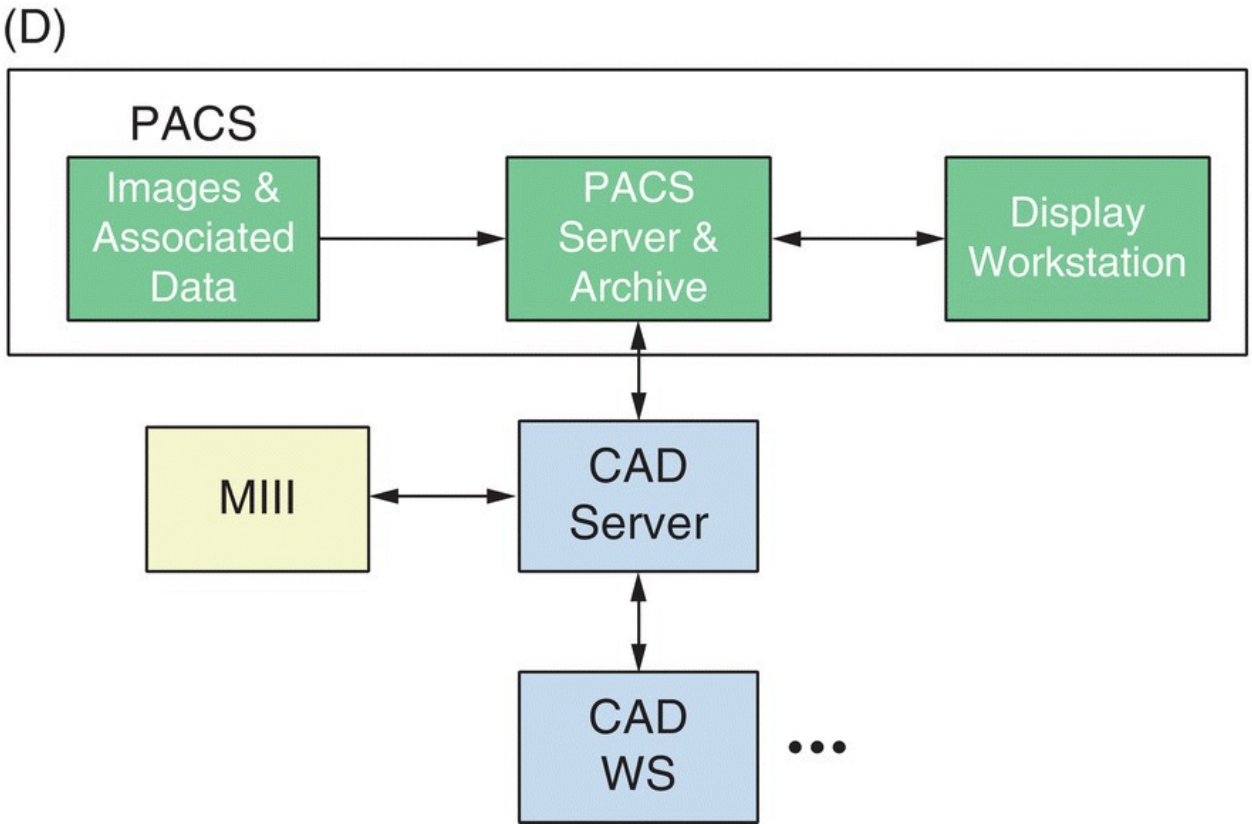

Figure 16.3 Methods of integrating CAD with DICOM PACS (see also Table 16.3). (A) PACS WS Q/R, CAD WS detect (C-GET is a DICOM service); (B) CAD WS Q/R and detect; (C) PACS WS has CAD software; (D) integration of CAD server with PACS and/or MIII.

Table 16.3 (A) CAD with DICOM PACS: PACS WS Q/R, CAD WS, and detect.

At the PACS server
• Connect CAD WS to PACS • Register CAD WS (IP address, port number, application entity [AE]) title to receive images
At the PACS WS
• Use DICOM query/retrieve to select patient/studies/images • Use DICOM C-get to select images from PACS server which pushes the images to CAD WS
At the CAD WS

- Develop DICOM storage class provider (SCP) to accept images
- CAD
- Develop database to archive CAD results

16.1.4.2 CAD WS Q/R and Detect

In the CAD WS Q/R and Detect approach, the CAD WS performs both Q/R and then the detection. This method only involves the PACS server and the CAD WS. The function of the PACS server is almost identical to that of the last method. The only difference is that the last method uses the PACS WS for Q/R images, whereas in this method the CAD WS performs the Q/R. For this reason, DICOM Q/R must be installed in the CAD WS. Table 16.3B and Figure 16.3B describe the steps.

Table 16.3 (B) CAD with DICOM PACS: CAD WS Q/R and detect.

At the PACS server:
• Connect CADWS to PACS • Register CADWS (IP address, port number, AE title) at PACS
At the CAD WS:
• Develop DICOM Q/R client and storage class to select/accept patient/study/images • CAD • Develop database to archive CAD results

16.1.4.3 PACS WS with CAD Software

The next approach is to install all CAD software into the PACS WS. Table 16.3C and Figure 16.3C show the steps involved.

Table 16.3 (C) CAD with PACS: PACS WS with diagnosis software.

- Install CAD software in the PACS WS
- PACS WS Q/R patient/study/images
- Establish software linkage in WS for CAD software to access DICOM

images

- Develop DICOM format decoder to convert images to CAD format
- CAD is performed at the PACS WS
- Develop CAD database in the WS to archive CAD results

16.1.4.4 Integration of CAD Server with PACS or MIII

The last method is to connect the CAD server to the PACS server, as described in Table 16.3D and Figure 16.3D. This server can also be attached to the MIII as a computational resource. The CAD server is used to perform at the PACS or MIII. The concept is similar to the distributed Web and computational grid servers (see Chapters 8 and 9).

Table 16.3 (D) Integration of CAD server with DICOM PACS and/or MIII.

- Connect CAD server to PACS and/or MIII
- CAD server performs Q/R Patient/study/images from PACS
- Archive in CAD server
- DICOM format decoder
- Distribute images to CAD WS

16.2 Integration of CAD with PACS-Based Multimedia Informatics

Integration of CAD with PACS-based multimedia informatics introduces new concepts and additional technical background, including DICOM screen captured (SC), structured reporting (SR) framework, some specific IHE workflow profiles, and the CAD–PACS toolkit.

16.2.1 The Need For CAD–PACS Integration

Among others, the main purpose in integrating CAD with PACS for daily clinical operation is to utilize CAD as a second reader. To recap from the last section, CAD software can be implemented within a stand-alone CAD WS, a CAD server, or to be integrated in PACS as PACS-based CAD. Currently,

several PACS and CAD companies have successfully integrated their CAD applications within the PACS operation, but these applications are either in a CAD-specific WS or embedded in a closed PACS operation environment with proprietary software. For example, in mammography, CAD has become an integral part of routine clinical assessment of breast cancer in many hospitals and clinics across the United States and elsewhere worldwide. However, the value and effectiveness of CAD applications are compromised by the inconvenience of the dedicated stand-alone CAD WS or server. The daily use of DICOM, PACS, and IHE technologies in the clinical environment may offer a clue as to how to work around these obstacles. The CAD–PACS integration has many distinct advantages:

1. PACS technology is mature. Integrating CAD with its powerful computers and high-speed networks dedicated to the storage, retrieval, distribution, and presentation of clinical images, will facilitate the daily operations of healthcare providers.
2. PACS-based easy Q/R tools provide the user with images and related patient data obtained from CAD WSs.
3. The DICOM SR and IHE workflow profiles can be readily applied to facilitate the CAD–PACS integration.
4. CAD–PACS integration results can be directly viewed and utilized at the PACS WS together with the PACS database.
5. The very large, dynamic, and up-to-date PACS database can be used by CAD to improve its diagnostic accuracy.

The usefulness of the CAD-PACS Toolkit is discussed in the next section, and some clinical examples are provided in Chapters 17 and 18.

16.2.2 DICOM Standard and IHE Workflow Profiles

Previous chapters in Part 2 of this edition described and illustrated the importance of CAD–HIS/RIS/PACS integration, which requires certain basic ingredients from HL7 standards for textual data, DICOM standards for image, and IHE workflow profiles in order to comply with Health Insurance Portability and Accountability Act (HIPAA)requirements. Among the DICOM standard and IHE workflow profiles, DICOM structured reporting (DICOM-SR), and IHE key image note (KIN), simple image and numeric report, and post-processing workflows (PWF), are important in CAD–HIS/RIS/PACS integration.

16.2.3 DICOM Structured Reporting (DICOM SR)

The scope of DICOM-SR is the standardization of structured reporting (SR) documents in the imaging environment. Structured reporting documents record observations made for an imaging-based diagnostic or interventional procedure, particularly information that describes or references images, waveforms, or specific regions of interest (ROI). DICOM-SR was introduced in 1994 and achieved major recognition when Supplement 23 was adopted into the DICOM standard in 1999 as the first DICOM-SR for clinical reports. The DICOM Committee has initiated more than 12 supplements to define specific SR document templates. Among these supplements, two related to capturing CAD results—the Mammography CAD SR (Supplement 50, 2000) and Chest CT CAD SR (Supplement 65, 2001)—have been ratified. In practice, the use of structured forms for reporting is known to be beneficial in reducing the ambiguity of natural language format reporting, by enhancing the precision, clarity, and value of the clinical document.

DICOM-SR is generalized by using DICOM information object definitions (IODs) and services for the storage and transmission of SRs. Figure 16.4 provides a simplified version of the DICOM model of the real world, showing where DICOM-SR objects are resided. The most important part of a SR object is the document content, which is a template that consists of different design patterns for various applications. Chapter 17, Section 17.2.2 describes the step-by-step summary on how to generate a SR based on two clinical examples. Figures 17.12 and 17.13 in Chapter 17 also delineate the image, diagnosis, and annotation along with the SR.

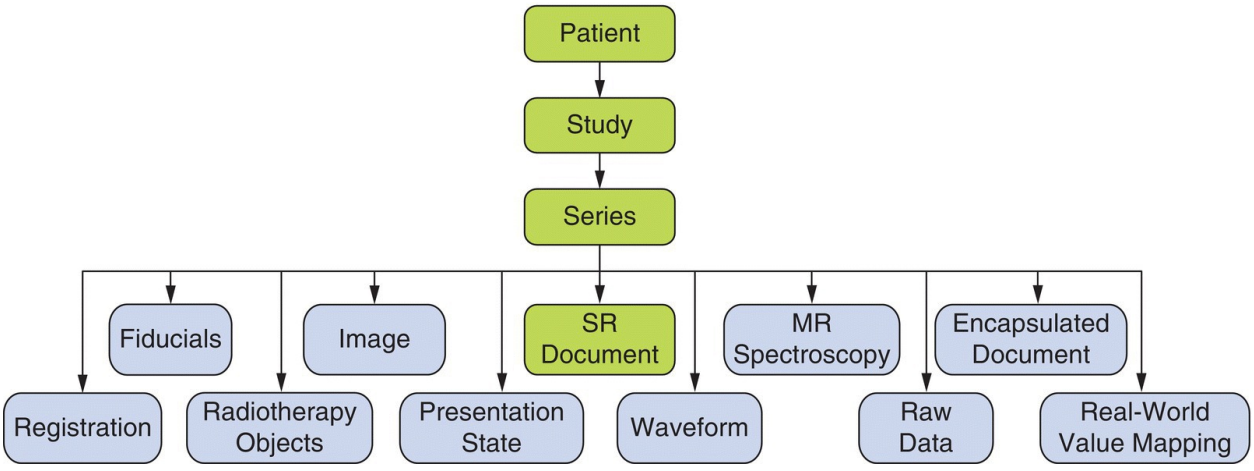

Figure 16.4 DICOM SR objects in the DICOM model of the real world. The green SR document is located in the DICOM data module (green box), which is

at the same level as the DICOM Image.

Once the CAD results with images, graphs, overlays, annotations, and text have been translated into a template designed for this application, the data in the specific template can be treated as a DICOM object stored in the work list of the data model (see Figure 16.4 boxes with light green background), and it can be displayed for review by a PACS WS with the display function. The viewing requires the original images from which the CAD results were generated, so that the results can be overlaid onto the images. The display function can link and download these images from the PACS archive and also display them on the WS.

16.2.4 IHE Profiles

Three IHE profiles are useful for CAD-PACS integration:

1. *Key image note (KIN) profile*: This profile allows users to flag images as significant (for referring, for surgery, etc.) and add a note.
2. *Simple image and numeric report (SINR) profile*: This profile specifies how diagnostic radiology reports (including images and numeric data) are created, exchanged, and used.
3. *Post-processing workflow (PWF) profile*: This profile provides a work list, status, and result tracking for post-acquisition tasks, such as CAD or image processing.

16.3 The CAD–PACS Integration Toolkit

CAD software can be in a stand-alone CAD WS, CAD server, or integrated within the PACS as PACS-based CAD (Section 16.1.4). Regardless of where the CAD software is installed, the goal is to integrate CAD results with the daily clinical PACS operation. In this section, the CAD workflow in current practice is first described, followed by a presentation of the CAD–PACS integration toolkit for extending the CAD workflow to the PACS environment. The CAD–PACS toolkit is a software package that was developed in 2006 at the Image Processing and Informatics Laboratory (IPILab). The CAD–PACS integration application was presented at the RSNA Annual Meetings in 2006 and 2007 [7].

16.3.1 Current CAD Workflow

Figure 16.5 depicts the PACS environment (blue box) and a CAD WS/server

location (red box) that is outside the realm of PACS. These two systems are usually disjointed. When an image is needed for CAD processing (see numerals in Figure 16.5), the workflow occurs as follows:

1. CAD processes the exam ordered through RIS, or directly from its modality.
2. A technologist or radiologist transmits the original images from the PACS or PACS WS to CAD WS for processing. Results are stored without the need to physically go to the CAD WS to view results.
3. The CAD–PACS toolkit (purple box), which can integrate with the PACS server, PACS WS, and the CAD server/WS together via the DICOM standard and IHE profiles, passes the CAD results to the PACS server for archiving and the PACS WS for viewing; and Q/R original images from the PACS server to PACS WS to be overlaid with the CAD results. In addition, it can automatically pass images directly from the PACS server or PACS WS to the CAD WS for processing.

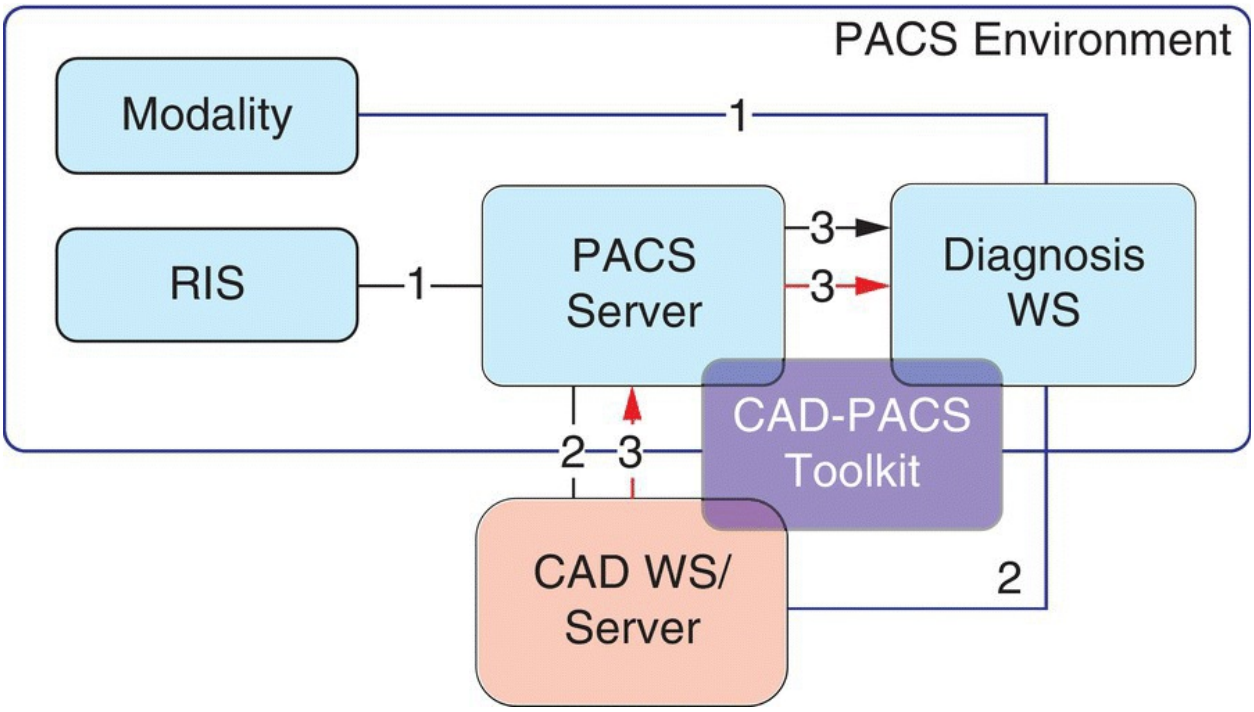

Figure 16.5 CAD workflow (red) in the PACS environment (blue) with the CAD–PACS toolkit (purple). See the color code used in Figure 16.6.

16.3.2 Concept

CAD-PACS is a software toolkit using the HL7 standard for textual information; the DICOM standard for various types of data formats, including images,

waveforms, graphics, overlays, and annotations; and IHE workflow profiles described in the aforementioned section for the integration of CAD results within the PACS workflow. This CAD software toolkit is modularized and its components can be installed in five different configurations:

1. in a stand-alone CAD WS;
2. in a CAD server;
3. in a PACS WS;
4. in a PACS server; or
5. in a mix of the previous four configurations.

In general, a CAD manufacturer would be more comfortable with the first two approaches, because there is very little collaboration needed for the PACS software, which is too complex for most CAD manufacturers. On the other hand, a PACS manufacturer would prefer to use an in-house CAD or acquire the CAD from outside and integrate it with its own PACS with the latter three approaches.

16.3.3 The Infrastructure

The CAD–PACS toolkit has three CAD-PACS editions: DICOM-SC, DICOM–PACS–IHE, and DICOM–CAD–IHE; as well as five software modules: i-CAD-SC, i-CAD, i-PPM, Receive-SR, and Display-SR. Each component contains some or all of the software modules. Figure 16.6 shows the architecture of the toolkit.

The toolkit is classified into three components for the different levels of PACS integration requirements, defining them as 1st edition, 2nd edition, and 3rd edition. Table 16.4 compares the three integration approaches. The 1st edition shows a simple screen-captured output, and the CAD data are not stored for future use. The 2nd edition is for full CAD–PACS integration requiring elaborate collaboration between the CAD developer and the PACS manufacturer. The 3rd edition does not require the elaborate integration efforts of the two parties, and proper use of the CAD-PACS toolkit is sufficient, which favors the independent CAD developer.

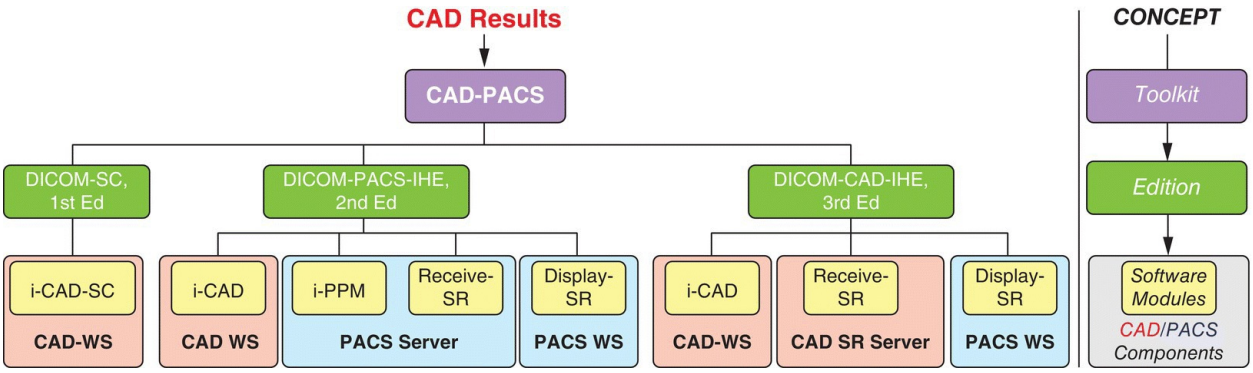

Figure 16.6 Rightmost: The concept of four-level CAD–PACS Integration toolkit. Left: CAD–PACS Integration toolkit (purple), Top levels: three CAD-PACS editions (green), and five distinct software modules (yellow), CAD components and results (red/orange), and PACS components (blue). Left: The 1st edition. DICOM-SC utilizes DICOM SC service to view CAD results. This edition is easy to integrate, but the CAD output is not in a database for future retrieval. Middle: The 2nd edition. DICOM-PACS-IHE is utilized for integration with a full PACS. It consists of four CAD-PACS software modules, and allows a PACS manufacturer to integrate an existing CAD into its own PACS. Right: The 3rd edition. DICOM-CAD-IHE is utilized for integration with the CAD server. This component is independent from the PACS manufacturer as long as the PACS WS is DICOM SR compliant. The CAD results can then be viewed at a PACS WS. The 3rd edition is favored by the CAD manufacturers or research laboratories for integration. The three modules i-CAD, Receive-SR, and Display-SR are the same as those in both the DICOM-PACS-IHE and DICOM-CAD-IHE editions. PPM (post-processing manager) allows the integration of CAD results with the PACS server, which are PACS specific and would require PACS vendor's assistance for implementation. In the lower level components, in either PACS or CAD, proper toolkit software modules can be installed in the corresponding system components for CAD-PACS integration.

Table 16.4 Comparison of the three CAD–PACS integration editions (SR: Structured Reporting).

Specifications	**CAD-PACS Edition**		
	DICOM-SC 1st Edition	**DICOM-PACS-IHE 2nd Edition**	**DICOM-CAD-IHE 3rd Edition**
Using secondary captured Image to store CAD results	✓		
Using DICOM SR		✓	✓

PACS without SR support	✓		✓
PACS with SR support		✓	
Display referenced image	✓	✓	✓
Toggling between image and annotation		✓	✓

16.3.4 Functions of the Three CAD-PACS Editions

16.3.4.1 DICOM-SC, First Edition

The first edition of DICOM-SC utilizes the i-CAD-SC software module, which relies on the DICOM SC service. Its design is simple to implement but has limited use in clinical research, because it uses SC to store CAD results for viewing purposes only.

16.3.4.2 DICOM–PACS–IHE, Second Edition

The second edition of DICOM–PACS–IHE consists of four software modules: i-CAD, i-PPM, Receive-SR, and Display-SR. It utilizes the DICOM structured reporting (DICOM-SR) service and several IHE workflow profiles; its methodology is elegant but requires installation of the four modules within the PACS server. The i-PPM module (post-processing manager) requires a thorough understanding of the entire PACS workflow, and would need intensive collaboration with the PACS manufacturer during integration. The integration could test the patience and perseverance of the integrator because of the protective culture of the PACS business.

16.3.4.3 DICOM–CAD–IHE, Third Edition

The third edition of DICOM–CAD–IHE comprises three software modules: i-CAD, Receive-SRTM, and Display-SRTM. This edition utilizes DICOM-SR and the KIN IHE profile, a method that reduces the necessity of altering the current PACS server, but CAD results are stored in the CAD server and not in PACS. DICOM SR links PACS image/data and CAD results for viewing.

This edition is favored by CAD manufacturers because they have the ability to install the toolkit in their CAD server and integrate CAD results with the PACS clinical workflow without the complexity of the previous edition. DICOM-SR provides the data format, allowing CAD results, text, images, graphics, and annotations to be directly archived within the DICOM-SR compliant CAD

server.

The second and the third editions provide the correct methods of integrating CAD with PACS. The availability of direct CAD results in the daily clinical workflow will enhance the PACS operation, as well as future PACS research possibilities.

16.4 Data Flow of the three CAD–PACS Editions Integration Toolkit

16.4.1 DICOM-SC, First Edition

The data flow within the DICOM-SC is simple and straightforward. The PACS WS sends the image to the CAD WS or CAD server. Results are captured on screen by the i-CAD-SC residing in the CAD WS as a DICOM image object and sent to the PACS server for archiving. This object can be viewed by the PACS WS. In this edition, results can only be viewed, and data cannot be used for other purposes. The display quality is marginal.

16.4.2 DICOM–PACS–IHE, Second Edition

Figure 16.7 shows the workflow of the second edition of DICOM–PACS–IHE. Four software modules (yellow) must be installed in the appropriate PACS and CAD components, if those PACS components do not have the required functions. The challenge of this version is that the CAD developer has to collaborate closely with the PACS server manufacturer to fully understand the PACS workflow, which is different from the CAD–PACS integration workflow. To integrate CAD results with the PACS workflow using i-PPMTM is an elaborate task.

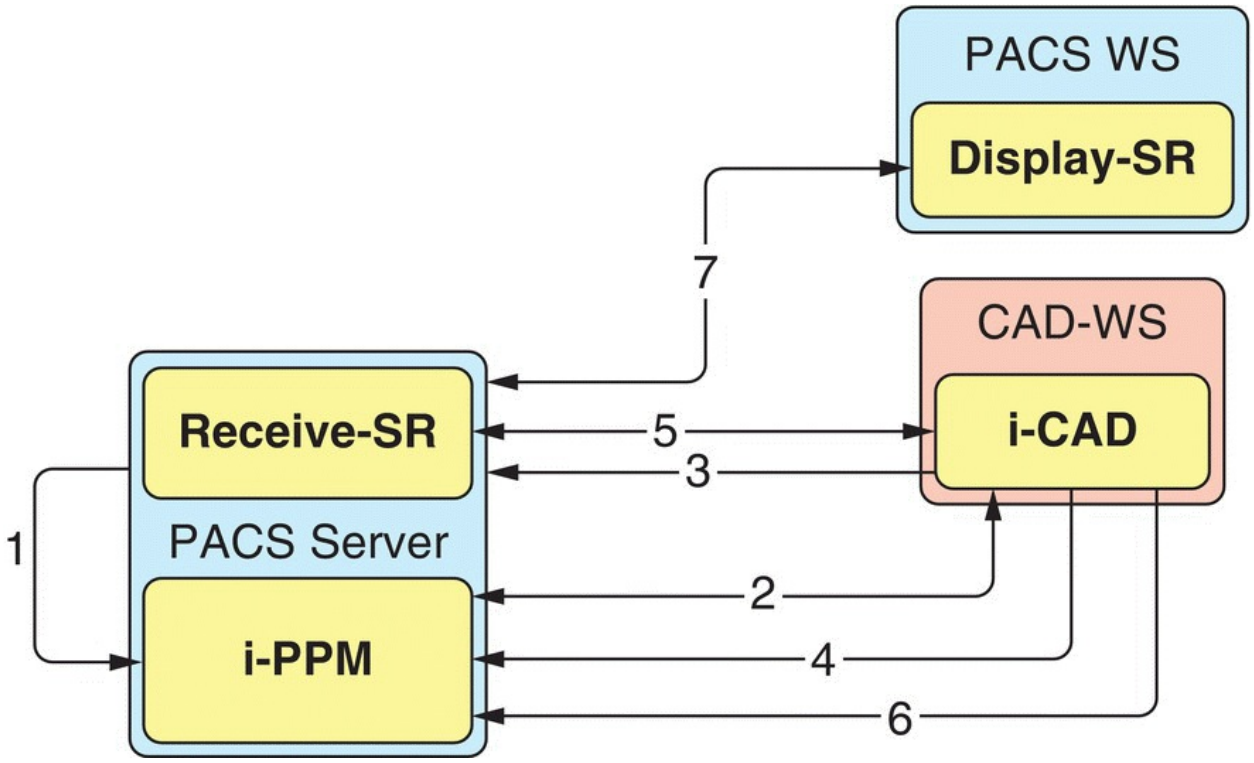

Figure 16.7 Data flow of the DICOM-PACS-IHE second edition and locations of the four modules (yellow) of DICOM-PACS-IHE in the CAD and PACS components (see also the color code used in Figure 16.4). Numbers represent data-flow steps during the integration. (1) CAD requests; (2) query CAD work list, work item claimed; (3) retrieve images for CAD; (4) work list purpose procedure step in PPM in the process; (5) CAD results; (6) work item PPS completed; (7) retrieve images/CAD results.

16.4.3 DICOM–CAD–IHE, Third Edition

Figure 16.8 shows the data workflow. In the third edition, the CAD has two components, the CAD WS and the CAD SR server. The latter takes care of monitoring and archiving of CAD results, and retrieving original images and data from PACS.

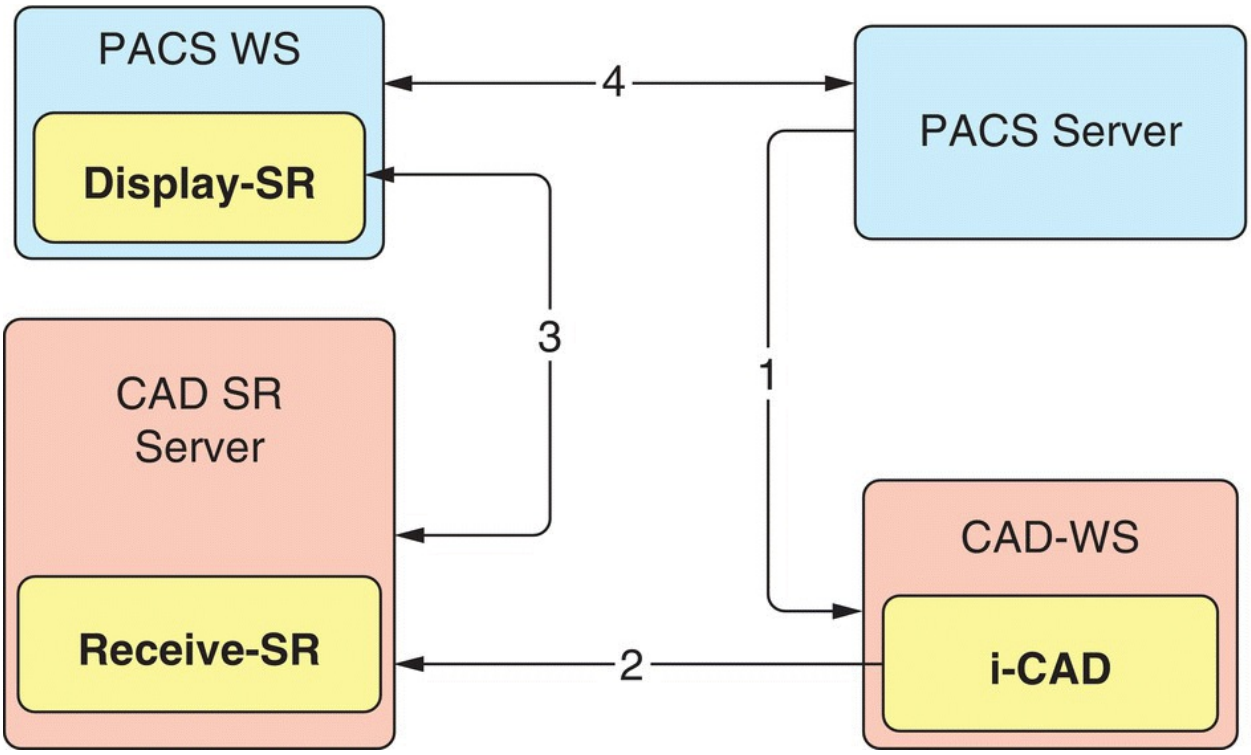

Figure 16.8 Data flow of the DICOM-CAD-IHETM third edition shows the locations of the three software modules (yellow) in the CAD SR server and PACS, respectively (see also the color code used in Figure 16.6). The data flow steps are (1) PACS server pushes the CT images to CAD WS for CAD process; (2) CAD WS pushes the DICOM SR CAD results to CAD SR server, which consists of the Receive-SRTM module with a SR database for archiving CAD results; (3) Web-based Display-SRTM at PACS WS queries/retrieves DICOM SR CAD results from CAD SR server; (4) the Display-SR automatically Q/R original images referenced in the DICOM SR CAD results in the PACS server for reviewing both original images and SR. In this edition, the CAD SR server also keeps all CAD results in SR format.

References

1 Andrade, R., Wangenheim, A. and Bortoluzzi, M.K. (2003) Wireless and PDA: a novel strategy to access DICOM-compliant medical data on mobile devices. *Int J Med Informat*, 71(2–3), 157–163.

2 Bosak, J. In: XML, Java, and the future of the Web. http://www.ibiblio.org/pub/sun-info/standards/xml/why/xmlapps.htm0000

3 Cao, X., Hoo, K.S., Zhang, H., *et al*. (2001) Web-based multimedia information retrieval for clinical application research, *SPIE Proc*, 4323, 350–358.

4 Cedara, I. View. http://www.cedara.com/0000

5 CORBA® BASICS. http://www.omg.org/gettingstarted/corbafaq.htm0000

6 Doi, K. and Huang, H.K. (2007) Computer-aided diagnosis (CAD) and image-guided decision support. Editorial, *J Computer Med Imag Graph*, 31, 195–197.

7 Le, A., Liu, B. and Huang, H.K (2009) Integration of computer-aided diagnosis/detection (CAD) results in a PACS environment using CAD–PACS toolkit and DICOM SR. *Intern J. Comp Asst Rad & Surg*, 4**,** 317–329

Further Reading

Huang, H.K., Wong, W.K., Lou, S.L., *et al*. (1996) Clinical experience with second-generation hospital integrated picture archiving and communication system. *J Digit Imag*, 9: 151–166.

Huang, H.K. (1999) Display workstation. In: *PACS Basic Principles and Applications*. New York: Wiley-Liss Press.

Huang, H.K., Cao, F., Liu, B.J., Zhang, J., Zhou, Z., et al. (2001) Fault-tolerant PACS server design. *SPIE Med Imag*, 4323–4314, 83–92.

Huang, H.K. and Huang, C. (2003) Internet 2. *Adv Imag Oncol Adm*, (October), 52–58.

Huang, H.K., Liu, B.J., Le, A. and Documet, J. (2011) PACS-based computer-aided detection and diagnosis. In: T.M. Deserno (ed.), *Biomedical Image Processing*, Chapter 18, Berlin: TM Springer-Verlag, pp. 455–469.

17
DICOM-Based CAD: Acute Intracranial Hemorrhage and Multiple Sclerosis

CHAPTER MENU

17.1 Computer-Aided Detection (CAD) of Small Acute Intracranial Hemorrhage on CT of the Brain

17.1.1 Clinical Aspect

17.2 Development of the CAD Algorithm for AIH on CT

17.2.1 Data Collection and Radiologist Readings

17.2.2 Evaluation of the CAD for AIH

17.2.3 From System Evaluation to Preclinical Practice

17.2.4 Summary of using CAD for AIH

17.3 CAD–PACS Integration

17.3.1 The DICOM-SR already available from the PACS Vendor

17.3.2 Integration of a Commercial CAD with PACS

17.4 Multiple Sclerosis (MS) on MRI

17.4.1 DICOM Structured Reporting (SR) and CAD–PACS-Based Integration Toolkit

17.4.2 Multiple Sclerosis Detection on MRI

17.4.3 Data Collection

17.4.4 Generation of the DICOM-SR Document from a CAD Report

17.4.5 Integration of CAD with PACS for Detection of Multiple Sclerosis (MS) on MRI

References

Further reading

This chapter presents two different CAD methods to address two different types

of diseases: acute intracranial hemorrhage and multiple sclerosis. Although computer-aided diagnosis (CAD) is the general terminology, these two methods are quite different.

17.1 Computer-Aided Detection (CAD) of Small Acute Intracranial Hemorrhage on CT of the Brain

17.1.1 Clinical Aspects

Acute intracranial hemorrhage (AIH) is a recent (less than 72 hours) bleed inside the skull. It can result from a stroke or be a complication of a head injury. The presence or absence of AIH requires different treatment strategies and its identification is of immediate importance for triage of patients presenting an acute neurological disturbance or a head injury. However, it is well recognized that clinical findings cannot accurately differentiate between symptoms of AIH and other neurological emergencies. Neuroimaging is thus essential for immediate decision making. CT has been the modality of choice for evaluating suspected AIH cases, because it is widely available, quick to perform, and compatible with most life-support devices. On CT images, an acute blood clot shows higher x-ray attenuation than normal brain parenchyma. The contrast between AIH and the adjacent structures depends on:

1. intrinsic physical properties of blood clot, including the density, volume, and location;
2. relationship to surrounding structures; and
3. technical factors, including scanning angle, slice thickness, and windowing.

Although diagnosis of AIH on CT is usually straightforward, identification of the demonstrable AIH on CT can become difficult when the lesion is inconspicuous, so small (≤1.00 cm) as to be masked by normal structures, or when the reader is inexperienced.

In most parts of the world outside the United States, acute care physicians, including emergency physicians, internists, and neural surgeons, are left to read the CT images at odd hours when radiologists' expertise is not immediately available. This is not a desirable arrangement, because the skill of acute care physicians in interpreting brain CT images has been shown to be imperfect. Even radiology residents can, albeit infrequently, overlook a hemorrhage on a brain

CT. Therefore, a CAD system has been developed that identifies a small AIH to help in the management of patients presenting with an acute neurological disturbance or a head injury in an emergency setting.

17.2 Development of the CAD Algorithm for AIH on CT

17.2.1 Data Collection and Radiologist Readings

To develop the CAD for AIH on a brain CT, extensive data collection was required. There were two data collection phases used for: i) working out the algorithm and validating the CAD system's effectiveness; and ii) a performance evaluation of CAD detection compared with radiologists' and physicians' readings. Phase one involved 186 brain CT studies, 62 cases of which were confirmed to be AIH (note that a single case can have multiple contiguous AIH volumes). The 124 cases showing no AIH were retrospectively retrieved from the PACS archive. All studies had used the CT scanner (HiSpeed CT, GE Medical Systems, Milwaukee, Wisconsin). All images were axial images obtained parallel to the orbitomeatal line (OML), at 120 kV and 80 to 200 mA. These cases were divided into 120 for training and 66 for validation.

The radiological diagnoses in all the cases were established by the consensus of two radiologists, one with 7 years and the other with 11 years of experience in reading brain CT. In addition, dimensions, locations, and type of individual disjoint AIH volumes were measured. Altogether there were 123 contiguous volumes of small AIH, 77 in the training cases and 46 in the validation dataset, with well-represented samples of each different type of AIH and different sizes (≤1.0 cm).

17.2.1.1 The CAD System Development

The dataflow of the CAD algorithm is illustrated in Figure 17.1. The image processing and analysis methods used in the scheme are listed in Table 17.1. All image processing methods were readily available in Mat-Lab Software Library (The Math Works, Inc., Natick, Massachusetts). The numerals in the figure correspond to the numerals in the table.

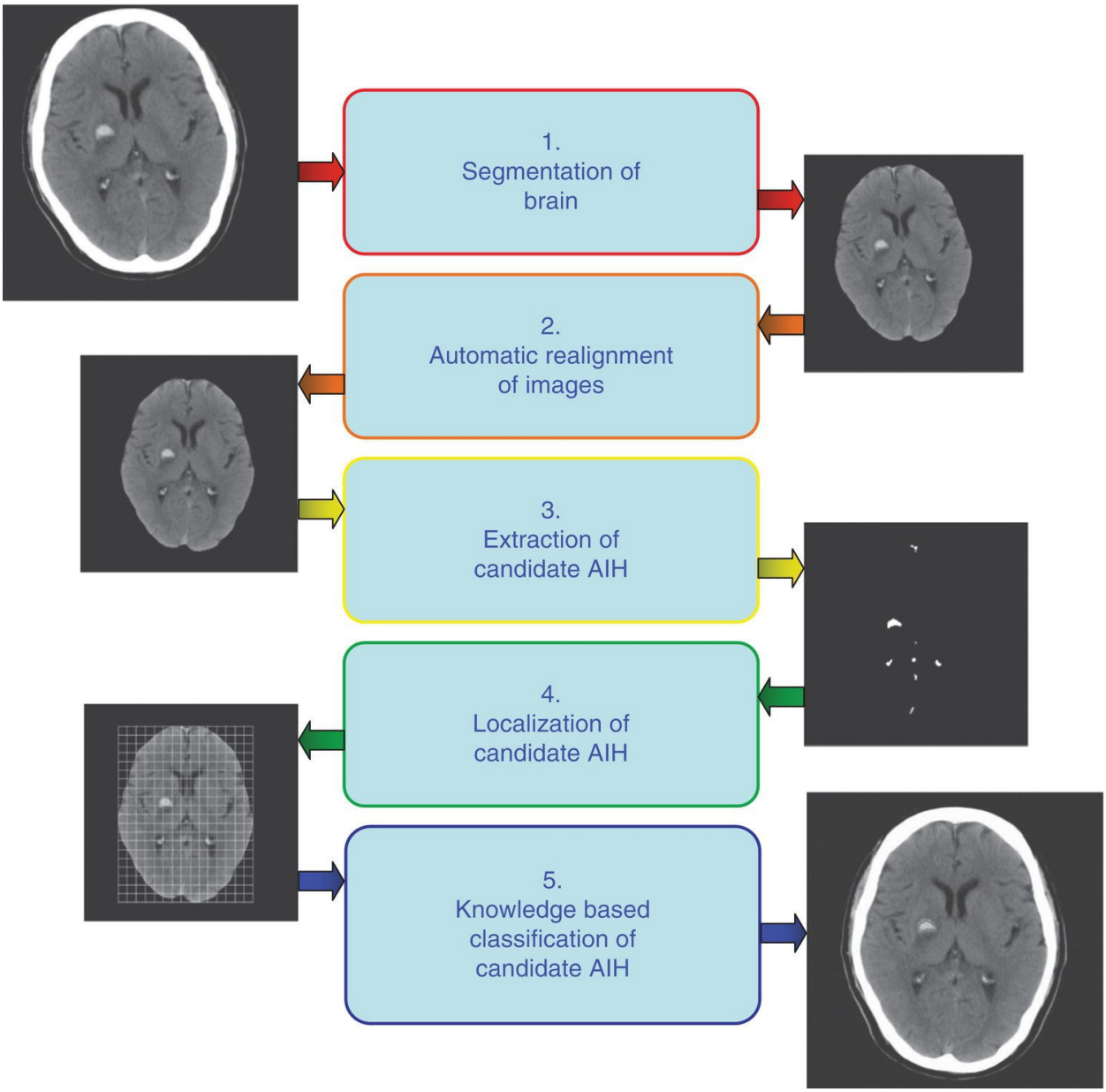

Figure 17.1 Schematic of the CAD system. Intermediary outputs of an image showing right basal ganglia hemorrhage illustrate the effect of individual steps. Details of individual steps are outlined in Table 17.1.

(courtesy of Dr T. Chan)

Table 17.1 Details of individual image processing and analysis steps of in the CAD for AIH algorithm, as outlined in Figure 17.1.

Steps	Methods	Purposes
1A. Segmentation	Global thresholding and morphological operations	Remove bones of skull and face

of intracranial contents		
	Remove structures not contiguous with the main central bulk of intracranial contents	Remove scalp, orbits, and other head and neck soft tissues
1B. Preprocessing of intracranial contents	Median filtering	De-noising
	Adjustment of intensity according to distance from the skull	Correct for CT cupping artifacts
2. Automatic realignment of images	Automatic localization of limits of brain, ventricles, floor of anterior intracranial fossa, mid-sagittal plane	Align the brain into the normal position
3. Extraction of candidate AIH	Top-hat view transformation	Highlight local high-density regions
	Subtraction between the two sides	Extract asymmetrically high-density regions
4. Localization of candidate AIH	Registration of the brain in question against a normalized coordinate system	Render the candidate AIH anatomical information
5. Knowledge based classification of AIH	Rule-based system with inputs of image features and anatomical coordinates of the extracted candidates	Distinguish genuine AIH from false positives resulting from noise, artifacts, and normal variants

17.2.1.1.1 Segmentation of the Brain

The skull, by virtue of its exceptionally high x-ray attenuation values, can be removed using global thresholding. A morphological opening algorithm is used to remove connections that may remain between the intracranial contents and the scalp. Afterwards, the scalp and other extrinsic structures become separated from

the centrally located intracranial contents by regions of void that represent the removed bones. The intracranial contents can subsequently be segmented by selectively removing elements that are not contiguous with the central component.

The segmented intracranial contents undergo pre-processing steps that include median filtering for noise reduction and adjustment for CT cupping artifacts. This produces a more homogeneous background against which abnormalities become more conspicuous (Figure 17.1).

17.2.1.1.2 Realignment of the Image

The brain is realigned into the conventional orientation after automatic localization of mid-sagittal plane and boundaries of the whole series of images. This is necessary as images obtained in an emergency clinical setting are often not optimally positioned. Figures 17.2 and 17.3 depict the process and the results of these operations.

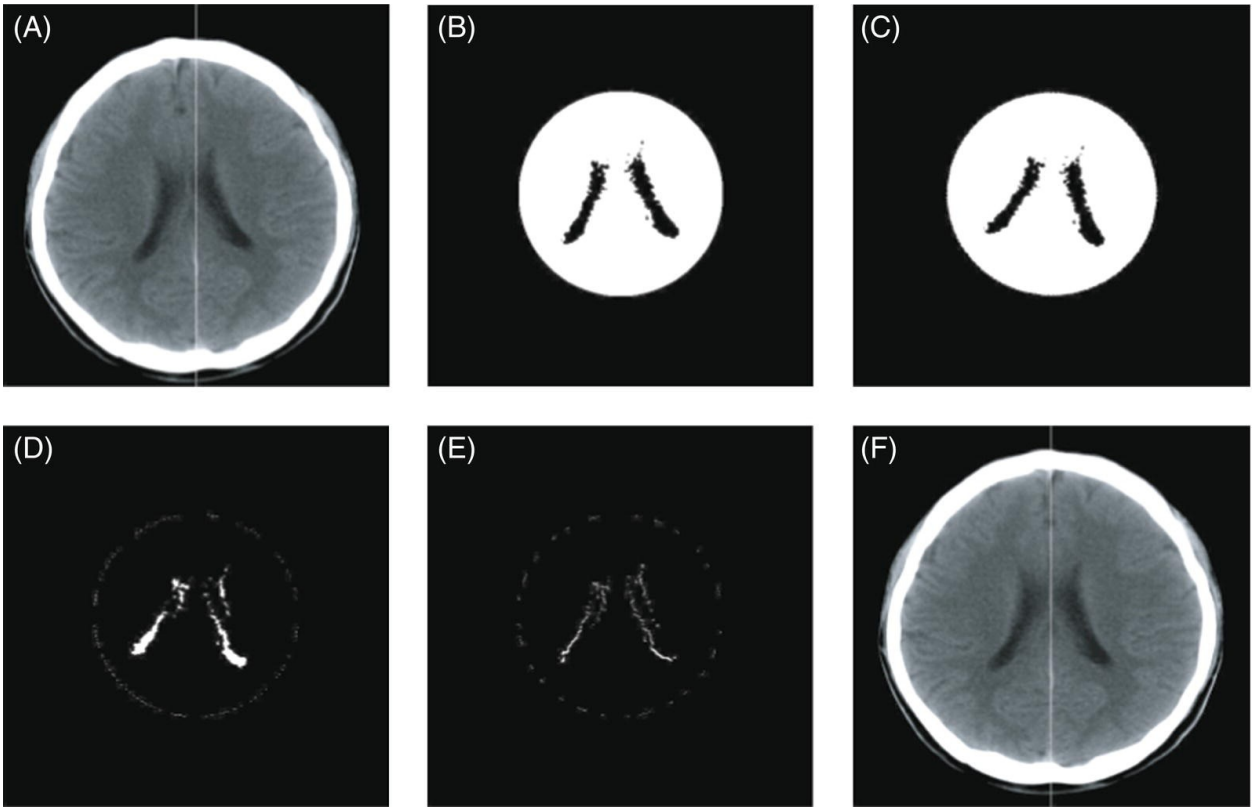

Figure 17.2 Angle of the mid-sagittal plane obtained by finding the line of symmetry of the body of lateral ventricles. The section containing the body of lateral ventricles (A) is automatically selected as described in text. The central portion of the image is binarized with threshold at CSF attenuation. It is rotated

over a range of angles. The differences between the rotated image (B) and its mirror image (C) are obtained (D). The angle that gives the least difference (E) is the angle of the mid-sagittal plane (F).

(courtesy of Dr T. Chan)

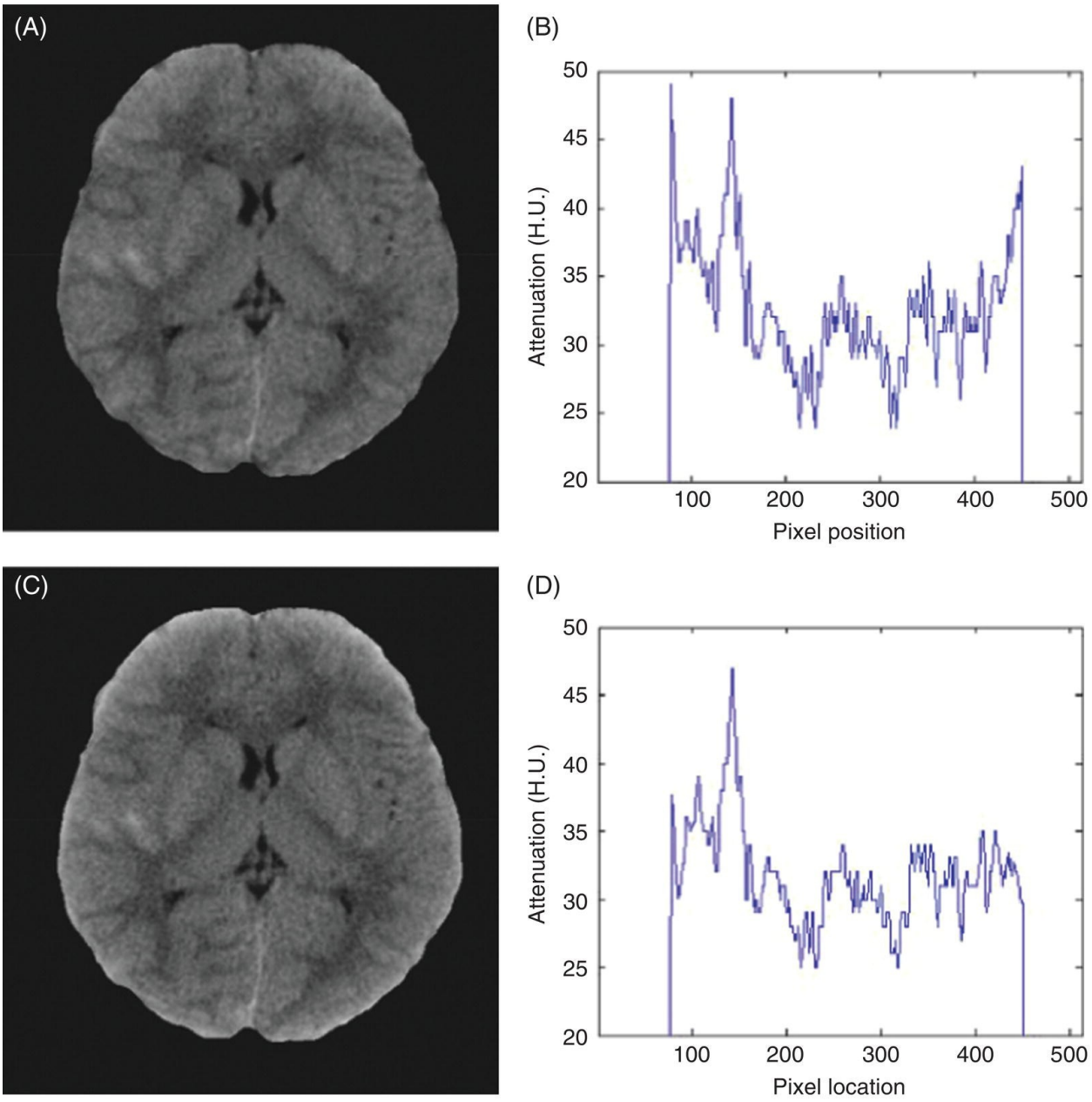

Figure 17.3 Original image with artifactual increase in signal intensity toward the brain skull interface (A). Horizontal line indicating the position from where the intensity profile (B) is obtained. Image after correction of cupping artifacts (C). Intensity profile along the same horizontal line (D). It can be appreciated by comparison of (B) and (D) that the peak intensity at the pixel position is around

140, because AIH is more prominent after correction of cupping artifacts.

(courtesy of Dr T. Chan)

17.2.1.1.3 Extract Candidates for AIH

High attenuation components are next segmented as candidate AIHs from each of the axial sections. The segmentation is based on combined:

1. top-hat view transformations, essentially selecting pixels of higher attenuation than those in their vicinity; and
2. subtraction between the two sides of the brain about the midline, which highlights regions of higher attenuation than the contralateral anatomical region.

The parameters are adjusted so that a good number of candidates for AIH are generated to avoid missing any small lesions. The processes are shown in Figures 17.4 and 17.5.

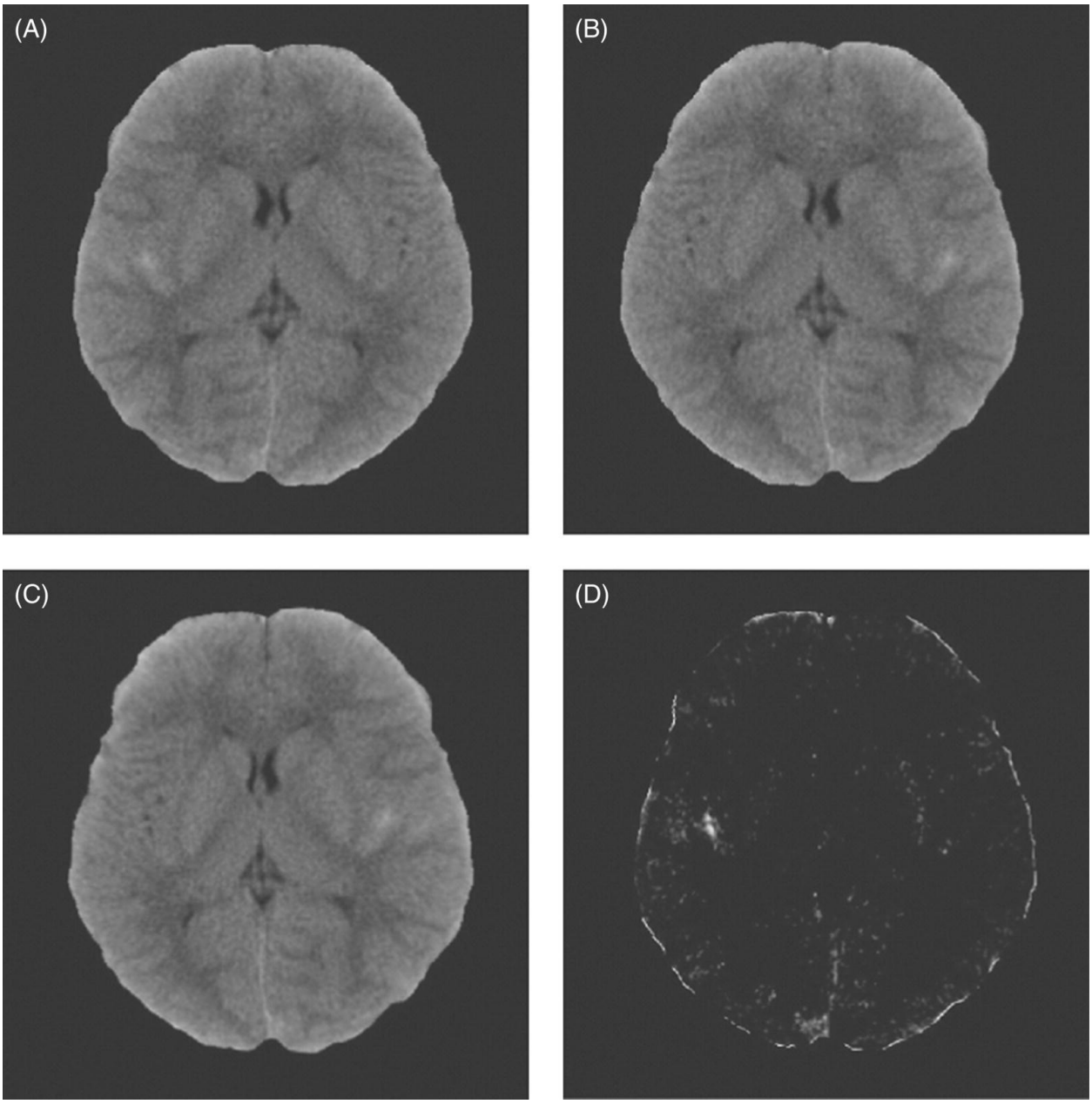

Figure 17.4 Procedure of highlighting asymmetrical high-density region illustrated by the intermediary outputs of the CAD scheme. Original is shown in (A). Flipped image (B) is elastically transformed to reduce the normal structural asymmetry between the two sides of the brain (C). Difference between (A) and the morphological closing transformation of (C) indicates that AIH within the right Sylvian fissure is of higher signal than CSF in the left contralateral Sylvian fissure (D).

(courtesy of Dr T. Chan)

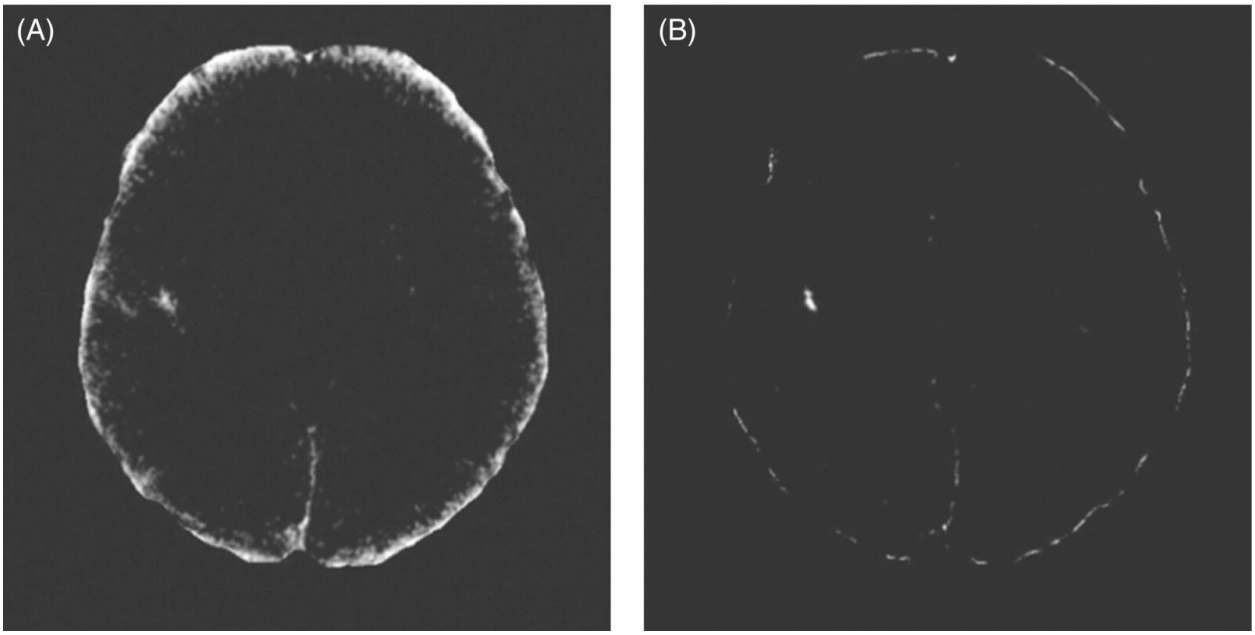

Figure 17.5 Comparison of global thresholding of original image after removal of skull and extracranial tissues (A), and thresholding of the combined processing steps including correction of cupping artifacts, image top-hat transformation, and left–right comparison (B). Notice that the result of (B) is much cleaner and more manageable for subsequent processing.

(courtesy of Dr T. Chan)

17.2.1.1.4 Localization of AIH Candidates

The many image features of the AIH candidates, including mean and variation of attenuation, area, long- and short-axis diameters, and relative orientation, are quantified. In addition, the candidate AIHs are given anatomical context by registration against a special coordinate system. This coordinate system is conceptually similar to the commonly-used Talairach coordinate system in anatomy, but is different in that it can be readily applicable for relatively thick section axial images obtained using ordinary clinical protocols.

Coordinates on the coordinate system have their own anatomical label as a result of a normalization procedure using axial brain CT normal subjects obtained using a clinical protocol. Through the registration process between the study in question and the normalized coordinate system, each pixel location of the brain in question is correlated with a coordinate location of the normalized brain and its embedded anatomical label.

17.2.1.1.5 Knowledge-Based Classification of AIH Candidates

The image features and coordinates of the AIH candidates provide the input for the rule-based classification system (Table 17.2), which primarily reduces false positives caused by normal variants and artifacts. The classification is possible because genuine AIH or normal variants tend to follow certain patterns at some typical anatomical locations.

Table 17.2 Sample rules used in the knowledge base classification in the CAD system for AIH on CT brain.

Anatomy Rules (P)[a]	**Imaging Feature Rules (Q)**[a]	**Interpretation**	**Probability of AIH**
Low probability of AIH for candidates presenting calcifications or normal high-density structures			
Mid-sagittal plane, supracranial fossa	Vertically aligned, ↑ attenuation, ↑ eccentricity, ↑ long axis length, ↓ short axis length	Falx calcification	↓
Mid-sagittal plane, supracranial fossa	Intermediate attenuation, intermediate eccentricity,	Superior sagittal sinus	↓
Periphery	↓ convex hull		
Medial portion of basal ganglia	↑ Attenuation (↑ if area ↑), ↓ area (↑ if symmetrical), symmetrical	Basal ganglia calcification	↓
Central portion of cerebellum	↑ Attenuation (↑ if area ↑), ↓ area (↑ if symmetrical), symmetrical	Dentate nuclei calcification	↓
Low probability of AIH for candidates presenting artifacts			
Posterior cranial fossa	↑ Eccentricity, ↑ long axis length, ↓ short axis length	Beam hardening artifact	↓
Above anterior cranial fossa	↑ Attenuation	Partial volume averaging	↓
Above temporal bone	↓ area beyond adjacent bone in contiguous section		

Periphery near vertex			
High probability of AIH for candidates presenting particular type of AIH			
Sylvian fissure	Vertically aligned, intermediate attenuation,↑ eccentricity, intermediate long axis length,↓ short axis length	Sylvian fissure subarachnoid hemorrhage	↑
Periphery	Perpendicular to perimeter of brain,↓ long axis length,↓ short axis length	Sulcal space subarachnoid hemorrhage	↑

[a] The rules that incorporate anatomical and imaging features information take the following form:

$$P \rightarrow Q$$

$$Q \rightarrow \Delta \text{ probability of AIH}$$

Sample rules used in the knowledge base classification system. P represents the set of rules used to check for the anatomical locations and Q the rules used to evaluate the imaging features appropriate for some particular anatomical positions. A candidate AIH is first checked for the anatomical position. If the position is one that satisfies a particular P, the corresponding Q will be invoked to evaluate the image features of the candidate AIH. If an appropriate pair of P and Q is satisfied, the probability of AIH for the candidate is adjusted accordingly.

The algorithm's output is displayed as images with red overlays at perimeters of the AIH determined by the system (Figure 17.6). The original images and the corresponding CAD output images are displayed side by side, one axial section at a time in the CT stack mode. The user can scroll through the whole series of synchronized original images and corresponding CAD output images. This arrangement is to facilitate comparison between the original and the CAD output images.

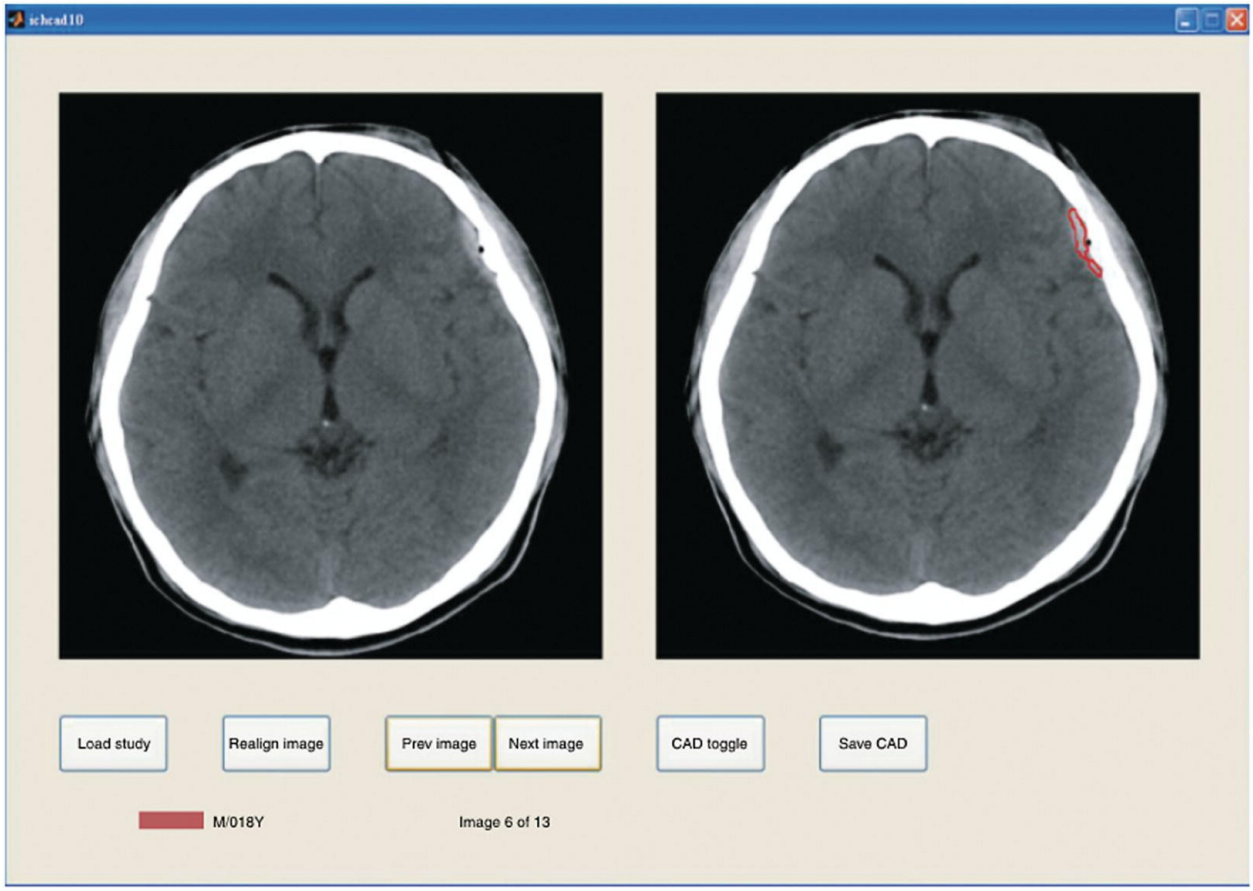

Figure 17.6 Screen capture of the CAD system graphical user interface. Original images are displayed at the left window, while the output images with the overlays of outlined AIH are displayed at the right. Original and output images are displayed in strip mode and linked such that they can be scrolled together for review of the whole image series.

(courtesy of Dr T. Chan)

17.2.1.1.6 Some Difficult AIH Cases

It is believed that the CAD system for AIH can detect lesions that are difficult to find by acute care physicians or even radiology residents. Some such lesions are shown in Figure 17.7. In the evaluation study to be discussed in the Section 17.1.3, such cases were included in a study that found emergency physicians and radiology residents to have missed them, whereas CAD could make the correct diagnosis using anatomically related lesion characteristics in accord with the knowledge-based rules discussed in the previous section.

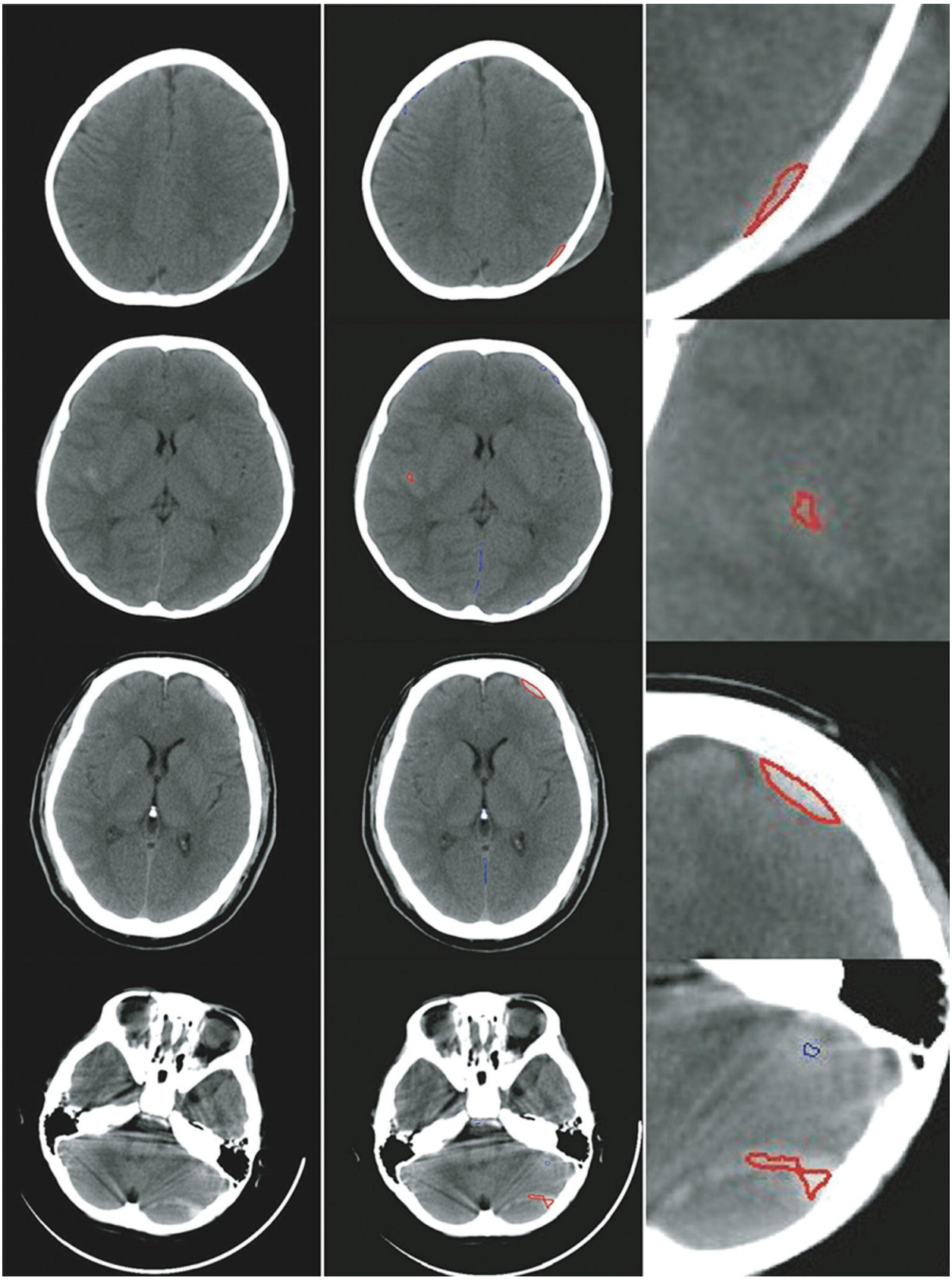

Figure 17.7 Difficult AIH cases. Small AIH are difficult to detect if they are of similar attenuation as adjacent structures or confused with normal variants and artifacts. Examples of some difficult cases (the left column) with their CAD results (the middle column) and magnified views (the right column) are shown. The system identifies AIH by red perimeter outlines. High-density regions that are segmented but subsequently classified as unlikely to be AIH are identified by blue perimeter outlines

(courtesy of Dr T. Chan).

17.2.1.1.7 Training and Validation of the CAD System

Training the CAD system involved using known clinical cases to improve the performance of the CAD; validating of the CAD, on the other hand, meant studying different known cases to validate the trained CAD method. There were two distinct sets of data and they could not be overlapped.

The system was trained with 40 AIH cases and 80 without AIH, and the validation used 22 positive cases and 44 controls, all obtained from the first phase of data collection. Some of the cases were not used in the collected data for CAD training or validation for various reasons, among these being cases used in training the human observers and cases where the AIH was larger than 1.00 cm. Table 17.3 shows the training and validation results. From the table, it can be seen that on a per patient basis, the sensitivity and specificity were 95% (38/40) and 88.8% (71/80), respectively, for the training cases. The system achieved sensitivity of 100% (22/22) and specificity of 84.1% (37/44) for the diagnosis of AIH for the validation cases.

Table 17.3 CAD results based on training data and validation data.

	Validation Positive	**Validation Negative**
A. Summary of CAD results on a per patient basis for training cases		
AIH present	38	2
AIH absent	9	71
Sensitivity = (38/40) 95.0%		
Specificity = (71/80) 88.9%		
Accuracy = 90.8%		
Positive predictive value = 80.8%		
Negative predictive value = 97.3%		

B. Summary of CAD results on a per patient basis for validation cases		
AIH present	22	0
AIH absent	7	37
Sensitivity = (22/22) 100.0%		
Specificity = (37/44) 84.1%		
Accuracy = 89.3%		
Positive predictive value = 75.9%		
Negative predictive value = 100.0%		

The speed of the current system was not optimized during the validation stage. It takes on average approximately 15 seconds per image to produce the output. But the time can vary substantially, depending on number of image and number of candidate AIH introduced, to be evaluated by the classification system.

17.2.2 Evaluation of the CAD for AIH

17.2.2.1 Rationale of Evaluation of a CAD System

The CAD system discussed in Sections 17.1 and 17.2 was evaluated after the system had been trained and validated. A new dataset (see Section 17.1.2.1, phase 2 of data collection) was then collected to compare the performance of the CAD with the human observers' performance, or to study if the CAD could help the human observers improve their performance.

In the AIH case, after the CAD algorithm was validated, the next step involved testing its performance by different healthcare providers who would use the CAD in a clinical situation or by physicians interested in improving their diagnostic skills. A CAD system can be useful if it proves to be beneficial to the human observer in making precise diagnoses. In other words, the CAD system should identify lesions that may otherwise be missed by the human observer. As opposed to early unsuccessful attempts to replace radiologists by computers in the 1960s and 1970s, current CAD schemes now aim to assist readers in making diagnoses by providing quantitative analyses of radiological images. Therefore, investigations of possible human–computer interaction such as the receiver operating characteristic (ROC) studies, are necessary.

For this purpose, the multiple-reader multiple-case (MRMC) ROC paradigm has been used in the evaluation of CAD systems. The MRMC is not only efficient in terms of resource requirement (i.e. fewer readers and cases are required for a

specified precision), but it also produces results that can generalize to the populations of readers and cases from which the samples were drawn. In the case of CAD for AIH on CT, the comparison is between CAD and emergency room physicians, attending physicians, radiology residents, fellows, radiologists, and neuroradiologists. The goal is to evaluate the effectiveness of CAD by way of the MRMC ROC, to potentially assist clinicians' performance in detection of small acute intracranial hemorrhage.

17.2.2.2 Multiple-Reader Multiple-Case Receiver Operating Characteristic Analysis for CAD Evaluation

17.2.2.2.1 Data Collection

The second phase of data collection was for the CAD evaluation study. All the readers and cases were recruited from a 1200-bed acute hospital in Hong Kong. Institute Review Board (IRB) approval was obtained for this study.

Sixty sets of axial brain CT images, of thicknesses between 5 and 10 mm, made up the test cases used in the observer performance study. All were emergency brain CT performed on a single detector CT scanner (HiSpeed CT, GE Medical Systems, Milwaukee, Wisconsin). All images were axial images obtained parallel to the orbitomeatal line (OML), at 120 kV and 80 to 200 mA. Thirty cases showed AIH, the radiological diagnosis being established by consensus of two experienced neuroradiologists, who did not participate in the observer study. In 26 of the cases, the presence of AIH was considered unambiguous by the radiologists. In the other four, the diagnoses were concluded with a follow-up CT/MRI. AIH of different types, including intracerebral hemorrhage (ICH), intraventricular hemorrhage (IVH), subarachnoid hemorrhage (SAH), subdural hemorrhage (SDH), and extradural hemorrhage (EDH), were included.

All intracerebral hematomas included in this study were smaller than 1.00 cm in the long-axis diameter, while all extra-axial hematomas were thinner than 1.00 cm. Only small hematomas were included, because detection of large hematomas is straightforward and unlikely to be problematic for clinicians. The other 30 cases revealed either normal findings or pathology other than hemorrhage, which included acute and chronic infarct, ischemia, and tumor.

17.2.2.2.2 ROC Observers

Seven emergency physicians (EP) with 5–9 years (average 6.4 years) of experience in emergency brain CT interpretation, 7 radiology residents (RR)

with 1–4 years of experience (average 2.3 years), and 6 board certified radiology specialists (RS) with 7–30 years of experience (average 17.8 years), were invited to participate in the evaluation of the CAD system. One of the specialists (subject 5) is a fellowship trained neuroradiologist with 12 years of experience.

17.2.2.2.3 ROC Procedure

The readers were provided with the original images and a graphical user interface (GUI) specifically implemented for this study, as shown on Figure 17.8. One axial section was displayed at a time. The readers could scroll through the images of a particular case back and forth, a total of 60 (with and without AIH cases with mixed orders) in the study. The experiment was conducted in a radiologist's reporting room, where ambient light was low. They were allowed to adjust the brightness of the screen to suit their individual needs, but image windowing was not provided, because this on its own could be considered one form of diagnostic aide. In particular, it was conceivable that pre-windowing could bias against people less familiar with its use, especially emergency physicians. The readers were instructed to record their confidence in detecting AIH on a scale from 1 (absolute absence of AIH) to 10 (absolute presence of AIH). Readers were also instructed to interpret the score of 5 and 6 as indeterminate, with 5 erring on the side of absent AIH and 6 otherwise.

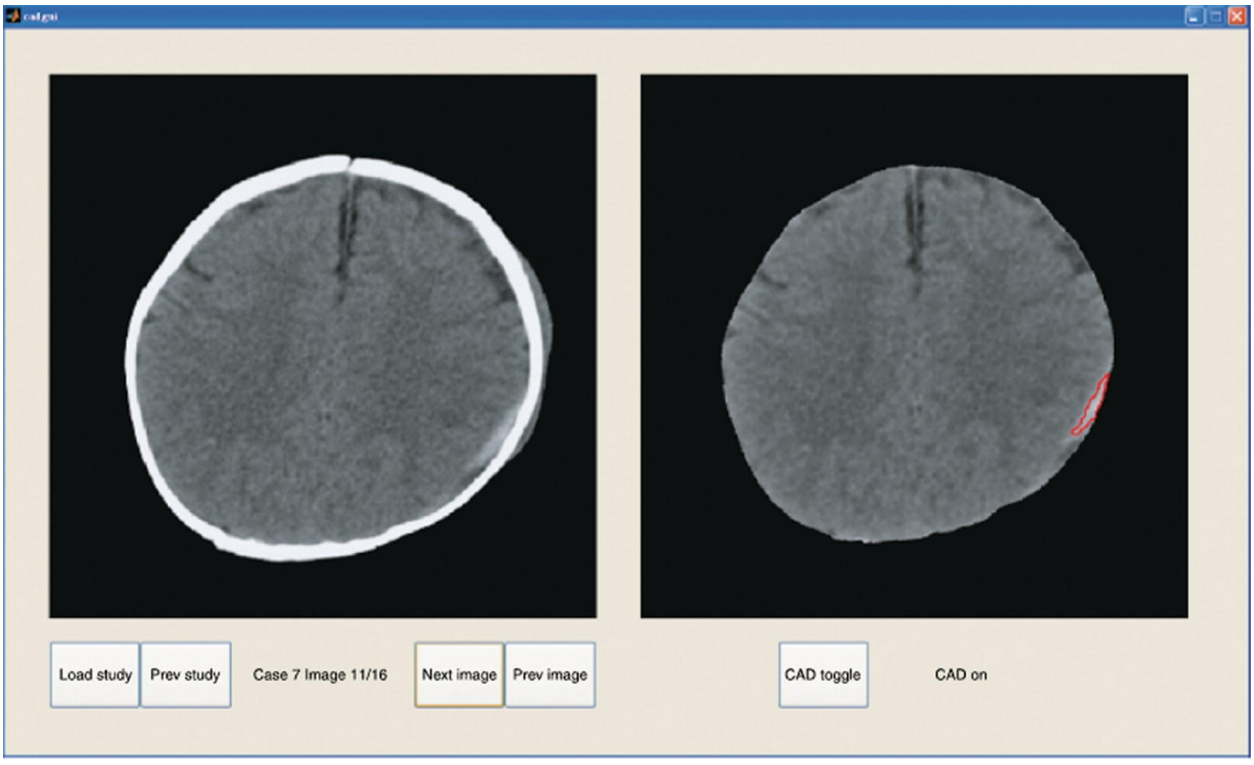

Figure 17.8 Screen capture of the graphical user interface used in the ROC observer study. The original images are displayed at the left window in stack mode. The second reading's output images of CAD are displayed at the right window. An output image that contained the segmented and realigned intracranial contents, and AIH, is outlined. The original and CAD output images are scrolled at the same time.

(courtesy of Dr T. Chan)

Immediately after they had finished all 60 cases and recorded the results, they could re-read the images, now with the CAD output images displayed side by side with the corresponding original images (Figure 17.8). Both the original and the CAD output images would scroll together in synchrony. They again recorded their confidence levels in the same way.

The readers were informed that during the CAD training and validation tests, the CAD had produced a sensitivity of 80–85% on a per lesion basis and a false positive rate of less than one in three cases in earlier tests, but performance for an individual case might depend on size and contrast difference of lesion(s) it contains. They were also reminded that the accuracy of the CAD output, in the sample cases during the ROC study that they were going to read, might be better or poorer than the quoted figures reflecting a difference in case selection.

17.2.2.2.4 ROC Data Analysis

The recorded data were subject to MRMC ROC analyses using the freely available software DBM MRMC developed by the University of Chicago group. The program was based on the Dorfman–Berhaum–Metz method, which allows generalization to the population of readers and cases. The ROC curve was obtained by a maximum likelihood estimation of the binormal distributions that best fit the rating data of the readers.

Since it was believed by many, including most of the participants in the test, that the diagnosis of AIH was an all-or-none question, it was also desirable to present the results in some conventional indicators that were more familiar to clinicians and were based on a yes/no type of response. The scores were placed into two categories of 1–5 and 6–10, which dichotomized the results into absence/presence of AIH. The sensitivity/specificity pair and positive/negative predictive values were calculated accordingly.

In addition, the frequency by which the use of CAD resulted in a change of diagnosis during the experiment, as opposed to mere change in confidence of

one particular diagnosis or another, was examined. The diagnosis of absence/presence of AIH for individual case was determined based on the aforementioned method of dichotomizing the score ratings. The frequency of change in diagnosis and the correctness of such changes were recorded. This information reflected the impact that the use of CAD might have in actual clinical practice where altered diagnostic decisions would affect management options.

17.2.2.3 Effect of CAD-Assisted Reading on Clinicians' Performance

All the results quoted in subsequent sections refer to those calculated on per case or per patient basis.

17.2.2.3.1 Clinicians Improved Performance with CAD

The area under the ROC curve (Az) values scored by individuals before and after CAD are presented in Figures 17.9. Figure 17.9A presents individual performance before and after using the CAD. Only 1 of the 20 observers (observer 4) scored marginally lower Az after CAD. The other 19 all attained a variable increment after use of CAD. Figure 17.9B depicts the three ROC curve pairs, where each pair shows the group's performance to have improved with the aid of CAD.

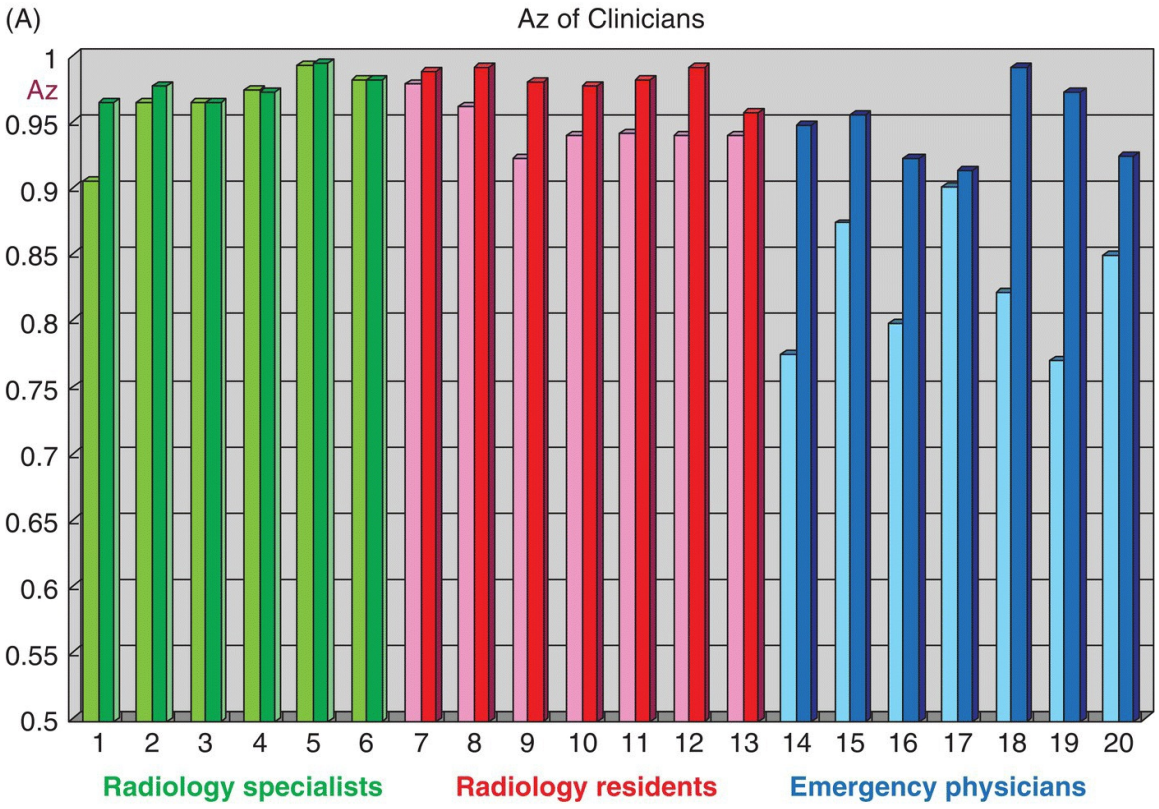
(A)
Az of Clinicians
Az
1
0.95
0.9
0.85
0.8
0.75
0.7
0.65
0.6
0.55
0.5
1 2 3 4 5 6 7 8 9 10 11 12 13 14 15 16 17 18 19 20
Radiology specialists
Radiology residents
Emergency physicians

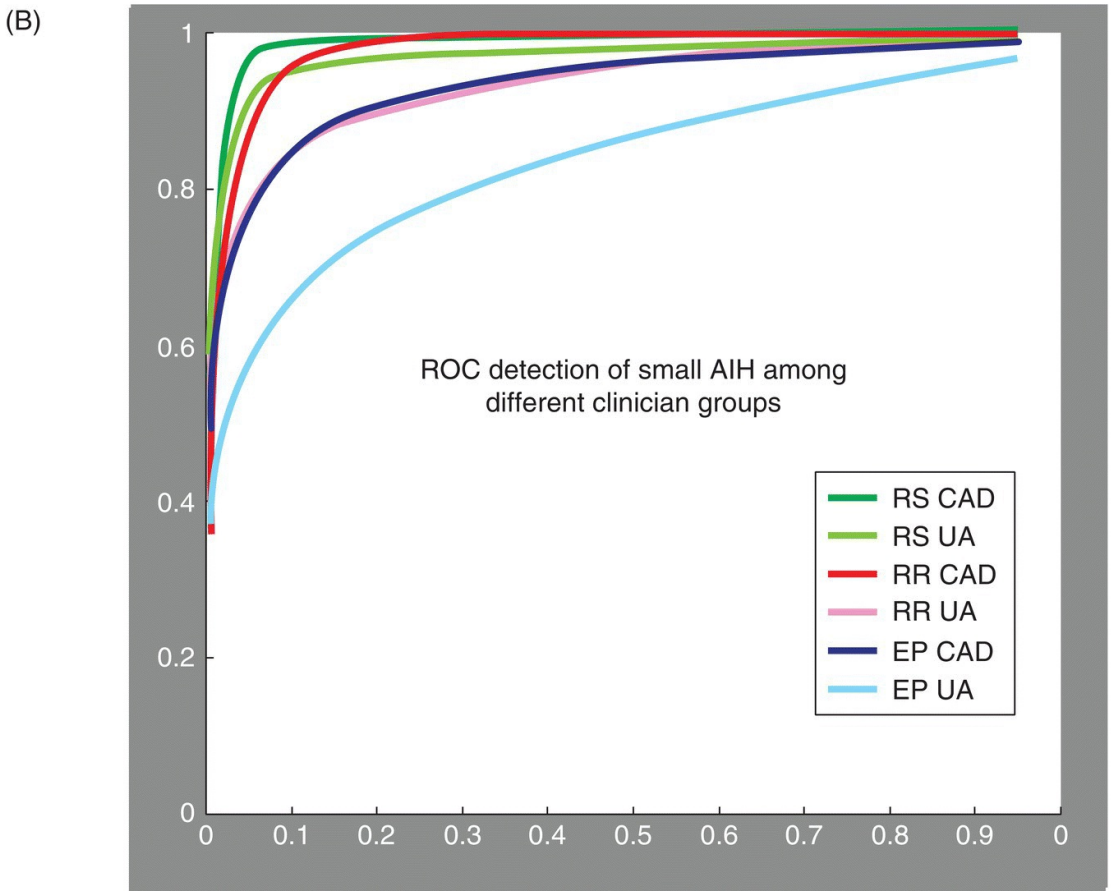
(B)
1
0.8
0.6
0.4
0.2
0
0 0.1 0.2 0.3 0.4 0.5 0.6 0.7 0.8 0.9 0
ROC detection of small AIH among
different clinician groups
RS CAD
RS UA
RR CAD
RR UA
EP CAD
EP UA

Figure 17.9 (A) ROC detection of AIH among different clinician groups. EP: emergency physicians; RR: radiology residents; RS: board certified radiology specialists. The lighter colored bars are unaided reading mode; the darker colored bars are CAD-assisted reading mode. Notice that among the 20 readers, all but reader 4 improved their performance with CAD-assisted reading. (B) Area under the ROC curves of all six curves. CAD can be used to improve the readings, which are the ROC (Az) values, in all three physician groups. Compare each of the three color groups: green, red, and blue. The lighter colored curves represent unaided reading mode (UA); the darker colored curves represent CAD–assisted reading mode.

Significantly improved performance is observed in the emergency physician (EP)average Az, which increased from 0.8422 to 0.9294 ($p = 0.0107$) when the diagnosis was made without and with the support of CAD. Az for the radiology resident (RR)increased from 0.9371 to 0.9762 ($p = 0.0088$). Az for the radiology specialist increased from 0.9742 to 0.9868 ($p = 0.1755$), but was statistically insignificant. The results are shown in Figure 17.9B.

It was clear that the performance of the EP with support of CAD approached that of the RR without CAD. The performance of the RR with CAD was close to that of RS in this experimental condition, since the readers were limited to viewing images without the benefit of windowing or tiling images. This result signifies that the CAD can improve reader performance as well as reduce variability among different clinician groups.

17.2.2.3.2 Sensitivity, Specificity, Positive and Negative Predictive Values

The sensitivity, specificity, positive, and negative predictive values were calculated for each reader, both before and after use of CAD (Table 17.4). It was demonstrated that both sensitivity and specificity improved for each group. The gain was the most remarkable for the EP, whose average sensitivity/specificity improved from 73.3/81.4% to 80.5/90.5%, and less for the RR, which was from 86.2/88.1% to 93.8/92.9%, and the least for the RS, which was from 92.2/93.3% to 95/94.4%.

Table 17.4 Average performance indicators included are sensitivity, specificity, positive predictive value, and negative predictive value for different clinician groups with and without CAD support.

	Emergency	**Radiology**	**Radiology**

	Physicians		Residents		Specialists	
	Unaided	CAD	Unaided	CAD	Unaided	CAD
Sensitivity	73.3	80.4	86.2	93.8	92.2	95.0
Specificity	81.4	90.5	88.1	92.9	93.3	94.4
Positive predictive value	80.0	89.5	88.4	93.0	93.3	94.5
Negative predictive value	75.7	82.5	86.7	93.8	92.6	95.1

Note: All indicators in all clinician groups are improved after use of CAD.

Again, it was clear that the EP results with support of CAD approached that of the RR without CAD, and the results of the residents with CAD approached those of the specialists without CAD.

After the use of CAD, the positive predictive values improved from 80.1% to 89.5% for EP, from 88.4% to 93.0% for RR, and from 93.3% to 94.5% for RS. The negative predictive values also improved from 75.7% to 82.5% for EP, from 86.7% to 93.8% for RR, and from 92.6% to 95.1% for RS.

Again, it was clear that these conventional indicators of diagnostic accuracy for the EP with support of CAD approached that of the RR without CAD, and the results of the RR with CAD approached those of the RS without CAD.

17.2.2.3.3 Change of Diagnostic Decision after CAD Assistance

When the diagnostic decision for each case was considered, it was found that use of CAD corrected the diagnosis far more frequently than misled the readers to a wrong diagnosis. For the EP, use of CAD led to 46 correct changes (beneficial effect) in diagnosis and 12 wrong changes (detrimental effect) out of the maximum number of possible change of 420 (7 readers out of 60 cases). For the RR, the figures were 29 versus 3 out of 420. For the RS, the figures were 7 and 0 of 360. Thus, use of CAD is associated with change in diagnosis in decreasing order of relative frequency from EP (13.8%), to RR (7.0%), to RS (1.9%). On the other hand, the relative frequency of correct change versus incorrect change shows an increasing trend from 79.3%:20.7% for EP, to 90.6%:19.4% for RR, to 100%:0% for RS (Table 17.5).

Table 17.5 Cases in which clinicians change their diagnostic decision after CAD.

	Emergency Physicians	Radiology Residents	Radiology Specialists
Correct change (% of actual number that change)	46 (79.3%)	29 (90.6%)	7 (100%)
Incorrect change (% of actual number that change)	12 (20.7%)	3 (9.4%)	0 (0%)
Frequency of change in decision	58	32	7
Change in decision/total possible change	13.8% (58/420)	7.6% (32/420)	1.9% (7/360)

Note: The proportion of correct change relative to incorrect change increased from EP to RR to RS. The total and relative number of change decreased from EP to RR to RS.

17.2.2.3.4 Some Clinical Considerations

17.2.2.3.4.1 Should CAD be used for AIH on CT

The previous section confirms that CAD for AIH can improve the diagnostic performance of all three types of physicians: emergency clinicians, radiology residents, and radiology specialists, and especially for the former two categories under the given environment and conditions. Unlike tumor detection in mammography, chest radiography, and CT, expert radiologists can diagnose AIH at very high accuracy. But this does not preclude the current system from becoming a clinical useful tool. This is because a patient's emergency brain CT often needs to be interpreted by acute care physicians to make an immediate judgment about the course of action when radiologists are not readily available to do the reading. The acute care physicians, however, cannot be expected to have honed the interpretation skills of a radiologist and thus to expertly detect small or difficult AIHs, or to distinguish a genuine AIH from a mimicking variant or artifact. For these reasons, the CAD system can be usefully implemented into daily clinical practice in the emergency room and other critical care environments. In the event of natural disasters, the CAD system can be depended upon to distinguish patients suffering from minor neurological disturbance from patients suffering head injury. After the CT is performed, clinicians can read the images with help from the CAD system. If AIH can be excluded, then the patients may be safely observed for a shorter period of time without admission to the neurological unit before discharge.

17.2.2.3.4.2 Integration CAD with PACS

CAD for AIH is different from most current CAD systems designed for routine clinical screening, such as in breast imaging, for which speed is of less concern. For urgent care applications, immediate availability without significant time delay is of critical importance, and AIH is one such critical area of application. Ways of integrating CAD for AIH may include an application server connected with the PACS system, or better still, direct incorporation of the system into clinical PACS. How to integrate the CAD into the workflow of the acute care physician or the emergency room will be addressed in the examples presented in Sections 17.2 and 17.3 of this chapter.

17.2.2.3.4.3 Further Evaluation

How to confirm that the CAD for AIH can perform as well in other clinical environments and different patient populations? How about when it is used on images from different CT scanners and scanning protocols, such as slice thickness or the 3-D CT dataset? These questions are discussed in Section 17.1.4.

17.2.3 From System Evaluation to Preclinical Practice

17.2.3.1 Further Clinical Evaluation

Questions were raised in the last section as to how will the CAD for AIH perform in other clinical environments with different patient populations, and how will it work on images from different CT scanners and scanning protocols. To address these issues, further evaluation studies are needed as follows.

AIH is often associated with head trauma, and it is a precipitant of acute neurological disturbances. Identification of AIH is of paramount clinical importance, as the nature of its presence dictates distinctive management and treatment strategies. In many parts of the world, emergency department physicians, internists, or neurosurgeons are the first to read emergency CT studies of a patient suffering head trauma, particularly when a radiologist’s expertise is not immediately available. The purpose of a CAD system for AIH is to provide a clinical decision support tool for clinicians, organizations confronting high volumes of potential AIHs, and resource-limited institutions. Up to this point we had completed the first step in creating such a system, used the data collected from Hong Kong, and trained, validated, and evaluated the CAD system with these data. The next step is to address the questions raised above.

A large-scale retrospective study is being performed of 300 cases with matched normals from the emergency department at the Los Angeles County and University of Southern California Hospital (LAC + USC) comprised of patients who had been previously diagnosed with AIH. Compared with the hospital in Hong Kong, where the validation and evaluation data were collected, LAC + USC is an entirely different clinical environment, serves different patient populations, and utilizes CT scanners from various manufacturers with different clinical protocols. For the questions raised above, the interim results are very promising, with 85% sensitivity, but a little bit lower in specificity. Further improvement is expected.

17.2.3.2 Next Steps for the Development of CAD for AIH in Clinical Environment

After the evaluation described in Section 14.1 is completed, the next logical step in the evolution of the system is actual integration of the CAD into a normal radiology infrastructure and workflow. It is important to implement the system such that future enhancements can readily be tested within a true clinical environment rather than in the isolation of a development or test environment. This next step will allow fine tuning aspects of the system design that must be optimized before a CAD system can be truly effective.

The CAD system must be integrated into the existing systems architecture to automatically run in real time, intercepting new studies and running prior to or in parallel with other existing workflow processes. Furthermore, the results of the CAD system must be stored as distinct files, preserving the original studies but remaining immediately accessible within the existing client software. Integration must therefore occur ahead of PACS or integrated with the PACS system.

Existing radiology and emergency department workflow must be altered to take advantage of the presence of the CAD system. However, acceptance testing of the CAD system within a clinical environment requires stringent confirmatory steps to ensure that no treatment decisions are made wholly based on the CAD system, until such time that the CAD system has been validated within the clinical environment. This specifically applies to clinicians who must be instructed to consult with a radiologist, despite the presence of CAD output during this next phase of development. Radiologists must also be recruited to facilitate validation in the clinical environment by modifying their existing workflow to reference CAD output and by assisting in documenting the successes and failures of both the algorithm and the system. Most important, the

system enhancements based on user input, from both clinicians and radiologists, is an essential next step in the evolution of the CAD system. Factors such as processing time, output visualization, accessibility, reporting, and logging, which may not have been primary drivers in the development and testing environments, become more important aspects of a production environment and must be developed and enhanced to deliver a complete CAD solution. Figure 17.10 summarizes these steps involved in the iterative process of clinical evaluation.

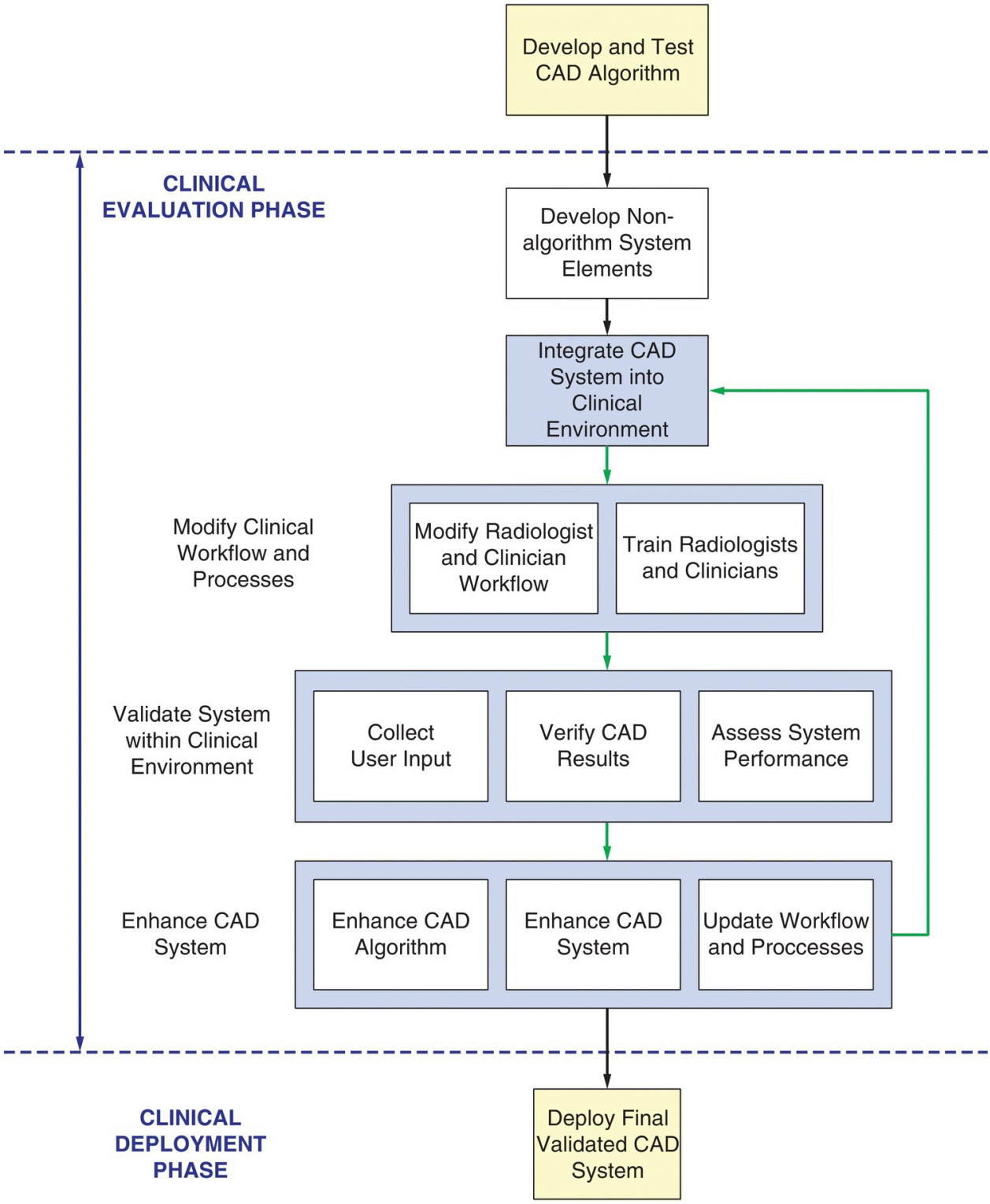

Figure 17.10 Iterative process in clinical evaluation. Once the CAD is installed in the clinical environment for evaluation, it goes through several phases of iterative processes, shown in green arrows. With this iterative process is completed, the CAD system can be deployed for clinical use.

(courtesy of Dr R. Lee)

Once these non-algorithmic elements are established, future iterations of the CAD system can focus on enhancement of the core algorithm and/or minor systems-related enhancements within the overall systems architecture. Figure 17.11 (see also Chapter 12) shows the prototype of the CAD–PACS integration in the laboratory environment before its deployment to the clinical environment for evaluation.

Figure 17.11 CAD–PACS integration prototype in the laboratory environment showing two systems: the CAD server for AIH, and the PACS simulator. The leftmost component is the CAD server running an AIH case study. Other components are the PACS simulator (see Chapters 7 and 8). The PACS simulator has all the essential components of a real PACS, including a modality simulator, DICOM gateway, PACS server, and PACS WS. It is used for PACS training and for testing the functionality of CAD-PACS integration. The PACS WS is located at the rightmost position, with the same AIH case shown on the monitor of the CAD server. A physician reads the case at the PACS WS with and without CAD-assistance (see also Chapter 12).

Another CAD system on bone age assessment of children, which will be discussed in Chapter 18, has passed many of the stages discussed above [1,2]. This system is presently being evaluated clinically in pediatric radiology, by integrating the CAD and radiologists' readings.

17.2.4 Summary of using CAD for AIH

This chapter presents the essentials of medical image-based CAD. This section starts with a brief review of the growth of CAD over the last 10 years. Then CAD is discussed, not in a mathematical algorithm context but from a medical

imaging informatics perspective. Conceptual methods of CAD-PACS integration are described that lead to the CAD-PACS integration toolkit discussed in Chapter 16.

A self-contained CAD method for AIH detection on CT is given to illustrate that CAD is not necessarily to be used for large-scale screening and daily radiological report generation, but also for particular clinical environments, such as the emergency room or in environments where a radiologist specialist may not be readily available. CAD may be able to assist in making a timely diagnosis to treat a patient with AIH. A step-by-step approach is used to illustrate all the basic ingredients, from the CAD problem definition, to algorithm development, data collection to training the CAD, validation of the CAD system, evaluation of CAD performance compared with human observers, and to deployment of the CAD for daily clinical use.

For CAD to be really useful to healthcare providers on a daily base, it has to be integrated with PACS. This chapter lays down the CAD basic foundation that will be picked up in Chapter 18, where we explain CAD-PACS system integration.

17.3 CAD–PACS Integration

In general, medical imaging and informatics examinations results are first reviewed then dictated by the physicians. These formal clinical reports are by no means structured, as shown and discussed in the cranial hemorrhage (AIH) example in Section 17.1.

17.3.1 The DICOM-SR already available from the PACS Vendor

This section presents two cases in which the CAD results are already integrated into the PACS clinical environment using the DICOM CAD–PACS integration toolkit. In both cases, the CAD outputs had been converted by the manufacturer to the DICOM-SR format, which is required by the CAD–PACS toolkit as the CAD output format for the integration of the exchange objects. In addition, it is assumed that the original images from the CAD results had already been stored in PACS, so that both the CAD ad PACS can use similar toolkit components to integrate the CAD system with the PACS system.

In order to have seamless integration between the CAD and PACS, the following

steps and components from the toolkit are required:

1. assign a DICOM node for the SR server;
2. establish connections between PACS and the SR server for image query and retrieval;
3. activate the CAD WS/server and the SR server to receive DICOM-SR objects; and
4. set up Display-SR at the PACS WS.

17.3.2 Integration of a Commercial CAD with PACS

The first CAD case considers the CAD detection of lesions on a chest CT image developed by a PACS manufacture (General Electric Medical Systems, Milwaukee, Wisconsin), and the second case is the CAD diagnosis of breast cancer on mammograms developed by another CAD manufacturer (R2/Hologic, Inc. Bedford, Massachusetts). In both cases, the available CAD outputs had already been converted to a DICOM-SR format by both manufacturers, and the original images were stored in two different PACS. The objective is to demonstrate that with the given CAD results in DICOM-SR format stored in a CAD WS, the CAD–PACS integration toolkit can integrate the CAD WS with the PACS for receiving and displaying the CAD results on the PACS WS. The steps include:

1. the CAD WS or server completes the CAD process and sends the DICOM-SR document containing the CAD results to the SR server (CAD–PACS toolkit);
2. the SR server utilizes the Receive-SR module (from the toolkit) to store the DICOM-SR CAD results and automatically pre-fetches reference images from PACS; and
3. CAD results are ready for viewing from a PACS WS using the Display-SR module (from the toolkit).

Figures 17.12 and 17.13 show the screenshots of a chest CT CAD and a mammogram CAD result in DICOM-SR format displayed on a PACS WS, respectively. These images in the PACS WS can be manipulated as DICOM images. The top of each image shows the patient information, the left side displays the structured report, and the right side is the DICOM images with nodule/lesion identified by overlaid annotations.

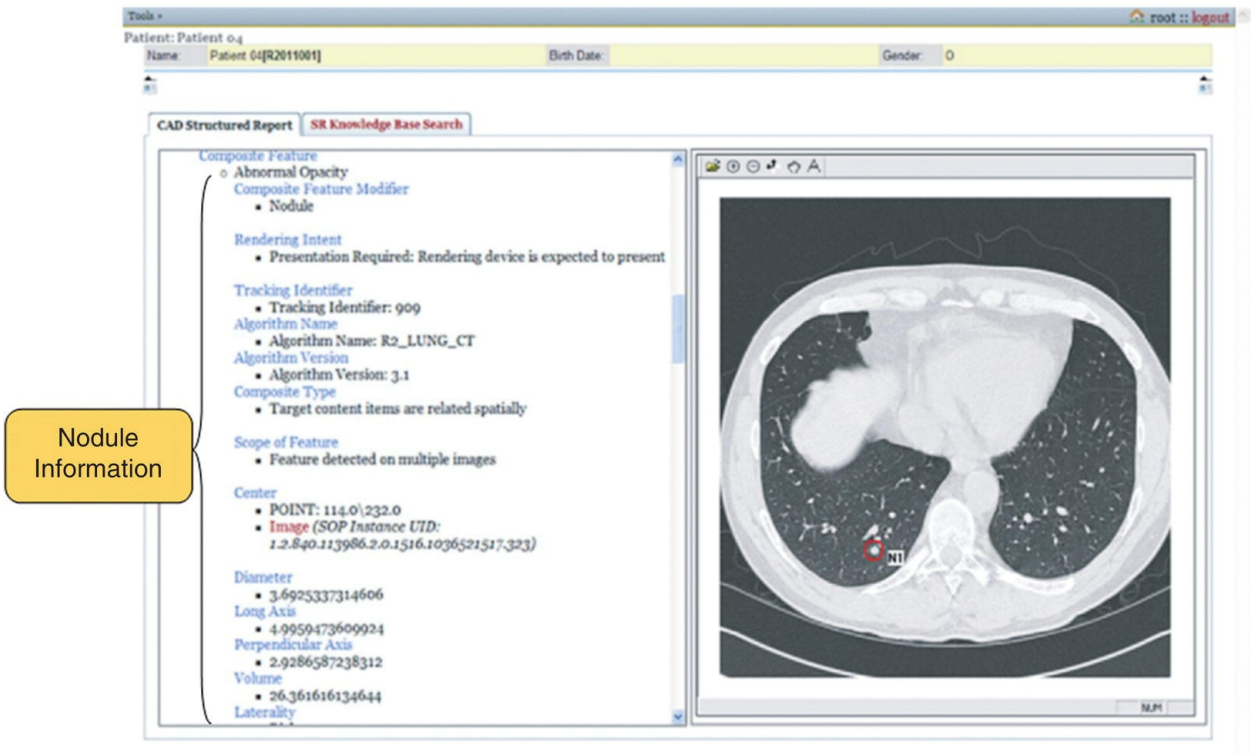

Figure 17.12 Manufacturer's chest CAD report already in DICOM-SR format (left) with referenced image and annotation (right). Annotation (small red circle) in the DICOM-SR allows the user to toggle it on or off (case materials courtesy of General Electric Medical Systems).

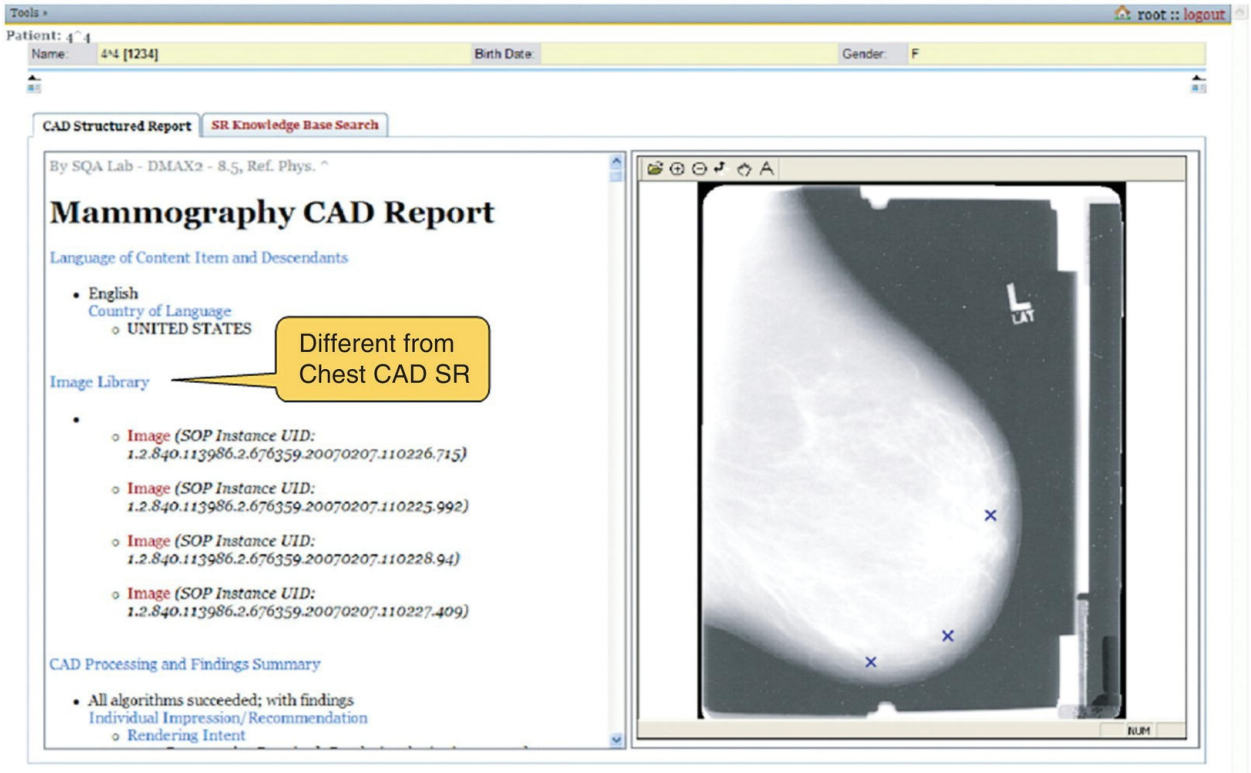

Figure 17.13 A manufacturer's mammography CAD report already in DICOM-SR (left) with referenced image and annotation (right). Note that the DICOM-SR format is different from that of the CAD on CT (red text, shown in Figure 17.12). Annotation (dark crosses) in the DICOM-SR allows the user to toggle it on or off (case materials courtesy of R2/Hologic, Inc).

As shown in Figure 17.12, the location of the chest nodule is identified from the DICOM-SR object and is sent to the Display-SR module for display as annotations (small red circle) on top of the original CT image stored in PACS. This information is stored separately from the original DICOM image and allows annotation to be toggled on/off from the original image that is displayed. The same is the case of the mammography CAD shown in Figure 17.13, in which the locations of the breast lesions determined by the CAD are indicated by the small dark crosses. The differences between the chest CT CAD and the small mammography CAD are that: i) the two CAD algorithms are different; and ii) the structures of the two DICOM-SR objects are also different (see rectangular box annotation on the left of each figure). For example, the chest CT CAD SR does not reference the whole CT chest study but only shows one CT image with a single nodule detected (red font) with a long structured report; whereas the mammography CAD DICOM-SR object includes all four images (left with red text) in a screening mammography study. One reason is that the CT study has

many images and the SR reference is the only image in which the single lesion was detected. Therefore each CAD algorithm or CAD for a different body region would have a different SR template to present complete and precise CAD results.

17.4 Multiple Sclerosis (MS) on MRI

17.4.1 DICOM Structured Reporting (SR) and CAD–PACS-Based Integration Toolkit

In Chapter 4, on Industrial Standards in DICOM, the concept of structured reporting (SR)was introduced as one of the DICOM extensions. In the small acute intracranial hemorrhage example shown in Section 17.1, the CAD results had already been converted to DICOM-SR format. The method of conversion from the CAD results to DICOM-SR format was straightforward, because the CAD was originally developed by the two manufacturers that had already converted the CAD results to DICOM-SR format. On the other hand, if the CAD result has not already been converted to DICOM-SR format, then the user, or the hospital clinician/researcher who is responsible for dictating the report, would have to convert the report to the SR format to comply with the DICOM standard and IHE workflow profiles (see Chapter 16, Section 16.2.2). The example used in Section 17.3, related to multiple sclerosis, does require the CAD results to be converted to the DICOM-SR format before or after dictation. The conversion method is discussed in this section (see Table 17.6, and the bone age assessment case discussed in Chapter 18, Figure 18.16).

Table 17.6 Tasks and requirements for integrating CAD with PACS systems in the three examples.

CAD Systems	Tasks and Requirements		
	CAD Algorithm	**CAD Output Format**	**Integration Tasks**
1. Commercial CAD: lesions on Chest CT and breast cancer on mammogram	Developed proprietary	DICOM-SR document	Store SR files in SR server and display SR on PACS WS
2. CAD for multiple sclerosis (MS) on MRI	Developed proprietary	Text or XML, images (DICOM/bitmap)	Create SR template and SR files

			Store SR files in SR server and display SR on PACS WS
3. CAD for bone age assessment	Developed proprietary	Text or XML, images (DICOM/bitmap)	Create SR template and SR files
			Store SR files in SR server and display SR on PACS WS

17.4.2 Multiple Sclerosis Detection on MRI

Multiple sclerosis (MS) is a progressive neurological disease affecting myelin pathways in the brain. Multiple lesions in the white matter can cause paralysis and severe motor disabilities of the affected patient. Symptoms are changes in sensation, visual problems, muscle weakness, and depression. Currently, MRI T1 and FLAIR pulse sequences are used for radiological diagnosis. In these images, MS appears as multiple white lesions in the white matter area of the brain. MRI is also used to follow up and monitor the progress of the disease and the effectiveness of therapy after the patient is treated with drugs. Since MRI provides excellent delineation of MS, it is fairly easy for radiologists to make the diagnosis. However, due to the possibility of a large number of multiple lesions in the MRI 3-D volume set of the brain, it is tedious and time-consuming to identify the 3-D aspect of each lesion and quantify the number and size of these lesions. Moreover, the quantitative reproducibility through human observers is poor. Augmenting CAD with imaging informatics methods, a 3-D CAD MS package would facilitate the physician's timely diagnosis, improve accuracy, and assess quantitatively the progress of therapy treatment.

17.4.3 Data Collection

Figure 17.14 shows the most common data obtained from 3-D CAD results. The data includes the original 3-D MRI dataset, Figure 17.14A shows an MRI FLAIR image, CAD detected multiple lesions (Figure 17.14B), radiologist identified lesions (Figure 17.14C), normally not shown in the results, depicted here only for comparison purposes); the detected MS lesions are color coded on each 2-D image (Figure 17.14D, one slice; Figure 17.14E two slices; and Figure

17.14F, all 26 slices). Figure 17.14G gives the quantitative result of all lesions detected by CAD. Figure 17.12H shows three 2-D oblique views of the brain overlaid with 26 MS lesions. The CAD results were generated through collaboration between IPILab, USC and Guardian Technologies, Inc., Dulles, Virginia.

(A)

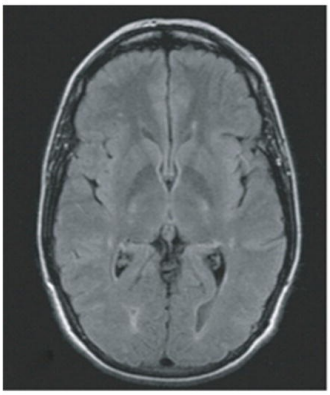

(B)

(C)

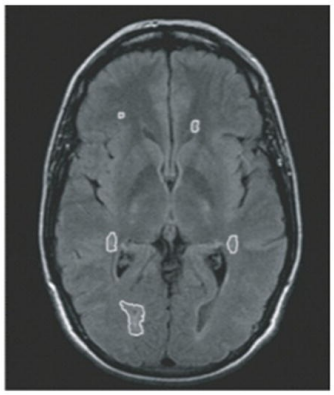

(D)

(E)

(F)

(G)

Lesion Name	Slice areas included in lesion	Total Count	Red	Yellow	Green	Cyan	Blue	Magenta
A	red 1, yellow 1	213	82	131				
B	red 2	172	172					
C	red 3	617	617					
D	red 4, yellow 2, Green 3	501	188	212	101			
E	red 5	24	24					
F	yellow 3	65		65				
G	yellow 4	194		194				
H	yellow 5	16		16				
I	yellow 6	79		79				
J	Green 1, Cyan 5, 8, 9-10, 6*, Blue 5*	1058			143	634	281	
K	Green 2	250			250			
L	Cyan 1	50				50		
M	Cyan 2	50				50		
N	Cyan 3	120				120		
O	Cyan 4	82				82		
P	Cyan 6	58				58		
Q	Cyan 7	55				55		
R	Cyan11, Blue 6-7, Magenta 2	393				151	170	72
S	Blue 1	37					37	
T	Blue 2	111					111	
U	Blue 3	0					fn	
V	Blue 4	102					102	
W	Blue 8	125					125	
X	Blue 9	52					52	
Y	Blue 10	88					88	
Z	Magenta 1	89						89

* Cyan 5 and 6 are not connected in slice 14 but join lesion J through Blue 5.

(H)

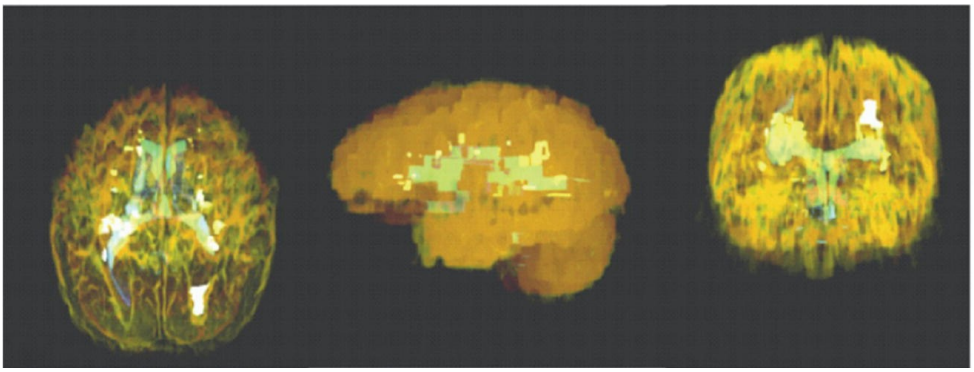

Figure 17.14 Commonly obtained data from 3-D multiple sclerosis (MS) CAD results. The data include the original 3-D MRI dataset: (A) MRI FLAIR image; (B) CAD detected multiple lesions; (C) radiologist identified lesions (normally not shown in the results, depicted here for comparison purpose only); (D) color-coded MS lesions on a 2-D image; (E) on two slices; (F) on all slices; (G) quantitative results of all 26 lesions detected by CAD; (H) three oblique views of 2-D images with all 26 MS lesions overlaid. Green color shows the ventricles.

(data: courtesy of Drs A. Gertych and B. Guo; and Guardian Technology, Inc)

Currently, these results can be shown only on the specialized MS detection CAD WS, but cannot be linked or viewed in the daily clinical PACS WS. The PACS database does not contain these results as DICOM objects, and the CAD WS or database does not know what other data the patient might have within the PACS. Sections 17.3.4 and 17.3.5 demonstrate how the CAD–PACS integration would allow this to happen, that is, to receive the CAD results from the CAD WS and display them on the PACS WS.

17.4.4 Generation of the DICOM-SR Document from a CAD Report

To convert the CAD results from a text file (i.e. the one shown in Figure 17.14) into DICOM-SR format, a special CAD template is first tailored to satisfy the specific need for presenting complete results. Figure 17.15 shows a SR template for the MS application. The template is similar to the two ratified CAD SR templates for mammography and chest CT in the DICOM standard shown in Figures 17.12 and 17.13. A new MS DICOM-SR object for this application based on the tree structure is defined, designed, and implemented. This design, which utilizes the DICOM Standard Supplement 23 and computer science terminologies, has a document root MS CAD (Figure 17.15) that branches into four parent nodes (detections, analyses, summary, and image library). Within this context, the detections performed can have one or more child nodes, detection performed (1 − n), with various detailed algorithms used for lesion detection. By the same token, the analyses performed parent node describes one or more methods of quantitative analysis performed on each lesion. Each analysis performed can be further branched to one or multiple (1 − n) grandchild nodes, single image finding. The finding summary parent node is the most important part of a SR, which includes CAD results. This node can branch into multiple child nodes (1 − n), each containing the name of the detection and analysis methods, together with detailed results of each lesion on each single image

finding. The detailed results include number, size, location, and referenced image. The image library parent node is optional; however, in the MS SR, it is used to reference original images where the CAD was performed. The data structure format of each child can be obtained directly from the DICOM Standard, Supplement 23.

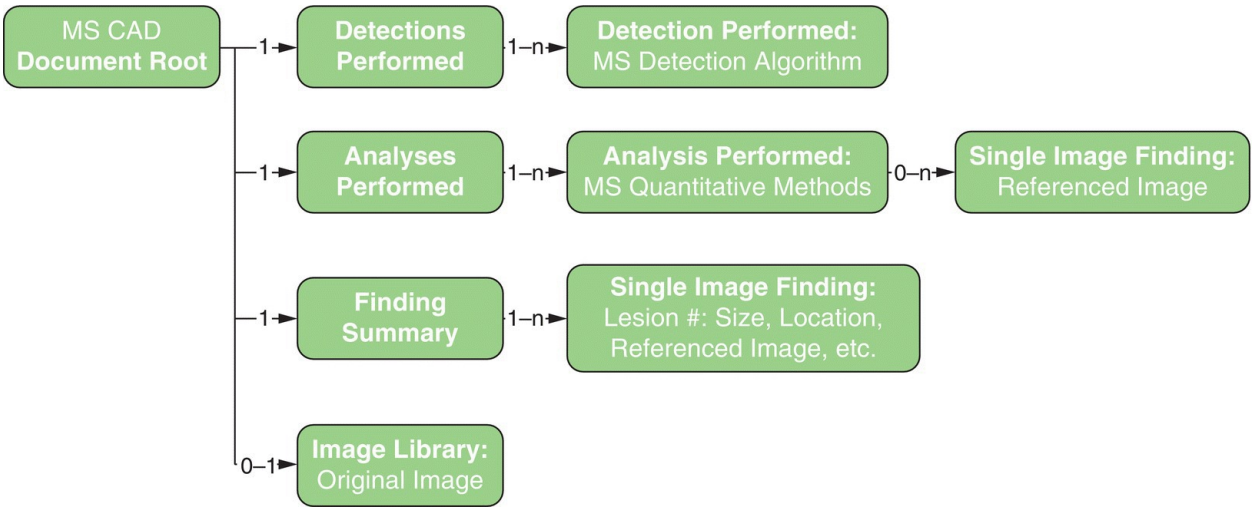

Figure 17.15 Multiple sclerosis (MS) computer-aided diagnosis (CAD) SR template. The SR template is designed following a tree structure starting from the document root, which branches into four parent nodes; each parent node branches to (1 − n) child nodes.

17.4.5 Integration of CAD with PACS for Detection of Multiple Sclerosis (MS) on MRI

17.4.5.1 Connecting the DICOM Structured Reporting (SR)with the CAD–PACS Toolkit

After the SR template is defined and designed, integrating the CAD with PACS can be implemented by using the toolkit. The first step is to use a PACS simulator to verify the data flow, as shown in Figure 17.16 (see Chapter 12). The PACS simulator has been used since 2000 in the IPILab, USC, as a training tool for PACS and imaging informatics research and development, and to verify compliance with the Health Insurance Portability and Accountability Act; the PACS simulator is currently utilized as a research tool in CAD–PACS integration.

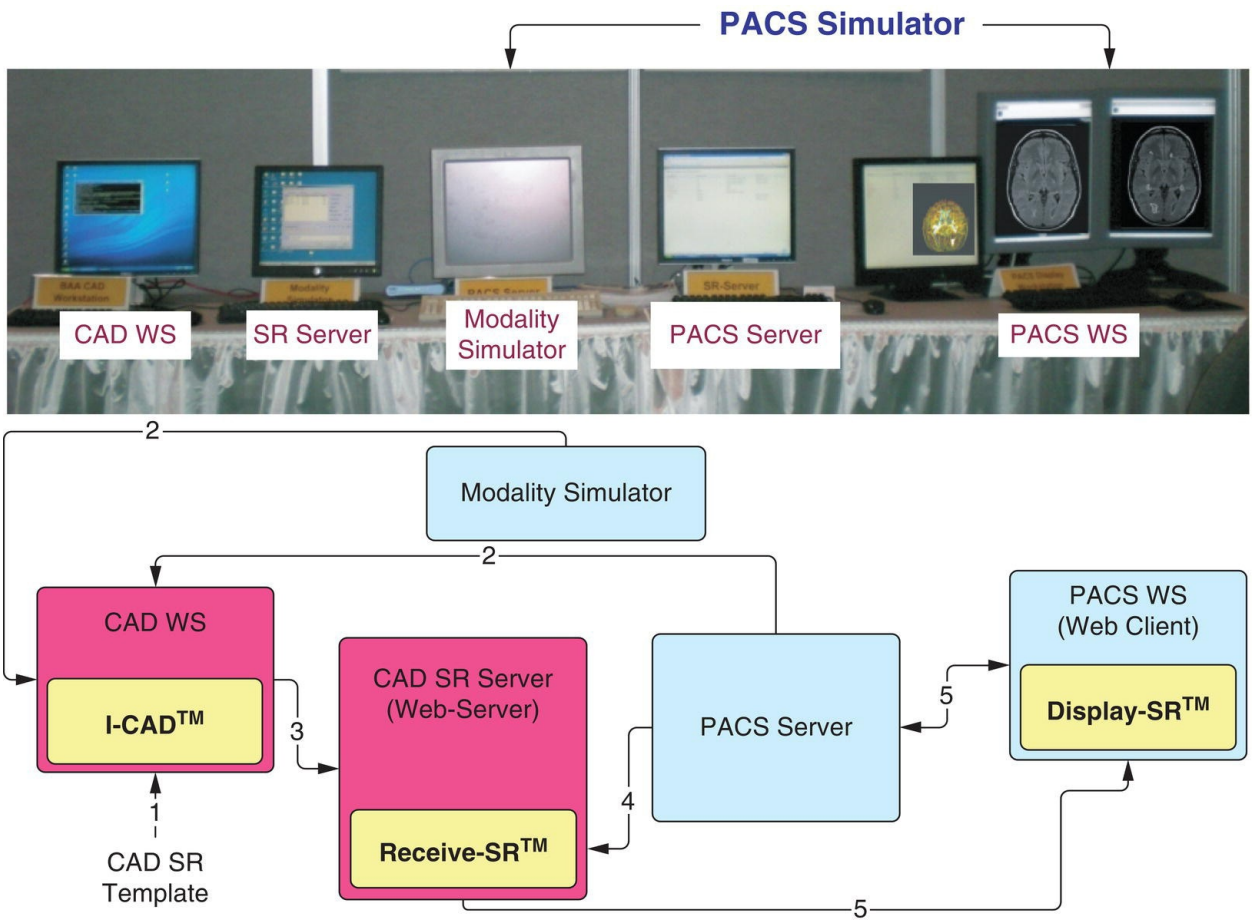

Figure 17.16 Use of the PACS simulator to verify the data flow between the integrated PACS and CAD system. Top: PACS simulator displayed at RSNA Annual Scientific Exhibit from 2000 to 2004. Bottom: Workflow of CAD–PACS integration: PACS simulator components (blue); CAD components (pink); CAD–PACS toolkit modules (yellow). The integration steps in numerals are described in the text. The PACS WS (the rightmost component) displays the original image (middle) from PACS, where the CAD results (right) were obtained. The left monitor shows the CAD–SR (see also Figure 17.17).

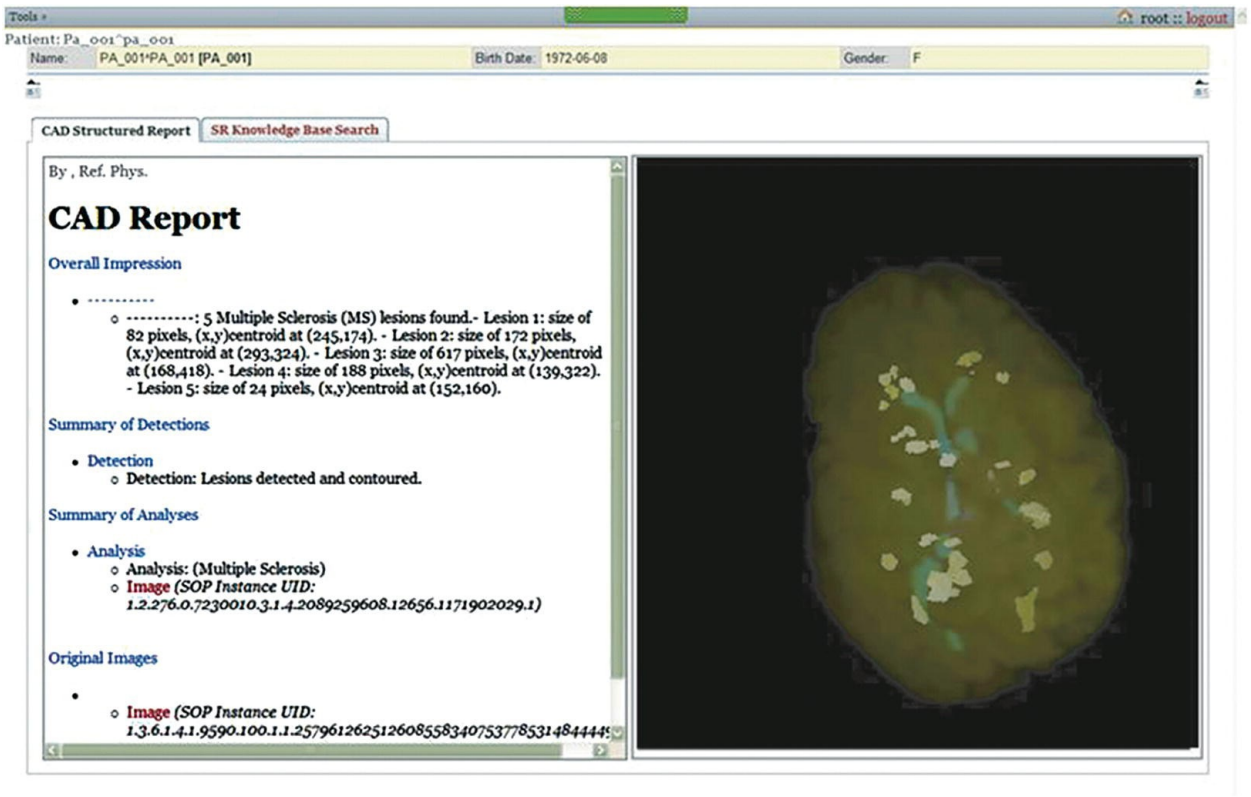

Figure 17.17 Multiple sclerosis CAD report in DICOM SR format (left) and a 2-D oblique image (right).

The integrating steps can be summarized as follows (see numerals in Figure 17.16):

1. the i-CAD module is configured with the MS SR template and all data (measurements, nodule images, and summary) to create the DICOM-SR object;
2. the CAD WS is configured to run the CAD application automatically after receiving DICOM images from modality simulator or PACS simulator;
3. based on the SR template, the i-CAD module automatically starts to create a SR upon completion of the CAD process, and the results are sent in DICOM-SR format to Receive-SR for storage;
4. the SR server pre-fetches the referenced images from the PACS server; and
5. the CAD results are ready for viewing on PACS WS.

In this case study, the CAD generates results as shown in Figure 17.14, among which are a number of lesions, 3-D coordinates of the lesions, the volume of each lesion, and their 2-D presentations in each detected MR slice at various

oblique angles. These 2-D presentations can be used for 3-D viewing on a 2-D monitor.

17.4.5.2 Integration of PACS with CAD for MS Detection

Figure 17.17 gives a screen shot of the CAD MS results at the PACS WS. The example shown is of an MS DICOM-SR object with one 3-D view of multiple oblique 2-D images obtained by DICOM SC (Figure 17.14H). Although this example only displays the 2-D oblique images, theoretically the DICOM-SR specification should include image references and CAD results that can be used to display real time 3-D rendered images.

References

1 Doi, K. (2007) Computer-aided diagnosis in medical imaging: Historical review, current status and future potential. *Comput Med Imag Graph*, 31(4–5), 198–211.

2 Gertych, A., Zhang, A., Sayre, J., Pospiech-Kurkowska, S. and Huang, H.K. (2007) Bone age assessment of children using a digital hand atlas. *Comput Med Imag Graph*, 31, 323–331.

Further Reading

Cao, F., Huang, H.K., Liu, B., Zhou, Z., Zhang, J. and Mogel, G. (2001) Fault-tolerant PACS server, InfoRAD Exhibit. 87th Scientific Assembly and Annual Meeting, November 25–30, Radiol Soc N Am, p. 737.

DICOM Standard (1999) Supplement 23: Structured Reporting Object.

DICOM Standard (2000) Supplement 50: Mammography CA.

DICOM Standard (2001) Supplement 65: Chest CAD SR SOP Class.

DICOM Standards (2008) http://medical.nema.org/medical/dicom/2008.

Greulich, W.W. and Pyle, S.I. (1959) *Radiographic Atlas of Skeletal Development of Hand Wrist*. Stanford: Stanford University Press, 1–36, 190, 194–5.

Health Level 7 (2008) http://www.hl7.org/

HHS, Office of Civil Rights, HIPAA (2008) http://www.hhs.gov/ocr/hipaa

Hologic R2 Home. http://www.r2tech.com/main/home/index.php

Huang, H.K and Doi, K. (2007) CAD and image-guided decision support. *Comput Med Imag Graph*, 31(4–5), 195–197.

Huang, H.K., Cao, F., Liu, B.J., Zhou. Z., *et al*. (2000) PACS simulator: a standalone educational tool. InfoRAD Exhibit (2000) 86th Scientific Assembly and Annual Meeting, November 26–December 1, *Radiol Soc N Am*, p. 688.

Huang, H.K. (2004) *PACS and Imaging Informatics: Basic principles and applications*, vol. 44. Hoboken, NJ: Wiley, pp. 504–507.

IHE (2008) http://www.ihe.net

Le, A., Mai, L., Liu, B. and Huang, H.K. (2008) The workflow and procedures for automatic integration of a computer-aided diagnosis workstation with a clinical PACS with real world examples. *Proc SPIE Med Imag*, 6919, 1–7.

Le, A.H.T., Liu, B. and Huang, H.K. (2009) Integration of computer-aided diagnosis/detection (CAD) results in a PACS environment using CAD-PACS toolkit and DICOM SR. *Intern J. Comp Asst Rad & Surg*, 4, 317–329.

Lee, J., Le, A.H.T., Liu, B.J. and Huang, H.K. (2008) Integration of content-based DICOM-SR for CAD in the medical imaging informatics Data Grid with examples in CT chest, mammography, and bone-age assessment. Education Exhibit, 94th Scientific Assembly and Annual Meeting, *Radiol Soc N Am*, November 30–December 5, p. 912.

Mamdani, E.H. (1974) Application of fuzzy algorithms for control of simple dynamic plant. *Proc IEEE*, 121, 1585–1588.

18
PACS-Based CAD: Digital Hand Atlas and Bone Age Assessment of children

CHAPTER MENU

18.1 Average Bone Age of a Child

18.1.1 Bone Age Assessment

18.1.2 Computer-Aided Diagnosis of Bone Age

18.2 Bone Age Assessment of Children

18.2.1 Classical Method of Bone Age Assessment of Children from a Hand Radiograph

18.2.2 Rationale for the Development of a CAD Method for Bone Age Assessment

18.2.3 Data Collection

18.2.4 The Digital Hand Atlas

18.2.5 CAD Module: Image Processing Algorithm

18.2.6 Fuzzy Logic in Computing Bone Age

18.3 Method of Analysis

18.3.1 Statistical Analysis

18.3.2 Radiologists' Interpretation

18.3.3 Cross-Racial Comparisons

18.3.4 Development of the Digital Hand Atlas for Clinical Evaluation

18.4 Integration of CAD with PACS-Based Multimedia Informatics for Bone Age Assessment ofChildren: The CAD System

18.4.1 The CAD System Based on Fuzzy Logic for Bone Age Assessment

18.4.2 Fuzzy System Architecture

18.4.3 Fuzzy Integration of Three Regions: Phalangeal, Carpal, and

Wrist
18.5 Validation of the CAD and Comparison of the CAD Result with Radiologists' Assessment
18.5.1 Validation of the CAD
18.5.2 Comparison of CAD versus Radiologists' Assessment of Bone Age
18.5.3 All Subjects Combined in the Digital Hand Atlas (DHA)
18.6 Clinical Evaluation of the CAD System for Bone Age Assessment (BAA)
18.6.1 BAA Evaluation in the Clinical Environment
18.6.2 Clinical Evaluation Workflow Design
18.6.3 Web-based BAA Clinical Evaluation System
18.6.4 Integration of the BAA CAD System at the Los Angeles County General Hospital
18.7 Integration CAD for Bone Age Assessment with Other Informatics Systems
18.7.1 BAA DICOM Structured Reporting (SR)
18.7.2 Integration of Content-Based DICOM-SR with CAD
18.7.3 Computational Services in Data Grid
18.7.4 Utilization of Data Grid Computational Service for Bone Age Assessment for Children
18.8 Research and Development Trends in CAD–PACS Integration
Acknowledgement
References
Further Reading

This chapter provides step-by-step guidelines to develop a CAD method for bone age assessment (BAA) of children from a hand and wrist radiograph. The data collection followed the Institutional Review Board data collection guidelines, including patient anonymity, CAD development, validation, evaluation, and HIPAA compliance. These guidelines are standard procedures for developing a CAD method from incubation, development, preliminary production, to clinical evaluation site deployment.

18.1 Average Bone Age of a Child

18.1.1 Bone Age Assessment

The assessment of the bone age of children is a common clinical procedure performed in pediatric radiology to evaluate the stage of skeletal maturation of the child. The clinical importance of bone age assessment (BAA) can help diagnose endocrinological problems and growth disorders in children. A difference between the chronological age and the skeletal age of the subject suggests abnormal development. BAA can also be used to monitor growth hormone therapies and may be used in pediatric surgery.

The current standard for BAA in the United States is for radiologists and clinicians to compare the patient's left hand radiograph with the *Greulich and Pyle (G&P*) *Hand Atlas* [1]. The atlas contains left-hand radiographs of normal children of both males and females ranging from newborn to 18 years of age. The *G&P Atlas*, while widely accepted, have some disadvantages. First, the atlas contains left-hand images that were collected over 50 years ago. Previous studies have shown that there have been discrepancies between the *G&P Atlas* and the development stages of modern children [2]. Second, the subjects were only Caucasians from the American Midwest region. In today's urban environment with its ethnic diversity, the atlas may not be adequate to evaluate children of different races and genders. Third, because BAA is based on visual comparison of closest matched image to the atlas, there are inter- and intra-personal reading discrepancies. Using the *G&P Atlas*, interobserver readings can differentiate from 0.37 to 0.6 years, and intra-observer differences can range from 0.25 to 0.47 years [3,4]. Based on these shortcomings, a solution is needed that both defines a more rigorous standard for today's ethnically diverse population and eliminates subjective comparison analysis for assessing bone age.

18.1.2 Computer-Aided Diagnosis of Bone Age

Consider an example of finding an average hand image from a large collection of x-ray hand images from normal young children (see later in this chapter). The following are the general steps by definitions, visualization) method (see also Section 18.4):

1. *State the problem*: To find the average hand image;
2. *Collect data*: A normal children hand radiographic image database;
3. *Preprocessing the data*: Each hand has over 20 quantitative parameters

extracted from the image by image processing methods. These parameters are used as a gauge to determine the average hand image in a subgroup in the hand database (see Section 3 on methods);

4. *Estimate the model*: Criteria are set up to discover the average hand in a subgroup of children based on these parameters from the database;
5. *Interpret and validate*: Comparing the discovered average image with all available hand images based on visualization.

Figure 18.1 depicts average hand images per year in a subgroup of African-American females from age 1 year to 12 years of age, in the hand database using the data-mining method (CAD).

Historically, large-scale data on children's bone age have been collected over the span of more than 10 years and the racial differences in bone age growth patterns of this dataset have been studied [5]. CAD for BAA of different age groups based on this dataset have been previously designed and implemented, including phalanges region of interest , carpal [6], and wrist joint ROI determination [7], and fuzzy logic subsystem design had been performed [8]. In this chapter, the detailed history and components of CAD BAA system are summarized, followed by development of the CAD method, the connection of the automatic computer-aided BAA system, the PACS operation of the Web-based pediatric radiology workstations (WSs) in the Department of Pediatrics, University of Southern California, and finally, the system clinical validation.

(A)

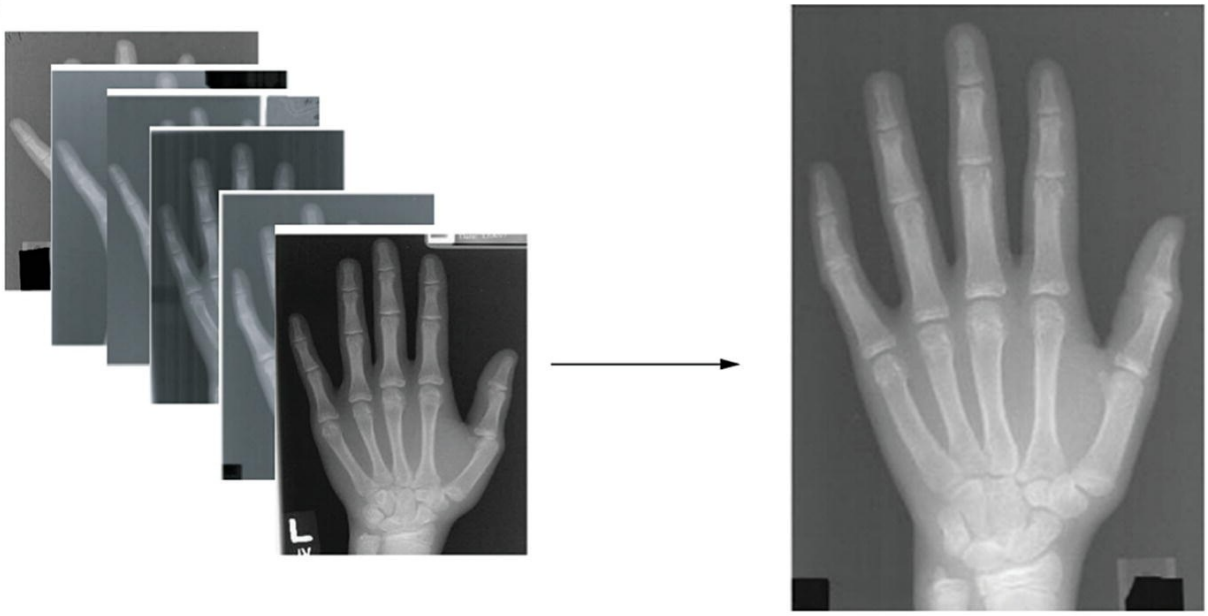

Average image (right) selected from a group of images (left)

(B)

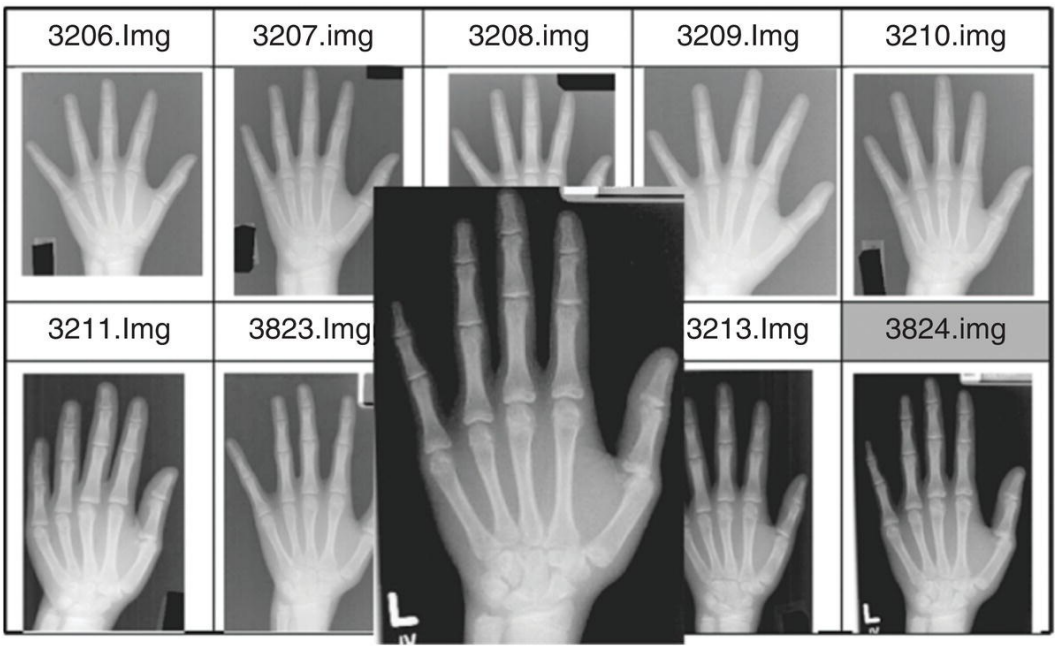

Example of average image of a AAF11 group

(C)

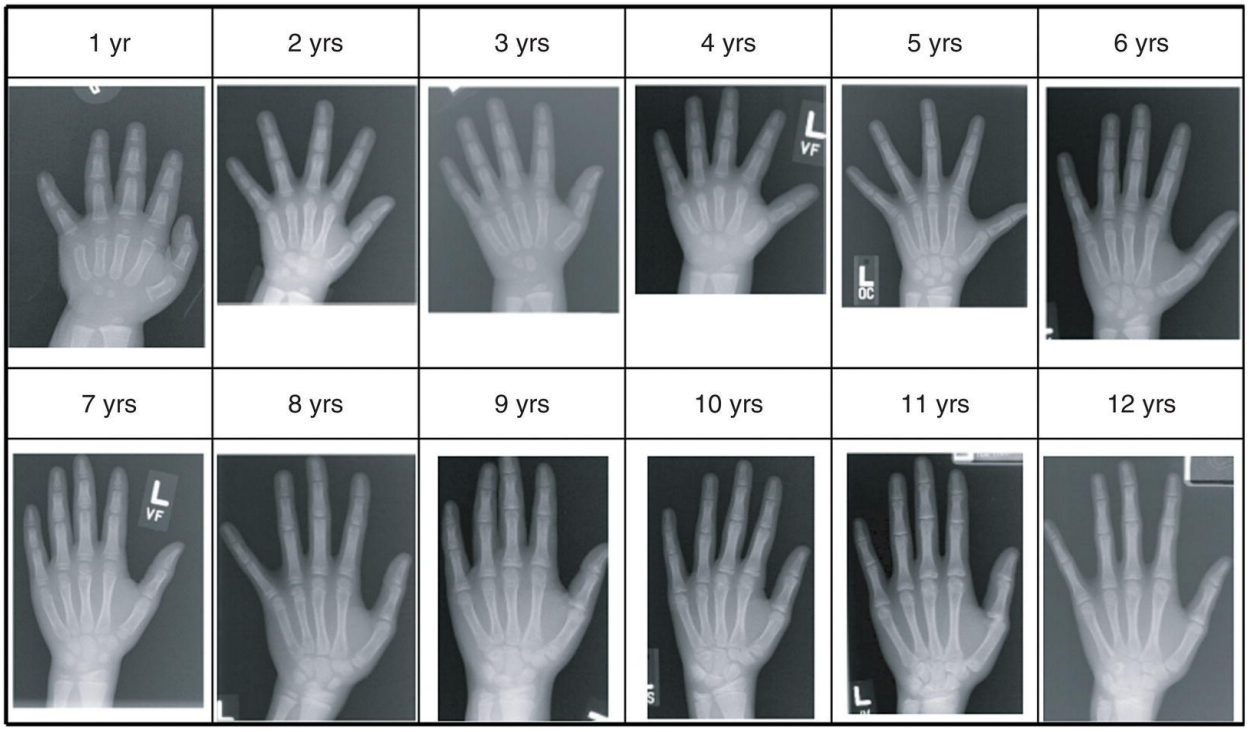

Average images of a group of African-American girls from one to 12 years old

Figure 18.1 An example of the data-mining process used to locate an average hand image of African-American females from 1 to 12 years of age. (A) The objective is to find the average image (right) from a group of images (left). (B) Example of the average image overlaid on a group of hand images of 11-year-old African-American girls from the database. (C) The average hand images of a group of African-American girls from 1 to 12 years old from a child hand database. One average image is provided per year group; see the example in (B) for the 11-year-old group.

18.2 Bone Age Assessment of Children

18.2.1 Classical Method of Bone Age Assessment of Children from a Hand Radiograph

BAA is a clinical procedure in pediatric radiology to evaluate the stage of skeletal maturity based on a left hand and wrist radiograph through bone growth observations. The determination of skeletal maturity (“bone age”) plays an important role in diagnostic and therapeutic investigations of endocrinological abnormality and growth disorders of children. In clinical practice, the most commonly-used BAA method is atlas matching by a left hand and wrist

radiograph against the *G&P Atlas*, which contains a reference set of standard hand images collected in 1950s with subjects exclusively from middle- and upper-class Caucasian populations. Figure 18.2 depicts the BAA method using the *G&P Atlas*. The atlas has been used for BAA around the world for more than 50 years.

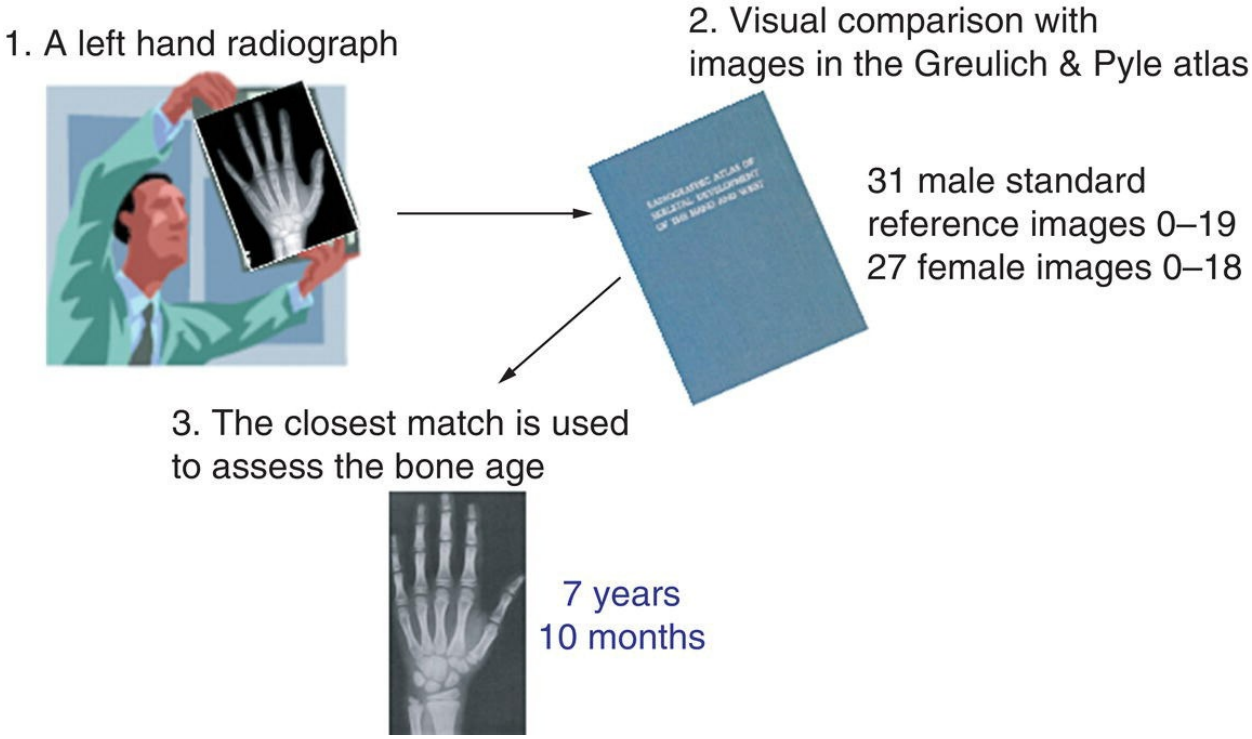

Figure 18.2 Procedure of current clinical practice in BAA for children that is based on comparing the child's hand radiograph with the Greulich & P*yle* Atlas (blue) with data over 70 years old.

18.2.2 Rationale for the Development of a CAD Method for Bone Age Assessment

Over the past 30 years, many studies have raised questions as to the appropriateness of using the *G&P Atlas* for BAA of contemporary children. In 1975, Roche showed that the average child in the United States was less mature than the 1959 standards of Greulich and Pyle [3]. In 1996, Ontell examined the applicability of the standards to the diverse ethnic origin of children. However, these studies along with others did not provide a large-scale and systematic method for validation. Thus, to meet the objective to replace the out-of-date *G&P Atlas*, the following steps were considered:

1. to collect up-to-date data on normal and healthy children to create a *Digital*

Hand Atlas (DHA);

2. to use the DHA to evaluate, on the basis of the *G&P Atlas* method, racial differences in skeletal growth patterns of Asian, African-American, Caucasian, and Hispanic children in the United States; and
3. to develop a CAD method to assess bone age of children based on the data collected.

18.2.3 Data Collection

The protocol of the retrospective data collection was approved by the Institutional Review Board and had been renewed annually; written informed consent was obtained from all participants or their legal guardians. This study was compliant with the Health Insurance Portability and Accountability Act (HIPPA). Patient anonymity was achieved by replacing the patient name and other traceable information with a data encryption method.

18.2.3.1 Subject Recruitment

Over 10 years (May 1997–March 2008), with support from the National Institutes of Health (R01 LM 06270 and R01 EB 00298), the DHA developed a database containing 1390 hand and wrist radiographs of healthy and normal Asian, African American, Caucasian, and Hispanic boys and girls was developed. All participants (age range, 1–18 years) were recruited from public schools in Los Angeles County, California.

18.2.3.2 Case Selection Criteria

Before the hand was examined with radiography, a physical examination was performed to determine the health and the Tanner maturity index of the subject, to ensure that he or she was healthy and that his or her skeletal development was normal. Height, trunk height, and weight were measured and used to calculate the body mass index (BMI).

18.2.3.3 Image Acquisition

Each radiograph of the hand and wrist was obtained using a strict data collection protocol. The radiographs were made using an x-ray generator (Polyphos 50; Siemens, Erlangen, Germany) at 55 kVp and 1.2 mAs (Figure 18.3A). The radiation dose delivered per image was less than 1 mrem, which is equivalent to approximately one day of natural background radiation. The hand was adjusted

to an exact position that required the subject to keep the fingers apart and maintain hand straightness as much as possible (Figure 18.3B); no hand jewelry was worn. The distance between the x-ray tube and the image cassette was 40 inches. The hand of a normal child was less than 1 inch thick; therefore the magnification factor of the image was approximately 1.

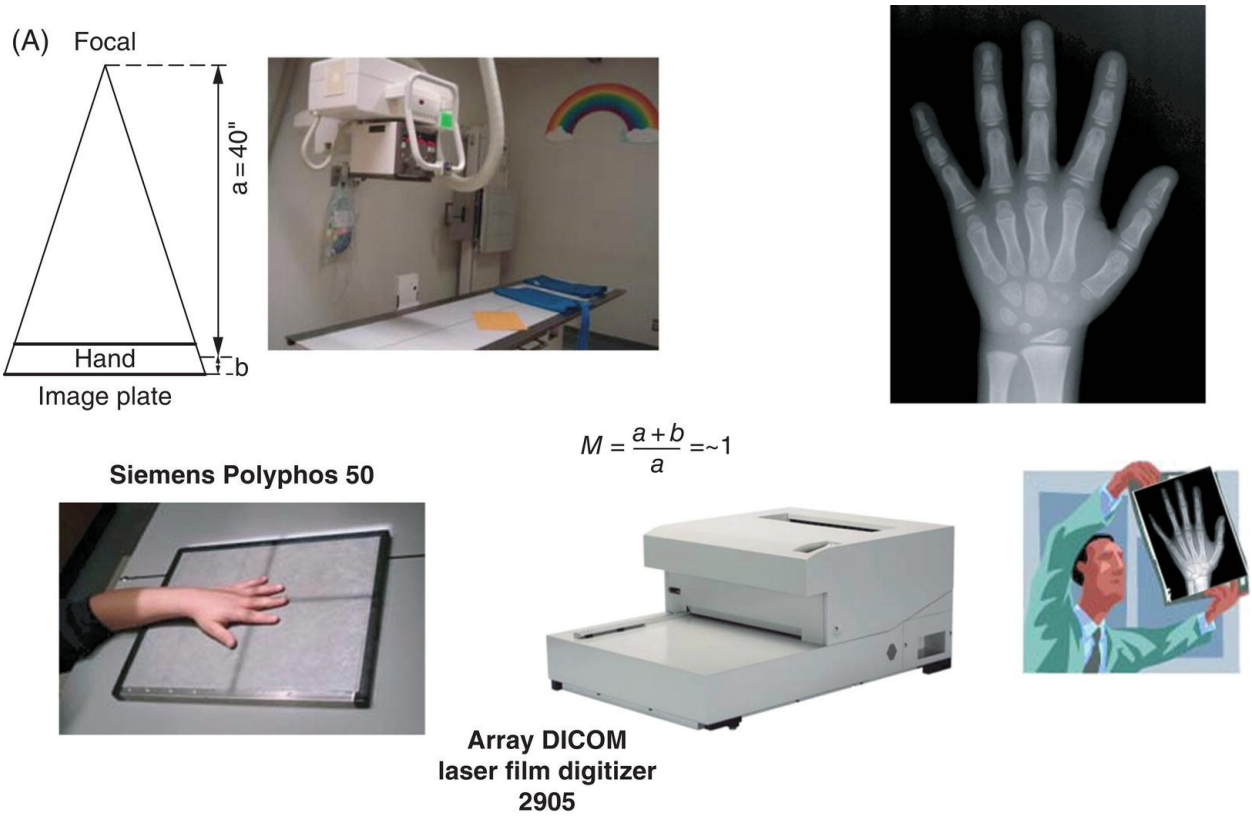

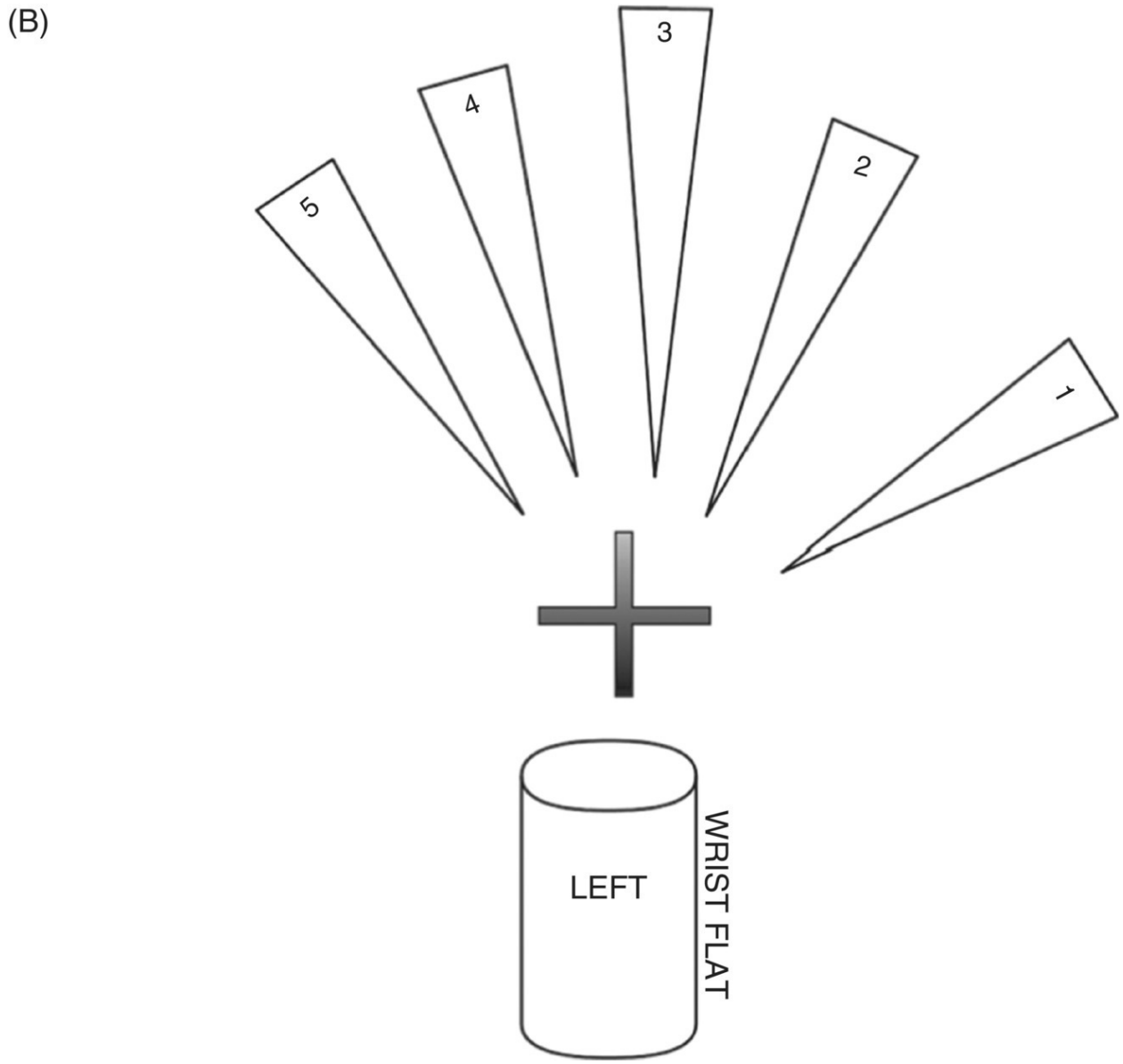

Figure 18.3 (A) Procedure for obtaining a hand radiograph and converting it to a digital image. (B) The protocol used to obtain the hand radiograph; the figure shows where the five fingers and the wrist joint should be placed. 1 represents the thumb.

(courtesy of Dr P. Moin)

18.2.3.4 Image Interpretation

After a radiograph of the hand was acquired from the child, two experienced pediatric radiologists (each with more than 25 years experience in BAA) performed independent readings based on the *G&P Atlas* standards. During the reading, radiologists were blind to the subject's chronologic age, racial group,

and other identifying information.

The child’s bone age, as determined by the radiologist, was compared with their chronologic age. The image was selected and accepted by the DHA only if the difference between the bone age, as determined by the radiologist, and the chronologic age was less than 3 years. The acceptance rate was higher than 90%.

18.2.3.5 Film Digitization

For data analysis, Web-based image and data distribution, and communication in the clinical environment and public domain, each accepted radiograph (the child's name and identification were covered with black tape) was digitized into DICOM format by using a laser film digitizer (Model 2905, Array Corporation, Tokyo, Japan); each participant’s information (excluding the name, as well as any other traceable identification data) was put in the DICOM header. The scanner parameters used were 12 bits per pixel, optical density 0.0 to 4.0, and 100 micron pixel spacing. The size of the image corresponded to the size of the original radiograph (Figure 18.3A). An example shown in Figure 18.4 displays four hand radiographs of 14-year-old boys from different races.

(A)

Asian

(B)

African-American

(C)

Caucasian

(D)

Hispanic

Figure 18.4 Examples of four 14-year-old boys from four different races; their corresponding demographic data and two radiologists' readings are included in the DICOM image header. (A) 14.13-year-old Asian boy; (B) 14.46-year-old African-American boy; (C) 14.79-year-old Caucasian boy; and (D) 14.64-year-old Hispanic boy.

(E)

Welcome to Digital Hand Atlas Database System!

Please select a race, a gender and an age group to query the subjects information and images:
note: ASI: Asian; BLK: African American; CAU: Caucasian; HIS: Hispanic.

Race ASI Gender Female Age Group 10 Submit

Image Name	Race	Gender	ChrAge	DOB	Exam Date	Tanner	Height(cm)	Weight(kg)	Trunk HT(cm)	Reading1	Reading2
5003	ASI	F	10.86	1989	2000	1.00	132.20	26.20	73.03	11.00	12.00
5007	ASI	F	10.61	1989	2000	2.00	143.50	50.70	73.66	11.00	11.50
5113	ASI	F	10.08	1990	2000	2.00	136.90	28.40	74.93	8.83	8.83
5151	ASI	F	10.10	1990	2000	1.00	125.70	21.40	66.04	7.25	7.25
5159	ASI	F	10.60	1989	2000	2.00	148.40	39.10	80.01	12.00	12.00
5163	ASI	F	10.84	1989	2000	2.00	146.10	40.30	74.93	11.00	12.00
5181	ASI	F	10.39	1990	2000	1.00	133.10	26.50	73.66	10.50	12.00
5233	ASI	F	10.49	1991	2001	1.00	138.00	38.00	73.66	11.50	11.00
5247	ASI	F	10.45	1991	2001	1.00	150.80	48.70	78.74	12.00	12.00
5260	ASI	F	10.22	1991	2001	1.00	133.50	29.10	71.76	8.83	8.83
7085	ASI	F	10.05	1995	2005	1.00	137.60	31.00	31.00	11.00	11.00
7095	ASI	F	10.03	1995	2005	1.00	135.00	26.40	26.40	8.83	8.83
7110	ASI	F	10.22	1995	2005	1.00	134.60	27.30	27.30	10.00	10.00
7222	ASI	F	10.24	1995	2005	2.00	148.40	41.40	41.40	12.00	12.00
7246	ASI	F	10.61	1994	2005	1.00	144.00	35.40	35.40	12.00	12.00

Figure 18.4 (E) A sample collection of hand images in digital atlas, available online.

18.2.3.6 Data Collection Summary

There were two cycles in data collection, each with eight categories (Asian girls, Asian boys, African-American girls, African-American boys, Caucasian girls, Caucasian boys, Hispanic girls, and Hispanic boys). Each category contains 19 age groups (one for subjects younger than 1 year and 18 sets at 1-year intervals for subjects aged 1–18 years). Two pediatric radiologists independently read all images obtained in each cycle. Cycle 1 consisted of 1103 digitized hand images with demographic data. Five cases for each younger age group (1–9 years) and

10 cases for each older age group (10–18 years) were included. The sample sizes were chosen to achieve a precision of approximately 0.20 for all age groups with 95% confidence interval when using the digital atlas to compare bone age with chronologic age. Precision was defined as the confidence interval width divided by the estimated mean value of the chronologic age. Subjects younger than 1 year were considered infants, and their data were not used for the analysis.

In order to study the active growth period in children aged 5–14 years more closely, data were collected in a further 287 children during the second cycle after the first cycle had been completed. Thus, a total of 1390 cases were included in the DHA. The breakdown of cases was as follows: 167 Asian girls, 167 Asian boys, 174 African-American girls, 184 African-American boys, 166 Caucasian girls, 167 Caucasian boys, 183 Hispanic girls, and 182 Hispanic boys. These 1390 cases, shown in Table 18.1, were used to develop the DHA described in this chapter.

Table 18.1 Images and data contained in the Digital Hand Atlas.

Cycle 1									Cycle 2								
	AS		AA		CA		HI			AS		AA		CA		HI	
Age Group/ Category	F	M	F	M	F	M	F	M	Age Group/ Category	F	M	F	M	F	M	F	M
00	1	2	4	5	3	3	1	4		3	4	4	4	2	5	5	4
01	5	5	5	5	5	5	5	5									
02	5	5	5	5	5	5	5	5									
03	5	5	5	5	5	5	5	5									
04	5	5	5	5	5	5	5	5									
05	5	5	5	5	5	5	5	5	05								
06	5	5	5	5	5	5	5	5	06	2	1	4	2	2	3	5	4
07	5	5	5	5	5	5	5	5	07	2	2	4	4	3	4	5	5
08	5	5	5	5	5	5	5	5	08	4	0	5	5	4	5	4	5
09	5	5	5	5	5	5	5	5	09	2	2	4	5	3	2	5	5
10	10	10	10	10	10	10	10	10	10	5	4	2	5	2	1	4	2
11	10	10	10	10	10	10	10	10	11	2	5	0	5	3	4	5	4
12	10	10	10	10	10	10	10	10	12	4	5	5	5	4	3	5	5
13	10	10	10	10	10	10	10	10	13	5	5	5	5	4	2	5	5
14	10	10	10	10	10	10	10	10	14	3	2	2	4	1	0	4	4
15	10	10	10	10	10	10	10	10									
16	10	10	10	10	10	10	10	10									
17	10	10	10	10	10	10	10	10									
18	10	10	10	10	10	10	10	10									
Subtotal	136	137	139	140	138	138	136	139	Subtotal	31	30	35	44	28	29	47	43

Note: Cycle 1: totaled 1103 cases with two readings per case; cycle 2: totaled 287 cases with 4 readings per case.

18.2.4 The Digital Hand Atlas

18.2.4.1 Research Supports

Over the past 10 years (May 1997–March 2008), the National Institutes of Health (R01 LM 06270 and R01 EB 00298) had supported the development of the DHA, as shown in Table 18.1. Figure 18.4 shows a sample of four hand images (ASI, Female, Age group: 10) in the DHA, which is available on line from the Website.

18.2.4.2 Digital Hand Atlas

In order to develop an objective BAA CAD system, data collection of normal children's left hand images is needed to replace the *G&P Atlas* as the standard and first option for BAA. The result is a DHA. The DHA is a collection of 1400 normal children's left-hand radiographs, and subjects include both male and female children of different ethnic backgrounds: African American, Asian American, Caucasian, and Hispanic. The subjects are aged from zero to 18 and are all from the Greater Los Angeles area. The result is an ethnically diverse and rich hand atlas that is more suitable for today's children in an urban setting. The data collection process began in the late 1990s and continued through to the middle of 2000s. The subjects were considered as having normal skeletal development based on trunk height, body height and weight, and tanner index, the latter of which was used by clinical endocrinologists.

The images are taken at the Children's Hospital of Los Angeles, and film images are digitized (50 × 50 microns) using a film scanner (Array, Tokyo, Japan). In DICOM header fields, patient's demographic information was manually entered, along with patient's physical measurements. The data was obtained in two cycles: the first cycle contained a set number of hand images per group, gender, and ethnicity, while the second cycle was completed to complement the first cycle results by increasing the number of cases for children between the ages of 5 and 14, due to the rapid development of bone features during this developmental stage.

The database of DHA is viewable online at http://ipilabmysql.usc.edu/newindex.php. The DICOM images are converted to JPEG format for online viewing. Figure 18.5 is a screenshot of the DHA database showing all cases of 10-year-old Asian girls.

Performance of DHA has been evaluated. Two radiologists read all of the images included using the *G&P Atlas* for Asian, African-American, and Hispanic children of both sexes, and the results have been stored in the database to show cross-racial reading discrepancies between the *G&P Atlas* and normal skeletal development.

18.2.5 CAD Module: Image Processing Algorithm

The BAA CAD system uses data collected from DHA to establish an objective and reliable algorithm that assesses bone age of children. The goal of CAD is to aid radiologists in performing BAA by offering a second opinion that is consistent for all cases. The system examines three regions of interest: carpal bones, phalanges, and wrist joint. Each region of interest displays different levels

of importance in evaluating bone age for different age groups. Table 18.2 displays the three regions of interest and the area of where they are most effective.

Table 18.2 Clinical reliability of using the three ROIs for BAA in different age groups.

Age Group	Phalangeal ROIs	Carpal ROI	Distal Radius ROI
0 – 5 (female)	Feature analysis of epi-metaphysis - **NOT reliable**	Size and shape analysis of carpal bones - **Reliable**	
0 – 7 (male)			
6 – 13 (female)	Feature analysis of epi-metaphysis - **Reliable**	Degree of overlapping of carpal bones - **NOT reliable**	
8 – 15 (male)			
14 – 18 (female)	Feature analysis of epi-metaphysis - **NOT sufficient**		Feature analysis of epi-diaphysis - **Reliable**
16 – 18 (male)			

The phalangeal ROI is one of the first criteria in assessing bone age. The shape, size, and development of the epiphysis in relation to metaphysis in the middle three fingers are used to evaluate bone development. During infancy, the epiphysis has not been formed and thus cannot be used in BAA. As bone ages, the epiphysis starts to increase in size, and finally fuses with the metaphysis when the subject enters adolescence. Therefore, the phalangeal ROI analysis is best suited for children in the middle age groups.

The carpal ROI is more reliable for younger children of less than 5 years old for females and less than 7 years old for males. Carpal bones grow as the infant grows, and the bones begin to overlap with each other starting at the age of 5 years. The difficulty in distinguishing different carpal bones in the ROI makes the method only suitable for BAA of younger children.

After the epiphysis and metaphysis have fused in the phalangeal ROI, epiphysis and metaphysis do not fully fuse in the wrist joint region until the child's development is fully mature. In other words, analysis on the degree of fusion

between epiphysis and metaphysis on radius is best used for BAA of older children.

18.2.6 Fuzzy Logic in Computing Bone Age

The CAD BAA system needs to weight results from the three ROI analyses intelligently to assess bone age accurately. The relationship between extracted features and assessed bone age is also nonlinear. The three components for analysis are arranged in a modular fuzzy logic system that integrates results and computes bone age for patients of different age, gender, and ethnicity. The fuzzy logic concept is derived from inherently imprecise measurements that exist in the natural, biological world [9]. A fuzzy logic system uses a set of rule-based classifications (various if … then … statements) and mathematical equations to derive outputs evaluating imprecise outcomes. Fuzzy logic is commonly used in engineering as a means for computing systems to output qualitative assessment, rather than quantitative data [10,11]. The principal investigator inserts references in the proper place.

For CAD BAA, a rule-based fuzzy logic system has been developed to compute outputs from feature analyses. The results need to be aggregated and a final bone age is computed from the integrated fuzzy logic system. An individual CAD algorithm was first developed for each ROI, with an integrated fuzzy logic for three regions of interest, phalanges ROI, carpal ROI, and wrist joint ROI. A fuzzy logic system integration of these three ROI analyses would be needed and is described in the next section.

18.3 Method of Analysis

18.3.1 Statistical Analysis

Statistical analyses were performed using SPSS, version 15.0 for Windows (SPSS Inc., Chicago, Illinois). Graphs were generated by third-party software groups (KaleidaGraph, Synergy Software, Reading, Pennsylvania). Two types of analyses, paired-samples t-test and analysis of variance (ANOVA), were conducted using the chronologic age as the reference standard. The age 0 group was not used for analysis. Two-cycle data were combined for each race and a given gender, with the entire ages ranging from 1 to 18; then paired samples t-tests were performed case by case to find the mean difference between the average of two readings and the chronologic age. The results were eight categories for comparison: Asian girls, Asian boys, African-American girls,

African-American boys, Caucasian girls, Caucasian boys, Hispanic girls, and Hispanic boys, each depicting the overall view of differences between the radiologists' average bone age reading against the chronologic age for subjects of each race and sex.

On the basis of the effects of growth factor and sex hormones, as well as our observations from phalangeal, carpal, and wrist joint regions, we divided the entire growth age ranging from age 1 year to 18 years into four age subsets, shown in Figure 18.5 (right column). These subsets were used to study the differences in growth patterns of children of different races for a given subset. ANOVA was used to study the cross-racial comparisons for a given subset of growth range based on the differences between chronologic age and bone age.

18.3.2 Radiologists' Interpretation

Table 18.3 shows the mean difference in age between the average bone age reading by two radiologists and the chronologic age for each of the eight categories by race and sex. Since data was collected in children with normal skeletal development, the differences showed with asterisks in Table 18.3 were within two standard deviations between the normal chronologic age and the average bone age (see Section 18.2.3.2) and may not be important from a clinical perspective, However, it was concluded that the radiologists had a slight tendency, which was statistically significant, to overestimate bone age in the Asian and Hispanic populations as a whole.

Table 18.3 Mean difference between bone age and chronologic age according to race and sex as assessed by radiologists.

	Asian		**African American**		**Caucasian**		**Hispanic**	
	Girls	**Boys**	**Girls**	**Boys**	**Girls**	**Boys**	**Girls**	**Boys**
Characteristics	**(F)**	**(M)**	**(F)**	**(M)**	**(F)**	**(M)**	**(F)**	**(M)**
Mean difference between bone age assessed by radiologists and chronological age	0.24[a]	0.41[a]	0.03	−0.02	−0.15[a]	0.01	0.24[a]	0.30[a]
Number of children[b]	166	165	170	179	163	164	182	178

[a] Indicates that mean difference between bone age assessed by radiologists and chronological ages was significant ($p \leq 0.05$).

[b] Infants (children younger than 1 year) were excluded from the analysis.

18.3.3 Cross-Racial Comparisons

The cross-racial differences assessed with ANOVA among the four races in the four divided age subsets are presented in Figure 18.5. The upper row shows that in girls, significant mean differences of average reading between races were observed in the third age subset (10–13 years, purple). Radiologists overestimated bone age in Asian girls in comparison with their African-American and Caucasian peers by approximately 0.59 year and 0.70 year, respectively. Similarly radiologists overestimated bone age by 0.58 year in Hispanic girls when compared with African-American girls. Figure 18.6 shows the plots of bone age versus chronologic age in Asian girls versus Caucasian girls, Asian girls versus African-American girls, and Hispanic girls versus African-American girls. In each comparison, the figure on the left covers the entire age range (1–18 years), whereas the figure on the right shows a close-up of the third age subset (10–13 years).

Similar patterns were observed in boys (Figure 18.5, chart in the lower row). In the third age subset (11–15 years, purple) significant overestimation of bone age of 0.97 year and 0.83 year was observed in Asian and Hispanic boys, respectively, when compared with African-American boys. Overestimation of 0.65 year continued until fourth age subset (16–18 years, orange), when Asian boys were compared with African-American boys. Furthermore, comparison of Caucasian boys with Asian boys and Hispanic boys in the third age subset (11–15 years) resulted in significant over reading of 0.59 year and 0.46 year, respectively. Figure 18.7 shows bone age versus chronologic age in four racial pairs:

1. Hispanic boys versus African-American boys;
2. Asian boys versus African-American boys;
3. Asian boys versus Caucasian boys; and
4. Hispanic boys versus Caucasian boys.

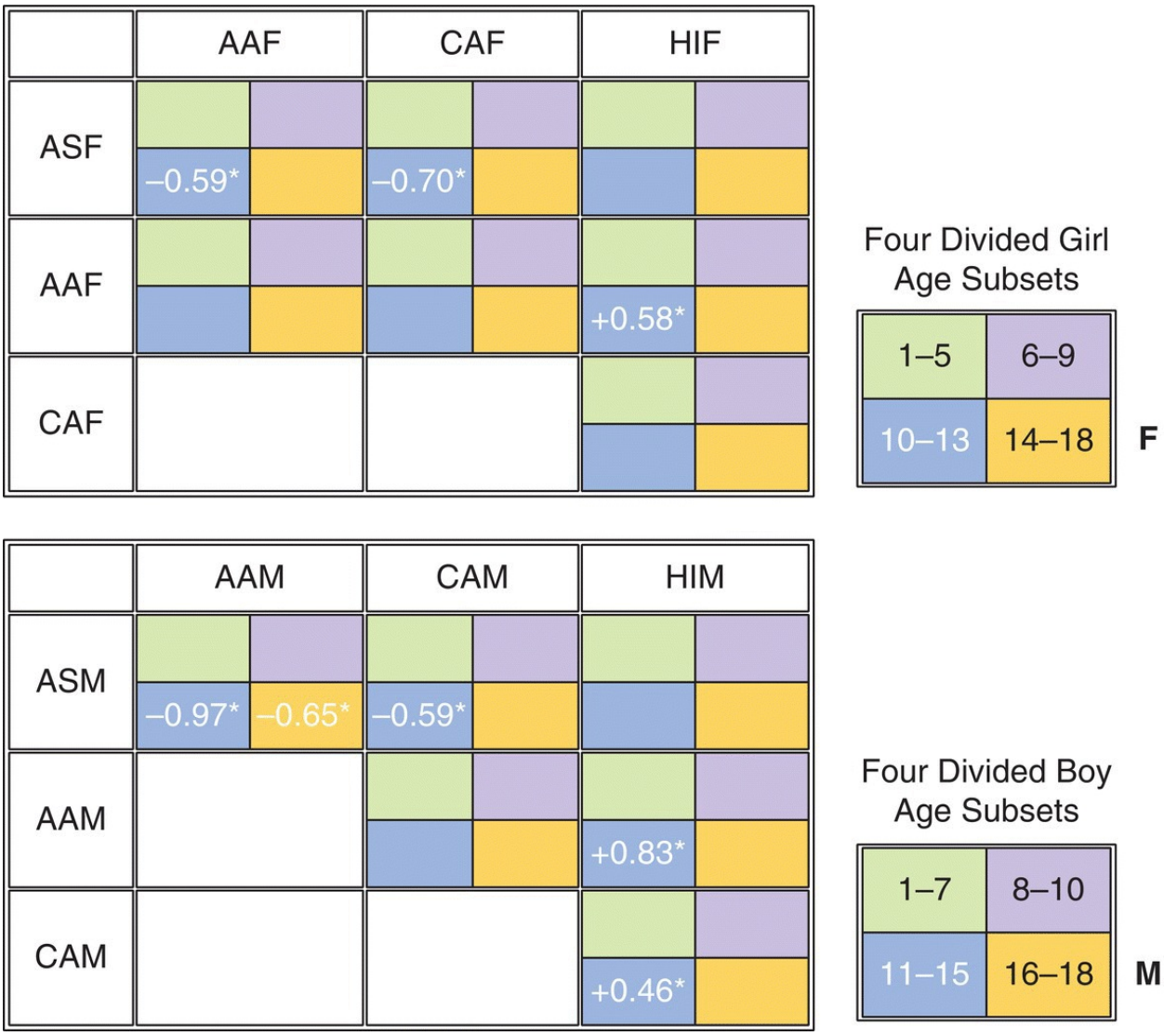

Figure 18.5 Right column: Small charts show the four divided age subsets for (F) girls and (M) boys. These charts provide a road map for use in the study of racial differences during different growth periods. (F) Green indicates 1–5 years of age; blue: 6–9 years; purple: 10–13 years; orange: 14–18 years. (M) Green indicates 1–7 years of age; blue: 8–10 years; purple: 11–15 years; orange: 16–18 years. Left column: Large charts show cross-racial comparison for (F) girls (upper chart), and (M) boys (lower chart). Data are shown only if differences are significant ($P \leq 0.05$). Each racial block was divided into the four age groups described. The plus and minus signs indicated under- and overestimation of bone age, respectively, by radiologists in comparing rows with columns. ASF: Asian girls; ASM: Asian boys; AAF: African-American girls; AAM: African-American boys; CAF: Caucasian girls; CAM: Caucasian boys; HIF: Hispanic girls; HIM: Hispanic boys.

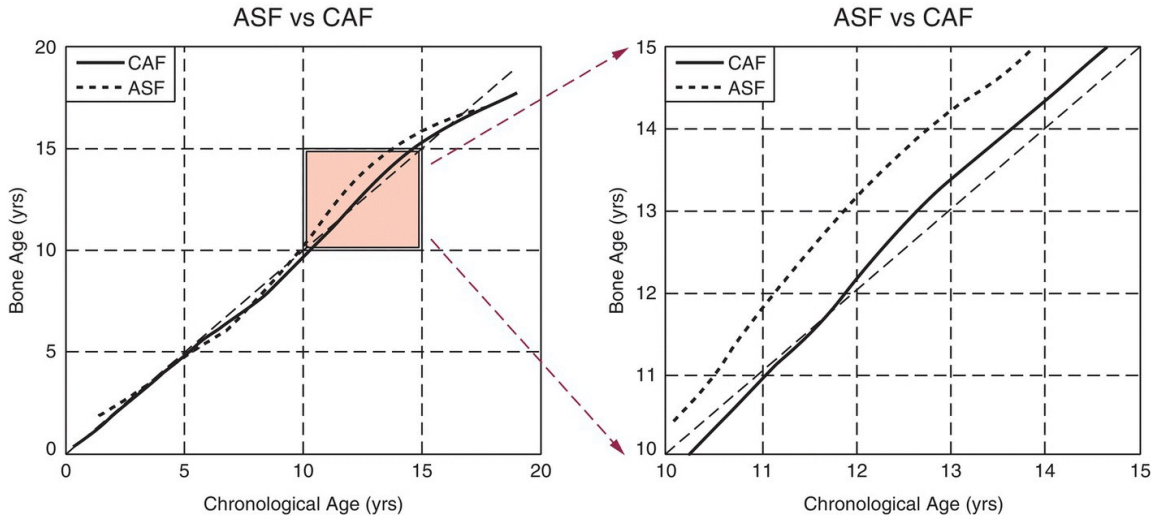

(A1) Female

(A2) Female

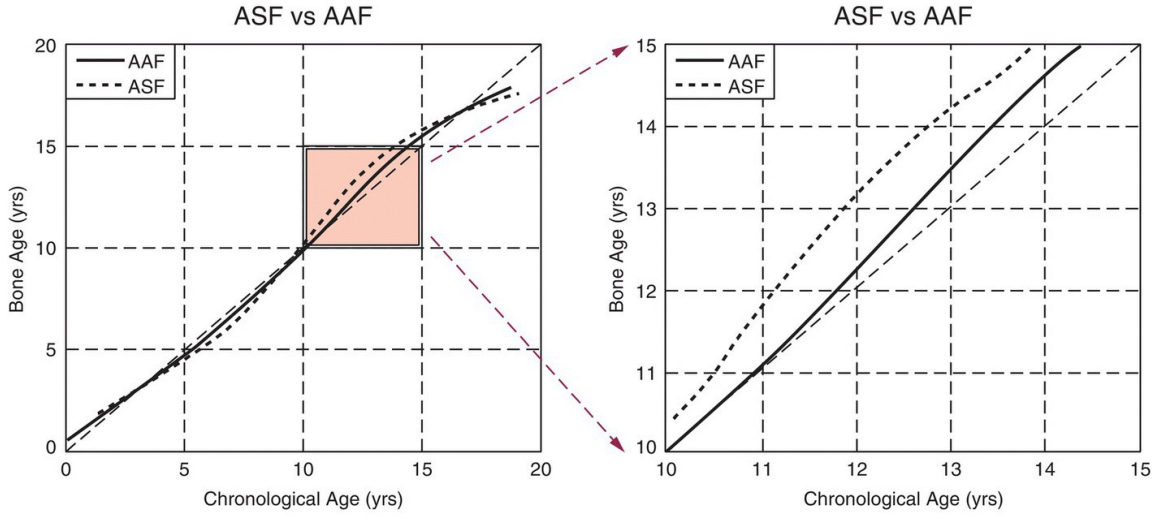

(B1) Female

(B2) Female

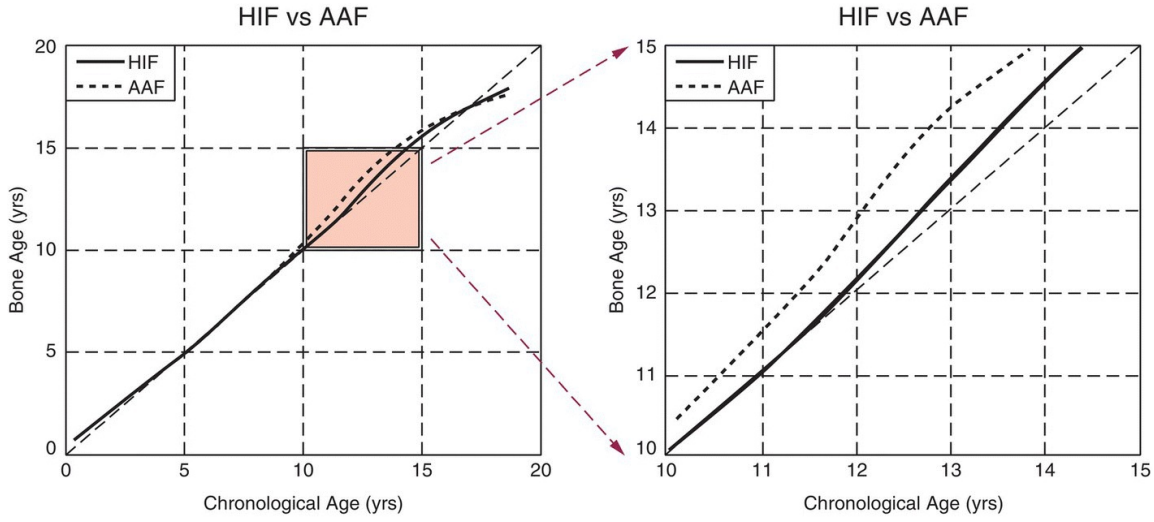

(C1) Female

(C2) Female

Figure 18.6 Comparisons of three racial female pairs. The *x*-axis shows the chronologic age, the *y*-axis shows the average bone age, and the 45° dotted line shows the normal standard comparison in (A1) Asian girls (ASF) versus Caucasian girls (CAF), (B1) Asian girls versus African-American girls (AAF), and (C1) Hispanic girls (HIF) versus African-American girls. The graphs on the left show the plots of the entire age (1–18 years) range, whereas the graphs on the right (A2, B2, C2) are close-up plots for the third age subset (10–13 years).

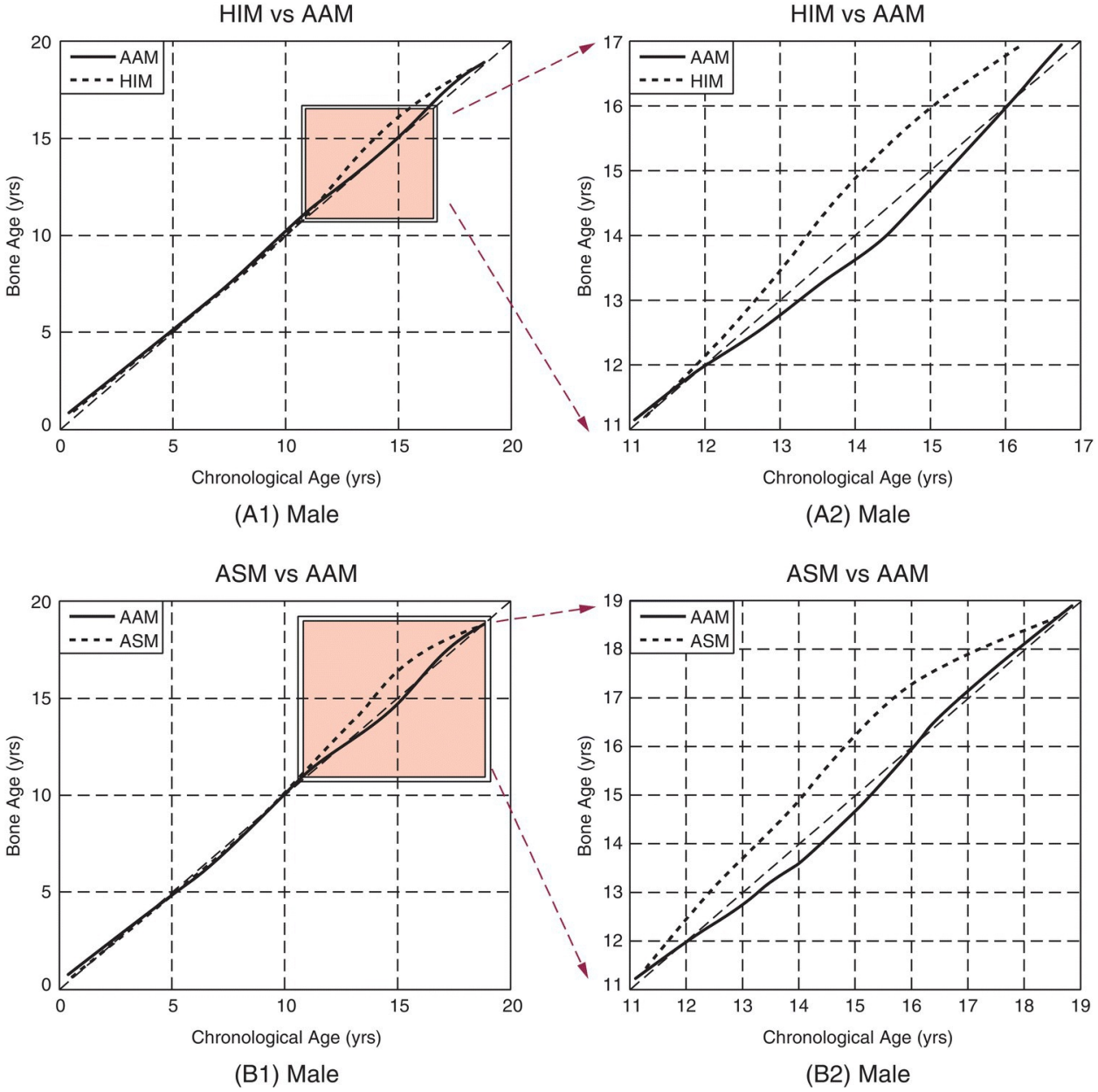

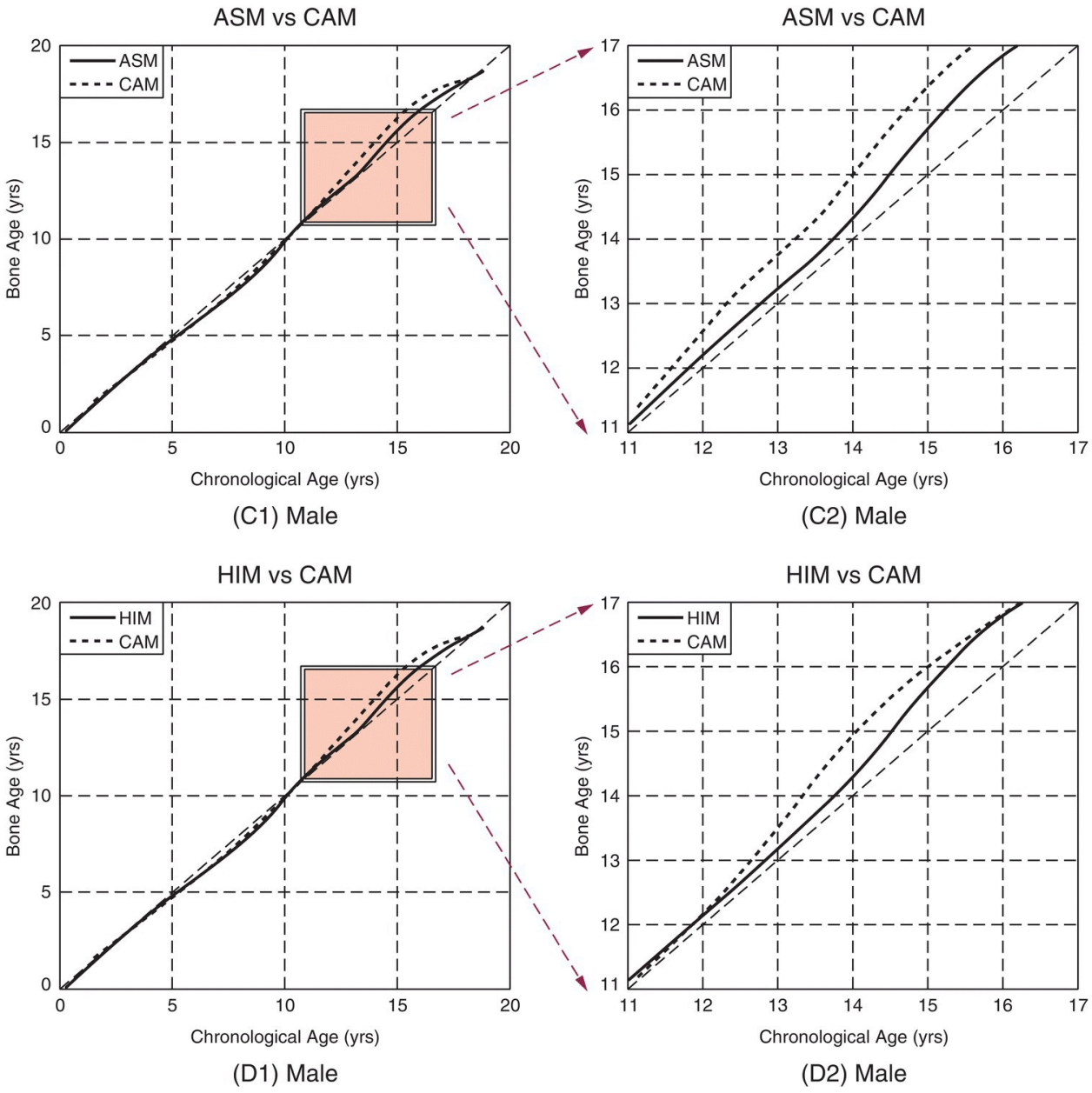

Figure 18.7 Comparisons among four racial male pairs: 1. (A1) Hispanic (HIM) versus African-American boys (AAM); 2. (B1) Asian (ASM) versus African American boys 3. (C1) Asian versus Caucasian boys (CAM); and 4. (D1) Hispanic versus Caucasian boys. Left: entire age range (1–18 years); Right: third age subset (11–15 years) (A2, C2, D2); and third and fourth age subsets (11–18 years) (B2).

18.3.4 Development of the Digital Hand Atlas for Clinical Evaluation

To recap, an up-to-date DHA for four ethnic groups was developed with 1390 hand and wrist radiographs obtained in Asian, African-American, Caucasian, and Hispanic boys and girls with normal skeletal development aged between 1 day and 18 years. Each case was read by two pediatric radiologists working independently on the basis of the Greulich and Pyle (G&P) atlas standard. The normality and consistency of the data were ensured by two radiologists' readings plus a rigorous quality assurance data collection protocol. Hand radiographs were digitized and stored in DICOM format, which facilitates image viewing and transmission in the clinical environment for training and image-assisted daily clinical operation.

Previous studies had been performed in which researchers examined the applicability of the *G&P Atlas* for use with contemporary children. Mora, *et al*. examined 534 children of European and African descent, and Ontell, *et al*. collected data in 765 trauma patients of four races. Both studies are close to this study in that they involved use and evaluation of the *G&P Atlas* in each of the racial groups. However, in neither study did the authors compare cross-ratio differences. In creating the DHA, this study observed differences in readings of two pediatric radiologists in subjects of four races on the basis of the *G&P Atlas* standard, and this study recorded these differences systematically. The study results show the cross-racial differences between skeletal growth patterns of Asian and Hispanic children and skeletal growth patterns of Caucasian and African-American children. Radiologists assessed the bone age that was relatively close to the chronologic age of African-American and Caucasian children.

The DHA provides an up-to-date standard with which to classify normal bone growth and development in children. Currently, the DHA is accessible from the World Wide Web for on'line learning and teaching. This study, even without the CAD to be discussed in the next few sections, can conclude that there are deficiencies in only using the *G&P Atlas* to assess bone age of children.

18.4 Integration of CAD with PACS-Based Multimedia Informatics for Bone Age Assessment of Children: The CAD System

18.4.1 The CAD System Based on Fuzzy Logic for Bone Age Assessment

A fully automatic CAD method for assessing the bone age of children based on the DHA has been modeled for boys and girls of four races. The CAD method is a fuzzy logic system applied to several ROI of the hand and wrist radiograph. A three-compartment model was used for the image analysis results, which included the phalangeal bones, carpal bones, and the distal radius. The three-compartment model was arranged in a modular and extensible fuzzy system integrating phalanges, carpals, and the distal radius for BAA. The DHA formed the knowledge base of the fuzzy system, under the assumption that bone age is equal to chronologic age, since the normality of children was ensured for each case during data collection for the atlas. The fuzzy logic concept is derived from the imprecise phenomena that commonly occur in real-world situations, such as in biological growth and incorporates a simple rule-based approach, thus making it suitable for the application of BAA. To address the imprecise nature of the relationship between bone growth and bone age, a rule-based fuzzy inference system was developed to provide alternative options for a set of unresolved issues in the current *G&P Atlas* matching method. The system was trained using the DHA to adapt to an individual's ethnicity and gender. To avoid subjectivity, two measurements were taken in sequence. First, a degree of membership was used to express the intermediate bone age from individual regions with quantitative measures. The final bone age was then aggregated from multiple regions and "defuzzified". The results obtained from the fuzzy system were validated using normal subjects in the DHA and evaluated with subjects in clinical environments. For details of the fuzzy logic concept, refer to references at the end of this chapter.

18.4.2 Fuzzy System Architecture [12–14]

18.4.2.1 Knowledge Base Derived from the Digital Hand Atlas (DHA)

The CAD system is based on three regions of interest: the phalanges, carpals, and distal radius. Table 18.2 summarizes the clinical reliability of using these three ROI for BAA. Based on this clinical knowledge, the CAD method's parameters were extracted from these regions. Phalangeal analysis is most reliable from late childhood to early adolescence, both in epi-metaphysis segmentation and the ability of extracted features to predict the bone age. During this range of ages, as carpal bones ossify, they overlap beginning at age 5 in females and at age 7 in males. Thus the use of carpal bones in the determination of bone age is most sensitive during infancy and early childhood. Prior to complete ossification and overlap in the anteroposterior projection, carpal bone

analysis has proved to be very reliable in both carpal bone segmentation and the use of the morphology of the segmented bones to predict the bone age for young children. For adolescents, the phalangeal and carpal regions lose a significant degree of sensitivity in the characterization of skeletal growth, while the wrist region, specifically the distal radius, provides more reliable growth information. These image analyses are further discussed in the literature at the end of this chapter.

Figure 18.8 shows the CAD algorithm workflow. After image preprocessing, three ROI—carpal bones (see left, large white rectangle), wrist joint (large white rectangle), and the phalangeal region, which has six sub-regions (six white rectangles)—are automatically located and extracted, as shown in the Figure 18.8. Anatomical features are then extracted from the segmented osseous structures from each of the ROI and input into the respective fuzzy subsystems. The results from the three regions are then aggregated to determine the final bone age. The following subsections describe fuzzy system development (see the four color boxes in Figure 18.8). For each subsystem, the generation methodology for membership functions and fuzzy rules refer to the references at the end of this chapter.

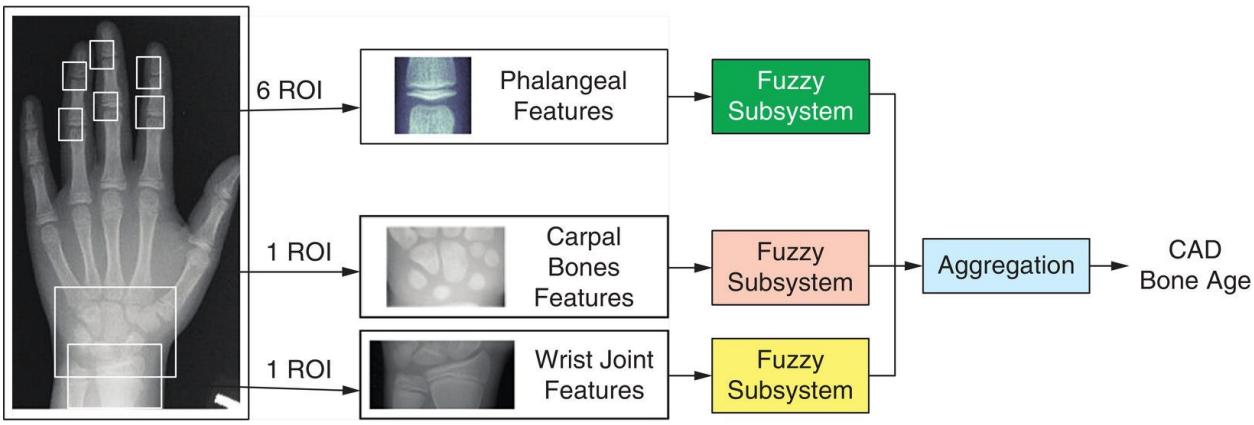

Figure 18.8 BAA fuzzy logic CAD algorithm workflow consists of eight regions of interest (ROI): six phalangeal, one carpal bone, and one wrist joint. All regions are automatically detected by the CAD. There are three fuzzy logic systems; the aggregation of the three systems gives the CAD bone age of the child.

18.4.2.2 Phalangeal Fuzzy Subsystem

The middle and distal epimetaphyseal regions of the second through fourth digits were localized and extracted from each hand radiograph. A total of six

phalangeal subregions of interest were thus isolated and acquired in the phalangeal ROI. Through image segmentation and feature extraction, eight quantitative size and shape features for those 0–12 years of age and 10 wavelet features for children of 10–18 were obtained from each phalangeal sub-ROI. As summarized at the top of Figure 18.9, size and shape features segmented and extracted, among these, the following features were found to contribute most to the bone growth: metaphsyeal diameter, epiphyseal diameter, epiphyseal–metaphyseal distance, horizontal epiphyseal diameter, and the distance between the more distal phalangeal metaphysis and the more proximal phalangeal epiphysis; these are the features also used for BAA. These features are then input into the fuzzy subsystem, which consists of six components in the fuzzy logic for phalangeal epimetaphyseal subregions (Figure 18.9, bottom). Each component includes two modules, one for shape and size features and another for wavelet features. The fuzzy bone age is assessed in two stages. First, each of the six components yields an intermediate output. Then, the six outputs are aggregated by finding their mean to obtain the fuzzy BA1, as shown in the base of Figure 18.9.

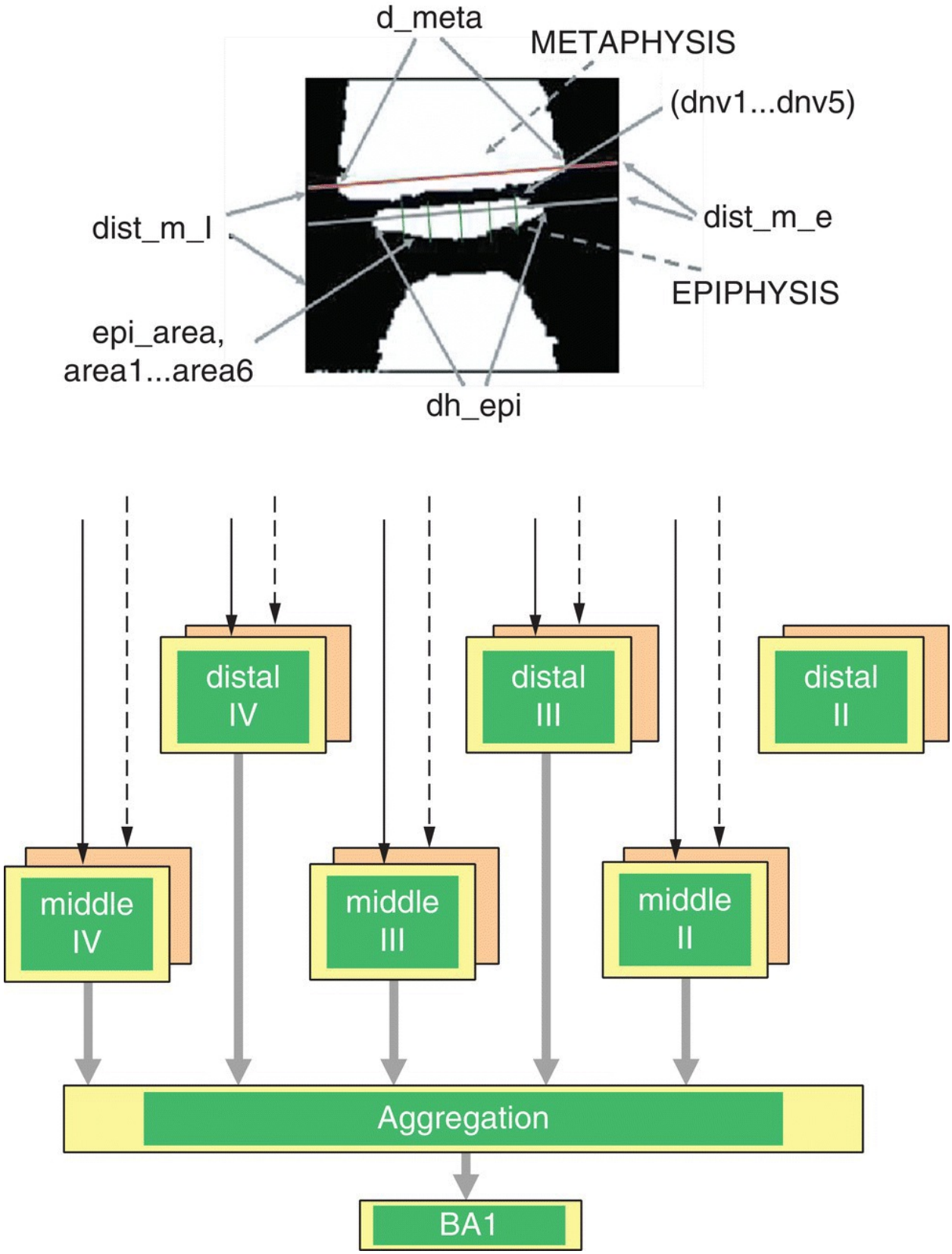

Figure 18.9 Top: Features extracted from a phalangeal sub-ROI segmentation

from which features are extracted. Bottom: Phalangeal fuzzy subsystems, consisting of six components, each with a module for shape and size features (solid lines), and wavelet features (dash lines). The aggregation of all features from six sub-regions yields the bone age, BA1, of the phalangeal.

18.4.2.3 Carpal Bone Fuzzy Subsystem

The carpal fuzzy subsystem consists of two components, the capitate and the hamate. After the carpal bones are segmented, the carpal ROI is extracted from the hand image, as shown in Figure 18.10. The capitate and the hamate, the first two bones to ossify in the carpal region during development, are identified using a knowledge-based model and used to assess the carpal bone age. One size (×1) and two shape features, eccentricity (×2), and triangularity (×3) features, are then extracted from both the capitate and the hamate. Hence a total of six features are input into the carpal bones fuzzy subsystem for BAA. The fuzzy bone age determined by the carpal bone region is assessed in two stages. First, each of the two carpal bones yields an intermediate output. Then, the two intermediate outputs are aggregated by finding their mean to obtain the fuzzy BA2.

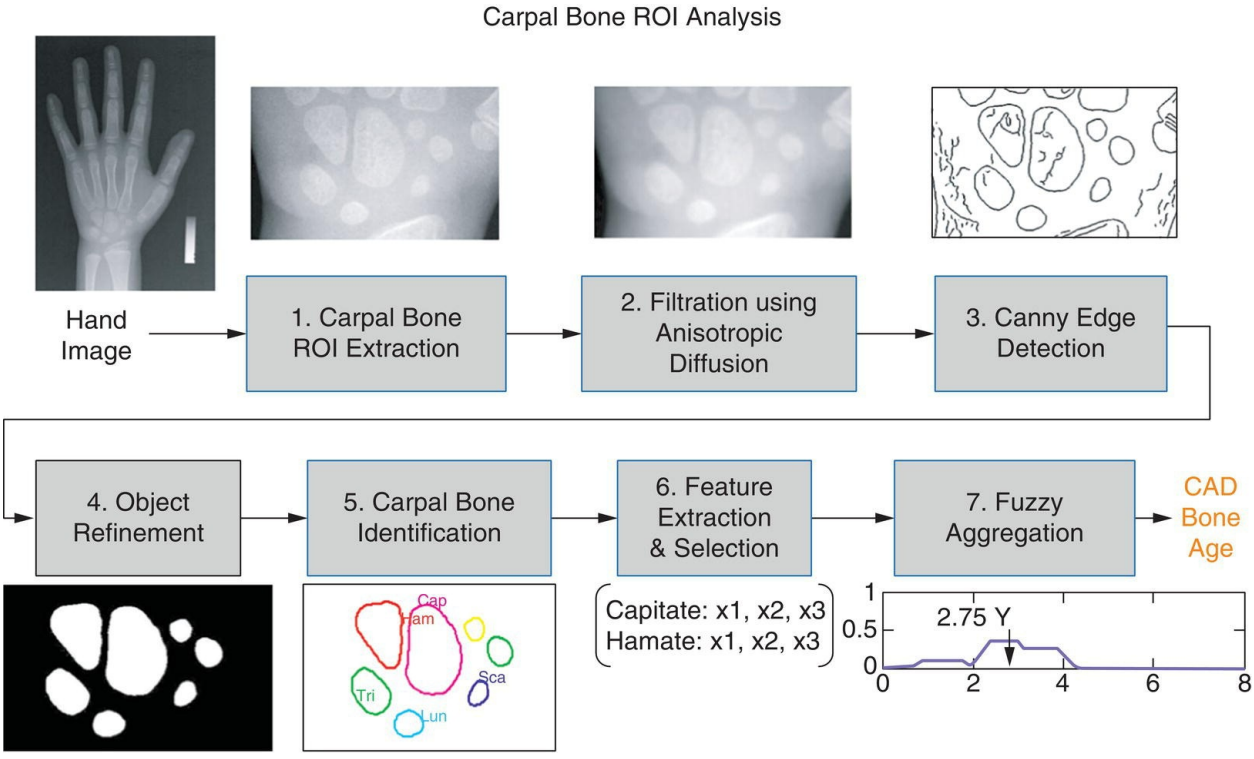

Figure 18.10 Example of using the carpal bones region alone to determine the bone age. Steps 1–7 describe the total procedure. The capitate (Cap) and hamate (Ham) bones provide sufficient information to assess the bone age, each with

three features: one size (×1), and two shapes, eccentricity (×2) and triangularity (×3). In this example, the bone age, BA2 is 2.75 years. ROI: region of interest; Y: years.

18.4.2.4 Wrist Joint Fuzzy Subsystem

The goal of wrist joint analysis is to yield higher accuracy for older children (girls: 14–18; boys: 16–18), based on the growth plate development and its separation from the radius. To perform wrist region assessment, the radius is first segmented based on the anatomical location, shape, and structure of the radius. The growth plate region is located and extracted. Wavelet features are obtained and then passed through the wrist joint fuzzy logic system to obtain the fuzzy BA3, as shown in Figure 18.11. It should be noted that the wrist region does not need an aggregate result, because it is a single ROI, unlike the six regions of the phalangeal subsystem and the two regions in the carpal subsystem. To obtain good features from the wrist joint, positioning of the hand while taking the radiograph has to adhere to the protocol shown in Figure 18.3B.

Figure 18.11 Result of wrist region analysis and growth plate segmentation, and the workflow of converting wavelet features into bone age BA3. ROI: region of interest.

18.4.3 Fuzzy Integration of Three Regions: Phalangeal, Carpal, and Wrist

The last step in BAA is to determine three fuzzy bone ages from the phalangeal subsystem (BA1), carpal subsystem (BA2), and distal radius subsystem (BA3). These three fuzzy output membership functions were aggregated into the final fuzzy bone age, as shown in Figure 18.12.

The final bone age is obtained through defuzzification, the conversion of fuzzy output from the integration procedure to determine a precise bone age. The center of gravity method is used. The completed BAA program with a three-region analysis and the corresponding fuzzy logic classifiers is applied to the DHA to determine a computer-aided BAA.

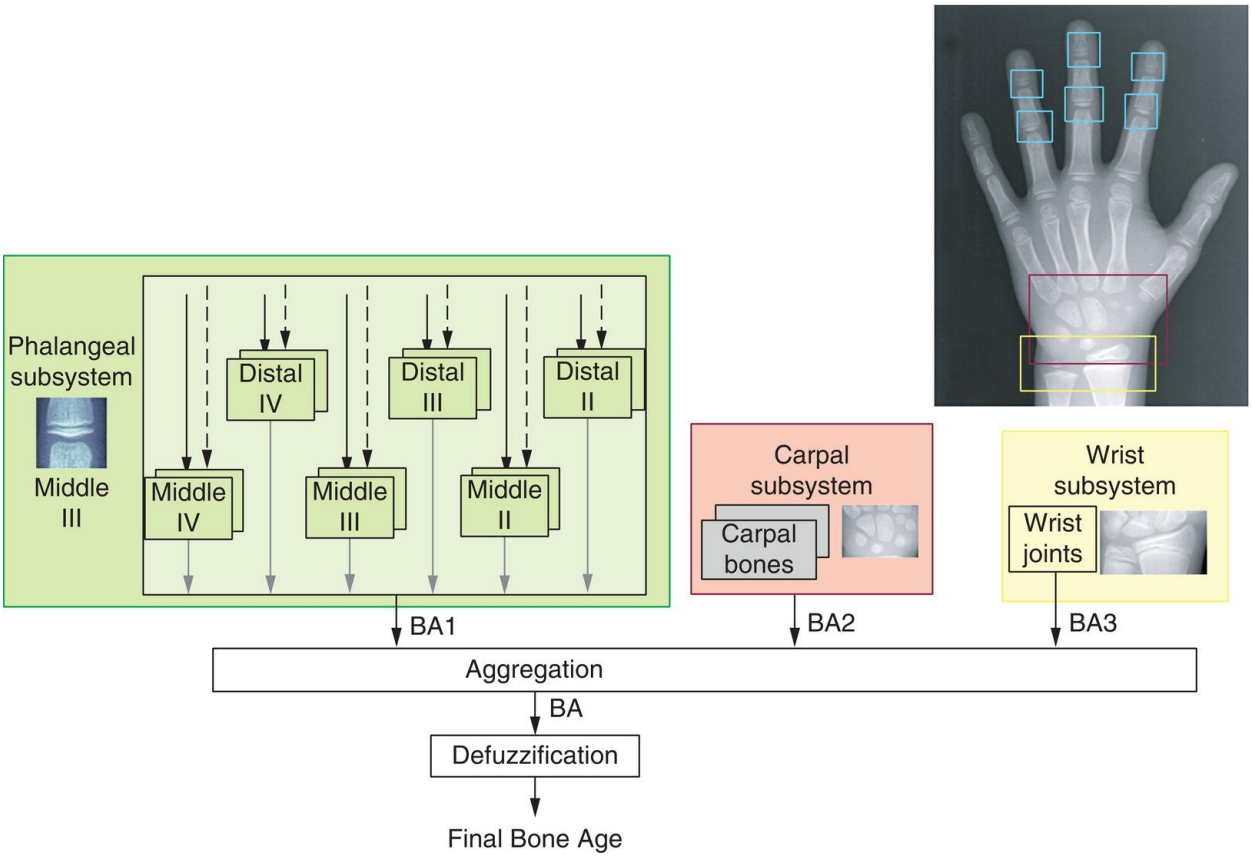

Figure 18.12 Fuzzy integration of eight ROIs, phanlangeal (6), carpal bones (1), and wrist (1), to determine the final BAA.

18.5 Validation of the CAD and the Comparison of CAD Result with Radiologists' Assessment

18.5.1 Validation of the CAD [15–19]

Sections 18.3 and 18.4 present the way in which the BAA was derived. This section validates the CAD BAA comparing the results with those obtained from the radiologists' assessment of bone age of children by reading from the DHA basis on the *G&P Atlas* standard. In the comparisons, it was discovered that for girls between 10 and 13 years, radiologists overestimated the bone age of Asian children compared to Caucasian, Asian girls compared with African-American girls, and Hispanic girls with African-American girls. For boys, radiologists also overestimated the bone age of Hispanic boys compared with African-American boys, Asian boys compared with to African-American boys, Asian boys compared to Caucasian boys, and Hispanic boys compared to Caucasian boys, in

the age group of 11 to 15 years. The over-estimated bone ages extended from 11 to 18 years for Asian compared to African-American. The knowledge gained from the DHA was incorporated into the design of the CAD fuzzy logic system for BAA. The validation of the CAD BAA as performed uses all data contained in the DHA.

The CAD fuzzy logic system described in Figure 18.13 was utilized to assess the bone age of all subjects contained in the DHA. An easy-to-use graphical user interface (GUI) was designed to cross-plot these results for comparison. The results are shown in Figure 13, A1, A2, …, A6, and B1, B2, …, B6.

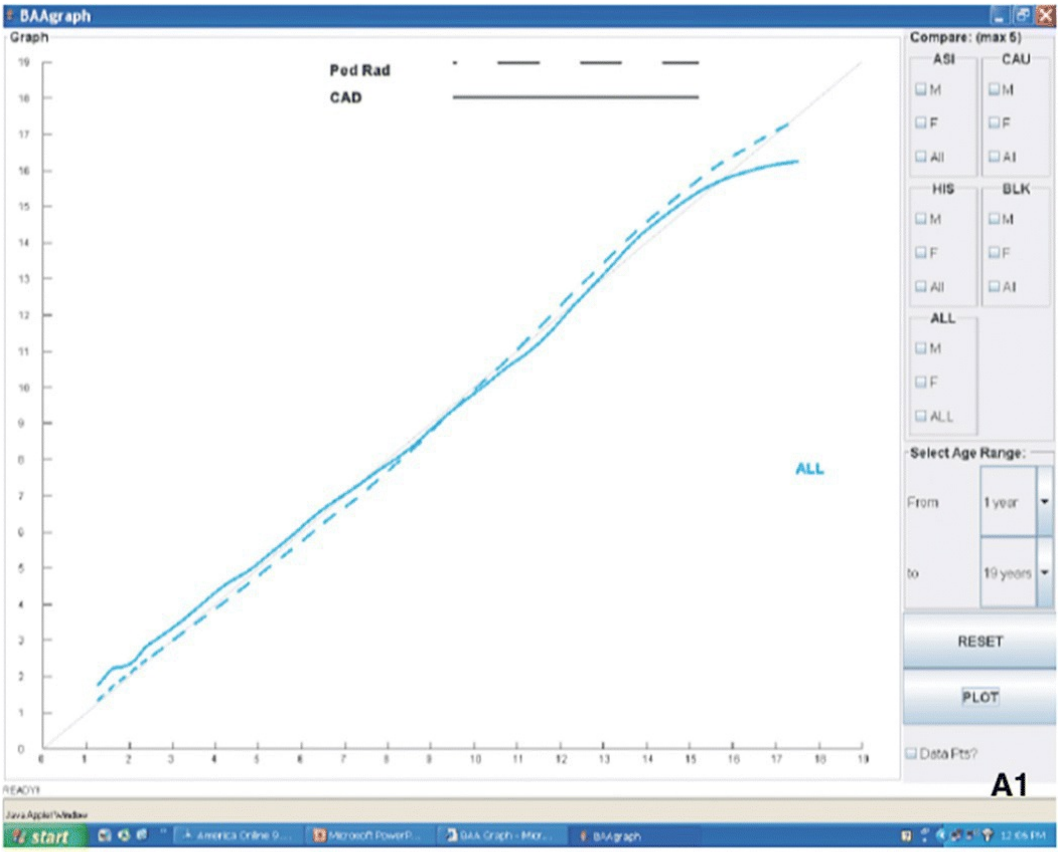
BAAgraph
Graph
Ped Rad
CAD
ALL
Compare: (max 5)
ASI
CAU
HIS
BLK
ALL
M
F
All
ALL
Select Age Range:
From
1 year
to
19 years
RESET
PLOT
Data Pts?
READY!
A1

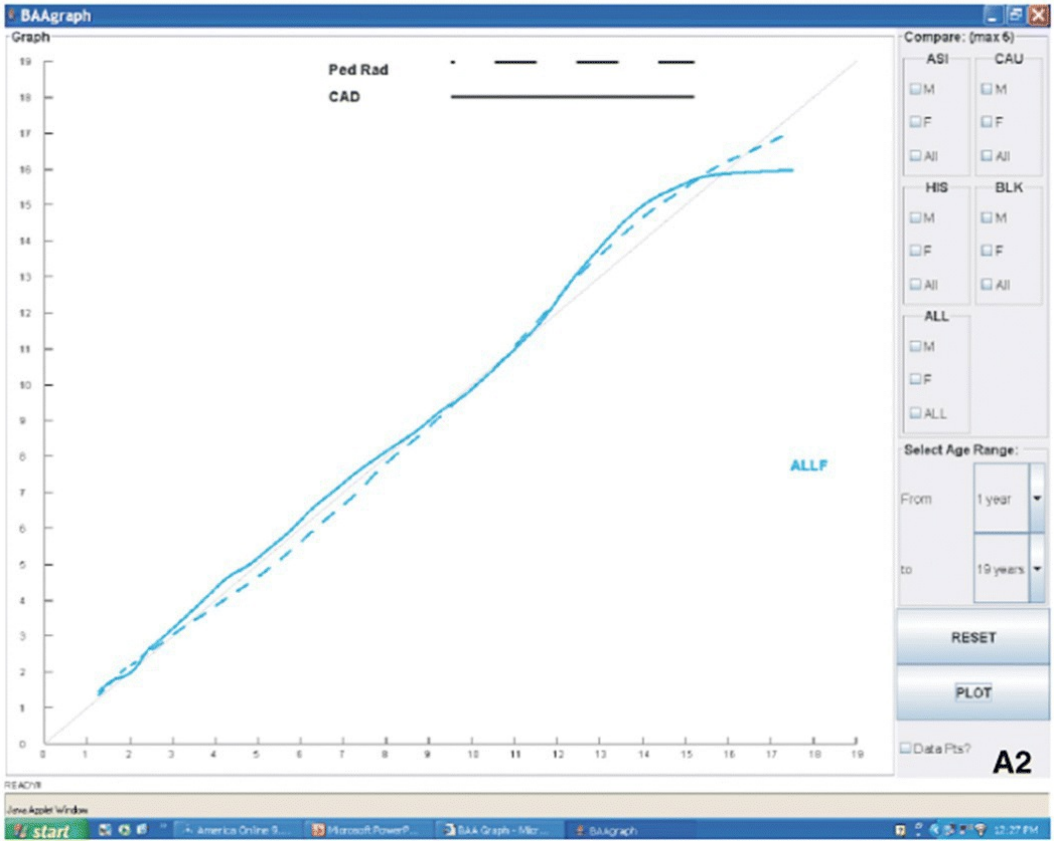
BAAgraph
Graph
Ped Rad
CAD
ALLF
Compare: (max 6)
ASI
CAU
HIS
BLK
ALL
M
F
All
ALL
Select Age Range:
From
1 year
to
19 years
RESET
PLOT
Data Pts?
READY!
A2

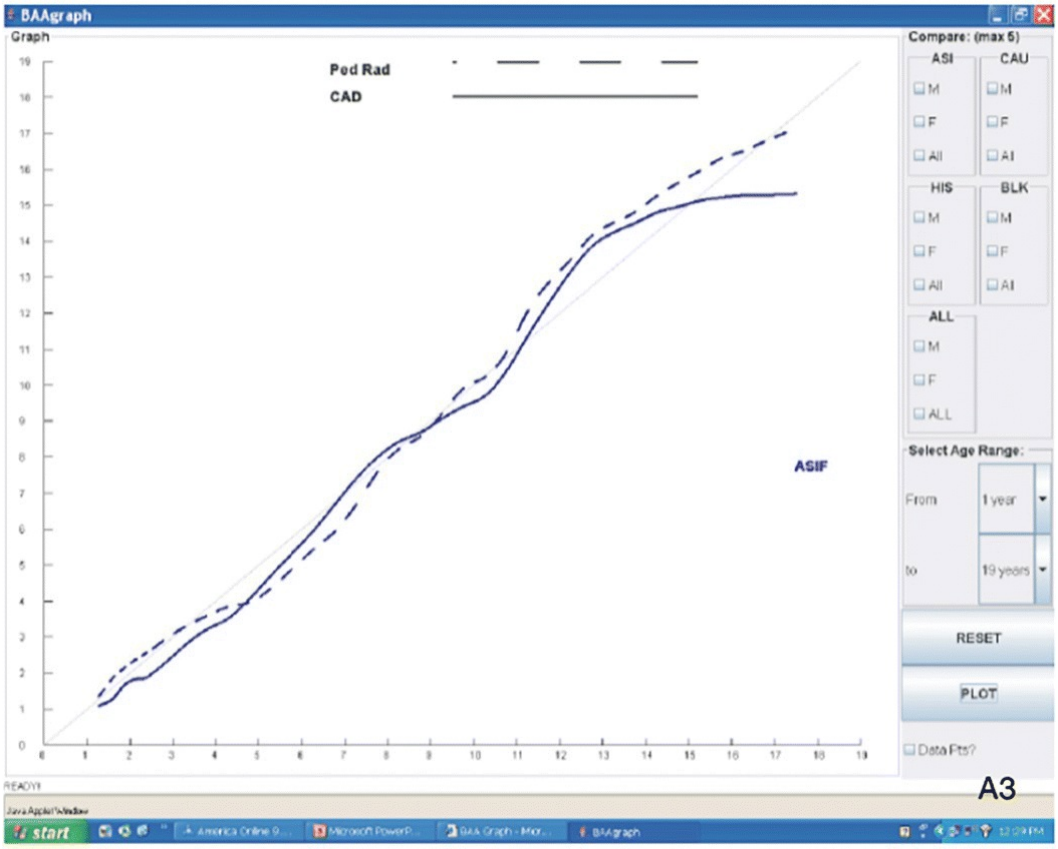
BAAgraph
Graph
Ped Rad
CAD
ASIF
Compare: (max 5)
ASI
CAU
HIS
BLK
ALL
M
F
All
AI
ALL
Select Age Range:
From
1 year
to
19 years
RESET
PLOT
Data Pts?
READY!
start
A3

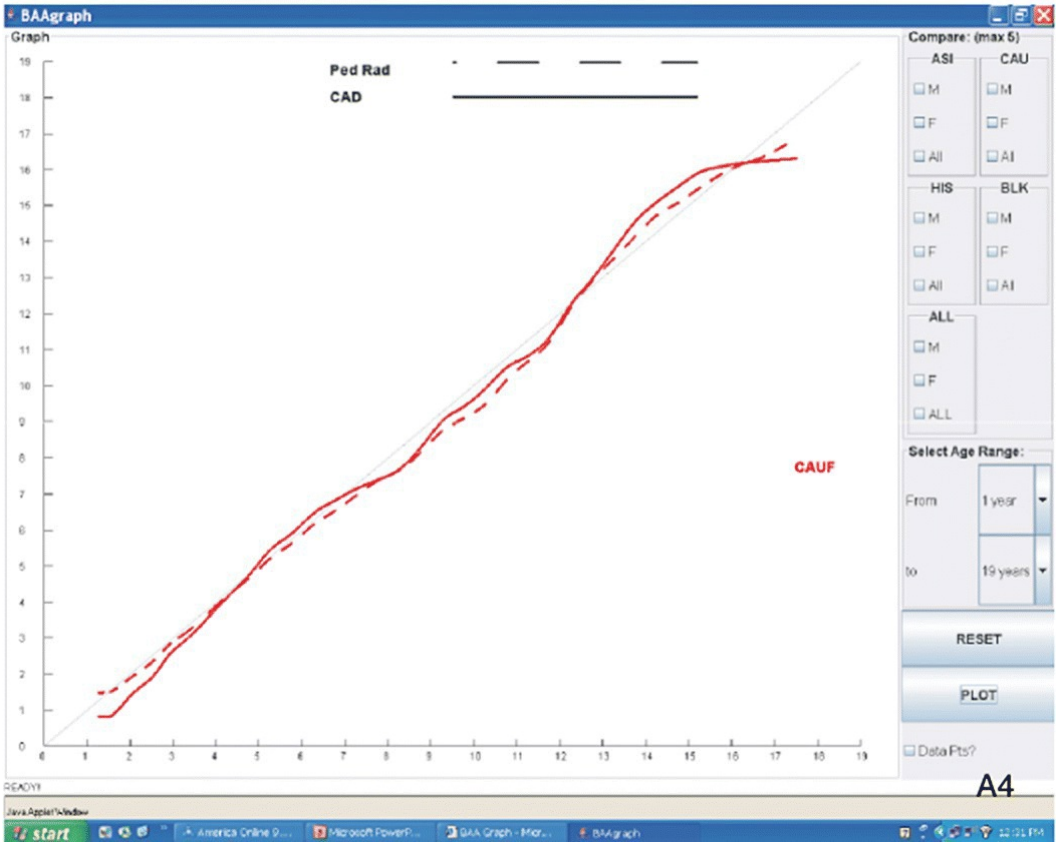
BAAgraph
Graph
Ped Rad
CAD
CAUF
Compare: (max 5)
ASI
CAU
HIS
BLK
ALL
M
F
All
AI
ALL
Select Age Range:
From
1 year
to
19 years
RESET
PLOT
Data Pts?
READY!
start
A4

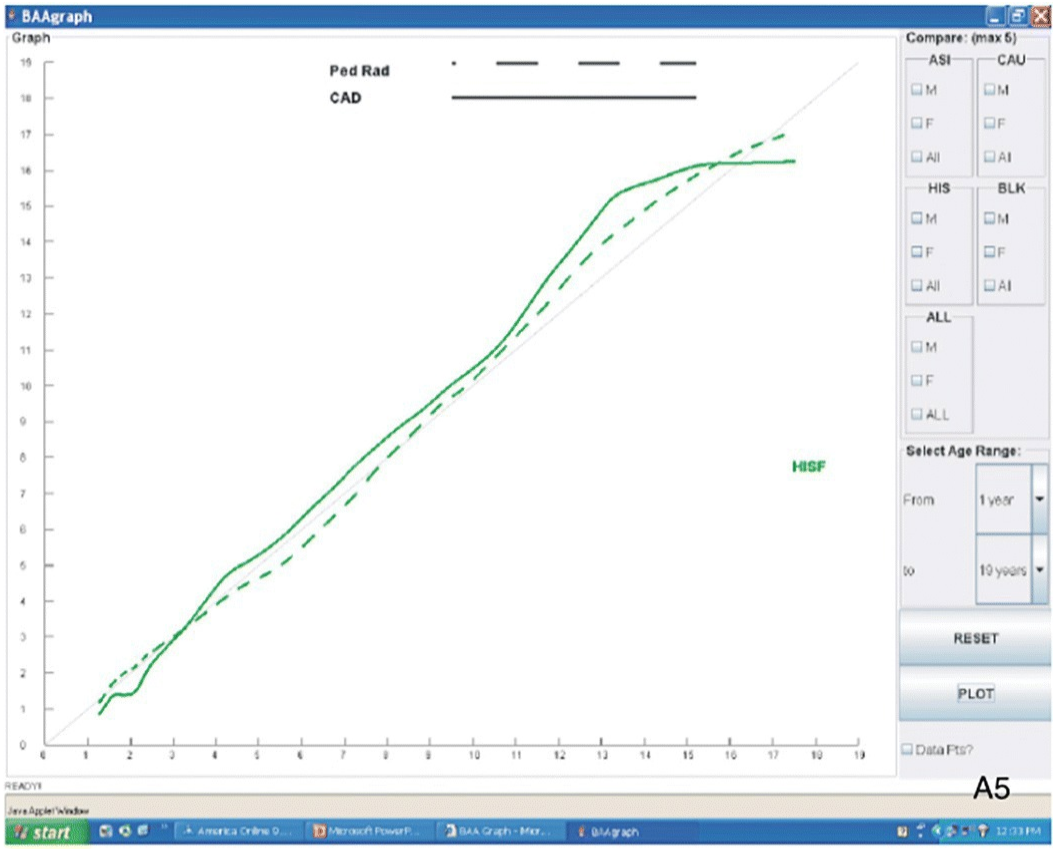
BAAgraph
Graph
Ped Rad
CAD
HISF
Compare: (max 5)
ASI
CAU
HIS
BLK
ALL
M
F
AI
All
Select Age Range:
From
1 year
to
19 years
RESET
PLOT
Data Pts?
READY!

A5

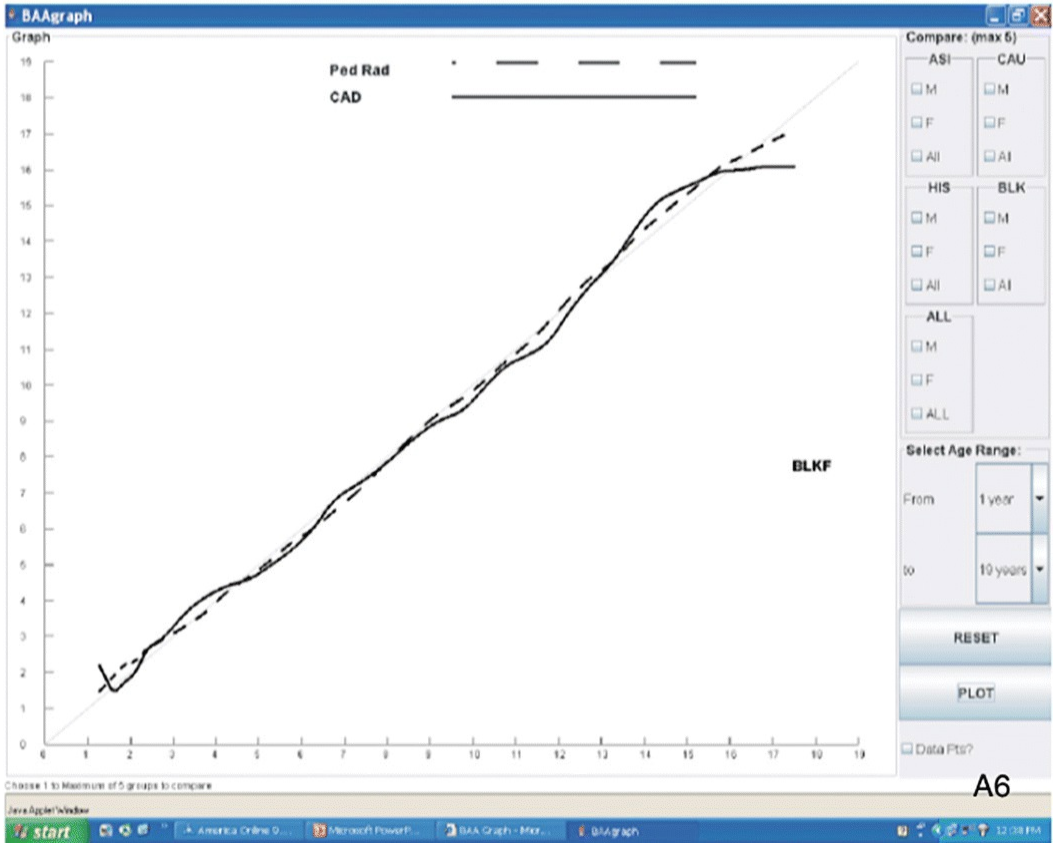
BAAgraph
Graph
Ped Rad
CAD
BLKF
Compare: (max 5)
ASI
CAU
HIS
BLK
ALL
M
F
AI
All
Select Age Range:
From
1 year
to
19 years
RESET
PLOT
Data Pts?

A6

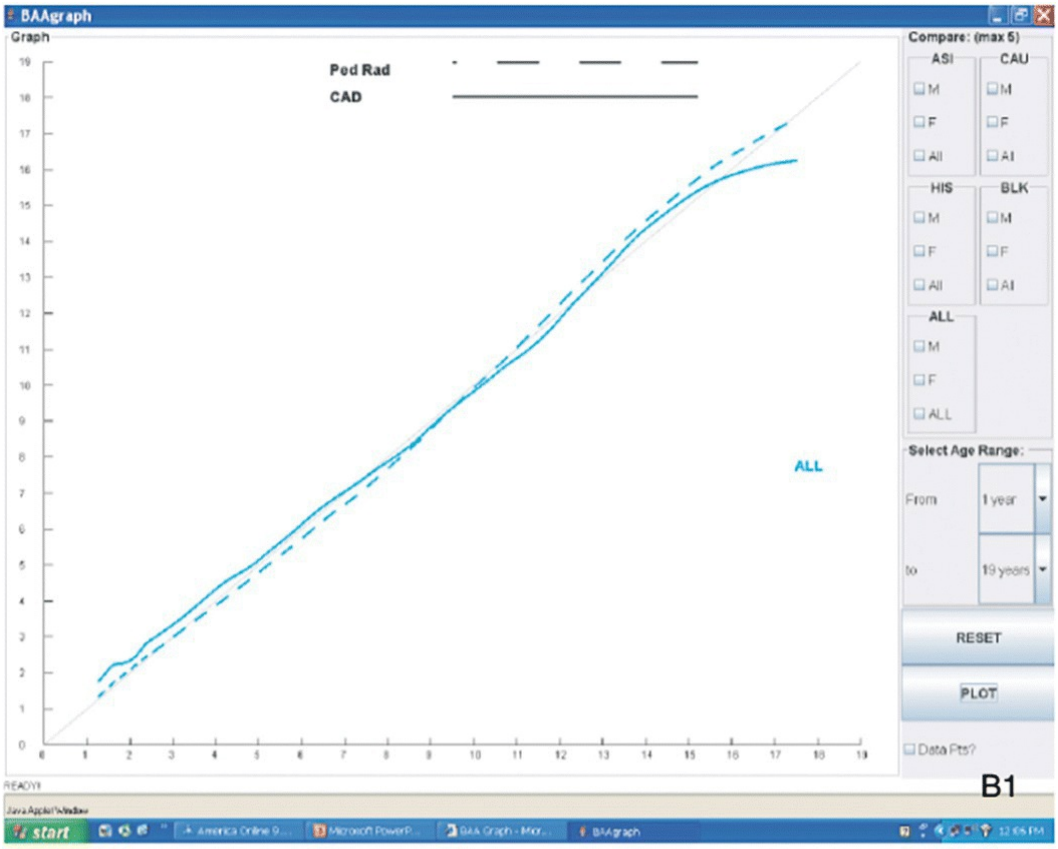
BAAgraph
Graph
Ped Rad
CAD
ALL
Compare: (max 5)
ASI
CAU
HIS
BLK
ALL
M
F
AI
Select Age Range:
From
1 year
to
19 years
RESET
PLOT
Data Pts?
READY!

B1

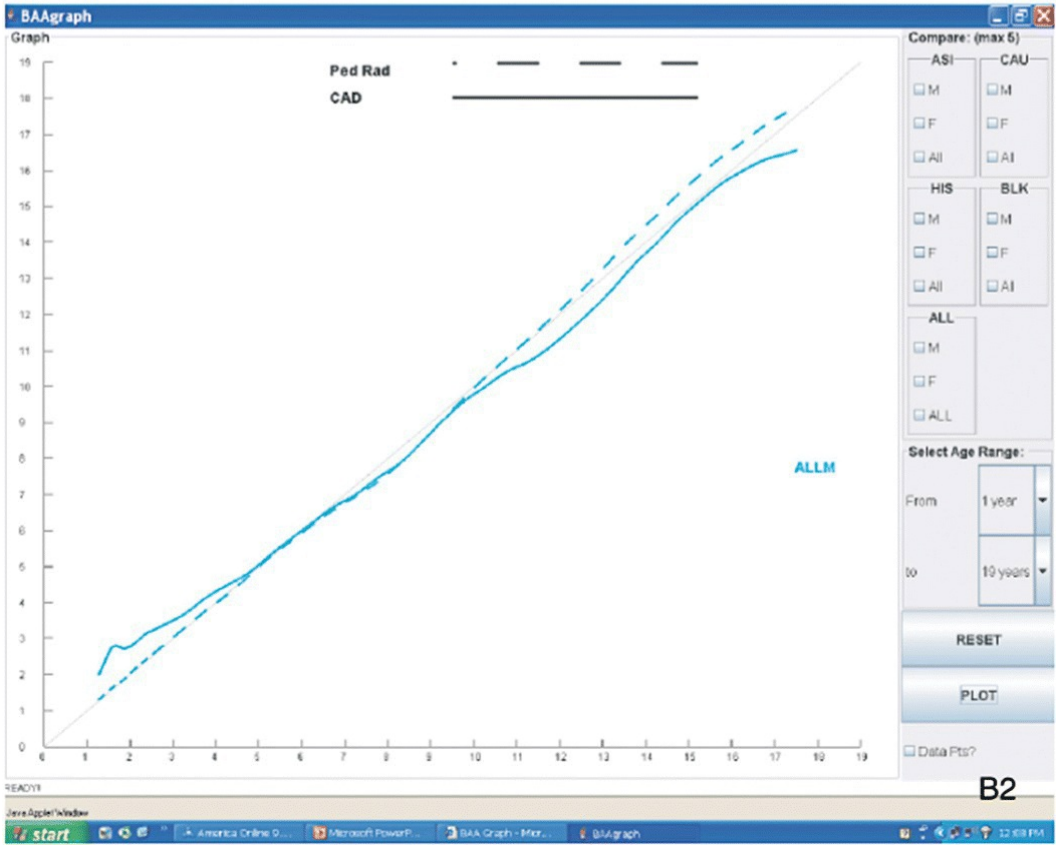
BAAgraph
Graph
Ped Rad
CAD
ALLM
Compare: (max 5)
ASI
CAU
HIS
BLK
ALL
M
F
AI
Select Age Range:
From
1 year
to
19 years
RESET
PLOT
Data Pts?
READY!

B2

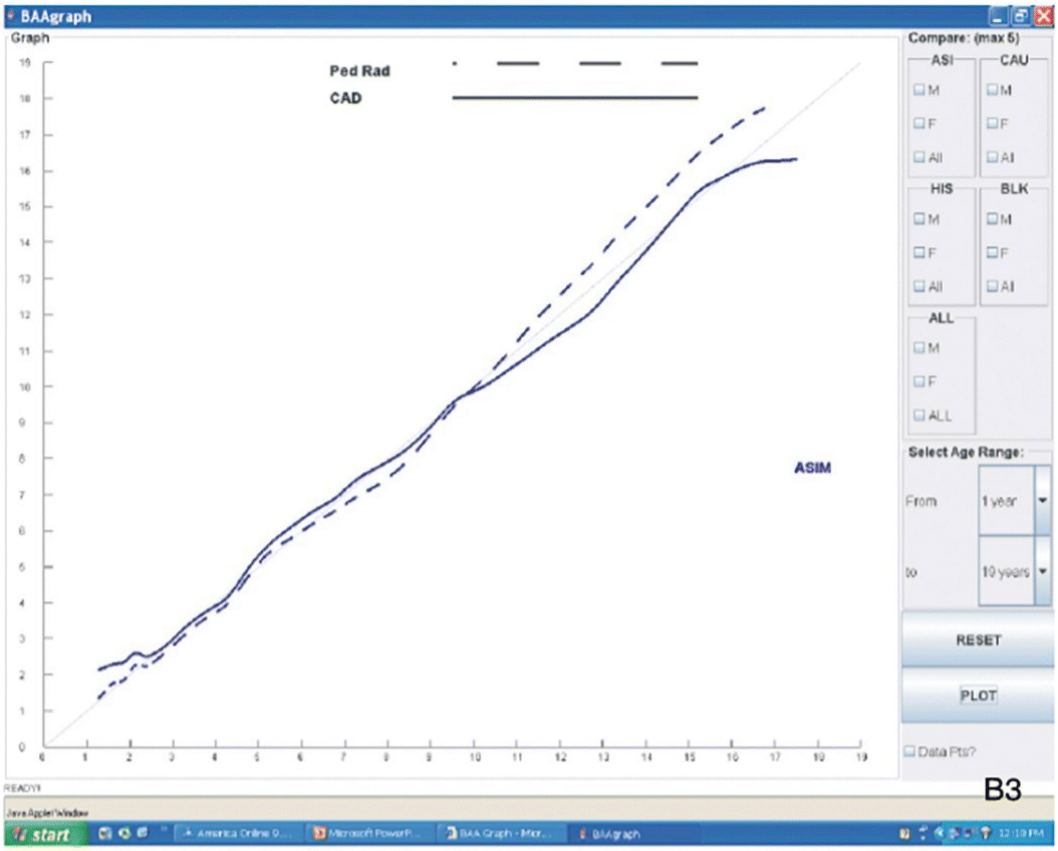
BAAgraph
Graph
Ped Rad
CAD
ASIM
Compare: (max 5)
ASI
CAU
HIS
BLK
ALL
M
F
AI
ALL
Select Age Range:
From
1 year
to
19 years
RESET
PLOT
Data Pts?
READY!
start

B3

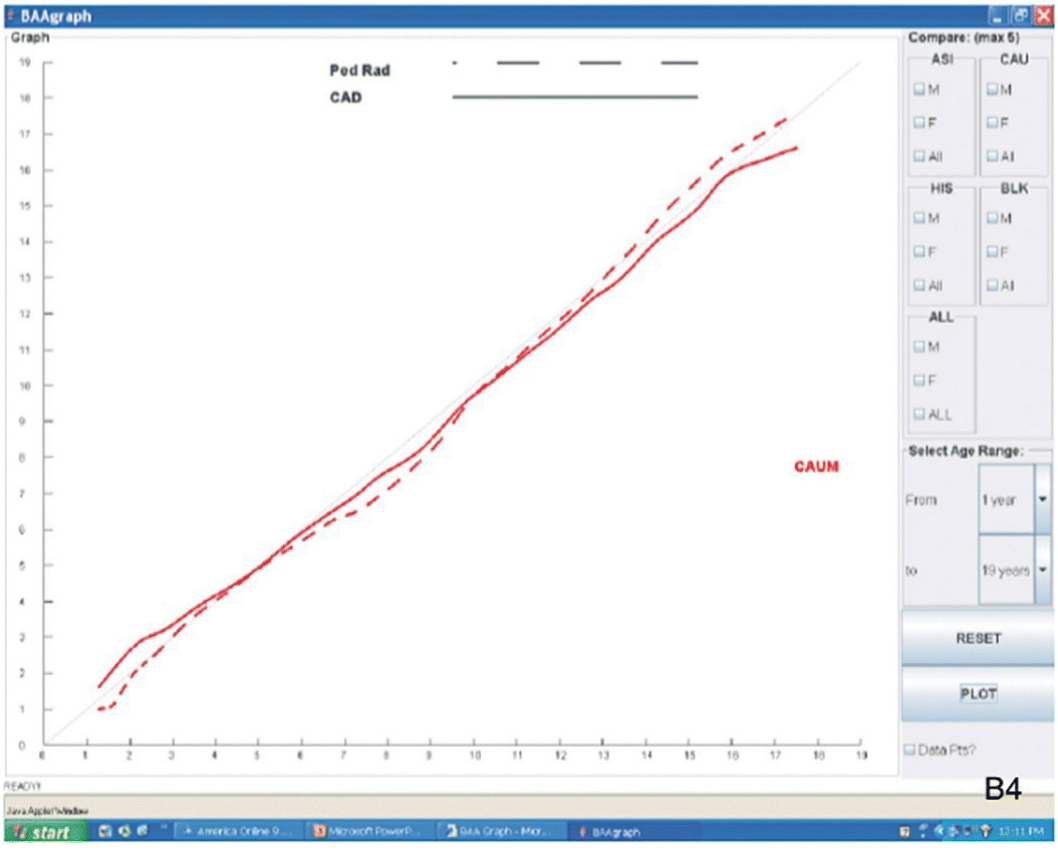
BAAgraph
Graph
Ped Rad
CAD
CAUM
Compare: (max 5)
ASI
CAU
HIS
BLK
ALL
M
F
AI
ALL
Select Age Range:
From
1 year
to
19 years
RESET
PLOT
Data Pts?
READY!
start

B4

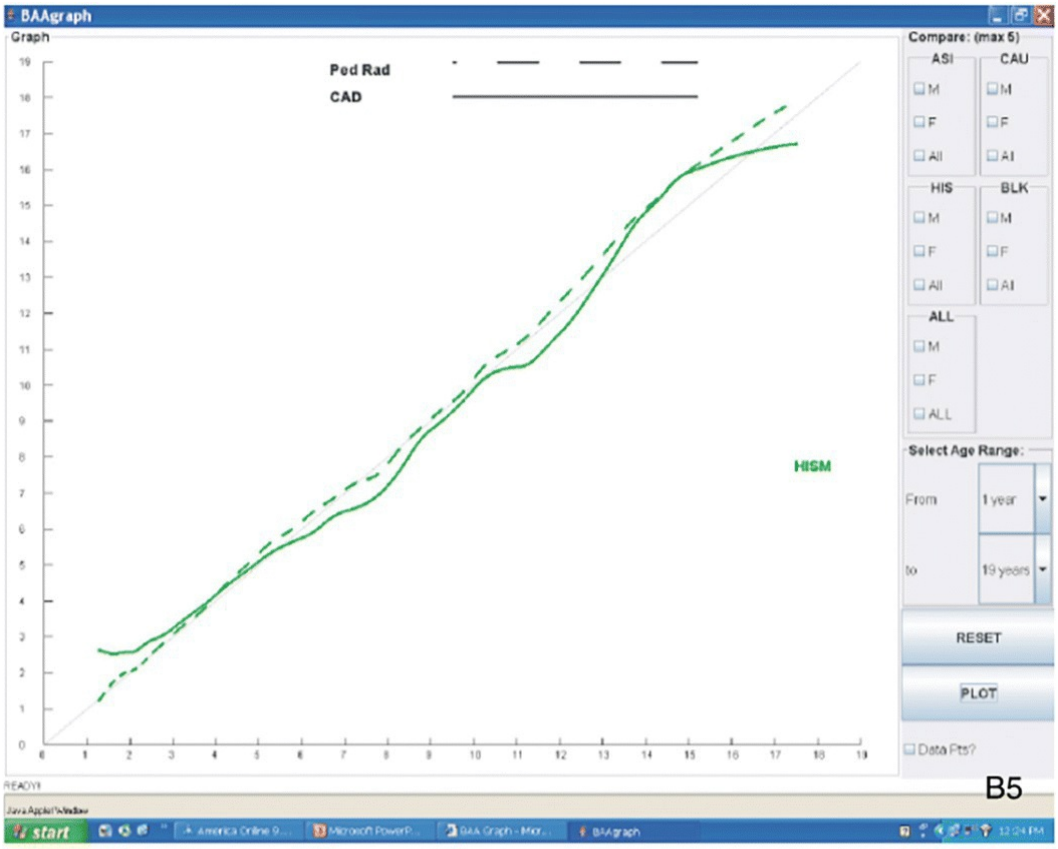
BAAgraph
Graph
Ped Rad
CAD
HISM
Compare: (max 5)
ASI
CAU
HIS
BLK
ALL
M
F
AI
ALL
Select Age Range:
From
1 year
to
19 years
RESET
PLOT
Data Pts?
READY!
start

B5

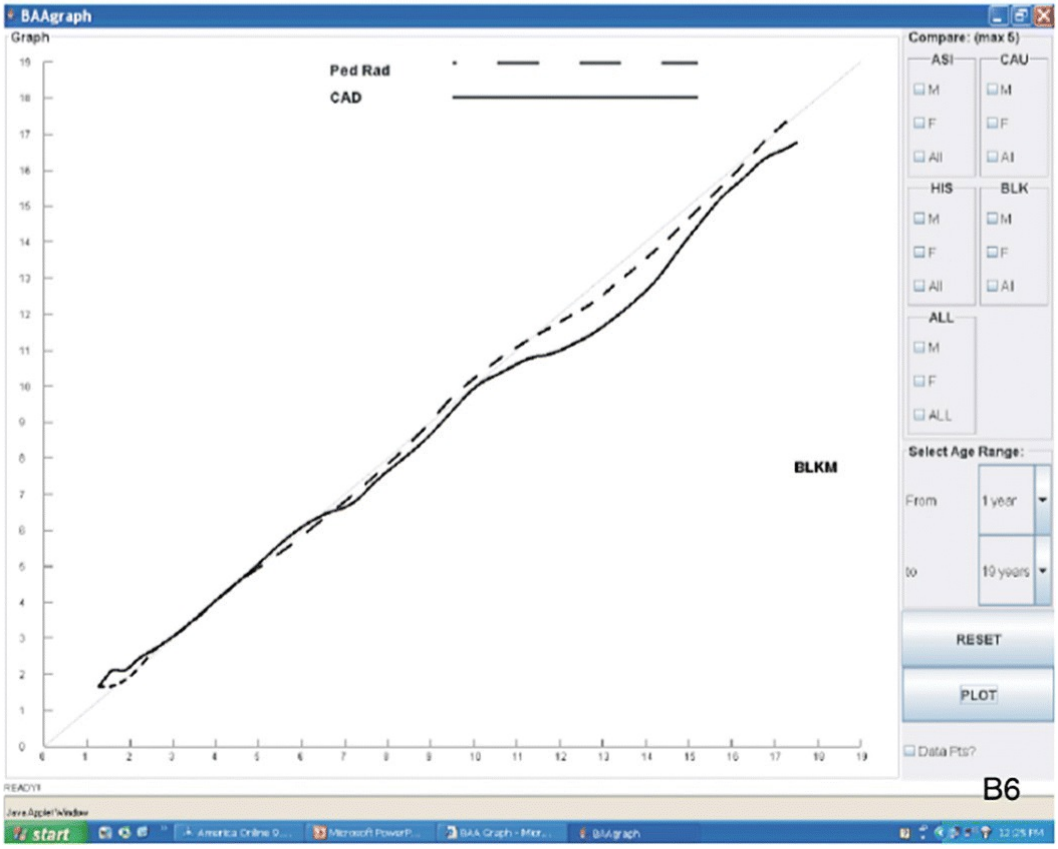
BAAgraph
Graph
Ped Rad
CAD
BLKM
Compare: (max 5)
ASI
CAU
HIS
BLK
ALL
M
F
AI
ALL
Select Age Range:
From
1 year
to
19 years
RESET
PLOT
Data Pts?
READY!
start

B6

Figure 18.13 Comparison between CAD and pediatric radiologists' (Ped Rad) assessment of bone age. Girls (A); boys (B). Each boy or girl group has six comparisons (1–6): A1, B1. All boys and girls images combined. A2, B2. All images from either all girls or boys. A3–6, B3–6:images from one race from the Digital Health Atlas (DHA). A screenshot from the GUI of the Digital Hand Atlas display component from http://ipilabmysql.usc.edu/newindex.php of the CAD system can assess the system. The user clicks icons on the screen (top right) to specify the data and format in the DHA to be plotted. Dotted line: Radiologists average reading, solid line: CAD assessment. Note that A1 and B1 are identical plots as they contain the same group data from the DHA.

18.5.2 Comparison of CAD versus Radiologists' Assessment of Bone Age

Figure 18.13 shows comparisons of the radiologists and the CAD method's assessments of bone age for the four racial pairs: Asian, Caucasian, Hispanic, and African-American, where A: Girls and B: Boys. In each plot, the dotted curve is the radiologist's assessment, and the solid curve is results from the CAD method. The plots of cross-comparisons between the radiologists and the CAD assessments were obtained from the GUI of BAA CAD system.

Results shown in Figure 18.13 demonstrate that the radiologist's readings (dotted line) of BAA tend to be higher than those of the *G&P Atlas* CAD method (solid line) for those children over 14 years of age. The discrepancy could be due to the fact that the bone growth of boys and girls over 14–15 years of age could have gradually matured earlier during the past 20–30 years than those of earlier decades. The additional bone assessment knowledge picked up by the radiologist's readings could have accumulated from their years of clinical experience. For this reason, the CAD method may require certain bone age adjustment to compensate for the older child bone age, which is discussed in Section 18.5.3.

18.5.3 All Subjects Combined in the Digital Hand Atlas(DHA)

Based on the experience accumulated from developing the DHA, it is observed that:

ALL Subjects Combined in the DHA

1. When combining all hand images of children in the DHA, CAD (solid line, Figure 18.13) underestimates the ages of those older than 8–10 years and overestimates the ages of children younger than 8–9 years, compared with the radiologists' assessments.
2. CAD underestimates the ages of all children combined, all girls, and all boys 15–18 years old, compared with the radiologists' assessments. This may be because the wrist joint bone assessment is more difficult for the CAD to perform, because radius joint separation requires good image quality to distinguish the joint space to obtain wavelet measurements.

Girls Only, Compared with the Radiologists' Assessments

1. When combining all girls in the DHA, CAD overestimates the 2–9 years age group, and the 13–15 years age group.
2. For all girls in each race, the two plot pairs, namely CAD compared with the radiologists' assessments, cross each other several times through different age groups. Among these, it seems that CAD exhibits the smallest differences in BAA in Caucasian and African-American children compared with the radiologists, and overestimates all girls older than 3-year-old Hispanic girls.

Boys Only, Compared with the Radiologists' Assessments

1. When combining all boys in the DHA, CAD overestimates the 2–5 years age group, and underestimates the 10–18 years age group, compared with the radiologists' assessments.
2. For all boys in each race, CAD underestimates all four races of subjects older than 10 years of age, compared with the radiologists' assessments. For the under 10 years age group, there are slight overestimations in Asian and Caucasian, underestimated in Hispanic boys, and a very close match with African-American boys.

18.6 Clinical Evaluation of the CAD System for Bone Age Assessment (BAA)

18.6.1 BAA Evaluation in the Clinical Environment

The next step after the validation was to bring the DHA and BAA CAD system

into a clinical setting for evaluation. The goal was to assist radiologists in their daily practice using the CAD results. To do this, a Web-based client–server system was designed with such a novel clinical implementation approach for on-line and real-time BAA. The DHA was already available on line in JPEG format http://ipilabmysql.usc.edu/newindex.php. The clinical validation system includes a stand-alone CAD WS that is connected with the clinical PACS, a Web-based GUI at the CAD WS, and a CAD workflow designed specifically for the clinical environment. The system is integrated at the radiology department of Los Angeles County Hospital (LAC), and cases were collected both in real time and retroactively to analyze the CAD system's performance. In addition, images in the *G&P Atlas* were digitized and stored in a *G&P Atlas* database for easy comparison.

18.6.2 Clinical Evaluation Workflow Design

The clinical workflow of BAA CAD had been previously designed by IPILab, USC, and tested within the laboratory environment. Figure 18.14 shows the clinical workflow diagram simulated as if it was in a clinical environment.

The workflow has six steps: the first three steps include conventional PACS workflow in radiology and the last three steps detail how data was transmitted in the presence of a CAD–PACS WS:

1. Hand image was sent from the modality simulator (which simulates a CR, DR, or film scanner) to the acquisition gateway;
2. Acquisition gateway transmitted the image to the PACS storage server;
3. PACS WS "queried and retrieved" the hand image from PACS and displayed the image on the PACS WS;
4. The modality sent a second copy of the hand image to the CAD WS/server. The server processed the CAD result;
5. CAD server sent CAD result to the PACS WS. Radiologists also assessed the bone age blindly from the WS, then compared the CAD results with their own readings;
6. Readings by radiologists were captured and sent back to CAD server for storage as the BAA evaluation results.

After laboratory validation, the BAA CAD system and WS were installed for clinical evaluation at the radiology department of the LAC, where the CAD WS could access the county's PACS and computed radiography images. The actual

clinical validation workflow is presented in Figure 18.15.

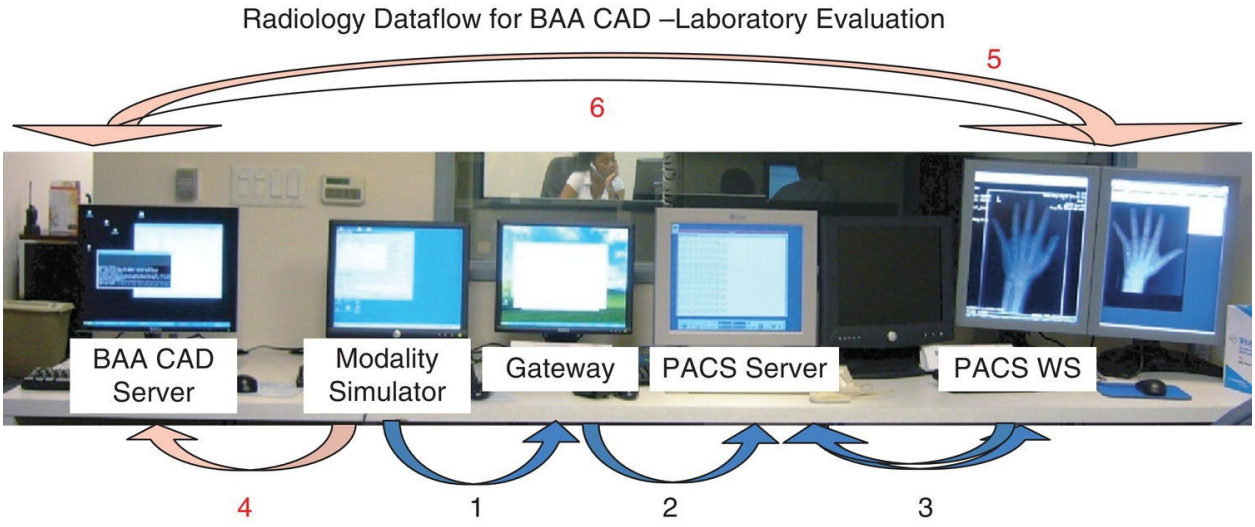

Figure 18.14 Simulated clinical workflow diagram of the BAA CAD system using the PACS simulator (see Chapter 12).

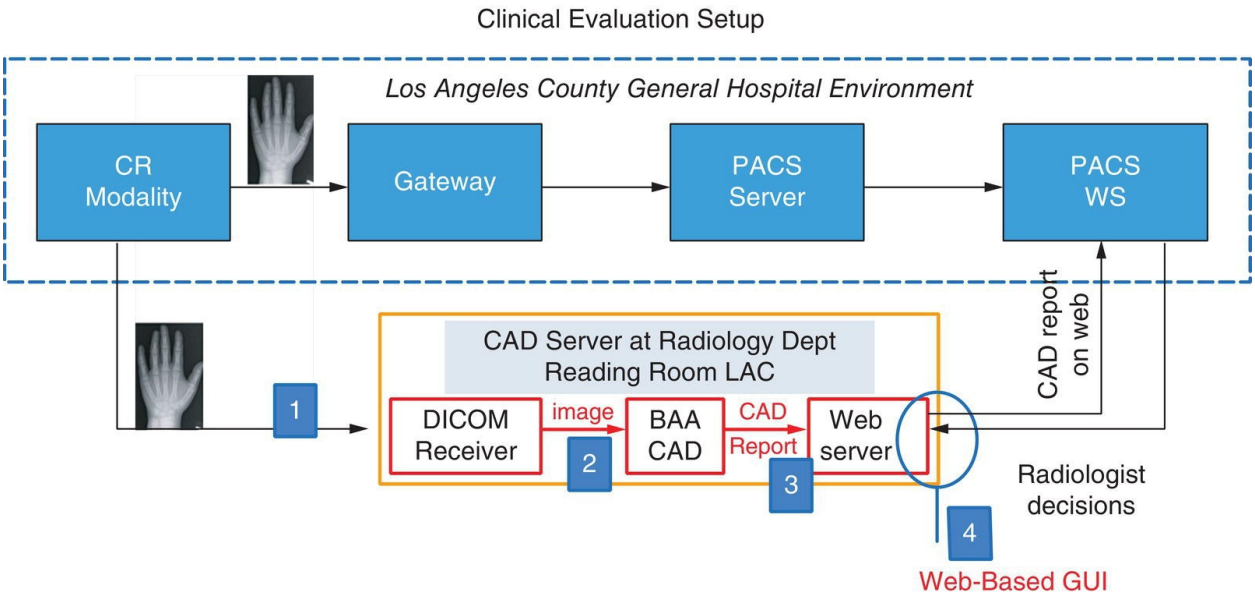

Figure 18.15 Clinical evaluation of the BAA CAD system. The workflow was implemented at the Los Angeles County Hospital (LAC) with the clinical PACS and CAD server.

18.6.3 Web-based BAA Clinical Evaluation System

The BAA CAD server has three components: a CAD server that performed automated BAA, a Web server that served as a database manager, and a GUI for display and a walk-through of the clinical validation process.

18.6.3.1 CAD Server

The BAA CAD program is written in MATLAB and then converted to an executable file for better integration and compatibility. The DICOM receiver and other necessary functions are handled by open-source DICOM Toolkit DCMTK.

18.6.3.2 Web Server

The Web server is set up such that the CAD results and the validation procedures can be accessed remotely via TCP/IP. A standard Apache Web server is used, and the Web user interface is designed in hypertext pre-processor(PHP). The database is handled by MySQL.

18.6.3.3 Graphical User Interface (GUI)

The Web user interface guides the radiologist through the validation process, which is separated into three steps. Figures 18.16A, B, and C are screenshots showing how the GUI works.

In step 1, the GUI displays the list of patients waiting to be evaluated. CAD results have already been stored (not displayed here). Each patient is anonymous, and their sex and ethnicity is displayed. Since ethnicities are not stored in the DICOM header, radiologists have to manually input the patient's ethnicity. The radiologist clicks on a patient ID to continue the evaluation process. For example, in Figure 18.16A, the user can select patient, for example, “2” from the work list.

Continuing at step 2, the GUI displays the patient’s hand image as well as the scanned hand images from the *G&P Atlas* (Figure 18.16B). The purpose of this stage is to allow radiologists to make an unbiased diagnosis using the current G&P standard. After the best-fit *G&P Atlas* image is selected by the radiologist, the result is saved into the database when the user clicks on the link to step 3.

In step 3, following Figure 18.16C, the GUI displays the patient’s original hand image (left), the *G&P Atlas* hand image selected in step 2 (middle), and the best-matched DHA image determined by CAD bone age (right). The CAD textual result is displayed at the right-hand top corner, as well as a normality graph that shows if the patient’s bone age falls within the range of normal determined by the mean and two standard deviations from the *G&P Atlas*. Here, the radiologist can choose whether the original diagnosis with the *G&P Atlas* is more accurate or the CAD result is more accurate. When the radiologist clicks on the “Save and Return to Step “1” link at the left-hand bottom corner of the GUI, the evaluation

of this patient is complete and ready for the next patient.

18.6.4 Integration of the BAA CAD System at the Los Angeles County General Hospital

After the laboratory validation, the BAA CAD system with the WS was installed for clinical evaluation at the Radiology Department of the hospital, where the CAD WS can access the county's PACS and computed radiography images. The actual clinical validation workflow is shown in Figure 18.16.

The CAD system was installed at the LAC Women and Children's Hospital in February 2008. A DICOM receiving node was created such that the CAD system on site could send copies of acquired left-hand images to the CAD server. The hospital was relocated to a new facility adjacent to the USC Medical Center in November 2008. The Department of Radiology PACS, together with the BAA CAD server, was reinstalled in the new outpatient clinical area. The DHA CAD validation restarted there in July 2012. The workflow is shown as follows:

1. CR sends a copy of the hand image to the CAD server located in the radiology outpatient reading room.
2. CAD program receives the image, performs BAA and records results in the server database.
3. The Web server searches the BAA database to locate the original hand image from PACS and links up with BAA results from the BAA database, as well as the best-matched DHA image (determined by the CAD BAA, see Figure 18.16B and C).
4. GUI in the WS displays the original image and the best-matched image from the DHA (Figure 18.1). Following these displays from the sequence will guide radiologists through the validation steps.

(A) Clinical Evaluation Workflow – Step 1

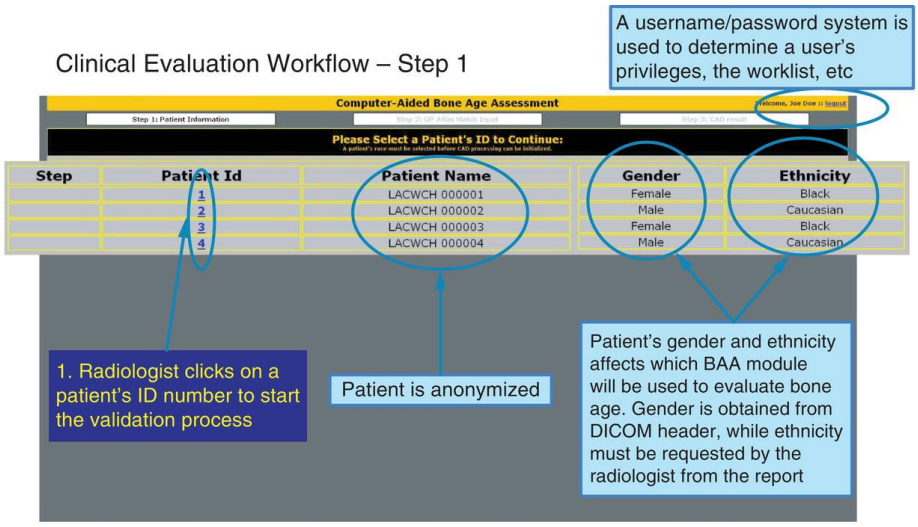

(B) Step 2

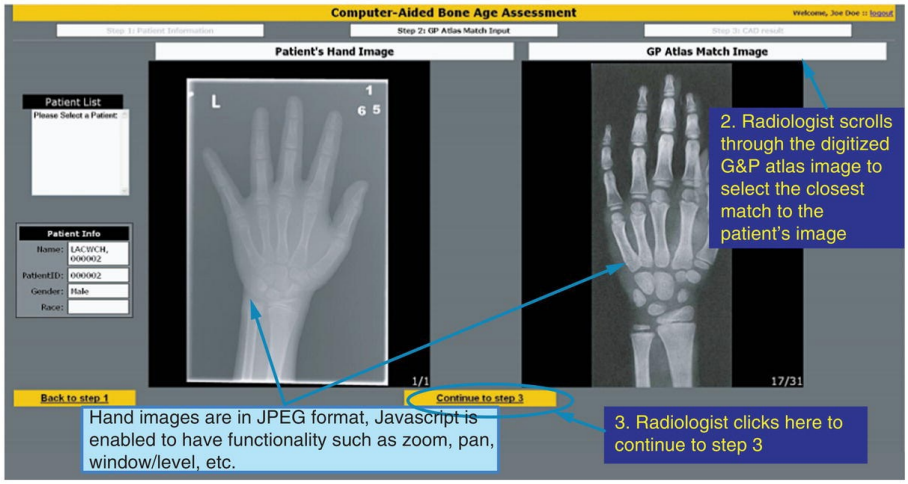

(C) GUI – Step 3

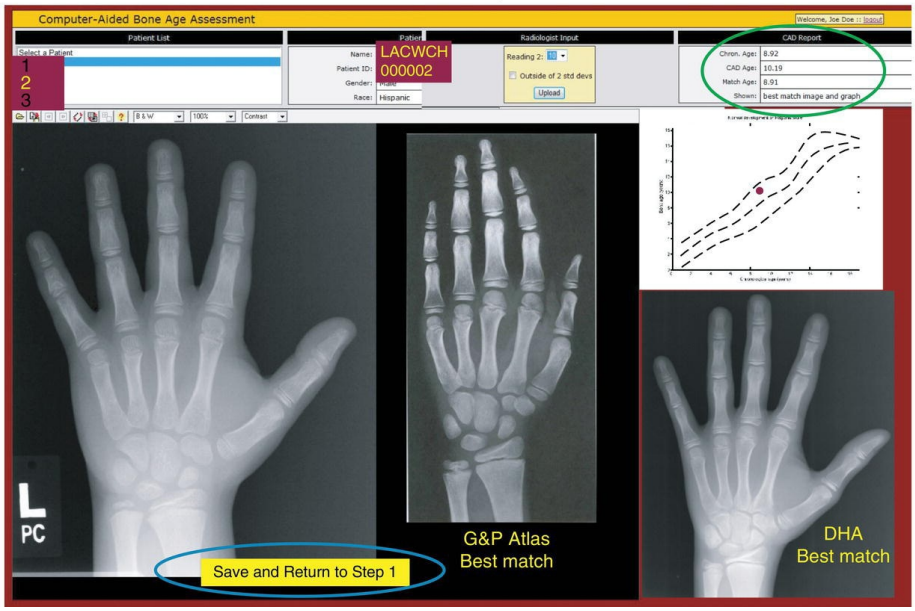

Figure 18.16 BAA CAD clinical evaluation Web GUI, as shown on the PACS WS monitor. (A) Step 1. Retrieve a patient's hand image from PACS, and link it with the CAD results in the CAD server database. (B) Step 2. Compare the original image (left) with the best matched Greulich & P*yle* (*G&P*) Atlas image (right). The match criterion is to use the patient's chronologic age to search the *G&P Atlas*, in the order of race, sex, and age, for the image with the closest age in the *G&P Atlas*. (C) Step 3. Compare the original image (left), with the best matched *G&P Atlas* image (center), and the best-matched DHA image (right). The chronologic age, bone age, and the matched DHA age are shown at the top right of the screen within the green ellipse. The CAD accessed child bone age (red dot) compared to the children in the normal range in the DHA is shown in the plot.

18.7 Integrating CAD for Bone Age Assessment with Other Informatics Systems

Up to this point, previous sections have described step-by-step the current clinical practice in BAA of children and its drawbacks, the rationale for the development of CAD, a method of data collection and analysis, background of the CAD system development, and its validation from clinical evaluation. Section 18.7 further extends the BAA CAD method of BAA with the content-based DICOM structured reporting (DICOM-SR) discussed in Chapter 6 and Data Grid (DG) discussed in Chapters 8 and 9, in which these concepts were introduced. This section discusses the power of PACS-based multimedia imaging informatics for clinical research and practice using the example of CAD BAA.

18.7.1 BAA DICOM Structured Reporting (SR)

In Chapters 6 and 17, the concept of DICOM-SR, and a clinical example using multiple sclerosis was introduced in Chapter 17. In particular:

1. to develop the SR format from a text file CAD report to the SR format;
2. to overlay the contents in SR on the original image; and
3. to display images and reports on the PACS WS.

In the case of BAA CAD, a similar method can also be used to convert the BAA CAD report to the DICOM-SR BAA and display both hand images and reports

on the PACS WS. The five Integration steps are as follows:

1. Create the DICOM-SR:
    a. Design the BAA SR template (each type of CAD should have its own template to accommodate specific requirements);
    b. Obtain the patient hand image and the matched image from the DHA in the *G&P Atlas* (JPEG format) to a DICOM SC image (a built-in module in the DICOM-SC edition of the CAD–PACS integration toolkit);
    c. Configure i-CAD (in the CAD–PACS integration toolkit with the defined BAA SR template applied on all available data (text file, plots, three DICOM images, i.e. the original image, the best-matched image from the DHA, and the best-matched image from the *G&P Atlas* to create the DICOM SR) ;
2. Configure SR-server to run i-CAD program 5 16 automatically when the CAD application finishes the CAD process;
3. Send DICOM-SR to SR-server (without user intervention);
4. Store DICOM-SR, query and retrieve referenced images in DICOM format from the two atlases (*DHA* and *G&P*) for PACS WS display;
5. CAD results are ready for viewing at PACS WS.

Figure 18.17 shows the BAA DICOM-SR template, and Figure 18.18 depicts CAD structured reporting (left) and the graph of the BAA value (right, red dot) of a child, within ± two standard deviations of the mean in the DHA18.16.

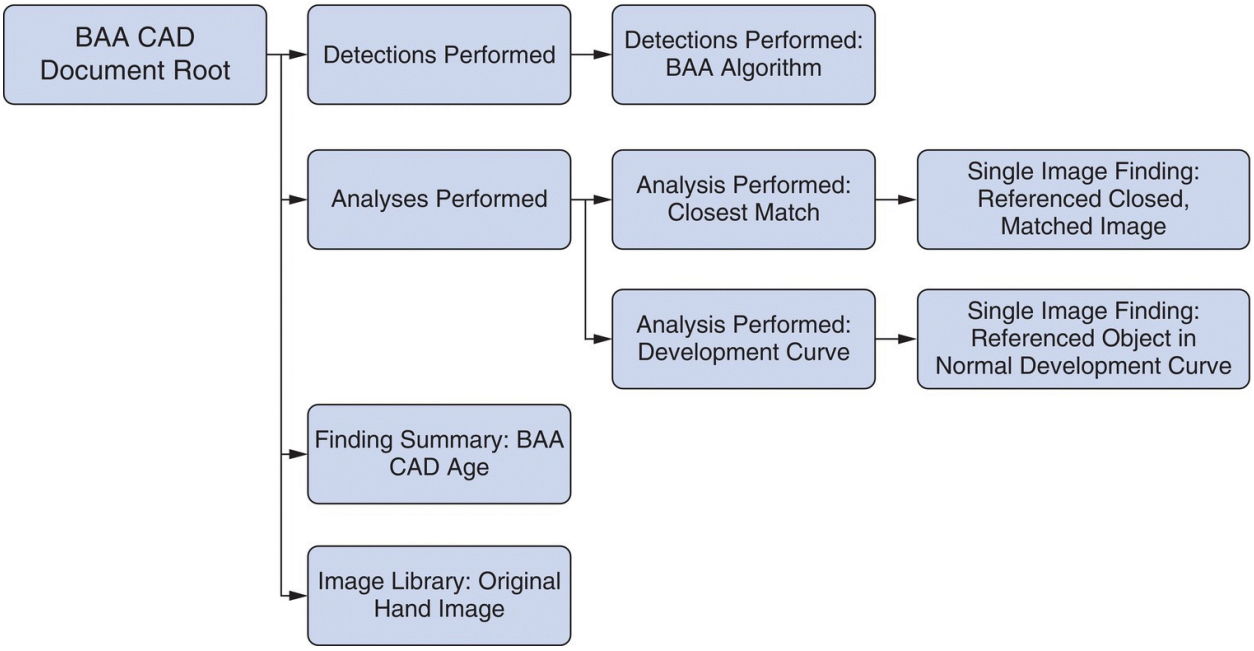

Figure 18.17 DICOM SR template for BAA CAD. The template is designed based on the types of output that radiologists require to review.

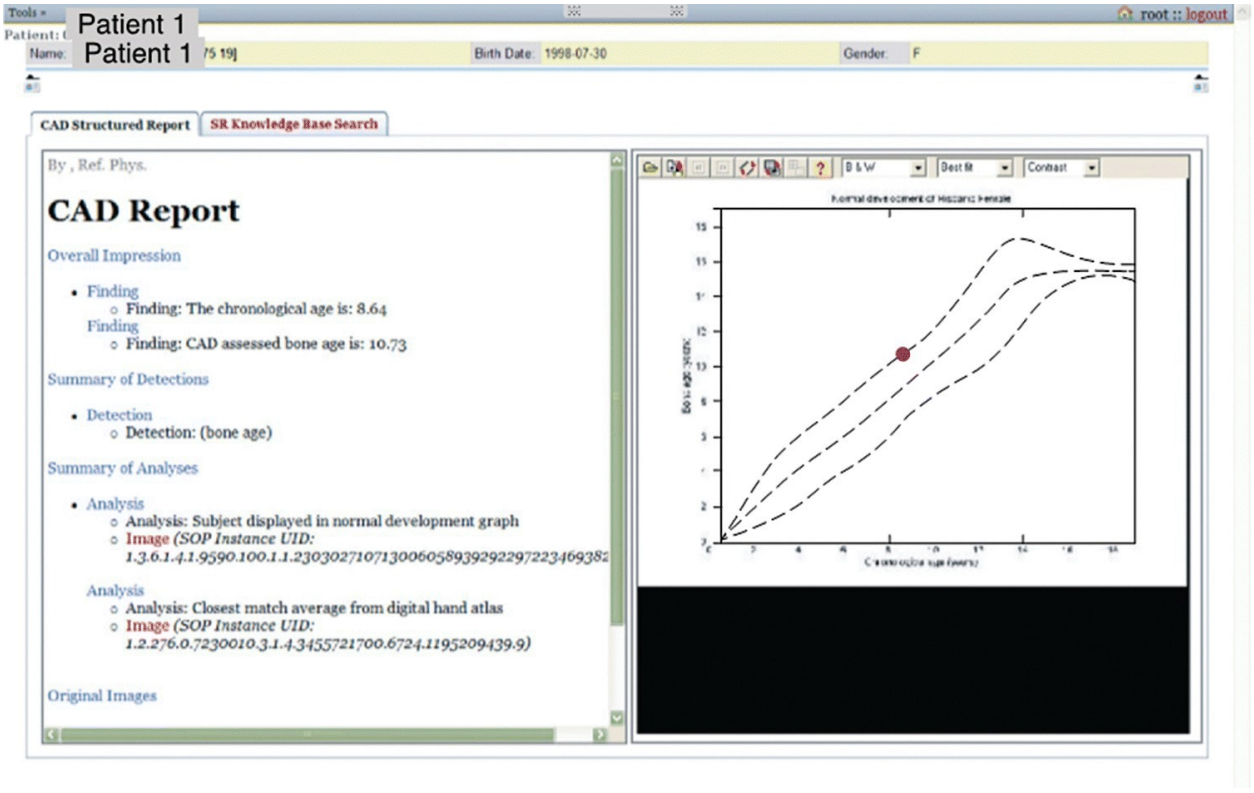

Figure 18.18 Integrating BAA CAD with DICOM-SR. Left: CAD report in DICOM-SR format based on the design of the SR template. Right: A component in the DICOM-SR that is a plot of the CAD BAA results of a patient (red dot)

compared with the normals and ± two standard deviations in the Digital Hand Atlas (see also Figure 18.16C).

18.7.2 Integration of Content-Based DICOM-SR with CAD

In Chapter 8, Data Grid technology is discussed as the preferred method for reliable image data storage. The Data Grid can also be integrated with DICOM-SR, which is content-based, for: i) improving the storage reliability of the DCIOM-SR data; and ii) utilizing the DICOM-SR for multiple site access data mining applications. In order to integrate with Data Grid, the following steps can be used:

1. Support CAD structured reports in the DICOM services layer of the Data Grid;
2. Extend Data Grid's database for CAD SR contents within a DICOM data model schema;
3. Design a recursive algorithm to extract specific contents of interest from CAD structured reports using a knowledge-based approach combined with the DICOM standard;
4. Implement Web-based client interfaces to allow remote data mining from the structured reports and link images archived in the Data Grid by quantitative retrieval method, rather than patient identifiers or study UIDs. The workflow of these steps is illustrated in Figure 8.19.

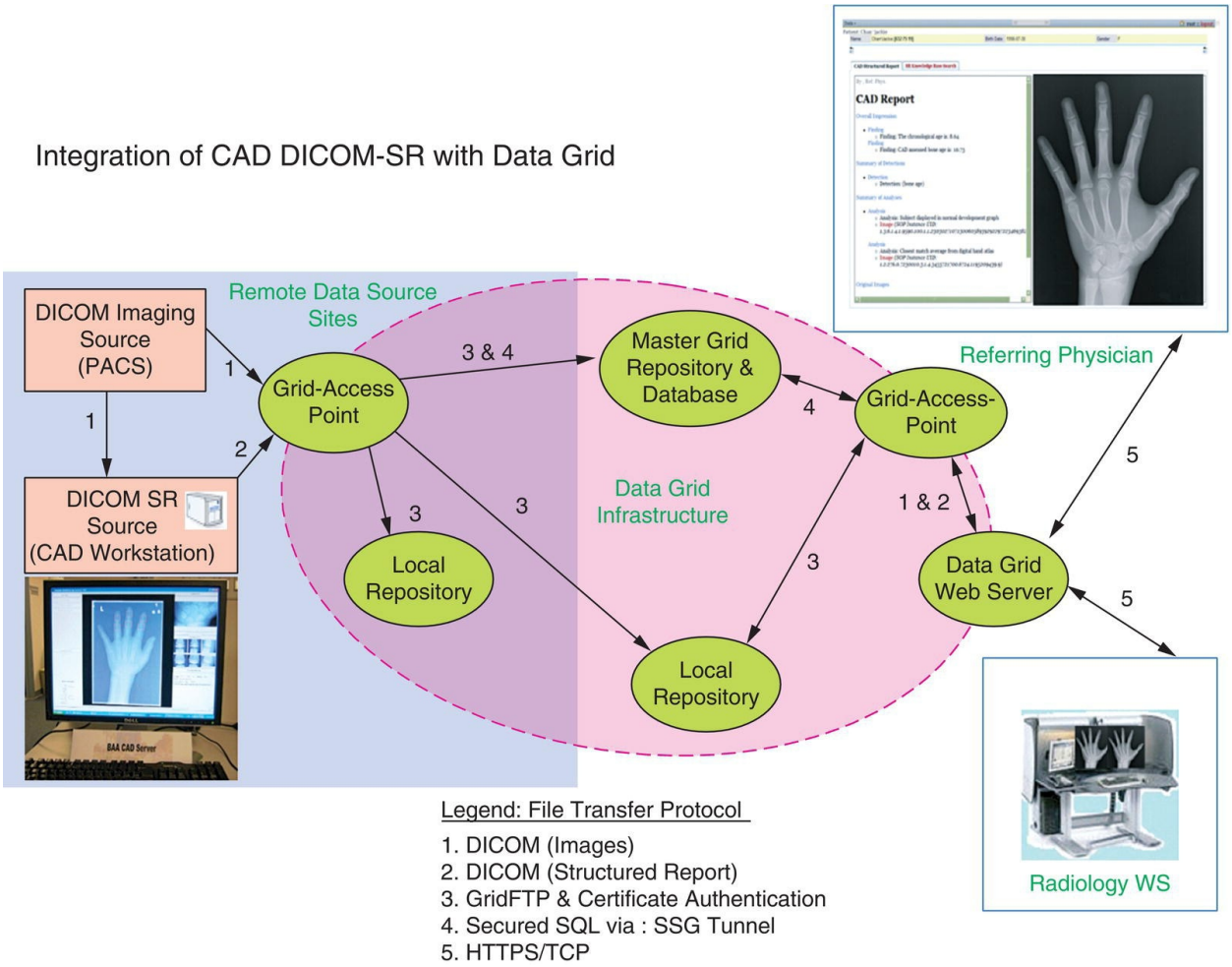

Figure 18.19 Workflow steps of integrating the CAD DICOM-SR with the Data Grid. Color code: Data sources and CAD (light blue); Data Grid infrastructure (pink); referring physician and radiology WS (blue); workflow processes (green). There is data Web server (right) and multiple grid access points (GAPs). Data flow: Input to the Data Grid—Images (1) and CAD results in DICOM-SR format (2) move across from left to right through the GAP (left), secured SQL via SSG tunnel requests data to be transmitted using GRIDFTP service for certificate authentication and stored in multiple local repositories (3), and metadata in master grid repository and database (3,4). Output–multiple sites where referring physicians and radiologists view images and DICOM-SR results from WSs by requesting the Data Grid Web server through the GAP (right), which fetches images, and CAD DICOM-SR data (3,4), and perform data mining using either HTTPS or TCP communication protocol (5). Data Grid provides both reliability and redundancy of images and DICOM-SR, and allows secured multiple user-accesses.

18.7.3 Computational Services in Data Grid

In Chapters 8 and 9, computational services architecture in the Data Grid, using the Globus Toolkit 4.02, was introduced, mainly for storage, and used mostly for data transfer and storage services, although other computational services in the Globus Toolkit are readily available. In the grid environment, an application component in computing can be implemented in different source files, each running in a different type of target architecture. Exact replicas of the executable file can be stored in many locations, which helps to reduce execution time. Data files can also be replicated in various locations. Each file has a description of its contents in terms of application-specific metadata. The metadata service, including the catalog service (see Chapter 8, Figure 8.4), responds to queries based on application-specific metadata and returns the logical names of files containing the required data, if they already exist. Given a logical file name that uniquely identifies a file without specifying a location, the replica location service (RLS) (Chapter 8, Figure 8.4) can be used to find the physical location for the file on the grid.

Figure 18.20A shows the operation architecture of the computational services in the grid environment. First, the client requests resources from monitoring and discovery system (MDS) server in the core middleware (step 1), which manages the resources and distributes the jobs to the computational services. The index service in the MDS finds resources appropriate to the requirements of application components and notifies the client to send the application to the grid resource allocation and management (GRAM) service (step 2). The GRAM service acknowledges MDS after it receives the application (step 3). After the GRAM service receives the application, jobs that are completely specified for execution are sent to schedulers that manage the resources and monitor execution progress. Execute acknowledges MDS server, the completion of the job in step 3, which in turn notifies the client (step 4).

18.7.4 Utilization of Data Grid Computational Service for Bone Age Assessment for Children

When BAA CAD becomes a daily clinical tool, many centers in pediatric radiology will use it as a method of subjective BAA for children. BAA CAD does require extensive computing that fits into the domain of the Data Grid for storage and computational services in the Globus for image processing. Following the discussion on BAA of children using the CAD, we model the computational aspect of the CAD BAA based on the Data Grid architecture,

which subdivides the entire hand image into multiple regions of interest, including six epimetaphyseal ROIs from three phalanges, the carpal bones ROI, and the wrist joint ROI. These ROIs are processed by remote grid resource nodes; all results are merged together through the Data Grid MDS server. For a child's hand image submitted to the Data Grid computational service, the overall operation workflow BAA is as shown in sequences 1, 2, and 3 in Figure 18.20C.

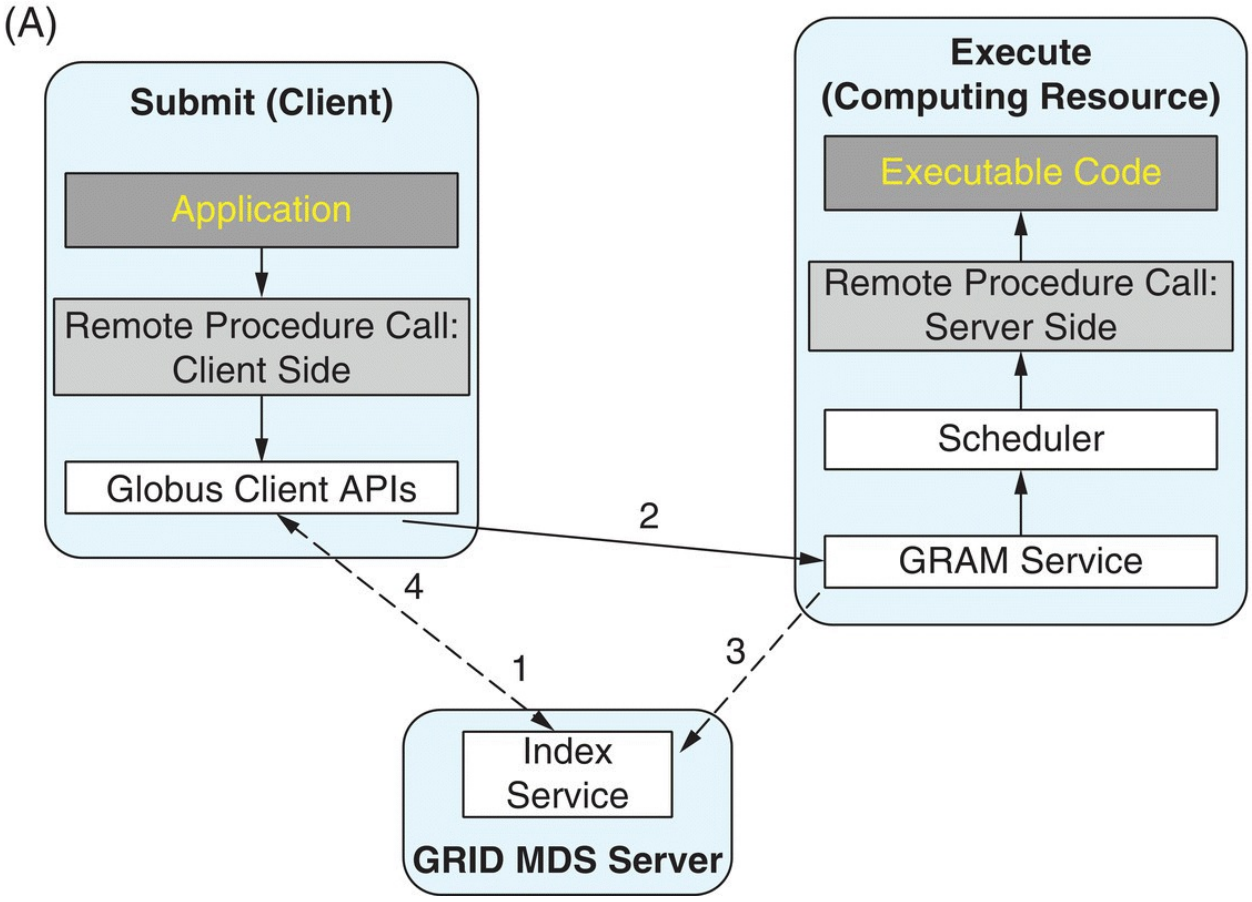

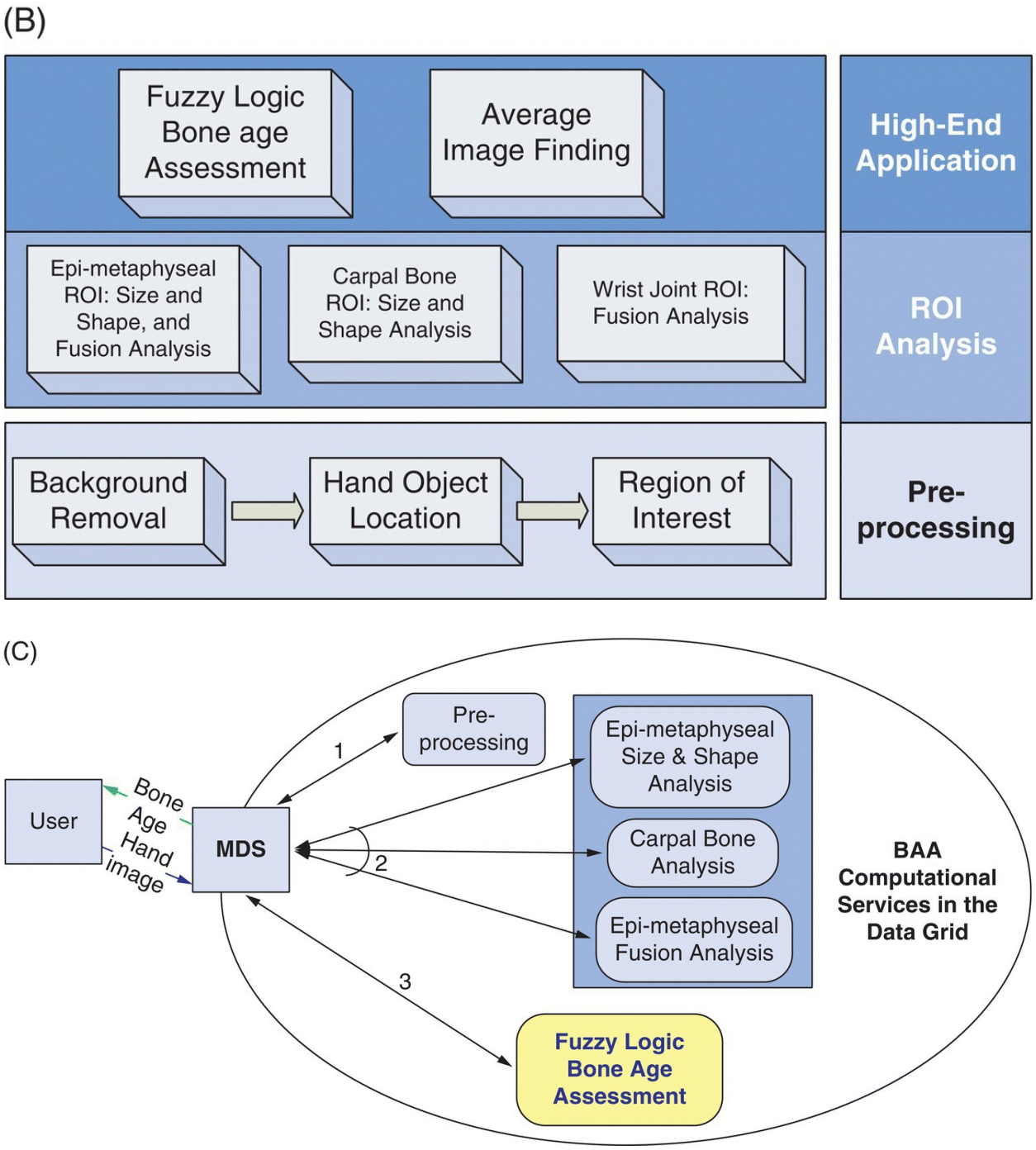

Figure 18.20 (A) Operation architecture of a computational grid. Numerals represent the workflow. (B) Three-layer procedure of BAA CAD. (C) Operation workflow of BAA computational services. The MDS allocates the computation requirements according to the available resources in the Data Grid. Numerals represent the workflow. API: application program interface; GRAM: grid resource allocation and management; ROI: region of interest.

18.8 Research and Development Trends in CAD–PACS Integration

Currently, CAD and PACS are two separate independent systems with only minimal communications between them. In Chapter 16, the concept of the CAD–PACS Integration toolkit as a universal method to push PACS and informatics data to CAD for computation was first introduced. The toolkit utilizes HL7 standards for textual data and the DICOM standard for imaging, so that it follows the industrial standard for data format and communications. The method needs the DICOM-SR standard to reformat CAD results in a SR template so that they can be integrated as a component in the DICOM data mode for viewing on the PACS WSs. It also uses three IHE workflow profiles: key image note (KIN), simple image and numeric report (SINR), and post-processing workflow profiles (PWF), to facilitate data transmission and communication in clinical workflow. In Chapters 17 and 18, two clinical examples: small acute intracranial hemorrhage and BAA of children using the CAD method are presented. How to use the CAD–PACS toolkit and to illustrate how to integrate existing CAD results into PACS daily clinical operation are discussed.

PACS-based imaging and informatics is a mature healthcare technology that continues to accumulate tremendous amount of imaging data daily. Unfortunately, the vast majority of this data in DICOM PACS is barely utilized, except for daily clinical service and some surgical applications.

There are many other advantages for integrating CAD results with PACS-based imaging informatics. CAD is a growing field, its applications ranging from specialties covering the chest to breast, colon, brain, liver, skeletal, and vascular disease. Doi, in his 2008 survey, reports that the number of presentations in CAD at the Annual Radiological Society of North America Scientific Assembly increased from 59 in 2000 to 227 in 2008. From the viewpoint of a CAD developer, PACS has tremendously large databases that can help to improve further the research and development of the new CAD methods. Integrating CAD results adds to these databases by providing quantified results that were previously unavailable through the standard DICOM image of a PACS study.

Because of the rich content in the DICOM-SR, it benefits CAD developers to produce a comprehensive and standardized results, findings, and quantitative values in DICOM-SR format. The DICOM standard and SR template can guide CAD developers in applying their knowledge to build high-quality and valuable reports for many other purposes.

Post-processing of medical images generated by imaging modalities is often done to enhance their diagnosis values. Post-processing of medical images is different from CAD in the sense that it produces some form of display, some quantitative measurements, but seldom provides direct detection and/or diagnosis. To this day, there are new technologies available for quantitative measurements obtained from post-processing or CAD that still reside within the post-processing WS or the CAD server in the clinical environment. There has been some collaboration between post-processing and CAD manufacturers with PACS manufacturers to improve PACS workflow by providing an integrated PACS WS. However, the integration has resulted in poor image quality performance and a return to stand-alone post-processing WSs.

With the introduction of the CAD–PACS toolkit, even these results could be converted to the DICOM-SR format and could be made readily available for direct query by PACS WS, thus revolutionizing clinical workflow from single-event patient-based queries to longitudinal-based queries on valuable metadata and quantitative measurements, such as the BAA of children discussed in this chapter.

The trend of CAD and PACS integration is to incorporate CAD findings and DICOM key image referencing into its DICOM-compliant databases and services in the form of DICOM-SR data objects. By way of DICOM-SR, content-based query/retrieval of DICOM imaging studies can be performed based on quantitative findings rather than patient identification and/or disease category. Query/retrieval of content-based imaging data can be advantageous for medical imaging research and clinical practice.

Acknowledgements

The Bone Hand Atlas project was supported by the National Institutes of Health (R01 LM 06270 and R01 EB 00298, May 1997–March 2008) for the development of the Digital DHA. Many faculty students and fellows had been involved, and supported this project. To name a few, Ewa Pietka initiated the project when she was Assistant Professor at UCSF, currently Chairperson and Professor at Silesian University of Technology, Poland, and several of her post doctoral fellows and students developed the mathematics. Professor Gilsanz Vicente helped to collect more than 1400 child hand x-rays images at the Childrens Hospital, Los Angeles. Aifeng (Lucy) Zhang completed her PhD Dissertation as the last component of the DHA, and implemented the BAA system at the Childrens Hospital, USC for clinical use. The DHA is open to the

public and has been used by many researchers and clinical users around the world.

References

1 Greulich, W. and Pyle, S. (1959) *Radiographic Atlas of Skeletal Development of Hand Wrist*. Stanford, CA: Stanford University Press.

2 Gertych, A., Zhang A., Sayre, J., *et al*. (2007) Bone age assessment of children using a digital hand atlas. *Computerized Medical Imaging and Graphics*, 31, 322–331.

3 Roch, A., Rochman, C. and Davila, G. (1970) Effect of training of replicability of assessment of skeletal maturity (Greulich-Pyle). *Am J Roentgenol*, 108, 511–515.

4 King, D., Steventon, D., O'Sullivan, M., *et al*. (1994) Reproducibility of bone ages when performed by radiology registrars: An audit of Tanner and Whitehouse II versus Greulich and Pyle methods. *Br J Radiol*, 67, 848–851.

5 Cao, F., Huang, H., Piettka, E., *et al*. (2000) Digital hand atlas and web-based bone age assessment: System design and implementation. *Comput Med Imag Graph*, 24, 297–307.

6 Cao, F., McNitt-Gray, M., Pietka, E., *et al*. (1991) Computer-assisted phalangeal analysis in skeletal age assessment. *IEEE Trans Med Imag*, 10, 616–620.

7 Pietka, E., Kaabi, L., Kuo, M., *et al*. (2001) Computer assisted bone age assessment: image preprocessing and ROI extraction. *IEEE Trans Med Imag*, 20, 715–729.

8 Pietka, E., Gertych, A., Pospiech, S., *et al*. (2001) Computer automated approach to the extraction of epiphyseal regions in hand radiographs. *J Digit Imag*, 14, 165–172.

9 Zadeh, L. (1989) Knowledge representation in fuzzy logic. *IEEE Trans Knowl Data Eng*, 1, 98–100.

10 Mamdani, E. (1974) Application of fuzzy algorithms for control of simple dynamic plant. *Proc IEEE*, 121, 1585–1588.

11 Baldwin, J. (1981) Fuzzy logic and fuzzy reasoning. In: *Fuzzy Reasoning and its Applications* (E.H. Mamdani and B.R. Gaines, eds). London: Academic Press.

12 Zhang, A., Gertych, A. and Liu, B. (2007) Automatic bone age assessment for young children from newborn to 7-year-olds using carpal bones. *Comput Med Imag Graph*, 31, 299–310.

13 Zhang, A. (2007) A Computer-aided Diagnosis (CAD) Method Combining Phalangeal and Carpal bone Features for Bone Age Assessment of Children, PhD Dissertation, Department of Biomedical Engineering, University of Southern California, May.

14 Zhang. A., Sayre, J.W., Vachon, L., Liu, B.J. and Huang, H.K. (2009) Cross-racial differences in growth patterns of children based on bone age assessment. *J Radiology*, 290(1), 228–235.

15 Huang, H.K. (2010) *PACS and Imaging Informatics: Principles and Applications*, 2nd Edition. Hoboken, NJ: Wiley & Blackwell, pp. 840–845.

16 Ma. W. and Manjunath, B. (1995) A comparison of wavelet transform features for texture image annotation. *Int Conf on Image Process*, 1995.

17 Ma, K.V., Zhang, A., *et al*. (2009) An online Real-time DICOM Web-based Computer-Aided Diagnosis System for Bone Age Assessment of Children in a PACS Environment, *SPIE*, February, pp. 58–65.

18 Ma, K.V., Moin, P., Zhang, A., *et al*. (2010) Computer aided Bone Age Assessment for Ethnically Diverse Older Children using Integrated Fuzzy Logic System, *SPIE*, February, pp. 84–92.

19 IPIlab: http://ipilabmysql.usc.edu/newindex.php

Further Reading

Mora, S., Boechat, M.I., Pietka, E., Huang and H.K., Gilsanz, V. (2001) Skeletal age determinations in children of European and African descent: Applicability of the Greulich and Pyle standards. *Pediat Res*, 50(5), 624–628.

Ontell, F.K., Ivanovic, M., Ablin, D.S. and Barlow, T.W. (1996) Bone age in children of diverse ethnicity. *American Journal of Roentgenology*, 167, 1395–

1398.

Pietka, E., Gertych, A., Pospiech, S., Cao, F., Huang, H.K. and Gilsanz, V. (2001) Computer assisted bone age assessment: image processing and epiphyseal/Metaphyseal ROI extraction. *IEEE Trans Med Imag*, 20, 715–729.

Pietka, E., Pospiech, S., Gertych, A., Cao, F., Huang, H.K. and Gilsanz, B. (2001) Computer automated approach to the extraction of epiphyseal regions in hand radiographs. *J Digit Imag*, 14, 165–172.

Pietka, E., Pospiech-Kurkowska, S., Gertych, A., Cao, F. and Huang, H.K. (2002) Computer-assisted bone age assessment: Image analysis and fuzzy classification. *Radiology*, 225, 751.

Roche, A.F., Roberts, J. and Harnill, P.V. (1975) Skeletal maturity of children 6–11 years: Racial, geographic area and socioeconomic differentials. In: *National Health Survey*, Rockville MD: Health Resources Administration, National Center for Health Statistics, pp. 1–38.

Ross, T. (2004) *Fuzzy Logic with Engineering Applications*, 2nd edition. Hoboken, NJ: Wiley.

Zadeh, L.A. (1988) Fuzzy logic. *Computer*, 1(4), 83–93.

Zadeh, L.A. (1965) Fuzzy sets and systems. *Information and Control*, 8, 338–353.

Zhang, A., Gertych, A. and Liu, B.J. (2007) Automatic bone age assessment for young children from newborn to 7-year-old using carpal bones. *Comput Med Imag Graph*, 31, 299–311.

Zhang, A., Uyeda, J., Tsao, S., Ma, K., Vachon, L., Liu, B. and Huang, H.K. (2008) Web-based computer-aided diagnosis (CAD) system for bone age assessment (BAA) of children. *Med Imag: PACS and Imaging Informatics*, vol. 4919.

Zhang, A., Zhou, Z., Gertych, A., Liu, B., Zheng, X. and Huang, H.K. (2006) Integration of bone age assessment CAD results with the PACS diagnostic workflow utilizing DICOM structure report. Scientific Poster, RSNA.

Zhang, A., Sayre, J.W., Vachon, L., Liu, B.J. and Huang, H.K. (2009) Cross-racial differences in growth patterns of children based on bone age assessment. *J*

Radiol, 290(1), 228–235.

Zhou, Z., Huang, H.K., Liu, B.J., Cao, .F, Zhang, J., Mogel, G. and Law, M. (2004) A RIS/PACS simulator with Web-based image distribution and display system for education. *Proc SPIE*, 5371, 372–381.

Zhou, Z., Huang, H.K., Cao, F., Liu, B.J., *et al*. (2003) An educational RIS/PACS simulator with Web-based image distribution and display system: InfoRad Exhibit, 89th Scientific Assembly and Annual Meeting, *Radiol Soc N Am*, November 30–December 5, p. 796.

Zhou, Z., Law, M., Huang, H.K., Cao, F., Liu, B. and Zhang, J. (2002) An educational RIS/PACS simulator. InfoRAD Exhibit. 88th Scientific Assembly and Annual Meeting, *Radiol Soc N Am*, December 1–6, p. 753.

Zhou, Z., Le, A., Liu, B. and Huang, H.K. (2007) PACS-CAD toolkit for integrating an independent CAD workstation to diagnosis workflow. *Proc SPIE Med Imag*, 6516, 1–8.

Zhou, Z., Liu, B.J., Huang, H.K. and Zhang, J. (2005) Educational RIS/PACS simulator integrated with the HIPAA compliant auditing (HCA) toolkit. *Proc SPIE*, 5748, 491–500.

Zhou, Z., Liu, B.J., Huang, H.K. and Zhang, J. (2004) Educational RIS/PACS simulator integrated with HIPAA compliant architecture (HCA) for auditing: InfoRad Exhibit. 90th Scientific Assembly and Annual Meeting, *Radiol Soc N Am*, November 28–December 3, p. 827.

Zhou, Z., Liu, B.J. and Le, A. (2007) CAD-PACS integration tool kit—based on DICOM screen capture (SC) and structured reporting (SR) and IHE workflow profiles. *J Comput Med Imag Graph*, 31(4–5), 346–352.

19
Intelligent ePR System for Evidence-Based Research in Radiotherapy

CHAPTER MENU

19.1 Introduction

19.1.1 Prostate Cancer and Proton Therapy

19.1.2 Challenges of Proton Therapy

19.1.3 Rationale for an Evidence-Based Electronic Patient Record System

19.2 Proton Therapy Clinical Workflow and Data

19.2.1 Workflow

19.2.2 Treatment Protocols

19.2.3 Defining Clinical Outcomes

19.3 Proton Therapy ePR System

19.3.1 System Architecture

19.3.2 Data Model

19.4 System Implementation

19.4.1 Web Technology

19.4.2 Database

19.4.3 Laboratory Implementation

19.5 Results

19.5.1 Data Collection

19.5.2 Characteristics of Clinical Information from Collected Data

19.5.3 Example of Knowledge Discovery of Evidence-Based Research

19.5.4 A Clinical Scenario

19.6 Conclusion and Discussion

19.6.1 The ePR System

19.6.2 Intelligent Decision Support Tools

19.6.3 Clinical Scenario Demonstrating Knowledge Discovery and Evidence-Based Treatment Plan

Acknowledgment

References

19.1 Introduction

19.1.1 Prostrate Cancer and Proton Therapy

Prostate cancer is a type of cancer that forms in tissues of the prostate (a gland in the male reproductive system found below the bladder and in front of the rectum). Prostate cancer usually occurs in older men. The National Cancer Institute (NCI) has estimated that there were 192 280 new cases and 37 360 deaths from prostate cancer in the United States in the year 2009 [1].

One of the methods to treat prostate cancer is proton therapy, which uses energized charged particles, protons, to deliver a dose to the target region. Protons are energized to specific velocities, which determine where they will deposit maximum energy within the body to destroy cancerous cells, allowing for maximum dose to the target region while minimizing dose to surrounding tissues. This is due to the fact that the proton depth dose (Bragg peak) is inversely proportional to the square of the particle velocity. This translates to fewer doses to normal healthy tissue in the body while depositing most of the energy within the target tumor located at a certain depth within the body. In addition, proton beams have no exit dose, which also minimizes damage to healthy tissue beyond the target tumor. However, the Bragg peak is just a peak or a spike that may only cover a few millimeters of tissue; therefore, a modulator is used to spread out the peak to the width of the target tumor. Figure 19.1 shows doses achieved by a proton beam in comparison to an x-ray beam in conventional radiation therapy [2]. The depth dose curve of the thin pencil of beam of protons is shown in red. The weighted superposition of proton beams of different energies (Bragg peaks with different proton ranges) makes it possible to deposit a homogenous dose in the target region. The resulting range modulated proton beam distribution is called spread out Bragg peak, shown in blue. This peak allows the dose to be confined around the tumor and the drop off right after the target, sparing the healthy tissue beyond it. The depth dose curve of an X-ray

beam, which shows the characteristic exponential decrease of the dose with depth, is shown in green.

Proton therapy is especially effective for types of cancer that require a controlled high concentration dose and tumors that are close to sensitive tissue. Some examples of the types of cancer treated include: prostate, brain, spinal cord, head and neck, base of skull, eye, lung, and tumors in children.[3].

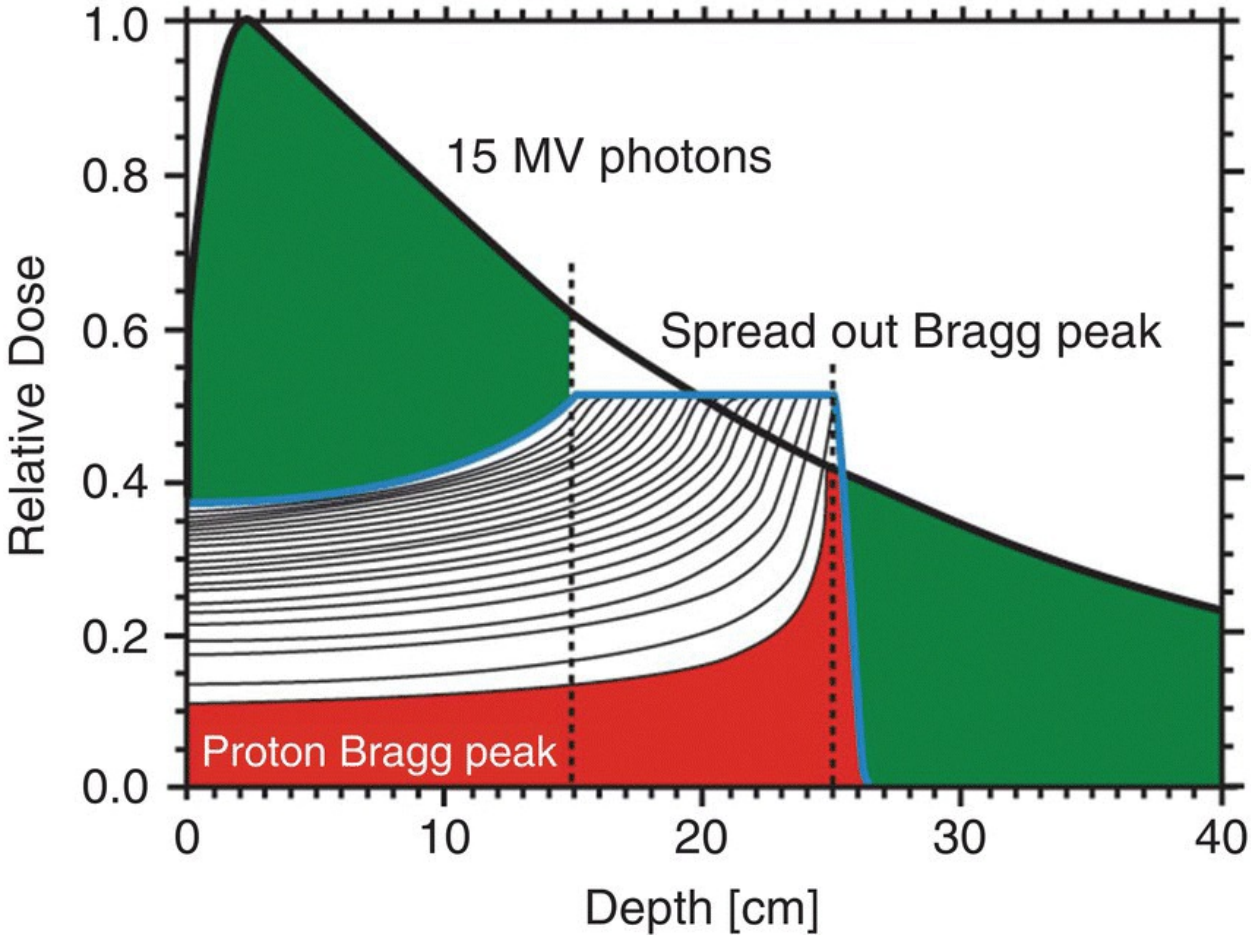

Figure 19.1 Graph showing a comparison between photon depth dose and proton depth dose. The depth dose curve of the thin pencil of beam of protons is shown in red. The blue line demonstrates the spread out proton beam Bragg peak, which allows the dose confined around the tumor and the drop off right after the target, sparing the healthy tissue beyond it. The depth dose curve of an x-ray beam (the modality used today in most hospitals for radiation therapy), which shows the characteristic exponential decrease of the dose with depth is shown in green.

19.1.2 Challenges of Proton Therapy

19.1.2.1 Uncertainty of Dose and Treatment Schedule

Conventional x-ray radiation therapy, given in sufficient doses, can control many cancers. However, because of the difficulty for physicians to adequately conform the irradiation pattern to the cancer, healthy tissues may receive a similar dose and can be damaged. Consequently, a less than desired dose is frequently used to reduce damage to healthy tissues and to avoid unwanted effects. On the other hand, in proton therapy, the treatment usually has greater tumor control than conventional radiation therapy. The power of protons is that higher doses of radiation can be used to control and manage cancer, while significantly reducing damage to surrounding healthy tissue and vital organs. Unfortunately, the tumor is not just a separate target that can be irradiated without side effects to other healthy tissues of nearby critical organs. In most cases, the tumor is in a position that is very close to other critical organs so that the acceptable margin is relatively small. Therefore, in close proximity, these critical organs are still exposed to a certain amount of radiation dose.

Similar to conventional radiation therapy, proton therapy(PT) has a long and established role in the curative treatment of organ-confined prostate cancer [4]. However, the optimal radiation dose and treatment schedule still remain unknown [5].

19.1.2.2 High Cost of Proton Treatment

Despite the superior physical characteristics of the proton, which allows the beam to radiate precisely to specific tumor targets without significant exit dose and minimizing damage to healthy tissue near the tumor, PT has limited popularity among other types of radiotherapy owing to the complexity in management and cost of proton facilities.

19.1.2.3 Data Scattered Among Many Systems

In general, there are different stand-alone and proprietary information systems in a proton therapy department. Each system has its own data “storage area” and proprietary data formats. Typically, the treatment plans are stored in a treatment planning system (TPS), treatment records stored in another information system or patient chart, and digital images stored in separate digital imaging devices. The patient’s medical history and initial treatment data are usually stored in an oncology information system. The patient’s outcomes data are usually collected and stored in another information system that is not readily available to physicians or researchers. Currently, all of these data is linked by paper records

or patient charts. Moreover, it is common practice for the hardcopy film images to be stored separately in the film library. Therefore, just like the case of radiology film, if the hard copy record is misplaced or lost, the patient's treatment information would not be available for review. Even more disturbing is that the treatment plans from an old TPS cannot be retrieved for comparison after a system upgrade, making historical review challenging.

19.1.2.4 Challenges in Data Comparison and Outcomes Analysis between Multiple Treatment Protocols

Proton therapy, along with other radiation treatment methods, faces common problems of disparate data as well as a lack of information technology readiness. Archiving, visualizing, and distributing treatment plans and patient outcomes is a big challenge for clinicians and researchers in the field. They require a system that can collect all relevant information for proton therapy treatment of prostate cancer. This system consolidates and makes centrally accessible all cancer patients' treatment related information. This information can be used to compare treatment plans and results of patients of the same treatment protocol or different treatment protocols, which ultimately improves treatment planning for new patients.

19.1.3 Rationale for an Evidence-based Electronic Patient Record System

Evidence-based decision making in medicine is an important subject in many therapeutic fields, including radiation therapy. Proton therapy is a promising radiation therapy modality, but clinical information about the outcomes observed is still insufficient to support the decision to use this expensive modality. Therefore, the development of an electronic patient record (ePR) system that supports the collection of relevant data, feeds them into centralized databases, and allows the synthesis of new evidence is an important task that has not yet been explored.

19.1.3.1 Proton Therapy ePR System

The ePR is an emerging concept to provide support for the hospital or clinic-based healthcare information system. The ePR combines image data from an image repository called the picture archiving and communication system (PACS) with other information systems and clinical services. An ePR consists of five major functions:

1. Accepts direct digital input of patient data;
2. Analyzes across patients and providers;
3. Provides clinical decision support;
4. Supports outcomes analysis and patient and physician profiling; and
5. Distributes information across different platforms and health information systems [6].

The ePR consists of a data model derived from existing clinical workflow, a database, a Web server and a graphical user interface (GUI). In addition, the ePR provides storage and a method to collect all relevant patient data, which equips the clinician with tools to improve treatment planning and achieve the goal of minimizing radiation toxicity in prostate cancer patients, while ultimately improving the patient's quality of life. There is no such current system available or developed for proton therapy. In addition, an intelligent ePR system with centralized PT-related data can facilitate the efficiency of the proton therapy workflow by providing clinicians with the ability to view imaging studies, evaluate proton treatment plans, and explore treatment outcomes. Specifically, the PT ePR can help to minimize radiation toxicity in prostate cancer patients through the utilization of data mining and the treatment plan navigation tool.

19.1.3.2 Goals of the ePR

The goals of this intelligent ePR system for prostate cancer patients are:

1. to design a system based on the above specifications tailored to proton therapy;
2. to improve efficiency in data collection and integration to facilitate outcomes analysis with this system; and
3. to utilize knowledge extracted from the collected data to help clinical decision-making processes for a better treatment plan of prostate cancer patients treated with the new development of hypofractionation treatment protocol.

In short, the purpose of this chapter is to present a novel ePR that will support the systematic collection data, analysis data, and perform data mining (Chapter 16) from a particular radiation modality, including but not limited to proton therapy.

19.2 Proton Therapy Clinical Workflow and Data

19.2.1 Workflow

Figure 19.2 shows the general clinical workflow model for proton therapy at the James M. Slater, MD, Proton Treatment and Research Center, Loma Linda University. This workflow shows steps after the patient has been diagnosed with cancer, consulted with the physicians, discussed available treatments, and determined to treat the tumor with proton therapy. The workflow, as shown in Figure 19.2, describes general procedures involved in the entire treatment from when the patient enters the oncology department for consultation to follow-up after the treatment for prostate cancer, which is similar to the general workflow of conventional radiation therapy [7,8].

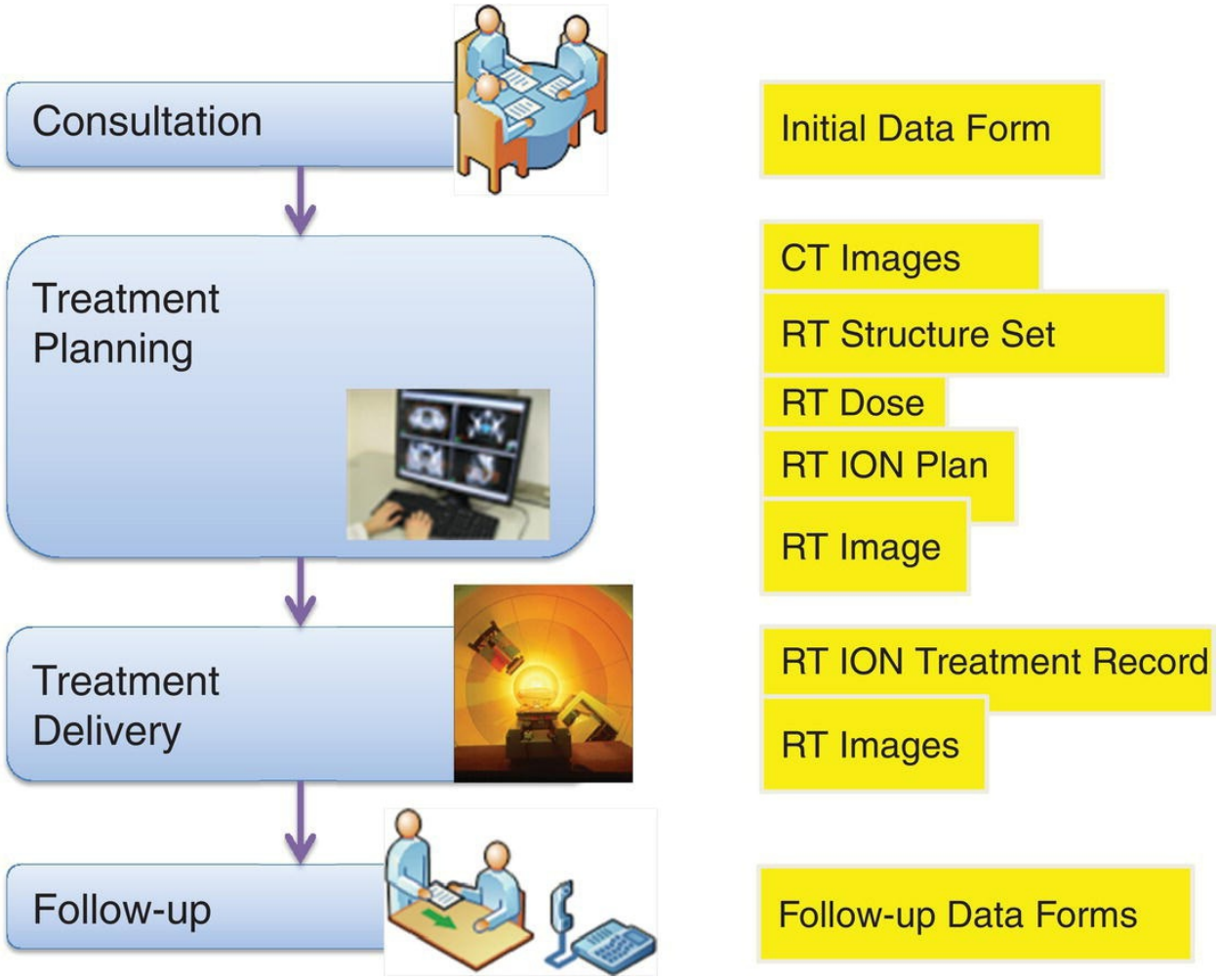

Figure 19.2 Illustration of the proton therapy workflow. Yellow boxes indicate the data (both DICOM objects and data forms) that are generated within the

workflow. CT: computed tomography; RT: radiotherapy DICOM object; RT-ION : radiotherapy ion, including protons and heavy ionized particles beam, DICOM object.

As shown in Figure 19.2 the yellow boxes indicate data generated and collected from the proton workflow. The data includes both textual data and DICOM objects, which is defined by the DICOM standard. Unless all equipment used in a department is from a single software vendor, it is necessary that images and other data should be transferable between different computing systems in a standardized fashion, so that it can be interpreted by different software applications. The DICOM standard facilitates interoperability of systems claiming conformance in a multi-vendor environment is the *de facto* standard for such data transfer in medical imaging and informatics. In addition to the DICOM standard formats for diagnostic images, such as CT, MR, US, etc., the DICOM standard has provided support for the transfer of radiotherapy-related data between devices found within and outside a radiotherapy department, by introducing seven DICOM-RT objects for x-ray radiotherapy (Supplement 11, 1996 and Supplement 29, 1998) and two more DICOM-RT-ION for proton therapy or ion therapy in general (Supplement 102, 2004) [7,8].

19.2.2 Treatment Protocols

External radiation beam therapy, including both x-ray and proton beam, has been used to treat more than 26 000 prostate patients in the United States annually [9]. Patients treated with conventional doses for prostate cancer receive the total dose in the range of 60–71 Gy. However, many studies suggest that the conventional dose is unable to eradicate prostate cancer in a significant proportion of cases, with a resultant increase in prostate-specific antigen (PSA) levels, secondary treatment, and, ultimately, clinical recurrence [10–12].

Many treatment protocols used in radiation therapy for prostate cancer need to go through an acceptance process to determine whether a protocol is adequate to deliver the total dose to the patient without new adverse effects or radiation toxicity. At the James M. Slater, MD, Proton Treatment and Research Center, the escalation dose treatment protocol, in which the current total dose has been increased to 81 Gy, has been utilized in clinical treatment for many years and this protocol has been proven to have minimum radiation toxicity compared with lower doses. The current practice is to give the patient one fraction, 1.8 Gy, of total dose each day, 5 days a week until the patient receives all prescribed dose. This treatment duration usually consists of 45 days, approximately 2 months.

The duration has been a problem for many patients, since most of them are not local. Another treatment protocol has been introduced and is undergoing evaluation and acceptance process. This new method, called hypofractionation dose protocol, allows patient to receive a higher dose per day, 3 Gy, for a total dose of 60 Gy; therefore, decreasing the total fractions of PT and the duration of treatment to nearly half [20].

In order to evaluate the new protocol for prostate cancer, therapists need to collect all the clinical information, images, and treatment plans data. The problem arises when the data are scattered among many systems. Furthermore, there is no system to collect all the data in one source for performing outcome analysis and quality assurance in treatment planning. The ePR is an effective system that provides a centralized archive for all data of prostate cancer patients treated with proton therapy.

19.2.3 Defining Clinical Outcomes

The outcomes of a treatment are generally measured by the radiation toxicity in addition to the local tumor control. Radiation toxicity is evaluated based on symptoms of the adverse effects developed after proton treatment and frequency or severity of these symptoms. The Cancer Radiation Therapy Program, National Cancer Institute, has published the Common Terminology Criteria for Adverse Events (CTCAE) (formerly known as the Common Toxicity Criteria) as standards used to grade, assign attribution, and report adverse effects or radiation toxicity experienced by patients on clinical trials. The latest version is CTCAE v.3, published on August 9, 2006, including all adverse events applicable to all oncology clinical trials, regardless of chronicity or modality [13].

For prostate cancer discussed in this chapter, adverse effects and symptoms exist in five categories, including dermatology/skin, gastrointestinal, renal/genitourinary, and sexual/reproductive function and constitutional symptoms, are collected at the James M. Slater, MD, Proton Treatment and Research Center to evaluate the radiation toxicity. In each category, there are many symptoms, in which each is described in five levels of frequency or severity. Each level is given a grade from 1 to 5, where grade 1 is the least toxicity and grade 5 is highest toxicity, normally resulting from death of a patient caused by the symptom. It is generally accepted in many studies that the highest grade toxicity of any of the nearby organs constitutes the overall radiation toxicity of the patient due to the proton therapy session.

19.3 Proton Therapy ePR System

19.3.1 System Architecture

The ePR is a Web-based system that complements the current TPS in a radiotherapy department. Its primary goal is to be integrated in the workflow of the current planning of prostate cancer radiotherapy, thus the ePR system should not be considered as a consolidation of all existing RT application software. The ePR system is designed with four main components: the data gateway, the ePR server, decision support tools, and visualization and display tools, shown in Figure 19.3:

A. The data gateway is responsible for receiving and queuing the data before the data is imported to the ePR server for storage and quantification. Two components of the data gateway is the DICOM module for receiving all DICOM objects and the non-DICOM module to handle other clinical data types, which are not covered in the DICOM standard currently, such as text data in initial data form and follow-up data forms.

B. The ePR server is the primary processing and monitoring engine of the whole ePR system. It provides the computational power for all modules and services, including storage, database, data quantification module, decision support tools, and future extra add-on modules. The ePR server also performs tasks to monitor and manage the entire system to ensure it is working properly.

C. Decision support tools utilize the processing modules and data residing inside the ePR server as an input for their applications. There are two decision support tools developed for the ePR system: i) the intelligent treatment plan navigator (ITPN) helps the user to evaluate treatment plans; and ii) the knowledge base (KB) data-mining search engine provides tools for the user to obtain and discover knowledge from previous patients' information in order to modify the treatment for new patients.

D. The visualization and display tools are the GUIs of the ePR, which facilitates user interactions with ePR tools to improve proton treatment plans and enhance patient outcomes.

The thick-line box in Figure 19.3 shows the architecture of the entire ePR system in which the modular design has taken into account the capability to add extra necessary modules in future, symbolized by the (…) in the figure.

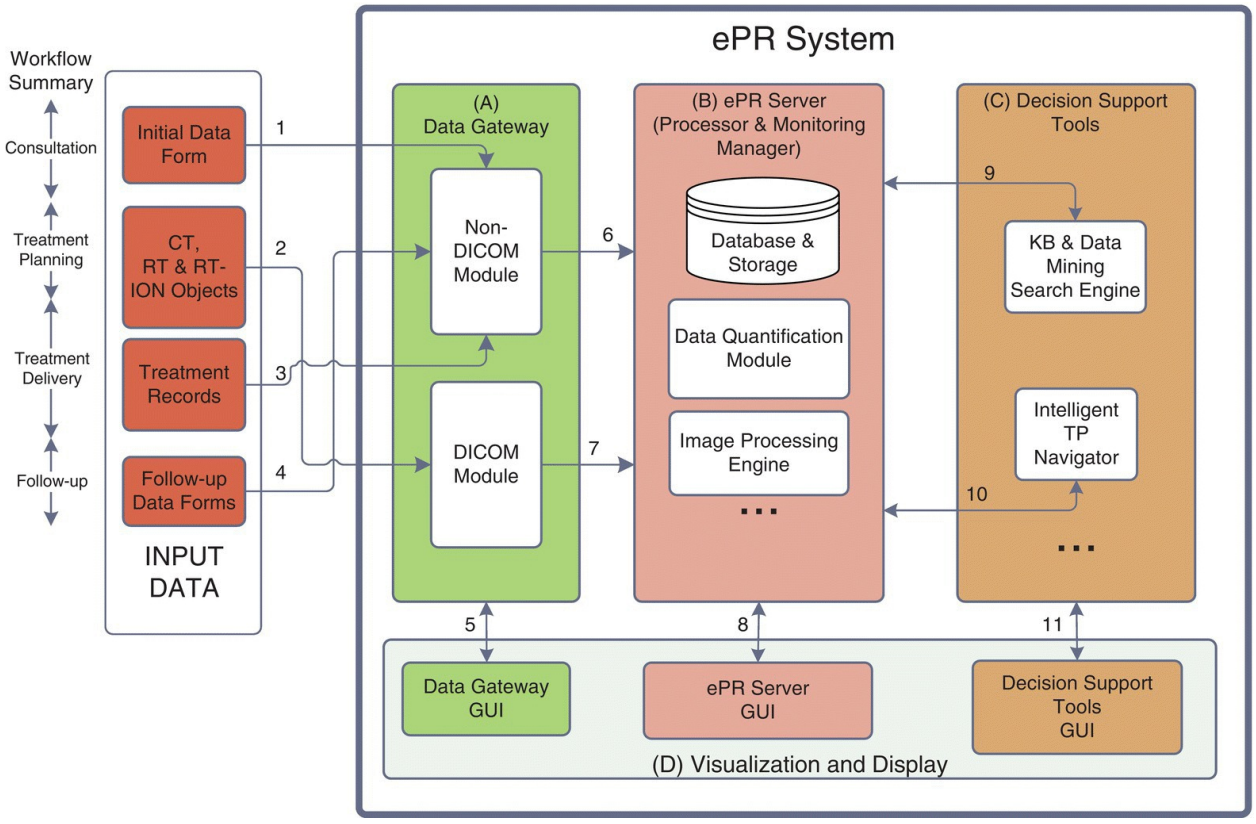

Figure 19.3 The architecture of the proton therapy ePR system and its data flow model. The data flow depicts a roadmap of how data can be integrated into the proton therapy ePR system. (A) The data gateway use to receive data. (B) The ePR server has the storage and database to archive and quantify stored data. (C) The decision support tools give users the ability to analyze and interact with treatment plans and patient data to improve treatment for future patient. (D) The visualization module contains all GUI for user interaction in data acquiring, data storage and display and decision support tools. The numerals represent the dataflow steps. CT: computed tomography; KB: knowledge base; RT: radiotherapy; RT ION: radiotherapy ions.

19.3.2 Dataflow Model

The design of the data flow model is based on the general proton therapy workflow, shown at the left of Figure 19.3. The right-hand side of the figure shows the four main components of the ePR: data gateway, ePR server, decision support tools, and visualization and display tools, described in the previous section.

19.3.2.1 Input Data

1. The initial data form is collected at the consultation section between the oncologist and prostate cancer patient. The data in this form will be input into the non-DICOM module residing within the data gateway.
2. The CT images and DICOM RT objects, such as structure set, plan, dose and image containing the digitally reconstructed radiographic image are sent from the TPS to the data gateway and received by the DICOM module. Another RT Image is the portal image sent from the digital portal system, residing in the treatment, to the DICOM module.
3. The treatment records collected from the patient chart are sent to the non-DICOM module.
4. The collected follow-up data forms are entered into the non-DICOM module in the data gateway.

19.3.2.2 Data Gateway

5. The data gateway GUI shows the status of data acquisition. The GUI is used to receive commands from physicists/oncologist/clinicians for data query/retrieve and entry.
6. The non-DICOM module converts treatment records to DICOM RT-ION treatment record objects, which are transferred to the DICOM module. Other clinical data from initial data forms and follow-up data forms, controlled by the non-DICOM module, are sent to ePR server for archival.
7. All DICOM objects from the DICOM module are sent to the ePR server for archival.

19.3.2.3 ePR Server

8. DICOM objects and data in the initial data form and follow-up data forms are displayed on the ePR server GUI. This GUI also shows the status of stored data and all the processes running on the ePR server.

19.3.2.4 Decision Support Tools

The decision support tools are user interactive and consist of the following:

9. The treatment plan data are accessed using the ITPN.
10. All the data residing in the ePR can also be accessed through the knowledge base and data mining search engine.

The clinicians and medical physicist can interact with the data and use the decision support tools through the Web-based decision support tools GUI.

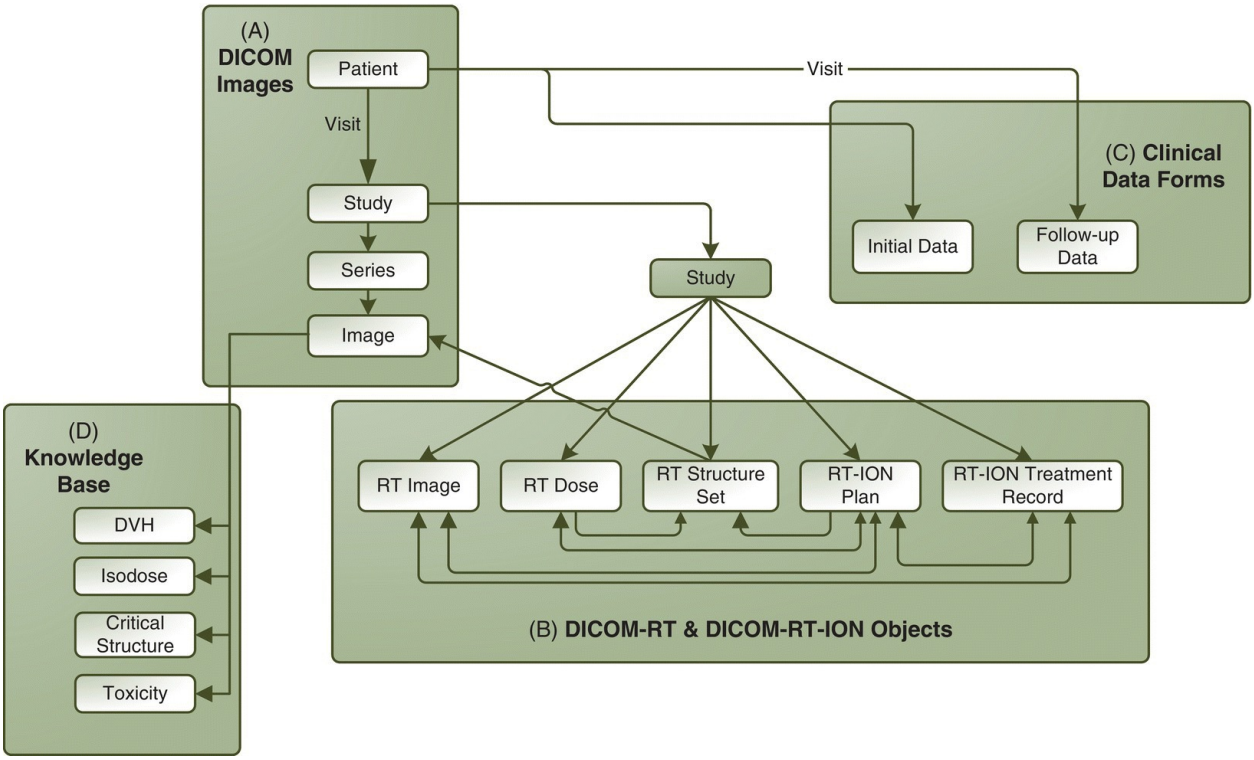

Figure 19.4 Data model consisting of three different primary data types: images, radiotherapy (RT) and RT-ION objects, and clinical data forms. The knowledge base data are added later when the primary data are analyzed and extracted for decision support purposes. DVH: dose–volume histogram.

Figure 19.4 shows the data model developed for the ePR system, which is based on the DICOM data model of the real world. This model depicts the relation of data objects organized for one patient consisting of four different primary data types (multimedia):

A. images;

B. RT and RT-ION objects;

C. clinical data forms; and

D. the knowledge base.

These are added after the extraction of the primary data and analysis from decision support tools.

19.4 System Implementation

19.4.1 Web Technology

The ePR system has been developed with current open source Web technology, image processing techniques, and DICOM Toolkit library. With the advantages of Web server-client architecture, including Apache Web server [14], MySQL database [15], hypertext pre-processor (PHP) scripting language [16] for the server side, and a combination of JavaScript, and ActiveX libraries for the client side, the patient data can be visualized through Web browsers and distributed across multiple locations by the local area network and Internet.

The WampServer version 2.0 [17], a package of Apache Web server 2.2, PHP 5.2 and MySQL 5.1, is utilized for development and distribution on a server running Windows operating system (OS). The development depends heavily on PHP scripts on the server side, jQuery JavaScript library [18], and Cascade Style Sheet (CSS) for graphical user interface on Web browsers.

19.4.2 Database

The database serving as the backbone of the ePR system has been developed using the Community version 5.1 of MySQL. The database was designed based on the data model shown in Figure 19.4, and consists of 68 tables: 8 tables for user management, 30 tables for DICOM data, 18 tables for DICOM knowledge extraction, and 12 tables for clinical data and knowledge discovery support.

19.4.3 Laboratory Implementation

The proton therapy ePR system for prostate cancer patients was developed at the Image Processing and Informatics Laboratory (IPILab), University of Southern California. The compliance and security requirements are satisfied, since the Web-based ePR system was developed based on the hypertext transfer protocol secured (HTTPS) and DICOM standards.

Figure 19.5 shows the hardware configuration. All the software components were installed in the ePR system, running Windows Server 2008, and verified to run properly. The TPS simulator, running Windows XP as well as the Odyssey treatment planning software non-clinical version 4.2, was used to test the data flow of DICOM objects. The client workstation (WS), running Windows 7 was used to verify data distribution, functionality of the electronic forms, treatment plan viewer, and search engine through the Web interface.

Figure 19.5 The system configuration at IPILab, University of Southern California for developing and evaluation.

19.5 Results

19.5.1 Data Collection

The ePR system is a centralized system that integrates all disparate data and provides a “one-stop-shop” for data of prostate cancer patients treated with proton therapy. All data utilized was collected at the James M. Slater, MD, Proton Treatment and Research Center, Loma Linda University Medical Center.

A prostate cancer patient’s dataset includes an Initial data form, CT images, a RT structure set object, a radiotherapy ion plan object, image objects, dose objects, a treatment record, and follow-up data forms. Table 19.1 summarizes all data collected from one patient. The ePR system contains a total of 39 patient datasets and 2 sample patients for testing and evaluation. These two sample patients were created by the expert in the field of proton therapy at the James M. Slater, MD, Proton Treatment and Research Center to depict sample cases of high radiation toxicity grade that has occurred at two organs at risk, bladder and rectum, in prostate cancer treatment. Therefore, a total of 41 patient datasets were imported into the ePR system for testing and evaluation.

Table 19.1 Proton therapy data collected from one prostate cancer patient.

Name	Media	Type	Digital Format	Originated Location
Patient Initial Data Form	Text	Pre-treatment Clinical Data	No	Research Spreadsheet
CT	DICOM	Image	Yes	PT Data Server

	Files			
RT Structure Set	DICOM File	Contours	Yes	TPS WS
RT-ION Plan	DICOM File	Plan	Yes	TPS WS
RT Image	DICOM File	RT Image	Yes	TPS WS
RT Dose	DICOM File	Dose Image	Yes	TPS WS
RT-ION Treatment Record[*]	DICOM File	Treatment Record	No	Patient Chart
Follow-up Data Form	Text	Outcome Data	No	Research Spreadsheet

[*] not currently collected since this data type is not significant for current status of the system

19.5.2 Characteristics of Clinical Information from Collected Data

As mentioned in Section 19.2.1, the initial patient data form allows the ePR to collect patient pretreatment data such as age, performance status, prior cancer, other diseases, prior prostate treatment, initial diagnosis with biopsies results, pathology condition (Gleason score), clinical T Stage (American Joint Committee on Cancer Cancer Staging Manual, 6th edition), and pre-diagnostic and pretreatment PSA level. These data are critical for physicians to evaluate treatment outcomes. An electronic form was developed so that the user can input the information directly into the ePR system and can be used in place of paper forms once the ePR system is deployed within the clinical environment. Table 19.2 summarizes the distribution of the main pretreatment clinical parameters collected on the initial data form.

Table 19.2 Summary of main pretreatment clinical data (n = 39 patients).

Characteristic	Mean	Standard Deviation	Range	Missing Data
Age (years)	62.59	8.85	33–75	0
Pretreatment PSA (ng/ml)	4.83	2.24	0.27–8.67	3

Gleason score	6	0	6–6	1
Percent biopsy scores (%)	23.12	21.35	5.26–100	7
Clinical State T Stage	T1c		T1a–T2c	1

The follow-up data form provides data for the ePR system regarding the treatment clinical outcome. These data includes PSA levels after the treatment and the five adverse event types identified in CTCAE to evaluate proton therapy radiation toxicity. The form collects patient's symptoms and frequency/severity of each symptom in five adverse events, which includes gastrointestinal, urinary, constitutional, skin, and sexual function. Adverse effects manifested within 90 days of initiation of proton therapy were considered "acute", with "late" being those manifested thereafter. For acute toxicity, the follow-up data were collected weekly after the first day of treatment for up to four weeks. For late toxicity, the form was collected every three months during the first two years, every six months for the subsequent three years, and annually thereafter. Similar to the initial data form, an electronic form was developed to have users input the clinical data on the follow-up data form directly to the ePR system through Web browsers. Table 19.3 summarizes follow-up characteristics in these forms.

Table 19.3 Summary of follow-up clinical data ($n = 39$ patients).

Characteristic	Mean	Standard Deviation	Range	Missing Data
Acute toxicity*	1.29	0.73	0–2	25
Late toxicity*	0.63	0.67	0–2	1
PSA 3 months after treatment (ng/ml)	2.1	1.27	0.02–5.4	6

* These data were calculated using the ePR

19.5.3 Example of Knowledge Discovery in Evidence-Based Research

The ePR system with integrated patient data provides an infrastructure for evidence-based research such as data integration and data-mining possibilities. The result included in this section is the utilization of knowledge that is collected and integrated to provide decision support in treating prostate cancer patients with a new hypofractionation treatment protocol in proton therapy. This decision

support capability of the ePR system with data-mining and navigation tools gives the physicists and oncologists the ability to optimize the treatment plan of a new patient, predict outcomes of the treatment plan in comparison to treatment plans of previous patients with the same protocol, and make necessary changes to improve the result.

An example of knowledge discovery utilizing the ePR system to improve treatment of a new patient based on treatment plans from previous patients is graphically explained using the step-by-step guideline shown in Figure 19.6.

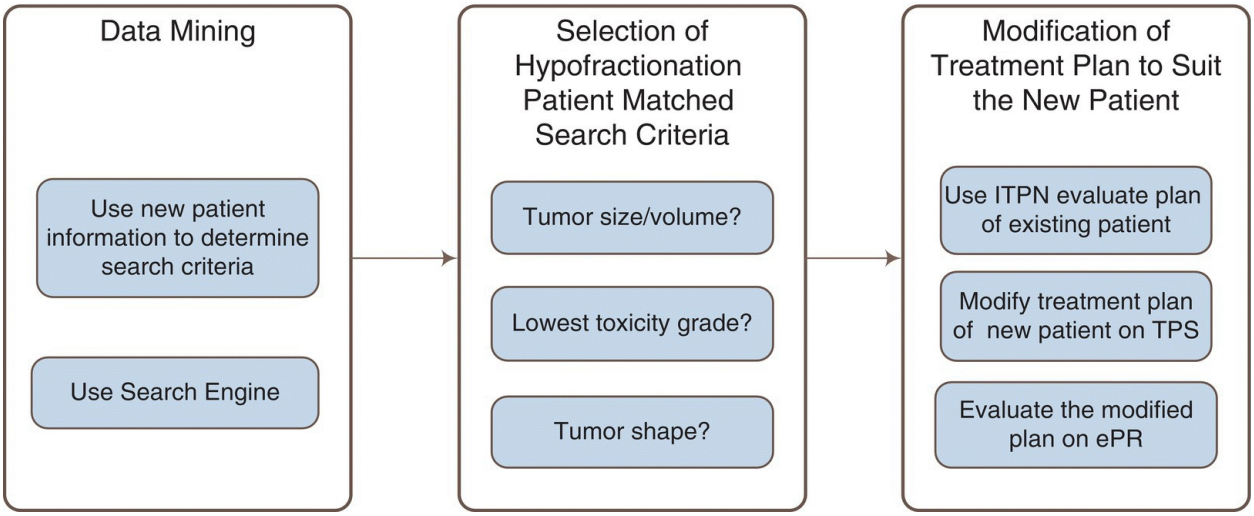

Figure 19.6 Step-by-step guideline of the clinical example. ePR: electronic patient records; ITPN: intelligent treatment plan navigator; TPS: treatment planning system.

19.5.4 A Clinical Scenario

Patient New (Pt. New), 60 years of age, was diagnosed with prostate cancer, and the decision was made to treat with proton therapy at LLUMC. The patient would prefer a shorter treatment time so he could go back home early. The patient chart shows that this 60-year-old patient was diagnosed with clinical stage T1c, entry PSA measurement of 5.2 ng/ml, and Gleason score of 6, which makes him eligible for hypofractionation protocol.

The oncologist at LLUMC introduces him to a new method that could save him 4 weeks of treatment, using 60 Gy of total dose and 3 Gy dose-per-fraction, in comparison with 9 weeks with the current clinically accepted proton therapy dose escalation protocol with a higher dose of 81 Gy. The patient is concerned whether this treatment would give him more side effects later, since the treatment time is shorter but dose is administered sooner and thus possibly not

allowing the patient to heal in time. The oncologist tries to optimize the plan for Pt. New with hypofractionation protocol using the ePR system, with the steps shown in Figure 10.6. These sections summarizes the steps involved and corresponding results (see [19] for more details).

19.5.4.1 Step 1: Data Mining

Table 19.4 shows Pt. New information in comparison with search criteria, which will be used to search for matched previous patients. The oncologist enters these querying parameters in the GUI of the search engine query command page, shown in Figure 19.7. The result of this search in the database described in Section 19.5.1 provides a list of seven patients, shown in Figure 19.8.

Table 19.4 Patient new information and treatment plan in comparison to search criteria.

	Patient New	**Search Criteria**
Age	60	55–65*
Clinical Condition	T1c	T1c
Gleason Score	6	<7*
Entry PSA Measurement	5.2 ng/ml	From 4.0 ng/ml and 6.0 ng/ml*
Total Dose	60Gy	60Gy
Dose per Fraction	3Gy	3Gy

*Wider search range to expand results to more closely match patients

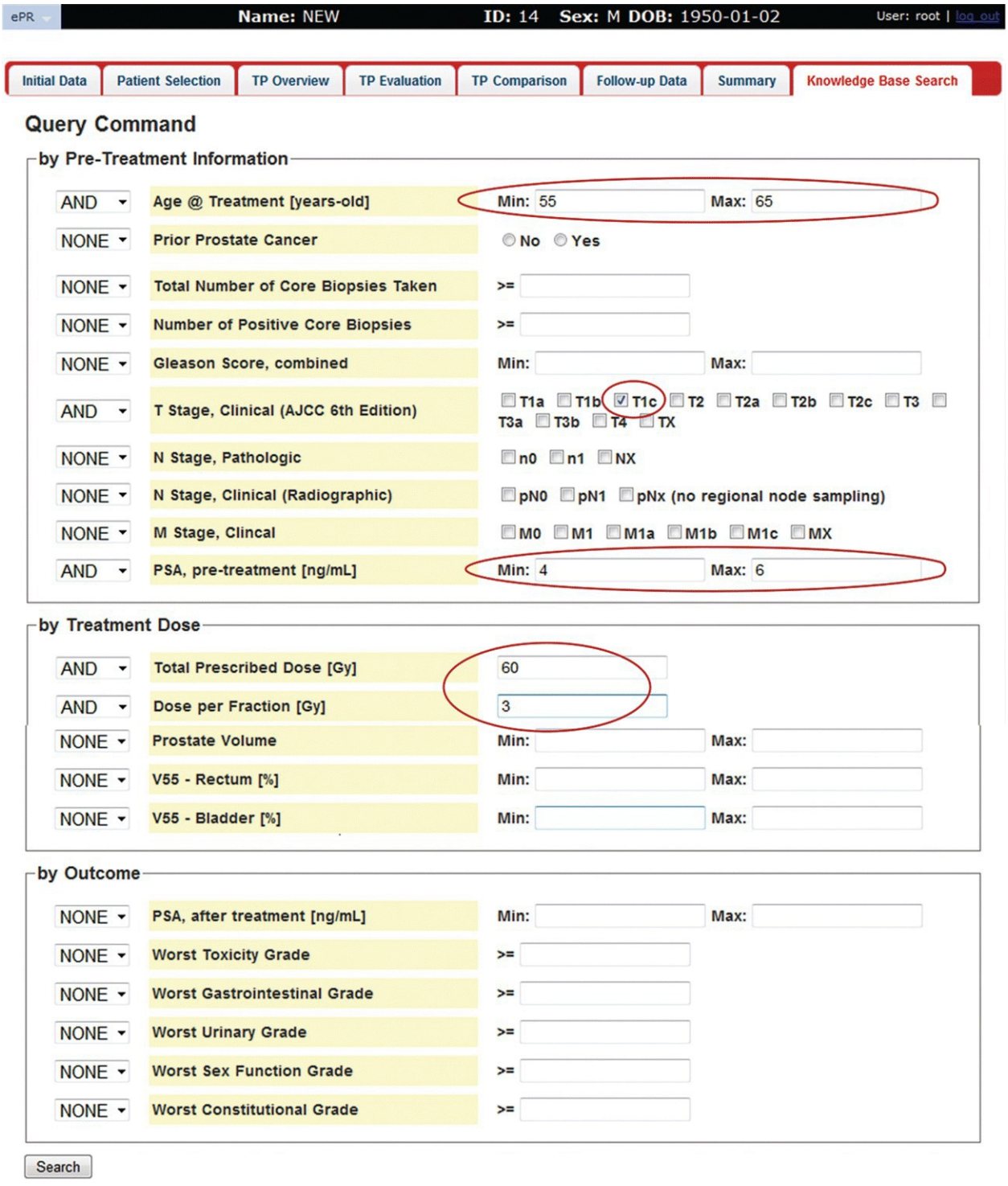

Figure 19.7 Screenshot of knowledge-based search engine query input for Patient New.

Number of results: 7

Search Results

NAME	AGE	PROSTATE VOLUME	RECTUM - V55	BLADDER-V55	TOXICITY GRADE
DEMO S	60	81.653	18.2	5.7	3
TWENTY-SIX H	59	47.79	5.6	1.7	2
THIRTY D	57	53.19	6.5	1.8	2
FOURTEEN S	56	70.11	8.5	2.2	1
EIGHTEEN B	63	66.713	4.4	2	0
TWENTY-ONE W	61	81.383	7.9	5.7	0
FORTY-TWO A	63	122.963	7.7	2.6	0

Figure 19.8 Screenshot of knowledge-based search results displaying previous patients that have undergone new hypofractionation treatment protocol who have toxicity grades ranging from 0 to 3.

19.5.4.2 Step 2: Selection of Hypofractionation Patients Matched Search Criteria

Once the query results are returned, the treatment plan will be chosen based on Pt. New's tumor size/volume, toxicity grade, and tumor shape. First, the tumor volume of Pt. New is 81 cc; hence, two patients among the seven matched this criterion of having similar prostate volumes, shown with red ellipses in Figure 19.8 (Pt. Demo and Pt. 21). These two matched previous patients have different toxicity grades, 3 and 0, but both are utilized to help the physicist to evaluate the treatment. Second, the patient who had lowest toxicity would be selected first. Therefore, Pt. 21, who had a positive outcome of rectal toxicity of 0, is the first patient to be utilized to create treatment plans for Pt. New. Lastly, when the tumor size is taken into consideration, the plan of Pt. 21 could not be used for Pt. New, because the shapes of the lower boundaries of the prostate tumors are different. Figure 19.9 shows the different shape of Pt. New's prostate (left), wrapping on top of the rectum, and Pt. 21's prostate (right). The oncologist rejects to adopt Pt. 21's treatment plan for Pt. New, because it would not provide good tumor coverage to achieve optimal tumor control, as the proton beam for Pt. New would be radiated to the two hip joints and create a possible higher toxicity grade (see green arrows in Figure 19.9).

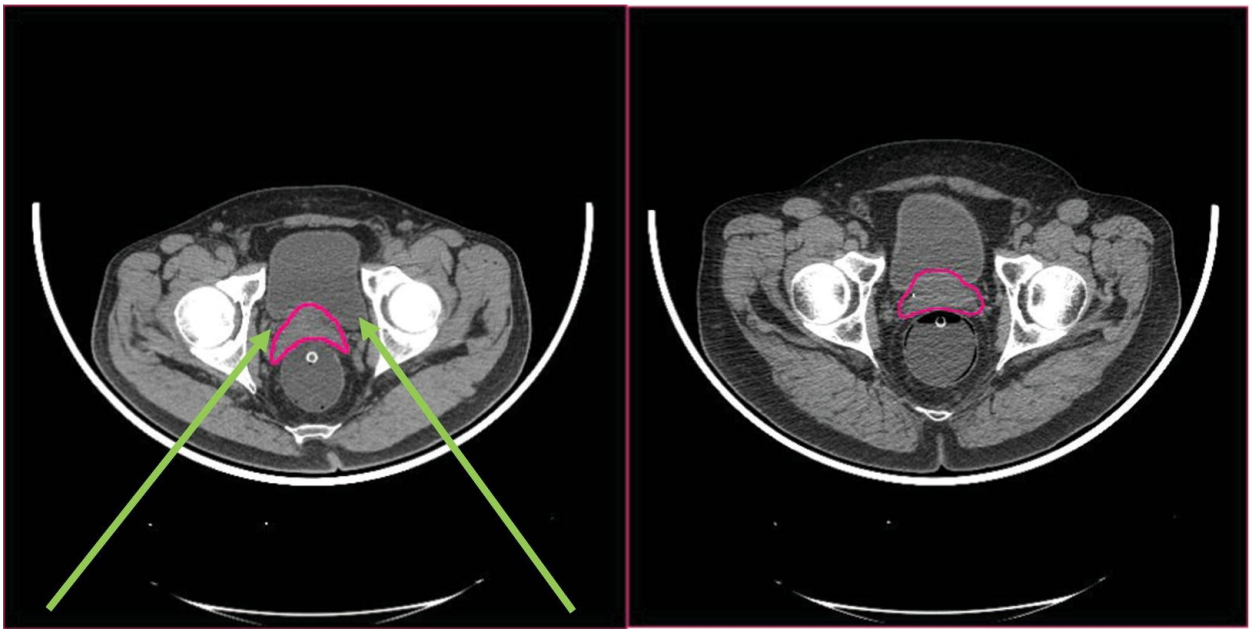

Figure 19.9 Difference in the shapes of the prostates, red contours, of Pt. New (left) and Pt. 21 (right).

19.5.4.3 Step 3: Modification of Treatment Plan to Suit the New Patient

Next, the oncologist considers Pt. Demo. However, while reviewing the results of the various treatment plans mined from the database, the treatment plan of Pt. Demo with toxicity grade 3 that had matching criteria with Pt. New was a concern. His treatment is loaded to the treatment plan evaluation page to evaluate Pt. Demo treatment plan, which is the first task in the right-hand box of Figure 19.6. The dose parameters from this treatment plan were utilized to guide the physicist in Pt. Demo's treatment to avoid a possible negative outcome of high toxicity. This GUI for the treatment plan evaluation page was implemented so that the physicist and oncologist could utilize knowledge discovered from the DICOM-RT objects as well as the quantified data to evaluate treatment plans. Also, from the treatment plan of Pt. Demo, the physicist learned that the margin of beam around the prostate was 10 mm. Figure 19.10 displays the beam configuration captured from the TPS system, and the beam margin around the prostate is in the red oval.

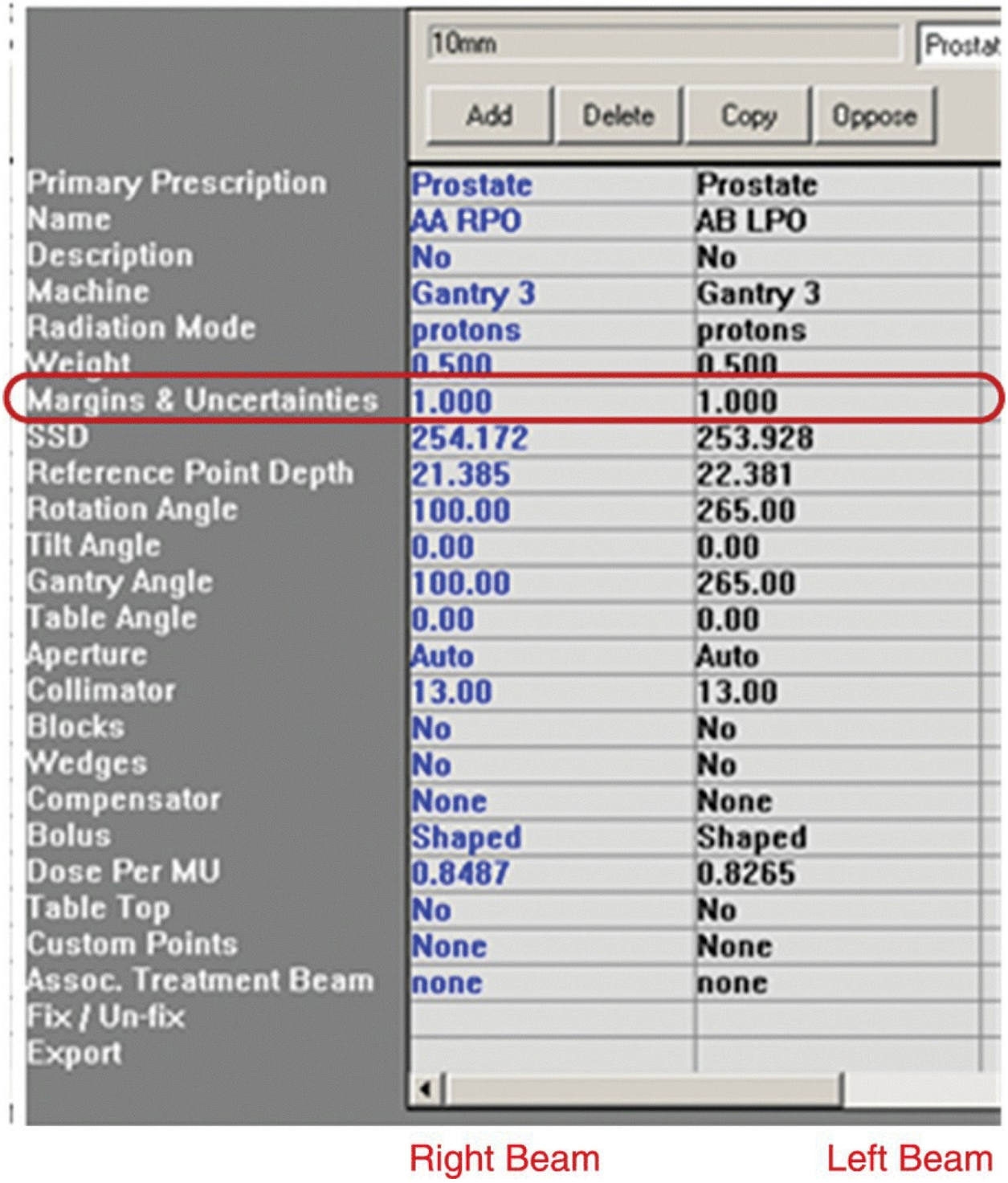

Figure 19.10 Screenshot of beam margin configuration of Pt. Demo showing the beam margin of 10 mm around prostate.

Upon reviewing the existing treatment plan, selected CT slices were showing areas of potential high dose to critical structures, i.e. rectum and bladder, using

the ITPN tool, as in Figure 19.11. Changes are then made to the treatment plan of Pt. New to try to reduce the quantitative amount of the rectum's and bladder's dose volume that would receive higher proton dose, which is the second task in the right-hand box of Figure 19.6. These changes are performed in the TPS and the results are sent to the ePR. In the modified plan of Pt. New, the beam margin was adjusted to 7 mm from the border of prostate.

Table 19.5 shows the dose volume difference in Pt. New' treatment plan: the maximum volume percentages of adjacent critical structures, which receive 60 Gy have been reduced from 6.4% to 1.9% for the rectum, and from 1.6% to 0% for the bladder. Note that the volume percentages in both plans are less than 15% of the dose limits for rectum and bladder. This reduction promises a better outcome for Pt. Demo with radiation toxicity of less than grade 3.

Table 19.5 Comparison of volume percentage of the tumor target and critical structures between previous plan and modified plan of Patient New.

	Prostate at 55Gy	**Rectum at 60Gy**	**Bladder at 60Gy**
Previous Plan	>95%	6.4%	1.6%
Modified Plan	>95%	1.9%	0%
Limit*	n/a	<15%	<15%

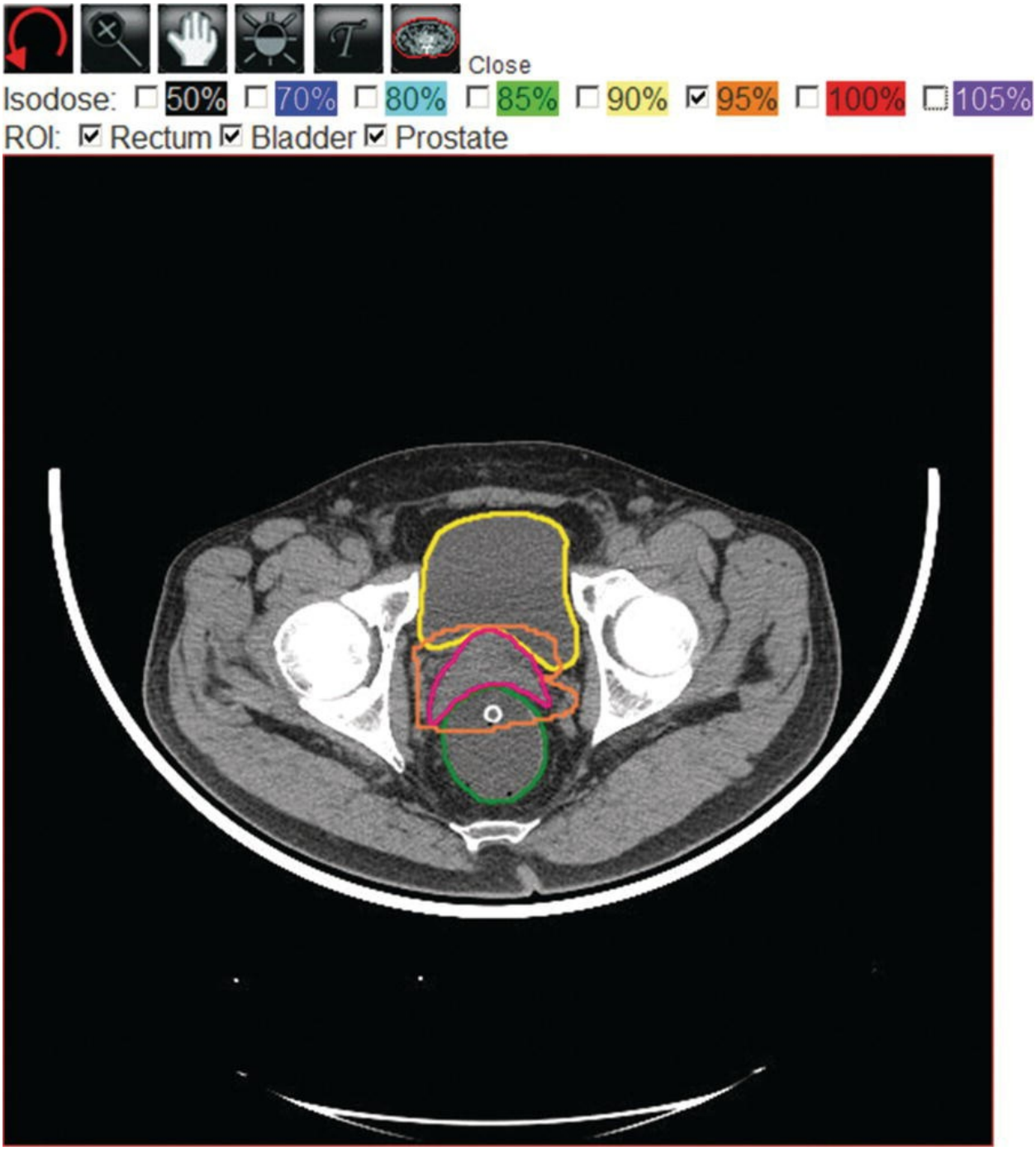

Figure 19.11 Screenshot of ITPN showing the overlapping region of the isodose curve 95% (orange), target prostate (pink), and critical organs: rectum (green) and bladder (yellow). The isodose 95% covered the entire prostate.

Figure 19.12 displays the DVH curves of two plans on the treatment planning viewer GUI of the ePR, which shows no change in target volume and a decreasing percentage rectum volume receiving 55 Gy from 25.7% to 18.18%.

After the treatment plan was finished with the new dose constraints and recalculated in the proton therapy TPS, the data were sent to the ePR for evaluation and validation, which is the last task in the right-hand box of Figure 19.6.

The example shown in this section demonstrates a concept of knowledge discovery in which simple data mining on doses and clinical conditions was performed to find a near match, in order to reduce the iterative process for optimal treatment plans according to the evidence provided in previous patient data. A more robust algorithm should be developed within the ePR system to perform data mining and identify the close match patient in the future.

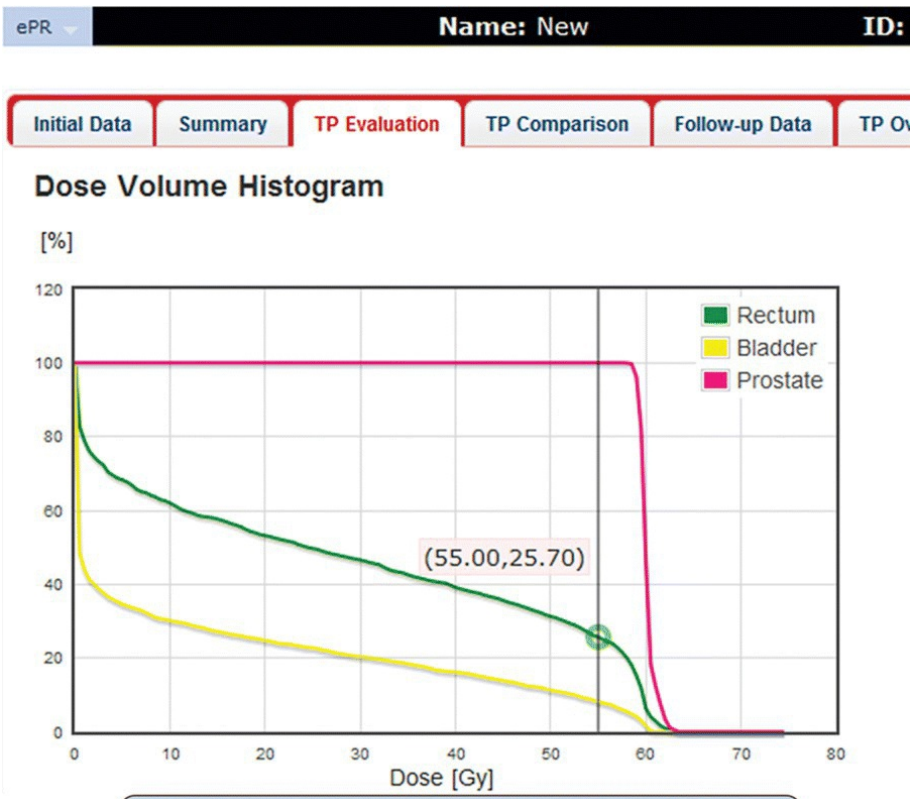

(a) Use existing hypofractionation plan of Pt. Demo on Pt. New with beam margin = 10mm

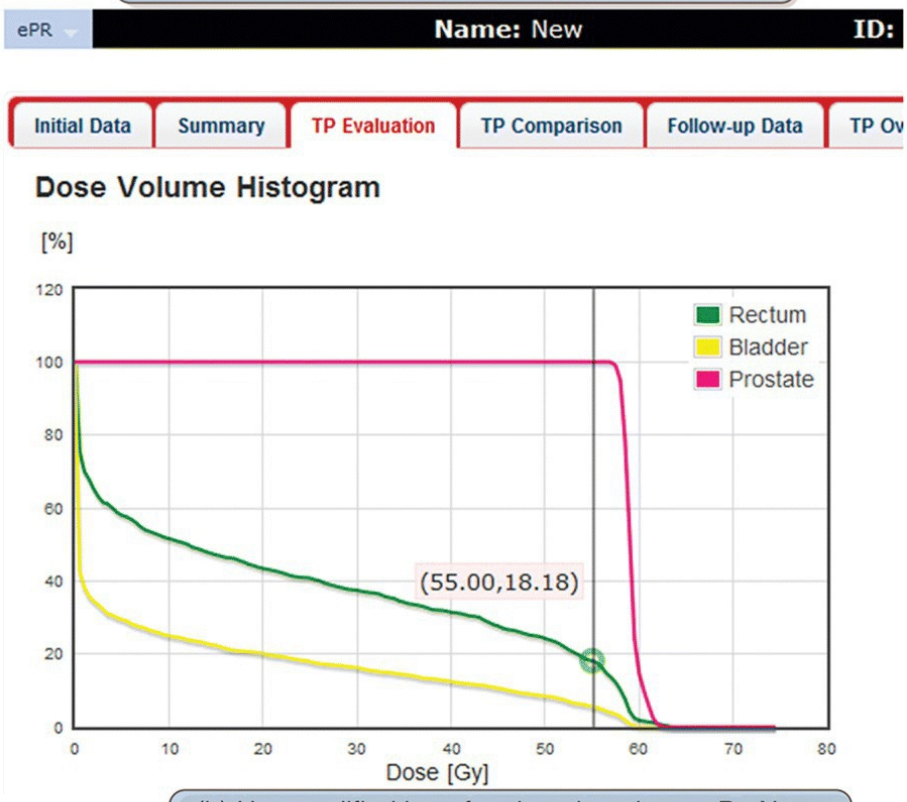

(b) Use modified hypofractionation plan on Pt. New, beam margin = 7mm

Figure 19.12 Screenshots DVH curves on the ITPN of Patient (Pt.). New shows 100% volume of prostate receiving 55 Gy, but a decreasing volume percentage of rectum receiving 55 Gy from 25.70% to 18.18%, with the modified hypofractionation plan of 7 mm beam margin being used. The computation is automatically computed by the ITPN shown in the right-hand-most column in Figure 19.3.

19.6 Conclusion and Discussion

19.6.1 The ePR System

In this chapter, the ePR system developed to support Web-based medical imaging intensive applications with server-client architecture was introduced. This architecture together with implementation of HTTPS and DICOM communication allows different data types, such as treatment plans and patient clinical data, to be archived, visualized, and distributed across multiple locations by the local area network and/or Internet. For example, with the Web-based design, the ePR can receive and exchange DICOM data and clinical data from a Web interface so that the outside institutions could benefit from the pool of patient data. The system was built with scalability architecture; that is, the database and the GUI are tightly integrated so that a new protocol can be easily adapted to this system.

The PT ePR system is DICOM and compliant with the Health Insurance Portability and Accountability Act. The system is evaluated to be able to handle and display text information collected from electronic forms, as well as perform DICOM communications to receive DICOM objects and display the relevant RT information, such as dose–volume curves, contours, and isodose curves on Web-based GUIs. This system promises a new frontier for research in proton therapy and medical imaging informatics, where all patient data is consolidated in a “one-stop-shop” repository. In addition, the ePR system allows users to find matched patient criteria using the knowledge driven search engine for evidence-based research and practice. It also includes the efficiency of collection patient data for hypofractionation protocol from weeks to hours. In general, data is archived in a secure system and easily accessed and retrieved by authorized clinicians and researchers. Beyond the efficiency for data collection, the more data is collected, the more knowledge can be derived and discovered to improve treatment plan for new patients.

19.6.2 Intelligent Decision Support Tools

The practice of radiation therapy involves decision making, where oncologists are challenged with evaluating treatment options for cancer patients to ensure optimal treatment for their disease. Traditionally, clinical experience and expert knowledge in the literature served as the basis for medical practice. However, experience and expertise alone may not necessarily prevent a negative result and promise an effective outcome [20]. Therefore, knowledge-based or evidence-based medicine is a new trend in current clinical practice, where disease management and decision making relies on clinical evidence in combination with clinician's experience and expertise, patients' preferences, and an easily accessible patient information and large clinical-based treatment plan database.

In the field of radiation oncology, this knowledge-based practice is manifested in the development and utilization of protocols based on treatment recommendations for a particular disease. In order to make such a recommendation, there is a rigorous process of research and evaluation of the effectiveness of new treatment protocols. The process for new treatment protocol evaluation requires the first step of acquiring relevant and complete information of the patient and then evaluating this information to maximize the positive effects in the treatment outcome. For example, if the research of proton therapy hypofractionation protocol treatment proves an equivalent or better result compared to existing dose escalation protocols, the shorter course of proton therapy would benefit not only prostate cancer patients coming from different geographic locations, but also those who need a high accuracy level of dose delivery as an alternative treatment option due to the overall cost and time.

19.6.3 Clinical Scenario Demonstrating Knowledge Discovery and Evidence-Based Treatment Plan

As discussed in Section 19.5.4, after the changes are made, the prostate cancer patient will have the option to follow the existing clinically accepted dose escalation treatment protocol or a refined hypofractionation protocol, or can even choose an alternative treatment approach outside the conventional realm of radiation therapy. This added value of the ePR system provides tremendous advantages to the new patient, because physicists and oncologists will have a better understanding and control over the treatment planning to deliver the best possible plan which the current workflow would not be able to do. For example, if patients elect for the hypofractionation treatment protocol, decision support tools can help physicians to determine whether this protocol is suitable for them,

based on prior knowledge obtained from the existing patients who had already undergone the hypofractionation protocol.

In addition, the standard clinical practice is normally based on scientific evidence generated from population studies. However, scientific evidence and standardized knowledge from large populations is not always effective in cancer management for individual patients with unique anatomical structures, tumor size and shapes, and clinical, psychological and social circumstances [20]. The proton therapy ePR system in this chapter provides clinicians with a new paradigm to utilize information in existing patient demographics and treatment data, allows knowledge discovery of this data to help oncologists and physicists make optimal decisions, and provide personalized care for prostate cancer patients in proton therapy. All the demographic, treatment plans, and outcomes data are stored in an easily accessible database. The clinical scenario example shown in this chapter illustrates the step-by-step reasoning and utilization of data-mining and navigation tools in the ePR to achieve a knowledge discovery and evidence-based treatment plan, which will be a valuable tool for clinical practitioners, scientists, and researchers in the field.

In fact, the development of the proton therapy ePR system can evolve to the next phase of clinical implementation and evaluation at a proton therapy facility. The clinical implementation will include training, users' feedback, and performance testing when the system acquires a larger cohort of patients and interacts with different type of users, such as nurses, oncologists, and physicists. The following evaluations can be achieved:

- user feedback from GUI to evaluate the effectiveness of the ePR when interacting with users;
- time performance to evaluate the efficiency of the ePR in data distribution; and
- stability and reliability of the ePR system in handling a larger cohort of patient cases, as well as multiple users' feedback for system improvement from different locations.

The implementation of such an ePR system in the clinical setting can result in treatment plans and protocols sharing between colleagues to foster peer-review and evidence-based practice, to improve treatment outcomes by improving the efficiency in data collection and integration for evaluating new treatment protocols. Beyond the treatment plans and patient data sharing, the collected data can be utilized for future large-scale outcome analysis, automatic knowledge

discovery, and data mining to improve treatment for better patient outcomes; that is, as to whether the change of treatment protocol and the modification of treatment plans provide better outcomes such as lower radiation toxicity. In short, the benefit of such an ePR system is that the more data collected, the more knowledge can be derived and discovered to improve treatment plans for new patients.

The workflow and dataflow are similar among many radiotherapy treatment protocols, therefore the implementation of this proton therapy ePR system can be extended beyond hypofractionation prostate cancer patients to other types of cancer and even to other radiotherapy methods.

Acknowledgements

The research in this chapter was partially supported by Subcontract USAMRMC 53-5149-5600. Contents of the chapter are from Anh Le's PhD Dissertation. She is now Assistant Professor and Medical Physicist, Department of Radiation Oncology, Jacobs School of Medicine & Biomedical Sciences, University at Buffalo, SUNY; and James M. Slater, MD, Proton Treatment and Research Center, Loma Linda University Medical Center.

References

1 National Cancer Institute (2009) *Prostate Cancer Home Page* [cited 2009 June 25] Available from: http://www.cancer.gov/cancertopics/types/prostate.

2 llc, A.F. *Advanced-Cancer-Therapy*. Available from: http://www.advanced-cancer-therapy.org/science_proton.html

3 Liu, B.J., *et al*. (2007) A knowledge-based imaging informatics approach to managing patients treated with proton beam therapy. In: *Medical Imaging: PACS and Imaging Informatics*. San Diego, CA: SPIE.

4 Hanks, G.E., *et al*. (1994) PSA confirmation of cure at 10 years of T1B, T2, N0, M0 prostate cancer patients treated in RTOG protocol 7706 with external beam irradiation. *Int J Radiat Oncol Biol Phys*, 30(2), 289–292.

5 Brenner, D.J. and Hall, E.J. (1999) *Fractionation and protraction for radiotherapy of prostate carcinoma. International Journal of Radiation Oncology*Biology*Physics*, 43(5), 1095–1101.

6 Huang, H.K. (2004) *Integration of HIS, RIS, PACS, and ePR, in PACS and Imaging Informatics*. Hokoben, NJ: John Wiley & Sons, p. 323.

7 Law, M.Y.Y. (2006) A model of DICOM-based electronic patient record in radiation therapy. In: *Computerized Medical Imaging and Graphics: the official journal of the Computerized Medical Imaging Society*, 29(2), 125–136.

8 Law, M.Y.Y. and Liu, B. (2009) Informatics in Radiology: DICOM-RT and its Utilization in Radiation Therapy. *Radiographics*, 29(3), 655–667.

9 Cooperberg, M.R., *et al*. (2004) *The Contemporary Management of Prostate Cancer in The United States: Lessons From The Cancer of the Prostate Strategic Urologic Research Endeavor (Capsure), A National Disease Registry*. pp. 1393–1401.

10 Kupelian, P.A., *et al*. (2004) Radical prostatectomy, external beam radiotherapy <72 Gy, external beam radiotherapy > =72 Gy, permanent seed implantation, or combined seeds/external beam radiotherapy for stage T1-T2 prostate cancer. *International Journal of Radiation Oncology*Biology*Physics*, 58(1), 25–33.

11 Vicini, F., *et al*. (2006) Radiation dose for prostate cancer: is more better? *Nat Clin Prac Oncol*, 3(6), 298–299.

12 Zietman, A.L., *et al*. (2004) *10-Year Outcome for Men with Localized Prostate Cancer Treated with External Radiation Therapy: Results of a Cohort Study*. pp. 210–214.

13 National Cancer Institute (2009) *Cancer Therapy Evaluation Program: Protocol Development* [cited June 25, 2009] Available from: http://ctep.cancer.gov/protocolDevelopment/electronic_applications/ctc.htm

14 The Apache Software Foundation. *Welcome! – The Apache HTTP Server Project* [cited April 18, 2010] Available from: http://httpd.apache.org/

15 Oracle Corporation and/or its affiliates. *MySQL: The world's most popular open source database* [cited April 18, 2010] Available from: http://www.mysql.com/.

16 The PHP Group. *PHP: Hypertext Preprocessor* [cited 2010 April 18] Available from: http://php.net/

17 Bourdon, R. *Install PHP 5 Apache MySQL on Windows: WampServer* [cited 2010 April 18, 1010] Available from: http://www.wampserver.com/en/.

18 The jQuery Project. *jQuery: The Write Less, Do More, JavaScript Library* [cited April 18, 2010] Available from: http://jquery.com/

19 Le, A. (2010) *Mining an ePR System Using a Treatment Plan Navigator for Radiation Toxicity to Evaluate Proton Therapy Treatment Protocol for Prostate Cancer, in Biomedical Engineering*. University of Southern California: Los Angeles. p. 123.

20 Lu, J.J. and Brady, L.W. (2008) Introduction, In: *Radiation Oncology: An Evidence-based Approach* (L.W. Brady, *et al*., eds). Berlin Heidelberg: Springer-Verlag:. pp. VII–XVI.

PERPUSTAKAAN PRIBADI AN-NUR SUNARYA

20
Multimedia Electronic Patient Record System for Minimally Invasive Image-Assisted Spinal Surgery

CHAPTER MENU

20.1 Integration of Medical Diagnosis with Image-Assisted Surgery Treatment

20.1.1 Bridging the Gap between Diagnostic Images and Surgical Treatment

20.1.2 Minimally Invasive Spinal Surgery

20.1.3 Minimally Invasive Spinal Surgery Procedure

20.1.4 The Algorithm of Spine Care

20.1.5 Rationale of the Development of the Multimedia ePR System for Image-Assisted MISS

20.1.6 The Goals of the ePR

20.2 Minimally Invasive Spinal Surgery Workflow

20.2.1 General MISS Workflow

20.2.2 Clinical Site for Developing the MISS

20.3 Multimedia ePR System for Image-Assisted MISS Workflow and Data Model

20.3.1 Data Model and Standards

20.3.2 The ePR Data Flow

20.4 ePR Miss System Architecture

20.4.1 Overall ePR MISS System Architecture

20.4.2 Four Major Components of the ePR MISS System

20.5 Pre-Op Authoring Module

20.5.1 Workflow Analysis

20.5.2 Participants in the Surgical Planning
20.5.3 Significance of Pre-Op Data Organization
20.5.4 Graphical User Interface
20.6 Intra-op Module
20.6.1 The Intra-Op Module
20.6.2 Participants in the Operating Room
20.6.3 Data Acquired during Surgery
20.6.4 Internal Architecture of the Integration Unit (IU)
20.6.5 Interaction with the Gateway
20.6.6 Graphical User Interface
20.6.7 Rule-Based Alert Mechanism
20.7 Post-Op Module
20.7.1 Post-Op Module Stage
20.7.2 Participants in the Post-Op Module Activities
20.7.3 Patient in the Recovery Area
20.7.4 Post-Op Documentation–The Graphical User Interface (GUI)
20.7.5 Follow-Up Pain Surveys
20.8 System Deployment, User Training and Support
20.8.1 System Deployment
20.8.2 Training and Supports for Clinical Users
20.9 Summary
References

This and the next chapter present image-assisted minimally invasive spinal surgery (MISS). Both chapters use the concept of the multimedia electronic patient record (ePR) system. The first chapter discusses the ePR for MISS, explaining how the patient information, including text, consent forms, images, waveforms, graphics, and reports, are acquired; as well as how the surgery is performed. The next chapter considers the integration of MISS in translational medicine. The word multimedia includes not only the preclinical data but also the real-time acquisition and data integration during the surgery. Multimedia ePR is classified as the “dynamic multimedia”, therefore the real-time component has

to be handled instantaneously and managed differently compared to the static multimedia.

In this chapter, the dynamic multimedia ePR system for MISS is discussed from scratch. It explains MISS step-by-step, why it needs ePR, and how to design the clinical workflow based on the existing image-assisted spinal surgery procedure. The chapter closes with the system implementation, deployment of the prototype system for daily clinical operation, and preliminary results. The California Spine Institute (CSI), Thousand Oaks, California, is the clinical partner in developing this system.

20.1 Integration of Medical Diagnosis with Image-Assisted Surgery Treatment

20.1.1 Bridging the Gap between Diagnostic Images and Surgical Treatment

Medical images are traditionally used for the patient diagnosis, from which a treatment plan is derived. The treatment can be any of different methods, or a combination of different methods, like radiation therapy, surgery, or drug treatment. This section discusses the concept of bridging the gap between diagnostic images and image-assisted surgical treatment, in the sense that real-time multimodality images are acquired continuously during the surgery, guiding the surgeon to perform the operation. The left-hand side of Figure 20.1 shows the diagnostic image domain and the right-hand side depicts the treatment domain. The red arrow in the bottom bridging the chasm between these two domains creates a continuum between the diagnosis and treatment in real time. There are various imaging modalities shown on the left-hand side, and different treatment methods shown on the right-hand side. To simplify the discussion of the concept of multimedia ePR for surgery, this section focuses on MISS. For this particular surgical procedure, in addition to the use of images, forms, waveforms, and textual data for planning the surgery, two real-time imaging techniques —digital fluoroscopic—endoscopic video images, and more than half a dozen live vital signs of the patient during surgery are needed to assist and monitor the surgery. These real-time data have to be acquired, displayed, and archived as well. The image data are shown in blue font in both the diagnosis and treatment domains.

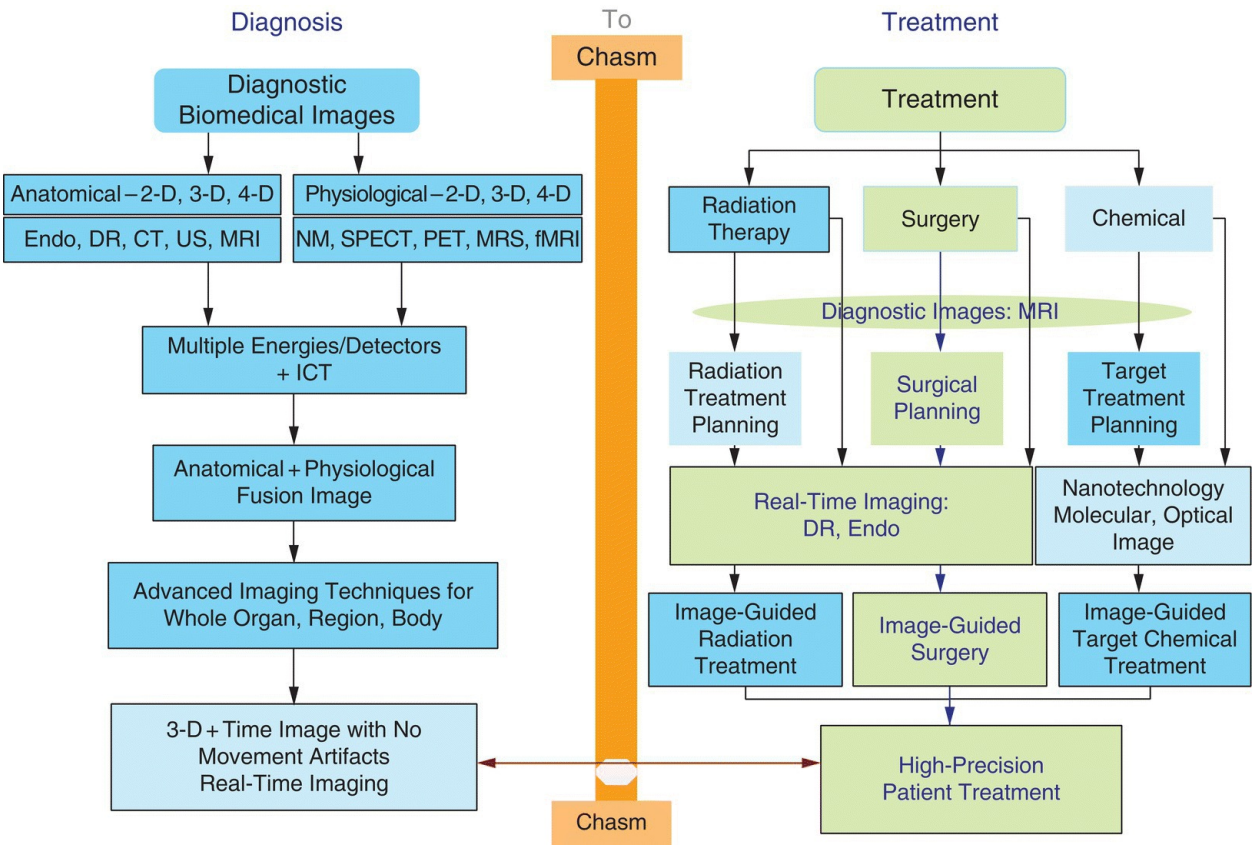

Figure 20.1 Creation of a continuum across the chasm from diagnostic images to treatment. Before, a patient was first diagnosed by imaging techniques, and the surgeon performed the surgery based on the diagnostic results; until recently, it was rare that the surgeon performed the surgery guided (or assisted) by real-time images. The example in MISS shows the surgeon performing the spinal surgery first based on diagnosis from 3-D MRI images (second row, leftmost column under diagnosis, dark blue background box), then under the guidance and assistance of two real-time imaging techniques: endoscope and DR (fifth row, leftmost column under treatment, light green background box). ICT: information and communication technology.

20.1.2 Minimally Invasive Spinal Surgery

Back and neck pain is the price human beings pay for poor posture, prolonged sitting, lifting, repeated bending, obesity, and injury from work or accidents. These ailments give the United States a massive economic headache. Approximately 85% of inhabitants of the Western world are afflicted with some degree of back or neck pain at some point in their lives. About 25% of our population has been incapacitated for two weeks or more due to back pain and an estimated 8–10 million people have a permanent disability. The economic

impact is obvious. In most cases, simple treatments such as bed rest, exercise, physiotherapy, and pain medication bring relief. Many sufferers are not so fortunate. If one or more of their vertebral discs ruptures and presses on nerve roots, the pain radiating from the back or neck and down the limbs can be incapacitating and severe. Until recently, the only treatment was surgical removal of part of the ruptured disc, a major operation that required general anesthesia, the dissection of muscle, removal of bone, manipulation of nerve roots, and, at times, bone fusion. In an effort to overcome the disadvantages of traditional surgical techniques, the scientific medical community began exploring the use of endoscopy (arthroscopy) for MISS. An endoscope provides clear visualization and magnification of deep structures in real time. With the advancement of scientific technology and miniaturization, including fiber optics, video imaging technology, laser treatment, and experience gained through MISS, there is a less traumatic discectomy procedure for some patients with disc problems. In recent years, development of image-guided surgery has improved the precision and reduced surgical tissue trauma. Figure 20.2 depicts the cervical, thoracic, and lumbar spines on MRI before (pre-op) and after (post-op) the endoscopic-guided spinal discectomy. The lesion(s) at each spinal region have clearly healed after the surgery.

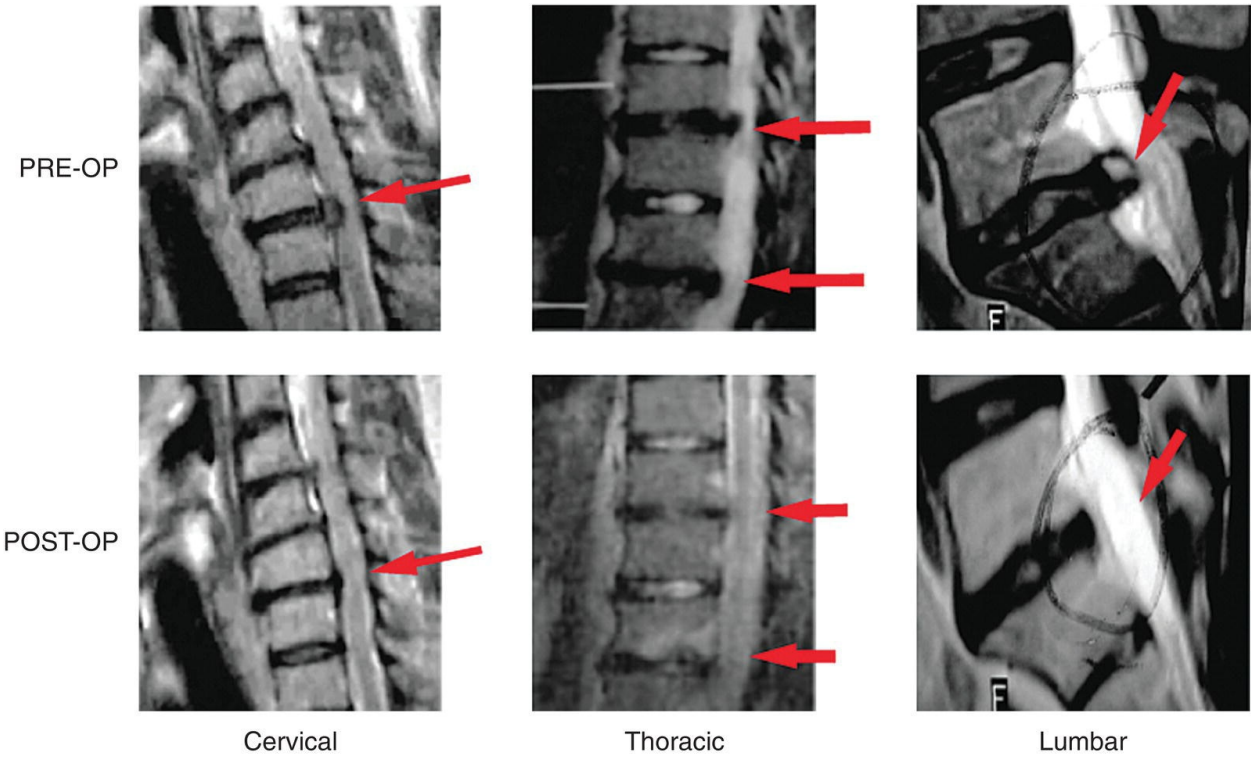

Figure 20.2 Minimally invasive spinal surgery on cervical, thoracic, and lumbar

spines. Upper row: Pre-operation arrows show the areas where the disc protrudes from the spine. Lower row: Post-endoscopy-assisted spinal surgery shows the lesions have been cured.

(courtesy of Dr J. Chiu, California Spine Institute, Thousand Oaks, California) [1,2]

(A)

(B)

Figure 20.3 (A) Surgical team assembles outside the OR reviewing the surgical plan before the operation. (B) Surgical team is inside the OR preparing for the MISS procedure.

20.1.3 Minimally Invasive Spinal Surgery Procedure

The patient scheduled for a MISS first went through a pre-op consultation after the surgeon determined they were fit for surgery. A pre-op consultation was done and all pertinent patient information and pre-op images were collected, studied, and entered into the patient's surgical file. A surgical team was then assembled, and met outside the operationg room (OR) to review the MISS plan (Figure 20.3A); after the review, the team entered the OR and prepared the patient for surgery (Figure 20.3B). The OR is shown in Figure 20.4 equipped with all necessary surgical devices, including the DF and endoscopic imaging equipment. Notice that the figure shows the same room crowded with equipment, display systems, and potential surgical personnel (color dots). External to the OR setup are the pre-op consultation information and images, as well as real-time devices to be connected to the patient for monitoring and assisting in the surgery. Many separate real-time devices, each with a separate display and archive, are also seen.

As the patient is readied for operation, all necessary live monitoring devices are connected to the patient (Figures 20.5A, 20.5B). Depending on the type of spinal surgery, the MISS procedure is performed with the patient under local anesthesia or in some situations, a brief general anesthesia. External real-time minimal exposure DF (Figure 20.5C) is used to guide the surgeon and pinpoint the exact location of the damaged disc based on the presurgical evaluation of the MRI spinal scans. After the location of the problem, the disc is marked on the skin of the patient, and a small hollow tube (about 6 mm) is inserted by the surgeon into the disc space (Figure 20.6A). An endoscope and a variety of MISS surgical instruments can be inserted through the hollow tube, including miniature forceps, curettes, trephines, rasps, burrs, cutters, and other types of probes (Figure 20.6B) for disc decompression guided by real-time continuous endoscopic video images (Figure 20.5D). Lasers are also used to shrink and tighten the disc and to remove portions of the protruded disc (Figure 20.7). The operation procedure takes about 30 minutes per disc on average. The discectome, a hollow probe, is used to cut, suction, and remove (Figure 20.8) small pieces of disc material until enough of the disc is removed to decompress the affected nerve root (Figure 20.8, bottom right). The supporting structure of

the disc is not disturbed.

Upon completion, several sutures and a small adhesive dressing are applied to the external incision. The patient is then relocated to the recovery area for monitoring, and is discharged in about 45 minutes to 1 hour. This endoscopic procedure is also used currently for bony decompression in spinal stenosis. Based on more than 5000 patient studies using MISS at the CSI, endoscopic spine surgery has a patient satisfaction score of 91%, and a 94% success rate (for a single level of disc problem). The complication rate is much less than 1%, and the mortality rate directly from spinal disc surgery is zero (Figure 20.9).

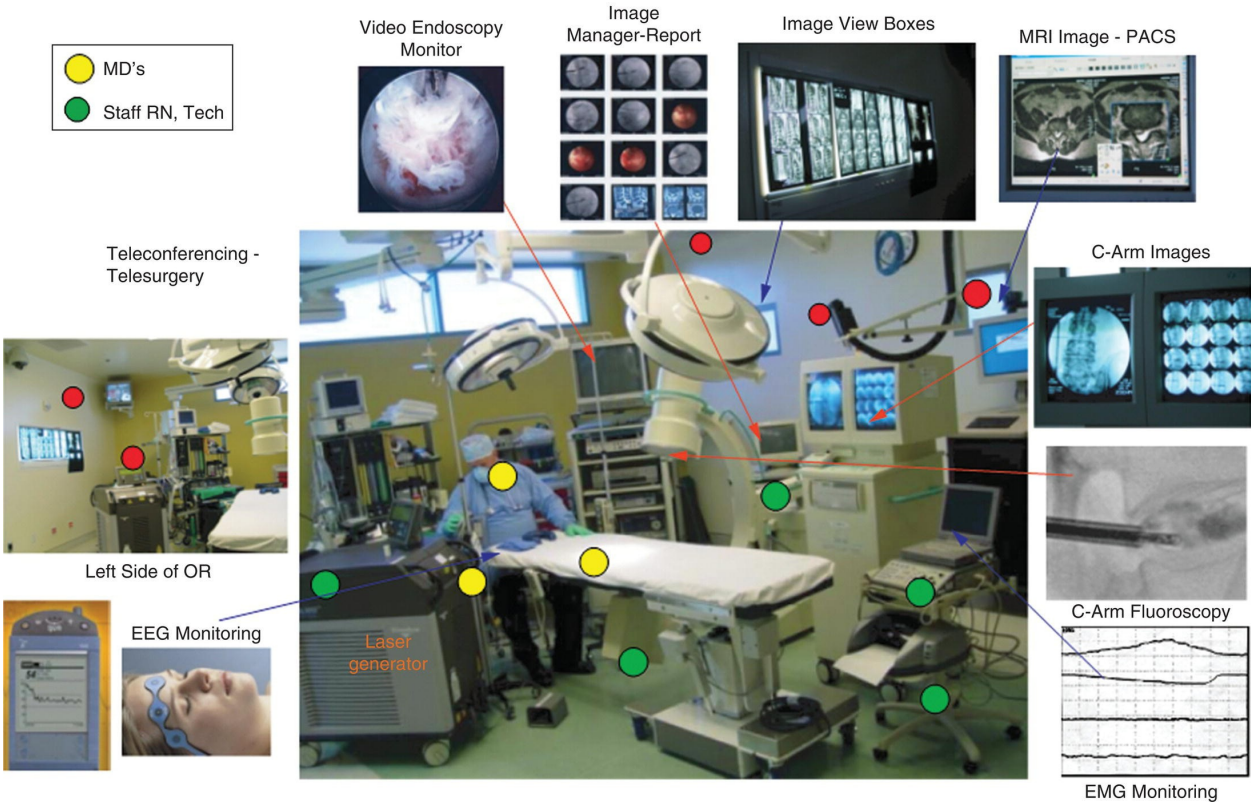

Figure 20.4 Traditional, present-day image-assisted OR suite for MISS operation with endoscopic imaging system and C-Arm DF for image-assisted operation. Notice the many live monitoring waveform devices scattered around the suite and the surgical video for documentation. In the periphery of the OR are the images, waveforms. and other information used during the operation. With the design and implementation of the ePR described in this chapter, today's suite becomes a real-time image-guided MISS OR (Figure 20.11).

(courtesy of Dr J. Chiu)

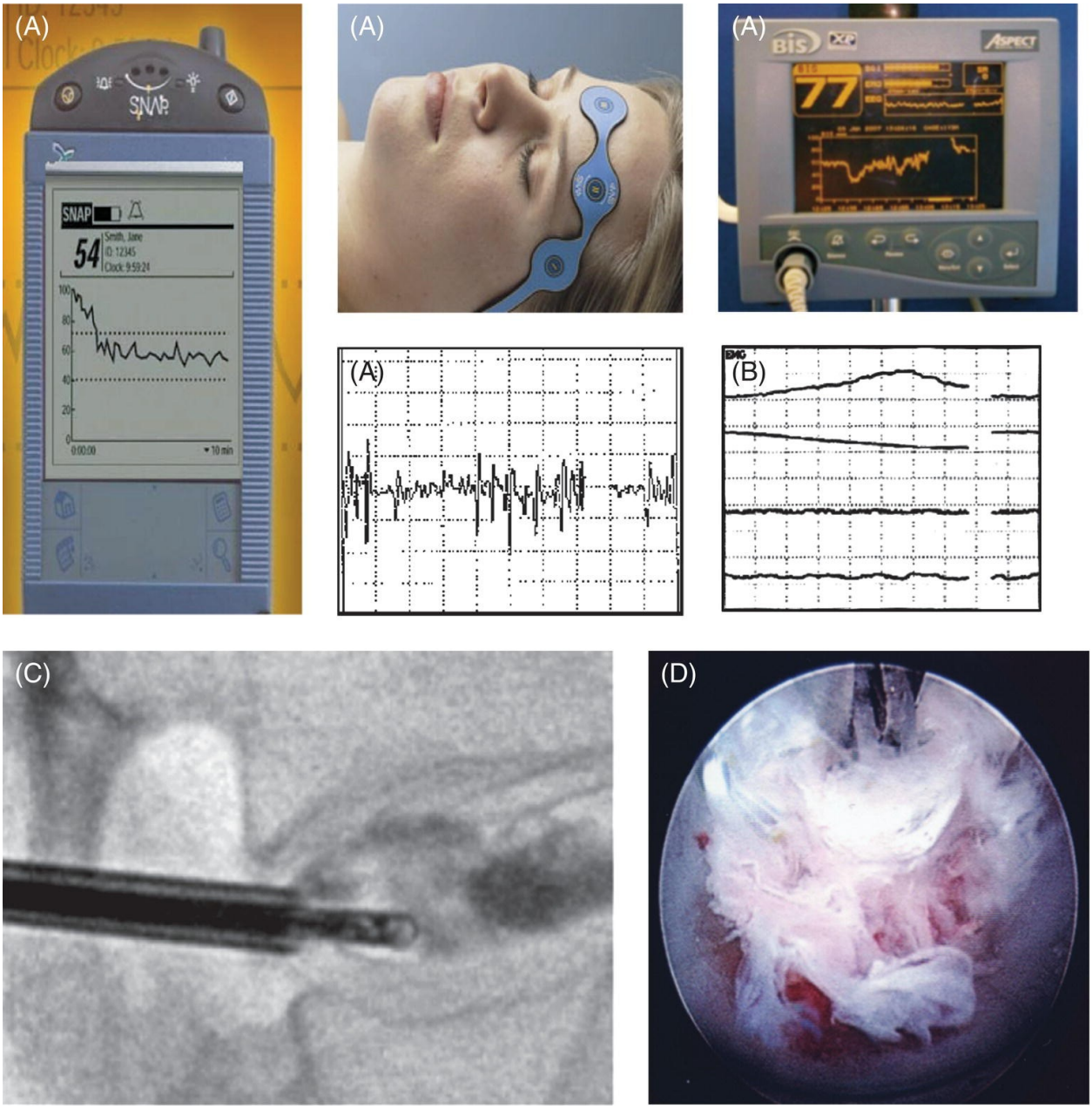

Figure 20.5 (A) Continuous conscious electroencephalogram monitoring with the computerized SNAP device (SNAP index or Bispectral Index monitor) improves anesthesia and reduces drug requirement. (B) Continuous intra-op electromyogram monitoring prevents undue trauma to the spinal nerve to be decompressed. (C) Real-time C-Arm fluoroscopy during surgery for positioning of the endoscopy. (D) Real-time digital video endoscopic images, both static images and video clips.

(courtesy of Dr J. Chiu)

(A)

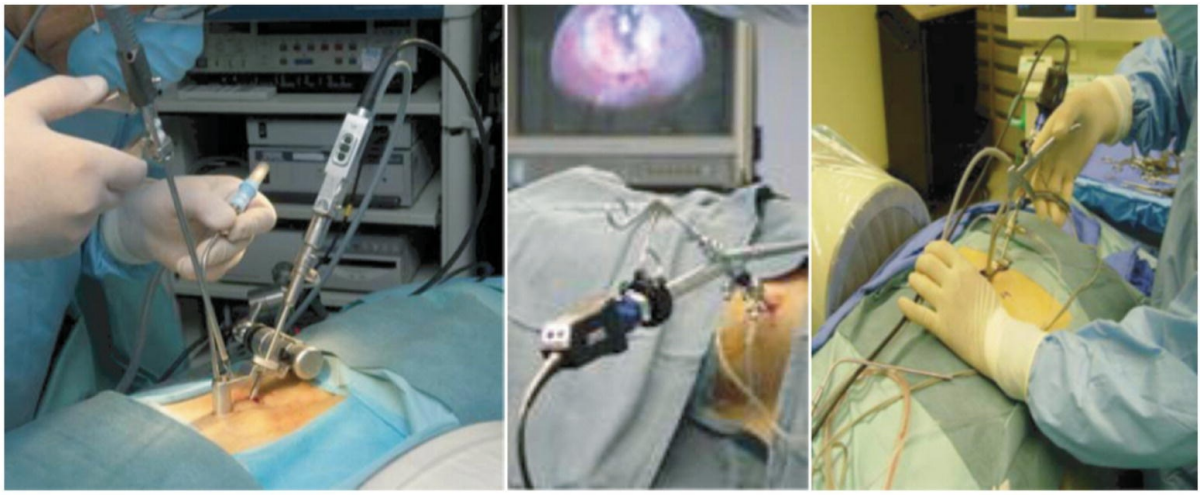

(B)

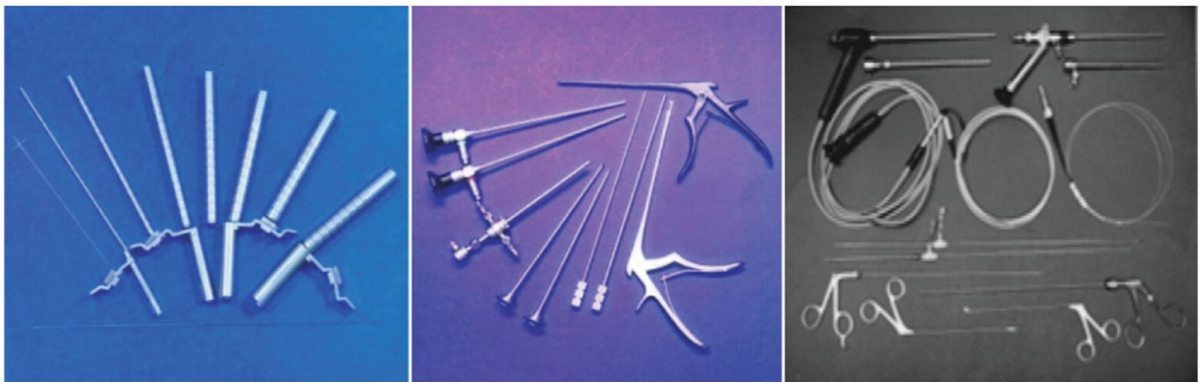

Figure 20.6 Location of problematic disc marked on the skin, with a small hollow tube (~6 mm) inserted by the surgeon into the disc space (A). The location is verified by the C-Arm image. An endoscope (see the endoscopic image shown in the middle above the insertion) and a variety of MISS surgical instruments can be inserted through the hollow tube, including mini-forceps, curettes, trephines, rasps, burrs, cutters, and other types of probes shown in (B) during the image-assisted operation.

(courtesy of Dr J. Chiu)

Figure 20.7 Tissue modulation technology, including Holmium yttrium aluminium garnet laser digital equipment and radiofrequency, are among technologies that can be used for thermodiskoplasty. The lasers are used to shrink and tighten the disc and to remove portions of a protruded disc. The figure shows the laser generators and the right-angle (side-firing) laser probe.

(courtesy of Dr J. Chiu)

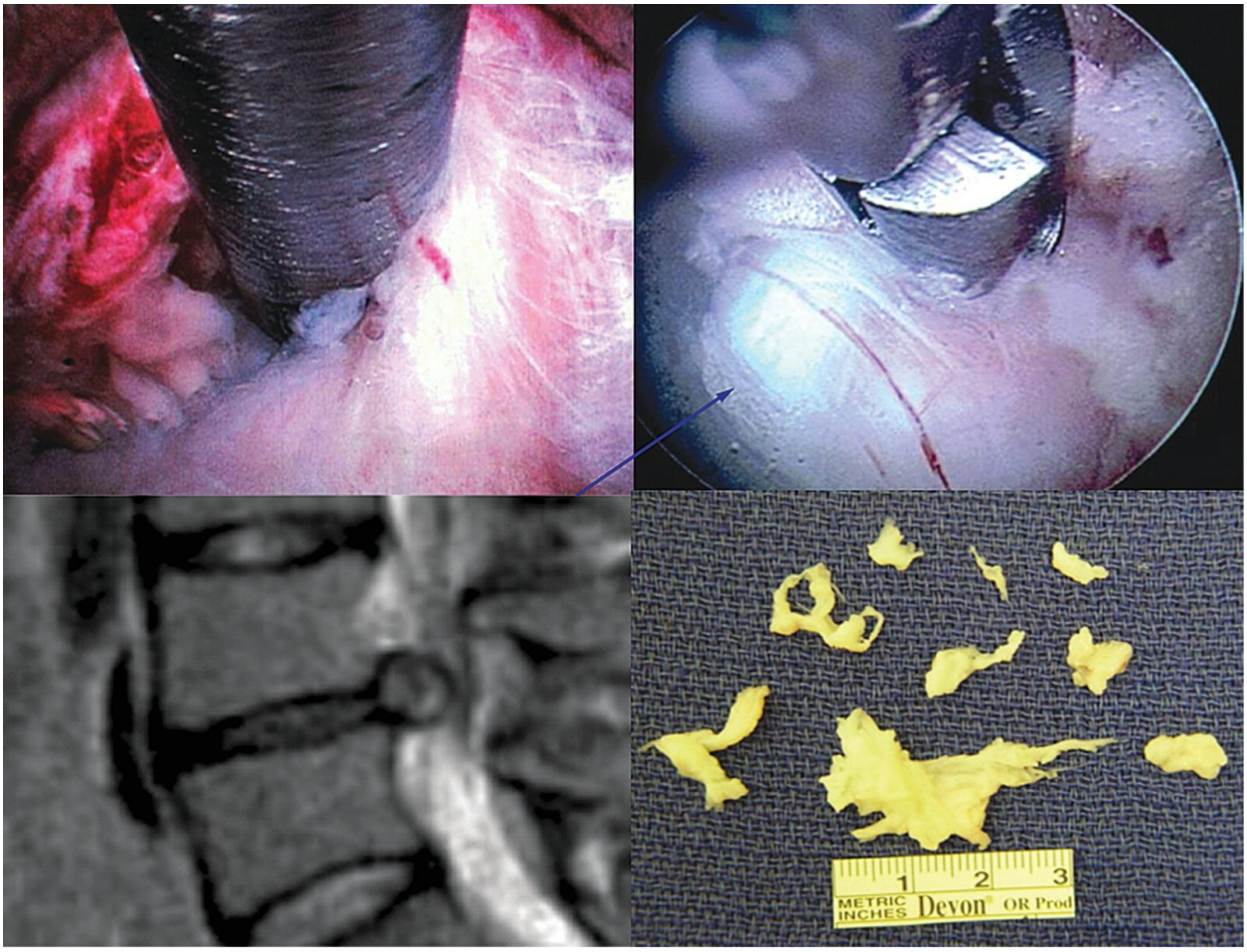

Figure 20.8 Lower left: MRI sagittal view showing the large extruded L4 disc. Upper left and right: The lumbar endoscopic posterior lateral approach showing two endoscopic lumbar discectomy images with the lumbar nerve root in close proximity. Lower right: Removed extruded disc fragments.

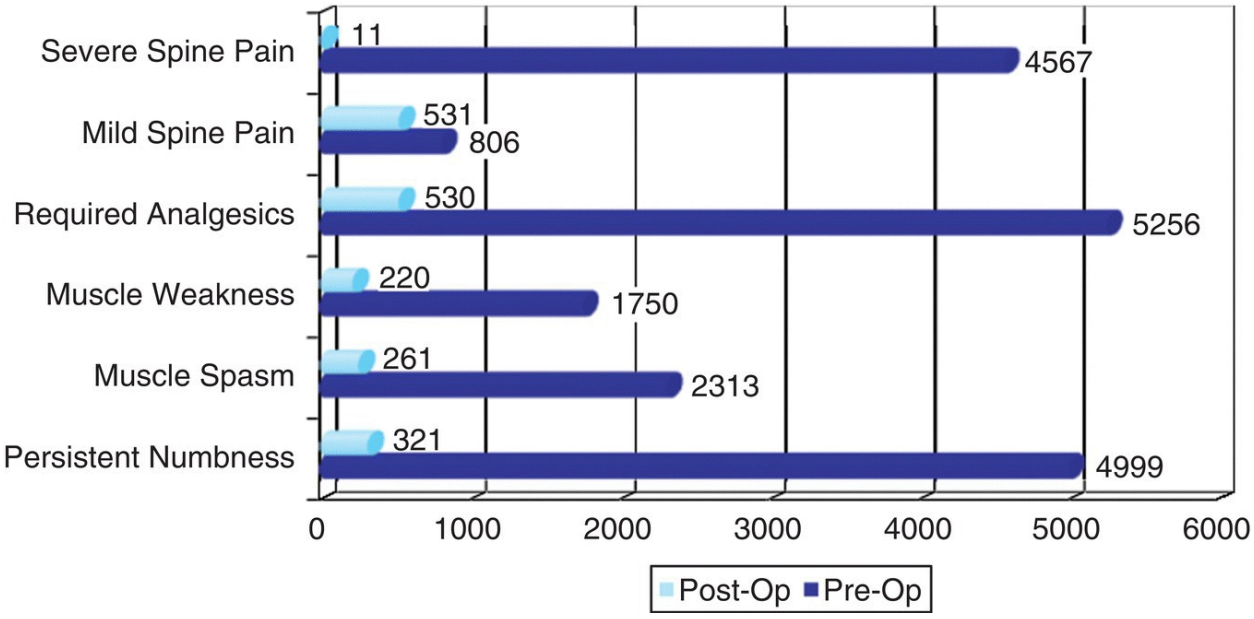

Figure 20.9 MISS patient surgical outcome (symptomatic improvements) from 5373 patients performed by Dr J. Chiu at the California Spinal Institute, Thousand Oaks, California.

20.1.4 The Algorithm of Spine Care

Image-guided MISS is a relatively new branch of neurosurgery that relies on multimodality images for guiding the surgical procedure. The surgical procedure is relatively simple and safe when performed by the expert, and with a rapid patient recovery time. The surgical procedure is much less painful, and the patient recovery time is shortened from months to days. MISS has therefore gradually replaced many unnecessary open spinal surgeries. Figure 20.10 shows the algorithm of spine care for degenerative and herniated spinal discs, and spinal stenosis; MISS has taken over the treatment of medium spinal disc aliments. With the multimedia ePR system, it will contribute further to the success of MISS.

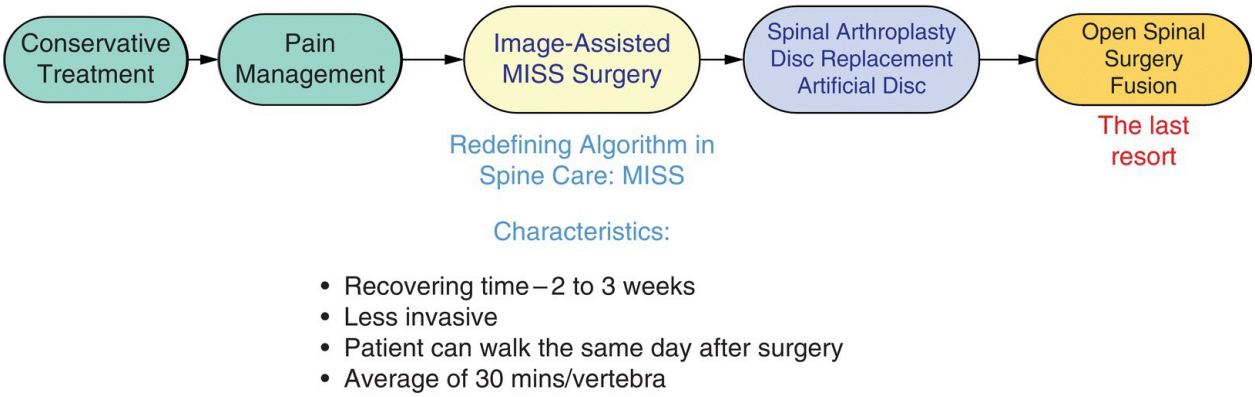

Figure 20.10 Algorithm of spine care for degenerative and herniated spinal discs, and spinal stenosis. Before MISS, spine care ranged from conservative treatment to pain management to spinal arthroplasty disc replacement or artificial disc, and to open spinal surgery fusion. With MISS, there exists an additional option (yellow ellipse) offered before the patient has to choose between the other two extremes.

20.1.5 Rationale of the Development of the Multimedia ePR System for Image-Assisted MISS

MISS will be the method of choice for future spinal surgery to treat cases of herniated lumbar discs, post-fusion junctional disc herniation, neural compression, osteophytes, spinal stenosis, vertebral compression fractures, spinal tumor, synovial cysts, and other types of spinal traumas. Over the past few decades, its popularity has been gaining as a preferred treatment option because of the benefits it provides against open surgery. Despite the overall advantages of MISS compared with conventional open spinal surgery, there are challenges remaining in MISS, owing to:

1. the scattered pre-, intra-, and post-op surgical data in data acquisition systems;
2. the difficulty of real-time data collection during the surgery; and
3. some lapses in the efficiency of surgical workflow.

An integrated dynamic mode multimedia ePR system promises to be an ideal way to overcome these challenges. It should take MISS to a higher level of excellence by which surgical expertise in MISS is combined with frontier advancements in imaging informatics. The outcomes will benefit those patients who, suffering from spinal pain, may recover much sooner with less cost and enjoy a better quality of life. In return, society benefits as a whole.

20.1.6 The Goals of the ePR

The two clear objectives of ePR are: i) to develop a totally integrated multimedia ePR system for image-assisted MISS; and ii) to deploy the ePR at CSI for daily clinical use. Multimedia integration means that all pre-, intra- and postoperative data collected for the patient will be acquired, displayed, and archived at each point of the surgical workflow. In intra-op, the data will be acquired, displayed, and archived in real time. Any record in the ePR can be retrieved instantaneously over the lifetime of the patient.

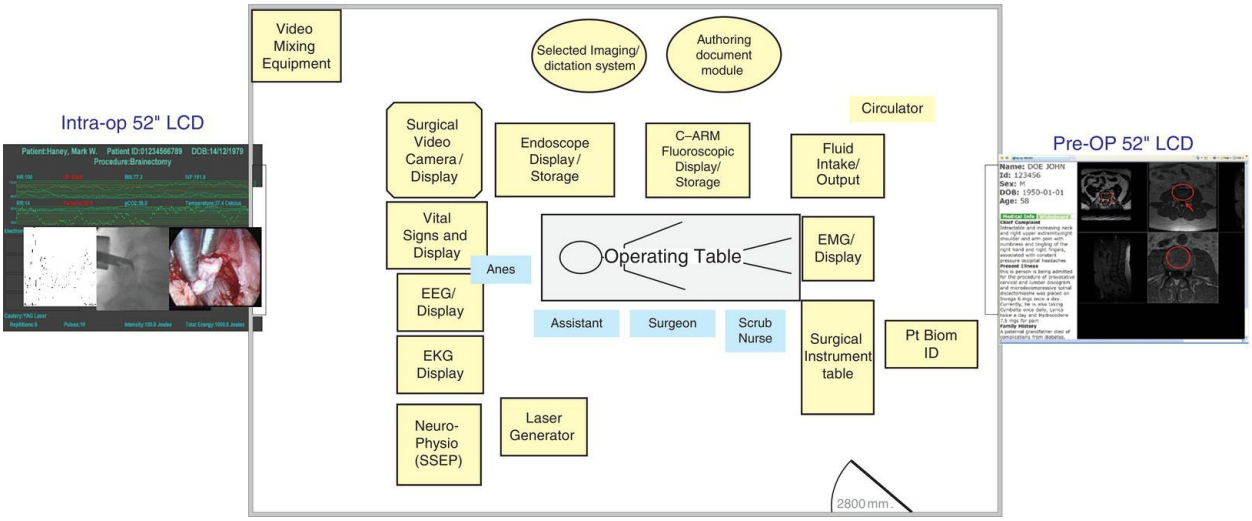

Figure 20.11 Schematic of the dynamic multimedia ePR system for image-assisted MISS. The prototype system is running at the MISS OR of CSI with two large liquid crystal displays (LCD), one for the pre-op consultation integrated display and the other for the live intra-op integrated display (compare to the current existing OR shown in Figure 20.4).

Figure 20.11 depicts the ePR prototype system running at the MISS OR of CSI, with two 52-inch liquid crystal displays, one for the pre-op consultation integrated display and the other for the live intra-op integrated display (compare with the existing OR small monitors shown in Figure 20.4).

20.2 Minimally Invasive Spinal Surgery Workflow

20.2.1 General MISS Workflow

The MISS current high-level operation workflow that starts from presurgical consultation, proceeds to pre-operation preparation, intra-operation imaging and vital signs acquisition and display, and post-surgery documentation, and ends

with patient recovery monitoring, is shown in Figure 20.12. The workflow can be broken down into three phases: i) before surgery; ii) during surgery (including the preparation); and (iii) post-surgery, discussed below.

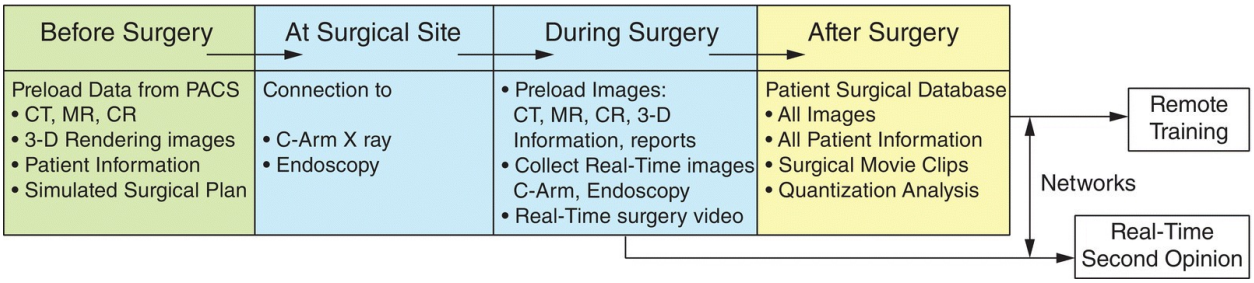

Figure 20.12 General workflow of the MISS procedure showing three different stages: before surgery (green), patient preparation at the surgical site and surgical operation (blue), and post-surgery (yellow) [3–18].

1. *Before surgery (pre-op)*: Prior to the actual surgical procedure, usually the patient presents with a problem and is evaluated by the physician to determine whether MISS is needed and whether it would be helpful to the patient. If this case is true, then a procedure is scheduled. At this stage, the surgeon or surgeons in combination with the physician's assistant plan the surgical procedure using digital diagnostic images such as CR, CT, and MRI. In addition to the information obtained from the medical studies, the patient fills out a set of questionnaires that determine the level of pain that they feel.
2. *During surgery (intra-op)*: As the surgeon(s) operate on the disc(s) that need to be corrected, there is a significant amount of data being acquired that helps to monitor the body responses of the patient to the procedure. Video and image data are also acquired with the endoscope. A single vertebrae procedure lasts 30 minutes on average.
3. *After surgery (post-op)*: As the patient recovers from surgery, the patient is continuously monitored in the recovery area to ensure all vitals signs are stable. In addition, a set of tests are performed to assess the outcome of the surgical procedure, which includes an additional set of forms that the patient fills out.

The recovery period after surgery lasts from 45 minutes to 1 hour. The patient is then discharged. Therapy can begin the next day and the patient can go back to work within 2–3 days.

The basic general concept of software organization follows the high- and low-level database schema, data model, and data flow model discussed in the Chapter

11.

20.2.2 Clinical Site for Developing the MISS

The design and implementation of the multimedia ePR MISS system had been in collaboration with the CSI. The CSI is a fully self-sufficient independent spinal surgery institute and performs between 10 and 20 MISS per week. It has its own diagnostic imaging facility, including conventional x-ray, CT, and MRI services and a commercial PACS. It also provides patients with the full in-house services for spinal surgery from pre-op consultation to post-op evaluation, check-up, and therapy. The concept of developing the multimedia ePR system for MISS was conceived in the mid-2000s, but technologies were not readily available until 2006. The go-ahead development decision was made in early 2007.

Many parameters used in the design were based on daily clinical experiences at CSI during the past seven years. The ePR system can be modified for MISS operations at other similar healthcare facilities, and other types of image-guided surgical OR. This concept will be discussed in the next chapter.

20.3 Multimedia ePR System for Image-Assisted MISS Workflow and Data Model

20.3.1 Data Model and Standards

The ePR for MISS at CSI was based on the extension of the DICOM data model, because its PACS used the DICOM model at that time. The ePR model follows the patient's record from before surgery, at surgical OR, during surgery, and after surgery, described in Figure 20.12. The data model includes all data used by DICOM, plus additional entities needed in MISS such as surgical procedure type, patient's real-time waveforms, recorded and real-time images, questionnaires on pain tolerance, and other patient related information. The data model is depicted in Figure 20.13, and is revisited in later sections.

The standards used in the data model include DICOM, hypertext transfer protocol secured (HTTPS), JPEG (Joint Photographic Expert Group), GIF (graphics interchange format), PNG (portable network graphics), and VGA (video graphics array, a display standard introduced in 1987 by IBM for use with IBM PC compatible personal computers). Recommended Standard 232 is used as the interface for each waveform device connected to the integration unit (IU) of the ePR.

20.3.2 The ePR Data Flow

The initial data flow in the ePR system is based on the concept of the workflow presented in Figure 20.12 and detailed in Figure 20.14, where each numeral represents a data flow event. The timeline shows three phases: the pre-op image/data module, the intra-op module, and the post-op module. Each of these modules has four components: input module, input gateway, ePR server, and the visualization and display module.

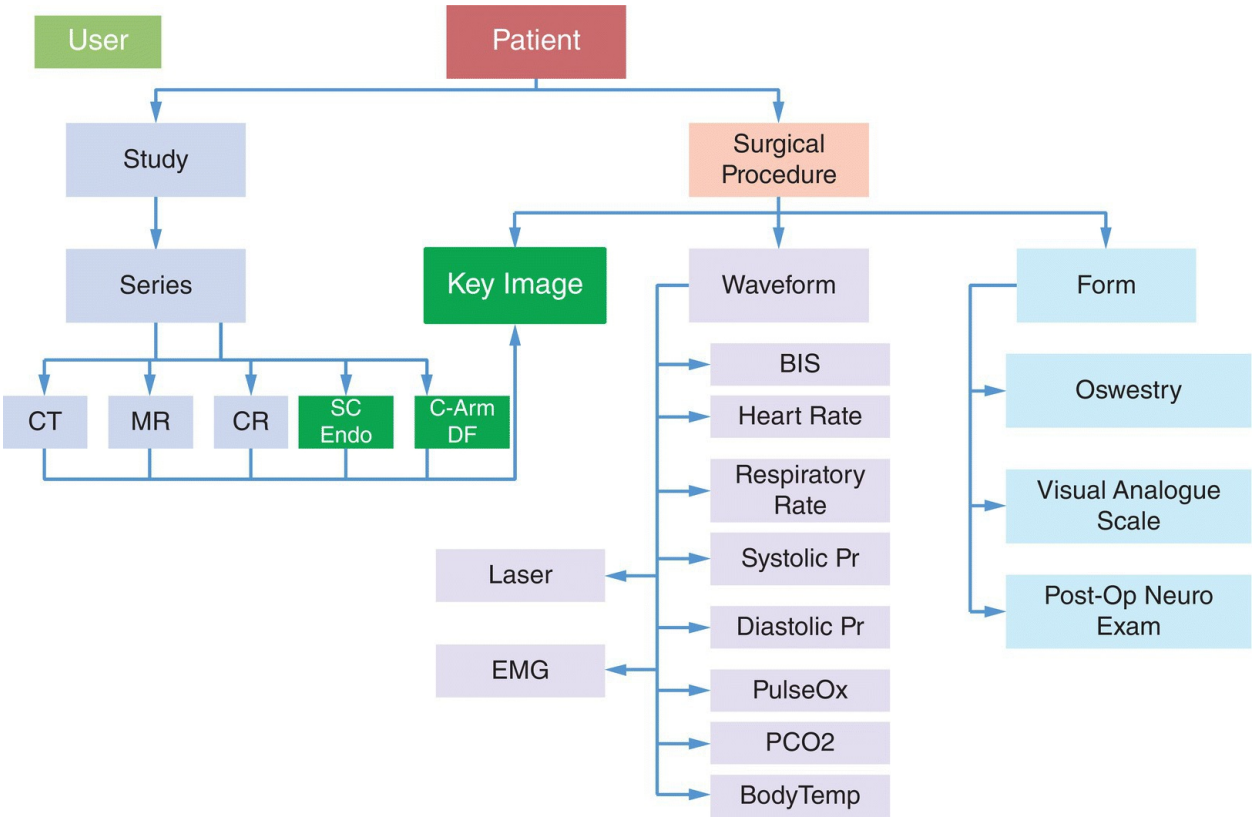

Figure 20.13 Data model of the ePR system. It extends the DICOM scheme to accommodate additional surgical information, including live patient waveforms and several standard surgical forms and real-time images. Additional entities (green) were augmented to the ePR imaged-assisted MASS data model [18].

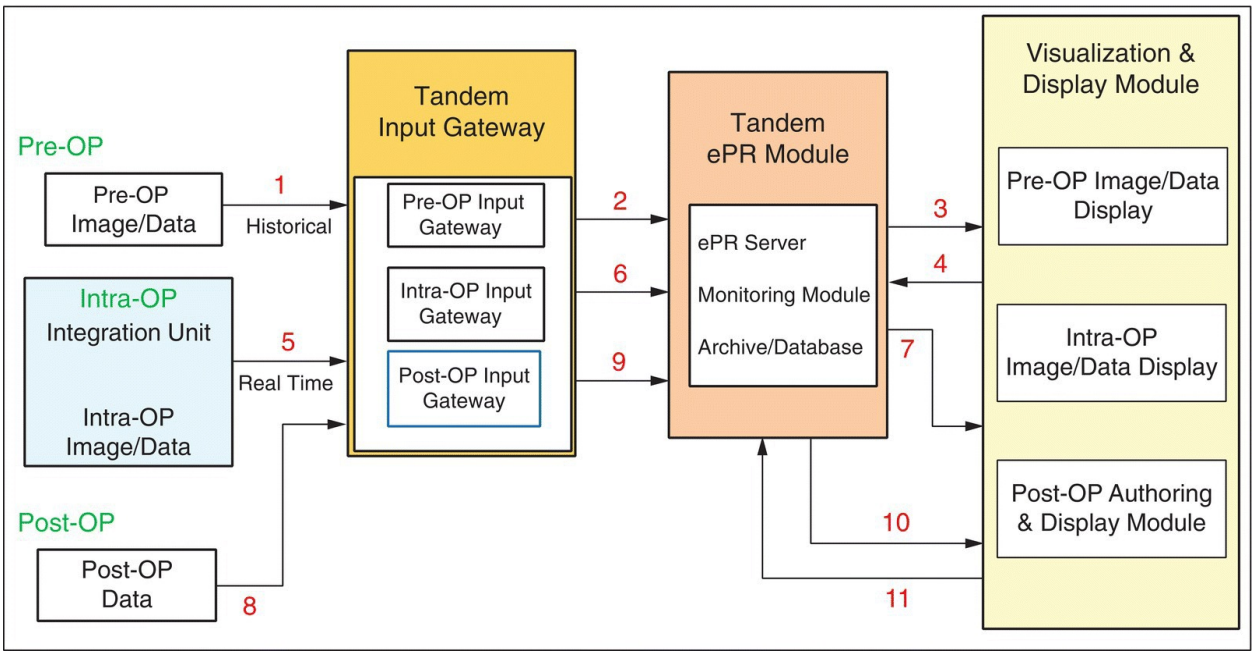

Figure 20.14 Data flow of the ePR system for MISS. There are three time stages—preoperative (Pre-OP), intraoperative (Intra-OP), and postoperative (Post-OP)—and four operational modules—input units, gateway, ePR server and database, and visualization and display, which forms a 3×4 matrix. Each numeral represents one event in the data flow [3–19].

20.3.2.1 Pre-Op Workflow

Following Figure 20.14 for the workflow:

1. Historical medical imaging studies in DICOM format are acquired from the PACS.
2. The gateway, which is a component of the ePR system, receives the DICOM images and processes them accordingly. The original image is kept in the ePR and a JPEG version is utilized for display purposes via the Web interface of the ePR. All DICOM header information and metadata are extracted and recorded in the database.
3. Pre-op authoring is performed by the surgeon(s) and the physician assistants. The surgical procedure information is entered into the ePR. At this stage, the patient's pain questionnaires are also entered into the system. The surgeon selects some key images and makes annotations on the key images that will ultimately be used during surgery. The authorized images/data are displayed in the OR on a 52-inch liquid crystal display (LCD) monitor.

4. Authorized images/data are archived in the ePR server and archive.

20.3.2.2 Intra-Op Workflow

In steps 5, 6, and 7, the integration unit is connected to all clinical devices in the OR and continuously gathers live data signals during the surgical procedure. These signals are displayed in real time on a second large 52-inch LCD monitor. At step 6, the gateway server receives the data from the IU and stores the data values and images in the database and the file system (Figure 20.15) temporarily.

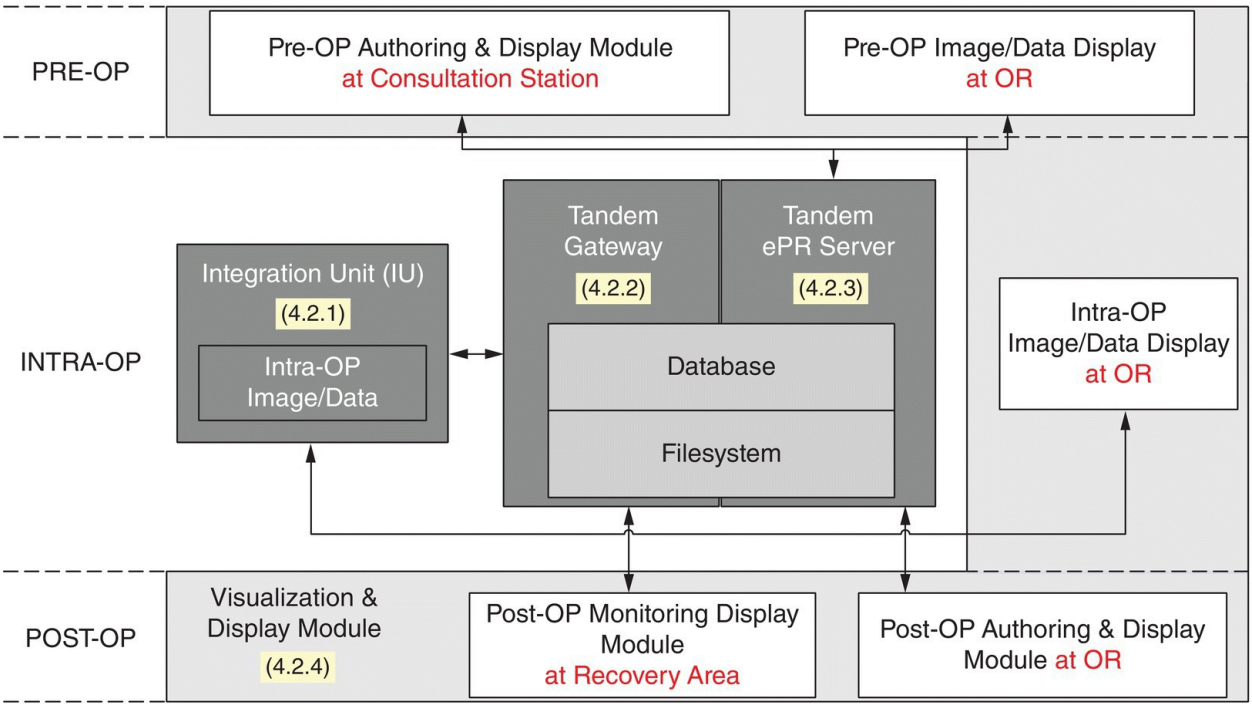

Figure 20.15 ePR system architecture showing three operation phases (first column), pre-op, intra-op, and post-op, as well as four operation modules (partitioned and scattered systematically). Some partitioned modules are bundled together for ease of data transfer and tandem backup. The arrows show the data flow during the three phases of operation. The outside light gray color large side-way U band is the display module backbone (Section 20.4.2.4) with five white rectangular box subunits. Inside the opening of the "U" in the dark gray are the integration unit (Section 20.4.2.1), tandem gateway (Section 20.4.2.2), and tandem ePR server (Section 20.4.2.3). Within the gateway and the ePR server, the database and file system software are interrelated and shared by both components.

20.3.2.3 Post-Op Workflow

1. While the patient is in the recovery area, the system continues gathering their vital signs that are transferred to the gateway server.
2. The gateway server receives the data and stores them into the database temporarily.
3. The surgeon uses the post-op authoring module to create a final report out of the data gathered during the pre-, intra-, and post-op stages.
4. The final report will be kept in digital format at the ePR server as the patient's permanent surgical record.

20.4 ePR MISS System Architecture

20.4.1 Overall ePR MISS System Architecture

Recall from Figure 20.14, where the workflow and data flow model of the ePR MISS system was represented by a 3 × 4 dimension matrix model. The three rows are pre-op, intra-op, and post-op workflow process stages, and the four columns are the input data IU, input gateway, ePR server, and image/data display. From the point of view of the system architecture, the ePR MISS system should be designed for efficiency, effectiveness, and reliability of system operations. For these reasons, although system workflow is separated into pre-op, intra-op, and post-op stages, some modules that handle multiple workflow stages may be combined to share system workload and reliability. For example, the fault-tolerant requirement of each component in the system is better designed to support other existing components of the system for easy system backup and cost containment. Also, although there are four major components and three operational workflow phases in the ePR system, many of the software have similarly designed backbones, and some software may be bundled together for easier programming effort and faster system execution time. For these reasons, the ePR system architecture is reorganized and modified from the data flow shown in Figures 20.14 and 20.15 for better system implementation and operation. Detailed examination of these two figures demonstrates the existence of four components and three operational workflow phases in both. However, some components in Figure 20.15 are bundled together for design and operational convenience. Section 20.4 describes the system design and architecture. Sections 20.5, 20.6, and 20.7 present the detailed technical descriptions of the pre-op, intra-op, and post-op modules, respectively.

20.4.2 Four Major Components of the ePR MISS System

Four major components in the ePR MISS system are:

1. data input integration unit;
2. fault-tolerant gateway server;
3. fault-tolerant ePR server; and
4. visualization and display.

Both the input gateway and the ePR server include data storage and archive, system database, system security, system fault tolerance, continuous availability, and failover. The graphical user interface (GUI) and display module resides within the ePR server. All data input systems such as medical imaging, surgical video, vital signs waveform recorders, and textual data recorder generate pre-op, intra-op, and post-op data, and they are all categorized as input data. The imaging and data systems that generate information are existing peripheral surgical supported equipment already within the OR, but they do not belong to the IG-MISS ePR system. However, the ePR system must integrate these systems in order to receive the input data that is acquired before, during, and after surgery to support the surgical procedure.

20.4.2.1 Integration Unit

20.4.2.1.1 Input Data and Archive

The integration unit is responsible for acquiring all data from different peripheral devices that are presented in the OR during surgery (intra-op) and to measure continuously all live vital signs, waveform signals, and surgical-related images of the patient undergoing a procedure. The data acquired by the IU from all input devices are synchronized through a master clock and displayed live onto a customized interface using a 52-inch LCD screen (called the intra-op live display) in the OR. The data gathered during surgery include the following:

- Digital C-arm fluorographic images;
- Digital endoscopic video images;
- Surgical video;
- Waveform signals: electromyography (EMG), BIS (bispectral Index), and vitals (blood pressure, heart rate, respiratory rate, pulse oxygen concentration, body temperature, and partial pressure of carbon dioxide).

The images, videos, and data points mentioned above are transferred automatically and continuously from the various input sources of the different data systems in the OR during operation that are attached to the data input IU. The data are immediately saved in the unit's memory. The integration unit's software displays the waveforms, images, and streamed videos properly every second (which is a default value) on the large intra-op LCD monitor, and also makes a copy from the memory to the IU local hard drive with 1.5 terabytes of storage space every 5 seconds (which is also a default value). These two default values can be adjusted interactively, depending on clinical demands.

Normal procedures for a single vertebra surgery takes about 30 minutes on average. The data are sent continuously to the gateway where the images are processed if needed and then placed in a data folder shared with the ePR server where they will be permanently archived. The data values are also extracted and saved to the ePR system database.

20.4.2.1.2 Out of Range Input Data Alert Message

In addition to the one-second input display described in the last section, the IU features a rules-based alert-software that checks each input waveform for data that is out of the normal range. The unit has a set of rules based on clinical accepted medical practice that determines when a given signal is considered within the normal range for a patient (Table 20.1). If at any given time during the surgical procedure, a signal falls outside the safe range, the unit will trigger an alert message on the intra-op live display (Figure 20.21). The alert message prompts the surgeon and key personnel in the OR to take necessary actions during the surgical procedure. The values shown in Table 20.1 are considered normal values within the safe ranges for the signals used in the IU. However, those values might not be considered normal for all patients, so during the pre-op patient consultation time, the default values of the patient need to be revised and properly adjusted as necessary.

Table 20.1 Default values for the safe ranges of the patient's vital signs during MISS operation used as indicators to set off alarms on the real-time intra-op display.

Signal	Lower Value	Upper Value	Units
Blood pressure	80	120	MmHg
Partial pressure	35	45	MmHg
Heart rate	60	100	Beats/minute

Respiratory rate	10	16	Breaths/minute
PulseOX	92		%
BIS	40	70	Score value
Body temperature	36.1	38	Celcius

20.4.2.2 The Tandem Gateway Server

The functions of the input gateway are receiving, staging, managing, and transferring input data during the three workflow stages of the surgery: pre-op, intra-op, and post-op.

20.4.2.2.1 Pre-Op Stage

The gateway receives DICOM images and diagnostic reports from PACS. Once images are received by the gateway, a pre-op script is automatically launched by the gateway to properly extract all the information from the headers of the DICOM files. The data are then saved in the database. This whole process is automated at the gateway and does not require any user intervention.

20.4.2.2.2 Intra-Op Stage

During intra-op, the gateway receives live data from the IU using an application program interface(API). The transfer protocol used is the HTTPS standard. Before any data is sent to the gateway, the IU needs to properly authenticate itself in order to avoid conflict with other possible input devices. Once the data are received by the gateway server, the API will place the data in a specific location in the ePR, where a script will be executed to process the data accordingly.

20.4.2.2.3 Post-Op Stage

During post-op, the patient is kept under observation in the recovery area by a nurse and the surgeon. The vital signs and other monitoring equipment are used to evaluate the patient’s post-op condition. During the 45 minutes to 1 hour observation period, live data of the patient are continuously received and displayed at the bedside monitor by the post-op module.

20.4.2.3 The Tandem ePR Server

The ePR server is the heart of the ePR MISS system, and the basic components are shown in Figure 20.16. The ePR server is the front end of the system where

the users will log in to perform all the necessary tasks during the surgical workflow. The ePR server allows access to the pre-op authoring module, the pre-op display in the OR. and the post-op authoring module (Figure 20.15). Administrative tasks such as providing the users access to the system, registration of patient information, scheduling, fingerprint registration, and identification are included.

The ePR, by its design, allows the users to obtain any necessary information about the patient from a single interface, and that the information follows the patient. The ePR goes beyond PACS, because it not only shows information about the medical examinations for the patients but also any other related data such as clinical history, pain surveys, biometric information, and data acquired during the surgical procedure.

The ePR is developed using hypertext preprocessor as the backend programming language. The data values are stored using an MySQL database. The Web pages are structured with hyper text markup language, and are styled using cascading style sheets. The interfaces are dynamically updated using JavaScript.

20.4.2.3.1 Data Storage and Archive and System Database

Managing the data acquired by the ePR system is a critical task. A dual-system backup mechanism is implemented as follows (Figure 20.16). First, the ePR server has the server hardware, and the gateway has the gateway hardware. Two identical server software packages are implemented, one in the ePR server hardware as the primary and the other in the gateway hardware as the backup. By the same token, two gateway software packages are implemented, the primary package is in the gateway hardware, and the secondary package is in the ePR server hardware as the backup. As shown in the middle row of Figure 20.15, the gateway and the ePR server each has its own hardware, where each hardware piece houses both the ePR server software and the gateway software; one is the backup of the other. Figure 20.16 depicts the dual-system backup mechanism.

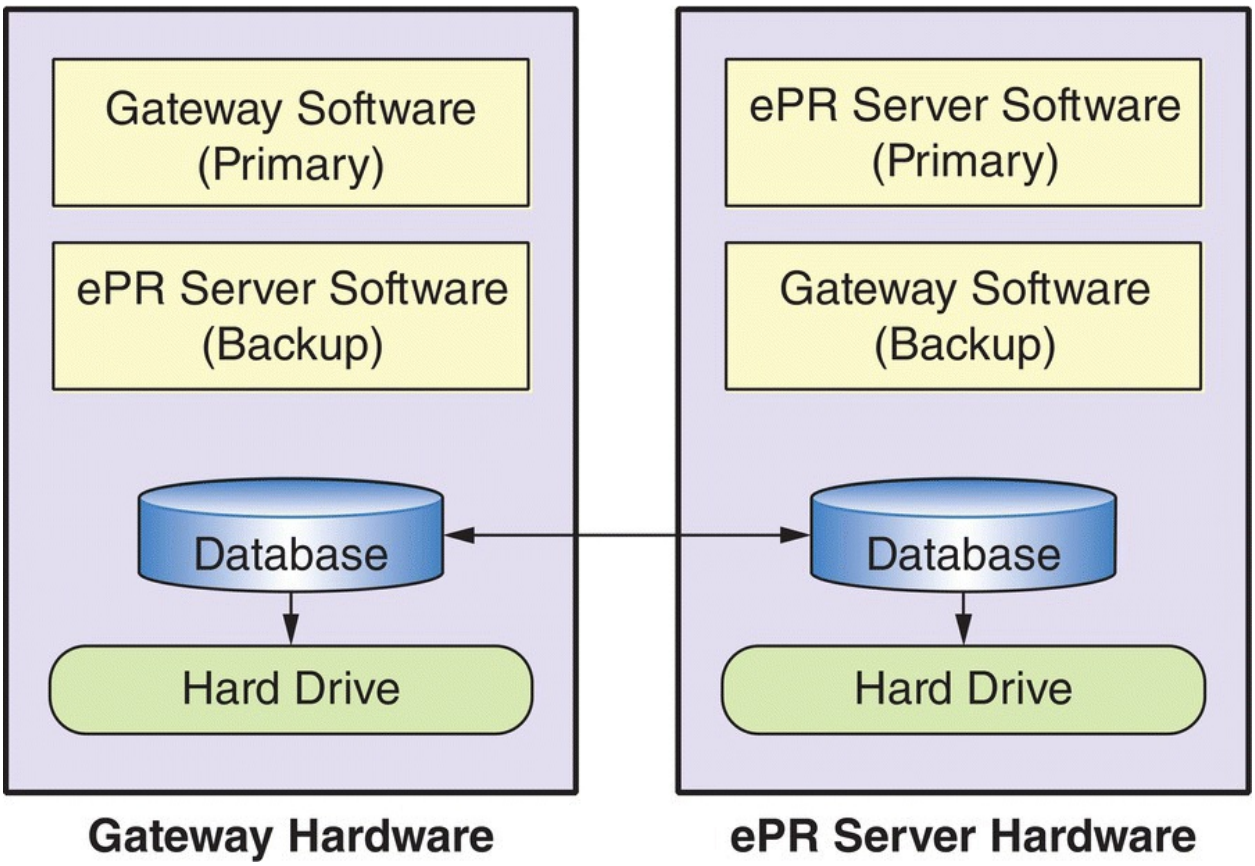

Figure 20.16 Tandem dual-system backup schema with two hardware pieces: gateway hardware and ePR server hardware. Each hardware piece has two softwares—ePR server software and gateway software—and a tandem database with hard drive for data and metadata archive [18].

The input data first comes to the gateway hardware, where the gateway software categorizes them by images, live waveform information, and textual information. Images include DICOM images in their original DICOM format as well as in JPEG format for Web display, along with endoscopic videos, endoscopic single frame images, and digital C-arm fluoroscopic images. The metadata in the DICOM images and other data are stored in the database disks. All acquired data and metadata are immediately backed up by the ePR server hardware.

20.4.2.3.2 Database Schema

The database schema is another important component of the system; it contains all values and relationships of the data objects that are stored. Figure 20.13 shows the database schema and all relationships among data tables based on the DICOM data model standard. The database schema is supported by the filesystem shown in Figure 20.15, where the images (DICOM, JPEG, GIF, etc.),

videos, and text files are stored. The database holds all metadata, data values, and pointers to the location of the objects stored in the filesystem as well. This database schema was first introduced for an ePR for radiation therapy for the decision-support purpose discussed in Chapter 11 and 19.

20.4.2.3.3 System Security

The system security has been considered carefully during the design, in order to comply with the Health Insurance Portability and Accountability Act requirement. Only users who have been granted permission are allowed access to the system. At the same time, the privacy of the communications are kept to prevent any unauthorized receiver from obtaining a patient's private information. To guarantee the security of the data, Web access to the ePR is established with HTTPS that encrypts all communication between the server and the clients (Web browsers). In addition, the ePR system handles permissions that allow users to perform different tasks on the system. Different user groups in the system have a different set of enabled permissions, but permission can be overwritten for an individual user by the system manager, if necessary, thus providing a level of flexibility.

20.4.2.3.4 Tandem System – Continuous Availability and Fail Over

The information kept in the ePR is unique and cannot be obtained from any other source if lost. Even images that were acquired from the PACS become unique once they were annotated in the ePR, so that they cannot be found anywhere else. To overcome any possible loss of data, a fault-tolerant solution that replicates the data of the ePR to more than one place has been implemented. The primary gateway serves as the backup for the primary ePR server, and vice versa.

In addition to storing the data with more than one copy, system redundancy with an automatic failover mechanism has been designed to access the data in case of failure of any component in the system and thus to guarantee system continuous availability.

20.4.2.4 Visualization and Display

The last of the four components in the ePR system is the GUI and display. In order for the ePR system to be utilized as an effective tool that can improve the workflow of the surgery department, it is important to have a user-friendly GUI that presents all the necessary contents for the surgery in an easy-to-use manner.

For this reason, the ePR system is designed to operate in three interrelated stages of a surgical procedure: planning (pre-op), surgery (intra-op), and patient recovery (post-op). The interface design between these three stages is critical. The display interface design (Figure 20.15) includes the main page, the pre-op display at the patient consultation room, the pre-op display at the OR, the intra-op display at the OR, the post-op display at the patient recovery area, the post-op display at the OR for surgical documentation, and the administrative pages.

Figure 20.17 shows the main page of the ePR system with three workflow steps as the pre-op list: the surgical patient's scheduled to be operated on; intra-op list: the next scheduled procedures of the patient; and post-op records: the procedures performed on the patient during intra-op.

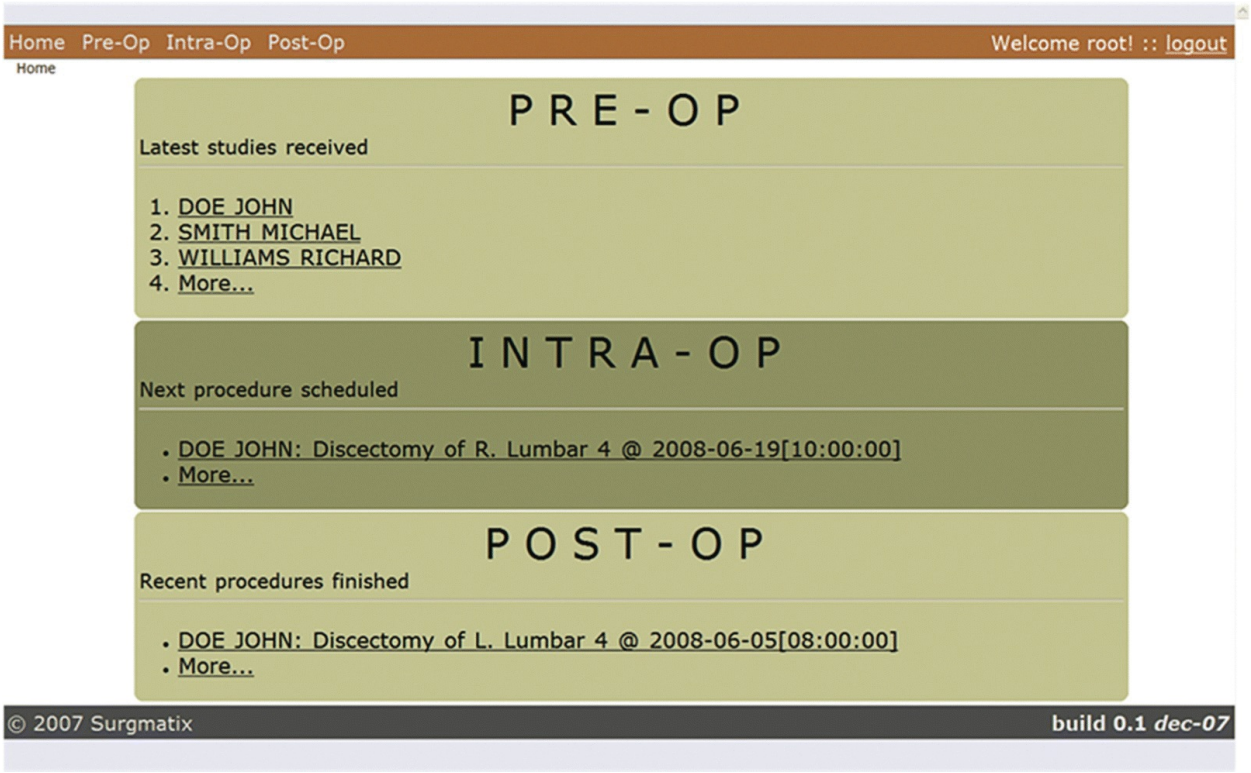

Figure 20.17 The home page of the ePR system showing three surgical stages: pre-op, intra-op, and post-op. The pre-op page shows that there are three patients with pre-op consultations; the intra-op and post-op pages show that patient John Doe is being operated on [17,18,20,21].

20.5 Pre-Op Authoring Module

The pre-op stage of a MISS procedure is where all necessary information prior

to the surgery procedure is collected and organized in a patient e-folder. This occurs days prior to the surgery, and involves querying, interviewing, collecting, and storing of presurgical medical images, patient demographic information, as well as other pertinent data that can assist the surgical procedure.

20.5.1 Workflow Analysis

The pre-op software module details the following steps:

1. The patient goes to the surgery planning center where proper medical examinations are performed. Usually, they are patient's x-ray and MRI exams that are stored in the PACS. These images are then reviewed by a medical specialist to determine the proper treatment course.
2. Once the patient has been recommended for an MISS procedure, they visit the surgeon for a consultation session. At this point, the patient registers in the MISS ePR system to have his/her fingerprint recorded for biometric verification and authentication. Also they fill out all the necessary forms on pain and clinical history, which are later entered into the ePR system.
3. Next the MISS clinical personnel create the surgical procedure planning in the ePR system (Figure 20.18A). The patient's ePR interface home pages allow the personnel to obtain their record and images from PACS and download them onto the ePR MISS server.
4. After the study is sent from the PACS to the ePR, the key images, including axial and sagittal MRI series images required, are selected and annotated by a physician assistant. The key images are labeled to identify the surgical region of the body.
5. The pre-op authoring phase is complete once all the necessary images and text information are entered into the ePR system; the information can be reviewed at the pre-op authoring and display module at the consultation workstation.

20.5.2 Participants in the Surgical Planning

Staff members at the MISS clinical site involved in the pre-op authoring module includes the following:

1. *Receptionist*s: Register the patient in the ePR system by entering the patient demographics, such as name, date of birth, sex, patient ID, and the accession number, as well as the pain questionnaire results. They also take a fingerprint

of the patient for biometric registration (used later at the OR for patient identification). They are in charge of scheduling the procedures and making sure there are no conflicts.

2. *Physician assistants*: Retrieve presurgical PACS images of the patient using a query/retrieve function in the pre-op authoring and display module of the ePR system. After the images of the patient have been transferred to the ePR system, they select the key images that are to be used during the intra-op stage. At the display module, they create the surgical procedures by entering annotations that would be later displayed with the images on the LCD monitor (52-inch) in the OR (Figure 20.11).
3. *Surgeon*: The surgeon approves the pre-op contents prior to display on the monitor in the OR. The surgeon works closely with the physician assistants to determine which images should be included in the procedures.
4. *Administrators*: In charge of assigning user access rights to the ePR system.

(A)

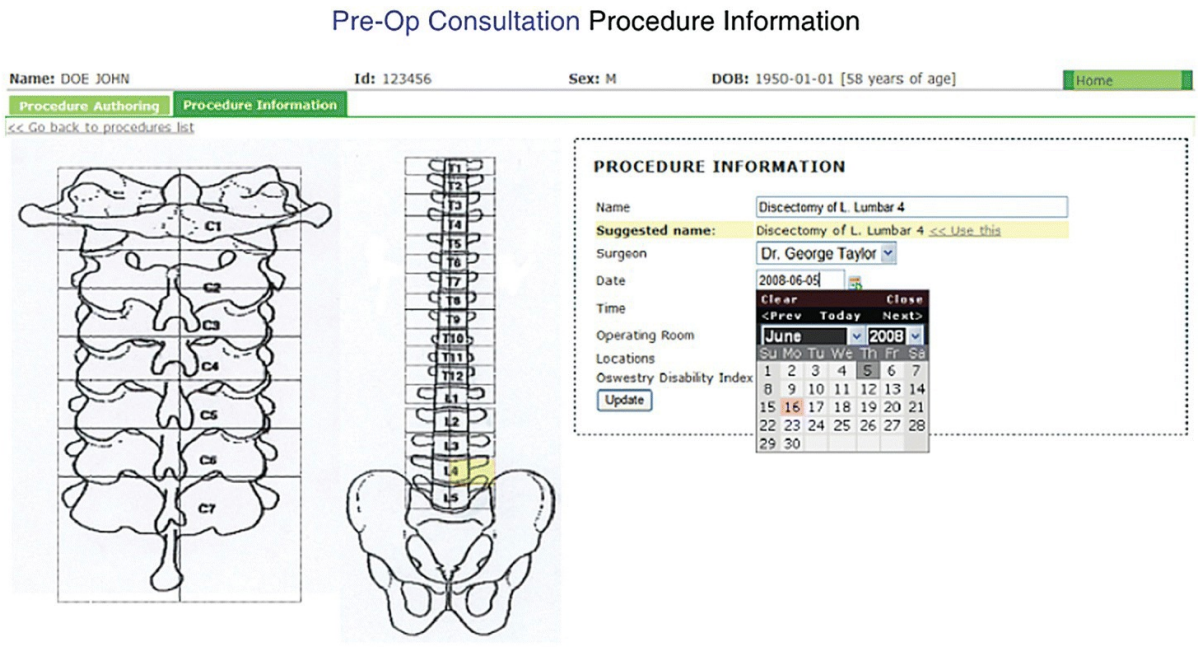

(B)

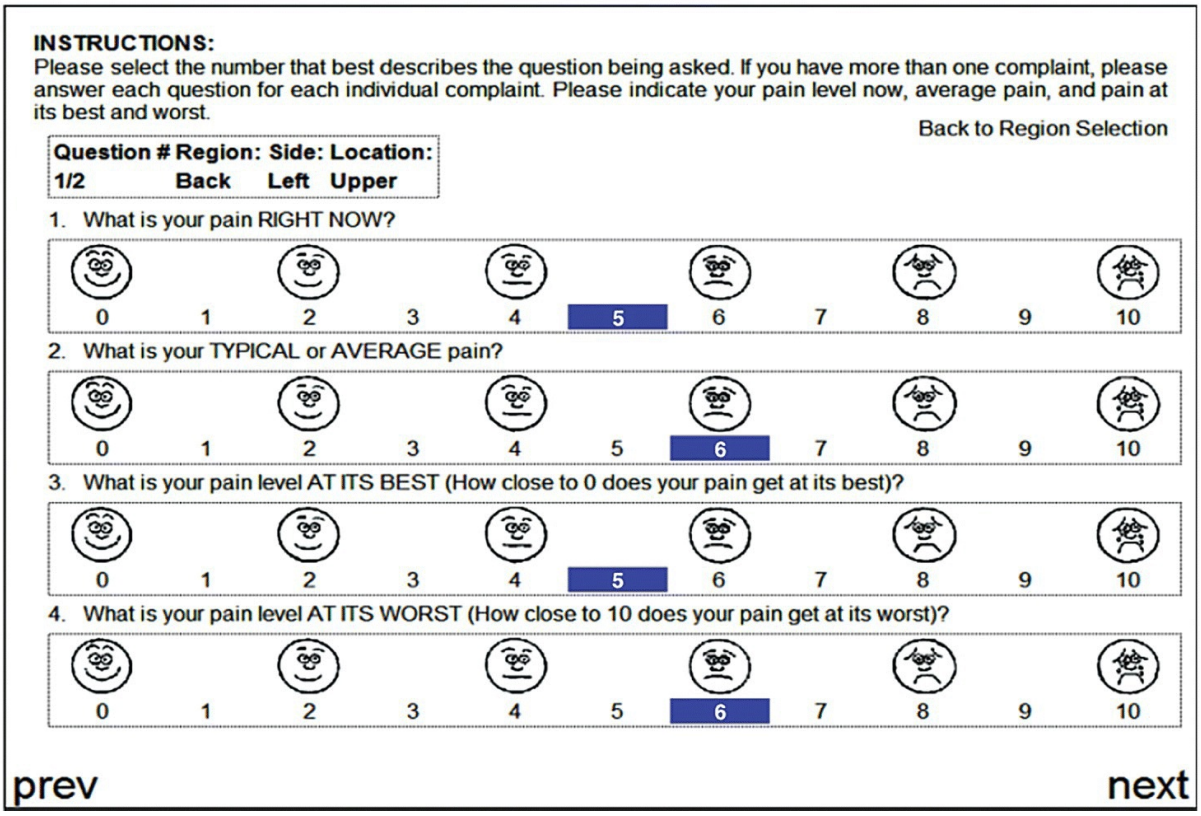

Figure 20.18 (A) Based on the patient examination, history, and recommendation, a physician assistant creates the surgical procedure planning in

the ePR system pre-op module. (B) Oswestry disability index, a survey to identify how the pain in the back or legs is affecting the patient in his/her daily activities.

20.5.3 Significance of Pre-Op Data Organization

20.5.3.1 Organization of the Pre-Op Data

Traditionally, surgeons rely on their memory to locate the body region where the procedure is to be performed. They review the MRI and x-ray images the day before surgery and study the approach to be taken during the procedure. These images are also brought to the OR for reference. But these images are displayed in hardcopy in an unorganized fashion scattered throughout the OR. The next few paragraphs focus on the organization of the pre-op patient information that requires the preparation process described earlier. This process is not done on the day of surgery; the information is saved days in advance with the display streamlined and organized for efficiency purposes.

20.5.3.2 Surgical Whiteboard Data

In addition to the input data described earlier, one type of pre-op data critical during surgery is the handwritten whiteboard information located at the entrance to the OR, with a very short summary of the patient such as name, sex, age, weight, height, any allergies, comorbidity, and pain. The pre-op authoring module described has been designed to integrate the whiteboard information onto the same pre-op screen for display in the OR during the surgery. The following survey measures are included in the ePR display:

1. *Visual analog scale (VAS)*: This a psychometric response scale to describe the amount of pain a patient is feeling from a specific part of her/his body.
2. *Oswestry disability index*: This is based on the patient's responses to the pain survey used to identify how the pain in the back or legs is affecting them in their daily activities (Figure 20.18B).

20.5.4 Graphical User Interface

The ePR system is designed to be user-friendly and effective at the same time. A criterion of the user interface is to minimize the number of mouse clicks needed to perform a certain task and to aggregate information adequately into a single interface whenever possible. The current pre-op authoring module is a self-contained interface where the users can download, edit, add, and delete the

contents as needed. The module has two major interfaces, one for editing and one for display on the monitor.

20.5.4.1 Editing

20.5.4.1.1 To Create a Procedure

The interface allows the users to create the surgical procedures by first selecting the key images as well as adding annotations to those key images, as shown in Figure 10.19A. On this screen, the MRI images and surgical procedures are combined into one display in the pre-op module. Image studies related to the surgical procedure are shown on the left-hand side based on the surgical data model (Figure 20.19A). To view an image in a study, the users can either drag the study shown in the list at the left to the viewing pane on the right-hand side or double-click on the study from the list at the left-hand side. Figure 20.19A displays a sagittal MRI image with the patient's unique identifier on top of the image. The toolbar with icons at the top of the viewing pane allows the users to perform certain tasks according to the current status of the editing module.

20.5.4.1.2 To Perform Editing

1. *To view images in a study*: The two icons on both the right-hand and left-hand sides allow the user to preview images in the study series.
2. *To perform image manipulation*: The toolbar includes some basic image manipulation tools, such as window/level, pan, and zoom. With this functionality, the images can be displayed optimally at the exact location of the lesion.

(A)

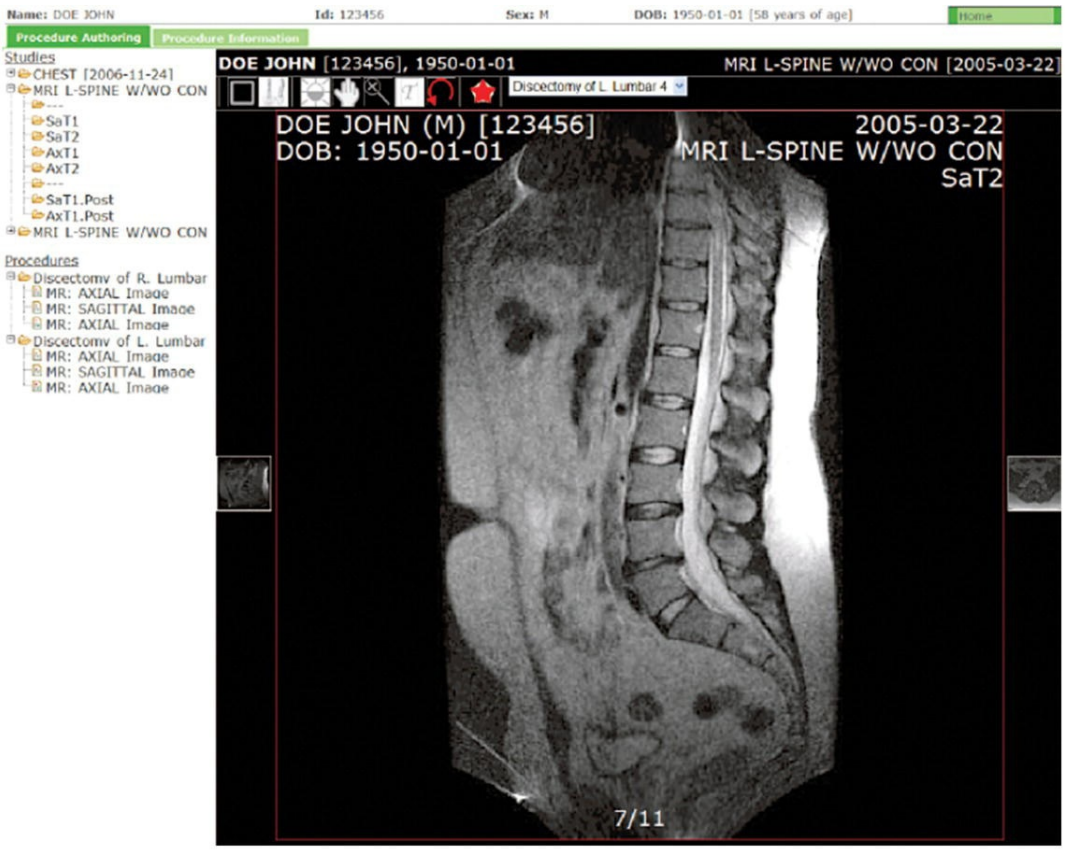
Name: DOE JOHN
Id: 123456
Sex: M
DOB: 1950-01-01 [58 years of age]
Home
Procedure Authoring
Procedure Information
Studies
CHEST [2006-11-24]
MRI L-SPINE W/WO CON

SaT1
SaT2
AxT1
AxT2

SaT1.Post
AxT1.Post
MRI L-SPINE W/WO CON
Procedures
Discectomy of R. Lumbar
MR: AXIAL Image
MR: SAGITTAL Image
MR: AXIAL Image
Discectomy of L. Lumbar
MR: AXIAL Image
MR: SAGITTAL Image
MR: AXIAL Image
DOE JOHN [123456], 1950-01-01
MRI L-SPINE W/WO CON [2005-03-22]
Discectomy of L. Lumbar 4
DOE JOHN (M) [123456]
DOB: 1950-01-01
2005-03-22
MRI L-SPINE W/WO CON
SaT2
7/11

(B)

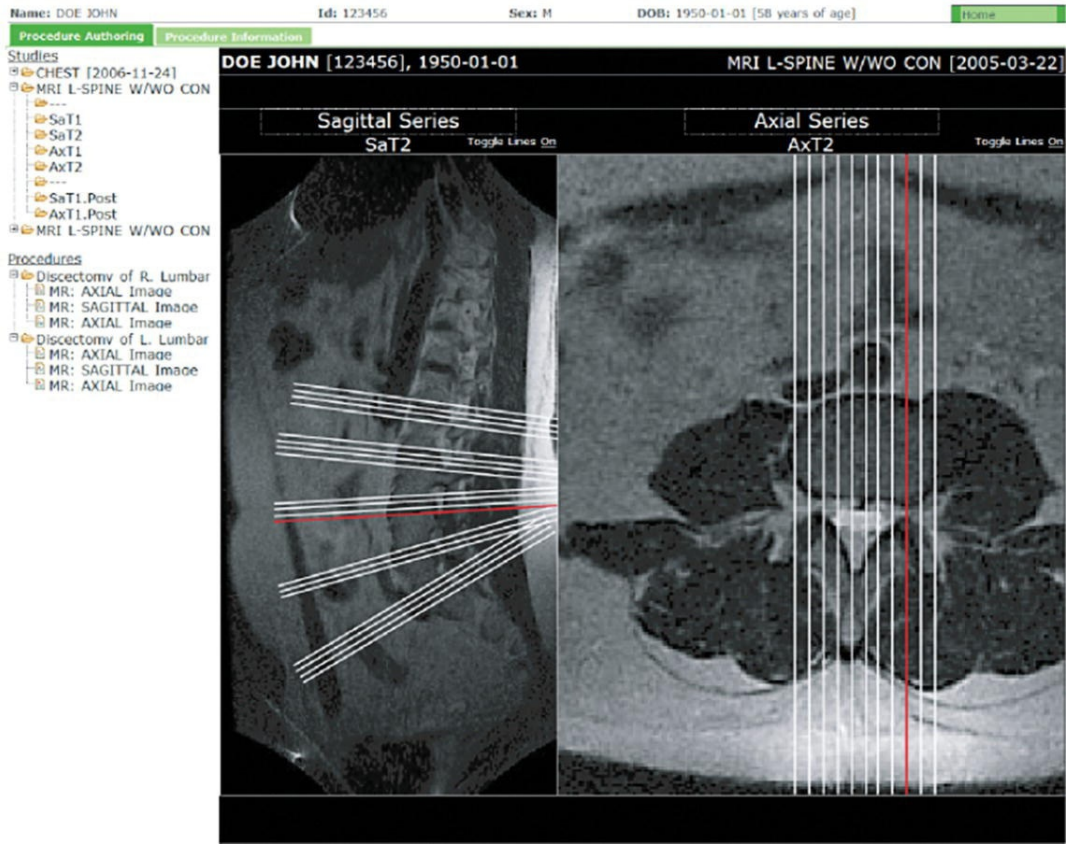
Name: DOE JOHN
Id: 123456
Sex: M
DOB: 1950-01-01 [58 years of age]
Home
Procedure Authoring
Procedure Information
Studies
CHEST [2006-11-24]
MRI L-SPINE W/WO CON

SaT1
SaT2
AxT1
AxT2

SaT1.Post
AxT1.Post
MRI L-SPINE W/WO CON
Procedures
Discectomy of R. Lumbar
MR: AXIAL Image
MR: SAGITTAL Image
MR: AXIAL Image
Discectomy of L. Lumbar
MR: AXIAL Image
MR: SAGITTAL Image
MR: AXIAL Image
DOE JOHN [123456], 1950-01-01
MRI L-SPINE W/WO CON [2005-03-22]
Sagittal Series
SaT2
Toggle Lines On
Axial Series
AxT2
Toggle Lines On

(C)

(D)

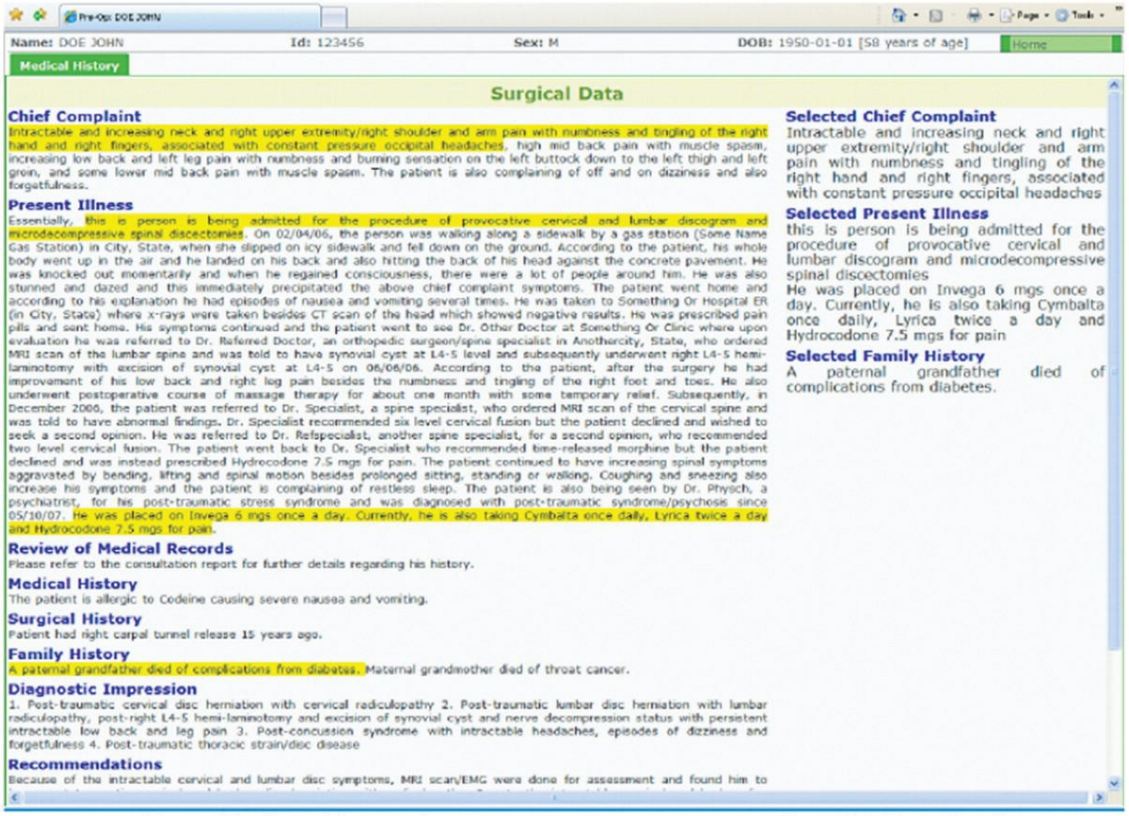

From Patient Record

On OR Pre-Op Screen

Figure 20.19 (A) Pre-op authoring module page. The upper left-hand text list depicts the surgical data model showing the studies and procedures. After the user clicks on an item in the list, the proper image, in this case a sagittal MRI, is shown on the right. (B) The neuronavigator tool allows the correlation of the position of the lesion in the sagittal (left) and the axial view (right). The red lines are the two corresponding sagittal and axial sections. (C) The pre-op display organized during patient consultation as seen on the monitor in the OR during intra-op. Top left: From the whiteboard information; Bottom left: Extracted from the patient history summary. Right: Images and annotation during the pre-op consultation (see also Figure 20.11, right). (D) Method of extracting pertinent and concise clinical history information by highlighting (yellow) from the full report during pre-op editing (compared with C, left). The extracted concise information is shown in (C) during intra-op.

20.5.4.2 Neuronavigator Tool for Image Correlation

During MISS, the axial view has to be correlated with the corresponding sagittal view of the MRI. The neuronavigator tool in the pre-op module allows such correlation from the display, as shown in Figure 20.19B.

20.5.4.3 Pre-Op Display

A MISS procedure requires multimedia data during the pre-op stage, including patient history, images, and consultation results. These data should be organized and displayed in the pre-op display during surgery. An example is shown in Figure 20.19C, which depicts the whiteboard information outside of the OR (top left), the extracted clinical history of the patient (bottom left), as well as the key images selected from the MRI study with their annotations during consultation (right). The term that is used for this display is the "pre-op display", since the authored data are actually displayed during the intra-op workflow stage.

20.5.4.4 Extraction of Clinical History for Display

Figure 20.19C depicts the extracted clinical history of the patient from a detailed report for display purpose during the intra-op. Figure 20.19D illustrates the method of extraction by highlighting (yellow) from the full report during pre-op editing (compared to Figure 20.19C, left).

20.6 Intra-Op Module

20.6.1 The Intra-Op Module

The intra-op stage is defined as the time the surgeon begins the MISS procedure to its finish at the OR. During the procedure, all information collected during the pre-op is displayed on the pre-op display in the OR. In addition, live data from different input devices during the surgery are collected by the IU and displayed on the intra-op monitor. Before the surgery starts, the patients' fingerprint is captured in the OR and verified with the biometric data acquired during the pre-op stage. This is an important step toward reducing error and ensuring correct patient identification prior to surgery.

20.6.2 Participants in the Operating Room

In addition to their standard assigned surgical tasks, personnel involved in the ePR intra-op include:

1. *Surgeons and medical staff*: The chief surgeon operates on the patient and makes decisions based on the ePR pre-op and intra-op displays while the procedure is taking place. Other surgeons and medical staff can discuss with the chief surgeon based on alert messages on the intra-op display. Thus, the ePR system facilitates their multiple tasking by displaying any relevant information in an organized and efficient easy-to-view way.
2. *An anesthesiologist*: Provides anesthesia to the patient and monitors the vital signs during the procedure.
3. *Nurses and technicians*: Each has preassigned duties to perform during the surgery. These duties include auto and manual surgical data acquisition if needed.

20.6.3 Data Acquired during Surgery

During surgery, while the surgeon is operating, all important live data are automatically acquired and saved by the IU (Figure 20.15). This acquired dataset forms the record of the patient's condition during the surgery:

1. *BIS (bispectral index system)*: BIS signals comes from an array of electrodes that are attached to the patient's forehead and monitor the patient consciousness. The value that comes out is in the range of 0–100, where zero means no brain activity and 100 is full consciousness. The safe range is considered to be between 40 and 70. Currently, the output data from this device is obtained from a serial port (RS 232).

2. *Vital signs*: The data obtained from the vital signs device includes the respiratory rate, heart beat rate, temperature, blood pressure, pulse oxygen and the CO_2 respiratory emission levels of the patient (see Table 20.1 for other possible data). Currently, the data output from this device is obtained from a serial port (RS 232).
3. *EMG*: The EMG device monitors the electrical activity of the muscles and nerves through a set of small needles inserted into the patient's body with the goal of preventing damage to the spinal cord while the surgeon is operating with the endoscope. Currently, the real-time output data from this device is obtained from an Ethernet connection.
4. *C-arm fluoroscopic images*: The C-arm imaging device takes x-ray images that assist the surgeon to pinpoint the exact position of the spinal column where the lesion is located in real time with respect to endoscopic probes. These images are also encapsulated in a DICOM file and sent to the ePR.
5. *Endoscopic images and video*: The MISS procedure is performed using an endoscope through a small incision (6 mm) made on the patient's body. The video stream of the camera inserted in the endoscope is displayed continuously on the intra-op live display and is also saved in the IU for later review. At the same time, the unit takes snapshots of the endoscopic video and saves them as images at the same preassigned default time interval as the other live data being acquired. The resolution of the video and images can vary from vendor to vendor; currently the ePR system is acquiring the output in the VGA standard with a resolution of 640 Å ~ 480 pixels. The output data from this device is obtained from an S-video port.
6. *Laser:* The laser is inserted in the endoscope and used to cauterize a wound inside the body for both cutting and healing purposes, but its usage depends on the type of treatment. The current available output from this device is from a serial port (RS 232).

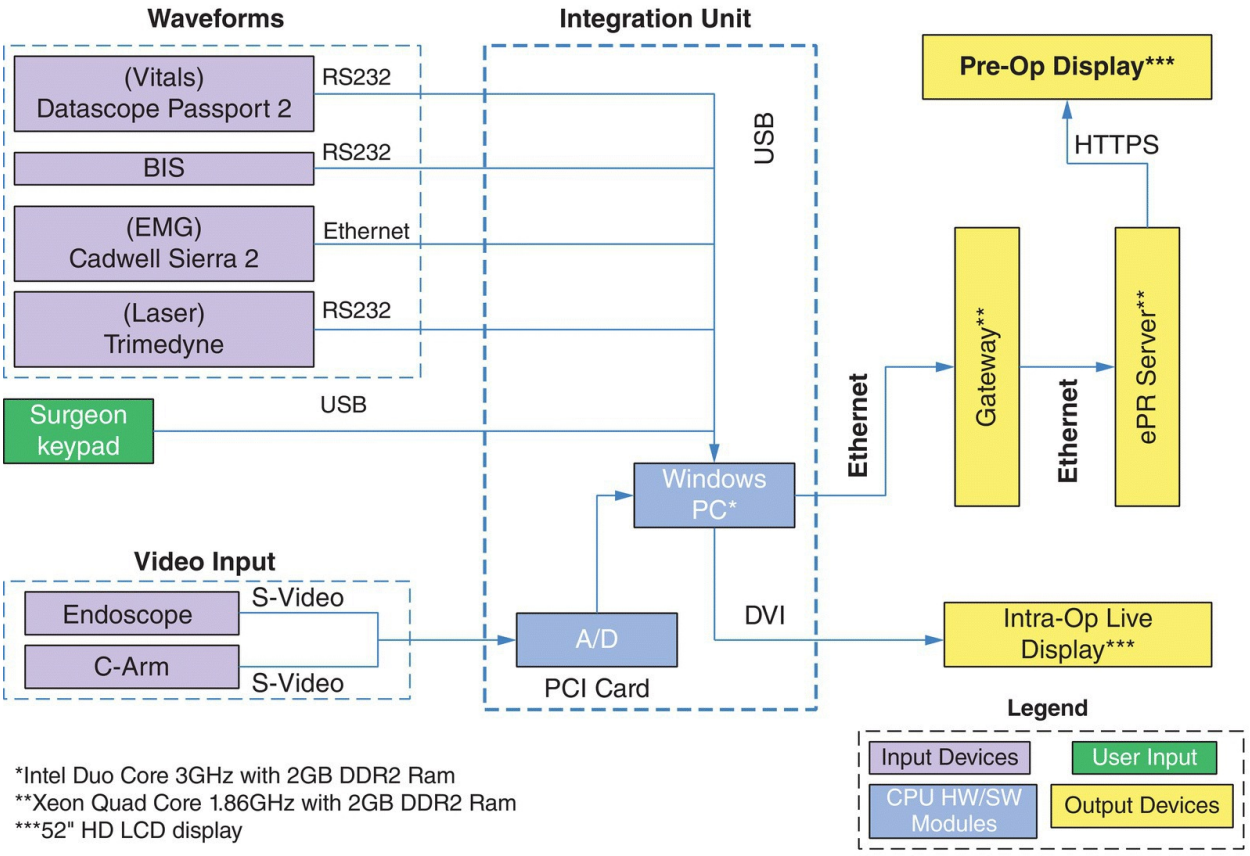

Figure 20.20 Hardware and software interconnectivity diagram for a MISS procedure using the ePR system. During intra-op, live data are continuously displayed on the intra-op monitor. A system default allows the live intra-op data to be acquired at a specific time interval. The surgeon has an option to acquire additional data during the entire course of the operation by pushing the surgeon keypad (green). The IU in the middle column accepts different input devices and sends them to the intra-op live display (lower-right, yellow) [17,18].

20.6.4 Internal Architecture of the Integration Unit (IU)

Figure 20.20 shows the interconnectivity between the existing input devices presented in the OR during surgery (see Figure 20.14, workflow step 5). The left-hand side shows the data inputs or sources, as explained in the previous section; the middle is the IU, and the right-hand side depicts the connectivity between the unit and the intra-op live display. The pre-op display shown at top right (yellow) also presents in the OR. The current setup allows the unit to support the available input devices at the implementation site at the California Spinal Institute, but the unit has been designed to be flexible enough to support various vendors' input devices using different interfaces (serial ports, VGA,

Ethernet, etc.).

As seen in Figure 20.20, there is an interactive input device called the surgeon keypad (left, green) that permits surgeons to manage some functionality of the IU. With this keypad, the surgeon can take a screenshot of all the data and images any time during the surgery if needed, and it can also be used to have a side-by-side freeze frame display of the endoscopic video with a prior endoscopic screenshot for comparison purposes. This feature facilitates the surgeon to reserve surgical data for the later post-op reporting.

20.6.5 Interaction with the Gateway

During the surgery, the IU saves all data acquired temporarily from different connected devices in its hard drive; after completion of the surgery, it automatically connects and sends all data to the gateway server. The protocol used to send the data is HTTPS. If the primary gateway is down, the unit will connect to the secondary gateway, which is the ePR server for failover (see Figure 20.16 for the data backup schema). To reduce the total sending time, the data are compressed and combined in a single zip file. Once the data is correctly received by the gateway server, the file is uncompressed and processed accordingly.

20.6.6 Graphical User Interface

Figure 20.21 shows the large intra-op live display of a patient with waveforms and images. The horizontal axis is time. There are eight groups of waveforms: six vital signs with heart rate, blood pressure, respiratory rate, pulse oxygen concentration, pCO_2, plus temperature, and BIS, intravenous fluid(IVF). Every dot in the waveform represents a data point over a 1-second interval. Also displayed are the C-arm fluoroscopic (right), the endoscopic video images (middle), and EMG waveforms (left). Lastly, laser energy in joules is shown in the bottom row. The video is updated on the intra-op live display with a frame rate of 30 per second (a default value).

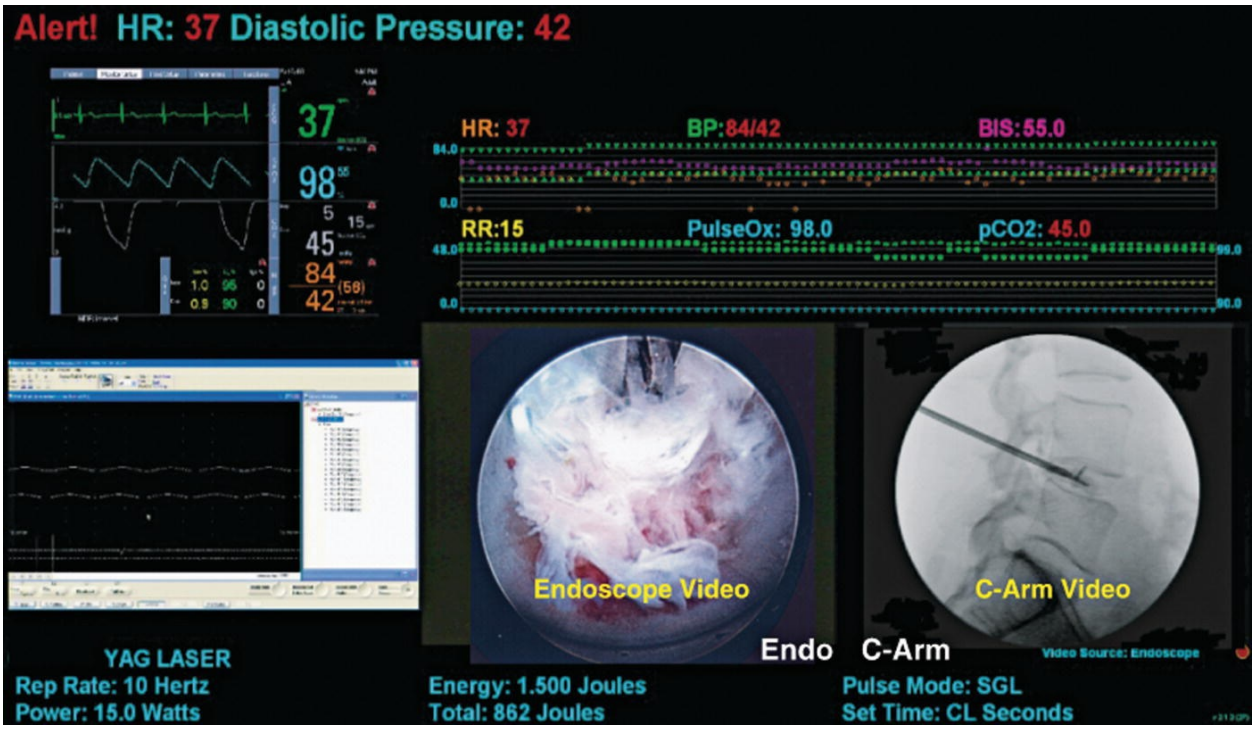

Figure 20.21 Example of the intra-op live display as seen on the large monitor in OR (see also Figure 20.11, right). (Top row) Eight waveforms of six vital signs, plus BIS, and IVF with digital values. Alert message on low heart rate (HR) and diastolic pressure; the horizontal axis is time. (Middle row from left to right) Waveform of EMG, endoscopic (Endo) images, and fluoroscopic image; (bottom row): Laser output values.

20.6.7 Rules-Based Alert Mechanism

If a signal falls outside its safe range, a three-stage mechanism will alert personnel in the OR about the situation:

1. *Warning mode*: If a numeral falls outside the safe range, it will change color to red (as seen with the pulse oxygen concentration and blood pressure in Figure 20.21, top line).
2. *Emergency mode*: If the condition falls to a value greater or lower in 25% of the safe range, then the live display will place an alert message at the top of the screen.
3. *Critical mode*: If the data signal value is either greater or lower in 50% to the values in the safe range, then the alert message will cover the whole screen.

20.7 Post-Op Module

20.7.1 Post-Op Module Stage

The post-op stage takes place after the completion of the surgical procedure. There are three substage times:

1. patient in the recovery area and then discharged;
2. the surgeon documents the surgical results; and
3. follow-up pain questionnaires.

20.7.2 Participants in the Post-op Module Activities

The personnel involved in the post-op module activities include the following:

1. *Surgeons*: The chief surgeon reviews the patient's ePR record, including pre-op, intra-op, and post-op files and images, and dictates the surgical report. The surgeon can also review the complete/partial intra-op digital file, including surgical images from the ePR for the report.
2. *Physician assistants*: Assist the surgeon in creating the surgical report.
3. *Nurses and front-desk personnel*: Perform follow-up surveys several times after the surgery, and enter the pain data from patient questionnaires into the ePR system as a follow-up on the progress of the patient.

20.7.3 Patient in the Recovery Area

While the patient is in the recovery area, some of the patient's vital signs (pulse oxygen, heart rate, and blood pressure) are still being recorded with the vitals devices and can be displayed on the recovery monitor within the recovery area (Figure 20.15). In addition, the patient will be questioned by a nurse about immediate pain levels before being discharged, as a follow-up monitoring of the surgery's effectiveness. These data are entered into the ePR post-op module for statistical outcome studies in the patient recovery record.

20.7.4 Post-Op Documentation – The Graphical User Interface (GUI)

The surgeon completing the post-op document can retrieve information from the post-op module pertinent to the surgery using the GUI. This process involves four major steps:

1. *Find the patient from the ePR system*: The correct patient can be found from the ePR by clicking on the first line of the bottom block section of GUI (Figure 20.17).
2. *Select images*: From this GUI, the surgeon can select endoscopic images that can be included in the final report by clicking on the star at the top left-hand corner of the viewing pane. Figure 20.22 shows the image is selected for the final report.
3. *Select waveforms*: The waveforms are displayed at the bottom of the GUI (see Figure 20.22, bottom). They can be dynamically selected by clicking on their corresponding boxes at the upper right-hand side of the interface.
4. *Data synchronization*: A blue slider at the bottom of the graph (Figure 20.22) allows for synchronized viewing of all the image and waveform data to be displayed.

Figure 20.22 presents a documentation page that has been authored by the surgeon from the ePR system using the post-op GUI. The data displayed and documented include an endoscopic image, heart rate, diastole and systole blood pressures, respiratory rate, BIS score value, oxygen pressure, partial pressure of CO_2, and temperature.

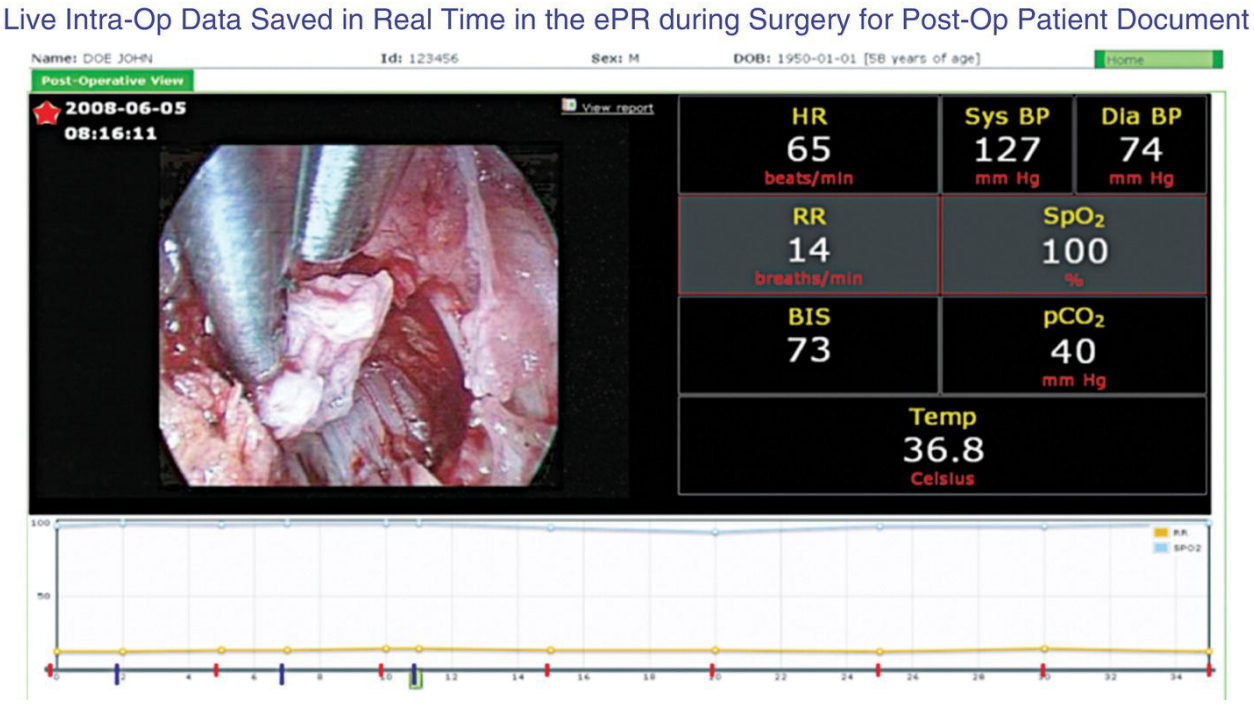

Figure 20.22 Post-op authoring module displaying a document showing data acquired during the surgery. This page can be synchronized by the surgeon's

post-op dictation. It is in PDF format for easy insertion into the report. The red time marks at the bottom are default intra-op data capture. Blue marks are additional data the surgeons saved during the surgery. The green mark represents the time frame when this page was captured.

There are also two curves shown at the bottom of Figure 20.22 (respiratory rate and pulse oxygen concentration); these are waveforms obtained from another intra-op device.

During the documentation, the surgeon also dictates the report, which will be synchronized with the authorized image and waveform paged.

20.7.5 Follow-up Pain Surveys

Nurses and front-desk personnel take pain surveys several times after the surgery and enter the survey data into the post-op module of the ePR system as a follow-up of the progress of the patient. The collective information can be used for future patient outcome analyses.

20.8 System Deployment, User Training and Support

The prototype system was deployed in August 2008 at the California Spinal Institute, which is the only clinical site in Southern California that performed MISS at that time. This section summarizes the highlights.

20.8.1 System Deployment

20.8.1.1 Planning and Design Phase

The ePR system for MISS was developed at the IPILab, Department of Radiology, University of Southern California, which has had close collaboration with the California Spinal Institute for more than five years. There are three phases of the implementation:

- *Phase 1*: To test the functionality of the ePR system. A prototype for each of the ePR components was developed and integrated at the California Spinal Institute research facility; in addition, mock-up data were collected at the Institute that included an intra-op signal simulator for the integration unit.
- *Phase 2*: Once the system was tested fully in the laboratory environment, it

was deployed at the OR at the Institute to obtain user feedback and clinical evaluation. The hardware and software components consisted of the gateway server, ePR server, IU, and fingerprint readers. Other software packages included the ePR Web pages, IU application, fingerprint application, database, and the Web server.

- *Phase 3*: The clinical implementation was to deploy the ePR system in the OR. This stage was challenging, since the OR was used for MISS daily; both the clinical and the engineering team had to work together to circumvent the clinical schedule, minimizing the risk of any possible clinical disruption. This working environment was especially difficult during the final stage of implementation, while the ePR was taking over some routine duties usually responsible by the regular surgical personnel.

20.8.1.2 Hardware Installation

The ePR and gateway servers were installed in the first and second OR at the California Spinal Institute. Figure 20.23A shows the location of the two servers where the installation was in progress.

(A)

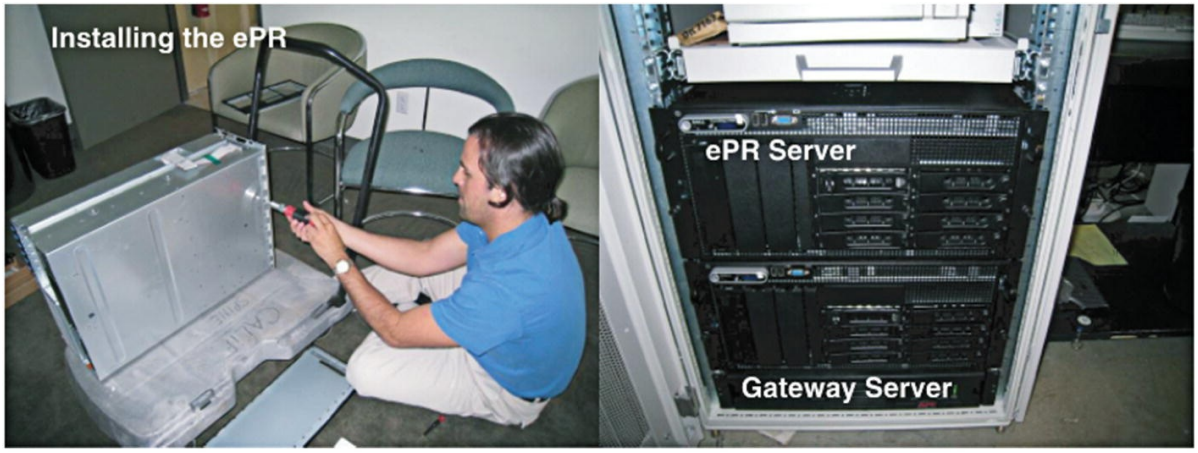

(B)

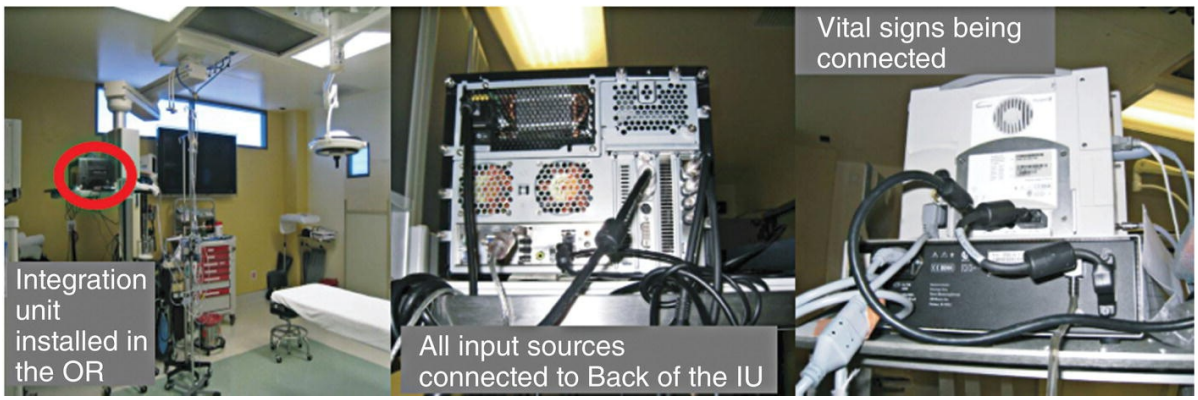

Figure 20.23 (A) ePR server installation at the server room of the California Spinal Institute. Dr J. Documet is shown installing the servers. (B) Left: the Integration unit (IU, inside the red ring) installed in the OR, it is connected to various input sources. Middle: Input units cables are connected to the back of the IU. Right: The back of the vital signs device is connected to the back of the IU [17,18].

Recall that the IU was connected to all required peripheral devices in the OR (Figure 20.20) for monitoring the real-time response of the patient during the clinical procedure shown in Figure 20.23B.

20.8.1.3 Software Installation

Once the servers were installed at the clinical facility, the next step was to configure all necessary software components of the ePR MISS system. These components included:

1. *ePR server*: A Web application that provides the user interface for the pre-op and post-op authoring module and the pre-op display (during surgery) as well.
2. In addition, this server requires the installation of the Web server (Apache) and the database (MySQL) [22].
3. *Gateway server*: A listener software that receives incoming DICOM studies sent from the PACS and a set of scripts to extract the metadata information and store it in the database. This server also receives the real-time surgical data, including live images and waveforms collected during a surgical procedure, which are sent by the IU using an API.
4. *Integration unit*: Acquires the surgical data in the form of data points, images, and videos from the surgical peripheral devices at the OR. A program developed in C++ is utilized to make low-level system calls to the different interfaces, depending on performance requirements to display real-time data in the OR.
5. *Fingerprint module*: The registration and identification of patients at the clinical facility is performed during the pre-op stage and the identification and verification at the intra-op stage. This module makes use of a fingerprint software development kit(SDK) from CrossMatch.

20.8.1.4 Special Software for Training

Training the users of the ePR system was a primary objective during deployment, and Section 20.8.2 explains this task in more detail. Training software was installed allowing the users to be trained more effectively and efficiently.

20.8.2 Training and Supports for Clinical Users

The following users were among those trained on the use of the ePR system:

1. *Surgeons*: Training was provided for the pre-op and post-op authoring modules (post-op was demonstrated using mock-up data), on how to use them to add, edit, and delete contents. In addition, surgeons were taught how to interpret the two pre-op and intra-op LCD monitors.
2. *Physician assistants*: Both “group” and “individual” training sessions were given using the pre-op authoring module, and topics included query/retrieve functionality, image manipulation, key image selection, procedure management, and annotations for key selected images.
3. *Nurses*: Nurses were trained on how to enter information related to the patient’s whiteboard data and survey forms.
4. *Front-desk assistants*: They received training on the scheduling of surgical procedures, input of pain surveys during pre-op and post-op stages, as well as patient registration including of patients’ fingerprints.
5. *Technicians*: The training given to technicians included verifying the patients’ identity at the OR using the fingerprint module. In addition, they were instructed on how to read the data presented on the LCD monitor at the OR.
6. *Administrative staff*: Administrative personnel learned how to add or remove a user from the ePR system and how to manage the consent documents for different procedures.

The engineering team provided three months' on-site training on the ePR system and assisted the duty staff in preparing the pre-op module. Figure 20.24 shows both the “group” and “individual” training for the pre-op and intra-op modules. The post-op module had been released to the surgeons and physician assistants for clinical use, and system refinement for report authoring was continuing.

(A)

(B)

(C)

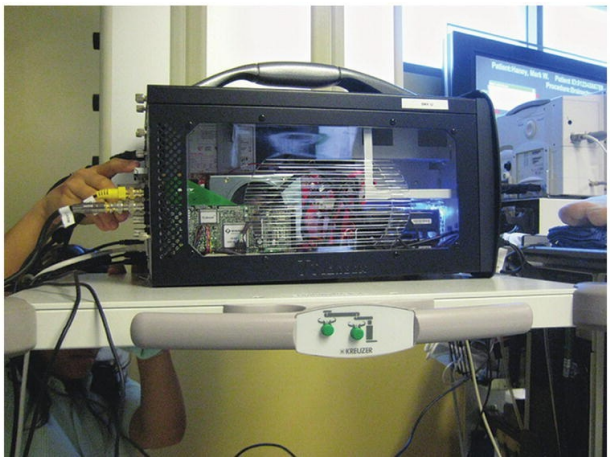

Figure 20.24 Training of the ePR system for the clinical staff at the California Spinal Institute. (A) Group training in pre-op authoring at the consultation room. (B) One-to-one training at the consultation room on GUI. (C) Training of the IU in the OR for input devices connectivity. The engineer is behind the unit.

20.9 Summary

A step-by-step approach is presented to develop a multimedia ePR system for imaging-guided-assisted MISS. It starts with the introduction of MISS, then the three stages of MISS workflow: pre-op, intra-op, and post op. The ePR architecture is developed using a three-part module: pre-op, intra-op, and post-op, plus the IPI Lab hardware and the software with four components: the input IU, fault-tolerant gateway server, fault-tolerant ePR server, and the visualization and display component. A prototype was built and deployed at an MISS clinical site with user training and support for daily use. Experience gained from the

clinical site provides valuable understanding and knowledge that form the basic ingredients for the planning and development of image-guided or -assisted MISS for other body regions, which is discussed in the next chapter.

References

1 Jensen, M., Brant-Zawadzki, M., Obuchowski, N., *et al*. (1994) Magnetic resonance imaging of the lumbar spine in people without back pain. *N Engl J Med*, 331: 69–116.

2 Vallfors, B. (1985) Acute, subacute and chronic low back pain: clinical symptoms, absenteeism and working environment. *Scan J Rehab Med*, 11(suppl), 1–98

3 Chiu, J.C. (2008) The decade of evolving minimally invasive spinal surgery (MISS) and technological considerations. *Internet J Mini Invasive Spinal Technol*, 2(3).

4 Chiu, J.C. (2006) Technological developments for computer assisted endoscopic minimally invasive spinal surgery (MISS). *Proc Comp Asst Rad Surg*, 20th International Congress, Osaka, Japan, June 28–July 1; CARS. Amsterdam, Netherland: Elsevier.

5 Chiu, J.C. and Savitz, M.H. (2005) Operating room of the future for spinal procedures. In: *The Practice of Minimally Invasive Spinal Technique* (Savitz, M.H., Chiu, J.C., Rauschning, W. and Yeung, A.T. eds). New York: AAMISS Press, pp. 645–648.

6 Chiu, J.C. and Savitz, M.H. (2005) Multicenter Study of Percutaneous Endoscopic Discectomy. In: *The Practice of Minimally Invasive Spinal Technique* (Savitz, M.H., Chiu, J.C., Rauschning, W. and Yeung, A.T. eds). New York: AAMISS Press, pp. 622–626.

7 Chiu, J.C. and Savitz, M.H. (2005) Use of laser in minimally invasive spinal surgery and pain management. In: *Arthroscopic and Endoscopic Spinal Surgery: Text and Atlas*, 2nd edition (Kambin, P. ed.). Totowa, NJ: Humana Press, pp. 259–269.

8 Chiu, J.C. (2004) Anterior endoscopic cervical microdiscectomy. In: *Endoscopic Spine Surgery and Instrumentation* (Kim, D., Fessler, R. and Regan, J. eds). New York: Thieme Medical, pp. 48–58.

9 Chiu, J.C. (2004) Endoscopic lumbar foraminoplasty. In: *Endoscopic Spine Surgery and Instrumentation* (Kim, D., Fessler, R. and Regan, J. eds). New York: Thieme Medical, pp. 212–229.

10 Chiu, J.C., Clifford, T. and Greenspan, M. (2000) Percutaneous microdecompressive endoscopic cervical discectomy with laser thermodiskoplasty. *Mt Sinai J Med*, 67, 278–282.

11 Huang, H.K. (2010) *PACS and Imaging Informatics: Principles and Applications*, 2nd edition. Hoboken, NJ: Wiley & Blackwell.

12 Huang, H.K. (2007) The role of imaging informatics in MISS. *Proc 21st CARS Intern Congress in Comp Asst Rad Surg*, Berlin, Germany, June 27–30.

13 Huang, H.K. (2004) *PACS and Imaging Informatics: Principles and Applications*. Hoboken, NJ: Wiley & Blackwell.

14 Huang, H.K. (2001) PACS, informatics, and the neurosurgery command module. *J Mini Invasive Spinal Tech*, 1, 62–67.

15 Chiu J and Huang HK, developed the Surgical Data Monitoring and Display System. USA, Trademark: 079977-0015: SURGMATIX; Canadian No. 1,423,071, 2010. US Patent 8,313,432 B2. Nov 20, 2012.

16 Huang, HK, Chief Consultant of the Honk Kong (HK) Hospital Authority, who developed the Enterprise-level total filmless operation for the HKHA healthcare delivery system, 01/2000 – 09/2012. He helped to implement a total (90%) filmless operation using the ePR-ID (with image distribution) platform for the HA healthcare delivery including 43 public hospitals and their connections to private physicians in Hong Kong.

17 Documet, J., Le, A., Liu, B.J., Chiu, J. and Huang, H.K. (2010) A multimedia Electronic Patient Record (ePR) system for Image-Assisted Minimally Invasive Spinal Surgery. *Intern J. Comp Asst Rad & Surg*, 5(3), 195–209.

18 Documet J, Ph.D, who participated in developing the Electronic Patient Record (EPR) System for the Imaging Assisted Minimally Invasive Spinal Surgery System. He receipted his Ph.D. Degree at the University of Southern California, USA, 2009.

19 Liu, B.J., Law, Y.Y., Documet, J. and Gertych, A. (2007) Image-assisted knowledge discovery and decision support in radiation therapy planning,

Comput Med Imag Graph, 31(4–5), 311–321.

20 CrossMatch Technologies, Inc. Available at: http://www.crossmatch.com

21 MySQL AB, Sun Solaris Microsystems Inc. Available at: http://dev.mysql.org

22 Apache Web server. Apache Software foundation. Available at: http://httpd.apache.org

21
From Minimally Invasive Spinal Surgery to Integrated Image-Assisted Surgery in Translational Medicine

CHAPTER MENU

21.1 Introduction

21.2 Integrated Image-Assisted Minimally Invasive Spinal Surgery

21.2.1 The Planning Stage

21.2.2 The Clinical IIA-MISS EMR System

21.2.3 Use of the IIA-MISS EMR System and Training

21.2.4 Pre-Op, Intra-Op, and Post-Op, and Data Archive, Display, and Document

21.3 IIA-MISS EMR System Evaluation

21.3.1 Data Collection

21.3.2 Statistical Analysis

21.3.3 Other Qualitative Advantages of the EMR system

21.4 To Fulfill some Translational Medicine Aims

21.4.1 Methods

21.4.2 Preliminary Results

21.4.3 A Mock-Up Intra-Op Mimicking Neurosurgery

21.5 Summary

21.6 Contribution from Colleagues

Acknowledgement

References

Surgery uses medical images to plan and guide the surgical procedure. The term “image-assisted surgery” emphasizes the importance of the image component in

planning and assisting the surgical procedure. Usage of real-time images to assist minimally invasive surgery allows the patient to return home on the same day, resulting in a lower-cost operation and shortening the patient's recovery time. For this reason, such surgery becomes favorable for non-complicated surgical procedures. This chapter starts by introducing minimally invasive spinal surgery (MISS), followed by integrated image-assisted (IIA) MISS. The combination of these two technologies is the IIA-MISS electronic medical record (EMR) system, which collects, displays, and archives relevant patient's EMR in real time, in this case the surgical record. Currently, it is an important national priority in healthcare delivery. This chapter first presents the development of the IIA-MISS in pictorial format, followed by its performance evaluation and to explain why the integrated system fulfills some of the translational medicine aims. The next topic further expands the IIA-MISS to integrated image-assisted surgery (IIAS) with EMR. A strategy to expand the IIA-MISS to other types of image-assisted surgery is presented. The methodology is introduced with an example in neurosurgery.

21.1 Introduction

Surgery often uses medical images to plan and guide the surgical procedures. With the advance of three-dimensional ultrasound(US), computed tomography (CT), and magnetic resonance imaging (MRI), the surgical plan and guidance becomes more detailed and precise. The term "image-assisted surgery" is commonly used to emphasize the importance of the imaging component in planning and assisting the surgical procedure. Usage of real-time imaging to assist minimally invasive surgery allows the patient to return home on the same day, resulting in lowering the cost of the operation and speeding up the patient's recovery time. For this reason, such surgery tends to be favorable for non-complicated surgical processes [1]. Figure 21.1 depicts IA-MISS.

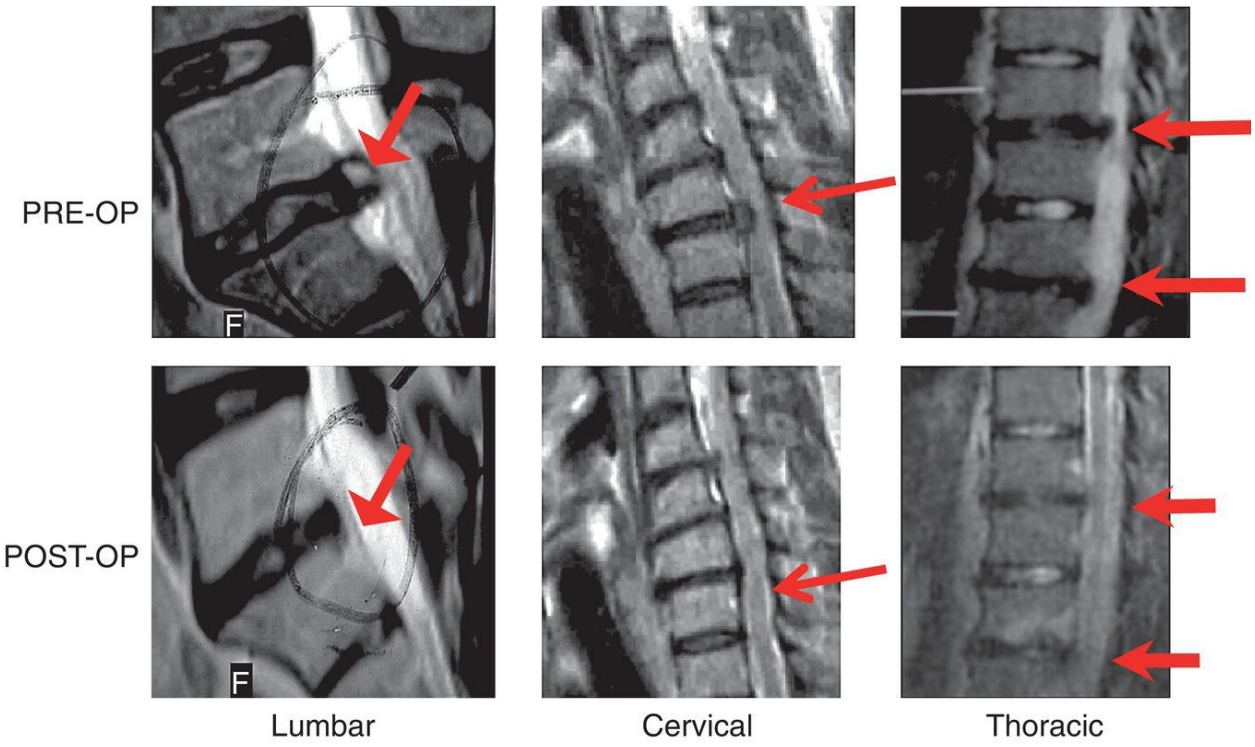

Figure 21.1 Some results of image-assisted minimally invasive spinal surgery at three anatomical locations: lumber, cervical, and thoracic. MRI was used to assist the surgery. Upper: pre-op, surgical planning. Lower: post-op, after surgery. Red arrows were annotated on the MRI digital images during the pre-op to identify the surgical plan. A greasy black pen was also used to mark the MRI film (left). These results were obtained without the integration of the electronic medical record system.

The concept of three time-phase surgical workflow in minimally invasive surgery was suggested in 2001; however, the necessary technologies were not readily available for experimental implementation [2]. In this concept, the surgical workflow has three phases:

1. pre-operation (pre-op) during the patient consultation;
2. intra-operation (intra-op) during the surgery; and
3. post-operation (post-op) during patient recovery and surgery documentation.

In each phase, data is collected in different forms and stored in different media at various times. For example, pre-op data can be collected during a patient's visit, which includes the patient's history, images, forms, the recommended surgical procedure, and surgical plan. Intra-op data are collected during the surgery; there are two components. The first is the patient's vital signs, images, and alert

signals, all in real time. The second component consists of the predetermined default collection of real-time surgical data, and surgeon selected data during the surgery. Post-op data consist of the already collected pre-op and intra-op data, as well as the surgeon's final report. These three datasets become the document of the surgical procedure.

During the past several years, due to the healthcare reform, two data collection terminologies are commonly used in the healthcare industry:

1. integration of image-assisted surgery (IAS)means the integration of all relevant data collected during a surgical operation; and
2. EMR is a system to collect relevant patient's electronic medical record.

An EMR system has two components, the computer hardware, and the software. A well-designed EMR can be used to evaluate and determine the reimbursement rate of a given surgical procedure.

This short review is to summarize the current status of IIA-MISS, including the methodology and its role in translational medicine. The review also discusses the potential of extending IIA-MISS concept to IIA neurosurgery.

21.2 Integrated Image-Assisted Minimally Invasive Spinal Surgery

21.2.1 The Planning Stage

IIA-MISS means that a patient's MISS data can be acquired in a three-phase workflow: pre-op, intra-op, and post-op [1–3]. The hypothesis of the study was that an EMR system can be designed and implemented to monitor, archive, and display in real time the patient's IIA-MISS data during the three surgical phases in the clinical environment. Based on this concept, an IIA-MISS prototype for laboratory evaluation was developed in 2007 to accomplish three tasks:

1. to understand the current MISS surgical workflow;
2. to accommodate the IIA-MISS clinical environment; and
3. to design the three-phase IIA-MISS workflow.

These three tasks were completed in 2008, with results shown in Figures 21.2 to 21.5. A prototype was immediately implemented in the laboratory environment for system evaluation [3].

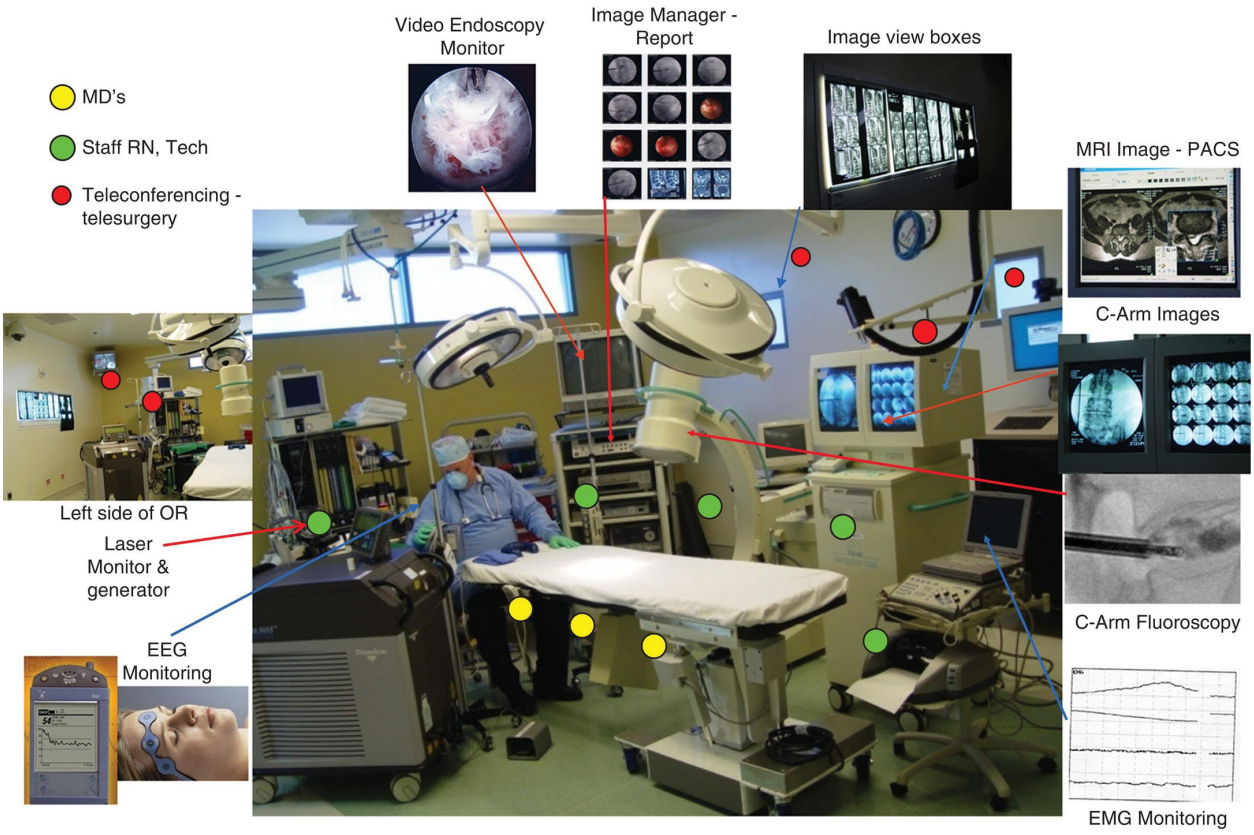

Figure 21.2 Image-assisted minimally spinal surgery (MISS) operating room (OR) with multiple signal and imaging systems and their corresponding display monitors before its integration with the electronic medical record system. Each staff member in the OR has his/her responsibility to monitor and view a given system(s) during the operation. C-arm x-rays (middle right) and endoscopic imaging (top middle) were used to assist the surgery in real time. PACS transmits MRI and other image data to the OR for viewing. EEG: electroencephalogram.

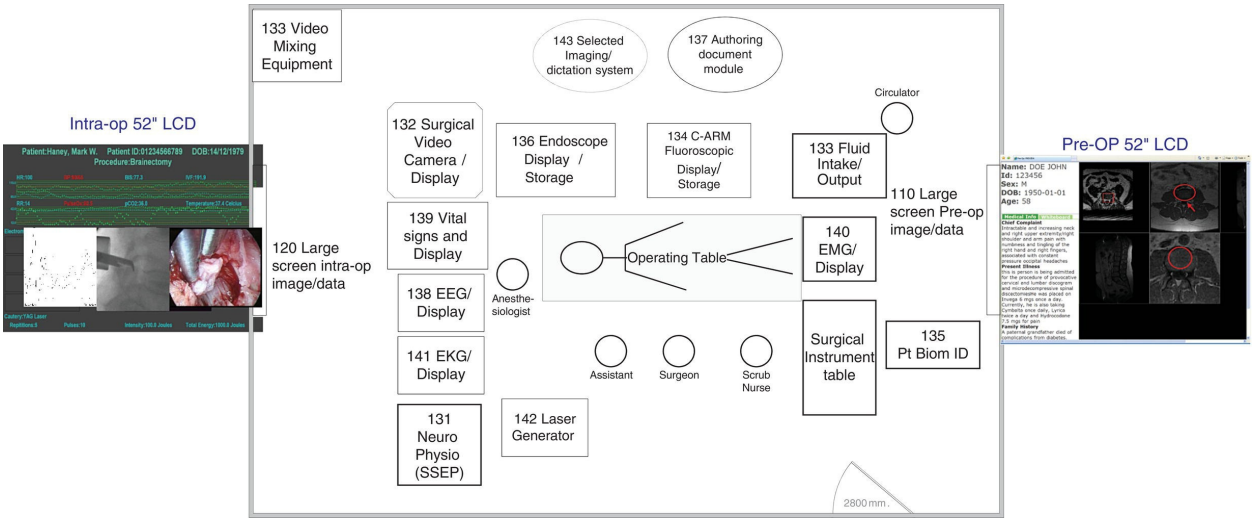

Figure 21.3 Integration of the EMR with the image assisted minimally invasive spinal surgery operating room. The locations of multiple signal and imaging systems are reorganized properly; two large display monitors were hanged strategically on two opposite walls of the room, one for pre-op data and the other for real-time intra-op data. Every staff member in the room can view both the pre-op and intra-op monitors simultaneously.

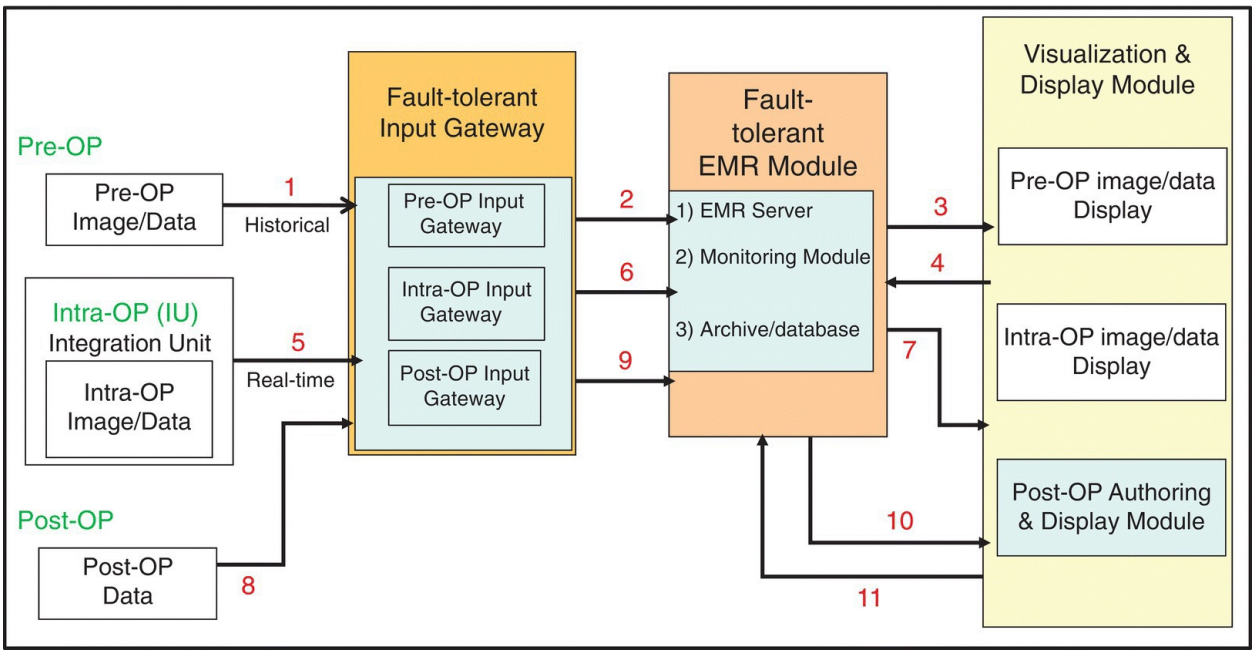

Figure 21.4 The workflow of the integrated image-assisted minimally invasive spinal surgery EMR) system in a 3×4 matrix. From left to right: Three rows delineate the pre-op, intra-op, and post-op phases. Input data moves through various components, first to the input gateway, the EMR module, and then to the pre-op, the intra-op (real-time), and the post-op (real-time) display monitors.

Numerals 1–12 portray the order of the data workflow. The left and the right monitors shown in Figure 21.3 are for the pre-op and intra-op modules. The post-op display shares the intra-op monitor since they are used at two different times. The input gateways are used to standardize all surgical data. The DICOM standard is used. The EMR module is the system that includes the EMR server, monitoring module, and archive database.

Figure 21.5 Integration unit installed in the operating room (left, green). All cables of the input data sources (middle and right) are connected to the unit's back panel.

21.2.2 The Clinical IIA-MISS EMR System

After the prototype was successfully evaluated, a clinical IIA-MISS EMR system was launched for clinical use at the California Spine Institute (CSI), Thousand Oaks, California, in 2009 [4], under the auspices of two institutional review board(IRB); the first was at the CSI, and the second at the University of Southern California [5,6]. The purposes of developing the clinical IIA-MISS EMR clinical system are:

1. to evaluate its efficacy and effectiveness in the MISS surgical environment;
2. to explore if IIA-MISS methodology can be expanded to other surgical procedures; and
3. to study if the concept of clinical IIA-MISS system is in parallel with translational medicine aims to expedite the discovery of new diagnostic tools and treatments by using a multidisciplinary, highly collaborate, "bench-to-bedside" approach.

It also compares whether the IIA-MISS, following the concept of translational medicine, can alleviate two major roadblocks in medicine, namely: i) to prevent

basic research findings from being tested in a clinical setting; and ii) to prevent proven interventions from becoming standard practice [7,8].

21.2.3 Use of the IIA-MISS EMR System and Training

There were little differences between MISS and IIA-MISS from the surgical point of view. To use the IIA-MISS EMR system, the surgeon would use an identical surgical set up, procedure, and equipment, but the surgeon would view real-time images and surgical signals from two much larger overhead monitors at the two opposite sides of the operating room (OR), instead of from scattered smaller specific monitors around the room. In the setup of the EMR system, its computer system chassis was housed at the back room of the OR. Each of all surgery-related input devices would have an extra permanent data cable connected to the EMR input gateway, so that the EMR system can continuously receive and display data from all surgical related equipment. Since this EMR is treated as an experimental clinical system in translation medicine, each existing input device remains as a backup and displays on the original small monitor (see Figure 21.4, columns 1–3 and Figure 21.5). As all input and output data are in digital format, all surgical staff members receive training on how to use necessary digital equipment and to view images and data from the two large monitors. In addition, some supporting staff members also learn to troubleshoot the EMR system if necessary [3].

21.2.4 Pre-Op, Intra-Op, and Post-Op, and Data Archive, Display, and Document

The concept, methodology, and results of the IIA-MISS clinical system, as well as some pre-op, intra-op, and post-op displays, are presented in Figures 21.6 to 21.10. In the intra-op displays, all data were received, acquired, and displayed in real time during the surgery.

Figure 21.6 A page of the pre-op display (see Figure 21.4, Numeral 3). Left: the patient history; Right: the surgical plan. The graphical user interface (GUI) in the pre-op screen can be used to switch to any other pages at the request of the surgeon at any time pre-op and intra-op.

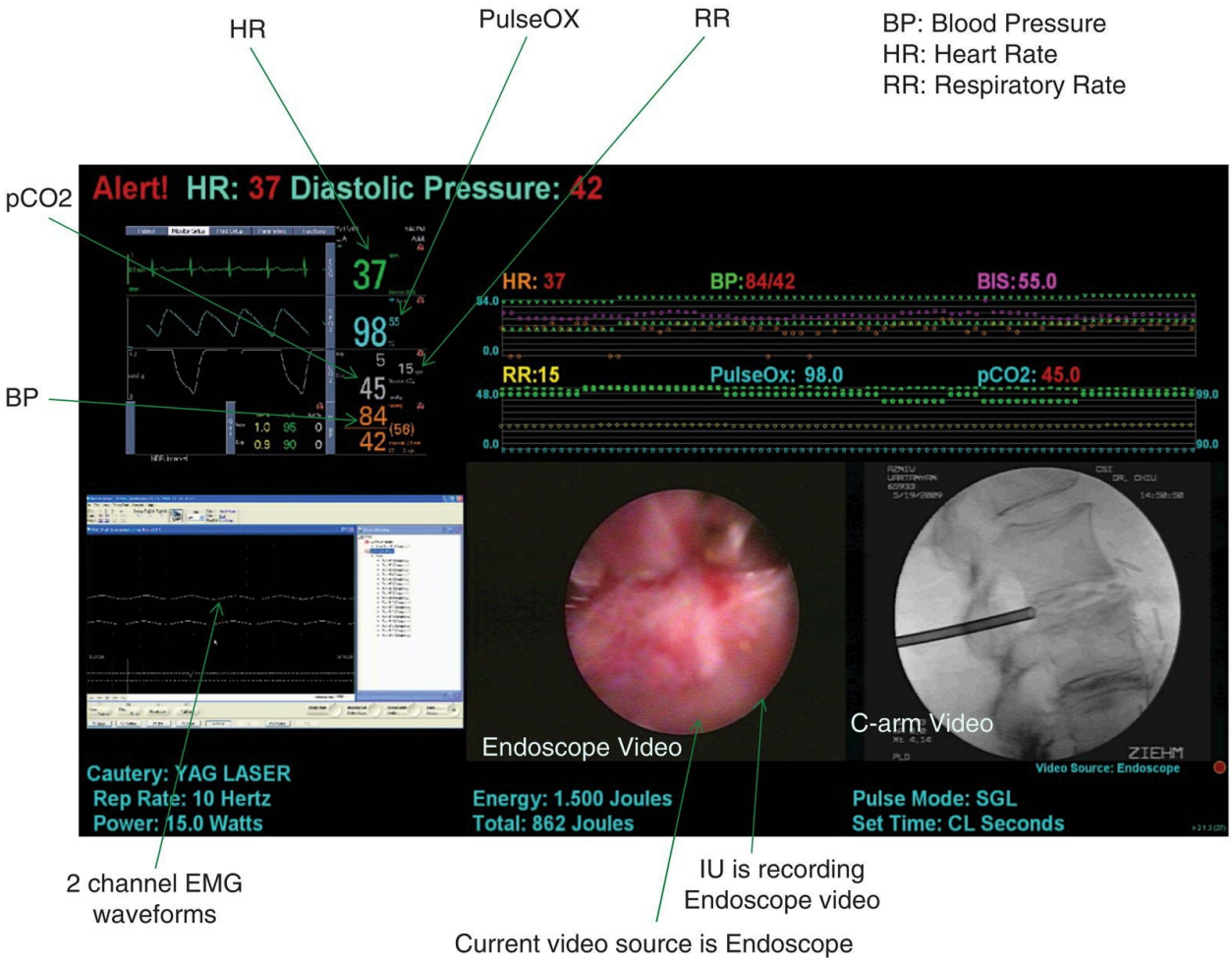

Figure 21.7 A snapshot of the intra-op monitor in which the anesthesiologist in the foreground is preparing a patient for the surgery. The monitor depicts some preliminary vital signs of the patient, and a C-arm image (right). The endoscopic display portion is not yet on line (see vertical color bars).

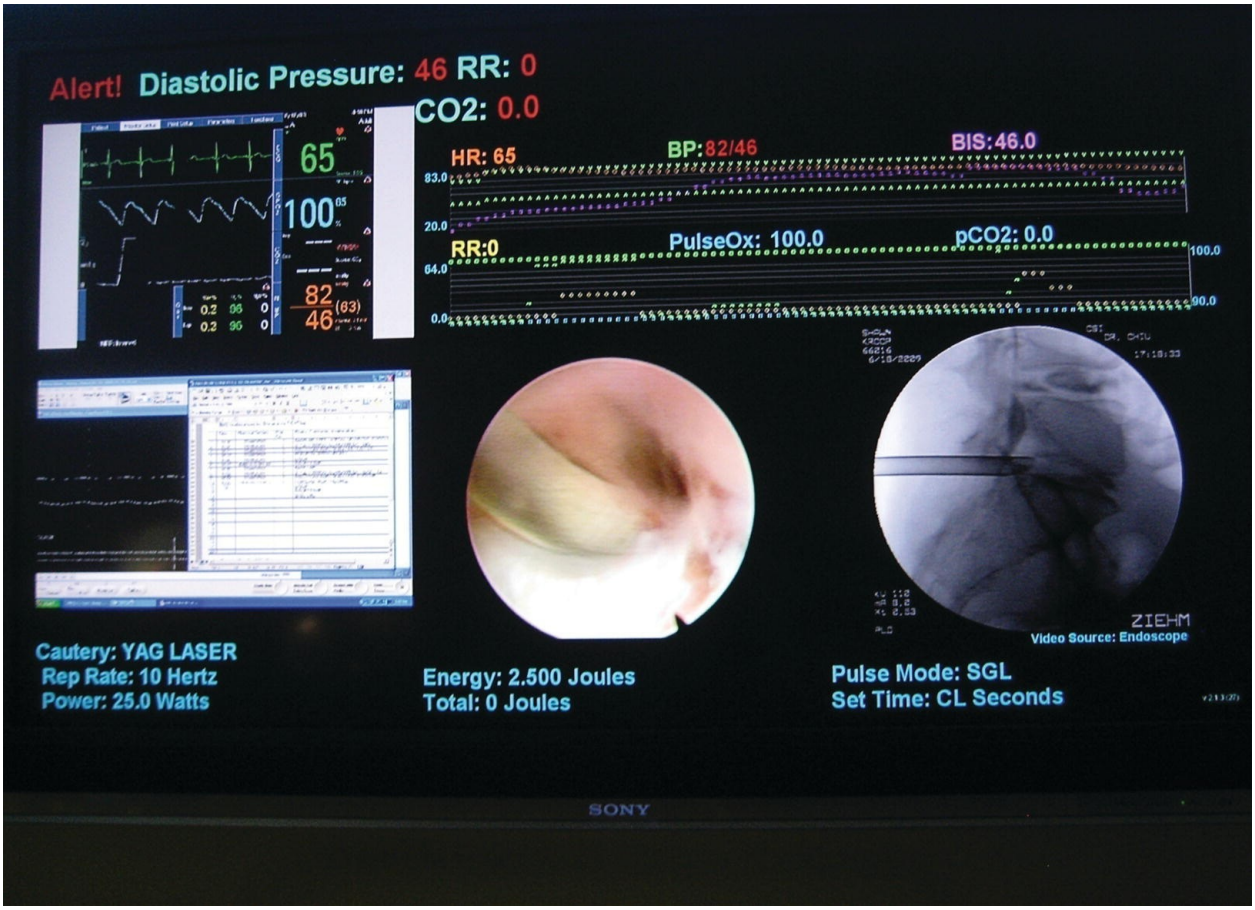

Figure 21.8 A snapshot of the intra-op monitor identifies the vital signs and other surgical related signals, as well as an endoscopic and a C-arm x-ray image of a patient.

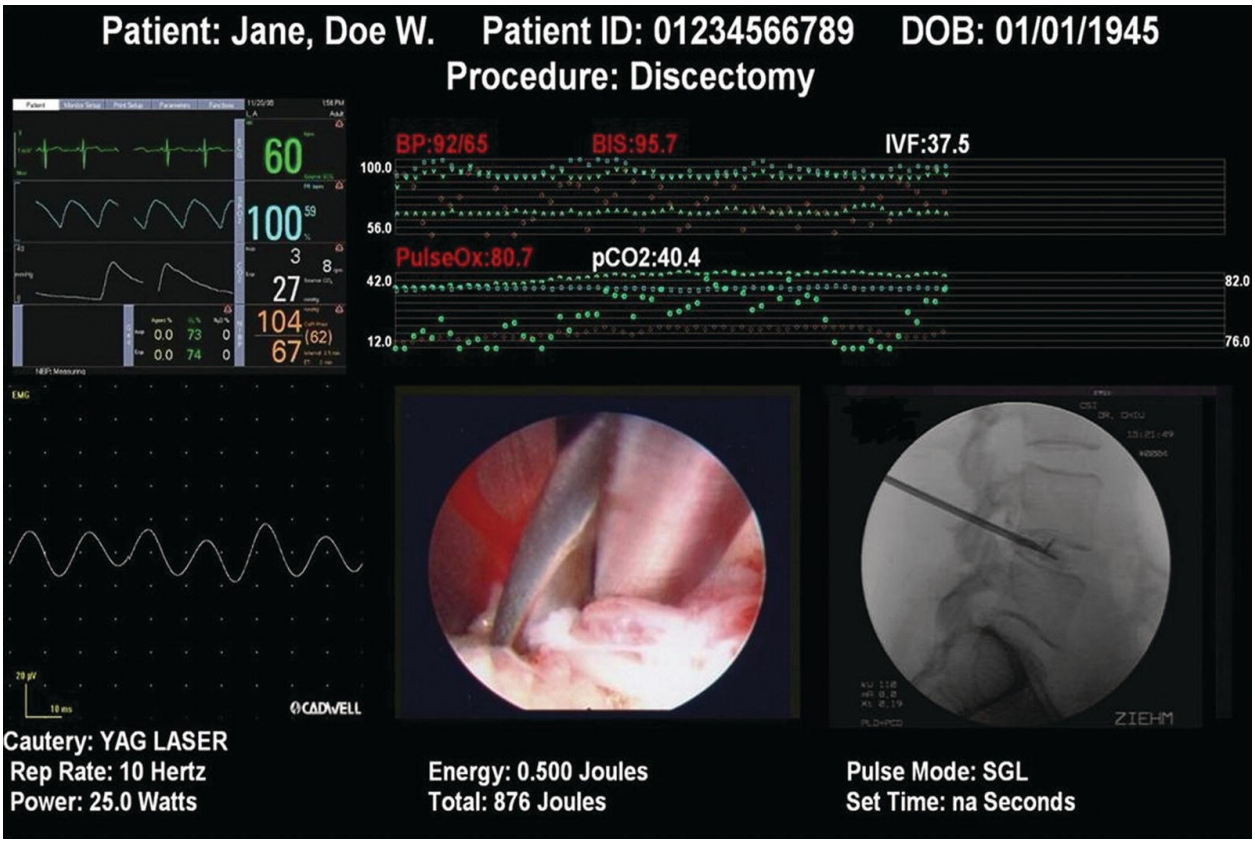

Figure 21.9 A snapshot depicting the intra-op display monitor of a patient during the minimally invasive spinal surgery with real-time surgical data (see also Figure 21.4, Numeral 7). The integrated EMR system records all information on the screen synchronized by a real-time master clock. Top: patient's vital signs, bispectral index system (BIS), and other related surgical signals. Right: the C-arm X-rays image shows the surgical site of the vertebra. Middle: the endoscopic image depicts a yttrium aluminum garnet (YAG) laser with characteristics shown in the last row, which was used to heat up the lesion. Left: the electromyogram signal shows that the spinal cord response is normal. This *in vivo* dataset had been recorded by the EMR as a part of the surgical document. The digital data including images of this page in the document was converted to an "open standard for electronic document exchange" Adobe Systems' PDF automatically by the EMR as an independent page. This page (can be more pages), along with other relevant data, and the surgeon's dictation comprise the final surgical report.

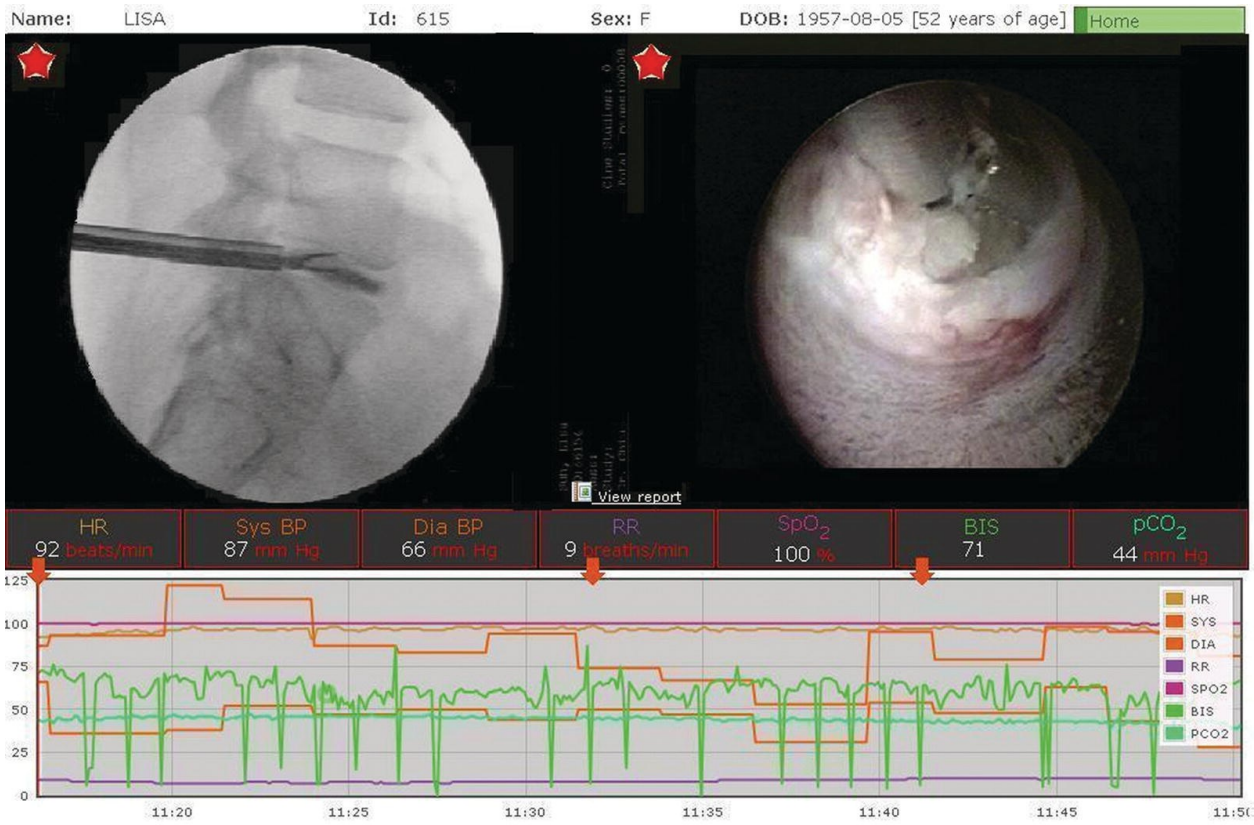

Figure 21.10 Post-op pages consisting of data from the EMR system default function, and those selected by the surgeon during the operation, which can be displayed and archived. This example is one of the selected pages consisting of two images (left: C-arm, right: endoscopic), seven waveforms, and time marks at a certain time during the surgery. Middle: three red vertical arrow time marks selected by the surgeon during the operation for inclusion in the surgical document (the three red arrows on the top of the waveforms). Bottom: seven waveforms, each color designating a surgical signal. Top: a C-arm x-ray and an endoscopic image at those selected time marks. Similar pages can also be generated for any system default time marks. The final patient report can be obtained by a click of the mark at the center of the display page. PDF files of this information can be generated automatically as part of the patient document. A red star at the upper left of each image indicates that the image had been included in the PDF file.

21.3 IIA-MISS EMR System Evaluation

As of 2010, the IIA-MISS EMR system had been used for over 300 patients for IIA-MISS, with encouraged qualitative results over the conventional MISS.

Among these are:

1. the system saves the operation time of the surgical team per patient;
2. automatic digital operation pre-op and real-time intra-op provides accurate on-line imaging data display and archive; and
3. the post-op document allows the surgeon to systematically generate timely efficient and accurate surgical reports.

The following study shows an example of a quantitative analysis of the EMR system, saving the surgical team operation time per patient.

21.3.1 Data Collection

The California Spinal Institute has two minimally invasive spinal surgery ORs, one equipped with the EMR system and the other without. During the data collection period of 18 months, patients were randomly assigned to one of the two ORs. Data collected from each surgical procedure in both ORs include patient's demographics, pain level before and after surgery, the region(s) of operation (cervical, thoracic, and lumbar), number of vertebrae (1 to 4) to be operated on at each operation, and operation time required for each operation per patient. Operation time began when the surgeon inserted the endoscopic cannula into the patient, and ended at the closure of the wound by the surgical tape and when the anesthesiologist turned off the patient monitoring system. Data was recorded by OR nurses manually and by the EMR system automatically. Thus, two sets of data were collected, one set consisted of patients operated with the help of the EMR system, and the other set without. The data was tabulated and compared against each set.

Data for 150 patients were collected from each set. The following criteria were used to match these two sets of patients for quantitative measures:

1. the anatomical region of operation and the numbers of vertebra to be operated on, and the patient's age and physical condition, but the patient's sex was not included; and
2. each matched pair should have the complete pre-op, intra-op, and post-op surgical data collected properly.

With these criteria, 80 matched pairs were selected to perform the preliminary quantitative study.

21.3.2 Statistical Analysis

Table 21.1 shows some preliminary results. The first column depicts the number of vertebrae operated on in each surgery. The third column shows the number of patients collected for the study corresponding to the first column. Each row compares the operation time required using MISS only (top line) versus that of EMR MISS (second line). The last column shows the *P*-value obtained by comparing the first and the immediate second mean time; a *P*-value close to 0.005 was statistically significant.

Table 21.1 Comparison of minimally invasive spinal surgery (MISS) operation times between the procedure with and without using the EMR system with different number of vertebrae per procedure.

No. of Vertebrae/ procedure	Without With EMR	No. of patients	Mean operative time (min)	Std. Deviation (min)	P value
1	MISS only	35	77.0	53.1	
	EMR used	21	70.0	32.1	.076
2	MISS only	43	76.2	40.9	
	EMR used	47	53.8	23.7	.005
3	MISS only	14	67.7	26.4	
	EMR used	6	68.1	12.0	.107
4	MISS only	0	–	–	
	EMR used	5	89.6	25.4	

Table 21.1 shows that there is an overall decrease in the operation time when the EMR system is used in the operation. For a two-vertebrae procedure, the *P*-value of 0.005 shows statistically significance in reducing the operation time. For a one-vertebra procedure, the *P*-value of 0.076 is also close to significant. This result, although preliminary, demonstrates that using the EMR system during the surgery does not delay the procedure time; on the contrary, it actually shortens the operation time despite it also collecting all necessary surgical data and images as well as displaying and archiving them in real time.

21.3.3 Other Qualitative Advantages of the EMR System

In addition to shortening the operation time based on the quantitative results, using the EMR system in MISS has several qualitative advantages over the traditional MISS practice. First, it provides an organized pre-op patient data

collection. Second, the post-op document allows the surgeon to systematically generate more efficient and precise surgical reports using the archived intra-op data by point-and–click relevant images, waveforms, and textual information from the EMR database. These data are automatically converted to PDF files and store in the patient report file. Third, the archived patient database includes pre-op, intra-op, and post-op data of the complete surgical operation, providing easily retrievable information for education and training.

21.4 To Fulfill some Translational Medicine Aims

This study using the IIA-MISS was a first attempt to test the efficacy of using such a digital EMR system for MISS. Its design was far from perfect to being efficient, effective, and reliable. However, the system does fulfill some translational medicine aims; first, it translates the method from research to clinical practice, which was actually implemented within the community; and it alleviates the two translational medicine roadblocks discussed earlier [7,8]. To continue the development of the IIA-MISS EPR concept, the next step is to extend the EMR system to other types of surgery by using the following strategy.

21.4.1 Methods

The next generation IIA-MISS EMR development should not only include the “MISS”, but also consider other types of IIAS EMR. The infrastructure of the IIAS EMR should have a common platform and customized components. Take neurosurgery as an example, which is not a simple surgical procedure. The first step is to identify common hardware and software components in general neurosurgery to form the basic IIAS platform. For a given special type of neurosurgery, other specific customized components would also be needed. The customized components would first be integrated with the platform to form a specific type of IIAS neurosurgery EMR. In the process of integration, imaging and informatics data of a patient acquired would cover the entire surgical workflow continuum from pre-op, intra-op to post-op (see also Figure 21.4) based on the DICOM (Digital imaging and communications in medicine) standard data model. To develop another specific type of neurosurgery, the basic IIAS platform can be reused, with only customized components needing to be changed [9].

21.4.2 Preliminary Results

Table 21.2 shows the common and the customized components required to develop a new specific surgical application. Column 1 is a list of all system components necessary. Column 2 identifies whether the component is hardware (HW) or software (SW). Column 3 with a “check mark” shows those components are common. And a check mark in column 4 indicates that the component is identified as common and no customization is required. Column 4 with a C shows the component is required for customization in a specific surgical application. This table demonstrates that almost all new customized components are software, which do not include computer system integration software.

Table 21.2 Comparison between the IIAS platform basic common components (columns 3 and 4) and the customized components in column 2 (SW) and column 4 (C) for a specific surgical application.

IIAS Platform Common Components	**Hardware/ Software**	**Common Components**	**Customized (C) components by modifying the IAS platform for a Specific Application**
Data Interface Software Module	SW		C
Basic Data Input Ports	HW	✓	✓
High Definition Input Ports	HW	✓	✓
Mobile Integration Unit	HW	✓	✓
Gateway	HW	✓	✓
ePR	HW	✓	✓
Basic Surgical DB	SW	✓	✓
Customized Surgical DB	SW		C
Pre- and Post-Op Authoring Toolkit	SW		C

Pre-Op and Intra-OP Display	SW		C
Post-Op Reports	SW		C

HW: hardware; SW: Software.

21.4.3 A Mockup Intra-Op Mimicking Neurosurgery

The design of a mock-up intra-op mimicking neurosurgery display is shown in Figure 21.11 [9]. The upper row is for patient real-time vital signs (common components). The bottom row shows the intra-op display of the neurosurgery system connected to three surgically related external systems (customized, left to right): the neuronavigation, microscopic, and surgical camera. The software of these three system integrations with the IIS is not listed in Table 21.2.

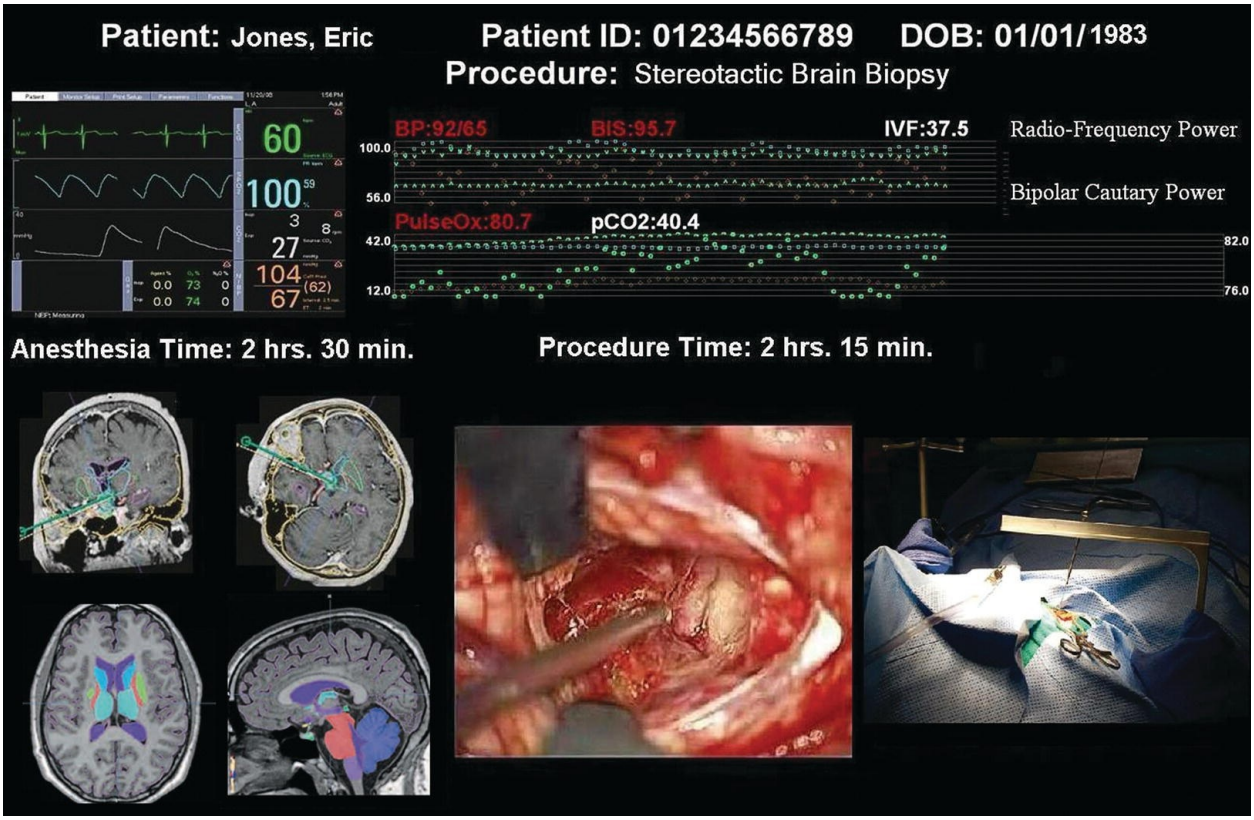

Figure 21.11 A mock-up intra-op screenshot mimicking a neurosurgical intra-op display of an integrated image-assisted neurosurgery EMR system. Additional real-time imaging data shown in the bottom are neuro-navigation system output with 3-D images on the left, microscopic image in the middle, and overhead camera image on the right.

21.5 Summary

An IIA-MISS EMR system has been developed for daily clinical operation. The role of the EMR is to systematically collect and manage the MISS data starting from the patient's visit to the recovery. This system acquires data in three phases pre-op, intra-op, and post-op, as shown in the MISS. The pre-op module is for data collection during the patient consultation. The intra-op module collects all surgical data and images in real time during the surgery and can be selected by the surgeon and by the EMR system default requested for surgical document. The post-op module is employed during patient recovery, surgical documentation and reporting. The surgical document system can download any pre-op and intra-up data in PDF format as a surgical document. A preliminary quantitative study demonstrates that the EMR system can shorten the surgical time; and qualitatively facilitate the surgical data archive, document, management, and education training. The operation of the proposed system satisfies certain translational medicine aims and has proven it is clinical viable in a community environment, since the California Spinal Institute is independent of any academic institution or from an enterprise level healthcare environment.

The next step to continue the IIA-MISS research and development effort is to expand the EMR system to IIAS. To this end, the design of a second-generation IIAS EMR system for neurosurgery application is at the planning stage. To begin with, defining EMR to a common platform and selecting customized components are essential. The common components platform can be duplicated for other image-assisted surgery systems. An example selecting neurosurgery was to treat it as a testbed for implementation. The single brain tumor excision was identified as the prototype system exploration. In terms of translational medicine, the research and clinical results shown in IIS-MISS demonstrate that the system fulfills several of the translational medicine aims [10].

21.6 Contribution from Colleagues

Jorge Documet, PhD, developed the MISS prototype in his PhD dissertation "An electronic patient record system for image-assisted minimally invasive spinal surgery" at the Biomedical Engineering Department, University of Southern California (USC), and later deployed the system for daily clinical use. He extends the MISS concept to other IIAS applications by defining the hardware requirement and implementing the system software. John C. Chiu, MD, DSc, Director and Chief Surgeon, California Spinal Institute, is the pioneer in image-

assisted minimally invasive spinal surgery, who shared the original concept of developing the IIA-MISS electronic EMR system. He provided the clinical data for the quantitative analysis. Bangxian Wu, MS, a PhD student at the Department of Diagnostic Radiology, The University of Hong Kong (UHK) obtained a fellowship from HKU to study IIA-MISS EMR under the guidance of Dr Documet at USC. He developed the software of the IIAS. Ali Maziad, MD, MS, was a surgical fellow in MISS with Dr Chu for two years. He assisted the MISS surgery and collected data to perform the quantitative study, and later guided by Professor James Sayre, Professor of Biostatistics, UCLA, to develop the statistical results. He is now a senior surgical fellow at the Department of Surgery, Boston University.

Acknowledgement

The development of this research was supported by SURGMATIX Inc.

References

1 Chiu, J.C. (2008) The decade of evolving minimally invasive spinal surgery (miss) and technological considerations. *The Internet Journal of Minimally Invasive Spinal Technology*, 2(3).

2 Huang, H.K. (2001) PACS, Informatics, and the Neurosurgery Command Module. *J. Mini Invasive Spinal Technique*, 1, 6–67.

3 Documet, J. (2009) An Electronic Patient Record (ePR) System for Image-assisted minimally invasive Spinal Surgery, PhD Dissertation, University of Southern California.

4 Documet, J., Le, A., Liu, B.J., Chiu, J. and Huang. H.K,.(2010) A multimedia Electronic Patient Record (ePR) system for Image-Assisted Minimally Invasive Spinal Surgery. *Intern J. Comp Asst Rad & Surg*, 5(3), 195–209.

5 Chiu, J.C. (2008) OR SurgMatix, An Electronic Patient Record (ePR) System for minimally invasive spinal surgery (MISS), WIRB Follow-up #202255 Western IRB, Exemption-B4-Chiu (August 8, 2008).

6 Huang, H.K. (2008) A Minimally Invasive Spinal Surgery (MISS) Clinical Database for Patient Outcomes Analysis, #HS-08-00476, USC IRB.

7 Woolf, S.H. (2008) The meaning of translational research and why it matters, *JAMA*, 299(2), 3140–3148.

8 Sung, N.S., Crowley, W.F., Genel, M., *et al*., (2003) Central challenges facing the national clinic research enterprise. *JAMA*, 289(10), 12, 78–87.

9 Huang, H.K., Documet, J., Wu, B. and Chiu, J.C. (2013) Architecture of an integrated image-assisted surgery system. (*IAS*), S191–S192, 8(Suppl. 1).

10 Chiu, J. and Huang, H.K. (2012) Surgical Data Monitoring and Display System. US Trademark: 079977-0015: SURGMATIX; Canadian No. 1,423,071, 2010. US Patent 8,313,432 B2. November 20, 2012.

PERPUSTAKAAN PRIBADI AN-NUR SUNARYA

22
Big Data in PACS-Based Multimedia Medical Imaging Informatics

CHAPTER MENU

22.1 Big Data in PACS-Based Multimedia Medical Imaging Informatics

22.1.1 Cloud Computing and Big Data

22.1.2 Medical Imaging and Informatics Data

22.2 Characters and Challenges of Medical Image Big Data

22.2.1 Volume

22.2.2 Value

22.2.3 Veracity

22.2.4 Variety

22.2.5 Velocity

22.3 Possible and Potential Solutions of Big Data in DICOM PACS-Based Medical Imaging and Informatics

22.3.1 Solutions for the Characters of Volume and Variety of Big Data in Medical Imaging and Informatics

22.3.2 Solutions for the Characters of Veracity and Value

22.3.3 Solutions for the Characters of Velocity

22.3.4 Security Privacy in Big Data

22.4 Research Projects Related to Medical Imaging Big Data

22.4.1 Grid-based IHE XDS-I Image Sharing Solution for Collaborative Imaging Diagnosis

22.4.2 Semantic Searching Engine (SSE) for RIS/PACS

22.4.3 3-D Enabled Visual Indexing for Medical Images and Reports

22.4.4 Segmentation and Classification of Lung CT Images with SPNs and GGO

22.4.5 High-Performance Computing Integrated Biomedical Imaging E-science Platform
22.5 Summary of Big Data
Acknowledgements
References

22.1 Big Data in PACS-Based Multimedia Medical Imaging Informatics

22.1.1 Cloud Computing and Big Data

Chapter 15, Sections 15.7.1, 15.7.2, and 15.7.3 present the rapid change in the PACS climate that leads to new concepts of cloud computing and big data in PACS-based multimedia medical imaging Informatics.

To recap on these sections in Chapter 15, cloud computing generally represents the practice of using a network of remote servers hosted on the Internet to store, manage, and process data, rather than using a local server or a personal computer. In the 1990s, telecommunications companies, that previously offered primarily dedicated point-to-point data circuits, began introducing virtual private network (VPN) services with comparable quality in service, but at a lower cost. By switching the communication traffic as they saw fit to balance server use, the network industry could use the overall network bandwidth more effectively and also began using the cloud symbol to denote the demarcation point between that which the provider was responsible for and that which users were responsible for. The cloud computing industry extended this boundary to cover all PACS-based servers as well as the network infrastructure. Since 2000, cloud computing has marched into industrial existence. Examples are: Amazon introduced its Elastic Compute Cloud in 2006; Microsoft announced its Azure in 2008, renamed to Microsoft Azure in 2014; IBM announced the IBM Smart Cloud in 2011; and Oracle introduced the Oracle Cloud in 2011, etc. (Content and examples *are* selectively extracted for PACS and Biomedical Informatics applications from Wikipedia, August, 2016). In Section 15.7.4, an example was given on how to use cloud storage for the DICOM-based archive. This chapter presents the directions of big data in PACS-based multimedia imaging informatics.

The issues of big data in PACS-based multimedia medical imaging informatics have special characteristics that need to be dealt with in healthcare service and research development. These characteristics lead to many technical challenges in medical imaging informatics. The dataset sizes and certain hidden functions of medical imaging are major factors that make the use of big data in medical imaging informatics different from other types of big data application. The possible and perspective solutions of big data issues in medical imaging informatics are discussed in this chapter, where some research and applications related to “the five V” features of big data in medical imaging and informatics are first introduced. In Section 22.2, the five V data related to PACS-based multimedia imaging informatics and three related topics are discussed.

22.1.2 Medical Imaging and Informatics Data

A massive amount of medical imaging and informatics data (e.g. medical images and electronic patient records, is generated daily in hospitals and healthcare organizations. By mining and analyzing these big data, generated from clinical operations, with large-scale population studies, a lot of valuable knowledge, technology, experience, and new business models can be achieved to bring huge benefits to facilitate patients and healthcare administration, and also to save healthcare costs [1–4].

Medical imaging services and research generate big data, not only because of the sheer volume of information but also due to the complexity, diversity, and rich context of the data that encompasses imaging discoveries of structures and functions from the molecular level to the organ level, with large-scale population studies on determinants of health status. Compared with other types of data, such as text-based structure and non-structure data, laboratory data, business cost data, pharmaceutical and medical products research and development data, and patient behavior and sentiment data, there are some special characters in PACS-based multimedia imaging and informatics data that can lead to difficult challenges to mine and discover more value from the data by using the common Hadoop solution [3]. In this chapter, characteristics of medical image datasets are first compared with other types of datasets, and some potential solutions to overcome obstacles of mining big data of medical images is discussed, which is then followed by some examples.

22.2 Characters and Challenges of Medical Image Big Data

In general, the concept of "big data" has five features: “volume”, “value”, “veracity”, “variety”, and “velocity” [5]:

- *Volume*: The quantity of data generated is very important in this context. It is the size of the data and its potential that determines whether the quantity can actually be considered as big data or not, that is, the name “big data” itself contains a term that is related to size and hence its character.
- *Value*: All big data are nothing if they cannot turn data into or use them for something valuable. Big data need to have the ability to predict meaningful positive outcomes.
- *Veracity*: The quality of the data being captured can vary greatly. Accuracy of analysis depends on the veracity of the source data.
- *Variety*: Variety means that the category to which big data belong is also an essential fact that needs to be known by the data analysts. This helps the users, who are closely analyzing the data they are associated with, to effectively use the data to their advantage and thus uphold the importance of the data.
- *Velocity*: The term velocity in this context refers to the speed of generation of data, or how fast the data are generated and processed to meet the demands and challenges that lie ahead in the path of growth and development.

In addition, there are two other features related to big data:

- *Vulnerability*: Experienced big data users are aware that the data they generate are being collected and then used by marketing to understand their behavior and, ultimately, used to sell different things. It may be that some people are okay with the process, but others see it as an invasion of privacy.
- *Complexity*: Data management can become a complex process, especially when large volumes of data originate from multiple sources. These data need to be linked, connected, and correlated in order to be able to grasp the information that is supposed to be conveyed by them.

Each of these features has certain special characteristics related to PACS-based multimedia imaging informatics, and these characteristics greatly impact on the scalability, heterogeneity, timeliness, storage, and complexity that may determine the big data processing and special barriers to values created from the data. The concept of these big data features is shown in Figure 22.1. There may be a risk of exposing a patient’s healthcare information by data sharing, or in data mining or crossing enterprise healthcare systems. Therefore, there may be

the need for one more “V” feature (the sixth one) to be considered in big data, which can be either “vulnerability” or “complexity”, discussed in Section 22.3.4. Sections 22.2.1–22.2.5 present the five V, the challenges of medical imaging healthcare practices and imaging informatics big data.

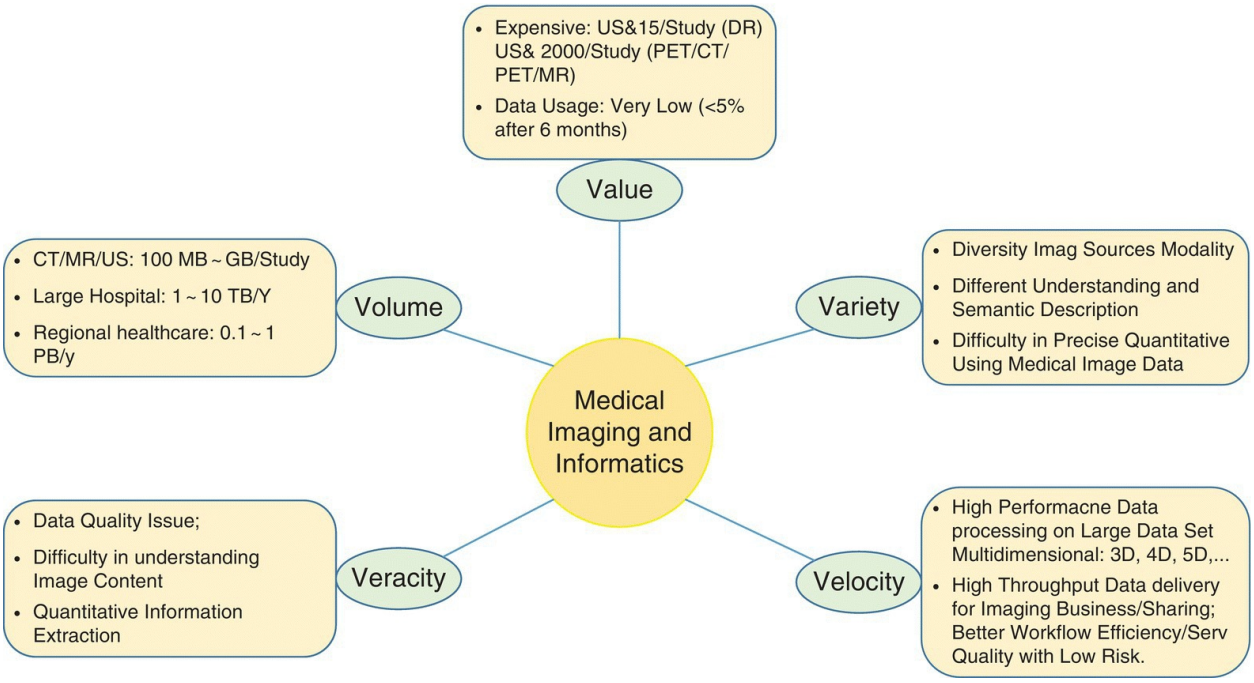

Figure 22.1 Special features of characters of the “five V” features: volume, value, veracity, variety, and velocity in big data of DICOM-based medical imaging informatics: PB: petabyte.

22.2.1 Volume

Since 2012, advanced digital medical imaging modalities (i.e. the 64/128/256 multi-row CT, high-field MRI; 3 T MRI), PET/CT and other imaging modalities (Chapter 2) had been promoted for use in large hospitals and healthcare enterprises that generated huge amounts of image data on a daily basis. As an example, Figure 22.2 shows the amount of image data stored in the hospital PACS per year from 2008 to 2013 (1–7 months) in the large Huadong Hospital, Shanghai, China (1200 beds). From Figure 22.2, it can be seen that the increasing ratio of PACS-based image data storage requirements is about 20–30% per year in this hospital alone. There are about 34 similar-sized hospitals in Shanghai; consider that 3–5 years later, each of these large hospitals would proportionally increase to the similar numbers of PACS-based image data requirement. This would lead to the petabyte (PB, a million gigabytes)-size image data in Shanghai, one city in China. This large number of imaging data

would create a major challenge to the city hospital's data management and costs.

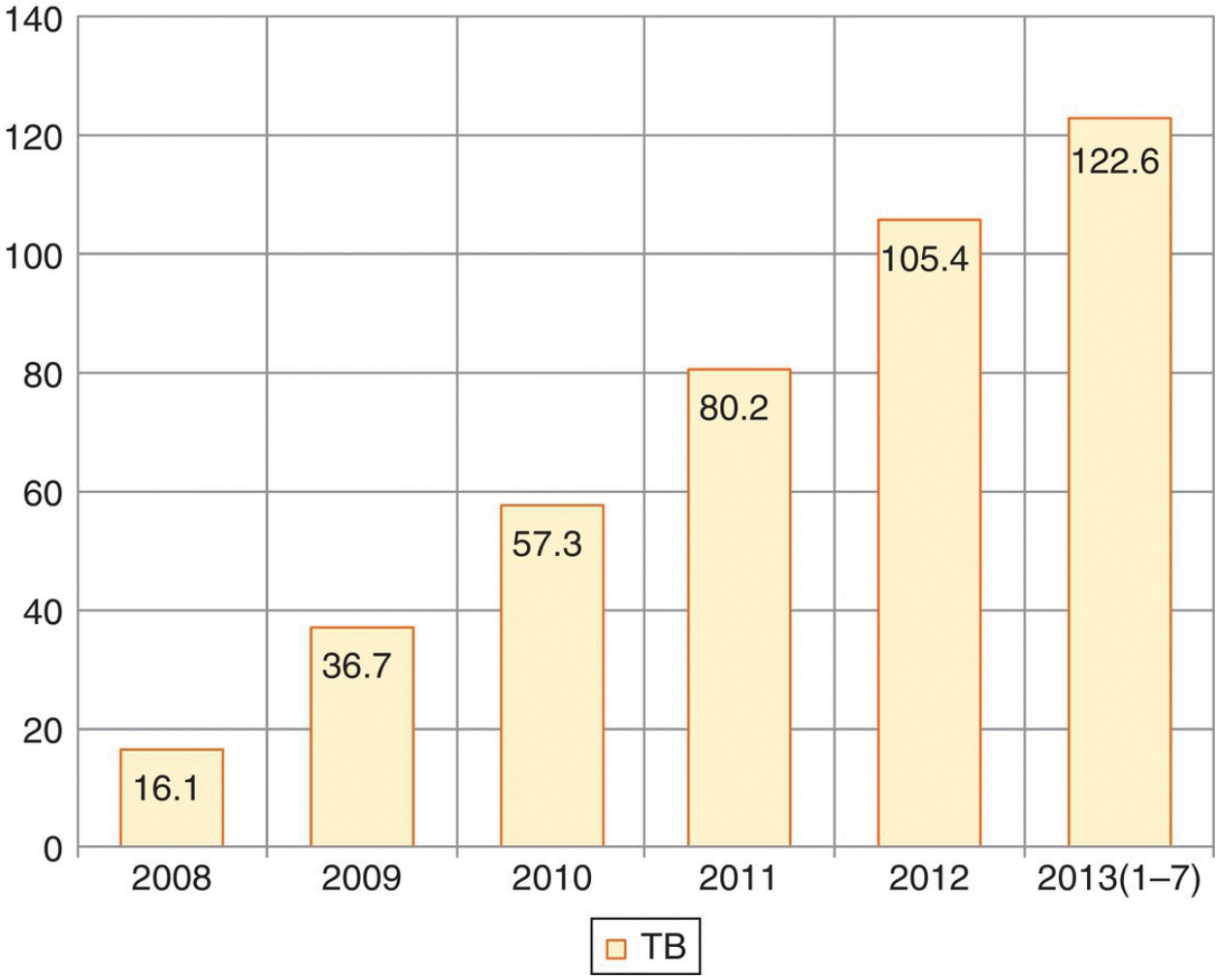

Figure 22.2 Amount of PACS-based image data (terabytes, TB) stored per year from 2008 to 2013 (only 7 months) in the Huadong Hospital, Shanghai. China.

Currently, most large datasets of DICOM-based PACS images are generated from CT and MRI. Frost & Sullivan predicted in 2016 that diagnostic imaging alone would generate nearly 1 exabyte (10^{18}) of data worldwide [6]. If emerging imaging modalities such as breast tomosynthesis for women, and other medical specialties like cardiology, digital pathology, endoscopy, ophthalmology, dermatology, and surgery, are also counted, the growth in medical image data volumes will accelerate more rapidly in the near future. In parallel to these imaging data volume is the increasing complexity of data management (including, but not limited to radiology), as well as the heightening the diversity of image data sources across healthcare enterprises, including image-using and image-producing clinical stakeholders. This evolution of the medical imaging

data landscape is bringing new challenges to traditional imaging informatics ecosystems and is required to innovatively build new solutions to deal with such challenges.

22.2.2 Value

Big data values include the business value, which is derived mostly from discovery of relationships with events, either explicitly or implicitly hidden within the big data, and creating a new business mode to generate potential new revenues. Another value of big data is usability. Researchers in this area found that there was a connection between data usability and financial performance in many industrial fields, especially usability of effective data that can greatly improve employee productivity [7].

Medical image data have great value and are widely used in disease prediction, diagnosis, treatment, and rehabilitation assessment. Image data are expensive to use and maintain; for example, in China, the cost of each radiology study, including imaging examination, diagnosis, and reporting, is around US$12 for digital radiography x-rays to US$1500 (PET/CT), depending on modality types and body parts. Also, the image data have to be archived for more than 10 years, and used as key evidence of medical records and for continuing healthcare services and medical research. For these reasons, each hospital in China, and also other countries, has to invest large resources to manage and maintain the huge amounts of image data.

But the usefulness/usability of the imaging data in a hospital is mostly during the new short-term studies of about 3–6 months. Most historical data remain in the long-term archive without retrieval. Figure 22.3 shows the percentage of retrieved historic imaging studies in the Huadong Hospital DICOM-based PACS system during the year 2013, measured statistically [8].

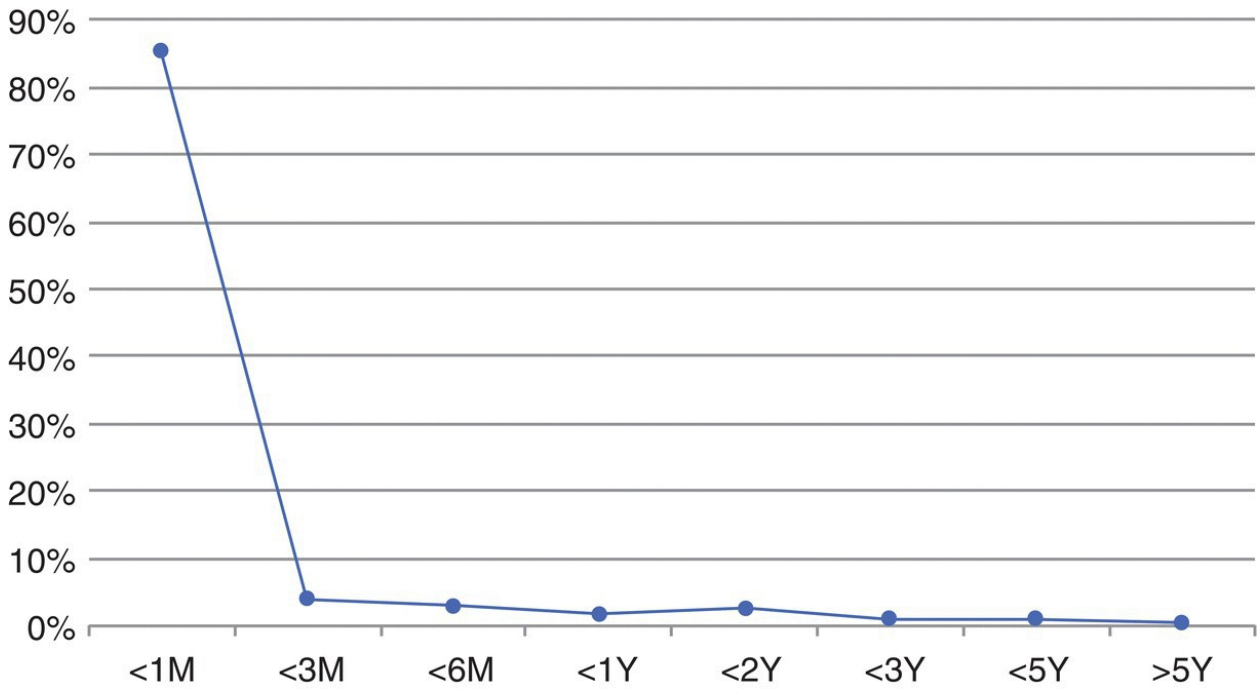

Figure 22.3 Percentage of retrieved historic imaging studies in Huadong Hospital PACS during 2013 (M: month, Y: year).

From Figure 22.3, it is clear that most historic image studies were not often used statistically if they were over 6 months or 1 year old. The primary value of the historic image is lost, even though they are expensive to keep, but it can still be valuable to the patient even though seldom used. However, the hospital has to pay for storage and maintenance costs to retain them. How to improve the usability of historic image studies by extracting quality values using data-mining knowledge from the image data is a tremendous challenge in PACS-based imaging informatics.

22.2.3 Veracity

Veracity in medical image big data is an important issue. It is not just about data quality, but about data understandability. Usually, it is difficult to understand the content of medical images if users are not trained in the specialty medical imaging area. In clinical practices, it is a big challenge for clinical physicians to read and use medical images if there is no radiologist to help. The challenges are mostly in the following aspects:

1. the uncertainty in understanding the images;
2. how to best use images heavily dependent on the doctor's experience; and

3. his or her professional knowledge and the complexity of image texture characteristics.

In order to efficiently use medical images, it needs radiologists semantically to interpret the content of images into a text report, so that other medical professionals can understand the meaning of medical images. Also, there is a lot of quantitative information (measurable aspects of images, length, area, volume of lesions, specific features and image biomarkers, and so on). The contents of the images need to be extracted by image processing tools for the use of imaging diagnosis, treatment, and evaluation.

As both images and reports mostly comprise non-structured data, it is difficult to use computing methods to process them directly in the same way as other kinds of big data. Current considerations are to use various image processing tools to extract quantitative information or computing imaging features. Others use biomarkers for research purposes only, but biomarkers have yet to be used in clinical services. As of now, veracity is a big challenge on how to develop efficient image processing tools to segment and extract quantitative information of images for quantitative imaging diagnosis, treatment, and evaluation.

22.2.4 Variety

The variety of medical image big data is mostly related to diversity of imaging sources or modalities, imaging protocols or parameters, times of imaging, etc. Although DICOM is dominant in radiological images, it is easier to transfer DICOM images to other resources and to use them in clinical operation. But there are still many other types of medical images that are not DICOM, such as JPEG, MPEG2/4, and GIF, which are being used in other clinical departments (Chapter 2).

As each modality or imaging protocol has its functions and specific characteristics to obtain the information of morphology structure and biological function, the content and interpretation of images are different for the same organ/body part scanned with different imaging modalities or protocols. Also, different radiologists or physicians may have a different understanding and semantic representation of the same image study, as their knowledge or medical experiences vary greatly. For these reasons, a major challenge of the variety of medical image big data is that it is difficult to precisely and quantitatively using medical image data in healthcare services and research. Another challenge is due to data exchange and sharing across healthcare enterprises based on the variety of image data. Because it is difficult to compare the studies between different

imaging modalities and protocols, it is also difficult to register and fuse images (Chapter 2) acquired from different kinds of modalities and protocols at different times.

22.2.5 Velocity

The velocity of medical images big data relates to two aspects. One aspect is about the imaging service workflow efficiency and the service quality. These two factors are determined by the data acquisition, transmission, archiving, display, and reporting during the whole process of the imaging diagnostic service. As data volume is generated daily in hospitals and is increasing continuously, the data complexity also becomes increasingly significant in clinical imaging services. The velocity is also a big challenge to healthcare/hospital organizations, on how to look for “best practice” methods driving down the risk, growth, profitability, patient retention, and above all, patient safety.

As the data sizes of single imaging studies become even large, such as from a hundred of MBs to a few GBs (e.g. CT/MRI for cardiology, breast tomosynthesis, etc.), more and more 3-D/4-D/5-D image datasets are being used in imaging diagnosis, imaging-guided surgery procedures, and treatment planning and evaluation. The image computation power on 3-D/4-D/5-D and network delivering speeds become key factors in the successful use of these big data for clinical services. How to build a powerful image computation and transmission platform to deliver data services to clinical imaging users in healthcare enterprises and cross-enterprises is another key issue in using DICOM-based medical image big data.

22.3 Possible and Potential Solutions of Big Data in DICOM PACS-Based Medical Imaging and Informatics

A wide variety of techniques and technologies have been developed and adapted to aggregate, manipulate, analyze, and visualize big data. These techniques and technologies drawn from several fields of research and technology, including statistics, computer science, applied mathematics, informatics, and economics. The purposes of using these techniques and technologies are to create, discover, or mine values from big data. There are usually three directions to create and discover the values:

1. The first direction is to create transparency to data consumers. This is significant in healthcare, such as sharing the medical records among healthcare providers across departments or enterprises, which can reduce the costs and risks, yet improve the healthcare quality and efficiency;
2. The second direction is to increase the data usage and quality significantly [7], especially medical image data, as the data is mostly used within the first few months of acquisition, but stored and rarely accessed again after six months [8];
3. The third direction is to quantitatively and efficiently analyze image data, and find out the data events and their relationships among massive amounts of image data. This direction would improve decision making, minimize risks, and unearth hidden values.

As with the five Vs features of big data discussed above, medical imaging and informatics big data have special characteristics and challenges compared to other types of big data. Some innovative research and technical solutions are required to be extracted and redeveloped. The following sections highlight some possible technical solutions and research being addressed.

22.3.1 Solutions for the Characters of Volume and Varity of Big Data in Medical Imaging and Informatics

Medical imaging big data have some special characters different from other types of large datasets that have been historically stored and analyzed. Most other big data are mostly made up of discrete, small, incremental data elements with real-time additions or modifications. However, PACS-based medical imaging services in healthcare enterprises have often been referred to as a three-tier architecture, which is close to acquisition (server), storage data, and presentation (user), in which the user provides security; reversibly, high-performance end user (presentation) goes back to the database or storage, as shown in Figure 22.4A. On the other hand, in big data, the data become more horizontally scaled and distributed throughout the middle layer network nodes, and traffic between server and storage nodes has become significantly greater than that between servers and end users, as shown in Figure 22.4B. As a result, to develop a new data processing infrastructure providing high-speed connections optimized for big data processing and analyzing is critical to realize scalable, high-performance big data implementations.

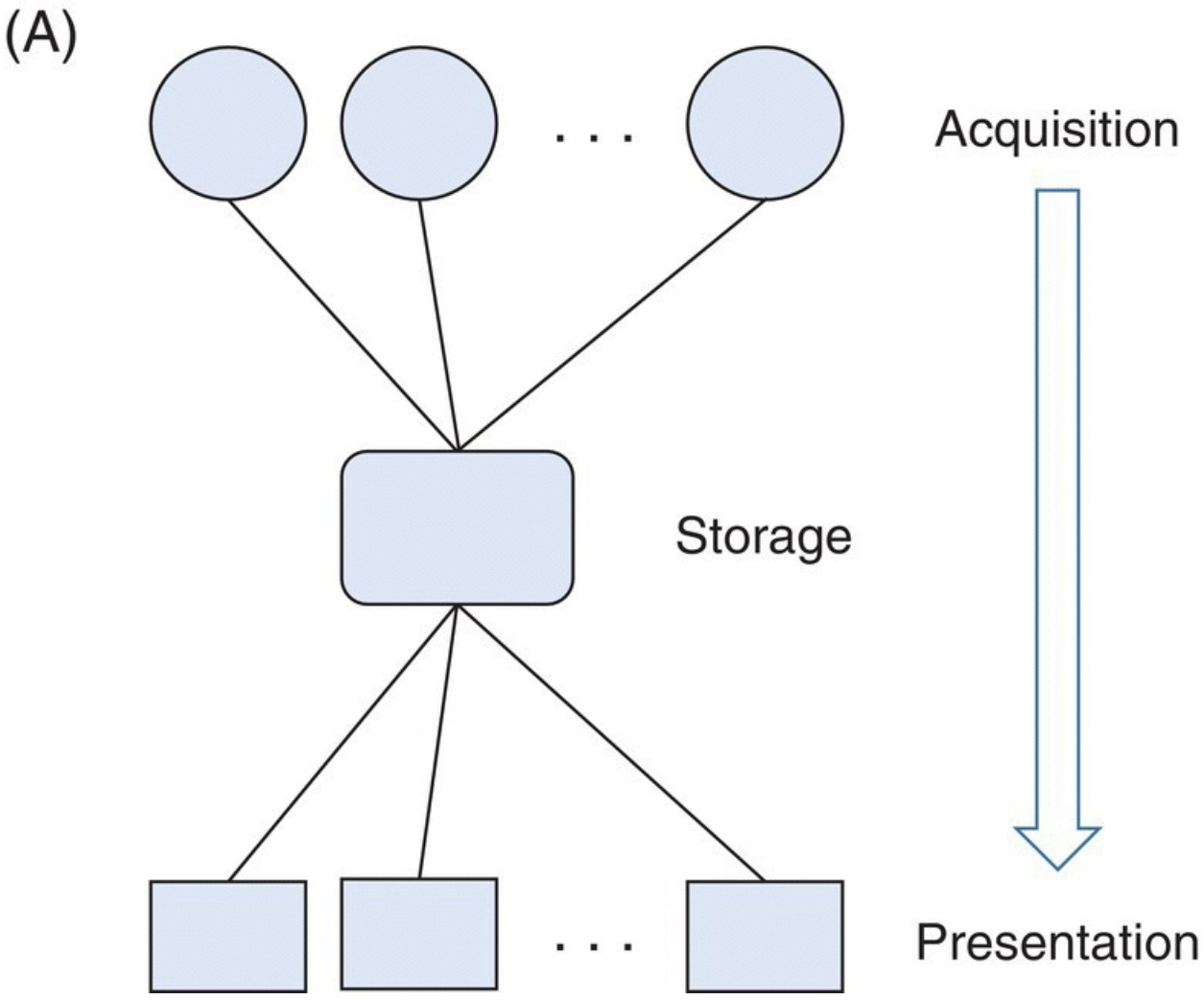
(A)
Acquisition
Storage
Presentation

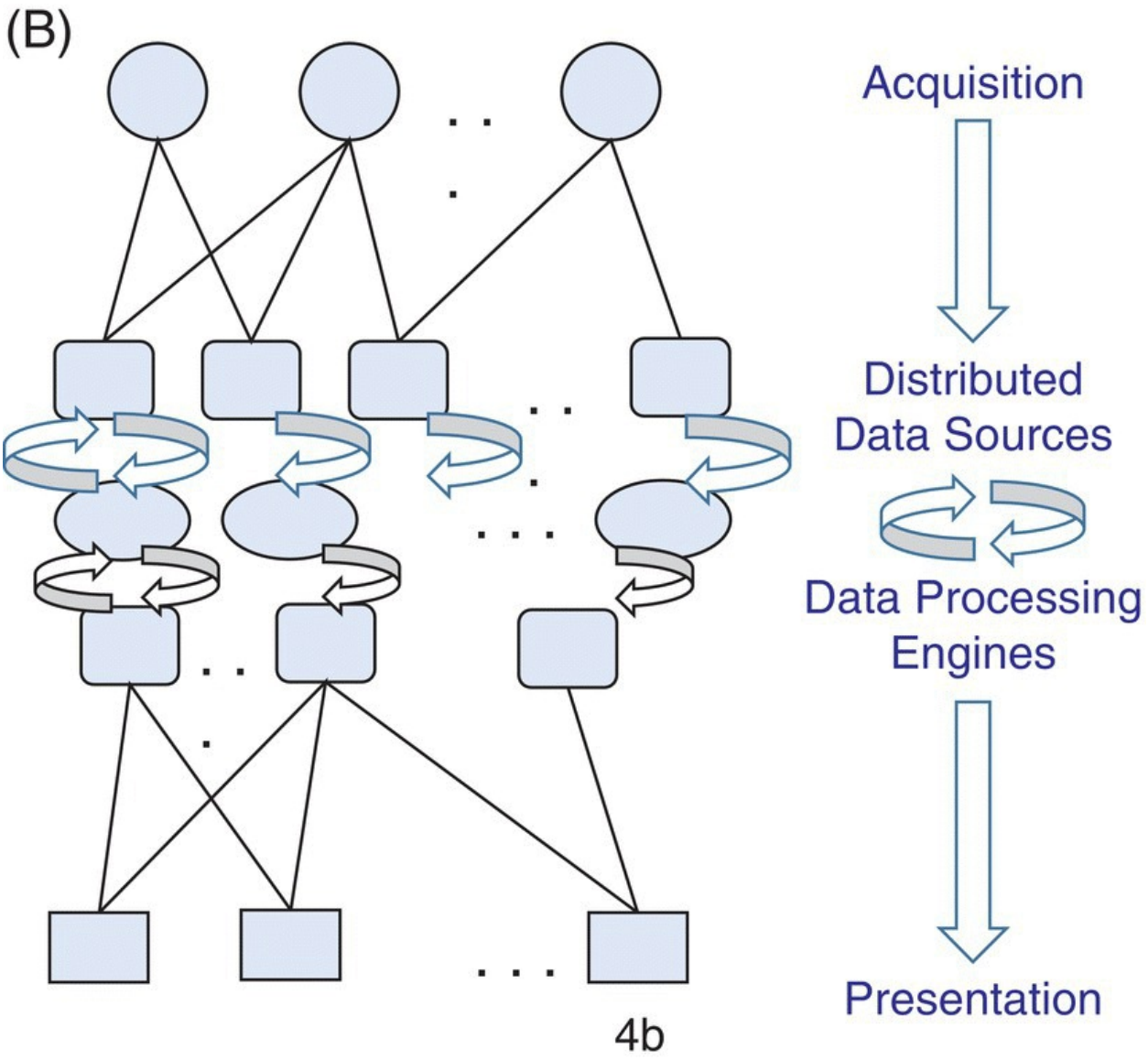

Figure 22.4 (A) The traditional data storing and processing three-tier infrastructure. (B) Big data in medical imaging and informatics: horizontally scaled and distributed big data processing architecture with multiple middle layers in between acquisition and presentation.

Hadoop [3] included a distributed file system known as the Hadoop distributed file sstem and MapReduce [4], suggesting a critical big data technology that provides a scalable file system infrastructure and allows for the horizontal scale of data for quick query, process, access, and data management. At its most basic level, Hadoop's implementation created four unique node types: data node, client node, name node, and job tracker for cataloging, tracking, and managing data throughout the infrastructure. Hadoop is now becoming the basic foundation of

technical solutions in big data business; however, it is difficult to use Hadoop architecture to deal with big data of medical images, because Hadoop splits files into large blocks (default 64 MB or 128 MB) and distributes the blocks amongst the nodes in the cluster that cannot be operated efficiently for clinical imaging services.

During the last few years, a new technology called vendor neutral archive (VNA) [9] (see Chapter 15) was introduced into medical imaging enterprise applications, that stores images and documents (and potentially any file of clinical relevance) in a standard format with a standard interface and can be accessed in a vendor-neutral manner by other systems. VNA can be used to store and distribute diverse data from multiple imaging sources to multiple departments to enhance image data interoperation in an enterprise or cross-enterprise. Also, another new technical solution for massive amounts of image data storage and processing is cloud computing, which provides the various kinds of services from software, platform, and infrastructure based on on-demand modes [10]. The cloud computing-based solutions are usually set in the Internet environment and can be accessed from anywhere at any time. Both VNA and cloud computing cannot only be used as a storage solution for the massive amounts of image data, but can also be promoted to function as an image data sharing solution if properly implemented and used with IHE XDS/XDS-I profiles [11]. Figure 22.5 shows architectures of a typical VNA solution (A), and cloud computing-based image storage and sharing solution (B).

(A)

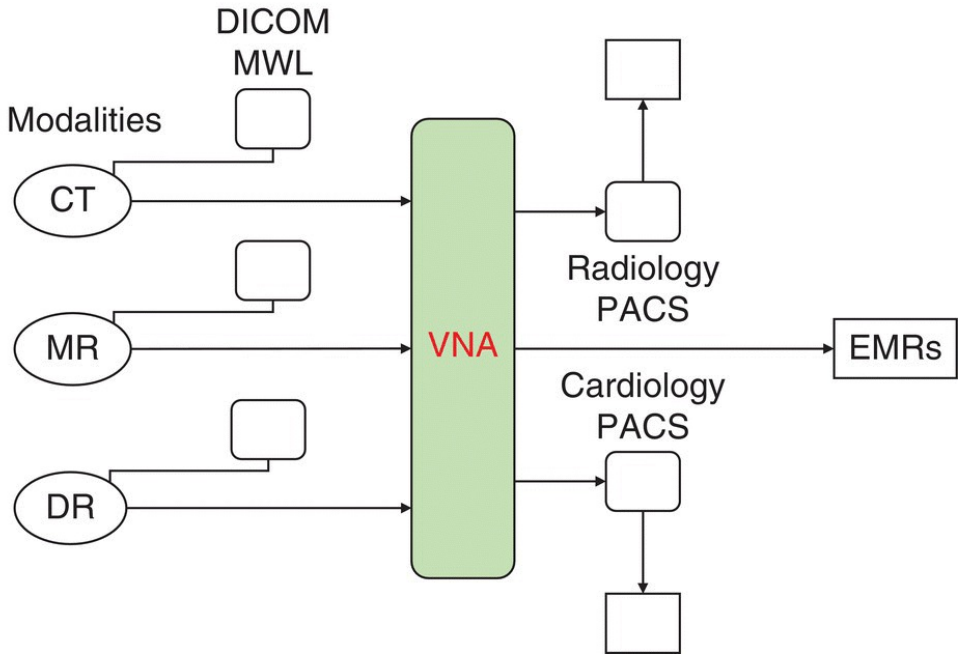

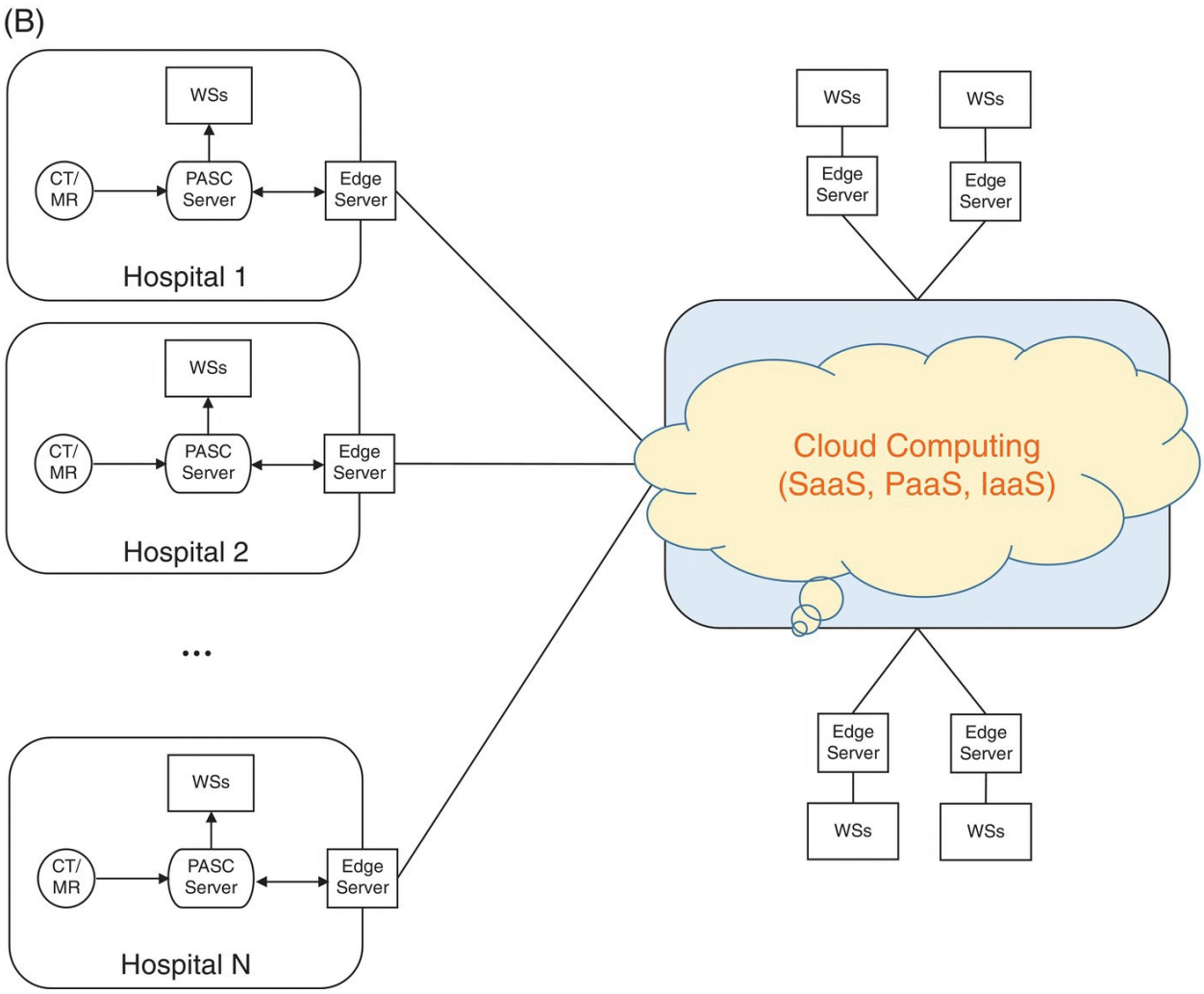

Figure 22.5 (A) A typical architecture of vendor neutral archive-based image storage and sharing solution; (B) Cloud computing-based image storage and sharing solution. See also Chapter 15 for VNA.

Compared to traditional PACS, both VNA and cloud computing solutions tend to resolve the issues of big data of medical imaging in volume and variety. But VNA would also present challenges in dealing with value, veracity, and velocity.

22.3.2 Solutions for the Characters of Veracity and Value

Veracity in medical imaging is about how to improve the data quality and to understand the meaning of image content correctly and precisely. In order to achieve these goals, the current research on quantitative imaging has become a hot topic in medical imaging informatics and there are a lot of research groups working in this area. In particular, quantitative imaging is the extraction of quantifiable features, also called imaging biomarkers, from medical images for

the assessment of:

- normal, or
- severity, degree of change, or
- status of a disease, injury, or
- chronic condition relative to normal.

Quantitative imaging includes the development, standardization, and optimization of anatomical, functional, and molecular imaging acquisition protocols, data analyses, display methods, and reporting structures [12].

As quantitative imaging provides clinicians with a more accurate picture of a disease state, by applying to medical images algorithms that precisely measure various aspects of an abnormality [13], it will be more precise and effective for clinicians to make diagnosis or perform treatment on patients. By accruing a sufficient database of measurements, comparisons between specific features from one case and similar features from other cases become possible, so quantitative imaging can profile patients based on information contained in medical images [14]. The questions are how to translate the research outputs of quantitative imaging into clinical services and how to store or link the quantifiable imaging biomarkers of images into proper image databases to later perform image data mining. These issues are crucial to tackle the veracity and value of big data in medical imaging and informatics.

Another approach to resolve veracity and value in big data is to improve the image data usability, and the content-based image retrieval. Although much research in this area, and many projects in medical imaging informatics are in progress, few research outputs have been translated to daily clinical imaging services or operation.

22.3.3 Solutions for the Characters of Velocity

The operations of 3-D/4-D/5-D medical image rendering and manipulation are computation intensive. Also, the faster image delivering and high-speed image processing throughput for a massive amount of image data in an enterprise healthcare networking environment are key factors for successful imaging applications. The solution to resolve the issue of velocity is related to two components: image computation and intercommunications among data sources, processing engines, and consumers.

During the past few decades, computational performance of graphics processing

units (GPU) has progressed more rapidly than that of central processing units (CPUs). And medical image processing on GPU has become popular for the following three reasons:

1. The technology makes it possible to apply more advanced algorithms;
2. It performs computationally demanding tasks quickly in clinical environments; and
3. Its “computes unified device architecture” programming language uses the Nvidia (this device designs GPUs for the gaming market), making general purpose calculations far easier.

The intersection between the medical imaging and high-performance computing has demonstrated the potential to make a significant impact on the translation of medical imaging research from the laboratory to the clinical environment. But there may still be some challenges in using GPUs for faster medical image computation, because high-performance computing technologies are complex to use and master, and their exploration in the medical imaging domain application may still be raw. However, GPUs have the potential and may lead to some new and interesting research areas in medical imaging big data challenges.

Within the past few years, a new generation of heterogeneous computing platforms for medical imaging big data processing includes nodes with multi-core CPUs, GPUs, and deep memory hierarchies. They emerged together and are now being widely deployed for large-scale scientific research. New trends, such as cloud infrastructures and interoperability between different high performance computers, augment the options to employ such infrastructures for medical imaging applications. Nevertheless, many challenges in synthesizing and managing information from large quantities of high-resolution imaging data remain. These challenges would require novel techniques in:

1. data management;
2. data retrieval and staging;
3. data processing and visualization to minimize input/output;
4. computation overheads;
5. exploit computing and memory capacity distributed across multiple types of devices and systems; and
6. maximize application throughput while reducing application development complexity.

22.3.4 Security Privacy in Big Data

PACS security and privacy has been discussed extensively in the Second Edition of *PACS and Imaging Informatics*, 2010. At that time, big data in PACS-based multimedia imaging informatics was not a primary issue, because the term “big data” was not ready to be discussed. However, as more hospitals are increasingly adopting electronic medical record (eMR) systems to enable the aggregation of patient data, including medical imaging data within the hospital and across the hospital system, use of healthcare big data is likely to provide the greatest benefit and impact to the healthcare community. Also, security and privacy concerns are growing as healthcare big data become increasingly accessible [15]. Currently, the use of deidentification or anonymization techniques to protect privacy in health practices in a hospital is regulated by HIPAA. In the past, healthcare big data were limited to large healthcare institutions that could afford to create and own the infrastructure necessary for hosting and mining large amounts of data, and these infrastructures were typically proprietary and were isolated from general networks. The potential use of healthcare big data is novel because hospitals of all sizes, medical researchers, and healthcare administrations will have access to big data and the means to employ it. Current deidentification or anonymization techniques may not be good enough to protect privacy for use of big data in public environment, and this was also of significant concern in the President’s Council of Advisors on Science and Technology reports on big data about the use of deidentification or anonymization techniques to protect privacy in health big data analytics [16].

22.4 Research Projects Related to Medical Imaging Big Data

This section lists five examples relating to the five "V" features of big data of DICOM-based multimedia imaging informatics medical imaging. These research projects were performed at the Laboratory for Medical Imaging Informatics, Shanghai Institute of Technical Physics (LMI/SITP) under Professor Jianguo Zhang’s supervision, who is the Director of the Laboratory for Medical Imaging Informatics, School of Biomedical Engineering, Shanghai Institute of Technical Physics, Chinese Academy of Sciences [25]. Figure 22.6 shows LMI/SITP research projects related to the five V features. These projects are discussed briefly in the section below.

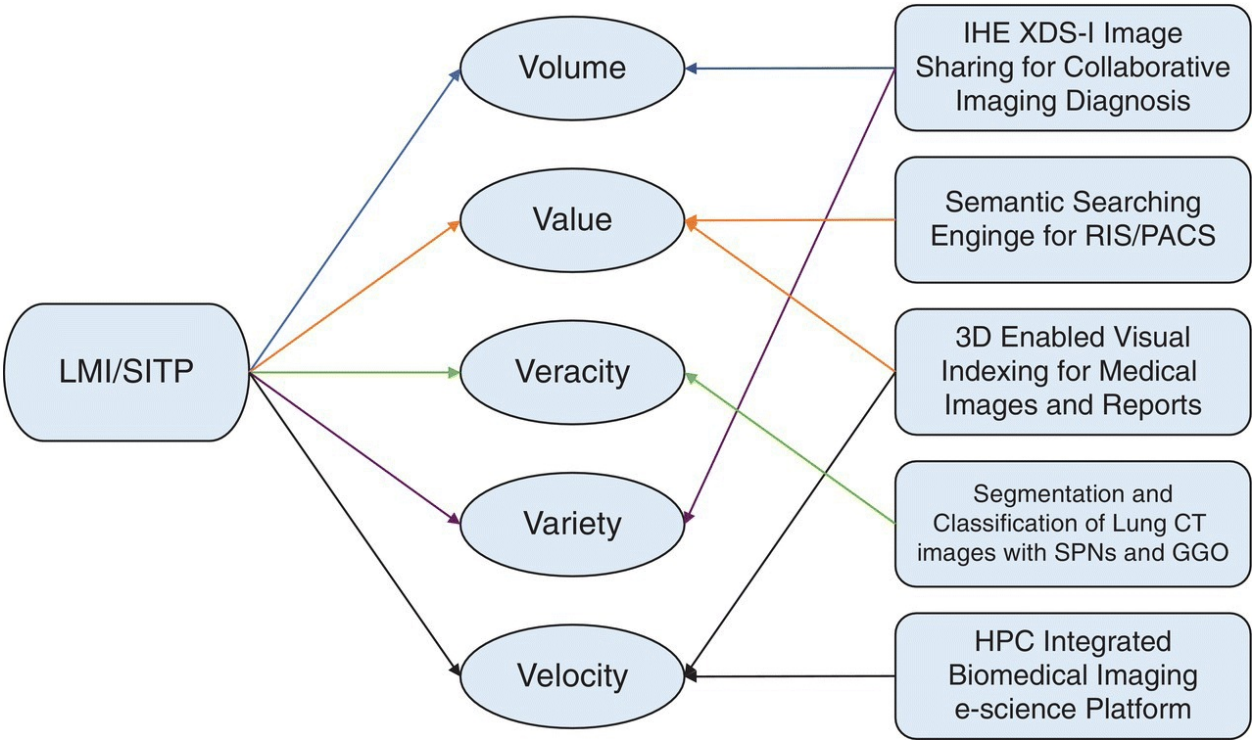

Figure 22.6 The five "V" features research performed at the Laboratory for Medical Imaging Informatics of The Shanghai Institute of Technical Physics (LMI/SITP).

22.4.1 Grid-based IHE XDS-I Image Sharing Solution for Collaborative Imaging Diagnosis

This project introduced the grid concept to implement the IHE XDS-I profile in regional healthcare to enable image sharing between hospitals in Shanghai, China, with a population of 24 million. The developed system has been implemented and operated in five districts of the city of Shanghai for regional collaborative imaging diagnostic services (see Chapter 7) [17,18].

22.4.2 Semantic Searching Engine (SSE) for RIS/PACS

This project was to design and develop a semantic searching engine (SSE) for radiologists to perform semantic searching of reports and related images in RIS-integrated PACS environment. SSE has been implemented for use in a large hospital in Shanghai for a term of four years. The evaluation results show that SEE can increase the 12% usage of historic studies of PACS, especially for those studies archived in PACS for more than 1 year longer [8].

22.4.3 3-D Enabled Visual Indexing (VI) for Medical Images and Reports

This project was to design an innovative visual indexing method to assign an anatomical 3-D structure object to every patient visually, to store indexes of the patients' historical imaging study information. The evaluation results showed that the visual indexing concept has a high potential to be used in RIS/PACS, to quickly search medical records, and provide a deep understanding of the healthcare status of patients with a large number of examinations [19,20].

22.4.4 Segmentation and Classification of Lung CT Images with SPNs and GGO

This project was to develop image processing algorithms to perform feature selection of support vector machine (SVM)-based classifier for differentiating benign and malignant solitary pulmonary nodules (SPNs) by CT [21], and to build Markov random field (MRF) algorithms to perform segmentation in lung CT images showing ground-glass opacities [22]. This research focused on finding a highly efficient feature index for CT images with SPNs and also to develop a method to quantitatively measure the lung nodule disease of ground glass opacity in lung CT images.

22.4.5 High-Performance Computing Integrated Biomedical Imaging E-Science Platform

This project was to design and develop high performance computing integrating an e-science platform to support intensively computing biomedical imaging research and application across multiple academic institutions and hospitals in Shanghai [23]. This platform was rich in image processing algorithms and executed more than 200 000 image processing jobs to support multidisciplinary collaborative research in the past two years [24].

22.5 Summary of Big Data

This chapter outlined five "V" features of big data in PACS-based multimedia imaging informatics. Compared with big data issues of other sectors such as social networking, e-commerce, and manufacturing, issues of big data in medical imaging informatics has special characteristics, which need to be dealt with in healthcare services and research. These characteristics lead to difficult technical

challenges in medical imaging informatics, such as:

1. requiring better methods and systems architecture to resolve the issues of volume and variety;
2. developing better image processing algorithms to perform difficult disease pattern recognition;
3. innovating new quantitative imaging methods to deal with the issues of veracity and value;
4. needing a high performance imaging computer platform to provide more effective mechanisms to overcome limitations of insufficient computing and time-consuming multidimensional medical imaging computation and intercommunication between imaging data sources, servers, and consumers; and
5. the current security and privacy solutions being widely used in current healthcare systems also need to be reinnovated, because the traditional solutions for security and privacy may not be good enough to resolve this issue in healthcare big data.

This chapter also summarizes some solutions to resolve the five V features of big data in medical imaging and informatics, and also lists some research projects relating to five V features of medical imaging big data.

Acknowledgements

This chapter on big data is based on Professor Jianguo Zhang's past and current works on the concept of big data when he chaired [25] the annual SPIE in 2015, 2016 and 2017, as well as his presentations at the RSNA in 2016 and 2017 in Chicago. His PhD student De-Zhong Zheng refined the drawings in Figures 22.1–6. This research was supported by Professor Zhang's grants from the Major State Basic Research Development Program of China (973 Program No: 2010CB834302) and Key Deployment Project of Chinese Academy of Sciences (Project No. KGZD-EW-T03-4).

References

1 Krisberg, K. (2014) Big Data Key to Improving Health Care, *AAMC Reporter*: January 2014.

2 Groves, P., *et al*. (2013) *The "Big Data" Revolution in Healthcare*. McKinsey & Co.

3 Hadoop. Available at: http://hadoop.apache.org

4 MapReduce. Available at: http://en.wikipedia.org/wiki/MapReduce

5 Defining the Big Data Architecture Framework (BDAF). Available at: bigdatawg.nist.gov/_uploadfiles/ M0055_v1_7606723276.pdf

6 Frost & Sullivan: US Medical Imaging Informatics Industry Reconnects with Growth in the Enterprise Image Archiving Market, November 1, 2012. Available at: http://www.frost.com/prod/servlet/ press-release.pag?docid=268728701

7 Barua, A., et al. Measuring the Business Impacts of Effective Data, Available at: www.sybase.dk/files/White_Papers/EffectiveDataStudyPt1-MeasuringtheBusinessImpac

8 Ling, T., Yang, Y. and Zhang, J. (2015) Clinical evaluation of using Semantic Searching Engine for Radiological Imaging Services in RIS-Integrated PACS. *Proc SPIE*, vol. 9418.

9 Vendor Neutral Archive. Available at: http://en.wikipedia.org/wiki/Vendor_Neutral_Archive;

10 The NIST Definition of Cloud Computing, NIST Special Publication 800-145, September, 2011.

11 Integrating the Healthcare Enterprise Cross Enterprise Document Sharing for imaging. Last viewed March 2014. Available at: http://wiki.ihe.net/index.php?title=Cross-enterprise _Document_ Sharing_for_Imaging

12 http://www.rsna.org/QIBA.aspx

13 Yeager, D. (2011) Quantitative Imaging – Going beyond displaying medical images. *Radiology Today*, 12(11), p. 6.

14 Eklund, A.1., Dufort, P., Forsberg, D. and LaConte, S.M. (2013) Medical image processing on the GPU – past, present and future. *Med Image Anal*, 17(8), 1073–1094.

15 Schmitt, C. (2014) Security and Privacy in the Era of Big Data. Available at: www.renci.org/wp-content/ uploads/ 2014/02/0213WhitePaper-SMW.pdf

16 Big Data and Privacy: *A Technological Perspective*, May 2014. Available at: www.whitehouse.gov/ ostp/pcast

17 Zhang, J., *et al*. (2011) Grid-Based implementation of XDS-I as part of Image-Enabled EHR for regional healthcare in Shanghai. *Int J CARS*, 6, 273–284.

18 Zhang, J., Yang, Y., Zhang, K., Sun, J. and Ling, T. (2014) Medical imaging document sharing solutions for various healthcare services based on IHE XDS/XDS-I profiles. *SPIE Proc*, vol. 9039-10.

19 Dong, W. and Zhang, J. (2011) Visualization index for image-enabled medical records. *Proc SPIE*, 7967, 79670Y-1.

20 Zheng, W., Dong W., Chen, X. and Zhang, J. (2012) Semantic extraction and processing of medical records for patient-oriented visual index. *SPIE*, 8, 319–331.

21 Zhu, Y., Tan, Y., Hua, Y., Wang, M., Zhang, G. and Zhang, J. (2101) Feature selection and performance evaluation of Support Vector Machine (SVM)-based classifier for differentiating benign and malignant pulmonary nodules by Computed Tomography. *Journal of Digital Imaging*, 23, 51–65.

22 Zhu, Y., Tan, Y., Hua, Y., Zhang, G. and Zhang, J. (2012) Automatic segmentation of ground-glass opacities in lung CT images by using Markov random field-based algorithms. *Journal of Digital Imaging*, 25, 409–422

23 Zhang, J., Zhang, K., Wang, T. and Yang, Y. (2012) Building Biomedical Imaging and Informatics e-Science platform for translational medical research. *Journal of Translational Medicine*, 1(Suppl. 2). A32.

24 Wang, T., *et al*. (2015) e-Science platform for translational biomedical imaging research: running, statistic and analysis. *Proc SPIE*, vol. 9418.

25 Zhang, J. (2016) Big Data Issues in Medical Imaging and Informatics, Keynote Speech. *SPIE*, 2016.

Index

a

Access to radiology information (ARI) 148

ACR-NEMA and DICOM 127–128

ACR-NEMA 2.0 version 128

ActiveX 127, 184

Acute intracranial hemorrhage (AIH)

- CAD–PACS integration 452–456
- CAD system development
  - acceptance testing within clinical environment 451–452
  - difficult cases 441, 444
  - extract candidates 439–441
  - knowledge-based classification 441–443
  - localization of AIH candidates 440–441
  - realignment of the image 437–439
  - segmentation of the brain 436–437
  - training and validation 441, 443, 445
- clinical aspects 435–436
- clinical evaluation 451–453
- evaluation of CAD
  - change of diagnostic decision 449–450
  - clinicians improved performance 447–449
  - on CT 450
  - integration CAD with PACS 450

rationale of 443, 445
sensitivity, specificity, positive and negative predictive values 449
AIH. *See* Acute intracranial hemorrhage (AIH)
American College of Radiology (ACR) 127
American National Standards Institute/International Standards Organization (ANSI/ISO) 115
American Standard Code for Information Interchange (ASCII) 101
Analysis workstation 261–262
Anatomic pathology workflow (PWF) 145
Antepartum Care Summary (APS) 147
Application layer, MIDG 353–355
Application servers 98, 100
ASCII text representation 102
"Association request and response" commands 137
Asynchronous transfer mode (ATM) technology 17, 100, 114, 115
Audit Trail and Node Authentication (ATNA) 146, 148
AURORA 3-D dedicated breast MRI images 240
Automatic computerized transverse axial (ACTA) scanner 8–9
Automatic image data recovery scheme, for DICOM conformance device
basis 162
general processing flow diagram 162–163
missing images and data 162
missing series/image recovery 164
missing study, recovery of 163–164
Average bone age of child
bone age assessment 464
computer-aided diagnosis 464–466

b

BAA DICOM structured reporting 494–495

Backup archive server 400

- data recovery procedure 403
- functions of 401
- using application service provider model
  - general architecture 402
  - short-term fault-tolerant 402

Basic patient privacy consents (BPPC) 147

Berkeley Software Distribution (BSD) 152

Big data

- and cloud computing 575–576
- features 577, 578
- in DICOM PACS-based medical imaging and informatics 581–586
- research projects 586–587
- security privacy 586
- values 577, 579–580
- variety 577, 580–581
- velocity 577, 581, 585
- veracity 577, 580, 583
- volume 577–579
- vulnerability and complexity 577

Biomedical informatics 29–30

Bispectral index system (BIS) 550

Blobstore 331

Bluetooth™1 116

Bluetooth Special Interest Group (SIG) 116

B-mode (brightness) ultrasound scanning 51–52
Bone age assessment (BAA) of children 464
CAD module 472–473
CAD–PACS integration 497, 499
CAD *vs.* radiologists' assessment of bone age 484–489
clinical evaluation of CAD system
clinical environment 489–490
workflow design 490–491
cross-racial comparisons 475–478
data collection
case selection criteria 467
film digitization 468–469
image acquisition 468–469
image interpretation 468
subject recruitment 467
summary 468
development of CAD method 466–467
digital hand atlas
all subjects combined in 486–489
boys only, compared with radiologists' assessments 488
for clinical evaluation 477–479
database of 471–472, 475
girls only, compared with radiologists' assessments 487
performance of 471–472
research supports 470–472
fuzzy logic 473
hand radiograph 466–467

integrating CAD with other informatics systems 493
BAA DICOM structured reporting 494–495
computational services in data grid 495–498
content-based DICOM-SR with CAD 495
data grid computational service 497–498
integration of CAD with PACS-based multimedia informatics
fuzzy integration 482–483
fuzzy logic 479
fuzzy system architecture 479–482
Los Angeles County General Hospital 493
radiologists' interpretation 474
research supports 470–472
statistical analysis 473–475
validation of the CAD 483–489
web-based BAA clinical evaluation system
CAD server 491
graphical user interface 491–493
Web server 491
BrainLab workstation 319
Breast MR angiogram 72, 75

C

CAD–PACS integration 425, 452–456
advantages 427–428
DICOM standard and IHE workflow profiles 428
DICOM structured reporting 428, 429
IHE profiles 429

in laboratory environment 452, 454
requirement/need for 427–428
security and 421
toolkit 429–432
CAD–PACS simulator 329
bone age assessment of children 333–335
CAD algorithm, evaluation of 332–333
characteristics 332
in clinical environment 333, 335
components and functions 332
integration 331–332
in laboratory environment 333, 334
CAD system
bone age assessment
clinical environment 489–490
content-based DICOM-SR 495
development of 466–467
workflow design 490–491
development in AIH
difficult cases 441, 444
extract candidates 439–441
knowledge-based classification 441–443
localization of AIH candidates 440–441
realignment of the image 437–439
segmentation of the brain 436–437
training and validation 441, 443, 445
C and C++ programming languages 101, 152

Cardiac Cath Workflow (CATH) 145
Carpal bone fuzzy subsystem 481
CAT-5 cables 116
Cathode ray tube (CRT) 255–256
Charge posting (CHG) 148
Chromosome karyotyping 30–31
Cine loop ultrasound 53–54
Classical PACS WS model 100
Clearinghouse 200–202
Client-server model 106–107
Cloud-based PACS archive
  cloud storage workflow 410, 412
  data query and retrieve functions 410, 413
  experiment 408–409
  PACS cloud architecture 410, 411
Cloud computing 413
  and big data 575–576
  and cloud storage 405
  NIST definition 406
  service models 404–405
  services in archive architecture 331
Cloud Storage 405
Color display 258
Color Doppler ultrasound imaging 53
Common Object Request Broker Architecture (CORBA@ BASIC) 184
Communication and networks
  network technologies (*See* Network technologies)

OSI and DOD 110, 112–113
Component-based Web Server
architecture of 184–185
component software technologies 183–184
display workstation 186–188
query/retrieve DICOM image/data
in PACS archive server 185–186
in Web Server 184–185
Component Object Model (COM) 184
Comprehensive electronic patient record 319–320
Compressed image file 85
Computed Maxillofacial Imaging Congress (CMI) 29
Computed radiography (CR) 17–18
examples of 46–48
Computer-aided detection/diagnosis (CAD/CADx)
average bone age of child 464–466
decision support 421
in mammography 420
research and development 421–423
system and evaluation 421
target applications 421
usefulness and practicality 420
with DICOM PACS and MIII 425
without PACS
with digital image 424
without digital image 423–424
workflow 429–430

Computer-assisted radiology and surgery (CARS) 29
Connectivity and open architecture 102
Consistent Presentation of Images (CPI) 148
Consistent time (CT) 146
Content mapping resource 140
Continuous conscious electroencephalogram monitoring 528, 531
Conventional direct Digital 2-D projection radiography 46
Convention transmission X-ray computed tomography (CT) 58
CORBA 127
Core middleware layer, MIDG 356
CR image information object class 133
Cross-enterprise document media interchange (XDM) 146
Cross-enterprise document reliable interchange (XDR) 146
Cross-enterprise document sharing (XDS) 146, 244
Cross-enterprise document sharing for imaging (XDS-I) 148
integration profile 192, 331, 366
description 193–194
implementation in second-generation MIDG 369–371
Cross-enterprise sharing of scanned documents (XDS-SD) 146

d

Data access interface (DAI) 225
Data and image acquisition gateways 98–99
Database GW 98
Database services 243
Database-to-database transfer method 172–173
Data flow

DICOM–CAD–IHE™, Third Edition 432, 433
DICOM–PACS–IHE™, Second Edition 432, 433
DICOM-SC, First Edition 431, 432
Data grid 222
clinical trials 233–234
data migration 236–238
dedicated breast MRI enterprise (*see* Dedicated breast (DB) MRI enterprise data grid)
for enterprise PACS 223–225
enterprise PACS daily clinical operation 224–226
image-based clinical trials 234
image/data security in 247–249
image storage and backup 236–237
independent clinical service 250
IPILab 222–224
multiple clinical trials 239
role of radiology core in imaging-based clinical trials 234–236
sociotechnical considerations 248, 250
Data Grid simulator (DGS)
with cloud computing design 331
components and connectivity 329
description 329
functions of 329
Data migration 236–238
Data persistence manager 356
Data reliability 102–103
Data security 103

Decoding 85
Dedicated breast (DB) MRI and DICOM Grid Access Point (GAP) 242–243
Dedicated breast (DB) MRI enterprise data grid
components 240–243
data grid for 239–240
functions of 240
IHE XDS-I workflow profile 244–24
image archive and backup, query/retrieve and disaster recovery 243
Deidentification/anonymization techniques 586
Density resolution 41, 43–44
Department of Radiological Sciences and the Biomedical Physics Graduate Program 10–11
Desktop workstation 263
Device Enterprise Communication (DEC) 147
Diagnostic workstation 260
Diagnostic WSs 99
DICOM. *See* Digital Imaging and Communications in Medicine (DICOM)
DICOM-based computer-aided detection
acute intracranial hemorrhage
CAD–PACS integration 452–456
CAD system development 436–443
clinical aspects 435–436
clinical evaluation 451
evaluation of the CAD 443–451
next steps for the development of CAD 451–454
multiple sclerosis
CAD-PACS toolkit 459–460

data collection 457–458
detection on MRI 456–457
DICOM-SR document 457–459
DICOM structured reporting and CAD–PACS-based integration toolkit 456–457
MS detection 460–461
DICOM-based image acquisition gateway
determination of the end of an image series 160–162
gateway computer components and database management 158–160
DICOM–CAD–IHE™, Third Edition 432, 433
DICOM-compliance image acquisition gateway 155–156
DICOM compliance PACS broker
concept 166–167
implementation 166–167
DICOM-compliant PACS-based archive server
advantages 397
hardware components 399, 400
image acquisition gateways 398, 399
image communication 397, 398
Q/R service class 397
software 400, 401
storage service class 397
workflow 400, 401
DICOM conformance PS 3.2–1996 136
DICOM Conversion Unit (DCU) 242
“DICOM message service elements” (DIMSEs) 134
DICOM–PACS–IHE, Second Edition 432, 433

DICOM PC-based display workstation software 269
software architecture 272–273
software modules
image communication 274
image display program 275
patient folder management 274–275
query and retrieve 275
software system 270, 272
DICOM-RT archive server 307–308
DICOM-RT-based ePR system architecture design 306–307
DICOM-RT gateway 306–307
DICOM-RT object input 306–307
DICOM-RT objects 304–306
DICOM-RT web-based ePR server 308–309
DICOM-SC, First Edition 431, 432
DICOM 3.0 Standard
DICOM communication 135–136
DICOM conformance 136
DICOM data format 129, 131, 132
DICOM file format 132–133
DICOM model of the real world 129, 131–132
DICOM services 134
object class and service class 133–134
query and retrieve 138–139
send and receive 136–137
Difference image 87
Diffusion tensor MRI (DTI) 75–76

Digital Electronic Computers in Biomedical Science 5
Digital hand atlas (DHA)
all subjects combined in 486–489
boys only, compared with radiologists' assessments 488
for clinical evaluation 477–479
database of 471–472, 475
girls only, compared with radiologists' assessments 487
performance of 471–472
research supports 470–472
Digital image 39–40
Digital Imaging and Communications in Medicine (DICOM) 124
acquisition gateway 156–157
communication protocol 101
compliance 157–158
data format 129, 131, 132
file format 132–133
model of the real world 129, 131–132
organizational structure
content mapping resource 140
current DICOM strategic document 141
mammography computer-aided detection 139
structured reporting 140
visible light images 139
waveform IOD 140
services 134
Digital Imaging and Communications in Medicine Standard PS 3.1 2008 128–129

Digital medical imaging
density resolution, spatial resolution, and signal-to-noise ratio 41, 43–44
digital image 39–40
digital medical image 40
image display 40, 42
image size 40–41
radiology workflow 44–45
Digital radiography 20
Digital scan converter (DSC) image memory 52
Digital subscriber lines (DSL) 117
Digital-to-analog (D/A) conversion 40
Digitized/digital medical images 40
Digitizing, printing, and CD copying workstation 261–262
Direct digital input, Fuji CR system 18–19
Direct sequence spread spectrum (DSSS) modulation 115
Displayable Reports (DRPT) 145
Display monitor 255–256
Display of 4-D medical images and fusion images 82–83
Display workstations 99–100, 186–188
analysis workstation 261–262
basic software functions 267–271
desktop workstation 263
diagnostic workstation 260
DICOM PC-based display workstation software 269–270, 272–25
digitizing, printing, and CD copying workstation 261–262
image display and measurement functions
distance, area, and average gray level measurements 265

histogram modification 263–264
image reverse 264
montage 267
optimization of image perception in soft display 265–267
window and level 263
zoom and scroll 263
intelligence workstation
characteristics of true 2½-D and true 3-D 282–283
true 3-D 283–285
“true 2½-D” and “true 3-D” image workstations 277–282
interactive teaching workstation 262
PACS-based (*see* PACS-based display workstations)
PACS-based multidimensional image display 276–278
post-processing workflow 276
review workstation 260–261
specialized post-processing workstation 277–280
3-D printing
technology 285
terminology and methods 285–286
use of 286–289
workstation user interface 268–271
Distributed computing
concept of 217–218
in PACS and medical imaging environment 218–219
Distributed image file server 179–181
Dose information object 304–305
Dose-volume histogram (DVH) 293, 296

Drum input to digital automatic computer (DRIDAC) 5–7
Drum scanner 17
Dynamic multimedia 321

e

Echocardiography Workflow (ECHO) 145
EchoPixel True 2½-D image 282
Echo-planar imaging (EPI) 73
Electronic healthcare record integration, in regional healthcare
  imaging sharing implementation 205–206
  overview 202–203
  results 207–208
  XDS-I-based regional collaborative imaging sharing solution 203–205
Electronic medical record (EMR) system 559, 561
  IIA-MISS
    advantages 569
    data collection 567–568
    qualitative results 565, 567
    statistical analysis 568–569
    use and training 564–565
Electronic patient record (ePR) MISS system architecture 538–540
  integration unit
    input data and archive 540
    out of range input data alert message 540–541
  tandem ePR server 541–542
    database schema 542–543
    data storage and archive and system database 542

system security 543
tandem system 543
tandem gateway server
intra-op stage 541
post-op stage 541
pre-op stage 541
visualization and display 543
Electronic patient record (ePR) system
data model 303–304
evidence-based 505–506
goals of 506
MISS ePR system 340–342
proton therapy (*See* Proton therapy ePR system)
software organization 300
Electronic portal imaging device (EPID) 297
Emergency department encounter record (EDER) 147
Emergency department referral (EDR) 147
Emission computed tomography (ECT) 61, 63, 65–67
Encoding 85
Endoscopic imaging 54–55
Enterprise PACS-based multimedia and ePR system with image distribution 110–111
Enterprise PACS daily clinical operation 224–226
Enterprise user authentication (EUA) 146
Enterprise-wide information systems (IHE) 177–178
Ethernet 116–117
Ethernet communication system 13–14

Evidence documents (ED) 145, 148
Exchange of personal health record content (XPHR) 147
Explicit value representations (VR) transfer syntax 132
Extensible access control markup language (XACML) 203
Extensible markup language (XML) 101, 153
External beam radiotherapy (RT) 292
Eye care displayable report (ECDR) 146
Eye care evidence document (ECED) 146
Eye care workflow (EYECARE) 146

f

Fabric layer, MIDG 356
Fail-safe gateway design 168–169
Failsafe tandem gateway system 169
Fast Ethernet 114
Fault-tolerance tests 366, 380
Fault-tolerant data grid 226–227
  archive and backup 227–228
  disaster recovery 229–230
  query/retrieve 228–229
Fiber optics 116
File transfer protocol (FTP) 110
Film-based CAD mammography 424
Film input to digital automatic computer (FIDAC) 5–7
512 image 40
Four-dimensional, multimodality, and fusion imaging
  display of 4-D medical images and fusion images 82–83

from 3-D to 4-D imaging 78–80
image fusion 82
image registration 82
medical imaging 83–87
multimodality 3-D and 4-D imaging 79, 81–82
Four-dimensional (4-D) PET-CT imaging 85–88
Four-dimensional (4-D) ultrasound imaging 83–84
Four-dimensional (4-D) X-ray CT imaging 83, 85
4K digital mammogram 40
Fuji computed radiography (FCR) system 17–18
Fuji computed radiography (FCR) XG5000 system 46–47
Full-field direct digital mammography (FFDDM)
screen/film cassette and digital mammography 46–47
slot-scanning full-field direct digital mammography 47–48, 50
Functional MRI (fMRI) 75
Functional status assessments (FSA) 147
Fused filament fabrication 285–286
Fuzzy logic, BAA 473
Fuzzy system architecture, BAA
carpal bone fuzzy subsystem 481
knowledge base derived from the digital hand atlas 479–480
phalangeal fuzzy subsystem 480–481
wrist joint fuzzy subsystem 481–482

g

Gamma camera and associated imaging system 51
GAP servers 355

Gateways (GW) 98
clinical operation and reliability of 168–169
data and image acquisition 98–99
fail-safe gateway design 168–169
weakness 168
Generic PACS-based multimedia architecture and workflow 98, 103–104
Gigabit Ethernet 114
Global superhighway 116
Globus Toolkit 221–222
Globus Toolkit 4.0 221
Graphical user interface (GUI) design 311–313
Greenfield, M. 11–12
Greulich and Pyle (G&P) Hand Atlas, 464
Grid-based IHE XDS-I image sharing solution 586
Grid computing
concept of 219
current technology 220–221
Globus Toolkit 4.0 221
integrating DICOM technology with the Globus Toolkit 221–222
Grid resource allocation and management (GRAM) service 497

h

Hadoop distributed file system 583
Hand radiograph, BAA 466–467
Healthcare big data 586
Health Insurance Portability and Accountability Act (HIPAA) 103, 467
Health Level 7 (HL7) standard

example 125–126
OSI model 124
trend in 126–127
user-vendor committee 124
Hierarchical storage systems 16
in PACS 391–392
High-definition multimedia interface (HDMI) 114
High-performance computing integrated biomedical imaging e-science platform 587
High-quality WSs 99
HI-PACS gateway 164–165
HL7 message development framework (MDF) 127
HL7 standard. *See* Health Level 7 (HL7) standard
HL7 Version 3 126–127
HL7 Version 2.X 126–127
Hospital Information System (HIS) 8, 98, 169–171
Hounsfield, Godfrey N. 8
Huang, H.K. 8, 12, 13, 30
Hypertext transfer protocol (HTTP) 181, 314
Hypofractionation dose protocol 508, 520

i

IAT simulators 329
IEEE 802.3 116
IHE 2020vision 151
IHE XDS/XDS-I profiles
brief description 193–194

comparison of three pilot studies 209–210
electronic healthcare record integration in regional healthcare 202–209
extension of XDS-I profile-based image sharing 211–212
image sharing for cross-enterprise healthcare with federated integration 194–199, 207
performance and storage 211
principles 191
security issues 210–211
XDS-I-based patient-controlled image sharing solution 200–202, 207
IIA-MISS. *See* Integrated image-assisted minimally invasive spinal surgery (IIA-MISS)
Image acquisition GW 98
Image-assisted knowledge discovery and decision making 320–321
Image-assisted minimally invasive spinal surgery (IA-MISS) 560
algorithm of spine care 531, 534
bridging the gap between diagnostic images and surgical treatment 526–527
on cervical, thoracic, and lumbar spines 527–528
clinical site 536
continuous conscious electroencephalogram monitoring 528, 531
endoscopic imaging system and C-Arm DF 528, 530
ePR MISS system architecture
major components 539–544
overall 538–539
general MISS workflow 535–536
goals of ePR 534–535
intra-op module 547, 549
data acquired during surgery 550
graphical user interface 552

interaction with the gateway 552
internal architecture of the integration unit 551
participants in the OR 550
rules-based alert mechanism 552–553
location of problematic disc marking 528, 532
MRI 529, 533
multimedia ePR system 534
data model and standards 536–537
intra-op workflow 538–539
preoperative workflow 537–538
patient surgical outcome 529, 533
post-op module
follow-up pain surveys 554
graphical user interface 553–554
participants 553
patient in the recovery area 553
stage 553
pre-op authoring module 543
graphical user interface 546–549
organization of the pre-op data 545
participants in the surgical planning 545
surgical whiteboard data 545–546
workflow analysis 544, 546
surgical team assembling 528–529
system deployment
hardware installation 555
planning and design phase 554–555

software installation 556
special software for training 556
tissue modulation technology 528, 532
training and supports for clinical users 556–557
Image-assisted surgery (IAS) ePR simulators 342–343
data flow 339
in laboratory environment 340
role 338–339
workflow
intra-op phase 339–340
post-op phase 340
pre-op phase 339
Image-based clinical trials 234
Image communication 274
Image compression 16
acceptable compression ratio 87–89
compressed image file 85
compression ratio 87
difference image 87
encoding and decoding 85
reconstructed image from a compressed image file 85
wavelet transform method 88, 90–93
Image data communication 117
Image display 40, 42
board 255–256
hardware 254–255
and measurement functions

distance, area, and average gray level measurements 265
histogram modification 263–264
image reverse 264
montage 267
optimization of image perception in soft display 265–267
window and level 263
zoom and scroll 263
program 275
Image-enabled EHR (iEHR) 194
Image fusion 82, 148
Image information object 304–305
Image pre-processing and display 167–168
Image processing algorithm 472–473
Image Processing and Informatics Laboratory (IPILab) 118, 222–224
Image Processing Laboratory (IPL) at UCLA 13–14
Image querying and retrieval 195–196
Image registering 196
Image registration 82
Image sharing for cross-enterprise healthcare with federated integration
background 194
image sharing architecture, components and workflows 195–196
image sharing models 197–198
key issues identified in pilot testing 196
performance 198–199
results 207
Image sharing models 197–198
Image size 40–41

Image workstation
analysis workstation 261–262
desktop workstation 263
diagnostic workstation 260
digitizing, printing, and CD copying workstation 261–262
interactive teaching workstation 262
review workstation 260–261
Imaging camera for medical applications 17
Imaging component
in treatment delivery 293–295, 297
in treatment planning 292–297
Imaging service workflow efficiency and quality 581
Implantable Device Cardiac Observation (IDCO) 145
Import Reconciliation Workflow (IRWF) 148
InCor 118, 120
Industry standards 101–102
Information object definitions (IODs) 309
Information sharing 319
Infrastructure as a service (IaaS) 405
Integrated image-assisted minimally invasive spinal surgery (IIA-MISS)
clinical EMR system 559, 561
advantages 569
data collection 567–568
qualitative results 565, 567
statistical analysis 568–569
use and training 564–565
intra-op display monitor 565–567

planning stage 561–564
post-op pages 565, 568
pre-op display 565
Integrating the Healthcare Enterprise (IHE) 102
data model, actors and integration profiles 144
examples 149–151
high-level information model 142
history 142
IHE activities 144
IHE Integration Workshop in 2006 142–143
IHE 2020Vision 151
international expansion 149, 151
multidisciplinary effort 149
profiles 144–148
Intelligent treatment plan navigator (ITPN) 509
Interactive display with multiple monitors 20–21
Interactive teaching workstation 262
Interface engine 172–174
International Society for Optical Engineering (SPIE) 27–28
International Standards Organization (ISO) 110
Internet 116–117, 181
Internet2 (I2)
connection of three international sites 118–120
image data communication 117
major international interconnection points 118
observations 120
Intra-op module, MISS 547, 549

data acquired during surgery 550
graphical user interface 552
interaction with the gateway 552
internal architecture of the integration unit 551
participants in the OR 550
rules-based alert mechanism 552–553
Intravascular ultrasound (IVUS) technology 68

j

Japan medical imaging technology 26–27
JavaBeans 184
Java (just another vague acronym) programming language platform 101
Journal of Applied Clinical Medical Physics (JACMP), 12

k

Kangarloo, H. 12
Key image note (KIN) profile 148, 429
Knowledge base (KB) data-mining search engine 509
Konica digital radiography system 20
Konica laser film scanner 17–18

l

Laboratory Scheduled Workflow (LSWF) 147
Large-capacity optical disk Jukebox 16
Laser film printer for X-ray images 16–17
Laser film scanner 17–18
Ledley, Robert S. 4–8

Light imaging 54–55, 76–77
Linear accelerator (LINAC) 297
Liquid crystal (LCD) 255–256
Liu, Brent 403
Local area network (LAN) 100
LOINC Test Codes Subset (LTCS) 147
Los Angeles County General Hospital 493
Lossless digital signature embedding (LDSE) procedure 247
Lung CT images, segmentation and classification of 587

m

Magnetic resonance angiography (MRA) imaging 261–262
Magnetic resonance imaging (MRI)
  basics 68–69
  image production 69–70
  MR angiography 72, 75
  pulse-sequence images 72–73, 75–76
  steps in producing 70–72
  3-D dedicated breast MR angiogram 71, 74
  3-D fetal 3 T MR images 71, 74
  T1 weighted images 71, 73
Mammography computer-aided detection (CADe) 139
Mammography Image (MAMMO) 148
Media access control (MAC) 116
Medical image big data. *See* Big data
Medical imaging. *See also* Three-dimensional (3-D) medical imaging; Two-dimensional (2-D) medical imaging

automatic computerized transverse axial 8–9
and informatics data 576
Ledley's contributions 4–7, 8
pattern recognition laboratory 4–7
Medical imaging informatics infrastructure (MIII) resource 423
Medical imaging informatics infrastructure (MIII) platform 326, 327
Medical imaging informatics (MII) simulator
defined 326
organization 326, 327
Medical summaries (MS) 147
Message header segment (MSH) 125–126
Micro-densitometer 17
Minimally invasive spinal surgery (MISS). *See* Image-assisted minimally invasive spinal surgery (IA-MISS)
Minimally invasive surgery 298–299
MISS ePR system 340–342
Modality integration unit (MIU) 98
Modulation transfer function (MTF) 257
Molecular imaging data grid (MIDG) 347
connectivity and workflow 356–358
current status and next-generation 360
experimental setup 358
implementation scenario 351
in healthcare informatics 360
objective 350
performance evaluation 359–360
sample preclinical molecular imaging datasets 358–359

simulator 329–331
software architecture 352
application layer 353–355
core middleware layer 356
fabric layer 356
user-level middleware layer 353, 355–356
MR angiography (MRA) 72, 75
MRI. *See* Magnetic resonance imaging (MRI)
MTOM/XOP 210
Multi-center MIDG implementation
data collection 375–377
data normalization 375–376
DICOM tags 375, 377
download performance 378, 380
evaluation steps 372, 374
fault tolerance 380
hardware requirements 374
network bandwidths 374, 375
purpose 371
software requirements 374
three site test-bed 372, 373
upload performance 378, 379
USC Image Processing and Informatics Lab 372
USC Molecular Imaging Center 372
USC Ultrasound Transducer Resource Center 372
Multimedia ePR system, in radiotherapy (RT)
communication between isolated information systems and archival of

information 319
comprehensive ePR model 319–320
database schema 309, 311
of RT archive server 311–312
data collection for the prototype system 314–315
DICOM-RT archive server 307–308
DICOM-RT-based ePR system architecture design 306–307
DICOM-RT gateway 306–307
DICOM-RT object input 306–307
DICOM-RT objects 304–306
DICOM-RT web-based ePR server 308–309
ePR data model 303–304
graphical user interface design 311–313
GUI in the WS 314
hardware and software 314
image-assisted knowledge discovery and decision making 320–321
information sharing 319
multimedia ePR system 315–318
background 299–300
database schema 300–301
data flow model 300
data model 300, 302
ePR software organization 300
minimally invasive surgery 298–299
multimodality 2-D and 3-D imaging
fusion of 3-D MRI and 3-D CT images 296, 298
image registration 293–295, 297–298

imaging component in treatment delivery 293–295, 297
imaging component in treatment planning 292–297
radiotherapy workflow 292
radiotherapy planning and treatment 301–303
RT ePR prototype 312, 314
RT web client workstation 309–310
workflow 302–303
Multimedia ePR system, MISS 534
data model and standards 536–537
intra-op workflow 538–539
preoperative workflow 537–538
Multimodality 2-D and 3-D imaging
fusion of 3-D MRI and 3-D CT images 296, 298
image registration 293–295, 297–298
imaging component in treatment delivery 293–295, 297
imaging component in treatment planning 292–297
radiotherapy workflow 292
Multimodality 3-D and 4-D imaging 79, 81–82
Multimodality Registration for Radiation Oncology (MMR-RO) 147
Multiple display controller 15
Multiple-reader multiple-case receiver operating characteristic analysis 445–447
Multiple sclerosis (MS)
CAD-PACS toolkit 459–460
data collection 457–458
detection on MRI 456–457
DICOM-SR document 457–459

DICOM structured reporting and CAD-PACS-based integration toolkit 456–457
MS detection 460–461
Multipurpose internet mail extension (MIME) message 184

n

National Electrical Manufacturers Association (NEMA) 127
NATO Advanced Science Institute (ASI) 23–25
Netherlands National Foundation 23
Network technologies
asynchronous transfer mode technology 114, 115
Ethernet 116–117
fast Ethernet and gigabit Ethernet 114
Internet 116–117
Internet2 117–120
standard Ethernet 113–114
wireless networks 115–116
Neuroimaging 435–436
Neurosurgery 570, 571
Next-generation Internet (NGI) 118
Non-DICOM files 314–315
Normalized information object classes 133
Normal treatment planning-simple (NTPL-S) 147
Nuclear medicine image (NM) 148
Nuclear medicine (NM) imaging 48–51
gamma camera and associated imaging system 51
principles of 48–49, 51

o

Object class 133–134

Open grid services architecture (OGSA) 220, 331

Open Group 406–408

Open systems interconnection (OSI) 110, 112–113

Optical carrier level 1 (OC-1) 115

Organizational root 133

Orthogonal frequency division multiplexing (OFDM) 115

Oswestry disability index 545–546

p

PACS-based architectures

- client-server model and data flow 106–107
- enterprise PACS-based multimedia and ePR system with image distribution 110–111
- stand-alone PACS-based model and data flow 105–106
- teleradiology model 108–110
- web-based model 107–108

PACS-based archive server

- DICOM 397–400
- system operations 396–397

PACS-based display workstations

- color display 258
- display monitor 255–256
- image display board 255–256
- image display hardware 254–255
- resolution 256–259

PACS-based multidimensional image display 276–278
PACS-based multimedia biomedical imaging informatics 390
PACS components and network
application servers 98, 100
components 97
data and image acquisition gateways 98–99
display workstations 99–100
PACS server and archive 99
system networks 100–101
PACS–ePR simulator
components and data flow 328
description 328
function and data flow 328
imaging informatics applications 329
PACS image management design concept 391–395
PACS infrastructure design concept
connectivity and open architecture 102
data reliability 102–103
industry standards 101–102
security 103
PACS modality gateway
and HI-PACS 164–165
ultrasound modality 165–166
PACS server and archive 99
functions of 395–396
positions of 391
RIS and HIS interface 396

system configuration 392
archive server 393–394
archive storage 394
backup archive system 394
communication networks 394–395
database system 394
PACS with HIS and RIS
common data 174–175
database-to-database transfer method 172–173
IHE patient information reconciliation profile 177–178
implementation of RIS-PACS interface 174–177
interface engine 172–174
rationale of interfacing 173
Parallel virtual machine (PVM) 218
Patient demographics query (PDQ) 146
Patient folder management 274–275
Patient identifier cross-reference and patient demographics query for HL7v3 146
Patient identifier cross referencing (PIX) 146
Patient information object class 133
Patient information reconciliation (PIR) 148
Patient record architecture (PRA) 127
Patient synchronized application (PSA) 146
Pattern recognition laboratory (PRL) 4–7, 10
Personal image filing system 16
Personnel white pages (PWP) 146
Phalangeal fuzzy subsystem 480–481

Picture archiving and communication system (PACS)
ATM communication technology 17
biomedical informatics 29–30
CARS 29
chromosome karyotyping 30–31
collaboration of the UCLA Team with the US Medical Imaging Industry 25
computed radiography 17–18
Department of Radiological Sciences and the Biomedical Physics Graduate Program 10–11
digital radiography 20
diligent contributors 34
direct digital input, Fuji CR 18–19
end users 33–34
EuroPACS 28–29
golden era of medical imaging technology research support 32–33
Greenfield’s contributions 11–12
hierarchical storage system 16
HIS/RIS/PACS system 8, 10
Image Compression project 16
image processing laboratory at UCLA 13–14
interactive display with multiple monitors 20–21
Japan medical imaging technology 26–27
Kangarloo’s contributions 12
laser film printer for X-ray images 16–17
laser film scanner 17–18
medical imaging informatics system 30, 32
multiple display controller 15

NATO Advanced Science Institute and the UCLA PACS 23–25
Netherlands National Foundation and the UCLA PACS 23
patents and copyrights 29
personal image filing system 16
SPIE 27–28
US Government Agencies 22–23
VAX 11/750 computer system 15
Picture element 39
Pixel 39
Plan information object 304–305
Platform as a service (PaaS) 405
PolyU 118, 120
Portable data for imaging (PDI) 148
Positron emission tomography (PET) 65–67
Post-op module, MISS
follow-up pain surveys 554
graphical user interface 553–554
participants 553
patient in the recovery area 553
stage 553
Post-processing workflow 148, 276, 429
Preclinical molecular imaging
data model 351–352
informatics 348–350, 361
modalities 348, 349
Pre-op authoring module, MISS 543
graphical user interface 546–549

organization of the pre-op data 545
participants in the surgical planning 545
surgical whiteboard data 545–546
workflow analysis 544, 546
“Presence of the next series” method 162
Presentation of Grouped Procedures (PGP) 148
Protocol 135
Proton therapy (PT)
challenges of 504–505
clinical outcomes 508
clinical workflow 506–507
dose uncertainty and treatment schedule 504–505
high cost of 505
and prostrate cancer 503–504
radiation toxicity 508
treatment protocols 507–508
Proton therapy ePR system 520
database 512
dataflow model 510–511
data gateway 508–509
decision support tools 509, 520
ePR server 509
laboratory implementation 512
for prostate cancer patients 506, 521
data collection 512, 513
follow-up data form 513, 514
knowledge-based search engine query input 515, 516

patient information and treatment plan 515
pretreatment clinical parameters 513
treatment plan modification 517–519
system architecture 508–509
visualization and display tools 509
WampServer version 2.0 511
web technology 511
Pure teleradiology model 108–109

q

Quantitative imaging 583–584
“Query and retrieve” images 136, 138
Query for existing data (QED) 147
Query/retrieve DICOM image/data
in PACS archive server 185–186
in Web Server 184–185
Queue software 101

r

Radiation therapy 504, 507, 520. *See also*Proton therapy (PT)
Radiation toxicity 508
Radiology information system (RIS) 8, 98, 171–172
Radiology workflow 44–45
Radiotherapy (RT) ePR simulator
architecture and data flow 335–337
components and features 335, 336
description 335

intelligent treatment plan navigator 337, 338
role 337
step-by-step simulation, of knowledge discovery 337
Radiotherapy planning and treatment 301–303
RAD-69/WADO hybrid image retrieval 193
Real-time, interactive virtual reality system 282
Reasoning Foundations of Medical Diagnosis 5
Reconstructed image 85
Redundant array of independent disks (RAID) 236
Reference information model (RIM) 127
Registry stored query transaction for cross-enterprise document sharing profile 146
Reporting workflow (RWF) 148
Request information for display (RID) 146
Research and development (R&D), CAD 421–423
Research projects, medical imaging big data
grid-based IHE XDS-I image sharing solution 586
high-performance computing integrated biomedical imaging e-science platform 587
lung CT images, segmentation and classification of 587
semantic searching engine, for RIS/PACS 586
3-D enabled visual indexing 587
Resolution 256–259
Retrieve form for data capture (RFD) 146
Retrieve Imaging Document set 69 (RAD-69) 192
Review workstation 99, 260–261
Rotating gamma camera system 63, 65
RT archive server 311–312

RT ePR prototype 312, 314
RT web client workstation 309–310

S

Sampling modes and image display 52–53
Scheduled workflow (SWF) 148
Screen/film cassette and digital mammography 46–47
Second-generation MIDG
  benefits 383
  centralized queue handling 369
  data transmission performance 380–381
  design architecture 366
  DICOM-compliant file management web-services 367
  distributed connectivity 368
  future research and development 384–386
  GUI Web server 381–382
  IHE XDS-i integration profile implementation 369–371
  implementation at molecular imaging facility 381–383
  improved research workflow 383
  intelligent routing service 371
  multi-center implementation 371–375
  with OGSA data grid infrastructure 369, 370
  performance 369
  preclinical imaging workflow 367–368
  rules-based backup 371
  service-oriented design 369
  system overview 368–369

Secure socket layer (SSL) 201
Security privacy, in big data 586
Semantic searching engine (SSE), for RIS/PACS 586
“Send and receive” images 136–137
Service 135
Service class 133–134
Service class provider (SCP) 136
Service class user (SCU) 136
Service-object pairs (SOPs) 129
Shanghai Shen-Kang Hospital Management Center (SSKHMC) 194
Sharing Laboratory Reports (XD*-LAB) 147
Signal-to-noise ratio 41, 43–44
Silva, L.B. 408
Simple Image and Numeric Report (SINR) 148, 429
Single photo emission CT (SPECT) 63, 65
Slot-scanning full-field direct digital mammography 47–48, 50
Soft-copy display 40
Software as a service (SaaS) 405
Software visualization toolkit (VTK) 277
Spatial resolution 41, 43–44
Specialized post-processing workstation 277–280
Specimen input to digital automatic computer (SPIDAC) 5–7
Spine care, algorithm of 531, 534
Spin echo free-induction-decay (FID) signals 71
Spin-echo pulsing sequence 71
Spiral imaging readout techniques 73
SRT structure set information object 304–305

Stand-alone PACS-based model and data flow 105–106
Stand-alone primary diagnostic WS 99
Standard Ethernet 113–114
Static multimedia 321
Stereolithography 285–286
Stored Query 146
Stress testing workflow (STRESS) 145
Structured English Query Language (SEQUEL) 152
Structured Query Language (SQL) 101, 152–153
Structured reporting (SR) 428, 429
  BAA DICOM 494–495
  DICOM organizational structure 140
Study information object class 133
System networks 100–101

t

TCP/IP communication protocols 102
Teaching File and Clinical Trial Export (TCE) 148
Teleradiology model
  PACS 109–110
  pure 108–109
Thick-client model. *See* Stand-alone PACS-based model and data flow
Thick-client PACS WS 100
Thin-client model. *See* Client-server model
Thin-client PACS WS 100
Three-cores data grid architecture 236–237
3-D CT scanner 59–60

3-D enabled visual indexing, for medical images and reports 587
3-D fluorescence confocal microscopy 76–77
Three-dimensional (3-D) medical imaging
emission computed tomography 61, 63, 65–67
magnetic resonance imaging (*see* magnetic resonance imaging (MRI))
3-D fluorescence confocal microscopy 76–77
three-dimensional ultrasound imaging 68–69
3-D micro imaging and small animal imaging 76, 79
transmission X-ray computed tomography (*see* transmission X-ray computed tomography)
two-dimensional transmission X-ray computed tomography 55–58
Three-dimensional (3-D) ultrasound imaging 68–69
3-D lossless digital signature embedding procedure 247
3-D micro imaging and small animal imaging 76, 79
3-D printing
technology 285
terminology and methods 285–286
use of 286–289
3-D wavelet transform 90–93
Tissue modulation technology 528, 532
Translational medicine 569–571
Transmission control protocol/internet protocol (TCP/IP) 101, 181
Transmission X-ray computed tomography
components and data flow of a 3-D CT scanner 59–60
convention 58
CT image data 60–63
whole body CT scan 59

Treatment workflow (TRWF) 147
"True 2½-D" and "true 3-D" image workstations 277–282
Two-dimensional (2-D) endoscopic imaging 54–55
Two-dimensional (2-D) light imaging 54
Two-dimensional (2-D) medical imaging
  computed radiography systems 46–48
  conventional direct Digital 2-D projection radiography 46
  full-field direct digital mammography 46–50
  light and endoscopic imaging 54–55
  nuclear medicine imaging 48–51
  ultrasound imaging (*see* two-dimensional (2-D) ultrasound imaging (US))
Two-dimensional (2-D) transmission X-ray computed tomography 55–58
Two-dimensional (2-D) ultrasound imaging (US)
  B-mode (brightness) ultrasound scanning 51–52
  cine loop ultrasound 53–54
  color Doppler ultrasound imaging 53
  sampling modes and image display 52–53
2-D wavelet transform 90

u

Ultrasound (US) PACS module 165–166
Ultrasound Transducer Resource Center (UTRC) 372
University Corporation for Advanced Internet Development (UCAID) 118
UNIX operating system 101, 152
USC Image Processing and Informatics Lab (IPILab) 372
USC Molecular Imaging Center 372
User-level middleware layer, MIDG 353

collision management 355–356
data persistence manager 356
GAP servers 355
US Government Agencies 22–23

V

Variety, of medical image big data 577, 580–581
VAX 11/750 computer system 15
Velocity, of medical image big data 577, 581, 585
Vendor neutral archive (VNA) 583, 584
Veracity, in medical image big data 577, 580, 583
Very high-speed backbone network service(vBNS) 118
Virtual private network (VPN) 195
Visible light (VL) images 139
Visual analog scale (VAS) 545
Voxel 40

W

Waveform IOD 140
Web Access to DICOM Persistent Objects (WADO) 129
hybrid image retrieval 192
Web-based BAA clinical evaluation system
CAD server 491
graphical user interface 491–493
Web server 491
Web-based data management and image distribution
component-based Web Server 183–188

distributed image file server 179–181
PACS-based data management 179–180
performance evaluation 188–189
Web Server 181–183
Web-based ePR system, for breast cancer screening 386
Web-based multi-modality multi-resource information integration (MIMI) system 361, 384
Web-based PACS model 107–108
Web Server
concept of 182–183
Web technology 181–182
Web 100 tuning protocol 118, 120
Whole body CT scan 59
Wi-Fi (IEEE 802.11) 116
Windows NT and XP operating systems 152
WINDOWS NT/XP operating system 101
Wireless Ethernet Compatibility Alliance (WECA) 116
Wireless fidelity (Wi-Fi) 115
Wireless LAN (WLAN) 115
Wireless networks 115–116
Workstation graphic user interface (GUI)
basic software functions 267–271
workstation user interface 268–271
Wrist joint fuzzy subsystem 481–482

X

XDS-I-based patient-controlled image sharing solution

background 200
key features 202
patient-controlled workflow 201
results 207
RSNA image sharing network solution 200–201
X WINDOW platform 101

WILEY END USER LICENSE AGREEMENT

Go to www.wiley.com/go/eula to access Wiley's ebook EULA.